UNIVERSITY OF CALIFORNIA,
IRVINE

Synthesis of Collision Induced Dissociation Cross-linkers for Cross-linking Mass Spectrometry Experiments; Work Towards the Synthesis of Indole Alkaloid Alstonlarsine A; Total Syntheses of Strasseriolides A and B, Antimalarial Macrolide Natural Products

DISSERTATION

submitted in partial satisfaction of the requirements
for the degree of

DOCTOR OF PHILOSOPHY

in Chemistry

by

Leah Jeannine Salituro

Dissertation Committee:
Professor Scott Rychnovsky, Chair
Professor Elizabeth Jarvo
Professor Christopher Vanderwal

2022

DEDICATION

To my mom and dad

TABLE OF CONTENTS

LIST OF FIGURES

Page

LIST OF SCHEMES

LIST OF TABLES

Page

LIST OF ABBREVIATIONS

Δ Heat

Å Angstroms

Ac Acetate

AIBN 2,2′-Azobis(2-methylpropionitrile)

aq. Aqueous

Atm Atmosphere

BMSO Bismaleimide sulfoxide

Bn Benzyl

Boc *tert*-Butyloxycarbonyl

bp Boiling point

BrASSO Bromoacetamide succinimidyl sulfoxide

BSA Bovine serum albumin

BTPP *tert*-Butylimino-tri(pyrrolidino)phosphorane

Bu Butyl

Bz Benzoate

°C Degree Celsius

cat. Catalytic

CI Chemical ionization

CID Collision induced dissociation

Cp* Pentamethylcyclopentadiene

cod Cycloocta-1,5-diene

CSA Camphorsulfonic acid

d day(s)

δ Chemical shift

dba Dibenzylideneacetone

DBrASO Dibromoacetamide sulfoxide

DBU 1,8-Diazabicycloundec-7-ene

DCC *N*, *N*′-Dicyclohexylcarbodiimide

DDQ 2,3-Dichloro-5,6-dicyano-1,4-benzoquinone

DHSO Dihydrazide sulfoxide

DIA Diisopropyl azodicarboxylate

DIBAL-H Diisobutylaluminium hydride

DIPEA *N,N*-Diisopropylethylamine

DMAP 4-Dimethylaminopyridine

DMF Dimethylformamide

DMP Dess-Martin periodinane

DMS Dimethylsulfide

DMSO Dimethyl sulfoxide

DSSO Disuccinimidyl sulfoxide

dr Diastereomeric ratio

EDC 1-Ethyl-3-(3-dimethylaminopropyl)carbodiimide

ee Enantiomeric excess

equiv Equivalents

ESI Electrospray ionization

Et Ethyl

Fmoc Fluorenylmethyloxycarbonyl

g Gram

h Hour(s)

hex hexanes

HF Hydrofluoric acid

HFIP Hexafluoro isopropanol

HMDS 1,1,1,3,3,3-Hexamethyldisilazane

HMPA Hexamethylphosphoramide

HPLC High pressure liquid chromatography

HRMS High resolution mass spectrometry

Hz Hertz

i iso

Imid Imidazole

IPA Isopropyl alcohol

IR Infrared spectrometry

J Coupling constant

L liter

LAH Lithium aluminum hydride

LDA Lithium diisopropylamide

LICA lithium isopropoylcyclohexylamine

LLS Longest linear sequence

µ micro

m milli

M Molar

m-CPBA 3-Chloroperoxybenzoic acid

Me methyl

MHz Megahertz

min Minute(s)

MMSO Monosuccinimide maleimide sulfoxide

MOM Methoxymethyl

MPS *p*-Methoxybenzyl sulfonate

Ms Methanesulfonyl

MS Molecular sieves

MS Mass spectrometry

MS/MS Tandem mass spectrometry

MTBE Methyl *tert*-butyl ether

MTM Methylthiomethyl

NBS *N*-Bromosuccinimide

NfF Nonafluorobutanesulfonyl fluoride

NHS *N*-hydroxy succinimide

NMO *N*-Methylmorpholine *N*-oxide

NMP N-Methyl-2-pyrrolidone

NMR Nuclear Magnetic Resonance

PCC Pyridinium chlorochromate

Ph Phenyl

PhH benzene

Pin Pinacol

PMB *p*-Methoxybenzyl ether

PMP *p*-Methoxyphenyl

ppm Parts per million

PPSE Trimethylsilyl polyphosphate

PPTS Pyridinium p-toluenesulfonate

Pr propyl

PTSA *p*-Toluenesulfonic acid

Py Pyridine

RCAM Ring closing alkyne metathesis

RCM Ring closing metathesis

rt Room temperature

rxn Reaction

SDASO Succinimidyl-diazirine sulfoxide

SEM Trimethylsilylethoxymethyl

t tert

TBAF Tetra-n-butylammonium fluoride

TBDPS *tert*-Butyldiphenylsilyl

TBS *tert*-Butydimethylsilyl

TC Thiophene-2-carboxylate

TCBC 2,4,6-Trichlorobenzoyl chloride

TES Triethylsilyl

TIPS Triisopropylsilyl

Tf Trifluoromethanesulfonate

TFA Trifluoroacetic acid

TFAA Trifluoroacetic anhydride

THF Tetrahydrofuran

THPO Tetrahydropyranone

TLC Thin-layer chromatography

TMEDA Tetrahmethylethylenediamine

TMS Trimethylsilyl

TOF Time of flight

Ts Tosyl

Tr 2,2-Trichloroethoxycarbonyl

XLMS Cross-linking mass spectrometry

ACKNOWLEDGEMENTS

First and foremost, I need to thank my supervisor, Scott Rychnovsky. I have learned so much from you over these past few years. I am very appreciative of the environment you have developed in the lab, as an encouraging place to ask questions and work collaboratively. I am also grateful for your flexibility as a supervisor; you helped me when I was struggling and left me alone when I needed to focus. Thank you for everything.

I would also like to thank Chris Vanderwal and Liz Jarvo for being on my dissertation and orals committees. I have enjoyed our insightful conversations about my chemistry and I really value the ideas and encouragement you have given me since my second year. I also would really like to acknowledge the environment within both of your research groups; the positivity, encouragement, and advice that I have received from your students has given me invaluable lessons that I will take on with me past graduate school.

I am also indebted to the current and former graduate students in the Rychnovsky lab. I did not have much organic chemistry research experience when I first joined and the older members of the lab, including Sunshine, Burtea, and Sarah helped me to learn not only proper techniques, but also how to approach an experimental problem. I need to especially thank Sunshine for taking time to really help me develop as an organic chemist, even as reluctant I could be at times. I would also like to thank Jess Pazienza for jumping on the strasseriolide project with me, and being able to finish it as quickly as we did. Chuck Dooley would also be mad if I did not acknowledge him here, but he really has helped me everyday since we joined the lab together in our first year. Any time I have had a question, or needed some advice on my project you were often the first person I would ask, so thank you for all of your advice throughout the years.

I would be remised if I did not thank my undergraduate advisor, Professor Bruce Branchini for allowing me to begin research as a freshman in college and work in his lab through my college

experience. He taught me how to keep an immaculate laboratory notebook and really encouraged me to apply to graduate school. I would also really like to thank my undergraduate organic chemistry professor, Timo Ovaska for encouraging me to pursue organic chemistry in graduate school.

I am also so grateful for my friends outside of the Rychnovsky lab. I am grateful for Bonnie and Ryan across the hall for always being available to chat with me about chemistry and non-chemistry things. I am also so thankful for my friends from my cohort Carly, Kirsten, Chuck, Justin, Tyler, and Taylor for going through all of the highs and lows of graduate school together. I will really miss living in such close proximity to such a smart, kind, and encouraging group of people.

Eric, you have been my rock and my best friend through this entire experience. As terrible as a day or week I could have had, you always knew how to make me smile. Your confidence in me has meant so much to me, and I am so thankful to have met you here. I cannot wait for our future together after graduate school. I love you.

To my mom, dad, and sister Alanna, I do not even have words to say how much you all mean to me and how much your support has helped me get to where I am today. I have missed being so close to you all these past few years, but now I will have more time to travel to see you all (even if I do have to go to Florida).

VITA

Leah Salituro

EDUCATION

University of California, Irvine — Irvine, CA

Ph.D., Organic Chemistry (expected Spring 2022) — 2017 - Present

GPA: 3.94

Connecticut College — New London, CT

B.A. Chemistry — 2013 - 2017

GPA: 3.65

RESEARCH EXPERIENCE

Graduate Student, Organic Chemistry, University of California, Irvine

2017 - Present

- Supervised by Professor Scott Rychnovsky
- Design and synthesis of novel MS-labile cross-linkers collaboratively used to capture protein structure information via proteomics analysis
- Route design and work towards the total syntheses of the antimalarial macrolide natural product strasseriolides A and B and the indole alkaloid alstonlarsine A, a kinase (DRAK2) inhibitor

Undergraduate Researcher, Biochemistry and Organic Chemistry, Connecticut College

2014 - 2017

- Supervised by Professor Bruce Branchini
- Synthesis and characterization of a near-infrared luciferin analogue for use in bioluminescent imaging (thesis)
- Collection of Blue Ghost fireflies (*Phausis reticulata*) and characterization of isolated luciferase protein by cloning the luciferase gene and examining the bioluminescent properties
- Purification of adenylated luciferin analogues through optimized HPLC methods

Summer Researcher, Organic Chemistry, University of Otago, New Zealand

Summer 2016

- Supervised by Professor Bill Hawkins
- Self-conceived summer internship, forged new collaborations between Branchini (Connecticut College) and Krause/Hawkins labs (Otago)
- Development of a synthesis of the proposed structure of the New Zealand Glowworm (*Arachnocampa luminosa*) luciferin

Summer Intern, Analytical Chemistry, Merck & Co.

Summer 2015

- Supervised by Dr. Michael Hicks
- Optimized operating conditions for coulometric array detector
- Application of coulometric array detector data to determine oxidative liabilities of drug like compounds

PUBLICATIONS

- **Salituro, L. J**.; Pazienza, J. E.; Rychnovsky, S. D. Total Syntheses of Strasseriolide A and B, Antimalarial Macrolide Natural Products. *Org. Lett*. **2022**, 24, 1190–1194.
- Gutierrez, C.; **Salituro, L. J**.; Yu, C.; Wang, X.; DePeter, S. F.; Rychnovsky, S. D.; Huang, L. Enabling Photoactivated Cross-linking Mass Spectrometric Analysis of Protein Complexes by Novel MS-cleavable Cross-linkers. *Mol. Cell. Proteom*. **2021**, 20, 100084.
- Branchini, B. R.; Southworth, T. L.; **Salituro, L. J.**; Fontaine, D. M.; Oba, Y. Cloning of the Blue Ghost (*Phausis reticulata*) Luciferase Reveals a Glowing Source of Green Light. *Photochem. Photobiol*. **2017**, 93, 473–478.
- Hicks, M. B.; **Salituro, L. J**.; Mangion, I.; Schafer, W.; Xiang, R.; Gong, X.; Welch, C. J. Assessment of Coulometric Array Electrochemical Detection Coupled with HPLC-UV for the Absolute Quantitation of Pharmaceuticals. *Analyst* **2017**, 142, 525–536.

TEACHING AND MENTORSHIP

- Teaching assistant for organic chemistry, advanced organic chemistry, organic chemistry lab, and honors organic chemistry lab
- Supervised two undergraduate student researchers on the synthesis of cross-linkers
- Tutored organic chemistry and general chemistry undergraduates

PRESENTATIONS

- **Salituro, L. J.**; Pazienza, J. E.; Rychnovsky, S. D. Progress towards the synthesis of antimalarial macrolide strasseriolide B. ACS Fall, 2021.

AWARDS

- NSF GRFP Honorable Mention (2018)
- ACS Undergraduate Award in Organic Chemistry (2017)
- ACS Connecticut Valley Section Award (2017)

OUTREACH

Summer intern and volunteer, Students 2 Science 2013 – 2017

- Designed hands-on and virtual STEM experiments for middle and high school students
- Developed lesson plans, and instructor and student guides for each experiment

ABSTRACT OF THE DISSERTATION

Synthesis of Collision Induced Dissociation Cross-linkers for
Cross-linking Mass Spectrometry Experiments
Work Towards the Synthesis of Indole Alkaloid Alstonlarsine A
Total Syntheses of Strasseriolides A and B, Antimalarial Macrolide Natural Products

by

Leah Jeannine Salituro

Doctor of Philosophy in Chemistry

University of California, Irvine, 2022

Professor Scott Rychnovsky, Chair

The first chapter details the synthesis of three collision induced dissociation cross-linkers that have been developed for cross-linking mass spectrometry experiments. One of the cross-linkers is a homobifunctional cysteine targeting linker denoted DBrASO. It exploits the selective reactivity of thiols with α-bromoacetamides; and it is currently being studied in protein-protein interaction experiments. Another cross-linker BrASSO, is a heteobifunctional cross-linker that targets cysteine and lysine residues. The final cross-linker that was synthesized is SDASO, which contains a diazirine ring that can be used for non-specific cross-linking. SDASO proved the ability to cross-link all twenty amino acids, and was able to be used in complex proteosome cross-linking mass-spectrometry studies. These new cross-linkers expands the capability of studying protein structure and protein-protein interactions in tandem with mass-spectrometry.

The second chapter details work towards the synthesis of indole alkaloid alstonlarsine A. Many approaches to the natural product were considered and pursued to the cyclohepta[*b*]indole natural product. Formation of the cycloheptane proved difficult and our initial cyclohepta[*b*]indole annulation resulted in an unproductive spriocycle. An alternative route targeted a cis-

octahydroindolone through many disconnections, but only the *trans* isomer was favored. This natural product was not pursued further.

The third chapter details the first total syntheses of strasseriolide A and B. Strasseriolide B exhibited potent antimalarial activity against the drug-sensitive and drug-resistant strains of malaria. The macrolides were synthesized through a convergent route targeting a carboxylic acid-aldehyde fragment and an alcohol-vinyl iodide fragment. The synthesis of the two fragments were completed by starting from commercially available terpenes. The fragments were coupled through a Yamaguchi esterification and the key macrocyclization event was accomplished via a Nozaki-Hiyama-Kishi cyclization. Strasseriolide B was synthesized in 16 steps (LLS) and strasseriolide A was synthesized in 17 steps (LLS).

Chapter 1. Synthesis of Collision Induced Dissociation Cleavable Cross-Linkers

1.1 Introduction

1.1.1 Protein structure and interaction elucidation techniques

Elucidating protein structure and protein-protein interactions (PPIs) is essential to understanding cell functions and overall biological processes. The ability to understand structural biology allows for drugs and proteins to be engineered for specific causes. As the number of sequenced proteins grows, so too does the number of unknown tertiary and quaternary structures. The methods for uncovering protein structure include NMR, X-ray crystallography, and cryo-electron microscopy, which are responsible for elucidating 99.8% of the proteins listed in the protein data bank (PDB); with X-ray crystallography alone responsible for 87%.[1] However, as with any method, there are limitations for each.

X-ray crystallography is limited in that the proteins that are analyzed need to be pure and crystallizable and therefore it is best used with rigid, ordered proteins.[2–3] Analyzing flexible proteins is possible but much more difficult. NMR is limited by the size of the protein or protein complex. Larger structures are more difficult to resolve due to overlapping peaks and protein mobility, which cause broad, weak signals.[4] Moreover, for an acceptable signal to noise ratio, a large quantity of the protein and high purity is necessary. Over the last decade, cryo-electron microscopy has blossomed as a revolutionary structural elucidation technique and received the Nobel prize in 2017 for these advances.[5–6] However, one of the main disadvantages of cryo-electron microscopy is the low signal to noise ratio that can occur when studying biomacromolecules since they are only made up of carbon, oxygen, nitrogen, and hydrogen.[7] Also, the machinery required can be very expensive and the analysis can be quite time-consuming.[8] All three of these structural elucidation methods require viewing the protein structure outside of its native state. Furthermore, cryo-electron microscopy and X-ray only give a static image. Complementary to these techniques is cross-linking mass spectrometry (XL-MS) which

can be used to help determine tertiary and quaternary structure in more native, or even *in vivo*, environments.[9–14]

Cross-linking mass spectrometry makes use of chemical cross-linkers, which are molecules of a defined length that are designed to covalently bind with specific amino acids. When reacted in a protein complex, the cross-linker will bind two (sometimes three) amino acids and the cross-linked sample can be subjected to mass spectrometry. Through data analysis of the mass spectrometry results, the amino acids that were cross-linked can be determined. Additional analysis including comparison of the known crystal structure of a protein determines the exact amino acids that were cross-linked. The length of the cross-linker used defines an upper limit to how near the linked residues can be to one another in space. This constraint is important for the data analysis to validate the plausibility of a cross-link to occur in the system that is being studied.

Some advantages that XL-MS provides are as follows. Cross-linking can be applied to a proteosome in its native environment to capture short-lived interactions or temporary tertiary and quaternary structures. Cross-linking studies can be performed on small amounts of protein that does not have to be completely pure. Even more remarkable, cross-linking can be done *in vivo* in whole tissue or organelle systems. Over the past few decades cross-linking mass spectrometry has seen more widespread use due to technological advances of mass spectrometry and data sequencing software as well as the development of collision-induced dissociation (CID) cleavable cross-linkers.[14]

1.1.2 CID cleavable cross-linkers and tandem MS

A sample is cross-linked by simply adding the cross-linker to a buffered solution of a protein or protein complex. Once cross-linked, it can be purified and subjected to tandem mass spectrometry (MS/MS) analysis, in which at least two mass analyzers are used in sequence. For protein sequencing, a collision cell is used in between the analyzers, which contains gaseous

neutral molecules. When an analyte is accelerated into the cell, it will collide with the neutral gases and an energy transfer will occur, causing the bonds within the analyte to fragment. This process is what is known as collision-induced dissociation (CID). By varying the acceleration speed of the analyte ions, different collision energies can be achieved, which causes different bonds to break; weaker bonds will break at lower energies. When a purified cross-linked sample is subjected to MS/MS, the first MS analysis (MS1) will indicate the mass to charge ratio (*m/z*) of the cross-linked peptides. This mass can be selected and subjected to the collision chamber, where the peptide bonds are fragmented, and the masses of these fragments are detected in the second mass analyzer (MS2), Figure 1.1b.[15]

For example, disuccinimidyl suberate (DSS) is one of the most widely used cross-linkers for proteomics experiments, Figure 1.1a.[16] DSS contains two *N*-hydroxy succinimide (NHS) esters that react almost exclusively with lysine (K) residues under biological conditions. When DSS is exposed to a short peptide fragment (Figure 1.1a) it will react with the lysine residue that will displace the NHS ester on each end of the linker to form two amide bonds. There will also be dead-end links in which one end of DSS reacts with the peptide and the other is hydrolyzed, (Figure 1.1d). The dead-end links can be detected in MS1 and not subjected for further analysis. From this mixture, the *m/z* of the desired cross-linked fragment is calculated, observed, and subjected to MS2, in which the peptide bonds are cleaved and the fragments are observed (Figure 1.1e). The sequencing analysis for a short peptide like the example shown in Figure 1.1 is straightforward, especially with the help of sequencing analysis software. However, when larger proteins and protein complexes are studied, the data analysis becomes extremely difficult and convoluted. When using a search algorithm that compares experimental MS/MS datasets with theoretical MS/MS spectra, a scaling problem is observed as the size of the system being studied grows; this is known as the n^2 problem.[17] CID-cleavable cross-linkers were developed to address this problem.

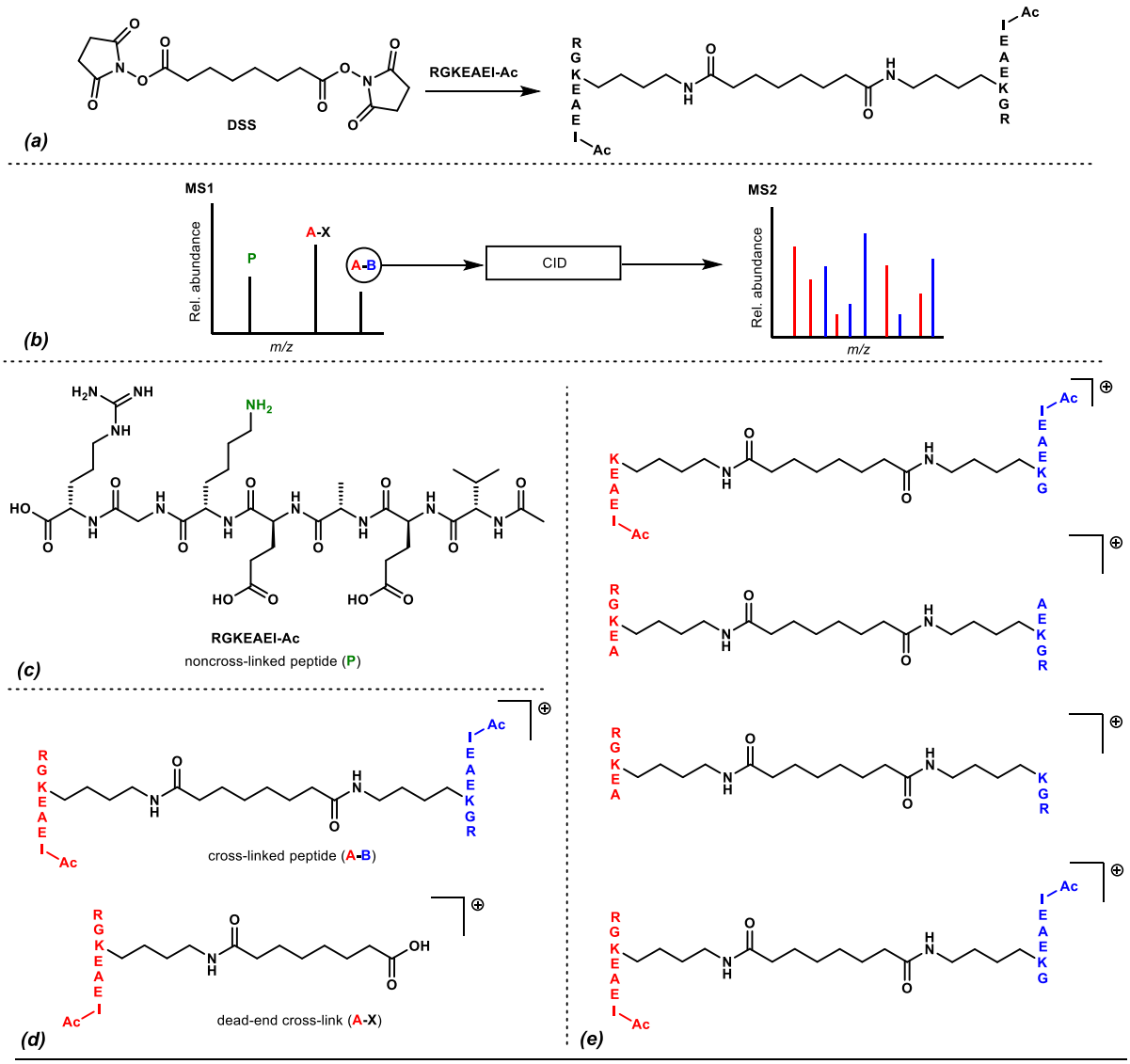

Figure 1.1 (a) Reaction of DSS with a short peptide ***(b)*** Tandem MS of the cross-linked peptide ***(c)*** Structure of peptide fragment ***(d)*** Structures of a cross-linked peptide and a dead-end cross-link ***(e)*** Examples of fragmented ions in MS2

Integrating a CID-cleavable moiety into a cross-linker will simplify the final data analysis by adding an additional collision chamber and mass analyzer to the MS/MS. The CID-cleavable moiety must be able to cleave at a lower energy than the energy it takes to break a peptide bond. The cross-linker is designed to cleave in the first collision chamber, while the peptide bonds will cleave in the second collision chamber. Figure 1.2b shows the tandem MS for a CID-cleavable cross linker.

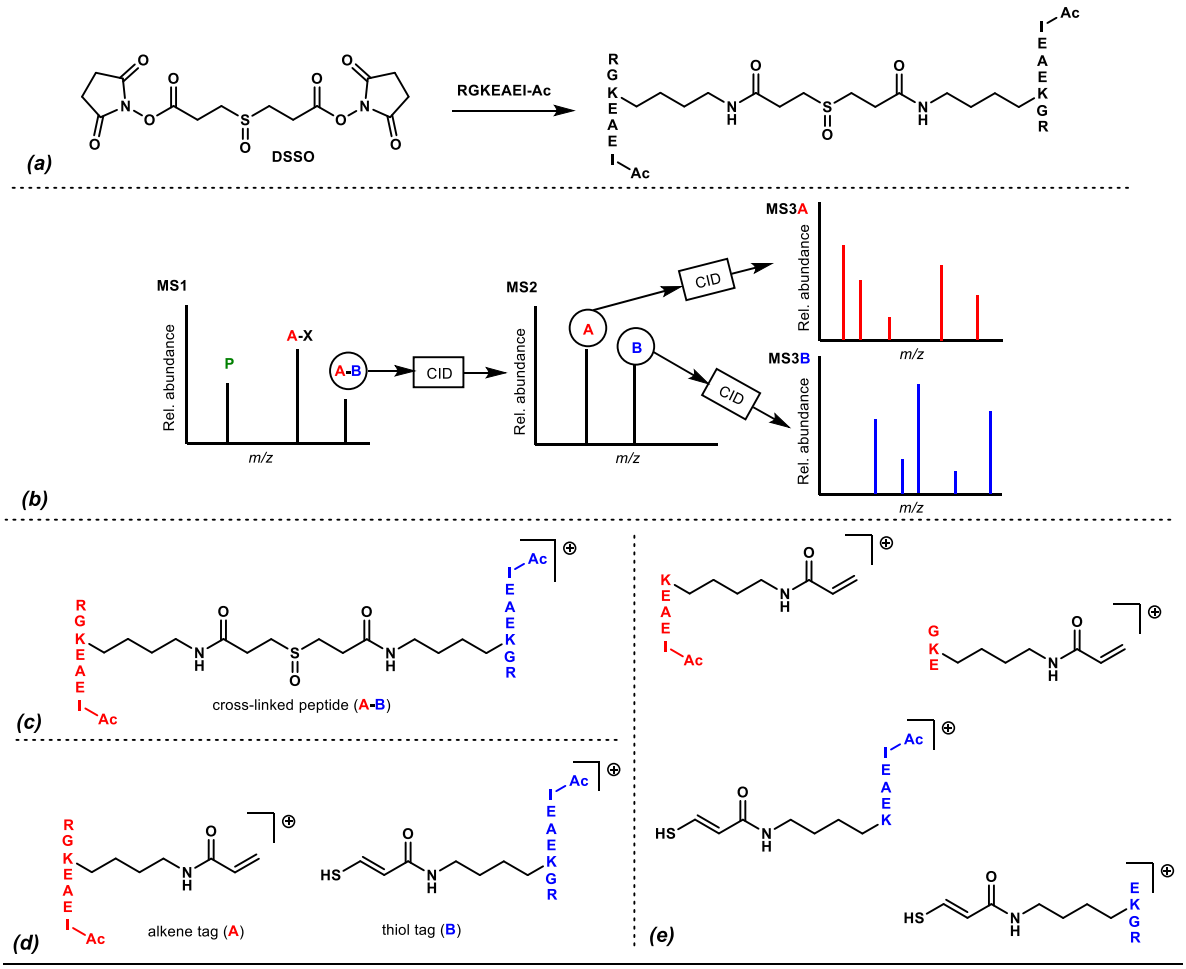

Figure 1.2 (a) Reaction of DSSO with a short peptide ***(b)*** Tandem MS of the cross-linked peptide ***(c)*** Structure of cross-linked peptide with DSSO ***(d)*** Structures of the tagged fragments after CID of cross-linker ***(e)*** Examples of fragmented ions in MS3

To meet this design requirement, the CID cleavable cross-linker disuccinimidyl sulfoxide, DSSO (Figure 1.1a) was developed in our lab, which is similar to DSS and contains two NHS esters to chemoselectively react with lysine residues.[18] In addition, the spacer region of DSSO contains a sulfoxide, which is the CID cleavable moiety (the cleavage mechanism will be discussed in section 1.1.3). The carbon-sulfur bonds can be fragmented at a lower energy in the MS compared to peptide bonds.[18] Analogous to the non-cleavable linkers, MS1 will detect the *m/z* of the cross-linked peptides. This specific ion will then be subjected to a collision chamber that is set at a collision energy that will break the CID-cleavable functional group within the cross-linker, but not the peptide bonds. Each peptide fragment will contain a portion of the cross-linker (MS2, Figure 1.2d) which are essentially tags on each peptide fragment. When using sulfoxide as the

CID-cleavable moiety, one fragment will contain an alkene while the other will contain a thiol (Figure 1.2d). Each fragment will be subjected to separate MS3 for peptide bond cleavage, Figure 1.2e. This data is sequenced with specialized software to determine which amino acids were cross-linked. CID-cleavable cross-linkers like DSSO have simplified the data processing aspect of cross-linking mass-spectrometry and have allowed for large organelles, and even tissues, such as a mouse heart (!) to be studied with this method.[19]

The workflow that is used by our collaborators, the Huang lab at UC, Irvine, for studying the more complex systems is shown in Figure 1.3. When studying short peptide fragments as shown in Figures 1.1 and 1.2, there is little purification that needs to be done before subjecting the sample to the MS/MS for analysis. However, when studying more complex systems like whole proteins or protein complexes, a more in-depth purification is needed before subjecting a sample to mass spectrometry.

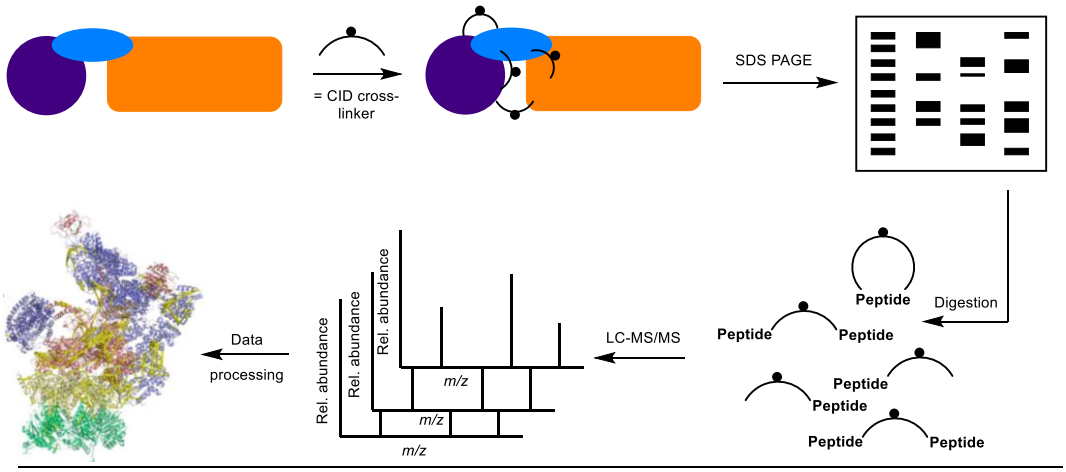

Figure 1.3. Work flow for cross-linking mass spectrometry

In step one, a protein complex is reacted with a CID cleavable cross linker resulting in a cross-linked protein complex. This protein complex is purified via sodium dodecyl sulphate–polyacrylamide gel electrophoresis (SDS-PAGE) to separate noncross-linked samples from cross-linked samples. The desired sample is excised and digested with trypsin or chymotrypsin.

This mixture is subjected to tandem LC-MS/MS and the data is processed using protein sequencing software to furnish a cross-linking map of the protein complex.

1.1.3 Mechanisms of CID cleavability

There are many different CID-cleavable functional groups that have been developed for cross-linking mass spectrometry. Our group, in collaboration with the Huang lab at UC, Irvine, has developed a number of sulfoxide containing CID cleavable cross-linkers. However, there are many other CID cleavable cross-linkers that contain NHS esters, but have different cleavable moieties. This section will discuss other CID cleavable cross-linkers that target lysine residues and compare the different fragmentation methods.

As a side note, the mechanisms described in this section are all only postulated, as the only mechanistic evidence is the observed *m/z* ratio of the highly energetic and short-lived intermediates, and the known structure of the cross-linker. Furthermore, multiple ions may be detected in MS2 after the fragmentation, complicating which ions should be considered for the mechanism. When designing a CID cleavable cross-linker, various fragmentation mechanisms should be considered. Ideally only one bond will fragment at a collision energy less than the energy it takes to break a peptide bond.

Bisuccinimidyl-succinamyl-aspartyl-proline (SuDP), Scheme 1.1a, was reported in 2006 and contained a proline-aspartic acid peptide bond as the CID cleavable group.[20] These particular peptide bonds are known to cleave at a lower energy than other peptide bonds during CID.[21,22] The authors developed the two step CID cleavage, in which the first CID cleaves the cross-linker and the second cleaves peptide bonds.[23] This technique paved the way for the development of additional MS-labile cross-linkers and the data processing thereof. The proposed fragmentation mechanism for SuDP is shown in Scheme 1.1b. After a proton shift from the aspartic acid to the

proline residue, the aspartyl group can cyclize on the proline peptide bond. Formation of the cyclic anhydride will eject the proline group to form the two fragments.

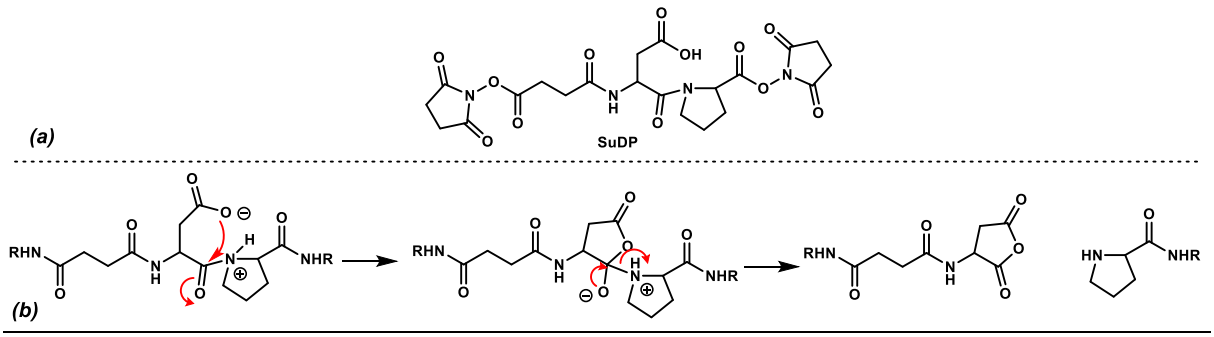

Scheme 1.1 (a) Structure of SuDP ***(b)*** Mechanism of fragmentation of SuDP; R refers to lysine residues on peptide fragments

CID cleavable cross-linker disuccinimidyldibutyric urea (DSBU) was reported by Sinz and coworkers in 2010.[24] This linker contains a urea moiety in the spacer region and there are two possible fragmentation mechanisms that result in the same *m/z* ion fragments. In the first mechanism, Scheme 1.2b, the amide resulting from the lysine linkage can attack the urea carbonyl through a 7-*exo-dig* cyclization. Cleavage of one of the urea amide bonds results in the primary amine fragment and the oxazepanone fragment. Alternatively, Scheme 1.2c, a 1,7-proton transfer could occur, followed by cleavage via isocyanate formation. The isocyante fragment and the oxazepanone fragment have the same exact mass so either mechanism is possible.[25]

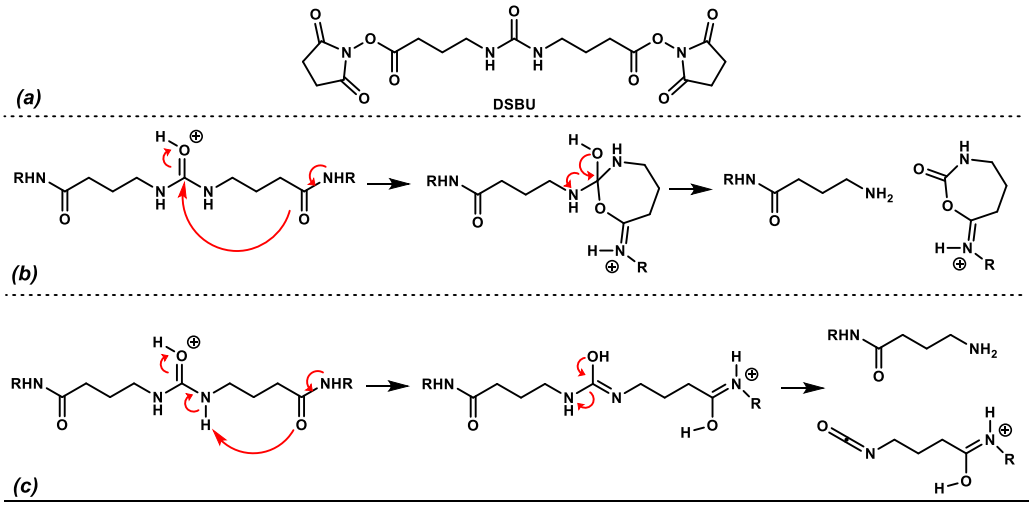

Scheme 1.2 (a) Structure of DSBU ***(b)*** One plausible fragmentation mechansim of DSBU ***(c)*** A second plausible fragmentation mechansim of DSBU; R refers to lysine residues on peptide fragments

In 2008, Reid and coworkers developed a sulfonium ion CID-cleavable cross-linker.[26] The linker was inspired by previous findings that sulfonium ion derivatives of sulfur containing amino acids (methionine and cysteine) undergo cleavage in the MS by loss of a dialkyl sulfide. This simple cleavage mechanism is postulated to go through attack of the amide carbonyl into the antibonding orbital of the carbon-sulfur bond to furnish a dialkyl thiol fragment and a six-membered oxazoline fragment. This cross-linker was also found to cross-link very efficiently in proteins, likely due to its increased water solubility.

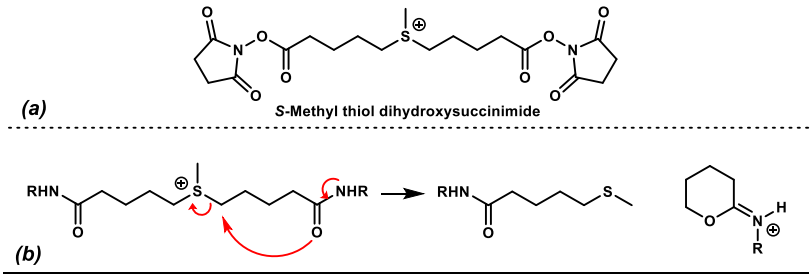

Scheme 1.3 (a) Structure of *S*-methyl thiol containing cross-linker ***(b)*** Mechanism of fragmentation; R refers to lysine residues on peptide fragments

The 1,4-diazabicyclo[2.2.2]octane (DABCO) containing cross-linker DC4 is a quaternary diamine that has two positive charges contributing to its great aqueous solubility.[27] The fragmentation proceeds via a straightforward mechanism: in MS2 one end of the linker undergoes a 5-*exo*-*tet* to kick our the DABCO moiety and result in the two fragments shown in Scheme 1.4b. When the DABCO-containing fragment is subjected to its individual MS3, it undergoes another cyclization to kick out DABCO (while the peptide bonds are also cleaved).

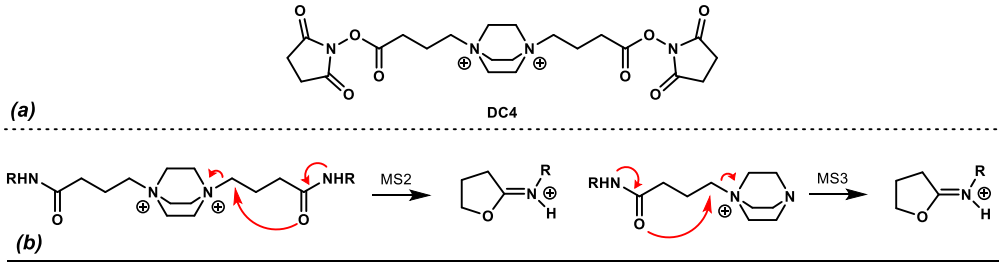

Scheme 1.4 (a) Structure of DC4 ***(b)*** Mechanism of fragmentation, the linker is cleaved in both MS2 and MS3; R refers to lysine residues on peptide fragments

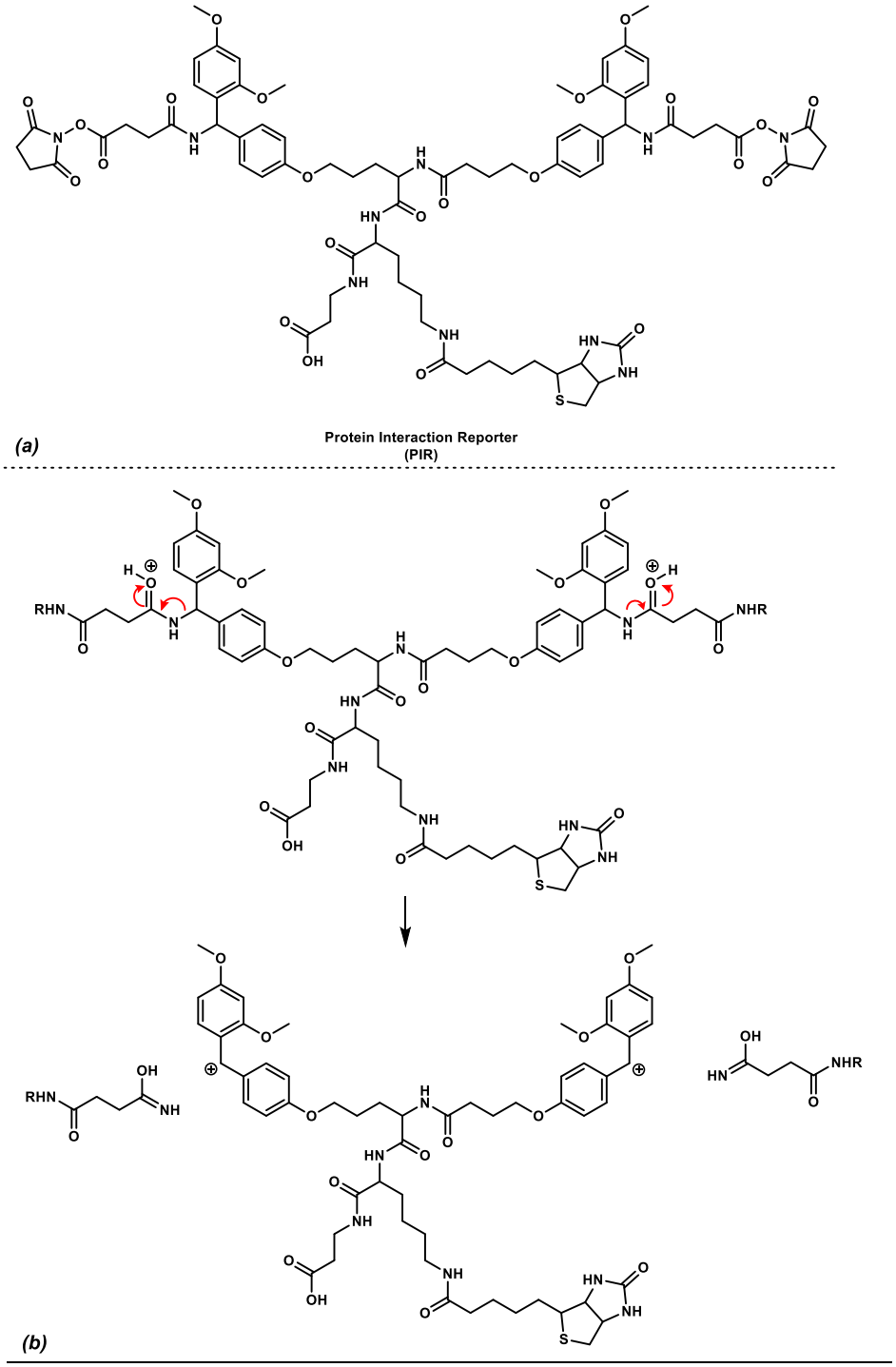

Scheme 1.5 (a) Structure of PIR ***(b)*** Mechanism of fragmentation;
R refers to lysine residues on peptide fragments

In 2005 Bruce and coworkers reported a CID cleavable cross-linker called protein interaction reporter (PIR), Scheme 1.5a.[28] The linker was designed with two NHS esters to react with lysine residues, a biotin moiety for affinity purification, and a spacer region that was designed

after solid phase peptide reagents. PIR has shown to be very successful for *in vivo* studies, while the biotin tag helps with enrichment.[29,30] The cleavage mechanism is shown in Scheme 1.5b, in which two benzylic amine bonds are broken resulting in two doubly benzylic carbocations and the two peptide containing fragments.

The final cleavage mechanism that will be discussed was developed in our lab. DSSO as discussed in section 1.1.2, contains a sulfoxide as the CID cleavable moiety. The sulfoxide can undergo a retro-ene type mechanism to form an enone fragment and a sulfenic acid containing fragment. The sulfenic acid often undergoes a dehydration to the resulting thioenol or thiol aldehyde. The cleavage can occur on either side of the cross-linker, leading to two possible ion pairs (if the cross-linked peptide fragments are not equivalent) DSSO is commercially available and has proven to be successful in many cross-linking mass spectrometry studies.[31–36] Through the success of DSSO, it became apparent that the sulfoxide moiety cleavability could be the basis for new cross-linkers to target different amino acids.

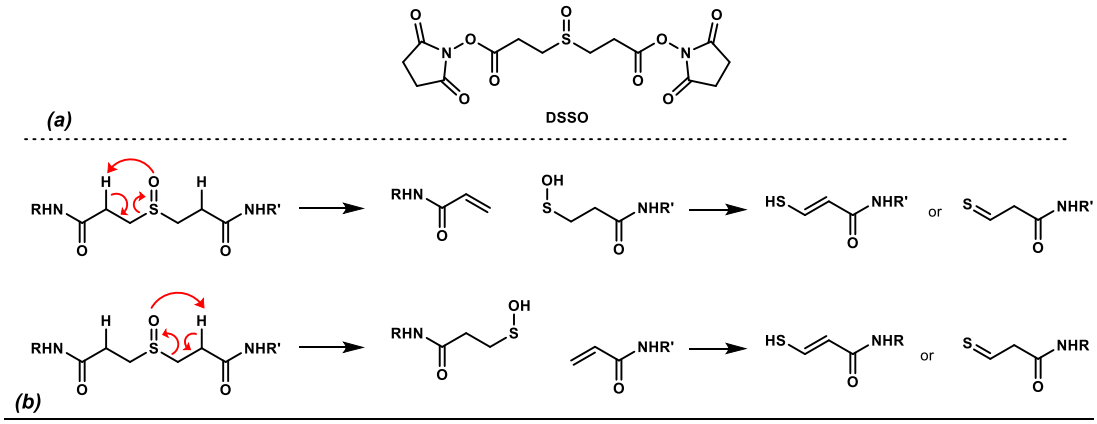

Scheme 1.6 (a) Structure of DSSO ***(b)*** Mechanism of fragmentation;
R refers to lysine residues on peptide fragments

1.1.4 Rychnovsky lab sulfoxide containing cross-linkers

DSSO is now commercially available, but the synthesis of this cross-linker is straightforward, Scheme 1.7. The commercially available 3,3' thiodipropionic acid is esterified with *N*-hydroxysuccinimide to form sulfide **1-1**, which can easily be oxidized to the corresponding sulfoxide when treated with *m*-CPBA.[18]

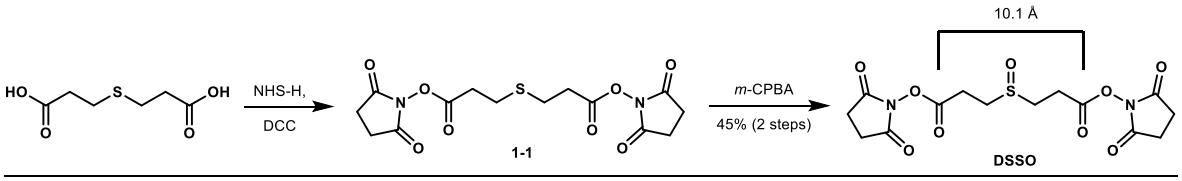

Scheme 1.7. Synthesis of DSSO

DSSO has a spacer length of 10.1 Å, which can be seen as a "molecular ruler" meaning that there is a distance range that the cross-linked lysine residues can be from each other. It was hypothesized that increasing the length of DSSO would give different or additional structural insight when studying a protein or protein complex. Our lab set out to synthesize DSSO derivatives of varying lengths to test this theory.

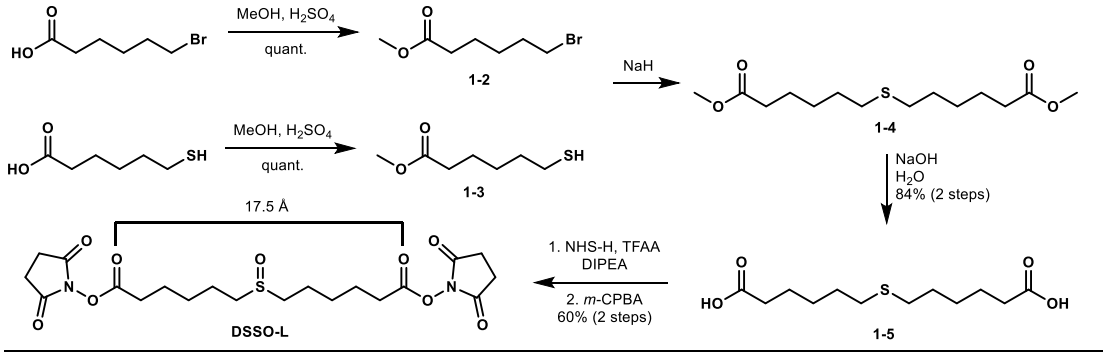

Scheme 1.8. Synthesis of DSSO-L

An analog of DSSO, DSSO-L was synthesized by a previous Rychnovsky lab member Eric Novitsky, Scheme 1.8, and was calculated to have a spacer length of 17.5 Å.[37,38] To study the viability of this cross-linker, it was initially studied with a short peptide. The tandem MS experiments showed that the carbon-sulfur bond fragmented at the same energy as the peptide

backbone. Also, the dehydration of the sulfenic acid fragment, **1-10,** to the thiol, **1-11**, Figure 1.4 was observed at a significantly lower abundance as compared to DSSO. The carbon-sulfur bond in DSSO is much more labile as compared with DSSO-L. This can be explained by comparing the different fragments that would result from the cleavage of DSSO and DSSO-L. Alkene **1-6**, which is the product of DSSO cleavage, is conjugated with the carbonyl group while alkene **1-9** is not. This same logic can also explain why less dehydration of the sulfenic acid is observed with DSSO-L (compare **1-8** and **1-11**). This conclusion paved the way for future designs of sulfoxide containing CID cleavable cross-linkers. It was decided that at least one side of the linker needed to have a carbonyl at the β-position of the sulfoxide for efficient cleavage at a higher energy than the peptide backbone.

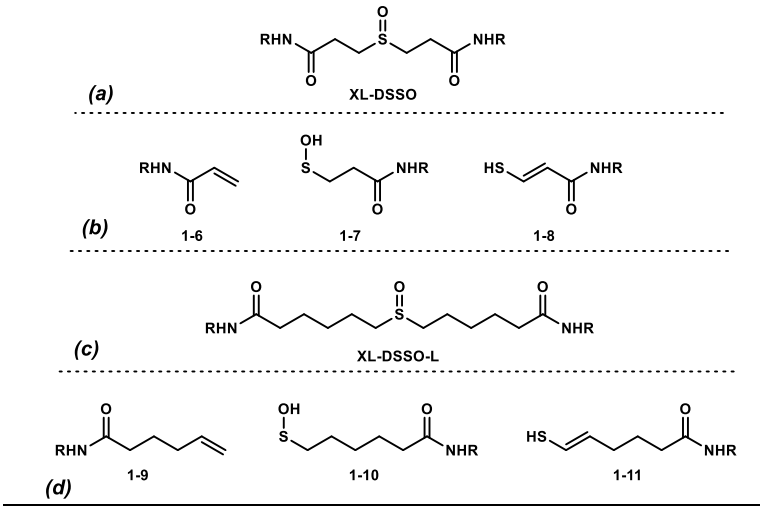

Figure 1.4 (a) Structure of DSSO cross-linked between two K residues (XL-DSSO) ***(b)*** MS2 fragments of XL-DSSO ***(c)*** Structure of DSSO-L cross-linked between two K residues (XL-DSSO-L) ***(d)*** MS2 fragments of XL-DSSO-L

To examine the reactivity of DSSO analogs in cross linking reactions, asymmetric DSSO derivatives **1-12**, **1-13**, and **1-14** were synthesized by Eric Novitsky.[37] The analogs contain ethylene glycol subunits in between the sulfoxide and the NHS ester on the long side of the chain, which have been shown in increase solubility and lysine reactivity of NHS esters compared to an all-carbon chain.[38,39] The short side of the cross-linker contains the required β-carbonyl. It was

postulated that these derivatives would only cleave on one side and therefore lead to just one pair of ion fragments in MS2.

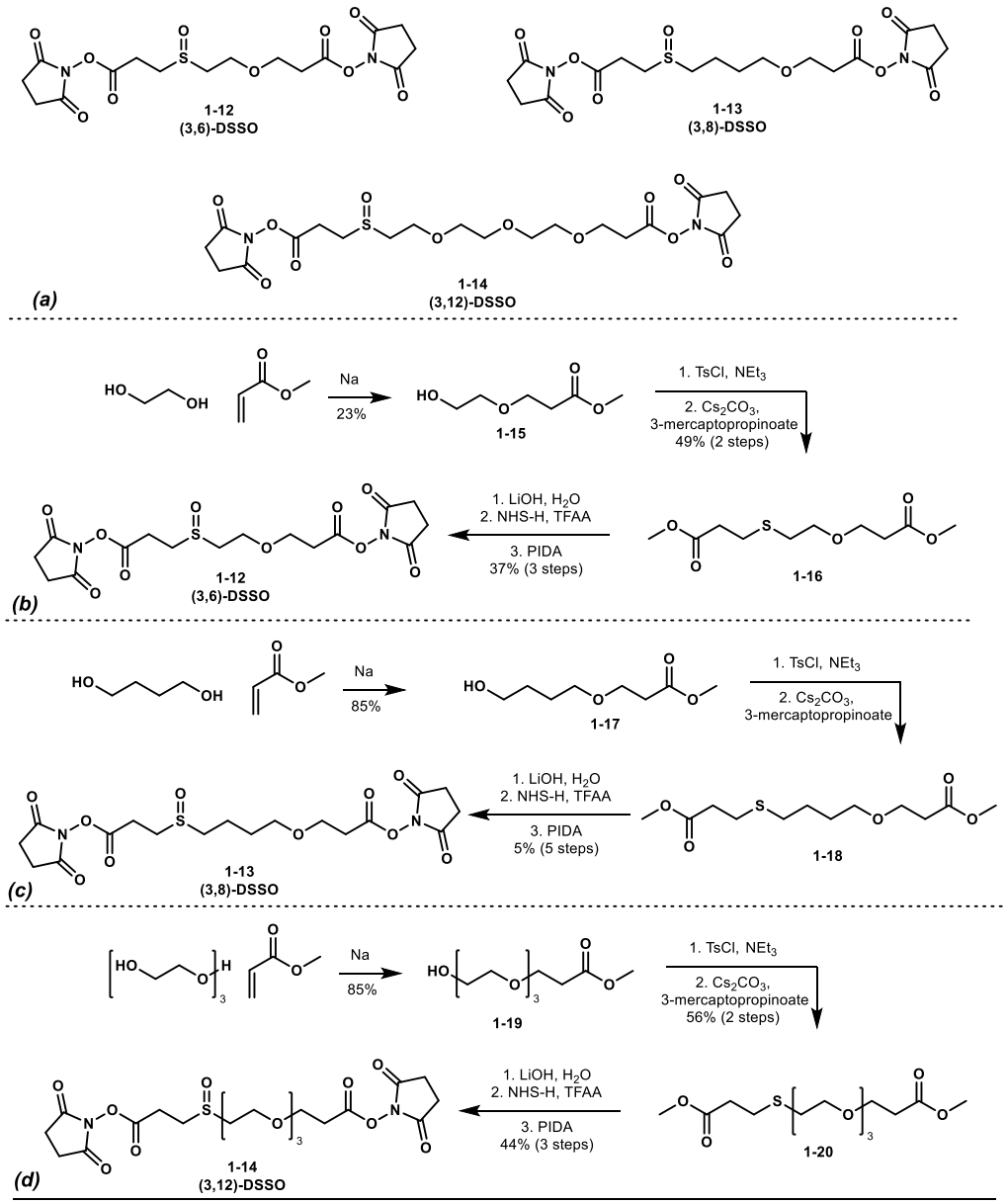

Scheme 1.9 (a) Structures of (3,6)-DSSO, (3.8)-DSSO, and (3,12)-DSSO
(b) Synthesis of (3,6)-DSSO ***(c)*** Synthesis of (3,8)-DSSO ***(d)*** Synthesis of (3,12)-DSSO

The syntheses of these analogs were similar, Scheme 1.9. First an oxa-Michael with a glycol, furnished the ethylene glycol side of the linker. Tosylation of the primary alcohol followed by displacement with 3-mercaptopropionate afforded the dimethyl ester intermediates. Each cross-linker was completed by hydrolysis, esterification, and sulfide oxidation. In reacting the four

cross-linkers with bovine serum albumin (BSA), different K-K linkages were observed with each. There were just 13 (out of the 44 unique linkages) that overlapped with all of the cross-linkers. (3,6)-DSSO and (3,8)-DSSO, which are quite similar in length shared about 75% of their linkages. Conversely, DSSO and (3,12)-DSSO only shared about 35% of their linkages. These data suggest that varying the cross-linker length result in different K-K linkages and therefore provides additional structural information on the same protein.

Seeking to further expand the cross-linker method, we reasoned that creating a toolbox of cross-linkers that vary in not only length but also amino acid selectivity would be beneficial for the structural biology community. It is not surprising that lysine residues have been the most commonly targeted amino acid with cross-linkers, as they have shown to react very selectively and efficiently with NHS esters under biological conditions.[40,41] Lysine is also an ideal target as it makes up about 6% of protein sequences and is concentrated on the surface of proteins. However, cross-linking data with different amino acids could give a larger picture and a unique view of protein structure and interactions. Our lab set out to synthesize CID cleavable cross-linkers that would target amino acids beyond lysine thus greatly expanding the number of observable cross-links.

In 2016, our lab reported a CID cleavable cross-linker that targeted acidic residues, aspartic acid and glutamic acid.[42] Dihydrazide sulfoxide (DHSO) was designed after DSSO; a symmetrical, homobifunctional (meaning the same reactivity on each end) cross-linker with a carbonyl at the β-position of the sulfoxide. In place of the NHS esters, DHSO contains two hydrazide moieties. The new cross-linker could be synthesized in one step from DSSO, as shown in Scheme 1.10a. In the presence of 4-(4,6-dimethoxy-1,3,5-triazin-2-yl)-4-methylmorpholin-4-ium chloride (DMTMM), DHSO was found to successfully cross-link proximal acidic amino acids. The cross-linking mechanism with this pair is shown in Scheme 1.10b. DMTMM is able to activate

carboxylic acids at a neutral pH,[43] while more traditional coupling reagents, such as 1-ethyl-3-(3-dimethylaminopropyl)carbodiimide (EDC) requires a lower pH, 5.5.[44]

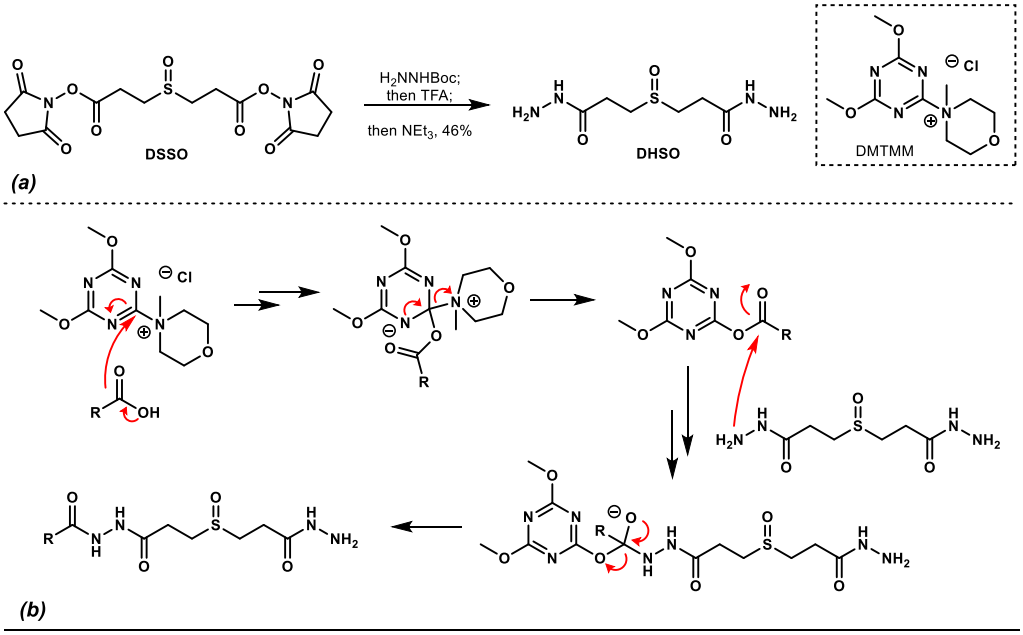

Scheme 1.10 (a) Synthesis of DHSO from DSSO ***(b)*** Mechanism of DMTMM activation of a carboxylic acid and cross-linking with DHSO; R = peptide fragment

Other appealing amino acids to target with this method were cysteine residues, which are major contributors to the tertiary structure of proteins. These thiols are very nucleophilic and therefore were targeted in the design of a new cross-linker. Bismaleimide sulfoxide (BMSO)[45] contains maleimide functional groups that are known to react with cysteine residues under biological conditions though a thiol-Michael addition.[40,46] BMSO was also designed after DSSO as a homobifunctional sulfoxide containing CID cross-linker. It was also synthesized in one step from DSSO, Scheme 1.11a. BMSO reacted as expected with short peptides and BSA. However, the cross-linked product after the Michael addition was extremely susceptible to hydration, Scheme 1.11c. A mixture of open and closed form of the cross-linked product made the data analysis more difficult. Additional cysteine targeting homobifunctional cross-linkers that do not have this issue will be discussed in section 1.2.

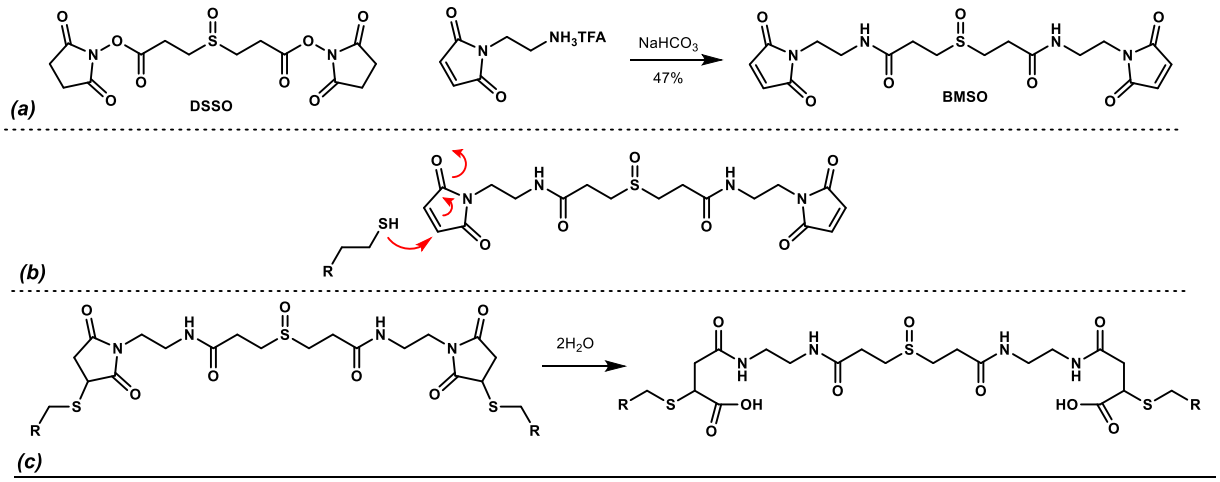

Scheme 1.11 (a) Synthesis of BMSO from DSSO ***(b)*** Thiol-Michael addition of cysteine into BMSO maleimide ***(c)*** Closed ring cross-linked BMSO and hydrated open ring cross-linked BMSO

The data from cross-linking BSA with DSSO, DHSO, and BMSO were compared. As shown in Figure 1.5, these three cross-linkers show distinct structural data.[45] These data inspired our lab to continue to synthesize cross-linkers with different reactivity profiles in order to expand the CID cleavable cross-linker toolbox.

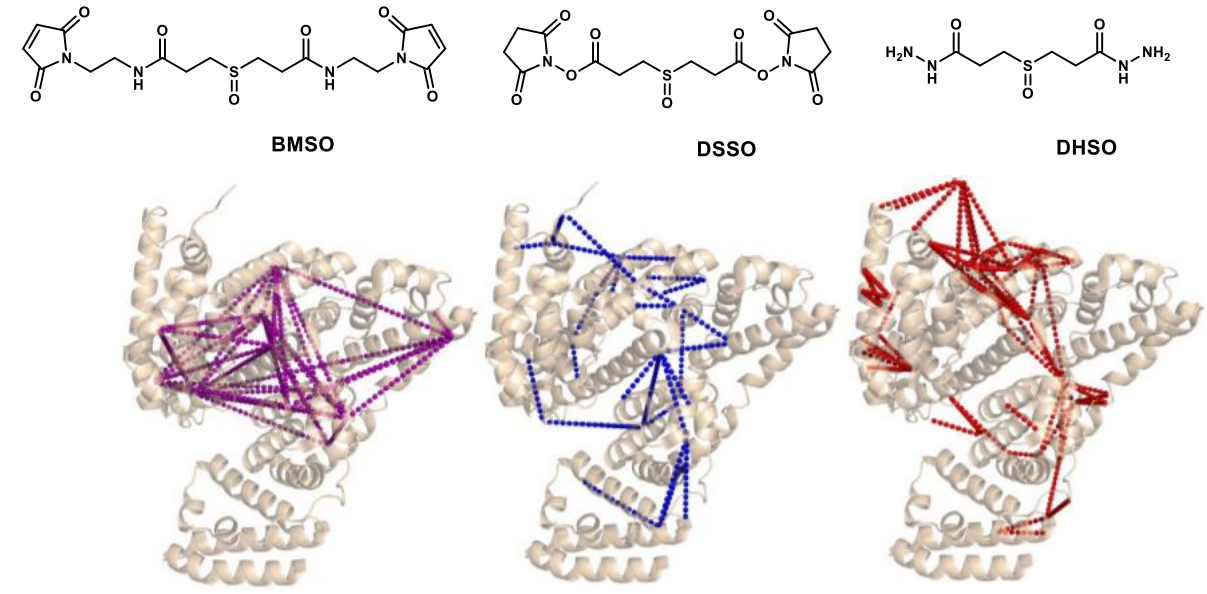

Figure 1.5. Comparison of XLMS maps of the BSA crystal strucutre with BMSO (purple), DSSO (blue), and DHSO (red)

1.1.5 Application of sulfoxide containing cross-linkers

As shown in Figure 1.5, by using the different reactivity of the cross-linkers (BMSO, DSSO, and DHSO) we were able to observe different structural information on BSA. The Huang lab wanted to further apply this reactivity to solve a larger structural biology quandary. The constitutive photomorphogenesis 9 (COP9) signalosome is a protein complex made up of eight subunits. It is responsible for removing ubiquitin-like proteins (deneddylation) from the largest enzyme class of ubiquitin-proteasome systems, called Cullin-RING E3 ligases. It is the only deactivator of Cullin-RING E3 ligases, and due to its essential functionality, it has been extensively studied biophysically. It has even been shown that inhibiting this protein complex can kill cancer cells and certain parasites.[47,48] However, the structural dynamics of the COP9 complex functionalization are still unknown and have been difficult to track with more conventional methods. It was recently discovered that the COP9 complex has a ninth subunit (CSN9), which may be important for the conformational changes of the complex during deneddylation.[49] The CSN9 is small and highly disordered and therefore has been difficult to study. The Huang group was able to employ our three cross-linkers, DSSO, DHSO, and BMSO to examine where on the COP9 the newly discovered subunit binds and how this might affect the structural changes of the entire complex.[34]

The three cross-linkers were reacted with the two separate complexes (one of just the COP9 complex and one of the COP9 complex with the CSN9 unit). The results are shown in Figure 1.6. Since the CSN9 subunit is highly acidic and does not contain any cysteine residues and very few lysine residues, cross-linking with this subunit was only observed with DHSO. Additionally, unique linkages with all three cross-linkers were observed between the eight original subunits when the CSN9 was added. This data infers that the conformation of the whole complex changes when the ninth unit is added. The cross-links that were observed are consistent with the known X-ray structure. The cross-linking data was also supported by additional structural modeling of the COP9 complex. The ninth subunit was found to interact with subunits one (CSN1)

and three (CSN3) through cross-linking with DHSO. Previously, it was reported that the CSN9 interacted with subunits five and six, but there were no cross-links observed with these subunits.

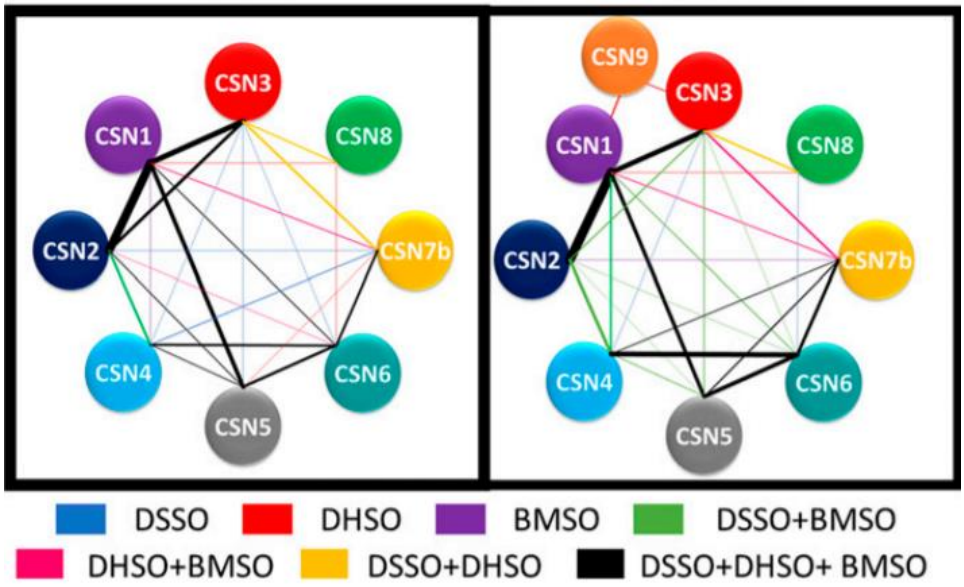

Figure 1.6. Cross-linking map of the COP9 complex without (left) and with (right) the CSN9 complex; the CSN9 only showed DHSO cross-links with subunits 1 and 3 (ref. 34)

Most of the core structure of the COP9 complex was maintained with the addition of the CSN9 unit. The largest changes in cross-links were observed with subunit two (CSN2). It is known that CSN2 within this complex is important for the interaction of the COP9 complex with the Cullin-RING E3 ligases; the structure of the COP9-enzyme complex has been previously studied.[50–53] Therefore, it is postulated that the addition of the ninth subunit induces structural changes to allow the COP9 to bind to the ligase. Without the addition of CSN9, the structural change the COP9 complex needs to induce in order to bind the ligase requires significant activation energy. Figure 1.7 shows the proposed structural changes of the COP9 complex when binding to the Cullin-RING E3 ligases without the CSN9 and with the CSN9 subunit.

This study shows the application of using cross-linkers with different reactivity to study structural biology. Adding to the toolbox of CID cleavable cross-linkers will allow for similar studies to be performed and additional physical biology questions to be examined.

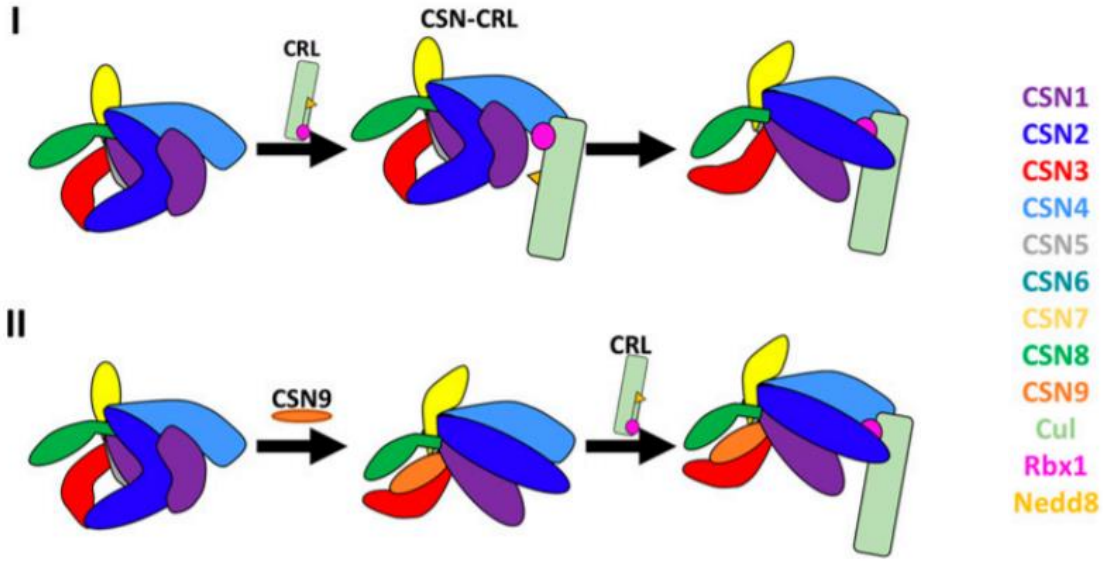

Figure 1.7. Proposed structural changes of the COP9 complex when (top) binding to Cullin-RING E3 ligases (CRL) and (bottom) binding to the CSN9 subunit and then binding to CRL (ref. 34)

1.2 Synthesis of DBrASO, a homobifunctional cysteine-cysteine cross-linker

1.2.1 Introduction to cysteine-cysteine cross-linkers and design of DBrASO

In our pursuit of expanding the toolbox of sulfoxide CID cleavable cross-linkers, we looked to improve upon BMSO, the cysteine-cysteine cross-linker. The thiol reactive maleimide group is prone to hydrolysis, which will complicate the MS data analysis with the closed and open form of the Michael addition product. Also, under biological conditions the Michael addition product could potentially undergo a retro-Michael and reform the maleimide, Scheme 1.12a, which is certainly unproductive for cross-linking.[54,55] By taking advantage of the known reactivity of acetylbromides with thiols under physiological conditions, we designed dibromoacetamide sulfoxide (DBrASO). α-Halocarbonyls have a long history of direct alkylation of cysteine residues.[56] The cysteine can displace the α-halo group through a simple irreversible S_N2 reaction, Scheme 1.12b. These electrophiles can also react with other nucleophilic amino acids, so it is slightly less chemoselective than maleimide groups for cysteine.[55] Nonetheless, we wanted to examine the reactivity and viability of DBrASO as a cross-linker.

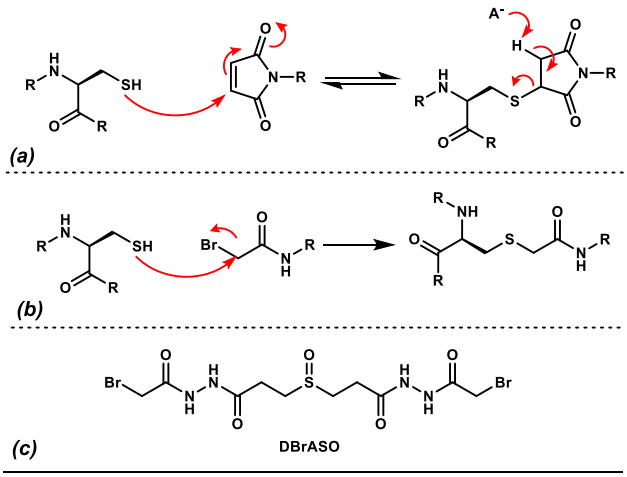

Scheme 1.12 (a) Reversible Michael addition of cysteine into maleimides ***(b)*** S_N2 addition of cysteine into α-bromoacetamides ***(c)*** Structure of DBrASO

1.2.2 Synthesis of DBrASO

Our initial synthetic plan was to react DHSO with bromoacetic acid to yield the new cross-linker DBrASO. However, DHSO is extremely polar which made it difficult to work with and to isolate the desired product. To decrease some of the polarity issues, we planned to go through the sequence with the sulfide as opposed to the sulfoxide. We began by modeling our route after the synthesis of DHSO. Treating NHS ester **1-1** with *t*-butyl carbazate afforded the protected hydrazide **1-22** in good yields, after optimization of the purification. Attempts to do an aqueous work-up of the reaction slurry left the product in the aqueous phase. Trying to purify the crude mixture on silica was also unsuccessful because the product is so polar and it would co-elute with *N*-hydroxysuccinimide. Gratifyingly, when the reaction was performed in CH_2Cl_2, the product would precipitate out of solution after a few minutes and a simple filtration furnished the pure product. Hydrazide **1-22** was then deprotected upon treatment with trifluoroacetic acid (TFA) to form the bis TFA salt of the hydrazide **1-23**. A one pot amide bond formation and deprotection was attempted, as was done in the DHSO synthesis, but the best mass recovery was observed through a two-pot transformation. Liberation of the salt to the free base form **1-24** was initially attempted similar to the synthesis of DHSO by treatment with NEt_3. DHSO would precipitate out of the solution under these conditions, however, the sulfide precursor did not precipitate out and another means of free-basing was explored. An aqueous workup was again not viable due to the high solubility of sulfide **1-24** in water. Therefore, a non-aqueous free-basing method was needed. A one pot aqueous-free approach to deprotecting and free-basing Boc protected amines with the Amberlyst A21 resin was reported in 2005.[57] The reactive part of the resin is a tertiary amine, similar to NEt_3. Stirring salt **1-23** with the resin afforded the free-based amine **1-24** with varying mass recoveries. The best results for the two step deprotection-free-basing were observed on smaller scale (about 0.5 mmol).

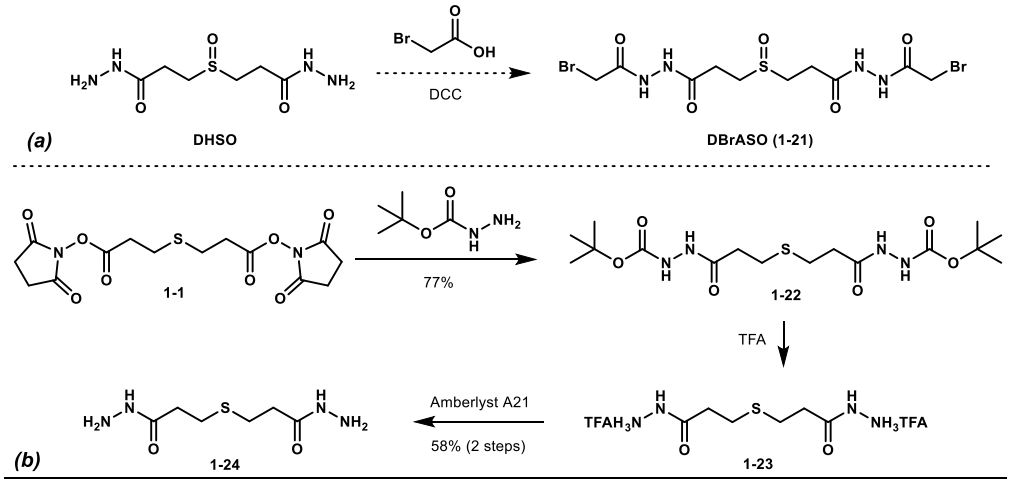

Scheme 1.13 (a) Initial proposed one-step route of DHSO to DBrASO ***(b)*** Three step sequence to the free bishydrazide, without the need for aqueous workup or chromatography

With the free amine in hand, we turned our attention to adding the bromoacetamide fragments. Treating the bisamine **1-24** with bromoacetyl bromide and NEt_3, resulted in decomposition. Alternatively, using NHS ester **1-25** as the acetyl bromide source afforded the desired bromoacetamide **1-26**. Purification of **1-26** was also challenging. Silica gel chromatography was unsuccessful due to the polarity of the product and therefore, reverse phase chromatography was explored. A gradient of MeCN in H_2O cleanly eluted the product, but it was observed that the product would precipitate out of the eluent. This observation led to a slight change in the reaction conditions of **1-26**. The solvent for the bromoacetamide formation was changed to a mixture of MeCN and H_2O and the product precipitated out of solution and was easily filtered off to obtain the pure bromoacetamide **1-26** without the need for reverse phase chromatography.

The final step to make the cross-linker was an oxidation of the sulfide to the sulfoxide. Initial oxidations were performed with *m*-CPBA and were found to be successful. The product could be purified through reverse phase chromatography, however, poor mass recovery from the purification was often observed, partially due to some over oxidation of the sulfoxide to the sulfone as well as some recovered starting material. Alternatively, oxidation with H_2O_2 in HFIP, only

afforded the desired sulfoxide **1-21** and none of the over oxidized byproduct. Quenching the oxidation with dimethylsulfide (DMS) surprisingly precipitated the cross-linker out of the reaction solution. Washing the precipitate with a MeCN and H_2O solution purified the mixture to obtain the desired cross-linker without the need for chromatography. This cross linker was synthesized in five steps from a known starting material and does not require any purification via chromatography.

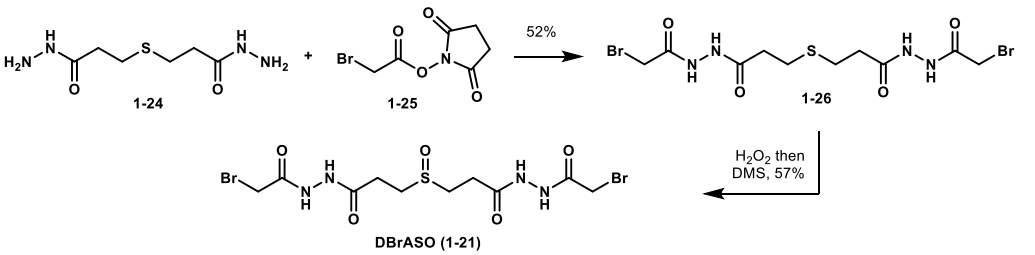

Scheme 1.14. Final steps in the synthesis of DBrASO

1.2.3 XLMS analysis with DBrASO

The cross-linker was delivered to the Huang lab for testing. It was initially reacted with a short cysteine containing peptide and successfully interlinked two equivalents of the peptide. The cross-linker also behaved as expected in the MS/MS experiments. When cross-linked with BSA, DBrASO showed 52 unique cross-links compared to 38 unique cross-links with BMSO. Only 23 of these links were shared between the two cross-linkers. This again proves that changing the reactivities and lengths of cross-linkers will result in additional structural information. DBrASO is currently being investigated in additional cross-linking mass spectrometry experiments by the Huang lab.

1.3 Synthesis of BrASSO, a heterobifunctional lysine-cysteine cross-linker

1.3.1 Introduction to heterobifunctional cross-linkers

In our group's pursuit of expanding the toolbox of cross-linking reagents, we wanted to examine heterobifunctional sulfoxide CID cross-linkers. This means that the two reactive functionalities on the cross-linker would target different amino acids. We would then be able to study interactions that would not otherwise be detected with our homobifunctional class of linkers. One of the first heterobifunctional cross-linkers that was synthesized in the Rychnovsky lab was monosuccinimide maleimide sulfoxide (MMSO). This cross-linker contains an NHS ester on one end to react with lysine residues and a maleimide functional group on the other side to react with cysteine residues. MMSO was initially synthesized by Sarah Block as shown in Scheme 1.15. It was shown to be a viable cross-linker however the synthesis was non-trivial and unreliable. Based on the success of DBrASO and the α-bromoacetamide functionality in targeting cysteine residues, we decided to design another heterobifunctional cross-linker that targets lysine and cysteine residues bromoacetamide succinimidyl sulfoxide (BrASSO).

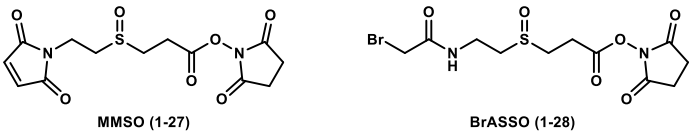

Figure 1.8. Structures of MMSO and BrASSO, cysteine-lysine heterobifunctional cross-linkers

These heterobifunctional cross-linkers also have the advantage of selectively cleaving only on one side within the MS. The NHS ester half of the cross-linkers have a carbonyl at the β-position of the sulfoxide, whereas the other side contains a nitrogen at this position. It was postulated and proven with MMSO that the cross-linker will only cleave on one side in MS2, as was also proven with the DSSO analogs **1-12**, **1-13**, and **1-14**. This selectivity also helped to simplify the MS data analysis. However, one drawback of the heterobifunctional cross-linkers is that the syntheses are more involved.

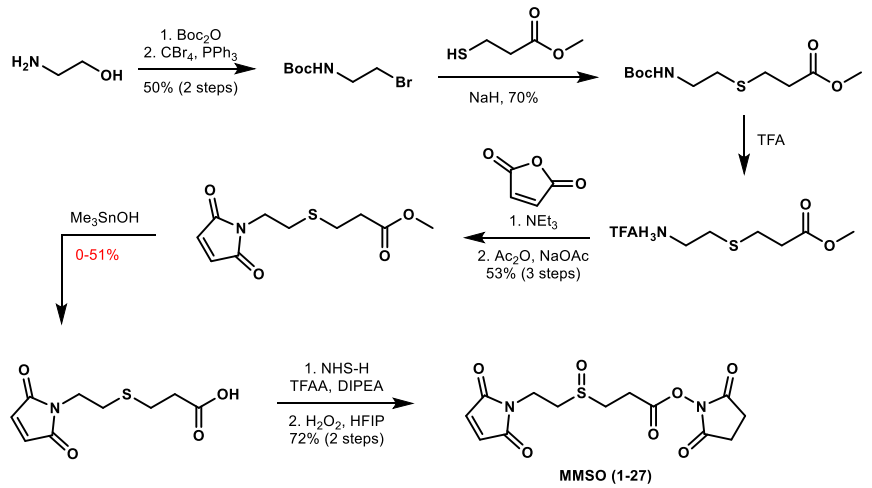

Scheme 1.15. Synthesis of MMSO by Sarah Block

1.3.2 First generation synthesis of BrASSO

The first generation synthesis of BrASSO was modeled after the MMSO synthesis. To start, ethanolamine was Boc protected and then tosylated to yield amine **1-29**. The coupling partner **1-30** was furnished through a thiol-Michael addition of thioacetic acid into *t*-butyl acrylate. An *in situ* deacylation and S_N2 displacement of tosylate **1-29** afforded sulfide **1-32** in moderate yields. Deprotection of the amine furnished **1-32** as the HCl salt. We were then able to take the salt and form the amide bond, however, the yields were often low and unreliable. We first explored using the Amberlyst A21 resin to free-base the amine and then add in the bromoacetyl NHS ester. Although this was successful, only yields of up to 31% were observed. Reacting the HCl salt **1-32** with NHS ester **1-25** and $NaHCO_3$ afforded amide **1-33** in 23% yield. Finally, switching the base from $NaHCO_3$ to NEt_3 resulted in a poor 3% yield. It was postulated that the low yields were resulting from poor conversion of the salt to the free-based amine. When the HCl salt **1-32** was separately stirred with each of these bases (Amberlyst A21, NEt_3, $NaHCO_3$) the mass recoveries of the free amine were all quite poor. To circumvent this problem, we envisioned changing the protecting group to one that could be removed under basic conditions, thus avaoiding the free-basing step.

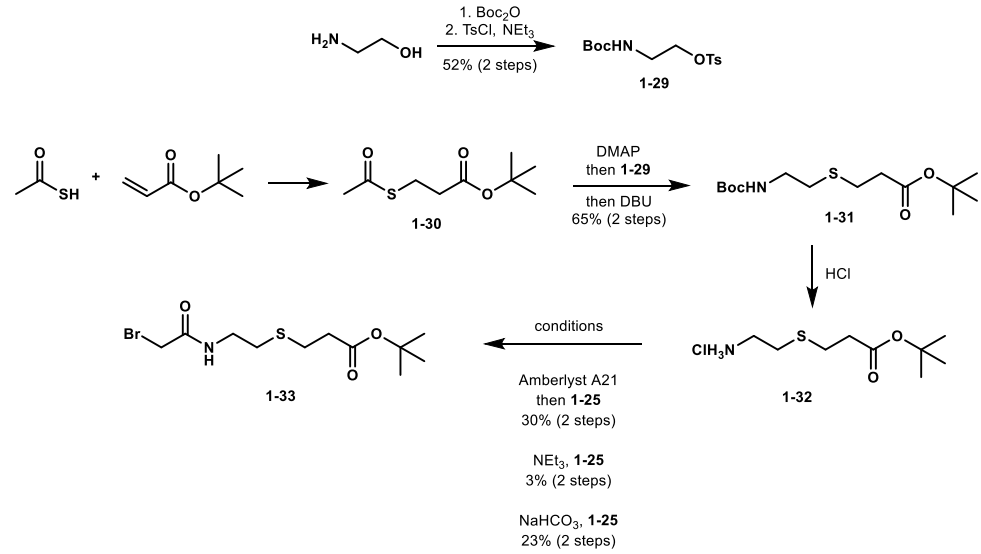

Scheme 1.16. Initial synthesis of BrASSO core

1.3.3 Second generation synthesis of BrASSO

Swapping the Boc protecting group to an Fmoc protecting group was envisioned to alleviate the deprotonation problem. Carbamate **1-34** was synthesized similarly to the Boc version, Scheme 1.17a. The deacylation, S_N2 step was more problematic with the Fmoc protecting group. Various bases were screened for the deacylation step to minimize deprotection of the amine. The best results were observed with NaOH in MeOH to yield the desired sulfide in up to 71% (brsm) yield (29% isolated yield). A significant side product that was observed was oxidation of the deacylated sulfide to the disulfide **1-36**. This product could be minimized with the use of degassed solvents. Another observable side product resulted from deprotection of the amine followed by addition of the thiol into the Fmoc alkene to form sulfide **1-37**, Scheme 1.17c. Attempts to perform the deacylation in a separate step and then subject it to the S_N2 substitution, just led to disulfide bond formation.

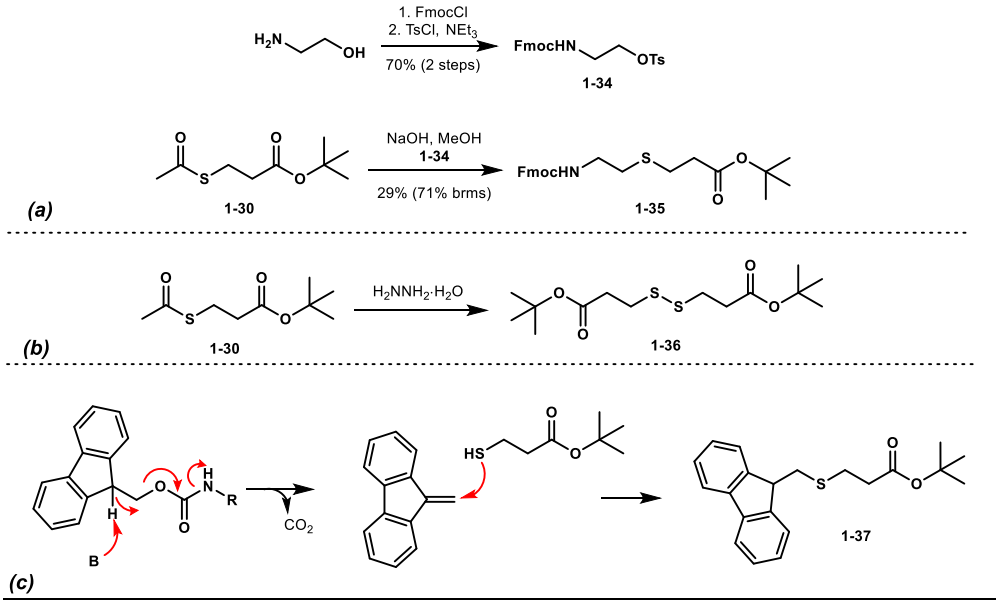

Scheme 1.17 (a) Synthesis towards BrASSO core with new protecting group ***(b)*** Disulfide formation in deacylation attempt ***(c)*** Mechanism of formation of sulfide side product

With the desired sulfide **1-35** in hand, we wanted to examine the amide bond formation in comparison to the previous Boc protected amine. Deprotection of the Fmoc group with piperidine followed by addition of the NHS ester **1-25**, afforded the desired amide **1-33** in 58% yield (over 2 steps). Although the amide bond formation was higher yielding, formation of the protected amine **1-33** was problematic. A different route to sulfide **1-33** was pursued.

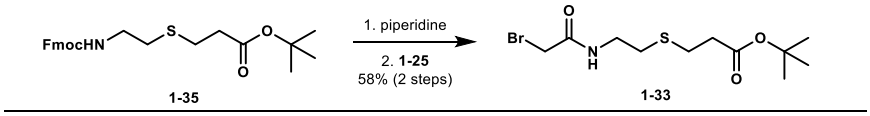

Scheme 1.18. Amide bond formation was more successful with the Fmoc protected amine compared to the Boc protected amine

1.3.4 Third generation synthesis of BrASSO

In order to forgo the problematic deacylation, S_N2 step, we envisioned starting from a primary sulfide and performing a conjugate addition into the Michael acceptor. Since a primary amine is a harder nucleophile than a thiol, we could also potentially circumvent the use of an amine protecting group. Therefore, a conjugate addition of cysteamine into *t*-butyl acrylate was executed. The desired product **1-38** was detected along with some of the double conjugate

addition product **1-39**. Addition of the NHS ester **1-25** resulted in the desired sulfide **1-33** in a 54% yield over 2 steps. Performing this reaction as a one pot procedure also resulted in the desired sulfide in yields up to 65%. The desired sulfide could now be easily made in one step from commercial reagents as opposed to the six step sequence we were previously implementing.

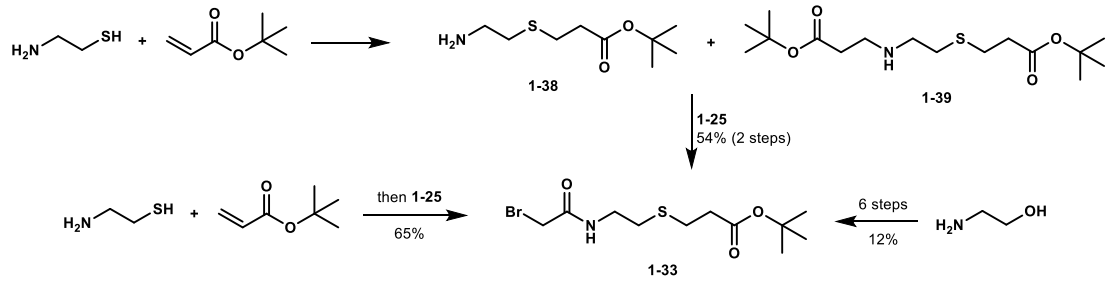

Scheme 1.19. Development of one pot Michael addition and amide bond formation

We could then turn our attention to installation of the NHS ester. Hydrolysis conditions were screened (aq. H_3PO_4; TMSOTf and 2,6 lutidine; KSF clay; HBr and AcOH; HFIP and Δ; SiO_2 and Δ; $ZnBr_2$; thermolysis) and the best results were obtained with the use of TFA. However, the formation of the NHS ester from carboxylic acid **1-40** was problematic. Product was occasionally isolated in moderate to low yields and most of the time no product was observed. Various conditions were screened, but the desired NHS ester **1-41** was only observed when subjecting carboxylic acid **1-40** to EDC·HCl and NHS-H. It is likely that this cross-linker precursor is susceptible to hydrolysis upon workup or chromatography. The best results were observed when the esterification was performed on small scale with a quick silica gel purification. Additional protocols for the purification and handling of this intermediate will be screened. Gratifyingly, with the material we had in hand, oxidation of sulfide **1-41** to the sulfoxide with *m*-CPBA afforded the cross-linker in moderate yields after purification. Higher yields, but less pure material was observed with an H_2O_2 oxidation without any column chromatography.

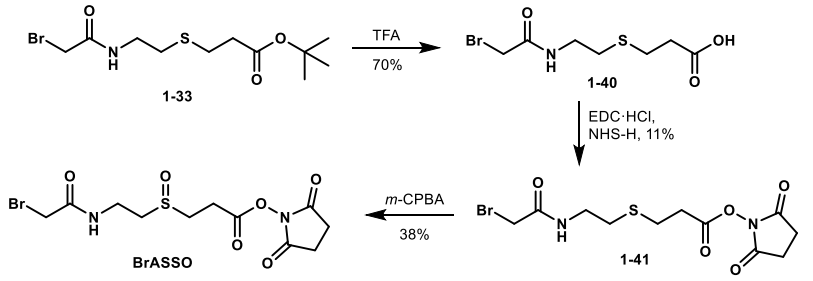

Scheme 1.20. Completion of BrASSO, cysteine-lysine heterobifunctional cross-linker

1.3.5 Fourth generation synthesis of BrASSO

To avoid the problematic esterification step another sequence was examined. We envisioned adding in the bromine of the bromoacetamide in the later stages of the route, and in its place would be a protected alcohol. We wanted to insert the bromine later in the sequence because we planned to do a conjugate addition of a sulfide into a Michael acceptor that already had the NHS ester in place. The bromoacetamide could not be in place during the conjugate addition because it is extremely reactive towards free thiols.

This route began with the displacement of bromoacetic acid with p-methoxy benzyl alcohol to install the protected α-alcohol **1-42**. Formation of the amide bond was easily achieved by NHS ester formation followed by displacement with cysteamine. Thiol **1-44** smoothly converted to sulfide **1-46** after a Michael addition into NHS ester **1-45**. Removal of the PMB protecting group with TfOH in 1,3-dimethoxy benzene unveiled the primary alcohol. An Appel reaction was attempted on the alcohol and could be achieved to afford the desired bromoacetamide. However, the product could not be separated from triphenylphosphine oxide. This route was not further pursued.

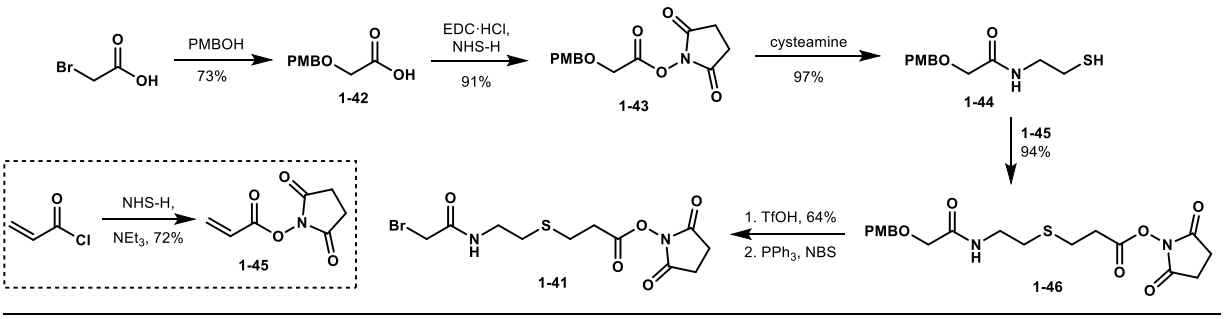

Scheme 1.21. Synthesis of the cross-linker precusor by implementing a protected alcohol in place of the bromide

1.3.6 MS analysis of BrASSO

Although not straightforward to synthesize, BrASSO was still able to be examined in cross-linking MS/MS experiments. It was found to successfully cross-link a lysine and cysteine residue on a short peptide and the MS cleavage resulted in the expected fragmentation. It was also examined in reduced BSA (BSA protein after being treated with tris(2-carboxyethyl)phosphine to reduce all the disulfide bridges). BrASSO was also found to be a viable cross-linker in the reaction with BSA. In comparison to MMSO (our other cysteine-lysine cross-linker) they shared 15 K-C linkages. BrASSO showed 41 unique cross-links compared to MMSO with 50 unique linkages. Since BrASSO was found to be a viable cross-linker the synthetic route to this linker will be examined in the future to develop a more reliable and reproducible outcome.

1.4 Synthesis of SDASO, a heterobifunctional lysine-X cross-linker

1.4.1 Introduction to photoactivated cross-linkers

Cross-linking mass spectrometry has proven to be a useful tool in the field of structural biology. However, only amino acids with nucleophilic or electrophilic side chains have been able to be targeted with classic cross-linking reagents. Aliphatic amino acids make up most of the proteosome and it would be extremely beneficial to be able to target these non-reactive residues. Recently, photoactivated cross-linkers have proven to successfully react nonspecifically with all amino acids, allowing hydrophobic regions to be studied with XL-MS.[58–67] All of these cross-linkers contain a photoreactive group and a lysine reactive moiety. Diazirine rings have been widely implemented as the photoreactive group because they are small in size, relatively photostable, and require a longer excitatory UV wavelength (~350 nm) compared to other photoreactive groups. When excited, the diazirine will either extrude N_2 and form a highly reactive carbene or it will rearrange to the linear diazo intermediate, Scheme 1.22. The linear diazo intermediate can further convert to the carbene, or react preferably with acidic residues. The carbene can undergo X-H insertion (X = C, N, O, S), but can also easily be quenched by the aqueous environment. The reactivity of diazirines is also highly dependent on its substituents (R groups in Scheme 1.22) and the pH of the cross-linking environment.[68]

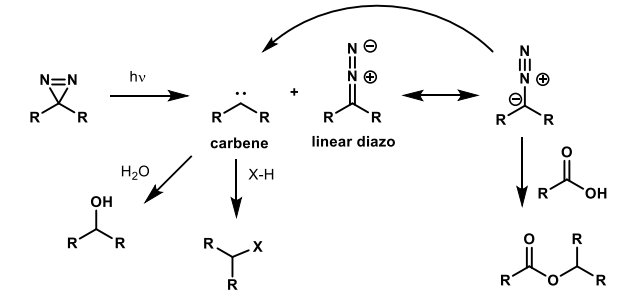

Scheme 1.22. Diazirine reactivity

Because of the nonspecific reactivity of the carbene intermediate and its facile quench in aqueous media, the cross-linking data analysis can be very complicated as there is low-

abundance of the cross-linked products. Therefore, implementing our sulfoxide CID cleavability to a photoreactive cross-linker will help this issue.

Succinimidyl-diazirine sulfoxide (SDASO) was designed similarly to BrASSO as a heterobifunctional cross-linker. One end of the cross-linker can react with lysine, while the other end contains the diazirine unit which can be photoexcited and undergo nonspecific reactivity.

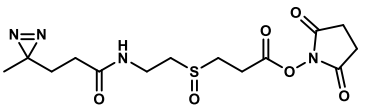

Figure 1.9. Structure of SDASO

1.4.2 First and second generation synthesis of SDASO

The first generation synthesis of SDASO began with the same intermediate from the first generation synthesis of BrASSO, sulfide **1-31**. The diazirine fragment of the cross-linker was synthesized according to known procedures from levulinic acid (see SI). Fragment **1-48** is a noncleavable photoactivated cross-linker that we envisioned implementing in our synthesis. Similar to the BrASSO synthesis, a few bases were screened for the amide bond formation step. Amberlyst A21 and NEt_3 gave similar yields at around 27%, while implementing $NaHCO_3$ almost doubled the yield. Although this was promising, the yield was still quite moderate for a simple coupling.

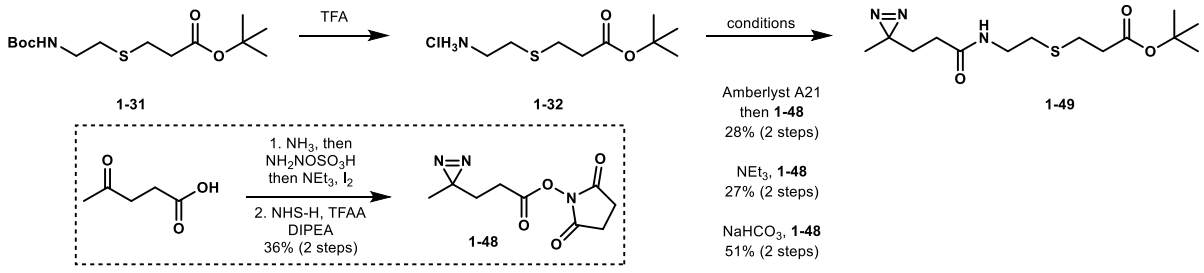

Scheme 1.23. Amide bond formation towards SDASO

I was working on the synthesis of BrASSO at the same time I was working on SDASO. As previously discussed, the amide bond formation in the initial BrASSO sequence was also problematic and therefore the amine protecting group was switched from Boc to Fmoc. Sulfide **1-35** was synthesized and subjected to deprotection conditions followed by the addition of diazirine fragment **1-48**. This amide bond formation resulted in about the same yield compared to the other protecting group.

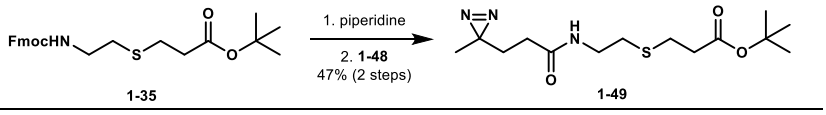

Scheme 1.24. Amide bond formation from the Fmoc protected amine

With the desired amide in hand, we next focused on introducing the NHS ester functionality. Hydrolysis of the *t*-butyl ester was unsuccessful under acidic conditions. After screening a couple of basic hydrolysis conditions, we found that subjecting the ester to TMSOTf and 2,6-lutidine afforded carboxylic acid **1-50**. Appending on the NHS ester through an EDC coupling was also successful. Although these transformations initially worked well, they proved to be unreliable. Often low yields, recovered starting material, or just decomposition was observed. With some of the sulfide **1-51** in hand, we were able to subject it to the oxidation conditions to afford the cross-linker in low yields. Purification of NHS ester **1-51** and the cross-linker on silica gel, also gave poor mass recovery, likely due to hydrolysis of the ester.

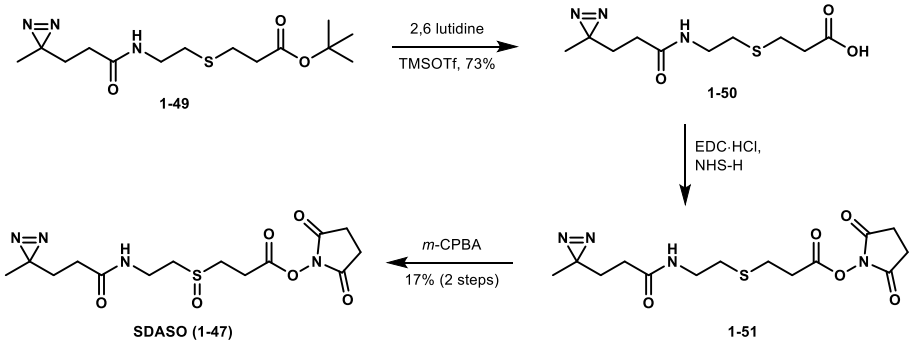

Scheme 1.25. Completion of SDASO cross-linker

1.4.3 Third generation synthesis of SDASO

Due to the problematic hydrolysis and NHS ester formation we wanted to design a route that began with the ester already installed. Inspired by the one pot, three component protocol that assembled the bromoacetamide **1-33**, I envisioned first forming the amide bond with cysteamine and the diazirine fragment, then a thiol Michael addition into the NHS acrylate would forge all the bonds needed for the chain.

The known diazirine fragment **1-48** was treated with cysteamine to cleanly afford sulfide **1-49** in good yield. This sulfide was subjected to a thiol Michael addition into acrylate **1-45** to afford the cross-linker precursor. Higher yields can be achieved for this transformation if chromatography is not performed, as the ester is prone to hydrolysis on silica gel. Finally, oxidation of the sulfide to the sulfoxide with H_2O_2 in HFIP furnished the cross-linker. This oxidation was much higher yielding compared to the oxidation with *m*-CPBA because there was no over oxidation under these conditions. The HFIP solvent strongly hydrogen bonds to the sulfoxide to prevent an additional oxidation.[69] This route improved the overall step count and yield. From a known intermediate **1-48**, the cross-linker was synthesized in three steps in a 22% overall yield. Comparatively, from the known tosylate **1-29**, SDASO was synthesized in 7 steps with an overall yield of 2%. This new route allowed us to make enough SDASO for our collaborators to perform additional cross-linking mass spectrometry studies.

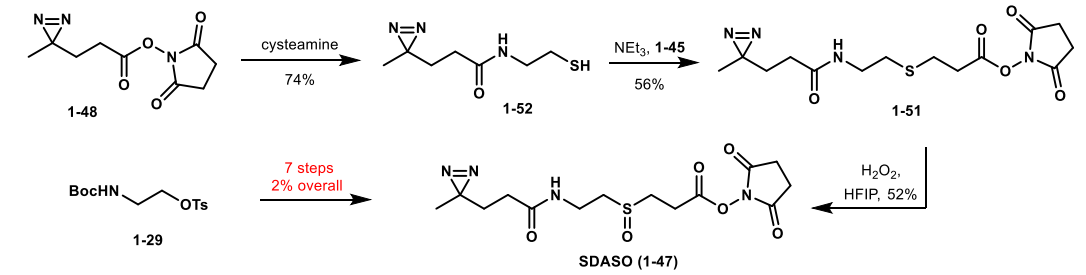

Scheme 1.26. Alternate route towards SDASO

1.4.4 XLMS analysis with SDASO

Another graduate student in our lab, Sadie DePeter, synthesized two derivatives of SDASO, as shown in Scheme 1-27, SDASO-S and SDASO-M. These two cross-linkers were designed shorter than SDASO to examine the utility of varying the lengths of these photoactivated linkers.

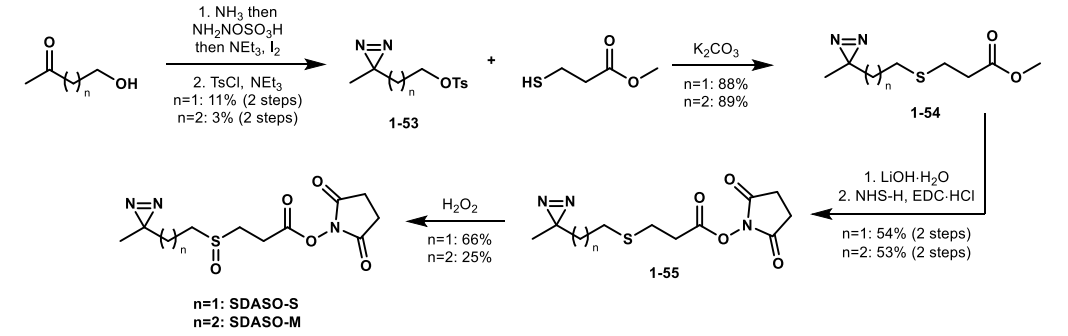

Scheme 1.27. Synthesis of SDASO derivatives by Sadie DePeter

The three SDASO linkers were examined for their cross-linking viability initially in BSA. Because this is a heterobifunctional cross-linker that can only cleave on one side, only one set of MS2 fragments were detected, which enhances sensitivity. Each were found to successfully cross-link with lysine residues and the photoactivated diazirine group showed cross-links to all 20 amino acids.[58] Unsurprisingly, SDASO showed preferential linkage to acidic residues as has been previously reported in the literature with diazirines.[65,70] This selectivity is due to the abundance of the linear diazo intermediate, Scheme 1.22, that readily forms esters with carboxylic acids. Of the two acidic residues, glutamic acid was cross-linked at a much higher rate compared to aspartic acid, even though BSA contains many more aspartic acid residues than glutamic acid. This observation may be due to the slightly longer chain or the slightly increased nucleophilicity glutamic acid. Other acidic targeting cross-linkers do not show this preferance.[42] SDASO also had preferential cross-links with tyrosine, valine, leucine, threonine, and histidine. SDASO, compared to the other three cross-linkers reported in our lab DSSO, DHSO, and BMSO, showed the highest

number of cross-links within BSA and therefore the most comprehensive interaction map, Figure 1.10.

Figure 1.10. Linkage maps of BSA with the SDASO cross-linkers compared to the overlaid linkage map of DSSO, DHSO, and BMSO (ref 58)

The three SDASO cross-linkers did not show much deviation when examined in BSA, however, when applied to a larger system, the yeast 26S proteosome, there was much more variability.[58] The longer the cross-linker, the more linkages were detected; also, the original SDASO, SDASO-L, showed more intersubunit linkages, followed by SDASO-M then SDASO-S. Because there was much less overlap between the detected linkages, a more comprehensive PPI map for the yeast 26S proteosome was obtained by implementing the three K-X cross-linkers, Figure 1.11.

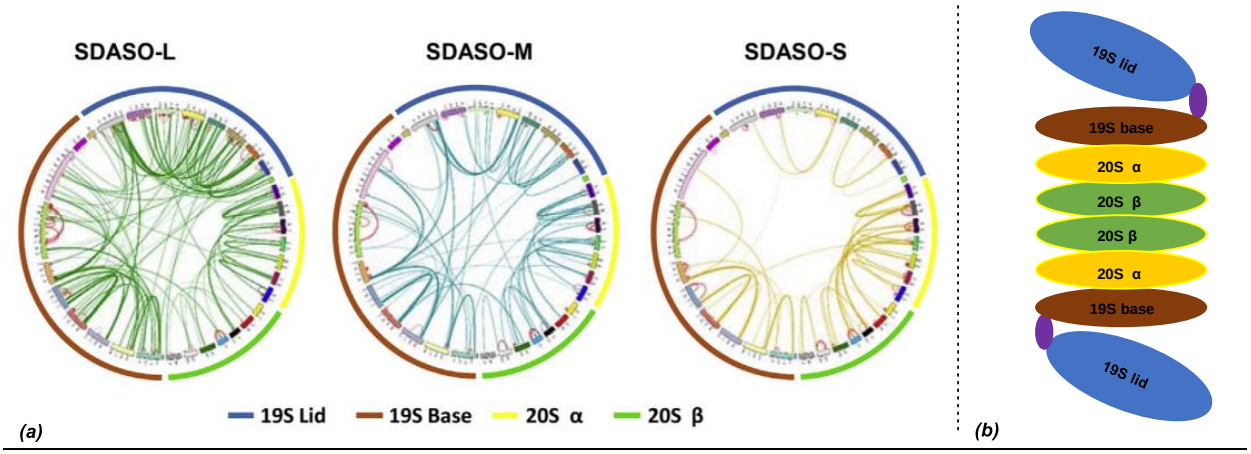

Figure 1.11 **(a)** Circular linkage maps of the yeast 26S proteosome with the SDASO cross-linkers (ref 58) ***(b)*** The yeast 26S proteosome outline

Interestingly, DSSO showed more linkages in the 26S proteosome compared to SDASO. However, the linkages were concentrated in different subunits. For example, SDASO was able to capture more interactions in the more rigid subunit 20S CP and less in the more flexible 19S RP subunit, Figure 1.12. All of this data demonstrates the value of using cross-linkers with different chemistries to study PPIs. The photoactivated functional group has been proven to be an invaluable tool within cross-linking mass spectrometry and our lab is continuing to design and synthesize additional photoactivated cross-linkers.

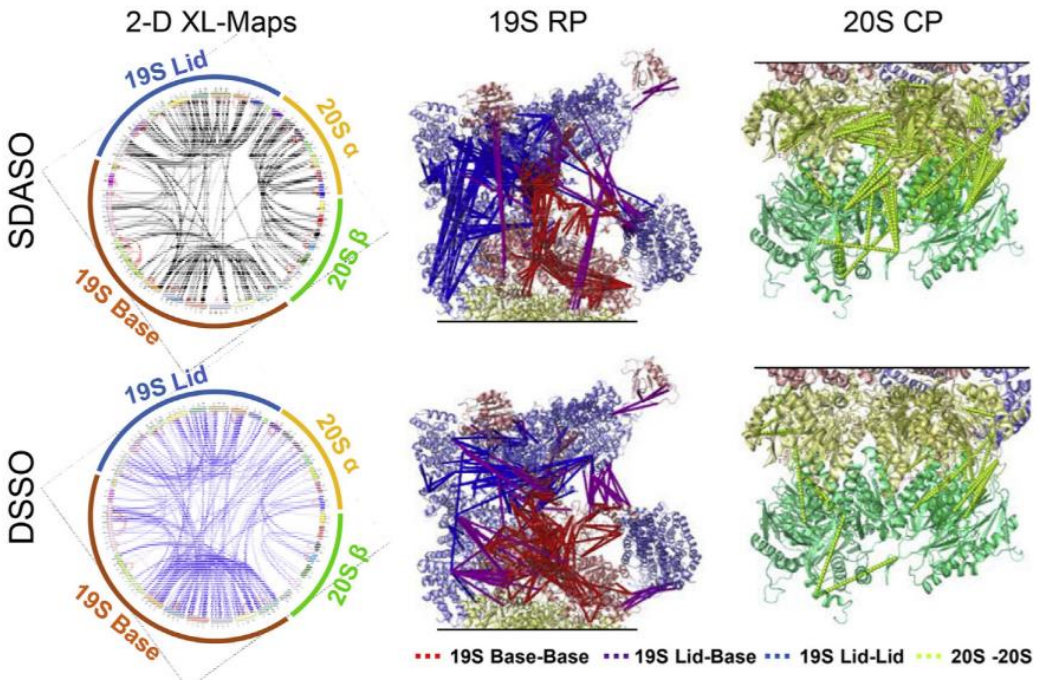

Figure 1.12. Linkage maps of the yeast 26S proteosome with the SDASO-L compared to DSSO (ref 58)

1.5 Supplemental Information

1.5.1 General Experimental

The ^{1}H NMR spectra were recorded at 500 MHz or 600 MHz using either a Bruker DRX500 (cryoprobe) or a Bruker AVANCE600 (cryoprobe) NMR, respectively. The ^{13}C NMR spectra were recorded at 126 MHz or 151 MHz on the Bruker DRX500 or Bruker AVANCE600 NMR, respectively. All NMR spectra were taken at 25 °C unless otherwise noted. Chemical shifts (δ) are reported in parts per million (ppm) and referenced to residual solvent peak at 7.26 ppm (^{1}H) or 77.16 ppm (^{13}C) for deuterated chloroform ($CDCl_3$), 3.31 ppm (^{1}H) or 49.15 ppm (^{13}C) for deuterated methanol (CD_3OD), 2.50 ppm (^{1}H) or 39.52 ppm (^{13}C) for deuterated dimethylsulfoxide (DMSO-d_6). The ^{1}H NMR spectral data are presented as follows: chemical shift, multiplicity (s = singlet, d = doublet, t = triplet, q = quartet, quint = quintet, m = multiplet, dd = doublet of doublets, ddd = doublet of doublet of doublets, dddd = doublet of doublet of doublet of doublets, dt = doublet of triplets, dq = doublet of quartets, ddq = doublet of doublet of quartets, app. = apparent), coupling constant(s) in hertz (Hz), and integration. High-resolution mass spectra (HRMS) were recorded on Waters LCT Premier TOF spectrometer with electrospray ionization (ESI) and chemical ionization (CI) sources. An internal standard was used to calibrate the exact mass of each compound. For accuracy, the peak selected for comparison was that which most closely matched the ion intensity of the internal standard.

Unless otherwise stated, synthetic reactions were carried out under an atmosphere of argon in flame- or oven-dried glassware. Thin layer chromatography (TLC) was carried out using glass plates coated with a 250 μm layer of 60 Å silica gel. TLC plates were visualized with a UV lamp at 254 nm, or by staining with Hanessian's stain or $KMnO_4$ stain. Liquid chromatography was performed using forced flow (flash chromatography) with an automated purification system on prepacked silica gel (SiO_2) columns unless otherwise stated.

All commercially available reagents were used as received unless stated otherwise. Solvents were purchased as ACS grade or better and as HPLC-grade and passed through a solvent purification system equipped with activated alumina columns prior to use. $CDCl_3$, CD_3OD, and DMSO-d_6 was purchased from Cambridge Isotope Laboratories.

1.5.2 Experimental procedures and compound characterization

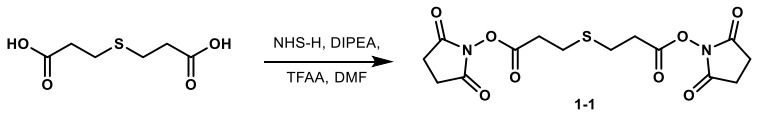

Bis(2,5-dioxopyrrolidin-1-yl) 3,3'-thiodipropionate (1-1):

To a solution of 3,3'-thiodipropionic acid (5.00 g, 28.1 mmol, 1.0 equiv), *N*-hydroxysuccinimide (12.9 g, 112 mmol, 4.0 equiv), and *N,N*-diisopropylethylamine (39.1 mL, 224 mmol, 8.0 equiv) in DMF (140 mL) at 0 °C was added trifluoroacetic anhydride (15.8 mL, 112 mmol, 4.0 equiv) dropwise. The orange solution was stirred for 2 h at 0 °C, and then partitioned between EtOAc and brine. The aqueous layer was extracted with EtOAc (2 X). The combined organic layers were washed with brine (5 X), dried over anhydrous Na_2SO_4, and concentrated *in vacuo*. The resulting residue was purified via flash chromatography (40% EtOAc in CH_2Cl_2) to obtain NHS ester **1-1** (8.21 g, 79%). Spectral data is in accordance with the reported literature.[18]

^{1}H NMR (500 MHz, DMSO-d_6) δ 3.01 (t, J = 7.0 Hz, 4H), 2.87 (t, J = 7.0 Hz, 4H), 2.82 (s, 8H).

^{13}C NMR (126 MHz, DMSO-d_6) δ 169.9, 167.6, 31.4, 25.6, 25.4.

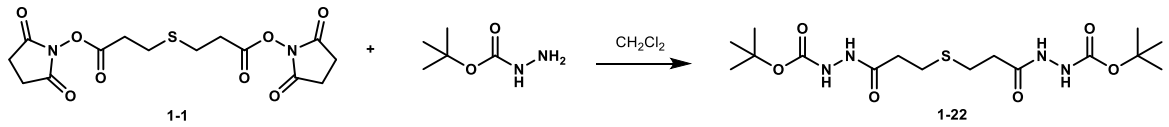

Di-*tert*-butyl 2,2'-(3,3'-thiobis(propanoyl))bis(hydrazine-1-carboxylate) (1-22):

To a slurry of NHS ester **1-1** (2.73 g, 7.33 mmol, 1.0 equiv) in CH_2Cl_2 (38 mL) was added *t*-butyl carbazate (1.94 g, 14.7 mmol, 2.0 equiv) to obtain a clear orange solution. After stirring for 15.5 h at rt, the slurry was vacuum filtered to obtain a white flakey precipitate. The precipitate was washed with additional CH_2Cl_2 and then dried further *in vacuo* to obtain sulfide **1-22** as a flakey white solid (2.28 g, 77%).

Melting point: 187–190 °C

^{1}H NMR (500 MHz, DMSO-d_6) δ 9.56 (s, 2H), 8.71 (s, 2H), 2.69 (t, J = 7.4 Hz, 4H), 2.352 (t, J = 7.0 Hz, 4H), 1.39 (s, 18H).

^{13}C NMR (125 MHz, DMSO-d_6) δ 170.1, 155.2, 79.0, 33.8, 28.1, 26.6.

IR (neat) 3217, 3041, 2981, 1650, 1503, 1155, 857, 604 cm^{-1}.

HRMS (ESI-TOF) *m/z* calculated for $C_{16}H_{30}N_4O_6SNa$ $(M+Na)^+$ 429.1779, found 429.1760.

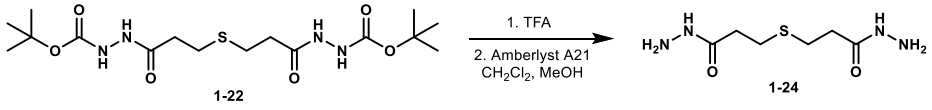

3,3'-Thiodi(propanehydrazide) (1-24):

Five separate vials each containing a solution of sulfide **1-22** (200 mg, 0.492 mmol, 1.0 equiv) in trifluoroacetic acid (1.0 mL) was stirred at rt for 16 h and then concentrated *in vacuo*. The resulting residue from each vial was dissolved in a 1:1 solution of MeOH:CH_2Cl_2, and added to a mixture of Amberlyst A21 resin (4.0 g, 10.0 equiv by mass of salt product) in CH_2Cl_2. The mixture was

stirred for 45 min at rt, after which the resin was filtered and washed with a 1:1 solution of MeOH:CH_2Cl_2. The filtrates were combined and concentrated *in vacuo* to obtain hydrazide **1-23** as a tan solid (293 mg, 58%).

^{1}H NMR (600 MHz, DMSO-d_6) δ 9.00 (s, 2H), 4.34 (s, br, 4H), 2.67 (t, J = 7.3 Hz, 4H), 2.28 (t, J = 7.3 Hz, 4H).

^{13}C NMR (151 MHz, DMSO-d_6) δ 169.9, 33.8, 26.9.

IR (neat) 3450, 3207, 2991, 1662, 1182, 1134, 798, 723 cm^{-1}.

HRMS (ESI-TOF) *m/z* calculated for $C_6H_{15}N_4O_6S$ $(M+H)^+$ 207.0911, found 207.0908.

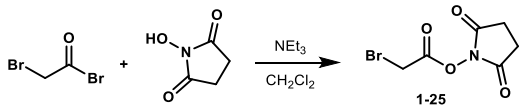

2,5-Dioxopyrrolidin-1-yl 2-bromoacetate (1-25):

To a solution of *N*-hydroxysuccinimide (1.32 g, 11.5 mmol, 1.0 equiv) in CH_2Cl_2 (15.0 mL) was added NEt_3 (1.92 mL, 13.8 mmol, 1.2 equiv) and a solution of bromoacetyl bromide (1.0 mL, 11.5 mmol, 1.0 equiv) in CH_2Cl_2 (15.0 mL) dropwise at 0 °C. After stirring at 0 °C for 1 h, the reaction was quenched with saturated $NaHCO_3$ solution. The organic phase was washed with saturated $NaHCO_3$ solution (2 X), 1 M HCl (3 X), and brine, dried over Na_2SO_4, and concentrated *in vacuo* to obtain NHS ester **1-25** as a tan solid (1.95 g, 72%). Spectral data is in accordance with the reported literature.[71]

^{1}H NMR (500 MHz, $CDCl_3$) δ 4.10 (s, 2H), 2.86 (s, 4H).

^{13}C NMR (126 MHz, $CDCl_3$) δ 168.6, 163.1, 25.7, 21.3.

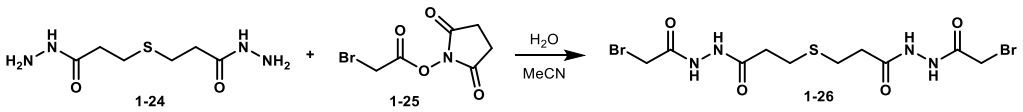

3,3'-Thiobis(N'-(2-bromoacetyl)propanehydrazide) (1-26):

To a solution of hydrazide **1-24** (293 mg, 1.42 mmol, 1.0 equiv) in H_2O (1.0 mL) was added a slurry of NHS ester **1-25** (671 mg, 2.84 mmol, 2.0 equiv) in MeCN (1.0 mL). The vial containing ester **1-25** was washed with MeCN:H_2O solution (1 mL) and the slurry was added to the reaction vial. After stirring at rt for 25 min the precipitate was vacuum filtered and washed with a 1:1 solution of MeCN:H_2O to obtain bromoacetamide **1-26** as an off white powder (333 mg, 52%)

Melting point: 166–170 °C

^{1}H NMR (500 MHz, DMSO-d_6) δ 10.38 (s, 2H), 10.12 (s, 2H), 3.91 (s, 4H), 2.72 (t, J = 7.3 Hz, 4H), 2.43 (t, J = 7.2 Hz, 4H).

^{13}C NMR (126 MHz, DMSO-d_6) δ 168.9, 164.5, 33.6, 27.1, 26.6.

IR (neat) 3429, 3199, 3042, 2943, 2847, 1698, 1601, 1215, 1078, 651 cm^{-1}.

HRMS (ESI-TOF) *m/z* calculated for $C_{10}H_{16}{}^{79}Br_2N_4O_4SNa$ $(M+Na)^+$ 468.9152, found 468.9170.

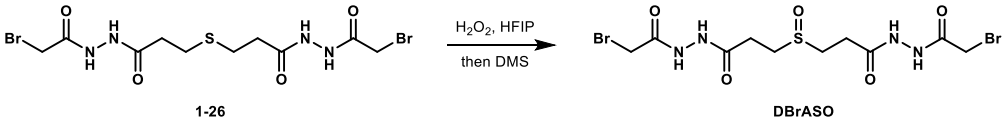

3,3'-Sulfinylbis(N'-(2-bromoacetyl)propanehydrazide) (DBrASO, 1-21):

To a solution of sulfide **1-26** (400 mg, 0.893 mmol, 1.0 equiv) in HFIP (4.5 mL) at rt was added 30% aqueous H_2O_2 (0.18 mL, 1.78 mmol, 2.0 equiv). The tan slurry became clear and after stirring for 25 min at rt the reaction was slowly quenched with DMS (0.20 mL, 2.70 mmol, 3.0 equiv). A white solid precipitated out of solution as the DMS was added, and the slurry was stirred for an

additional 10 min. The reaction mixture was vacuum filtered and the white precipitate was further dried *in vacuo* to obtain **DBrASO** as a white powder (235 mg, 57%).

Melting point: 175–178 °C

^{1}H NMR (600 MHz, DMSO-d_6) δ 10.38 (s, 2H), 10.22 (s, 2H), 3.92 (s, 4H), 3.09–3.02 (m, 2H), 2.86–2.79 (m, 2H), 2.58 (t, J = 6.8 Hz, 4H).

^{13}C NMR (151 MHz, DMSO-d_6) δ 168.6, 164.7, 46.1, 27.0, 25.8.

IR (neat) 3390, 3199, 3048, 2985, 2929, 1592, 1492, 1130, 1030, 645 cm^{-1}.

HRMS (ESI-TOF) *m/z* calculated for $C_{10}H_{16}{}^{79}Br_2N_4O_5SNa$ $(M+Na)^+$ 484.9101, found 484.9118.

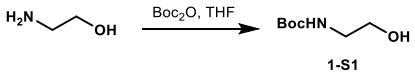

1-S1

***tert*-Butyl (2-hydroxyethyl)carbamate (1-S1):**

To a solution of di-*t*-butyl dicarbonate (17.8 g, 81.8 mmol, 1.0 equiv) in CH_2Cl_2 (250 mL) at 0 °C was added ethanolamine (5.0 mL, 81.8 mmol, 1.0 equiv) dropwise. The reaction was stirred at rt for 3 h and then concentered *in vacuo*. The resulting residue was purified through a silica plug (100% hex then 100% EtOAc) to yield alcohol **1-S1** as a clear oil (12.6 g, 96%). The spectral data is in accordance with the reported literature.[72]

^{1}H NMR (500 MHz, $CDCl_3$) δ 5.33 (s, br, 1H), 3.73 (s, br, 1H), 3.59 – 3.52 (m, 2H), 3.21 – 3.11 (m, 2H), 1.36 (s, 9H).

^{13}C NMR (126 MHz, $CDCl_3$) δ 156.8, 79.4, 61.9, 43.0, 28.3.

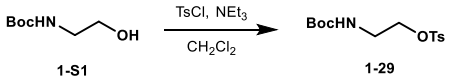

1-S1 1-29

2-((*tert*-Butoxycarbonyl)amino)ethyl 4-methylbenzenesulfonate (1-29):

To a solution of alcohol **1-S1** (12.6 g, 78.2 mmol, 1.0 equiv) in CH_2Cl_2 (156 mL) at 0 °C was added TsCl (22.3 g, 117 mmol, 1.5 equiv) in aliquots followed by the dropwise addition of NEt_3 33 mL, 235 mmol, 3.0 equiv). The solution was warmed to rt and then stirred for 2.5 h. The reaction solution was washed with H_2O (3 X) then brine, dried with Na_2SO_4, filtered, and concentrated *in vacuo*. The resulting residue was purified via flash chromatography (30% EtOAc in hex) to obtain tosylate **1-29** as a clear oil (13.4 g, 52%). The spectral data is in accordance with the reported literature.[73]

^{1}H NMR (600 MHz, $CDCl_3$) δ 7.77 (d, *J* = 8.3 Hz, 2H), 7.33 (d, *J* = 8.1 Hz, 2H), 4.88 (s, br, 1H), 4.05 (t, *J* = 4.8 Hz, 2H), 3.40 – 3.32 (m, 2H), 2.43 (s, 3H), 1.39 (s, 9H).

^{13}C NMR (151 MHz, $CDCl_3$) δ 155.7, 145.1, 132.8, 130.1, 128.0, 79.9, 69.6, 39.8, 28.4, 21.7.

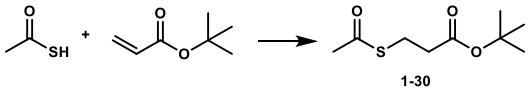

1-30

***tert*-Butyl 3-(acetylthio)propanoate (1-30):**

To a flask containing *t*-butyl acrylate (13.0 mL, 89.5 mmol, 1.0 equiv) was added thioacetic acid (6.3 mL, 89.5 mmol, 1.0 equiv). The solution was stirred overnight and then concentrated *in vacuo* to obtain thioester **1-30** as a clear oil (15.0 g, 82%).

^{1}H NMR (500 MHz, $CDCl_3$) δ 2.96 (t, J = 7.3, 2H), 2.42 (t, J = 7.3, 2H), 2.22 (s, 3H), 1.35 (s, 9H).

^{13}C NMR (126 MHz, $CDCl_3$) δ 195.2, 170.7, 80.8, 35.4, 30.4, 28.0, 24.3.

HRMS (ESI-TOF) *m/z* calculated for $C_9H_{16}O_3SNa$ $[M+Na]^+$ 227.0718, found 227.0724.

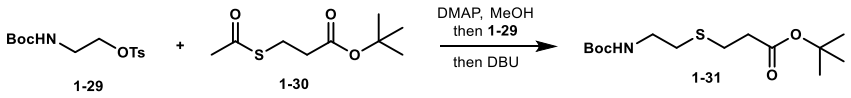

***tert*-Butyl 3-((2-((*tert*-butoxycarbonyl)amino)ethyl)thio)propanoate (1-31):**

To a solution of thioester **1-30** (7.78 g, 38.1 mmol, 1.0 equiv) in MeOH (28 mL) at rt was added DMAP (465 mg, 3.81 mmol, 0.1 equiv). The solution was stirred for 30 min and then a solution of tosylated **1-29** (12.0 g, 38.1 mmol, 1.0 equiv) in MeOH (10 mL) was added followed by DBU (5.5 mL, 38.1 mmol, 1.0 equiv). The reaction was stirred for 3.5 h and then concentrated *in vacuo*. The resulting yellow oil was dissolved in CH_2Cl_2 and washed with H_2O (3 X), then brine, dried with Na_2SO_4, filtered, and concentrated *in vacuo*. The resulting yellow residue was purified via flash chromatography (10% EtOAc in hex) to obtain sulfide **1-31** as a clear oil (7.58 g, 65%).

^{1}H NMR (500 MHz, $CDCl_3$) δ 5.03 (s, br, 1H), 3.27 – 3.19 (m, 2H), 2.67 (t, *J* = 7.3 Hz, 2H), 2.58 (t, *J* = 6.6 Hz, 2H), 2.43 (t, *J* = 7.4 Hz, 2H), 1.45 – 1.31 (m, 18H).

^{13}C NMR (126 MHz, $CDCl_3$) δ 171.1, 155.8, 80.8, 79.2, 39.7, 36.0, 32.3, 28.4, 28.1, 26.8.

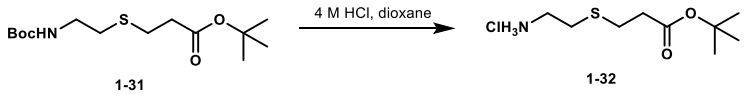

***tert*-Butyl 3-((2-(chloro-λ^5-azaneyl)ethyl)thio)propanoate (1-32):**

A solution of sulfide **1-31** (3.35 g, 11.0 mmol, 1.0 equiv) in 4 M HCl in dioxane (13.7 mL) was stirred at rt for 19 h. The solution was concentrated *in vacuo* to obtain HCl salt **1-32** which was taken onto the next step without further purification.

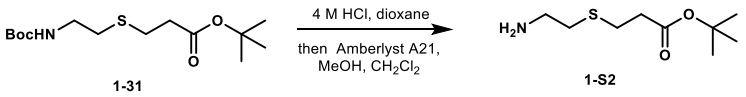

***tert*-Butyl 3-((2-aminoethyl)thio)propanoate (1-S2):**

To a flask containing sulfide **1-31** (2.0 g, 6.55 mmol, 1.0 equiv) was added 4 M HCl in dioxane (6.3 mL, 25.2 mmol, 3.8 equiv). The solution was stirred at rt overnight and the clear solution had turned cloudy white. The reaction solution was concentrated *in vacuo*. The resulting residue was dissolved in a 1:1 solution of CH_2Cl_2:MeOH (10 mL) and added to a flask containing Amberlyst A21 (1.7 g) and CH_2Cl_2 (50 mL). The mixture was stirred for 1 h and then filtered. The filtrate was concentrated *in vacuo* to obtain amine **1-S2** (923 mg, 69% over 2 steps).

^{1}H NMR (500 MHz, $CDCl_3$) δ 4.39 (s, br, 2H), 3.01 – 2.91 (m, 2H), 2.77 – 2.68 (m, 4H), 2.55 – 2.46 (m, 2H), 1.43 (s, 9H).

^{13}C NMR (126 MHz, $CDCl_3$) δ 171.3, 81.1, 40.4, 36.1, 34.0, 28.2, 27.0.

HRMS (ESI-TOF) *m/z* calculated for $C_9H_{20}NO_2S$ $(M+H)^+$ 206.1210, found 206.1214.

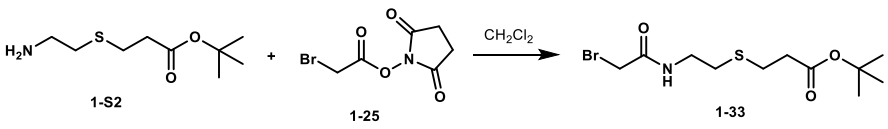

***tert*-Butyl 3-((2-(2-bromoacetamido)ethyl)thio)propanoate (1-33):**

To a solution of ester **1-25** (460 mg, 1.95 mmol, 2.0 equiv) in CH_2Cl_2 (2.0 mL) at rt was added amine **1-S2** (200 mg, 0.976 mmol, 1.0 equiv) in CH_2Cl_2 (1.3 mL). The solution was stirred for 1 h at rt and then concentrated *in vacuo*. The resulting residue was purified via flash chromatography (10 → 100% EtOAc in hex) to obtain bromoacetamide **1-33** as a clear oil (98 mg, 31% over 2 steps).

^{1}H NMR (500 MHz, $CDCl_3$) δ 6.95 (s, br, 1H), 3.88 (s, 2H), 3.50 (dd, *J* = 12.6, 6.1 Hz, 2H), 2.77 (t, *J* = 7.2 Hz, 2H), 2.71 (t, *J* = 6.4 Hz, 2H), 2.52 (t, *J* = 7.2 Hz, 2H), 1.46 (s, 9H).

^{13}C NMR (126 MHz, $CDCl_3$) δ 171.2, 165.7, 81.2, 39.2, 36.0, 31.8, 29.2, 28.2, 27.0.

IR (neat) 3232, 2978, 2935, 1704, 1213, 1152, 1075, 652 cm^{-1}.

HRMS (ESI-TOF) *m/z* calculated for $C_{11}H_{20}{}^{79}BrNO_3SNa$ $(M+Na)^+$ 348.0240, found 348.0240.

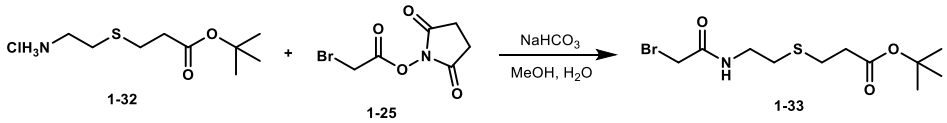

***tert*-Butyl 3-((2-(2-bromoacetamido)ethyl)thio)propanoate (1-33):**

To a solution of HCl salt **1-32** (340 mg, 1.41 mmol, 1.0 equiv) in MeOH (3.5 mL) and H_2O (3.5 mL) at rt was added ester **1-25** (500 mg, 2.12 mmol, 1.5 equiv) followed by $NaHCO_3$ (1.18 g, 14.1 mmol, 10.0 equiv). The reaction was stirred for 4 h and then diluted with EtOAc. The organic phase was washed with H_2O (3 X). The combined aqueous phase was extracted with EtOAc (2 X). The combined organic phase was washed with brine, dried with Na_2SO_4, filtered, and concentrated *in vacuo*. The resulting residue was purified via flash chromatography (40% EtOAc in hex) to obtain bromoacetamide **1-33** (105 mg, 23% over 2 steps). The spectral data matches the data reported *vide supre*.

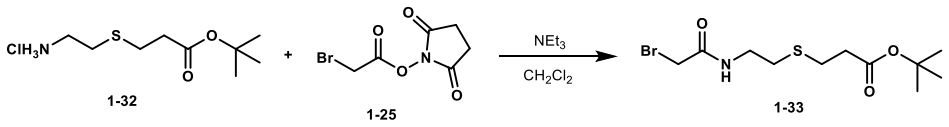

***tert*-Butyl 3-((2-(2-bromoacetamido)ethyl)thio)propanoate (1-33):**

To a solution of HCl salt **1-32** (560 mg, 2.32 mmol, 1.0 equiv) in CH_2Cl_2 (7.7 mL) at rt was added ester **1-25** (547 mg, 2.32 mmol, 1.0 equiv) followed by $NaHCO_3$ (1.6 mL, 11.6 mmol, 5.0 equiv). The solution was stirred for 30 min at rt and then the reaction solution was washed with 1 M HCl then brine. The combined aqueous phase was extracted with CH_2Cl_2. The combined organic phase was dried with Na_2SO_4, filtered, and concentrated *in vacuo*. The resulting residue was purified via flash chromatography (30 → 70% EtOAc in hex) to obtain bromoacetamide **1-33** (21 mg, 3% over 2 steps). The spectral data matches the data reported *vide supre*.

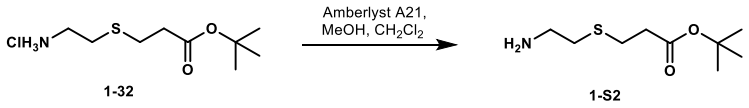

***tert*-Butyl 3-((2-aminoethyl)thio)propanoate (1-S2):**

To a mixture of Amberlyst A21 (2.3 g) in CH_2Cl_2 (50 mL) was added a solution of HCl salt **1-32** (196 mg, 0.820 mmol, 1.0 equiv) in MeOH (2 mL). The mixture was stirred for 30 min and then filtered and the filtrate was concentrated *in vacuo* to obtain amine **1-S2** (85 mg, 50% over 2 steps). The spectral data matches the data reported *vide supre*.

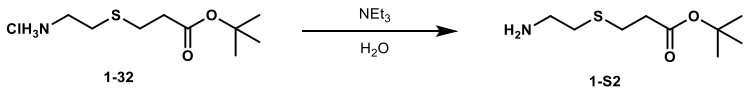

***tert*-Butyl 3-((2-aminoethyl)thio)propanoate (1-S2):**

To a solution of HCl salt **1-32** (197 mg, 0.824 mmol, 1.0 equiv) in H_2O (1.0 mL) was added NEt_3 (1.7 mL). The mixture was stirred for 4 h and then extracted with CH_2Cl_2 (4 X). The combined organic phase was dried with Na_2SO_4, filtered, and concentrated *in vacuo* to obtain amine **1-S2** (32 mg, 19% over 2 steps). The spectral data matches the data reported *vide supre*.

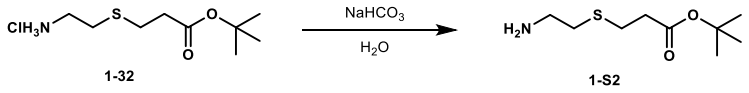

***tert*-Butyl 3-((2-aminoethyl)thio)propanoate (1-S2):**

To a solution of HCl salt **1-32** (204 mg, 0.853 mmol, 1.0 equiv) in H_2O (2.0 mL) was added $NaHCO_3$ (750 mg, 8.93 mmol, 10.0 equiv). The mixture was stirred for 4 h and then extracted with CH_2Cl_2 (4 X). The combined organic phase was dried with Na_2SO_4, filtered, and concentrated *in vacuo* to obtain amine **1-S2** (56 mg, 32% over 2 steps). The spectral data matches the data reported *vide supre*.

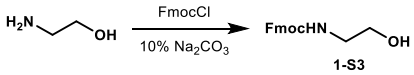

(9*H*-Fluoren-9-yl)methyl (2-hydroxyethyl)carbamate (1-S3):

To a solution of Na_2CO_3 (16.5 g) in H_2O (165 mL) was added ethanolamine (2.0 mL, 33.1 mmol, 1.0 equiv) followed by fluorenylmethyloxycarbonyl chloride (9.40 g, 36.4 mmol, 1.1 equiv). The cloudy solution was stirred for 21 h at rt and then extracted with EtOAc (3 X). The combined

organic phase was washed with brine, dried with Na_2SO_4, filtered, and concentrated *in vacuo* to obtain alcohol **1-S3** as a white fluffy powder (9.30 g, 99%). Spectral data is in accordance with the reported literature.[74]

^{1}H NMR (500 MHz, $CDCl_3$) δ 7.76 (d, *J* = 7.6 Hz, 2H), 7.59 (d, *J* = 7.5 Hz, 2H), 7.40 (t, *J* = 7.5 Hz, 2H), 7.31 (t, *J* = 7.5 Hz, 2H), 5.20 (s, br, 1H), 4.43 (d, *J* = 6.6 Hz, 2H), 4.21 (t, *J* = 6.5 Hz, 1H), 3.77 – 3.66 (m, 2H), 3.41 – 3.30 (m, 2H), 2.10 (s, 1H).

^{13}C NMR (126 MHz, $CDCl_3$) δ 144.0, 141.5, 127.8, 127.2, 125.1, 120.1, 66.9, 62.4, 47.4, 43.6.

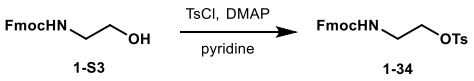

2-((((9*H*-Fluoren-9-yl)methoxy)carbonyl)amino)ethyl 4-methylbenzenesulfonate (1-34):

To a solution of alcohol **1-S3** (9.30 g, 33.1 mmol, 1.0 equiv) in pyridine (55 mL) at 0 °C was added DMAP (404 mg, 3.31 mmol, 0.1 equiv) followed by TsCl (12.6 g, 66.2 mmol, 2.0 equiv) in aliquots. The reaction was stirred for 5.5 h and then diluted with EtOAc. The solution was washed with 1 M HCl (3 X), saturated $CuSO_4$ solution, and brine (2 X) and then dried with Na_2SO_4, filtered, and concentrated *in vacuo*. The resulting residue was purified via flash chromatography (30% EtOAc in hex) to obtain tosylate **1-34** (10.1 g, 70%).

^{1}H NMR (500 MHz, $CDCl_3$) δ 7.80 – 7.75 (m, 4H), 7.57 (d, *J* = 7.4 Hz, 1H), 7.41 (t, *J* = 7.4 Hz, 1H) 7.34 – 7.28 (m, 4H) 5.13 (s, br, 1H), 4.33 (d, *J* = 7.1 Hz, 2H), 4.18 (t, *J* = 7.0 Hz, 1H), 4.14 – 4.09 (m, 2H), 3.47 (dd, *J* = 10.2, 5.0 Hz, 2H), 2.39 (s, 3H).

^{13}C NMR (126 MHz, $CDCl_3$) δ 156.3, 145.3, 143.9, 141.4, 132.7, 130.1, 128.1, 127.9, 127.2, 125.2, 120.1, 69.2, 67.2, 47.2, 40.4, 21.7.

HRMS (ESI-TOF) *m/z* calculated for $C_{24}H_{23}NO_5SNa$ $(M+Na)^+$ 460.1195, found 460.1205.

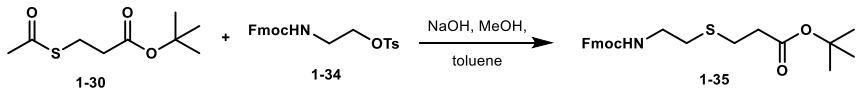

***tert*-Butyl 3-((2-((((9*H*-fluoren-9-yl)methoxy)carbonyl)amino)ethyl)thio)propanoate (1-35):**

To a solution of tosylate **1-34** (7.00 g, 16.0 mmol, 1.0 equiv) and thioester **1-30** (9.80 g, 48.0 mmol, 3.0 equiv) in degassed toluene (32 mL) and MeOH (76 mL) at rt was slowly added a solution of NaOH (576 mg, 14.4 mmol, 0.9 equiv) in MeOH (20 mL). The solution turned a bright yellow and was stirred for 16.5 h at rt. The solution was diluted with benzene and washed with 1 M HCl, H_2O, then brine; it was then dried with Na_2SO_4, filtered, and concentrated *in vacuo*. The resulting residue was purified via flash chromatography (30% EtOAc in hex) to obtain sulfide **1-35** as a clear oil (1.95 g, 29%) and recovered starting material **1-34** (4.20 g).

^{1}H NMR (500 MHz, $CDCl_3$) δ 7.76 (d, *J* = 7.7 Hz, 2H), 7.60 (d, *J* = 7.5 Hz, 2H), 7.39 (t, *J* = 7.5 Hz, 2H), 7.31 (t, *J* = 7.4 Hz, 2H), 5.36 (s, br, 1H), 4.40 (d, *J* = 6.9 Hz, 2H), 4.22 (t, *J* = 6.6 Hz, 1H), 3.44 – 3.36 (m, 2H), 2.76 (t, *J* = 6.9 Hz, 2H), 2.68 (t, *J* = 5.7 Hz, 2H), 2.52 (t, *J* = 7.0 Hz, 2H), 1.46 (s, 9H).

^{13}C NMR (126 MHz, $CDCl_3$) δ 171.2, 156.4, 144.0, 141.4, 127.7, 127.1, 125.1, 120.0, 81.0, 66.8, 47.3, 40.2, 36.0, 32.3, 28.2, 26.9.

HRMS (ESI-TOF) *m/z* calculated for $C_{24}H_{29}NO_4SNa$ $(M+Na)^+$ 450.1715, found 450.1718.

A separate run of this reaction resulted in sulfide **1-37**, the Fmoc alkenes, and other unidentified impurities.

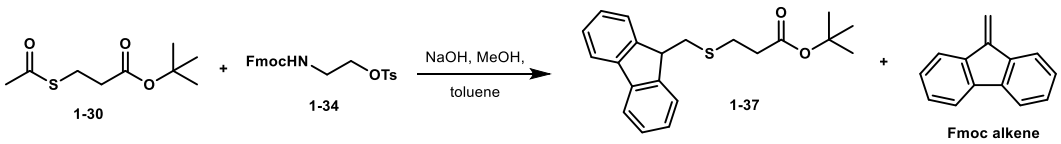

***tert*-Butyl 3-(((9*H*-fluoren-9-yl)methyl)thio)propanoate (1-37):**

^{1}H NMR (500 MHz, $CDCl_3$) δ 7.81 – 7.74 (m, 4H), 7.44 – 7.38 (m, 4H), 4.13 (t, *J* = 6.6 Hz, 1H), 3.10 (d, *J* = 6.7 Hz, 2H), 2.82 (t, *J* = 7.4 Hz, 2H), 2.54 (t, *J* = 7.4 Hz, 2H), 1.51 (2, 9H).

Fmoc alkene:

^{1}H NMR (500 MHz, $CDCl_3$) δ 7.74 – 7.70 (m, 4H), 7.38 – 7.31 (m, 4H), 6.10 (s, 2H).

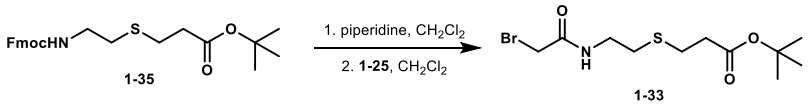

***tert*-Butyl 3-((2-(2-bromoacetamido)ethyl)thio)propanoate (1-33):**

To a solution of sulfide **1-35** (50 mg, 0.117 mmol, 1.0 equiv) in CH_2Cl_2 (0.24 mL) was added piperidine (0.10 mL). The solution was stirred for 45 min and then concentrated *in vacuo*. The resulting residue was redissolved in CH_2Cl_2 (0.40 mL) and NHS ester **1-25** (28 mg, 0.117 mmol, 1.0 equiv) was added. The reaction solution was concentrated *in vacuo* and the resulting residue was purified via flash chromatography to obtain bromoacetamide **1-33** as a clear oil (22 mg, 58%). The spectral data matches the data reported *vide supre*.

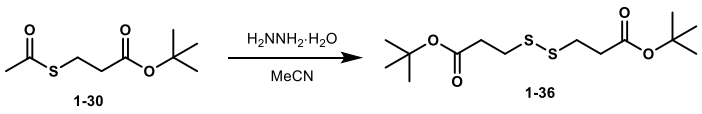

Di-*tert*-butyl 3,3'-disulfanediyldipropionate (1-36):

To a solution of thioester 1-30 (100 mg, 0.489 mmol, 1.0 equiv) in MeCN (2.9 mL) at rt was added hydrazine monohydrate (0.07 mL, 1.47 mmol, 3.0 equiv) in MeCN (1.5 mL). The solution was stirred for 28 h and was quench with 1 M HCl solution. The solution was extracted with CH_2Cl_2. The combined organic phase was washed with H_2O (2 X), then brine, dried with Na_2SO_4, filtered, and concentrated *in vacuo* to obtain disulfide **1-36** as a clear oil.

^{1}H NMR (600 MHz, $CDCl_3$) δ 2.88 (t, *J* = 7.2 Hz, 4H), 2.63 (t, *J* = 7.2 Hz, 4H), 1.45 (s, 18H).

^{13}C NMR (151 MHz, $CDCl_3$) δ 171.1, 81.1, 35.5, 33.7, 28.2.

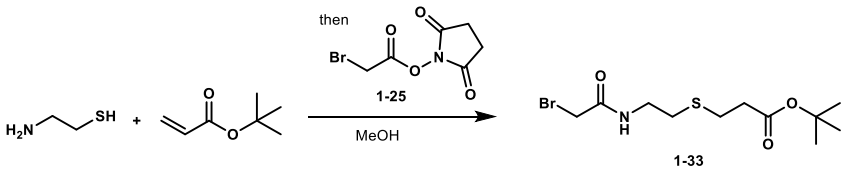

***tert*-Butyl 3-((2-(2-bromoacetamido)ethyl)thio)propanoate (1-33):**

To a solution of cysteamine (2.29 g, 29.7 mmol, 1.0 equiv) in MeOH (150 mL) at rt was added *t*-butyl acrylate (4.3 mL, 29.7 mmol, 1.0 equiv). The solution was stirred for 45 min and then NHS ester **1-25** (7.00 g, 29.7 mmol, 1.0 equiv) was added. The solution was stirred for 10 min and then concentrated *in vacuo*. The resulting residue was purified through a silica plug (40% EtOAc in hex) to obtain bromoacetamide **1-33** as a clear oil (6.33 g, 65%). The spectral data matches the data reported *vide supre*.

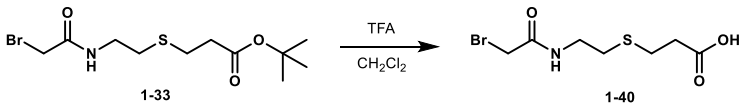

1-33 1-40

3-((2-(2-Bromoacetamido)ethyl)thio)propanoic acid (1-40):

To a solution of ester **1-33** (1.50 g, 4.60 mmol, 1.0 equiv) in CH_2Cl_2 (23 mL) was added TFA (1.8 mL, 23.0 mmol, 5.0 equiv). The solution was concentrated *in vacuo* after stirring at rt for 17 h. The resulting residue was purified via flash chromatography (0 → 15% MeOH in CH_2Cl_2) to obtain carboxylic acid **1-40** as a clear oil (871 mg, 70%).

^{1}H NMR (500 MHz, $CDCl_3$) δ 6.95 (s, br, 1H), 3.91 (s, 2H), 3.51 (q, *J* = 6.2 Hz, 2H), 2.82 (t, *J* = 7.1 Hz, 2H), 2.73 (t, *J* = 6.5 Hz, 2H), 2.67 (t, *J* = 7.1 Hz, 2H).

^{13}C NMR (126 MHz, $CDCl_3$) δ 176.1, 166.6, 39.4, 34.6, 31.6, 29.0, 26.6.

HRMS (ESI-TOF) *m/z* calculated for $C_7H_{12}{}^{79}BrNO_3SNa$ $(M+Na)^+$ 291.9614, found 291.9617.

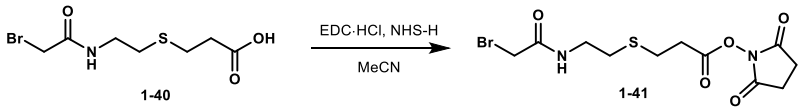

1-40 1-41

2,5-Dioxopyrrolidin-1-yl 3-((2-(2-bromoacetamido)ethyl)thio)propanoate (1-41):

To a solution of carboxylic acid **1-40** (871 mg, 3.22 mmol, 1.0 equiv) in MeCN (16 mL) was added EDC·HCl (679 mg, 3.54 mmol, 1.1 equiv) and NHS-H (371 mg, 3.22 mmol, 1.0 equiv). The solution was stirred for 15 h and then it was diluted with EtOAc. The solution was washed with H_2O and the aqueous layer was extracted with EtOAc (2 X). The combined organic phase was washed with brine, dried with Na_2SO_4, filtered, and concentrated *in vacuo*. The resulting residue

was purified via flash chromatography (0 → 100% EtOAc in hex) to obtain NHS ester **1-41** (125 mg, 11%).

^{1}H NMR (500 MHz, $CDCl_3$) δ 7.02 (s, br, 1H), 4.06 (s, 2H), 3.56 – 3.49 (m, 2H), 2.96 – 2.89 (m, 4H), 2.89 – 2.81 (m, 4H), 2.76 (t, J = 6.4 Hz, 2H).

^{13}C NMR (126 MHz, $CDCl_3$) δ 169.1, 167.2, 166.3, 42.8, 38.9, 32.3, 31.9, 26.3, 25.7.

HRMS (ESI-TOF) *m/z* calculated for $C_{11}H_{15}{}^{79}BrN_2O_5SNa$ $(M+Na)^+$ 388.9778, found 388.9784.

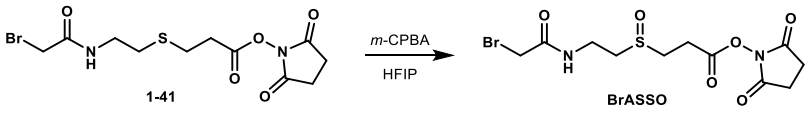

BrASSO (1-28):

To a solution of sulfide **1-41** (65 mg, 0.180 mmol, 1.0 equiv) in HFIP (0.90 mL) at rt was added *m*-CPBA (30 mg, 0.170 mmol, 0.95 equiv). The solution was stirred for 45 min and then concentrated *in vacuo*. The resulting residue was purified via flash chromatography (0 → 10% MeOH in CH_2Cl_2) to obtain cross-linker **BrASSO** as a white solid (25 mg, 38%).

^{1}H NMR (500 MHz, CD_3OD) δ 3.85 (s, 2H), 3.73–3.58 (m, 2H), 3.36–3.32 (m, 1H), 3.22–3.07 (m, 4H), 3.04–2.94 (m, 1H), 2.85 (s, 4H).

^{13}C NMR (126 MHz, CD_3OD) δ 171.7, 170.0, 168.9, 52.6, 46.9, 35.3, 28.7, 26.6, 25.0.

HRMS (ESI-TOF) *m/z* calculated for $C_{11}H_{15}{}^{79}BrN_2O_6SNa$ $(M+Na)^+$ 404.9727, found 404.9725.

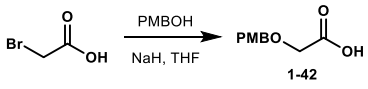

1-42

2-((4-Methoxybenzyl)oxy)acetic acid (1-42):

To a slurry of NaH (432 mg, 18.0 equiv, 2.5 equiv) in THF (29 mL) was added bromoacetic acid (1.00 g, 7.2 mmol, 1.0 equiv). When the bubbling subsided, 4-methoxybenzyl alcohol (1.00 g, 7.27 mmol, 1.01 equiv) was added and then the reaction was heated to reflux for 18 h. Once cooled to rt, the mixture was diluted with EtOH and then concentrated *in vacuo*. The resulting residue was partitioned between Et_2O and a saturated $NaHCO_3$ solution. The organic phase was washed with saturated $NaHCO_3$ solution (3 X). The combined aqueous phase was acidified to pH 1 with concentrated HCl. The acidified aqueous phase was then extracted with Et_2O and the combined organic phase was washed with brine, dried with $MgSO_4$, filtered, and concentrated *in vacuo* to obtain carboxylic acid **1-42** (1.03 g, 73%). The spectral data is in accordance with the reported literature.[75]

^{1}H NMR (500 MHz, $CDCl_3$) δ 7.26 (d, *J* = 8.6 Hz, 2H), 6.86 (d, *J* = 8.7 Hz, 2H), 4.54 (s, 2H), 4.05 (s, 2H), 3.78 (s, 3H).

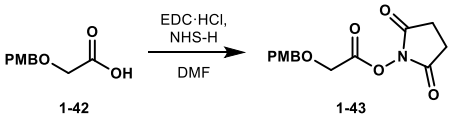

1-42 1-43

2,5-Dioxopyrrolidin-1-yl 2-((4-methoxybenzyl)oxy)acetate (1-43):

To a solution of carboxylic acid **1-42** (500 mg, 2.55 mmol, 1.0 equiv) in DMF (8.5 mL) was added EDC·HCl (537 mg, 2.80 mmol, 1.1 equiv) followed by NHS-H (293 mg, 2.55 mmol, 1.0 equiv). The solution was stirred for 24 h and then it was diluted with EtOAc. The mixture was washed

with H_2O (5 X) then brine. The organic phase was dried with Na_2SO_4, filtered, and concentrated *in vacuo* to obtain NHS ester **1-43** as a clear oil (678 mg, 91%).

^{1}H NMR (500 MHz, $CDCl_3$) δ 7.30 (d, *J* = 8.4 Hz, 2H), 6.89 (d, *J* = 8.5 Hz, 2H), 4.61 (s, 2H), 4.39 (s, 2H), 3.81 (s, 3H), 2.85 (s, 4H).

^{13}C NMR (126 MHz, $CDCl_3$) δ 168.9, 166.1, 159.9, 130.1, 128.4, 114.1, 73.4, 64.6, 55.4, 25.7.

HRMS (ESI-TOF) *m/z* calculated for $C_{14}H_{15}NO_6Na$ $(M+Na)^+$ 316.0797, found 316.0792.

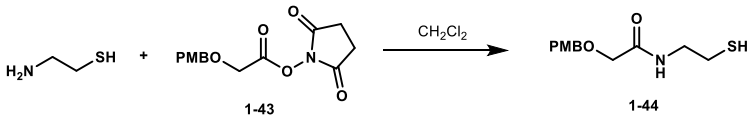

***N*-(2-Mercaptoethyl)-2-((4-methoxybenzyl)oxy)acetamide (1-44):**

To a solution of NHS ester **1-43** (600 mg, 2.05 mmol, 1.0 equiv) in CH_2Cl_2 (10 mL) was added cysteamine (158 mg, 2.05 mmol, 1.0 equiv). The solution was stirred for 15 min and then it was washed with H_2O, and brine. The organic phase was dried with Na_2SO_4, filtered, and concentrated *in vacuo* to obtain sulfide **1-44** (507 mg, 97%).

^{1}H NMR (500 MHz, $CDCl_3$) δ 7.30 (d, *J* = 8.6 Hz, 2H), 6.94 (d, *J* = 8.6 Hz, 2H), 4.54 (s, 2H), 4.00 (s, 2H), 3.84 (s, 3H), 3.49 (q, *J* = 6.5 Hz, 2H), 2.69 (dd, *J* = 15.0, 6.6 Hz, 2H), 1.41 (t, *J* = 8.5 Hz, 2H).

^{13}C NMR (126 MHz, $CDCl_3$) δ 170.0, 159.8, 129.8, 128.9, 114.1, 73.4, 69.3, 55.4, 41.8, 24.6.

HRMS (ESI-TOF) *m/z* calculated for $C_{12}H_{17}NO_3SNa$ $(M+Na)^+$ 278.0827, found 278.0823.

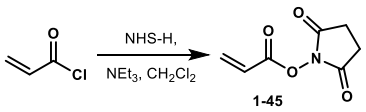

2,5-Dioxopyrrolidin-1-yl acrylate (1-45):

To a solution of NHS-H (5.18 g, 45.0 mmol, 1.0 equiv) in CH_2Cl_2 (90 mL) at 0 °C was added NEt_3 (6.3 mL, 45.0 mmol, 1.0 equiv) followed by acryloyl chloride (4.0 mL, 49.5 mmol, 1.1 equiv). The solution was stirred for 3 h and it was then filtered. The filtrate was washed with H_2O (2 X) and brine, dried with Na_2SO_4, filtered, and concentrated *in vacuo* to obtain acrylate **1-45** as a white flakey solid (5.52 g, 72%). The spectral data is in accordance with the reported literature.[76]

^{1}H NMR (500 MHz, $CDCl_3$) δ 6.70 (d, *J* = 17.3 Hz, 1H), 6.32 (dd, *J* = 17.3, 10.7 Hz, 1H), 6.16 (d, *J* = 10.7 Hz, 1H), 2.86 (s, 4H).

^{13}C NMR (126 MHz, $CDCl_3$) δ 169.2, 161.2, 136.3, 123.1, 25.8.

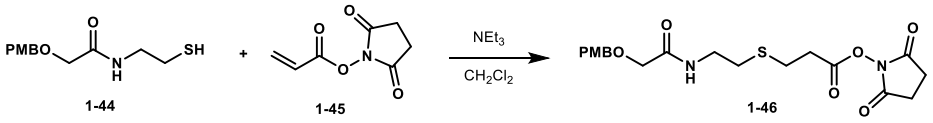

2,5-Dioxopyrrolidin-1-yl 3-((2-(2-((4-methoxybenzyl)oxy)acetamido)ethyl)thio)propanoate (1-46):

To a solution of sulfide **1-44** (500 mg, 1.96 mmol, 1.0 equiv) and acrylate **1-45** (331 mg, 1.96 mmol, 1.0 equiv) in CH_2Cl_2 (10 mL) at rt was added NEt_3 (0.27 mL). The solution was stirred for 10 min and then it was washed with 1 M HCl (2 X) and brine. The organic phase was dried with Na_2SO_4, filtered, and concentrated *in vacuo* to obtain sulfide **1-46** (794 mg, 94%) and some recovered acrylate **1-45**.

^{1}H NMR (500 MHz, $CDCl_3$) δ 7.24 (d, *J* = 8.4 Hz, 2H), 6.86 (d, *J* = 8.4 Hz, 2H), 4.47 (s, 2H), 3.93 (s, 2H), 3.77 (s, 3H), 3.45 (q, *J* = 6.4 Hz, 2H), 2.91 – 2.83 (m, 4H), 2.75 (s, 4H), 2.68 (t, *J* = 6.6 Hz, 2H).

^{13}C NMR (126 MHz, $CDCl_3$) δ 170.0, 169.0, 167.2, 159.8, 129.8, 129.1, 114.1, 73.4, 69.4, 55.5, 38.1, 32.2, 32.1, 26.3, 25.7.

HRMS (ESI-TOF) *m/z* calculated for $C_{19}H_{24}N_2O_7SNa$ $(M+Na)^+$ 447.1202, found 447.1198.

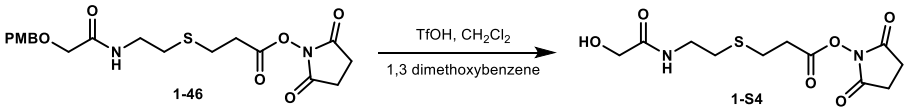

2,5-Dioxopyrrolidin-1-yl 3-((2-(2-hydroxyacetamido)ethyl)thio)propanoate (1-S4):

To a solution of sulfide **1-46** (50 mg, 0.118 mmol, 1.0 equiv) in CH_2Cl_2 (0.60 mL) at rt was added 1,3 dimethoxybenzene (0.05 mL, 0.354 mmol, 3.0 equiv) and TfOH (0.01 mL, 0.059 mmol, 0.5 equiv). The solution was stirred at rt for 20 min and was then concentrated *in vacuo*. The resulting residue was purified via flash chromatography (100% EtOAc) to obtain alcohol **1-S4** (23 mg, 64%).

^{1}H NMR (500 MHz, $CDCl_3$) δ 7.12 (s, br, 1H), 4.10 (s, 2H), 3.52 (dd, *J* = 12.2, 6.1 Hz, 2H), 2.96 – 2.88 (m, 4H), 2.85 (s, 4H), 2.76 (t, *J* = 6.3 Hz, 2H).

^{13}C NMR (126 MHz, $CDCl_3$) δ 172.5, 169.4, 167.3, 62.2, 38.2, 32.3, 32.2, 26.4, 25.7.

HRMS (ESI-TOF) *m/z* calculated for $C_{11}H_{16}N_2O_6SNa$ $(M+Na)^+$ 327.0627, found 327.0624

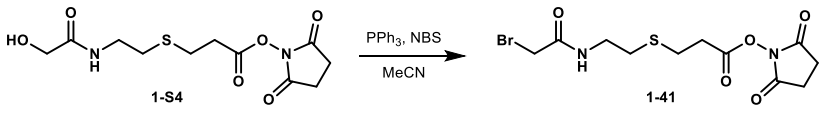

2,5-Dioxopyrrolidin-1-yl 3-((2-(2-bromoacetamido)ethyl)thio)propanoate (1-41):

To a solution of alcohol **1-S4** (50 mg, 0.164 mmol, 1.0 equiv) in MeCN (0.8 mL) at rt was added PPh_3 (47 mg, 0.181 mmol, 1.1 equiv) and NBS (32 mg, 0.181 mmol, 1.1 equiv). After stirring for 3 h at rt, the solution was concentrated *in vacuo*. The resulting residue was purified via flash chromatography (70 → 100% EtOAc in hex) to obtain bromoacetamide **1-41** as a mixture with triphenylphosphine oxide (11 mg).

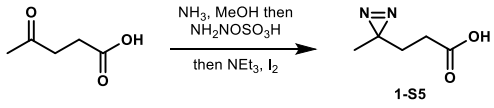

3-(3-Methyl-3*H*-diazirin-3-yl)propanoic acid (1-S5):

To a solution of levulinic acid (1.0 mL, 9.77 mmol, 1.0 equiv) in MeOH (2.3 mL) at 0 °C was added 7 N NH_3 in MeOH (7.4 mL). The solution was stirred for 3 h at 0 °C, then a slurry of hydroxylamine-O-sulfonic acid (1.27 g, 11.2 mmol, 1.15 equiv) in MeOH (7 mL) was added. The mixture was allowed to warm to rt overnight. The milky white solution was carefully concentrated *in vacuo*. The resulting residue was redissolved in MeOH (15 mL), cooled to 0 °C, and then NEt_3 (2.0 mL, 14.6 mmol, 1.5 equiv) was added. The solution was stirred for 10 min then I_2 (4.46 g, 17.6 mmol, 1.8 equiv) was added in aliquots. The slurry was diluted with EtOAc and then washed with 1 M HCl solution and saturated $Na_2S_2O_3$ solution. The combined aqueous phase was extracted with EtOAc. The combined organic phase was washed with brine, dried with Na_2SO_4, filtered, and

concentrated *in vacuo* to obtain carboxylic acid **1-S5** (792 mg, 63%). The spectral data is in accordance with the reported literature.[77]

^{1}H NMR (500 MHz, $CDCl_3$) δ 11.18 (s, br, 1H), 2.11 (t, *J* = 7.7 Hz, 2H), 1.57 (t, *J* = 7.7 Hz, 2H), 0.90 (s, 3H).

^{13}C NMR (126 MHz, $CDCl_3$) δ 178.5, 29.2, 28.4, 24.9, 19.4.

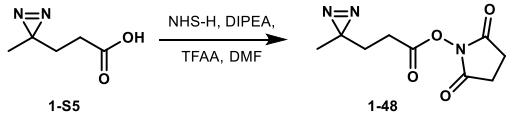

1-S5 1-48

2,5-Dioxopyrrolidin-1-yl 3-(3-methyl-3*H*-diazirin-3-yl)propanoate (1-48):

To a solution of carboxylic acid **1-S5** (790 mg, 6.17 mmol, 10 equiv) in DMF (31 mL) at 0 °C was added NHS-H (1.42 g, 12.3 mmol, 2.0 equiv) followed by DIPEA (4.3 mL, 24.7 mmol, 4.0 equiv) and TFAA (1.7 mL, 12.3 mmol, 2.0 equiv). The reaction was stirred for 2 h at 0 °C and was then diluted with EtOAc. The solution was washed with H_2O (7 X) then brine, dried with Na_2SO_4, filtered, and concentrated *in vacuo*. The resulting residue was purified via flash chromatography (0 → 70% EtOAc in hex) to obtain NHS ester **1-48** as a clear oil (797 mg, 57%). The spectral data is in accordance with the reported literature.[78]

^{1}H NMR (500 MHz, $CDCl_3$) δ 2.28 (s, 4H), 2.50 (t, *J* = 7.7 Hz, 2H), 1.79 (t, *J* = 7.7 Hz, 2H), 1.06 (s, 3H).

^{13}C NMR (126 MHz, $CDCl_3$) δ 169.1, 167.7, 29.6, 25.8, 25.7, 24.8, 19.6.

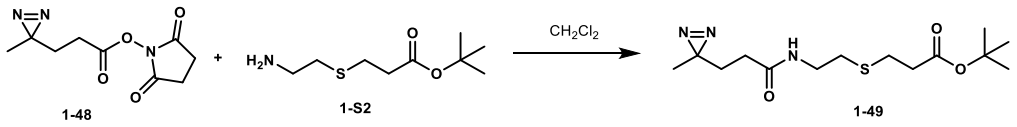

***tert*-Butyl 3-((2-(3-(3-methyl-3*H*-diazirin-3-yl)propanamido)ethyl)thio)propanoate (1-49):**

To a solution of amine **1-S2** (82 mg, 0.400 mmol, 1.0 equiv) in CH_2Cl_2 (1.3 mL) at rt was added NHS ester **1-48** (90 mg, 0.400 mmol, 1.0 equiv). After stirring for 1 h at rt the solution was concentrated *in vacuo*. The resulting residue was purified via flash chromatography (0 → 100% EtOAc in hex) to obtain sulfide **1-49** as a white solid (35 mg, 28% over 2 steps).

^{1}H NMR (600 MHz, $CDCl_3$) δ 6.18 (s, br, 1H), 3.43 (q, *J* = 6.1 Hz, 2H), 2.73 (t, *J* = 7.1 Hz, 2H), 2.66 (t, *J* = 6.3 Hz, 2H), 2.49 (t, *J* = 7.1 Hz, 2H), 2.01 (t, *J* = 7.8 Hz, 2H), 1.74 (t, *J* = 7.8 Hz, 2H), 1.44 (s, 9H), 1.01 (s, 3H).

^{13}C NMR (151 MHz, $CDCl_3$) δ 171.6, 171.4, 81.2, 38.5, 35.9, 32.0, 30.7, 30.1, 28.2, 26.8, 25.5, 20.0.

IR (neat) 3306, 2977, 2929, 1725, 1650, 1538, 1139, 843, 664 cm^{-1}.

HRMS (ESI-TOF) *m/z* calculated for $C_9H_{11}N_3O_4Na$ $(M+Na)^+$ 248.0642, found 248.0644.

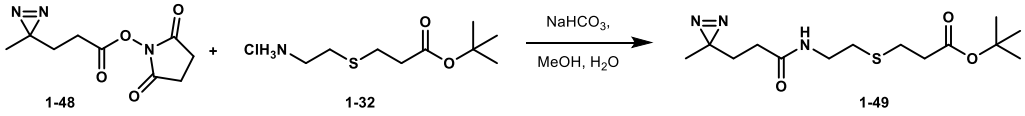

***tert*-Butyl 3-((2-(3-(3-methyl-3*H*-diazirin-3-yl)propanamido)ethyl)thio)propanoate (1-49):**

To a solution of salt **1-32** (91 mg, 0.444 mmol, 1.0 equiv) in MeOH (1.1 mL) and H_2O (1.1 mL) at rt was added $NaHCO_3$ (187 mg, 2.22 mmol, 5.0 equiv) followed by ester **1-48** (100 mg, 0.444

mmol, 1.0 equiv). The solution was stirred for 13.5 h and it was then diluted with EtOAc. The organic phase was washed with H_2O, and the aqueous phase was extracted with EtOAc (3 X). The combined organic phase was dried with Na_2SO_4, filtered, and concentrated *in vacuo* to obtain sulfide **1-49** (72 mg, 51% over 2 steps). The spectral data matches the data reported *vide supre*.

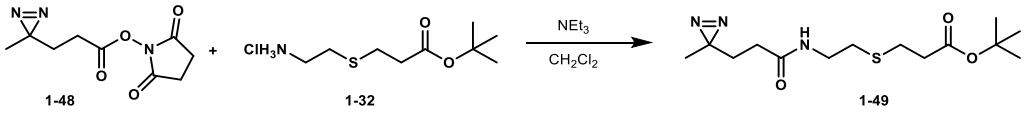

1-48 1-32 1-49

***tert*-Butyl 3-((2-(3-(3-methyl-3*H*-diazirin-3-yl)propanamido)ethyl)thio)propanoate (1-49):**

To a solution of salt **1-32** (500 mg, 2.44 mmol, 1.0 equiv) in CH_2Cl_2 (8.1 mL) at rt was added NEt_3 (0.90 mL) followed by ester **1-48** (825 mg, 3.66 mmol, 1.5 equiv). The solution was stirred for 1.5 h and it was then washed with H_2O (2 X). The aqueous phase was extracted with CH_2Cl_2 (2 X). The combined organic phase was dried with Na_2SO_4, filtered, and concentrated *in vacuo.* The resulting residue was purified via flash chromatography (30 → 70% EtOAc in hex) to obtain sulfide **1-49** (206 mg, 27% over 2 steps). The spectral data matches the data reported *vide supre*.

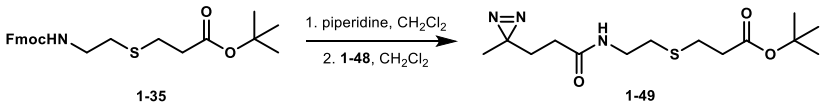

1-35 1-49

***tert*-Butyl 3-((2-(3-(3-methyl-3*H*-diazirin-3-yl)propanamido)ethyl)thio)propanoate (1-49):**

To a solution of sulfide **1-35** (159 mg, 0.372 mmol, 1.0 equiv) in CH_2Cl_2 (0.75 mL) was added piperidine (0.15 mL). The solution was stirred for 1 h and it was then concentrated *in vacuo*. The resulting residue was dissolved in CH_2Cl_2 (1.24 mL) and ester **1-48** (126 mg, 0.558 mmol, 1.5 equiv) was added. The solution was stirred for 1.5 h and then it was concentrated *in vacuo*. The

resulting residue was purified via flash chromatography (0 → 50% EtOAc in hex) to obtain sulfide **1-49** (55 mg, 47% over 2 steps). The spectral data matches the data reported *vide supre*.

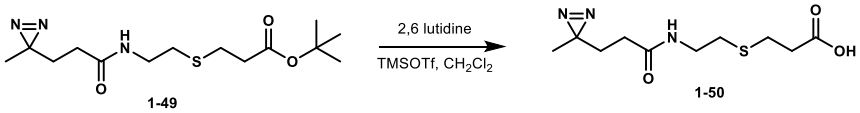

3-((2-(3-(3-Methyl-3*H*-diazirin-3-yl)propanamido)ethyl)thio)propanoic acid (1-50):

To a solution of ester **1-49** (262 mg, 0.830 mmol, 1.0 equiv) in CH_2Cl_2 (8.3 mL) at 0 °C was added 2,6-lutidine (0.21 mL, 1.80 mmol, 2.1 equiv) followed by TMSOTf (0.35 mL, 1.90 mmol, 2.3 equiv). The reaction was allowed to warm to rt and was stirred at rt for 1.5 h. The reaction was quenched with 1 M HCl solution and the organic phase was extracted. The aqueous phase was extracted with CH_2Cl_2 (3 X). The combined organic phase was washed with brine, dried with Na_2SO_4, filtered, and concentrated *in vacuo* to obtain carboxylic acid **1-50** (157 mg, 73%).

^{1}H NMR (500 MHz, $CDCl_3$) δ 6.23 (s, br, 1H), 3.45 (dd, *J* = 12.4, 6.2 Hz, 2H), 2.80 (t, *J* = 7.1 Hz, 2H), 2.69 (t, *J* = 6.5 Hz, 2H), 2.65 (t, *J* = 7.0 Hz, 2H), 2.06 – 2.01 (m, 2H), 1.77 – 1.69 (m, 2H), 1.02 (s, 3H).

^{13}C NMR (126 MHz, $CDCl_3$) δ 176.1, 172.2, 38.7, 34.7, 31.9, 30.7, 30.2, 26.5, 25.6, 20.0.

IR (neat) 3367, 2928, 1703, 1651, 1557, 1364, 1231, 992, 646 cm^{-1}.

HRMS (ESI-TOF) *m/z* calculated for $C_{10}H_{17}N_3O_3SNa$ $(M+Na)^+$ 282.0883, found 282.0895.

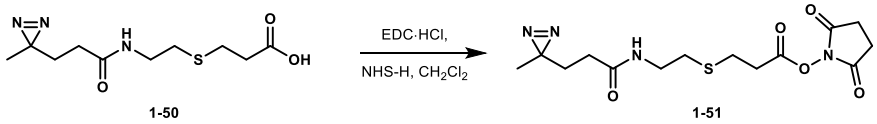

1-50 1-51

2,5-Dioxopyrrolidin-1-yl 3-((2-(3-(3-methyl-3*H*-diazirin-3-yl)propanamido)ethyl) thio) propanoate (1-51):

To a solution of carboxylic acid **1-50** (150 mg, 0.580 mmol, 1.0 equiv) in CH_2Cl_2 (2.0 mL) at rt was added EDC·HCl (122 mg, 0.640 mmol, 1.1 equiv) and NHS-H (67 mg, 0.580 mmol, 1.0 equiv). The solution was stirred for 17 h at rt and it was then washed with H_2O. The aqueous phase was extracted with CH_2Cl_2 (3 X). The combined organic phase was washed with brine, dried with Na_2SO_4, filtered, and concentrated *in vacuo* to obtain NHS ester **1-51** (198 mg), which was taken onto the next step without further purification.

^{1}H NMR (500 MHz, $CDCl_3$) δ 6.32 (s, br, 1H), 3.42 (dd, *J* = 12.2, 6.0 Hz, 2H), 2.94 – 2.82 (m, 8H), 2.70 (t, *J* = 6.2 Hz, 2H), 2.05 – 1.95 (m, 2H), 1.77 – 1.69 (m, 2H), 1.00 (s, 3H).

^{13}C NMR (126 MHz, $CDCl_3$) δ 171.6, 169.2, 167.1, 38.4, 31.99, 31.96, 30.4, 30.0, 26.2, 25.6, 25.5, 19.7.

HRMS (ESI-TOF) *m/z* calculated for $C_{14}H_{20}N_4O_5SNa$ $(M+Na)^+$ 379.1047, found 379.1043.

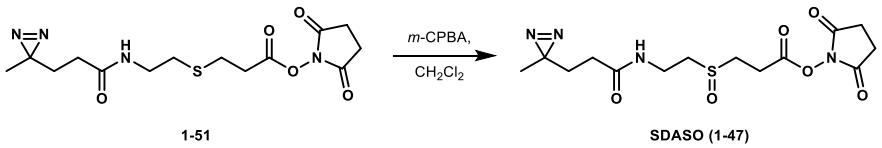

1-51 SDASO (1-47)

SDASO (1-47):

To a solution of sulfide **1-51** (80 mg, 0.220 mmol, 1.0 equiv) in CH_2Cl_2 (1.1 mL) was added *m*-CPBA (36 mg, 0.210 mmol, 0.95 equiv). The solution was stirred for 10 min and it was then quenched with saturated $Na_2S_2O_3$ solution and saturated $NaHCO_3$ solution. The organic layer was extracted and dried with Na_2SO_4, filtered, and concentrated *in vacuo*. The resulting residue was purified via flash chromatography (0 → 15% MeOH in CH_2Cl_2) to obtain **SDASO** as a white solid (13 mg, 17% over 2 steps).

^{1}H NMR (600 MHz, $CDCl_3$) δ 6.67 (s, 1H), 3.85 – 3.66 (m, 2H), 3.22 – 3.13 (m, 3H), 3.12 – 3.03 (m, 2H), 2.92 – 2.80 (m, 5H), 2.02 (t, *J* = 7.8 Hz, 2H), 2.02 (t, *J* = 7.8 Hz, 2H), 1.02 (s, 3H).

^{13}C NMR (151 MHz, $CDCl_3$) δ 172.1, 168.9, 167.0, 51.5, 46.1, 34.4, 30.6, 30.0, 25.7, 25.6, 24.3, 19.9.

HRMS (ESI-TOF) *m/z* calculated for $C_{14}H_{20}N_4O_6SNa$ $(M+Na)^+$ 395.0996, found 395.0995.

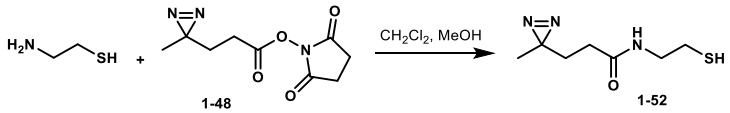

1-48 1-52

***N*-(2-mercaptoethyl)-3-(3-methyl-3*H*-diazirin-3-yl)propenamide (1-52):**

To a solution of cysteamine (1.0 g, 4.44 mmol, 1.0 equiv) in CH_2Cl_2 (22 mL) and MeOH (2.0 mL) at rt was added NHS ester **1-48** (343 mg, 4.44 mmol, 1.0 equiv). The solution was stirred for 15

min and then it was washed with H_2O and brine. The organic phase was dried with Na_2SO_4, filtered, and concentrated *in vacuo* to obtain sulfide **1-52** as a pink-orange oil (617 mg, 74%).

^{1}H NMR (500 MHz, $CDCl_3$) δ 5.88 (s, br, 1H), 3.43 (q, *J* = 6.2 Hz, 2H), 2.68 (dt, *J* = 8.5, 6.4 Hz, 2H), 2.00 (t, *J* = 7.6 Hz, 2H), 1.78 (t, *J* = 7.6 Hz, 2H), 1.37 (t, *J* = 8.5 Hz, 1H), 1.03 (s, 2H).

^{13}C NMR (126 MHz, $CDCl_3$) δ 171.5, 42.5, 30.8, 30.1, 25.6, 24.8, 20.1.

HRMS (ESI-TOF) *m/z* calculated for $C_7H_{13}N_3OSNa$ $(M+Na)^+$ 210.0677, found 210.0676.

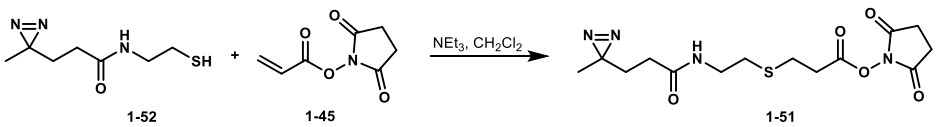

1-52 1-45 1-51

2,5-dioxopyrrolidin-1-yl 3-((2-(3-(3-methyl-3*H*-diazirin-3-yl)propanamido)ethyl) thio) propanoate (1-51):

To a solution of sulfide **1-52** (600 mg, 3.20 mmol, 1.0 equiv) and acrylate **1-45** (542 mg, 3.20 mmol, 1.0 equiv) in CH_2Cl_2 (16 mL) at rt was added NEt_3 (0.49 mL, 3.52 mmol, 1.1 equiv). The solution was stirred for 15 at rt and then it was washed with H_2O (2 X). The combined aqueous phase was extracted with CH_2Cl_2. The combined organic phase was dried with Na_2SO_4, filtered, and concentrated *in vacuo*. The resulting residue was purified via flash chromatography (0 → 100% EtOAc in hex) to obtain sulfide **1-51** (643 mg, 56%). The spectral data matches the data reported *vide supre*.

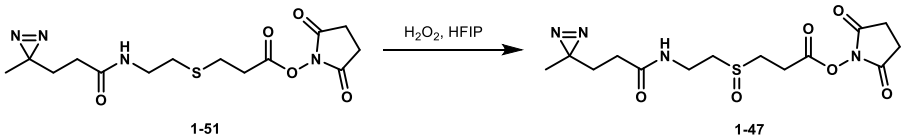

1-51 1-47

SDASO (1-47):

To a solution of sulfide **1-51** (640 mg, 1.80 mmol, 1.0 equiv) in HFIP (4.5 mL) at rt was added 30% aqueous H_2O_2 (0.37 mL, 3.59 mmol, 2.0 equiv). The solution was stirred for 10 min and then was quenched with DMS (1.4 mL). The reaction solution was concentrated *in vauco* and the resulting residue was redissolved in EtOAc. The solution was washed with H_2O and brine, dried with Na_2SO_4, filtered, and concentrated *in vacuo* to obtain **SDASO** (349 mg, 52%). The spectral data matches the data reported *vide supre*.

References

[1] Berman, H. M.; Westbrook, J.; Feng, Z.; Gilliland, G.; Bhat, T. N.; Weissig, H.; Shindyalov, I. N.; Bourne, P. E. The Protein Data Bank. *Nucleic Acids Research*, **2000**, *28*, 235–242. https://www.rcsb.org/stats/summary

[2] Shi, Y. A Glimpse of Structural Biology through X-Ray Crystallography. *Cell* **2014**, *159*, 995–1014.

[3] Su, X.; Zhang, H.; Terwilliger, T. C.; Lijas, A.; Xiao, J.; Dong, Y. Protein Crystallogrpahy from the Perspective of Technological Developments. *Crystallogr. Rev*. **2015**, *21*, 122–153.

[4] Wüthrich, K. Protein Structure Determination in Solution by NMR Spectroscopy. *J. Biol. Chem*. **1990**, *265*, 22059–22062.

[5] Cressey, D.; Callaway, E. Cryo-electron microscopy wins chemistry Nobel. *Nature* **2017**, *550*, 167.

[6] Callaway, E. The Protein-Imaging Technique Taking Over Structural Biology. *Nature* **2021**, *578*, 210.

[7] Milne, J. L. S.; Borgnia, M. J.; Bartesaghi, A.; Tran, E. E. H.; Earl, L. A.; Schauder, D. M.; Lengyel, J.; Pierson, J.; Patwardhan, A.; Subramaniam, S. Cryo-electron microscopy – a primer for the non-microscopist. *FEBS Journal* **2013**, *280*, 28–45.

[8] Benjin, X.; Ling, L. Developments, applications, and prospects of cryo-electron microscopy. *Protein Sci*. **2019**, *29*, 872–882.

[9] Schneider, M.; Belsome, A.; Rappsilber, J. Protein Tertiary Structure by Crosslinking/Mass Spectrometry. *Trends Biochem. Sci*. **2018**, *43*, 157–169.

[10] Iacobucci, C.; Götze, M.; Sinz, A. Cross-linking/mass spectrometry to get a closer view on protein interaction networks. *Curr. Opin. Biotechnol*. **2020**, *63*, 48–53.

[11] *In vivo* protein complex topologies: Sights through a cross-linking lens. *Proteomics* **2012**, *12*, 1565–1575.

[12] Chavez, J. D.; Bruce, J. E. Chemical cross-linking with mass spectrometry: a toll for systems structural biology. *Curr. Opin. Chem. Bio*. **2019**, *48*, 8–18.

[13] Wheat, A.; Yu, C.; Wang, X.; Burke, A. M.; Chemmana, I. E.; Kaake, R. M.; Baker, P.; Rychnovsky, S. D.; Yang, J.; Huang, L. Protein interaction landscapes revealed by advanced in vivo cross-linking–mass spectrometry. *Proc. Natl. Acad. Sci*. **2021**, *118*, e2023360118.

[14] Piersimoni, L.; Kastritis, P. L.; Arlt, C.; Sinz, A. Cross-Linking Mass Spectrometry for Investigating Protein Conformations and Protein–Protein Interactions─ A Method for All Seasons. *Chem. Rev*. **2021**, https://pubs.acs.org/doi/10.1021/acs.chemrev.1c00786.

[15] Skoog, D. A.; Holler, F. J.; Crouch, S. R. *Principles of Instrumental Analysis*, 6th ed.; Thomson, 2007.

[16] Steigenberger, B.; Albanese, P.; Heck, A. J. R.; Scheltema, R. A. To Cleave or Not to Cleave in XL-MS? *J. Am. Soc. Mass Spectrom*. **2020**, *31*, 196–206.

[17] Liu, F.; Rijkers, D. T. S.; Post, H.; Heck, A. J. R. Proteome-wide profiling of protein assemblies by cross-linking mass spectrometry. *Nature Methods* **2015**, *12*, 1179–1184.

[18] Kao, A.; Chiu, C.; Vellucci, D.; Yang, Y.; Patel, V. R.; Guan, S.; Randall, A.; Baldi, P.; Rychnovsky, S. D.; Luang, L. Development of a novel cross-linking strategy for fast and accurate identification of cross-linked peptides of protein complexes. *Mol. Cell. Proteomics* **2011**, M110.002212.

[19] Chavez, J. D. Lee, C. F.; Caudal, A.; Keller, A.; Tian, R.; Bruce, J. E. Chemical Crosslinking Mass Spectrometry Analysis of Protein Conformations and Supercomplexes in Heart Tissue. *Cell Systems* **2018**, *6*, 136–141.

[20] Soderblom, E. J.; Goshe, M. B. Collision-Induced Dissociative Chemical Cross-Linking Reagents and Methodology: Applications to Protein Structural Characterization Using Tandem Mass Spectrometry Analysis. *Anal. Chem.* **2006**, *78*, 8059–8068.

[21] Yu, W.; Vath, J. E.; Huberty, M. C.; Martin, S. A. Identification of the Facile Gas-Phase Cleavage of the Asp-Pro and Asp-Xxx Peptide Bonds in Matrix-Assisted Laser Desorption Time-of-Flight Spectrometry. *Anal. Chem*. **1993**, *65*, 3015–3023.

[22] Skribanek, Z.; Mezö, G.; Mák, M.; Hudecz, F. Mass spectrometric and chemical stability of the Asp-Pro bond in herpes simplex virus epitope peptides compared with X-Pro bonds of related sequences. *J. Pept. Sci.* **2002**, *8*, 398–406.

[23] Liu, F.; Wu, C.; Sweedler, J. V.; Goshe, M. B. An enhanced protein crosslink identification strategy using CID-cleavable chemical crosslinkers and LC/MS^n analysis. *Proteomics* **2012**, *12*, 401–405.

[24] Müller, M. Q.; Dreiocker, F.; Ihling, C. H.; Schäfer, M.; Sinz, A. Cleavable Cross-Linker for Protein Structure Analysis: Reliable Identification of Cross-Linking Products by Tandem MS. *Anal. Chem*. **2010**, *82*, 6958–6968.

[25] Sinz, A. Divide and conquer: cleavable cross-linkers to study protein conformation and protein-protein interactions. *Anal. Bioanal. Chem*. **2017**, *409*, 33–44.

[26] Lu, Y.; Tanasova, M.; Borhan, B.; Reid, G. E. Ionic Reagent for Controlling the Gas-Phase Fragmentation Reactions of Cross-Linked Peptides. *Anal. Chem.* **2008**, *80*, 9279–9287.

[27] Clifford-Nunn, B.; Showalter, H. D. H.; Andrews, P. C. Quaternary Diamines as Mass Spectrometry Cleavable Crosslinkers for Protein Interactions. *J. Am. Soc. Mass Spectrom.* **2012**, *23*, 201–212.

[28] Tang, X.; Munske, G. R.; Siems, W. F.; Bruce, J. E. Mass Spectrometry Identifiable Cross-Linking Strategy for Studying Protein−Protein Interactions. *Anal. Chem.* **2005**, *77*, 311–318.

[29] Tang, X.; Bruce, J. E. A new cross-linking strategy: protein interaction reporter (PIR) technology for protein–protein interaction studies. *Mol. Biosyst*. **2010**, *6*, 939–947.

[30] Chavez, J. D.; Mohr, J. P.; Mathay, M.; Zhong, X.; Keller, A.; Bruce, J. E. Systems structural biology measurements by in vivo cross-linking with mass spectrometry. *Nature Protocols* **2019**, *14*, 2318–2343.

Select recent examples of DSSO used in XL-MS experiments (31-35):

[31] Klykov, O.; Steigenberger, B.; Pektas, S.; Fasci, D.; Heck, A. J. R.; Scheltema, R. A. Efficient and robust proteome-wide approaches for cross-linking mass spectrometry. *Nature Protocols* **2018**, *13*, 2964–2990.

[32] Yugandhar, K.; Wang, T.; Leung, A. K.; Lanz, M. C.; Motorykin, I.; Liang, J.; Shayhidin, E. E.; Smolka, M. B.; Zhang, S.; Yu, H. MaXLinker: Proteome-wide Cross-link Identifications with High Specificity and Sensitivity. *Mol. Cell. Proteomics* **2020**, *19*, 554–568.

[33] Yu, C.; Wang, X.; Huszagn, A. S.; Viner, R.; Novitsky, E.; Rychnovsky, S. D.; Huang, L. Probing H_2O_2-mediated structural dynamics of the human 26S proteasome qusing quantitative cross-linking mass spectrometry. *Mol. Cell. Proteomics* **2019**, *18*, 954–967.

[34] Gutierrez, C.; Chemmama, I. E.; Mao, H.; Yu, C.; Echeverria, I.; Block, S. A.; Rychnovsky, S. D.; Zheng, N.; Sali, A.; Huang, L. Structural dynamics of the human COP9 signalosome revealed by cross-linking mass spectrometry and integrative modeling. *Proc. Natl. Acad. Sci*. **2020**, *117*, 4088–4098.

[35] Wang, X.; Cimermancic, P.; Yu, C.; Schweitzer, A.; Chopra, N.; Engel, J. L.; Greenberg, C.; Huszagh, A. S.; Beck, F.; Sakata, E.; Yang, Y.; Novitsky, E. J.; Leitner, A.; Nanni, P.; Kahraman, A.; Guo, X.; Dixon, J. E.; Rychnovsky, S. D.; Aebersold, R.; Baumeister, W.; Sali, A.; Huang, L. Molecular Details Underlying Dynamic Structures and Regulation of the Human 26S Proteasome. *Mol. Cell. Proteomics* **2017**, *16*, 840–854.

[36] Gonzalez-Lozano, M. A.; Koopmans, F.; Sullivan, P. F.; Protze, J.; Krause, G.; Verhage, M.; Li, K. W.; Liu, F.; Smit, A. B. Stitching the synapse: Cross-linking mass spectrometry into resolving synaptic protein interactions. *Science Advances* **2020**, *6*, eaax5783.

[37] Novitsky, E. J. Expanding the Scope of Collision-Induced Dissociation-Cleavable Protein Cross-Linkers. University of California, Irvine, 2017.

[38] Yu, C.; Novitsky, E. J.; Cheng, N. W.; Rychnovsky, S. D.; Huang, L. Exploring Spacer Arm Structures for Designs of Asymmetric Sulfoxide-Containing MS-Cleavable Cross-Linkers. *Anal. Chem.* **2020**, *92*, 6026–6033.

[39] Roberts, M. J.; Bentley, M. D.; Harris, J. M. Chemistry for peptide and protein PEGylation. *Adv. Drug Delivery Rev.* **2002**, *54*, 459–476.

[40] Mattson, G.; Conklin, E.; Desai, S.; Nielander, G.; Savage, M. D.; Morgensen, S. A practical approach to crosslinking*. Mol. Bio. Reports* **1993**, *17*, 167–183.

[41] Mädler, A.; Bich, C.; Touboul, D.; Zenobi, R. Chemical cross-linking with NHS esters: a systematic study on amino acid reactivities. *J. Mass Spectrom*. **2009**, *44*, 694–706.

[42] Gutierrez, C. G.; Yu, C.; Novitsky, E. J.; Huszagh, A. S.; Rychnovsky, S. D.; Huang, L. Developing an Acidic Residue Reactive and Sulfoxide-Containing MS-Cleavable Homobifunctional Cross-Linker for Probing Protein–Protein Interactions. *Anal. Chem.* **2016**, *88*, 8315–8322.

[43] Leitner, A.; Joachimiak, L. A.; Unverdorben, P.; Walzthoeni, T.; Frydman, J.; Förster, F.; Aeberosld, R. Chemical cross-linking/mass spectrometry targeting acidic residues in proteins and protein complexes. *Proc. Natl. Acad. Sci*. **2014**, *111*, 9455–9460.

[44] Novak, P.; Kruppa, G. H. Intra-Molecular Cross-Linking of Acidic Residues for Protein Structure Studies. *Eur. Mass Spectrom*. **2008**, *14*, 355− 365.

[45] Gutierrez, C. B.; Block, S. A.; Yu, C.; Soohoo, S. M.; Huszagh, A. S.; Rychnovsky, S. D.; Huang, L. Development of a Novel Sulfoxide-Containing MS-Cleavable Homobifunctional Cysteine-Reactive Cross-Linker for Studying Protein–Protein Interactions. *Anal. Chem.* **2018**, *90*, 7600–7607.

[46] Ishikawa, E.; Imagawa, M.; Hashida, S.; Yoshitake, S.; Hamaguchi, Y.; Ueno, T. Enzyme-Labeling of Antibodies and Their Fragments for Enzyme Immunoassay and Immunohistochemical Staining. *J. Immunoassay* **1983**, *4*, 209–327.

[47] Ghosh, S.; Farr, L.; Singh, A.; Leaton, L.; Padalia, J.; Shirley, D.; Sullivan, D.; Moonah, S. COP9 signalosome is an essential and druggable parasite target that regulates protein degradation. *PLoS Pathogens* **2020**, *16*, e1008952.

[48] Schlierf, A.; Altmann, E.; Quancard, J.; Jefferson, A. B.; Assenberg, R.; Renatus, M.; Jones, M.; Hassiepen, U.; Schaefer, M.; Kiffe, M.; Weiss, A.; Wiesmann, C.; Sedrani, R.; Eder, J.; Martoglio, B. Targeted inhibition of the COP9 signalosome for treatment of cancer. *Nat. Commun*. **2016**, *7*, 13166.

[49] Rozen, S.; Füzesi-Levi, M. G.; Ben-Nissan, G.; Mizrachi, L.; Gabashvili, A.; Levin, Y.; Ben-Dor, S.; Eisenstein, M.; Sharon, M. CSNAP is a Stoichiometric Subunit of the COP9 Signalosome. *Cell Reports* **2015**, *13*, 585–598.

[50] Enchev, R. I.; Scott, D. C.; da Fonseca, P. C. A.; Schreiber, A.; Monda, J. K.; Schulman, B. A.; Peter, M.; Morris, E. P. Structural Basis for a Reciprocal Regulation between SCF and CSN. *Cell Reports* **2012**, *2*, 616–627.

[51] Ligaraju, G. M.; Bunker, R. D.; Cavadini, S.; Hess, D.; Hassiepen, U.; Renatus, M.; Fischer, E. S.; Thonä, U. H. Crystal structure of the human COP9 singlosome. *Nature* **2014**, *512*, 161–165.

[52] Cavadini, S.; Fischer, E. S.; Bunker, R. D.; Potenza, A.; Ligaraju, G. M.; Goldie, K. N.; Mohamed, W. I.; Fatsy, M.; Petzold, G.; Beckwith, R. E. J.; Tichkule, R. B.; Hassiepen, U.; Adbulrahman, W.; Pantelic, R. S.; Matsumoto, S.; Sugasawa, K.; Stahlberg, H.; Thomä, N. H. Cullin-RING ubiquitin E3 ligase regulation by the COP9 singlosome. *Nature* **2016**, *531*, 598–603.

[53] Mosadeghi, R.; Reichermeier, K. M.; Winkler, M.; Schreiber, A.; Reitsma, J. M.; Zhang, Y.; Stengel, F.; Cao, J.; Kim, M.; Sweredoski, M. J.; Hess, S.; Leitner, A.; Aebersold, R.; Peter, M.; Deshaies, R. J.; Enchev, R. Structural and kinetic analysis of the COP9-signalosome activation and the cullin-RING ubiquitin ligase deneddylation cycle. *eLife* **2016**, *5*, e12102.

[54] Szijj, P. A.; Bahou, C.; Chudasama, V. Minireview: Addressing the Retro-Michael Instability of Maleimide Bioconjugates. *Drug Discovery Today: Technologies* **2018**, *30*, 27–34.

[55] Schelté, Philippe; Boeckler, C.; Frisch, B.; Schuber, F. Differential Reactivity of Maleimide and Bromoacetyl Functions with Thiols: Application to the Preparation of Liposomal Diepitope Constructs. *Bioconjugate Chem*. **2000**, *11*, 118–123.

[56] Chalker, J. M.; Bernardes, G. J. L.; Lin, Y. A.; Davis, B. G. Chemical Modification of Proteins at Cysteine: Opportunities in Chemistry and Biology. *Chem. Asian J*. **2009**, *4*, 630–640.

[57] Srinivasan, N.; Yurek-George, A.; Ganesan, A. *Mol. Divers*. **2005**, *9*, 291–293.

[58] Gutierrez, C.; Salituro, L. J.; Yu, C.; Wang, X.; DePeter, S. F.; Rychnovsky, S. D.; Huang, L. Enabling Photoactivated Cross-Linking Mass Spectrometric Analysis of Protein Complexes by Novel MS-Cleavable Cross-Linkers. *Mol. Cell. Proteomics* **2021**, *20*, 100084.

[59] Iacobucci, C., Piotrowski, C., Rehkamp, A., Ihling, C. H., and Sinz, A. The first MS-cleavable, photo-thiol-reactive cross-linker for protein structural studies. *J. Am. Soc. Mass Spectrom*. **2019**, *30*, 139–148.

[60] Schneider, M., Belsom, A., and Rappsilber, J. Protein tertiary structure by crosslinking/mass spectrometry. *Trends Biochem. Sci*. **2018**, *43*, 157–169.

[61] Brodie, N. I., Makepeace, K. A., Petrotchenko, E. V., and Borchers, C. H. Isotopically-coded short-range hetero-bifunctional photo-reactive crosslinkers for studying protein structure. *J. Proteomics* **2015**, *118*, 12–20.

[62] Brodie, N. I., Petrotchenko, E. V., and Borchers, C. H. The novel isotopically coded short-range photo-reactive crosslinker 2,4,6-triazido1,3,5-triazine (TATA) for studying protein structures. *J. Proteomics* **2016**, *149*, 69–76.

[63] Brodie, N. I., Popov, K. I., Petrotchenko, E. V., Dokholyan, N. V., and Borchers, C. H. Solving protein structures using short-distance cross-linking constraints as a guide for discrete molecular dynamics simulations. *Sci. Adv*. **2017**, *3*, e1700479.

[64] Belsom, A., Mudd, G., Giese, S., Auer, M., and Rappsilber, J. Complementary benzophenone cross-linking/mass spectrometry photochemistry. *Anal. Chem*. **2017**, *89*, 5319–5324.

[65] Iacobucci, C., Gotze, M., Piotrowski, C., Arlt, C., Rehkamp, A., Ihling, C., Hage, C., and Sinz, A. Carboxyl-photo-reactive MS-cleavable cross-linkers: Unveiling a hidden aspect of diazirine-based reagents. *Anal. Chem*. **2018**, *90*, 2805–2809.

[66] Liu, J., Cai, L., Sun, W., Cheng, R., Wang, N., Jin, L., Rozovsky, S., Seiple, I. B., and Wang, L. Photocaged quinone methide crosslinkers for light-controlled chemical crosslinking of protein-protein and protein-DNA complexes. *Angew. Chem. Int. Ed.* **2019**, *58*, 18839–18843.

[67] Ziemianowicz, D. S., Ng, D., Schryvers, A. B., and Schriemer, D. C. Photo-cross-linking mass spectrometry and integrative modeling enables rapid screening of antigen interactions involving bacterial transferrin receptors. *J. Proteome Res*. **2019**, *18*, 934–946.

[68] West, A. V.; Mucipinto, G.; Wu, H.; Huang, A. C. Labenski, M. T.; Jones, L. H.; Woo, C. M. Labeling Preferences of Diazirines with Protein Biomolecules. *J. Am. Chem. Soc*. **2021**, *143*, 6691–6700.

[69] Ravikumar, K. S.; Zhang, Y. M.; Bégue, J.; Bonnet-Delpon, D. Role of Hexa-fluoro-2-propanol in Selective Oxidation of Sulfide to Sulfoxide: Efficient Preparation of Glycosyl Sulfoxides. *Eur. J. Org. Chem*. **1998**, *12*, 2937–2940.

[70] Ziemianowicz D.S.; Bomgarden, R.; Etienne, C.; Schriemer, D. C. Amino acid insertion frequencies arising from photoproducts generated using aliphatic diazirines. *J. Am. Soc. Mass Spectrom*. **2017**, *28*, 2011-2021.

[71] Trmčić, M.; Hodgson, D. R. W. Kinetic studies and predictions on the hydrolysis and aminolysis of esters of 2-S-phosphorylacetates. *Beilstein J. Org. Chem*. **2010**, *6*, 732–741.

[72] Zhang, R.; McIntyre, P. J.; Collins, P. M.; Foley, D. J.; Arter, C.; von Delft, F.; Bayliss, R.; Warriner, S.; Nelson, A. Consturction of a Shape-Diverse Fragment Set: Design, Synthesis and Screen against Aurora-A Kinase. *Chem. Eur. J.* **2019**, *25*, 6831–6839.

[73] McGouran, J. F.; Kramer, H. B.; Mackeen, M. M.; di Gleria, K.; Altun, M.; Kessler, B. M. Fluorescence-based active site probes for profiling deubiquitinating enzymes. *Org. Biomol. Chem.* **2012**, *10*, 3379–3383.

[74] Porcheddu, A.; Giacomelli, G.; Piredda, I.; Carta, M.; Nieddu, G. A Practical and Efficient Approach to PNA Monomers Compatible with Fmoc-Mediated Solid-Phase Synthesis Protocols. *Eur. J. Org. Chem*. **2008**, *34*, 5786–5797.

[75] Lücke, D.; Linne, Y.; Hempel, K.; Kalesse, M. Total Synthesis of Pericoannosin A. *Org. Lett.* **2018**, *20*, 4475–4477.

[76] Ma, L.; Tu, C.; Le, P.; Chitoor, S.; Lim, S. J.; Zahid, M. U.; Teng, K. W.; Ge, P.; Selvin, P. R.; Smith, A. M. Multidentate Polymer Coatings for Compact and Homogeneous Quantum Dots with Efficient Bioconjugation. *J. Am. Chem. Soc.* **2016**, *138*, 3382–3394.

[77] Ahad, A. M.; Jensen, S. M.; Jewett, J. C. A Traceless Staudinger Reagent To Deliver Diazirines. *Org. Lett.* **2013**, *15*, 5060–5063.

[78] Arguello, A. E.; DeLiberto, A. N.; Kleiner, R. E. RNA Chemical Proteomics Reveals the N^6-Methyladenosine (m^6A)-Regulated Protein–RNA Interactome. *J. Am. Chem. Soc.* **2017**, *139*, 17249–17252.

Chapter 2. Work Towards the Synthesis of Indole Alkaloid Alstonlarsine A

2.1 Introduction

2.1.1 Introduction to cyclohepta[*b*]indoles

Cyclohepta[b]indole refers to a seven-membered ring fused with an indole. This is a large class of the indole alkaloid natural products and they display a wide variety of biological activity including anti-inflammatory,[1] anti-tuberculosis,[2] and cytotoxicity against cancer cells.[3–5] Due to the interesting and diverse biological activity, there has been development of potential pharmaceuticals bearing this core structure.[1,6–11] Figure 2.2 shows all of the isolated indole alkaloids bearing the cyclohepta[*b*]indole core.

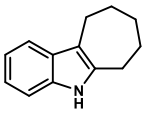

Figure 2.1. Cyclohepta[*b*] indole structure

Ajmaline was isolated in the 1930s and is the first known cyclohepta[*b*]indole to be reported.[12] The structure was revised by Woodward in 1956[13] and it was first synthesized in 1967 by Masamume and coauthors.[14] Since then, there have been three total syntheses of this alkaloid reported.[15–17] These syntheses will be discussed more in depth in section 2.1.3. Ajmaline is an approved pharmaceutical in some countries to treat heart arrythmia.

Actinophyllic acid is another well-known cyclohepta[*b*]indoles; it contains an unprecedented carbon skeleton that has shown potent biological activity.[18] This unique architecture has received much attention from the synthetic community, resulting in four total syntheses to date.[19–22] Recently, there have been many natural products isolated with the ajmaline core. Vincamaginine,[23,24] alstiphyllanine,[25] dihydrovinorine,[26] and isoajmaline[27] all contain the ajmaline core with varying oxidation and substituents about the piperidine ring.

Arcyriacyanin and dihydroarcyriacyanin are bis-indole containing natural products in which one of the indoles is bound at the [*cd*] carbons.[28,29] The highly conjugated arcyriacyanin was found to inhibit protein kinase C and protein tyrosine kinase.[30] Another highly conjugated bisindole,

caulersine, was isolated from algae that disrupts marine habitats in the South China Sea; the cyclohepta[*b*]indole was found to inhibit plant growth.[31] Exotines A and B comprise of a cyclohepta[*b*]indole core bearing a coumarin moiety.[32] These structures are quite unusual as indoles and coumarins are very common in natural products but are rarely seen in the same molecule.

The ambiguines are a class of hapalindole natural products, many of which contain the cyclohepta[*b*]indole core.[33] The first ambiguine was isolated in 1992 and since then a total of 18 ambiguine natural products have been reported.[34–38] Of these 18, the cyclohepta[*b*]indole core is present in 13 and more than half of these contain a chlorine at the C13 position. They possess a wide range of biological activity including cytotoxicity against colon and breast cancer cell lines.[36,39]

Ervitsine–ervatamine alkaloids are another large class of cyclohepta[*b*]indole natural products that contain a piperidine fused to the cycloheptane ring.[40] They exhibit various biological activities and are all isolated from the genus *Ervatamia*, which are flowering plants that have been used in traditional Chinese medicine to treat hypertension, scabies, and headaches.

The kopsifolines were originally isolated in 2004 and bear a bridged hexacyclic ring system.[5,41] The bicyclo[3.2.1] octane core consists of fully substituted bridgehead carbons. Some of these cyclohepta[*b*]indoles show potent cytotoxicity against human cancer cell lines.

The final cyclohepta[*b*]indole that will be discussed is alstonlarsine A. Reported in 2019, this structure possess a unique 9-azatricyclo[4.3.1.$0^{3,8}$]decane skeleton, which has not previously been reported in the literature.[42] It was found to exhibit DRAK2 inhibitory activity. This molecule will be discussed more in depth in section 2.2.

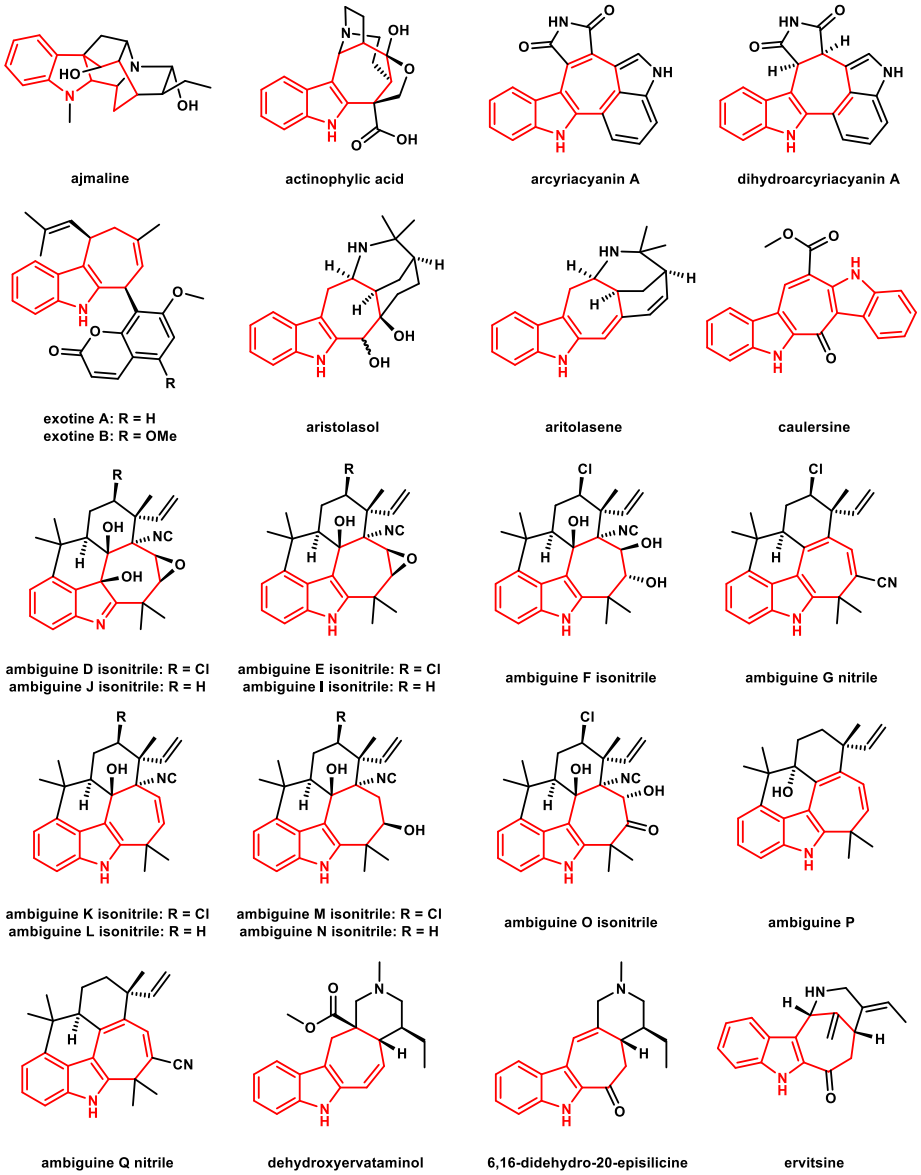

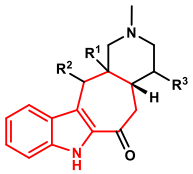

R^1	R^2	R^3	
β-CO_2Me	H,H	β-Et	**ervatamine**
β-CO_2Me	H,H	α-Et	**20-epiervatamine**
β-H	H,H	α-Et	**silicine**
α-H	H,H	α-Et	**16-episilicine**
β-H	H,H	β-Et	**20-episilicine**
α-H	H,H	β-Et	**16,20-diepisilicine**
β-H	O	α-Et	**6-oxosilicine**
α-H	O	α-Et	**6-oxo-16-episilicine**
α-H	O	β-Et	**6-oxo-16,20-diepisilicine**

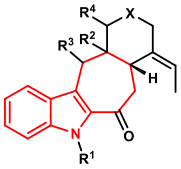

R^1	R^2	R^3	R^4	X^-	
H	β-CO_2Me	H,H	H,H	NMe	**19,20-didehydroervatamine**
OMe	β-CO_2Me	H,H	H,H	NMe	**19,20-didehydro-N^1-methoxyervatamine**
H	β-CO_2Me	H,H	O	NMe	**19,20-didehydro-5-oxoervatamine**
H	β-CO_2Me	α-OH	H,H	NMe	**19,20-didehydro-6α-hydroxyervatamine**
H	β-H	H,H	H,H	NMe	**methuenine**
H	α-H	H,H	H,H	NMe	**16-epimethuenine**
H	β-H	H,H	H,H	N(O)Me	**methuenine N^{18}-oxide**
H	α-H	H,H	H,H	N(O)Me	**16-epimethuenine N^{18}-oxide**
H	β-H	O	H,H	NMe	**6-oxomethuenine**
OMe	β-H	H,H	H,H	NMe	**N^1-methoxymethuenine**

Figure 2.2. Structures of cyclohepta[*b*]indole natural products

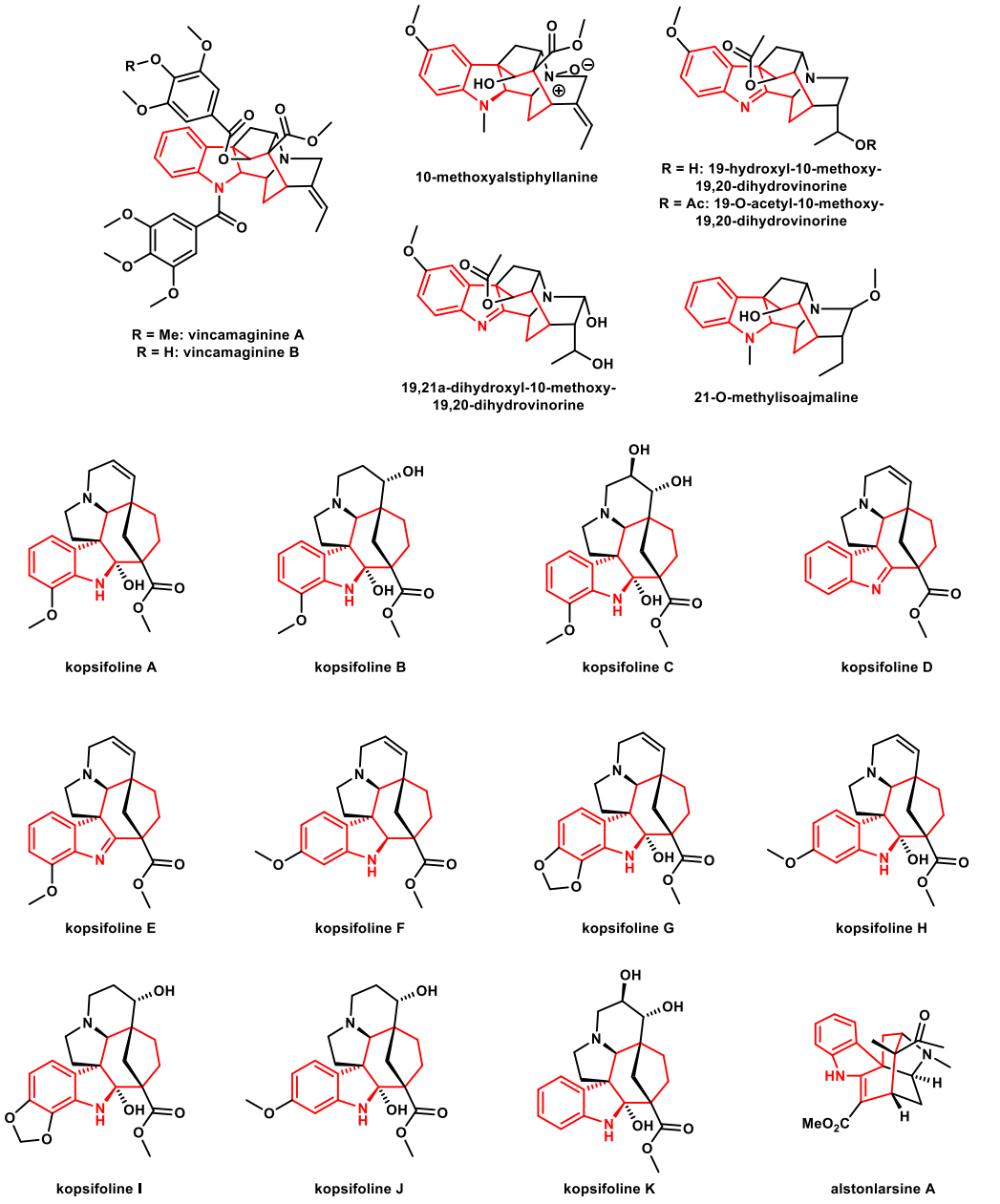

Figure 2.2 (cont.) Structures of cyclohepta[*b*]indole natural products

Of the 62 reported cyclohepta[*b*]indole natural products only a handful have been synthesized see (section 2.1.3). Due to the interesting biological activity and the wide range of structures within this class there have been many methods developed to make these cores. However, almost none of these methods have been used in total synthesis, showing a real disconnect within the literature. The next section will explore some of these methodologies.

2.1.2 Methodologies to synthesize cyclohepta[*b*]indoles

There has been a myriad of methods developed to build the cyclohepta[*b*]indoles. Classically the Fischer indole synthesis can be implemented, but there are limitations: the synthesis of the hydrazide and ketone synthons may not be functional group compatible and when using unsymmetrical ketones, there are regioselectivity issues. Over the last couple of decades there have been many novel methods developed, which will be briefly discussed in this section. There have been reviews on this topic that discuss these methods more in depth.[43,44]

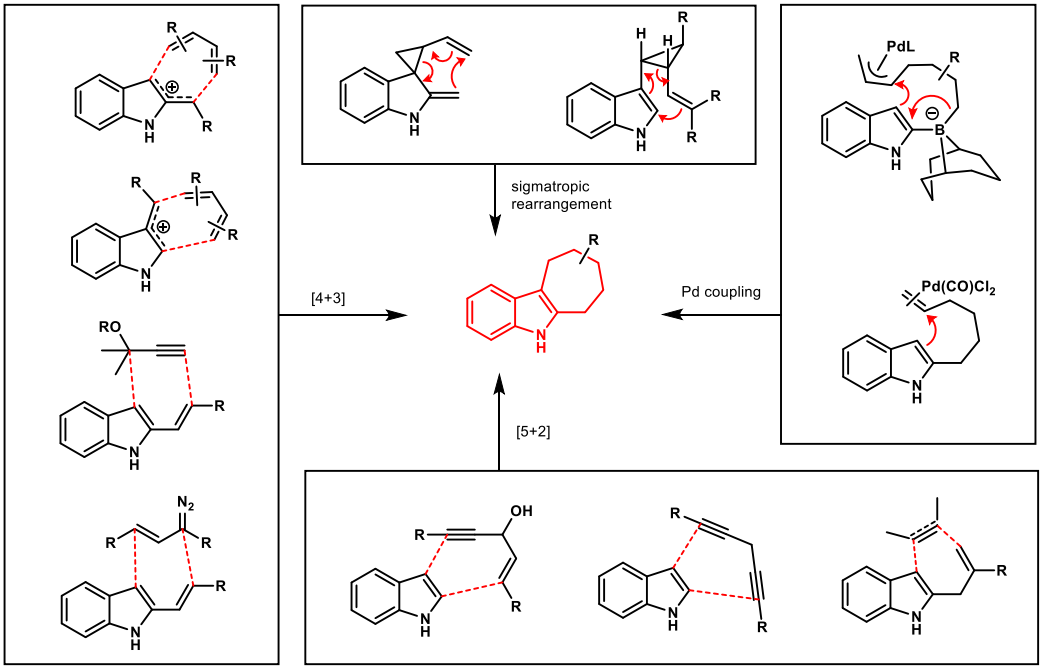

Figure 2.3. Four general methods to approach cyclohepta[b]indoles

The recent method development can generally be broken up into four major categories: [4+3] cycloadditions, [5+2] cycloadditions, palladium couplings, and sigmatropic rearrangements, which are shown in Figure 2.3. One additional category is miscellaneous transformations including photochemistry,[45–47] benzyne chemistry,[48] cascade annulations,[49,50] and asymmetric C-H alkylations.[51] This list is not comprehensive but references the more broadly used chemistry.

The most common method exploited is the [4+3] cycloaddition. One example of a [4+3] cycloaddition is shown in Scheme 2.1. Developed by Li and coauthors and reported in 2014,[52] easily prepared propargyl alcohol **2-1** was treated with catalytic silver salt to promote a hydroamination to enamine **2-2**. In the same pot, $ZnCl_2$ and butadiene were added to the allylic alcohol to form indoyl cation intermediate **2-3** which could then undergo a [4+3] cycloaddition to furnish cyclohepta[*b*]indole **2-4** in excellent yield. When the diene was swapped with silyl enol ether **2-6**, enone **2-7** was observed after hydrolysis to the ketone and elimination of the protected alcohol. These carbon skeletons can be mapped onto ervatamine and other alkaloids within this family, although elaboration to the natural product is not straight forward. There are many other [4+3] cycloadditions to furnish the cyclohepta[*b*]indole skeletons.[53–64]

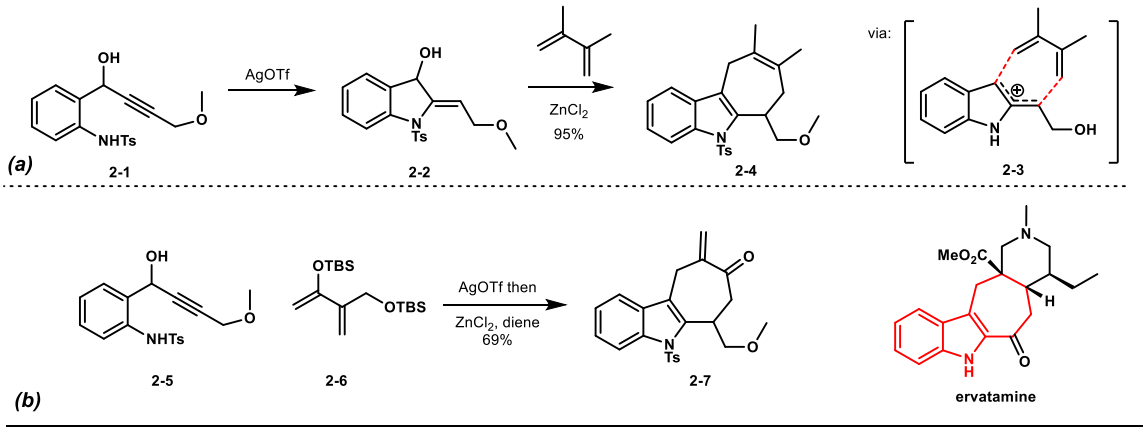

Scheme 2.1. [4+3] cycloaddition developed by Li and coauthors towards the ervatamine core

Another cycloaddition was utilized by Nishida and coauthors and reported in 2018 (Scheme 2.2).[65] Indium (III) salts were employed to promote this formal [5+2] because they can act as both pi and sigma Lewis acids. The indium (III) binded to the alkyne for addition of indole **2-6** through a Friedel-Craft type alkylation to furnish intermediate **2-9**. The Lewis acid then coordinated to the carbonyl oxygen for the 7-*endo-dig* cyclization (red arrow) which occurred much faster than the potential 5-*endo-dig* (blue arrow). The resulting cycloheptane was achieved in excellent yields. However, the substrate scope for this transformation was fairly limited. Only

aryl substitution on the alkyne was tolerated, and limited substitution on the alkene of the indole was reported. This substrate does not map onto any of the isolated cyclohepta[*b*]indoles shown in Figure 2.2. Additional [5+2] cycloadditions are reported in the literature.[66–71]

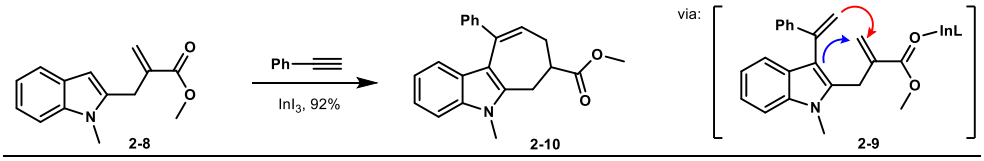

Scheme 2.2. [5+2] cycloaddition developed by Nishida and coauthors

Sigmatropic rearrangements have also been used to make cyclohepta[*b*]indoles.[72] The initial report of this pericyclic reaction is shown in Scheme 2.3. After adding the allylic chloride to the 3-position of the heterocycle furnished indole **2-11**, the carbamate protecting group was hydrolyzed. Treatment of the carbamate with NaOH yielded intermediate **2-12** which decarboxylated and promoted cyclopropane formation to form allylic cyclopropane **2-13**. This intermediate was primed for a ring-expanding [3,3] sigmatropic rearrangement and afforded the desired cyclohepta[*b*]indole. The substrate scope for this transformation was again quite limited, with only simple alkyl chains and protected alcohols at the 2-position of the indole. An enantioselective variation of this rearrangement has also been reported.[8]

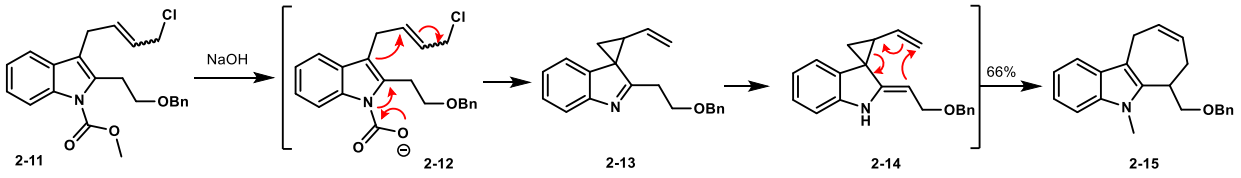

Scheme 2.3. Allylic cyclopropane formation and subsequent [3,3] sigmatropic rearrangement developed by Sinha and coauthors

In a particularly interesting cyclohepta[*b*]indole synthesis, Ishikura and Keto reported an intramolecular alkyl migration and Tsuji-Trost type cross-coupling.[73] Lithiation of *N*-methyl indole furnished lithium reagent **2-16**. Treatment of the lithium reagent with borane **2-17** yielded intermediate **2-18**. A 1,2 migration of the alkyl group from the borane onto the indole promoted an intramolecular Tsuji-Trost allylation to form the cycloheptane ring **2-19**. A limited substrate scope

was also reported with this cyclization. A tandem palladium catalyzed cyclization and carboalkoxylation has also been reported to make cyclohepta[*b*]indoles.[74]

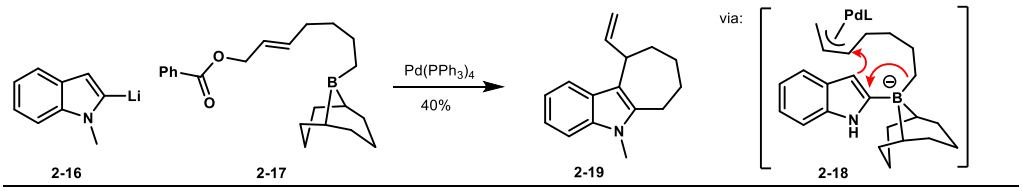

Scheme 2.4. Intramolecular alkyl migration and Tusji-Trost type cyclization developed by Ishikura and Kato

Although the methods shown in this section cleverly build cyclohepta[b]indole cores, very few have been implemented in total synthesis. There are only a couple of reported total synthesis of cyclohepta[*b*]indole natural products that uses cycloadditions to make the core. None of these reports apply the specific methods cited in this section. Also, there are very few methods for the enantioselective formation of cyclohepta[*b*]indoles. Despite this class of natural products being quite large there are not many total syntheses reported. The next section will describe these total syntheses and the strategies used to make the cyclohepta[*b*]indole skeleton.

2.1.3 Total synthesis of cyclohepta[*b*]indole natural products – ajmaline

As previously mentioned, ajmaline was the first cyclohepta[*b*]indole isolated and synthesized, with the first synthesis reported in 1967 by Masamune and coauthors.[14] All of the syntheses of this natural product take the same general approach to the cage structure.

Masamune's synthesis of ajmaline began with formation of β-keto ester **2-21** from a substituted indole. Notably this first step installed all but two of the carbons of the natural product. Amination of the ketone and a global reduction furnished amino-alcohol **2-22**, which was benzyl protected to intermediate **2-23**. A Johnson-Lemieux oxidation cleaved the alkene to form a dialdehyde intermediate which immediately cyclized to form hemiaminal **2-24**. Treatment of the hemiaminal with acetic acid closed the C ring to afford tetracycle **2-25**. Through a series of steps, the aldehyde of **2-25** was converted to a nitrile and the final two carbons of the natural product

were installed. The protected alcohol was converted to an aldehyde to afford **2-26**, which was treated with acid to promote cyclization of the indole onto the aldehyde to close the seven-membered ring. The final series of steps involved deprotections and closure of the final ring to afford ajmaline (the final step of the synthesis is not actually reported and instead refers to a degradation study of ajmaline, which converts one of Masamune's intermediates to the natural product).[75] Although not all of Masamune's steps are reported, the route efficiently constructed the caged structure. This synthesis also set the stage and provided precedent for future syntheses.

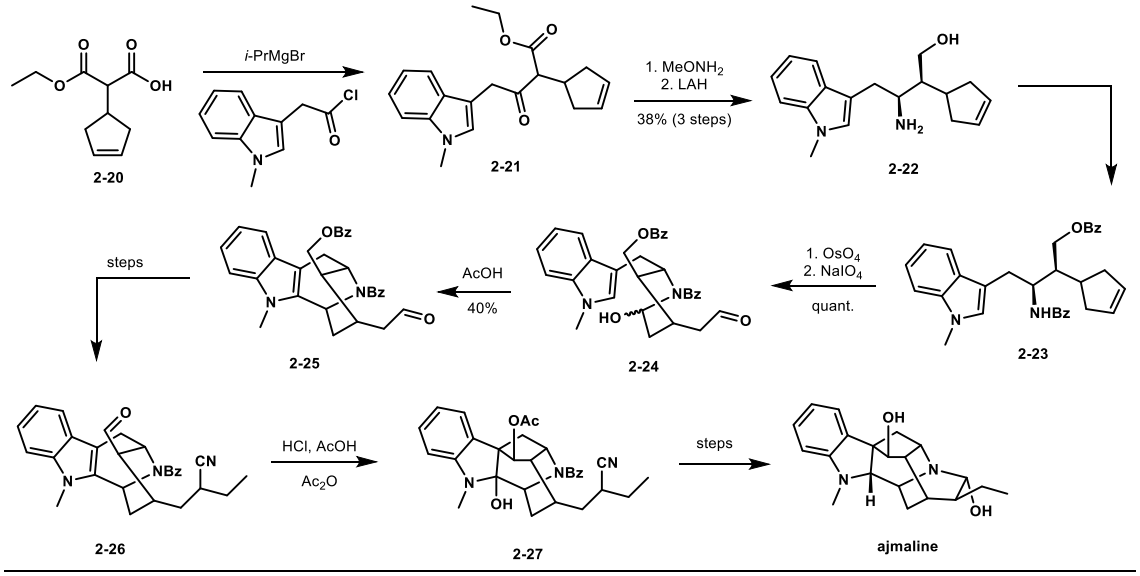

Scheme 2.5. Masamune's synthesis of ajmaline

Two years later, Mashimo and Sato reported their synthesis of isoajmaline, which is an epimer of ajmaline at C20 and C21.[76] The synthesis began with a protected derivative of tryptophan **2-28**. Exposure of the amine to methyl-4-oxobutanoate promoted a Pictet-Spengler cyclization to tricycle **2-29**. A Dieckmann cyclization closed the fourth ring to β-keto ester **2-30**. A series of eight steps converted the β-keto ester to alcohol **2-31**, similar to intermediate **2-26** in Masamune's synthesis, but was epimeric at the C16 position. An Albright–Goldman oxidation yielded the aldehyde and the α-position was epimerized with alumina to afford at 3:2 ratio of the

desired epimer to the undesired. The cycloheptane ring was closed under the same acidic conditions reported by Masamune and cyclohepta[*b*]indole **2-33** was reportedly converted to isoajmaline (Mashimo's paper references the same degradation study of ajmaline and isoajmaline that converts nitrile **2-33** to isoajmaline in one step).[75] Although not particularly efficient due to the unfavorable epimerization step and the low-yielding ring closure, this synthesis was the base for the next couple of reported syntheses of ajmaline. Mashimo and Sato also reported a formal synthesis of ajmaline soon after. They synthesized one of Masamune's intermediates by utilizing a similar approach to their synthesis of isoajmaline.[77]

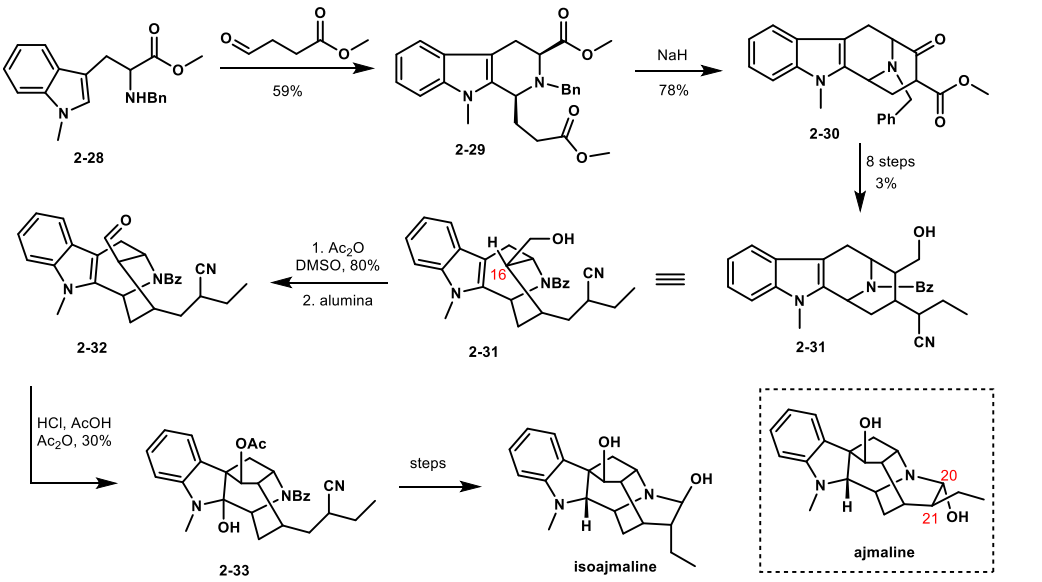

Scheme 2.6. Mashimo and Kato's synthesis of isoajmaline

One year later, van Tamelen and Oliver reported a biomimetic synthesis of ajmaline.[17] Aldehyde **2-35** was prepared in 12 steps from cyclopentadiene. When the aldehyde was treated with *N*-methyl tryptophan under reductive conditions produced amine **2-36**. Saponification and oxidative cleavage of the diol to the bis-aldehyde promoted an intramolecular Pictet-Spengler type cyclization to tetracycle **2-37** as a mixture of many diastereomers. Aldehyde **2-37** was then treated with DCC and TsOH. The esterified intermediate **2-38** could undergo a decarbonylation to iminium ion **2-39**. After deprotonation of the α-carbon of the aldehyde a cyclization event yielded aldehyde

2-40. Unfortunately, the undesired epimer at C16 was observed and attempts to epimerize this position resulted in a ratio of 85:15 of the undesired to the desired diastereomer. van Tamalen and Oliver then referred to two different degradation studies of the natural product and stated that intermediate **2-41** has previously been elaborated to ajmaline.[78,79] This route was particularly inefficient, as it requires 12 steps to afford one of their intermediates and the key cyclization step is quite low yielding (18%). According to the degradation studies it takes at least seven steps to transform aldehyde **2-41** to the natural product.

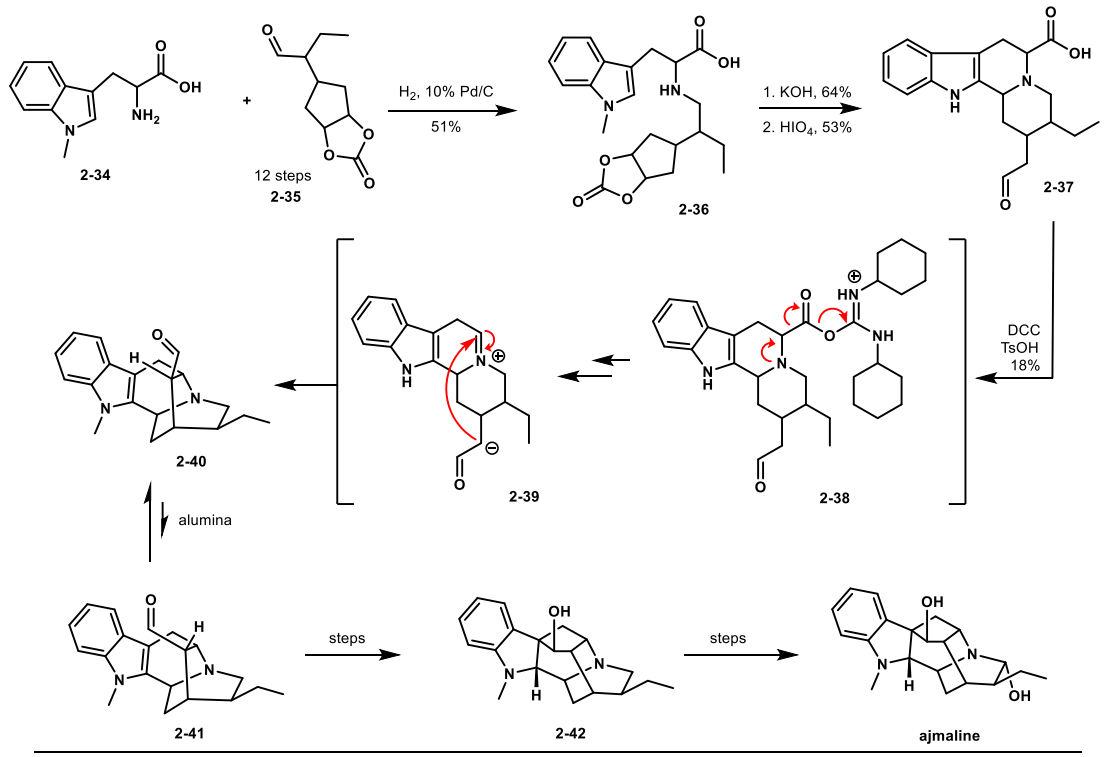

Scheme 2.7. van Tamelen and Oliver's synthesis of ajmaline

About three decades later, Cook and coauthors reported an enantioselective synthesis of ajmaline starting from tryptophan.[15] Amine **2-43** was protected through a reductive amination and then a Pictet-Spengler cyclization afforded piperidine **2-44**. Similar to Mashimo's synthesis, di-ester **2-44** was treated with NaH to promote a Dieckmann cyclization. A hydrolysis and decarbonylation furnished ketone **2-45**. This ketone was elaborated to aldehyde **2-46** in six steps. Next, a hydrogenation removed the amine protecting group and promoted a reductive amination

to close the D ring of the natural product. Closure of the final ring was accomplished similar to the previous syntheses by treating the protected aldehyde under acidic conditions; two additional steps afforded the natural product.

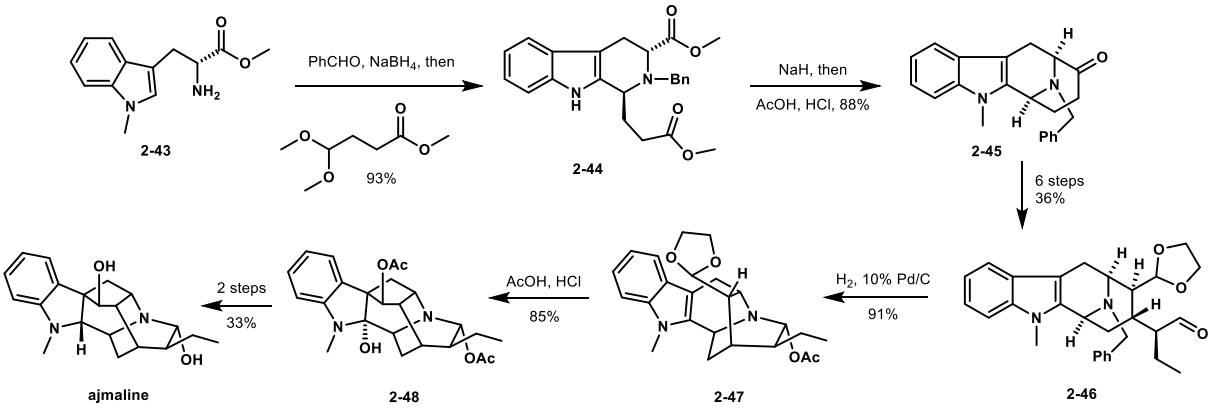

Scheme 2.8. Cook and coauthors' synthesis of ajmaline

2.1.4 Total synthesis of cyclohepta[*b*]indole natural products – actinophyllic acid

The isolation of actinophyllic acid was reported in 2005.[80] The unique carbon skeleton and its interesting bioactivity inspired many total syntheses since the initial report. In 2008, the Overman group reported the first racemic total synthesis.[81] One year later, Overman confirmed the absolute configuration after a series of experimental and theoretical experiments.[82] In 2010, the same group reported the first enantioselective synthesis of actinophyllic acid (Scheme 2.9).[19]

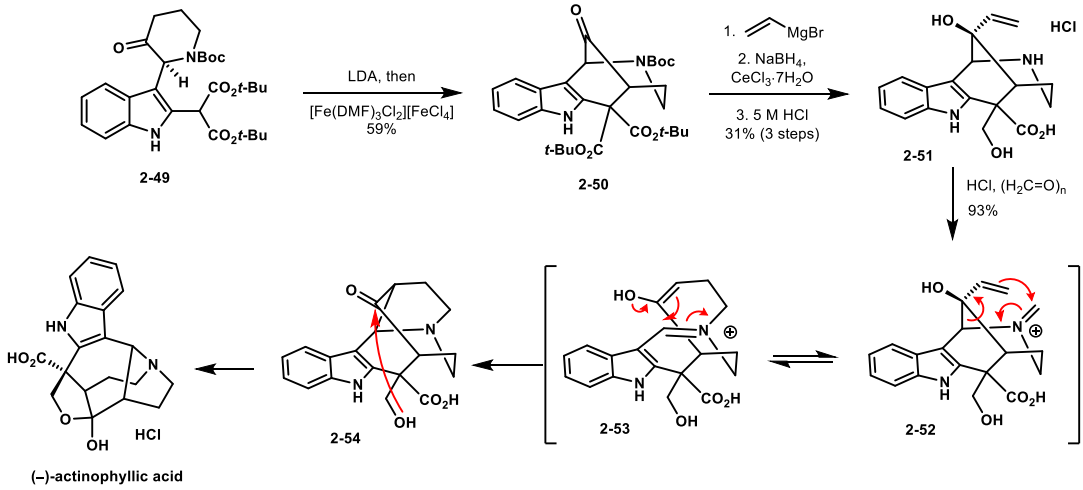

Scheme 2.9. Overman's enantioselective synthesis of actinophyllic acid featuring an aza-cpoe mannich cyclization

Indole **2-49** was prepared in seven steps from a commercially available amino acid derivative. An oxidative dienolate coupling was performed on the diester **2-49** to furnish tetracycle **2-50**. A Grignard addition, Luche reduction, and hydrolysis afforded the precursor to the key step in the synthesis, indole **2-51**. Condensation of formaldehyde onto the amine furnished intermediate **2-52** which was primed for an aza-Cope rearrangement. The resulting enol could then undergo a Mannich cyclization to yield ketone **2-54**, which spontaneously forms the lactol of the natural product. This impressive aza-Cope, Mannich cascade efficiently forged the natural product in just 12 steps from commercial materials.

In 2013, Martin reported a racemic synthesis of actinophyllic acid featuring a key cyclization cascade to form the cyclohepta[*b*]indole core.[19] Indole **2-55** was prepared in five transformations from indole, and silyl enol ether **2-56** was prepared in two steps from a commercially available enone. Upon treatment of the mixture with TMSOTf and 2,6-di-*t*-butylpyridine, carbocation **2-57** was quenched by the silyl enol ether to furnish iminium ion **2-58**. Cyclization of the indole onto the iminium afforded amine **2-59** in excellent yields. In just one step the tetracyclic core was formed and it was easily elaborated to the natural product in just six steps.

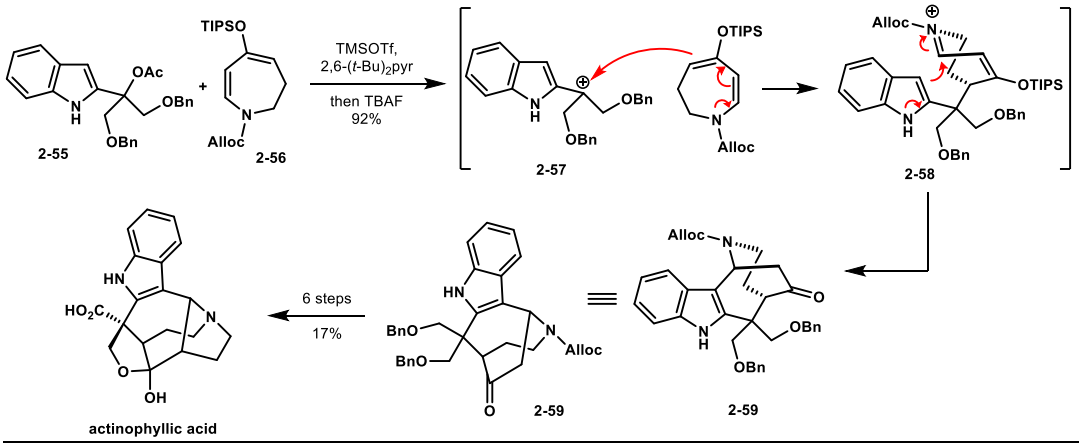

Scheme 2.10. Martin's racemic synthesis of actinophyllic acid

The next synthesis of actinophyllic acid was reported in 2016 by the Kwon group.[21] To set the initial stereochemistry in their sequence, the authors exploited an enantioselective phosphine

catalyzed [3+2] annulation. Addition of phosphine catalyst **2-62** in the presence of (*R*)- or (*S*)-BINOL, to iminium **2-60** and allene **2-61** cleanly yielded the desired pyrrolidine in a near quantitative yield with great enantioselectivity. This pyrrolidine was elaborated to indole **2-63**, which when treated with CuI cyclized to the desired seven-membered ring. Swapping the benzyl ester to the chloromethyl ester allowed for another cyclization to occur to furnish keto-ester **2-67**. A pinacol coupling of the ketone and ester closed the last of the rings of the natural product and furnished hemiacetal **2-68**. A three step dehydroxylation of the tertiary alcohol yielded actinophyllic acid.

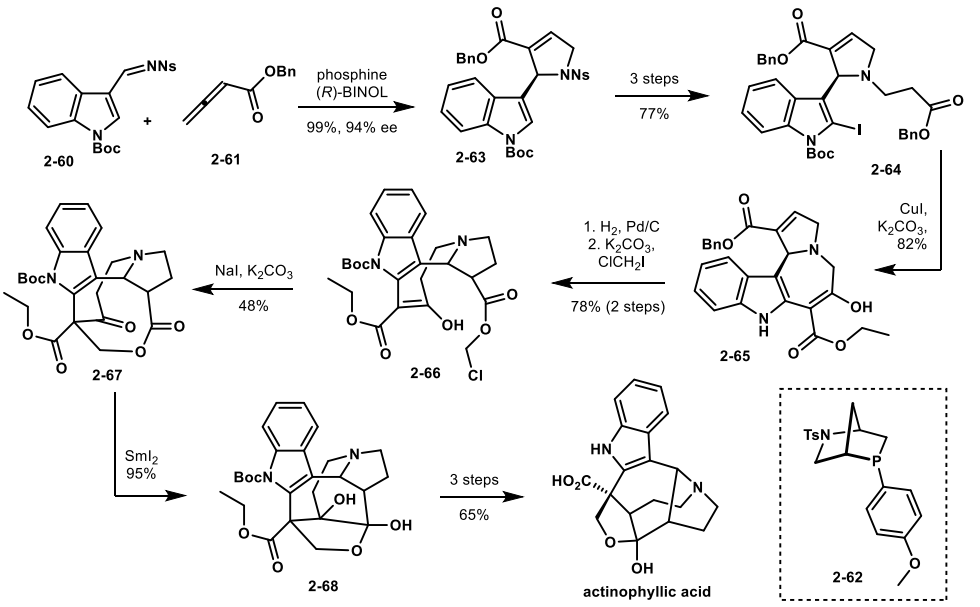

Scheme 2.11. Kwon's synthesis of actinophyllic acid

The most recent synthesis of actinophyllic acid was reported by the Chen group in 2017.[20] In a novel approach to the natural product they envisioned a desymmetrization route, which would begin from the meso compound trienone **2-69**. An initial regioselective dihydroxylation resulted in diol **2-70**. The diol was oxidatively cleaved and in the same pot, a reductive amination afforded amine **2-71**. The key desymmetrization event was then employed. Dibromooxime formed bromonitrileoxide *in situ* which performed a regioselective [3+2] cycloaddition to furnish isooxazoline **2-72** as a single stereoisomer. The remaining alkene was then poised for an

aminoarylation to input the carbons needed for the indole and close the caged structure. A palladium catalyzed hydrogenation furnished the desired indole **2-74**. The enol of ester **2-74** accomplished an aldol addition with formaldehyde which was followed by a lactolization to yield actinophyllic acid.

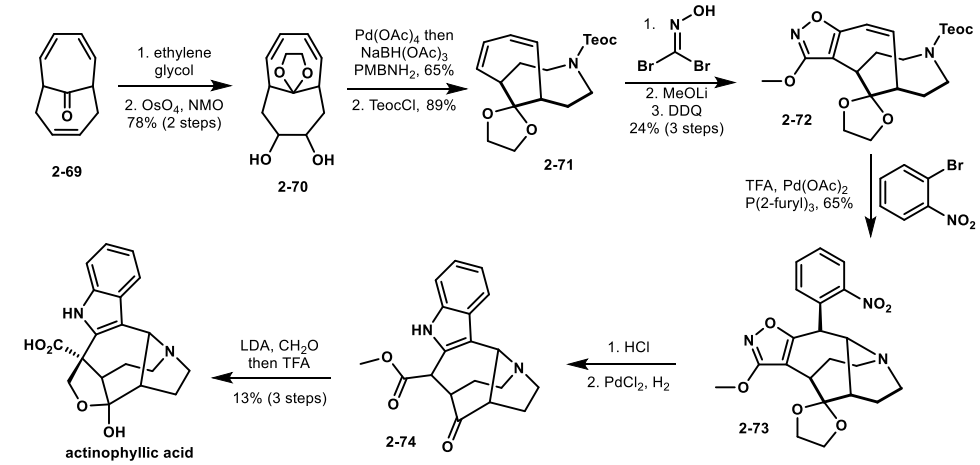

Scheme 2.12. Chen's synthesis of actinophyllic acid

2.1.5 Total synthesis of cyclohepta[*b*]indole natural products – aristolasene

Aristolasol and aristolasene were isolated as two minor alkaloids from *Aristotelia australasica*, a shrub found in New South Wales, Australia.[83] One total synthesis of aristolasene was reported in 1992 from the Borschberg group (Scheme 2.13).[84] The synthesis began with (*S*)-perilla alcohol, and through a series of simple transformations amine **2-75** was obtained.[85] The thiol was required in place of the alcohol for the cyclization step to occur; the cyclization was unsuccessful with the protected alcohol equivalent. The amine was condensed onto protected indole **2-76**, and intermediate **2-77** then cyclized to piperidine **2-78**. In seven steps the thiol was converted to an aldehyde and the indole protecting group was removed (MPS = *p*-methoxybenzyl sulfonate) to produce **2-79**. The final cyclization was promoted with TsOH and trimethylorthoformate to close the cycloheptane ring and forge the natural product in modest yield.

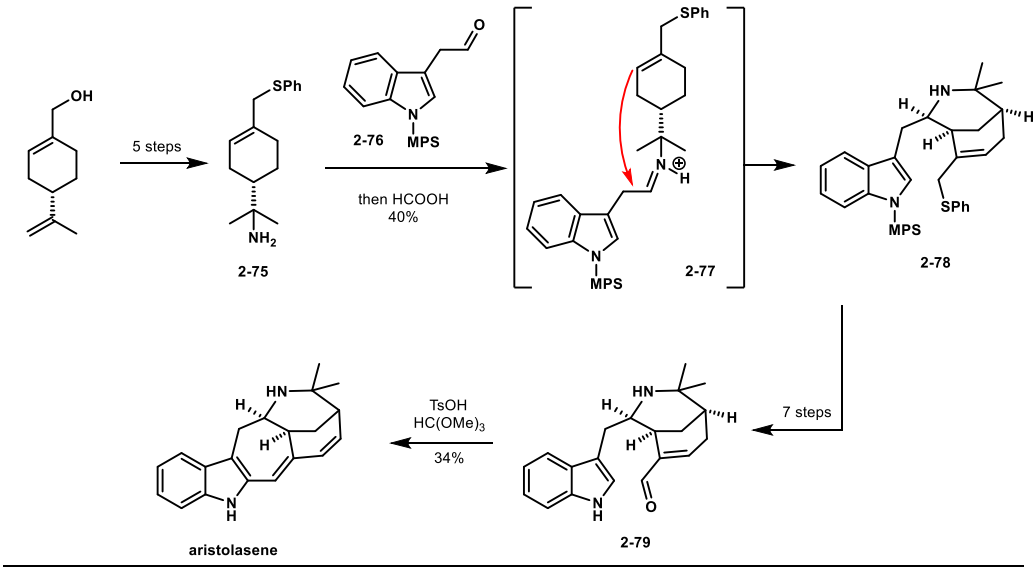

Scheme 2.13. Borschberg group's synthesis of aristolasene

2.1.6 Total synthesis of cyclohepta[*b*]indole natural products – caulersin

Caulersine is a highly conjugated bisindole natural product that was isolated from the algea *Caulerpa serrulate.*[26] The cyclohepta[*b*]indole was found to inhibit plant growth. Three total syntheses of caulersine have been reported to date. Each synthesis used a bisindole intermediate and closed the cycloheptene ring as one of the final steps. The first reported synthesis, Scheme 2.14a, closed the ring through a displacement of the chlorine with the enolate of methyl ketone **2-80**.[86] The final alkene was installed through an oxidation and the resulting methyl ketone was converted to the methyl ester.

The second synthesis reported employed the Vilsmeier reagent to engage the cyclization.[87] Initial addition of the reagent to the ketone after deprotonation at the ester α-carbon resulted in intermediate **2-83**.[88] An additional equivalent of the Vilsmeier reagent was then displaced to input the final carbon of the cycloheptane ring (between the α-ester carbon and the indole C3 carbon) to afford vinyl chloride **2-84**, which was hydrolyzed to the desired ketone.

The Miki synthesis employed a simple aldol condensation with aldehyde **2-85** to forge the triene.[89] The natural product can then be obtained after deprotection of the indoles.

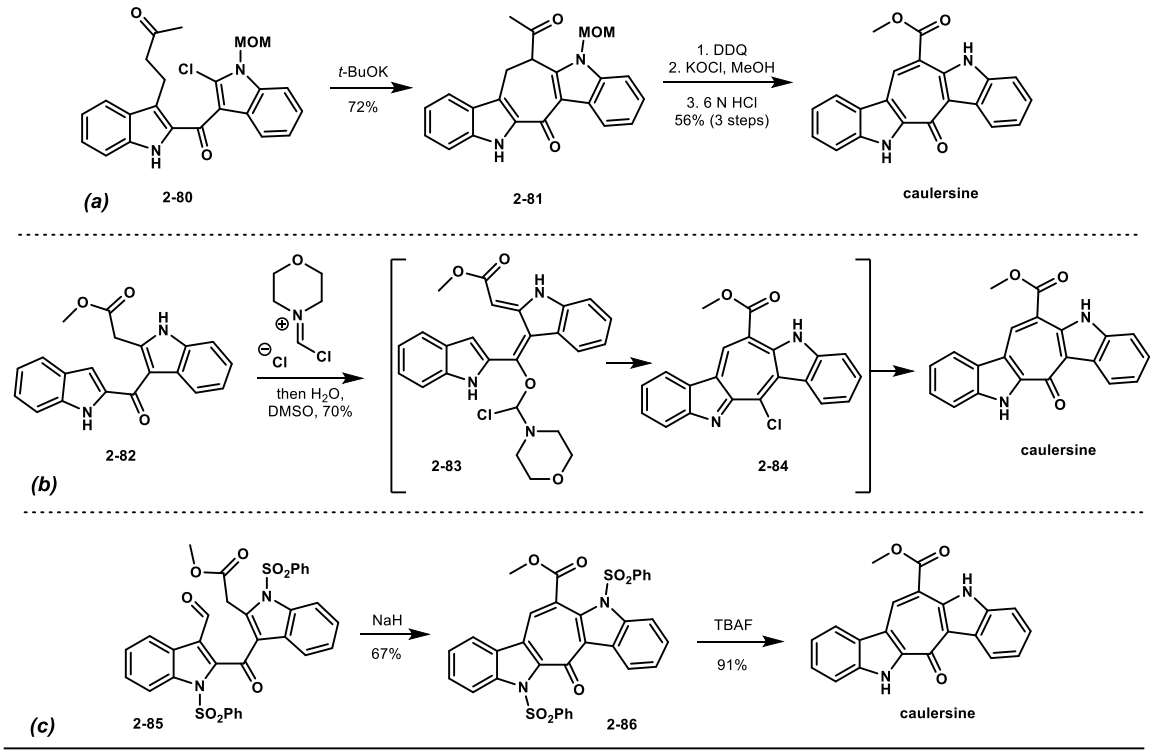

Scheme 2.14 (a) Synthesis of caulersine by the Molina group ***(b)*** Synthesis of caulersine by the Bergman group ***(c)*** Synthesis of caulersine by the Miki group

2.1.7 Total synthesis of cyclohepta[*b*]indole natural products – arcyriacyanin A

Arcyriacyanin A is an unsymmetrical bisindole that is highly conjugated and was isolated from the slime mold, *Arcyria abvelata*.[28] It was found to inhibit protein kinase C and protein tyrosine kinase.[30] In 1997, the Steglich lab reported one route to arcyriacyanin A and two routes to *N*-methyl arcyriacyanin A (Scheme 2.15).[90] 3,4-Dibromomaleimide, **2-88**, was added to the bisbromomagnesium salt of **2-87** to furnish arcyriacyanin A in 41% yield. The *N*-methyl derivative of the natural product was produced through a Heck cyclization of bisindole **2-89**, which was prepared in seven steps. The authors noted that *N*-methyl arcyriacyanin could be transformed into arcyriacyanin using standard methods, but did not report this step.

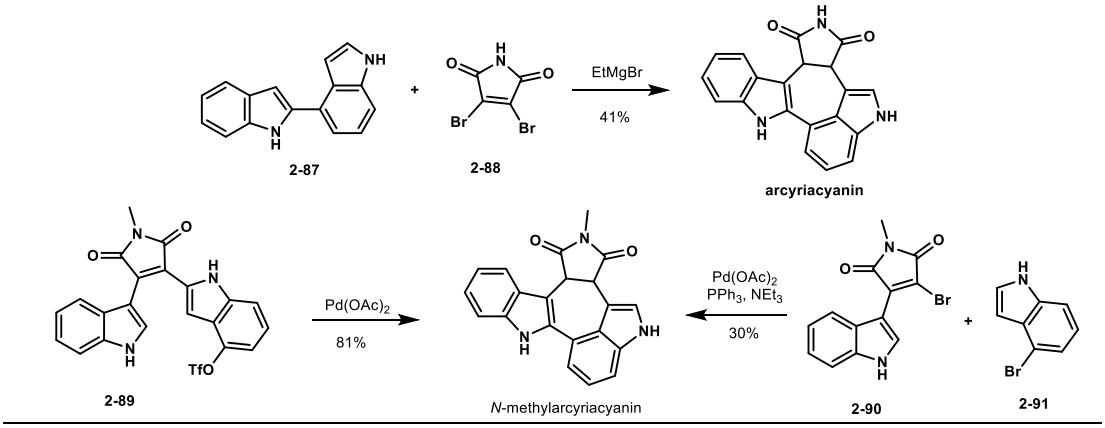

Scheme 2.15. Three approaches taken by the Steglich group to synthesize arcyriacyanin and *N*-methylarcyriacyanin

Finally, a domino Heck cyclization was employed with bromomaleimide **2-90** and bromoindole **2-91** to form the cycloheptane ring of *N*-methyl arcyriacyanin. A few years later the Murase group also reported a synthesis of arcyriacyanin A that utilized an analogous addition of bisindole **2-87** to maleimide **2-88**.[91,25]

2.1.8 Total synthesis of cyclohepta[*b*]indole natural products – ervatamine and ervitsine alkaloids

The Bosch group has reported the only total syntheses of the large group of ervatamine and ervitsine alkaloids. These cyclohepta[*b*]indoles bear a piperidine ring fused with the cycloheptane ring and do not contain the more alkaloid like tryptamine derivation (Figure 2.2). The group's first synthesis of this class of alkaloids was reported in 1996 (Scheme 2.16a).[92] The enolate of indole **2-92** was added to pyridinium salt **2-93** and the resulting dihydropyridine was trapped with an anhydride to add in the final carbon needed for the carbon skeleton of the natural product. The methyl ester **2-94** was hydrogenated to take the α,β-γ,δ ester to the fully saturated ester, which was then treated with trimethylsilyl polyphosphate (PPSE) to promote the ring closure. Diketone **2-95** was taken onto 6-oxo-16-episilicine in five additional steps.

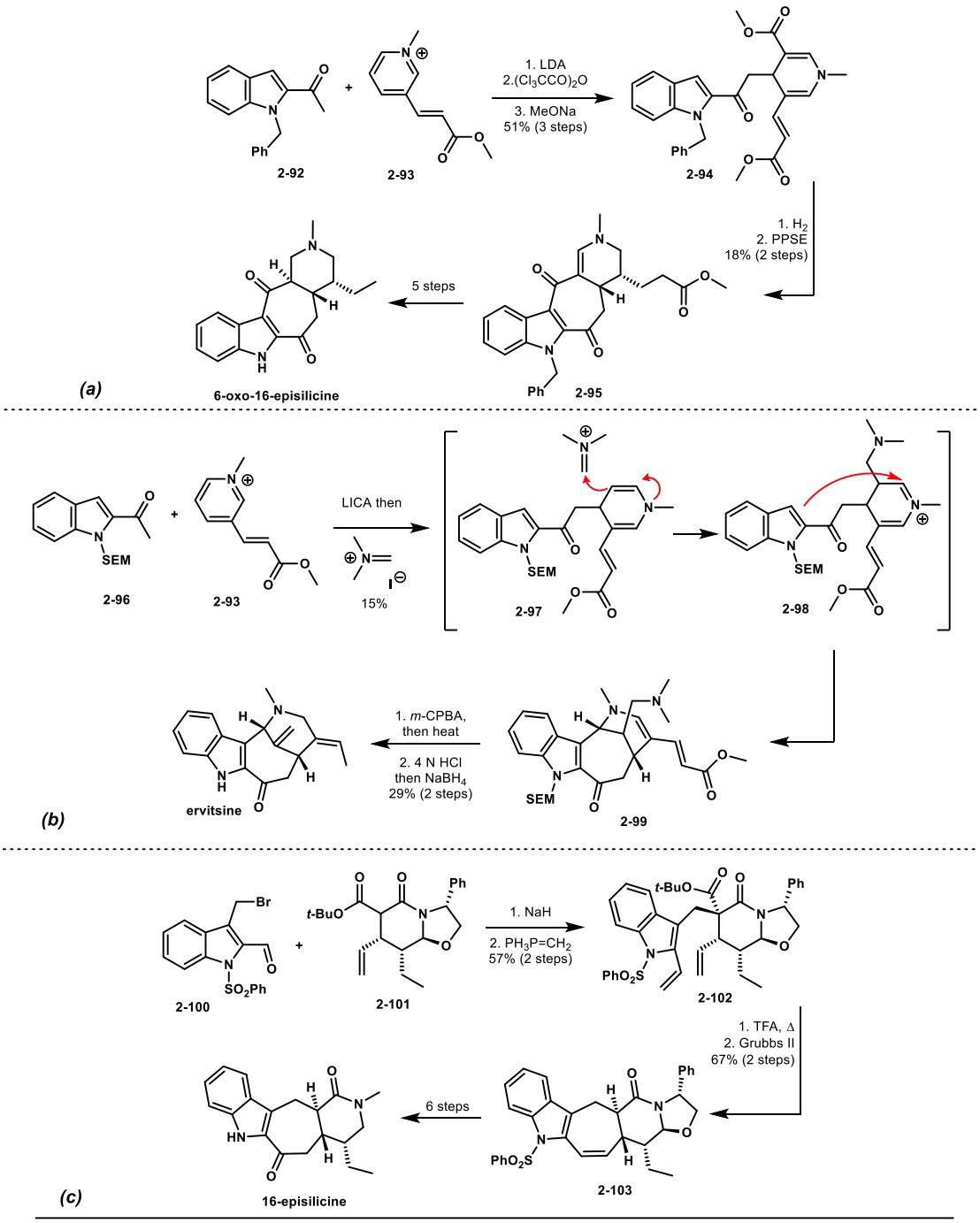

Scheme 2.16 (a) Synthesis of 6-oxo-16-episilicine ***(b)*** Synthesis of ervitsine ***(c)*** Synthesis of 16-episilicine

One year later the same group reported the synthesis of ervitisine, and implemented similar chemistry (Scheme 2.16b).[93] The enolate of indole **2-96** was added to pyridinium salt **2-93**, but in this case the dihydropyridine intermediate **2-97** was captured with Eschenmoser's salt. The indole was closed onto the iminium ion to forge tetracycle **2-99** in low yields (LICA = lithium

isopropoylcyclohexylamine). A Cope elimination of the tertiary amine furnished the exocyclic alkene and elimination of the ester group completed the synthesis.

In 2010 the Bosch group reported an enantioselective synthesis of 16-episilicine, which envisioned a new disconnection (Scheme 2.16c).[94] The highly decorated lactam **2-101** was previously synthesized[95] by the group starting from an unnatural amino acid. The β-keto ester **2-101** was alkylated with indole **2-100** and the aldehyde was subsequently methylenated to the corresponding alkene, **2-102**. Hydrolysis and decarboxylation of the ester followed by a ring closing metathesis (RCM) resulted in cycloheptene **2-103**. The natural product was obtained in six steps from this intermediate. This was the first synthesis of the cyclohepta[*b*]indoles that employed an RCM to close the seven-membered ring.

2.1.9 Total synthesis of cyclohepta[*b*]indole natural products – exotine A and B

Exotine A and B are cyclohepta[*b*]indoles that bear a coumarin moiety on the cycloheptane ring. This unusual structure was synthesized in one step by the Martin group utilizing a three-component formal [4+3] addition.[96] The proposed mechanism for the transformation is shown in Scheme 2.17.

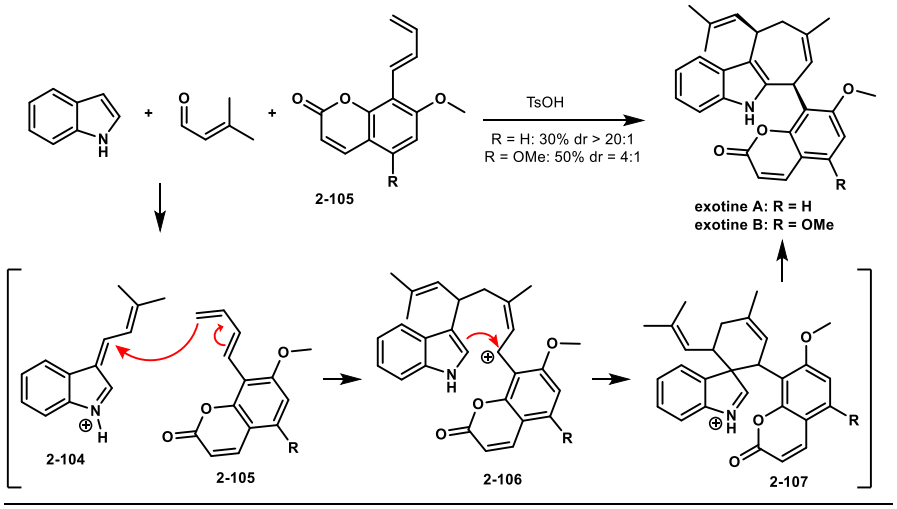

Scheme 2.17. Synthesis of exotines A and B through a one-step, biomimetic procedure

Prenyl aldehyde condensed onto indole to afford the highly electrophilic iminium ion **2-104**. The diene of coumarin **2-105** added into iminium ion **2-104** to form benzylic carbocation **2-106**, which was captured with the indole to form spirocycle **2-107**. A 1,2 shift, then resulted in the two natural products in modest yields. A synthesis of exotine B was also reported by Trauner.[97]

2.1.10 Total synthesis of cyclohepta[*b*]indole natural products – ambiguines

The ambiguines make up a large portion of the cyclohepta[*b*]indole natural products, and display a wide variety of biological activities.[34,37] In 2019 both the Sarpong group and the Rawal group reported total syntheses of ambiguine P (Scheme 2.18). They implemented similar chemistry to make the core of the pentacycle. The Sarpong synthesis began with an oxidative coupling between indole and (*S*)-carvone.[98,99] An alkynylation followed by a Dauben-Michno oxidative rearrangement[100] resulted in enyne **2-108**. An intramolecular Nicolas reaction prompted reactivity at the indole C2 position to close the cycloheptane ring. The resulting cobalt complex **2-109** was not cleaved in order to protect the latent alkene. The final ring of the core was closed through a Friedel-Crafts alkylation at the C4 of the indole furnishing pentacycle **2-110**.

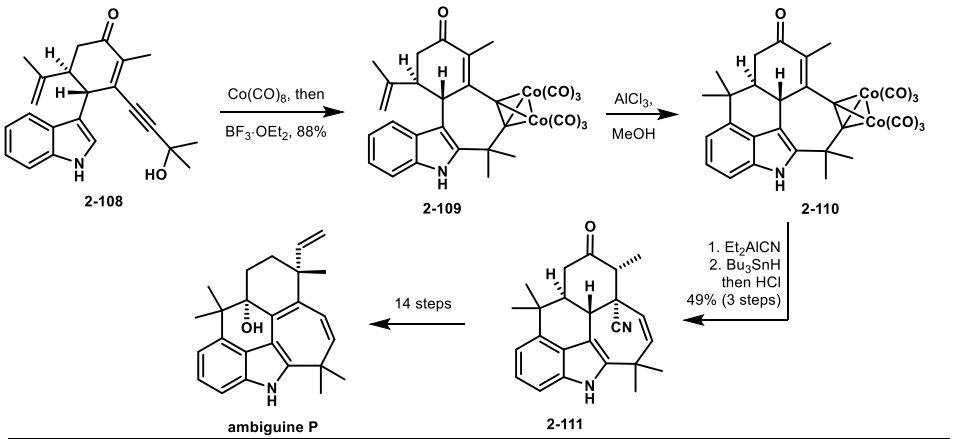

Scheme 2.18. Synthesis of ambiguine P by the Sarpong group

A conjugate addition with Nagata's reagent installed a nitrile group that would later be used as a handle to install the quaternary center and the final alkene of the cyclohepatriene. The cobalt complex was then removed with tributyltin hydride and acid to afford diene **2-111**. An

additional 14 steps were required to set the quaternary center, remove the ketone, and install the final alkene and alcohol moieties.

Shortly thereafter, the Rawal group reported their synthesis of ambiguine P (Scheme 2.19).[101] Instead of setting the quaternary center in the later stages of the synthesis, the authors began with diene **2-112** which already had the quaternary center installed. They envisioned a [4+3] cycloaddition to install the cycloheptane ring, however, when they treated diene **2-112** and indole **2-113**, they only observed partial addition to produce enone **2-114**.

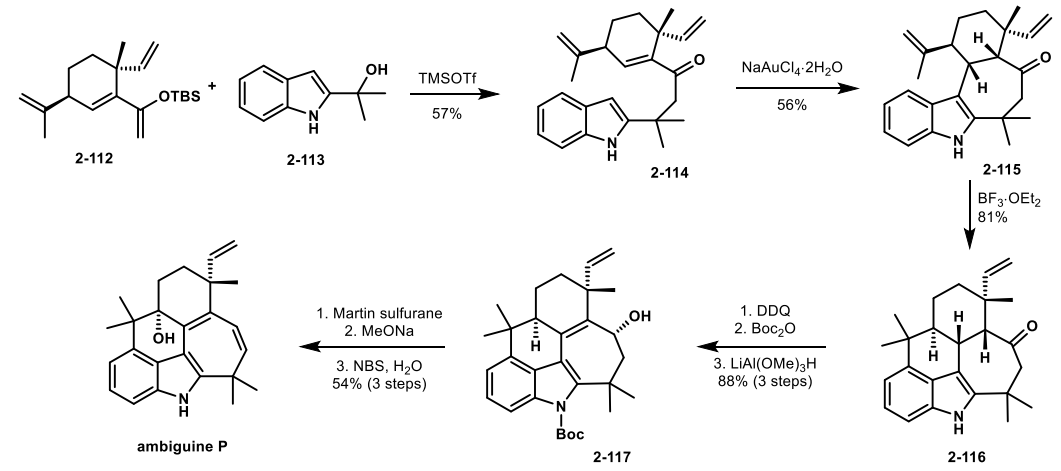

Scheme 2.19. Synthesis of ambiguine P by the Rawal group

To promote reactivity at the indole C3 and to finish the step-wise [4+3], the enone was treated with gold salts to close the tetracycle. Similar to Sarpong, a Friedel-Crafts alkylation at the C4 of the indole closed the final ring of the core. Ketone **2-116** was oxidized to the corresponding enone and then reduced to allylic alcohol **2-117**. The natural product was obtained after a dehydration, deprotection, and allylic oxidation.

The Rawal group has also reported a total synthesis of ambiguine G, which contains the same core but it is decorated with additional functionalization around the pentacycle.[102] The authors used the same approach to make the core as was implemented in their synthesis of

ambiguine P. The synthesis began with a [4+3] cycloaddition of diene **2-118** with indole **2-119**. A Friedel-Crafts alkylation forged the final ring of the core.

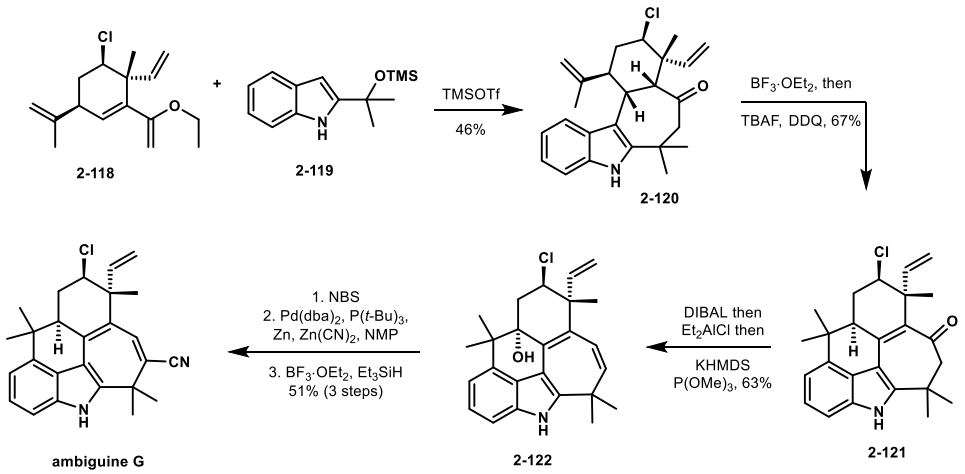

Scheme 2.20. Synthesis of ambiguine G by the Rawal group

This route was an expedient route to the core of these cyclohepta[*b*]indoles. In the same pot as the Friedel-Crafts, the Lewis acid was quenched with TBAF and an oxidation of the ketone successfully furnished enone **2-121**. The ketone was then reduced and eliminated to the corresponding alkene. The C15 carbon was extremely electron rich and therefore also needed to be protected to allow the nitrile that is present in the natural product to be installed. Therefore, in a single pot reaction, reduction, elimination, and air oxidation yielded alcohol **2-122**. Finally, the nitrile was installed and the alcohol was removed to afford ambiguine G.

2.1.11 Total synthesis of cyclohepta[*b*]indole natural products – kopsifolines

The kopsifolines were first isolated in 2004 and the cyclohepta[*b*]indole variants of this class are distinguished by the bridged hexacycle.[41] There have been a few syntheses of this class and each closes the final ring to form the cycloheptane in the late stages of the synthesis. In 2014 the Boger group reported a synthesis of kopsifoline D (Scheme 2.21).[103] They planned to assemble the natural product through a [4+2]–[3+2] cascade. Heating 1,3,4-oxadiazole **2-123** initiated a [4+2] with the appending alkene to furnish cycloaddition adduct **2-124**. After loss of N_2,

zwitterion **2-125** underwent a [3+2] cycloaddition with the indole to furnish the pentacyclic ring system **2-126** in good yields. Elaboration of the lactam to alkyl iodide **2-127** was accomplished in nine steps. Indole deprotection and a subsequent transannular ring closure forged the final ring to afford kopsifoline D.

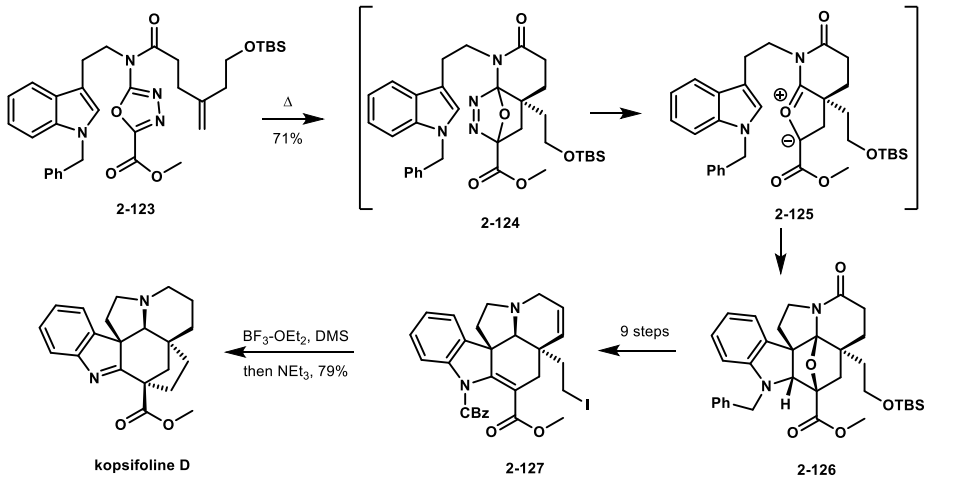

Scheme 2.21. Synthesis of kopsifoline D by the Boger group

Recently, the Movassaghi group reported the syntheses of three of the kopsifoline natural products.[104] The known tetracycle **2-128** was reduced to the corresponding hemiaminal and a transannular ring closure formed the pentacyclic ring system. Installation of the ester group furnished indole **2-129**. Kopsifiline D was completed by desilylation and an intramolecular Mitsunobu with DIA (diisopropyl azodicarboxylate) and triphenylphosphine.

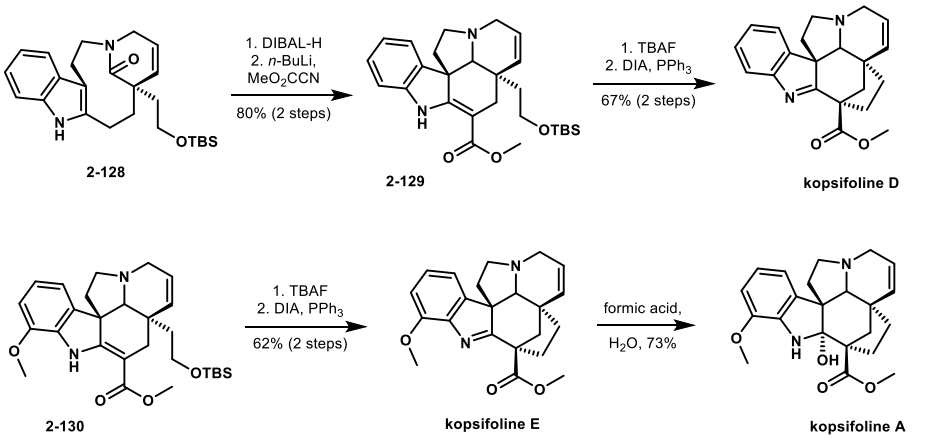

Scheme 2.22. Synthesis of three kopsifolines by the Movassaghi group

Kopsifiline A and E were also targeted. Pentacycle **2-130** was synthesized similarly to **2-129**, and the same two step sequence was implemented to afford kopsifiline E. Hydration of the indole under acidic conditions converted kopsifiline E to A in good yields.

2.2 Work towards the synthesis of alstonlarsine A

2.2.1 Introduction

Alstonlarsine A is a cyclohepta[*b*]indole that was reported in 2019 and was isolated from the roots and bark of *Alstonia scholaris*.[42] It contains a unique 9-azatricyclo[4.3.1.$0^{3,8}$] decane core and the structure was determined with NMR and X-ray crystallography. The proposed biosynthetic synthesis is shown in Scheme 2.23. The biosysnthesis was proposed to begin with *N*-demethylalstogustine, which is a monoterpene indole alkaloid that has been found in large quantities in *Alstonia scholaris*.[42,105] A dehydration and oxidation afforded allylic alcohol **2-131**, which can undergo a ring cleavage to **2-132**. Another oxidation event and *N*-methylation resulted in hemiaminal **2-133**, which dehydrates to iminium ion **2-134**. Addition of H_2O and a Mannich type addition closed the caged structure to **2-135**. The alcohol was then oxidized to β-keto acid **2-136**. A decarboxylation afforded enol **2-137**, which was methylated with *S*-adenosylmethionine (Ad = adenosine) to furnish alstonlarsine A.

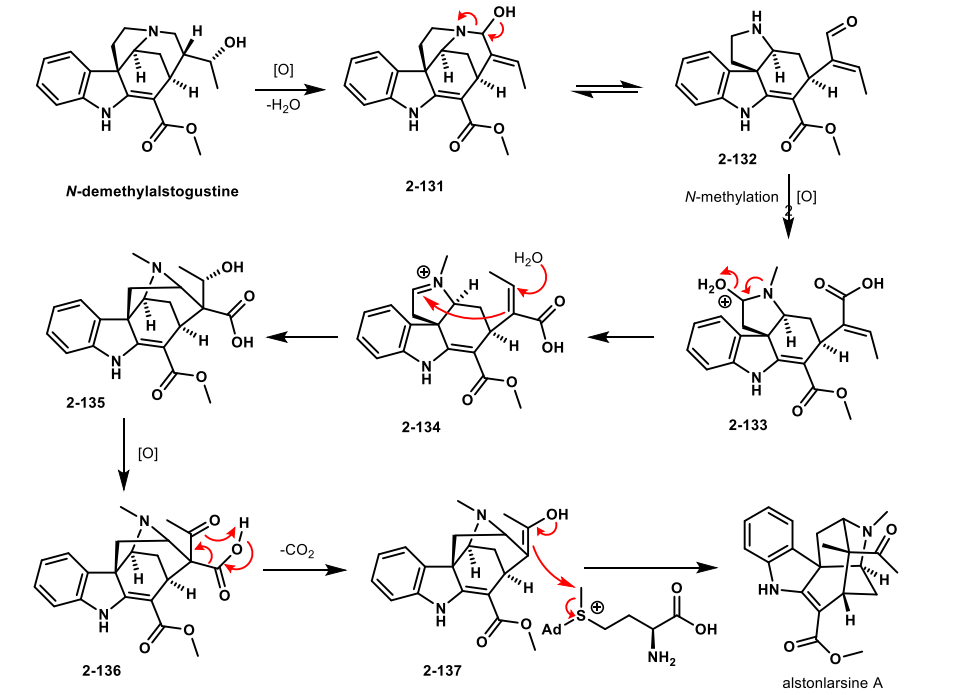

Scheme 2.23. Proposed biosynthetic pathway of alstonlarsine A

The indole alkaloid was tested for its inhibitory effects against DAP kinase-related apoptosis protein kinase-2 (DRAK2). DRAK2 is a protein kinase that is required for initiating and inducing programmed cell death. Alstonlarsine A was found to have an IC_{50} value of 11.65 ± 0.63 μM against DRAK2. The natural product was only examined for this inhibitory affect, but monoterpene indole alkaloids have a wide range of biological activity. Our lab set out to synthesize alstonlarsine A due to its interesting structure and to examine additional biological activities.

2.2.2 First generation route to alstonlarsine A

This initial route was a collaboration between myself and Dr. Sunshine Burns. Our initial retrosynthetic analysis is shown in Scheme 2.24. We planned to install the quaternary center in the late stages of the synthesis from ketone **2-138**. The core of the structure was planned to be set during an intramolecular Diels-Alder from triene **2-139**. The cycloheptene ring was planned to be forged through a gold catalyzed annulation of ynone **2-140**, which is easily accessible from tryptophan.

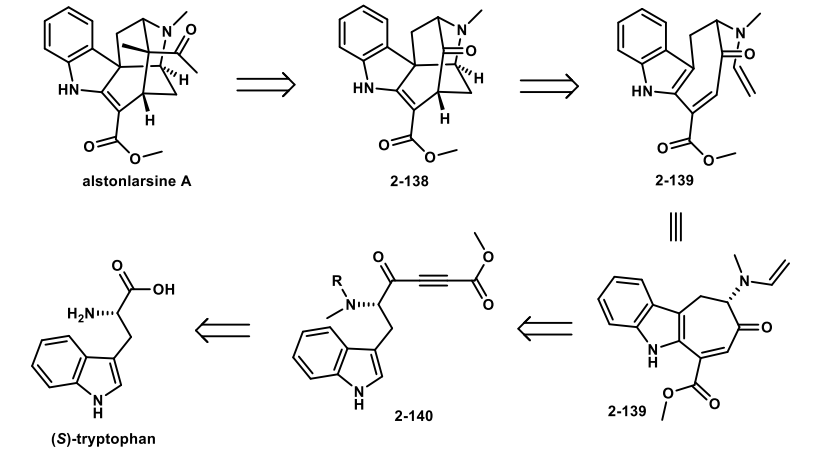

Scheme 2.24. Initial retrosynthetic analysis of alstonlarsine A

In the forward direction, Sunshine prepared ynone **2-143** from Boc-(*S*)-tryptophan in four steps, Scheme 2.25. The acid was esterified to the Weinreb amide and the indole was protected with TBS to furnish amide **2-141**. The amine was methylated and the lithiated alkyne **2-142** was

added into the Weinreb amide to afford ynone **2-143**. Attempts to alkylate with an alkyne bearing an ester group were unfruitful. We next examined the cyclization of the ynone to the cycloheptene ring. The cyclization was modeled after a gold catalyzed ynone annulation that was reported by the Carbery group.[106]

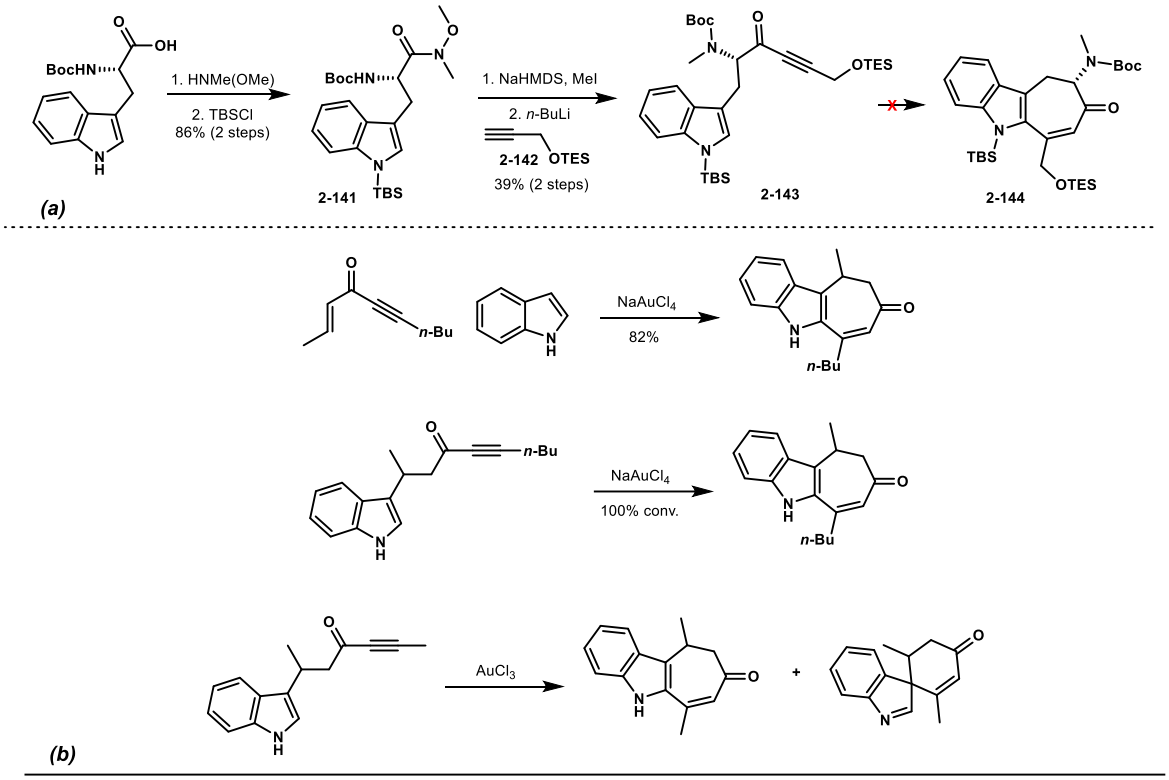

Scheme 2.25 (a) Ynone synthesis and attempted annulation
(b) Double gold-catalyzed annulation of ynones onto indoles (ref 106)

When subjecting ynone **2-143** to gold salts under heat, only decomposition was observed. At room temperature, no reaction was observed. Longer reaction times at room temperature resulted in cleavage of the TES protecting group. It was postulated that there was too much steric bulk around the reactive site and so the indole protecting group was removed. The TES protecting group on the alcohol was swapped for the slightly more stable TBS group. Ynone **2-147** was prepared and subjected to the gold salts. No cyclization product was observed. However, when silver (I) salts were added a new product was observed, spirocycle **2-149**.

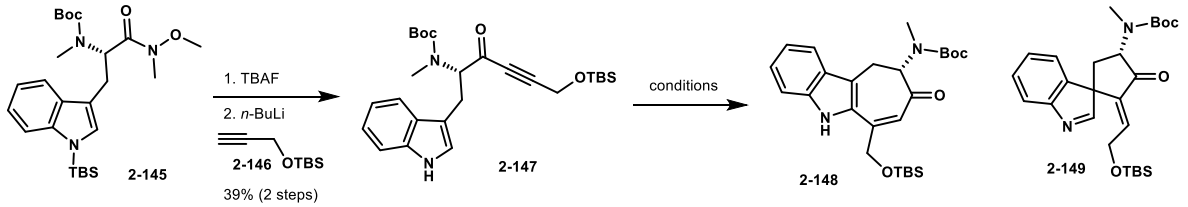

catalyst	solvent	result	catalyst	solvent	result
$AuCl_3$	CH_2Cl_2	**2-147**	Au(JohnPhos)Cl	CH_2Cl_2	**2-147**
$Au(PPh_3)Cl$	CH_2Cl_2	**2-147**	$Ag(CF_3CH_2COO)$	CH_2Cl_2	**2-149**
$Au[P(C_6F_5)_3]Cl$	CH_2Cl_2	**2-147**	$Ag(PF_6)$	CH_2Cl_2	**2-149**
$AuCl_3$	THF	**2-147**	$AgBF_4$	CH_2Cl_2	**2-149**
$Au(PPh_3)Cl$	THF	**2-147**	Ag(OTs)	CH_2Cl_2	**2-147**
$Au[P(C_6F_5)_3]Cl$	THF	**2-147**	$Sc(OTf)_3$	$CDCl_3$	**2-147**
$AuCl_3$/AgOTf	CH_2Cl_2	decomposition	AgOTf	MeCN	**2-147**
$Au(PPh_3)Cl$/AgOTf	CH_2Cl_2	**2-147**	AgOTf	toluene	**2-149**
$Au[P(C_6F_5)_3]Cl$/AgOTf	CH_2Cl_2	**2-149**	$Cu(OTf)_2$	CH_2Cl_2	**2-149**
$AuCl_3$/AgOTf	THF	decomposition	$Zn(OTf)_2$	CH_2Cl_2	**2-147**
$Au(PPh_3)Cl$/AgOTf	THF	decomposition	$FeCl_3$	CH_2Cl_2	**2-147**
$Au[P(C_6F_5)_3]Cl$/AgOTf	THF	decomposition	$Pd(OAc)_2$	CH_2Cl_2	**2-147**
$PtCl_4$	DMSO	**2-147**	$Y(OTf)_3$	CH_2Cl_2	**2-147**
$PtCl_4$	DMSO	decomposition	$Pt(en)_2Cl_2$	CH_2Cl_2	**2-147**
AgOTf	CH_2Cl_2	**2-149**	$[RuCl_2(p\text{-cymene})]_2$	CH_2Cl_2	**2-147**
$GaCl_3$	$CDCl_3$	**2-147**	$InBr_3$	CH_2Cl_2	**2-147**
$BF_3{\cdot}OEt_2$	CH_2Cl_2	**2-147**	$Hg(TFA)_2$	THF	**2-147**
$SnCl_4$	CH_2Cl_2	**2-147**			

Scheme 2.26. Lewis acid screen for annulation

Unfortunately, this could not be elaborated to the desired cycloheptene ring. An exhaustive screen of Lewis acids was performed, Scheme 2.27, but the only cyclization product observed was the exocyclic alkene. During this time Sunshine synthesized enone **2-150** and attempted an RCM to close the cycloheptane ring, but this was also unfruitful. At this point we considered other disconnections to the natural product.

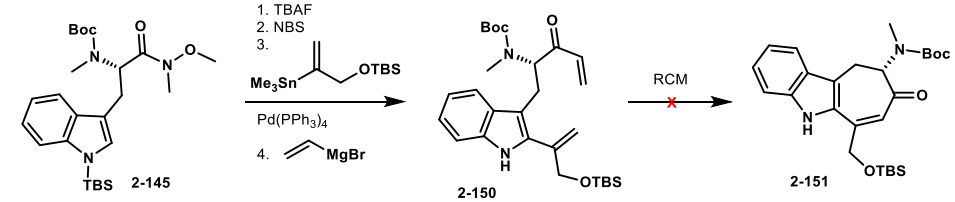

Scheme 2.27. Attempted RCM to close the cycloheptene ring

2.2.3 Second generation route to alstonlarsine A

In considering a new disconnection, we thought to set the quaternary center earlier in the sequence. Through retrosynthetic analysis we still planned to attempt the Diels-Alder reaction to forge the caged structure, but in this case, we would already have the quaternary center in place. We envisioned closing the cycloheptene ring through an asymmetric RCM from diene **2-153**, to close the ring and set the quaternary center in one step. The indole was envisioned to be closed through a Fukuyama annulation from aniline derivative **2-154**, which can be mapped back to the commercially available (*E*)-3-(2-nitrophenyl)acrylaldehyde.

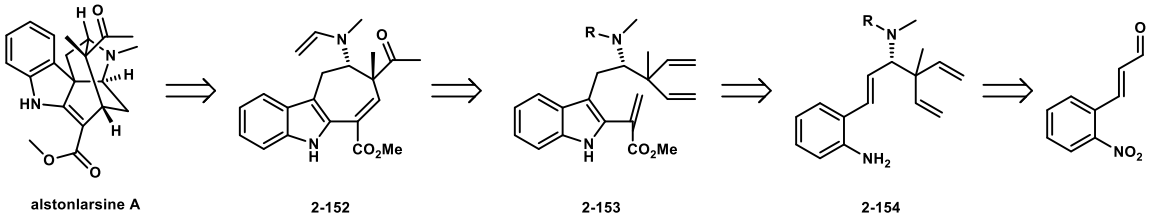

Scheme 2.28. Second retrosynthesis of alstonlarsine A

In the forward direction, amine **2-154** was targeted, starting from the commercially available aldehyde. There were many methods attempted to install a six carbon unit onto the aldehyde. The only successful route is shown in Scheme 2.29. The commercially available 3-methylpenta-1,4-diene was metallated and treated with an electrophilic boronate to afford allylic borane **2-155**. Upon treatment of the borane with 3-(2-nitrophenyl)acrylaldehyde, exclusive formation of the skipped diene **2-156** was observed, and a simple oxidation of the alcohol to the ketone afforded enone **2-157**. The low yield observed for this sequence was a result of the low yield in the boronation step. Attempts to perform an enantioselective reductive amination on enone **2-157** resulted in either no reaction or decomposition. Iminium formation was also investigated and was unsuccessful. This route was not explored further because of the problematic amination, the low yielding boronation, and the skipped diene starting material was quite expensive. Due to these difficulties a new route to the natural product was explored.

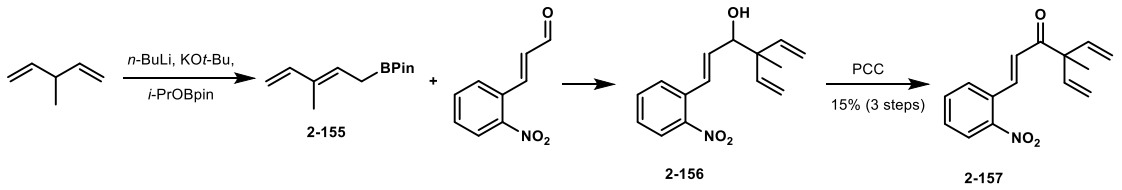

Scheme 2.29. Synthesis of enone for reductive amination

2.2.4 Third generation route to alstonlarsine A

Due to the difficulties in forming the cycloheptene early in the sequence, we instead envisioned forming the 6-5 ring system first and then closing the caged structure. Our third retrosynthetic analysis is shown in Scheme 2.30. We sought to form the indole late in the synthesis from the corresponding ketone and aryl amine. The quaternary center was envisioned also to be set late stage from an alkylation of the methyl ketone, which could arise from alkene **2-158**. The seven-membered ring was envisioned to be closed through an intramolecular Sakurai addition of allylic silane **2-159**, which can be mapped back to ketone **2-160**. This ketone was planned to be made through an aza-Cope rearrangement from allylic alcohol **2-161** and formaldehyde.

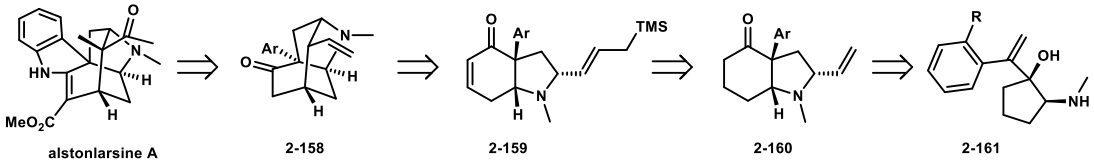

Scheme 2.30. Third retrosynthesis of alstonlarsine A with a Sakurai addition proposed to close the caged structure

To make the amino alcohol, we started from cyclopentene oxide and opened the epoxide with dimethylamine. The corresponding alcohol could be oxidized and then addition of the aryl group to the ketone afforded a 9:1 mixture of *cis*:*trans* amino alcohol **2-164**. The phenyl group was used as a model system in place of the planned ortho-nitro vinyl bromide coupling partner. Unfortunately, demethylation of the amine was unsuccessful. The benzyl protected amine **2-166** was also synthesized but could not be deprotected in the presence of the alkene.

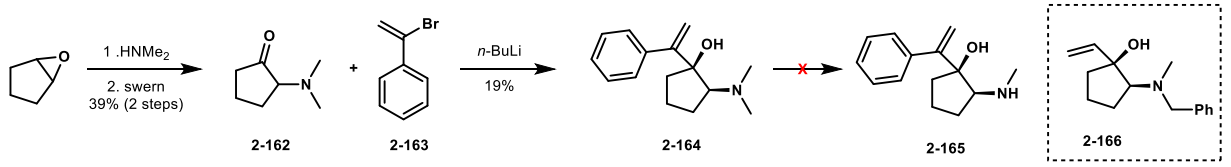

Scheme 2.31. Attempts to make the aza-Cope prescursor

Alternatively, we envisioned that synthon **2-158** could be made through a Sakurai addition in the other direction from the allylic silane into the imine of **2-167**. This would simplify the synthesis of the bicycle, as the ketone **2-168** (with the othro-nitro benzyl as Ar) is a known intermediate.

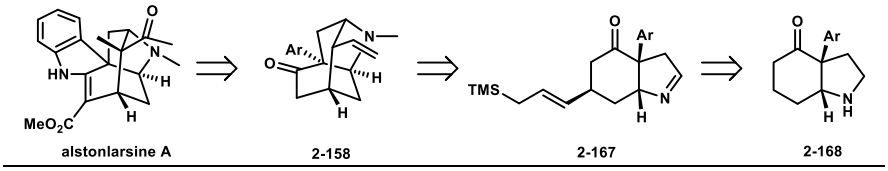

Scheme 2.32. Retrosynthetic analysis with a new proposed Sakurai addition

The synthesis of this fragment began from 1,3-cyclohexanedione. A three step sequence was utilized to make alkene **2-169**: *C*-alkylation of the diketone with the commercially available aryl iodide, followed by *O*-allylation with allyl bromide resulted in an intermediate that was heated to effect a Claisen rearrangement forming **2-169**.[107] The resulting alkene was ozonolyzed to the corresponding aldehyde and a reductive amination with methylamine afforded a diastereomeric mixture of bicycles **2-170** and **2-171**. Unfortunately, the ratio was not in our favor; a 2:1 mixture of *trans*:*cis* was observed. A large screening of reductants and amine sources was performed and the ratio did not improve.

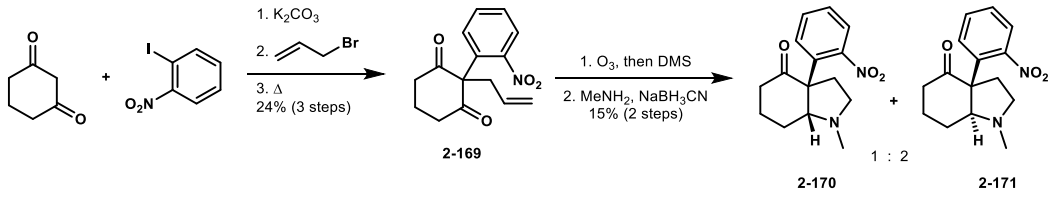

Scheme 2.33. Synthesis of known bicycle

In an attempt to correct the stereochemistry of the mixture and funnel the mixture to the desired *cis* conformation, the amine was oxidized to the *N*-oxide **2-172** and eliminated to the corresponding iminium. The reductant shown in Scheme 2.34 has been shown to reduce the mixture to the desired *cis* conformation, but when we applied it, we only observed the undesired *trans* conformation.[108]

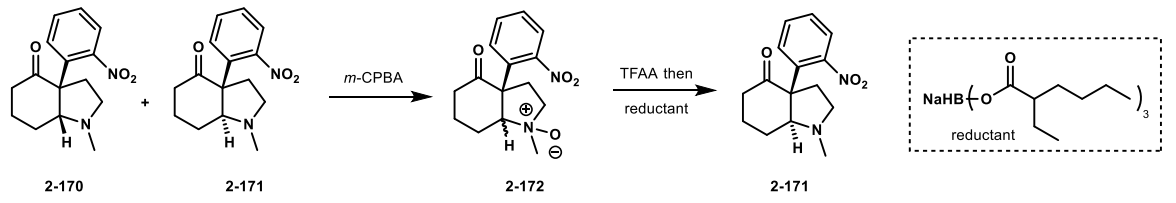

Scheme 2.34. Attempt to funnel diastereomeric mixture to the desired *cis* conformation, but only afforded the *trans*

Alternative approaches to the bicycle are shown in Scheme 2.35. We envisioned incorporating the ethylamine fragment as one unit of the bicycle to favor the desired *cis* product. First an aza-Michael alkylation cascade from enone **2-173** with Boc protected 2-chloroethan-1-amine was attempted but only resulted in recovered starting material. Vinyl aziridine **2-176** was synthesized and a ring expansion to the bicycle was attempted. Treating the aziridine with iodide, which has been reported on a similar substrate,[109] only resulted in ring opening of the aziridine. It was that this point we decided to pause the project as many approaches to the natural product were taken, but none have been successful so far.

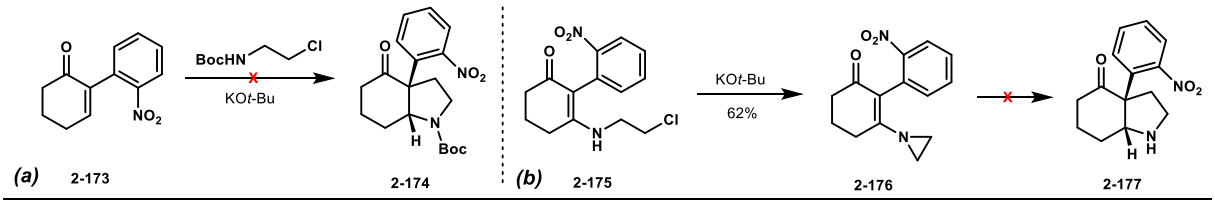

Scheme 2.35 (a) Attempted aza-Michael, alkylation cascade ***(b)*** Attempted ring expansion of vinyl aziridine

2.2.5 Conclusions

Herein we reported several approaches towards the synthesis of alstonlarsine A. There is certainly additional work that can be done with these disconnections. The key cyclization events to make the cage were not attempted, as the necessary precursors were not successfully synthesized. It was at this point in my graduate career that I began working on another project and did not have time to return to this work. Moving forward, hopefully another graduate student will successfully make these synthons to examine the key transformations.

2.3 Supplemental Information

2.3.1 General Experimental

The ^{1}H NMR spectra were recorded at 500 MHz or 600 MHz using either a Bruker DRX500 (cryoprobe) or a Bruker AVANCE600 (cryoprobe) NMR, respectively. The ^{13}C NMR spectra were recorded at 126 MHz or 151 MHz on the Bruker DRX500 or Bruker AVANCE600 NMR, respectively. All NMR spectra were taken at 25 °C unless otherwise noted. Chemical shifts (δ) are reported in parts per million (ppm) and referenced to residual solvent peak at 7.26 ppm (^{1}H) or 77.16 ppm (^{13}C) for deuterated chloroform ($CDCl_3$), 3.31 ppm (^{1}H) or 49.15 ppm (^{13}C) for deuterated methanol (CD_3OD), 2.50 ppm (^{1}H) or 39.52 ppm (^{13}C) for deuterated dimethylsulfoxide (DMSO-d_6). The ^{1}H NMR spectral data are presented as follows: chemical shift, multiplicity (s = singlet, d = doublet, t = triplet, q = quartet, quint = quintet, m = multiplet, dd = doublet of doublets, ddd = doublet of doublet of doublets, dddd = doublet of doublet of doublet of doublets, dt = doublet of triplets, dq = doublet of quartets, ddq = doublet of doublet of quartets, app. = apparent), coupling constant(s) in hertz (Hz), and integration. High-resolution mass spectra (HRMS) were recorded on Waters LCT Premier TOF spectrometer with electrospray ionization (ESI) and chemical ionization (CI) sources. An internal standard was used to calibrate the exact mass of each compound. For accuracy, the peak selected for comparison was that which most closely matched the ion intensity of the internal standard.

Unless otherwise stated, synthetic reactions were carried out under an atmosphere of argon in flame- or oven-dried glassware. Thin layer chromatography (TLC) was carried out using glass plates coated with a 250 μm layer of 60 Å silica gel. TLC plates were visualized with a UV lamp at 254 nm, or by staining with Hanessian's stain or $KMnO_4$ stain. Liquid chromatography was performed using forced flow (flash chromatography) with an automated purification system on prepacked silica gel (SiO_2) columns unless otherwise stated.

All commercially available reagents were used as received unless stated otherwise. Solvents were purchased as ACS grade or better and as HPLC-grade and passed through a solvent purification system equipped with activated alumina columns prior to use. $CDCl_3$, CD_3OD, and DMSO-d_6 was purchased from Cambridge Isotope Laboratories.

2.3.2 Experimental procedures and compound characterization

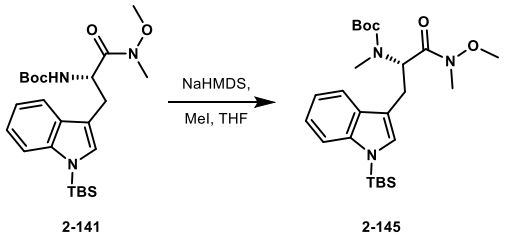

2-141 2-145

***tert*-Butyl (*S*)-(3-(1-(tert-butyldimethylsilyl)-1*H*-indol-3-yl)-1-(methoxy(methyl)amino)-1-oxopropan-2-yl)(methyl)carbamate (2-145):**

To a solution of indole **2-141** (3.70 g, 8.02 mmol, 1.0 equiv) in THF (25 mL) at –78 °C was added a solution of NaHMDS (2.79 g, 15.2 mmol, 1.9 equiv) in THF (20 mL) dropwise. The solution was stirred at this temperature for 1 h and then MeI (1.4 mL, 22.8 mmol, 3.0 equiv) was added. The solution was allowed to warm to rt overnight and the next day TLC indicated the incomplete conversion. The solution was cooled back to –78 °C and a solution of NaHMDS (1.78 g, 9.70 mmol, 1.2 equiv) in THF (15 mL) was added. After stirring for 1 h at this temperature, MeI (1.4 mL) was added. The solution was stirred for 1 h at –78 °C and it was then warmed to rt and stirred for an additional 1 hr. The reaction was quenched with saturated NH_4Cl solution, and was extracted with Et_2O. The organic phase was washed with H_2O then brine, dried with $MgSO_4$, filtered, and concentrated *in vacuo* to obtain tertiary amine **2-145** as a 1.25:1 mixture of rotamers, and was taken onto the next step without further purification (3.65 g).

^{1}H NMR (500 MHz, $CDCl_3$) δ 7.59 (d, *J* = 7.0, 1H), 7.46 (d, *J* = 7.5 Hz, 1H), 7.17 – 7.08 (m, 2H), 6.95 (s, 1 H), 3.54 (s, 3H), 3.34 – 3.20 (m, 1H), 3.19 – 3.04 (m, 4H), 2.90 (s, 3H), 2.53 – 2.36 (m, 1H), 1.10 (s, 9H), 0.90 (s, 9H), 0.56 (s, 6H), 0.14 (s, 6H).

^{13}C NMR (126 MHz, $CDCl_3$, one rotamer is reported, Weinreb amide carbonyl peak is missing) δ 155.2, 141.6, 131.0, 130.0, 121.5, 119.5, 118.6, 114.1, 113.4, 79.7, 61.5, 54.9, 53.4, 32.2, 28.1, 26.3, 25.0, 19.5, -3.8.

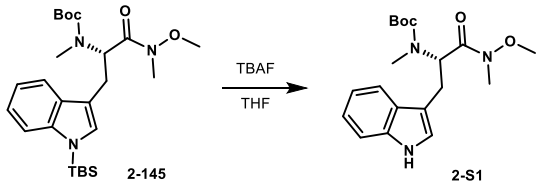

***tert*-Butyl (*S*)-(3-(1*H*-indol-3-yl)-1-(methoxy(methyl)amino)-1-oxopropan-2-yl)(methyl) carbamate (2-S1):**

To a solution of indole **2-145** (3.00 g, 6.31 mmol, 1.0 equiv) in THF (12.6 mL) at rt was added a solution of TBAF (1.0 M in THF; 6.3 mL, 1.0 equiv). The solution was stirred for 20 min at rt and was then diluted with Et_2O. The solution was washed with H_2O (2 X) then brine. The organic phase was dried with $MgSO_4$, filtered, and concentrated *in vacuo*. The resulting residue was purified via flash chromatography (50% EtOAc in hex) to obtain indole **2-S1** (1.44 g, 63%).

^{1}H NMR (500 MHz, $CDCl_3$) δ 8.34 (s, 1H), 7.63 (d, *J* = 7.7 Hz, 1H), 7.34 (t, *J* = 10.8 Hz, 1H), 7.17 (t, *J* = 7.2 Hz, 1H), 7.11 (t, *J* = 7.4 Hz, 1H), 6.98 (s, 1H), 3.61 (s, 3H), 3.36 – 3.22 (m, 1H), 3.20 (s, 2H), 3.17 – 3.06 (m, 1H), 2.92 (s, 3H), 1.09 (s, 9H).

^{13}C NMR (126 MHz, $CDCl_3$, one rotamer is reported, Weinreb amide carbonyl peak is missing) δ 155.4, 136.4, 127.6, 123.1, 121.9, 119.3, 118.8, 118.5, 111.3, 79.8, 61.4, 55.3, 53.7, 32.3, 27.9, 24.8.

HRMS (ESI-TOF) *m/z* calculated for $C_{19}H_{27}N_3O_4Na^+$ $(M+Na)^+$ 384.1899, found 384.1881.

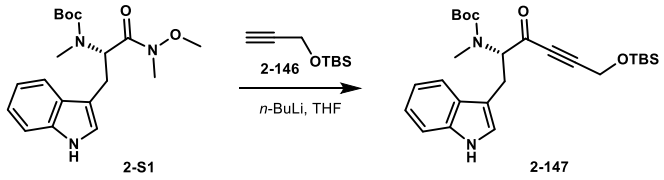

***tert*-Butyl (*S*)-(6-((tert-butyldimethylsilyl)oxy)-1-(1*H*-indol-3-yl)-3-oxohex-4-yn-2-yl)(methyl) carbamate (2-147):**

To a solution of alkyne **2-146** (1.13 g, 6.64 mmol, 2.0 equiv) in THF (6.6 mL) at –78 °C was added *n*-BuLi. The solution was stirred at –78 °C for 20 min and then it was warmed to 0 °C and stirred for an additional 20 min. The solution was cooled back to –78 °C and a solution of indole **2-S1** (1.20 g, 3.32 mmol, 1.0 equiv) in THF (10 mL) was added. The reaction was stirred for 1.5 h at –78 °C and then it was warmed to 0 °C and stirred for 20 min, after which it was quenched with saturated NH_4Cl solution. The slurry was extracted with Et_2O, and the combined organic phase was washed with H_2O, then brine, dried with $MgSO_4$, filtered, and concentrated *in vacuo*. The resulting residue was purified via flash chromatography (0 → 100% EtOAc in hex) to obtain ynone **2-147** as a mixture of rotamers (970 mg, 62%).

^{1}H NMR (600 MHz, DMSO-d_6) δ 10.85 (s, 1H), 7.55 (d, *J* = 7.8 Hz, 1H), 7.36 – 7.31 (m, 1H), 7.12 – 7.03 (m, 2H), 7.01 – 6.93 (m, 1H), 4.66 (dd, *J* = 10.1, 3.7 Hz, 1H), 4.56 (s, 2H), 3.36 – 3.28 (m, 1H), 3.07 (dd, *J* = 14.7, 10.7 Hz, 1H), 2.58 (s, 3H), 1.18 (s, 9H), 0.86 (s, 9H), 0.09 (s, 6H).

^{13}C NMR (151 MHz, DMSO, one rotamer is reported) δ 185.4, 154.0, 136.2, 127.0, 123.7, 120.9, 118.3, 118.1, 111.4, 109.6, 91.8, 82.6, 79.4, 67.6, 51.0, 33.2, 27.6, 25.6, 23.4, 17.8, -5.4.

HRMS (ESI-TOF) *m/z* calculated for $C_{26}H_{38}N_2O_4SiNa^+$ $(M+Na)^+$ 493.2498, found 493.2479.

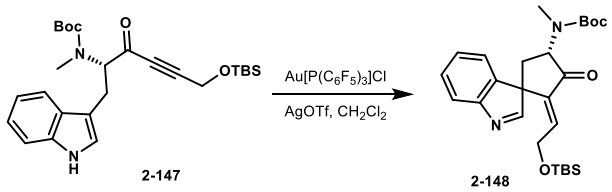

***tert*-Butyl ((4*S*,*E*)-2-(2-((tert-butyldimethylsilyl)oxy)ethylidene)-3-oxospiro[cyclopentane-1,3'-indol]-4-yl)(methyl)carbamate (2-149):**

A solution of ynone **2-147** (15 mg, 0.0319 mmol, 1.0 equiv) and $Au[P(C_6F_5)_3]Cl$ (2 mg, 0.0032 mmol, 0.1 equiv) in CH_2Cl_2 (0.32 mL) was stirred at rt for 24 h, no reaction was observed by TLC. To the solution was added AgOTf (2 mg, 0.0078 mmol, 0.2 equiv) and it was stirred for an additional 5.5 h. The solution was concentrated *in vacuo* and the resulting residue was purified via flash chromatography (0 → 65% EtOAc in hex) to presumably obtain spirocycle **2-148**. Due to the small amount of material and rotamers in the spectra, only diagnostic NMR peaks were evaluated.

Diagnostic ^{1}H NMR for spirocycloe 2-148:

^{1}H NMR (600 MHz, $CDCl_3$) δ 6.80 (dd, *J* = 9.7, 5.3 Hz, 1H), 4.88 (dd, *J* = 12.5, 9.3 Hz, 1H), 4.36 (dd, *J* = 12.5, 9.3 Hz, 1H).

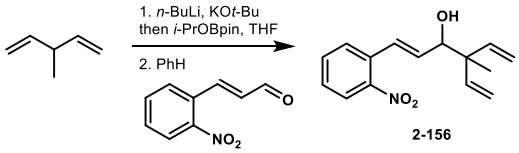

(*E*)-4-Methyl-1-(2-nitrophenyl)-4-vinylhexa-1,5-dien-3-ol (2-156):

To a slurry of KO*t*-Bu (1.12 g, 10.0 mmol, 1.0 equiv) and *n*-BuLi solution (2.2 M in hex; 4.8 mL, 10.5 mmol, 1.05 equiv) at 0 °C was added 3-methylpenta-1,4-diene (1.22 mL, 10.0 mmol, 1.0 equiv). The suspension was stirred for 20 min at 0 °C and it was then concentrated *in vacuo*. The

resulting residue was dissolved in THF (50 mL) and the solution was cooled to –78 °C. To the cooled solution was added *i*-PrOBpin (2.0 mL, 10.0 mmol, 1.0 equiv). The solution was stirred at –78 °C for 1 h and it was then quenched with saturated NH_4Cl solution. The slurry was extracted with Et_2O (3 X). The combined organic phase was washed with brine, dried with $MgSO_4$, filtered, and concentrated *in vacuo*. The resulting residue was taken onto the next step without further purification.

The resulting residue (852 mg) was dissolved in benzene (24 mL) and (*E*)-3-(2-nitrophenyl)acrylaldehyde (1.0 g, 4.81 mmol, 1.0 equiv) was added. The solution was stirred for 41 h and then it was then concentrated *in vacuo*. The resulting residue was purified via flash chromatography (10% EtOAc in hex) to obtain alcohol **2-156** (322 mg, 26%).

^{1}H NMR (500 MHz, $CDCl_3$) δ 7.92 (d, *J* = 8.2 Hz, 1H), 7.57 – 7.53 (m, 2H), 7.43 – 7.35 (m, 1H), 7.06 (d, *J* = 15.7 Hz, 1H), 6.18 (dd, *J* = 15.7, 6.3 Hz, 1H), 6.03 (dd, *J* = 17.6, 10.8 Hz, 1H), 5.96 (dd, *J* = 17.5, 10.8 Hz, 1H), 5.24 (t, *J* = 11.2 Hz, 2H), 5.16 (dd, *J* = 17.6, 3.1 Hz, 2H), 4.16 (d, *J* = 5.7 Hz, 1H), 1.19 (s, 3H).

^{13}C NMR (126 MHz, $CDCl_3$) δ 148.0, 142.0, 141.5, 134.0, 133.2, 132.9, 129.1, 128.2, 127.7, 124.6, 115.7, 115.5, 77.7, 49.0, 19.1.

HRMS (ESI-TOF) *m/z* calculated for $C_{15}H_{17}NO_3Na^+$ $(M+Na)^+$ 282.1106, found 282.1100.

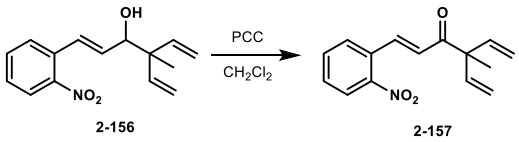

2-156 2-157

(*E*)-4-Methyl-1-(2-nitrophenyl)-4-vinylhexa-1,5-dien-3-one (2-157):

To a solution of alcohol **2-156** (270 mg, 1.0 mmol, 1.0 equiv) in CH_2Cl_2 (5.2 mL) was added PCC (561 mg, 2.60 mmol, 2.5 equiv). The solution was stirred for 4 h at rt after which it was filtered through celite. The cake was washed with additional CH_2Cl_2 and the filtrate was *concentrated in vacuo*. The resulting residue was purified via flash chromatography (15% EtOAc in hex) to obtain enone **2-157** (125 mg, 57%).

^{1}H NMR (500 MHz, $CDCl_3$) δ 8.06 – 7.97 (m, 2H), 7.67 – 7.57 (m, 2H), 7.56 – 7.48 (m, 1H), 6.89 (d, *J* = 15.6 Hz, 1H), 6.09 (dd, *J* = 17.6, 10.7 Hz, 2H), 5.29 (d, *J* = 10.7 Hz, 2H), 5.21 (d, *J* = 17.6 Hz, 2H), 1.39 (s, 3H).

^{13}C NMR (126 MHz, $CDCl_3$) δ 197.9, 148.8, 139.6, 137.9, 133.5, 131.2, 130.3, 129.2, 127.3, 125.0, 116.6, 56.9, 21.2.

HRMS (ESI-TOF) *m/z* calculated for $C_{15}H_{15}NO_3Na^+$ $(M+Na)^+$ 280.0950, found 280.0948.

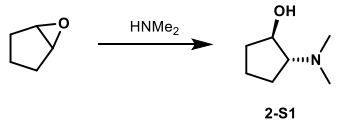

2-S1

2-(Dimethylamino)cyclopentan-1-ol (2-S2):

A solution of cyclopentene oxide (1.0 mL, 11.5 mmol, 1.0 equiv) and 40% aqueous dimethylamine (3.8 mL) was stirred for 16 h at rt. The solution was diluted with H_2O and extracted with Et_2O (3 X). The combined organic phase was washed with brine, dried with $MgSO_4$, filtered, and

concentrated *in vacuo* to obtain amino alcohol **2-S2** as a clear oil (862 mg, 58%). The spectral data is in accordance with the reported literature.[110]

^{1}H NMR (500 MHz, $CDCl_3$) δ 3.90 (dd, *J* = 12.4, 5.5 Hz, 1H), 2.33 (td, *J* = 8.2, 5.8 Hz, 1H), 2.12 (s, 6H), 1.80 – 1.72 (m, 1H), 1.68 (ddd, *J* = 11.9, 7.5, 3.9 Hz, 1H), 1.53 (ddd, *J* = 15.9, 10.0, 6.1 Hz, 1H), 1.48 – 1.38 (m, 2H), 1.31 (ddd, *J* = 16.8, 12.5, 8.6 Hz, 1H).

^{13}C NMR (126 MHz, $CDCl_3$) δ 74.9, 74.7, 43.2, 34.4, 27.0, 21.5.

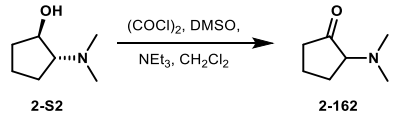

2-S2 **2-162**

2-(Dimethylamino)cyclopentan-1-one (2-162):

To a solution of oxalyl chloride (0.37 mL, 4.26 mmol, 1.1 equiv) in CH_2Cl_2 (10.5 mL) at –78 °C was added DMSO (0.33 mL, 4.64 mmol, 1.2 equiv). The solution was stirred at this temperature for 10 min and then a solution of alcohol **2-S2** (500 mg, 3.87 mmol, 1.0 equiv) in CH_2Cl_2 (5 mL) was added. The solution was stirred for 15 min, then NEt_3 (2.7 mL, 19.4 mmol, 5.0 equiv) was added. The solution was warmed to rt and then was washed with H_2O and brine. The organic phase was dried with Na_2SO_4, filtered, and concentrated *in vacuo* to obtain ketone **2-162** (337 mg, 68%).

^{1}H NMR (500 MHz, $CDCl_3$) δ 2.96 (dd, *J* = 11.4, 7.8 Hz, 1H), 2.29 (s, 6H), 2.28 – 2.22 (m, 1H), 2.10 – 2.04 (m, 1H), 2.02 – 1.94 (m, 2H), 1.78 (dd, *J* = 11.7, 5.8 Hz, 1H), 1.70 – 1.62 (m, 1H).

^{13}C NMR (126 MHz, $CDCl_3$) δ 217.2, 71.7, 45.9, 42.4, 37.2, 23.5, 18.2, 10.5.

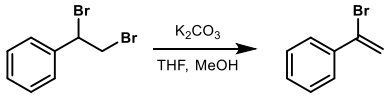

2-163

(1-Bromovinyl)benzene (2-163):

To a solution of (1,2-dibromoethyl)benzene (1.00 g, 3.79 mmol, 1.0 equiv) in THF (7.5 mL) and MeOH (7.5 mL) was added K_2CO_3 (1.05 g, 7.58 mmol, 2.0 equiv). The solution was stirred overnight at rt and then it was concentrated in vacuo. The resulting residue was diluted with H_2O and extracted with Et_2O (3 X). The combined organic phase was washed with brine, dried with $MgSO_4$, filtered, and concentrated *in vacuo* to obtain vinyl bromide **2-163** as a yellow oil (662 mg, 95%). The spectral data is in accordance with the reported literature.[111]

^{1}H NMR (500 MHz, $CDCl_3$) δ 7.68 – 7.57 (m, 2H), 7.43 – 7.29 (m, 3H), 6.14 (d, *J* = 1.9 Hz, 1H), 5.81 (d, *J* = 1.9 Hz, 1H).

^{13}C NMR (126 MHz, $CDCl_3$) δ 138.7, 131.1, 129.2, 128.4, 127.4, 117.8.

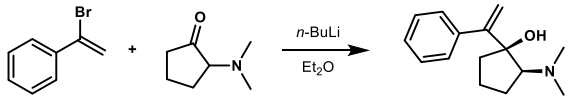

2-163 2-162 2-164

2-(Dimethylamino)-1-(1-phenylvinyl)cyclopentan-1-ol (2-164):

To a solution of vinyl bromide **2-163** (216 mg, 1.18 mmol, 1.5 equiv) in Et_2O (1.8 mL) at –78 °C was added *n*-BuLi (2.5 M in hex; 1.1 mL, 2.75 mmol, 3.5 equiv). The solution was stirred at –78 °C for 1 h and it was then warmed to 0 °C and stirred for an additional hr. The solution was cooled back to –78 °C and ketone **2-162** (100 mg, 0.786, 1.0 equiv) in Et_2O (1.2 mL) was added. The reaction was stirred for 1.25 h at this temperature and it was quenched with saturated NH_4Cl solution. The slurry was extracted with Et_2O (2 X) and the combined organic phase was washed

with brine, dried with $MgSO_4$, filtered, and concentrated *in vacuo*. The resulting residue was purified via flash chromatography (0 → 20% EtOAc in hex, 1% NEt_3) on a neutralized silica gel column to obtain amino alcohol **2-164** (35 mg, 19%).

^{1}H NMR (600 MHz, $CDCl_3$) δ 7.33 – 7.27 (m, 4H), 7.27 – 7.22 (m, 1H), 5.63 (d, *J* = 1.9 Hz, 1H), 5.06 (d, *J* = 1.9 Hz, 1H), 2.78 (dd, *J* = 10.0, 6.8 Hz, 1H), 2.26 (s, 6H), 2.24 – 2.18 (m, 1H), 1.99 (dt, *J* = 14.2, 8.5 Hz, 1H), 1.82 – 1.75 (m, 2H), 1.73 – 1.68 (m, 1H), 1.45 – 1.37 (m, 1H).

^{13}C NMR (151 MHz, $CDCl_3$) δ 157.0, 141.7, 128.8, 127.9, 127.0, 113.5, 80.0, 72.1, 44.7, 42.3, 30.2, 22.2.

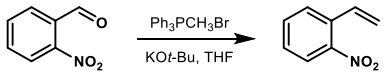

2-S3

1-Nitro-2-vinylbenzene (2-S3):

To a solution of Ph_3PCH_3Br (911 mg, 2.55 mmol, 1.7 equiv) in THF (3.0 mL) at 0 °C was added KO*t*-Bu (286 mg, 2.55 mmol, 1.7 equiv) in two portions. The slurry became clear yellow upon addition. The solution was warmed to rt and stirred for 30 min, after which it was cooled back to 0 °C. To the cooled solution 2-nitrobenzaldehyde (227 mg, 1.50 mmol, 1.0 equiv) was added and the reaction was allowed to warm to rt. The solution was stirred for 22 h and then it was concentrated *in vacuo* and the resulting residue was purified via flash chromatography (0 → 10% EtOAc in hex) to obtain alkene **2-S3** (80 mg, 36%). The spectral data is in accordance with the reported literature.[112]

^{1}H NMR (500 MHz, $CDCl_3$) δ 7.92 (d, *J* = 8.2 Hz, 1H), 7.62 (d, *J* = 7.8 Hz, 1H), 7.57 (t, *J* = 7.6 Hz, 1H), 7.44 – 7.37 (m, 1H), 7.17 (dd, *J* = 17.3, 11.0 Hz, 1H), 5.74 (d, *J* = 17.3 Hz, 1H), 5.48 (d, *J* = 11.0 Hz, 1H).

^{13}C NMR (126 MHz, $CDCl_3$) δ 133.5, 133.2, 132.6, 128.6, 128.5, 124.5, 119.0, 119.0.

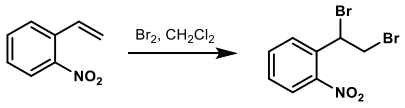

2-S3 2-S4

1-(1,2-Dibromoethyl)-2-nitrobenzene (2-S4):

To a solution of alkene **2-S3** (80 mg, 0.537 mmol, 1.0 equiv) in CH_2Cl_2 (2.7 mL) at 0 °C was added Br_2 (0.03 mL, 0.591 mmol, 1.1 equiv). The solution was stirred for 10 min and then it was washed with $Na_2S_2O_3$ solution, then brine. The organic phase was dried with Na_2SO_4, filtered, and concentrated *in vacuo* to obtain dibromide **2-S4**, which was taken onto the next step without further purification.

^{1}H NMR (500 MHz, $CDCl_3$) δ 7.92 (d, *J* = 8.2 Hz, 1H), 7.78 – 7.73 (m, 1H), 7.69 (t, *J* = 7.6 Hz, 1H), 7.51 (t, *J* = 8.2 Hz, 1H), 5.96 (dd, *J* = 10.1, 5.7 Hz, 1H), 4.12 – 3.97 (m, 2H).

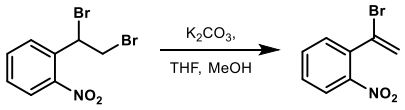

2-S4 2-S5

1-(1-Bromovinyl)-2-nitrobenzene (2-S5):

To a solution of dibromide **2-S4** (166 mg, 0.537 mmol, 1.0 equiv) in THF (1.0 mL) and MeOH (1.0 mL) was added K_2CO_3 (148 mg, 1.07 mmol, 2.0 equiv). The solution was stirred overnight at rt and then it was concentrated in vacuo. The resulting residue was diluted with H_2O and extracted with Et_2O (3 X). The combined organic phase was washed with brine, dried with $MgSO_4$, filtered,

and concentrated *in vacuo* to obtain vinyl bromide **2-S5** as a yellow oil (100 mg, 82% over 2 steps).

^{1}H NMR (500 MHz, $CDCl_3$) δ 7.91 (d, *J* = 8.1 Hz, 1H), 7.59 (td, *J* = 7.7, 1.0 Hz, 1H), 7.52 – 7.43 (m, 2H), 5.87 (dd, *J* = 4.3, 2.1 Hz, 2H).

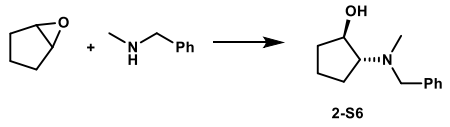

2-S6

2-(Benzyl(methyl)amino)cyclopentan-1-ol (2-S6):

A neat solution of cyclopentene oxide (0.25 mL, 2.87 mmol, 1.0 equiv) and methylbenzylamine (0.41 mL, 3.16 mmol, 1.1 equiv) was stirred at rt for 18 h. Subsequently it was heated to 100 °C for 17.5 h. NMR analysis of the reaction mixture showed only starting material so additional methylbenzylamine (0.60 mL, 4.66 mmol, 1.6 equiv) was added. The solution was heated to 120 °C for 26 h. NMR analysis indicated a mixture of starting material and desired product, so the reaction was heated to 170 °C for 21 h. The solution was cooled to rt and purified via flash chromatography (100% EtOAc) to obtain amino alcohol **2-S6** (391 mg, 66%). The spectral data is in accordance with the reported literature.[113]

^{1}H NMR (500 MHz, $CDCl_3$) δ 7.36 – 7.28 (m, 4H), 7.23 (t, *J* = 6.9 Hz, 1H), 4.18 – 4.09 (m, 1H), 3.5 (s, 2H), 2.82 – 2.70 (m, 2H), 2.18 (s, 3H), 1.92 (dt, *J* = 14.4, 7.2 Hz, 1H), 1.83 (ddd, *J* = 11.9, 7.7, 4.1 Hz, 1H), 1.75 – 1.67 (m, 1H), 1.67 – 1.60 (m, 1H), 1.60 – 1.51 (m, 2H).

^{13}C NMR (126 MHz, $CDCl_3$) δ 139.4, 129.1, 128.3, 127.0, 74.8, 73.5, 60.0, 38.7, 33.4, 25.1, 21.1.

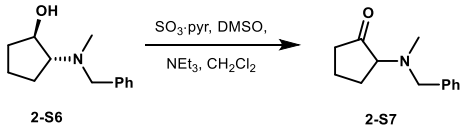

2-S6 2-S7

2-(Benzyl(methyl)amino)cyclopentan-1-one (2-S7):

To a solution of amino alcohol **2-S6** (50 mg, 0.244 mmol, 1.0 equiv) in CH_2Cl_2 (1.6 mL) at 0 °C was added DMSO (0.83 mL, 11.7 mmol, 48.0 equiv), NEt_3 (0.20 mL, 1.46 mmol, 6.0 equiv), and SO_3·pyridine (97 mg, 0.610 mmol, 2.5 equiv). The solution was allowed to warm to rt overnight and then it was quenched with saturated NH_4Cl solution. The slurry was extracted with CH_2Cl_2 (3 X). The combined organic phase was washed with brine, dried with Na_2SO_4, filtered, and concentrated *in vacuo*. The resulting residue was purified via flash chromatography (20 → 60% EtOAc in hex) to obtain ketone **2-S7** (22 mg, 44%).

^{1}H NMR (500 MHz, $CDCl_3$) δ 7.35 (d, *J* = 7.5 Hz, 2H), 7.29 (t, *J* = 7.5 Hz, 2H), 7.22 (t, *J* = 7.2 Hz, 1H), 3.68 (dd, *J* = 38.8, 13.1 Hz, 2H), 3.16 (dd, *J* = 11.8, 8.1 Hz, 1H), 2.34 – 2.22 (m, 4H), 2.16 – 2.05 (m, 2H), 2.01 – 1.92 (m, 1H), 1.86 (ddd, *J* = 23.6, 11.9, 6.2 Hz, 1H), 1.72 – 1.59 (m, 1H).

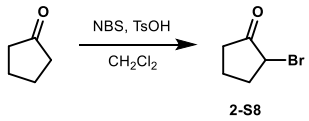

2-S8

2-Bromocyclopentan-1-one (2-S8):

A microwave vial containing cyclopentanone (0.50 mL, 5.65 mmol, 1.0 equiv), NBS (1.21 g, 6.78 mmol, 1.2 equiv), and TsOH (97 mg, 0.565 mmol, 0.1 equiv) in CH_2Cl_2 (5.6 mL) was heated to 55 °C for 13 h. After cooling toch rt the reaction solution was washed with H_2O. The aqueous phase was extracted with CH_2Cl_2 (2 X). The combined organic phase was washed with saturated $NaHCO_3$ solution, then brine, dried with Na_2SO_4, filtered, and concentrated *in vacuo*. The resulting

residue was purified via flash chromatography (0 → 20% EtOAc in hex) to obtain bromide **2-S8** (485 mg, 53%). The spectral data is in accordance with the reported literature.[114]

^{1}H NMR (500 MHz, $CDCl_3$) δ 4.17 – 4.11 (m, 1H), 2.34 – 2.19 (m, 2H), 2.17 – 2.02 (m, 3H), 1.98 – 1.87 (m, 1H).

^{13}C NMR (126 MHz, $CDCl_3$) δ 211.0, 48.3, 34.8, 33.7, 20.0.

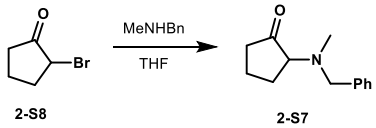

2-S8 2-S7

2-(Benzyl(methyl)amino)cyclopentan-1-one (2-S6):

A solution of bromide **2-S8** (480 mg, 2.94 mmol, 1.0 equiv) and methylbenzylamine (1.1 mL, 8.83 mmol, 3.0 equiv) in THF (6.0 mL) was stirred at rt for 1.25 h. The solution was diluted with H_2O and extracted with CH_2Cl_2 (2 X). The combined organic phase was washed with brine, dried with Na_2SO_4, filtered, and concentrated *in vacuo*. The resulting residue was purified via flash chromatography (0 → 25% EtOAc in hex) to obtain amine **2-S7** (103 mg, 17%). The spectral data matches the data reported *vide supre*.

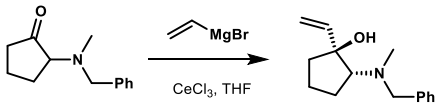

2-S6 2-166

2-(Benzyl(methyl)amino)-1-vinylcyclopentan-1-ol (2-166):

A slurry of $CeCl_3$ (30 mg, 1.0 equiv) in THF (0.25 mL) was stirred at rt overnight. The slurry was cooled to –78 °C and vinyl Grignard (0.7 M in THF; 0.53 mL, 0.369 mmol, 3.0 equiv) was added

and the reaction was stirred at this temperature for 1.5 h. To the solution ketone **2-S7** (25 mg, 0.123 mmol, 1.0 equiv) in THF (0.5 mL) was added and it was stirred at –78 °C for 18.5 h. The reaction was quenched with NH_4Cl solution. The slurry as extracted with Et_2O and the organic phase was washed with brine, dried with Na_2SO_4, filtered, and concentrated *in vacuo* to obtain alcohol **2-166** (18 mg, 64%).

^{1}H NMR (500 MHz, $CDCl_3$) δ 7.34 – 7.27 (m, 5H), 7.25 – 7.22 (m, 1H), 5.97 (dd, *J* = 17.1, 10.6 Hz, 1H), 5.45 (d, *J* = 17.1 Hz, 1H), 4.99 (d, *J* = 10.6 Hz, 1H), 3.82 (d, *J* = 13.2 Hz, 1H), 3.42 (d, *J* = 13.1 Hz, 1H), 2.77 – 2.65 (m, 1H), 2.16 (s, 3H), 2.01 – 1.91 (m, 1H), 1.91 – 1.79 (m, 4H), 1.60 – 1.53 (m, 1H).

^{13}C NMR (126 MHz, $CDCl_3$) δ 146.4, 142.5, 127.0, 128.5, 127.2, 111.2, 73.5, 61.1, 40.6, 40.0, 29.9, 21.0.

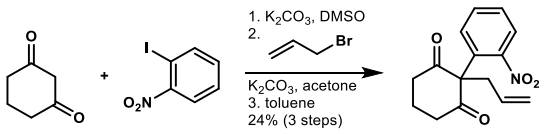

2-169

2-Allyl-2-(2-nitrophenyl)cyclohexane-1,3-dione (2-169):

A solution of 1,3-cyclohexanedione (900 mg, 8.03 mmol, 2.0 equiv), 1-iodo-2-nitrobenzene (1.00 g, 4.02 mmol, 1.0 equiv), and K_2CO_3 (1.39 g, 2.5 equiv) in DMSO (12.5 mL) was heated to 90 °C and was stirred at this temperature for 4 h. After cooling to rt, the solution was diluted with H_2O and acidified with concentrated HCl. The solution was extracted with Et_2O (3 X) and the combined organic phase was dried with Na_2SO_4, filtered, and concentrated *in vacuo*. A small aliquot was reserved for characterization (The spectral data is in accordance with the reported literature[107]). The resulting residue was dissolved in acetone (20 mL) and allyl bromide (0.38 mL, 4.42 mmol, 1.1 equiv) and K_2CO_3 (1.11 g, 8.04 mmol, 2.0 equiv) was added. The solution was refluxed for 3

h, and then the solution was concentrated *in vacuo*. The resulting residue was partitioned between CH_2Cl_2 and H_2O. The organic phase was extracted, washed with brine, dried with Na_2SO_4, filtered, and concentrated *in vacuo*. A small aliquot was reserved for characterization (The spectral data is in accordance with the reported literature[107]). The resulting residue was dissolved in toluene (5.0 mL) and heated to 185 °C. The reaction was stirred at this temperature for 12 h and then it was concentrated *in vacuo*. The resulting residue was purified via flash chromatography to obtain diketone **2-169** as a brown solid (264 mg, 24% over 3 steps). The spectral data is in accordance with the reported literature.[107]

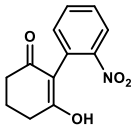

2-S9

6-Hydroxy-2'-nitro-4,5-dihydro-[1,1'-biphenyl]-2(3H)-one (2-S9):

^{1}H NMR (600 MHz, $CDCl_3$) δ 7.99 – 7.85 (m, 1H), 7.59 –7.48 (m, 1H), 7.44 – 7.32 (m, 1H), 7.25 –7.15 (m, 1H), 4.22 – 4.01 (m, 1H), 2.15 – 1.90 (m, 4H), 1.38 – 1.16 (m, 2H).

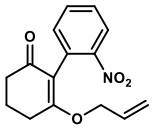

2-S10

6-(Allyloxy)-2'-nitro-4,5-dihydro-[1,1'-biphenyl]-2(3*H*)-one (2-S10):

^{1}H NMR (600 MHz, $CDCl_3$) δ 7.91 (d, *J* = 8.2 Hz, 1H), 7.51 (t, *J* = 7.5 Hz, 1H), 7.36 (t, *J* = 7.8 Hz, 1H), 7.24 (d, *J* = 7.7 Hz, 1H), 5.74 (ddd, *J* = 16.0, 10.2, 4.9 Hz, 1H), 5.17 – 5.08 (m, 2H), 4.49 – 4.41 (m, 2H), 2.67 (t, *J* = 6.2 Hz, 2H), 2.46 – 2.41 (m, 2H), 2.14 – 2.06 (m, 1H), 2.06 – 1.98 (m, 1H).

2-Allyl-2-(2-nitrophenyl)cyclohexane-1,3-dione (2-169):

^{1}H NMR (600 MHz, $CDCl_3$) δ 8.12 (d, *J* = 8.1 Hz, 1H), 7.69 (t, *J* = 7.7 Hz, 1H), 7.58 (d, *J* = 7.9 Hz, 1H), 7.50 (t, *J* = 7.7 Hz, 1H), 5.59 (ddt, *J* = 16.8, 10.2, 6.6 Hz, 1H), 5.26 (d, *J* = 17.0 Hz, 1H), 5.16 (d, *J* = 10.2 Hz, 1H), 3.07 (d, *J* = 6.6 Hz, 2H), 2.88 – 2.75 (m, 4H), 2.44 – 2.32 (m, 1H), 2.22 – 2.14 (m, 1H).

^{13}C NMR (151 MHz, $CDCl_3$) δ 205.3, 147.8, 133.8, 132.4, 131.4, 130.9, 128.7, 126.1, 120.0, 38.0, 36.9, 17.1.

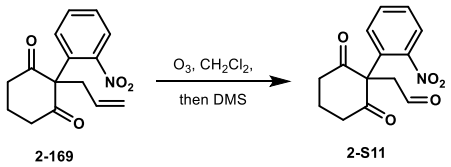

2-169 2-S11

2-(1-(2-Nitrophenyl)-2,6-dioxocyclohexyl)acetaldehyde (2-S11):

A solution of alkene **2-169** (200 mg, 0.732 mmol, 1.0 equiv) in CH_2Cl_2 (2.5 mL) at –78 °C was treated with O_3 until the solution turned blue in color. The flask was purged with O_2 until the blue color dissipated, and then DMS (0.54 mL, 7.32 mmol, 10.0 equiv) was added. The solution was allowed to slowly warm to rt overnight. The solution was diluted with brine, and extracted with CH_2Cl_2 (4 X). The combined organic phase was washed with brine, dried with Na_2SO_4, filtered, and concentrated *in vacuo* to obtain aldehyde **2-S11** (200 mg, 98%)**.** The spectral data is in accordance with the reported literature.[115]

^{1}H NMR (500 MHz, $CDCl_3$) δ 9.48 (t, *J* = 1.8 Hz, 1H), 8.04 (d, *J* = 8.1 Hz, 1H), 7.67 (t, *J* = 7.7 Hz, 1H), 7.53 (t, *J* = 7.8 Hz, 1H), 7.36 (d, *J* = 7.9 Hz, 1H), 3.20 (d, *J* = 2.1 Hz, 2H), 2.89 – 2.78 (m, 4H), 2.35 – 2.25 (m, 1H), 2.17 – 2.09 (m, 1H).

^{13}C NMR (126 MHz, $CDCl_3$) δ 204.24, 197.64, 147.86, 133.98, 130.88, 129.45, 126.29, 77.41, 77.16, 76.91, 45.48, 37.14, 17.25.

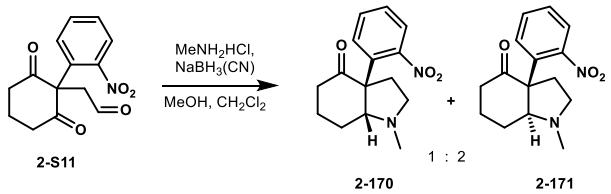

2-S11 2-170 2-171

1-Methyl-3a-(2-nitrophenyl)octahydro-4H-indol-4-one (2-170 and 2-171):

To a solution of aldehyde **2-S11** (402 mg, 1.46 mmol, 1.0 equiv) in MeOH (5.0 mL) and CH_2Cl_2 (1.0 mL) was added dimethylamine-HCl salt (394 mg, 5.84 mmol, 4.0 equiv) and $NaB(CN)H_3$ (229 mg, 3.65 mmol, 2.5 equiv). The solution was stirred at rt for 29 h and then it was concentrated *in vacuo*. The resulting residue was diluted CH_2Cl_2 and was washed with saturated $NaHCO_3$ solution (2 X). The combined aqueous phase was extracted with CH_2Cl_2 (4 X). The combined organic phase was washed with brine, dried with Na_2SO_4, filtered, and concentrated *in vacuo* to obtain a mixture of bicycle **2-170** and **2-171** (1:2 of **2-170**:**2-171**; 59 mg, 15%). The resulting residue was purified via flash chromatography (0 → 10% MeOH in CH_2Cl_2) to separate the diastereomers. The *trans* isomer (**2-171**) is reported below; the *cis* isomer was isolated with many impurities, but the spectral data is in accordance with the reported literature.[107]

^{1}H NMR (600 MHz, $CDCl_3$) δ 8.77 (d, *J* = 8.1 Hz, 1H), 7.55 (t, *J* = 7.3 Hz, 1H), 7.50 (d, *J* = 7.9 Hz, 1H), 7.37 (t, *J* = 7.6 Hz, 1H), 3.20 (dd, *J* = 16.7, 8.5 Hz, 1H), 2.83 (ddd, *J* = 13.6, 10.9, 6.9 Hz, 1H), 2.35 (s, 3H), 2.34 – 2.28 (m, 2H), 2.28 – 2.21 (m, 2H), 2.03 – 1.97 (m, 1H), 1.96 – 1.87 (m, 3H), 1.54 (ddd, *J* = 18.9, 10.7, 5.4 Hz, 1H).

^{13}C NMR (151 MHz, $CDCl_3$) δ 207.2, 150.7, 133.6, 132.8, 131.4, 127.8, 124.1, 78.7, 63.6, 53.6, 41.2, 38.9, 30.5, 26.1, 23.2.

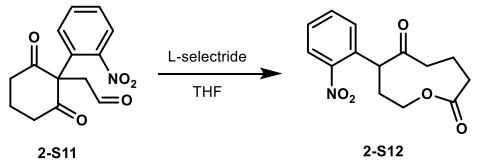

7-(2-Nitrophenyl)oxonane-2,6-dione (2-S12):

To a solution of aldehyde **2-S11** (50 mg, 0.183 mmol, 1.0 equiv) in THF (1.8 mL) at –78 °C was added L-selectride (1.0 M in THF; 0.18 mL, 0.183 mmol, 1.0 equiv) dropwise. The solution was stirred at –78 °C for 20 min and then it was quenched with H_2O and warmed to rt. The solution was extracted with Et_2O (3 X) and the combined organic phase was washed with brine, dried with Na_2SO_4, filtered, and concentrated *in vacuo* to obtain lactone **2-S12**. The spectral data is in accordance with the reported literature.[115]

^{1}H NMR (500 MHz, $CDCl_3$) δ 7.78 (d, *J* = 8.1 Hz, 1H), 7.71 (d, *J* = 7.9 Hz, 1H), 7.59 (t, *J* = 7.7 Hz, 1H), 7.38 (t, *J* = 7.8 Hz, 1H), 4.47 (ddd, *J* = 11.1, 6.4, 1.4 Hz, 1H), 4.37 (dd, *J* = 11.2, 1.8 Hz, 1H), 4.19 (td, *J* = 11.5, 5.0 Hz, 1H), 3.01 – 2.95 (m, 1H), 2.93 – 2.85 (m, 1H), 2.55 (ddd, *J* = 14.6, 8.0, 1.6 Hz, 1H), 2.48 – 2.41 (m, 1H), 2.41 – 2.35 (m, 1H), 2.33 – 2.25 (m, 1H), 1.97 – 1.92 (m, 1H).

^{13}C NMR (126 MHz, $CDCl_3$) δ 211.1, 172.2, 149.3, 133.4, 133.2, 130.3, 127.9, 124.0, 61.8, 50.49, 42.5, 36.1, 33.7, 22.4.

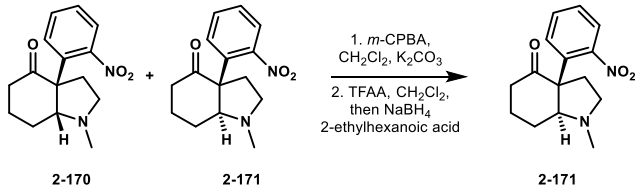

1-Methyl-3a-(2-nitrophenyl)octahydro-4H-indol-4-one (2-171):

To solution of bicycles **2-170** and **2-171** (59 mg, 0.215 mmol, 1.0 equiv) in CH_2Cl_2 (2.5 mL) at –10 °C was added a solution of *m*-CPBA (56 mg, 0.323 mmol, 1.5 equiv) in CH_2Cl_2 (1.5 mL). The

solution was stirred for 2 h at –10 °C after which a scoop of K_2CO_3 was added. The solution was allowed to warm to rt and the slurry was filtered through celite. The cake was washed with additional CH_2Cl_2 and the filtrate was concentrated *in vacuo*. The resulting residue was dissolved in CH_2Cl_2 (2.2 mL) and was cooled to 0 °C. To this cooled solution was added TFAA (0.06 mL, 0.430 mmol, 2.0 equiv) and it was stirred at this temperature for 1 h and then it was warmed to rt and stirred at rt for 15 min. The solution was basified to pH 5 with 10 M NaOH and then a solution of $NaBH_4$ (28 mg, 0.753 mmol, 3.5 equiv) and 2-ethylhexanoic acid (0.42 mL, 2.64 mmol, 12.3 equiv) in CH_2Cl_2 (2.0 mL) that had been stirred at rt overnight was added. The reaction was stirred at rt overnight and then it was washed with $NaHCO_3$ solution. The organic phase was washed with brine, dried with Na_2SO_4, filtered, and concentrated *in vacuo* to obtain exclusively the undesired trans isomer **2-170**. The spectral data matches the data reported *vide supre*.

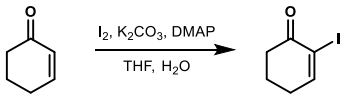

2-S13

2-Iodocyclohex-2-en-1-one (2-S13):

To a solution of cyclohexenone (0.30 mL, 3.12 mmol, 1.0 equiv) in THF (3.0 mL) and H_2O (3.0 mL) was added I_2 (1.19 g, 4.68 mmol, 1.5 equiv), K_2CO_3 (517 mg, 3.74 mmol, 1.2 equiv), and DMAP (76 mg, 0.624 mmol, 0.2 equiv). The solution was stirred for 1 h at rt and then it was diluted with H_2O and extracted with EtOAc (2 X). The combined organic phase was washed with saturated $Na_2S_2O_3$ solution and brine, then it was dried with Na_2SO_4, filtered, and concentrated *in vacuo* to obtain vinyl iodide **2-S13** (613 mg, 88%). The spectral data is in accordance with the reported literature.[116]

^{1}H NMR (500 MHz, $CDCl_3$) δ 7.77 (t, *J* = 4.4 Hz, 1H), 2.70 – 2.63 (m, 2H), 2.44 (dd, *J* = 10.5, 5.8 Hz, 2H), 2.14 – 2.05 (m, 2H).

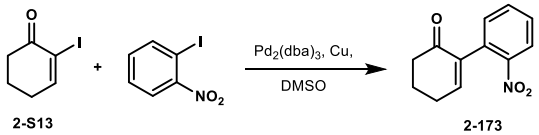

2-S13 2-173

2'-Nitro-4,5-dihydro-[1,1'-biphenyl]-2(3*H*)-one (2-173):

To a Schlenk flask containing $Pd_2(dba)_3$ (41 mg, 0.0450 mmol, 0.10 equiv) was added vinyl iodide **2-S13** (100 mg, 0.450 mmol, 1.0 equiv), 1-iodo-2-nitrobenzene (182 mg, 0.901 mmol, 2.0 equiv), and copper powder (286 mg, 4.50 mmol, 10.0 equiv). The mixture was diluted with DMSO (1.4 mL) and the slurry was heated to 70 °C for 1 h. After cooling to rt, the slurry was diluted with Et_2O and filtered through a plug of celite. The cake was washed with additional Et_2O. The filtrate was washed with H_2O then brine, and it was dried with Na_2SO_4, filtered, and concentrated *in vacuo*. The resulting residue was purified via flash chromatography to obtain enone **2-173** as a yellow oil (48 mg, 79%).

^{1}H NMR (500 MHz, $CDCl_3$) δ 8.01 (dd, *J* = 8.2, 0.9 Hz, 1H), 7.59 (td, *J* = 7.5, 1.1 Hz, 1H), 7.49 – 7.43 (m, 1H), 7.25 (dd, *J* = 7.7, 1.4 Hz, 1H), 7.00 (t, *J* = 4.2 Hz, 1H), 2.62 – 2.54 (m, 4H), 2.18 – 2.11 (m, 2H).

^{13}C NMR (126 MHz, $CDCl_3$) δ 196.7, 148.8, 146.7, 139.6, 133.4, 132.3, 131.8, 128.9, 124.4, 38.5, 26.4, 22.7.

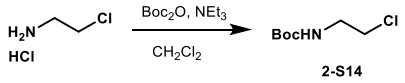

2-S14

***tert*-Butyl (2-chloroethyl)carbamate (2-S14):**

To a solution of 2-chloroethan-1-amine HCl salt (500 mg, 4.31 mmol, 1.0 equiv) in CH_2Cl_2 (9.0 mL) at 0 °C was added NEt_3 (0.78 mL, 5.60 mmol, 1.3 equiv) followed by Boc_2O (1.03 g, 4.74 mmol, 1.1 equiv). The solution was allowed to warm to rt an stirred at rt for 15 h. The reaction solution was washed with H_2O and the aqueous phase was extracted with CHCl3 (2 X). The combined organic phase was washed with H_2O (2 X) and brine, then it was dried with Na_2SO_4, filtered, and concentrated *in vacuo* to obtain protected amine **2-S14** (774 mg, 100%).

^{1}H NMR (500 MHz, $CDCl_3$) δ 4.96 (s, br, 1H), 3.64 – 3.54 (m, 2H), 3.51 –3.39 (m, 2H), 1.45 (s, 9H).

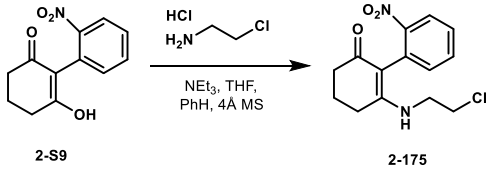

2-S9 2-175

6-((2-Chloroethyl)amino)-2'-nitro-4,5-dihydro-[1,1'-biphenyl]-2(3H)-one (2-175):

A solution of 2-chloroethan-1-amine HCl salt (60 mg, 0.515 mmol, 1.2 equiv) in THF (0.40 mL) was stirred with NEt_3 (0.05 mL, 0.386 mmol, 0.9 equiv) at rt for 5 min, after which ketone **2-S9** (100 mg, 0.429 mmol, 1.0 equiv), benzene (1.0 mL), and 4 Å molecular sieves was added. The solution was heated to 90 °C, and it was stirred at this temperature for 29.5 h. After cooling to rt the slurry was filtered through a pad of celite and the cake was washed with MeOH. The filtrate was concentrated *in vacuo* and the resulting residue was purified via flash chromatography (80 → 95% EtOAc in hex) to obtain enamine **2-175** as a yellow oil (18 mg, 14%)

^{1}H NMR (500 MHz, $CDCl_3$) δ 7.98 (d, *J* = 8.1 Hz, 1H), 7.61 (t, *J* = 7.5 Hz, 1H), 7.46 (t, *J* = 8.4 Hz, 1H), 7.29 (d, *J* = 7.6 Hz, 1H), 4.76 (s, br, 1H), 3.61 – 3.44 (m, 4H), 2.64 – 2.57 (m, 2H), 2.42 (t, *J* = 6.6 Hz, 2H), 2.16 – 2.05 (m, 2H).

HRMS (ESI-TOF) *m/z* calculated for $C_{14}H_{15}ClN_2O_3Na^+$ $(M+Na)^+$ 317.0669, found 317.0668.

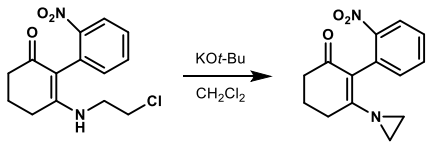

2-175 **2-176**

6-(Aziridin-1-yl)-2'-nitro-4,5-dihydro-[1,1'-biphenyl]-2(3*H*)-one (2-176):

To a solution of amine **2-175** (15 mg, 0.0510 mmol, 1.0 equiv) in CH_2Cl_2 (0.25 mL) was added KO*t*-Bu. The solution turned dark purple and was stirred at rt overnight. The solution was washed with H_2O and the aqueous phase was extracted with CH_2Cl_2 (2 X). The combined organic phase was washed with H_2O (2 X) then brine, and it was dried with Na_2SO_4, filtered, and concentrated *in vacuo*. The resulting residue was purified via flash chromatography (70 → 100% EtOAc in hex) to obtain aziridine **2-176** (8 mg, 62%).

^{1}H NMR (600 MHz, $CDCl_3$) δ 7.98 (d, *J* = 8.1 Hz, 1H), 7.57 (t, *J* = 7.5 Hz, 1H), 7.46 – 7.37 (m, 2H), 2.66 (dt, *J* = 17.5, 5.1 Hz, 1H), 2.55 (ddd, *J* = 17.5, 8.9, 5.4 Hz, 1H), 2.48 (dt, *J* = 16.5, 5.4 Hz, 1H), 2.45 – 2.38 (m, 1H), 2.14 – 2.04 (m, 2H), 1.93 (d, *J* = 6.3 Hz, 2H), 1.88 (d, *J* = 6.2 Hz, 2H).

^{13}C NMR (151 MHz, $CDCl_3$) δ 195.2, 166.9, 149.8, 133.5, 132.5, 129.9, 128.2, 124.1, 121.5, 37.2, 30.0, 28.3, 21.6.

HRMS (ESI-TOF) *m/z* calculated for $C_{14}H_{14}N_2O_3Na^+$ $(M+Na)^+$ 281.0902, found 281.0895.

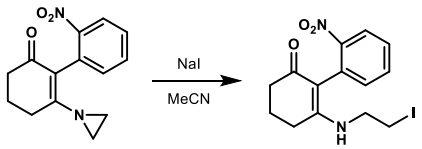

2-176 2-S15

6-((2-Iodoethyl)amino)-2'-nitro-4,5-dihydro-[1,1'-biphenyl]-2(3H)-one (2-S15):

A solution of aziridine **2-176** (7 mg, 0.0270 mmol, 1.0 equiv) and NaI (12 mg, 0.0810 mmol, 3.0 equiv) in MeCN (0.15 mL) was heated to 80 °C for 13 h. Then additional NaI (14 mg, 0.0934 mmol, 3.5 equiv) was added because there was still starting material by TLC. The reaction was heated again to 90 °C and it was stirred at this temperature for 2.5 h. The solution was cooled to rt and it was then concentrated *in vacuo*. The resulting residue was purified via flash chromatography to obtain alkyl iodide **2-S15**.

^{1}H NMR (600 MHz, $CDCl_3$) δ 8.00 (d, *J* = 8.1 Hz, 1H), 7.62 (t, *J* = 7.5 Hz, 1H), 7.47 (t, *J* = 7.8 Hz, 1H), 7.33 (d, *J* = 7.6 Hz, 1H), 4.71 (s, br, 1H), 3.57 – 3.47 (m, 2H), 3.19 (dt, *J* = 10.2, 6.5 Hz, 1H), 3.13 (dt, *J* = 10.2, 6.8 Hz, 1H), 2.61 (td, *J* = 5.6, 2.3 Hz, 2H), 2.43 (t, *J* = 6.6 Hz, 2H), 2.13 (dd, *J* = 12.5, 6.5 Hz, 1H), 2.08 (dd, *J* = 13.7, 6.5 Hz, 1H).

^{13}C NMR (151 MHz, $CDCl_3$) δ 193.2, 160.2, 150.8, 133.9, 133.4, 129.5, 128.8, 125.0, 110.4, 45.1, 36.4, 21.1, 4.5, 0.1.

References

[1] Kuehm-Caubère, C.; Caubère, P.; Jamart-Grégoire, B.; Pfeiffer, B.; Guardiola-Lemaître, B.; Manechez, D.; Renard, P. Novel Thiopyrano[3, 2-` b] And Cycloalkeno[1, 2-*b*] Indole Derivatives with High Inhibitory Properties in LTB4 Production. *Eur. J. Med. Chem*. **1999**, *34*, 51– 61.

[2] Yamuna, E.; Kumar, R. A.; Zeller, M.; Prasad, K. J. R. Synthesis, Antimicrobial, Antimycobacterial and Structure-Activity Relationship of Substituted Pyrazolo-, Isoxazolo-, Pyrimido- and Mercaptopyrimidocyclohepta[*b*]indoles. *Eur. J. Med. Chem*. **2012**, *47*, 228−238.

[3] Murase, M.; Watanabe, K.; Yoshida, T.; Tobinaga, S. A New Concise Synthesis of Arcyriacyanin A and Its Unique Inhibitory Activity Against a Panel of Human Cancer Cell Line. *Chem. Pharm. Bull*. **2000**, *48*, 81−84.

[4] Yeap, J. S.; Tan, C.; Yong, K.; Lim, K.; Lim, S.; Low, Y.; Kam, T. Macroline, talpinine, and sarpagine alkaloids from *Alstonia penangiana*. An NMR-based method for differentiating between *A. penangiana* and *A. macrophylla*. *Phytochemistry* **2020**, *176*, 112391.

[5] Long, S.; Li, C.; Hu, J.; Zhao, Q.; Chen, D. Indole alkaloids from the aerial parts of *Kopsia fruticosa* and their cytotoxic, antimicrobial and antifungal activities. *Fitoterapia* **2018**, *129*, 145–149.

[6] Barf, T.; Lehmann, F.; Hammer, K.; Haile, S.; Axen, E.; Medina, C.; Uppenberg, J.; Svensson, S.; Rondahl, L.; Lundback, T. N-BenzylIndolo Carboxylic Acids: Design and Synthesis of Potent and Selective Adipocyte Fatty-Acid Binding Protein (A-FABP) Inhibitors. *Bioorg. Med. Chem. Lett*. **2009**, *19*, 1745−1748.

[7] Napper, A. D.; Hixon, J.; McDonagh, T.; Keavey, K.; Pons, J.-F.; Barker, J.; Yau, W. T.; Amouzegh, P.; Flegg, A.; Hamelin, E.; Thomas, R. J.; Kates, M.; Jones, S.; Navia, M. A.; Saunders, J. O.; DiStefano, P. S.; Curtis, R. Discovery of Indoles as Potent and Selective Inhibitors of the Deacetylase SIRT1. *J. Med. Chem*. **2005**, *48*, 8045−8054.

[8] Gritsch, P. J.; Stempel, E.; Gaich, T. Enantioselective Synthesis of Cyclohepta[b]indoles: Gram-Scale Synthesis of (*S*)-SIRT1-Inhibitor IV. *Org. Lett.* **2013**, *15*, 5472−5475.

[9] Yamuna, E.; Kumar, R. A.; Zeller, M.; Prasad, K. J. R. Synthesis, Antimicrobial, Antimycobacterial and Structure-Activity Relationship of Substituted Pyrazolo-, Isoxazolo-, Pyrimido- and Mercaptopyrimidocyclohepta[*b*]indoles*. Eur. J. Med. Chem*. **2012**, *47*, 228−238.

[10] Joseph, B.; Alagille, D.; Merour, J.-Y.; Leonce, S. Synthesis and in Vitro Cytotoxic Evaluation of N-Substituted Benzo[5,6]cyclohepta- [*b*]indoles. *Chem. Pharm. Bull*. **2000**, *48*, 1872−1876.

[11] Ishikawa, K.; Mochizuki, Y.; Hirayama, S.; Nemoto, T.; Nagai, K.; Itoh, K.; Fujii, H. Synthesis and Evaluation of Novel Opioid Ligands with a C-Homomorphinan Skeleton. *Bioorg. Med. Chem*. **2016**, *24*, 2199−2205.

[12] Itallie, L.; Steenhauer,A. J. Rauwsolfia serpentina Benth. *Arch. Pharm*. **1932**, *270*, 313–322.

[13] Woodward, R. B. Neuere Entwicklungen in der Chemie der Naturstoffe. *Angew. Chem*. **1956**, *68*, 13–20.

[14] Masamune, S.; Ang, S. K.; Egli, C.; Nakatsuka, N.; Sarkar, S. K.; Yasunari, Y. Synthesis of ajmaline. *J. Am. Chem. Soc*. **1967**, *89*, 2506–2507.

[15] Li, J.; Wang, T.; Yu, P.; Peterson, A.; Weber, R.; Soerens, D.; Grubisha, D.; Bennett, D.; Cook, J. M. General Approach for the Synthesis of Ajmaline/Sarpagine Indole Alkaloids: Enantiospecific Total Synthesis of (+)-Ajmaline, Alkaloid G, and Norsuaveoline via the Asymmetric Pictet−Spengler Reaction. *J. Am. Chem. Soc*. **1999**, *121*, 6998–7010.

[16] Mashimo, K.; Sato, Y. Synthesis of isoajmaline. *Tetrahedron Lett*. **1969**, *10*, 901–904.

[17] Van Tamelen, E. E.; Oliver, L. K. The Biogenetic-type Total Synthesis of Ajmaline. *J. Am. Chem. Soc*. **1990**, *92*, 2136–2137.

[18] Carroll, A. R.; Hyde, E.; Smith, J.; Quinn, R. J.; Guymer, G.; and Forster, P. I. Actinophyllic Acid, a Potent Indole Alkaloid Inhibitor of the Coupled Enzyme Assay Carboxypeptidase U/Hippuricase from the Leaves of *Alstonia actinophylla* (Apocynaceae). *J. Org. Chem*. **2005**, *70*, 1096– 1099.

[19] Martin, C. L.; Overman, L. E.; Rohde, J. M. Total Synthesis of (±)- and (−)-Actinophyllic Acid. *J. Am. Chem. Soc.* **2010**, *132*, 4894–4906.

[20] Yoshii, Y.; Tokuyama, H.; Chen, D. Y. K. Total Synthesis of Actinophyllic Acid. *Angew. Chem. Int. Ed*. **2017**, *56*, 12277–12281.

[21] Cai, L.; Zhang, K.; Kwon, O. Catalytic Asymmetric Total Synthesis of (–)-Actinophyllic Acid. *J. Am. Chem. Soc.* **2016**, *138*, 3298–3301.

[22] Granger, B. A.; Jewett, I. T.; Butler, J. D.; Hua, B.; Knezevic, C. E.; Parkinson, E. I.; Hergenrother, P. J.; Martin, S. F. Synthesis of (±)-Actinophyllic Acid and Analogs: Applications of Cascade Reactions and Diverted Total Synthesis. *J. Am. Chem. Soc.* **2013**, *135*, 12984–12986.

[23] Yeap, J. S.; Navanesan, S.; Sim, K.; Yong, K.; Gurusamy, S.; Lim, S.; Low, Y; Kam, T. Ajmaline, Oxindole, and Cytotoxic Macroline–Akuammiline Bisindole Alkaloids from *Alstonia penangiana*. *J. Nat. Prod*. **2018**, *81*, 1266−1277.

[24] Yeap, J. S.; Tan, C.; Yong, K.; Lim, K.; Lim, S.; Low, Y.; Kam, T. Macroline, talpinine, and sarpagine alkaloids from *Alstonia penangiana.* An NMR-based method for differentiating between *A. penangiana* and *A. macrophylla. Phytochemistry* **2020**, *176*, 112391.

[25] Hu, J.; Mao, X.; Shi, X.; Jin, N.; Shi, J. Monoterpenoid Indole Alkaloids from the Leaves of *Alstonia scholaris*. *Chem. Nat. Prod*. **2018**, *54*, 934−937.

[26] Zhang, Z.; Du, R.; He, J.; Wu, X.; Li, Y.; Li, R. Three new monoterpenoid indole alkaloids from Vinca major. *J. Asian Nat. Prod. Res*. **2015**, *18*, 328−333.

[27] Rukachaisirikul, T.; Chokchaisiri, S.; Suebsakwong, P.; Suksamrarn, A.; Tocharus, C. A New Ajmaline-type Alkaloid from the Roots of *Rauvolfia serpentina*. *Nat. Prod. Commun*. **2017**, *12*, 495−498.

[28] Steglich, W. Slime moulds (Myxomycetes) as a source of new biologically active metabolites. *Pure App. Chem*. **1989**, *61*, 281–288.

[29] Kamata, K.; Suetsugu, T.; Yamamoto, Y.; Hayashi, M.; Komiyama, K.; Ishibashi, M. Bisindole Alkaloids From Myxomycetes *Arcyria Denudata* And *Arcyria Obvelata*. *J. Nat. Prod*. **2006**, *69*, 1252−1254.

[30] Murase, M.; Watanabe, K.; Yoshida, T.; Tobinaga, S. A New Concise Synthesis of Arcyriacyanin A and Its Unique Inhibitory Activity against a Panrl of Human Cancer Cell Line. *Chem. Pharm. Bull*. **2000**, *48*, 81−84.

[31] Su, J.-Y.; Zhu, Y.; Zeng, L.-M.; Xu, X.-H. A New Bisindole From Alga Caulerpa Serrulata. *J. Nat. Prod*. **1997**, *60*, 1043−1044.

[32] Liu, B.-Y.; Zhang, C.; Zeng, K.-W.; Li, J.; Guo, X.-Y.; Zhao, M.- B.; Tu, P.-F.; Jiang, Y. Exotines a and B, Two Heterodimers of Isopentenyl-Substituted Indole and Coumarin Derivatives From Murraya Exotica. *Org. Lett*. **2015**, *17*, 4380−4383.

[33] Hohlman, R. M.; Sherman, D. H.; Recent advances in hapalindole-type cyanobacterial alkaloids: biosynthesis, synthesis, and biological activity. *Nat. Prod. Rep*. **2021**, *38*, 1567−1588.

[34] Smitka, T. A.; Bonjouklian, R.; Doolin, L.; Jones, N.; Deeter, J. B.; Yoshida, W. Y.; Prinsep, M. R.; Moore, R. E.; Patterson, G. M. L. Ambiguine Isonitriles, Fungicidal Hapalindole-Type Alkaloids From Three Genera of Blue-Green Algae Belonging to the Stigonemataceae. *J. Org. Chem*. **1992**, *57*, 857−861.

[35] Huber, U.; Moore, R. E.; Patterson, G. M. L. Isolation of a Nitrile-Containing Indole Alkaloid From the Terrestrial Blue-Green Alga Hapalosiphon Delicatulus. *J. Nat. Prod*. **1998**, *61*, 1304−1306.

[36] Raveh, A.; Carmeli, S. Antimicrobial Ambiguines From the Cyanobacterium Fischerella Sp. *J. Nat. Prod*. **2007**, *70*, 196−201.

[37] Mo, S.; Krunic, A.; Chlipala, G.; Orjala, J. Antimicrobial Ambiguine Isonitriles From the Cyanobacterium Fischerella Ambigua. *J. Nat. Prod*. **2009**, *72*, 894−899.

[38] Mo, S.; Krunic, A.; Santarsiero, B. D.; Franzblau, S. G.; Orjala, J. Hapalindole-Related Alkaloids From the Cultured Cyanobacterium Fischerella Ambigua. *Phytochemistry* **2010**, *71*, 2116−2123.

[39] Acuña, U. M.; Zi, J.; Orjala, J.; Carcache de Blanco, E. J. Ambiguine I isonitrile from Fischerella ambigua induces caspaseindependent cell death in MCF-7 hormone dependent breast cancer cells. *Int. J. Cancer Res*. **2015**, *49*, 1655−1662.

[40] *Dictionary of Alkaloids with CD-ROM*, Vol 2. Buckingham, J.; Baggaley, K. H.; Roberts, A. D.; Szabo, L. F. Eds. CRC Press: Boca Raton. **2012**, https://doi.org/10.1201/EBK1420077698.

[41] Kam, T.; Choo, Y. Kopsifolines A–F: a New Structural Class of Monoterpenoid Indole Alkaloids from Kopsia. *Helv. Chim. Acta*. **2004**, *87*, 991–998.

[42] Zhu, X.; Fan, Y.; Xu, L.; Liu, Q.; Wu, J.; Li, J.; Gao, K.; Yue, J. Alstonlarsines A–D, Four Rearranged Indole Alkaloids from *Alstonia scholaris*. *Org. Lett.* **2019**, *21*, 1471–1474.

[43] Stempel, E.; Gaich, T. Cyclohepta[*b*]indoles: A Privileged Strucutre Motif in Natural Products and Drug Design. *Acc. Chem. Res*. **2016**, *49*, 2390–2402.

[44] Gierok, J.; Benedix, L.; Hiersemann, M. An Update on Cyclohepta[*b*]indoles. *Eur. J. Org. Chem*. **2021**, *2021*, 3748–3758.

[45] Tymann, D.; Tymann, D. C.; Bednarzick, U.; Iovkova-Berends, L.; Rehbein, J.; Heirsemann, M. Development of an Alkyne Analogue of the de Mayo Reaction: Synthesis of Medium-Sized Carbacycles and Cyclohepta[*b*]indoles. *Angew. Chem. Int. Ed.* **2018**, *57*, 15553–15557.

[46] Tymann, D. C.; Benedix, L.; Iovkova, L.; Pallach, R.; Henke, S.; Tymann, D.; Hiersemann, M. Photochemical Approach to the Cyclohepta[*b*]indole Scaffold by Annulative Two-Carbon Ring-Expansion. *Chem. Eur. J.* **2020**, *26*, 11974–11978.

[47] Mu, X.; Li, Y.; Zheng, N.; Long, J.; Chen, Si.; Liu, B.; Zhao, C. Stereoselective Synthesis of Cyclohepta[*b*]indoles by Visible-Light-Induced [2+2]-Cycloaddition/retro-Mannich-type Reactions. *Angew. Chem. Int. Ed*. **2021**, *60*, 11211–11216.

[48] Wang, Z.; Addepalli, Y.; He, Y. Construction of Polycyclic Indole Derivatives via Multiple Aryne Reactions with Azaheptafulvenes. *Org. Lett*. **2018**, *20*, 644–647.

[49] Mishra, U. K.; Yadav, S.; Ramasastry, S. S. V. One-Pot Multicatalytic Approaches for the Synthesis of Cyclohepta[b]indoles, Indolotropones, and Tetrahydrocarbazoles. *J. Org. Chem*. **2017**, *82*, 6729–6737.

[50] Zeng, Q.; Dong, K.; Huang, J.; Qiu, L.; Xu, X. Copper-catalyzed carbene/alkyne metathesis terminated with the Buchner reaction: synthesis of dihydrocyclohepta[b]indoles. *Org. Biomol. Chem*. **2019**, *17*, 2326–2330.

[51] Dhawa, U.; Connon, R.; Oliveira, J. C. A.; Ackerman, L. Enantioselective Ruthenium-Catalyzed C–H Alkylations by a Chiral Carboxylic Acid with Attractive Dispersive Interactions. Org. Lett. 2021, 23, 2760-2765.

[52] Zhang, J.; Shao, J.; Xur, J.; Wang, Y.; Li, Y. One pot hydroamination/[4 + 3] cycloaddition: synthesis towards the cyclohepta[*b*]indole core of silicine and ervatamine. RSC Adv. 2014, 4, 63850–63854.

[53] Joseph, B.; Cornec, O.; Merour, J.-Y. Intramolecular Heck Reaction: Synthesis of Benzo[4,5]cyclohepta[*b*]indole Derivatives. *Tetrahedron* **1998**, *54*, 7765−7776.

[54] He, S.; Hsung, R. P.; Presser, W. R.; Ma, Z.-X.; Haugen, B. J. An Approach to Cyclohepta[*b*]indoles Through an Allenamide [4+3] Cycloaddition−Grignard Cyclization−Chugaev Elimination Sequence. *Org. Lett*. **2014**, *16*, 2180−2183.

[55] Shu, D.; Song, W.; Li, X.; Tang, W. Rhodium- and PlatinumCatalyzed [4 + 3] Cycloaddition with Concomitant Indole Annulation: Synthesis of Cyclohepta[*b*]indoles. *Angew. Chem. Int. Ed*. **2013**, *52*, 3237−3240.

[56] Kusama, H.; Sogo, H.; Saito, K.; Suga, T.; Iwasawa, N. Construction of Cyclohepta[b]indoles Via Platinum-Catalyzed Intermolecular Formal [4 + 3]-Cycloaddition Reaction of α,β-Unsaturated Carbene Complex Intermediates with Siloxydienes. *Synlett* **2013**, *24*, 1364−1370.

[57] Liu, J.; Wang, L.; Wang, X.; Xu, L.; Hao, Z.; Xiao, J. Fluorinated alcohol-mediated [4 + 3] cycloaddition reaction of indolyl alcohols with cyclopentadiene. *Org. Biomol. Chem.* **2016**, *14*, 11510–11517.

[58] Zhang, H.; Zhu, Z.; Fan, T.; Liang, J.; Shi, F. Intermediate-Dependent Unusual [4+3], [3+2] and Cascade Reactions of 3-Indolylmethanols: Controllable Chemodivergent and Stereoselective Synthesis of Diverse Indole Derivatives. *Adv. Synth. Catal*. **2016**, *358*, 1259–1288.

[59] Li, Y.; Zhu, C.; Zhang, J. Gold-Catalyzed [4+3] Cycloaddition/C–H Functionalization Cascade: Regio- and Diastereoselective Route to Cyclohepta[*b*]indoles. *Eur. J. Org. Chem*. **2017**, *2017*, 6609–6613.

[60] Xu, G.; Chen, L.; Sun, J. Rhodium-Catalyzed Asymmetric Dearomative [4 + 3]-Cycloaddition of Vinylindoles with Vinyldiazoacetates: Access to Cyclohepta[*b*]indoles. *Org. Lett*. **2018**, *20*, 3408–3412.

[61] Gelis, C.; Levitre, G.; Merad, J.; Retailleau, P.; Neuville, L.; Masson, G. Highly Diastereo- and Enantioselective Synthesis of Cyclohepta[*b*]indoles by Chiral-Phosphoric-Acid-Catalyzed (4+3) Cycloaddition. *Angew. Chem. Int. Ed*. **2018**, *130*, 12297–12301.

[62] Zheng, X.; Sun, H.; Yang, W.; Deng, W. Elaboration of phosphoramidite ligands enabling palladium-catalyzed diastereo- and enantioselective all carbon [4+3] cycloaddition. *Sci. China Chem*. **2020**, *63*, 911–916.

[63] Pirovano, V.; Brambilla, E.; Moretti, A.; Rizzato, S.; Abbiati, G.; Nava, D.; Rossi, E. Synthesis of Cyclohepta[b]indoles by (4 + 3) Cycloaddition of 2-Vinylindoles or 4H-Furo[3,2-*b*]indoles with Oxyallyl Cations. *J. Org. Chem*. **2020**, *85*, 3265–3276.

[64]Yang, W.; Li, W.; Yang, Z.; Deng, W. Organocatalytic Regiodivergent Ring Expansion of Cyclobutanones for the Enantioselective Synthesis of Azepino[1,2-*a*]indoles and Cyclohepta[*b*]indoles*. Org. Lett*. **2020**, *22*, 4026–4032.

[65] Takeda, T.; Harada, S.; Okabe, A.; Nishida, A. Cyclohepta[*b*]indole Synthesis through [5 + 2] Cycloaddition: Bifunctional Indium (III)-Catalyzed Stereoselective Construction of 7-Membered Ring Fused Indoles. *J. Org. Chem*. **2018**, *83*, 11541–11551.

[66] Hamada, N.; Yoshida, Y.; Oishi, S.; Ohno, H. Gold-Catalyzed Cascade Reaction of Skipped Diynes for the Construction of a Cyclohepta[*b*]pyrrole Scaffold. *Org. Lett*. **2017**, *19*, 3875–3878.

[67] Kaufmann, J.; Jäckel, E.; Haak, E. Ruthenium-Catalyzed Cascade Annulation of Indole with Propargyl Alcohols. *Angew. Chem. Int. Ed.* **2018**, *57*, 5908–5911.

[68] Jadhav, A. S.; Pankhade, Y. A.; Anand, R. V. Exploring Gold Catalysis in a 1,6-Conjugate Addition/Domino Electrophilic Cyclization Cascade: Synthesis of Cyclohepta[*b*]indoles. *J. Org. Chem.* **2018**, *83*, 8615–8626.

[69] Parker, A. N.; Martin, C.; Shenje, R.; Fance, S. Calcium-Catalyzed Formal [5 + 2] Cycloadditions of Alkylidene β-Ketoesters with Olefins: Chemodivergent Synthesis of Highly Functionalized Cyclohepta[*b*]indole Derivatives. *Org. Lett*. **2019**, *21*, 7268-7273.

[70] Mei, G.; Yuan, H.; Gu, Y.; Chen, W.; Chung, L. W.; Li, C.-C. Dearomative Indole [5 + 2] Cycloaddition Reactions: Stereoselective Synthesis of Highly Functionalized Cyclohepta[*b*]indoles. *Angew. Chem. Int. Ed*. **2014**, *53*, 11051−11055.

[71] Wender, P. A.; Mascarenas, J. L. A New [5 + 2] Cycloaddition Method and Its Application to the Synthesis of BC Ring Precursors of Phorboids. *J. Org. Chem*. **1991**, *56*, 6267−6269.

[72] Chakraborty, A.; Goswami, K.; Adiyala, A.; Sinha, S. Syntheses of Spiro[cyclopent[3]ene-1,3′-indole]s and Tetrahydrocyclohepta[*b*]indoles from 2,3-Disubstituted Indoles through Sigmatropic Rearrangement. *Eur. J. Org. Chem*. **2013**, *2013*, 7117−7127.

[73] Ishikura, M.; Kato, H. A synthetic use of the intramolecular alkyl migration process in indolylborates for intramolecular cyclization: a novel construction of carbazole derivatives. *Tetrahedron* **2002**, *58*, 9827−9838.

[74] Liu, C.; Widenhoefer, R. A. Palladium-Catalyzed Cyclization/ Carboalkoxylation of Alkenyl Indoles. *J. Am. Chem. Soc*. **2004**, *126*, 10250−10251.

[75] Anet, F. A. L.; Chakravarti, D.; Robinson, R.; Schlittler, E. Ajmaline. Part I. *J. Chem. Soc*. **1954**, 1242−1260.

[76] Mashimo, K.; Sato, Y. Synthesis of isoajmaline. *Tetrahedron Lett*. **1969**, *10*, 901−904.

[77] Mashimo, K.; Sato, Y. A Contribution to the Synthesis of Ajmaline. *Chem. Pharm. Bull*. **1970**, *18*, 353−355.

[78] Bartlett, M. F.; Lambert, B. F.; Werblood, H. M.; Taylor, W. I. Rauwolfia Alkaloids. XLIII.[1] A Facile Ring Closure of Deoxyajmalal-A to Deoxyajmaline. *J. Am. Chem. Soc.* **1963**, *85*, 475–477.

[79] Hobson, J. D.; McCluskey, J. G. Cleavage of tertiary bases with phenyl chloroformate: the reconversion of 21-deoxyajmaline into ajmaline. *J. Chem. Soc. C* **1967**, 2015–2017.

[80] Carroll, A. R.; Hyde, E.; Smith, J.; Quinn, R. J.; Guymer, G.; Forster, P. I. Actinophyllic Acid, a Potent Indole Alkaloid Inhibitor of the Coupled Enzyme Assay Carboxypeptidase U/Hippuricase from the Leaves of *Alstonia actinophylla* (Apocynaceae). *J. Org. Chem*. **2005**, *70*, 1096–1099.

[81] Martin, C. L.; Overman, L. E.; Rohde, J. M. Total Synthesis of (±)-Actinophyllic Acid. *J. Am. Chem. Soc.* **2008**, *130*, 7568–7569.

[82] Taniguchi, T.; Martin, C. L.; Monde, K.; Nakanishi, K.; Berova, N.; Overman, L. E. Absolute Configuration of Actinophyllic Acid As Determined through Chiroptical Data. *J. Nat. Prod.* **2009**, *72*, 430–432.

[83] Quirion, J. C.; Kan-Fan, C.; Bick, I. R. C.; Husson, H. P. Aristolasol and aristolasene: Indole alkaloids from *Aristotelia australasica*. *Phytochemistry* **1988**, *27*, 3337–3339.

[84] Dobler, M.; Beerli, R.; Weissmahr, W. K.; Borschberg, H. Synthesis of *Aristotelia*-type alkaloids. Part XI. Total syntheses of (+)-sorelline and (+)-aristolasene. *Tetrahedron: Asymm*. **1992**, *3*, 1411–1420.

[85] Beerli, R.; Borschberg, H. Synthesis of *Aristotelia*-type alkaloids. Part VI. Biomimetic Synthesis of (+)-Aristofruticosine. *Helv. Chim. Acta*. **1991**, *74*, 110–116.

[86] Fresneda, P. M.; Molina, P.; Saez, M. A. The First Synthesis of the (Bis)indole Marine Alkaloid Caulersin. *Synlett*. **1999**, 1651–1653.

[87] Wahlström, N.; Stensland, B.; Bergman, J. Synthesis of the marine alkaloid caulersin. *Tetrahedron* **2004**, *60*, 2147–2153.

[88] Bergman, J. Stålhandske, C. Cyclization of N-Acylanthranilic Acids with Vilsmeier Reagents. Chemical and Structure Studies. *Tetrahedron* **1996**, *52*, 753–770.

[89] Miki, Y.; Aoki, Y.; Miyatake, H.; Minematsu, T.; Hibino, H. Synthesis of caulersin and its isomers by reaction of indole-2,3-dicarboxylic anhydrides with methyl indoleacetates. *Tetrahedron Lett.* **2006**, *47*, 5215–5218.

[90] Brenner, M.; Mayer, G.; Terpin, A.; Steglich, W. Total Syntheses of the Slime Mold Alkaloid Arcyriacyanin A. *Chem. Eur. J*. **1997**, *3*, 70–74.

[91] Murase, M.; Matanabe, K.; Kurihara, T.; Tobinaga, S. A Synthesis of Arcyriacyanin A, an unsymmetrical Substituted Indole Pigment of the Slime Mould by Palladium Catalyzed Cross-Coupling Reaction. *Chem. Pharm. Bull*. **1998**, *46*, 889–892.

[92] Bennasar, M.; Vidal, B.; Bosch, J. A synthetic route to the alkaloids of the ervatamine group. First total synthesis of (+)-6-oxo-16-episilicine. *Chem. Commun*. **1996**, 2755–2756.

[93] Bennasar, M.; Vidal, B.; Bosch, J. Biomimetic Total Synthesis of Ervitsine and Indole Alkaloids of the Ervatamine Group via 1,4-Dihydropyridines. *J. Org. Chem*. **1997**, *62*, 3597–3609.

[94] Amat, M.; Llor, N.; Checa, B.; Molins, E.; Bosch, J. A Synthetic Approach to Ervatamine-Silicine Alkaloids. Enantioselective Total Synthesis of (−)-16-Episilicine. *J. Org. Chem*. **2010**, *75*, 178–189.

[95] Amat, M.; Llor, N.; Hidalgo, J.; Bosch, J. A concise procedure for the preparation of enantiopure 3-alkylpiperidines. *Tetrahedron: Asymm*. **1997** *8*, 2237–2240.

[96] Lepovitz, L. T.; Martin, S. F. Biomimetically Inspired, One-Step Synthesis of Exotine A and Exotine B. *J. Org. Chem*. **2021**, *86*, 10946–10953.

[97] Cheng, B.; Volpin, G.; Morstein, J.; Trauner, D. Total Synthesis of (±)–Exotine B. *Org. Lett.* **2018**, *20*, 4358–4361.

[98] Johnson, R. E.; Ree, H.; Hartmnn, M.; Lang, L.; Sawano, S.; Sarpong, R. Total Synthesis of Pentacyclic (−)-Ambiguine P Using Sequential Indole Functionalizations. *J. Am. Chem. Soc*. **2019**, *141*, 2233−2237.

[99] Baran, P. S.; Richter, J. M. Direct Coupling of Indoles with Carbonyl Compounds: Short, Enantioselective, Gram-Scale Synthetic Entry into the Hapalindole and Fischerindole Alkaloid Families. *J. Am. Chem. Soc.* **2004**, *126*, 7450–7451.

[100] Dauben, W. G.; Michno, D. M. Direct oxidation of tertiary allylic alcohols. A simple and effective method for alkylative carbonyl transposition. *J. Org. Chem*. **1977**, *42*, 682–685.

[101] Xu, J.; Rawal, V. H. Total Synthesis of (−)-Ambiguine P. *J. Am. Chem. Soc*. **2019**, *141*, 4820−4823.

[102] Hu, L.; Rawal, V. H. Total Synthesis of the Chlorinated Pentacyclic Indole Alkaloid (+)-Ambiguine G. *J. Am. Chem. Soc*. **2021**, *143*, 10872−10875.

[103] Lee, K.; Boger, D. Total Syntheses of (−)-Kopsifoline D and (−)-Deoxoapodine: Divergent Total Synthesis via Late-Stage Key Strategic Bond Formation. *J. Am. Chem. Soc*. **2014**, *136*, 3312–3317.

[104] Myeong, I.; Avci, N. H.; Movassaghi, M. Total Synthesis of (−)-Kopsifoline A and (+)-Kopsifoline E. *Org. Lett*. **2021**, *23*, 9118–9112.

[105] Gan, L.; Yang, S.; Wu, Y.; Ding, J.; Yue, J. Terpenoid Indole Alkaloids from *Winchia calophylla*. *J. Nat. Prod.* **2006**, *69*, 18–22.

[106] Heffernan, S. J.; Tellam, J. P.; Queru, M. E.; Silvanus, A. C.; Benito, D.; Mahon, M. F.; Hennessy, A. J.; Andrews, B. I.; Carbery, D. R. Double Gold-Catalysed Annulation of Indoles by Enynones. *Adv. Synth. Cat*. **2013**, *355*, 1149–1159.

[107] Solé, D.; Bosch, J.; Bonjoch, J. 3a-(o-Nitrophenyi)octahydroindol-4-ones: Synthesis and Spectroscopic Analysis. *Tetrahedron* **1996**, *52*, 4013−4028.

[108] Bonjoch, J.; Solé, D.; García-Rubio, S.; Bosch, J. A General Synthetic Entry to Strychnos Alkaloids of the Curan Type via a Common 3a-(2-Nitrophenyl)hexahydroindol-4-one Intermediate. Total Syntheses of (±)- and (−)-Tubifolidine, (±)-Akuammicine, (±)-19,20-Dihydroakuammicine, (±)-Norfluorocurarine, (±)-Echitamidine, and (±)-20-Epilochneridine. *J. Am. Chem. Soc.* **1997**, *119*, 7230–7240.

[109] Whitlock, H. W.; Smith, G. L. The Total Synthesis of *dl*-Crinine. *J. Am. Chem. Soc*. **1967**, *89*, 3600–3606.

[110] Calogeropoulou, T.; Angelou, P.; Detsi, A.; Fragiadaki, I.; Scoulica, E. Design and Synthesis of Potent Antileishmanial Cycloalkylidene-Substituted Ether Phospholipid Derivatives. *J. Med. Chem*. **2008**, *51*, 897–908.

[111] Cain, D. L.; McLaughlin, C.; Molloy, J. J.; Carpenter-Warren, C.; Anderson, N. A.; Watson, A. J. B. A Cascade Suzuki–Miyaura/Diels–Alder Protocol: Exploring the Bifunctional Utility of Vinyl Bpin. *Synlett* **2019**, *30*, 787–791.

[112] Boelke, A.; Caspers, L. D.; Nachtsheim, B. J. NH_2-Directed C–H Alkenylation of 2-Vinylanilines with Vinylbenziodoxolones. *Org. Lett*. **2017**, *19*, 5344–5347.

[113] González-Sabín, J.; Gotor, V.; Rebolledo, F. Optically active *trans*-2-aminocyclopentanols: Chemoenzymatic preparation and application as chiral ligands. *Biotechnol. J*. **2006**, *1*, 835–841.

[114] Sharley, J. S.; Collado Pérez, A. M.; Ferri, E. E.; Miranda, A. F.; Baxendale, I. R. α, β-Unsaturated ketones via copper(II) bromide mediated oxidation. *Tetrahedron* **2016**, *72*, 2947–2954.

[115] Loya, D. R.; Jean, A.; Cormier, M.; Fressigné, C.; Nejrotti, S.; Blanchet, J.; Maddaluno, J.; De Paolis, M. Domino Ring Expansion: Regioselective Access to 9-Membered Lactones with a Fused Indole Unit from 2-Nitrophenyl-1,3-cyclohexanediones. *Chem. Eur. J*. **2018**, *24*, 2080–2084.

[116] Smith, A. B.; Kürti, L.; Davulcu, A. H.; Cho, Y. S.; Ohmoto, K. Indole Diterpene Synthetic Studies: Development of a Second-Generation Synthetic Strategy for (+)-Nodulisporic Acids A and B. *J. Org. Chem.* **2007**, *72*, 4611–4620.

Chapter 3. Total Syntheses of Strasseriolide A and B, Antimalarial Macrolide Natural Products

3.1 Introduction

3.1.1 Malaria and antimalarial drugs

Malaria is a highly infectious and deadly disease, but can be prevented with proper treatments. This disease is concentrated in underdeveloped sub-tropical regions. According to the World Health Organization (WHO), there were about 241 million cases of the disease in 2020.[1] About 627 thousand deaths were recorded, most of whom were children; this is a large increase from the previous year, partially due to the COVID-19 pandemic.[1] The parasitic species *Plasmodium falciparum* is responsible for the most virulent strain of malaria in humans. One of the most concerning data points is that over the past few decades resistance to antimalarial treatments has been on the rise.[2–5] Chloroquine was one of the first drugs used to treat and prevent malaria; however, just a couple decades after widespread use, chloroquine resistant strains of *P. falciparum* became prevalent.[5] Due to chloroquine's significant decrease in effectiveness, it is not recommended to be used alone to treat malaria.[4] Artemisinin, and its derivatives, in combination with a partner drug is the current front-line therapy against mild to serve cases of malaria.[1] Even though much precaution has been taken with this combination therapy, resistance to artemisinin (and its derivatives) was feared and has recently been discovered.[2] This report is extremely worrisome as artemisinin-based treatments are the last line of defense against the drug resistant parasites. The lack of structural diversity within antimalarial treatments and the rise of drug resistant strains inspired a high throughput screening (HTS) study that was performed by Pérez-Moreno and co-authors to discover a potential new class of antimalarial treatments.[6]

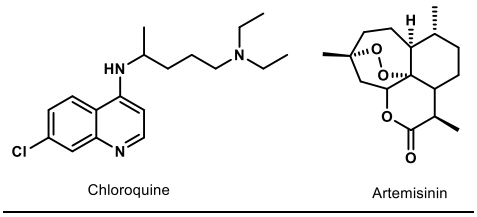

Figure 3.1. Structures of antimalarial agents chloroquine and artemisinin.

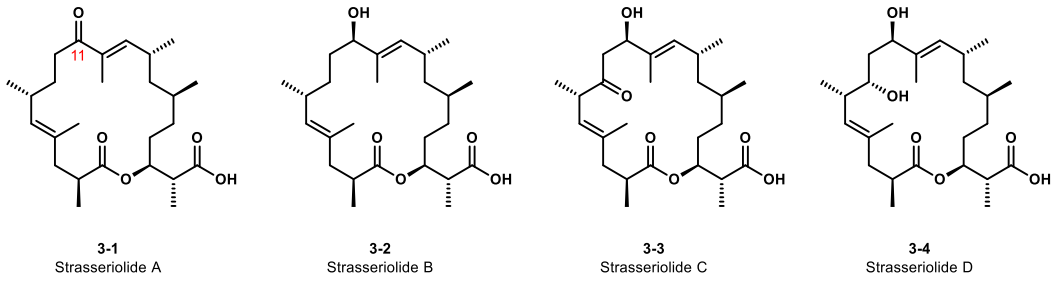

Figure 3.2. Structures of strasseriolides A–D

The group screened 22,000 microbial extracts from Fundacioń MEDINA's natural product collection and isolated strasseriolides A–D from an extract produced by the fungus, *Strasseria geniculata* CF-247251.[7] This microbe was originally isolated as an axenic culture from the root of an unnamed plant in New Zealand. The structures of the macrolides were elucidated by NMR, and the absolute configuration was determined by X-ray crystallography (Figure 3.2). Strasseriolides A–D were examined for their biological activity against the drug-sensitive strain of the parasite, *P. falciparum* parasite 3D7, and were found to have IC_{50} values of 9.810, 0.013, 0.123, and 0.128 μM respectively (Table 3.1). Strasseriolide B (**3-2**) was additionally tested against chloroquine-resistant *P. falciparum* strain Dd2 and was found to have an IC_{50} value of 0.0322 μM. These values are comparable with chloroquine and artemisinin.[8] The macrolide was also found to be non-cytotoxic against HepG2 cells proving that it was selective for the parasite.

Antimalarial	IC_{50} 3d7 (nM)	IC_{50} Dd2 (nM)
Chloroquine	12 nM	125 nM
Artemisinin	11 nM	12 nM
3-1	9810 nM	-
3-2	13 nM	32 nM
3-3	123 nM	-
3-4	128 nM	185 nM

Table 3.1. IC_{50} values of chloroquine, artemisinin, and strassiolides A–D against *P. falciparum* 3d7 and Dd2.

The hydroxy group at C11 is imperative for the potency against the parasite. Strasseriolide A, which has a ketone in place of the C11 alcohol is 750X less potent than B. Although the mode of action for the strasseriolides is currently unknown, this data suggests that the macrolides might inhibit the *P. falciparum* lactate dehydrogenase enzyme and hinder glycolysis of the parasite.[7] In order to better understand the mode of action, our group set out to synthesize strasseriolides A and B, which is a promising starting point for a new class of antimalarial treatments.

3.1.2 Macrocycles and drug discovery

Macrocycles, or molecules with rings containing 12 atoms or more, are common in nature, but less prevalent in drug discovery. Almost all of the approved macrocyclic pharmaceuticals are natural products or are derived from natural products.[9–10] However, synthetic macrocycles are an underexplored and unexploited class of potential drugs. Although they do not follow the "rule of five" that is typical of most small molecules in drug discovery,[11] there is a lot of potential within this space. Macrocycles are flexible, but often have some conformational bias. These molecules are also able to span a larger surface area of a target and can mold to a target area better than small molecules due to their plasticity.[9–10] These characteristics allow for more a potent and selective substrate and the synthetic macrocycles deserve more attention in drug discovery.

One of the many reasons macrocycles have been underexplored is due to the difficulty in forming medium to large sized rings. However, over the past couple of decades, there have been huge strides in the development of robust macrocyclization methods beyond the widely used macrolactonization and macrolactamization.[12–21] In this section, I will discuss examples of macrocyclization strategies that were considered for our route to the strasseriolides.

3.1.3 Ring closing alkyne metathesis

Our initial disconnection to close the macrocycle of strasseriolide B was a ring closing alkyne metathesis (RCAM). This method has been made popular and extensively used by the Fürstner group.[22] The group has developed new RCAM catalysts (**3-6** to **3-10**) that are more active, more functional group tolerant, and easier to use (stable in air) compared to the earlier Schrock alkyne metathesis catalysts **3-5** (Figure 3).[23–28] They have applied these catalysts to a wide variety of total syntheses of macrocyclic natural products (examples shown below). In addition to successfully making the macrocyclic rings, the group has also developed post-

macrocyclization methods, beyond just simple alkyne reduction.[29–36] These strategies have further enhanced the synthesis of macrocycles.

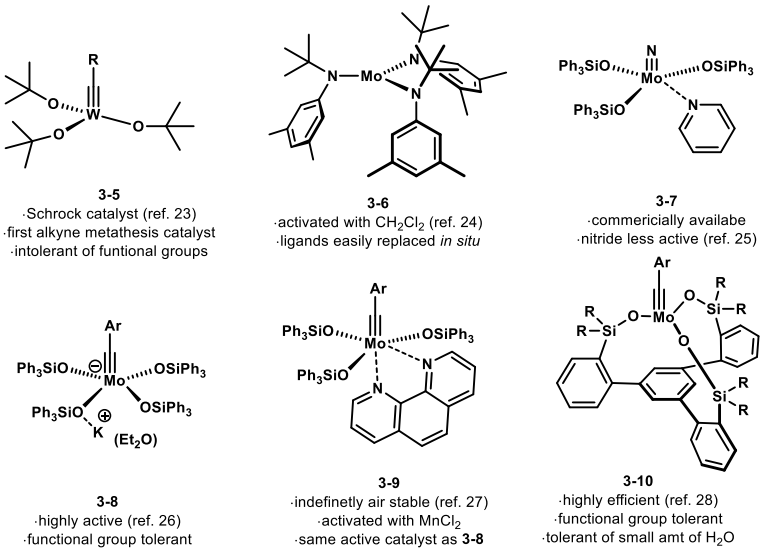

Figure 3.3. Structures of alkyne metathesis catalysts and their characteristics

It is relevant to discuss why RCAM is useful beyond ring closing alkene metathesis (RCM). The extensive use of RCM in natural product synthesis,[15] and in industry,[37] shows how easily accessible, user friendly, and efficient these catalysts are. Rings of all sizes have been forged by this methodology, however, there are limitations. It is not straightforward to predict the E:Z selectivity of the resulting alkene, and often a stereochemical mixture is observed. In some unfortunate cases, the undesired alkene isomer is obtained and isomerization is not always facile.[38] RCAM has the advantage that the resulting alkyne can be selectively reduced to exclusively form one alkene diastereomer. Additionally, olefin metathesis catalysts can react with both double and triple bonds (as shown by ene-yne metathesis),[39] yet alkyne metathesis catalysts are highly selective for alkynes, reducing the potential for undesired side reactions. The alkyne created from the metathesis is also a great handle for additional functionalization, other than just reduction. This section will cover examples of RCAM in total synthesis with focus on two main post-cyclization strategies: π-acid activation of alkynes and hydrometallation of alkynes.

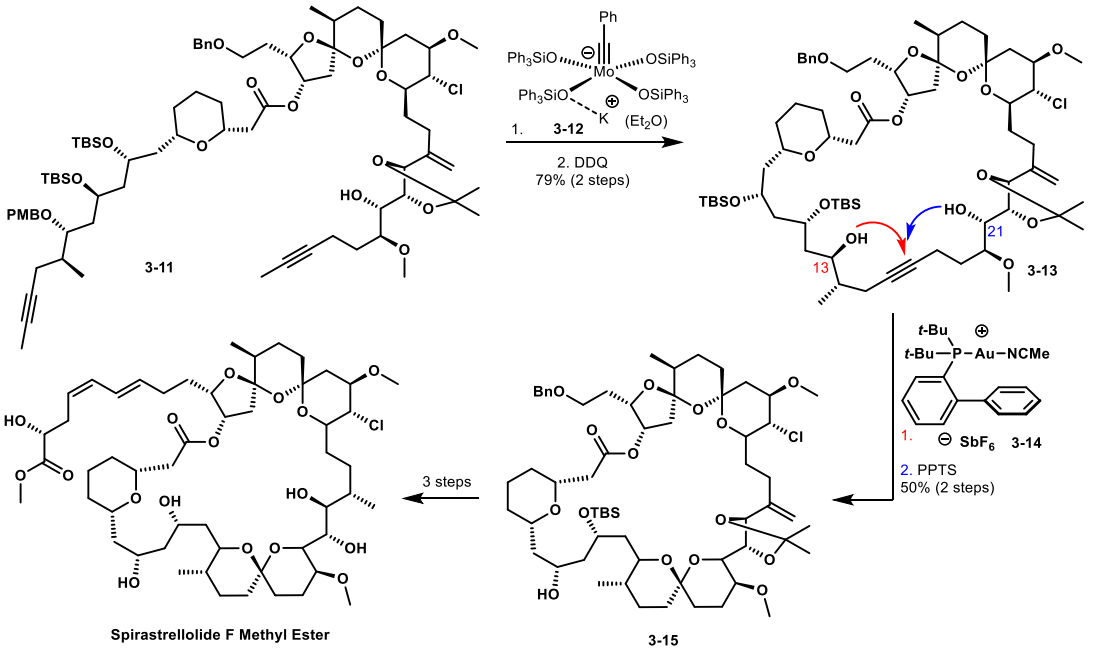

Scheme 3.1. Ring closing alkyne metathesis and transannular Au-activated hydroalkoxylation ring contraction in the Fürstner group's second-generation synthesis of spirastrellolide F methyl ester

One of the first examples of a postmetathetic strategy implemented by the Fürstner group was in their second-generation synthesis of spirastrellolide F methyl ester.[40] The first-generation synthesis closed the macrolide *via* a Yamaguchi esterification.[41–42] In their second report, the authors envisioned a RCAM followed by a π-acid activation of the resulting alkyne to promote a ring contraction and formation of the southern acetal spirocycle. The advanced intermediate diyne **3-11** was subjected to Mo catalyst **3-10** and exclusively produced the desired metathesis product (Scheme 3.1). The triphenylsilanolate ligated catalyst has an effective balance of Lewis acidity at the metal center. This balance allows for efficiency (the reaction occurring at room temperature), functional group tolerance (not disturbing any of the acid-labile moieties), and high selectivity (not reacting with the available alkenes). The alkyne metathesis mechanism shown in Scheme 3.2 suggests that the metal center needs to shift between an

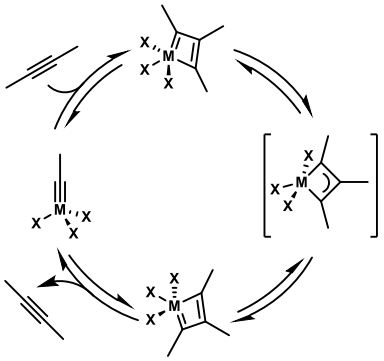

Scheme 3.2. Alkyne metathesis general mechanism

electronically poor center for substrate binding and an electronically rich center for the retro–[2+2]. The silanolate ligands are ideal for this mechanism, as they are flexible and can therefore vary their π-donor ability throughout the metathesis.[26–27] The PMB protecting group was reduced and diol **3-13** was treated with gold catalyst **3-14**. The C13 alcohol closed onto the alkyne *via* a 6-*endo-dig* cyclization. The 5-*exo-dig* regioisomer was also detected and could be separated by chromatography. Treatment of the 3,4–dihydropyran product with pyridinium *p*-toluenesulfonate (PPTS) resulted in the C21 alcohol closing onto the enol ether to furnish spirocycle **3-15**. Spirastrellolide F methyl ester was synthesized in three additional steps.

In 2016 the Fürstner group reported their synthesis of (–)-enigmazole A.[43] Previous syntheses of this potential anti-cancer agent have furnished the macrolide through macrolactonizations[44–45] and an RCM.[46] Implementing a similar idea from their previous work, the Fürstner group envisioned a transannular ring contraction from an alkyne metathesis product. Treatment of diyne **3-16** with Mo catalyst **3-17**, smoothly afforded the desired alkyne while conserving the sensitive adjacent acetyl group (Scheme 3.3a). The desired ring contraction and pyran formation was achieved upon exposure of the substrate to gold catalyst **3-19** in an impressive 91% yield. The next sequence was initiated by a [3,3]–sigmatropic rearrangement that resulted in allenyl acetate intermediate **3-20**, which was primed for addition of the adjacent alcohol via a 6-*exo-dig* cyclization to form pyran **3-21**.

Interestingly, although the stereochemistry of the propargylic alcohol is quickly lost upon rearrangement to the allene, the C7 epimer of **3-18** did not undergo the same reactivity (Scheme 3.3b). The major product isolated from this reaction was benzene derivative **3-22**. After allene formation, it is postulated that the *exo*-methylene can attack as a competing nucleophile to form the tertiary carbocation. Elimination of acetic acid and proto-demetalation resulted in the undesired product. Thankfully matching the stereochemistry at C7 with the correct enantiomer of

the gold catalyst **3-19** furnished their desired product in exceptional yields. Subsequently, pyran **3-21** was further elaborated to the phosphorylated natural product.

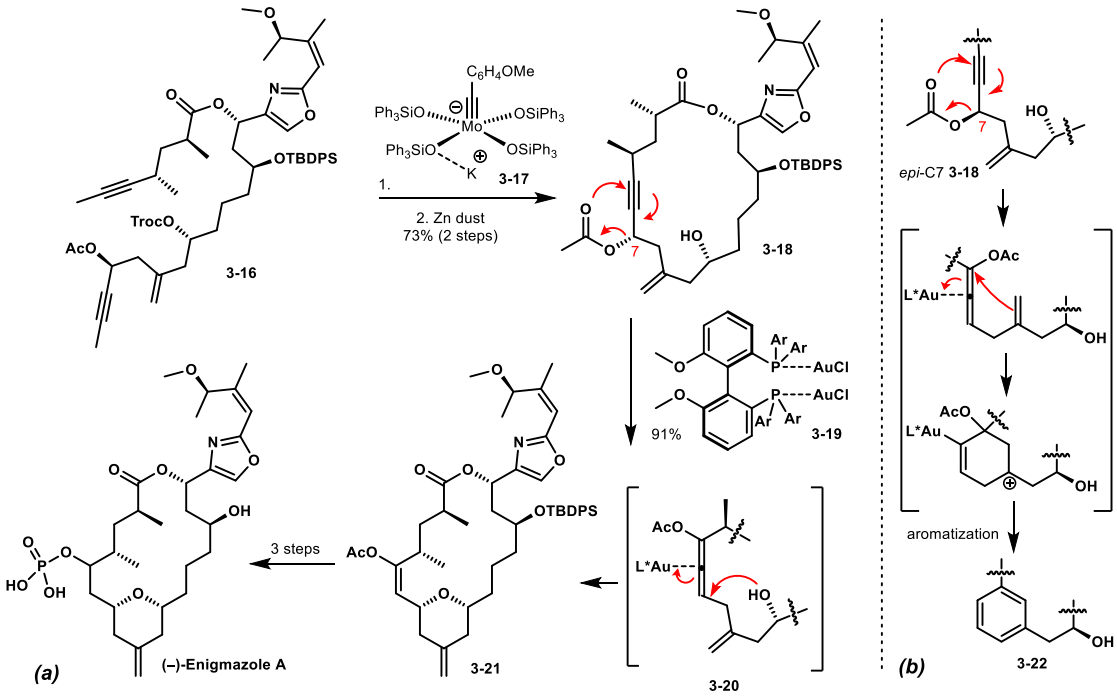

Scheme 3.3 (a) Ring closing alkyne metathesis and gold catalyzed [3,3]-sigmatropic rearrangement and transannular hydroalkoxylation of the resulting allenyl acetate ***(b)*** Failed pyran formation with C7 epimer and mechanistic rational for the major isolated product

In 2014, the Fürstner group completed the first enantioselective synthesis of (–)-lythranidine.[47] The authors envisioned an aza-Michael transannular ring contraction to afford the piperidine within the natural product. En route to synthesize the precursor for the aza-Michael, the triphenylsilanolate ligated molybdenum catalyst **3-24** accomplished the metathesis of diyne **3-23** in a 78% yield. It is of note that the metathesis was not hindered by the protic sites from the alcohol, phenol, and amine moieties, again proving the remarkable functional group tolerance of these catalysts. Next, a redox isomerization and *in situ* aza-Michael cascade was envisioned. A dual metal catalyzed redox isomerization, that was initially developed by Trost,[48] was able to take propargylic alcohol **3-25** exclusively to enone **3-26**; however, the amine did not undergo the Michael addition in the same pot as was originally anticipated. The proposed mechanism for the redox isomerization is shown in Scheme 3.4b. After initial coordination of the ruthenium catalyst

to the propargyl alcohol, a 1,2-hydride shift promoted oxidation of the propargylic carbon to the ketone and subsequent proto-demetalation afforded the desired *E*-enone. The role of $InCl_3$ in the mechanism is unclear, but it is postulated to be a halide scavenger or to relieve some ring strain of intermediate **3-25A**, forming the indium bridged intermediate **3-25B**.[48] The aza-Michael addition was triggered by treatment of the enone with *p*-TsOH to furnish a separable mixture of diastereomers (*trans*:*cis* at the piperidine junction). The natural product was obtained after a simple ketone reduction and removal of the protecting groups.

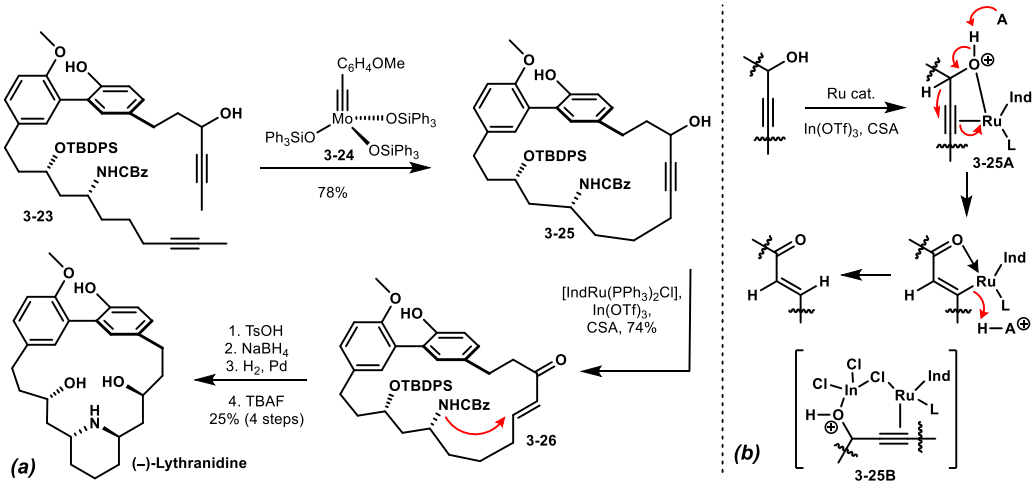

Scheme 3.4 (a) Ring closing alkyne metathesis and redox isomerization followed by an aza-Michael addition en route to (–)-lythranidine ***(b)*** Proposed mechanism for the redox isomerization and role of $InCl_3$

The final π-acid activation example that will be discussed in this section is the Fürstner group's amphidinolide F synthesis.[49] The 1,4-diketone umpolung type moiety within the natural product at C15 and C18 was an interesting challenge to approach, as this functionality is rarely seen in polyketides. After a successful RCAM of diyne **3-27**, the alkyne was treated with $[(C_2H_4)PtCl_2]_2$ to promote a regioselective hydroalkoxylation of the alkyne and exclusively afforded the dihydrofuran intermediate **3-28** in excellent 97% yield.[50] There was no detection of the unexpected 4-*exo*-*dig* cyclization product and both dienes within the intermediate remained untouched. Treatment of the enol ether with PPTS promoted the hydration of the alkene to the

1,4-ketol **3-29**. Oxidation of the remaining alcohol and deprotection of the silyl groups cleanly afforded the 1,4-diketone containing natural product.

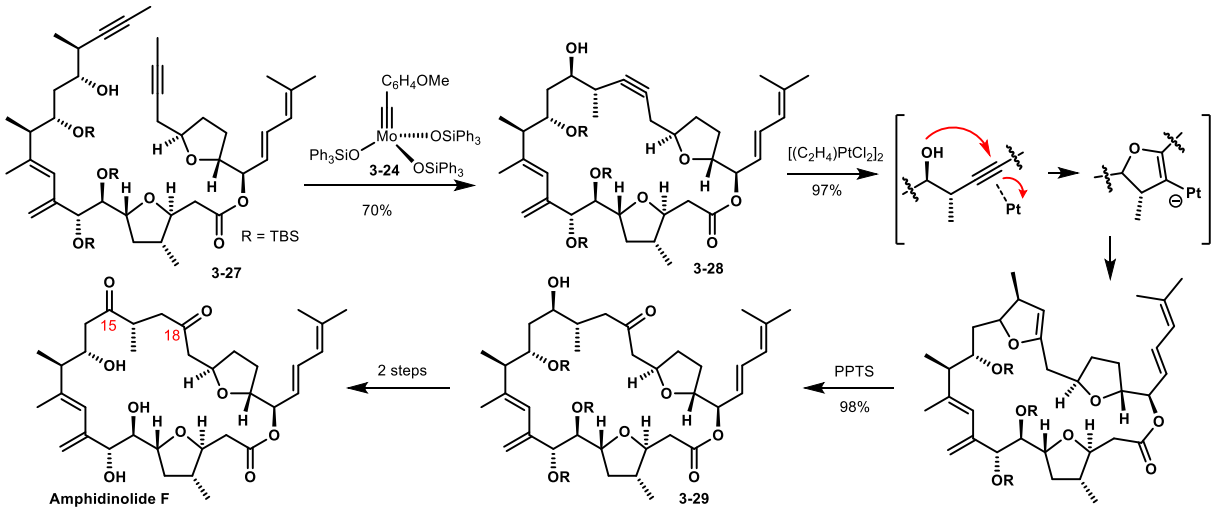

Scheme 3.5. Ring closing alkyne metathesis, platinum promoted hydroalkoxylation of the resulting alkyne, and elaboration to the 1,4-diketone containing macrolide, amphidinolide F

The next group of examples explore applications of Fürstner's regioselective hydrometalation of propargylic alcohols to afford trisubstituted alkenes. The group discovered that treating a propargylic alcohol with a ruthenium catalyst in the presence of a metal-hydride will promote a *trans*-hydrometalation of the alkyne with excellent regioselectivity (Scheme 3.6).[51–53]

In the first total synthesis of antibiotic disciformycin B, the Fürstner group targeted diyne **3-30**.[54] The C-silylated alkene was necessary up to this point to prevent isomerization of the alkene, a known decomposition pathway of the natural product. The RCAM was achieved with catalyst precursor **3-6** in the presence of the solvent CH_2Cl_2. This cyclization is particularly impressive due to the strain within the 12-membered ring product and the steric hindrance around the reactive site. The alcohol protecting groups were removed and the hydrostannation was attempted on the free diol. However, the only detectable product was cleavage of the macrocycle, due to the immense strain of the ring. The authors found to promote the hydrostannation, some of the strain within the ring needed to be relaxed by removing the C-silyl group.

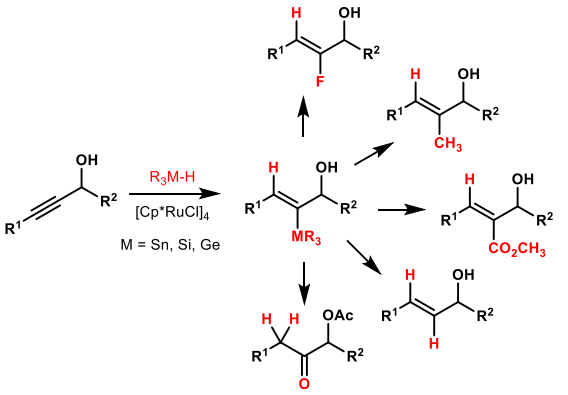

Scheme 3.6. Regioselective *trans*-hydrometalation of propargylic alcohols and further elaboration of the products

The alkyne metathesis product was converted to ester **3-32**. The propargyl alcohol was subjected to the hydrostannation conditions to produce the desired vinyl stannane **3-33**. The authors state that the regioselectivity of this transformation was due to the ruthenium catalyst binding to the alcohol and alkyne, thus delivering the hydride to the distal carbon of the alkyne (Scheme 3.7).[51] Unfortunately, in this particular case, the other vinyl stannane regioisomer was also observed (the stannane was installed at the distal carbon). This outcome was very uncommon with this hydrometalation hydrostannation transformation; often exquisite regioselectivity was observed.[36,55] This selectivity issue was likely due to the hydrogen-bonding interaction of the propargyl alcohol with the adjacent ester group, hindering the formation of the hydrometalation intermediate. A stoichiometric Stille with the desired regioisomer afforded alkene **3-34**. This sensitive product was further elaborated to disiformycin B by addition of a sugar moiety onto the free alcohol.

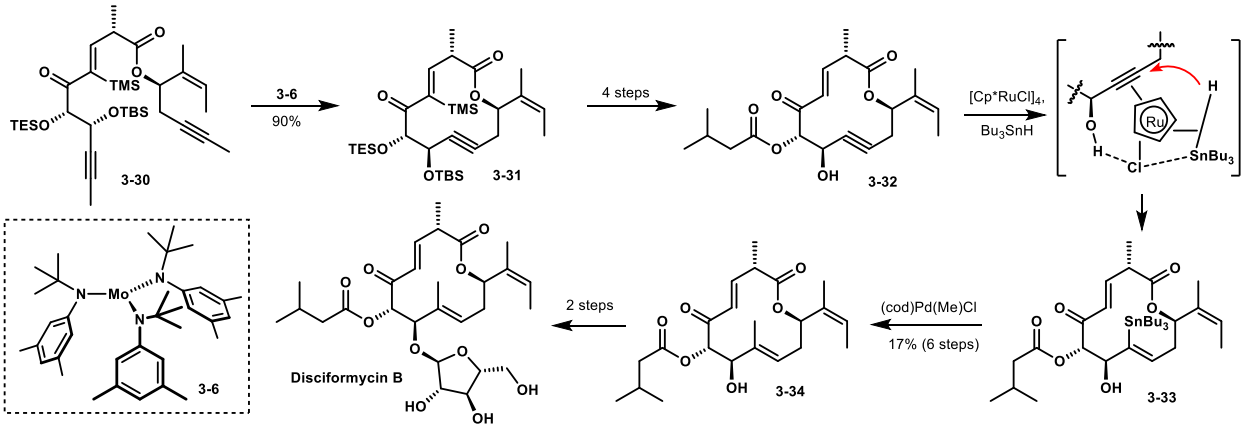

Scheme 3.7. Ring closing alkyne metathesis and regioselective *trans*-hydrostannation of the propargylic alcohol en route to disciformycin B

In 2019, the Fürstner group targeted the nine-membered lactone (−)-sinulariadiolide via a transannular ring contraction.[56] The precursor to the ring contraction was envisioned to be made from a RCAM product. Diyne **3-35** was synthesized in order to mask the 1,3-dicarbonyl at C3 and C5, which is one of the few functional groups that is not tolerated by alkyne metathesis catalysts.[57] Exposure of the masked β-ketoester to catalyst precursor **3-6** and chelating silanol ligand **3-36** cleanly afforded the 13-membered macrocycle in good yield. This catalyst and ligand pair is a part of the new canopy catalyst system that was developed by this group and offers even more functional group tolerance and selectivity.[58] Removal of the tetramethylpiperidine (TMP) protecting group afforded diol **3-37**, which underwent the regioselective *trans*-hydrostannation when treated with Bu_3SnH and catalytic $[Cp^*RuCl]_4$. A Stille carbonylation followed by protection of the diol afforded α-β unsaturated ester **3-38**, the precursor to the envisioned ring contraction. Upon treatment of intermediate **3-38** with Cs_2CO_3, the ester not only underwent the Michael addition, but also an unexpected (but welcomed) elimination of CO_2 to yield the carbon skeleton of the natural product (Scheme 3.8). The cascade afforded the methyl ether of sinulariadiolide, which could be demethylated with BBr_3 to furnish (–)-sinulariadiolide.

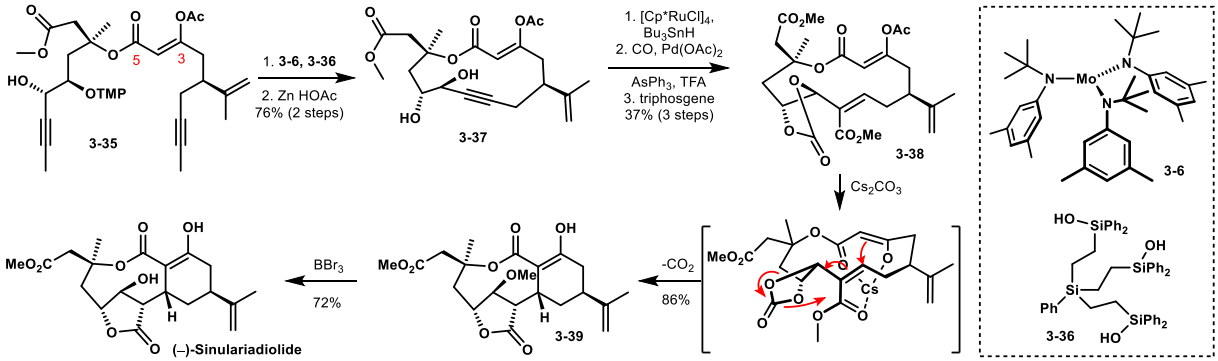

Scheme 3.8. Ring closing alkyne metathesis and regioselective *trans*-hydrostannation followed by a transannular Michael addition ring contraction cascade

The final example in this section I will discuss is the Fürstner group's recent synthesis of a couple of the casbane diterpenes, eurphorhylonal and depressin.[59] The envisioned alkyne metathesis was planned to be done on a propargylic cyclopropane, which could potentially lead to scrambling of the cyclopropane stereochemistry or just complete decomposition (Scheme 3.9b). Propargylic cyclopropane **3-40** was synthesized in ten steps (LLS) and was subjected to the same catalyst precursor **3-6** and chelating silanol **3-36** as previously discussed. Although the transformation required refluxing conditions the impressive RCAM afforded alkyne **3-41** without any observed scrambling of stereochemistry of the cyclopropane or decomposition of the substrate. The highly strained 14-membered ring contains two trisubstituted *E*-alkenes, a propargylic alkyne, and the cyclopropane moiety. The alcohol diastereomers could be separated by chromatography and the desired α-face alcohol was subjected to the *trans*-hydrostannylation to afford the desired regioisomer of vinylstannane **3-42**. Lithiation of the vinylstannane followed by exposure to DMF afforded the nominal eurphorhylonal. Alternatively, a Stille coupling with **3-42** followed by oxidation of the allylic alcohol resulted in the natural product depressin.

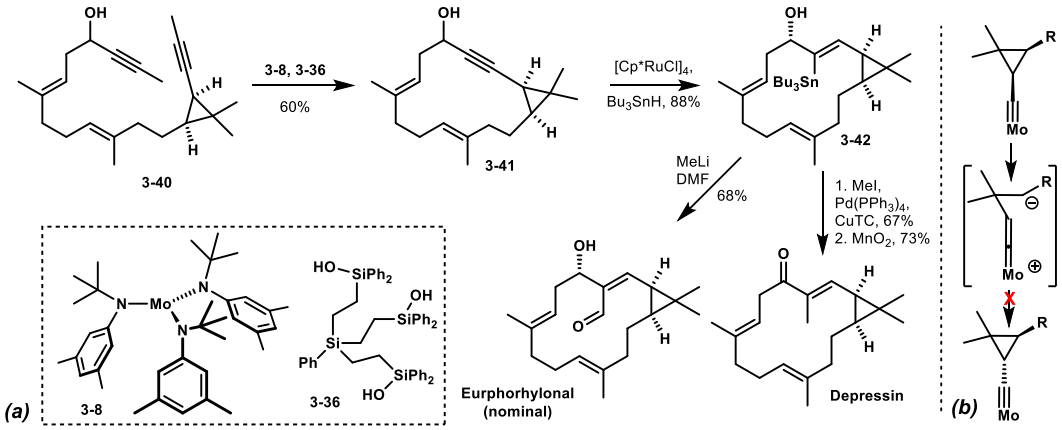

Scheme 3.9. (a) Ring closing alkyne metathesis of propargylic cyclopropane and *trans*-hydrostannation en route to the casbane diterpenes ***(b)*** Potential scrambling of the cyclopropane stereochemistry during the RCAM

3.1.4 Nickel catalyzed reductive cyclization of ynals

Another useful, yet less exploited disconnection to make macrocyclic allylic alcohols is the nickel catalyzed reductive cyclization of an ynal. This chemistry has been developed by both the Jamison and Montgomery groups and has been used in multiple total syntheses as an intermolecular coupling as well as a cyclization strategy.[60–63] This section will discuss the use of this technique as a macrocyclization strategy in total synthesis as well as some limitations of the method.

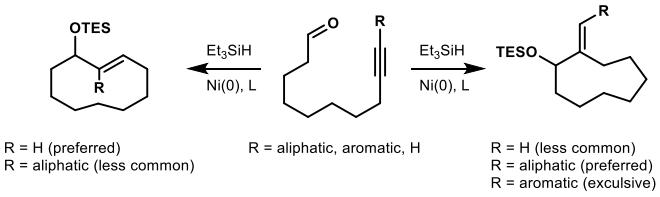

Scheme 3.10. Regioselectivity of nickel catalyzed reductive ynal cyclizations with varying alkyne substitution

The substituents on an alkyne within an ynal substrate is the main factor in the regioselectivity of an intramolecular nickel catalyzed reductive coupling. Alkynes bearing aromatic groups at the distal position will almost exclusively form exocyclic alkenes (Scheme 3.10). This cannot be inherently overridden by varying the ligands on the catalyst. On the other hand, 1,2-aliphatic substituted alkynes can lend itself to ligand control for the macrocyclization to produce

either the exo- or endocyclic olefin. Terminal alkynes often prefer to form endocyclic *trans*-alkenes, but can be forced to form 1,1 disubstituted exocyclic alkenes by varying the ligands on the catalyst. However, the regioselectivity issue is also greatly influenced by the conformational bias of a particular substrate. This preorganization can also dictate the stereochemical outcome of the resulting allylic alcohol. Some care must be taken when considering this disconnection as it can occasionally lead to dead end routes.

An interesting example of ligand controlled regioselectivity was shown by the Montgomery group's synthesis of 10-deoxymethynolide.[64] The envisioned cyclization would result in the desired endocyclic enone, but the group also wanted to examine if changing the NHC ligand on the catalyst would promote cyclization to the exocyclic alkene product. Terminal alkyne **3-43** was prepared in 12 steps and subjected to previously developed conditions for the reductive cyclization.[65] Using triethylsilane as a reductant, $Ni(cod)_2$ as the nickel source, and NHC derivative IMes as the ligand, the cyclization formed exclusively the desired endocyclic *trans*-alkene product **3-46** as a mixture of diastereomers at the C7 alcohol position. The orientation of the transition state is shown in Scheme 3.11a. The aryl groups on the NHC ligand were able to be oriented parallel to the aldehyde, essentially removing steric hinderance of the ligand from the reactive sites. This allowed for the substitution on the alkyne to align the less substituted distal, and more electronically favored, end of the alkyne towards the electrophilic aldehyde, to form metallocycle **3-45**. On the other hand, when the ligand was switched to DP-IPr (Scheme 3.11b), the larger ortho substituents on the aryl group greatly influenced the orientation of the transition state. The steric demand of the isopropyl groups as well as the phenyl groups on the NHC ring forced the alkyne into the position to form metallocycle **3-48**, and resulted in exclusive formation of the exocyclic product **3-49**.[66] Fortunately, the endocyclic product was easily elaborated to 10-deoxymethynolide after a silyl deprotection and a chemoselective oxidation.

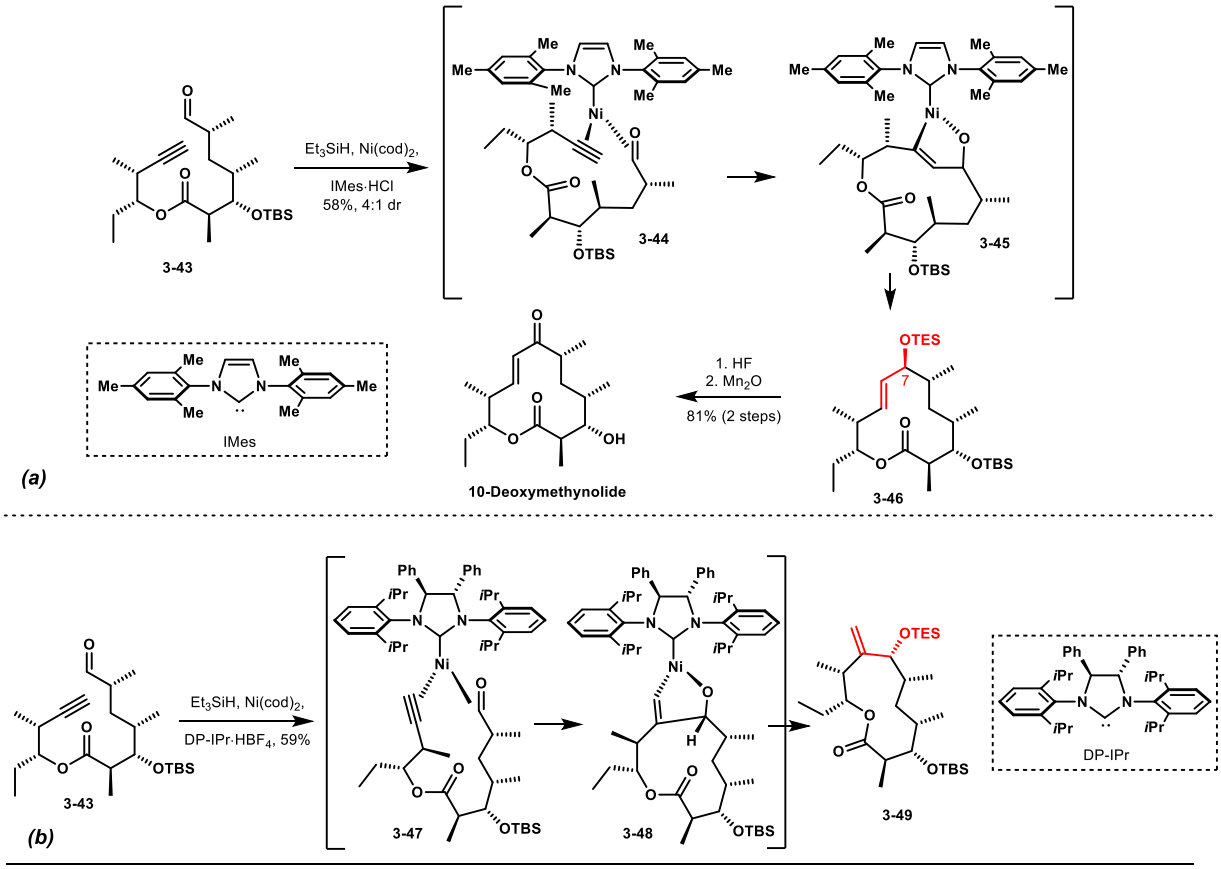

Scheme 3.11. Ligand controlled regioselectivity of a nickel catalyzed reductive ynal cyclization

A straightforward example of exclusive formation of an exocyclic olefin from a nickel catalyzed reductive cyclization was shown in the total synthesis of amphidinolide T1 by the Jamison group.[67] Through retrosynthetic analysis the authors envisioned making the α-hydroxy ketone within the macrolide from the product of a regioselective reductive cyclization followed by an oxidative cleavage of the resulting exocyclic olefin. En route to the cyclization precursor, the authors implemented an intermolecular nickel catalyzed reductive coupling. The benzylic alkyne **3-50** and epoxide **3-51** fragments were subjected to previously developed conditions to forge the homoallylic alcohol as one regioisomer.[68] Alcohol **3-52** was successfully elaborated to the cyclization precursor, ynal **3-53**, which bears a phenyl group on the distal end of the alkyne, in order help obtain the desired regioselectivity from the cyclization. Previous work of intramolecular couplings found that an alkyne with an aryl group on one end and an aliphatic group on the other

coupled the aliphatic bearing carbon to the aldehyde carbon.[65] Treatment of the ynal with the known conditions produced the desired exocyclic product **3-54** in moderate yields. Ozonolysis of the resulting exocyclic alkene afforded the α-hydroxy ketone that was further elaborated to the natural product in a few additional steps.

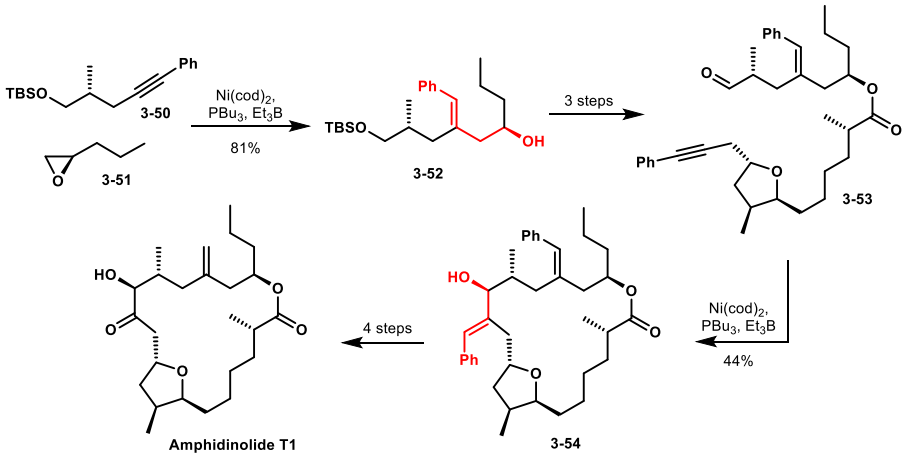

Scheme 3.12. Nickel catalyzed intermolecular reductive coupling and ynal cyclization en route to amphidinolide T1

In their efforts towards the antibiotic gulmirecin A, the Ichikawa group utilized this reductive cyclization strategy with a 1,2-dialkyl substituted alkyne.[69] Alcohol **3-55** was prepared and then oxidized to the corresponding aldehyde. Due to the ease of an intermolecular aldol reaction of the aldehyde, the intermediate needed to be taken crude into the key cyclization step. Fortunately, the macrocyclization afforded a single diastereomer and regioisomer of their desired allylic alcohol. Removal of the silyl group, furnished alcohol **3-56** in a 30% yield over three steps. This example showed the importance of substrate preorganization prior to cyclization in the transition state. Although this was the desired outcome for the reaction, the other regioisomer was essentially unobtainable due to the conformational restrictions of this particular substrate. A screen of varying ligands and reductants showed that no other cyclization products could be obtained from this transformation. Moreover, slight variations in the substrate, such as differing protecting groups, did not result in any cyclization product under the same conditions. This was

an interesting case study for these types of macrocyclizations, and although the outcome was favorable, this is not always the case.

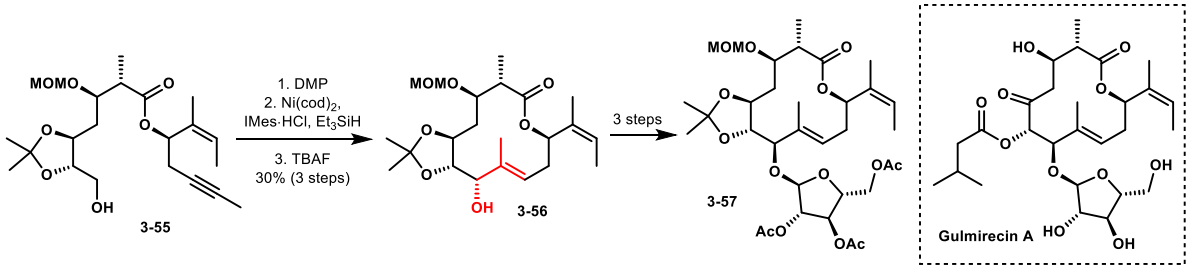

Scheme 3.13. Regioselective and stereoselective nickel catalyzed reductive macrocyclization of an ynal

In the Jamison group's pursuit of (–)-terpestacin they envisioned a reductive macrocyclization of ynal **3-58**, in which the alkyne bears two aliphatic substituents, to afford the 15-membered carbocycle.[70] Unfortunately, exposure of ynal **3-58** to the reductive cyclization conditions afforded only the undesired 14-membered macrocycle **3-59** as opposed to the desired 15-membered macrocycle **3-60**. Slight changes to the substrate (removal of the α-methyl group, reduction of the ketone, etc.) resulted in the same outcome. It was initially postulated that the quaternary center at C1 was causing too much steric hinderance or that the *trans* relationship between C1 and C15 was too much a barrier to overcome; however, removal of the α-methyl group did not result in any of the desired 15-membered ring product. Attempts to make the epimer of this substrate, to force a *cis* relationship between C1 and C15, were unfruitful. In analyzing the two metallocycle intermediates,[71] it is possible that the bicyclo[13.3.0] metallocycle **3-61**, the intermediate that would form the 14-membered product, has a lower activation energy as opposed to the bicyclo[12.2.1] **3-62** that would form the desired 15-membered carbocycle. Unfortunately, this route to the natural product had to be abandoned. An alternative route using an enantioselective intermolecular reductive coupling forged the allylic alcohol (blue disconnection), and the macrocycle was formed via an alkylation of the ketone (red disconnection). Although the reductive ynal cyclizations has shown to be useful in the formation of macrocyclic allylic alcohols,

some precaution must be taken when implementing the cyclization in total synthesis especially with 1,2-aliphatic substituted alkynes.

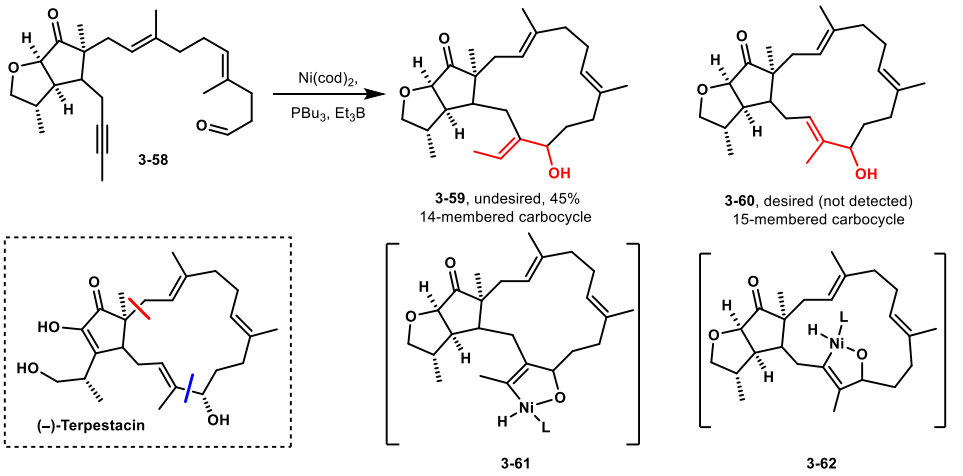

Scheme 3.14. Nickel catalyzed reductive cyclization afforded exclusively the undesired regioisomer towards the synthesis of (–)-terpestacin

3.1.5 Nozaki–Hiyama–Kishi cyclization

The Nozaki–Hiyama–Kishi (NHK) has been widely and successfully used in total synthesis as both an inter- and intramolecular transformation.[14] The mild conditions, chemoselectivity, diastereoselectivity, and functional group tolerance has made this reaction broadly useful for a wide variety of substrates. The mechanism for this transformation is shown in Scheme 3.15.

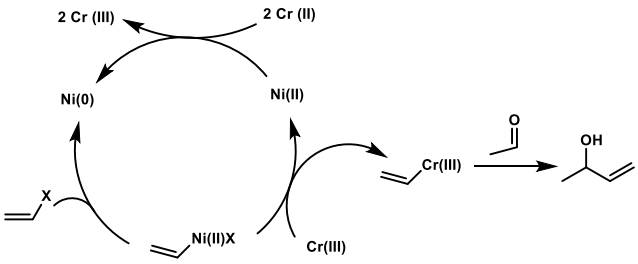

Scheme 3.15. Mechanism of the Nozaki-Hiyama-Kishi coupling using stoichiometric chromium

The intramolecular variation of this reaction has advantages over the intermolecular counterpart: (1) substrate preorganization will often lead to higher stereoselectivity (2) polymerization products are not observed (3) the haloalkene and aldehyde substrate is

straightforward to synthesize (4) as there is just one substrate, there is no need for excess of one fragment over another (5) these reactions can be run at higher concentrations than other macrocyclizations. The haloalkene synthon can be made through traditional methods. For disubstituted alkenes the desired alkene geometry is set prior to the NHK and the geometry is retained during the coupling. Trisubstituted alkenes however will rearrange to give exclusively the *E*-alkene product.[72] The regio- and diastereoselectivity (of the alkene) is easily predictable, however, the stereochemistry of the resulting alcohol position is usually dependent on the conformational bias of the structure. There have been chiral ligands developed for asymmetric NHK reactions to control the stereochemistry of the alcohol as well.[73–74] One drawback of the NHK is the stoichiometric amounts of toxic chromium required. Variations of the NHK reaction have been developed that are catalytic in chromium, by using manganese to reduce the chromium (III) back to chromium (II), however this will not be discussed in this chapter.[75–76] This section will present applications of the NHK (using stoichiometric amounts of chromium) as a macrocyclization strategy.

In 2012, the Kigoshi group developed a novel hybrid compound that was found to have actin-depolymerizing activity, an interesting target for potential anticancer agents.[77] It was a combination of the macrolactone of aplyronine A and the side chain from mycalolide B; two natural products that have shown potent actin-depolymerizing activity.[7879] The hybrid was synthesized and evaluated for its biological activity.

In the first total synthesis of aplyronine A, the macrolide was closed via a Yamaguchi macrolactonization.[80] This reaction required high dilution conditions (0.39 mM) and resulted in a moderate 44% yield. In the synthesis of this hybrid compound, the authors approached the cyclization through an NHK disconnection instead. Subjecting ester **3-62** to the NHK reaction conditions afforded allylic alcohol **3-63** in an impressive 95% yield. The reaction was initially run at a concentration of 1.0 mM, yet it was found that the yield did not suffer and the

diastereoselectivity remained the same when the reaction was run at 10 mM. Unfortunately, due to the lack of steric hinderance around the reactive site and the floppiness of this intermediate, the product was essentially a 1:1 mixture of diastereomers at the newly formed alcohol position. The undesired diastereomer could be separated and funneled to the desired diastereomer through an oxidation and chiral reduction sequence. The desired β-face alcohol could be taken on to the aplyronine A derivative, which was evaluated for its bioactivity. The hybrid compound was found to retain potent for actin-depolymerization, and it was considerably less cytotoxic than the natural aplyronine A.

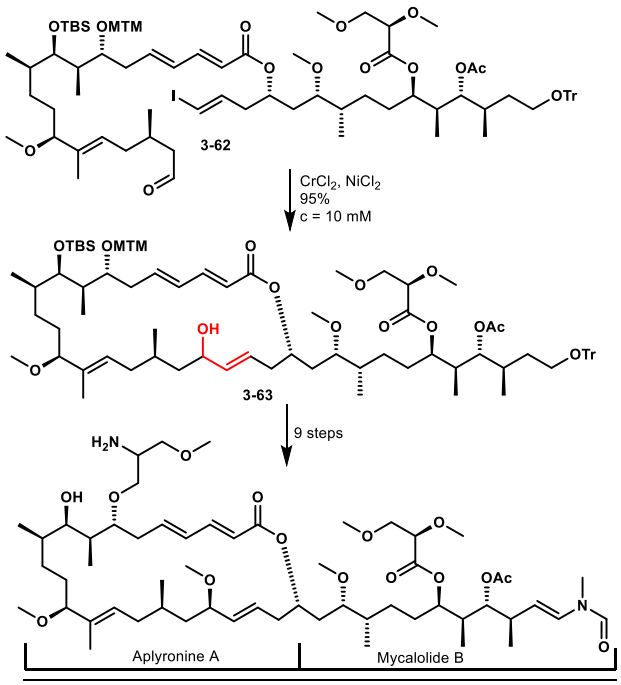

Scheme 3.16. NHK cyclization resulted in a 1:1 diastereomeric mixture of the 24-membered lactone

The next example that will be discussed is the Fürstner group's synthesis of aspercyclide B.[81] In their initial route, an RCM was attempted to close the macrocycle. Subjecting diene **3-64** to Hoyveda-Grubbs catalyst II (HG II) did result in some of the desired RCM product, however a significant amount of side product **3-66** was isolated. Because the reaction required a stoichiometric amount (100 mol%) of the catalyst, this side product could not be avoided.

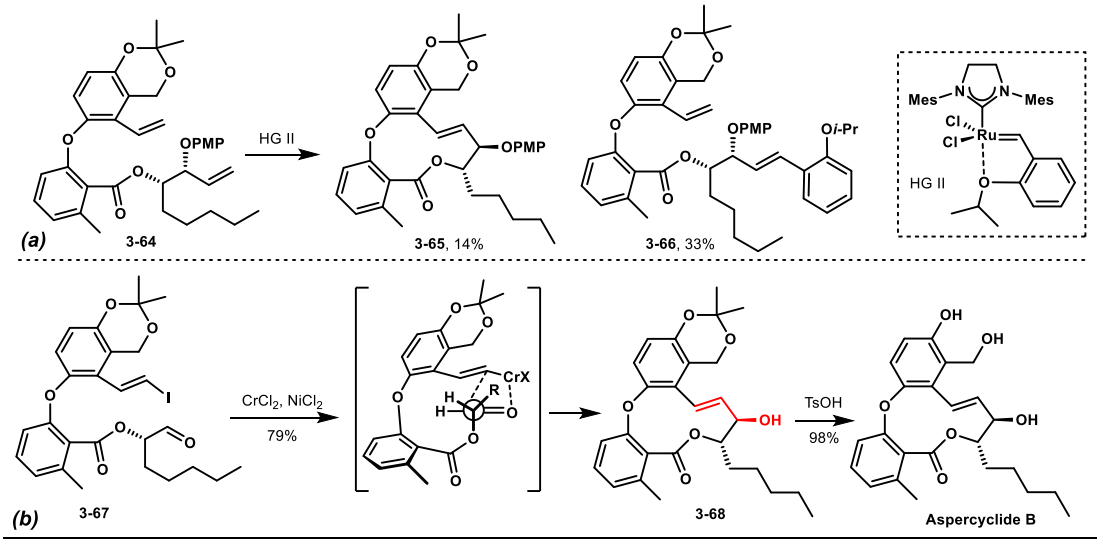

Scheme 3.17 (a) RCM apprach resulted in low yields of the desired macrolide ***(b)*** NHK cyclization resulted in one stereoisomer due to the conformational resitrictions and Felkin-Ahn transition state

Therefore, an alternate route was considered. The allylic alcohol within the natural product was instead envisioned be forged through an intramolecular NHK. Vinyl iodide **3-67** was prepared in ten steps and subjected to the NHK reaction conditions. To the author's delight, only a single diastereomer was isolated from the cyclization. The selectivity can be partially explained by the transition state shown in Scheme 3.17. The preferred pathway for organochromium reagents to add to aldehydes (that have a heteroatom at the β-position) is through a Felkin-Anh transition state.[82] This restricted transition state only allowed for the addition to occur from the α-face of the aldehyde. The substrate was also conformational restricted because the ester group was forced out of planarity with the aromatic ring due to the *bis*-ortho groups on the ring. This conformational bias essentially pre-organized the linear intermediate to help with the selectivity of the addition. Removal of the acetal protecting group of alcohol **3-68** afforded aspercyclide B in 12 steps.

The final example that will be discussed is the synthesis of the FDA-approved metastatic breast cancer treatment eribulin, which is brand named Halaven®.[83–85] It is a fully synthetic analog of the marine natural product halichondrin B, and it is one of the longest synthetic sequences of an approved drug.[86] Since it is an FDA-approved drug, it must be regularly synthesized on kilogram scale. In the industrial scale sequence, the NHK reaction not only closes the macrocycle

(Scheme 3.18), but it is also used to forge two other bonds within the molecule (disconnections shown in red).

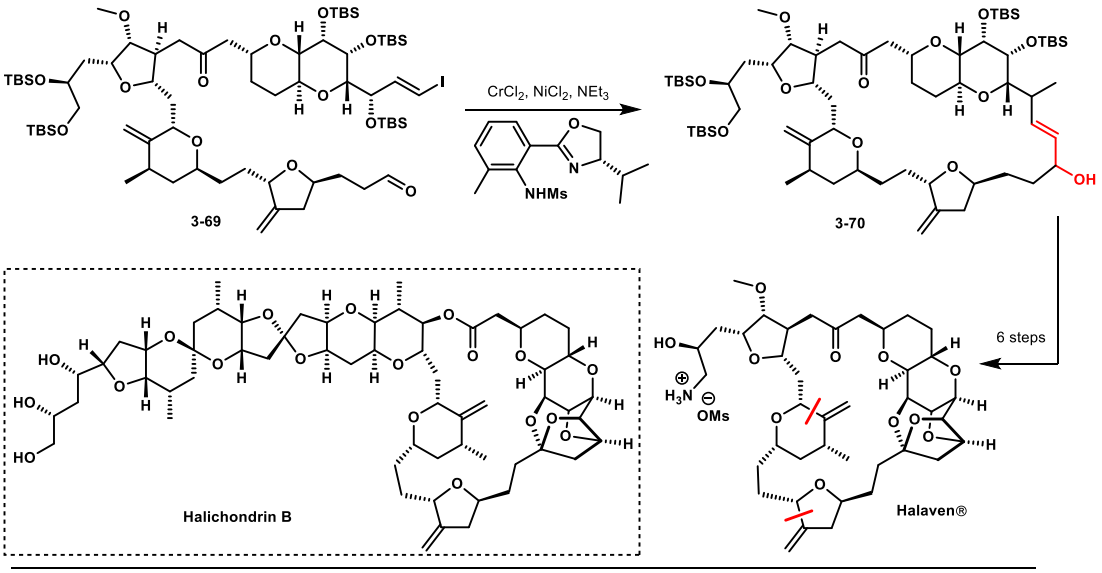

Scheme 3.18. NHK macrocyclization in the process scale route of the FDA approved Halaven® which is a synthetic derivative of the marine natural product halichondrin B

Subjecting vinyl iodide **3-69** to the optimized conditions cleanly afforded the desired product **3-70**, under non-high dilution conditions and was just six steps away from the final compound. The ligand used in this reaction was added for efficiency and does not lend itself to any diastereocontrol. The stereochemistry at the alcohol position was inconsequential as it was oxidized in the next step to the corresponding enone. Although the reaction was stoichiometric in chromium, the metal was easily filtered off upon workup. The synthesis displayed the powerful NHK transformation on a complex system in the presence of multiple sensitive functionalities. Halaven® is a feat of total synthesis in drug discovery; it is one of the longest synthetic sequences that is applied on industrial scale at a longest linear sequence of 35 steps.

As shown in this section, the NHK reaction as a macrocyclization strategy has been used in a wide variety of total syntheses. It has shown the ability to forge di- and trisubstituted alkenes with great regio- and diastereoselectivity. There are a limited number of examples of an NHK cyclization with tetrasubstituted alkenes, none of which forge macrocycles.[87] Additional examples

of the NHK cyclization in total synthesis are shown in Figure 3.4 (the red bonds were forged *via* an NHK macrocyclization).[88–95]

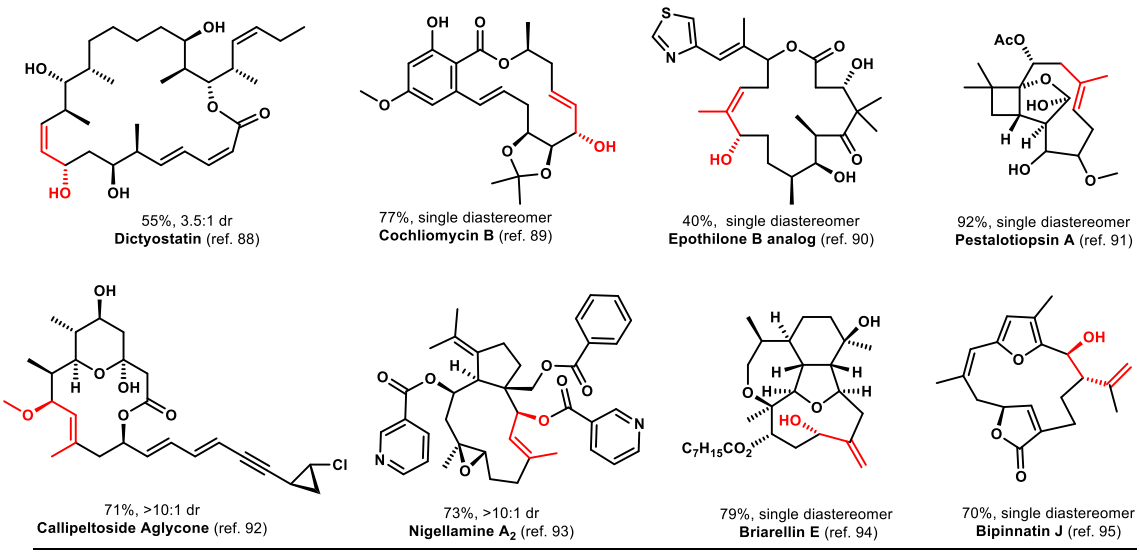

Figure 3.4. Representative examples of NHK macrocyclizations with varying alkene substitution; % yields and dr for the NHK are shown

3.1.6 Macrolactonizations

The lactonization of seco-acids is the most widely used approach to form macrocyclic lactones. There are a number of great reviews on this topic and will not be covered in depth in this section.[20–21] Since the strasseriolides are macrolides, macrolactonization cannot be ignored as a potential disconnection. Only acid activation techniques were considered for the macrolactonization towards the strasseriolides because the stereochemistry of the alcohol was planned to be set prior to this transformation. This section will briefly touch upon various macrolactonization strategies *via* acid activation. Alcohol activation to forge macrocycles will not be discussed, as it was not considered in this synthesis.

A list of acid activation methods is shown in Figure 3.5 (this list is not exhaustive). The use of thioesters as an activation technique was reported by Corey and Nicolaou in 1974.[96] Biosynthetically, macrolactones are forged through activation of the acid by thioester intermediates, therefore applying this in a laboratory setting was also successful. The 2-pyridine

thioester (labeled Corey-Nicolaou) is able to form a “doubly activated” intermediate which will electrostatically drive the reaction towards ring closure. Improvements to the initial Corey-Nicolaou reagent are shown in Figure 3.5; thioester activation has been used in many macrolactonizations, but is used less often than newer activation reagents.

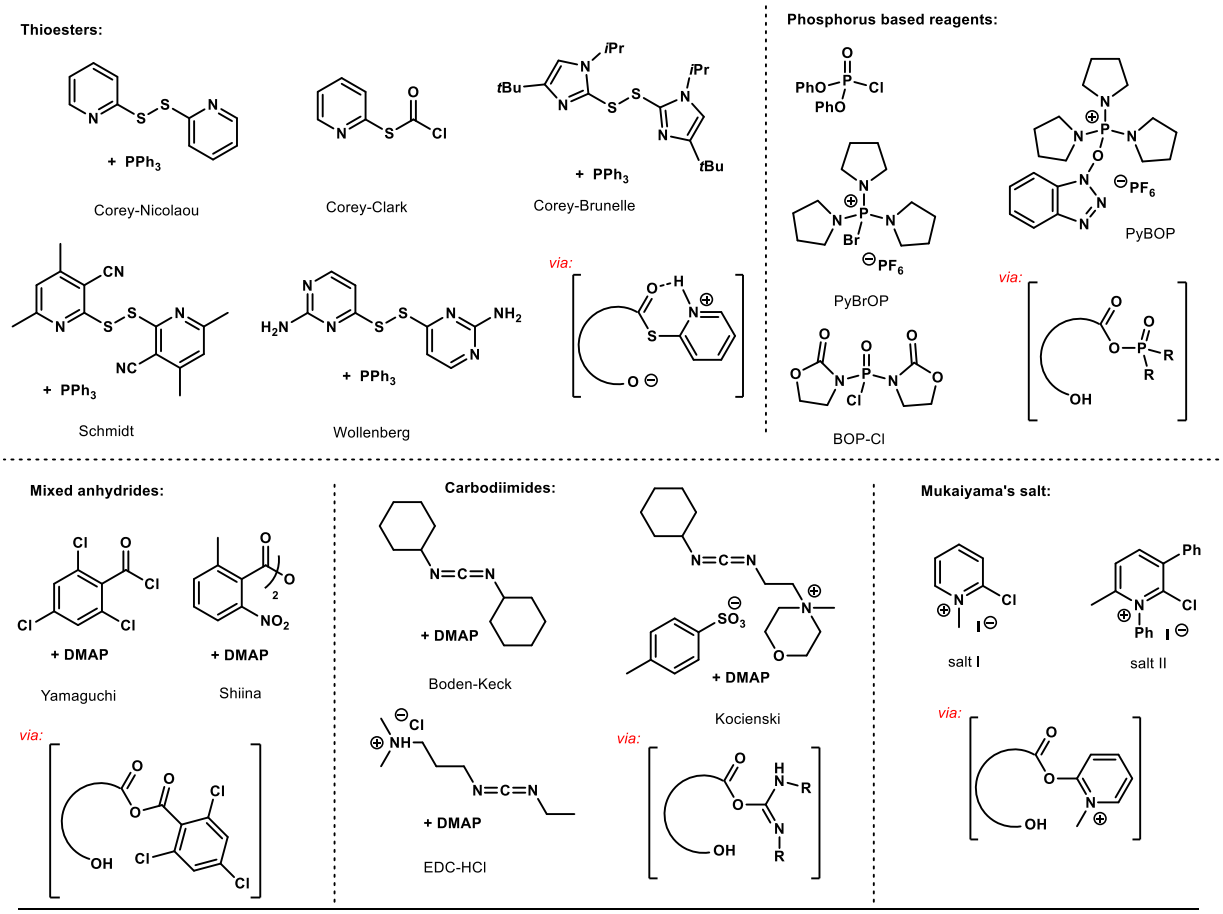

Figure 3.5. Acid activation reagents for macrolactonizations

Phosphorous based reagents have commonly been used in peptide synthesis and macrolactamizations, but they have also been applied in macrolactonizations.[20,97–99] One drawback of these reagents is caused by heating the acyl-oxy-phosphonium intermediate, which could lead to dimerization of the acid to form the undesired anhydride. Therefore, these macrolactonizations should be performed below 80 °C.[100–101]

The formation of mixed anhydrides *in situ* under basic conditions has been the most widely used method of macrolactonization, the Yamaguchi reagent being the most popular.[102] The initial report of this reagent has over 2600 citations and the reagent has been used in countless total syntheses since the 1979 report. The Shiina reagent was published more recently and has shown to promote macrolactonizations at room temperature with great selectivity.[103] The drawback of these methods is the need for highly basic DMAP, which could potentially lead to side products and epimerizations.

Carbodiimides are some of the oldest esterification reagents. The initial report of DCC as a lactonization tool was by Woodward in 1958 in his group's synthesis of reserpine.[104] One main drawback of DCC is removal of the urea by-product. The resulting urea is not very water-soluble and therefore chromatography if often required which is not ideal, especially on large scale. Alternative carbodiimides EDC and the Kocienski reagent form urea by-products that are water soluble and therefore can be removed through standard aqueous work-up procedures.[105] These reagents, most often DCC, have been used in many total syntheses of macrolides.

The original Mukaiyama salt was found to be an efficient macrolactonization reagent.[106] Through *ipso*-substitution at the aryl chloride position, the ester intermediate can undergo the cyclization to yield the desired lactone and a pyridone by-product. Since Mukaiyama salt **I** can readily decompose in the presence of amine bases, Mukaiyama salt **II** was reported and shown to not undergo the same decomposition pathways.[107] One drawback of this method is the potential of decomposition of the ester intermediate to the corresponding ketene which can undergo a variety of unproductive side reactions.[108] This reagent has however been successful in many total syntheses. Analogous to the other macrocyclization strategies discussed in this section, the conformation bias of the linear cyclization precursor is the most important factor in the successful of a macrolactonization. Figure 3.6 shows a select few examples of macrolides that have been synthesized via a macrolactonization.[45,88,100,109–122]

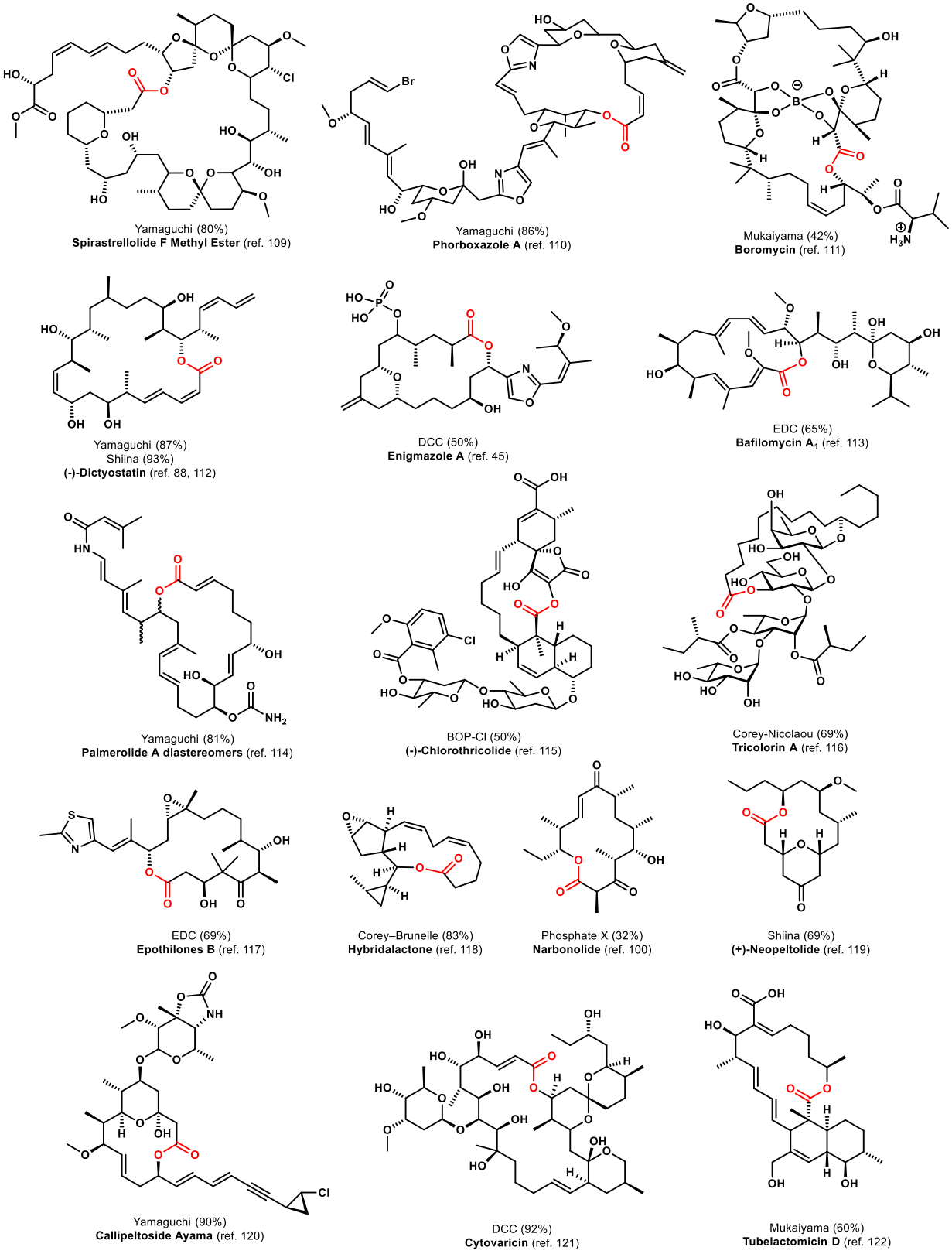

Figure 3.6. Examples of macrolides synthesized through various macrolactonization techniques

3.2 Syntheses of strasseriolides A and B

3.2.1 Introduction

The strasseriolides are a new class of macrolides that were isolated from an axenic culture produced by the fungus, *Strasseria geniculata* CF-247251. The fungus was obtained from the root of an unnamed plant in Mimiha, New Zealand. Strasseriolide B is an 18-membered macrolide containing six methyl substituents around the ring, two trisubstituted (*E*)-alkenes, and a challenging *anti*-1,3 dimethyl array. It was found to have potent activity against two strains of *P. falciparum* (section 3.1.1). While its protein target and mode of action are unknown, the presence of the hydroxyl group at C11 dramatically increases the macrolide's bioactivity and is postulated to play a role in its potency. In contrast, strasseriolide A contains a contains a ketone in this position and shows a significant decrease in bioactivity. Intrigued by its bioactivity and structural complexity, we decided to pursue the synthesis of strasseriolide B.

3.2.2 Alkyne metathesis route

Our initial retrosynthetic analysis proposed the key macrocyclization event occurring though an alkyne metathesis, Scheme 3.19. The resulting propargyl alcohol **3-71** could then be subjected to Fürstner's (*E)*-selective hydrostannation to set the final alkene within the ring.[36] A subsequent Stille coupling with the vinyl stannane would add in the final methyl group of the natural product. The RCAM precursor was envisioned to converge from western carboxylic acid **3-73** and eastern alcohol fragment **3-74**. Within fragment **3-73**, the alkyne could be installed and the alcohol stereocenter set in one step with Carreria's enantioselective alkynylation.[123] The ester group would be installed *via* a palladium catalyzed coupling reaction. [124] The trisubstituted (*E)*-alkene within fragment **3-75** would be accessed using a regio- and diasteroselective hydroiodination whose precursor, alkyne **2-76** is a known intermediate. As for the eastern esterification precursor, alkyne **3-74**, the alcohol and adjacent methyl sterocenter are primed to

be set *via* an Evans aldol addition. We envisioned installing the *anti*-1,3-dimethyl array within alkyne **3-77** using Feringa's iterative enantioselective conjugate addition. This conjugate addition would require the easily accessible α-β unsaturated thioester **3-78** as a starting point.[125]

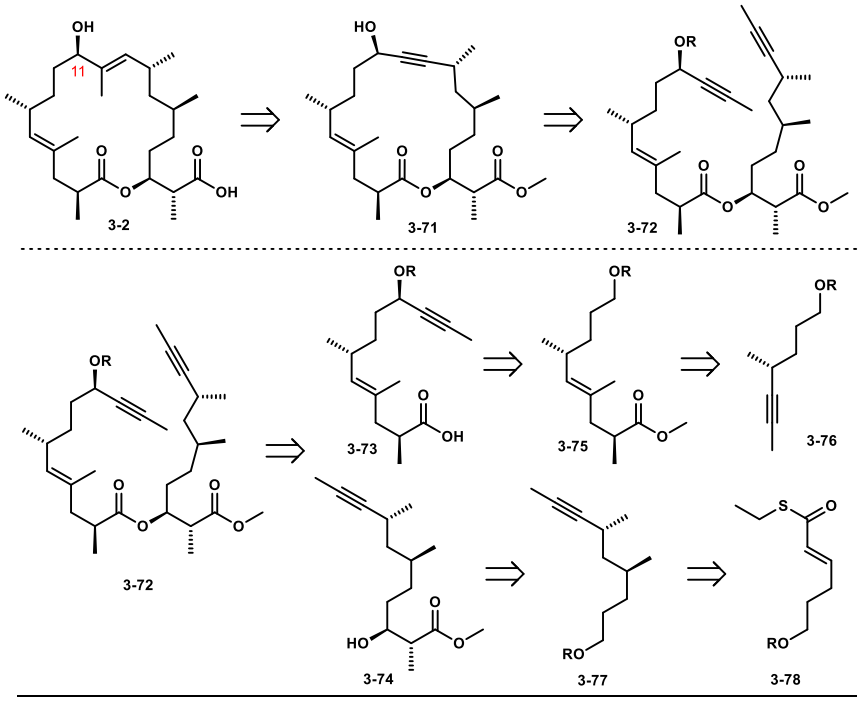

Scheme 3.19. Initial retrosynthetic analysis of strasseriolide B

Alkyne **3-79** was initially targeted. A Myers alkylation[126] using readily available intermediates afforded amide **3-81** in a 59% yield. Reduction of the auxiliary directly to the aldehyde only resulted in trace amounts of product; therefore, amide **3-81** was reduced to the corresponding alcohol and oxidized to the desired aldehyde **3-82**. A few different homologations were attempted to furnish the desired alkyne (Corey-Fuchs, Seyferth–Gilbert) but the Ohira-Bestmann reagent provided consistently good yields.[127] Although this route was reliable and the yields were modest, the starting material required (pseudoephedrine) is a controlled substance, which presents complications in a scale-up process. Therefore, a different route was explored.

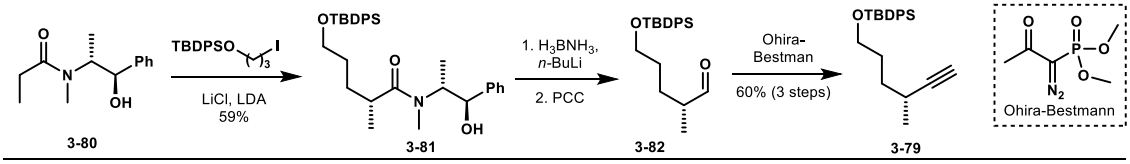

Scheme 3.20. Initial route to known alkyne

Alternatively, the desired stereocenter in this fragment could be set using Feringa's enantioselective conjugate addition.[125] Thioester **3-83** was prepared *via* a Wittig homologation and was then subjected to the conjugate addition conditions using the (*R,S*)-Josiphos ligand. Although this protocol has previously been reported to achieve excellent enantioselectivity, it only resulted in about 81% *ee* on this substrate. Other ligands were not explored for this transformation. The resulting thioester was reduced to aldehyde **3-86**, which was then elaborated to the desired alkyne in two additional steps (*vide infra*). This route was also abandoned because I was only observing moderate *ee*'s with the expensive (*R,S*)-Josiphos ligand.

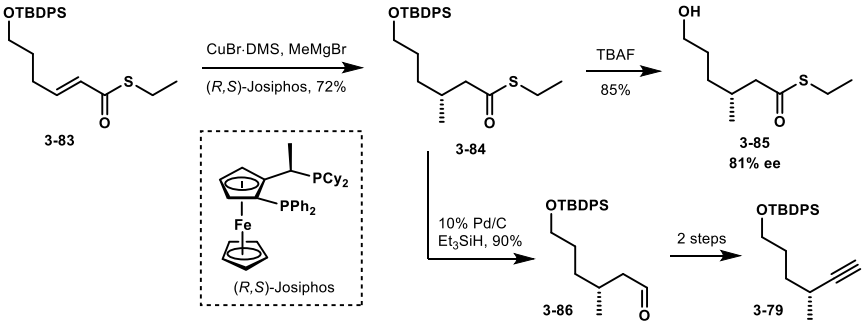

Scheme 3.21. Conjugate addition route to alkyne

Returning to route design, we were inspired to start the synthesis from an available chiral pool terpene, which already has this stereocenter in place instead of having to set this stereocenter within the fragment ourselves. Through a reductive cleavage of the alkene, (*R*)-citronellal could be mapped onto aldehyde **3-86**. Unfortunately, at the time we began the synthesis, the terpene was not commercially available. We could alternately begin with (*R*)-citronellic acid from which a simple reduction, oxidation sequence afforded the desired starting material. To obtain the previously synthesized alkyne **3-79**, we needed to install an alkyne

between the carbonyl carbon and the appending methylene. A one step formal dehydration using *tert*-butylimino-tri(pyrrolidino)phosphorane (BTPP) and nonafluorobutanesulfonyl fluoride (NfF) was implemented and successfully furnished the desired aldehyde.[128]

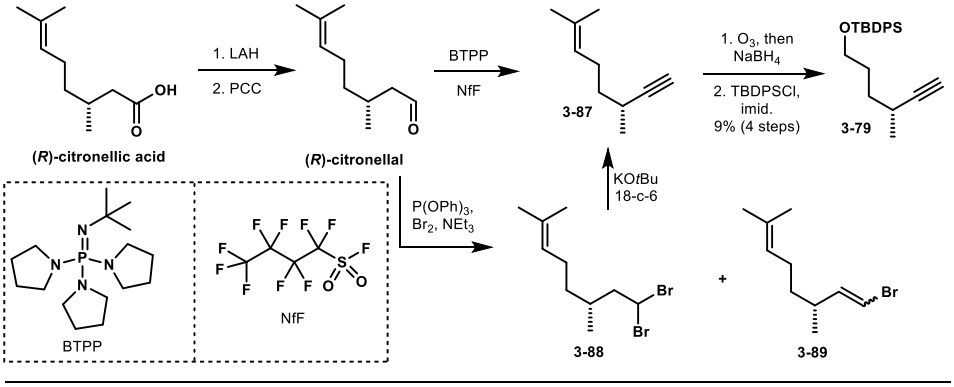

Scheme 3.22. Terpene route to alkyne

Even though this method was successful an alternative route was explored. The elimination required at least two equivalents of BTPP; the synthesis of this base was quite hazardous and required large quantities of *tert*-butyl azide which is potentially explosive. An alternative a two-step debromination and elimination procedure to take aldehydes to terminal alkynes has been successfully demonstrated in previous total syntheses.[129,130] Subjecting (*R*)-citronellal to the bromination conditions afforded the desired geminal dibromide **3-88** along with the vinyl bromide diastereomers **3-89**. The mixture was subjected to the reported elimination conditions to afford the desired terminal alkyne **3-87** along with unidentified and inseparable impurities. Ozonolysis of the alkene and subsequent silyl protection afforded alkyne **3-79** in 9% yield over four steps.

The poor yields for this new route can partially be attributed to the low molecular weight of all of the intermediates and the unidentified side products from the elimination. For ease of preparation and isolation of intermediates, a slightly different route was executed. Adding the protecting group earlier in the sequence would allow for easier isolation of intermediates. First, methylation of the acid, ozonolysis of the alkene, and silyl protection of the resulting alcohol,

afforded ester **3-90** in 83% yield over three steps. This ester was converted to the corresponding aldehyde through a reduction, oxidation sequence. To install the alkyne between the carbonyl carbon and the adjacent methylene, the BTPP, NfF elimination was again considered, however the silyl protecting group was incompatible and the safety concern was still an issue. Therefore, the two step dibromination, elimination was explored. The dibromination proceeded smoothly to afford the desired geminal dibromide **3-91** that was isolated as an inseparable mixture with vinyl bromide diastereomers **3-92**. Fortunately, the next step was elimination of the bromides, and therefore these side products were inconsequential. The reported literature for this elimination implemented KO*t*-Bu and 18-crown-6 to furnish the alkyne.[129–130] However, when applied to our system, the rearranged allene isomer **3-93** was often observed as a significant side-product. Optimization of the elimination by screening various bases (*n*-BuLi, LiHMDS, KH and $H_2N(CH_2)_3NH_2$, etc.) found that treatment with LDA efficiently afforded the terminal alkyne without generation of any detectable side products. Presumably the lithiated alkyne intermediate was resistant to isomerization. Subsequent methylation of the terminal alkyne afforded internal alkyne **3-94**. A one step elimination, methylation was explored; however, higher yields were obtained in the two-step transformation. The one-pot procedure often stalled out at the terminal alkyne intermediate.

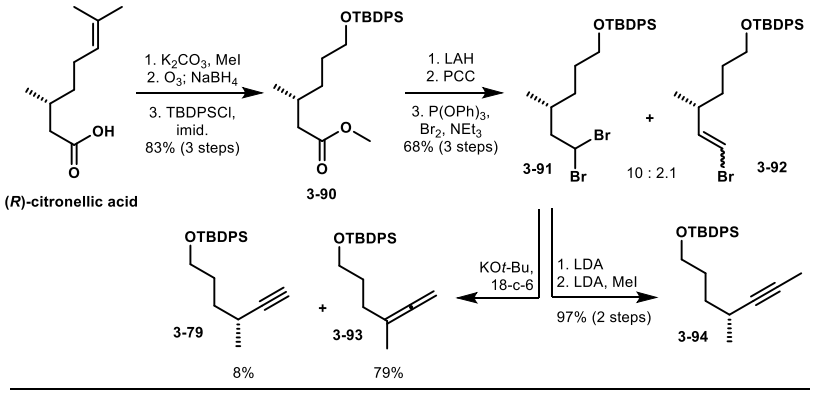

Scheme 3.23. Alternative terpene route to alkyne

Next, a regioselective and diastereoselective hydroiodination was achieved using Schwartz reagent (Cp_2ZrHCl), and the resulting vinyl zirconium species captured with iodide to exclusively form the desired alkene isomer **3-95**.[124] Various batches of Schwartz reagent would result in a minor amount of the undesired regioisomer. The best results were obtained using Cp_2ZrHCl that was made in-lab (and stored in a nitrogen filled glovebox) as opposed to the bottle purchased from Sigma-Aldrich. At least two equivalents of Schwartz reagent were required (Scheme 3.24b).[131–132] The vinyl iodide product was subjected to a Negishi cross-coupling with the zinc homoenolate reagent generated from ester **3-96** to afford (*E*)-alkene **3-97**.[133,134] Turning our attention to inserting the alkyne needed for the planned metathesis, deprotection of the silyl alcohol followed by oxidation to aldehyde **3-98** afforded the substrate needed for the alkynylation.

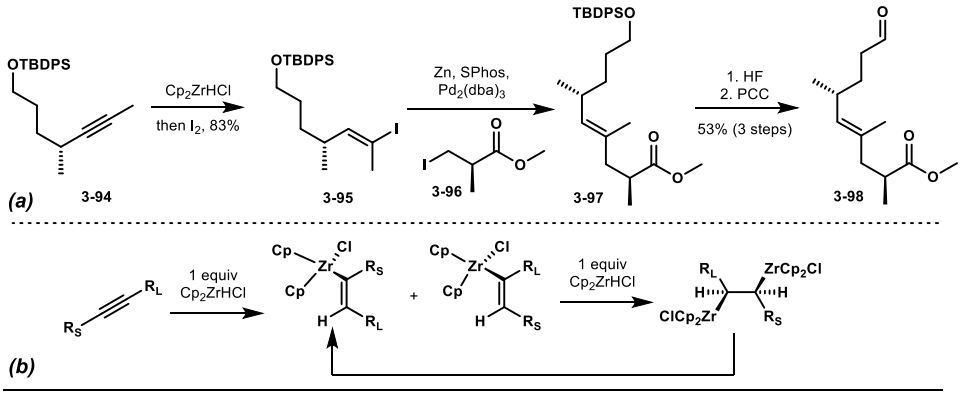

Scheme 3.24 (a) Hydroiodination and Negishi coupling installed the E-alkene ***(b)*** At least two equivalents of Schwartz reagent was needed for good regioselectivity of the hydrozirconation

Following Carreria's alkynlation conditions, treatment of aldehyde **3-98** with propyne, $Zn(OTf)_2$, and pseudoephedrine only resulted in recovered starting material.[123] Switching from gaseous propyne to TMS-acetylene did result in some desired product, however, it was isolated as a 2.5:1 inseparable mixture of diastereomers. Alternatively, the alcohol stereochemistry and the alkyne could be installed stepwise. Aldehyde **3-98** was treated with propynylmagnesium bromide and the resulting alcohol was oxidized to the corresponding ynone **3-100**. Ynone **3-100** was then treated with Noyori hydrogenation catalyst to obtain the desired propargyl alcohol **3-101** as well as 15% of the propyl ketone (**3-S13**, *vide infra*), which is a side product that has not been

previously reported under these conditions; see the experimental section for details.[135] A simple silyl protection and hydrolysis afforded the desired carboxylic acid **3-102** for the western fragment.

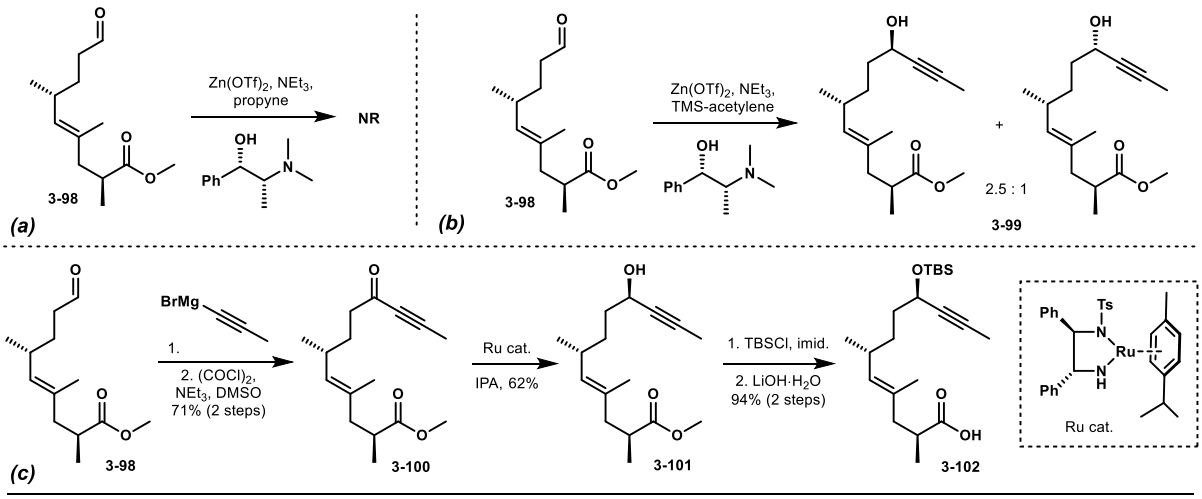

Scheme 3.25 (a) Attempted Carreria alkynylation with propyne ***(b)*** Carreria alkynylation with TMS-acetylene ***(c)*** Enone formation, Noyori hydrogenation, and completion of the western fragment

The synthesis of the eastern fragment was developed in a collaboration between myself and a colleague, Jessica Pazienza. The yields and observations reported in this section were performed by myself and the literature reported yields were optimized by Jess.[136]

Initially, the synthesis of the eastern fragment was planned to begin by performing two iterations of Feringa's enantioselective conjugate addition to install the *anti*-1,3 dimethyl array within the fragment, Scheme 3.26a.[125] However, inspired by the synthesis of the western fragment, we could alternatively begin with (*S*)-citronellal which already contains one of the methyl groups for the 1,3-dimethyl array. A Wittig homologation of the terpene afforded the α,β-unsaturated thioester.[137] The thioester was subjected to the conjugate addition conditions and afforded a single diastereomer of the desired *anti*-1,3 dimethyl motif **3-104**. A straightforward ozonolysis and silyl protection furnished thioester **3-105**. Next, we wanted to install the alkyne needed for the envisioned metathesis between the carbonyl carbon and the adjacent methylene. To do so, the thioester was reduced to the corresponding aldehyde **3-106** using Fukuyama's conditions[138] and then subjected to the three step dibromination, elimination, methylation

sequence that was optimized for the western fragment. Similar outcomes were observed in this sequence; the dibromination always resulted in an inconsequential mixture with the vinyl bromide diastereomers, and the two-step elimination-methylation sequence was higher yielding than the one step procedure. Turning our attention to the southern portion of the fragment, removal of the silyl protecting group and oxidation to the aldehyde **3-108** cleanly afforded the precursor to the Evan's aldol addition. Exposure of the aldehyde to the boron enolate of oxazolidinone **3-109** under standard Evan's aldol conditions furnished the alcohol as a single diastereomer. The eastern fragment was completed through a hydrolysis and methylation sequence that proceeded in moderate yield.

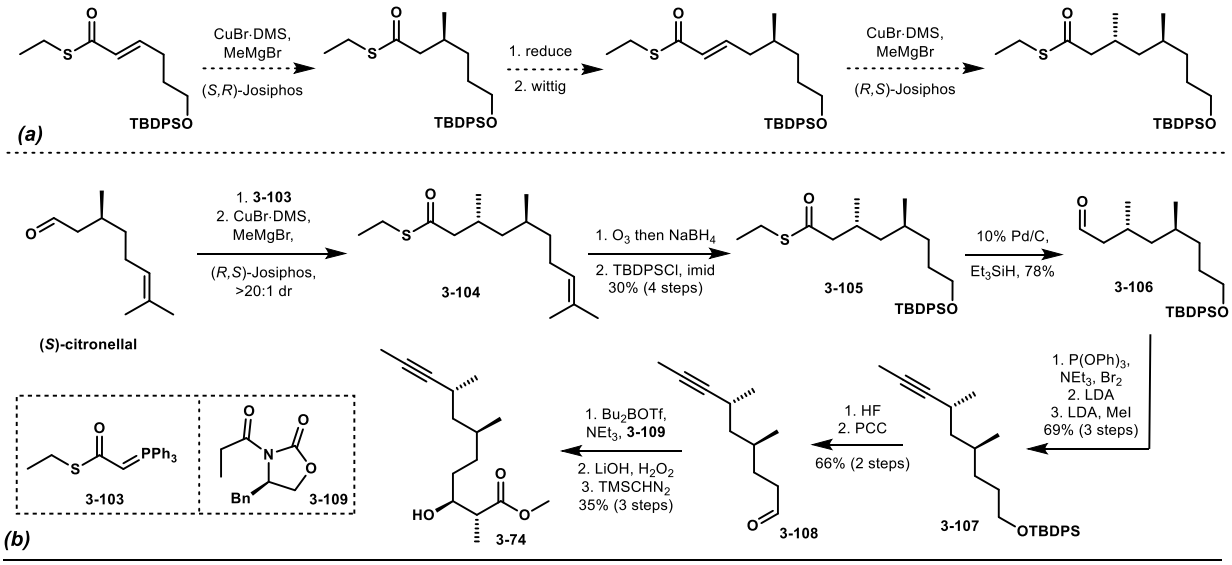

Scheme 3.26 (a) Envisioned iterative conjugate addition ***(b)*** Synthesis of the eastern fragment

We next turned our attention to the key alkyne metathesis. The fragments were coupled through a Yamaguchi esterification and the metathesis precursor **3-110** was obtained. Unfortunately, subjecting the diyne to the commercially available Mo catalyst **3-7**, did not result in any of the desired macrolide. Reports show that addition of $B(C_6F_5)_3$ with the molybdenum-nitride catalysts promotes the initial [2+2] and retro [2+2] through *N*-ligation.[139] However, addition of the Lewis acid also did not promote the cyclization. Mo catalyst precursor **3-112** was synthesized and the catalyst was attempted to be prepared *in situ* by the addition of triphenylsilanol, but this also

only led to recovered starting material.[25] The metathesis was also attempted with the free alcohol at the propargylic position and no reaction was observed. It is postulated that the nitride-molybdenum catalysts are much less active than their carbene counterparts.[140] It is likely that equilibrium between the nitride-molybdenum catalyst and the Mo complex **3-113** is heavily favoring the nitride catalyst. The alkynes are decently far apart from one another in space (~10 Å in the ground state) and therefore the Mo complex **3-113** might not have been able to exist long enough in solution to reach the other alkyne. Other alkyne metathesis catalysts (that were discussed in section 3.1.3) were targeted, but attempts to synthesize those catalysts were unsuccessful. Due to this unfortunate outcome, other macrocyclization strategies were explored.

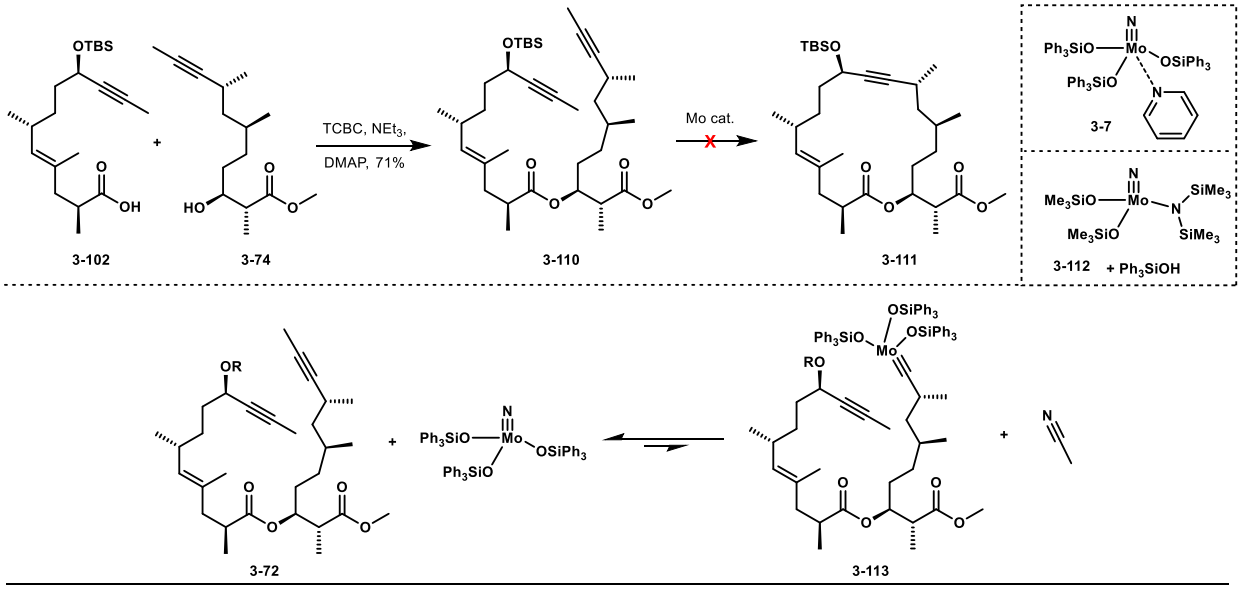

Scheme 3.27 (a) Combining the fragments and attempted alkyne metathesis
(b) Molybdeum nitride complex could be heavily favored in the equilibrium

3.2.3 Exploration into other macrocyclization strategies

With alkyne metathesis unfruitful in our system, we evaluated alternative macrocyclization strategies. The next strategy explored was the nickel catalyzed reductive cyclization. The two fragments that needed to be coupled for this route could be intercepted from intermediates in the previous sequences. To explore this strategy a model system was initially synthesized, Scheme 3.28. Subjecting the model system **3-116** to the reductive cyclization conditions that have been reported in the literature to make endocyclic alkenes only resulted in recovered starting material. Various reductants and ligands were screened, giving the same unsuccessful result. It is unclear why the starting material does not react. Since only starting material was recovered, the nickel did not do an initial oxidative insertion into the ynal, or else we would have observed linear reduction products. The model substrate is quite floppy and therefore the nickel might not have been able to coordinate to both the alkyne and the aldehyde to undergo the oxidative insertion and form the metallocycle. The problem with the reaction also may be due to the sensitivity of all of the reagents needed for the transformation. This route was not explored further as there was no clear conclusion that could be made about the shortcomings of the transformation on our substrate; also, there was very limited precedent for the cyclization with 1,2-aliphatic disubstituted alkynes forming the desired endocyclic alkene.

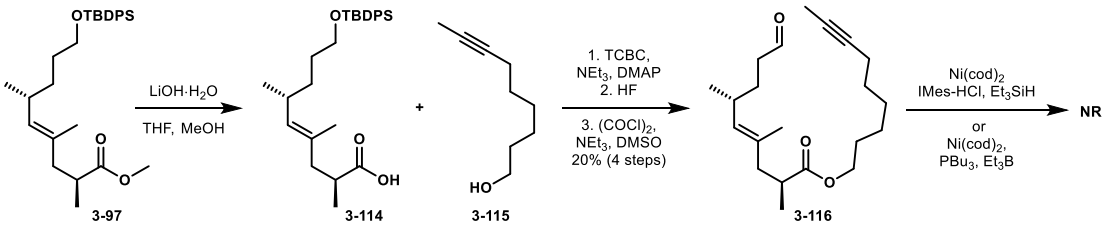

Scheme 3.28. Synthesis of model system and attempted nickel catalyzed reductive cyclization

With the same model substrate still readily available, another reductive cyclization procedure was explored. The Oppolzer group in 1993 reported an enantioselective reductive ynal macrocyclization in their synthesis of the perfume ingredient (*R*)-muscone.[141] The

macrocyclization proceeded through an initial hydroboration of the terminal alkyne **3-117** followed by a transmetallation to the alkenylzinc species which could then cyclize onto the aldehyde in the presence of amine **3-118**. The resulting allylic alcohol **3-119** was elaborated to the natural product through a cyclopropanation of the alkene, oxidation of the alcohol, and then subsequent reduction of the cyclopropane ring. The precedent was promising however, there are no examples of macrocyclizations under these conditions with an internal alkyne. The alkyl borane was likely not going to be regio- or diastereoselective in the initial reduction of our internal alkyne. To achieve better regio- and diastereoselectivity from the initial hydrometallation, the borane was replaced with Schwartz reagent. Alkyl zirconium have shown to readily undergo transmetallation in the presence of alkyl zinc reagents, so this was a viable change.[142] Treatment of our model ynal with Cp_2ZrHCl, followed by slow addition into a solution of Et_2Zn only resulted in reduction of the aldehyde to alcohol **3-120**. Altering the protocol to slow addition of Schwartz reagent into a flask containing the ynal and a silver salt (silver salts are known to dramatically accelerate a Grignard-type addition of alkenylzirconium intermediates into carbonyls), resulted in the same outcome.[143]

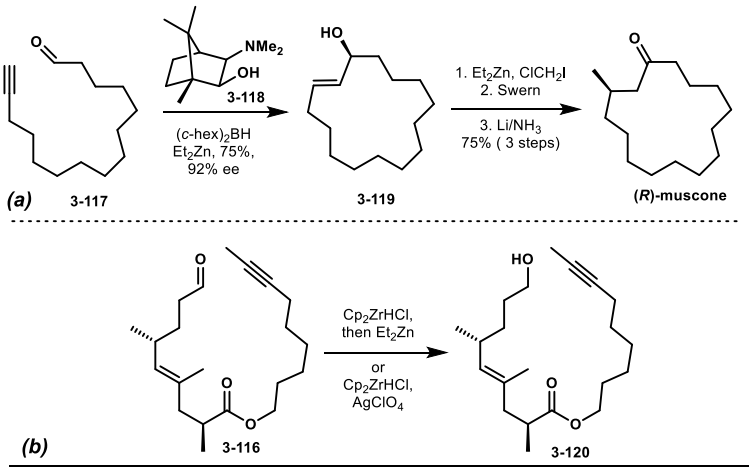

Scheme 3.29 (a) Synthesis of (R)-muscone by Oppolzer (ref. 140)
(b) Attempted reductive cyclization

In order to mitigate the undesired aldehyde reduction, an alternative macrocyclization strategy was explored. We envisioned first making the allylic alcohol using the intermolecular variant of the reductive ynal method (Scheme 3.30). By performing this reaction intermolecularly,

the Schwartz regent would first react with the internal alkyne before the aldehyde is introduced into the system. This transformation has been shown to proceed enantioselectively by the use of chiral ligands (as seen in the synthesis of (*R*)-muscone, Scheme 3.29) so that the stereochemistry of the alcohol could also be set at this step. After formation of the allylic alcohol, the seco acid could be unveiled and a macrolactonization would close the ring. This route seemed promising as macrolactonization is one of the most widely used methods of forging macrocycles. Treatment of our model alkyne with (less than two equivalents) of Cp_2ZrHCl followed by Et_2Zn, and finally the aldehyde **3-98**, afforded some of the desired allylic alcohol product **3-124** (as a mixture of diasteromers). The undesired regioisomer **3-125** was also isolated. This outcome is likely due to the amount of Schwartz regent in the reaction. There were less than two equivalents of Cp_2ZrHCl in the reaction because excess reductant would result in the undesired aldehyde reduction. Alkylation of the aldehyde directly from the alkyl zinc reagent was also observed, **3-126**. Although we observed promising data from this outcome, the regioselectivity issue could be mitigated by forming the allylic alcohol through a two-step procedure, as will be discussed with the next disconnection.

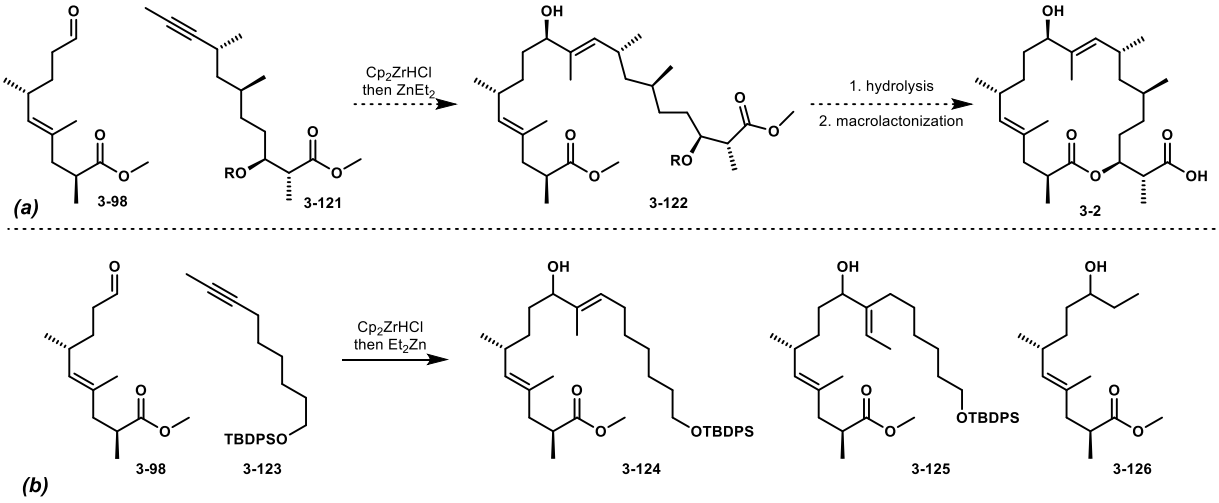

Scheme 3.30 (a) Revised retrosynthetic analysis ***(b)*** Hydrozirconation, transmetalation, and Grignard-type addition resulted in some desired product

Instead of trying to do a hydrometallation and Grignard-type addition into the aldehyde in one pot, we envisioned forming the vinyl iodide from the alkyne first and then doing a Grignard type addition in a second step. This disconnection allows for a variety of conditions to be screened for the addition (i.e. forming a Grignard reagent, lithium-halogen exchange, NHK, etc.). The hydroiodination could also be done earlier in the sequence to avoid any side reactivity with other functional groups on the alkyne fragment (*ie*. the ester could potentially get reduced), Scheme 3.31a. The product from the addition **3-129** could then be subjected to a macrolactonization.

Alkyne **3-107** was treated with Schwartz reagent followed by iodine to obtain vinyl iodide **3-130** as a single alkene regioisomer. Vinyl iodide **3-130** was treated with *t*-BuLi and then aldehyde **3-98** was introduced to the presumed vinyl lithium. This reaction resulted in many spots by TLC and upon isolation, the only observable product was addition of *t*-BuLi into the aldehyde and ester moieties, **3-131**. To avoid these side products, an intermolecular NHK was alternatively explored. A mixture of aldehyde **3-98** and vinyl iodide **3-124** was treated with excess $CrCl_2$ and catalytic $NiCl_2$. The desired allylic alcohol **3-133** was obtained as a mixture of diastereomers at the C7 alcohol position along with diene **3-134**, the cross-electrophile coupling product. This was a very promising result. It is well known that the cross-electrophile coupling diene product could be mitigated by performing the reaction intramolecularly (the dilution of an intramolecular NHK will moderate this reactivity). Moreover, if this reaction is done intramolecularly, there may be some conformational bias for the ring closure to aid in the stereochemical outcome at C7. There are also many variations of the asymmetric NHK that would help to set this stereocenter.

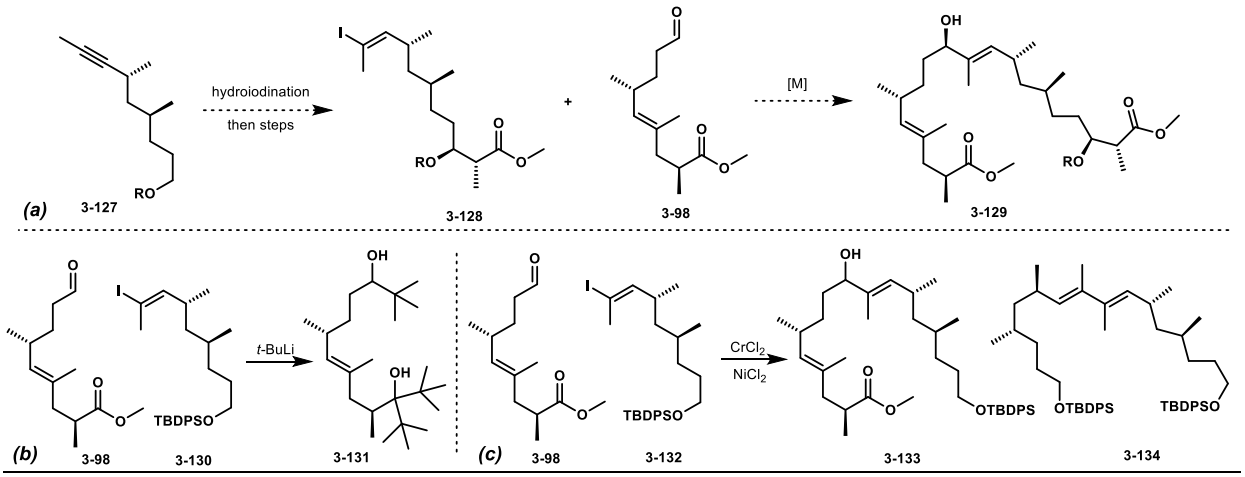

Scheme 3.31 (a) Envisioned allylic alcohol formation ***(b)*** Attempted lithium-halogen exchange ***(c)*** NHK addition resulted in desired product

3.2.4 Successful NHK macrocyclization and completion of the natural products

The results from the intermolecular NHK addition inspired the successful route to the strasseriolides. As discussed earlier, intramolecular NHK cyclizations have advantages over the intermolecular additions. Since a large side product from this reaction was the homo coupling product, we instead decided to combine the fragments through an esterification and then close the macrocycle *via* an NHK. From this planned route we could intercept two intermediates from our initial alkyne metathesis sequence. The western fragment was easily synthesized; aldehyde **3-98** was hydrolyzed to carboxylic acid **3-134** with trimethyltin hydroxide, Scheme 3.31.[144]

Modifications to the synthesis of the eastern fragment were performed by myself and Jessica Pazienza. To insert the vinyl iodide needed for the NHK cyclization, the same protocol to make vinyl iodide **3-95** was planned. Since Schwartz reagent is known to reduce Evan's auxiliaries to the corresponding aldehydes,[145] we planned to insert the iodide prior to the aldol reaction. Alkyne **3-107** was treated with excess Schwartz reagent and quenched with iodide to obtain **3-130** as a single regioisomer. Removal of the silyl protecting group, and oxidation afforded the Evan's aldol precursor. Subjecting the aldehyde to the boron enolate of **3-109** afforded the desired alcohol in moderate yield. The auxiliary was removed and converted to the corresponding methyl ester, but the hydrolysis and methylation were low yielding (34% over two steps). Also,

the auxiliary masked the desired carboxylic acid already and therefore removal of the oxazolidinone at this point was unnecessary, and was planned for after the macrocyclization.

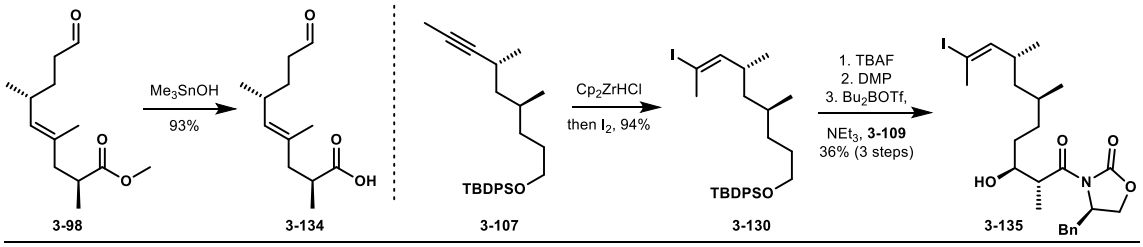

Scheme 3.32. Completion of eastern and western fragments for the NHK cyclization route

Coupling alcohol **3-135** with carboxylic acid **3-134** was surprisingly challenging. Many unsuccessful esterification methods were explored (Shiina, EDCI, DCC, PyBOP, HBTU); ultimately, we saw the best yields, although still modest, through a Yamaguchi esterification (39%).[102] Closure of the macrolide was achieved *via* an intramolecular NHK cyclization to afford a 1.1:1 mixture of diastereomers at the C11 alcohol. The diastereomers were separated by chromatography and assigned by hydrolysis of each alcohol. An asymmetric NHK cyclization was briefly explored, but its results were unfruitful. Lithium hydroxide/hydrogen peroxide hydrolysis cleaved the auxiliary from the more polar alcohol diastereomer **3-137** to afford strasseriolide B (**3-2**). The α-face alcohol **3-136** from the NHK reaction was oxidized with DMP and subsequently hydrolyzed to produce strasseriolide A (**3-1**). The spectral data for both natural products matched those reported and the optical rotations were consistent with the assigned absolute configurations. This is the first reported synthesis of the strasseriolides. :)

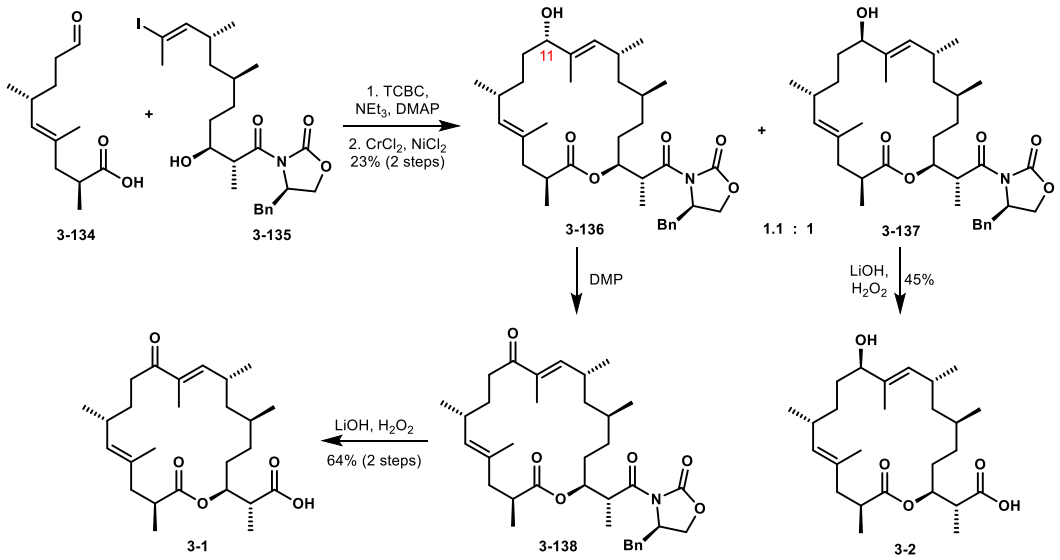

Scheme 3.33. Completion of the total syntheses of strasseriolides A and B

Initial evaluation of synthetic samples of strasseriolide A and B were odd—they were missing several peaks in their respective carbon spectra. The carbon NMR spectra of strasseriolide A was investigated in detail, as shown in Table 3.2. In a dilute CD_3OD solution, the ^{13}C peaks for C1 and C2 were missing, and the chemical shifts for C3 and C20 were slightly off. The C2 peak was observed in the HSQC spectra in the appropriate region, which suggested that the peaks were shifted and broadened by an exchange process.

Carbon #	lit	no AcOH	5 equiv AcOH	10 equiv AcOH
1	177.5	absent	absent	177.5
2	43.0	absent	43.0	43.0
3	75.4	75.9	75.4	75.4
20	13.7	14.3	13.7	13.7

Table 3.2. Carbon chemical shifts and the effect of acetic acid-d_4; Carbon NMR spectra acquired in CD_3OD at 151 MHz, concentration of strasseriolide A was 10 mM

All the discrepancies were localized around the free carboxylic acid (C1). If the effect arose from a monomer-dimer exchange of the carboxylic acid, it would be very sensitive to acid concentration. We added acetic acid-d_4 and found that it progressively returned the carbon spectrum expected for the natural product. Presumably we are generating a mixed carboxylic

acid dimer and increasing the exchange rate between different forms, Scheme 3.34. The spectra reported for the natural products also showed reduced intensity at C2, suggesting that line broadening was also observed under their conditions. Similar to alkaloids spectra being very sensitive to conditions and concentrations, it appears that carboxylic acids also show some sensitivity to concentration and that their spectra can be stabilized with added acetic acid-d_4.

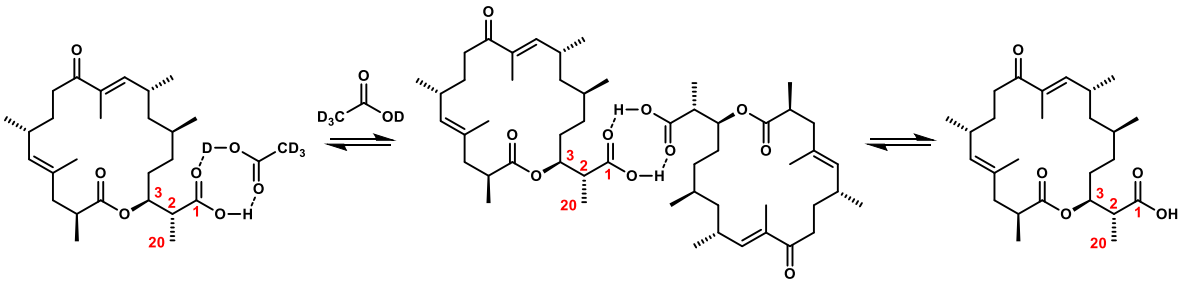

Scheme 3.33. Dimerization of strasseriolide A and the effect of acetic acid-d_4

3.3 Conclusions

This chapter details the first reported total syntheses of strasseriolides A and B. Strasseriolide B was prepared in a convergent synthetic sequence with a longest linear sequence of 16 steps from (*R*)-citronellic acid. Many macrocyclization techniques were explored and the NHK cyclization successfully forged the macrolide, which could be elaborated to the two natural products. Characterization of the molecule demonstrates hydrogen bonding monomers that form carboxylic acids, causing unique changes in the NMR spectra. This phenomenon is underrepresented in the literature. The initial isolation paper of the strasseriolides performed *in vitro* studies on the *Plasmodium falciparum* parasite. As previously mentioned, strasseriolide B was found to have an IC_{50} value of 13 nM against the drug-sensitive strain of malaria and 32 nM against the chloroquine-resistant strain. It also did not show any *in vitro* toxicity with human liver cells and no inhibition of cytochrome P450, or potassium ion channels.

Recently, the isolation team performed additional *in vivo* studies on strasseriolides A–D.[146] Interestingly, when mice were treated with strasseriolide B, they all immediately showed signs of toxicity and died. Additional studies showed that even a dosage as low as 1 mg/Kg was fatal. There were no further studies done with strasseriolide B as its toxicity levels to mice were significant. Interestingly, strasseriolide D, Figure 3.2, was much more promising. It was not toxic to the mice at a dosage as high as 25 mg/Kg and it had modest pharmacokinetic parameters. Even though strasseriolide B was found to be highly toxic to mice, this family of natural products shows progress in identifying a new structural class of anti-malarial compounds. These biological studies and our convergent synthesis of strasserioldes A and B are a promising start.

Moving forward, a sample of strasseriolide B has been sent to the La Roche lab at the University of California, Riverside to be tested again for the IC_{50} value against various malaria strains. If the results are promising, we will move forward by synthesizing strasseriolide B and its analogues for the collaborators to examine first the protein target of the macrolide and then its

mode of action within the parasite. This project will open a door to synthesizing derivatives of these natural products to further improve the toxicity, metabolic stability, and potency.

3.4 Supplemental Information

3.4.1 General Experimental

The ^{1}H NMR spectra were recorded at 500 MHz or 600 MHz using either a Bruker DRX500 (cryoprobe) or a Bruker AVANCE600 (cryoprobe) NMR, respectively. The ^{13}C NMR spectra were recorded at 126 MHz or 151 MHz on the Bruker DRX500 or Bruker AVANCE600 NMR, respectively. All NMR spectra were taken at 25 °C unless otherwise noted. Chemical shifts (δ) are reported in parts per million (ppm) and referenced to residual solvent peak at 7.26 ppm (^{1}H) or 77.16 ppm (^{13}C) for deuterated chloroform ($CDCl_3$), 3.31 ppm (^{1}H) or 49.15 ppm (^{13}C) for deuterated methanol (CD_3OD), 2.50 ppm (^{1}H) or 39.52 ppm (^{13}C) for deuterated dimethylsulfoxide (DMSO-d_6). The ^{1}H NMR spectral data are presented as follows: chemical shift, multiplicity (s = singlet, d = doublet, t = triplet, q = quartet, quint = quintet, m = multiplet, dd = doublet of doublets, ddd = doublet of doublet of doublets, dddd = doublet of doublet of doublet of doublets, dt = doublet of triplets, dq = doublet of quartets, ddq = doublet of doublet of quartets, app. = apparent), coupling constant(s) in hertz (Hz), and integration. High-resolution mass spectra (HRMS) were recorded on Waters LCT Premier TOF spectrometer with electrospray ionization (ESI) and chemical ionization (CI) sources. An internal standard was used to calibrate the exact mass of each compound. For accuracy, the peak selected for comparison was that which most closely matched the ion intensity of the internal standard.

Unless otherwise stated, synthetic reactions were carried out under an atmosphere of argon in flame- or oven-dried glassware. Thin layer chromatography (TLC) was carried out using glass plates coated with a 250 μm layer of 60 Å silica gel. TLC plates were visualized with a UV lamp at 254 nm, or by staining with Hanessian's stain or $KMnO_4$ stain. Liquid chromatography was performed using forced flow (flash chromatography) with an automated purification system on prepacked silica gel (SiO_2) columns unless otherwise stated. Optical rotations were performed on a JACSO P-1010 spectrometer using a glass 10 mm cell with the sodium D-line at 589 nm.

All commercially available reagents were used as received unless stated otherwise. Solvents were purchased as ACS grade or better and as HPLC-grade and passed through a solvent purification system equipped with activated alumina columns prior to use. $CDCl_3$, CD_3OD, and DMSO-d_6 was purchased from Cambridge Isotope Laboratories. (*R*)-(+)-citronellic acid and (*R,S*)-Josiphos was purchased from Sigma Aldrich. (*S*)-(–)-citronellal was purchased from TCI Chemicals.

3.4.2 Experimental procedures and compound characterization

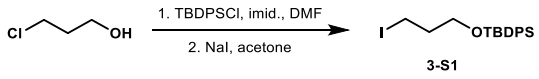

3-S1

***tert*-Butyl(3-iodopropoxy)diphenylsilane (3-S1):**

Iodide **3-S1** was prepared according to a modified literature procedure:[147]

To a solution of 3-chloro-1-propanol (0.84 mL, 10.0 mmol, 1.0 equiv) in DMF (20 mL) at rt was added imidazole (2.04 g, 30.0 mmol, 3.0 equiv) followed by TBDPSCl (3.1 mL, 12.0 mmol, 1.2 equiv). The reaction was stirred at rt overnight and then diluted with Et_2O. The organic phase was washed with H_2O (4 X) then brine, dried with $MgSO_4$, filtered, and concentrated *in vacuo*. The resulting residue was dissolved in acetone and then treated with NaI and heated to reflux for 44 h. After cooling to rt, the solution was concentrated *in vacuo*. The resulting residue was diluted with H_2O and extracted with Et_2O (2 X). The combined organic phase was washed with brine, dried with $MgSO_4$, filtered, and concentrated *in vacuo* to obtain iodide **3-S1** (3.54 g, 83%). Spectral data is in accordance with the reported literature.[147]

^{1}H NMR (500 MHz, $CDCl_3$) δ 7.70 (d, *J* = 8.0 Hz, 4H), 7.48 – 7.39 (m, 6H), 3.75 (t, *J* = 5.7 Hz, 2H), 3.37 (t, *J* = 6.8 Hz, 2H), 2.06 (quint, *J* = 6.3 Hz, 2H) 1.09 (s, 9 H).

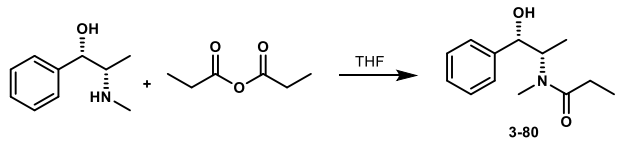

***N*-((*1S,2S*)-1-Hydroxy-1-phenylpropan-2-yl)-*N*-methylpropionamide (3-80):**

Amine **3-80** was prepared according to a modified literature procedure:[148]

To a solution of (*1S,2S*)-(+)-pseudoephedrine (500 mg, 3.03 mmol, 1.0 equiv) in THF (6 mL) was added propanoic anhydride (0.42 mL, 3.33 mmol, 1.1 equiv). After stirring for 30 min at rt, the reaction was quenched with saturated $NaHCO_3$ solution. The slurry was extracted with EtOAc (4 X). The combined organic phase was washed with brine, dried with Na_2SO_4, filtered, and concentrated *in vacuo* to obtain amine **3-80** as a white solid. Spectral data is in accordance with the reported literature.[148]

^{1}H NMR (3:1 ratio of rotamers, asterisk denotes minor rotamer; 500 MHz, $CDCl_3$) δ 7.38 – 7.32 (m, 5H), 4.63 – 4.57 (m, 1H), 4.48 – 4.39 (m, 1H), 4.06 – 3.96* (m, 1H), 2.93* (s, 3H), 2.81, (s, 3H), 2.58 – 2.49* (m, 1H), 2.44 – 2.37* (m, 1H), 2.36 – 2.24 (m, 2H), 1.15 – 1.09 (m, 6H), 0.98* (d, J = 6.8 Hz, 3H).

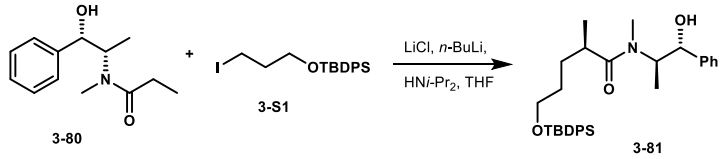

(*R*)-5-((*tert*-Butyldiphenylsilyl)oxy)-*N*-((*1R,2R*)-1-hydroxy-1-phenylpropan-2-yl)-*N*,2-dimethylpentanamide (3-81):

Amine **3-81** was prepared according to a modified literature procedure:[149]

To a solution of anhydrous LiCl (3.0 g, 70.8 mmol, 6.0 equiv) and HN*i*-Pr_2 (5.0 mL, 35.4 mmol, 3.0 equiv) in THF (17 mL) at –78 °C was added *n*-BuLi (2.5 M in hex; 11.8 mL, 29.5 mmol, 2.5 equiv). The flask was removed from the cooling bath for a couple min before cooling back to –78 °C. A solution of amine **3-80** (2.61 g, 11.8 mmol, 1.0 equiv) in THF (25 mL) was added and the

reaction was stirred for 2 h before warming to 0 °C. A solution of iodide **3-S1** (10.0 g, 23.6 mmol, 2.0 equiv) in THF (10 mL) was added and the reaction was stirred at 0 °C for 15 h. The reaction was quenched with NH_4Cl solution and extracted with Et_2O (2 X). The combined organic phase was washed with brine, dried with $MgSO_4$, filtered, and concentrated *in vacuo*. The resulting residue was purified via flash chromatography (0 → 70% EtOAc in hex) to obtain amine **3-81** (3.58 g, 59%).

^{1}H NMR (600 MHz, 395 K, DMSO-d_6) δ 7.66 (d, *J* = 6.8 Hz, 4H), 7.49 – 7.41 (m, 6H), 7.35 (d, *J* = 7.3 Hz, 2H), 7.31 (t, *J* = 7.6 Hz, 2H), 7.24 (t, *J* = 7.1 Hz, 1H), 4.61 (d, *J* = 7.0 Hz, 1H), 3.70 (t, *J* = 6.4 Hz, 2H), 3.03 – 2.89 (m, 2H), 2.83 (s, 3H), 2.76 – 2.66 (m, 1H), 1.65 (dd, *J* = 13.1, 7.3 Hz, 1H), 1.56 – 1.49 (m, 2H), 1.37 (dd, *J* = 13.5, 7.3 Hz, 1H), 1.07 (s, 9H), 0.99 (d, *J* = 6.1 Hz, 3H), 0.95 (d, *J* = 6.5 Hz, 3H).

^{13}C NMR (126 MHz, $CDCl_3$) δ 178.9, 142.7, 135.7, 135.6, 134.0, 129.6, 128.3, 127.7, 126.4, 77.4, 76.4, 63.7, 36.3, 30.3, 30.1, 27.0, 19.3, 17.3, 14.5.

HRMS (ESI-TOF) *m/z* calculated for $C_{32}H_{43}NO_3SiH^+$ $(M+H)^+$ 518.3090, found 518.3098.

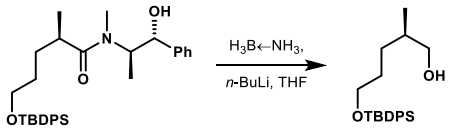

3-81 3-S2

(*R*)-5-((*tert*-Butyldiphenylsilyl)oxy)-2-methylpentan-1-ol (3-S2):

To a solution of $H_3B{\leftarrow}NH_3$ (874 mg, 28.3 mmol, 4.1 equiv) in THF (14 mL) at 0 °C was added *n*-BuLi (2.5 M in hex; 11.1 mL, 27.7 mmol, 4.0 equiv). The flask was removed from the ice bath for a few min then cooled back to 0 °C. A solution of amine **3-81** (3.58 g, 6.91 mmol, 1.0 equiv) in THF (20 mL) was added and the reaction was allowed to warm to rt overnight. After stirring for 15 h, the reaction was quenched with H_2O. The solution was extracted with Et_2O and the combined organic phase was washed with brine, dried with $MgSO_4$, filtered, and concentrated *in vacuo*. The

resulting residue was purified via flash chromatography (10% EtOAc in hex) to obtain alcohol **3-S2** (2.02 g, 82%).

^{1}H NMR (500 MHz, $CDCl_3$) δ 7.67 (d, *J* = 6.6 Hz, 4H), 7.45 – 7.36 (m, 6H), 3.66 (t, *J* = 6.5 Hz, 2H), 3.48 (dd, *J* = 10.6, 5.3 Hz, 1H), 3.41 (dd, *J* = 10.8, 5.4 Hz, 1H), 1.69 – 1.53 (m, 2H), 1.46 (ddd, *J* = 13.3, 10.6, 5.3 Hz, 1H), 1.21 – 1.12 (m, 1H), 1.05 (s, 9H), 0.90 (d, J = 6.7 Hz, 3H).

^{13}C NMR (126 MHz, $CDCl_3$) δ 135.7, 134.2, 129.7, 127.7, 68.5, 64.3, 35.6, 30.1, 29.4, 27.0, 19.4, 16.7.

HRMS (CI-TOF) *m/z* calculated for $C_{22}H_{32}O_2SiH^+$ $(M+H)^+$ 357.2250, found 357.2242.

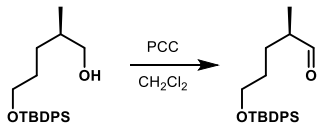

3-S2 3-82

(*R*)-5-((*tert*-Butyldiphenylsilyl)oxy)-2-methylpentanal (3-82):

To solution of alcohol **3-S2** (2.02 g, 5.66 mmol, 1.0 equiv) in CH_2Cl_2 (28 mL) was added PCC (2.20 g, 10.2 mmol, 1.8 equiv). The slurry was stirred for 2 h at rt and then filtered through a pad a silica. The cake was thoroughly washed with CH_2Cl_2 after which the filtrated was concentrated *in vacuo* to obtain aldehyde **3-82** (1.72 g, 86%).

^{1}H NMR (500 MHz, $CDCl_3$) δ 9.62 (s, 1H), 7.68 (d, *J* = 7.4 Hz, 4H), 7.48 – 7.31 (m, 6H), 3.70 (t, *J* = 6.1 Hz, 2H), 2.34 (dd, *J* = 13.7, 6.8 Hz, 1H), 1.87 – 1.77 (m, 1H), 1.67 – 1.55 (m, 2H), 1.53 – 1.42 (m, 1H), 1.14 – 1.00 (m, 12H).

^{13}C NMR (125 MHz, $CDCl_3$) δ 205.2, 135.7, 134.0, 129.7, 127.8, 63.7, 46.1, 29.9, 27.0, 26.9, 19.3, 13.5.

HRMS (CI-TOF) *m/z* calculated for $C_{22}H_{29}O_2Si^+$ $(M-H_2+H)^+$ 353.1937, found 353.1933.

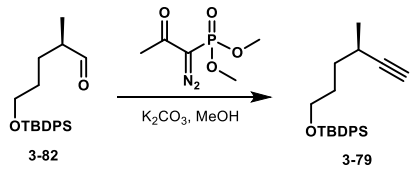

(*R*)-*tert*-Butyl((4-methylhex-5-yn-1-yl)oxy)diphenylsilane (3-79):

To a solution aldehyde **3-82** (10 mg, 0.282 mmol, 1.0 equiv) in MeOH (1.4 mL) at 0 °C was added the Ohira-Bestmann reagent (65 mg, 0.338 mmol, 1.2 equiv) followed by K_2CO_3 (78 mg, 0.564 mmol, 2.0 equiv). The solution was stirred at 0 °C for 6.5 h and then concentrated *in vacuo*. The resulting residue was partitioned between H_2O and Et_2O. The organic phase was extracted and washed with brine, dried with $MgSO_4$, filtered and concentrated *in vacuo* to obtain terminal alkyne **3-79** (84 mg, 85%). The spectral data is in accordance with the reported literature.[149]

^{1}H NMR (500 MHz, $CDCl_3$): δ 7.68 (d, *J* = 6.5 Hz, 4H), 7.46 – 7.36 (m, 6H), 3.69 (t, *J* = 6.3 Hz, 2H), 2.48 – 2.39 (m, 1H), 2.03 (d, *J* = 2.3 Hz, 1H), 1.81 – 1.72 (m, 1H), 1.72 – 1.63 (m, 1H), 1.61 – 1.49 (m, 1H), 1.18 (d, *J* = 6.9 Hz, 3H), 1.06 (s, 9H).

^{13}C NMR (126 MHz, $CDCl_3$): δ 135.7, 134.2, 129.7, 127.8, 89.2, 68.4, 63.8, 33.2, 30.4, 27.0, 25.6, 21.1, 19.4.

HRMS (CI-TOF) *m/z* calculated for $C_{23}H_{30}OSiH^+$ $(M+H)^+$ 351.2144, found 351.2137.

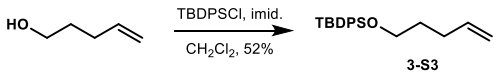

***tert*-Butyl(pent-4-en-1-yloxy)diphenylsilane (3-S3):**

To a solution of 4-penten-1-ol (2.0 mL, 19.4 mmol, 1.0 equiv) in CH_2Cl_2 (19 mL) at rt was added imidazole (1.45 g, 21.3 mmol, 1.1 equiv) followed by TBDPSCl (5.5 mL, 21.3 mmol, 1.1 equiv). The reaction was stirred at rt for 18.5 h and then washed with H_2O (2 X) and brine. The organic phase was dried with Na_2SO_4, filtered, and concentrated *in vacuo*. The resulting residue was purified through a silica pad (100% hex) to obtain alkene **3-S3** as a clear oil (3.31 g, 52%). Spectral data is in accordance with the reported literature.[150]

^{1}H NMR (500 MHz, $CDCl_3$): 7.80 – 7.72 (m, 4H), 7.50 – 7.40 (m, 6H), 5.93 – 5.80 (m, 1H), 5.07 (ddd, *J* = 17.1, 3.5, 1.7 Hz, 1H), 5.03 – 4.96 (m, 1H), 3.75 (qd, *J* = 6.2, 2.4 Hz, 2H), 2.23 (dd, *J* = 9.4, 3.9 Hz, 2H), 1.77 – 1.69 (m, 2H), 1.13 (s, 9H).

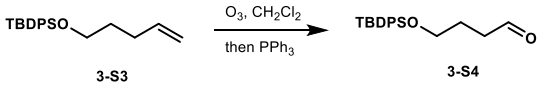

3-S3 3-S4

4-((*tert*-Butyldiphenylsilyl)oxy)butanal (3-S4):

A solution of alkene **3-S3** (1.50 g, 4.62 mmol, 1.0 equiv) in CH_2Cl_2 (23 mL) at –78 °C was treated with O_3 until the solution turned blue in color. The flask was purged with O_2 until the blue color dissipated, and then PPh_3 (3.64 g, 13.9 mmol, 3.0 equiv) was added. The solution was allowed to slowly warm to rt overnight. The reaction mixture was concentrated *in vacuo* and the resulting residue was purified via flash chromatography (0 → 20% EtOAc in hex) to obtain aldehyde **3-S4** as a clear oil (1.27g, 84%).

^{1}H NMR (500 MHz, $CDCl_3$) δ 9.81 (s, 1H), 7.70 (d, *J* = 6.8 Hz, 4H), 7.48 – 7.38 (m, 6H), 3.73 (t, *J* = 5.9 Hz, 2H), 2.57 (t, *J* = 7.0 Hz, 2H), 1.92 (p, *J* = 6.5 Hz, 2H), 1.10 (s, 9H).

^{13}C NMR (125 MHz, $CDCl_3$) δ 202.5, 135.6, 133.7, 129.8, 127.8, 63.0, 40.8, 26.9, 25.4, 19.3.

HRMS (ESI-TOF) *m/z* calculated for $C_{20}H_{26}O_2SiNa^+$ $(M+Na)^+$ 349.1600, found 349.1606.

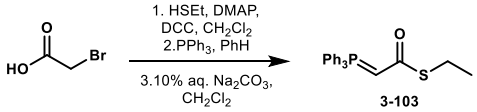

3-103

***S*-Ethyl 2-(triphenyl-λ^5-phosphaneylidene)ethanethioate (3-103):**

Thioester **3-103** was prepared according to a known literature procedure:[151]

To a solution of bromoacetic acid (2.0 g, 14.4 mmol, 1.0 equiv) in CH_2Cl_2 (50 mL) was added ethanethiol (1.3 mL, 18.7 mmol, 1.3 equiv), DCC (3.12 g, 15.1 mmol, 1.05 equiv), and DMAP (176 mg, 1.44 mmol, 1.05 equiv). The solution was stirred at rt overnight and then filtered through a

pad of celite and the cake was washed with additional CH_2Cl_2. The filtrate was then washed with saturated $NaHCO_3$ solution, H_2O, then brine. The organic phase was dried with Na_2SO_4, filtered, and concentrated *in vacuo*. The resulting residue was diluted with benzene (15 mL) and filtered through filter paper. The precipitate was washed additional benzene (15 mL). To the filtrate was added PPh_3. The slurry was allowed to rest at rt (without stirring) for 2 d. The slurry was then vacuum filtered and the precipitate was washed with toluene. The resulting white crystals were diluted with CH_2Cl_2 (27 mL) and 10% aqueous Na_2CO_3 solution (18 mL). The slurry was stirred for 20 min and then the organic phase was extracted. The aqueous layer was extracted with CH_2Cl_2 (2 X). The combined organic phase was concentrated *in vacuo* and the resulting residue was diluted with pentanes. The slurry was vacuum filtered to obtain thioester **3-103** as white crystals (3.61 g, 69% over 3 steps). Spectral data is in accordance with the reported literature.

^{1}H NMR (500 MHz, $CDCl_3$) δ 7.68 – 7.59 (m, 6H), 7.59 – 7.52 (m, 3H), 7.50 – 7.43 (m, 6H), 3.66 (d, *J* = 22.1 Hz, 1H), 2.84 (q, *J* = 7.3 Hz, 2H), 1.25 (t, *J* = 7.3 Hz, 3H).

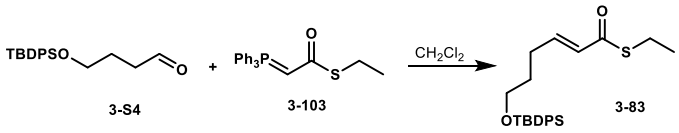

_S_-Ethyl (_E_)-6-((_tert_-butyldiphenylsilyl)oxy)hex-2-enethioate (3-83):

A solution of aldehyde **3-S4** (868 mg, 2.66 mmol, 1.0 equiv) and Wittig reagent **3-103** (1.26g, 3.46 mmol, 1.3 equiv) in CH_2Cl_2 (13 mL) was heated to reflux and stirred for 23 h. The solution was concentrated *in vacuo* and the resulting residue was purified via flash chromatography (0 → 10% EtOAc in hex) to obtain thioester **3-83** (693 mg, 63%).

^{1}H NMR (500 MHz, $CDCl_3$) δ 7.68 (dd, *J* = 8.0, 1.4 Hz, 2H), 7.47 – 7.35 (m, 6H), 6.96 – 6.87 (m, 1H), 6.12 (d, *J* = 15.5 Hz, 1H), 3.70 (t, *J* = 6.1 Hz, 2H), 2.96 (dd, *J* = 14.9, 7.4 Hz, 2H), 2.33 (dd, *J* = 14.8, 7.1 Hz, 1H), 1.77 – 1.68 (m, 2H), 1.30 (t, *J* = 7.5 Hz, 3H), 1.08 (s, 9H).

^{13}C NMR (126 MHz, $CDCl_3$) δ 190.2, 145.0, 135.7, 133.9, 129.8, 129.1, 127.8, 63.0, 31.0, 28.7, 27.0, 23.2, 19.3, 15.0.

HRMS (ESI-TOF) *m/z* calculated for $C_{24}H_{32}O_2SiSNa^+$ $(M+Na)^+$ 435.1790, found 435.1790.

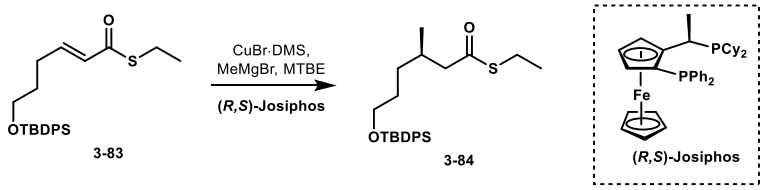

***S*-Ethyl (*R*)-6-((*tert*-butyldiphenylsilyl)oxy)-3-methylhexanethioate (3-84):**

A solution of CuBr·DMS (6 mg, 0.0292 mmol, 0.03 equiv) and (*R,S*)–Josiphos (25 mg, 0.0390 mmol, 0.04 equiv) in MTBE (8 mL) was stirred at rt for 30 min and then cooled to –78 °C. To the cooled solution was added MeMgBr (3.0 M in Et_2O, 0.48 mL, 1.45 mmol, 1.5 equiv) followed by a slow addition of thioester **3-83** (400 mg, 0.969 mmol, 1.0 equiv) in MTBE (2 mL) via syringe pump over 2 h (0.5 mL/ hr). The reaction was stirred at –70 °C for 19 h and then quenched with MeOH. The solution was partitioned between saturated NH_4Cl solution and Et_2O and additional extractions were performed with Et_2O. The combined organic phase was washed with brine, dried with $MgSO_4$, filtered, and concentrated *in vacuo* to obtain thioester **3-84** (300 mg, 72%).

^{1}H NMR (500 MHz, $CDCl_3$) δ 7.69 (d, *J* = 7.7 Hz, 4H), 7.46 – 7.36 (m, 6H), 3.67 (t, *J* = 6.5 Hz, 2H), 2.88 (q, *J* = 7.4 Hz, 2H), 2.53 (dd, *J* = 14.4, 6.0 Hz, 1H), 2.36 (dd, *J* = 14.5, 8.1 Hz, 1H), 2.04 (dd, *J* = 13.5, 6.8 Hz, 1H), 1.68 – 1.50 (m, 1H), 1.48 – 1.39 (m, 1H), 1.33 – 1.20 (m, 4H), 1.07 (s, 9H), 0.94 (d, J = 6.8 Hz, 3H).

^{13}C NMR (126 MHz, $CDCl_3$) δ 199.2, 135.7, 134.2, 129.7, 127.7, 64.1, 51.5, 32.9, 31.0, 30.0, 27.0, 23.4, 19.6, 19.3, 14.9.

HRMS (ESI-TOF) *m/z* calculated for $C_{25}H_{36}O_2SSiNa^+$ $(M+Na)^+$ 451.2103, found 451.2104.

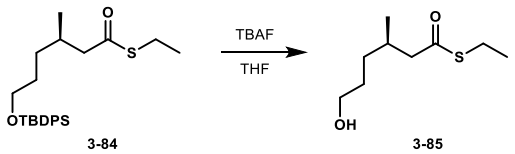

3-84 3-85

***S*-Ethyl (*R*)-6-hydroxy-3-methylhexanethioate (3-85):**

To a solution of thioester **3-84** (30 mg, 0.070 mmol, 1.0 equiv) in THF (0.35 mL) was added TBAF (1.0 M in THF; 0.14 mL, 0.14 mmol, 2.0 equiv). The solution was stirred for 1.5 h at rt and then concentrated *in vacuo* and subjected to flash chromatography (0 → 50% EtOAc in hex) to obtain alcohol **3-85** (11 mg, 85%).

^{1}H NMR (500 MHz, $CDCl_3$) δ 3.63 (t, J = 6.6 Hz, 2H), 2.87 (q, *J* = 7.4 Hz, 2H), 2.53 (dd, *J* = 14.6, 6.3 Hz, 1H), 2.38 (dd, *J* = 14.6, 7.8 Hz, 1H), 2.10 – 1.99 (m 1H), 1.67 – 1.58 (m, 1H), 1.57 – 1.50 (m, 1H), 1.41 (ddd, *J* = 13.4, 8.0, 4.0 Hz, 1H), 1.30 – 1.19 (m, 4H), 0.95 (d, *J* = 6.7 Hz, 3H).

^{13}C NMR (126 MHz, $CDCl_3$) δ 199.4, 63.1, 51.4, 32.7, 30.9, 30.1, 23.5, 19.6, 14.9.

HRMS (ESI-TOF) *m/z* calculated for $C_9H_{18}O_2SNa^+$ $(M+Na)^+$ 213.0925, found 213.0928.

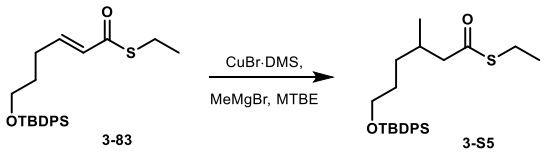

3-83 3-S5

***S*-Ethyl 6-((*tert*-butyldiphenylsilyl)oxy)-3-methylhexanethioate (3-S5):**

To a slurry of CuBr·DMS (53 mg, 0.257 mmol, 1.0 equiv) in MTBE (2.2 mL) at –78 °C was added MeMgBr (2.7 M in Et_2O, 0.19 mL, 0.514 mmol, 2.0 equiv) followed by a dropwise addition of thioester **3-83** (106 mg, 0.257 mmol, 1.0 equiv) in MTBE (0.4 mL). The reaction was stirred at –70 °C for 20 h and then additional MeMgBr (2.7 M in Et_2O, 0.2 mL, 0.514 mmol, 2.0 equiv) was added. The reaction continued to stir at –70 °C for 17 h and was then quenched with MeOH. The solution was partitioned between saturated NH_4Cl solution and Et_2O and additional extractions were performed with Et_2O. The combined organic phase was washed with brine, dried with

$MgSO_4$, filtered, and concentrated *in vacuo*. The resulting residue was subjected to flash chromatography (0 → 5% EtOAc in hex) to obtain thioester **3-S5** (26 mg, 24%).

^{1}H NMR (500 MHz, $CDCl_3$) δ 7.66 (dd, *J* = 7.8, 1.4 Hz, 4H), 7.45 – 7.35 (m, 6H), 3.64 (t, *J* = 6.4 Hz, 2H), 2.87 (q, *J* = 7.4 Hz, 2H), 2.51 (dd, *J* = 14.4, 6.0 Hz, 1H), 2.34 (dd, *J* = 14.4, 8.1 Hz, 1H), 2.02 (dd, *J* = 13.4, 6.8 Hz, 1H), 1.64 – 1.48 (m, 2H), 1.41 (ddd, *J* = 10.7, 7.8, 5.4 Hz, 1H), 1.29 – 1.19 (m, 4H), 1.05 (s, 9H), 0.92 (d, *J* = 6.7 Hz, 3H).

^{13}C NMR (126 MHz, $CDCl_3$) δ 199.3, 135.7, 134.2, 129.7, 127.7, 64.1, 51.5, 32.9, 31.1, 30.0, 27.0, 23.4, 19.6, 19.4, 14.9.

HRMS (ESI-TOF) *m/z* calculated for $C_{25}H_{36}O_2SSiNa^+$ $(M+Na)^+$ 451.2103, found 451.2082.

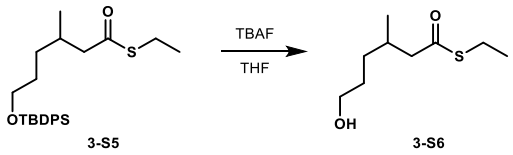

3-S5 3-S6

***S*-Ethyl 6-hydroxy-3-methylhexanethioate (3-S6):**

To a solution of thioester **3-S5** (26 mg, 0.0606 mmol, 1.0 equiv) in THF (0.30 mL) was added TBAF (1.0 M in THF; 0.12 mL, 0.121 mmol, 2.0 equiv). The solution was stirred for 1.5 h at rt and then concentrated *in vacuo* and subjected to flash chromatography (0 → 50% EtOAc in hex) to obtain alcohol **3-S6** (6 mg, 55%).

^{1}H NMR (500 MHz, $CDCl_3$) δ 3.64 (t, *J* = 6.6 Hz, 2H), 2.88 (q, *J* = 7.4 Hz, 2H), 2.54 (dd, *J* = 14.6, 6.3 Hz, 1H), 2.38 (dd, *J* = 14.6, 7.8 Hz, 1H), 2.05 (dd, *J* = 13.4, 6.8 Hz, 1H), 1.68 – 1.49 (m, 2H), 1.46 – 1.38 (m, 2H), 1.31 – 1.20 (m, 4H), 0.96 (d, *J* = 6.7 Hz, 1H).

^{13}C NMR (126 MHz, $CDCl_3$) δ 199.4, 63.1, 51.4, 32.7, 30.9, 30.2, 23.5, 19.7, 14.9.

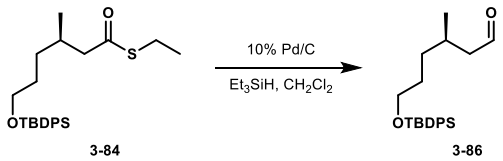

3-84 3-86

(*R*)-6-((*tert*-Butyldiphenylsilyl)oxy)-3-methylhexanal (3-86):

To a solution of thioester **3-84** (140 mg, 0.327 mmol, 1.0 equiv) and Et_3SiH (0.16) in CH_2Cl_2 (1.0 mL) at rt, open to air, was added 10% Pd/C (500 mg). The slurry was stirred for 1 h and then additional Et_3SiH (0.15 mL) and 10% Pd/C (~100 mg) was added. The slurry was stirred for 15 min and then filtered over celite and the cake was rinsed thoroughly with CH_2Cl_2. The filtrated was concentrated *in vacuo* to obtain aldehyde **3-86** (108 mg, 90%) which was subjected to the next reaction without further purification.

Optical rotation: $[\alpha]^{22}_D$ = +6.2 (*c* = 10.0, $CHCl_3$).

^{1}H NMR (500 MHz, $CDCl_3$): δ 9.74 (s, 1H), 7.68 (d, *J* = 6.8 Hz, 4 H), 7.46 – 7.37 (m, 6H), 3.67 (t, *J* = 6.4 Hz, 2H), 2.38 (dd, *J* = 16.1, 5.5 Hz, 1H), 2.22 (ddd, *J* = 16.1, 8.0, 2.4 Hz, 1H), 2.10 – 2.00 (m, 1H), 1.66 – 1.50 (m, 2H), 1.46 – 1.36 (m, 1H), 1.36 – 1.25 (m, 1H), 1.07 (s, 9H), 0.96 (d, *J* = 6.7 Hz, 3H).

^{13}C NMR (126 MHz, $CDCl_3$): δ 203.1, 135.7, 134.1, 129.7, 127.8, 64.0, 51.1, 33.1, 30.0, 28.0, 27.0, 20.1, 19.3.

HRMS (ESI-TOF) *m/z* calculated for $C_{23}H_{32}O_2SiNa+$ $(M+Na)^+$ 391.2069, found 391.2072.

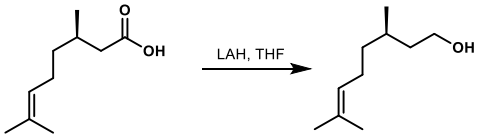

(*R*)-Citronellol:

To a solution of (*R*)-(+)-citronellic acid (2.0 mL, 10.9 mmol, 1.0 equiv) in THF (36 mL) at 0 °C was added lithium aluminum hydride (454 mg, 12.0 mmol, 1.1 equiv) portionwise. When the bubbling ceased, the reaction was warmed to rt and stirred at rt for 3 h after which an additional portion of

lithium aluminum hydride was added (~300 mg). The slurry was then stirred at rt overnight. The reaction was slowly quenched with 1 M HCl, and then diluted with H_2O and EtOAc. The slurry was vacuum filtered over filter paper. The slurry was extracted with EtOAc (3 X). The combined organic phase was washed with H_2O, then brine, dried with Na_2SO_4, filtered, and concentrated *in vacuo* to obtain (*R*)-citronellal which was subjected to the next reaction without further purification.

^{1}H NMR (500 MHz, $CDCl_3$) δ 4.98 (t, *J* = 7.1 Hz, 1H), 3.60 – 3.47 (m, 2H), 1.90 – 1.79 (m, 2H), 1.56 (s, 3H), 1.52 – 1.42 (m, 5H), 1.30 – 1.19 (m, 2H), 1.10 – 1.00 (m, 1H), 0.79 (d, *J* = 6.9 Hz, 3H).

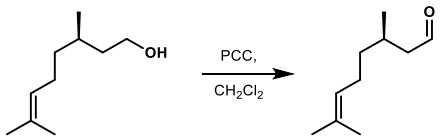

(*R*)-Citronellal:

To a solution of (*R*)-citronellol in CH_2Cl_2 at rt was added PCC (3.31 g, 15.4 mmol, 1.4 equiv). The slurry was stirred for 2 h at rt and then filtered through a pad a silica. The cake was thoroughly washed with CH_2Cl_2 after which the filtrate was concentrated *in vacuo* to obtain (*R*)-citronellal (876 mg, 53% over 2 steps).

^{1}H NMR (500 MHz, $CDCl_3$) δ 9.72 (s, 1H), 5.05 (t, *J* = 6.5 Hz, 1H), 2.37 (dd, *J* = 16.0, 5.4 Hz, 1H), 2.19 (dd, *J* = 16.1, 7.9 Hz, 1H), 2.10 – 1.91 (m, 3H), 1.65 (s, 3H), 1.57 (s, 3H), 1.38 – 1.29 (m, 1H), 1.29 – 1.19 (m, 1H), 0.94 (d, *J* = 7.0 Hz, 3H).

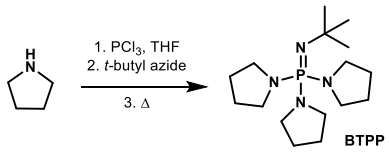

***tert*-Butylimino-tri(pyrrolidino)phosphorane (BTPP):**

BTPP was prepared according to a known literature procedure:[129]

To a solution of pyrrolidine (20 mL, 241 mmol, 8.4 equiv) in THF (80 mL) at –78 °C was added PCl_3 (2.5 mL, 28.6 mmol, 1.0 equiv) dropwise. The solution was allowed to warm to rt and stirred at rt for 20 h. The reaction was then cooled to 0 °C and *t*-butyl azide (3.68 g, 37.3 mmol, 1.3 equiv) was added after which it was allowed to warm to rt and stirred at rt overnight. Next, the solution was poured into a separatory funnel containing cold H_2O (60 mL), hex (63 mL), toluene (32 mL), and NEt_3 (5 mL). The organic layer was extracted and additional extractions were performed with hex. The combined organic phase was dried over KOH pellets with stirring for 2 h and then placed in the freezer for 3 h. The solvent was decanted and concentrated *in vacuo* to obtain the phosphazide as a light-yellow solid, which was kept on the high-vac for a few hours. The neat solid was then heated under argon while stirring at 150 °C for 3 days to obtain BTPP as a cloudy viscous oil, which was used without further purification.

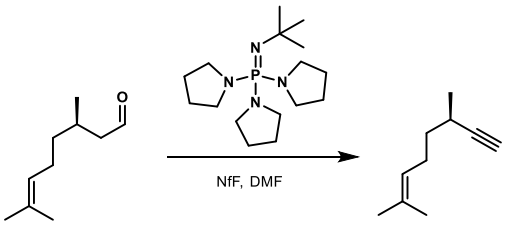

3-87

(*R*)-3,7-Dimethyloct-6-en-1-yne (3-87):

To a solution of (*R*)-citronellal (1.0 g, 6.48 mmol, 1.0 equiv) and NfF (1.4 mL, 7.78 mmol, 1.2 equiv) in DMF (13 mL) at –10 °C was added BTPP (4.79 g, 15.3 mmol, 2.4 equiv). The solution was allowed to warm to rt and was stirred at rt overnight. The reaction solution was directly subjected to flash chromatography (100% hex) to obtain terminal alkyne **3-87**, which was subjected to the next reaction without further purification.

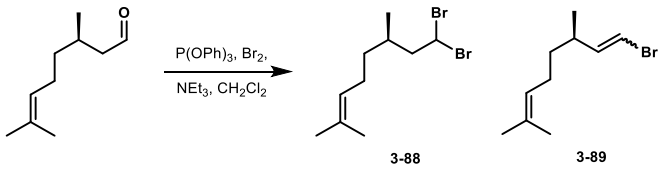

(*R*)-8,8-Dibromo-2,6-dimethyloct-2-ene (3-88):

Dibromide **3-88** was synthesized according to a modified literature procedure:[129]

To a solution of triphenyl phosphite (0.51 mL, 1.94 mmol, 1.5 equiv) in CH_2Cl_2 (10 mL) at –78 °C was added Br_2 (0.09 mL, 1.69 mmol, 1.3 equiv) followed by NEt_3 (0.54 mL, 3.90 mmol, 3.0 equiv) dropwise. When the foggy vapor disappeared from the head space, a solution of (*R*)-citronellal (200 mg, 1.30 mmol, 1.0 equiv) in CH_2Cl_2 (3 mL) was added dropwise. The reaction was warmed to rt and stirred for 2.5 h. The reaction solution was concentrated *in vacuo* and subjected to flash column chromatography (100% hex) to obtain **3-88** and **3-89** as mixture of geminal dibromo alkane, and *cis* and *trans* vinyl bromide diastereomers (10 : 0.5 : 1.0) and some $P(OPh)_3$ (3 % by ^{1}H NMR) (208 mg). This mixture was subjected to the next step without further purification. Spectral data for dibromide **3-88** is in accordance with the reported literature.[129]

^{1}H NMR (500 MHz, $CDCl_3$) δ 5.72 (dd, *J* = 8.5, 5.8 Hz, 1H), 5.09 (t, *J* = 7.1 Hz, 1H), 2.44 (ddd, *J* = 14.3, 8.5, 5.5 Hz, 1H), 2.25 – 2.17 (m, 1H), 2.07 – 1.94 (m, 2H), 1.83 – 1.74 (m, 1H), 1.69 (s, 3H), 1.62 (s, 3H), 1.41 – 1.31 (m, 1H), 1.27 – 1.16 (m, 1H), 0.92 (d, *J* = 6.8 Hz, 3H).

^{13}C NMR (126 MHz, $CDCl_3$) δ 131.9, 124.2, 52.9, 45.0, 36.3, 32.3, 25.9, 25.3, 18.6, 17.9.

Diagnostic data for *cis* and *trans* vinyl bromide:

^{1}H NMR (500 MHz, $CDCl_3$) δ 6.11 (d, *J* = 6.9 Hz, 1H, *cis*), 6.06 (dd, *J* = 13.5, 8.1 Hz, 1H, *trans*), 5.87 (d, *J* = 13.6 Hz, 1H, *trans*), 5.87 (dd, *J* = 9.2, 7.0 Hz, 1H, *cis*).

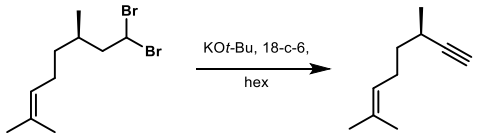

3-88 3-87

(*R*)-3,7-Dimethyloct-6-en-1-yne (3-87):

Terminal alkyne **3-87** was synthesized according to a modified literature procedure:[129]

To a solution of the crude dibromide (200 mg, 0.671, 1.0 equiv) in hex (1.6 mL) was added KO*t*-Bu (271 mg, 2.42 mmol, 3.6 equiv) followed by 18-crown-6 (9 mg, 0.034 mmol, 0.05 equiv). This slurry was heated to reflux in a microwave vial for 15 h. After cooling to rt, the slurry was washed with H_2O and the aqueous phase was back extracted with hex (3 X). The combined organic phase was dried with Na_2SO_4, filtered, and concentrated *in vacuo*. The resulting residue was subjected to the next step without further purification. Spectral data is in accordance with the reported literature.[129]

^{1}H NMR (500 MHz, $CDCl_3$) δ 5.10 (t, *J* = 7.2 Hz, 1H), 2.48 – 2.40 (m, 1H), 2.18 – 2.08 (m, 2H), 2.04 (d, *J* = 2.4 Hz, 1H), 1.69 (s, 3H), 1.63 (s, 3H), 1.54 – 1.42 (m, 2H), 1.18 (d, *J* = 7.0 Hz, 3H).

^{13}C NMR (126 MHz, $CDCl_3$) δ 132.3, 124.0, 89.3, 68.3, 37.0, 25.9, 25.9, 25.4, 21.1, 17.8.

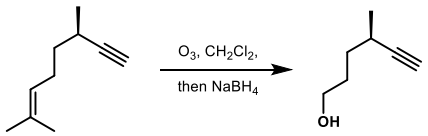

3-87 3-S7

(*R*)-4-Methylhex-5-yn-1-ol (3-S7):

A solution of the crude alkyne **3-87** (91 mg, 1.0 equiv) in CH_2Cl_2 (3.3 mL) at –78 °C was treated O_3 until the solution turned blue in color (~5 min). The flask was purged with O_2 until the blue color dissipated, and then $NaBH_4$ (252 mg, 6.71 mmol, 10.0 equiv) was added. The solution was allowed to slowly warm to rt overnight before it was slowly quenched with H_2O. The slurry was diluted with brine and the organic phase was extracted, dried with Na_2SO_4, filtered, and

concentrated *in vacuo*. The resulting residue was subjected to the next step without further purification.

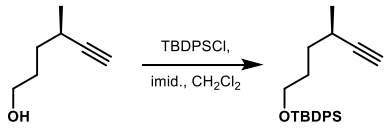

3-S7 3-79

(*R*)-*tert*-Butyl((4-methylhex-5-yn-1-yl)oxy)diphenylsilane (3-79):

To a solution of the crude alcohol **3-S7** (75 mg, 1.0 equiv) in CH_2Cl_2 (3.3 mL) at rt was added imidazole (136 mg, 2.00 mmol, 3.0 equiv) followed by TBDPSCl (0.21 mL, 0.802 mmol, 1.2 equiv). The reaction was stirred at rt overnight and then diluted with H_2O. The organic layer was extracted and additional extractions were performed with CH_2Cl_2 (2 X). The combined organic phase was dried with $MgSO_4$, filtered, and concentrated *in vacuo*. The resulting residue was purified via flash chromatography (100% hex) to afford X as a clear oil (39 mg, 9% over 4 steps). The spectral data matches the data reported *vide supre*.

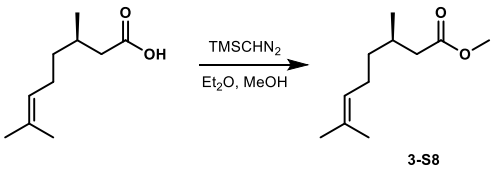

3-S8

Methyl (*R*)-3,7-dimethyloct-6-enoate (3-S8):

To a solution of (*R*)-(+)-citronellic acid (3.4 mL, 18.4 mmol, 1.0 equiv) in Et_2O (150 mL) and MeOH (30 mL) at 0 °C was added (trimethylsilyl)diazomethane (2.0 M in Et_2O; 18 mL, 36.9 mmol, 2.0 equiv). The reaction was allowed to warm to rt over 6 h after which it was quenched with AcOH (20 mL). When the yellow color dissipated and the bubbling stopped, the solution was concentrated *in vacuo*. The resulting residue was diluted with H_2O (100 mL) and extracted with pentanes (3 x 100 mL). The combined organic phase was washed with brine, dried with $MgSO_4$,

filtered, and concentrated *in vacuo* to obtain ester **3-S8**. The resulting oil was subject to the next step without further purification.

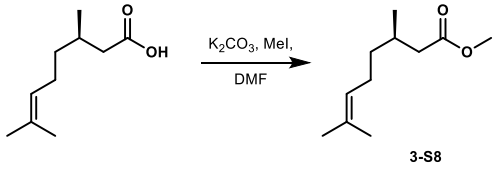

3-S8

Methyl (*R*)-3,7-dimethyloct-6-enoate (3-S8):

To a solution of (*R*)-(+)-citronellic acid (4.0 mL, 21.7 mmol, 1.0 equiv) in DMF (43 mL) at rt was added K_2CO_3 (9.62 g, 69.9 mmol, 3.2 equiv), followed by iodomethane (4.7 mL, 76.1 mmol, 3.5 equiv). After stirring at rt for 16 h, the solution was diluted with H_2O (100 mL), and extracted with Et_2O (5 x 100 mL). The combined organic phase was washed with brine, dried with $MgSO_4$, filtered, and concentrated *in vacuo* to obtain ester **3-S8**. The resulting clear oil was subject to the next step without further purification. The spectral data is in accordance with the reported literature.[152]

^{1}H NMR (500 MHz, $CDCl_3$): δ 5.03 (t, *J* = 6.4 Hz, 1H), 3.60 (s, 3H), 2.26 (dd, *J* = 14.8, 5.9 Hz, 1H), 2.06 (ddd, *J* = 14.7, 8.3, 1.6 Hz, 1H), 2.01 – 1.85 (m, 3H), 1.34 – 1.24 (m, 1H), 1.22 – 1.11 (m, 1H), 0.88 (d, J = 6.9 Hz, 3H).

^{13}C NMR (126 MHz, $CDCl_3$) δ 173.7, 131.5, 124.3, 51.3, 41.6, 36.8, 30.0, 25.7, 25.4, 19.6, 17.6.

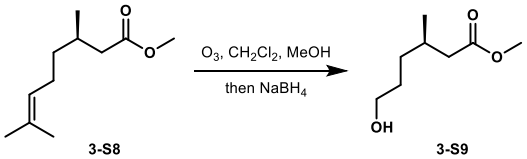

3-S8 **3-S9**

Methyl (*R*)-6-hydroxy-3-methylhexanoate (3-S9):

A solution of alkene **3-S8** (4.0 g, 21.7 mmol, 1.0 equiv) in CH_2Cl_2 (80 mL) and MeOH (20 mL) at –78 °C was treated with O_3 until the solution turned blue in color. The flask was purged with O_2 until the blue color dissipated, and then $NaBH_4$ (2.46 g, 65.1 mmol, 3.0 equiv) was added. The

solution was allowed to slowly warm to rt overnight before it was slowly quenched with H_2O (100 mL). The slurry was extracted with CH_2Cl_2 (4 x 50 mL) and the combined organic phase was washed with brine, dried with $MgSO_4$, filtered, and concentrated *in vacuo* to obtain **3-S9**. The resulting clear oil was subject to the next step without further purification.

^{1}H NMR (500 MHz, $CDCl_3$) δ 3.63 (s, 3H), 3.59 (t, *J* = 6.5 Hz, 2H), 2.28 (dd, *J* = 14.9, 6.3 Hz, 1H), 2.12 (dd, *J* = 14.9, 7.8 Hz, 1H), 1.99 – 1.89 (m, 1H), 1.88 (s, br, 1H), 1.63 – 1.55 (m, 1H), 1.55 – 1.46 (m, 1H), 1.42 – 1.33 (m, 1H), 1.26 – 1.19 (m, 1H), 0.92 (d, *J* = 6.8 Hz, 3H).

^{13}C NMR (126 MHz, $CDCl_3$) δ 173.8, 53.5, 51.5, 41.6, 32.7, 30.1, 30.1, 19.8.

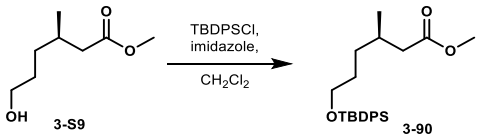

Methyl (*R*)-6-((*tert*-butyldiphenylsilyl)oxy)-3-methylhexanoate (3-90):

To a solution of alcohol **3-S9** (3.45 g, 21.7 mmol, 1.0 equiv) in CH_2Cl_2 (100 mL) at rt was added imidazole (4.43 g, 65.1 mmol, 3.0 equiv) followed by TBDPSCl (8.5 mL, 32.6 mmol, 1.5 equiv). The reaction was stirred at rt for 18 h and then diluted with H_2O (100 mL). The organic layer was extracted and additional extractions were performed with CH_2Cl_2 (2 x 50 mL). The combined organic phase was washed with brine, dried with $MgSO_4$, filtered, and concentrated *in vacuo*. The resulting residue was purified via flash chromatography (2% EtOAc in hex) to obtain ester **3-90** as a clear oil (7.22 g, 83% yield over 3 steps). The spectral data is in accordance with the reported literature.[153]

Optical rotation: $[\alpha]^{22}_D$ = +4.7 (*c* = 10.0, $CHCl_3$)

^{1}H NMR (500 MHz, $CDCl_3$): δ 7.67 (d, J = 7.3 Hz, 4H), 7.46 – 7.36 (m, 6H), 3.70 – 3.62 (m, 5H), 2.30 (dd, *J* = 14.7, 5.9 Hz, 1H), 2.12 (dd, *J* = 14.7, 8.2 Hz, 1H), 2.01 – 1.91 (m, 1H), 1.65 – 1.50 (m, 2H), 1.40 (ddd, *J* = 16.1, 11.3, 5.5 Hz, 1H), 1.26 (ddd, *J* = 18.6, 10.4, 6.9 Hz, 1H), 1.06 (s, 9H), 0.93 (d, *J* = 6.6 Hz, 3H).

^{13}C NMR (126 MHz, $CDCl_3$): δ 173.8, 135.7, 134.2, 129.7, 127.7, 64.2, 51.5, 41.8, 33.0, 30.3, 30.1, 27.0, 19.8, 19.4.

HRMS (ESI-TOF) *m/z* calculated for $C_{24}H_{35}O_3Si^+$ $(M+H)^+$ 399.2355, found 399.2353.

3-90 3-S10

(*R*)-6-((*tert*-Butyldiphenylsilyl)oxy)-3-methylhexan-1-ol (3-S10):

To a solution of ester **3-90** (7.22 g, 18.8 mmol, 1.0 equiv) in THF at rt (60 mL) was added lithium aluminum hydride solution (1.0 M in THF; 22 mL, 22.6 mmol, 1.2 equiv). The reaction was stirred for 15 h at rt and then slowly quenched with H_2O (100 mL). The slurry was extracted with Et_2O (4 X 100 mL) and the combined organic phase was washed with brine, dried with $MgSO_4$, filtered, and concentrated *in vacuo* to yield alcohol **3-S10** as a clear oil (6.40 g, 95%). The spectral data is in accordance with the reported literature.[154]

Optical rotation: $[\alpha]^{22}_D$ = +3.3 (*c* = 10.0, $CHCl_3$).

^{1}H NMR (500 MHz, $CDCl_3$): δ 7.68 (d, *J* = 7.8 Hz, 4H), 7.46 – 7.34 (m, 6H), 3.72 – 3.60 (m, 4H), 1.67 – 1.50 (m, 4H), 1.43 – 1.34 (m, 2H), 1.25 – 1.20, (m, 1H), 1.06 (s, 9H), 0.89 (d, *J* = 6.6 Hz, 3H).

^{13}C NMR (126 MHz, $CDCl_3$): δ 135.7, 134.3, 129.7, 127.7, 64.3, 61.3, 40.0, 33.2, 30.1, 29.4, 27.0, 19.8, 19.4.

HRMS (ESI-TOF) *m/z* calculated for $C_{23}H_{34}O_2SiNa^+$ $(M+Na)^+$ 393.2226, found 393.2216.

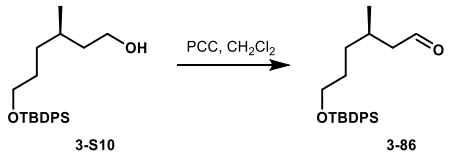

(*R*)-6-((*tert*-Butyldiphenylsilyl)oxy)-3-methylhexanal (3-86):

To a solution of alcohol **3-S10** (6.40 g, 17.3 mmol, 1.0 equiv) in CH_2Cl_2 (80 mL) at rt was added PCC (6.70 g, 31.1 mmol, 1.8 equiv). The reaction was stirred at rt for 2 h, then it was filtered through a silica plug. The cake was washed with additional CH_2Cl_2 (300 mL) and the filtrate was concentrated *in vacuo* to yield aldehyde **3-86** as a clear oil (5.74 g, 90%). The spectral data matches the data reported *vide supre*.

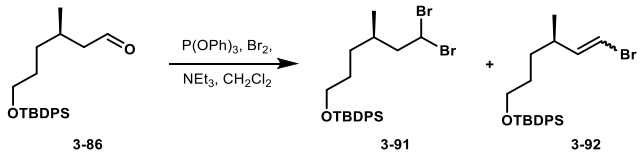

(*R*)-*tert*-Butyl((6,6-dibromo-4-methylhexyl)oxy)diphenylsilane (3-91):

To a solution of triphenyl phosphite (6.1 mL, 23.4 mmol, 1.5 equiv) in CH_2Cl_2 (100 mL) at –78 °C was added Br_2 (1.0 mL, 20.3 mmol, 1.3 equiv) followed by NEt_3 (6.5 mL, 46.8 mmol, 3.0 equiv) dropwise. When the foggy vapor disappeared from the head space, a solution of aldehyde **3-86** (5.74 g, 15.6 mmol, 1.0 equiv) in CH_2Cl_2 (50 mL) was added via cannula transfer. The reaction was stirred for 2 h at –78 °C, then warmed to rt and stirred for an additional 2 h. The reaction solution was concentrated *in vacuo* and subjected to flash column chromatography (1% EtOAc in hex) to obtain **3-91** and **3-92** as an inconsequential and inseparable mixture of geminal dibromo alkane, and *cis* and *trans* vinyl bromide diastereomers (10 : 0.8 : 1.3). (6.32 g, 79%). To remove excess $P(OPh)_3$, for a simpler purification, the crude oil was stirred with 30% aq. H_2O_2 in THF for 20 min. The solution was diluted with brine and extracted with Et_2O. The combined organic phase was washed with brine, dried with $MgSO_4$, filtered, and concentrated *in vacuo*. The resulting residue was purified via silica plug (10% EtOAc in hex) to obtain **3-91** and **3-92** as an

inconsequential and inseparable mixture of geminal dibromo alkane, and *cis* and *trans* vinyl bromide diastereomers (10 : 0.8 : 1.3).

Dibromide 3-91:

^{1}H NMR (500 MHz, $CDCl_3$): δ 7.68 (dd, *J* = 7.9, 1.4 Hz, 4H), 7.46 – 7.36 (m, 6H), 5.70 (dd, *J* = 8.4, 5.9 Hz, 1H), 3.67 (t, *J* = 6.3 Hz, 2H), 2.41 (ddd, *J* = 14.3, 8.4, 5.6 Hz, 1H), 2.21 (ddd, *J* = 15.0, 8.0, 5.5 Hz, 1H), 1.76 (dd, *J* = 13.0, 6.3 Hz, 1H), 1.64 – 1.51 (m, 2H), 1.45 – 1.36 (m, 1H), 1.29 – 1.20 (m, 1H), 1.07 (s, 9H), 0.90 (d, *J* = 6.7 Hz, 3H).

^{13}C NMR (125 MHz, $CDCl_3$) δ 135.7, 134.2, 129.7, 127.8, 64.0, 52.9, 45.0, 32.4, 32.2, 29.7, 27.0, 19.4, 18.7.

HRMS (CI-TOF) *m/z* calculated for $C_{23}H_{32}Br_2OSiH^+$ $(M+H)^+$ 513.0649, found 513.0637.

Diagnostic data for cis and trans vinyl bromides (3-92):

^{1}H NMR (500 MHz, $CDCl_3$) δ 6.09 (d, *J* = 6.9 Hz, 1H, *cis*), 6.04 (dd, *J* = 13.5, 8.1 Hz, 1H, *trans*), 5.96 (d, *J* = 13.6 Hz, 1H, *trans*), 5.85 (dd, *J* = 9.2, 7.0 Hz, 1H, *cis*), 1.12 (d, *J* = 6.0 Hz, 3H, *cis*), 1.00 (d, *J* = 6.7 Hz, 3H, *trans*).

HRMS (CI-TOF) *m/z* calculated for $C_{19}H_{22}BrOSi^+$ $(M–t\text{-butyl})^+$ 373.0623, found 373.0634.

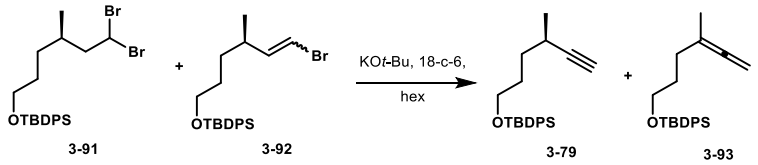

(*R*)-*tert*-Butyl((4-methylhex-5-yn-1-yl)oxy)diphenylsilane (3-79) and *tert*-Butyl((4-methylhexa-4,5-dien-1-yl)oxy)diphenylsilane (3-93):

To a solution of bromides **3-91** and **3-92** (2.95 g, 5.75, 1.0 equiv) in hex (15 mL) was added KO*t*-Bu (2.32 g, 20.7 mmol, 3.6 equiv) followed by 18-crown-6 (152 mg, 0.575 mmol, 0.10 equiv). This slurry was heated to reflux for 14 h. After cooling to rt, the slurry was washed with H_2O (3 X) and the aqueous phase was back extracted with hex (3 X). The combined organic phase was dried with Na_2SO_4, filtered, and concentrated *in vacuo*. The resulting residue was subjected to flash

chromatography (100% hex) to obtain allene **3-93** (1.59g, 79%) and alkyne **3-79** (163 mg, 8%). The spectral data for terminal alkyne **3-79** matches the data reported *vide supre*.

Allene 3-93:

^{1}H NMR (500 MHz, $CDCl_3$) δ 7.71 (dd, *J* = 8.0, 1.6 Hz, 4H), 7.47 – 7.38 (m, 6H), 4.58 (dd, *J* = 6.4, 3.2 Hz, 2H), 3.73 (t, *J* = 6.4 Hz, 2H), 2.11 – 2.01 (m, 2H), 1.80 – 1.72 (m, 2H), 1.70 (t, *J* = 3.1 Hz, 3H), 1.09 (s, 9H).

^{13}C NMR (126 MHz, $CDCl_3$) δ 206.2, 135.7, 134.3, 129.7, 127.7, 98.3, 74.3, 63.6, 30.6, 29.8, 27.0, 19.4, 19.0.

HRMS (CI-TOF) *m/z* calculated for $C_{23}H_{30}O_2SiH^+$ $(M+H)^+$ 351.2144, found 351.2157.

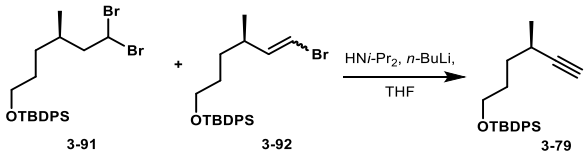

(*R*)-*tert*-Butyl((4-methylhex-5-yn-1-yl)oxy)diphenylsilane (3-79):

To a solution of HN*i*-Pr_2 (7.0 mL, 49.3 mmol, 4.0 equiv) in THF (20 mL) at –78 °C was added *n*-BuLi (2.5 M in hex.; 17.0 mL, 43.2 mmol, 3.5 equiv). The solution was warmed to 0 °C then cooled back to –78 °C after which a solution of bromides **3-91** and **3-92** (6.32 g, 12.3 mmol, 1.0 equiv) in THF (20 mL) was added. The reaction was stirred for 2 h at –78 °C, then warmed to rt and stirred for an additional 3 h, after which it was quenched with saturated NH_4Cl solution (100 mL). The mixture was extracted with Et_2O (3 X 40 mL), and the combined organic phase was washed with brine, dried with $MgSO_4$, filtered, and concentrated *in vacuo*. The oil was taken on to the next step without further purification. For characterization, an aliquot of the resulting residue was purified through a silica plug (10% EtOAc in hex) to obtain terminal alkyne **3-79**. The spectral data for terminal alkyne **3-79** matches the data reported *vide supre*.

Optical rotation: $[\alpha]^{22}_D$ = –10.81 (*c* = 10.0, $CHCl_3$).

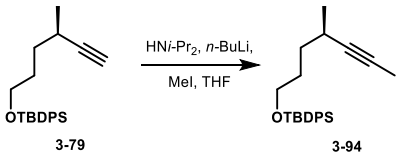

3-79 3-94

(*R*)-*tert*-butyl((4-methylhept-5-yn-1-yl)oxy)diphenylsilane (3-94):

To a solution of HN*i*-Pr$_2$ (5.2 mL, 49.3 mmol, 3.0 equiv) in THF (20 mL) at –78 °C was added *n*-BuLi (2.5 M in hex.; 12.0 mL, 30.8 mmol, 2.5 equiv). The solution was warmed to 0 °C then cooled back to –78 °C after which a solution of terminal alkyne **3-79** (4.31 g, 12.3 mmol, 1.0 equiv) in THF (40 mL) was added. The solution was warmed to rt and stirred for 1 h before it was cooled to –78 °C and iodomethane (5.3 mL, 86.1 mmol, 7.0 equiv) was added. The reaction was allowed to warm to rt over 14 h and then quenched with saturated NH_4Cl solution (100 mL). The mixture was extracted with Et_2O (3 X 40 mL), and the combined organic phase was washed with brine, dried with $MgSO_4$, filtered, and concentrated *in vacuo*. The resulting residue was purified through a plug of silica gel (10% EtOAc in hex) to obtain internal alkyne **3-94** as a clear oil (4.36 g, 97% over 2 steps).

Optical rotation: $[\alpha]^{22}_D$ = –9.11 (*c* = 10.0, $CHCl_3$).

^{1}H NMR (500 MHz, $CDCl_3$): δ 7.70 (d, *J* = 6.9 Hz, 4H), 7.47 – 7.36 (m, 6H), 3.71 (t, *J* = 6.4 Hz, 2H), 2.43 – 2.34 (m, 1H), 1.80 (d, *J* = 2.2 Hz, 3H), 1.78 – 1.72 (m, 1H), 1.71 – 1.62 (m, 1H), 1.52 (ddd, *J* = 15.4, 11.9, 5.6 Hz, 1H), 1.46 (ddd, *J* = 13.1, 8.8, 5.1 Hz, 1H), 1.15 (d, *J* = 6.9 Hz, 3H), 1.08 (s, 9H).

^{13}C NMR (126 MHz, $CDCl_3$): δ 135.7, 134.3, 129.6, 127.7, 83.9, 75.8, 64.0, 33.7, 30.6, 27.0, 25.8, 21.6, 19.4, 3.64.

HRMS (CI-TOF) *m/z* calculated for $C_{24}H_{32}OSiH^+$ $(M+H)^+$ 365.2301, found 365.2305.

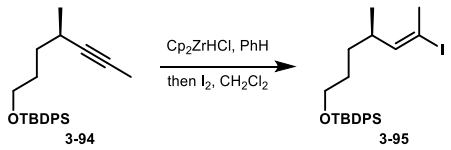

(*R,E*)-*tert*-Butyl((6-iodo-4-methylhept-5-en-1-yl)oxy)diphenylsilane (3-95):

A Schlenk flask containing Cp_2ZrHCl (6.16 g, 24.0 mmol, 2.0 equiv) was removed from the glove box, and a solution of internal alkyne **3-94** (4.36 g, 12.0 mmol, 1.0 equiv) in benzene (120 mL) was added at rt. After stirring for 17 h at rt, a saturated solution of I_2 in CH_2Cl_2 was added to the cloudy yellow mixture until the purple color persisted in the solution. A saturated $Na_2S_2O_3$ solution was added and the mixture was vigorously stirred until purple color dissipated. The slurry was diluted with brine and extracted with CH_2Cl_2 (4 X 200 mL). The combined organic phase was dried with Na_2SO_4, filtered, and concentrated *in vacuo*. The resulting residue was purified via flash chromatography (0% → 15% EtOAc in hex) to obtain vinyl iodide **3-95** as a yellow/orange oil (4.92 g, 83%).

Optical rotation: $[\alpha]^{22}_D = -24.80$ (*c* = 1.0, $CHCl_3$).

^{1}H NMR (500 MHz, $CDCl_3$): δ 7.66 (d, *J* = 6.6 Hz, 4H), 7.45 – 7.36 (m, 6H), 5.92 (dd, *J* = 9.9, 1.2 Hz, 1H), 3.63 (t, *J* = 6.4 Hz, 2H), 2.39 – 2.33 (m, 1H), 2.32 (d, *J* = 1.3 Hz, 3H), 1.58 – 1.44 (m, 2H), 1.38 (dd, *J* = 15.8, 9.3, 5.5 Hz, 1H), 1.27 (dd, *J* = 18.7, 9.1, 4.4 Hz, 1H), 1.05 (s, 9H), 0.94 (d, *J* = 6.7 Hz, 3H).

^{13}C NMR (126 MHz, $CDCl_3$): δ 147.5, 135.7, 134.2, 129.7, 127.8, 92.8, 63.9, 35.6, 33.2, 30.5, 27.9, 27.0, 20.6, 19.4.

HRMS (CI-TOF) *m/z* calculated for $C_{24}H_{33}OISiH^+$ $(M+H)^+$ 493.1424, found 493.1447.

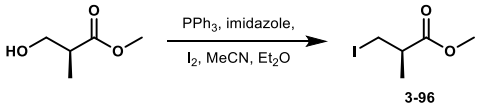

Methyl (*R*)-3-iodo-2-methylpropanoate (3-96):

Iodide **3-96** was prepared according to a modified literature procedure:[155]

To a solution of PPh_3 (2.78 g, 10.6 mmol, 1.25 equiv) and imidazole (749 mg, 11.0 mmol, 1.3 equiv) in MeCN (8.5 mL) and Et_2O (25 mL) at rt was added iodide (2.79 g, 11.0 mmol, 1.3 equiv) portionwise followed by methyl (*S*)-3-hydroxy-2-methyl propanoate (0.93 mL, 8.47 mmol, 1.0 equiv). The slurry was stirred for 2 h at rt and then concentrated *in vacuo*. The resulting residue was purified via flash chromatography (10% EtOAc in hex) to obtain ester **3-96** as a light green volatile oil (1.52 g, 79%). The spectral data is in accordance with the literature reported.[155]

^{1}H NMR (500 MHz, $CDCl_3$) δ 3.67 (s, 3H), 3.36 – 3.30 (m, 1H), 3.24 – 3.19 (m, 1H), 2.79 – 2.70 (m, 1H), 1.22 (d, *J* = 7.2 Hz, 3H).

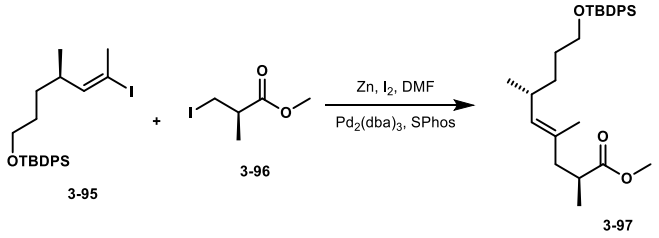

Methyl (*2S,6R,E*)-9-((*tert*-butyldiphenylsilyl)oxy)-2,4,6-trimethylnon-4-enoate (3-97):

A Schlenk flask containing Zn dust (<10 micron; 2.60 g, 40.0 mmol, 4.0 equiv) was heated with a heat gun under vacuum for 10 min. The flask was purged with Ar and was allowed to cool to rt. To the flask containing the Zn dust, DMF (Sparged with Ar for 1 h, 10 mL) and I_2 (380 mg) was added at rt and was stirred until the purple color dissipated. To this slurry, ester **3-96** (2.96 g, 13.0 mmol, 1.3 equiv) in DMF (15 mL) was added followed by an additional portion of I_2 (380 mg). The slurry was stirred for 30 min, then $Pd_2(dba)_3$ (916 mg, 1.0 mmol, 0.10 equiv) and SPhos (821 mg, 2.0 mmol, 0.20 equiv) was added followed by vinyl iodide **3-95** (4.92 g, 10.0 mmol, 1.0 equiv) in DMF (35 mL). The reaction was heated to 57 °C in an oil bath for 14 h. After cooling to rt, the slurry was diluted with EtOAc (100 mL) and then filtered through a pad of celite and the cake washed with additional EtOAc. The filtrate was washed with brine (4 X 100 mL) and the combined organic phase was dried with Na_2SO_4, filtered, and concentrated *in vacuo*. The resulting residue was purified via flash chromatography (5% EtOAc in hex) to obtain ester **3-97** (4.28 g), which was isolated with an unknown impurity and subjected to the next step without further purification.

^{1}H NMR (500 MHz, $CDCl_3$): δ 7.70 (d, *J* = 7.9 Hz, 4H), 7.47 – 7.38 (m, 6H), 4.95 (d, *J* = 9.4 Hz, 1H), 3.69 – 3.65 (m, 5H), 2.70 – 2.60 (m, 1H), 2.41 – 2.28 (m, 2H), 2.05 (dd, *J* = 13.5, 7.8 Hz, 1H), 1.59 (s, 3H), 1.57 – 1.47 (m, 2H), 1.44 – 1.37 (m, 1H), 1.28 – 1.24 (m, 1H), 1.13 (d, *J* = 7.0 Hz, 3H), 1.08 (s, 9H), 0.92 (d, *J* = 6.7 Hz, 3H).

^{13}C NMR (126 MHz, $CDCl_3$): δ 177.1, 135.7, 134.3, 134.1, 130.7, 129.6, 127.7, 64.2, 51.5, 44.3, 38.1, 33.8, 32.3, 30.7, 27.0, 21.4, 19.3, 16.7, 16.0.

HRMS (ESI-TOF) *m/z* calculated for $C_{29}H_{42}O_3SiH^+$ $(M+H)^+$ 467.2982, found 467.2978.

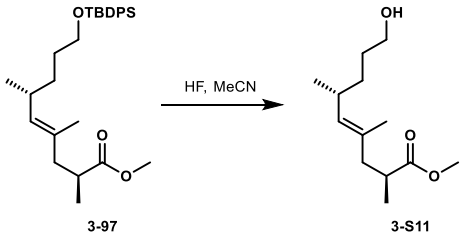

3-97 3-S11

Methyl (*2S,6R,E*)-9-hydroxy-2,4,6-trimethylnon-4-enoate (3-S11):

To a plastic bottle containing ester **3-97** (4.28 g, 9.17 mmol, 1.0 equiv) in MeCN (37 mL) was added HF (50% aq. soln; 1.0 mL). After stirring for 1 h, an additional portion of HF (2 mL) was added. After stirring for 3 h, an additional portion of HF (5 mL) was added. After stirring for 4.5 h, an additional portion of HF (2 mL) was added. After stirring for 5 h total, the reaction was slowly quenched with saturated $NaHCO_3$ solution and extracted with ether (3 X 50 mL). The combined organic phase was washed with brine, dried with $MgSO_4$, filtered, and concentrated *in vacuo*. The resulting residue was purified through a silica plug (30% EtOAc in hex then 100% EtOAc) to obtain alcohol **3-S11** (1.51 g, 72% over 2 steps) as a clear oil.

Optical rotation: $[\alpha]^{22}_D$ = –6.25 (*c* = 10.0, $CHCl_3$).

^{1}H NMR (500 MHz, $CDCl_3$): δ 4.83 (d, *J* = 9.5 Hz, 1H), 3.56 (s, 3H), 3.50 (t, *J* = 6.7 Hz, 2H), 2.60 – 2.50 (m, 1H), 2.34 (s, br, 1H), 2.28 – 2.19 (m, 2H), 1.95 (dd, *J* = 13.6, 7.4 Hz, 1H), 1.51 (s, 3H), 1.47 – 1.36 (m, 2H), 1.28 (ddd, *J* = 16.0, 9.2, 5.5 Hz, 1H), 1.13 (ddd, *J* = 13.4, 8.7, 5.1 Hz, 1H), 1.03 (d, *J* = 7.1, 3H), 0.83 (d, *J* = 6.9, 3H).

^{13}C NMR (126 MHz, $CDCl_3$): δ 177.1, 133.7, 130.8, 62.9, 51.4, 44.1, 38.0, 33.7, 32.2, 30.8, 21.2, 16.6, 15.9.

HRMS (ESI-TOF) *m/z* calculated for $C_{13}H_{24}O_3Na^+$ $(M+Na)^+$ 251.1623, found 251.1624.

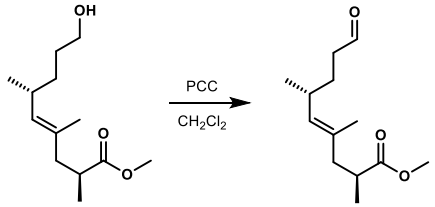

3-S11 3-98

Methyl (*2S,6R,E*)-2,4,6-trimethyl-9-oxonon-4-enoate (3-98):

To a solution of alcohol **3-S11** (300 mg, 1.31 mmol, 1.0 equiv) in CH_2Cl_2 (6.6 mL) at rt was added PCC (510 mg, 2.37 mmol, 1.8 equiv). The reaction was stirred at rt for 1 h, then it was filtered through a silica plug. The cake was washed with additional CH_2Cl_2 (30 mL) and the filtrate was concentrated *in vacuo* to yield aldehyde **3-98** as a clear oil (217 mg, 73%).

Optical rotation: $[\alpha]^{22}_D$ = –4.5 (*c* = 10.0, $CHCl_3$).

^{1}H NMR (500 MHz, $CDCl_3$): δ 9.72 (s, 1H), 4.86 (d, *J* = 9.6 Hz, 1H), 3.63 (s, 3H), 2.66 – 2.57 (m, 1H), 2.40 – 2.28 (m, 4H), 2.02, (dd, *J* = 13.6, 7.3 Hz, 1H), 1.71 – 1.62 (m, 1H), 1.56 (s, 3H), 1.50 – 1.40 (m, 1H), 1.10 (d, *J* = 7.0 Hz, 1H), 0.92 (d, *J* = 6.7 Hz, 1H).

^{13}C NMR (126 MHz, $CDCl_3$): δ 202.8, 177.0, 132.5, 132.3, 51.5, 44.2, 42.3, 38.1, 32.1, 29.7, 21.3, 16.9, 16.2.

HRMS (ESI-TOF) *m/z* calculated for $C_{13}H_{22}O_3Na^+$ $(M+Na)^+$ 249.1467, found 249.1477.

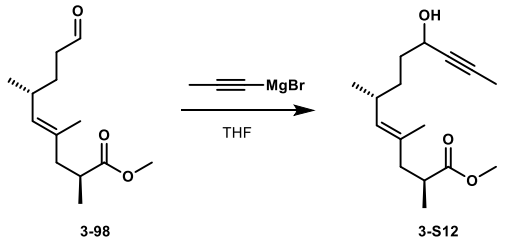

3-98 3-S12

Methyl (*2S,6R,E*)-9-hydroxy-2,4,6-trimethyldodec-4-en-10-ynoate (3-S12):

To a solution of 1-propynyl magnesium bromide (0.5 M in THF; 22 mL, 11.2 mmol, 1.7 equiv) in THF (18 mL) at –78 °C was added aldehyde **3-98** (1.49 g, 6.57 mmol, 1.0 equiv) in THF (15 mL) and was stirred at this temperature for 45 min. After warming to rt, the reaction was quenched with saturated NH_4Cl solution and extracted with Et_2O (2 X 50 mL). The combined organic phase was washed with H_2O (50 mL) then brine, dried with $MgSO_4$, filtered, and concentrated *in vacuo* to obtain alcohol **3-S12** as a mixture of diastereomers (1.56 g, 89%). Diastereomers were indistinguishable in the ^1H NMR.

^{1}H NMR (500 MHz, $CDCl_3$): δ 4.89 (d, *J* = 9.4 Hz, 1H), 4.29 – 4.21 (m, 1H), 3.61 (s, 3H), 2.60 (dd, *J* = 14.6, 7.4 Hz, 1H), 2.30 (dd, *J* = 13.5, 7.7 Hz, 2H), 2.05 (s, br, 1H), 2.00 (dd, *J* = 13.6, 7.4 Hz, 1H), 1.81 (d, *J* = 2.2 Hz, 3H), 1.64 – 1.51 (m, 5H), 1.42 (ddd, *J* = 13.5, 10.0, 4.4 Hz, 1H), 1.32 – 1.21 (m, 1H), 1.08 (d, *J* = 7.0 Hz, 3H), 0.89 (d, *J* = 6.8 Hz, 3H).

^{13}C NMR β-face alcohol diastereomer reported: (126 MHz, $CDCl_3$): δ 171.2, 133.6, 131.1, 80.8, 80.6, 62.8, 51.5, 44.2, 38.1, 36.3, 33.1, 32.3, 21.4, 16.8, 16.1, 3.6.

HRMS (ESI-TOF) *m/z* calculated for $C_{16}H_{26}O_3Na^+$ $(M+Na)^+$ 289.1780, found 289.1786.

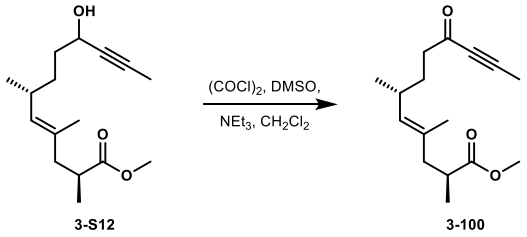

Methyl (*2S,6R,E*)-2,4,6-trimethyl-9-oxododec-4-en-10-ynoate (3-100):

To a solution of oxalyl chloride (0.630 mL, 7.03 mmol, 1.2 equiv) in CH_2Cl_2 (15 mL) at –78 °C was added DMSO (1.0 mL, 14.1 mmol, 2.4 equiv). The mixture was stirred at this temperature for 5 min. after which alcohol **3-S12** (1.56 g, 5.86 mmol, 1.0 equiv) in CH_2Cl_2 (15 mL) was added followed by NEt_3 (4.1 mL, 29.3 mmol, 5.0 equiv). The solution was warmed to rt, stirred for 10 min, then quenched with saturated NH_4Cl solution. The slurry was extracted with CH_2Cl_2 (3 X 40 mL), and the combined organic phase was washed with brine, dried with Na_2SO_4, filtered, and concentrated *in vacuo* to obtain ynone **3-100** as a clear oil (1.24 g, 80%).

^{1}H NMR (500 MHz, $CDCl_3$): δ 4.88 (d, *J* = 8.7 Hz, 1H), 3.64 (s, 3H), 2.67 – 2.58 (m, 1H), 2.48 – 2.42 (m, 2H), 2.37 – 2.30 (m, 2H), 2.06 – 2.02 (m, 1H), 2.01 (s, 3H), 1.74 – 1.65 (m, 1H), 1.58 (d, *J* = 1.2 Hz, 1H), 1.53 – 1.43 (m, 1H), 1.12 (d, *J* = 6.9 Hz, 3H), 0.92 (d, *J* = 6.6 Hz, 3H).

^{13}C NMR (126 MHz, $CDCl_3$): δ 188.5, 177.1, 132.8, 132.2, 89.9, 80.4, 51.6, 44.7, 43.7, 38.1, 32.0, 31.7, 21.3, 16.9, 16.1, 4.2.

HRMS (ESI-TOF) *m/z* calculated for $C_{16}H_{24}O_3H^+$ $(M+H)^+$ 265.1804, found 265.1806.

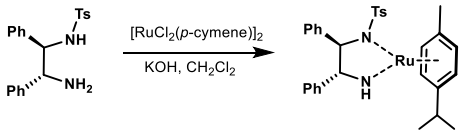

Noyori ruthenium catalyst was prepared according to a known literature procedure:[156] To a solution of $[RuCl_2(p\text{-cymene})]_2$ (83 mg, 0.136 mmol, 1.0 equiv) in CH_2Cl_2 (2.0 mL) was added (*1R,2R*)-(–)-N-(4-toluenesulfonyl)-1,2-diphenylethylenediamine (100 mg, 0.273 mmol, 2.0 equiv) and KOH (114 mg, 2.04 mmol, 15 equiv). The solution was stirred for 5 min then washed with

H_2O. The purple organic phase was dried with CaH_2, filtered, and concentrated *in vacuo* to obtain Noyori ruthenium catalyst.

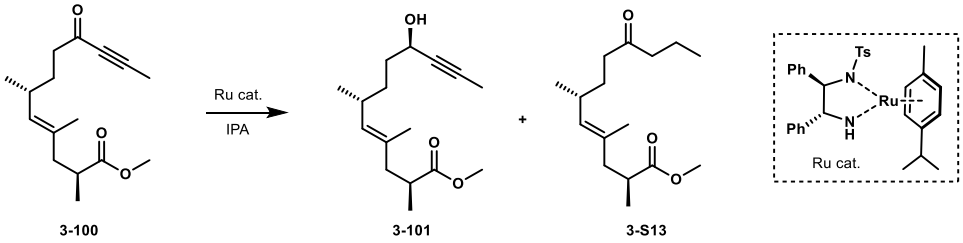

Methyl (*2S,6R,9R,E*)-9-hydroxy-2,4,6-trimethyldodec-4-en-10-ynoate (3-101):

To a solution of ynone **3-101** (1.20 g, 4.54 mmol, 1.0 equiv) in isopropanol (45 mL) was added Ru. cat. (177 mg, 0.294 mmol, 0.06 equiv). The solution was stirred for 2 h at rt and then concentrated *in vacuo*. The residue was purified via flash chromatography (0 → 30% EtOAc in hex) to obtain alcohol **3-101** as a clear oil (752 mg, 62%) and ketone **3-S13** (184 mg, 15%).

Ynone 3-101:

^{1}H NMR (500 MHz, $CDCl_3$): δ 4.91 (d, *J* = 9.5 Hz, 1H), 4.32 –4.25 (m, 1H), 3.64 (s, 3H), 2.67 – 2.56 (m, 1H), 2.38 – 2.25 (m, 2H), 2.02 (dd, *J* = 13.5, 7.4 Hz, 1H), 1.83 (d, *J* = 2.0 Hz, 3H), 1.78 (s, br, 1H), 1.62 – 1.57 (m , 5H), 1.45 (ddd, *J* = 13.4, 10.5, 5.5 Hz, 1H), 1.27 (ddd, *J* = 15.9, 13.3, 8.6 Hz, 1H), 1.10 (d, *J* = 7.0 Hz, 3H), 0.91 (d, *J* = 6.7 Hz, 1H).

^{13}C NMR (126 MHz, $CDCl_3$): δ 177.2, 133.6, 131.2, 81.1, 80.6, 63.0, 51.5, 44.2, 38.2, 36.3, 33.1, 32.3, 21.4, 16.8, 16.1, 3.7.

HRMS (ESI-TOF) *m/z* calculated for $C_{16}H_{26}O_3H^+$ $(M+H)^+$ 267.1960, found 267.1953.

Ketone 3-S13:

^{1}H NMR (500 MHz, $CDCl_3$): δ 4.84 (d, *J* = 9.5 Hz, 1H), 3.60 (s, 3H), 2.65 – 2.54 (m, 1H), 2.39 – 2.21 (m, 6H), 2.00 (d, *J* = 13.6, 7.4 Hz, 1H), 1.66 – 1.46 (m, 6H), 1.42 – 1.29 (m, 1H), 1.07 (d, *J* = 7.1 Hz, 3H), 0.93 – 0.76 (m, 6H).

^{13}C NMR (126 MHz, $CDCl_3$): δ 211.5, 177.0, 133.1, 131.8, 51.5, 44.8, 44.1, 40.9, 38.1, 32.0, 31.4, 21.2, 17.4, 16.8, 16.1, 13.8.

HRMS (ESI-TOF) *m/z* calculated for $C_{16}H_{28}O_3H^+$ $(M+H)^+$ 269.2117, found 269.2127.

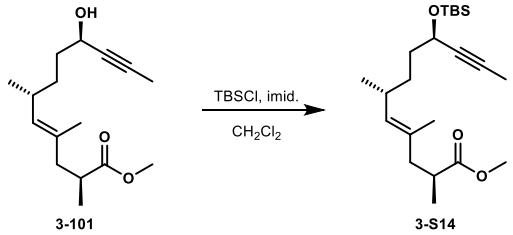

Methyl (*2S,6R,9R,E*)-9-((*tert*-butyldimethylsilyl)oxy)-2,4,6-trimethyldodec-4-en-10-ynoate (3-S14):

To a solution of alcohol **3-101** (500 mg, 1.88 mmol, 1.0 equiv) in CH_2Cl_2 (9.4 mL) at rt was added imidazole (384 mg, 5.64 mmol, 3.0 equiv) followed by TBSCl (424 mg, 2.82 mmol, 1.5 equiv). The solution was stirred for 13 h at rt and then washed with H_2O (2 X 10 mL), then brine. The organic phase was dried with Na_2SO_4, filtered, and concentrated *in vacuo* to obtain alkyne **3-S14** as a clear oil (674 mg, 94%).

^{1}H NMR (500 MHz, $CDCl_3$): δ 4.91 (d, *J* = 9.4 Hz, 1H), 4.26 (ddd, *J* = 8.4, 4.4, 2.0, 1H), 3.64 (s, 3H), 2.66 – 2.57 (m, 1H), 2.36 – 2.24 (m, 2H), 2.01 (dd, *J* = 13.4, 7.6 Hz, 1H), 1.81 (d, *J* = 2.0 Hz, 3H), 1.58 (s, 3H), 1.57 – 1.50 (m, 2H), 1.48 – 1.39 (m, 1H), 1.29 – 1.20 (m, 1H), 1.10 (d, *J* = 6.9 Hz, 3H), 0.89 (m, 12 H), 0.10 (s, 3H), 0.08 (s, 3H).

^{13}C NMR (126 MHz, $CDCl_3$): δ 177.2, 134.0, 130.9, 81.2, 80.0, 63.5, 51.5, 44.4, 38.1, 37.1, 33.3, 32.3, 26.0, 21.4, 18.4, 16.8, 16.0, 3.7, -4.4, -4.9.

HRMS (CI-TOF) *m/z* calculated for $C_{22}H_{40}O_3Si^+$ $(M)^+$ 380.2747, found 380.2746.

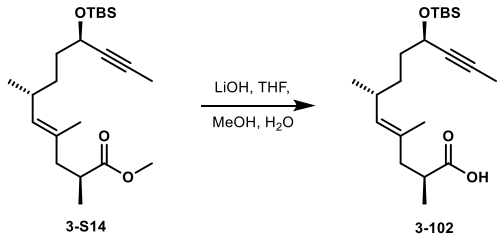

(*2S,6R,9R,E*)-9-((*tert*-Butyldimethylsilyl)oxy)-2,4,6-trimethyldodec-4-en-10-ynoic acid (**3-102**):

To a solution of ester **3-S14** (100 mg, 0.263 mmol, 1.0 equiv) in THF (0.75 mL), MeOH (0.50 mL), and H_2O (0.25 mL) was added $LiOH \cdot H_2O$ (44 mg, 1.05 mmol, 4.0 equiv). The solution was stirred for 24 h and then diluted with EtOAc (5 mL). The slurry was washed with saturated NH_4Cl solution (5 mL), then brine. The combined aqueous phase was extracted with EtOAc (5 mL). The combined organic phase was dried with Na_2SO_4, filtered, and concentrated *in vacuo* to obtain carboxylic acid **3-102** as a clear oil, which was taken on to the next step without further purification.

^{1}H NMR (600 MHz, $CDCl_3$) δ 4.96 (d, *J* = 9.4 Hz, 1H), 4.30 – 4.23 (m, 1H), 2.62 (dd, *J* = 14.4, 7.1 Hz, 1H), 2.38 (dd, *J* = 13.4, 6.9 Hz, 1H), 2.33 (dd, *J* = 13.6, 7.5 Hz, 1H), 2.04 (dd, *J* = 13.4, 8.2 Hz, 1H), 1.81 (d, *J* = 1.4 Hz, 3H), 1.59 (s, 3H), 1.58 – 1.52 (m, 2H), 1.48 – 1.40 (m, 1H), 1.28 (d, *J* = 9.6 Hz, 1H), 1.13 (d, J = 6.9 Hz, 3H), 0.89 (s, 12H), 0.10 (s, 3H), 0.08 (s, 3H).

^{13}C NMR (151 MHz, $CDCl_3$) δ 182.3, 134.5, 130.5, 81.2, 80.0, 63.5, 44.0, 37.9, 37.1, 33.3, 32.4, 26.0, 21.4, 18.4, 16.4, 15.9, 3.7, -4.3, -4.9.

HRMS (ESI-TOF) *m/z* calculated for $C_{21}H_{38}O_3SiNa^+$ $(M+Na)^+$ 389.2488, found 389.2490.

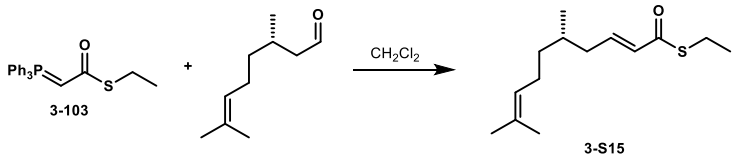

***S*-Ethyl (*S,E*)-5,9-dimethyldeca-2,8-dienethioate (3-S15):**

A solution of (*S*)-citronellal (0.50 mL, 2.77 mmol, 1.0 equiv) and Wittig reagent **3-103** (1.31 g, 3.60 mmol, 1.3 equiv) in CH_2Cl_2 was heated to reflux for 17.5 h. The solution was cooled to rt and

concentrated *in vacuo*. The resulting residue was purified via flash chromatography (0 → 5% EtOAc in hex) to obtain thioester **3-S15** (499 mg, 75%).

Optical rotation: $[\alpha]^{22}_{D}$ = +3.8 (*c* = 10.0, $CHCl_3$).

^{1}H NMR (500 MHz, $CDCl_3$) δ 6.84 (dt, *J* = 15.2, 7.5 Hz, 1H), 6.07 (dd, *J* = 15.5, 1.2 Hz, 1H), 5.06 (td, *J* = 7.1, 1.2 Hz, 1H), 2.91 (dd, *J* = 14.9, 7.4 Hz, 2H), 2.18 (ddd, *J* = 12.9, 7.0, 5.8 Hz, 1H), 2.04 – 1.89 (m, 3H), 1.65 (s, 3H), 1.64 – 1.59 (m, 1H), 1.57 (s, 3H), 1.38 – 1.29 (m, 1H), 1.25 (t, *J* = 7.5 Hz, 3H), 1.22 – 1.12 (m, 1H), 0.88 (d, *J* = 6.9 Hz, 3H).

^{13}C NMR (126 MHz, $CDCl_3$) δ 190.0, 144.1, 131., 129.89, 124.4, 39.7, 36.8, 32.2, 25.8, 25.6, 23.1, 19.6, 17.7, 14.9.

HRMS (CI-TOF) *m/z* calculated for $C_{14}H_{24}OSH^+$ $(M+H)^+$ 241.1626, found 241.1620.

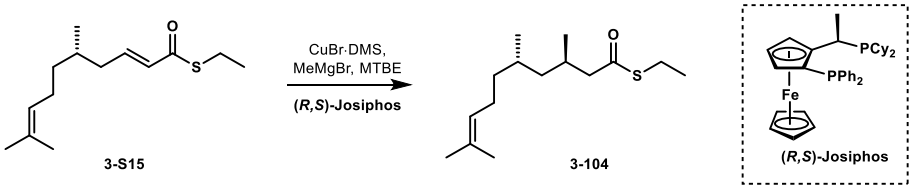

***S*-Ethyl (3*R*,5*S*)-3,5,9-trimethyldec-8-enethioate (3-104):**

A solution of CuBr·DMS (4 mg, 0.0187 mmol, 0.03 equiv) and (*R,S*)–Josiphos (16 mg, 0.0250 mmol, 0.04 equiv) in MTBE (5.2 mL) was stirred at rt for 30 min and then cooled to–78 °C. To the cooled solution was added MeMgBr (3.0 M in Et_2O, 0.31 mL, 0.936 mmol, 1.5 equiv) followed by a slow addition of thioester **3-S15** (150 mg, 0.624 mmol, 1.0 equiv) in MTBE (1.0 mL) via syringe pump over 2 h (0.5 mL/ hr). The reaction was stirred at –70 °C for 17.5 h and then quenched with MeOH. The solution was partitioned between saturated NH_4Cl solution and Et_2O and additional extractions were performed with Et_2O. The combined organic phase was washed with brine, dried with $MgSO_4$, filtered, and concentrated *in vacuo.* The resulting residue was purified via flash chromatography (100% hex) to obtain thioester **3-104** along with a small amount of starting material (9 mol% by ^{1}H NMR; 10% mass frac) (53 mg total, 48 mg of pdt, 30%).

Optical rotation: $[\alpha]^{22}_D$ = +22.3 (*c* = 10.0, $CHCl_3$).

*an analytical sample prepared by Jess Pazienza was used for optical rotation

^{1}H NMR (500 MHz, $CDCl_3$) δ 5.08 (t, *J* = 6.4 Hz, 1H), 2.86 (q, *J* = 7.4 Hz, 2H), 2.47 (dd, *J* = 14.4, 6.1 Hz, 1H), 2.34 (dd, *J* = 14.4, 7.9 Hz, 1H), 2.10 (dd, *J* = 13.9, 6.8 Hz, 1H), 2.01 – 1.91 (m, 2H), 1.67 (s, 3H), 1.59 (s, 3H), 1.47 (dd, *J* = 13.4, 6.8 Hz, 1H), 1.28 (dd, *J* = 11.5, 4.2 Hz, 1H), 1.24 (t, *J* = 7.5 Hz, 3H), 1.18 – 1.05 (m, 3H), 0.89 (d, *J* = 6.6 Hz, 3H), 0.85 (d, *J* = 6.6 Hz, 3H).

^{13}C NMR (126 MHz, $CDCl_3$) δ 199.3, 131.2, 125.0, 52.3, 44.2, 37.8, 29.8, 28.8, 25.8, 25.6, 23.4, 19.4, 19.4, 17.8, 15.0.

HRMS (CI-TOF) *m/z* calculated for $C_{15}H_{28}OSH^+$ $(M+H)^+$ 257.1939, found 257.1940.

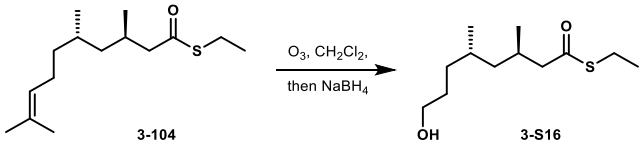

***S*-Ethyl (3*R*,5*S*)-8-hydroxy-3,5-dimethyloctanethioate (3-S16):**

A solution of the alkene **3-104** (45 mg, 0.176 mmol, 1.0 equiv) in CH_2Cl_2 (0.70 mL) and MeOH (0.30 mL) at –78 °C was treated O_3 until the solution turned blue in color (~5 min). The flask was purged with O_2 until the blue color dissipated, and then $NaBH_4$ (20 mg, 0.528 mmol, 3.0 equiv) was added. The solution was allowed to slowly warm to rt overnight before it was slowly quenched with H_2O. The slurry was diluted with brine and the organic phase was extracted, dried with Na_2SO_4, filtered, and concentrated *in vacuo*. The resulting residue was purified via flash chromatography (0 → 35% EtOAc in hex) to obtain alcohol **3-S16** as a clear oil (23 mg, 56% over 2 steps)

Optical rotation: $[\alpha]^{22}_D$ = +13.9 (*c* = 1.0, $CHCl_3$).

^{1}H NMR (500 MHz, $CDCl_3$) δ 3.61 (t, *J* = 6.4 Hz, 2H), 2.86 (q, *J* = 7.3 Hz, 2H), 2.47 (dd, *J* = 14.5, 6.2 Hz, 1H), 2.35 (dd, *J* = 14.3, 7.7 Hz, 1H), 2.11 (dq, *J* = 13.4, 6.8 Hz, 1H), 1.63 – 1.46 (m, 3H),

1.37 – 1.28 (m, 1H), 1.24 (t, *J* = 7.1 Hz, 3H), 1.20 – 1.08 (m, 3H), 0.90 (d, *J* = 6.6 Hz, 3H), 0.86 (d, *J* = 6.4 Hz, 3H).

^{13}C NMR (126 MHz, $CDCl_3$) δ 199.5, 63.4, 52.2, 44.3, 33.6, 30.4, 30.0, 28.7, 23.4, 19.5, 19.4, 14.9.

HRMS (ESI-TOF) *m/z* calculated for $C_{12}H_{24}O_2SNa^+$ $(M+Na)^+$ 255.1395, found 255.1391.

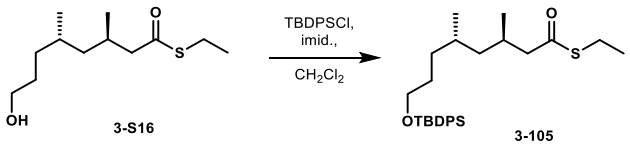

***S*-Ethyl (3*R*,5*S*)-8-((*tert*-butyldiphenylsilyl)oxy)-3,5-dimethyloctanethioate (3-105):**

To a solution of alcohol **3-S16** (23 mg, 0.0990 mmol, 1.2 equiv) in CH_2Cl_2 (0.50 mL) at rt was added imidazole (11 mg, 0.165 mmol, 2.0 equiv) followed by TBDPSCl (0.02 mL, 0.0825 mmol, 1.0 equiv). The reaction was stirred at rt for 17.5 h and then diluted with CH_2Cl_2. The organic phase was washed with brine, dried with $MgSO_4$, filtered, and concentrated *in vacuo*. The resulting residue was purified via flash chromatography (100% hex) to obtain thioester **3-105** as a clear oil (34 mg, 72%).

Optical rotation: $[\alpha]^{22}_D$ = +8.9 (*c* = 10.0, $CHCl_3$).

^{1}H NMR (500 MHz, $CDCl_3$) δ 7.67 (d, *J* = 7.8 Hz, 4H), 7.45 – 7.34 (m, 6H), 3.64 (t, *J* = 6.6 Hz, 2H), 2.87 (q, *J* = 7.4 Hz, 2H), 2.47 (dd, *J* = 14.4, 6.2 Hz, 1H), 2.35 (dd, *J* = 14.4, 7.9 Hz, 1H), 2.14 – 2.05 (m, 1H), 1.62 – 1.51 (m, 2H), 1.49 – 1.41 (m, 1H), 1.34 – 1.27 (m, 1H), 1.25 (t, *J* = 7.4 Hz, 3H), 1.21 – 1.15 (m, 1H), 1.13 – 1.08 (m, 2H), 1.05 (s, 9H), 0.88 (d, *J* = 6.6 Hz, 3H), 0.83 (d, *J* = 6.6 Hz, 3H).

^{13}C NMR (126 MHz, $CDCl_3$) δ 199.4, 135.7, 134.3, 129.6, 127.7, 64.4, 52.3, 44.2, 33.8, 30.1, 29.9, 28.7, 27.0, 23.4, 19.4 (2X), 19.3, 15.0.

HRMS (ESI-TOF) *m/z* calculated for $C_{28}H_{42}O_2SSiNa^+$ $(M+Na)^+$ 493.2573, found 493.2565.

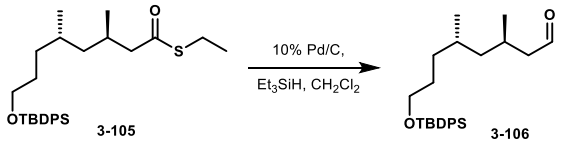

(3*R*,5*S*)-8-((*tert*-Butyldiphenylsilyl)oxy)-3,5-dimethyloctanal (3-106):

To a solution of thioester **3-105** (150 mg, 0.319 mmol, 1.0 equiv) and Et_3SiH (0.15 mL, 0.956 mmol, 3.0 equiv) in CH_2Cl_2 open to air was added 10% Pd/C (25 mg) portionwise. The slurry was stirred for 20 min after which it was filtered over celite and the cake was thoroughly washed with CH_2Cl_2. The filtrate was concentrated in vacuo and the resulting residue was purified via flash chromatography (100% hex) to obtain aldehyde **3-106** (102 mg, 78%).

Optical rotation: $[\alpha]^{22}_D$ = +15.6 (*c* = 10.0, $CHCl_3$).

^{1}H NMR (500 MHz, $CDCl_3$) δ 9.75 (t, *J* = 2.2 Hz, 1H), 7.68 (d, *J* = 6.6 Hz, 4H), 7.46 – 7.36 (m, 6H), 3.66 (t, *J* = 6.5 Hz, 2H), 2.35 (ddd, *J* = 15.9, 5.8, 1.9 Hz, 1H), 2.24 (ddd, *J* = 15.9, 7.6, 2.5 Hz, 1H), 2.19 – 2.11 (m, 1H), 1.63 – 1.46 (m, 3H), 1.38 – 1.29 (m, 1H), 1.24 – 1.16 (m, 2H), 1.13 – 1.09 (m, 1H), 1.07 (s, 9H), 0.93 (d, *J* = 6.6 Hz, 3H), 0.87 (d, *J* = 6.6 Hz, 3H).

^{13}C NMR (126 MHz, $CDCl_3$) δ 203.1, 135.7, 134.3, 129.7, 127.7, 64.3, 51.9, 44.6, 33.7, 30.1, 29.9, 27.0, 25.7, 19.8, 19.43, 19.35.

HRMS (CI-TOF) *m/z* calculated for $C_{26}H_{38}O_2SiH^+$ $(M+H)^+$ 411.2719, found 411.2729.

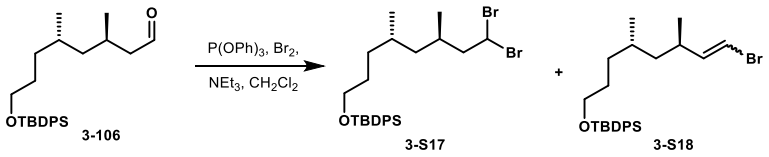

***tert*-Butyl(((4*S*,6*R*)-8,8-dibromo-4,6-dimethyloctyl)oxy)diphenylsilane (3-S17):**

To a solution of triphenyl phosphite (0.09 mL, 0.329 mmol, 1.5 equiv) in CH_2Cl_2 (1.0 mL) at –78 °C was added Br_2 (0.02 mL, 0.285 mmol, 1.3 equiv) followed by NEt_3 (0.09 mL, 0.657 mmol, 3.0 equiv) dropwise. When the foggy vapor disappeared from the head space, a solution of aldehyde **3-106** (90 mg, 0.219 mmol, 1.0 equiv) in CH_2Cl_2 (1.2 mL) was added dropwise. The reaction was

stirred for 2 h at –78 °C, then warmed to rt and stirred for an additional 2 h. The reaction solution was concentrated *in vacuo* and subjected to flash column chromatography (100% hex) to obtain bromides **3-S17** and **3-S18** as an inconsequential and inseparable mixture of geminal dibromo alkane, and *cis* and *trans* vinyl bromide diastereomers (10 : 1.0 : 1.3) (107 mg, 88%).

^{1}H NMR (500 MHz, $CDCl_3$) δ 7.68 (d, *J* = 6.8 Hz, 4H), 7.45 – 7.35 (m, 6H), 5.72 (dd, *J* = 8.0, 6.3 Hz, 1H), 3.66 (t, *J* = 6.5 Hz, 2H), 2.37 (ddd, *J* = 14.2, 8.1, 5.9 Hz, 1H), 2.27 – 2.19 (m, 1H), 1.83 (dd, *J* = 14.0, 7.1 Hz, 1H), 1.64 – 1.46 (m, 4H), 1.38 – 1.30 (m, 1H), 1.21 (ddd, *J* = 13.2, 9.0, 4.6 Hz, 1H), 1.15 – 1.09 (m, 1H), 1.07 (s, 9H), 0.87 (d, *J* = 6.6 Hz, 3H), 0.85 (d, *J* = 6.5 Hz, 3H).

^{13}C NMR (126 MHz, $CDCl_3$) δ 135.7, 134.3, 129.7, 127.7, 64.4, 53.7, 45.1, 43.7, 33.8, 30.2, 30.1, 29.8, 27.1, 19.47, 19.37, 18.6.

HRMS (CI-TOF) *m/z* calculated for $C_{26}H_{38}Br_2OSiH^+$ $(M+H)^+$ 553.1137, found 553.1163.

Diagnostic data for *cis* and *trans* vinyl bromides (3-S18):

^{1}H NMR (500 MHz, $CDCl_3$) δ 5.97 (d, *J* = 13.6 Hz, 1H, *trans*), 5.85 (dd, *J* = 9.1, 7.0 Hz, 1H, *cis*).

HRMS (CI-TOF) *m/z* calculated for $C_{26}H_3BrOSiH^+$ $(M+H)^+$ 473.1875, found 473.1878.

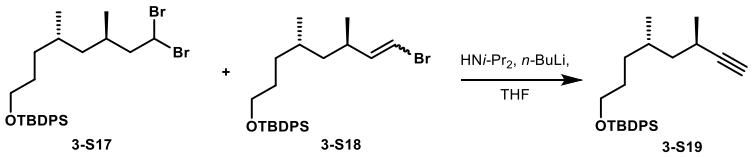

***tert*-Butyl(((4*S*,6*R*)-4,6-dimethyloct-7-yn-1-yl)oxy)diphenylsilane (3-S19):**

To a solution of HN*i*-Pr_2 (1.6 mL, 11.4 mmol, 4.5 equiv) in THF (3.0 mL) at –78 °C was added *n*-BuLi (2.5 M in hex.; 4.0 mL, 10.0 mmol, 4.0 equiv). The solution was removed from cooling bath for a couple min. and then cooled back to –78 °C after which bromides **3-S17** and **3-S18** (1.30 g, 2.54 mmol, 1.0 equiv) in THF (5.5 mL) was added. The reaction was allowed to slowly warm to rt over 3 h and then stirred at rt for an additional 1.5 h, after which it was quenched with saturated NH_4Cl solution (100 mL). The mixture was extracted with Et_2O (2 X), and the combined organic phase was washed with brine, dried with $MgSO_4$, filtered, and concentrated *in vacuo* to obtain

terminal alkyne **3-S19**. The oil was taken on to the next step without further purification. An aliquot was removed and purified for characterization.

Optical rotation: $[\alpha]^{22}_{D}$ = –21.6 (*c* = 1.0, $CHCl_3$).

^{1}H NMR (500 MHz, $CDCl_3$) δ 7.67 (d, *J* = 6.5 Hz, 4H), 7.45 – 7.35 (m, 6H), 3.65 (t, *J* = 6.5 Hz, 2H), 2.52 – 2.42 (m, 1H), 2.00 (d, *J* = 2.2 Hz, 1H), 1.68 – 1.56 (m, 2H), 1.54 – 1.47 (m, 1H), 1.45 – 1.27 (m, 3H), 1.19 – 1.10 (m, 4H), 1.05 (s, 9H), 0.87 (d, *J* = 6.7 Hz, 3H).

^{13}C NMR (126 MHz, $CDCl_3$) δ 135.7, 134.3, 129.6, 127.7, 89.7, 68.0, 64.4, 44.4, 32.3, 30.5, 29.9, 27.0, 23.5, 21.2, 20.0, 19.4.

HRMS (CI-TOF) *m/z* calculated for $C_{26}H_{36}OSiH^+$ $(M+H)^+$ 393.2614, found 393.2624.

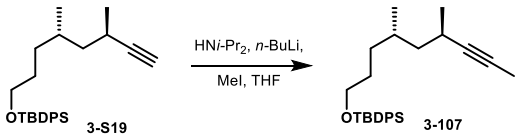

***tert*-Butyl(((4*S*,6*R*)-4,6-dimethylnon-7-yn-1-yl)oxy)diphenylsilane (3-107):**

To a solution of HN*i*-Pr_2 (1.4 mL, 9.76 mmol, 4.0 equiv) in THF (4.0 mL) at –78 °C was added *n*-BuLi (2.5 M in hex.; 2.9 mL, 7.31 mmol, 3.0 equiv). The solution was removed from cooling bath and while warming to rt, terminal alkyne **3-S19** (957 mg, 2.44 mmol, 1.0 equiv) in THF (8.0 mL) was added. The solution was stirred at rt for 1 h and then cooled back to –78 °C and iodomethane (0.91 mL, 14.6 mmol, 6.0 equiv) was added. The reaction was allowed to warm to rt over 15.5 h after which it was quenched with saturated NH_4Cl solution. The mixture was extracted with Et_2O (3 X), and the combined organic phase was washed with brine, dried with $MgSO_4$, filtered, and concentrated *in vacuo*. The resulting residue was purified via flash chromatography (100% hex) to obtain internal alkyne **3-107** (770 mg, 78% over 2 steps).

Optical rotation: $[\alpha]^{22}_{D}$ = –10.1 (*c* = 1.0, $CHCl_3$).

^{1}H NMR (500 MHz, $CDCl_3$) δ 7.73 (dd, *J* = 8.0, 1.7 Hz, 4H), 7.48 – 7.40 (m, 6H), 3.71 (t, J = 6.7 Hz, 2H), 2.52 – 2.43 (m, 1H), 1.80 (d, *J* = 2.6 Hz, 3H), 1.70 – 1.62 (m, 2H), 1.58 (ddd, *J* = 12.9,

10.8, 6.4 Hz, 1H), 1.47 – 1.43 (m, 1H), 1.40 – 1.35 (m, 2H), 1.22 – 1.18 (m, 1H), 1.15 (d, *J* = 6.9 Hz, 3H), 1.11 (s, 9H), 0.92 (d, *J* = 6.8 Hz, 3H).

^{13}C NMR (126 MHz, $CDCl_3$) δ 135.7, 134.3, 129.6, 127.7, 84.3, 75.3, 64.5, 45.0, 32.4, 30.5, 29.9, 29.9, 27.0, 23.7, 21.6, 20.0, 19.4, 3.6.

HRMS (CI-TOF) *m/z* calculated for $C_{27}H_{38}OSiH^+$ $(M+H)^+$ 407.2770, found 407.2785.

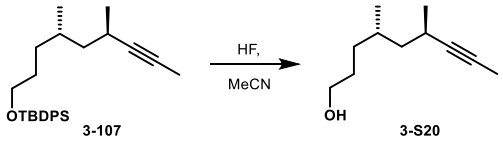

(*4S,6R,E*)-8-Iodo-4,6-dimethylnon-7-en-1-ol (3-S20):

To a plastic bottle containing internal alkyne **3-107** (770 mg, 1.89 mmol, 1.0 equiv) in MeCN (7.6 mL) was added HF (50% aq. soln; 0.13 mL). After stirring for 30 min, an additional portion of HF (0.5 mL) was added. After stirring for 1.5 h, an additional portion of HF (0.25 mL) was added. After stirring for 15 min, the reaction was slowly quenched with saturated $NaHCO_3$ solution and extracted with EtOAc (3 X). The combined organic phase was washed with brine, dried with $MgSO_4$, filtered, and concentrated *in vacuo*. The resulting residue was purified via flash chromatography (0 → 100% EtOAc in hex) to obtain alcohol **3-S20** (264 mg, 83%).

^{1}H NMR (500 MHz, $CDCl_3$) δ 3.56 (t, *J* = 6.8 Hz, 2H), 2.45 – 2.34 (m, 1H), 2.07 (s, br, 1H), 1.73 (d, *J* = 2.9 Hz, 3H), 1.63 – 1.51 (m, 2H), 1.51 – 1.42 (m, 1H), 1.41 – 1.33 (m, 1H), 1.31 – 1.19 (m, 2H), 1.13 – 1.07 (m, 1H), 1.05 (d, *J* = 7.4 Hz, 3H), 0.85 (d, *J* = 7.4 Hz, 3H).

^{13}C NMR (126 MHz, $CDCl_3$) δ 84.2, 75.4, 63.2, 44.8, 32.1, 30.4, 30.0, 23.6, 21.5, 19.9, 3.5.

HRMS (CI-TOF) *m/z* calculated for $C_{11}H_{20}ONH_4^+$ $(M+NH_4)^+$ 186.1858, found 186.1856.

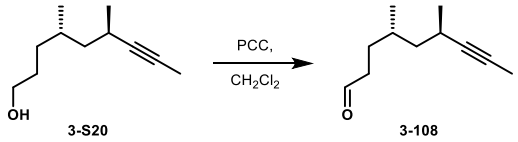

3-S20 3-108

(*4S,6R,E*)-8-Iodo-4,6-dimethylnon-7-enal (3-108):

To a solution of alcohol **3-S20** (189 mg, 1.12 mmol, 1.0 equiv) in CH_2Cl_2 (5.6 mL) at rt was added PCC (435 mg, 2.02 mmol, 1.8 equiv). The slurry was stirred for 2 h at rt and then filtered through a pad a silica. The cake was thoroughly washed with CH_2Cl_2 after which the filtrated was concentrated *in vacuo* to obtain aldehyde **3-108** (148 mg, 80%).

^{1}H NMR (500 MHz, $CDCl_3$) δ 9.71 (s, 1H), 2.44 – 2.31 (m, 3H), 1.70 (d, *J* = 2.7 Hz, 3H), 1.67 – 1.55 (m, 2H), 1.38 – 1.15 (m, 3H), 1.04 (d, *J* = 7.0 Hz, 3H), 0.84 (d, *J* = 6.9 Hz, 3H).

^{13}C NMR (126 MHz, $CDCl_3$) δ 202.9, 83.8, 75.7, 44.5, 41.6, 30.4, 28.2, 23.6, 21.6, 19.8, 3.5.

HRMS (CI-TOF) *m/z* calculated for $C_{11}H_{18}O^+$ $(M)^+$ 166.1358, found 166.1356.

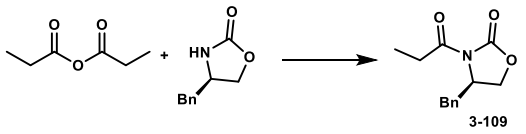

3-109

(*R*)-4-benzyl-3-propionyloxazolidin-2-one (3-109):

To a solution of (*R*)-4-benzyloxazolidin-2-one (500 mg, 2.82 mmol, 1.0 equiv) in THF (3.0 mL) was added propionic anhydride (0.72 mL, 5.64 mmol, 2.0 equiv), NEt_3 (0.43 mL, 3.10 mmol, 1.1 equiv), and DMAP (17 mg, 0.141 mmol, 0.05 equiv). The solution was stirred for 14 h and then concentrated *in vacuo*. The resulting residue was dissolved in CH_2Cl_2 and then washed with 1 M NaOH solution then saturated $NaHCO_3$ solution. The combined aqueous phase was back extracted with CH_2Cl_2 (2 X). The combined organic phase was dried with Na_2SO_4, filtered, and concentrated *in vacuo*. The resulting residue was purified via flash chromatography (0 → 25% EtOAc in hex) to obtain oxazolidinone **3-109** as a white solid (650 mg, 99%). Spectral data is in accordance with the reported literature.[157]

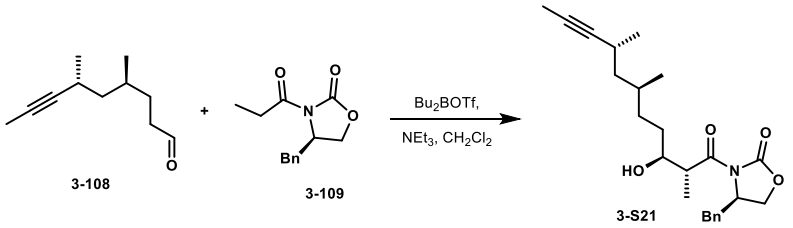

(*R*)-4-Benzyl-3-((*2R,3S,6S,8R*)-3-hydroxy-2,6,8-trimethylundec-9-ynoyl)oxazolidin-2-one (3-S21):

To a solution of oxazolidinone **3-109** (64 mg, 0.273 mmol, 1.0 equiv) in CH_2Cl_2 (0.75 mL) at 0 °C was added freshly distilled Bu_2BOTf (0.10 mL, 0.328 mmol, 1.2 equiv) followed by NEt_3 (0.05 mL, 0.355 mmol, 1.3 equiv). The solution was cooled to –78 °C and aldehyde X (50 mg, 0.301 mmol, 1.0 equiv) in CH_2Cl_2 (0.1 mL) was added. The reaction was stirred at –78 °C for 30 min and then warmed to 0 °C and stirred for 2.75 h. To quench the reaction, a solution of pH 7 phosphate buffer (0.5 mL) and MeOH (1.5 mL) was added followed by a solution of 30% aq. H_2O_2 (1.0 mL) and MeOH (0.5 mL). The slurry was vigorously stirred for 45 min and then extracted with Et_2O (3 X). The combined organic phase was washed with brine, dried with MgSO4, filtered, and concentrated *in vacuo*. The resulting residue was purified via flash chromatography (0 → 25% EtOAc in hex.) to obtain alcohol **3-S21** (75 mg, 69%).

^{1}H NMR (500 MHz, $CDCl_3$) δ 7.33 (t, *J* = 7.3 Hz, 2H), 7.29 – 7.25 (m, 1H), 7.20 (d, *J* = 7.5 Hz, 2H), 4.70 (t, *J* = 8.4 Hz, 1H), 4.27 – 4.14 (m, 2H), 3.97 – 3.88 (m, 1H), 3.83 – 3.73 (m, 1H), 3.24 (d, *J* = 13.4 Hz, 1H), 2.84 – 2.74 (m, 1H), 2.48 – 2.40 (t, *J* = 16.4 Hz, 1H), 1.77 (s, 3H), 1.68 – 1.61 (m, 1H), 1.59 – 1.53 (m, 1H), 1.44 – 1.35 (m, 2H), 1.33 – 1.28 (m, 2H), 1.28 – 1.21 (m, 4H), 1.10 (d, *J* = 6.9 Hz, 3H), 0.89 (d, *J* = 6.8 Hz, 3H).

^{13}C NMR (126 MHz, $CDCl_3$) δ 177.7, 153.2, 135.2, 129.6, 129.1, 127.6, 84.3, 75.5, 71.9, 66.3, 55.2, 44.8, 42.3, 37.9, 32.5, 31.2, 30.6, 23.7, 21.6, 20.0, 10.6, 3.6.

HRMS (ESI-TOF) *m/z* calculated for $C_{24}H_{33}NO_4Na^+$ $(M+Na)^+$ 422.2307, found 422.2323.

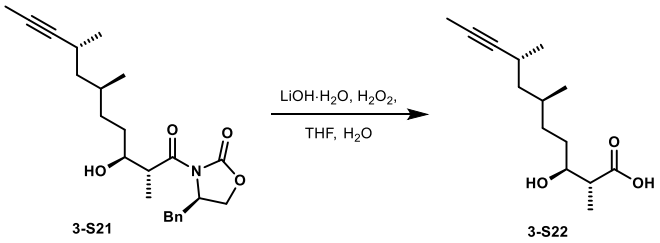

(*2R,3S,6S,8R*)-3-Hydroxy-2,6,8-trimethylundec-9-ynoic acid (3-S22):

To a solution of oxazolidinone **3-S21** (75 mg, 0.188 mmol, 1.0 equiv) in THF (1.4 mL) and H_2O (0.5 mL) was added $LiOH·H_2O$ (16 mg, 0.375 mmol, 2.0 equiv) followed by 30% aq. H_2O_2 (0.19 mL). The reaction was stirred for 1 h and then quenched with saturated $Na_2S_2O_3$ solution. The volatiles were removed *in vacuo*. The resulting solution was acidified to pH 1 with 3 M HCl and then extracted with EtOAc (6 X). The combined organic phase was dried with Na_2SO_4, filtered, and concentrated *in vacuo* to obtain carboxylic acid **3-S22**. The resulting residue was taken on to the next step without further purification.

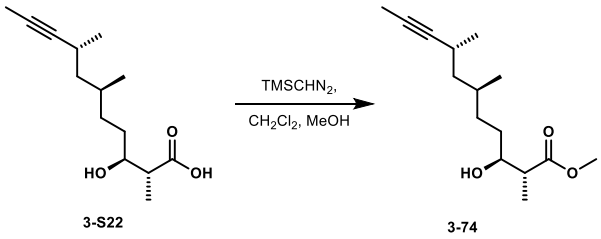

Methyl (2R,3S,6S,8R)-3-hydroxy-2,6,8-trimethylundec-9-ynoate (3-74):

To a solution of carboxylic acid **3-S22** (45 mg, 0.188 mmol, 1.0 equiv) in Et_2O (1.3 mL) and MeOH (0.6 mL) at rt was added $TMSCHN_2$ (2.0 M in hex.; 0.21 mL, 0.414 mmol, 2.2 equiv) dropwise. The reaction was stirred for 2.5 h at rt and then slowly quenched with AcOH until the yellow color dissipated in the solution. The slurry was diluted with H_2O and then extracted with Et_2O (2 X). The combined organic phase was washed with brine, dried with $MgSO_4$, filtered, and concentrated *in vacuo* to obtain ester **3-74** (27 mg, 56% over 2 steps).

^{1}H NMR (500 MHz, $CDCl_3$) δ 3.88 (dd, *J* = 8.2, 4.0 Hz, 1H), 3.71 (s, 3H), 2.55 (qd, *J* = 7.2, 3.7 Hz, 1H), 2.50 – 2.40 (m, 2H), 1.78 (d, *J* = 2.4 Hz, 3H), 1.64 (dd, *J* = 11.6, 7.2 Hz, 1H), 1.52 – 1.48 (m, 1H), 1.42 – 1.34 (m, 2H), 1.33 – 1.23 (m, 3H), 1.19 (d, *J* = 7.2 Hz, 3H), 1.10 (d, *J* = 6.8 Hz, 3H), 0.88 (d, *J* = 6.7 Hz, 3H).

^{13}C NMR (126 MHz, $CDCl_3$) δ 176.7, 84.2, 75.6, 72.1, 51.9, 44.8, 44.4, 32.3, 31.1, 30.6, 23.7, 21.6, 20.0, 10.9, 3.6.

HRMS (ESI-TOF) *m/z* calculated for $C_{15}H_{26}ONa^+$ $(M+Na)^+$ 277.1780, found 277.1783.

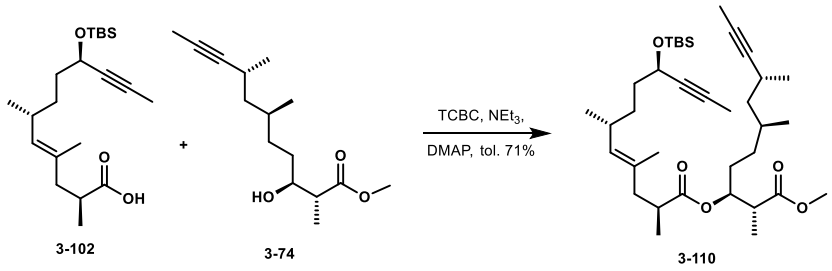

(*2R,3S,6S,8R*)-1-Methoxy-2,6,8-trimethyl-1-oxoundec-9-yn-3-yl (*2S,6R,9R,E*)-9-((*tert*-butyldimethyl silyl)oxy)-2,4,6-trimethyldodec-4-en-10-ynoate (3-110): To a solution of carboxylic acid **3-102** (16 mg, 0.0433 mmol, 1.1 equiv) in toluene (0.25 mL) at rt was added 2,4,6-trichlorobenzoyl chloride (10 µL, 0.0591 mmol, 1.5 equiv) followed by NEt_3 (10 µL, 0.0591 mmol, 1.5 equiv). The reaction was stirred for 30 min at rt then DMAP (5 mg, 0.034 mmol, 1.0 equiv) and alcohol **3-74** was added. The reaction was stirred for 18 h at rt then DMAP (10 mg, 0.0788 mmol, 2.0 equiv) was added and stirred for an additional 2 h. The reaction was quenched with citric acid solution and extracted with EtOAc (2 X 3 mL). The combined organic phase was dried with Na_2SO_4, filtered, and concentrated *in vacuo* to obtain diyne **3-110** as a clear oil (17 mg, 71%).

^{1}H NMR (500 MHz, $CDCl_3$) δ 5.12 – 5.08 (m, 1H), 4.95 (d, *J* = 9.4 Hz, 1H), 4.29 – 4.23 (m, 1H), 3.67 (s, 3H), 2.72 – 2.65 (m, 1H), 2.57 (dd, *J* = 14.5, 7.0 Hz, 1H), 2.44 – 2.37 (m, 2H), 2.35 – 2.29 (m, 1H), 1.97 (dd, *J* = 13.3, 9.2 Hz, 1H), 1.81 (s, 3H), 1.77 (s, 3H), 1.67 – 1.50 (m, 9H), 1.47 –

1.41 (m, 1H), 1.36 – 1.23 (m, 4H), 1.15 (d, *J* = 7.0 Hz, 3H), 1.11 – 1.06 (m, 6H), 0.91 (d, *J* = 6.6 Hz, 3H), 0.89 (s, 9H), 0.87 (d, *J* = 6.7 Hz, 3H), 0.10 (s, 3H), 0.08 (s, 3H).

^{13}C NMR (126 MHz, $CDCl_3$) δ 176.0, 174.5, 134.3, 130.7, 81.2, 80.0, 75.6, 74.1, 63.5, 51.9, 44.8, 43.9, 43.1, 38.1, 37.1, 33.3, 32.4, 31.8, 30.6, 29.2, 26.0, 23.6, 21.6, 21.4, 19.8, 18.4, 16.5, 15.9, 12.1, 3.7, 3.6, -4.3, -4.9.

HRMS (ESI-TOF) *m/z* calculated for $C_{36}H_{62}O_5SiNa^+$ $(M+Na)^+$ 625.4265, found 625.4265.

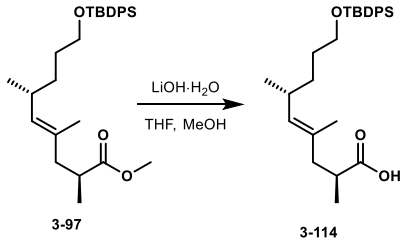

(2S,6R,E)-9-((tert-butyldiphenylsilyl)oxy)-2,4,6-trimethylnon-4-enoic acid (3-114):

To a solution of ester **3-97** (100 mg, 0.214 mmol, 1.0 equiv) in THF (0.6 mL), MeOH (0.4 mL), H_2O (0.2 mL) at rt was added $LiOH·H_2O$ (45 mg, 1.07 mmol, 5.0 equiv). The slurry was stirred at rt overnight and then acidified to pH 3 with 3 M HCl. The solution was extracted with EtOAc (5 X) and the combined organic phase was washed with brine, dried with Na_2SO_4, filtered, and concentrated *in vacuo* to obtain **3-114**. The resulting residue was subjected to the next step without further purification.

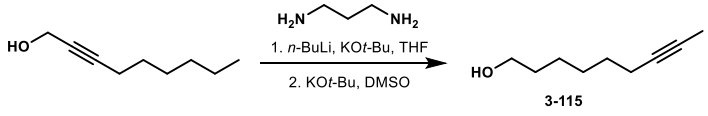

Non-7-yn-1-ol (3-115):

To a solution of 1,3-diaminopropane (1.4 mL, 16.8 mmol, 5.4 equiv) in THF (5 mL) at 0 C was added *n*-BuLi (6.7 mL, 16.8 mmol, 5.4 equiv) dropwise. The solution was stirred for 20 min then KO*t*-Bu (1.47 g, 13.1 mmol, 4.2 equiv) in THF (13 mL) was added followed by non-2-yn-1-ol (0.5

mL, 3.11 mmol, 1.0 equiv). The solution was warmed to rt and stirred for 2 h. The solution was diluted with saturated NH4Cl solution and then extracted with EtOAc (3 X). The combined organic phase was washed with 1 M HCl solution, saturated $NaHCO_3$ solution, then brine and then dried with Na_2SO_4, filtered, and concentrated *in vacuo*. The resulting residue was dissolved in DMSO and KO*t*-Bu was added at rt. The solution was stirred overnight and then diluted with 1 M HCl, which was then extracted with Et_2O (3 X). The combined organic phase was washed with H_2O (3 X), then brine, dried with $MgSO_4$, filtered, and concentrated in vacuo to obtain alcohol **3-115**. The spectral data is in accordance with the reported literature.[158]

^{1}H NMR (500 MHz, $CDCl_3$) δ 3.63 (t, *J* = 6.6 Hz, 2H), 2.14 – 2.09 (m, 2H), 1.77 (t, *J* = 2.4 Hz, 3H), 1.60 – 1.53 (m, 2H), 1.51 – 1.44 (m, 2H), 1.43 – 1.33 (m, 4H).

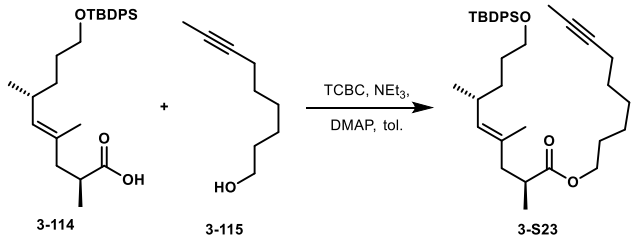

Non-7-yn-1-yl (*2S,6R,E*)-9-((*tert*-butyldiphenylsilyl)oxy)-2,4,6-trimethylnon-4-enoate (3-S23):

To a solution of carboxylic acid **3-114** (97 mg, 0.214 mmol, 1.0 equiv) in toluene (1.0 mL) was added 2,4,6-trichlorobenzoyl chloride (50 µL, 0.321 mmol, 1.5 equiv) followed by NEt_3 (40 µL, 0.321 mmol, 1.5 equiv). The solution was stirred for 30 min then alcohol **3-115** (30 mg, 0.214 mmol, 1.0 equiv) in toluene (1.1 mL) was added followed by DMAP (131 mg, 1.07 mmol, 5.0 equiv). After stirring for 1.5 h at rt, the reaction was quenched with 1 M HCl and then extracted with Et_2O (2 X). The combined organic phase was washed with brine, dried with $MgSO_4$, filtered, and concentrated *in vacuo* to obtain ester **3-S23**. The resulting residue was subjected to the next step without further purification.

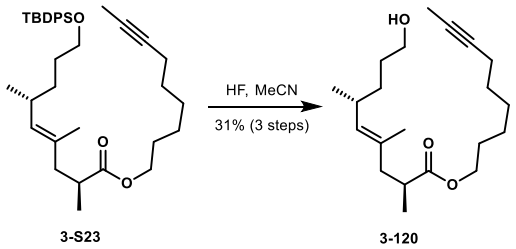

Non-7-yn-1-yl (*2S,6R,E*)-9-hydroxy-2,4,6-trimethylnon-4-enoate (3-120):

To a solution of ester **3-S23** (123 mg, 0.214 mmol, 1.0 equiv) in MeCN (1.1 mL) at rt was added HF (0.5 mL). The solution was stirred at rt for 1.5 h and then slowly quenched with a saturated $NaHCO_3$ solution. Once bubbling ceased, the solution was extracted with Et_2O (2 X). The combined organic phase was washed with brine, dried with $MgSO_4$, filtered, and concentrated *in vacuo*. The resulting residue was purified via flash chromatography (0 → 80% EtOAc) to obtain alcohol **3-120** as a clear oil (22 mg, 31% over 3 steps).

^{1}H NMR (500 MHz, $CDCl_3$) δ 4.92 (dd, *J* = 9.5, 1.0 Hz, 1H), 4.03 (td, *J* = 6.7, 3.7 Hz, 2H), 3.61 (t, *J* = 6.6 Hz, 2H), 2.60 (dd, *J* = 14.4, 7.3 Hz, 1H), 2.34 (dd, *J* = 13.9, 7.0 Hz, 2H), 2.12 (ddt, *J* = 9.5, 7.1, 2.3 Hz, 2H), 2.06 (s, br, 1H), 2.02 (dd, *J* = 13.6, 7.7 Hz, 1H), 1.77 (t, *J* = 2.5 Hz, 3H), 1.63 (dd, *J* = 14.3, 7.1 Hz, 2H), 1.59 (d, *J* = 1.2 Hz, 3H), 1.54 – 1.45 (m, 4H), 1.43 – 1.32 (m, 5H), 1.21 (ddd, *J* = 9.8, 8.7, 3.9 Hz, 1H), 1.09 (d, *J* = 6.9 Hz, 3H), 0.91 (d, *J* = 6.7 Hz, 3H).

^{13}C NMR (126 MHz, $CDCl_3$) δ 176.8, 133.7, 131.1, 793, 75.7, 64.4, 63.3, 44.1, 38.3, 33.8, 32.4, 331.0, 29.1, 28.7, 28.6, 25.7, 21.4, 18.8, 16.8, 16.1, 3.6.

HRMS (ESI-TOF) *m/z* calculated for $C_{21}H_{36}O_3Na^+$ $(M+Na)^+$ 359.2562, found 359.2556.

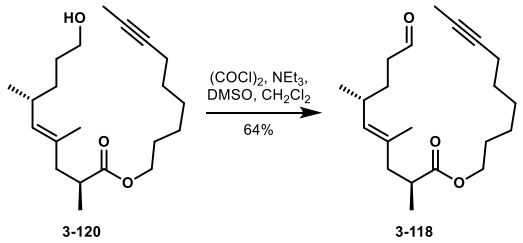

Non-7-yn-1-yl (*2S,6R,E*)-2,4,6-trimethyl-9-oxonon-4-enoate (3-118):

To a solution of oxalyl chloride (10 µL, 0.0785 mmol, 1.2 equiv) in CH_2Cl_2 (0.2 mL) at –78 °C was added DMSO (10 µL, 0.157 mmol, 2.4 equiv) followed by alcohol **3-120** (22 mg, 0.654 mmol, 1.0 equiv) in CH_2Cl_2 (0.2 mL). The solution was stirred for 5 min at this temperature and then NEt_3 (50 µL, 0.327 mmol, 5.0 equiv) was added. The reaction was warmed to rt and stirred for an additional 30 min after which it was diluted CH_2Cl_2. The solution was washed with saturated NH_4Cl solution, and brine, and then it was dried with Na_2SO_4, filtered, and concentrated *in vacuo* to obtain aldehyde **3-118** (14 mg, 64%).

^{1}H NMR (500 MHz, $CDCl_3$) δ 9.73 (t, *J* = 1.7 Hz, 1H), 4.87 (dd, *J* = 9.6, 1.1 Hz, 1H), 4.06 – 3.97 (m, 2H), 2.60 (dd, *J* = 14.4, 7.2 Hz, 1H), 2.38 – 2.30 (m, 4H), 2.11 (ddd, *J* = 9.6, 4.8, 2.6 Hz, 2H), 2.02 (dd, *J* = 13.6, 7.5 Hz, 1H), 1.76 (t, *J* = 2.5 Hz, 3H), 1.70 – 1.58 (m, 4H), 1.57 (d, *J* = 1.3 Hz, 3H), 1.50 – 1.44 (m, 3H), 1.38 – 1.32 (m, 3H), 1.09 (d, *J* = 6.9 Hz, 3H), 0.93 (d, *J* = 6.6 Hz, 3H).

^{13}C NMR (126 MHz, $CDCl_3$) δ 202.8, 176.6, 132.5, 132.4, 79.2, 75.6, 64.4, 44.1, 42.3, 38.2, 32.1, 29.8, 29.0, 28.7, 28.6, 25.7, 21.3, 18.8, 16.9, 16.2, 3.6.

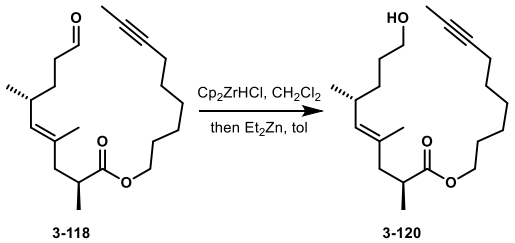

Non-7-yn-1-yl (*2S,6R,E*)-9-hydroxy-2,4,6-trimethylnon-4-enoate (3-120):

To a solution of aldehyde **3-118** (7 mg, 0.0209 mmol, 1.0 equiv) in CH_2Cl_2 (0.10 mL) at rt was added Cp_2ZrHCl (13 mg, 0.0523 mmol, 2.5 equiv). The slurry was stirred until the cloudiness dissipated to a clear yellow solution (45 min) and the solution was concentrated *in vacuo*. The residue was redissolved in toluene (0.50 mL) and added via syringe pump over 2 h to a cooled solution of Et_2Zn (2.0 M in hex; 10 µL, 0.0209 mmol, 1.0 equiv) in toluene (0.5 mL) at –65 °C. The reaction was allowed to warm to rt overnight and then concentrated *in vacuo* the next day. The resulting residue was purified via flash chromatography (0 → 40% EtOAc in hex) to obtain alcohol **3-120**. The spectral data matches the data reported *vide supre*.

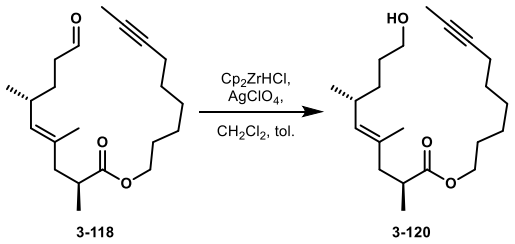

Non-7-yn-1-yl (*2S,6R,E*)-9-hydroxy-2,4,6-trimethylnon-4-enoate (3-120):

To a solution of aldehyde **3-118** (8 mg, 0.0239 mmol, 1.0 equiv) and $AgClO_4$ (2 mg, 0.0119, 0.5 equiv) in toluene (0.2 mL) at rt was added Cp_2ZrHCl (7 mg, 0.0263 mmol, 1.1 equiv) in CH_2Cl_2 (0.3 mL) via syringe pump over 1 h. The solution was stirred for an additional 3 h at rt and was then filtered over celite. The cake was washed with additional CH_2Cl_2 and the filtrate was concentrated *in vacuo* to obtain alcohol **3-120**. The spectral data matches the data reported *vide supre*.

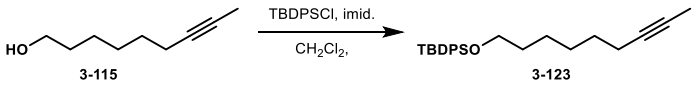

***tert*-Butyl(non-7-yn-1-yloxy)diphenylsilane (3-123):**

To a solution of alcohol **3-115** (100 mg, 0.713 mmol, 1.0 equiv) in CH_2Cl_2 (3.6 mL) at rt was added imidazole (146 mg, 2.14 mmol, 3.0 equiv) followed by TBDPSCl (0.28 mL, 1.07 mmol, 1.5 equiv). The reaction was stirred at rt overnight and then washed with H_2O (2 X) and brine. The organic phase was dried with Na_2SO_4, filtered, and concentrated *in vacuo*. The resulting residue was purified through a silica pad (100% hex) to obtain alkyne **3-123** as a clear oil.

^{1}H NMR (500 MHz, $CDCl_3$) δ 7.71 (dd, *J* = 7.7, 1.2 Hz, 4H), 7.47 – 7.38 (m, 6H), 3.70 (t, *J* = 6.5 Hz, 2H), 2.14 (ddd, *J* = 9.7, 4.8, 2.6 Hz, 2H), 1.80 (t, *J* = 2.5 Hz, 3H), 1.65 – 1.58 (m, 2H), 1.53 – 1.46 (m, 2H), 1.44 – 1.35 (m, 2H), 1.09 (s, 9H).

^{13}C NMR (126 MHz, $CDCl_3$) δ 135.7, 134.3, 129.6, 127.7, 79.5, 75.5, 64.0, 32.6, 29.2, 28.8, 27.0, 25.5, 19.4, 18.8, 3.6.

HRMS (CI-TOF) *m/z* calculated for $C_{21}H_{25}OSi^+$ (M–*t*-butyl)$^+$ 321.1675, found 321.1690.

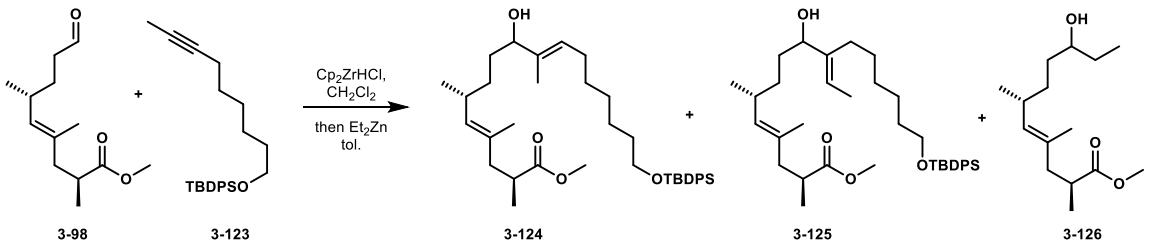

Methyl (*2S,4E,6R,10E*)-17-((*tert*-butyldiphenylsilyl)oxy)-9-hydroxy-2,4,6,10-tetramethylheptadeca-4,10-dienoate (3-124), Methyl (*2S,4E,6R,10E*)-16-((*tert*-butyldiphenylsilyl)oxy)-10-ethylidene-9-hydroxy-2,4,6-trimethylhexadec-4-enoate (3-125), and Methyl (*2S,6R,E*)-9-hydroxy-2,4,6-trimethylundec-4-enoate (3-126):

To a Schlenk flask containing Cp_2ZrHCl (15 mg, 0.0581 mmol, 1.1 equiv) at rt was added alkyne **3-123** (20 mg, 0.0528 mmol, 1.0 equiv) in CH_2Cl_2 (0.20 mL) and the solution was stirred at rt for 2 h. The solution was concentrated *in vacuo* and then redissolved in toluene (0.20 mL) and cooled

to –65 °C. A solution of Et_2Zn (1.0 M in hex; 50 µL, 0.0528 mmol, 1.0 equiv) was added dropwise. The reaction was then warmed to 0 °C and aldehyde **3-98** (12 mg, 0.0528 mmol, 1.0 equiv) was added. The solution was allowed to warm to rt and then concentrated *in vacuo*. The resulting residue was purified via flash chromatography (0 → 25% EtOAc in hex) to obtain alcohol **3-124**, alcohol **3-125**, and alcohol **3-126**.

Diagnostic ^{1}H NMR data for alcohol **3-124**:

^{1}H NMR (600 MHz, $CDCl_3$) δ 5.34 (t, *J* = 6.5 Hz, 1H), 4.91 (d, *J* = 7.2 Hz, 1H), 3.93 (t, *J* = 6.4 Hz, 1H), 1.59 (s, 3H).

Diagnostic ^{1}H NMR data for alcohol **3-125**:

^{1}H NMR (600 MHz, $CDCl_3$) δ 5.45 (q, J = 6.5 Hz, 1H), 4.90 (d, 9.2 Hz, 1H), 3.94 (t, J = 6.4 Hz, 1H) 1.61, (d, J = 6.7 Hz, 3H).

Diagnostic ^{1}H NMR data for alcohol **3-126**:

^{1}H NMR (600 MHz, $CDCl_3$) δ 4.91 (dd, J = 9.1, 5.3 Hz, 1H), 3.50 – 3.46 (m, 1H).

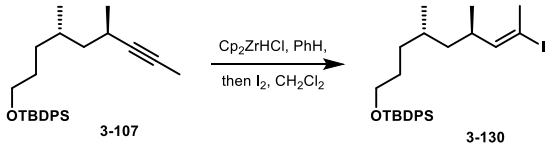

***tert*-Butyl(((4*S*,6*R*,*E*)-8-iodo-4,6-dimethylnon-7-en-1-yl)oxy)diphenylsilane (3-130):**

A Schlenk flask containing Cp_2ZrHCl (95 mg, 0.369 mmol, 3.0 equiv) was removed from the glove box, and a solution of internal alkyne **3-107** (50 mg, 0.123 mmol, 1.0 equiv) in benzene (1.2 mL) at rt was added. After stirring for 17.5 h at rt, a saturated solution of I_2 in CH_2Cl_2 was added to the cloudy yellow mixture until the purple color persisted in the solution. A saturated $Na_2S_2O_3$ solution was added and the mixture was vigorously stirred until purple color dissipated. The slurry was diluted with brine and extracted with CH_2Cl_2 (3 X). The combined organic phase was dried with Na_2SO_4, filtered, and concentrated *in vacuo*. The resulting residue was purified via silica plug (10% EtOAc in hex) to obtain vinyl iodide **3-130** (62 mg 94%).

Optical rotation: $[\alpha]^{22}_D$ = –20.2 (*c* = 10.0, $CHCl_3$).

^{1}H NMR (500 MHz, $CDCl_3$) δ 7.68 (d, *J* = 6.6 Hz, 4H), 7.46 – 7.36 (m, 6H), 5.94 (dd, *J* = 9.8, 0.9 Hz, 1H), 3.64 (t, *J* = 6.5 Hz, 2H), 2.45 (ddd, *J* = 14.1, 9.6, 7.0 Hz, 1H), 2.34 (d, *J* = 1.1 Hz, 3H), 1.62 – 1.55 (m, 1H), 1.52 – 1.45 (m, 1H), 1.42 – 1.31 (m, 2H), 1.18 (dd, *J* = 13.5, 6.7 Hz, 1H), 1.14 – 1.08 (m, 2H), 1.06 (s, 9H), 0.91 (d, *J* = 6.7 Hz, 3H), 0.84 (d, *J* = 6.5 Hz, 3H).

^{13}C NMR (126 MHz, $CDCl_3$) δ 148.0, 135.7, 134.3, 129.7, 127.7, 92.2, 64.5, 44.5, 33.4, 32.9, 30.3, 30.0, 27.8, 27.0, 20.4, 20.1, 19.4.

HRMS (ESI-CI) *m/z* calculated for $C_{27}H_{39}OISiH^+$ $(M+H)^+$ 535.1893, found 535.1875.

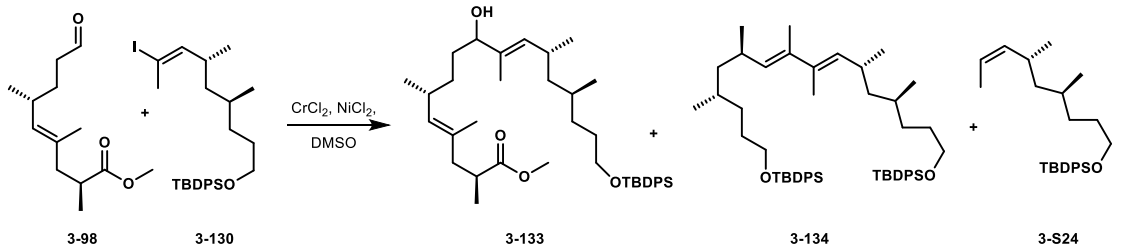

Methyl (*2S,4E,6R,10E,12R,14S*)-17-((*tert*-butyldiphenylsilyl)oxy)-9-hydroxy-2,4,6,10,12,14-hexamethylheptadeca-4,10-dienoate (3-133):

A Schlenk flask containing $CrCl_2$ (14 mg, 0.112 mmol, 1.0 equiv) and $NiCl_2$ (7 mg, 0.056 mmol, 0.5 equiv) was removed from the glovebox, and a solution of aldehyde **3-98** (25 mg, 0.112 mmol, 1.0 equiv) and iodide **3-123** (60 mg, 0.112 mmol, 1.0 equiv) in DMSO (1.1 mL) was added. The slurry was stirred at rt for 21 h and then diluted with H_2O. The slurry was extracted with Et_2O (2 X); the combined organic phase was washed with H_2O (3 X) and then brine, dried with $MgSO_4$, filtered, and concentrated *in vacuo*. The resulting residue was purified via flash chromatography (0 → 10% EtOAc in hex) to obtain alcohol **3-124** (11 mg, 16%) and diene **3-134**.

One diastereomer of the alcohol was characterized:

^{1}H NMR (500 MHz, $CDCl_3$) δ 7.67 (d, *J* = 6.7 Hz, 4H), 7.45 – 7.34 (m, 6H), 5.11 (d, *J* = 9.3 Hz, 1H), 4.91 (d, *J* = 9.3 Hz, 1H), 3.90 (t, *J* = 6.0 Hz, 1H), 3.66 – 3.60 (s, 5H), 2.61 (dd, *J* = 14.3, 7.2

Hz, 1H), 2.47 – 2.39 (m, 1H), 2.37 –2.28 (m, 2H), 2.02 (dd, *J* = 13.4, 7.7 Hz, 1H), 1.58 (s, 3H), 1.52 – 1.33 (m, 6H), 1.32 – 1.29 (m, 1H), 1.24 – 1.17 (m, 3H), 1.15 – 1.12 (m, 1H), 1.10 (d, *J* = 6.9 Hz, 3H), 1.05 (s, 9H), 0.90 (d, *J* = 6.6 Hz, 3H), 0.86 (d, *J* = 6.6 Hz, 3H), 0.83 (d, *J* = 6.5 Hz, 3H).

^{13}C NMR (126 MHz, $CDCl_3$) δ 135.7, 135.2, 134.3, 134.0, 133.8, 130.9, 129.6, 127.7, 78.2, 64.6, 51.5, 45.1, 44.3, 38.1, 33.7, 33.1, 32.9, 32.4, 30.4, 30.1, 29.6, 27.0, 21.3, 20.9, 20.1, 19.4, 16.7, 16.1, 11.5.

*missing carbonyl peak due to low concentration of sample

HRMS (ESI-TOF) *m/z* calculated for $C_{40}H_{62}O_4SiNa^+$ $(M+Na)^+$ 657.4315, found 657.4323.

Diene **3-134** was indistinguishable via NMR from the proto-demetalated alkene **3-S24** and was distinguished by HRMS.

HRMS (ESI-TOF) *m/z* calculated for $C_{54}H_{78}O_2Si_2Na^+$ $(M+Na)^+$ 838.5467, found 838.5559.

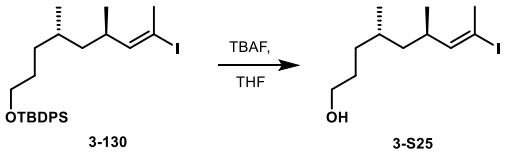

3-130 3-S25

(4*S*,6*R*,*E*)-8-iodo-4,6-dimethylnon-7-en-1-ol (3-S25):

To a solution of vinyl iodide **3-130** (500 mg, 0.935 mmol, 1.0 equiv) in THF (4.7 mL) was added TBAF (1.0 M in THF; 1.9 mL, 1.87 mmol, 2.0 equiv). The reaction was stirred for 1 h at rt and then quenched with saturated NH_4Cl solution. The solution was extracted with Et_2O (2 X) and the combined organic phase was washed with brine, dried with $MgSO_4$, filtered, and concentrated *in vacuo*. The resulting residue was purified via flash chromatography (0 → 35% EtOAc in hex) to obtain alcohol **3-S25** as a clear oil (204 mg, 74%).

Optical rotation: $[\alpha]^{22}_D$ = –47.7 (*c* = 1.0, $CHCl_3$).

^{1}H NMR (500 MHz, $CDCl_3$) δ 5.94 (d, *J* = 9.8 Hz, 1H), 3.62 (t, *J* = 6.2 Hz, 2H), 2.48 (ddd, *J* = 14.1, 9.4, 6.9 Hz, 1H), 2.38 (s, 3H), 1.65 – 1.55 (m, 1H), 1.55 – 1.46 (m, 1H), 1.43 (dd, *J* = 13.1, 6.8 Hz, 1H), 1.37 (ddd, *J* = 12.8, 10.9, 5.3 Hz, 1H), 1.21 (dd, *J* = 13.6, 6.8 Hz, 1H), 1.16 – 1.07 (m, 2H), 0.92 (d, *J* = 6.7 Hz, 3H), 0.87 (d, *J* = 6.6 Hz, 3H).

^{13}C NMR (126 MHz, $CDCl_3$) δ 147.9, 92.2, 63.5, 44.5, 33.4, 32.8, 30.4, 30.3, 27.8, 20.4, 20.0.

HRMS (ESI-TOF) *m/z* calculated for $C_{11}H_{21}OINa^+$ $(M+Na)^+$ 319.0535, found 319.0538.

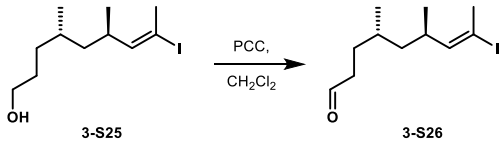

3-S25 3-S26

(4*S*,6*R*,*E*)-8-iodo-4,6-dimethylnon-7-enal (3-S26):

To a solution of alcohol **3-S25** (5.2 mg, 0.0176 mmol, 1.0 equiv) in CH_2Cl_2 (0.2 mL) was added PCC (7 mg, 0.0316 mmol, 1.8 equiv). The reaction was stirred at rt for 30 min, then it was filtered through a silica plug. The cake was washed with additional CH_2Cl_2 and the filtrate was concentrated *in vacuo* to yield aldehyde **3-S26** (4.8 mg, 92%).

Optical rotation: $[\alpha]^{22}_D$ = –47.7 (*c* = 1.0, $CHCl_3$).

^{1}H NMR (500 MHz, $CDCl_3$) δ 9.77 (t, *J* = 1.6 Hz, 1H), 5.94 (dd, *J* = 9.8, 1.3 Hz, 1H), 2.53 – 2.39 (m, 3H), 2.38 (d, J = 1.4 Hz, 3H), 1.72 – 1.63 (m, 1H), 1.46 (dd, *J* = 10.4, 4.1 Hz, 1H), 1.40 – 1.34 (m, 1H), 1.21 (dd, *J* = 13.6, 6.8 Hz, 1H), 1.18 – 1.11 (m, 1H), 0.93 (d, *J* = 6.6 Hz, 3H), 0.88 (d, *J* = 6.5 Hz, 3H).

^{13}C NMR (126 MHz, $CDCl_3$) δ 202.8, 147.6, 92.1, 44.2, 41.7, 33.3, 30.2, 28.7, 27.8, 20.3, 19.7.

HRMS (ESI-CI) *m/z* calculated for $C_{11}H_{19}OI^+$ $(M)^+$ 294.0481, found 294.0472.

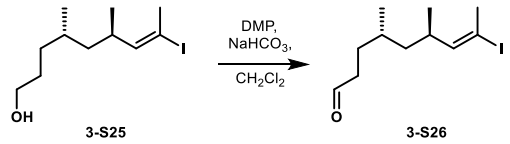

(4*S*,6*R,E*)-8-iodo-4,6-dimethylnon-7-enal (3-S26):

To a solution of alcohol **3-S25** (120 mg, 0.405 mmol, 1.0 equiv) in CH_2Cl_2 (2.0 mL) was added Martin's reagent (258 mg, 0.608 mmol, 1.5 equiv) and $NaHCO_3$ (102 mg, 1.22 mmol, 3.0 equiv). After stirring for 1 h at rt, saturated $Na_2S_2O_3$ solution was added and the slurry was vigorously stirred for an additional 1 h. The slurry was extracted with CH_2Cl_2 (3 X) and the combined organic phase was washed with brine, dried with Na_2SO_4, filtered, and concentrated *in vacuo* to obtain aldehyde **3-S26**. The resulting residue was subjected to the next step without further purification.

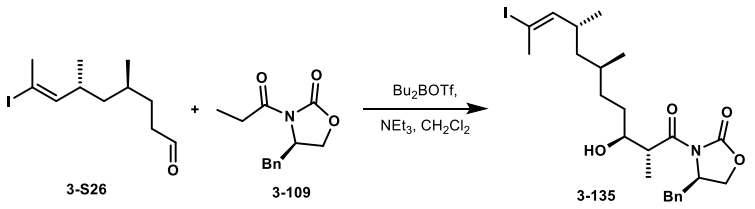

(*R*)-4-benzyl-3-((2*R*,3*S*,6*S*,8*R,E*)-3-hydroxy-10-iodo-2,6,8-trimethylundec-9-enoyl)oxazolidin-2-one (3-135):

To a solution of oxazolidinone **3-109** (84 mg, 0.359 mmol, 1.1 equiv) in CH_2Cl_2 (0.50 mL) at 0 °C was added freshly distilled Bu_2BOTf (0.13 mL, 0.424 mmol, 1.3 equiv) followed by NEt_3 (0.06 mL, 0.456 mmol, 1.4 equiv). The solution was cooled to –78 °C and aldehyde **3-S26** (96 mg, 0.326 mmol, 1.0 equiv) in CH_2Cl_2 (0.60 mL) was added. The reaction was stirred at –78 °C for 30 min and then warmed to 0 °C and stirred for 1.5 h. To quench the reaction, a solution of pH 7 phosphate buffer (1.0 mL) and MeOH (2.0 mL) was added followed by a solution of 30% aq. H_2O_2 (2.0 mL) and MeOH (1.0 mL). The slurry was vigorously stirred for 45 min and then extracted with Et_2O (3 X). The combined organic phase was washed with brine, dried with $MgSO_4$, filtered, and

concentrated *in vacuo*. The resulting residue was purified via flash chromatography (10% → 35% EtOAc in hex) to obtain **3-135** (84 mg, 49% over 2 steps).

Optical rotation: $[\alpha]^{22}_{D} = -46.8$ (*c* = 1.0, $CHCl_3$)

^{1}H NMR (500 MHz, $CDCl_3$) δ 7.33 (t, *J* = 7.4 Hz, 2H), 7.30 – 7.25 (m, 1H), 7.20 (d, *J* = 7.4 Hz, 2H), 5.93 (d, *J* = 9.8 Hz, 1H), 4.71 (dd, *J* = 13.9, 5.6 Hz, 1H), 4.27 – 4.16 (m, 2H), 3.93 – 3.87 (m, 1H), 3.75 (dd, *J* = 7.1, 2.0 Hz, 1H), 3.24 (dd, *J* = 13.4, 3.0 Hz, 1H), 2.79 (dd, *J* = 13.4, 9.4 Hz, 1H), 2.49 (dd, *J* = 9.3, 7.1 Hz, 1H), 2.38 (s, 3H), 1.70 (d, *J* = 7.1 Hz, 1H), 1.62 – 1.52 (m, 1H), 1.46 – 1.40 (m, 1H), 1.39 – 1.30 (m, 2H), 1.25 (d, *J* = 7.1 Hz,3), 1.23 – 1.18 (m, 1H), 1.12 (dd, *J* = 13.8, 7.0 Hz, 1H), 0.92 (d, *J* = 6.6 Hz, 3H), 0.87 (d, *J* = 6.6 Hz, 3H).

^{13}C NMR (126 MHz, $CDCl_3$) δ 177.7, 153.1, 147.8, 135.1, 129.5, 129.1, 127.6, 92.3, 71.8, 66.3, 55.2, 44.4, 42.2, 37.9, 33.4, 32.8, 31.2, 30.4, 27.8, 20.4, 20.0, 10.5.

HRMS (ESI-TOF) *m/z* calculated for $C_{24}H_{34}O_4NINa^+$ $(M+Na)^+$ 550.1430, found 550.1455.

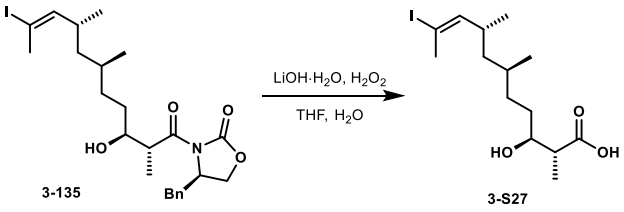

(*2R,3S,6S,8R,E*)-3-Hydroxy-10-iodo-2,6,8-trimethylundec-9-enoic acid (3-S27):

To a solution of alcohol **3-135** (mixture of diastereomers from aldol addition; 60 mg, 0.114 mmol, 1.0 equiv) in THF (0.8 mL) and H_2O (0.3 mL) was added $LiOH·H_2O$ (10 mg, 0.228 mmol, 2.0 equiv) followed by 30% aq. H_2O_2 (0.12 mL). The reaction was stirred overnight at rt and then acidified to pH 5 with 3 M HCl. The aqueous phase was extracted with Et_2O (2 X). The aqueous phase was further acidified to pH 1 with 3 M HCl and then extracted with EtOAc (3 X). The combined organic phase was washed with brine, dried with Na_2SO_4, filtered, and concentrated *in vacuo* to obtain carboxylic acid **3-S27**. The resulting residue was taken on to the next step without further purification.

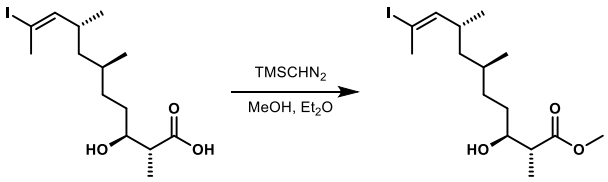

3-S27 3-S28

Methyl (*2R,3S,6S,8R,E*)-3-hydroxy-10-iodo-2,6,8-trimethylundec-9-enoate (3-S28):

To a solution of **3-S27** (42 mg, 0.114 mmol, 1.0 equiv) in Et_2O (0.8 mL) and MeOH (0.4 mL) at 0 °C was added $TMSCHN_2$ (2.0 M in hex.; 0.10 mL, 0.251 mmol, 2.0 equiv) dropwise. The reaction was stirred for 1 h at 0 °C and then slowly quenched with AcOH until the yellow color dissipated in the solution. The slurry was diluted with H_2O and then extracted with Et_2O (2 X). The combined organic phase was washed with brine, dried with $MgSO_4$, filtered, and concentrated *in vacuo.* The resulting residue was purified via flash chromatography (0 → 25% EtOAc in hex) to obtain **3-S28** as a mixture of diastereomers (15 mg, 34% over 2 steps). One diastereomer is reported:

^{1}H NMR (500 MHz, $CDCl_3$) δ 5.94 (d, *J* = 9.8 Hz, 1H), 3.89 – 3.81 (m, 1H), 3.71 (s, 3H), 2.58 – 2.51 (m, 1H), 2.50 – 2.44 (m, 1H), 2.38 (s, 3H), 1.56 –1.47 (m, 1H), 1.47 –1.35 (m, 3H), 1.30 – 1.23 (m, 1H), 1.22 –1.20 (m, 1H), 1.18 (d, *J* = 7.2 Hz, 3H), 1.16 – 1.08 (m, 1H), 0.91 (t, *J* = 5.1 Hz, 3H), 0.87 (d, *J* = 5.7 Hz, 3H).

HRMS (ESI-TOF) *m/z* calculated for $C_{15}H_{27}O_3INa^+$ $(M+Na)^+$ 405.0903, found 405.0903.

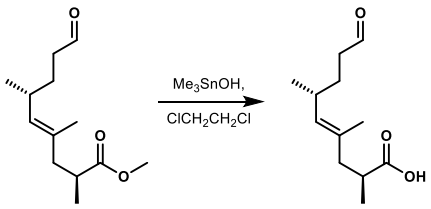

3-98 3-134

(*2S,6R,E*)-2,4,6-trimethyl-9-oxonon-4-enoic acid (3-134):

To a solution of ester **3-98** (270 mg, 1.19 mmol, 1.0 equiv) in dichloroethane (6.0 mL) was added trimethyltin hydroxide (2.0 g, 11.1 mmol, 9.3 equiv) and the slurry was heated to 85 °C for 18.5 h. The solution was cooled to rt, diluted with CH_2Cl_2 (10 mL), and washed with 3 M HCl solution (3

X 10 mL). The organic phase was dried with Na_2SO_4, filtered, and concentrated *in vacuo* to obtain carboxylic acid **3-134** (236 mg, 93%) which was taken on to the next step without further purification.

Optical rotation: $[\alpha]^{22}_D$ = –14.0 (c = 10.0, $CHCl_3$).

^{1}H NMR (500 MHz, $CDCl_3$): δ 9.73 (t, *J* = 1.6 Hz, 1H), 4.91 (d, *J* = 9.6 Hz, 1H), 2.64 – 2.60 (m, 1H), 2.40 – 2.32 (m, 4H), 2.06 (dd, *J* = 13.6, 7.6 Hz, 1H), 1.68 (ddd, *J* = 10.0, 7.7, 4.1 Hz, 1H), 1.59 (s, 3H), 1.48 (ddd, *J* = 11.2, 8.2, 6.1 Hz, 1H), 1.13 (d, *J* = 6.9 Hz, 3H), 0.93 (d, *J* = 6.7 Hz, 3H).

^{13}C NMR (126 MHz, $CDCl_3$): δ 203.0, 182.7 (br), 132.9, 132.1, 43.8, 42.3, 38.0, 32.2, 29.7, 21.3, 16.6, 16.2. Carboxylic acid carbon peak is very broad due to carboxylic acid dimer formation.

HRMS (ESI-TOF) *m/z* calculated for $C_{12}H_{19}O_3^-$ $(M+Na)^-$ 211.1334, found 211.1335.

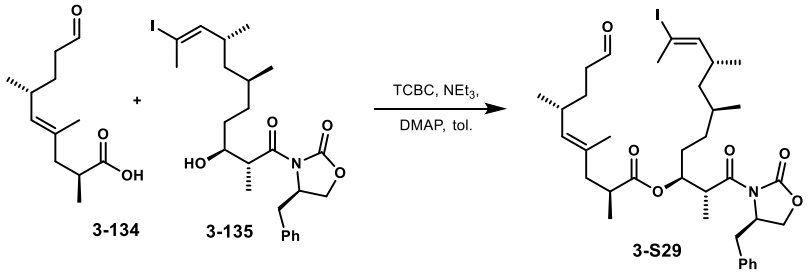

(*2R*,*3S*,*6S*,*8R*,*E*)-1-((*R*)-4-Benzyl-2-oxooxazolidin-3-yl)-10-iodo-2,6,8-trimethyl-1-oxoundec-9-en-3-yl (*2S*,*6R*,*E*)-2,4,6-trimethyl-9-oxonon-4-enoate (S29):

To a solution of carboxylic acid **3-134** (24 mg, 0.112 mmol, 1.2 equiv) in toluene (0.5 mL) was added 2,4,6-trichlorobenzoyl chloride (20 µL, 0.139 mmol, 1.5 equiv) followed by NEt_3 (20 µL, 0.139 mmol, 1.5 equiv). The solution was stirred for 30 min then alcohol **3-135** (49 mg, 0.0929 mmol, 1.0 equiv) in toluene (0.5 mL) was added followed by DMAP (34 mg, 0.279 mmol, 3.0 equiv). After stirring for 20 min at rt, the reaction was quenched with saturated NH_4Cl solution and then extracted with Et_2O (2 x 5 mL). The combined organic phase was washed with brine, dried

with $MgSO_4$, filtered, and concentrated *in vacuo*. The resulting residue was purified via flash chromatography (0 → 35% EtOAc in hex) to obtain ester **3-S29** as a clear oil (26 mg, 39%).

Optical rotation: $[\alpha]^{22}_D$ = –37.3 (c = 1.0, $CHCl_3$).

^{1}H NMR (500 MHz, CDCl3): δ 9.75 (s, 1H), 7.32 (t, *J* = 7.3 Hz, 2H), 7.29 – 7.26 (m, 1H), 7.19 (d, *J* = 7.3 Hz, 2H), 5.93 (d, *J* = 9.8 Hz, 1H), 5.18 (dt, *J* = 8.4, 4.3 Hz, 1H), 4.92 (d, *J* = 9.5 Hz, 1H), 4.57 – 4.49 (m, 1H), 4.28 (t, *J* = 8.3 Hz, 1H), 4.15 (dd, *J* = 8.9, 2.0 Hz, 1H), 4.00 – 3.92 (m, 1H), 3.26 (dd, *J* = 13.4, 2.9 Hz, 1H), 2.77 (dd, *J* = 13.4, 9.7 Hz, 1H), 2.61 – 2.53 (m, 1H), 2.52 – 2.41 (m, 2H), 2.41 – 2.32 (m, 6H), 1.98 (dd, *J* = 13.6, 9.3 Hz, 1H), 1.73 – 1.62 (m, 2H), 1.60 – 1.55 (m, 4H), 1.56 – 1.46 (m, 2H), 1.45 – 1.36 (m, 1H), 1.29 (ddd, *J* = 12.8, 9.9, 3.3 Hz, 1H), 1.22 – 1.15 (m, 4H), 1.12 – 1.06 (m, 4H), 0.95 (d, *J* = 6.6 Hz, 3H), 0.91 (d, *J* = 6.6 Hz, 3H), 0.86 (d, *J* = 6.6 Hz, 3H).

^{13}C NMR (126 MHz, $CDCl_3$) δ 202.8, 176.3, 174.1, 153.8, 147.8, 135.6, 132.9, 132.1, 129.6, 129.1, 127.4, 92.4, 73.4, 66.5, 56.0, 44.4, 43.8, 42.3, 41.5, 38.1, 38.0, 33.4, 32.7, 32.2, 30.4, 30.0, 29.8, 27.8, 21.3, 20.2, 19.8, 16.5, 16.0, 10.1.

HRMS (ESI-TOF) *m/z* calculated for $C_{36}H_{52}NO_6INa^+$ $[M+Na]^+$ 744.2737, found 744.2716.

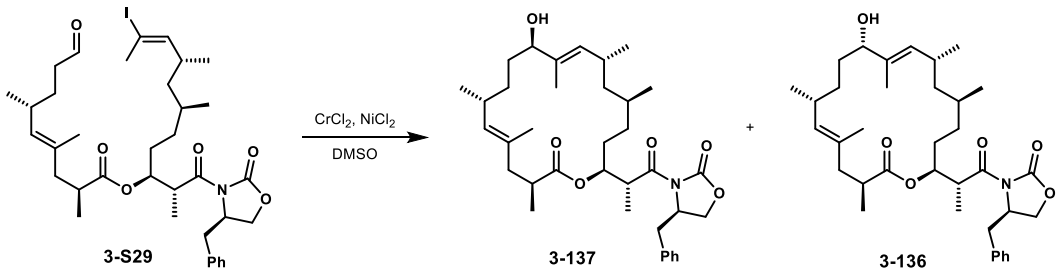

(*R*)-4-benzyl-3-((*R*)-2-((*2S*,*5S*,*7R*,*8E*,*10R*,*13R*,*14E*,*17S*)-10-hydroxy-5,7,9,13,15,17-hexamethyl-18-oxooxacyclooctadeca-8,14-dien-2-yl)propanoyl)oxazolidin-2-one (3-137) and (*R*)-4-benzyl-3-((*R*)-2-((*2S,5S,7R,8E,10S,13R,14E,17S*)-10-hydroxy-5,7,9,13,15,17-hexamethyl-18-oxooxacyclooctadeca-8,14-dien-2-yl)propanoyl)oxazolidin-2-one (3-136):

To a solution of aldehyde **3-S29** (32 mg, 0.0444 mmol, 1.0 equiv) in DMSO (4.4 mL), in a nitrogen filled glovebox, was added $CrCl_2$ (109 mg, 0.888 mmol, 20 equiv) followed by $NiCl_2$ (1 mg, 0.00772 mmol, 0.17 equiv). The solution was stirred overnight at rt in the glovebox, and removed the next morning. The black solution was diluted with H_2O (15 mL) and extracted with EtOAc (5 x 5 mL). The combined organic phase was washed with H_2O (5 X 5 mL) and brine, dried with Na_2SO_4, filtered, and concentrated *in vacuo.* The resulting residue was purified via flash chromatography (20% EtOAc in hex) to obtain the diastereomers as a mixture 1.1:1 dr of α:β face alcohol (19 mg, 73%). The diastereomers were separated via a second flash column (20% → 30% EtOAc in hex; 500 wt% of silica to mixture mass) to obtain β-face alcohol **3-137** (6 mg, 23%) as a white amorphous solid and α-face alcohol **3-136** (8 mg, 31%) white amorphous solid.

Alcohol 3-137:

Optical rotation: $[\alpha]^{22}_D$ = –12.4 (c = 0.59, $CHCl_3$).

R_f = 0.34 (7/3; hex/EtOAc)

^{1}H NMR (600 MHz, $CDCl_3$): δ 7.32 (t, *J* = 7.3 Hz, 2H), 7.29 – 7.26 (m, 1H), 7.20 (d, *J* = 7.0 Hz, 2H), 5.25 – 5.21 (m, 1H), 5.12 (d, *J* = 8.8 Hz, 1H), 4.71 (d, *J* = 8.8 Hz, 1H), 4.59 –4.54 (m, 1H), 4.26 (t, *J* = 8.3 Hz, 1H), 4.17 (dd, *J* = 9.0, 2.3 Hz, 1H), 4.03 – 3.98 (m, 1H), 3.86 – 3.82 (m, 1H),

3.26 (dd, *J* = 13.4, 3.2 Hz, 1H), 2.77 (dd, *J* = 13.4, 9.7 Hz, 1H), 2.64 (ddd, *J* = 11.6, 7.0, 3.1 Hz, 1H), 2.52 (dt, *J* = 14.8, 7.4 Hz, 1H), 2.27 (dd, *J* = 14.3, 11.8 Hz, 1H), 2.23 – 2.17 (m, 1H), 2.02 (dd, *J* = 14.5, 2.4 Hz, 1H), 1.68 – 1.62 (m, 1H), 1.60 – 1.58 (m, 6H), 1.43 – 1.35 (m, 2H), 1.35 – 1.29 (m, 2H), 1.27 – 1.25 (m, 2H), 1.27 – 1.22 (m, 5H), 1.21 (d, *J* = 6.9 Hz, 3H), 1.11 – 1.03 (m, 1H), 0.95 (d, *J* = 6.7 Hz, 3H), 0.90 – 0.85 (m, 5H), 0.83 (d, *J* = 6.7 Hz, 3H).

^{13}C NMR (151 MHz, $CDCl_3$) δ 174.8, 174.2, 153.6, 135.6, 135.5, 134.8, 133.2, 132.1, 129.6, 129.1, 127.5, 79.5, 73.3, 66.5, 55.9, 45.2, 43.8, 40.6, 38.0, 33.6, 32.7, 32.0, 30.5, 30.4, 29.9, 29.6, 29.4, 21.8, 21.6, 21.3, 18.7, 17.0, 11.4, 10.0.

HRMS (ESI-TOF) *m/z* calculated for $C_{36}H_{53}NO_6Na^+$ $[M+Na]^+$ 618.3771, found 618.3763.

Alcohol 3-136:

Optical rotation: $[\alpha]^{22}_D$ = –19.8 (c = 1.0, $CHCl_3$).

Rf = 0.40 (7/3; hex/EtOAc)

^{1}H NMR (600 MHz, $CDCl_3$) δ 7.32 (t, *J* = 7.3 Hz, 2H), 7.27 (d, *J* = 7.3 Hz, 1H), 7.20 (d, *J* = 7.1 Hz, 2H), 5.28 – 5.25 (m, 2H), 4.70 (d, *J* = 8.9 Hz, 1H), 4.61 – 4.56 (m, 1H), 4.26 (t, *J* = 8.3 Hz, 1H), 4.17 (dd, J = 9.0, 2.2 Hz, 1H), 4.13 – 4.11 (m, 1H), 4.04 – 3.99 (m, 1H), 3.26 (dd, *J* = 13.4, 3.1 Hz, 1H), 2.77 (dd, *J* = 13.4, 9.7 Hz, 1H), 2.65 (ddd, *J* = 11.7, 7.0, 3.1 Hz, 1H), 2.60 – 2.53 (m, 1H), 2.28 – 2.22 (m, 1H), 2.21 – 2.14 (m, 1H), 2.02 (dd, *J* = 13.9, 2.2 Hz, 1H), 1.77 – 1.65 (m, 2H), 1.59 (s, 3H), 1.54 (s, 3H), 1.48 – 1.40 (m, 2H), 1.36 – 1.30 (m, 3H), 1.29 – 1.26 (m, 2H), 1.24 (d, *J* = 6.9 Hz, 3H), 1.21 (d, *J* = 6.9 Hz, 3H), 1.11 – 1.04 (m, 2H), 0.95 (d, *J* = 6.7 Hz, 3H), 0.86 (d, *J* = 6.8 Hz, 3H), 0.84 (d, *J* = 6.7 Hz, 3H).

^{13}C NMR (151 MHz, $CDCl_3$) δ 174.7, 174.3, 153.6, 135.5, 135.4, 133.6, 132.1, 129.8, 129.6, 129.1, 127.5, 74.5, 73.4, 66.5, 55.9, 45.5, 44.3, 40.8, 40.7, 38.0, 32.4, 30.5, 30.3, 30.3, 29.7, 29.5, 29.3, 22.0, 22.0, 21.3, 18.7, 16.8, 15.1, 11.8.

HRMS (ESI-TOF) *m/z* calculated for $C_{36}H_{53}NO_6Na^+$ $[M+Na]^+$ 618.3771, found 618.3780.

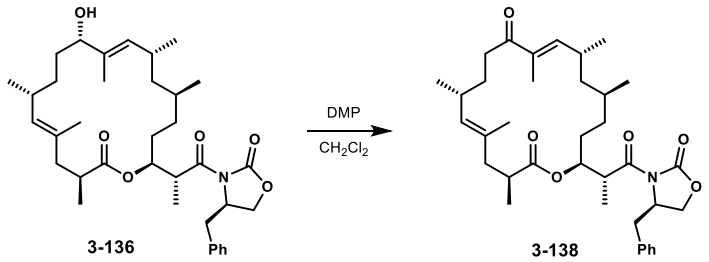

(*3S,5E,7R,11E,13R,15S,18S*)-18-((*R*)-1-((*R*)-4-benzyl-2-oxooxazolidin-3-yl)-1-oxopropan-2-yl)-3,5,7,11,13,15-hexamethyloxacyclooctadeca-5,11-diene-2,10-dione (3-136):

To a solution of alcohol **3-136** (4.9 mg, 0.008224 mmol, 1.0 equiv) in CH_2Cl_2 (0.10 mL) at rt was added Martin's reagent (5 mg, 0.0126, 1.5 equiv) and the solution was stirred for 1.5 h at rt. The slurry was concentrated *in vacuo* and to the resulting residue was added Et_2O (3 mL). The solution was stirred for 5 min and then filtered and concentrated *in vacuo* to obtain enone **3-138**. The resulting residue was taken on to the next step without further purification.

HRMS (ESI-TOF) *m/z* calculated for for $C_{36}H_{51}NO_6Na^+$ $[M+Na]^+$ 616.3614, found 616.3602.

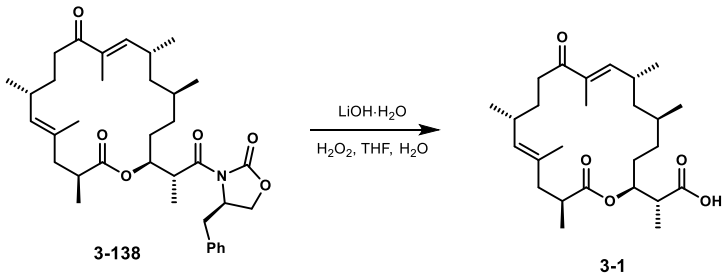

Strasseriolide A (3-1):

To a solution of ketone **3-138** (4.9 mg, 0.008224 mmol, 1.0 equiv) in THF (0.1 mL) and H_2O (0.5 mL) was added $LiOH{\cdot}H_2O$ (2.0 mg) followed by 30% aq. H_2O_2 solution (10 µL). The solution was stirred for 40 min and then quenched with 3 M HCl. The solution was extracted with EtOAc (3 x 3 mL). The combined organic phase was washed with brine, dried with Na_2SO_4, filtered, and concentrated *in vacuo*. The resulting residue was purified via prep TLC (50/50/1

EtOAc/hex/AcOH) to obtain strasseriolide A (2.3 mg, 64% over 2 steps) as a white amorphous solid.

Optical rotation: $[\alpha]^{22}_{D}$ = +6.3 (c = 1.0, CH_3OH). Literature reported:[7] $[\alpha]^{25}_{D}$ = +8.0 (c = 0.45, CH_3OH).

^{1}H NMR (600 MHz, CD_3OD) δ 6.60 (d, *J* = 9.2 Hz, 1H), 5.14 – 5.09 (m, 1H), 4.79 (d, *J* = 9.3 Hz, 1H), 2.99 (ddd, *J* = 15.5, 7.7, 4.5 Hz, 1H), 2.86 – 2.77 (m, 1H), 2.72 – 2.66 (m, 1H), 2.58 (ddd, *J* = 10.5, 7.1, 3.2 Hz, 1H), 2.43 – 2.34 (m, 2H), 2.20 (dd, *J* = 14.2, 11.6 Hz, 1H), 2.00 (dd, *J* = 14.4, 2.7 Hz, 1H), 1.87 – 1.79 (m, 2H), 1.75 (s, 3H), 1.71 – 1.66 (m, 1H), 1.61 – 1.55 (m, 3H), 1.53 (s, 3H), 1.51 – 1.40 (m, 3H), 1.18 (d, *J* = 6.9 Hz, 3H), 1.13 – 1.07 (m, 4H), 1.03 (d, *J* = 6.8 Hz, 3H), 0.94 (d, *J* = 6.6 Hz, 3H), 0.90 (d, *J* = 6.8 Hz, 3H).

^{13}C NMR (151 MHz, CD_3OD) δ 205.5, 177.5 176.9, 150.8, 137.1, 134.2, 133.0, 75.5, 45.9, 44.6, 43.1, 42.7, 36.9, 34.9, 33.1, 31.9, 31.7, 30.7, 30.3, 22.2, 21.3, 20.9, 19.2, 17.8, 13.8, 11.8.

^{13}C NMR contains ~10 equiv of acetic acid-D4 to resolve carboxylic acid peak

HRMS (ESI-TOF) *m/z* calculated for $C_{26}H_{42}O_5Na^+$ $[M+Na]^+$ 457.2930, found 457.2919.

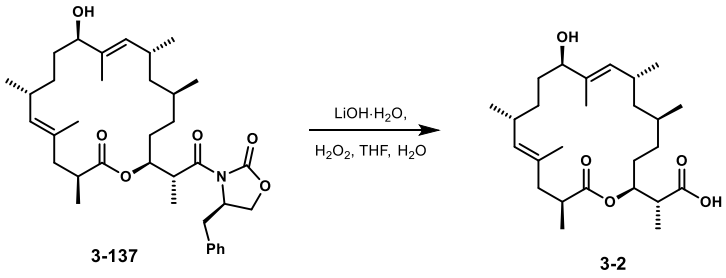

3-137 3-2

Strasseriolide B (3-2):

To a solution of alcohol **3-137** (2.6 mg, 0.00436 mmol, 1.0 equiv) in THF (0.10 mL) and H_2O (0.05 mL) was added $LiOH·H_2O$ (1.0 mg, 0.0175 mmol, 4.0 equiv) followed by 30% aq. H_2O_2 solution (10 µL). The solution was stirred for 1 h and then quenched with 3 M HCl. The solution was extracted with EtOAc (3 x 3 mL). The combined organic phase was washed with brine, dried with Na_2SO_4, filtered, and concentrated *in vacuo*. The resulting residue was combined with 1.0 mg of

crude material from a previous reaction and was purified via prep TLC (50/50/1 EtOAc/hex/AcOH) to obtain strasseriolide B (1.3 mg, 45%) as a white amorphous solid.

Optical rotation: $[\alpha]^{22}_{D}$ = +20.0 (c = 0.25, CH_3OH). Literature reported: $[\alpha]^{25}_{D}$ = +32.6 (c = 0.25, CH_3OH)

^{1}H NMR (600 MHz, CD3OD) δ 5.17 – 5.13 (m, 1H), 5.06 (d, J = 9.1 Hz, 1H), 4.73 (d, J = 8.8 Hz, 1H), 3.77 (dd, J = 10.2, 4.7 Hz, 1H), 2.75 – 2.69 (m, 1H), 2.65 – 2.55 (m, 2H), 2.28 – 2.20 (m, 2H), 2.09 (dd, J = 13.7, 2.8 Hz, 1H), 1.79 – 1.73 (m, 1H), 1.62 (d, J = 0.9 Hz, 3H), 1.59 (d, J = 1.2 Hz, 3H), 1.54 – 1.48 (m, 3H), 1.44 – 1.40 (m, 1H), 1.33 – 1.30 (m, 3H), 1.20 (d, J = 6.9 Hz, 4H), 1.13 (d, J = 6.9 Hz, 4H), 1.08 – 1.05 (m, 1H), 0.97 (d, J = 6.7 Hz, 3H), 0.92 – 0.90 (m, 1H), 0.89 (d, J = 6.7 Hz, 3H), 0.85 (d, J = 6.7 Hz, 3H).

^{13}C NMR (151 MHz, CD_3OD) δ 177.6, 176.6, 136.9, 135.9, 134.9, 133.7, 80.4, 75.5, 48.2, 45.2, 42.9, 42.5, 35.0, 34.1, 33.3, 31.8, 30.8, 30.7, 30.4, 22.4, 22.3, 21.8, 18.9, 17.2, 14.1, 10.6.

HRMS (ESI-TOF) *m/z* calculated for $C_{26}H_{42}O_5Na^+$ $[M+Na]^+$ 459.3087, found 459.3078.

References

[1] World malaria report 2021. Geneva: World Health Organization, 2021. https://www.who.int/teams/global-malaria-programme/reports/world-malaria-report-2021

[2] Balikagala, B.; Fukuda, N.; Ikeda, M.; Katuro, O. T.; Tachibana, S.; Yamauchi, M.; Opio, W.; Emoto, S.; Anywar, D. A.; Kimura, E.; Palacpac, N. M. Q.; Odongo-Aginya, E. I.; Ogwang, M.; Horii, T.; Toshihiro Mita, T. Evidence of Artemisinin-Resistant Malaria in Africa. *N. Engl. J. Med.* **2021**, *385*, 1163–1171.

[3] White, N. J. Antimalarial drug resistance. *J. Clin. Invest*. **2004**, *113,* 1084–1092.

[4] Plowe C.V. Antimalarial Drug Resistance in Africa: Strategies for Monitoring and Deterrence. In*: Malaria: Drugs, Disease and Post-genomic Biology*. Sullivan, D.J., Krishna, S., Eds. Springer: Berlin, Heidelberg. **2005**, 55–79.

[5] Hyde, J. E. Drug-resistant malaria. *Trends Parasitol.* **2005**, *21*, 494–498.

[6] Pérez-Moreno, G.; Cantizani, J.; Sánchez-Carrasco, P.; Ruiz-Pérez, L. M.; Martín, J.; Aouad, N. el; Pérez-Victoria, I.; Tormo, J. R.; González-Menendez, V.; González, I.; Pedro, N. de; Reyes, F.; Genilloud, O.; Vicente, F.; González-Pacanowska, D. Discovery of New Compounds Active against Plasmodium Falciparum by High Throughput Screening of Microbial Natural Products. *PLOS One* **2016**, *11*, e0145812.

[7] Annang, F.; Pérez-Moreno, G.; González-Menéndez, V.; Lacret, R.; Pérez-Victoria, I.; Martín, J.; Cantizani, J.; Pedro, N. de; Choquesil-lo-Lazarte, D.; Ruiz-Pérez, L. M.; González-Pacanowska, D.; Ge-nilloud, O.; Vicente, F.; Reyes, F. Strasseriolides A–D, A Family of Antiplasmodial Macrolides Isolated from the Fungus Strasseria Geniculata CF-247251. *Org. Lett*. **2020**, *22*, 6709–6713.

[8] Baniecki, M. L.; Wirth, D. F.; Clardy, J. High-throughput Plasmodium falciparum growth assay for malaria drug discovery. *Antimicrob. Agents Chemother*. **2007**, *51*, 716–723.

[9] Marsault, E.; Peterson, M. L. Macrocycles Are Great Cycles: Applications, Opportunities, and Challenges of Synthetic Macrocycles in Drug Discovery. *J. Med. Chem*. **2011**, *54*, 1961–2004.

[10] Driggers, E.; Hale, S.; Lee, J.; Terrett, N. K. The exploration of macrocycles for drug discovery — an underexploited structural class. *Nat. Rev. Drug Discov*. **2008**, *7*, 608–624.

[11] Lipinski, C. A.; Lombardo, F.; Dominy, B. W.; Feeney, P. J. Experimental and computational approaches to estimate solubility and permeability in drug discovery and development settings. *Adv. Drug Deliv. Rev*. **2001**, *46*, 3–26.

For excellent reviews of macrocyclization strategies, refer to 12–21

[12] Yu, X.; Sun, D. Macrocyclic Drugs and Synthetic Methodologies toward Macrocycles. *Molecules* **2013**, *18*, 6230–6268.

[13] Martí-Centelles, V.; Pandey, M. D.; Burguete, M. I.; Luis, S. V. Macrocyclization Reactions: The Importance of Conformational, Configurational, and Template-Induced Preorganization. *Chem. Rev.* **2015**, *115*, 8736–8834.

[14] Gil, A.; Albericio, F.; Álvarez, M. Role of the Nozaki−Hiyama−Takai−Kishi Reaction in the Synthesis of Natural Products. *Chem. Rev*. **2017**, *117*, 8420–8446.

[15] Lecourt, C.; Dhambri, S.; Allievi, L.; Sanogo, Y.; Zeghbib, N.; Othman, R. B.; Lannou, M. I.; Sorin, G.; Ardisson, J. Natural products and ring-closing metathesis: synthesis of sterically congested olefins. *Nat. Prod. Rep*. **2018**, *35*, 105–124.

[16] Donald, J. R.; Unsworth, W. P. Ring-Expansion Reactions in the Synthesis of Macrocycles and Medium-Sized Rings. *Chem. Eur. J.* **2017**, *23*, 8780–8799.

[17] Zheng, K.; Hong, R. Stereoconfining macrocyclizations in the total synthesis of natural products. *Nat. Prod. Rep*. **2019**, *36*, 1546–1575.

[18] Agouridas, V.; Mahdi, O. E.; Diemer, V.; Cargoet, M.; Monbaliu, J. M.; Melnyk, O. Native Chemical Ligation and Extended Methods: Mechanisms, Catalysis, Scope, and Limitations. *Chem. Rev*. **2019**, *119*, 7328–7443.

[19] Fürstner, A. Lessons from Natural Product Total Synthesis: Macrocyclization and Postcyclization Strategies. *Acc. Chem. Res*. **2021**, *54*, 861–874.

[20] Parenty, A.; Moreau, X.; Niel, G.; Campagne, J. M. Update 1 of: Macrolactonizations in the Total Synthesis of Natural Products. *Chem. Rev*. **2013**, *113*, PR1–PR40.

[21] Li, Y.; Yin, X.; Dai, M. Catalytic macrolactonizations for natural product synthesis. *Nat. Prod. Rep.* **2017**, *34*, 1185–1192.

[22] Fürstner, A. The Ascent of Alkyne Metathesis to Strategy-Level Status. *J. Am. Chem. Soc*. **2021**, *143*, 15538–15555.

[23] Wengrovius, J. H.; Sancho, J.; Schrock, R. R. Metathesis of Acetylenes by Tungsten(VI)-Alkylidyne Complexes. *J. Am. Chem. Soc*. **1981**, *103*, 3934–3935.

[24] Fürstner, A.; Mathes, C.; Lehmann, C. W. Mo[N(*t*-Bu)(Ar)]$_3$ Complexes As Catalyst Precursors: In Situ Activation and Application to Metathesis Reactions of Alkynes and Diynes. *J. Am. Chem. Soc*. **1999**, *121*, 9453–9454.

[25] Bindl, M.; Stade, R.; Heilmann, E. K.; Picot, A.; Goddard, R.; Fürstner, A. Molybdenum Nitride Complexes with Ph_3SiO Ligands Are Exceedingly Practical and Tolerant Precatalysts for Alkyne Metathesis and Efficient Nitrogen Transfer Agents. *J. Am. Chem. Soc*. **2009**, *131*, 9468–9470.

[26] Heppekausen, J.; Stade, R.; Goddard, R.; Fürstner, A. Practical New Silyloxy-Based Alkyne Metathesis Catalysts with Optimized Activity and Selectivity Profiles. *J. Am. Chem. Soc*. **2010**, *132*, 11045–11057.

[27] Heppekausen, J.; Stade, R.; Kondoh, A.; Seidel, G.; Goddard, R.; Fürstner, A. Optimized Synthesis, Structural Investigations, Ligand Tuning and Synthetic Evaluation of Silyloxy-Based Alkyne Metathesis Catalysts. *Chem. Eur. J*. **2012**, *18*, 10281–10299.

[28] Hillenbrand, J.; Leutzsch, M.; Yiannakas, E.; Gordon, C. P.; Wille, C.; Nöthling, N.; Copéret, C.; Fürstner, A. "Canopy Catalysts" for Alkyne Metathesis: Molybdenum Alkylidyne Complexes with a Tripodal Ligand Framework. *J. Am. Chem. Soc*. **2020**, *142*, 11279–11294.

[29] Rummelt, S. M.; Radkowski, K.; Rosca, D.-A.; Fürstner, A. Interligand Interactions Dictate the Regioselectivity of *trans*-Hydrometalations and Related Reactions Catalyzed by [Cp*RuCl]. Hydrogen Bonding to a Chloride Ligand as Steering Principle in Catalysis. *J. Am. Chem. Soc*. **2015**, *137*, 5506–5519.

[30] Rosca, D.-A.; Radkowski, K.; Wolf, L. M.; Wagh, M.; Goddard, R.; Thiel, W.; Fürstner, A. Ruthenium-catalyzed Alkyne *trans*-Hydrometalation: Mechanistic Insights and Preparative Implications. *J. Am. Chem. Soc*. **2017**, *139*, 2443–2455.

[31] Huwyler, N.; Radkowski, K.; Rummelt, S. M.; Fürstner, A. Two Enabling Strategies for the Stereoselective Conversion of Internal Alkynes into Trisubstituted Alkenes. *Chem. Eur. J*. **2017**, *23*, 12412–12419.

[32] Jin, H.; Fürstner, A. Regioselective *Trans*-Carboboration of Propargyl Alcohols. *Org. Lett*. **2019**, *21*, 3446–3450.

[33] Leutzsch, M.; Wolf, L. M.; Gupta, P.; Fuchs, M.; Thiel, W.; Farès, C.; Fürstner, A. Formation of Ruthenium Carbenes by Gem-Hydrogen Transfer to Internal Alkynes: Implications for Alkyne *Trans*-Hydrogenation. *Angew. Chem. Int. Ed*. **2015**, *54*, 12431–12436.

[34] Longobardi, L. E.; Fürstner, A. *trans*-Hydroboration of Propargyl Alcohol Derivatives and Related Substrates. *Chem. Eur. J.* **2019***, 25,* 10063–10068.

[35] Sommer, H.; Hamilton, J. Y.; Fürstner, A. A Method for the Late-Stage Formation of Ketones, Acyloins, and Aldols from Alkenylstannanes: Application to the Total Synthesis of Paecilonic Acid A. *Angew. Chem. Int. Ed.* **2017**, *56*, 6161–6165.

[36] Rummelt, S. M.; Fürstner, A. Ruthenium-Catalyzed *Trans*-Selective Hydrostannation of Alkynes. *Angew. Chem. Int. Ed*. **2014**, *53*, 3626–3630.

[37] Yu, M.; Lou, S.; Gonzalez-Bobes, F. Ring-Closing Metathesis in Pharmaceutical Development: Fundamentals, Applications, and Future Directions. *Org. Process Res. Dev*. **2018**, *22*, 918–946.

[38] Fürstner, A. Teaching Metathesis "Simple" Stereochemistry. *Science* **2013**, *341*, 1229713.

[39] Fischmeister, C.; Bruneau, C. Ene-yne cross-metathesis with ruthenium carbene catalysts. *Beilstein J. Org. Chem*. **2011**, *7*, 156–166.

[40] Benson, S.; Collin, M.; Arlt, A.; Gabor, B.; Goddard, R.; Fürstner, A. Second-Generation Total Synthesis of Spirastrellolide F Methyl Ester: The Alkyne Route. *Angew. Chem. Int. Ed*. **2011**, *50*, 8739–8744.

[41] O'Neil, G. W.; Ceccon, J.; Benson, S.; Collin, M.; Fasching, B.; Fürstner, A. Total Synthesis of Spirastrellolide F Methyl Ester—Part 1: Strategic Considerations and Revised Approach to the Southern Hemisphere**.** *Angew. Chem. Int. Ed*. **2009,** *48*, 9940–9945.

[42] Benson, S.; Collin, M.; O'Neil, G. W.; Ceccon, J.; Bernhard, F.; Fenster, M. D. B.; Godbout, C.; Radkowski, K.; Goddard, R.; Fürstner, A. Total Synthesis of Spirastrellolide F Methyl Ester—Part 2: Macrocyclization and Completion of the Synthesis. *Angew. Chem. Int. Ed*. **2009**, *48*, 9946–9950.

[43] Ahlers, A.; de Haro, T.; Gabor, B.; Fürstner, A. Concise Total Synthesis of Enigmazole A. *Angew. Chem. Int. Ed*. **2016**, *55*, 1406–1411.

[44] Ai, Y.; Zozytska, M. V.; Zou, Y.; Khartulyari, A. S.; Smith, A. B. Total Synthesis of (−)-Enigmazole A. *J. Am. Chem. Soc*. **2015**, *137*, 15426–15429.

[45] Skepper, C. K.; Quach, T.; Molinski, T. F. Total Synthesis of Enigmazole A from *Cinachyrella enigmatica*. Bidirectional Bond Constructions with an Ambident 2,4-Disubstituted Oxazole Synthon. *J. Am. Chem. Soc*. **2010**, *132*, 10286–10292.

[46] Keisuke, K.; Sasaki, M.; Fuwa, H. Total Synthesis of (−)-Enigmazole A. *Angew. Chem. Int. Ed*. **2018**, *57*, 5143–5146.

[47] Gebauer, K.; Fürstner, A. Total Synthesis of Biphenyl Alkaloid (–)-Lyranidine. *Angew. Chem. Int. Ed*. **2014**, *53*, 6393–6396.

[48] Trost, B. M.; Livingston, R. C. Two-Metal Catalyst System for Redox Isomerization of Propargyl Alcohols to Enals and Enones. *J. Am. Chem. Soc*. **1995**, *117*, 9586–9587.

[49] Valot, G.; Regens, C. S.; O'Malley, D. P.; Godineau, E.; Takikawa, H.; Fürstner, A. Total Synthesis of Amphidinolide F. *Angew. Chem. Int. Ed*. **2013**, *52*, 9534–9538.

[50] Liu, B.; De Brabander, J. K. Metal-Catalyzed Regioselective Oxy-Functionalization of Internal Alkynes: An Entry into Ketones, Acetals, and Spiroketals. *Org. Lett*. **2006**, *8*, 4907–4910.

[51] Rummelt, S. M.; Radkowski, K.; Roşca, D.; Fürstner, A. Interligand Interactions Dictate the Regioselectivity of *trans*-Hydrometalations and Related Reactions Catalyzed by [Cp*RuCl]. Hydrogen Bonding to a Chloride Ligand as a Steering Principle in Catalysis. *J. Am. Chem. Soc*. **2015**, *137*, 5506–5519.

[52] Roşca, D.; Radkowski, K.; Wolf, L. M.; Wagh, M.; Goddard, R.; Thiel, W.; Fürstner, A. Ruthenium-Catalyzed Alkyne *trans*-Hydrometalation: Mechanistic Insights and Preparative Implications. *J. Am. Chem. Soc*. **2017**, *139*, 2443–2455.

[53] Fürstner, A. *trans*-Hydrogenation, *gem*-Hydrogenation, and *trans*-Hydrometalation of Alkynes: An Interim Report on an Unorthodox Reactivity Paradigm. *J. Am. Chem. Soc*. **2019**, *141*, 11–24.

[54] Kwon, Y.; Schulthoff, S.; Dao, Q. M. Wirtz, C.; Fürstner, A. Total Synthesis of Disciformycin A and B: Unusually Exigent Targets of Biological Significance. *Chem. Eur. J*. **2018**, *24*, 109–114.

[55] Frihed, T. G.; Fürstner, A. Progress in the *trans*-Reduction and *trans*-Hydrometalation of Internal Alkynes. Applications to Natural Product Synthesis. *Bull. Chem. Soc. Jpn*. **2016**, *89*, 135–160.

[56] Meng, Z.; Fürstner, A. Total Synthesis of (−)-Sinulariadiolide. A Transannular Approach. *J. Am. Chem. Soc*. **2019**, *141*, 805–809.

[57] Persich, P.; Llaveria, J.; Lhermet, R.; de Haro, T.; Stade, R.; Kondoh, A.; Fürstner, A. Increasing the Structural Span of Alkyne Metathesis. *Chem. Eur. J*. **2013**, *19*, 13047–13058.

[58] Schaubach, S.; Gerbauer, K.; Ungeheuer, F.; Hoffmeister, L.; Ilg, M. K.; Wirtz, C.; Fürstner, A. A Two-Component Alkyne Metathesis Catalyst System with an Improved Substrate Scope and Functional Group Tolerance: Development and Applications to Natural Product Synthesis. *Chem. Eur. J*. **2016**, *22*, 8494–8507.

[59] Loffler, L. E.; Wirtz, C.; Fürstner, A. Collective Total Synthesis of Casbane Diterpenes: One Strategy, Multiple Targets. *Angew. Chem. Int. Ed*. **2021**, *60*, 5316–5322.

[60] Montgomery, J. Nickel-Catalyzed Reductive Cyclizations and Couplings. *Angew. Chem. Int. Ed*. **2004**, *43*, 3890–3908.

[61] Montgomery J.; Sormunen G. J. Nickel-Catalyzed Reductive Couplings of Aldehydes and Alkynes. In: *Metal Catalyzed Reductive C–C Bond Formation*. *Topics in Current Chemistry*, Vol. 279. Krische M. J., Ed. Springer: Berlin, Heidelberg. **2007** 1–23.

[62] Malik, H. A.; Baxter, R. D.; Montgomery, J. Nickell-Catalyzed Reductive Couplings and Cyclizations. In: *Cataysis without Precious Metals*. Bullock, R. M., Ed. Wiley-VCH: Weinheim, Germany. **2010**, 181– 210.

[63] Standley, E. A.; Tasker, S. Z.; Jensen, K. L.; Jamison, T. F. Nickel Catalysis: Synergy between Method Development and Total Synthesis. *Acc. Chem. Res*. **2015**, *48*, 1503–1514.

[64] Shareef, A.; Sherman, D. H.; Montgomery, J. Nickel-catalyzed regiodivergent approach to macrolide motifs. *Chem. Sci*. **2012**, *3*, 892–895.

[65] Knapp-Reed, B.; Mahandru, G. M.; Montgomery, J. Access to Macrocyclic Endocyclic and Exocyclic Allylic Alcohols by Nickel-Catalyzed Reductive Cyclization of Ynals. *J. Am. Chem. Soc*. **2005**, *127*, 13159–13157.

[66] Liu, P.; Montgomery, J.; Houk, K. N. Ligand Steric Contours To Understand the Effects of N-Heterocyclic Carbene Ligands on the Reversal of Regioselectivity in Ni-Catalyzed Reductive Couplings of Alkynes and Aldehydes. *J. Am. Chem. Soc*. **2011**, *133*, 6956–6959.

[67] Colby, E. A.; O'Brien, K. C.; Jamison, T. F. Total Syntheses of Amphidinolides T1 and T4 via Catalytic, Stereoselective, Reductive Macrocyclizations. *J. Am. Chem. Soc*. **2005**, *127*, 4297–4307.

[68] Molinaro, C.; Jamison, T. F. Nickel-Catalyzed Reductive Coupling of Alkynes and Epoxides. *J. Am. Chem. Soc*. **2003**, *125*, 8076–8077.

[69] Kitahata, S.; Katsuyama, A.; Ichikawa, S. A Synthesis Strategy for the Production of a Macrolactone of Gulmirecin A via a Ni(0)-Mediated Reductive Cyclization Reaction. *Org. Lett*. **2020**, *22*, 2697–2701.

[70] Chan, J.; Jamison, T. F. Enantioselective Synthesis of (–)-Terpestacin and Structural Revision of Siccanol Using Catalytic Stereoselective Fragment Couplings and Macrocyclizations. *J. Am. Chem. Soc*. **2004**, *126*, 10682–10691.

[71] Mahandru, G. M.; Lui, G.; Montgomery, J. Ligand-Dependent Scope and Divergent Mechanistic Behavior in Nickel-Catalyzed Reductive Couplings of Aldehydes and Alkynes. *J. Am. Chem. Soc*. **2004**, *126,* 3698–3699.

[72] Takai, K.; Kimura, K.; Kuroda, T.; Hiyama, T.; Nozaki, H. Selective grignard-type carbonyl addition of alkenyl halides mediated by chromium(II) chloride. *Tetrahedron Lett*. **1983**, *24*, 5281–5284.

[73] Tian, Q.; Zhang, G. Recent Advances in the Asymmetric Nozaki–Hiyama–Kishi Reaction. *Synthesis* **2016**, *48*, 4038–4049.

[74] Hargaden, G. C.; Guiry, P. J. The Development of the Asymmetric Nozaki–Hiyama–Kishi Reaction. *Adv. Synth. Catal*. **2007**, *349*, 2407–2424.

[75] Fürstner, A.; Shi, N. Nozaki–Hiyama–Kishi Reactions Catalytic in Chromium. *J. Am. Chem. Soc*. **1996**, *118*, 12349–12357.

[76] Namba, K.; Kishi, Y. New Catalytic Cycle for Couplings of Aldehydes with Organochromium Reagents. *Org. Lett*. **2004**, *6*, 5031–5033.

[77] Kobayashi, K.; Fujii, Y.; Hirayama, Y.; Kobayashi, S.; Hayakawa, I.; Kigoshi, H. Design, Synthesis, and Biological Evaluations of Aplyronine A–Mycalolide B Hybrid Compound. *Org. Lett*. **2012**, *14*, 1290–1293.

[78] Ojika, M.; Kigoshi, H.; Yoshida, Y.; Ishigaki, T.; Nisiwaki, M.; Tsukada, I.; Arakawa, M.; Ekimoto, H.; Yamada, K. Aplyronine A, a potent antitumor macrolide of marine origin, and the congeners aplyronines B and C: isolation, structures, and bioactivities. *Tetrahedron* **2007**, *63*, 3138–3167.

[79] Fusetani, N.; Yasumuro, K.; Matsunaga, S.; Hashimoto, K. Mycalolides A – C, hybrid macrolides of ulapualides and halichondramide, from a sponge of the genus Mycale. *Tetrahedron Lett*. **1989**, *30*, 2809–2812.

[80] Kigoshi, H.; Ojika, M.; Ishigaki, T.; Suenaga, K.; Mutou, T.; Sakakura, A.; Ogawa, T.; Yamada, K. Total Synthesis of Aplyronin A, a Potent Antitumor Substance of Marine Origin. *J. Am. Chem. Soc*. **1994**, *116*, 7443–7444.

[81] Pospíšil, J.; Müller, C.; Fürstner, A. Total Synthesis of the Aspercyclides. *Chem. Eur. J*. **2009**, *15*, 5956–5968.

[82] Lewis, M. D.; Kishi, Y. Further studies on chromium(II)-mediated homoallylic alcohol syntheses. *Tetrahedron Lett*. **1982**, *23*, 2343–2346.

[83] Chase, C. E.; Fang, F. G.; Lewis, B. M.; Wilkiw, G. D.; Schanderbeck, M.J.; Zhu, X. Process Development of Halaven®: Synthesis of the C1–C13 Fragment from d-(–)-Gulono-1,4-lactone. *Synlett*. **2013**, *24*, 323–326.

[84] Brian C. Austad, B. C.; Benayoud, F.; Calkins, T. L.; Campagna, S.; Chase, C. E.; Choi, H.; Christ, W.; Costanzo, R.; Cutter, J.; Endo, A.; Fang, F. G.; Hu, Y.; Lewis, B. M.; Lewis, M. D.; McKenna, S.; Noland, T. A.; Orr, J. D.; Pesant, M.; Schnaderbeck, M. J.; Wilkie, G. D.; Abe, T.; Asai, N.; Asai, Y.; Kayano, A.; Kimoto, Y.; Komatsu, Y.; Kubota, M.; Kuroda, H.; Mizuno, M.; Nakamura, T.; Omae, T.; Ozeki, N.; Suzuki, T.; Takigawa, T.; Watanabe, T.; Yoshizawab, K. cluster Process Development of Halaven®: Synthesis of the C14–C35 Fragment via Iterative Nozaki–Hiyama–Kishi Reaction–Williamson Ether Cyclization. *Synlett* **2013**, *24*, 327–332.

[85] Austad, B. C.; Calkins, T. L.; Chase, C. E.; Fang, F. G.; Horstmann, T. E.; Hu, Y.; Lewis, B. M.; X.; Noland, T. A.; Orr, J. D.; Schnaderbeck, M. J.; Zhang, H.; Asakawa, N.; Asai, N.; Chiba, H.; Hasebe, T.; Hoshino, Y.; Ishizuka, H.; Kajima, T.; Kayano, A.; Komatsu, Y.; Kubota, M.; Kuroda, H.; Miyazawa, M.; Tagami, K.; Watanabeb, T. Commercial Manufacture of Halaven®: Chemoselective Transformations En Route to Structurally Complex Macrocyclic Ketones. *Synlett*. **2013**, *24*, 333–337.

[86] For the remarkable whole story of Halaven see: Bauer, A. Story of Eribulin Mesylate: Development of the Longest Drug Synthesis. In: *Synthesis of Heterocycles in Contemporary Medicinal Chemistry*, Vol. 44. Maes, B.; Cossy, J.; Polanc, S. Eds. Springer: Berlin, Heidelberg. **2016**, 209–270.

[87] Pelphrey, P. M.; Bolstad, D. B.; Wright, D. L. Versatile Oxabicyclic Synthons: Studies on C8-Oxygenated Eunicellin Diterpenes. *Synlett*. **2007**, *17*, 2647–2650.

[88] Zhu, W.; Jiménez, M.; Jung, W.; Camarco, D. P.; Balachandran, R.; Vogt, A.; Day, B. W.; Curran, D. P. Streamlined Syntheses of (−)-Dictyostatin, 16-Desmethyl-25,26-dihydrodictyostatin, and 6-epi-16-Desmethyl-25,26-dihydrodictyostatin. *J. Am. Chem. Soc*. **2010**, *132*, 9175–9187.

[89] Bolte, B.; Basutto, J. A.; Bryan, C. S.; Garson, M. J.; Banwell, M. G.; Ward, J. S. Modular Total Syntheses of the Marine-Derived Resorcylic Acid Lactones Cochliomycins A and B Using a Late-Stage Nozaki–Hiyama–Kishi Macrocyclization Reaction. *J. Org. Chem*. **2015**, *80*, 460–470.

[90] Njardarson, J. T.; Biswas, K.; Danishefsky, S. J. Application of hitherto unexplored macrocyclization strategies in the epothilone series: novel epothilone analogs by total synthesis. *Chem. Commun*. **2002**, *23*, 2759–2761.

[91] Takao, K.; Hayakawa, N.; Yamada, R.; Yamaguchi, T.; Morita, U.; Kawasaki, S.; Tadano, K. Total Synthesis of (−)-Pestalotiopsin A. *Angew. Chem. Int. Ed*. **2008**, *47*, 3426–3429.

[92] Marshall, J. A.; Eidam, P. M. A Formal Synthesis of the Callipeltoside Aglycone. *Org. Lett*. **2008**, *10*, 93– 96.

[93] Bian, J.; Van Wingerden, M.; Ready, J. M. Enantioselective Total Synthesis of (+)- and (−)-Nigellamine A2. *J. Am. Chem. Soc*. **2006**, *128*, 7428–7429.

[94] Corminboeuf, O.; Overman, L. E.; Pennington, L. D. Enantioselective Total Synthesis of Briarellins E and F: The First Total Syntheses of Briarellin Diterpenes. *J. Am. Chem. Soc*. **2003**, *125*, 6650–6652.

[95] Tang, B.; Bray, C. D.; Pattenden, G. Total Synthesis of (+) -Intricarene Using a Biogenetically Patterned Pathway from (−) -Bipinnatin J, Involving a Novel Transannular. *Org. Biomol. Chem*. **2009**, *7*, 4448–4457.

[96] Corey, E. J.; Nicolaou, K. C. Efficient and mild lactonization method for the synthesis of macrolides. *J. Am. Chem. Soc*. **1974**, *96*, 5614–5616.

[97] White, C. J.; Yudin, A. K. Contemporary strategies for peptide macrocyclization. *Nat. Chem*. **2011**, *3*, 509–524.

[98] Davies, J.S. The cyclization of peptides and depsipeptides. *Pept. Sci*. **2003**, *9*, 471–501.

[99] El-Faham, A.; Albericio, F. Peptide Coupling Reagents, More than a Letter Soup. *Chem. Rev.* **2011**, *111*, 6557–6602.

[100] Kaiho, T.; Masamune, S.; Toyoda, T. Macrolide synthesis: narbonolide. *J. Org. Chem*. **1982**, *47*, 1612–1614.

[101] Arrieta, A.; García, T.; Lago, J. M.; Palomo, C. Reagents and Synthetic Methods 28. Modified Procedures for Anhydrization, Esterification and Thiolesterification of Carboxylic Acids by Means of Available Phosphorus Reagents. *Synth. Commun*. **1983**, *13*, 471–487.

[102] Inanaga, J.; Hirata, K.; Saeki, H.; Katsuki, T.; Yamaguchi, M. A Rapid Esterification by Means of Mixed Anhydride and Its Application to Large-ring Lactonization. *Bull. Chem. Soc. Jpn.* **1979**, *52*, 1989–1993.

[103] Shiina, I.; Kubota, M.; Ibuka, R. A novel and efficient macrolactonization of ω-hydroxycarboxylic acids using 2-methyl-6-nitrobenzoic anhydride (MNBA). *Tetrahedron Lett*. **2002**, *43*, 7535–7539.

[104] Woodward, R. B.; Bader, F. E.; Bickel, H.; Frey, A. J.; Kierstead, R. W. The total synthesis of reserpine. *Tetrahedron* **1958***, 2*, 1-57.

[105] Ashworth, P.; Broadbelt, B.; Jankowski, P.; Kocienski, P.; Pimm, A.; Bell, R. A Synthesis of Jaspamide Based on 1,2 Metallate Rearrangements of α-Heteroalkenylmetal Derivates. *Synthesis* **1995**, *2*, 199–206.

[106] Narasaka, K.; Maruyama, K.; Mukaiyama, T. A Useful Method for the Synthesis of Macrocyclic Lactone. *Chem. Lett.* **1978**, *7*, 885–888.

[107] Mukaiyama, T. New Synthetic Reactions Based on the Onium Salts of Aza-Arenes. *Angew. Chem. Int. Ed*. **1979**, *18*, 707–721.

[108] Funk, R. L.; Abelman, M. M.; Jellison, K. M. Generation of Ketenes From Carboxylic Acids Using the Mukaiyama Reagent. *Synlett*. **1989**, *1*, 36–37.

[109] Arlt, A.; Benson, S.; Schulthoff, S.; Gabor, B.; Fürstner, A. A Total Synthesis of Spirastrellolide A Methyl Ester. *Chem. Eur. J*. **2013**, *19*, 3596–3608.

[110] Evans, D. A.; Fitch, D. M.; Smith, T. E.; Cee, V. J. Application of Complex Aldol Reactions to the Total Synthesis of Phorboxazole B. *J. Am. Chem. Soc.* **2000**, *122*, 10033–10046.

[111] White, J. D.; Avery, M. A.; Choudhry, S. C.; Dhingra, O. P.' Gray, B. D.; Kang, M. C.; Kuo, S. C.; Whittle, A. J. Total synthesis of boromycin. *J. Am. Chem. Soc*. **1989**, *111*, 790–792.

[112] Paterson, I.; Britton, R.; Delgado, O.; Gardner, N. M.; Meyer, A.; Naylor, G. J.; Poullennec, K. G. Total synthesis of (−)-dictyostatin, a microtubule-stabilising anticancer macrolide of marine sponge origin. *Tetrahedron* **2010**, *66*, 6534–6545.

[113] Hanessian, S.; Ma, J.; Wang, W. Total Synthesis of Bafilomycin A1 Relying on Iterative 1,2-Induction in Acyclic Precursors. *J. Am. Chem. Soc.* **2001**, *123*, 10200–10206.

[114] Nicolaou, K. C.; Sun, Y.; Guduru, R.; Banerji, B.; Chen, D. Y. K. Total Synthesis of the Originally Proposed and Revised Structures of Palmerolide A and Isomers Thereof. *J. Am. Chem. Soc.* **2008**, *130*, 3633–3644.

[115] Roush, W. R.; Sciotti, R. J. Enantioselective Total Synthesis of (−)-Chlorothricolide via the Tandem Inter- and Intramolecular Diels−Alder Reaction of a Hexaenoate Intermediate. *J. Am. Chem. Soc.* **1998**, *120*, 7411–7419.

[116] Lu, S.; O'yang, Q.; Guo, Z.; Yu, B.; Hui, Y. Total Synthesis of Tricolorin A. *J. Org. Chem.* **1997**, *62*, 8400–8405.

[117] Mulzer, J.; Mantoulidis, A.; Öhler, E. Total Syntheses of Epothilones B and D. *J. Org. Chem.* **2000**, *65*, 7456–7467.

[118] Corey, E. J.; De, B. Total synthesis and stereochemistry of hybridalactone. *J. Am. Chem. Soc.* **1984**, *106*, 2735–2736.

[119] Kim, H.; Park, Y.; Hong, J. Stereoselective Synthesis of 2,6-cis-Tetrahydropyrans through a Tandem Allylic Oxidation/Oxa-Michael Reaction Promoted by the gem-Disubstituent Effect: Synthesis of (+)-Neopeltolide Macrolactone. *Angew. Chem. Int. Ed*. **2009**, *48*, 7577–7581.

[120] Huang, H.; Panek, J. S. Total Synthesis of Callipeltoside A. O*rg. Lett.* 2004, 6, 23, 4383–4385

[121] Evans, D. A.; Kaldor, S. W.; Jones, T. K.; Clardy, J.; Stout, T. J. Total synthesis of the macrolide antibiotic cytovaricin. *J. Am. Chem. Soc.* **1990**, *112*, 7001–7031.

[122] Sawamura, K.; Yoshida, K.; Suzuki, A.; Motozaki, T.; Kozawa, I.; Hayamizu, T.; Munakata, R.; Takao, K.; Tadano, K. Total Syntheses of Natural Tubelactomicins B, D, and E: Establishment of Their Stereochemistries. *J. Org. Chem*. **2007**, *72*, 6143–6148.

[123] Frantz, D. E.; Fässler, R.; Carreira, E. M. Facile Enantioselective Synthesis of Propargylic Alcohols by Direct Addition of Terminal Alkynes to Aldehydes. *J. Am. Chem. Soc*. **2000**, *122*, 1806–1807.

[124] Hart, D. W.; Schwartz, J. Hydrozirconation. Organic synthesis via organozirconium intermediates. Synthesis and rearrangement of alkylzirconium(IV) complexes and their reaction with electrophiles. *J. Am. Chem. Soc*. **1974**, *96*, 8115–8116.

[125] Mazery, R. D.; Pullez, M.; López, F.; Harutyunyan, S. R.; Minnaard, A. J.; Feringa, B. L. An Iterative Catalytic Route to Enantiopure Deoxypropionate Subunits: Asymmetric Conjugate Addition of Grignard Reagents to α,β Unsaturated Thioesters. *J. Am. Chem. Soc.* **2005**, *127*, 9966–9967.

[126] Myers, A. G.; Yang, B. H.; Chen, H.; McKinstry, L.; Kopecky, D. J.; Cleason, J. L. Pseudoephedrine as a Practical Chiral Auxiliary for the Synthesis of Highly Enantiomerically Enriched Carboxylic Acids, Alcohols, Aldehydes, and Ketones. *J. Am. Chem. Soc.* **1997**, *119*, 6496–6511.

[127] Ohira, S. Methanolysis of Dimethyl (1-Diazo-2-oxopropyl) Phosphonate: Generation of Dimethyl (Diazomethyl) Phosphonate and Reaction with Carbonyl Compounds. *Synth. Commun.* **1989**, *19*, 561–564.

[128] Lyapkalo, I.; Vogel, M.; Boltukhina, E.; Vavřík, J. Thieme Chemistry Journal Awardees - Where Are They Now? A General One-Step Synthesis of Alkynes from Enolisable Carbonyl Compounds. *Synlett* **2009**, *2009*, 558–561.

[129] Lu, H.-H.; Martinez, M. D.; Shenvi, R. A. An Eight-Step Gram-Scale Synthesis of (−)-Jiadifenolide. *Nat. Chem.* **2015**, *7*, 604–607.

[130] Zhou, Q.; Chen, X.; Ma, D. Asymmetric, Protecting-Group-Free Total Synthesis of (−)-Englerin A. *Angew. Chem. Int. Ed.* **2010**, *49*, 3513–3516.

[131] Hart, D. W.; Blackburn, T. F.; Schwartz, J. Hydrozirconation. III. Stereospecific and Regioselective Functionalization of Alkylacetylenes via Vinylzirconium(IV) Intermediates. *J. Am. Chem. Soc*. **1974**, *97*, 679–680.

[132] Buchwald, S. L.; LaMaire, S. J.; Nielsen, R. B.; Watson, B. T.; King, S. M. Schwartz's Reagent. *Org. Synth.* **1993**, *71*, 77.

[133] Lang, J. H.; Lindel, T. Synthesis of the Polyketide Section of Seragamide A and Related Cyclodepsipeptides via Negishi Cross Coupling. *Beilstein J. Org. Chem*. **2019**, *15*, 577–583.

[134] Nakamura, E.; Aoki, S.; Seki-ya, K.; Oshino, H.; Kuwajima, I. Carbon-Carbon Bond-Forming Reactions of Zinc Homoenolate of Esters. A Novel Three-Carbon Nucleophile with General Synthetic Utility. *J. Am. Chem. Soc*. **1987**, *109*, 8056–8066.

[135] Matsumura, K.; Hashiguchi, S.; Ikariya, T.; Noyori, R. Asymmetric Transfer Hydrogenation of α, β-Acetylenic Ketones. *J. Am. Chem. Soc*. **1997**, *119*, 8738–8739.

[136] Salituro, L. J.; Pazienza, J. E.; Rychnovsky, S. D. Total Syntheses of Strasseriolides A and B, Antimalarial Macrolide Natural Products. *Org. Lett*. **2022**, *24*, 1190–1194.

[137] Keck, G. E.; Boden, E. P.; Mabury, S. A. A Useful Wittig Reagent for the Stereoselective Synthesis of Trans α, β-Unsaturated Thiol Esters. *J. Org. Chem.* **1985**, *50*, 709–710.

[138] Tokuyama, H.; Yokoshima, S.; Lin, S.-C.; Li, L.; Fukuyama, T. Reduction of Ethanethiol Esters to Aldehydes. *Synthesis* **2002**, *2002*, 1121–1123.

[139] Finke, A. D.; Moore, J. S. Lewis acid activation of molybdenum nitrides for alkyne metathesis. *Chem. Commun*. **2010**, *46*, 7939–7941.

[140] Dehnicke, K.; Strähle, J. Nitrido Complexes of Transition Metals. *Angew. Chem. Int. Ed.* **1992**, *31*, 955–978.

[141] Oppolzer, W.; Radinov, R. N. Synthesis of (*R*)-(–)-Muscone by an Asymmetrically Catalyzed Macrocyclization of ω-Alkynal. *J. Am. Chem. Soc*. **1993**, *115*, 1593–1594.

[142] Wipf, P.; Xu, W. Preparation of allylic alcohols by alkene transfer from zirconium to zinc. *Tetrahedron Lett*. **1994**, *35*, 5197–5200.

[143] Maeta, H.; Hashimoto, T.; Hasegawa, T.; Suzuki, K. Grignard-type addition of alkenyl- and alkylzirconocene chloride to aldehyde: Remarkable catalytic acceleration effect of $AgClO_4$. *Tetrahedron Lett.* **1992**, *33*, 5965–5968.

[144] Nicolaou, K. C.; Estrada, A. A.; Zak, M.; Lee, S. H.; Safina, B. S. A Mild and Selective Method for the Hydrolysis of Esters with Trimethyltin Hydroxide. *Angew. Chem. Int. Ed*. **2005**, *44*, 1378–1382.

[145] White, J. M.; Tunoori, A. R.; Georg, G. I. A Novel and Expeditious Reduction of Tertiary Amides to Aldehydes Using $Cp_2Zr(H)Cl$. *J. Am. Chem. Soc*. **2000**, *122*, 11995–11996.

[146] Annang, F.; Pérez-Moreno, G.; Díaz, C.; González-Menéndez, V.; de Pedro Montejo, N.; Pérez del Palacio, J.; Sáanchez, P.; Tanghe, S.; Rodriguez, A.; Pérez-Victoria, I.; Cantizani, J.; Ruiz,Pérez, L. M.; Genilloud, O.; Reyes, F.; Vicente, F.; González-Pacanowska, D. Preclinical evaluation of strasseriolides A–D, potent antiplasmodial macrolides isolated from *Strasseria geniculata* CF-247,251. *Malaria Journal* **2021**, 20:457.

[147] Douchez, A.; Lubell, W. D. Chemoselective Alkylation for Diversity-Oriented Synthesis of 1,3,4-Benzotriazepin-2-ones and Pyrrolo[1,2][1,3,4]benzotriazepin-6-ones, Potential Turn Surrogates. *Org. Lett*. **2015**, *17*, 6046–6049.

[148] Speck, K.; Wildermuth, R.; Magauer, T. Convergent Assembly of the Tetracyclic Meroterpenoid (−)-Cyclosmenospongine by a Non-Biomimetic Polyene Cyclization. *Angew. Chem. Int. Ed*. **2016**, *55*, 14131–14135.

[149] Schultz, E. E.; Sarpong, R. Application of In Situ-Generated Rh-Bound Trimethylenemethane Variants to the Synthesis of 3,4-Fused Pyrroles. *J. Am. Chem. Soc.* **2013**, *135,* 4696–4699.

[150] Tejeda-Serrano, M.; Lloret, V.; Márkus, B. G.; Simon, F.; Hauke, F.; Hirsch, A.; Doménech-Carbó, A.; Abellán, G.; Leyva-Pérez, A. Few-layer Black Phosphorous Catalyzes Radical Additions to Alkenes Faster than Low-valence Metals. *Chem. Cat. Chem*. **2020**, *12*, 2226–2232.

[151] Keck, G. E.; Boden, E. P.; Mabury, S. A. A useful Wittig reagent for the stereoselective synthesis of *trans*-α,β-unsaturated thiol esters. *J. Org. Chem.* **1985**, *50*, 709–710.

[152] Comeau, C.; Ries, B.; Stadelmann, T.; Tremblay, J.; Poulet, S.; Fröhlich, U.; Côté, J.; Boudreault, P.; Derbail, R. M.; Sarret, P.; Grandbois, M.; Leclair, G.; Riniker, S.; Marsault, É. Modulation of the Passive Permeability of Semipeptidic Macrocycles: N- and C-Methylations Fine-Tune Conformation and Properties. *J. Med. Chem.* **2021**, *64*, 5365–5383.

[153] Wang, T.; Pinard, E.; Paquette, L. A. Asymmetric Synthesis of the Diterpenoid Marine Toxin (+)-Acetoxycrenulide. *J. Am. Chem. Soc.* **1996**, *118*, 1309–1318.

[154] Wang, T.; Pinard, E.; Paquette, L. A. Asymmetric Synthesis of the Diterpenoid Marine Toxin (+)-Acetoxycrenulide. *J. Am. Chem. Soc.* **1996**, *118*, 1309–1318.

[155] Featherston, A. L.; Miller, S. J. Synthesis and evaluation of phenylalanine-derived trifluoromethyl ketones for peptide-based oxidation catalysis. Bioorganic Med. Chem. 2016, 24, 4871–4874.

[156] Yamani, K.; Pierre, H.; Archambeau, A.; Meyer, C.; Cossy, J. Asymmetric Transfer Hydrogenation of *gem*-Difluorocyclopropenyl Esters: Access to Enantioenriched *gem*-Difluorocyclopropanes. *Angew. Chem. Int. Ed*. **2020**, *59*, 18505–18509.

[157] Weber, S. E.; Gaß, J.; Zend, H.; Erb-Brinkmann, M.; Schobert, R. Synthesis and Bioactivity of a Macrocidin B Stereoisomer. *Org. Lett*. **2021**, *23*, 8273–8276.

[158] Lehr, K.; Schulthoff, S.; Ueda, Y.; Mariz, R.; Leseurre, L.; Gabor, B.; Fürstner, A. A New Method for the Preparation of Non-Terminal Alkynes: Application to the Total Syntheses of Tulearin A and C. *Angew. Chem. Int. Ed.* **2015**, *21*, 219–227.

Appendix A: NMR Spectra for Chapter 1

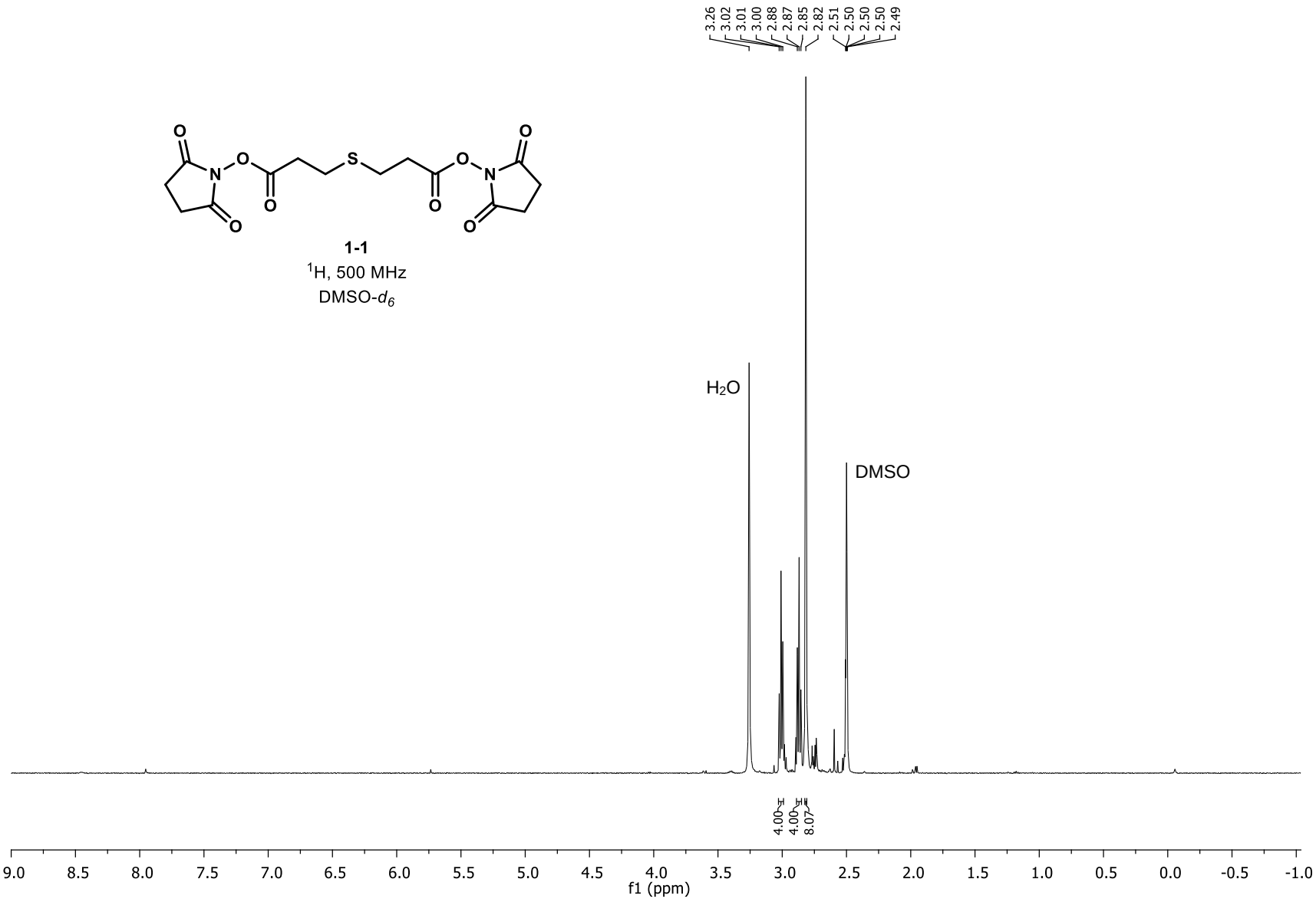

1-1

^{1}H, 500 MHz

DMSO-d_6

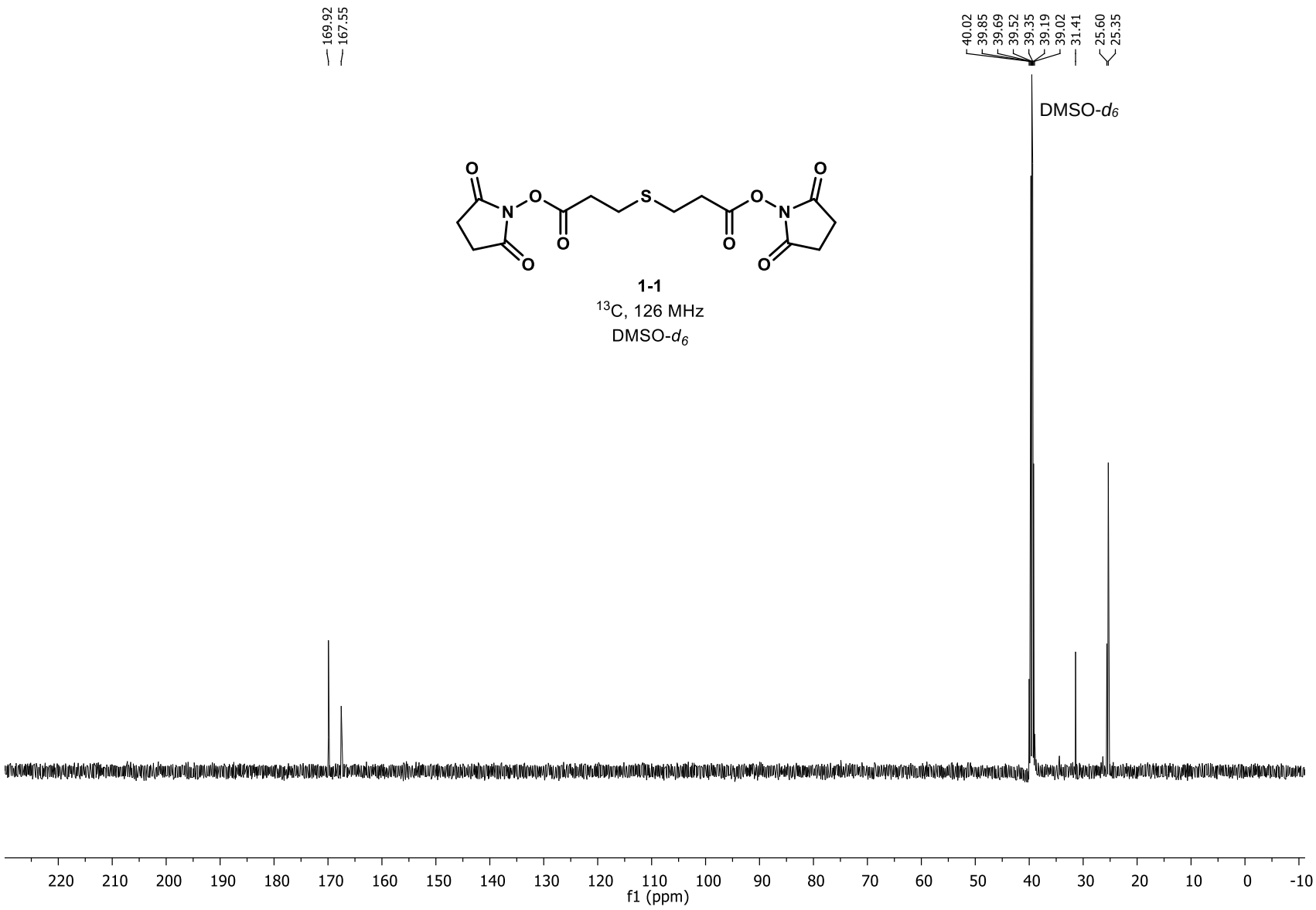
169.92
167.55
40.02
39.85
39.69
39.52
39.35
39.19
39.02
31.41
25.60
25.35
DMSO-d_6
O
N
O
O
S
O
O
N
O
O
O
O
1-1
^{13}C, 126 MHz
DMSO-d_6
220
210
200
190
180
170
160
150
140
130
120
110
100
90
80
70
60
50
40
30
20
10
0
-10
f1 (ppm)

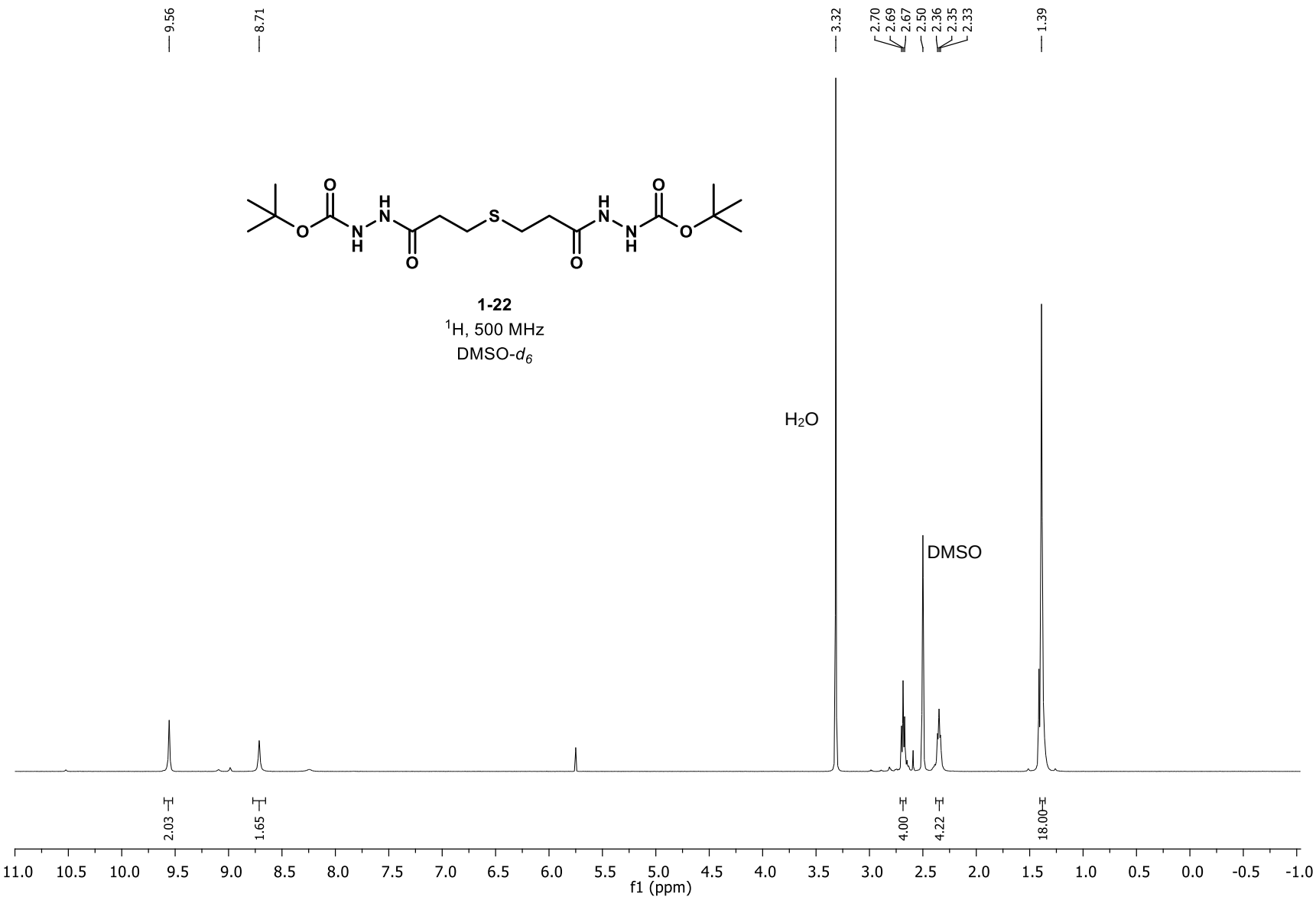
9.56
8.71
3.32
2.70
2.69
2.67
2.50
2.36
2.35
2.33
1.39
1-22
1H, 500 MHz
DMSO-d6
H2O
DMSO
2.03
1.65
4.00
4.22
18.00
f1 (ppm)

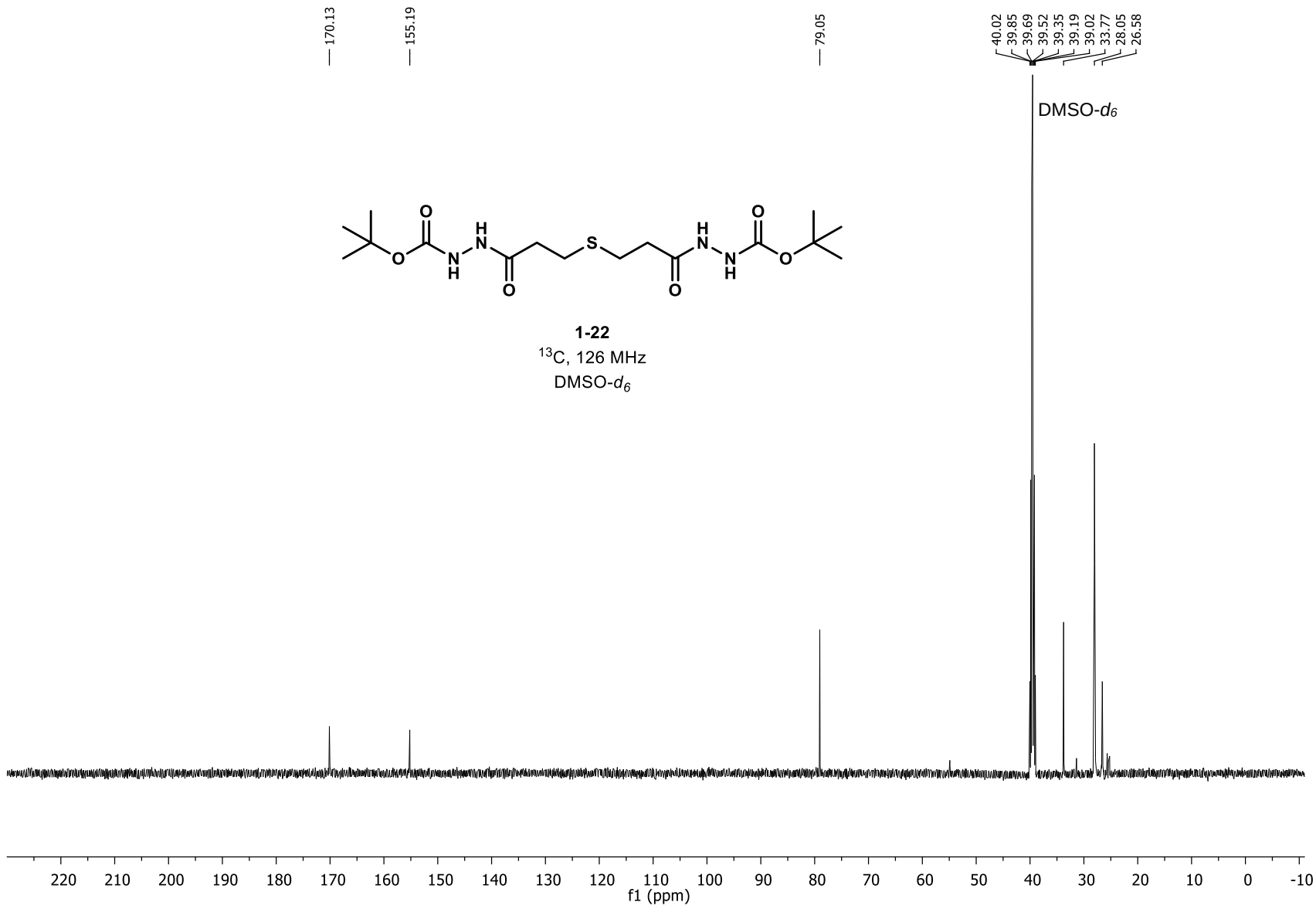
170.13
155.19
79.05
40.02
39.85
39.69
39.52
39.35
39.19
39.02
33.77
28.05
26.58
DMSO-d6
1-22
13C, 126 MHz
DMSO-d6
220 210 200 190 180 170 160 150 140 130 120 110 100 90 80 70 60 50 40 30 20 10 0 -10
f1 (ppm)

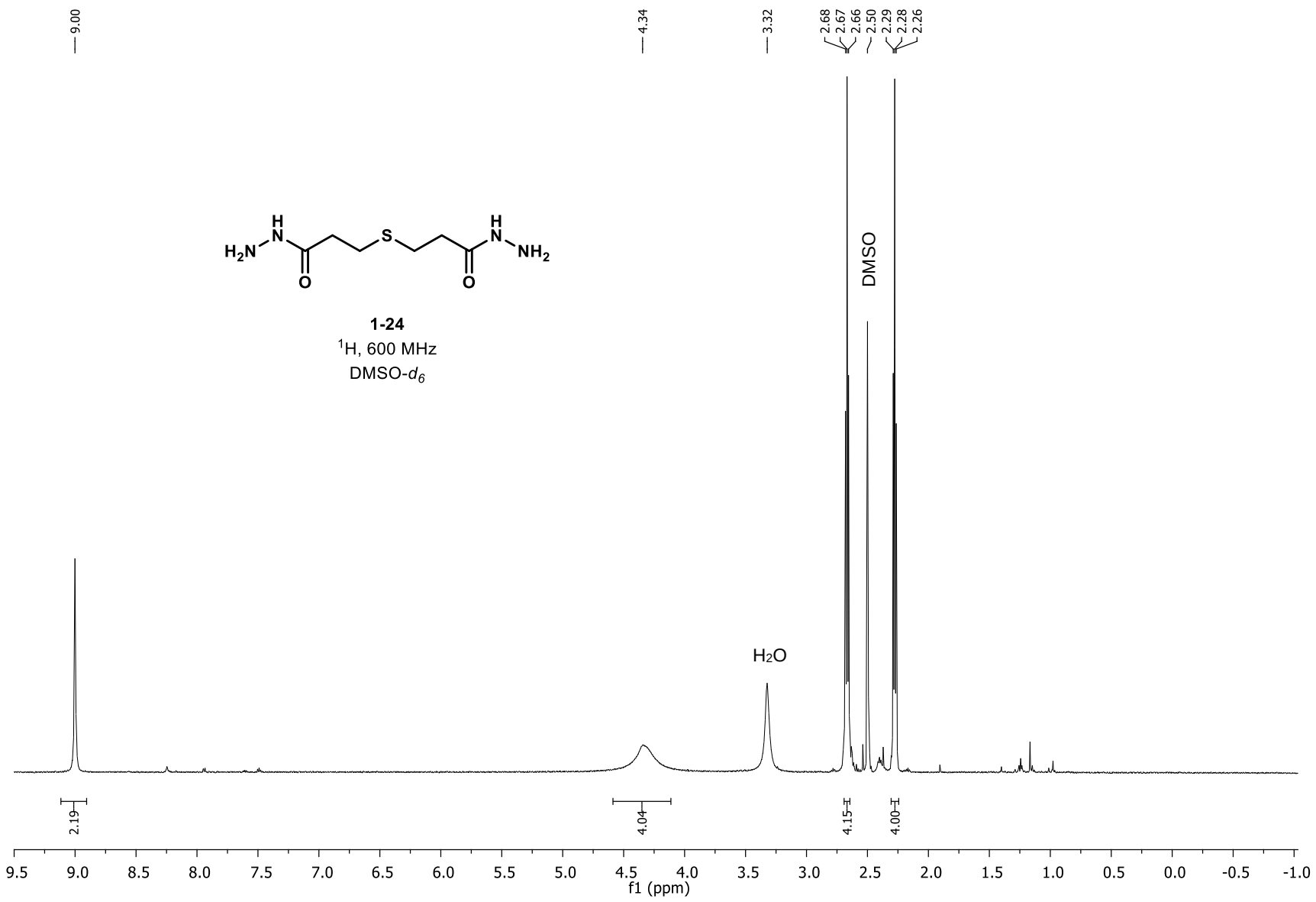

1-24

^{1}H, 600 MHz

DMSO-d_6

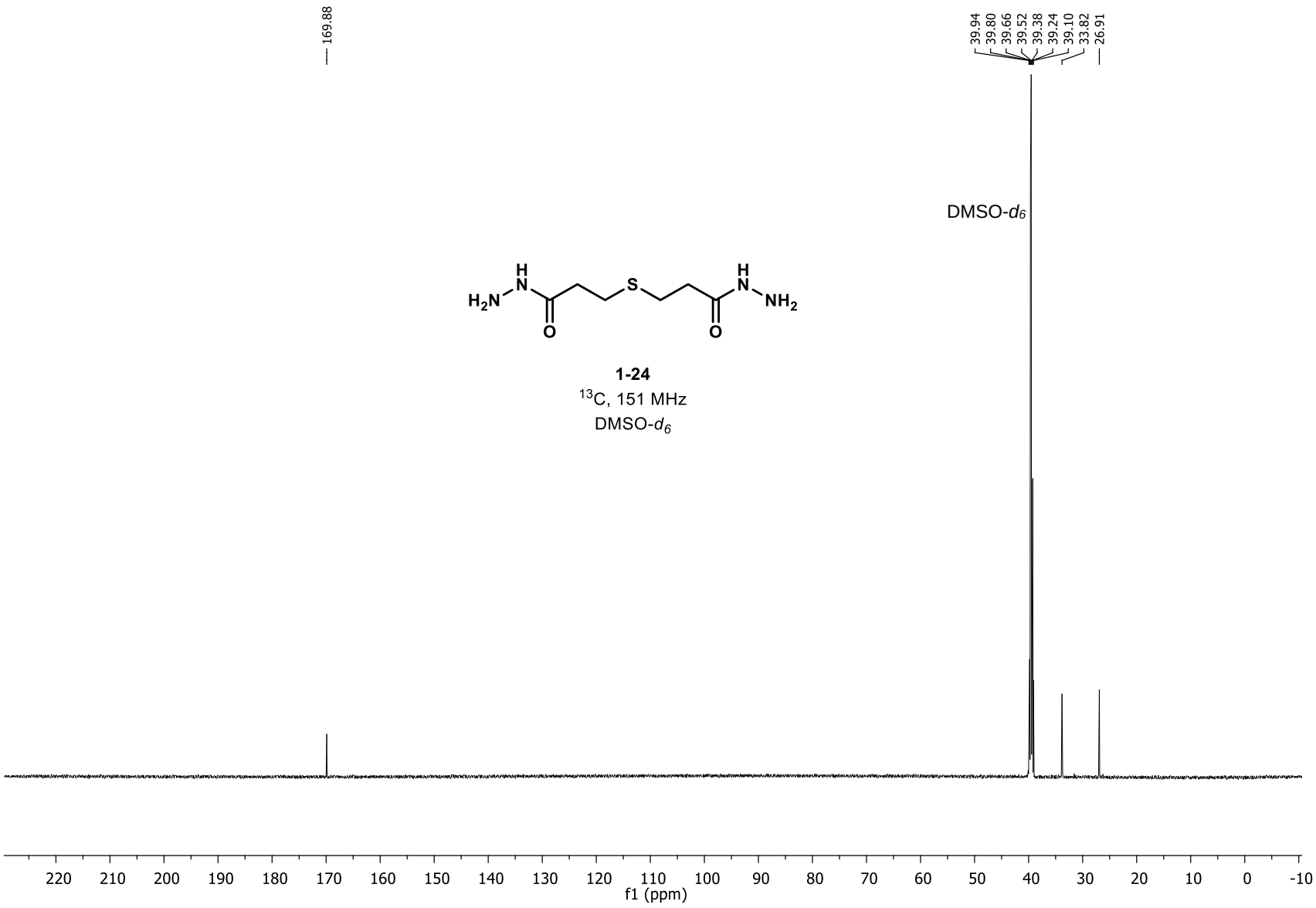
169.88
39.94
39.80
39.66
39.52
39.38
39.24
39.10
33.82
26.91
DMSO-d6
1-24
13C, 151 MHz
DMSO-d6
220 210 200 190 180 170 160 150 140 130 120 110 100 90 80 70 60 50 40 30 20 10 0 -10
f1 (ppm)

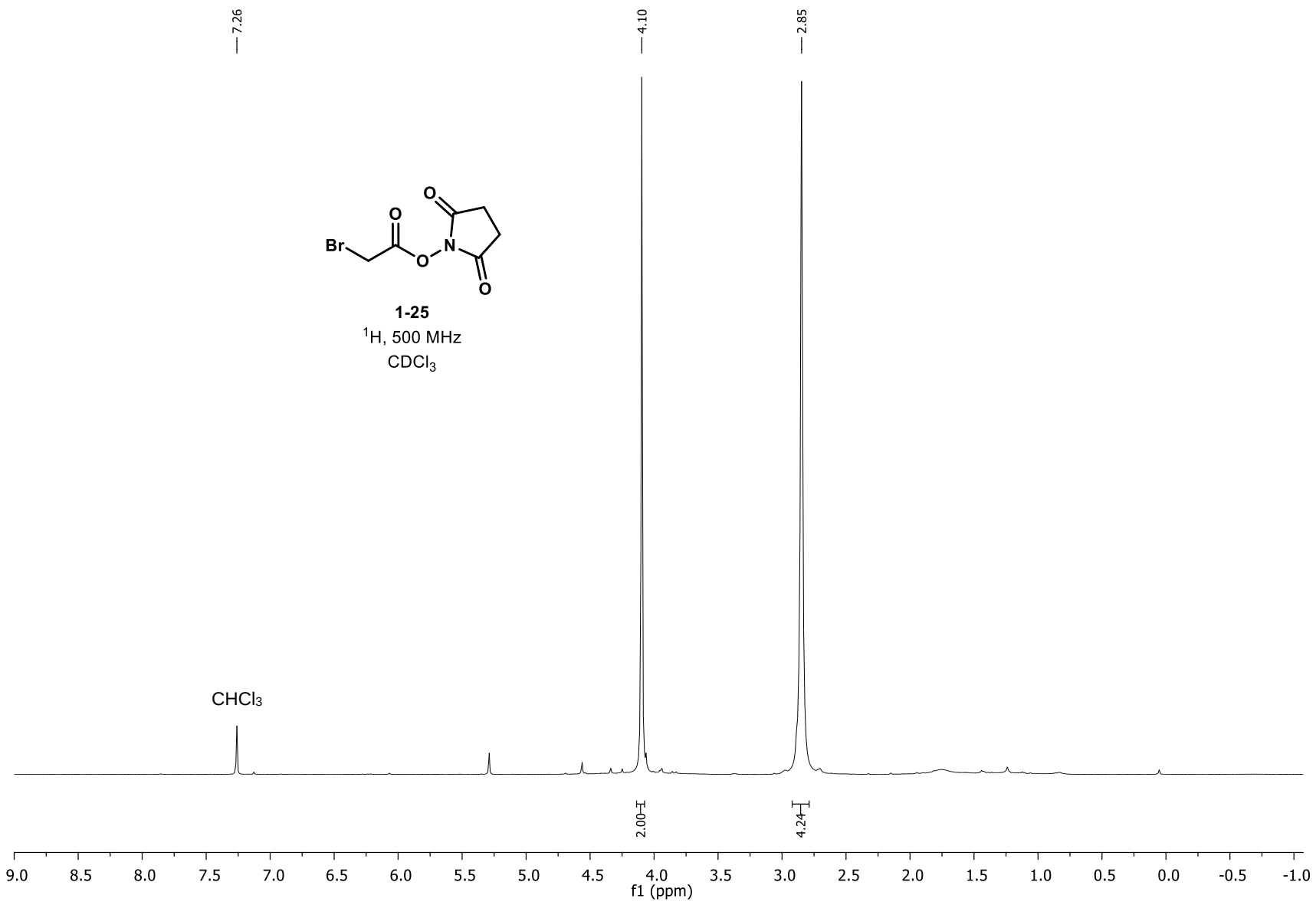
7.26
4.10
2.85
Br
O
O
N
O
O
O
1-25
1H, 500 MHz
CDCl3
CHCl3
2.00
4.24
9.0
8.5
8.0
7.5
7.0
6.5
6.0
5.5
5.0
4.5
4.0
3.5
3.0
2.5
2.0
1.5
1.0
0.5
0.0
-0.5
-1.0
f1 (ppm)

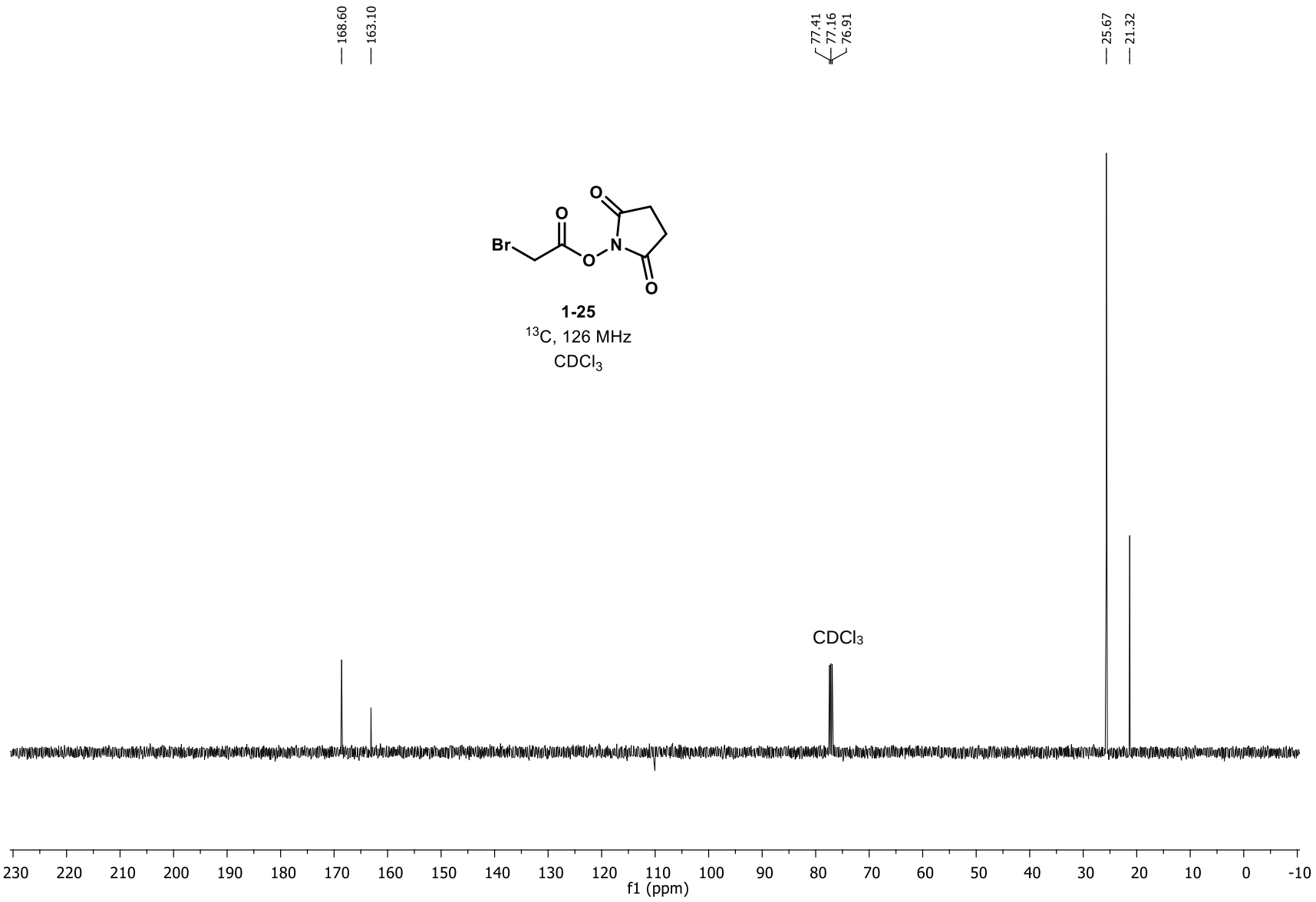
168.60
163.10
77.41
77.16
76.91
25.67
21.32
Br
O
O
O
N
O
O
1-25
13C, 126 MHz
CDCl3
CDCl3
230
220
210
200
190
180
170
160
150
140
130
120
110
100
90
80
70
60
50
40
30
20
10
0
-10
f1 (ppm)

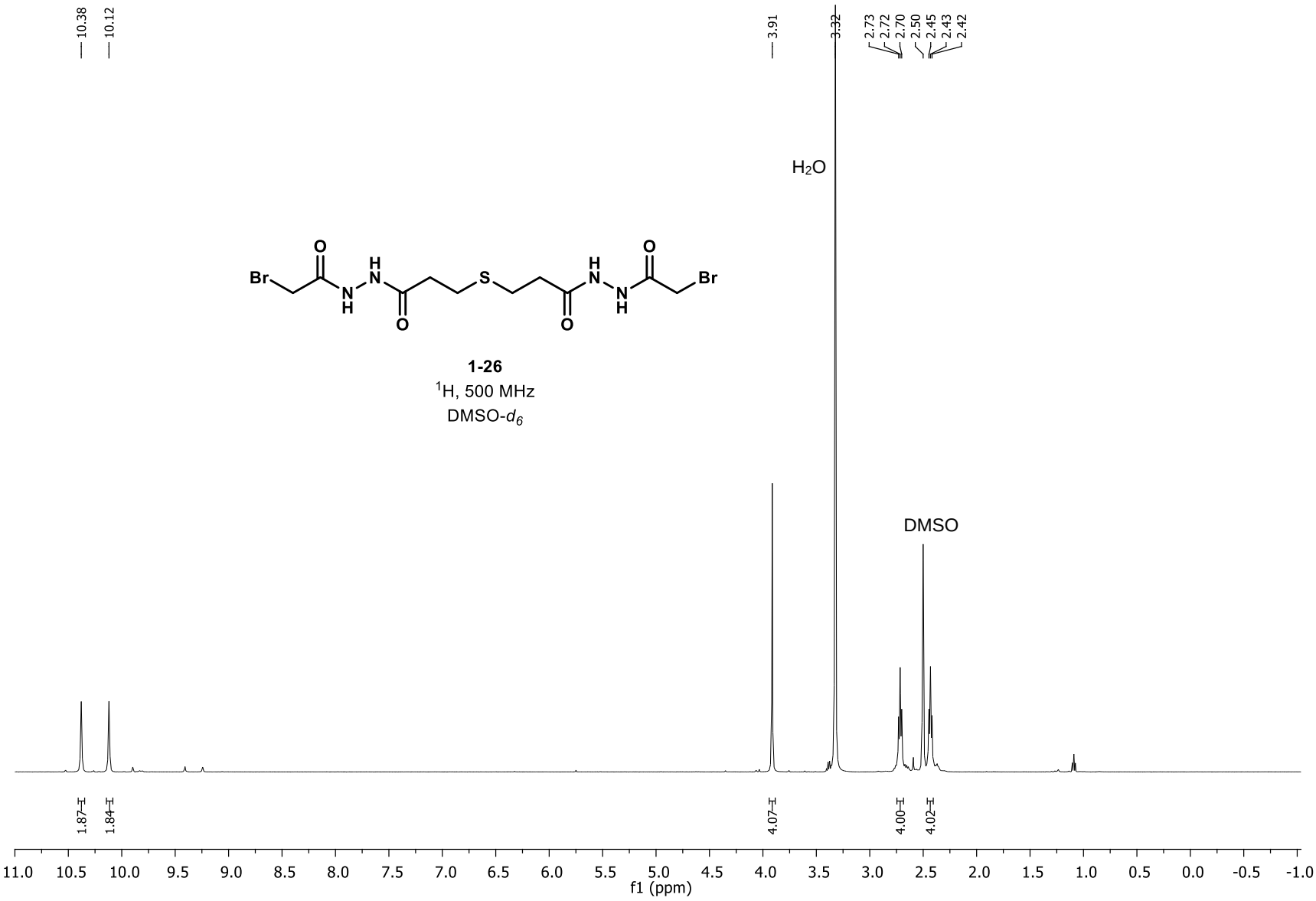
10.38
10.12
3.91
3.32
2.73
2.72
2.70
2.50
2.45
2.43
2.42
H2O
DMSO
1-26
1H, 500 MHz
DMSO-d6
1.87
1.84
4.07
4.00
4.02
11.0 10.5 10.0 9.5 9.0 8.5 8.0 7.5 7.0 6.5 6.0 5.5 5.0 4.5 4.0 3.5 3.0 2.5 2.0 1.5 1.0 0.5 0.0 -0.5 -1.0
f1 (ppm)

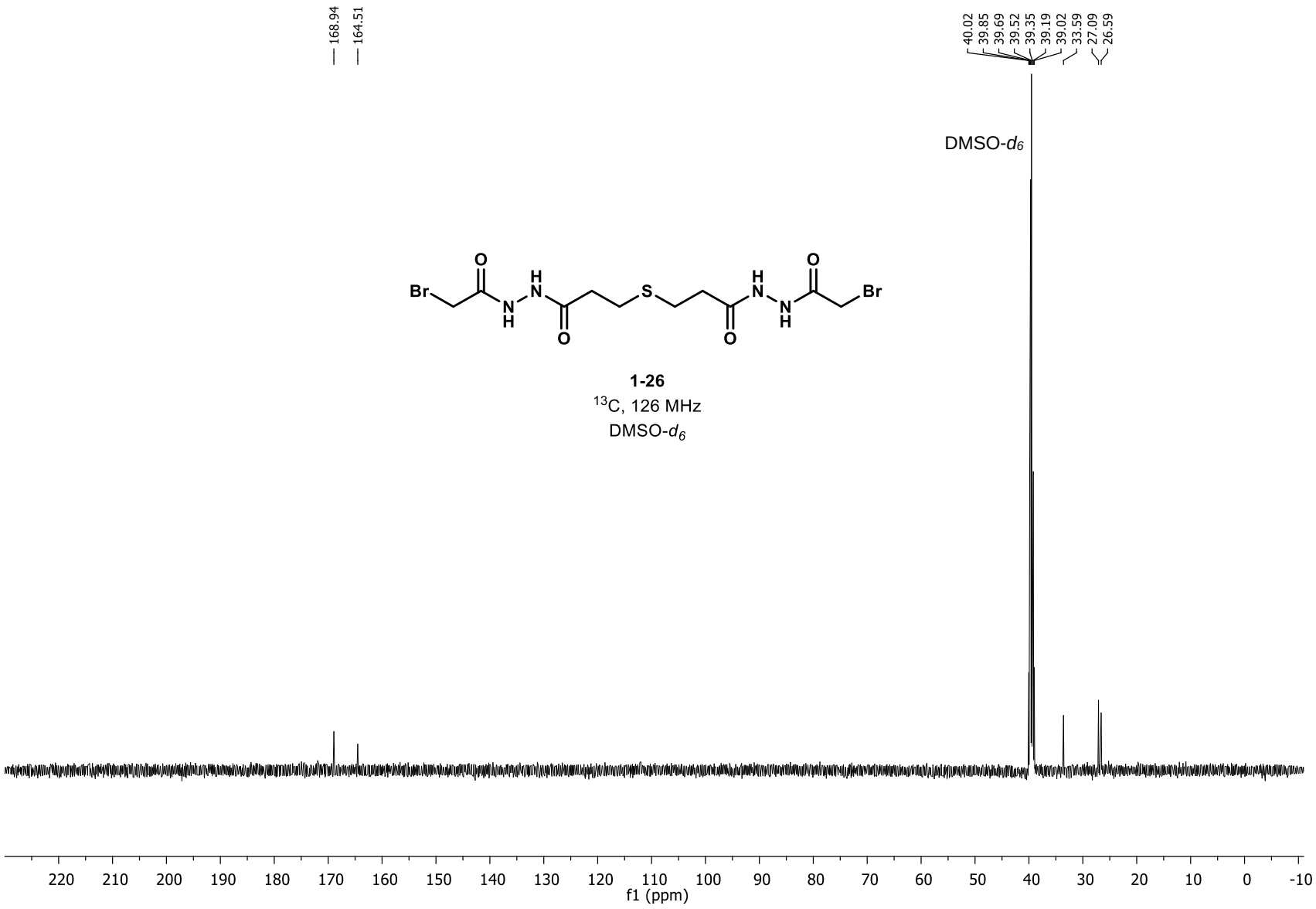
168.94
164.51
40.02
39.85
39.69
39.52
39.35
39.19
39.02
33.59
27.09
26.59
DMSO-d6
Br
O
H
N
N
H
O
S
O
H
N
N
H
O
Br
1-26
13C, 126 MHz
DMSO-d6
220
210
200
190
180
170
160
150
140
130
120
110
100
90
80
70
60
50
40
30
20
10
0
-10
f1 (ppm)

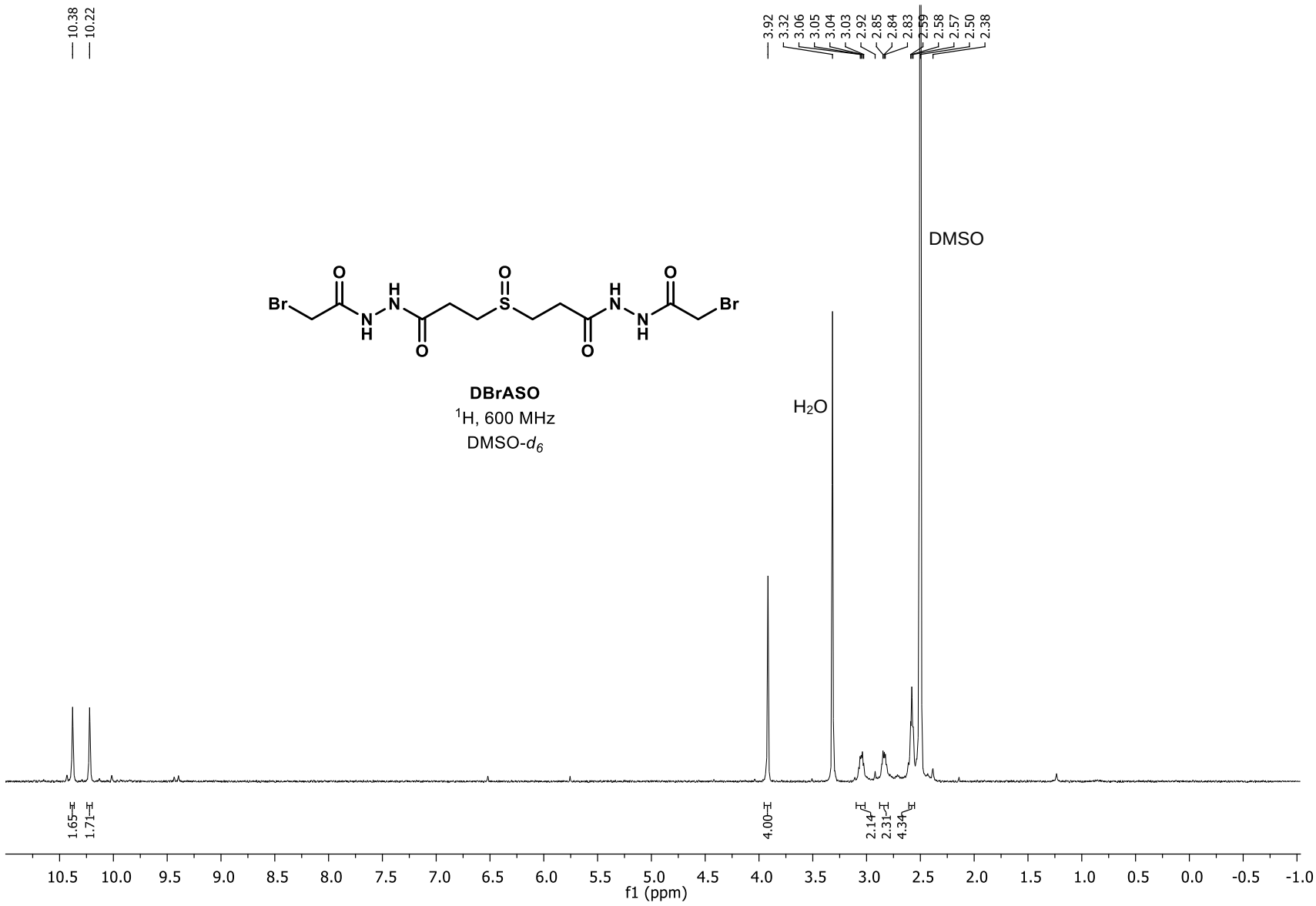
10.38
10.22
3.92
3.32
3.06
3.05
3.04
3.03
2.92
2.85
2.84
2.83
2.59
2.58
2.57
2.50
2.38
DMSO
H2O
DBrASO
1H, 600 MHz
DMSO-d6
1.65
1.71
4.00
2.14
2.31
4.34
f1 (ppm)

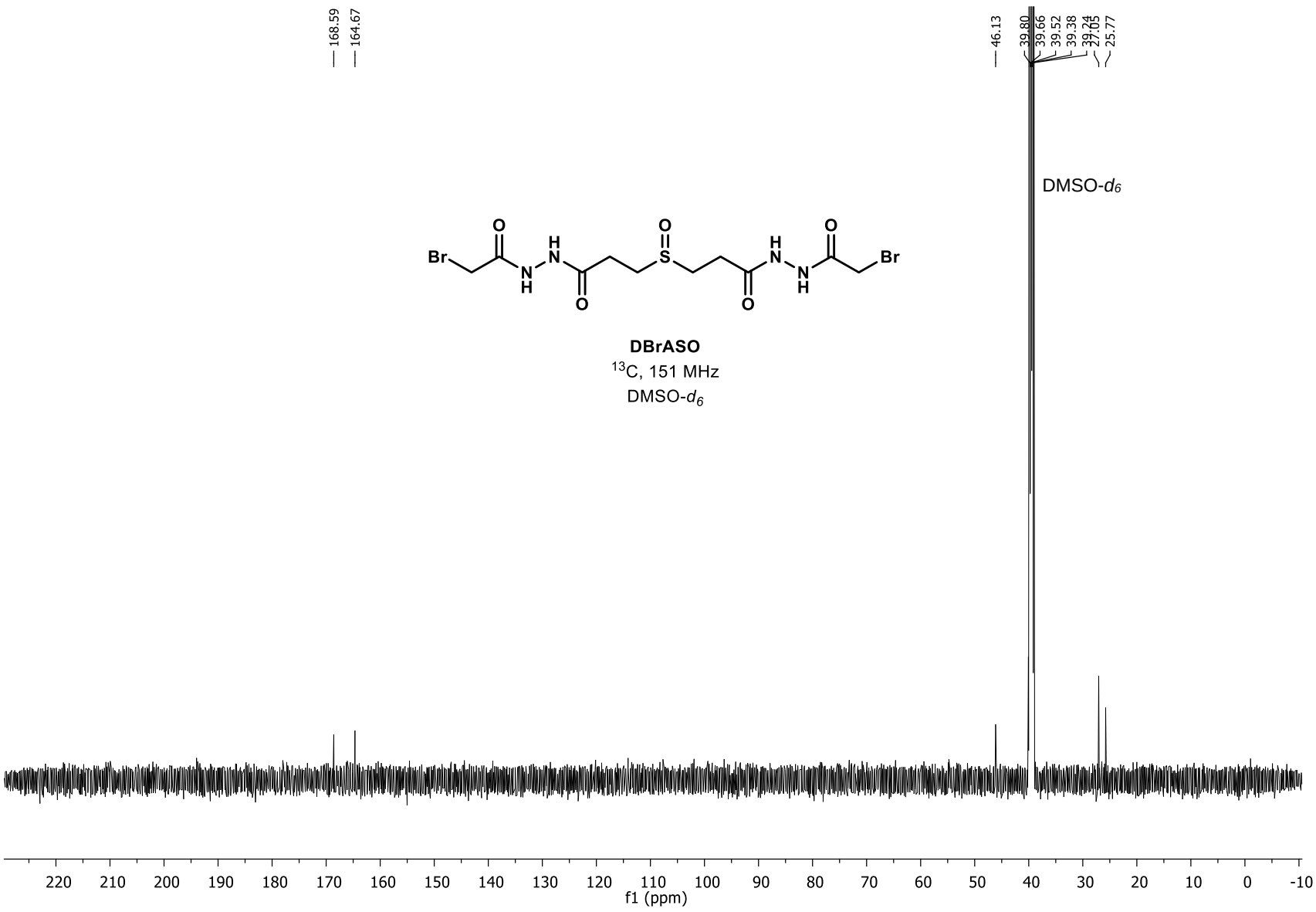
168.59
164.67
46.13
39.80
39.66
39.52
39.38
39.24
27.05
25.77
DMSO-d6
Br
Br
DBrASO
13C, 151 MHz
DMSO-d6
220 210 200 190 180 170 160 150 140 130 120 110 100 90 80 70 60 50 40 30 20 10 0 -10
f1 (ppm)

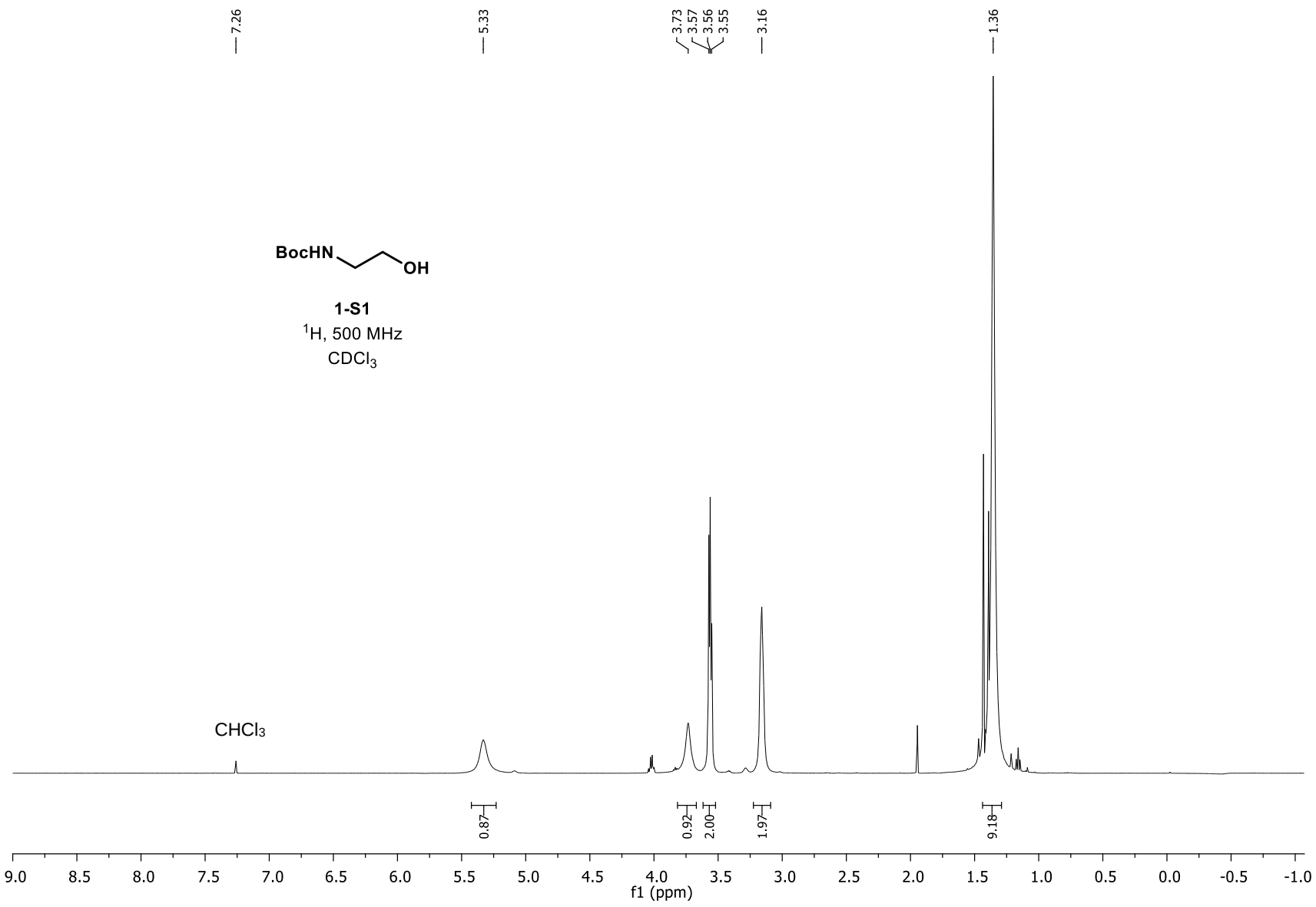
7.26
5.33
3.73
3.57
3.56
3.55
3.16
1.36
BocHN
OH
1-S1
1H, 500 MHz
CDCl3
CHCl3
0.87
0.92
2.00
1.97
9.18
9.0
8.5
8.0
7.5
7.0
6.5
6.0
5.5
5.0
4.5
4.0
3.5
3.0
2.5
2.0
1.5
1.0
0.5
0.0
-0.5
-1.0
f1 (ppm)

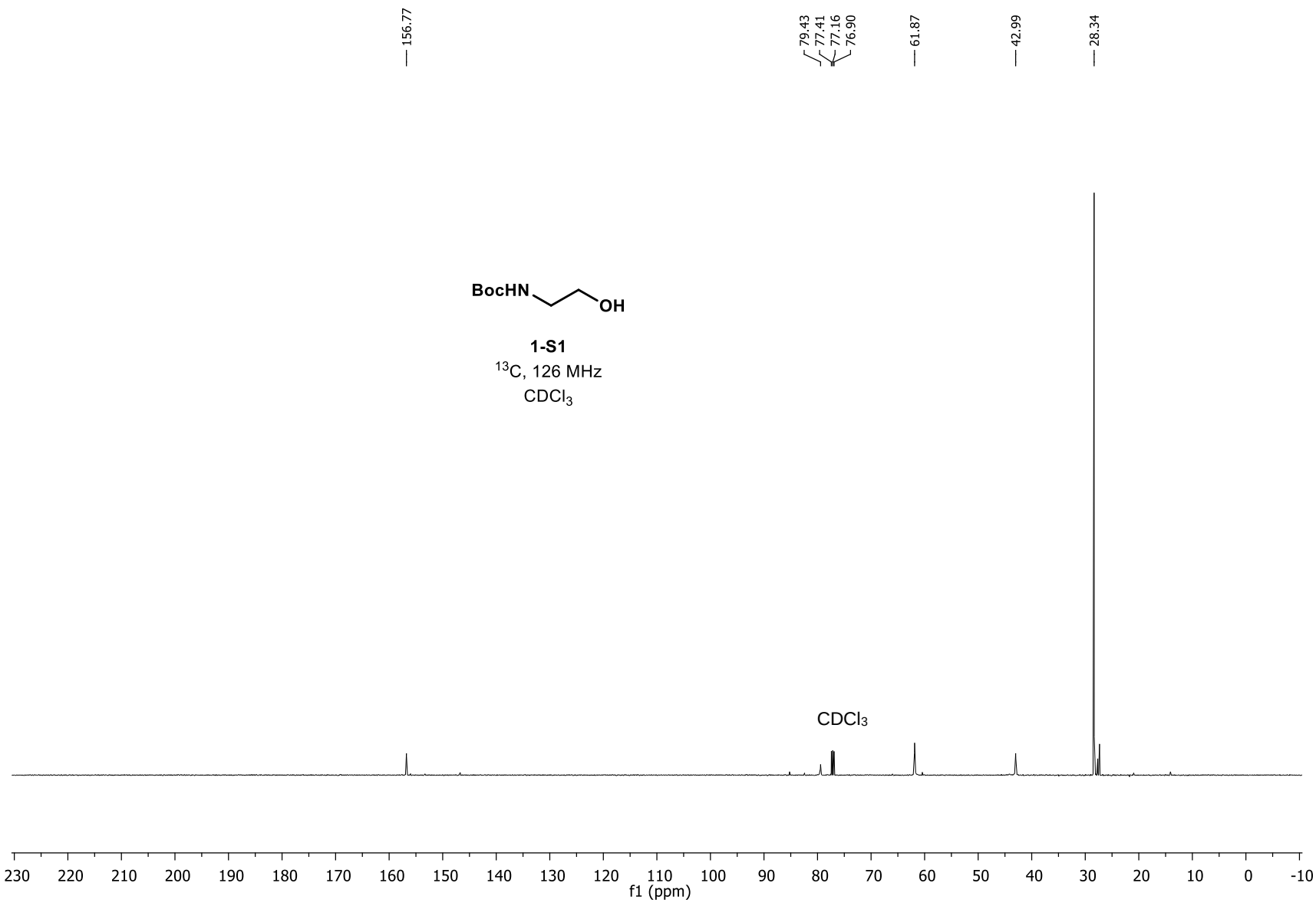
156.77
79.43
77.41
77.16
76.90
61.87
42.99
28.34
BocHN
OH
1-S1
13C, 126 MHz
CDCl3
CDCl3
230 220 210 200 190 180 170 160 150 140 130 120 110 100 90 80 70 60 50 40 30 20 10 0 -10
f1 (ppm)

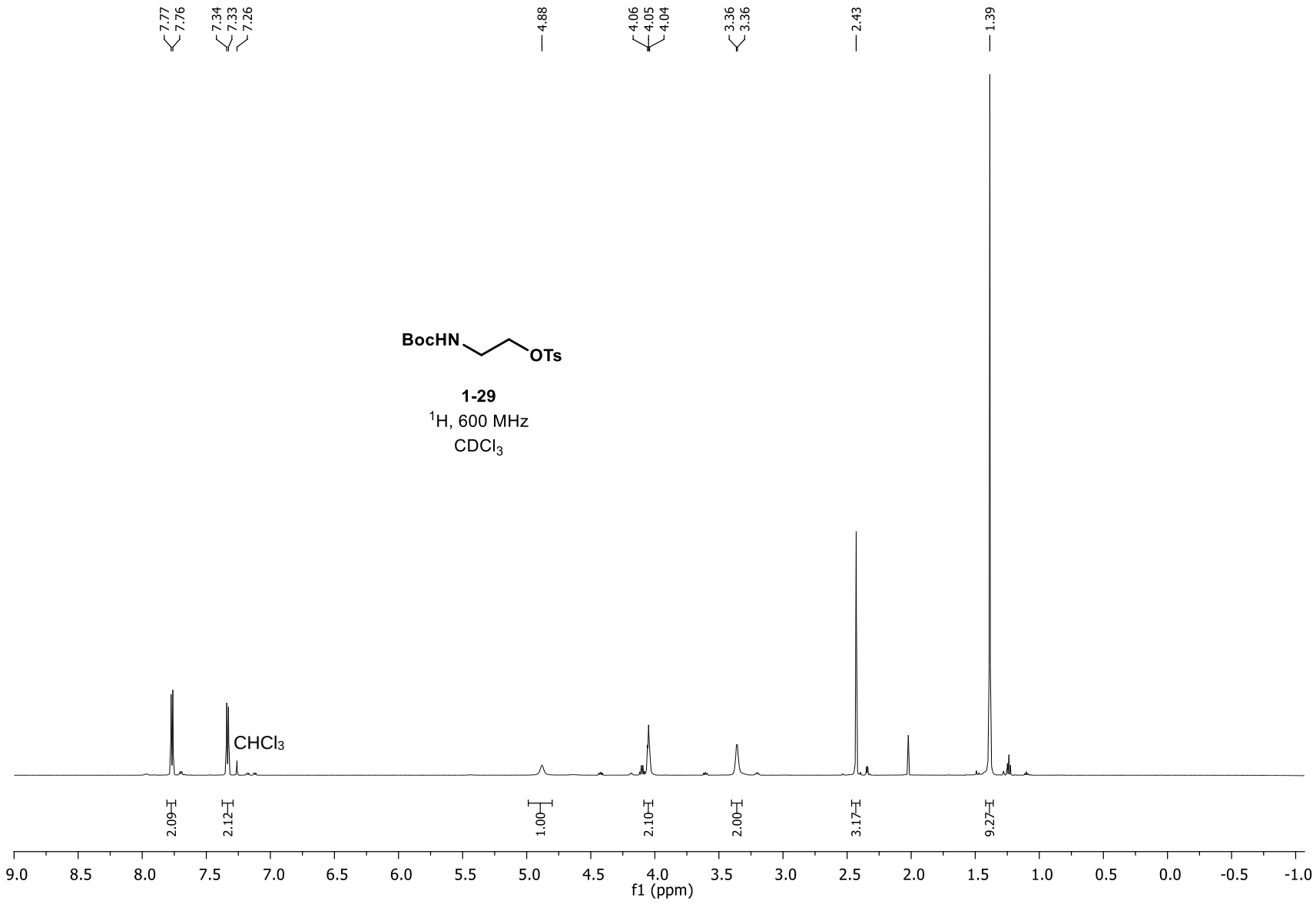
7.77
7.76
7.34
7.33
7.26
4.88
4.06
4.05
4.04
3.36
3.36
2.43
1.39
BocHN
OTs
1-29
1H, 600 MHz
CDCl3
CHCl3
2.09
2.12
1.00
2.10
2.00
3.17
9.27
9.0
8.5
8.0
7.5
7.0
6.5
6.0
5.5
5.0
4.5
4.0
3.5
3.0
2.5
2.0
1.5
1.0
0.5
0.0
-0.5
-1.0
f1 (ppm)

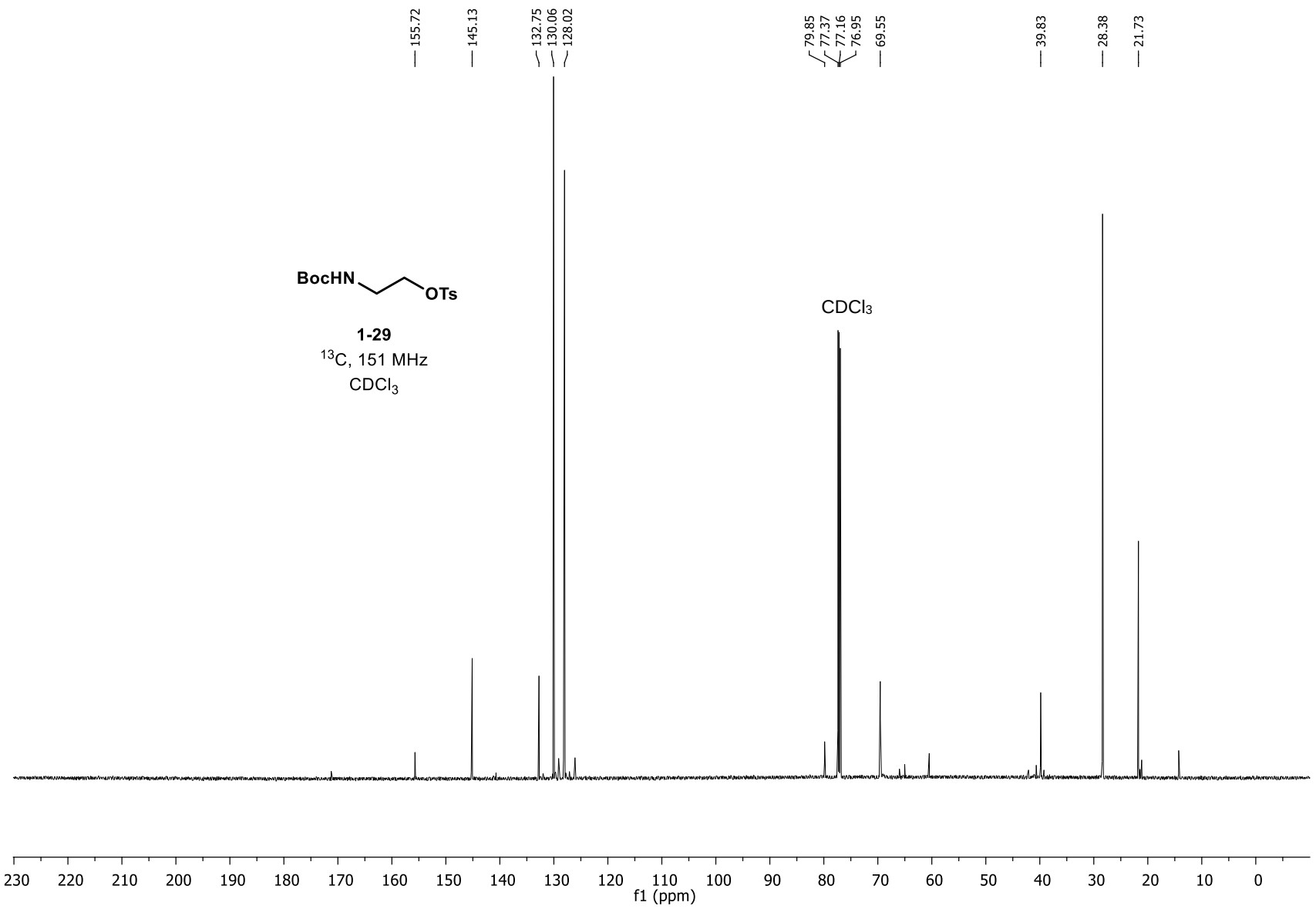
155.72
145.13
132.75
130.06
128.02
79.85
77.37
77.16
76.95
69.55
39.83
28.38
21.73
BocHN
OTs
1-29
13C, 151 MHz
CDCl3
CDCl3
230 220 210 200 190 180 170 160 150 140 130 120 110 100 90 80 70 60 50 40 30 20 10 0
f1 (ppm)

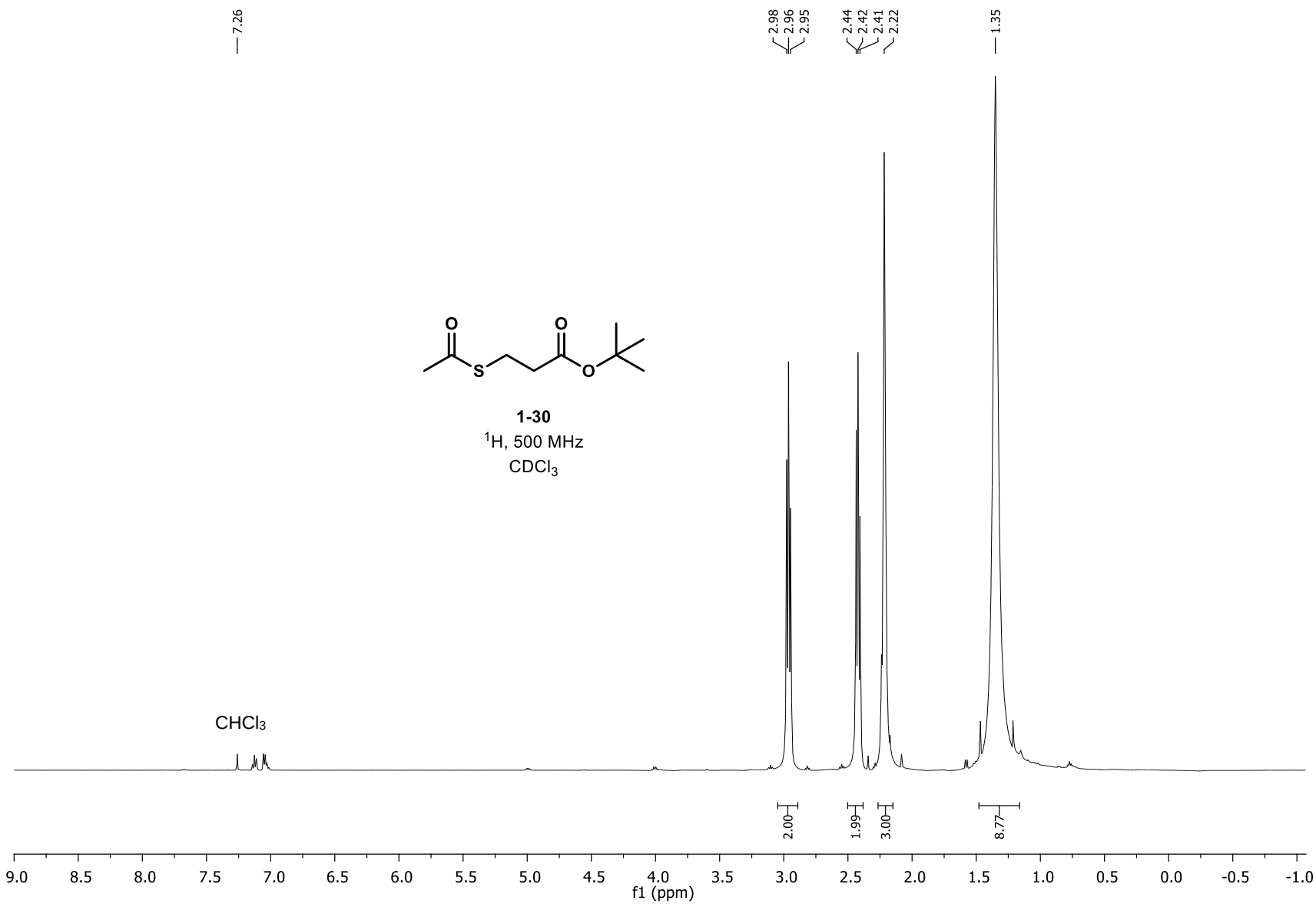
7.26
2.98
2.96
2.95
2.44
2.42
2.41
2.22
1.35
O
O
S
O
1-30
1H, 500 MHz
CDCl3
CHCl3
2.00
1.99
3.00
8.77
9.0
8.5
8.0
7.5
7.0
6.5
6.0
5.5
5.0
4.5
4.0
3.5
3.0
2.5
2.0
1.5
1.0
0.5
0.0
-0.5
-1.0
f1 (ppm)

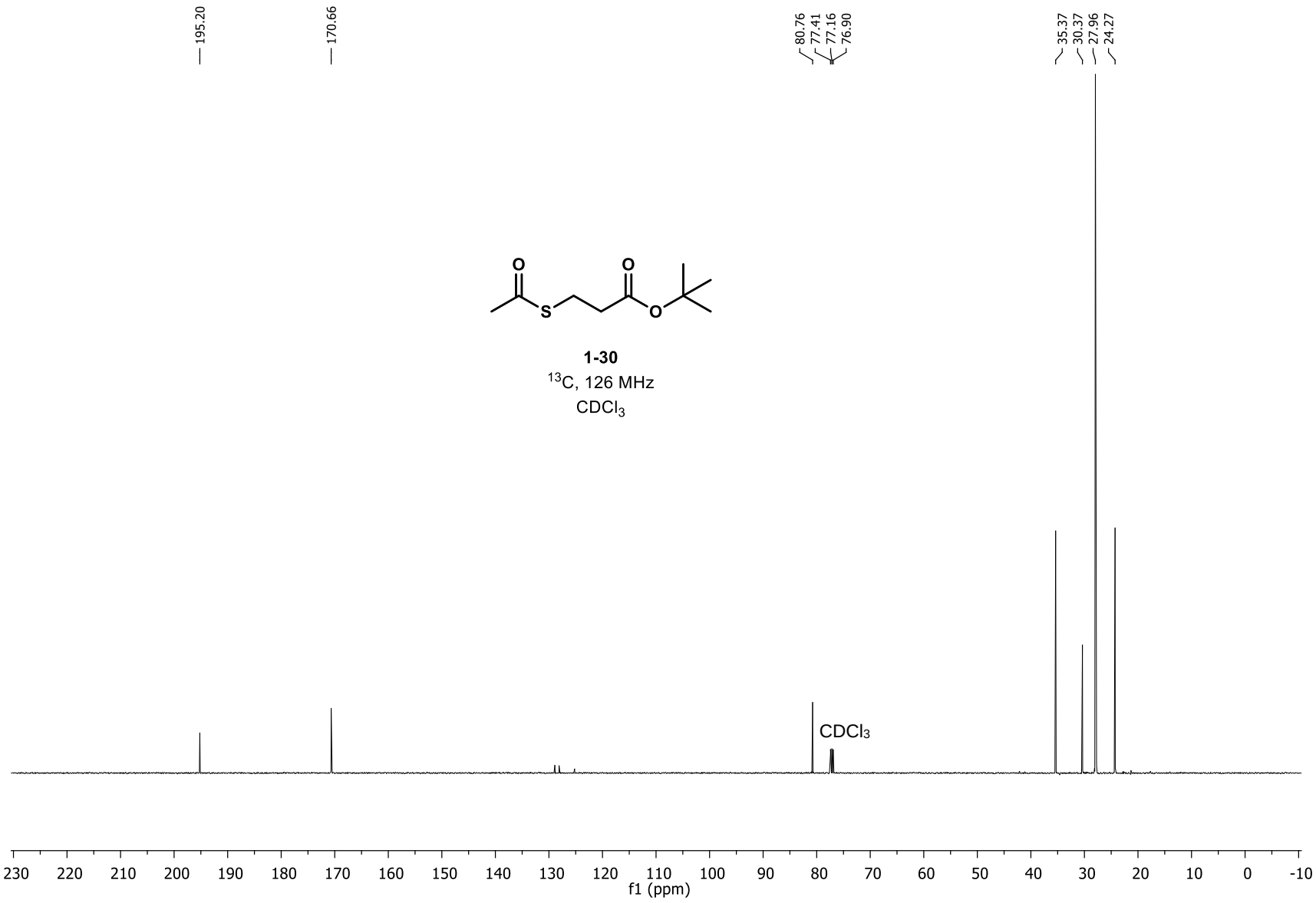
195.20
170.66
80.76
77.41
77.16
76.90
35.37
30.37
27.96
24.27
O
O
S
O
1-30
13C, 126 MHz
CDCl3
CDCl3
230 220 210 200 190 180 170 160 150 140 130 120 110 100 90 80 70 60 50 40 30 20 10 0 -10
f1 (ppm)

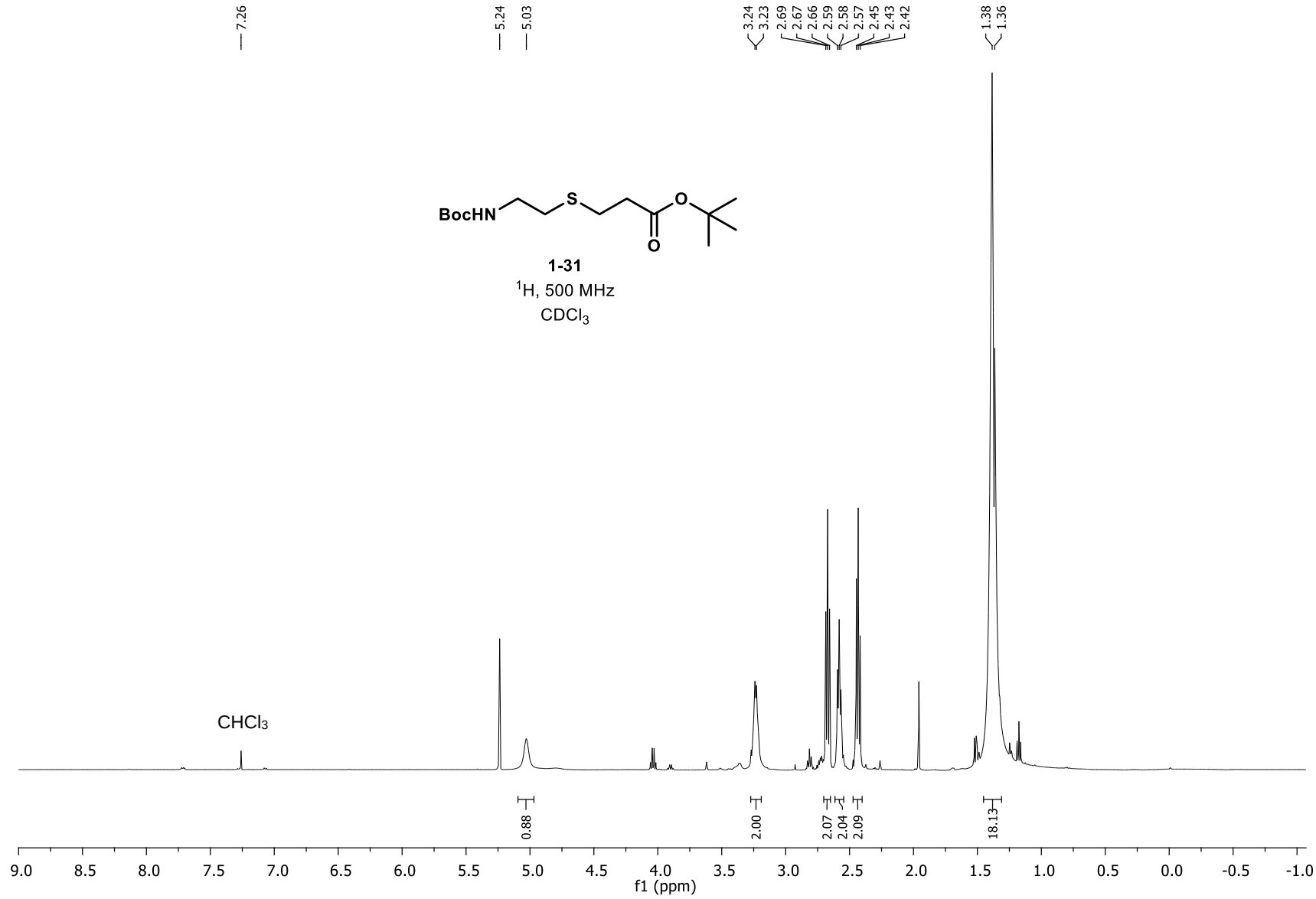
7.26
5.24
5.03
3.24
3.23
2.69
2.67
2.66
2.59
2.58
2.57
2.45
2.43
2.42
1.38
1.36
BocHN
S
O
O
1-31
1H, 500 MHz
CDCl3
CHCl3
0.88
2.00
2.07
2.04
2.09
18.13
9.0
8.5
8.0
7.5
7.0
6.5
6.0
5.5
5.0
4.5
4.0
3.5
3.0
2.5
2.0
1.5
1.0
0.5
0.0
-0.5
-1.0
f1 (ppm)

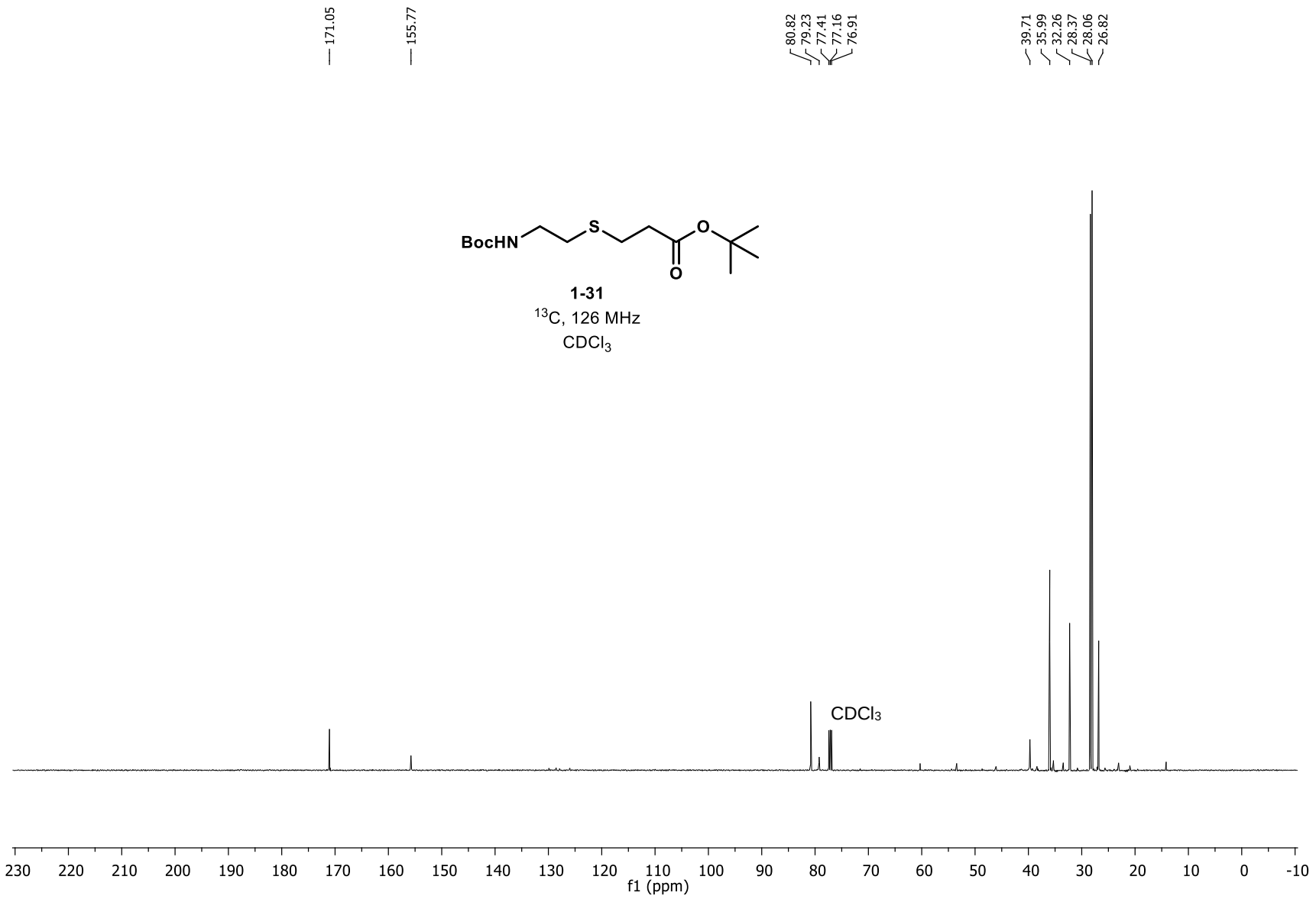
171.05
155.77
80.82
79.23
77.41
77.16
76.91
39.71
35.99
32.26
28.37
28.06
26.82
BocHN
S
O
O
1-31
13C, 126 MHz
CDCl3
CDCl3
230 220 210 200 190 180 170 160 150 140 130 120 110 100 90 80 70 60 50 40 30 20 10 0 -10
f1 (ppm)

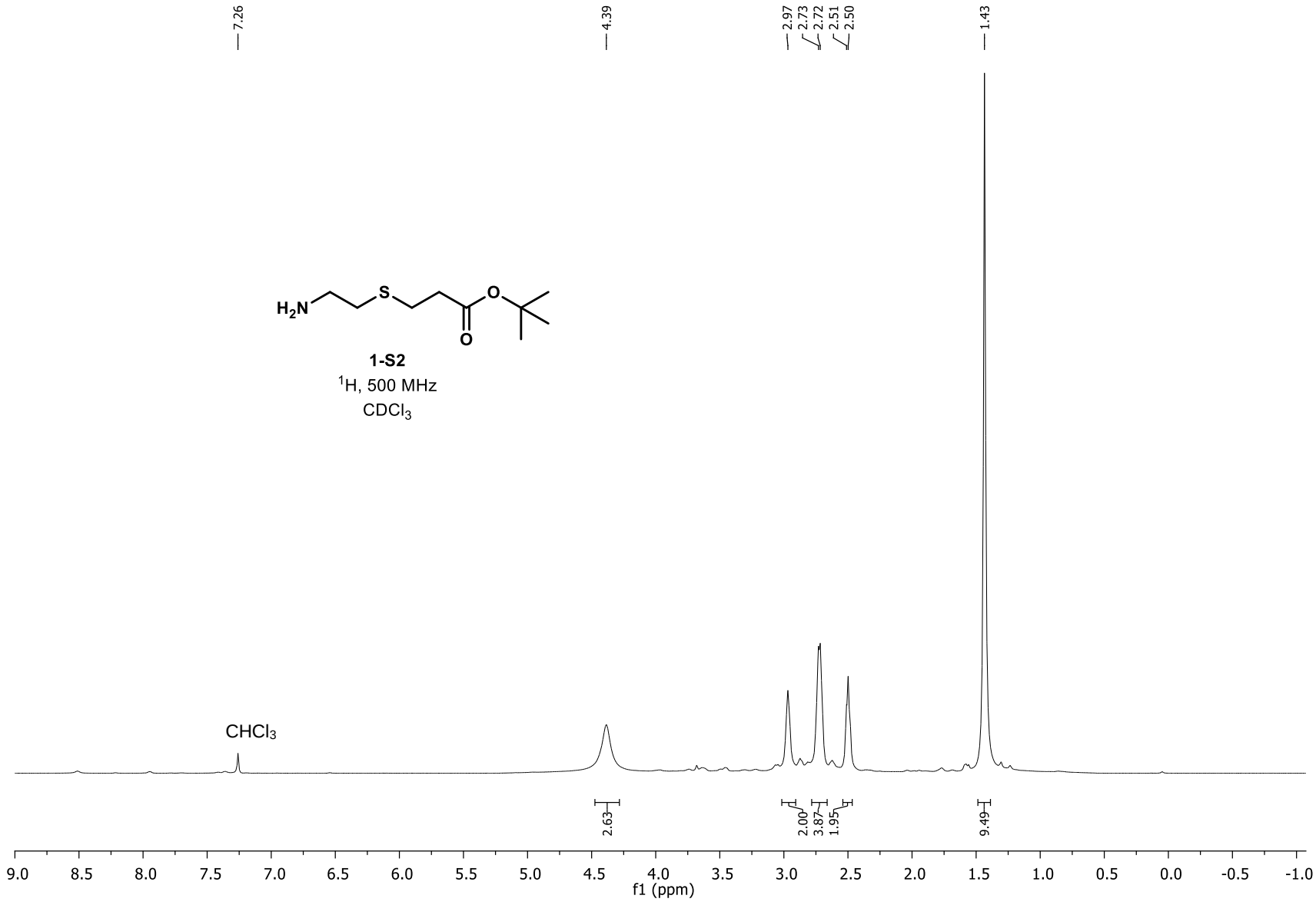
7.26
4.39
2.97
2.73
2.72
2.51
2.50
1.43
H2N
S
O
O
1-S2
1H, 500 MHz
CDCl3
CHCl3
2.63
2.00
3.87
1.95
9.49
9.0
8.5
8.0
7.5
7.0
6.5
6.0
5.5
5.0
4.5
4.0
3.5
3.0
2.5
2.0
1.5
1.0
0.5
0.0
-0.5
-1.0
f1 (ppm)

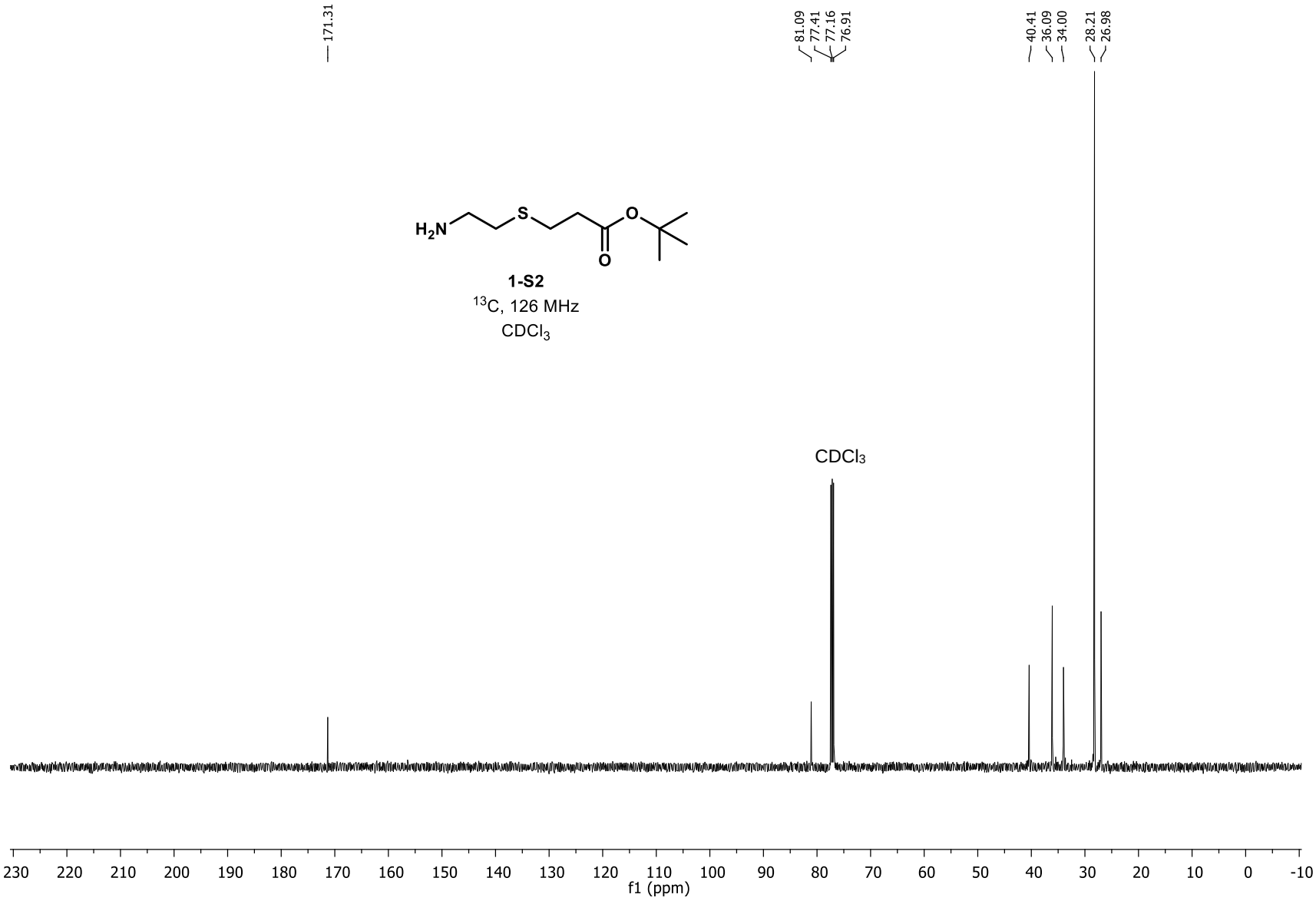
171.31
81.09
77.41
77.16
76.91
40.41
36.09
34.00
28.21
26.98
CDCl3
H2N
S
O
O
1-S2
13C, 126 MHz
CDCl3
230 220 210 200 190 180 170 160 150 140 130 120 110 100 90 80 70 60 50 40 30 20 10 0 -10
f1 (ppm)

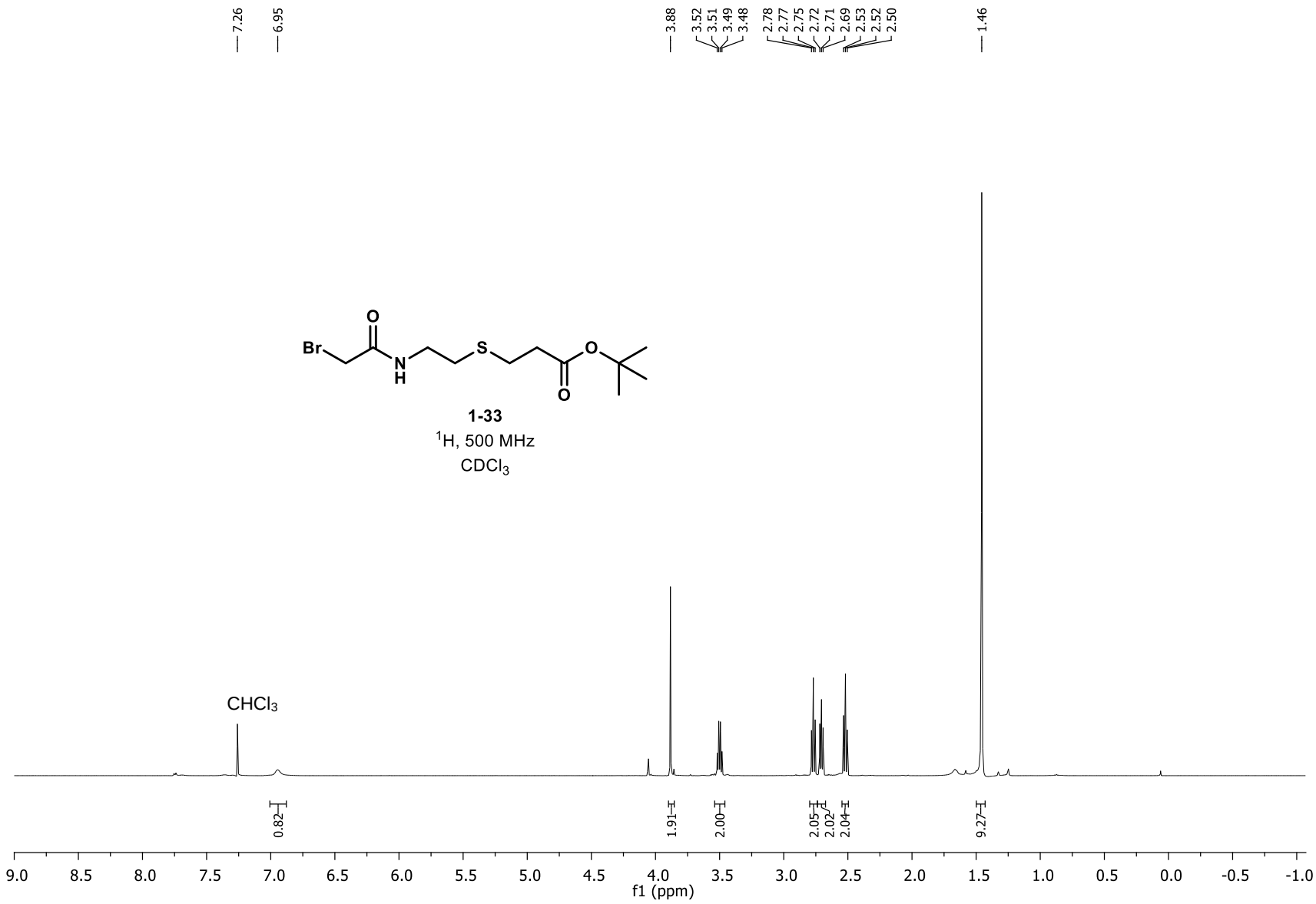
7.26
6.95
3.88
3.52
3.51
3.49
3.48
2.78
2.77
2.75
2.72
2.71
2.69
2.53
2.52
2.50
1.46
Br
O
N
H
S
O
O
1-33
1H, 500 MHz
CDCl3
CHCl3
0.82
1.91
2.00
2.05
2.02
2.04
9.27
9.0
8.5
8.0
7.5
7.0
6.5
6.0
5.5
5.0
4.5
4.0
3.5
3.0
2.5
2.0
1.5
1.0
0.5
0.0
-0.5
-1.0
f1 (ppm)

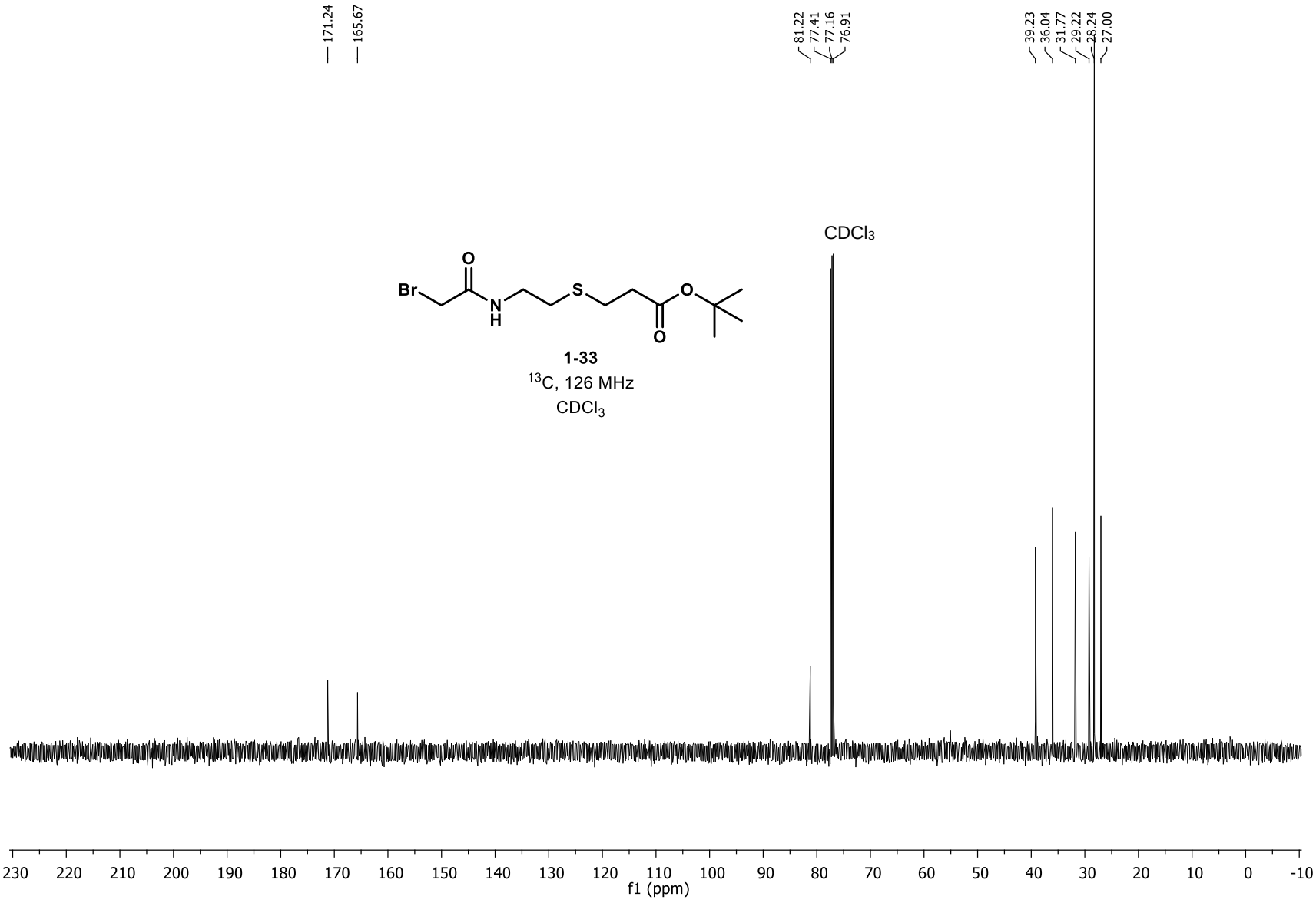
171.24
165.67
81.22
77.41
77.16
76.91
39.23
36.04
31.77
29.22
28.24
27.00
CDCl3
Br
O
N
H
S
O
O
1-33
13C, 126 MHz
CDCl3
230 220 210 200 190 180 170 160 150 140 130 120 110 100 90 80 70 60 50 40 30 20 10 0 -10
f1 (ppm)

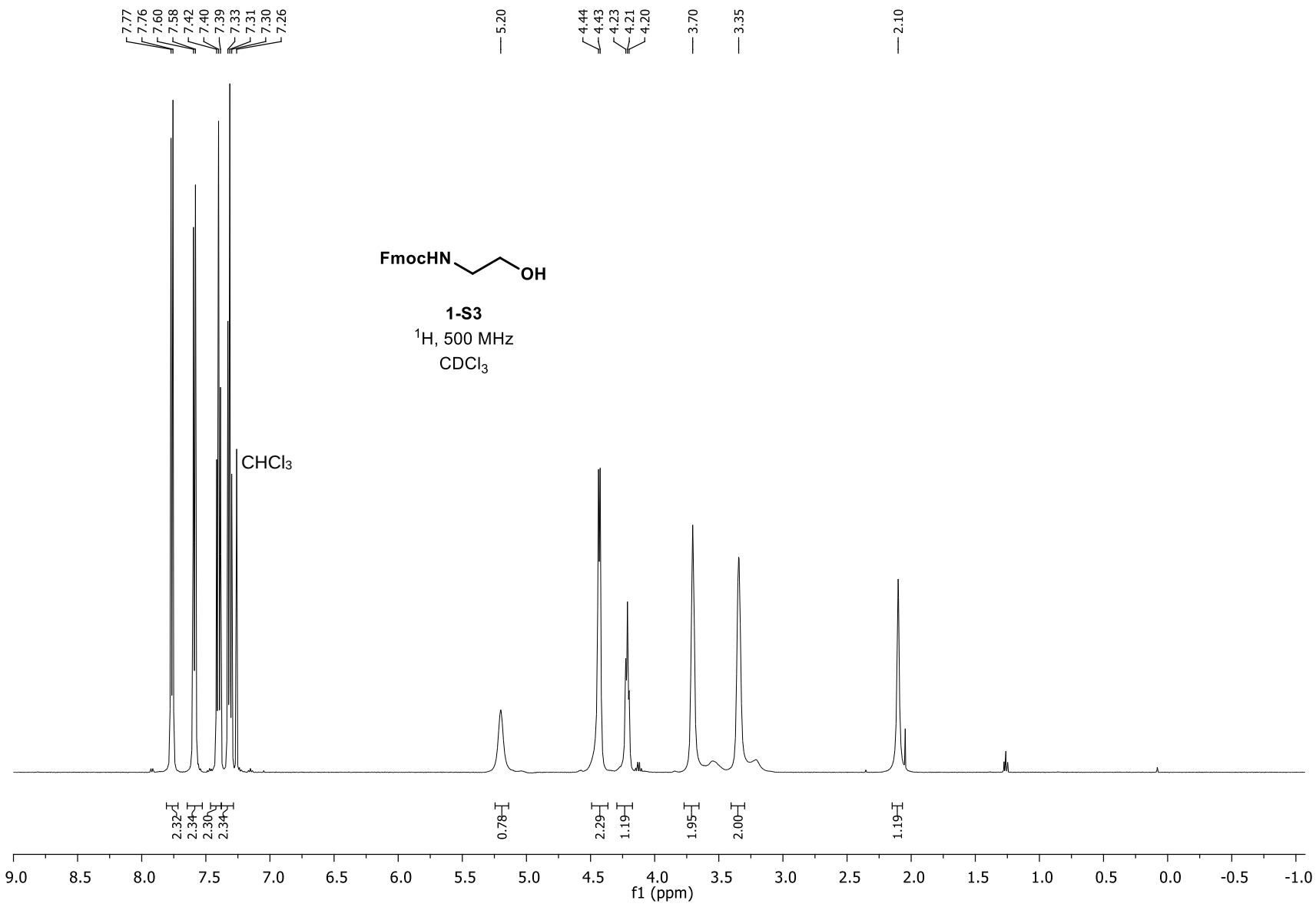
7.77
7.76
7.60
7.58
7.42
7.40
7.39
7.33
7.31
7.30
7.26
5.20
4.44
4.43
4.23
4.21
4.20
3.70
3.35
2.10
FmocHN
OH
1-S3
1H, 500 MHz
CDCl3
CHCl3
2.32
2.34
2.30
2.34
0.78
2.29
1.19
1.95
2.00
1.19
9.0
8.5
8.0
7.5
7.0
6.5
6.0
5.5
5.0
4.5
4.0
3.5
3.0
2.5
2.0
1.5
1.0
0.5
0.0
-0.5
-1.0
f1 (ppm)

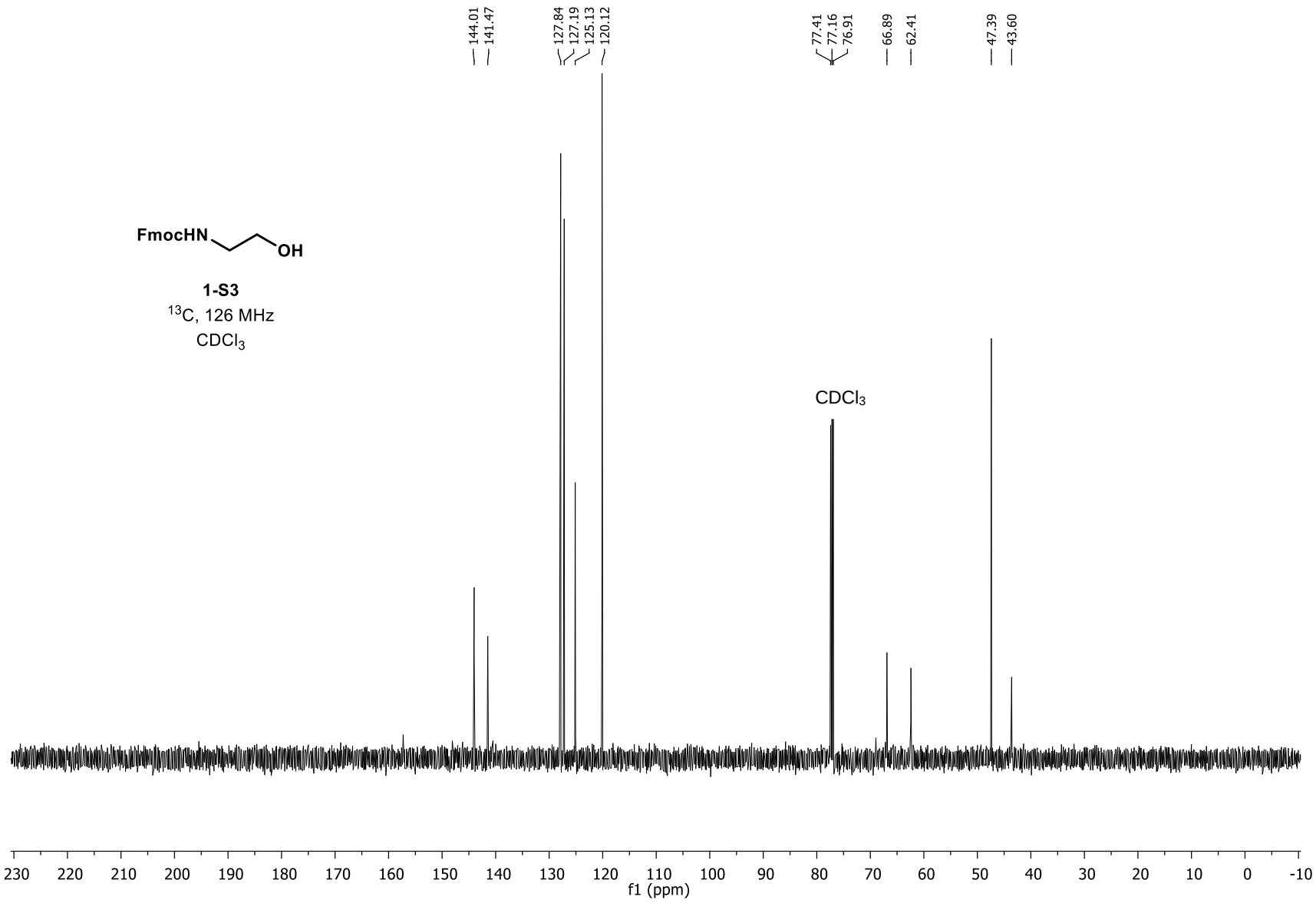
144.01
141.47
127.84
127.19
125.13
120.12
77.41
77.16
76.91
66.89
62.41
47.39
43.60
FmocHN
OH
1-S3
13C, 126 MHz
CDCl3
CDCl3
230 220 210 200 190 180 170 160 150 140 130 120 110 100 90 80 70 60 50 40 30 20 10 0 -10
f1 (ppm)

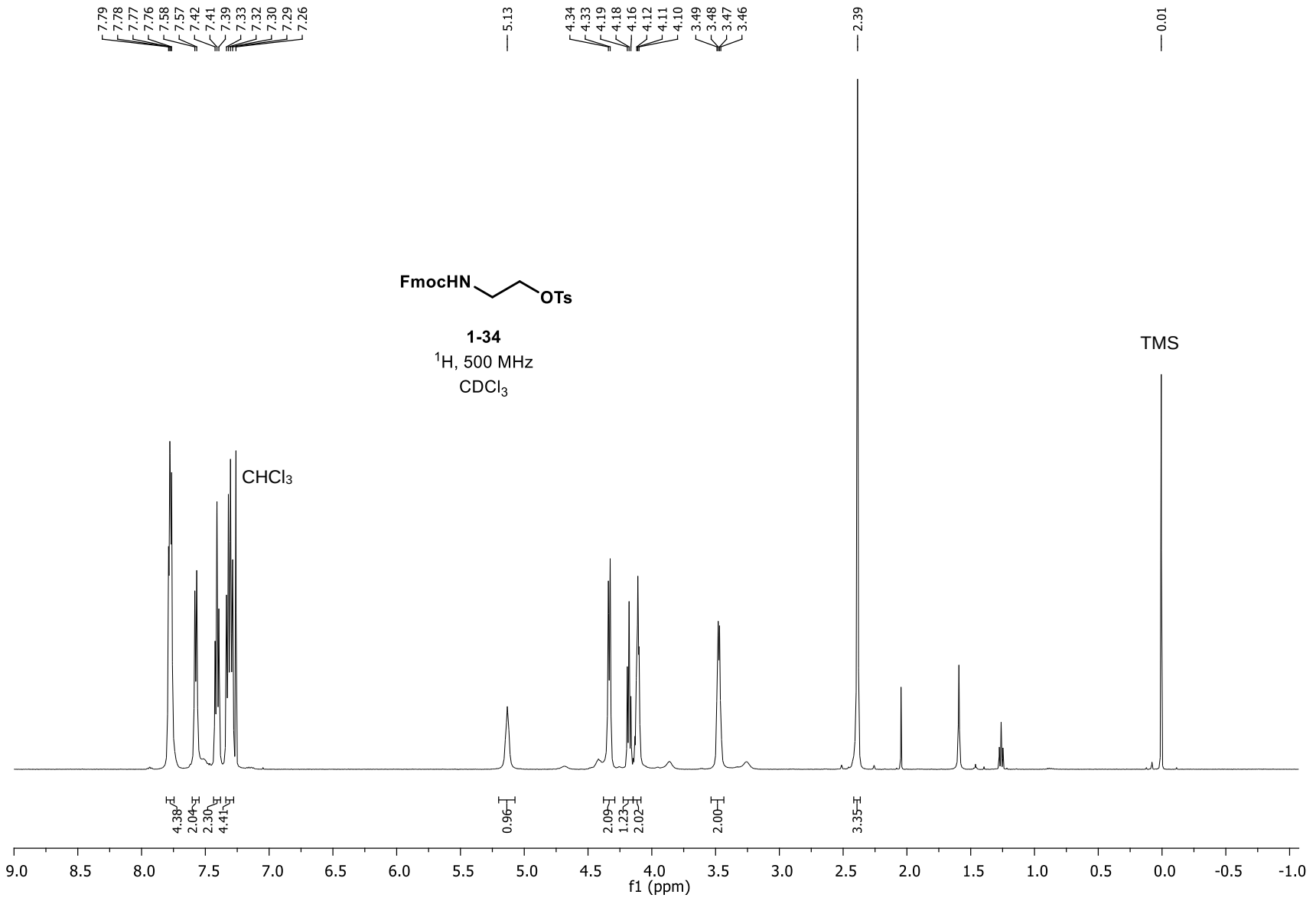
7.79
7.78
7.77
7.76
7.58
7.57
7.42
7.41
7.39
7.33
7.32
7.30
7.29
7.26
5.13
4.34
4.33
4.19
4.18
4.16
4.12
4.11
4.10
3.49
3.48
3.47
3.46
2.39
0.01
FmocHN
OTs
1-34
1H, 500 MHz
CDCl3
TMS
CHCl3
4.38
2.04
2.30
4.41
0.96
2.09
1.23
2.02
2.00
3.35
9.0
8.5
8.0
7.5
7.0
6.5
6.0
5.5
5.0
4.5
4.0
3.5
3.0
2.5
2.0
1.5
1.0
0.5
0.0
-0.5
-1.0
f1 (ppm)

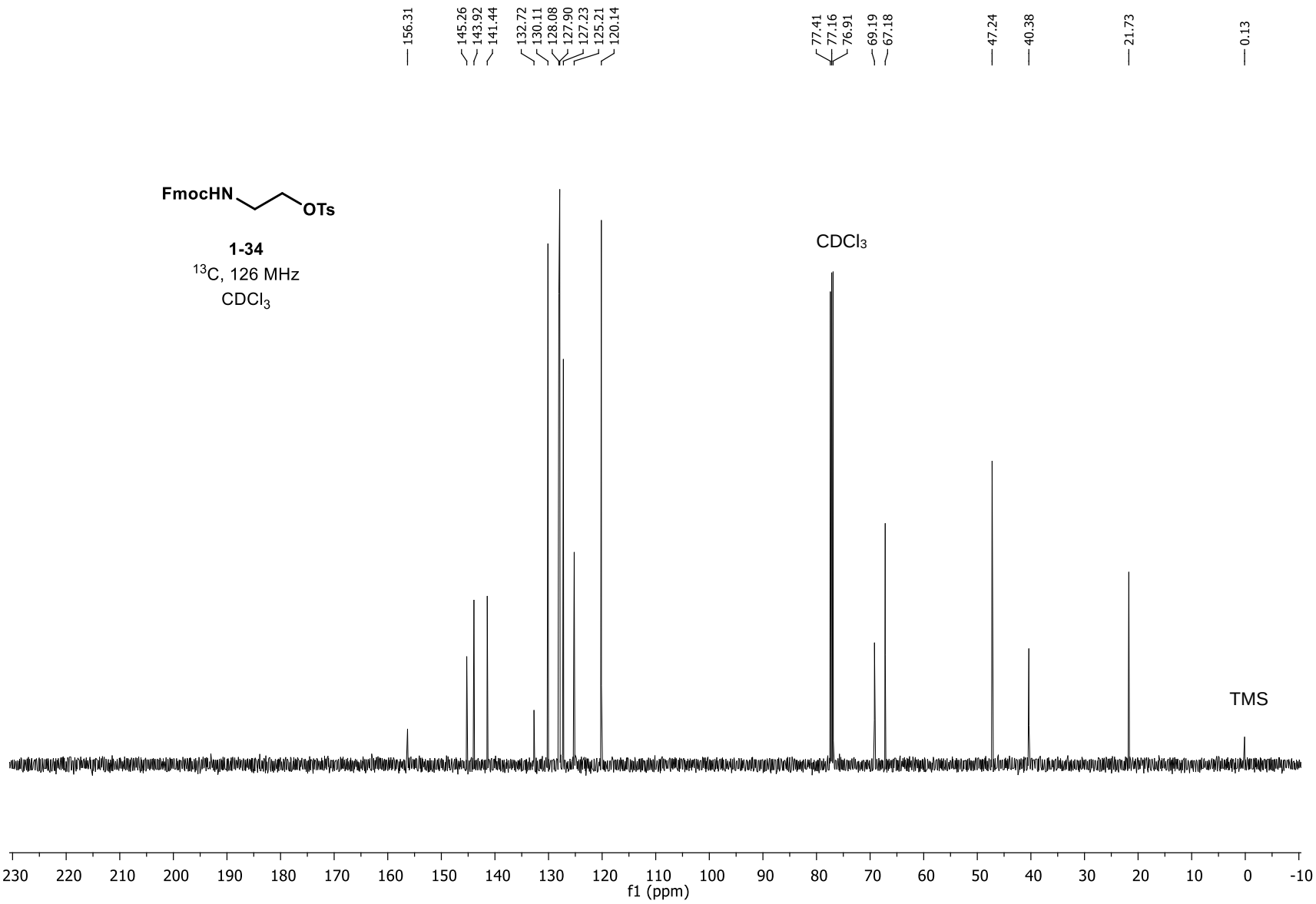
156.31
145.26
143.92
141.44
132.72
130.11
128.08
127.90
127.23
125.21
120.14
77.41
77.16
76.91
69.19
67.18
47.24
40.38
21.73
0.13
FmocHN
OTs
1-34
13C, 126 MHz
CDCl3
CDCl3
TMS
230 220 210 200 190 180 170 160 150 140 130 120 110 100 90 80 70 60 50 40 30 20 10 0 -10
f1 (ppm)

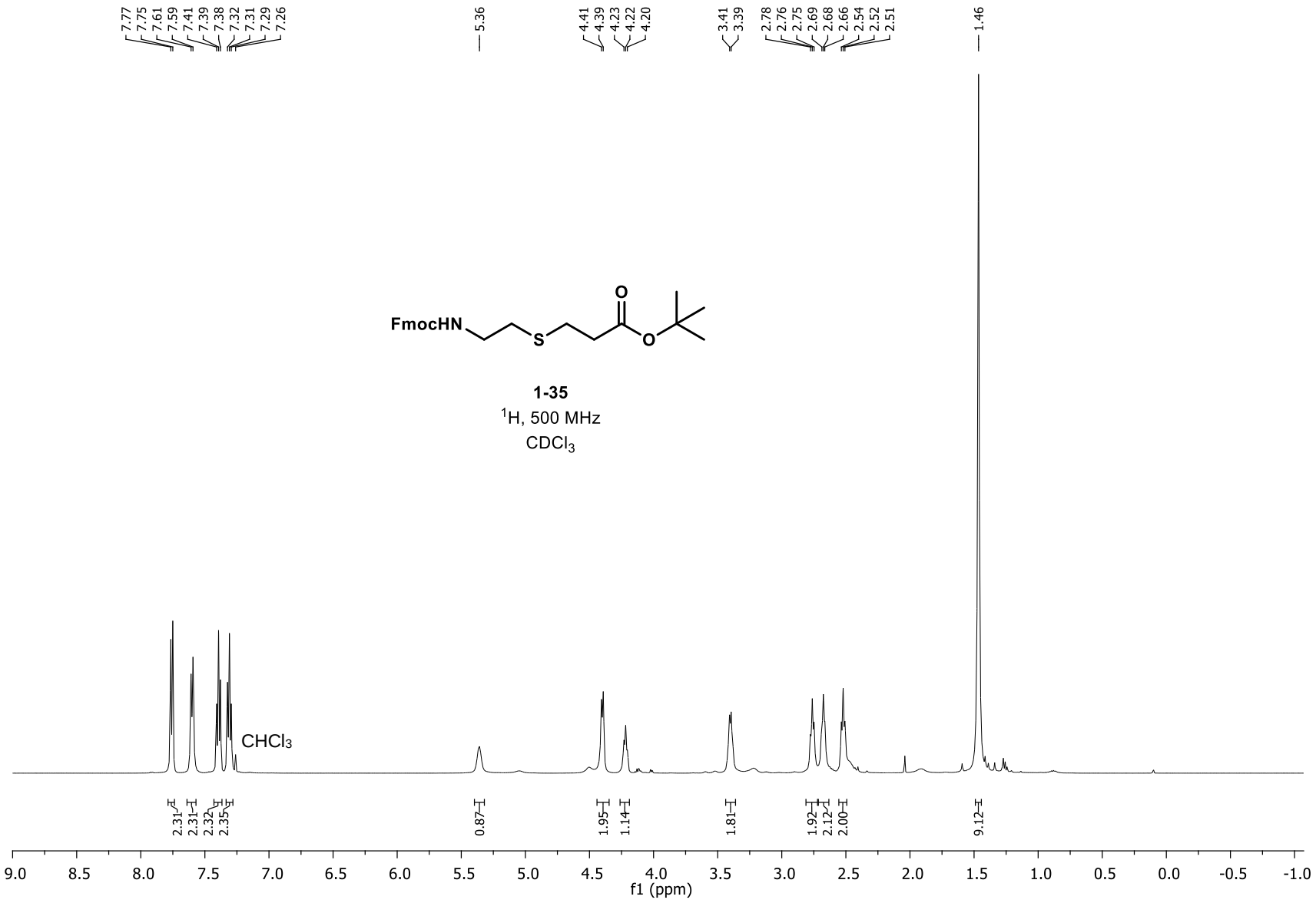
7.77
7.75
7.61
7.59
7.41
7.39
7.38
7.32
7.31
7.29
7.26
5.36
4.41
4.39
4.23
4.22
4.20
3.41
3.39
2.78
2.76
2.75
2.69
2.68
2.66
2.54
2.52
2.51
1.46
FmocHN
S
O
O
1-35
1H, 500 MHz
CDCl3
CHCl3
2.31
2.31
2.32
2.35
0.87
1.95
1.14
1.81
1.92
2.12
2.00
9.12
9.0
8.5
8.0
7.5
7.0
6.5
6.0
5.5
5.0
4.5
4.0
3.5
3.0
2.5
2.0
1.5
1.0
0.5
0.0
-0.5
-1.0
f1 (ppm)

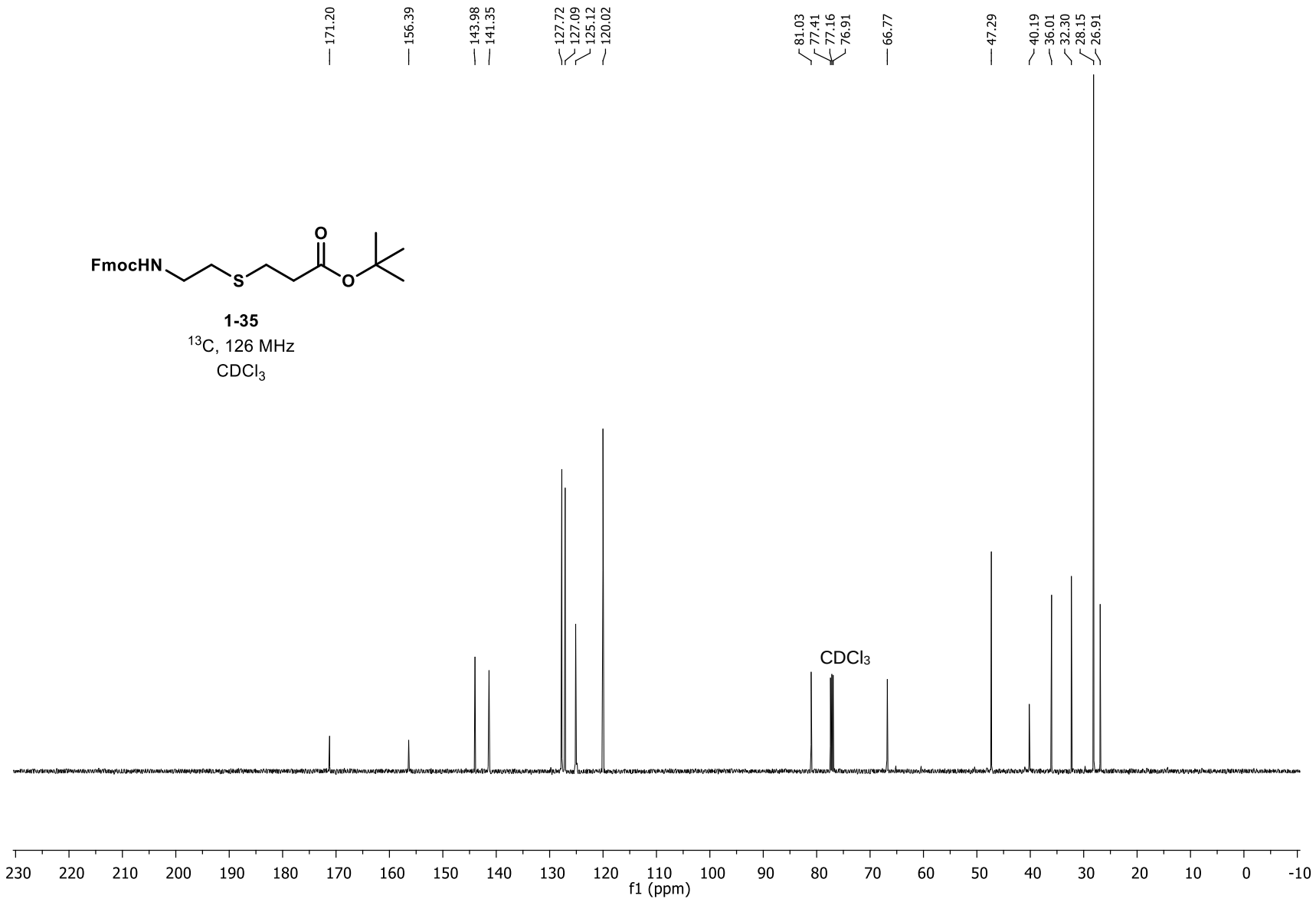
171.20
156.39
143.98
141.35
127.72
127.09
125.12
120.02
81.03
77.41
77.16
76.91
66.77
47.29
40.19
36.01
32.30
28.15
26.91
FmocHN
S
O
O
1-35
13C, 126 MHz
CDCl3
CDCl3
230 220 210 200 190 180 170 160 150 140 130 120 110 100 90 80 70 60 50 40 30 20 10 0 -10
f1 (ppm)

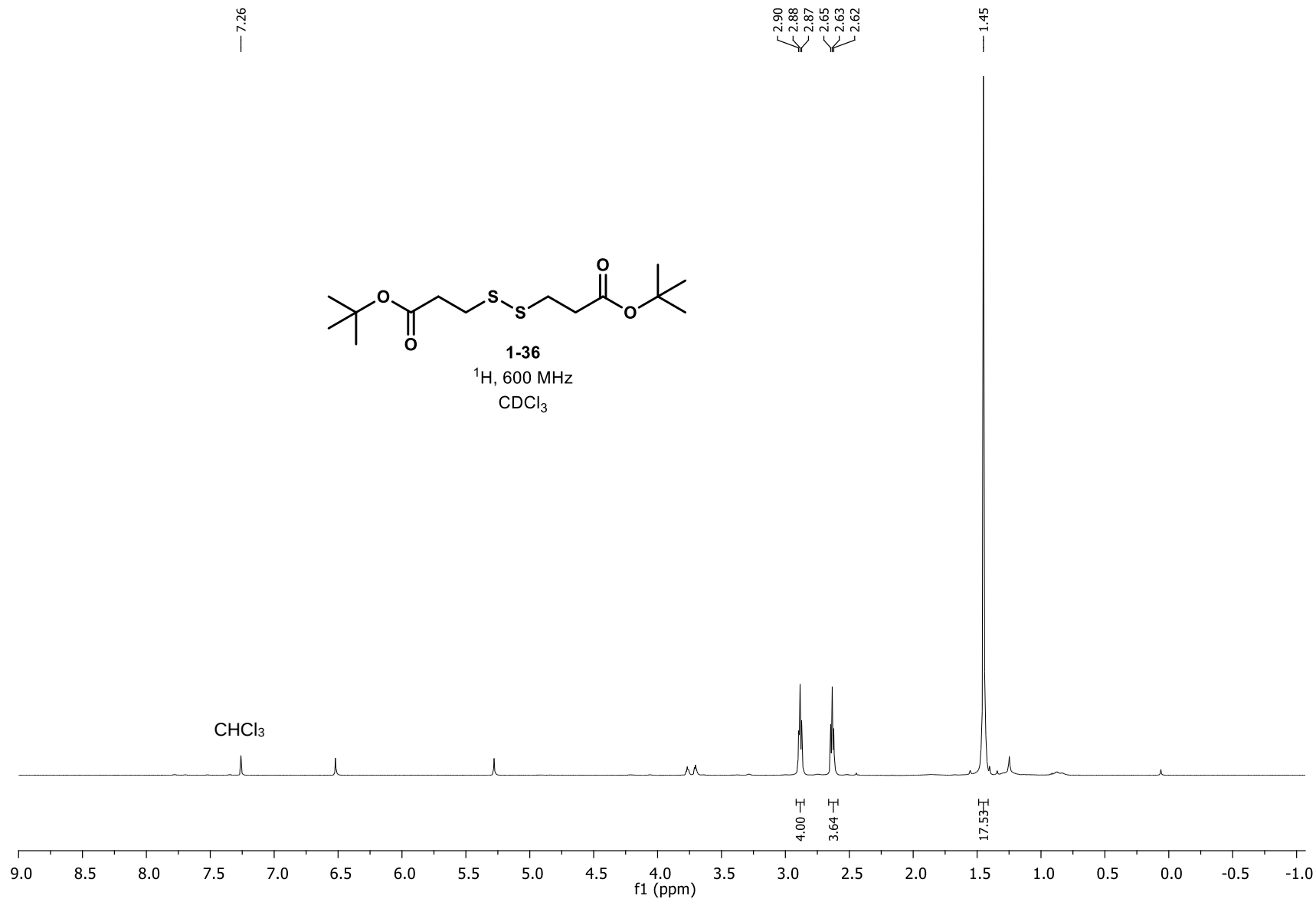
7.26
2.90
2.88
2.87
2.65
2.63
2.62
1.45
O
O
S
S
O
O
O
1-36
1H, 600 MHz
CDCl3
CHCl3
4.00
3.64
17.53
9.0
8.5
8.0
7.5
7.0
6.5
6.0
5.5
5.0
4.5
4.0
3.5
3.0
2.5
2.0
1.5
1.0
0.5
0.0
-0.5
-1.0
f1 (ppm)

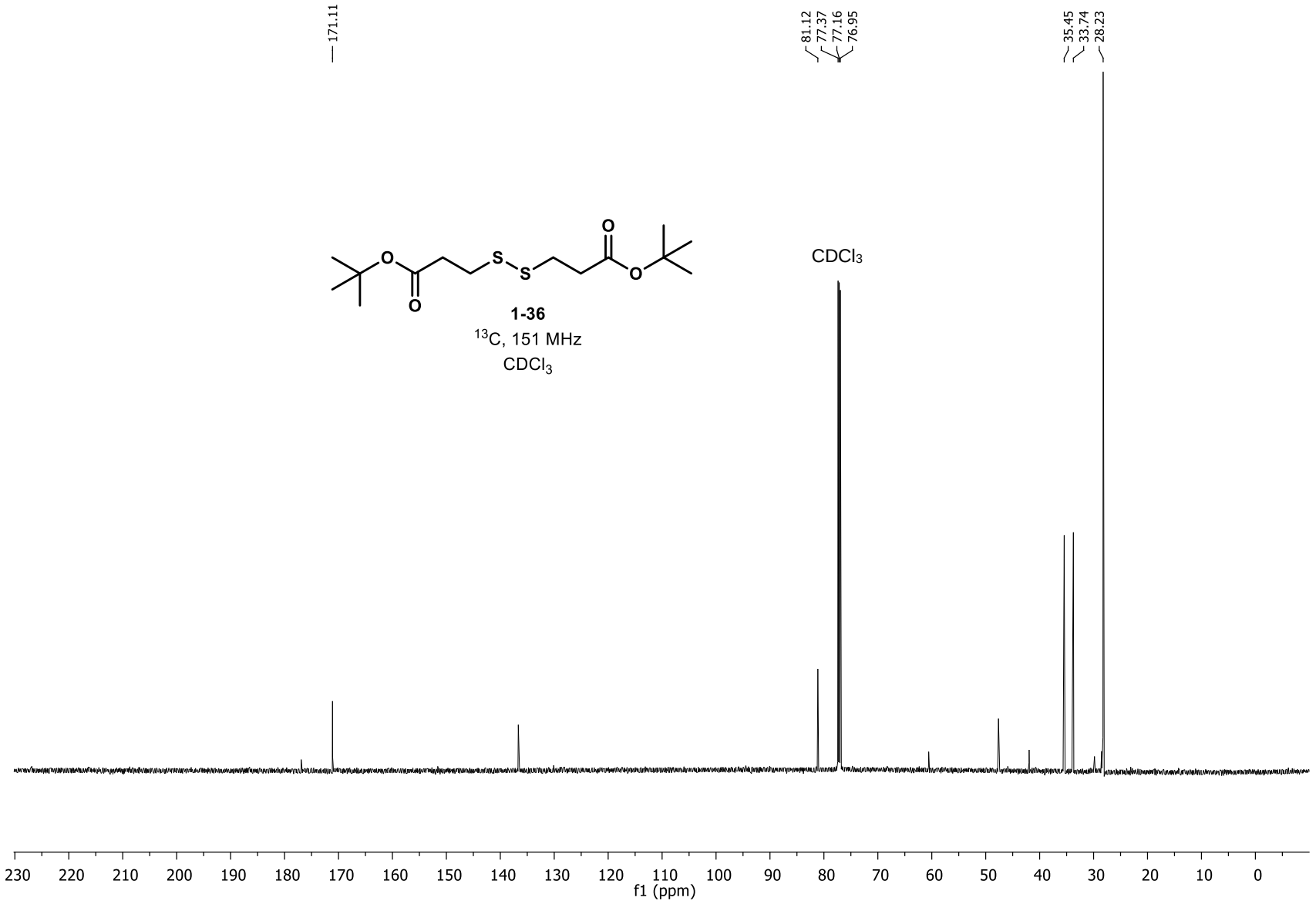
171.11
81.12
77.37
77.16
76.95
35.45
33.74
28.23
CDCl3
O
O
S
S
O
O
1-36
13C, 151 MHz
CDCl3
230
220
210
200
190
180
170
160
150
140
130
120
110
100
90
80
70
60
50
40
30
20
10
0
f1 (ppm)

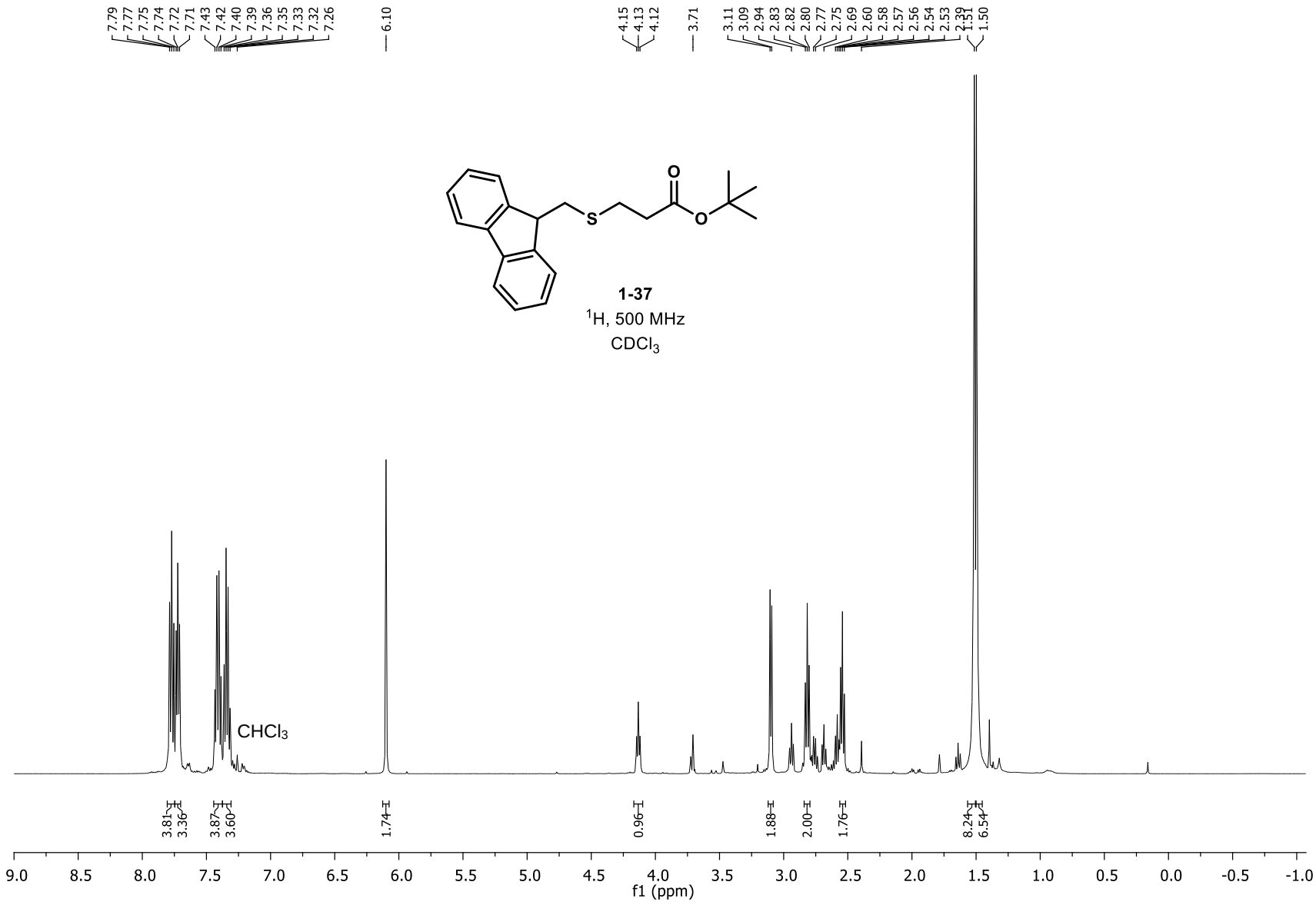
7.79
7.77
7.75
7.74
7.72
7.71
7.43
7.42
7.40
7.39
7.36
7.35
7.33
7.32
7.26
6.10
4.15
4.13
4.12
3.71
3.11
3.09
2.94
2.83
2.82
2.80
2.77
2.75
2.69
2.60
2.58
2.57
2.56
2.54
2.53
1.51
1.50
O
S
O
1-37
1H, 500 MHz
CDCl3
CHCl3
3.81
3.36
3.87
3.60
1.74
0.96
1.88
2.00
1.76
8.24
6.54
9.0
8.5
8.0
7.5
7.0
6.5
6.0
5.5
5.0
4.5
4.0
3.5
3.0
2.5
2.0
1.5
1.0
0.5
0.0
-0.5
-1.0
f1 (ppm)

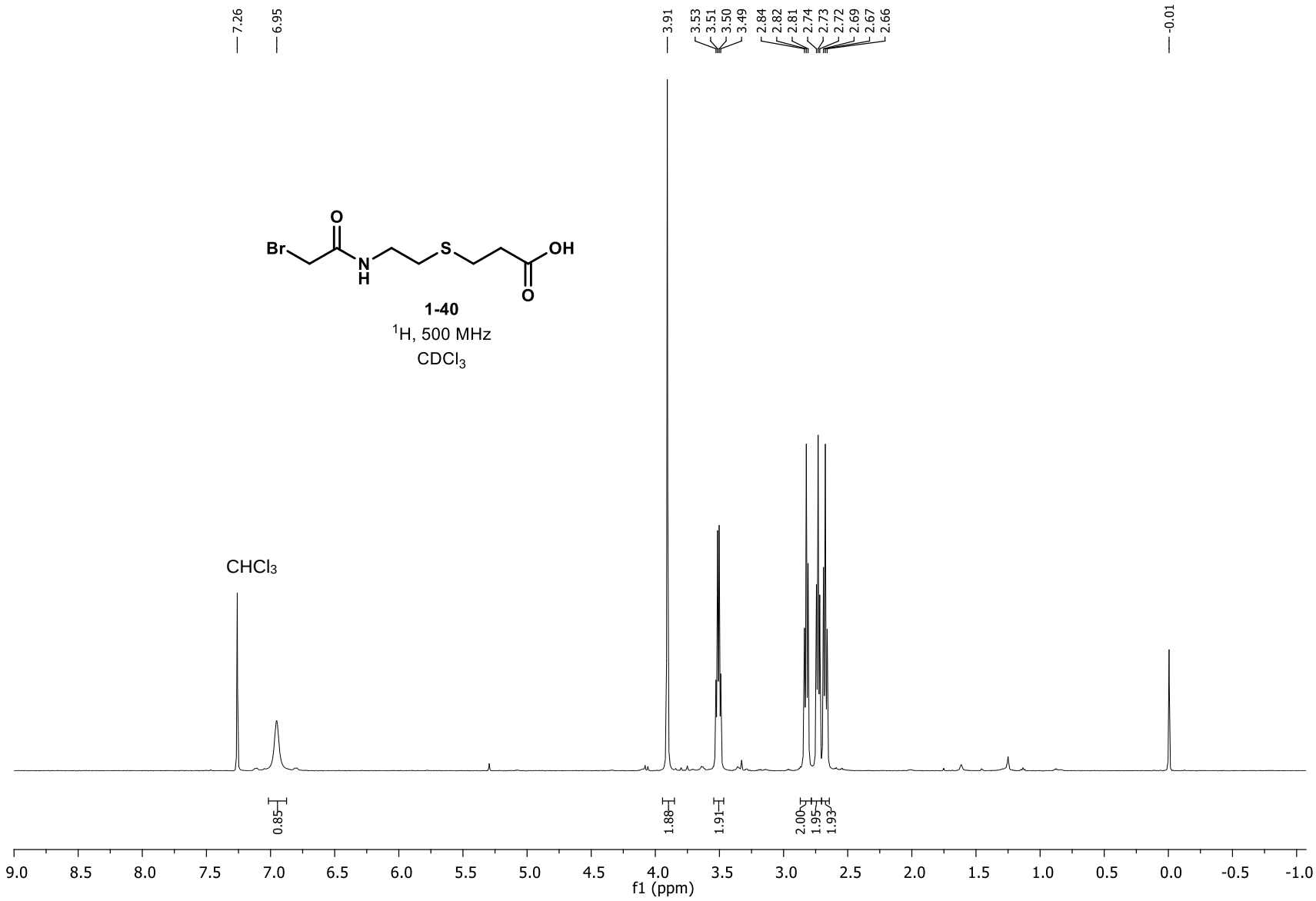
7.26
6.95
3.91
3.53
3.51
3.50
3.49
2.84
2.82
2.81
2.74
2.73
2.72
2.69
2.67
2.66
-0.01
Br
O
N
H
S
OH
O
1-40
1H, 500 MHz
CDCl3
CHCl3
0.85
1.88
1.91
2.00
1.95
1.93
9.0
8.5
8.0
7.5
7.0
6.5
6.0
5.5
5.0
4.5
4.0
3.5
3.0
2.5
2.0
1.5
1.0
0.5
0.0
-0.5
-1.0
f1 (ppm)

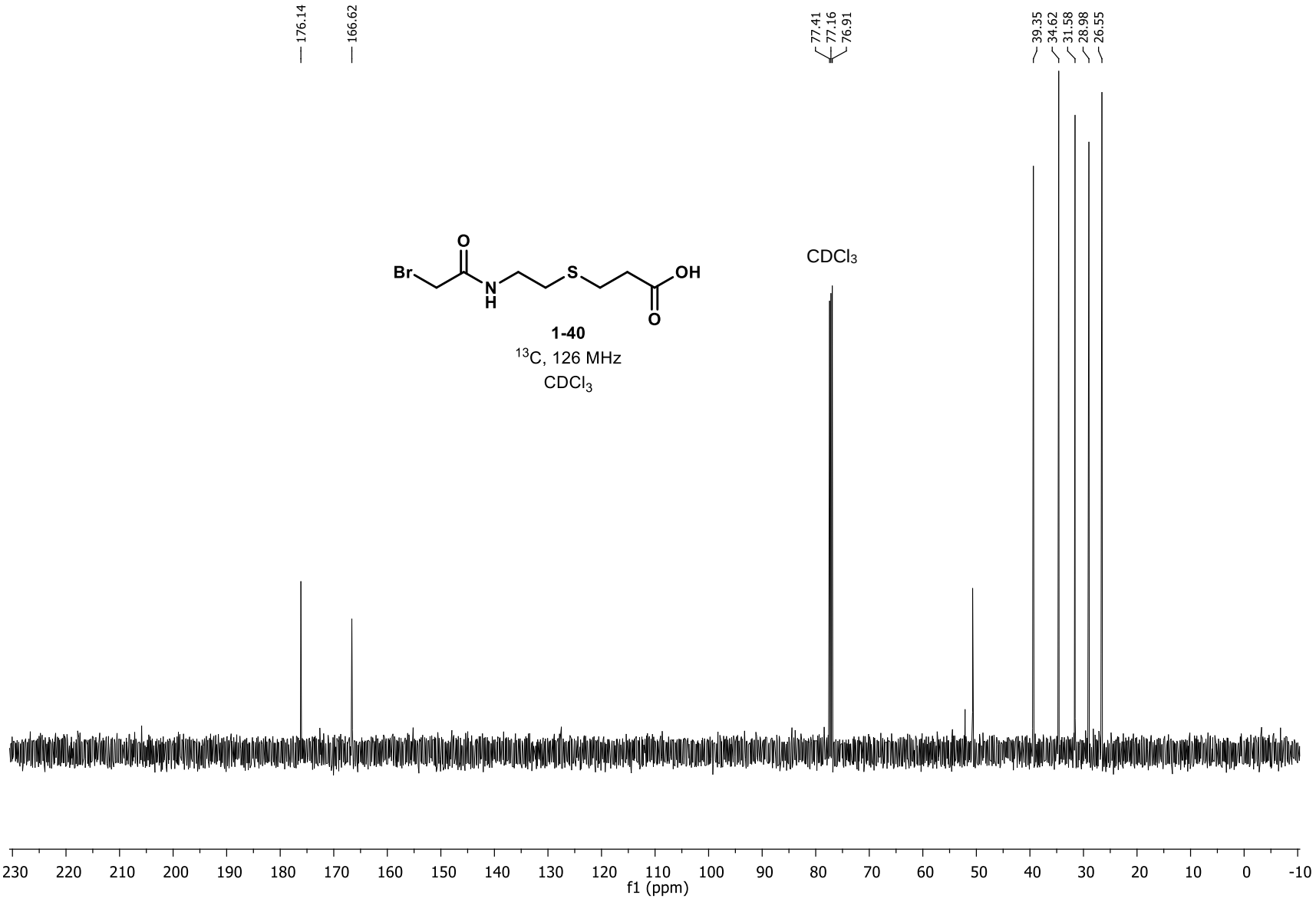
176.14
166.62
77.41
77.16
76.91
39.35
34.62
31.58
28.98
26.55
CDCl3
Br
O
N
H
S
OH
O
1-40
13C, 126 MHz
CDCl3
230 220 210 200 190 180 170 160 150 140 130 120 110 100 90 80 70 60 50 40 30 20 10 0 -10
f1 (ppm)

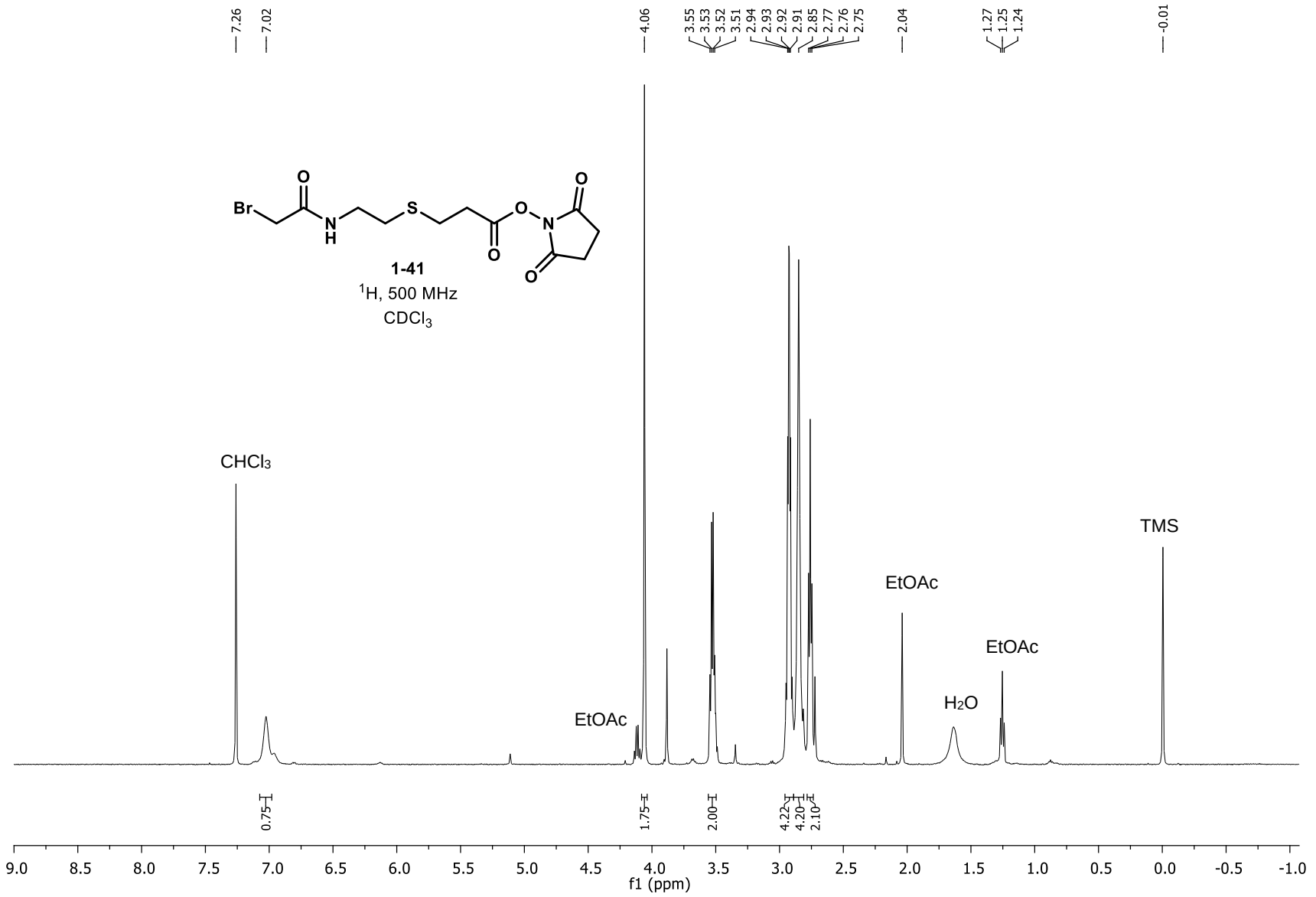
7.26
7.02
4.06
3.55
3.53
3.52
3.51
2.94
2.93
2.92
2.91
2.85
2.77
2.76
2.75
2.04
1.27
1.25
1.24
-0.01
Br
O
N
H
S
O
O
N
O
O
O
1-41
1H, 500 MHz
CDCl3
CHCl3
EtOAc
EtOAc
H2O
EtOAc
TMS
0.75
1.75
2.00
4.22
4.20
2.10
9.0
8.5
8.0
7.5
7.0
6.5
6.0
5.5
5.0
4.5
4.0
3.5
3.0
2.5
2.0
1.5
1.0
0.5
0.0
-0.5
-1.0
f1 (ppm)

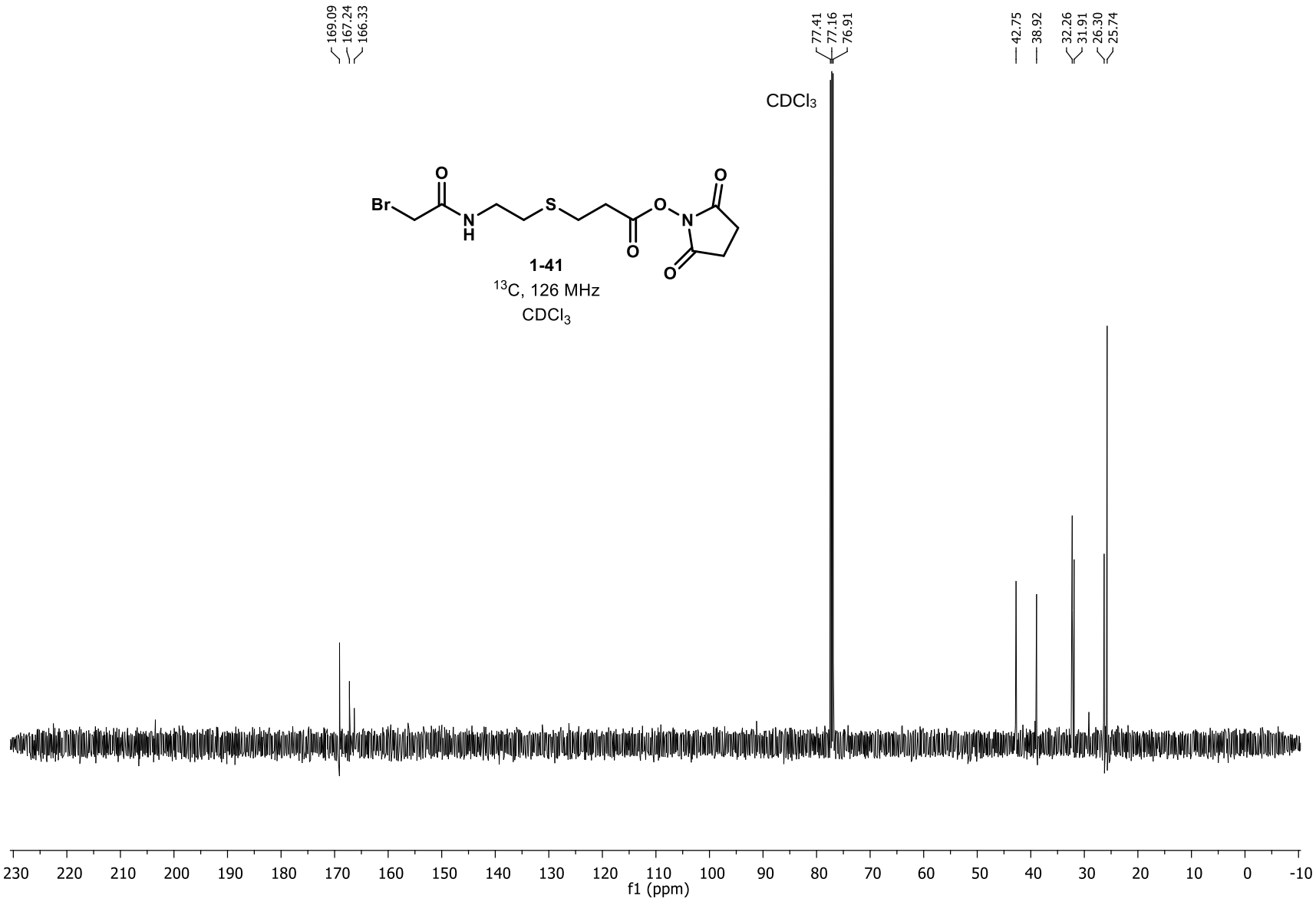
169.09
167.24
166.33
77.41
77.16
76.91
42.75
38.92
32.26
31.91
26.30
25.74
CDCl3
Br
O
N
H
S
O
O
N
O
O
O
1-41
13C, 126 MHz
CDCl3
230 220 210 200 190 180 170 160 150 140 130 120 110 100 90 80 70 60 50 40 30 20 10 0 -10
f1 (ppm)

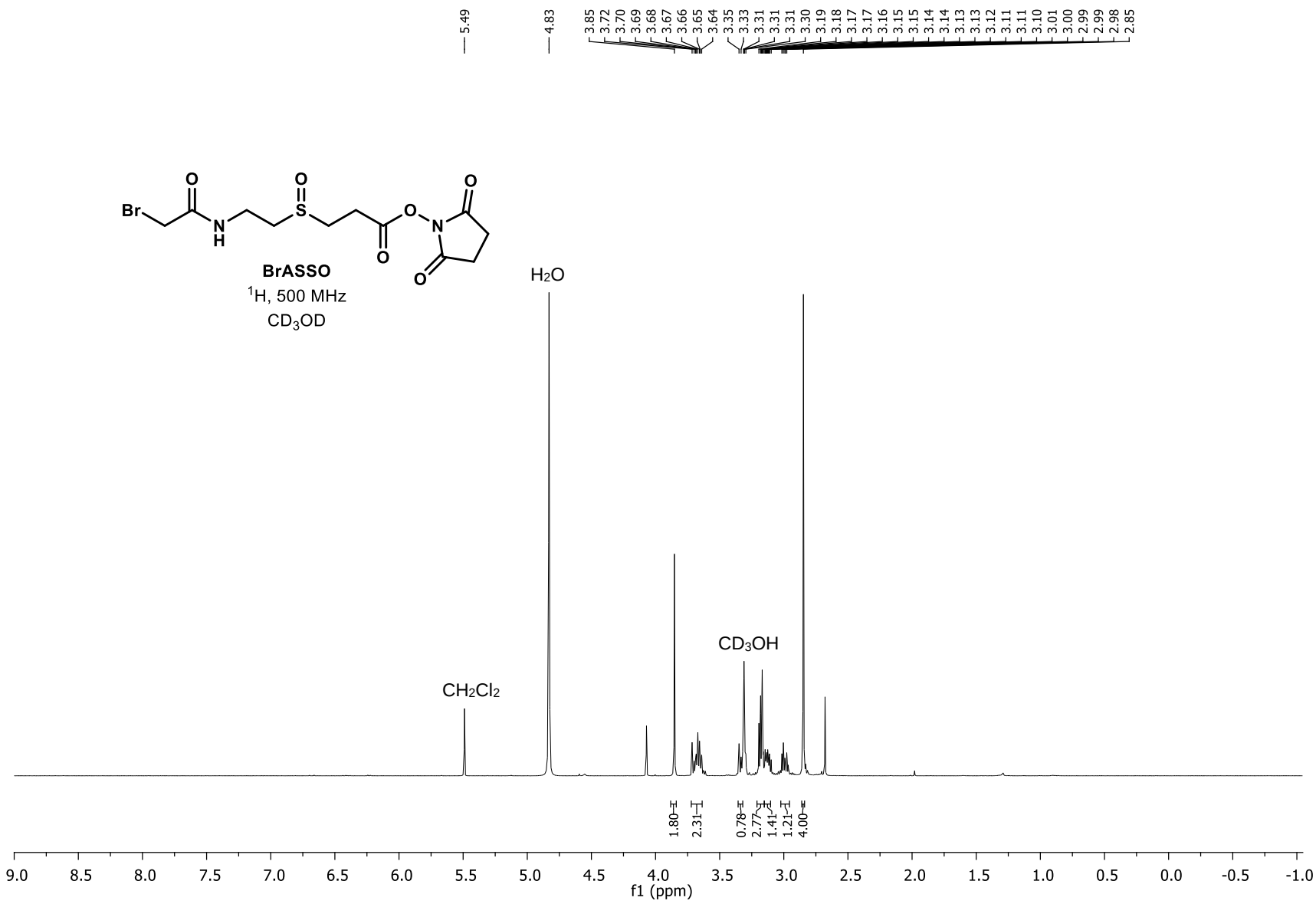
5.49
4.83
3.85
3.72
3.70
3.69
3.68
3.67
3.66
3.65
3.64
3.35
3.33
3.31
3.31
3.31
3.30
3.19
3.18
3.17
3.17
3.16
3.15
3.15
3.14
3.14
3.13
3.13
3.12
3.11
3.11
3.10
3.01
3.00
2.99
2.99
2.98
2.85
Br
O
N
H
S
O
O
O
N
O
O
BrASSO
1H, 500 MHz
CD3OD
H2O
CD3OH
CH2Cl2
1.80
2.31
0.78
2.77
1.41
1.21
4.00
9.0
8.5
8.0
7.5
7.0
6.5
6.0
5.5
5.0
4.5
4.0
3.5
3.0
2.5
2.0
1.5
1.0
0.5
0.0
-0.5
-1.0
f1 (ppm)

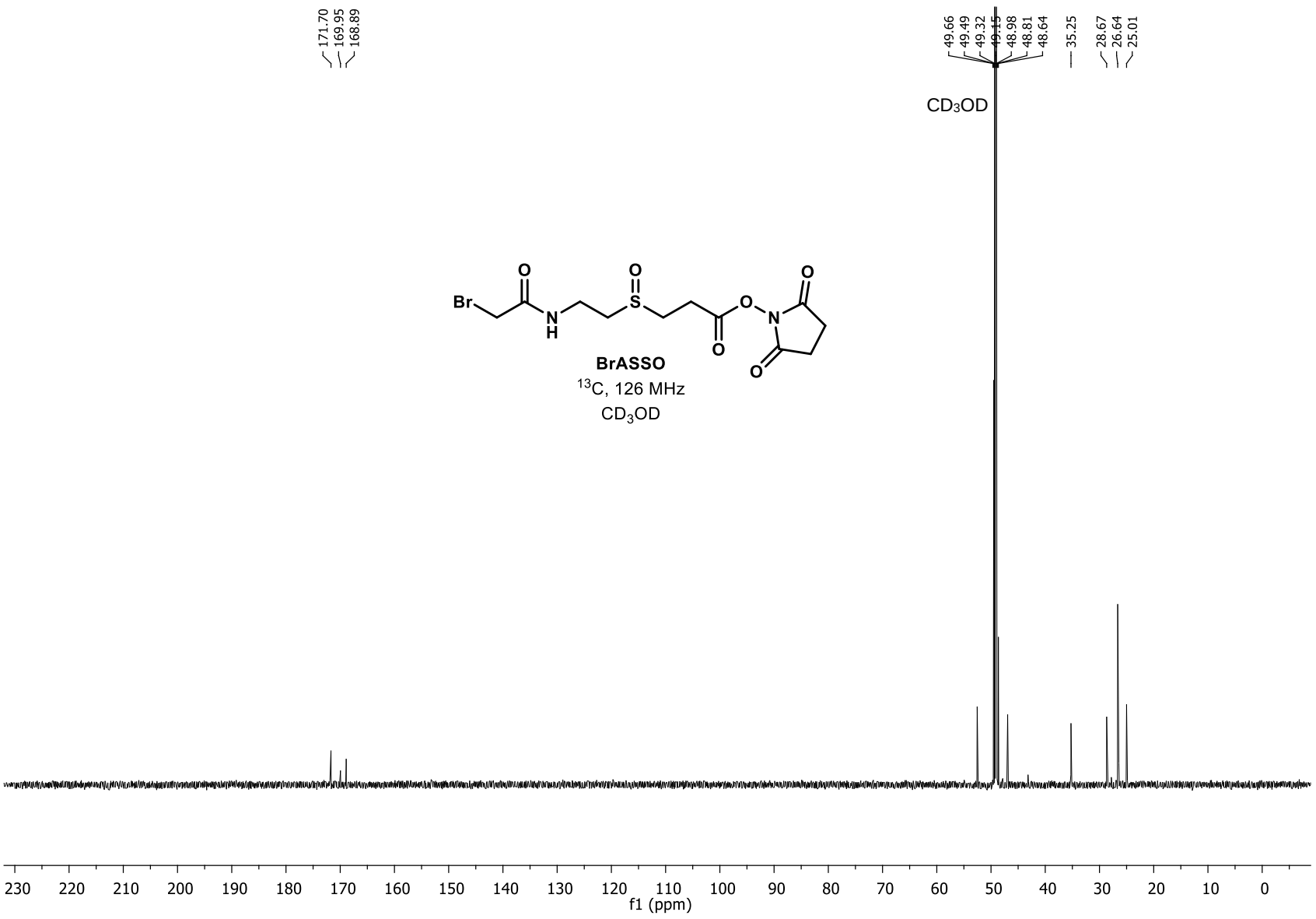
171.70
169.95
168.89
49.66
49.49
49.32
49.15
48.98
48.81
48.64
35.25
28.67
26.64
25.01
CD3OD
Br
O
N
H
S
O
O
O
N
O
O
BrASSO
13C, 126 MHz
CD3OD
230
220
210
200
190
180
170
160
150
140
130
120
110
100
90
80
70
60
50
40
30
20
10
0
f1 (ppm)

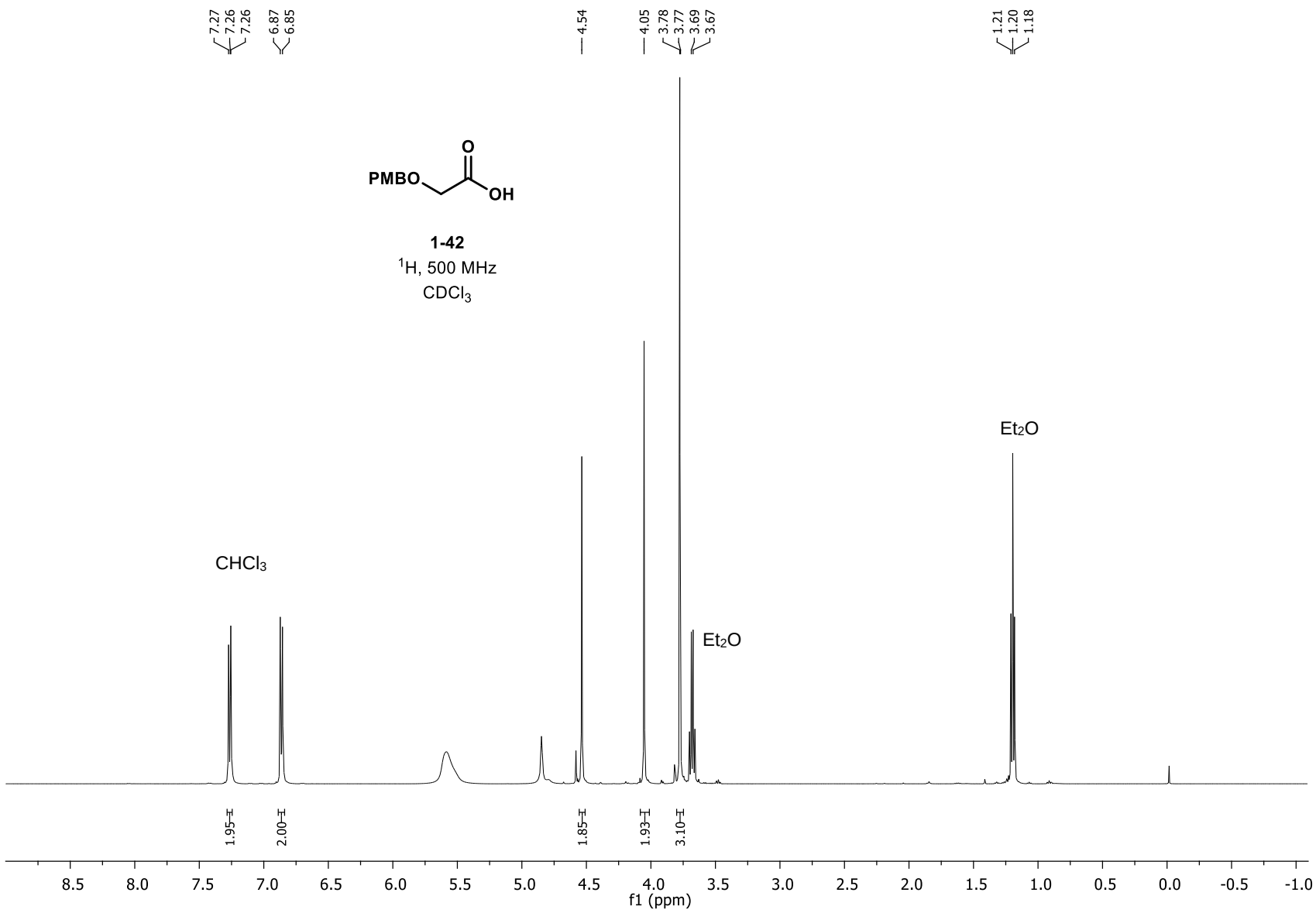
7.27
7.26
7.26
6.87
6.85
4.54
4.05
3.78
3.77
3.69
3.67
1.21
1.20
1.18
PMBO
O
OH
1-42
1H, 500 MHz
CDCl3
Et2O
CHCl3
Et2O
1.95
2.00
1.85
1.93
3.10
8.5
8.0
7.5
7.0
6.5
6.0
5.5
5.0
4.5
4.0
3.5
3.0
2.5
2.0
1.5
1.0
0.5
0.0
-0.5
-1.0
f1 (ppm)

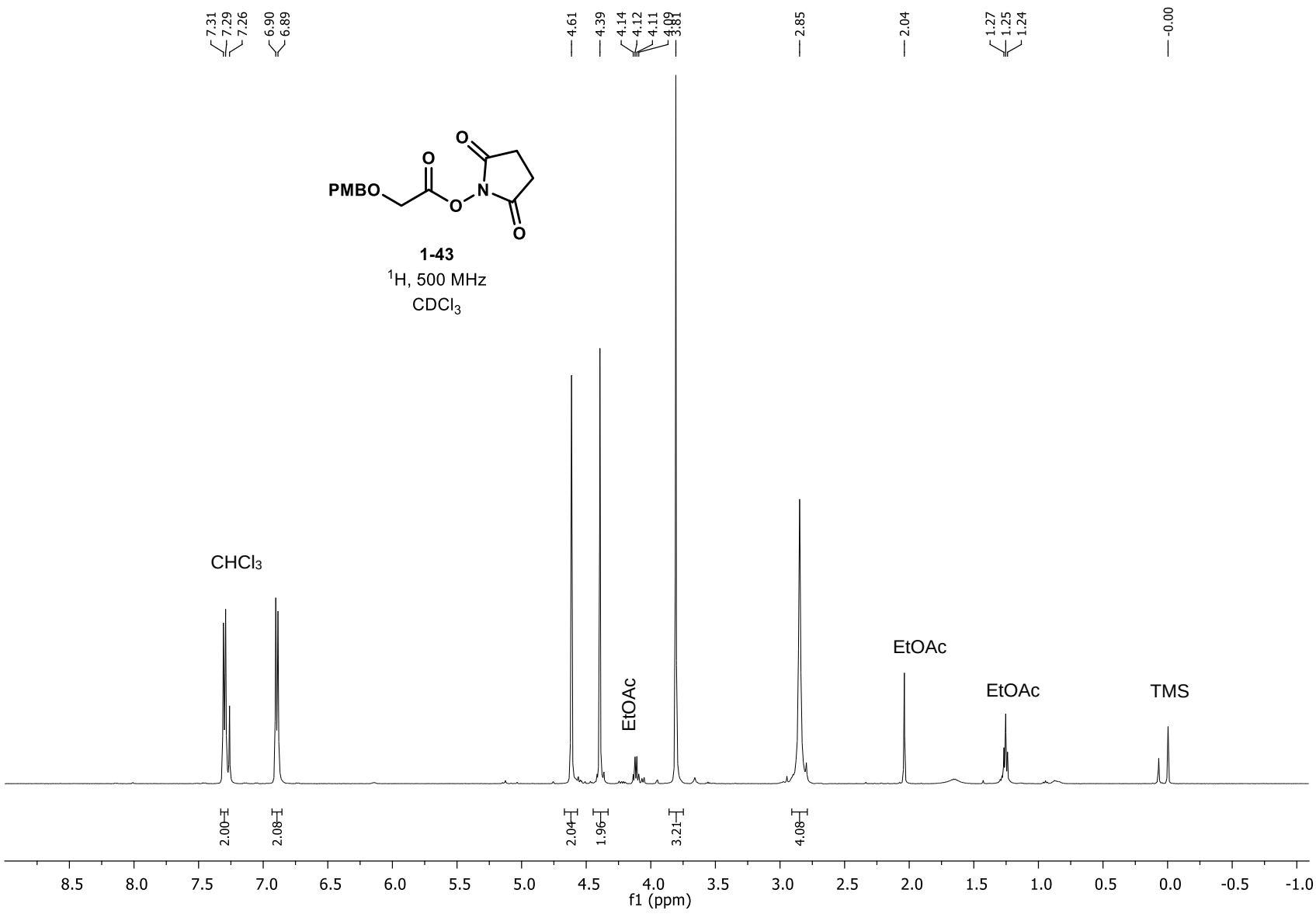
7.31
7.29
7.26
6.90
6.89
4.61
4.39
4.14
4.12
4.11
4.09
3.81
2.85
2.04
1.27
1.25
1.24
-0.00
PMBO
O
O
O
N
O
O
1-43
1H, 500 MHz
CDCl3
CHCl3
EtOAc
EtOAc
EtOAc
TMS
2.00
2.08
2.04
1.96
3.21
4.08
8.5
8.0
7.5
7.0
6.5
6.0
5.5
5.0
4.5
4.0
3.5
3.0
2.5
2.0
1.5
1.0
0.5
0.0
-0.5
-1.0
f1 (ppm)

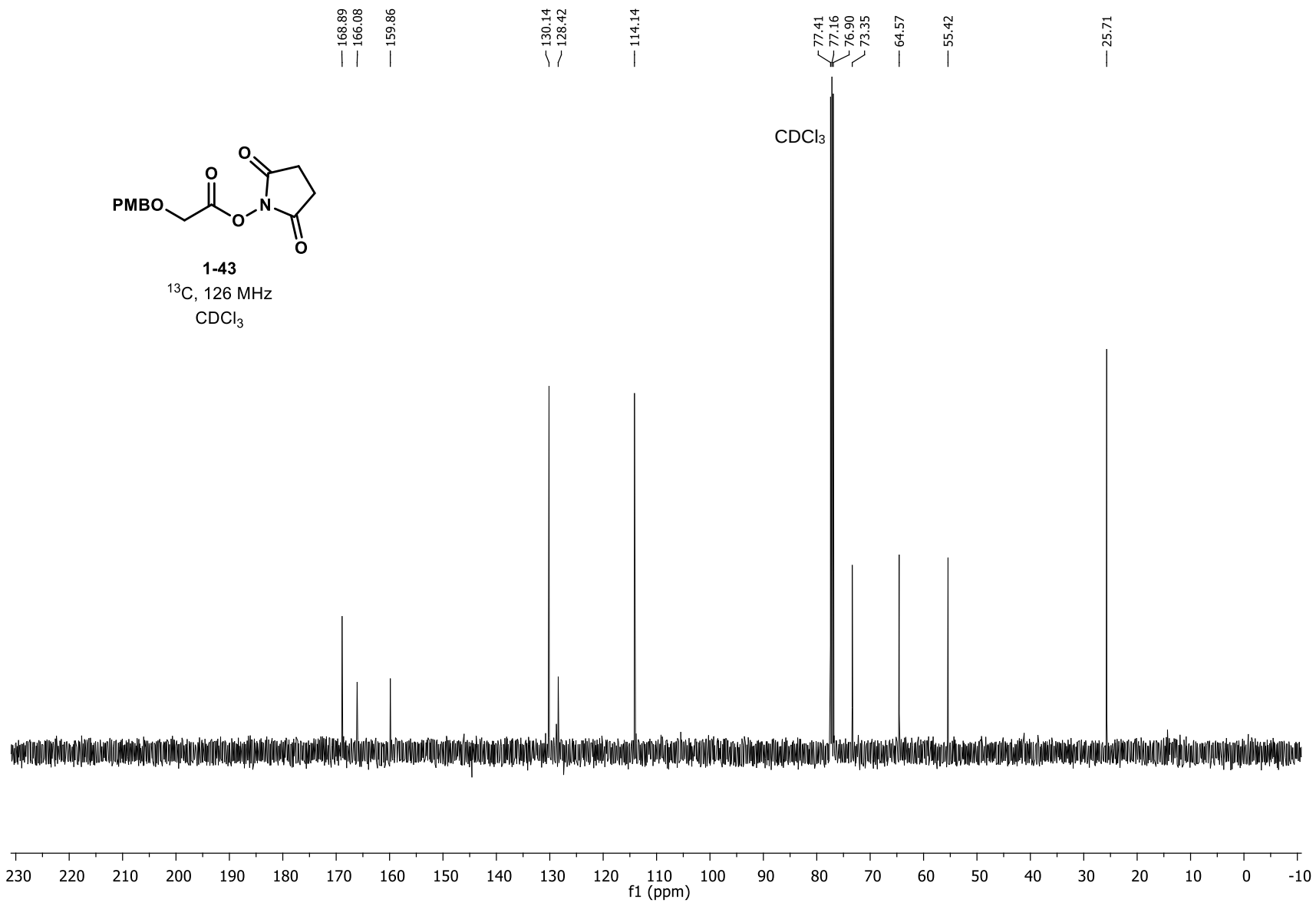
168.89
166.08
159.86
130.14
128.42
114.14
77.41
77.16
76.90
73.35
64.57
55.42
25.71
CDCl3
PMBO
O
O
O
N
O
O
1-43
13C, 126 MHz
CDCl3
230 220 210 200 190 180 170 160 150 140 130 120 110 100 90 80 70 60 50 40 30 20 10 0 -10
f1 (ppm)

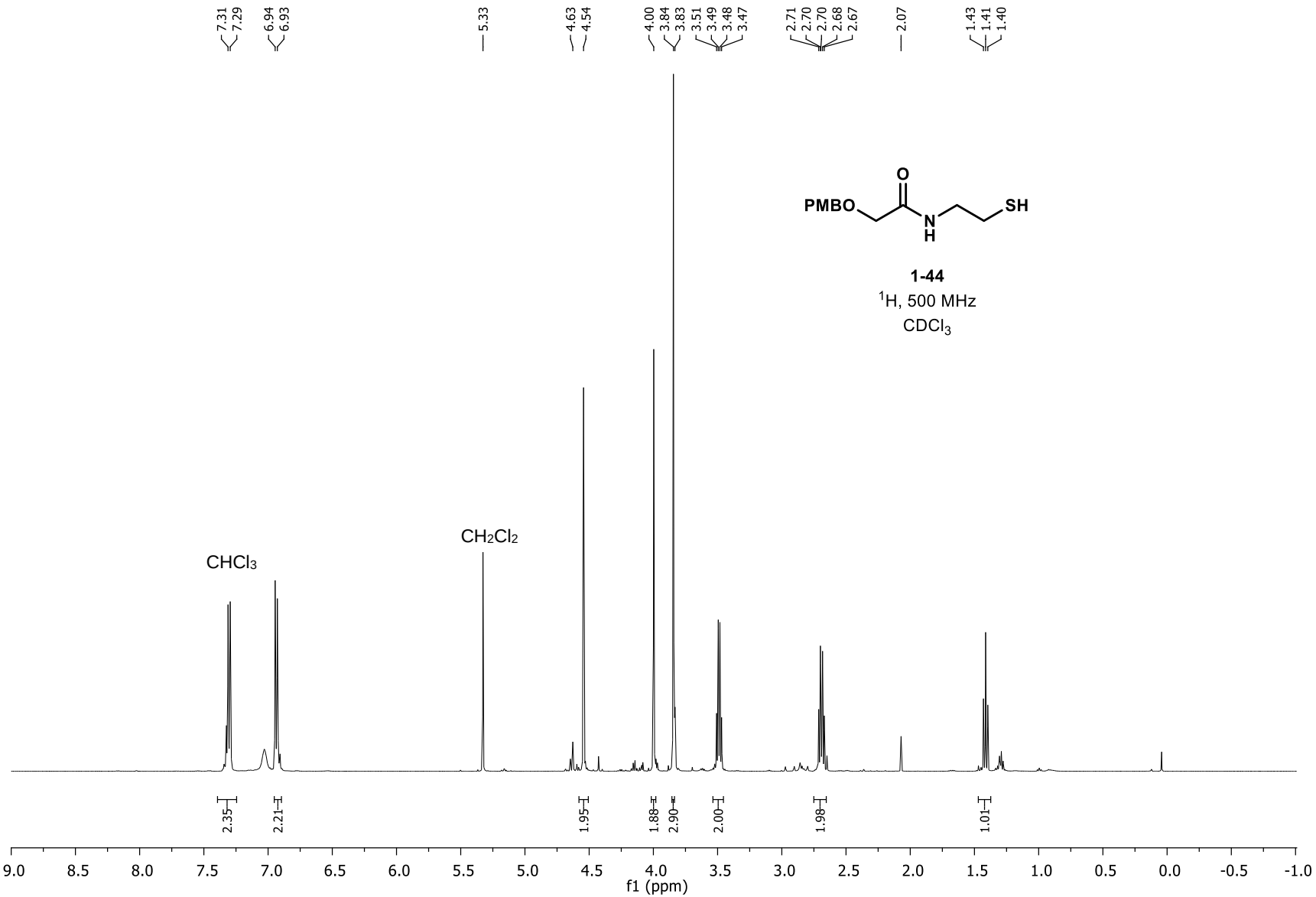
7.31
7.29
6.94
6.93
5.33
4.63
4.54
4.00
3.84
3.83
3.51
3.49
3.48
3.47
2.71
2.70
2.70
2.68
2.67
2.07
1.43
1.41
1.40
O
PMBO
N
H
SH
1-44
1H, 500 MHz
CDCl3
CHCl3
CH2Cl2
2.35
2.21
1.95
1.88
2.90
2.00
1.98
1.01
9.0
8.5
8.0
7.5
7.0
6.5
6.0
5.5
5.0
4.5
4.0
3.5
3.0
2.5
2.0
1.5
1.0
0.5
0.0
-0.5
-1.0
f1 (ppm)

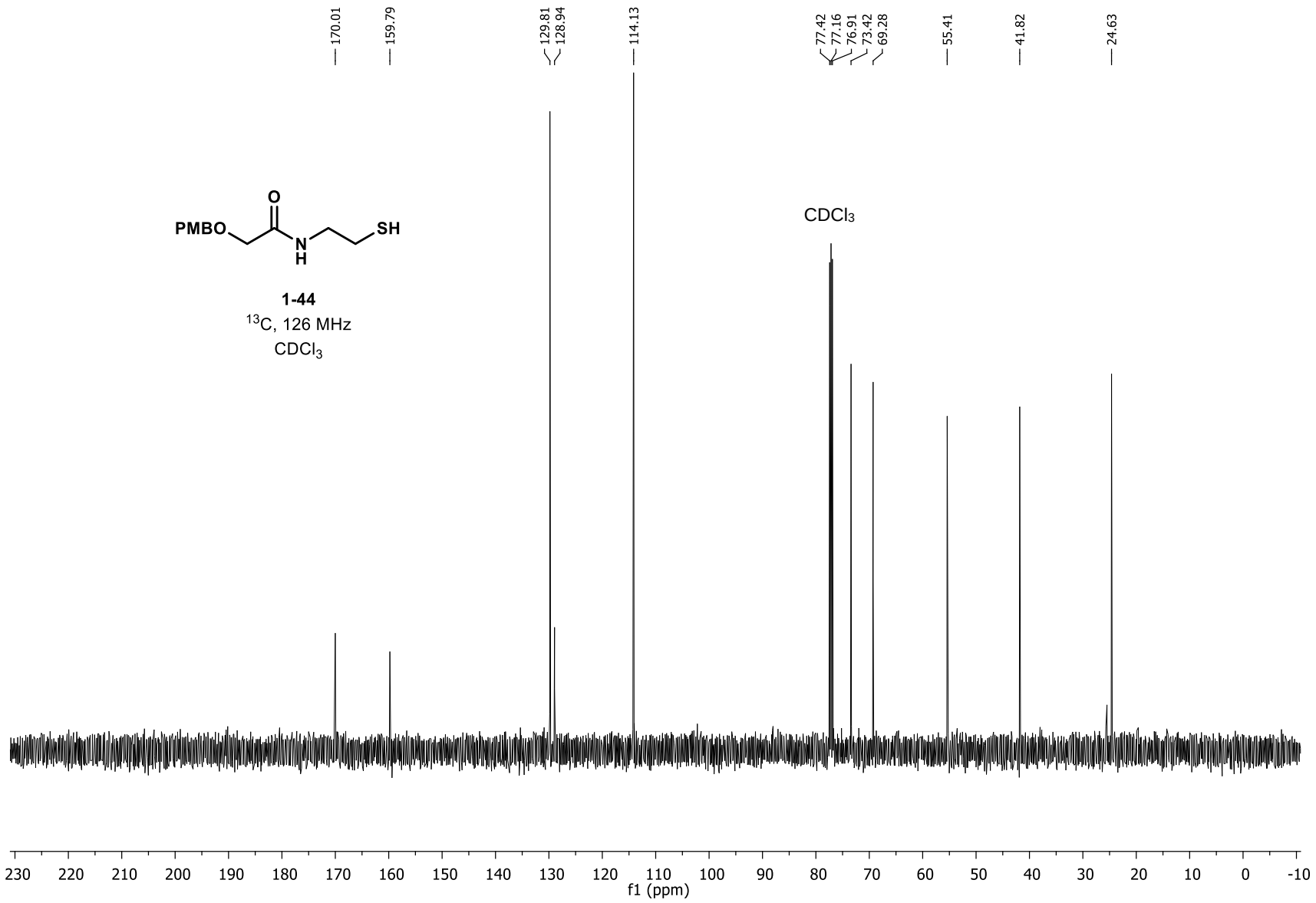
170.01
159.79
129.81
128.94
114.13
77.42
77.16
76.91
73.42
69.28
55.41
41.82
24.63
CDCl3
PMBO
O
N
H
SH
1-44
13C, 126 MHz
CDCl3
230 220 210 200 190 180 170 160 150 140 130 120 110 100 90 80 70 60 50 40 30 20 10 0 -10
f1 (ppm)

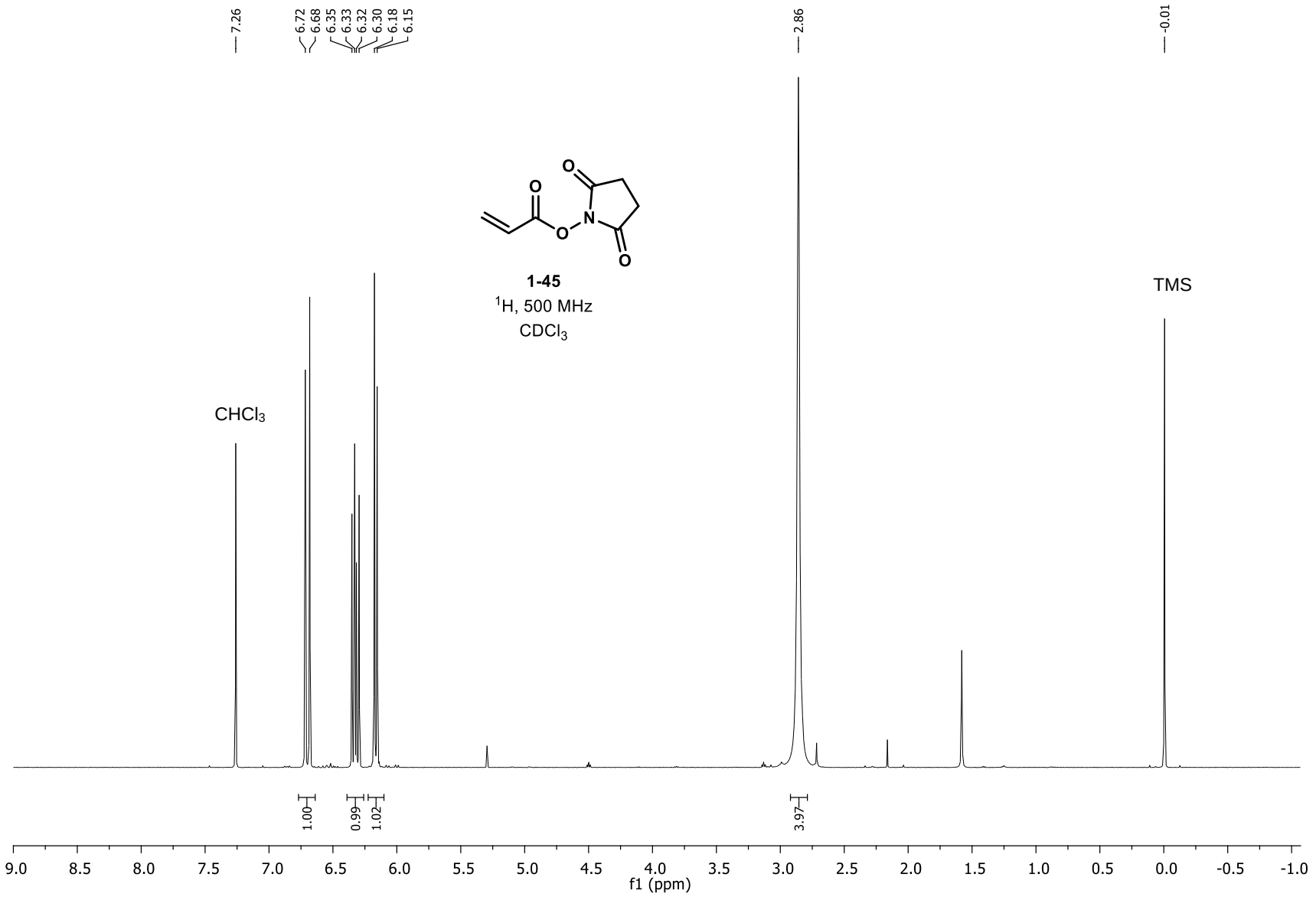
7.26
6.72
6.68
6.35
6.33
6.32
6.30
6.18
6.15
2.86
-0.01
1-45
1H, 500 MHz
CDCl3
CHCl3
TMS
1.00
0.99
1.02
3.97
9.0
8.5
8.0
7.5
7.0
6.5
6.0
5.5
5.0
4.5
4.0
3.5
3.0
2.5
2.0
1.5
1.0
0.5
0.0
-0.5
-1.0
f1 (ppm)

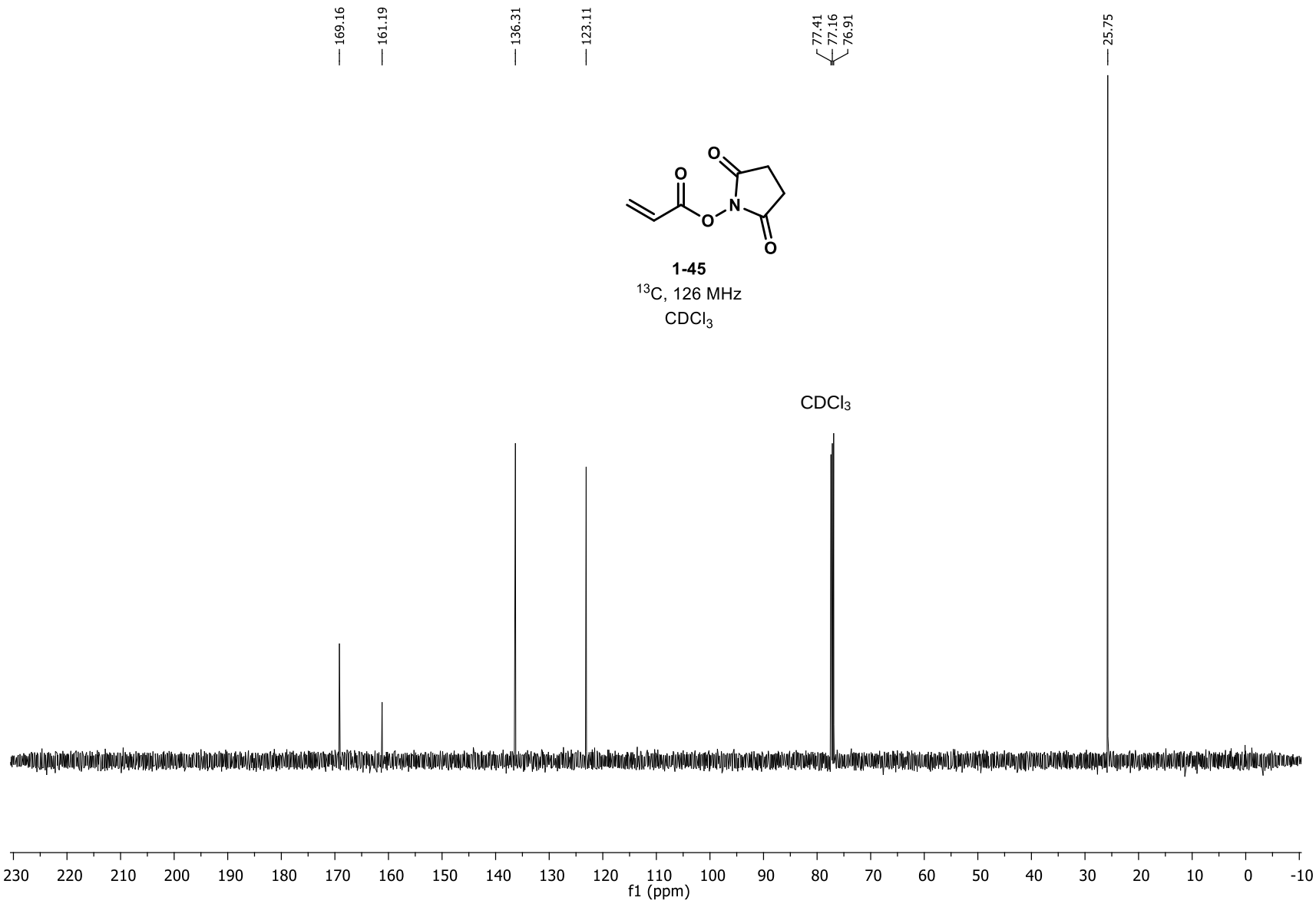
169.16
161.19
136.31
123.11
77.41
77.16
76.91
25.75
O
O
N
O
O
1-45
13C, 126 MHz
CDCl3
CDCl3
230 220 210 200 190 180 170 160 150 140 130 120 110 100 90 80 70 60 50 40 30 20 10 0 -10
f1 (ppm)

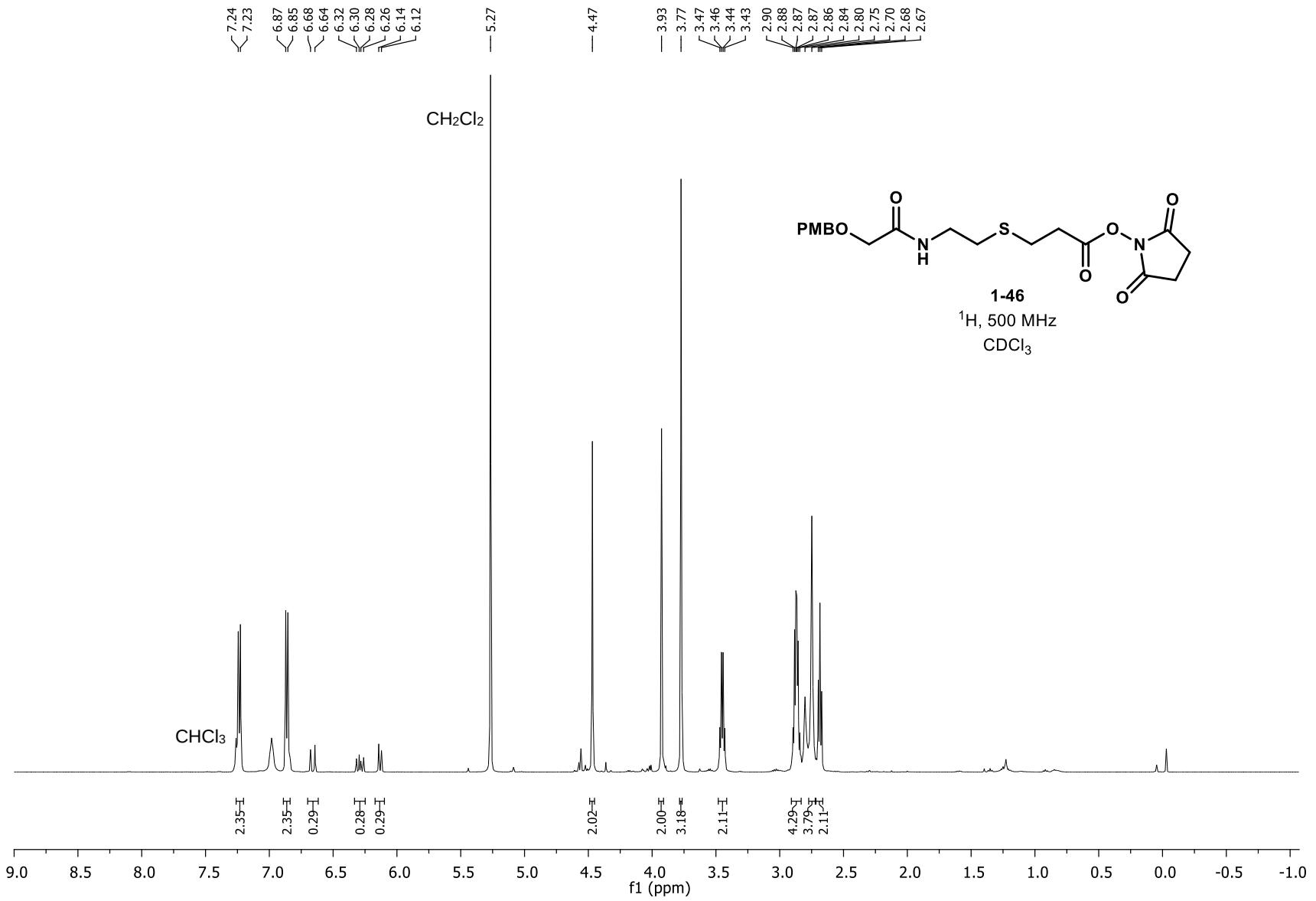
7.24
7.23
6.87
6.85
6.68
6.64
6.32
6.30
6.28
6.26
6.14
6.12
5.27
4.47
3.93
3.77
3.47
3.46
3.44
3.43
2.90
2.88
2.87
2.87
2.86
2.84
2.80
2.75
2.70
2.68
2.67
CH2Cl2
CHCl3
PMBO
O
N
H
S
O
O
N
O
O
O
1-46
1H, 500 MHz
CDCl3
2.35
2.35
0.29
0.28
0.29
2.02
2.00
3.18
2.11
4.29
3.79
2.11
9.0
8.5
8.0
7.5
7.0
6.5
6.0
5.5
5.0
4.5
4.0
3.5
3.0
2.5
2.0
1.5
1.0
0.5
0.0
-0.5
-1.0
f1 (ppm)

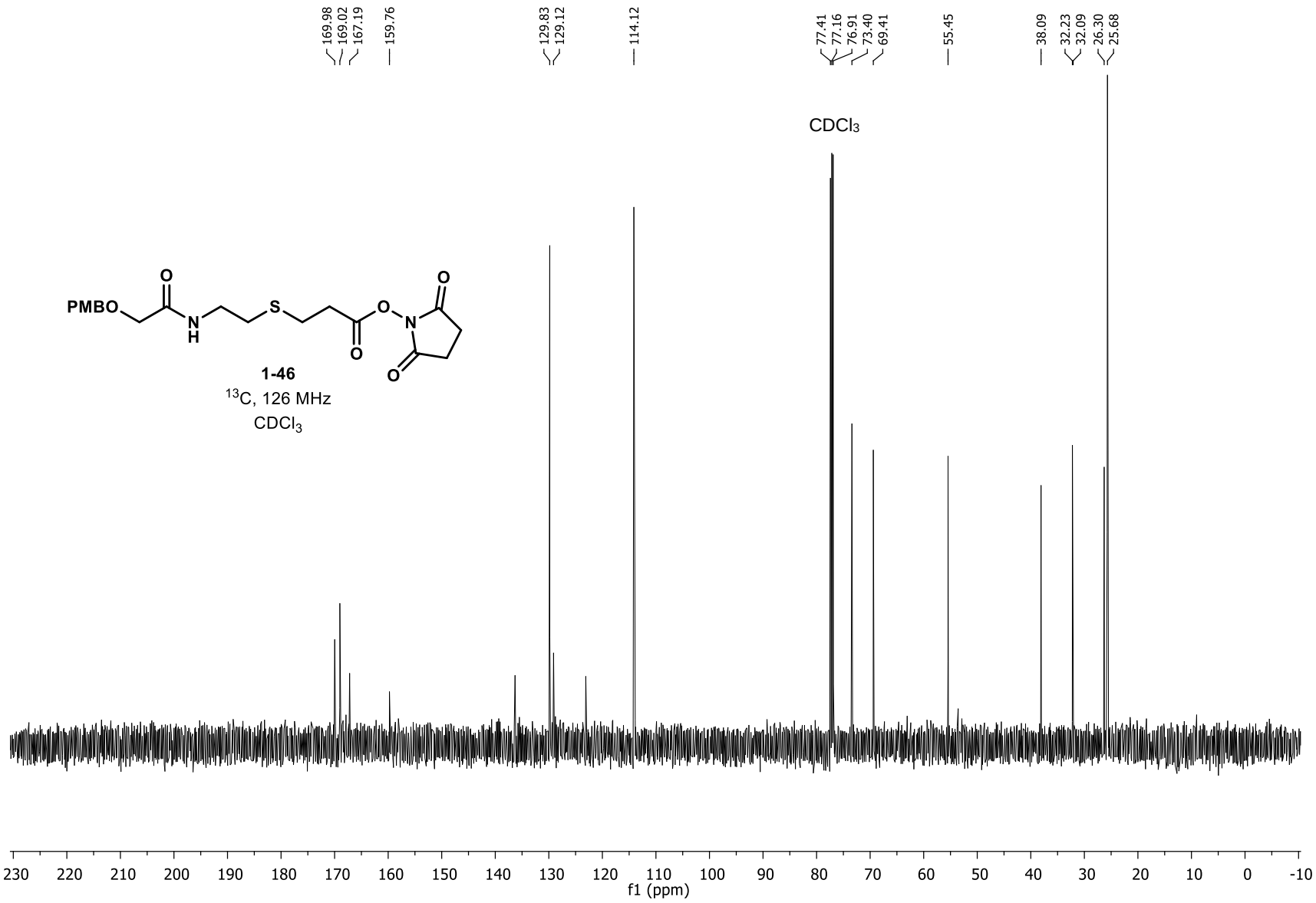
169.98
169.02
167.19
159.76
129.83
129.12
114.12
77.41
77.16
76.91
73.40
69.41
55.45
38.09
32.23
32.09
26.30
25.68
CDCl3
PMBO
O
N
H
S
O
O
N
O
O
O
1-46
13C, 126 MHz
CDCl3
230 220 210 200 190 180 170 160 150 140 130 120 110 100 90 80 70 60 50 40 30 20 10 0 -10
f1 (ppm)

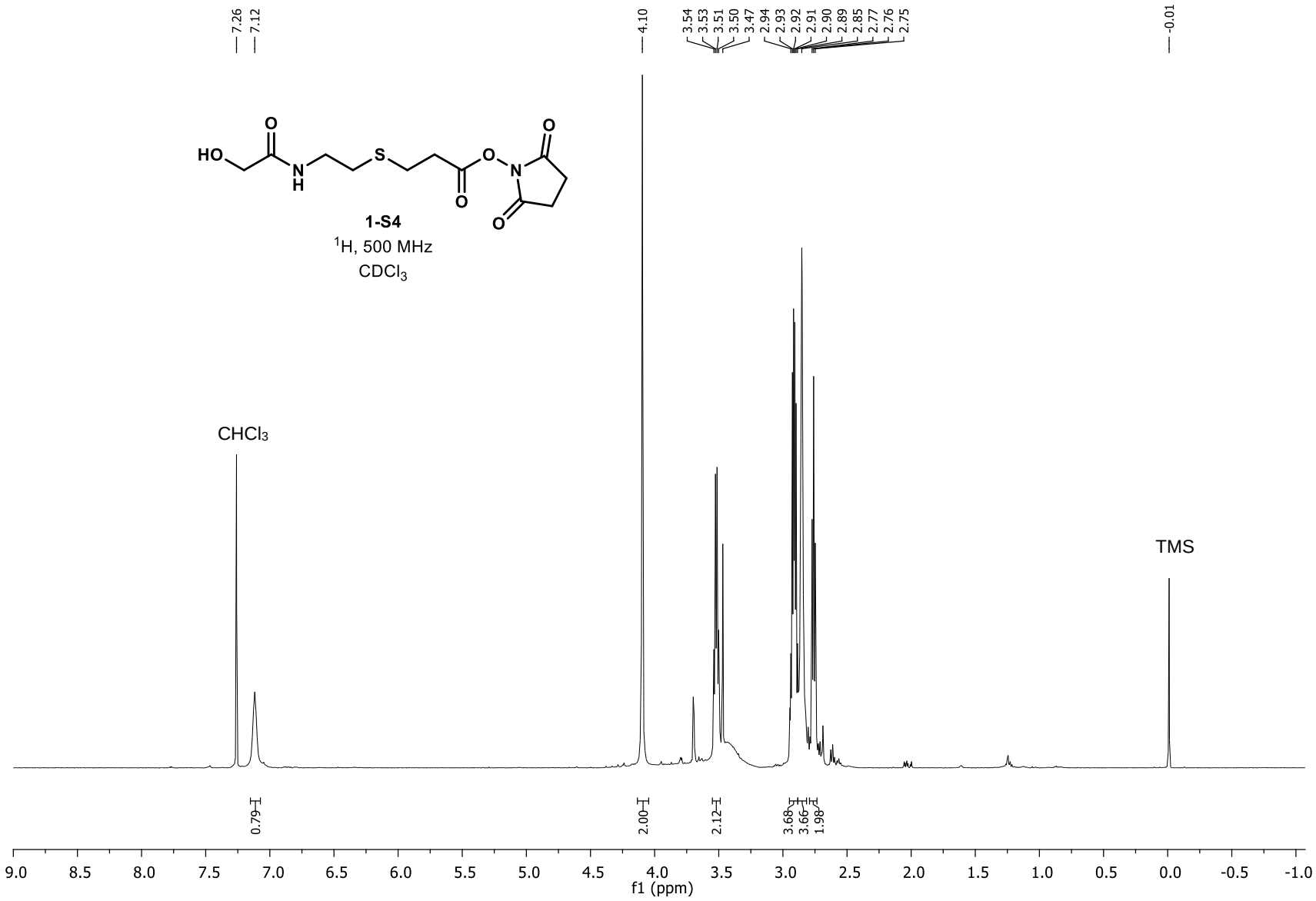
7.26
7.12
4.10
3.54
3.53
3.51
3.50
3.47
2.94
2.93
2.92
2.91
2.90
2.89
2.85
2.77
2.76
2.75
-0.01
HO
O
N
H
S
O
O
N
O
O
O
1-S4
1H, 500 MHz
CDCl3
CHCl3
TMS
0.79
2.00
2.12
3.68
3.66
1.98
9.0
8.5
8.0
7.5
7.0
6.5
6.0
5.5
5.0
4.5
4.0
3.5
3.0
2.5
2.0
1.5
1.0
0.5
0.0
-0.5
-1.0
f1 (ppm)

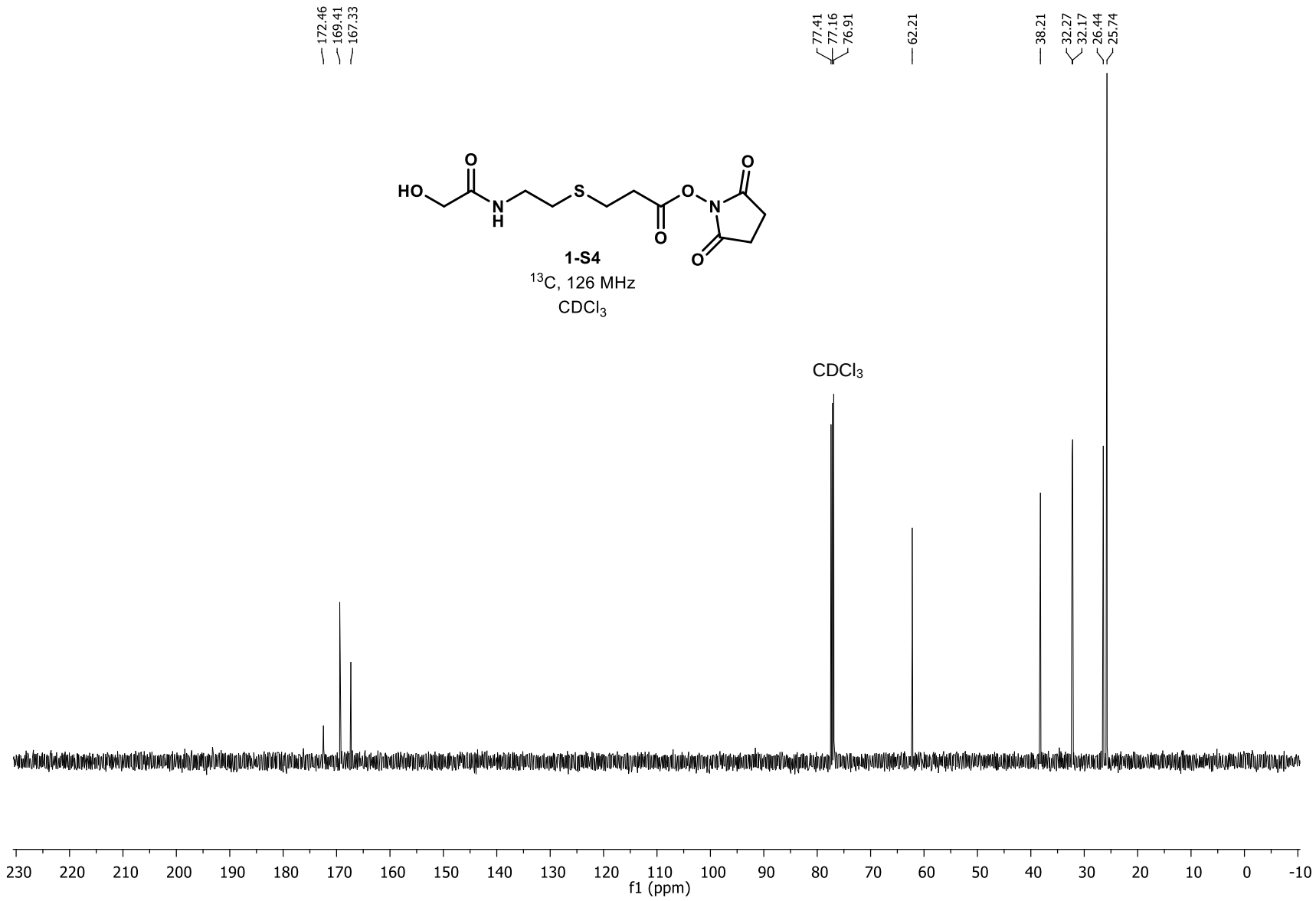
172.46
169.41
167.33
77.41
77.16
76.91
62.21
38.21
32.27
32.17
26.44
25.74
HO
O
N
H
S
O
N
O
O
O
O
1-S4
13C, 126 MHz
CDCl3
CDCl3
230 220 210 200 190 180 170 160 150 140 130 120 110 100 90 80 70 60 50 40 30 20 10 0 -10
f1 (ppm)

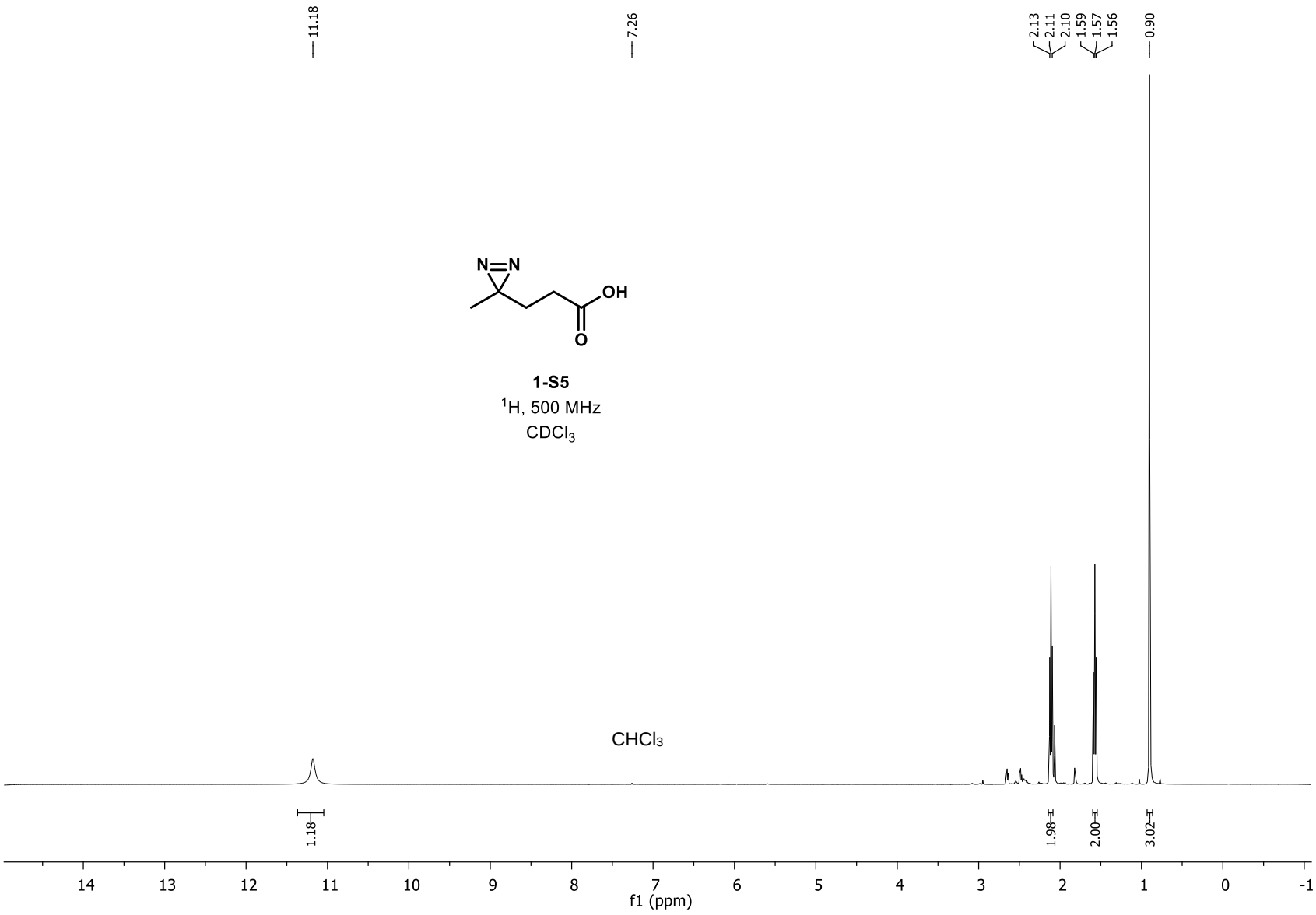
11.18
7.26
2.13
2.11
2.10
1.59
1.57
1.56
0.90
N=N
OH
O
1-S5
1H, 500 MHz
CDCl3
CHCl3
1.18
1.98
2.00
3.02
14
13
12
11
10
9
8
7
6
5
4
3
2
1
0
-1
f1 (ppm)

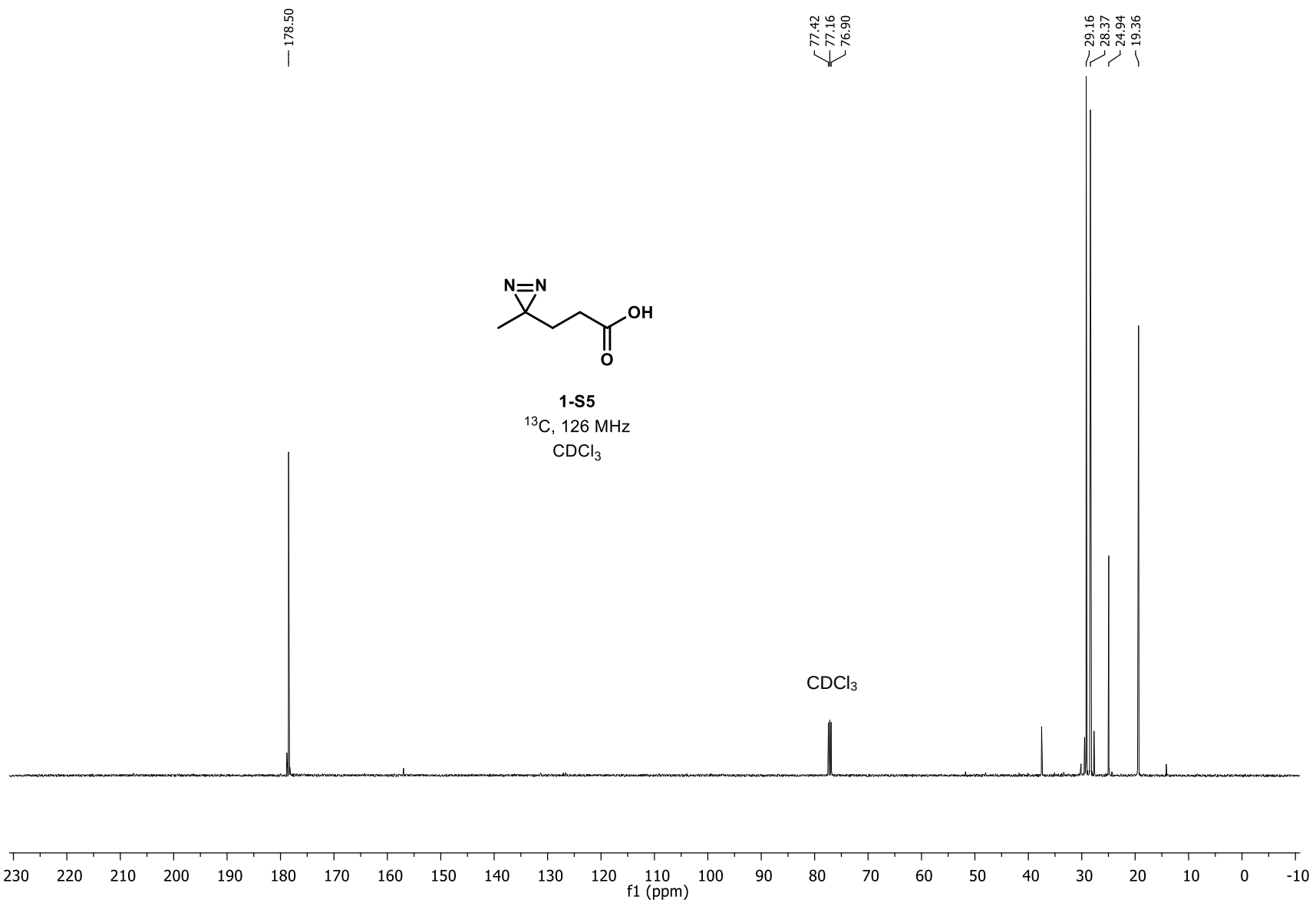
178.50
77.42
77.16
76.90
29.16
28.37
24.94
19.36
N=N
OH
O
1-S5
13C, 126 MHz
CDCl3
CDCl3
230 220 210 200 190 180 170 160 150 140 130 120 110 100 90 80 70 60 50 40 30 20 10 0 -10
f1 (ppm)

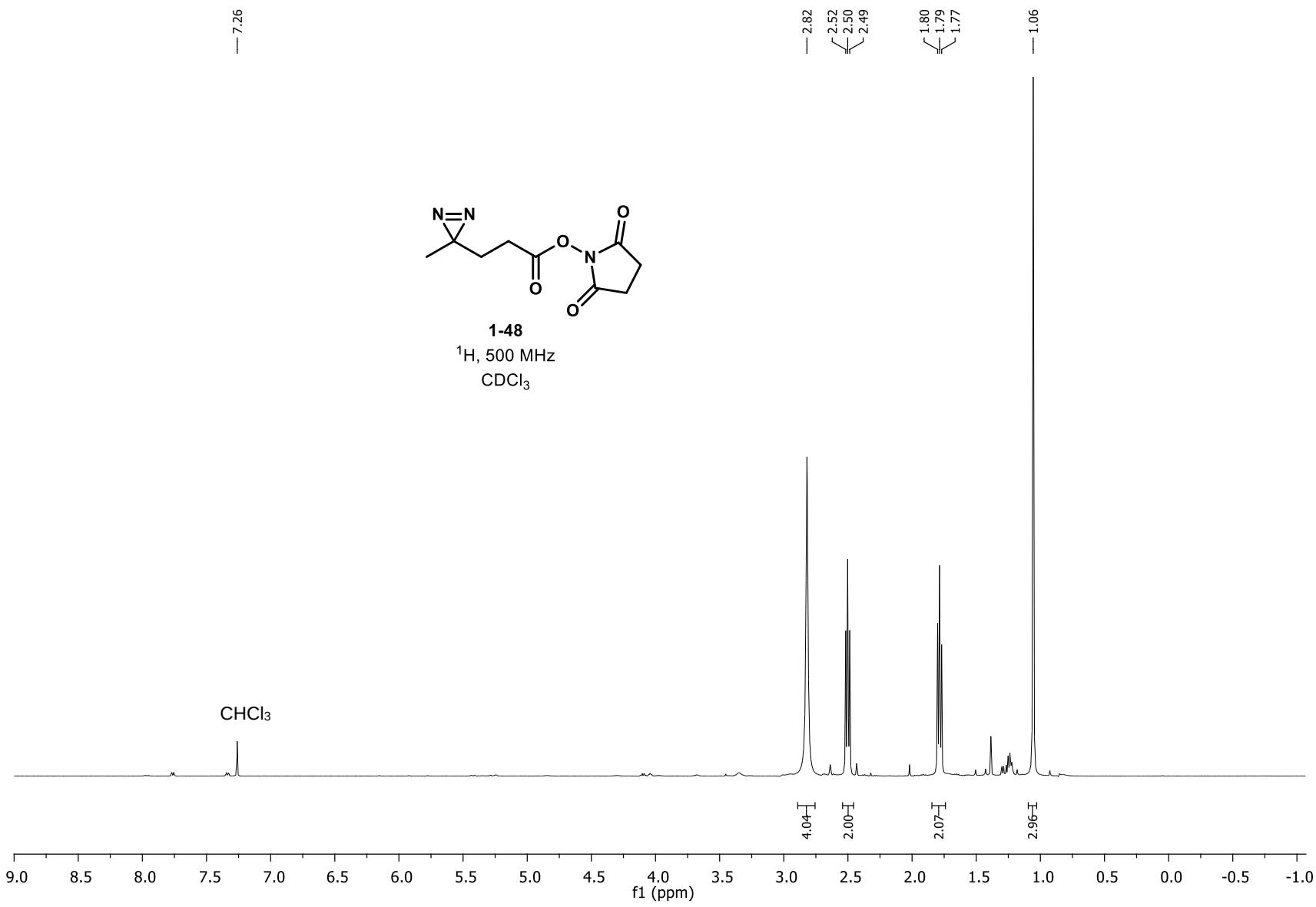
7.26
2.82
2.52
2.50
2.49
1.80
1.79
1.77
1.06
N=N
O
O
N
O
O
1-48
1H, 500 MHz
CDCl3
CHCl3
4.04
2.00
2.07
2.96
9.0
8.5
8.0
7.5
7.0
6.5
6.0
5.5
5.0
4.5
4.0
3.5
3.0
2.5
2.0
1.5
1.0
0.5
0.0
-0.5
-1.0
f1 (ppm)

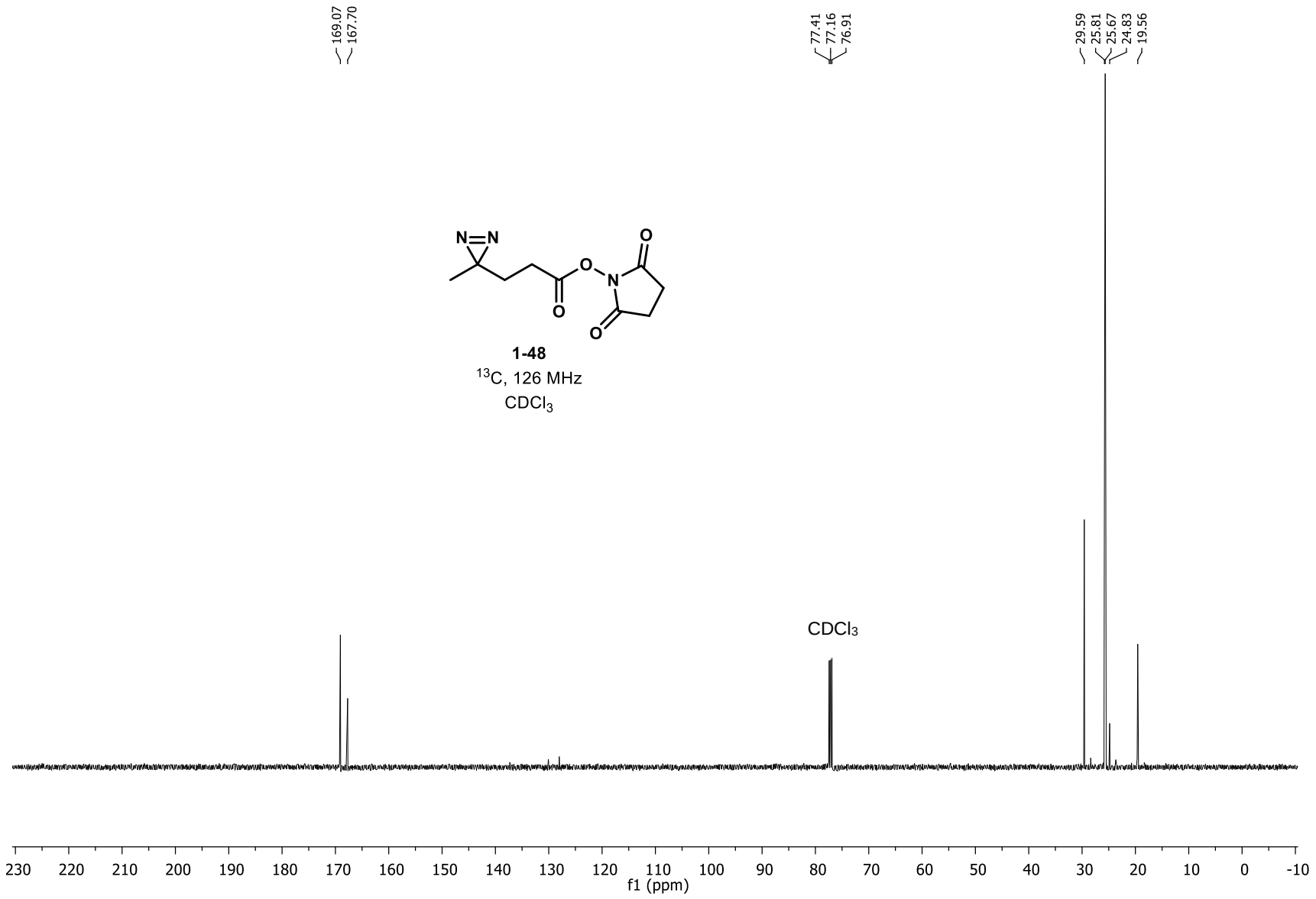
169.07
167.70
77.41
77.16
76.91
29.59
25.81
25.67
24.83
19.56
N=N
O
O
N
O
O
O
1-48
13C, 126 MHz
CDCl3
CDCl3
230 220 210 200 190 180 170 160 150 140 130 120 110 100 90 80 70 60 50 40 30 20 10 0 -10
f1 (ppm)

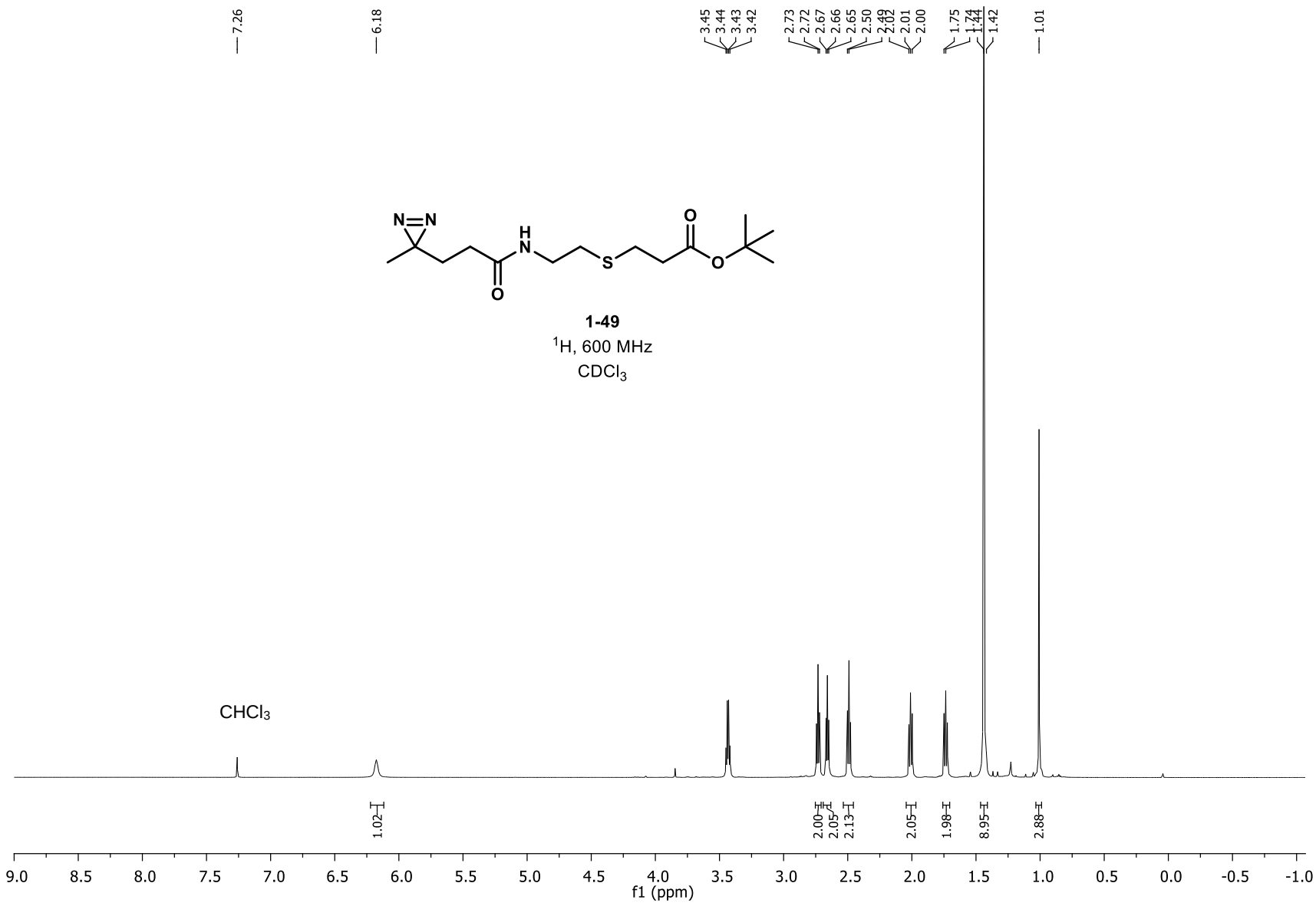
7.26
6.18
3.45
3.44
3.43
3.42
2.73
2.72
2.67
2.66
2.65
2.50
2.01
2.00
1.75
1.74
1.44
1.42
1.01
N=N
H
N
O
S
O
O
1-49
1H, 600 MHz
CDCl3
CHCl3
1.02
2.00
2.05
2.13
2.05
1.98
8.95
2.88
9.0
8.5
8.0
7.5
7.0
6.5
6.0
5.5
5.0
4.5
4.0
3.5
3.0
2.5
2.0
1.5
1.0
0.5
0.0
-0.5
-1.0
f1 (ppm)

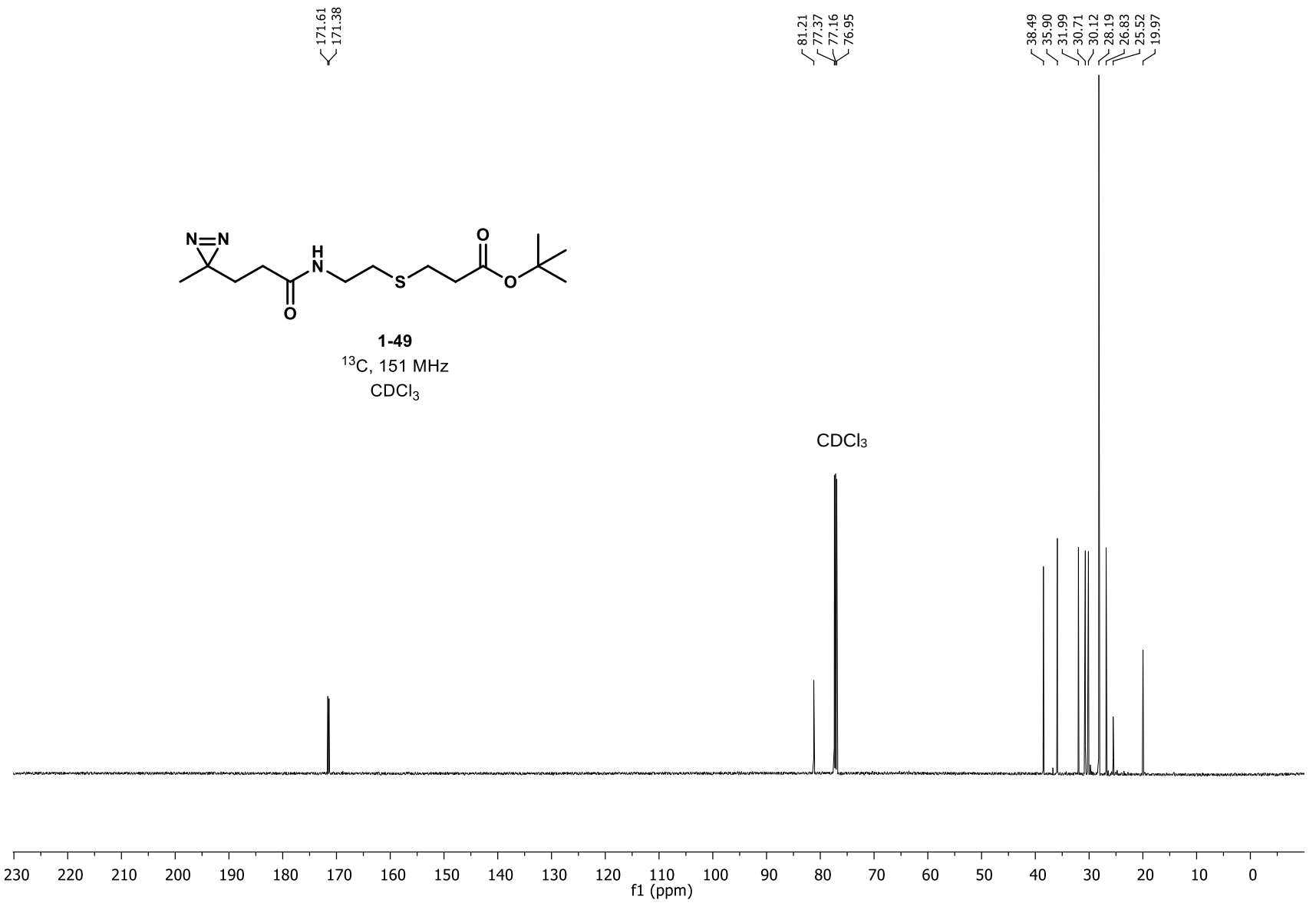
171.61
171.38
81.21
77.37
77.16
76.95
38.49
35.90
31.99
30.71
30.12
28.19
26.83
25.52
19.97
N=N
H
N
O
S
O
O
1-49
13C, 151 MHz
CDCl3
CDCl3
230 220 210 200 190 180 170 160 150 140 130 120 110 100 90 80 70 60 50 40 30 20 10 0
f1 (ppm)

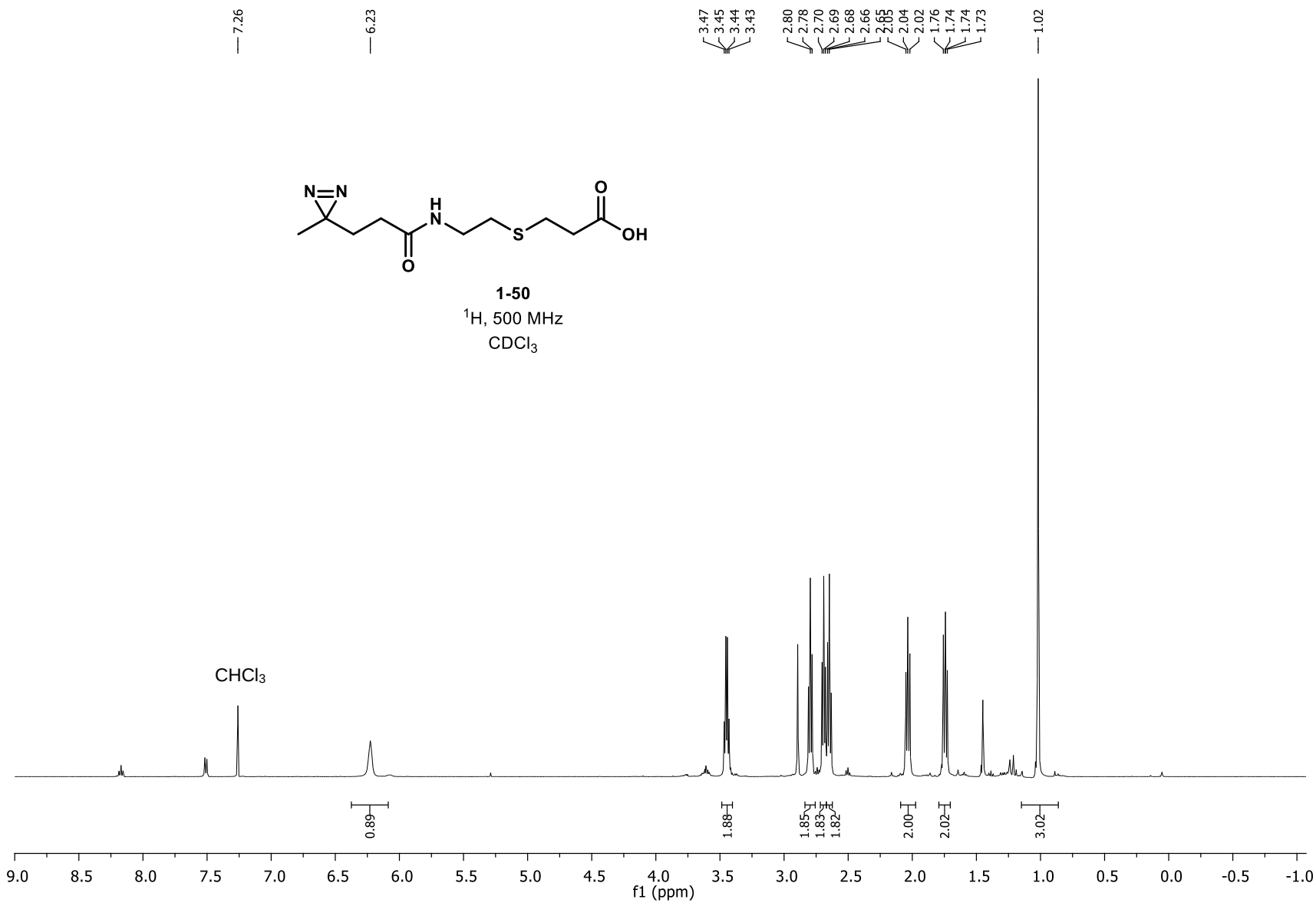
7.26
6.23
3.47
3.45
3.44
3.43
2.80
2.78
2.70
2.69
2.68
2.66
2.65
2.05
2.04
2.02
1.76
1.74
1.74
1.73
1.02
N=N
H
N
O
S
OH
O
1-50
1H, 500 MHz
CDCl3
CHCl3
0.89
1.88
1.85
1.83
1.82
2.00
2.02
3.02
9.0
8.5
8.0
7.5
7.0
6.5
6.0
5.5
5.0
4.5
4.0
3.5
3.0
2.5
2.0
1.5
1.0
0.5
0.0
-0.5
-1.0
f1 (ppm)

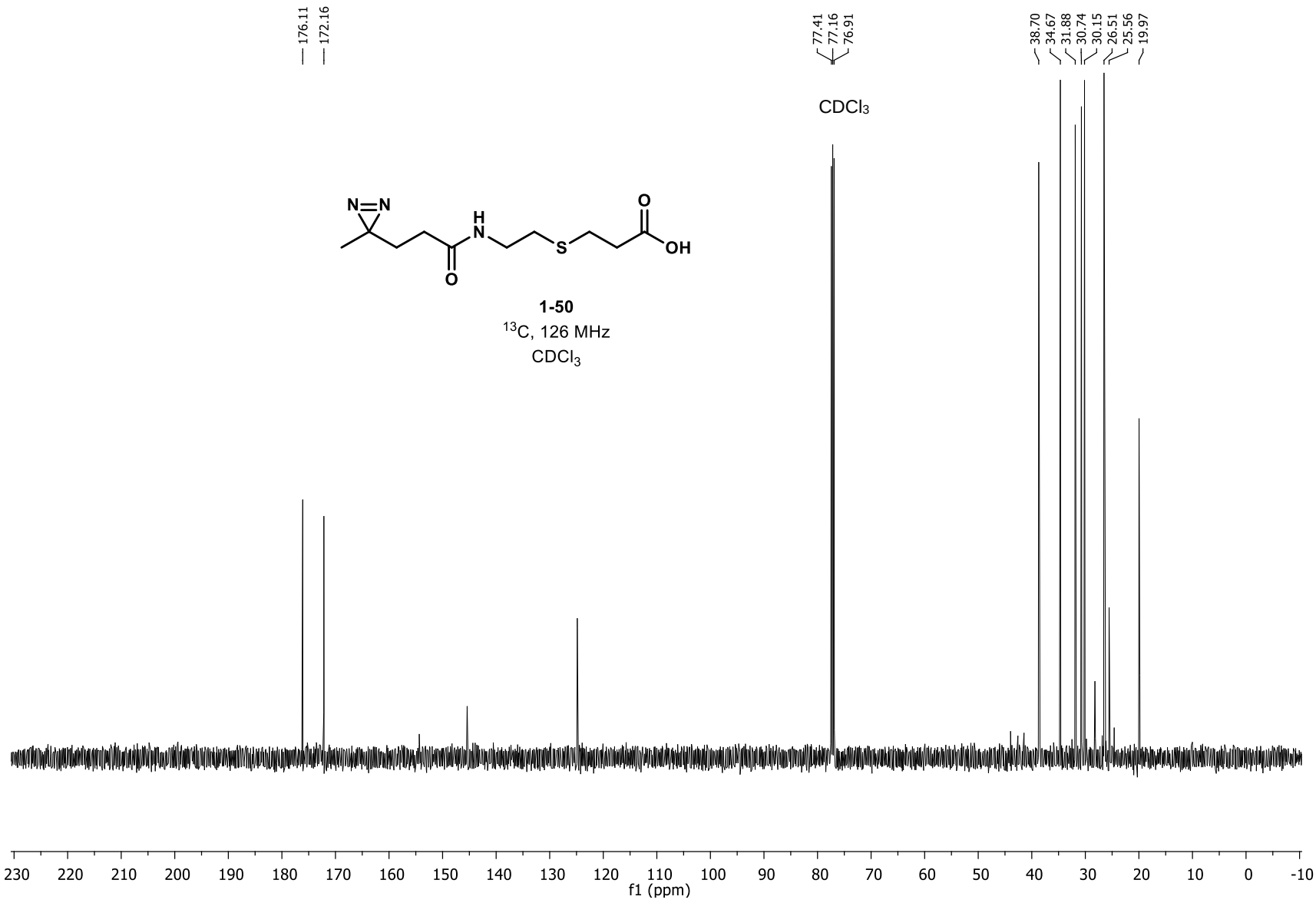
176.11
172.16
77.41
77.16
76.91
38.70
34.67
31.88
30.74
30.15
26.51
25.56
19.97
CDCl3
N=N
H
N
S
O
OH
O
1-50
13C, 126 MHz
CDCl3
230 220 210 200 190 180 170 160 150 140 130 120 110 100 90 80 70 60 50 40 30 20 10 0 -10
f1 (ppm)

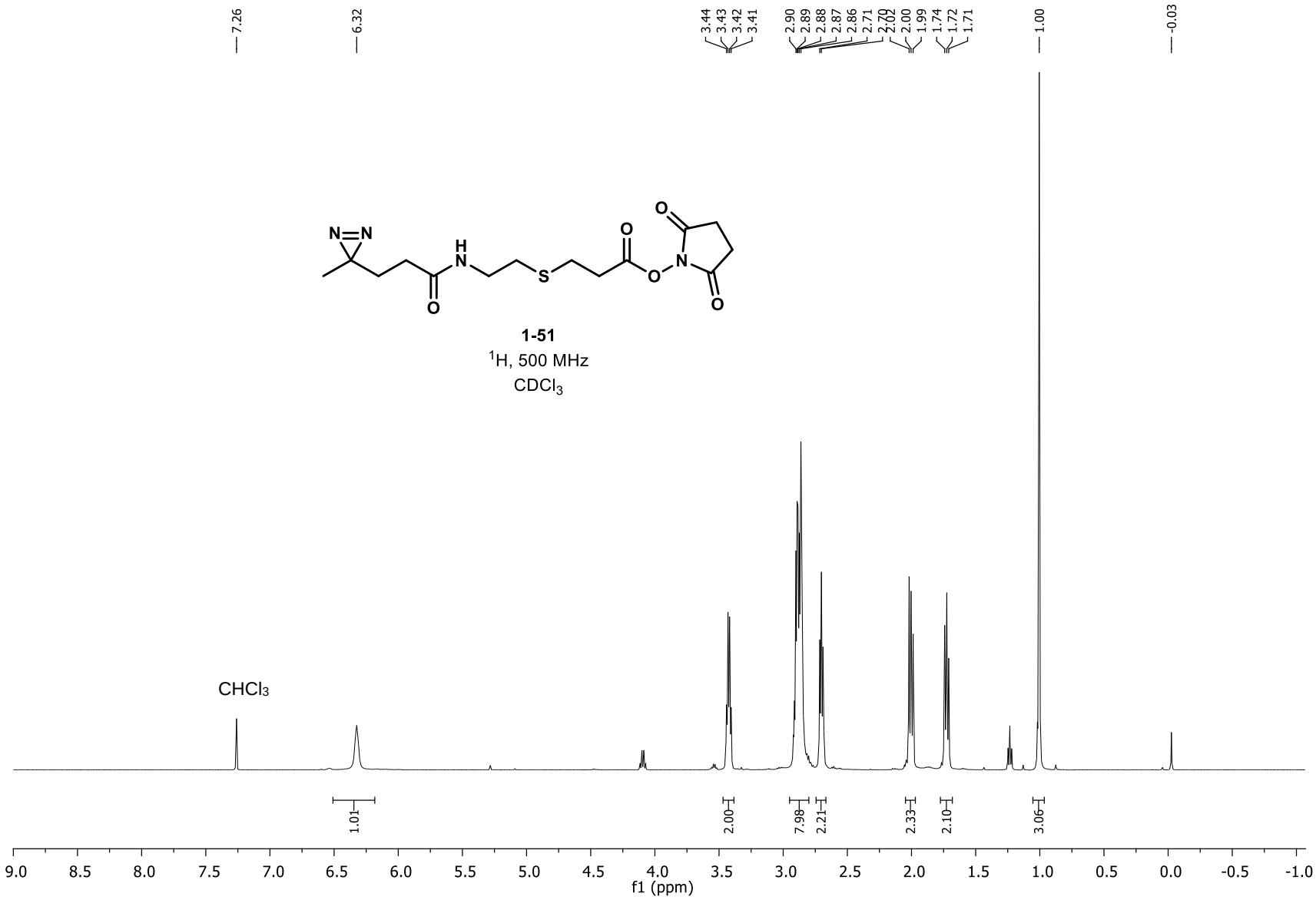
7.26
6.32
3.44
3.43
3.42
3.41
2.90
2.89
2.88
2.87
2.86
2.71
2.70
2.02
2.00
1.99
1.74
1.72
1.71
1.00
-0.03
1-51
1H, 500 MHz
CDCl3
CHCl3
1.01
2.00
7.98
2.21
2.33
2.10
3.06
f1 (ppm)

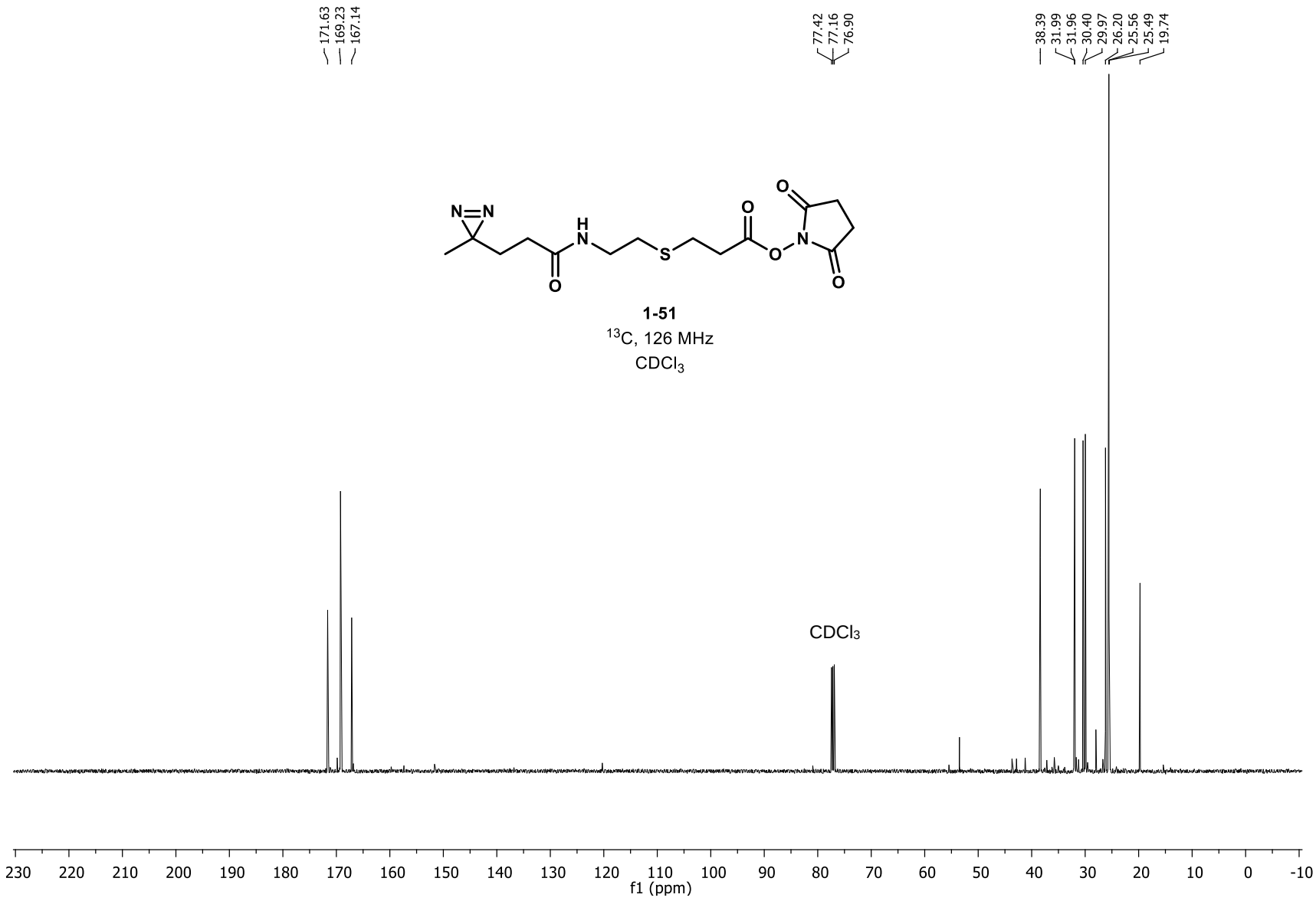
171.63
169.23
167.14
77.42
77.16
76.90
38.39
31.99
31.96
30.40
29.97
26.20
25.56
25.49
19.74
N=N
H
N
S
O
O
O
N
O
O
O
1-51
13C, 126 MHz
CDCl3
CDCl3
230 220 210 200 190 180 170 160 150 140 130 120 110 100 90 80 70 60 50 40 30 20 10 0 -10
f1 (ppm)

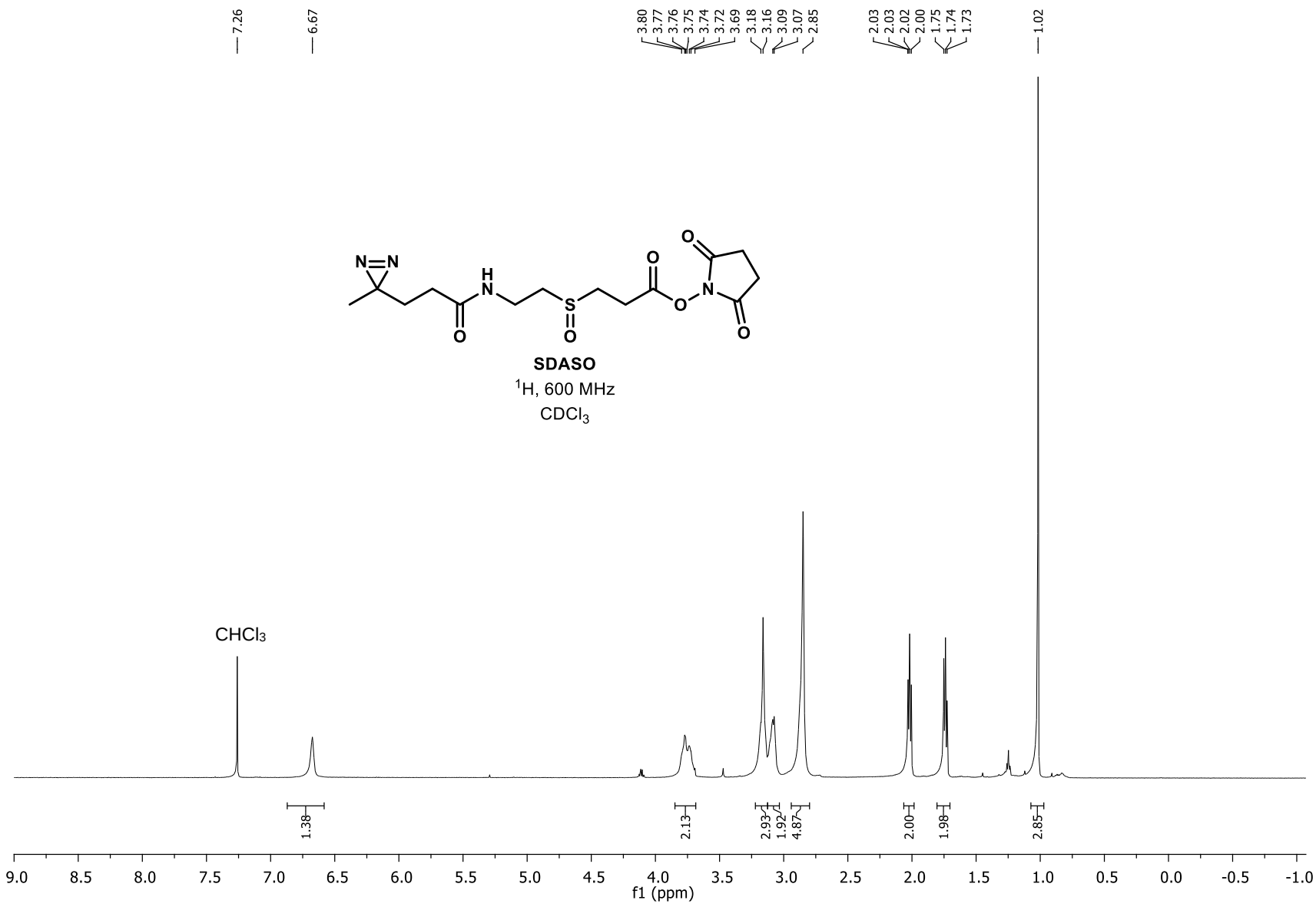
7.26
6.67
3.80
3.77
3.76
3.75
3.74
3.72
3.69
3.18
3.16
3.09
3.07
2.85
2.03
2.03
2.02
2.00
1.75
1.74
1.73
1.02
SDASO
1H, 600 MHz
CDCl3
CHCl3
1.38
2.13
2.93
1.92
4.87
2.00
1.98
2.85
f1 (ppm)

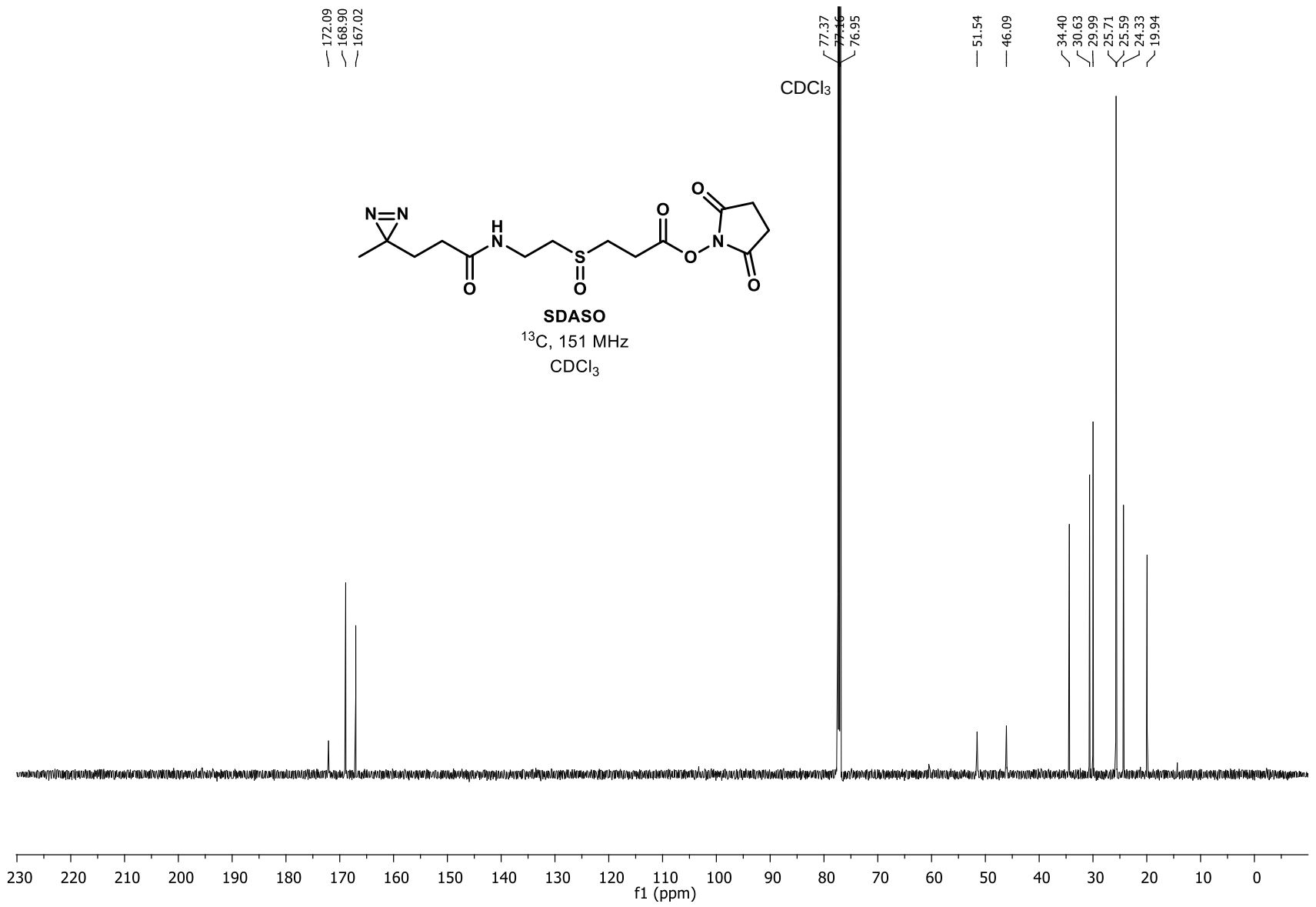
172.09
168.90
167.02
77.37
77.16
76.95
51.54
46.09
34.40
30.63
29.99
25.71
25.59
24.33
19.94
CDCl3
SDASO
13C, 151 MHz
CDCl3
230 220 210 200 190 180 170 160 150 140 130 120 110 100 90 80 70 60 50 40 30 20 10 0
f1 (ppm)

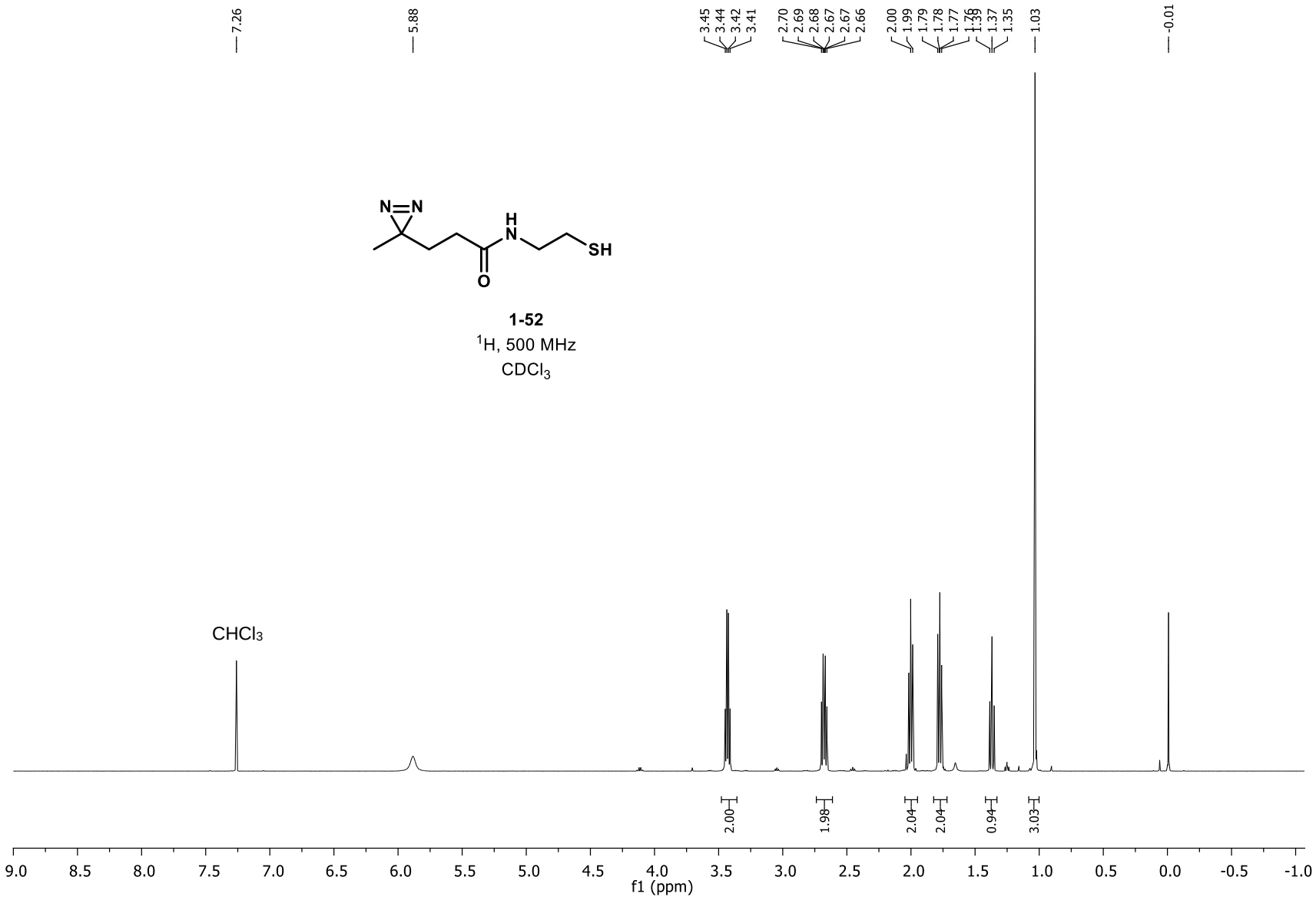
7.26
5.88
3.45
3.44
3.42
3.41
2.70
2.69
2.68
2.67
2.67
2.66
2.00
1.99
1.79
1.78
1.77
1.38
1.37
1.35
1.03
-0.01
N=N
H
N
SH
O
1-52
1H, 500 MHz
CDCl3
CHCl3
2.00
1.98
2.04
2.04
0.94
3.03
9.0
8.5
8.0
7.5
7.0
6.5
6.0
5.5
5.0
4.5
4.0
3.5
3.0
2.5
2.0
1.5
1.0
0.5
0.0
-0.5
-1.0
f1 (ppm)

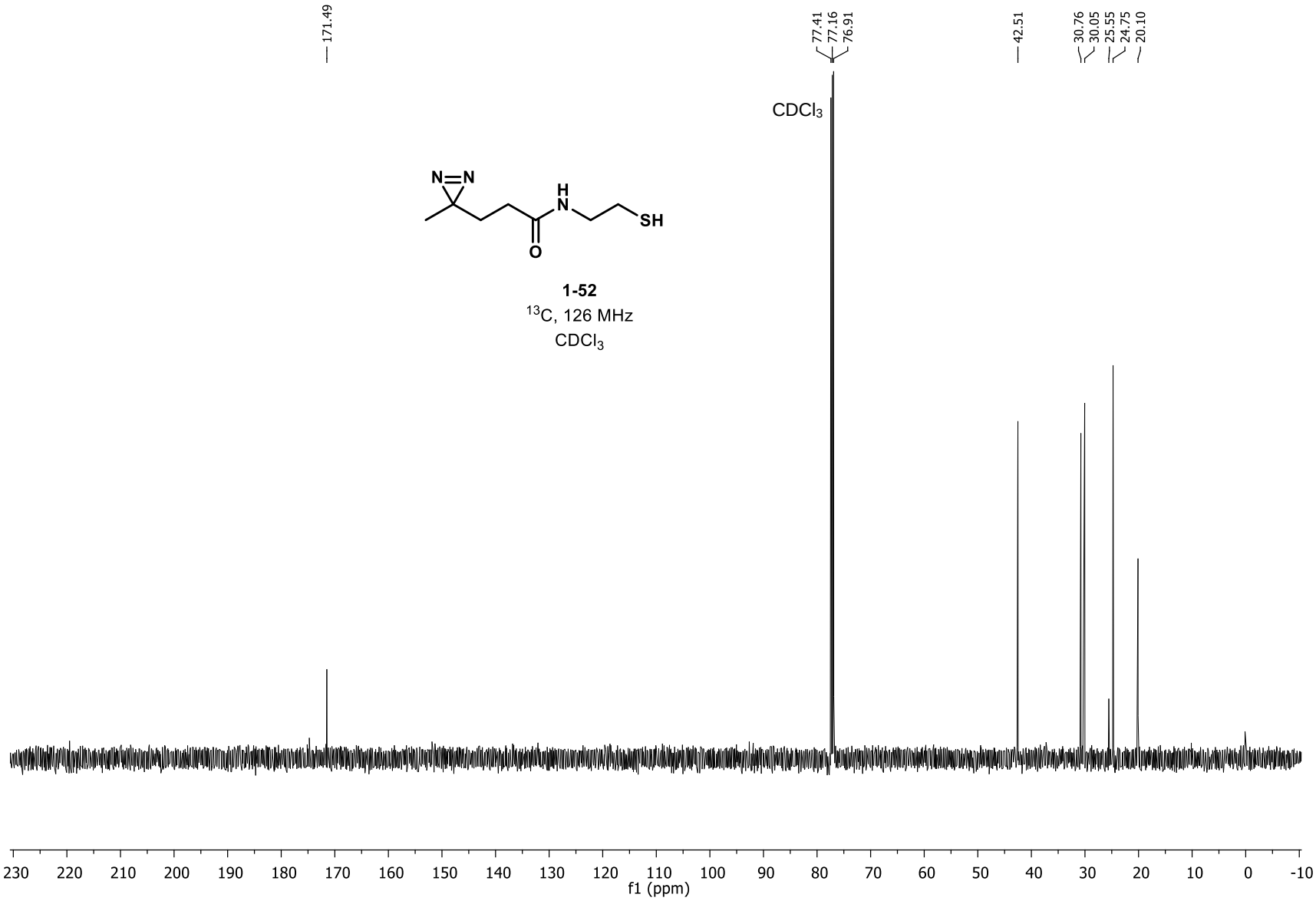
171.49
77.41
77.16
76.91
42.51
30.76
30.05
25.55
24.75
20.10
CDCl3
N=N
H
N
SH
O
1-52
13C, 126 MHz
CDCl3
230 220 210 200 190 180 170 160 150 140 130 120 110 100 90 80 70 60 50 40 30 20 10 0 -10
f1 (ppm)

Appendix B: NMR Spectra for Chapter 2

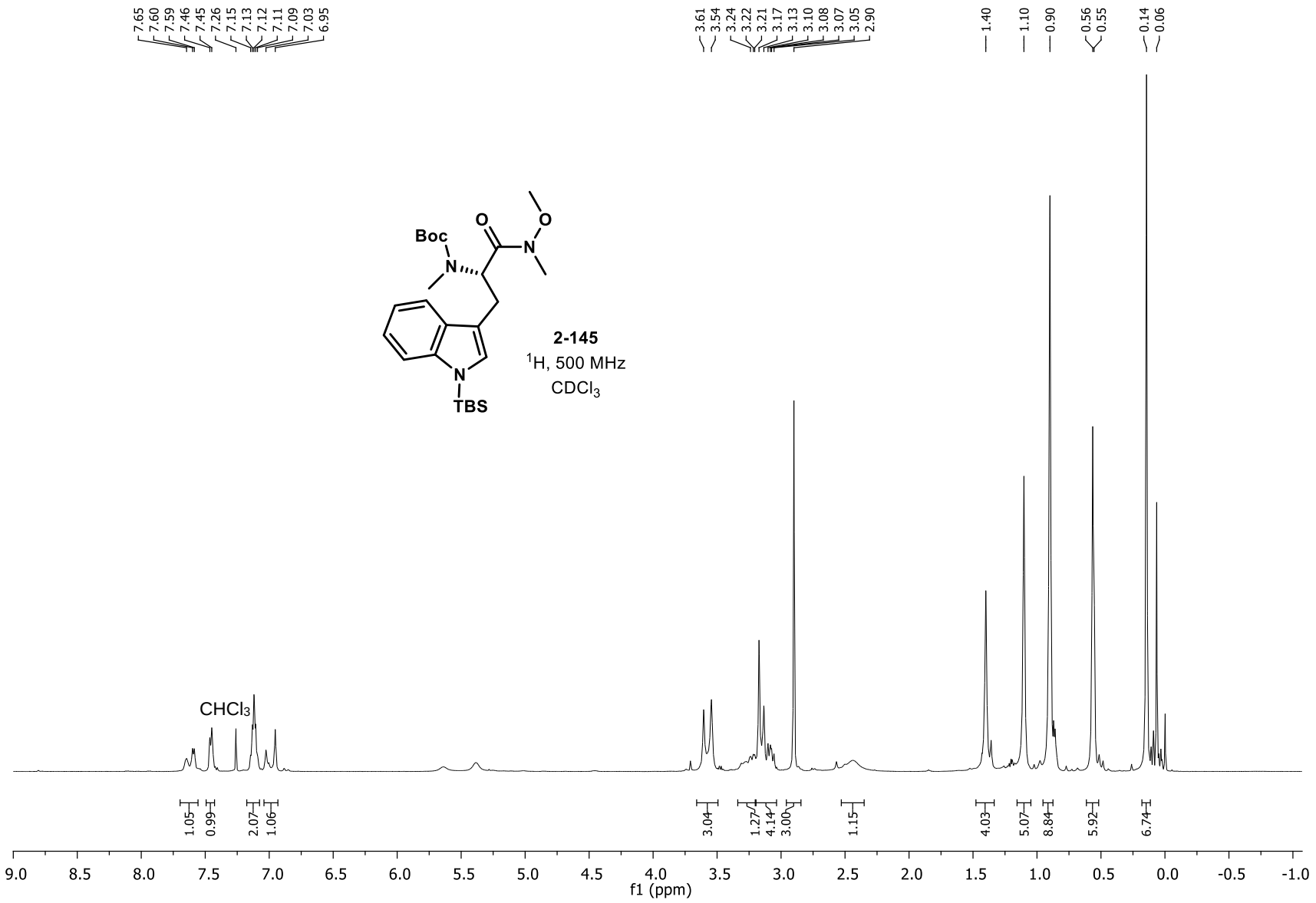
7.65
7.60
7.59
7.46
7.45
7.26
7.15
7.13
7.12
7.11
7.09
7.03
6.95
3.61
3.54
3.24
3.22
3.21
3.17
3.13
3.10
3.08
3.07
3.05
2.90
1.40
1.10
0.90
0.56
0.55
0.14
0.06
Boc
N
O
O
N
N
TBS
2-145
1H, 500 MHz
CDCl3
CHCl3
1.05
0.99
2.07
1.06
3.04
1.27
4.14
3.00
1.15
4.03
5.07
8.84
5.92
6.74
9.0
8.5
8.0
7.5
7.0
6.5
6.0
5.5
5.0
4.5
4.0
3.5
3.0
2.5
2.0
1.5
1.0
0.5
0.0
-0.5
-1.0
f1 (ppm)

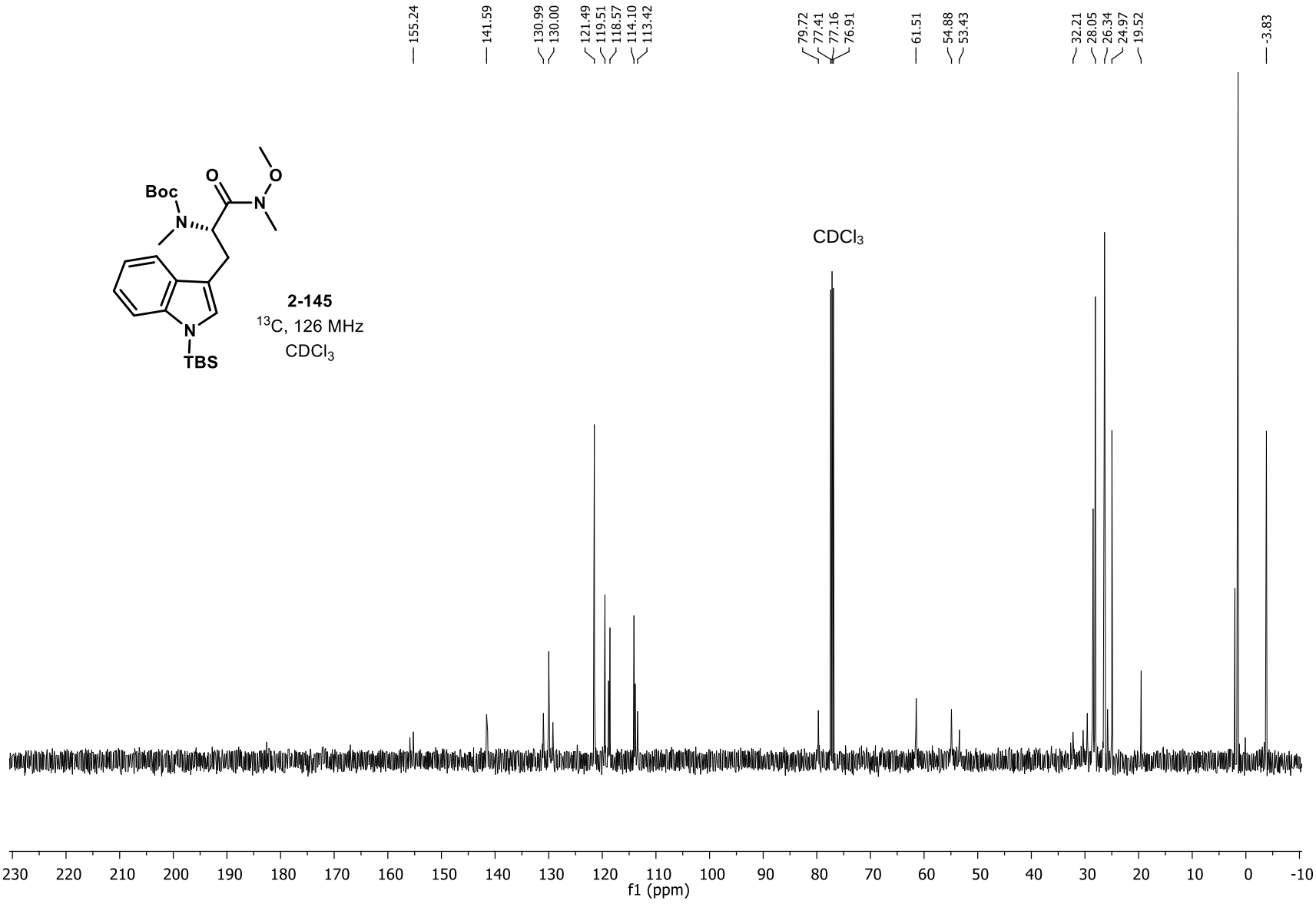
155.24
141.59
130.99
130.00
121.49
119.51
118.57
114.10
113.42
79.72
77.41
77.16
76.91
61.51
54.88
53.43
32.21
28.05
26.34
24.97
19.52
-3.83
CDCl3
Boc
N
O
O
N
N
TBS
2-145
13C, 126 MHz
CDCl3
230
220
210
200
190
180
170
160
150
140
130
120
110
100
90
80
70
60
50
40
30
20
10
0
-10
f1 (ppm)

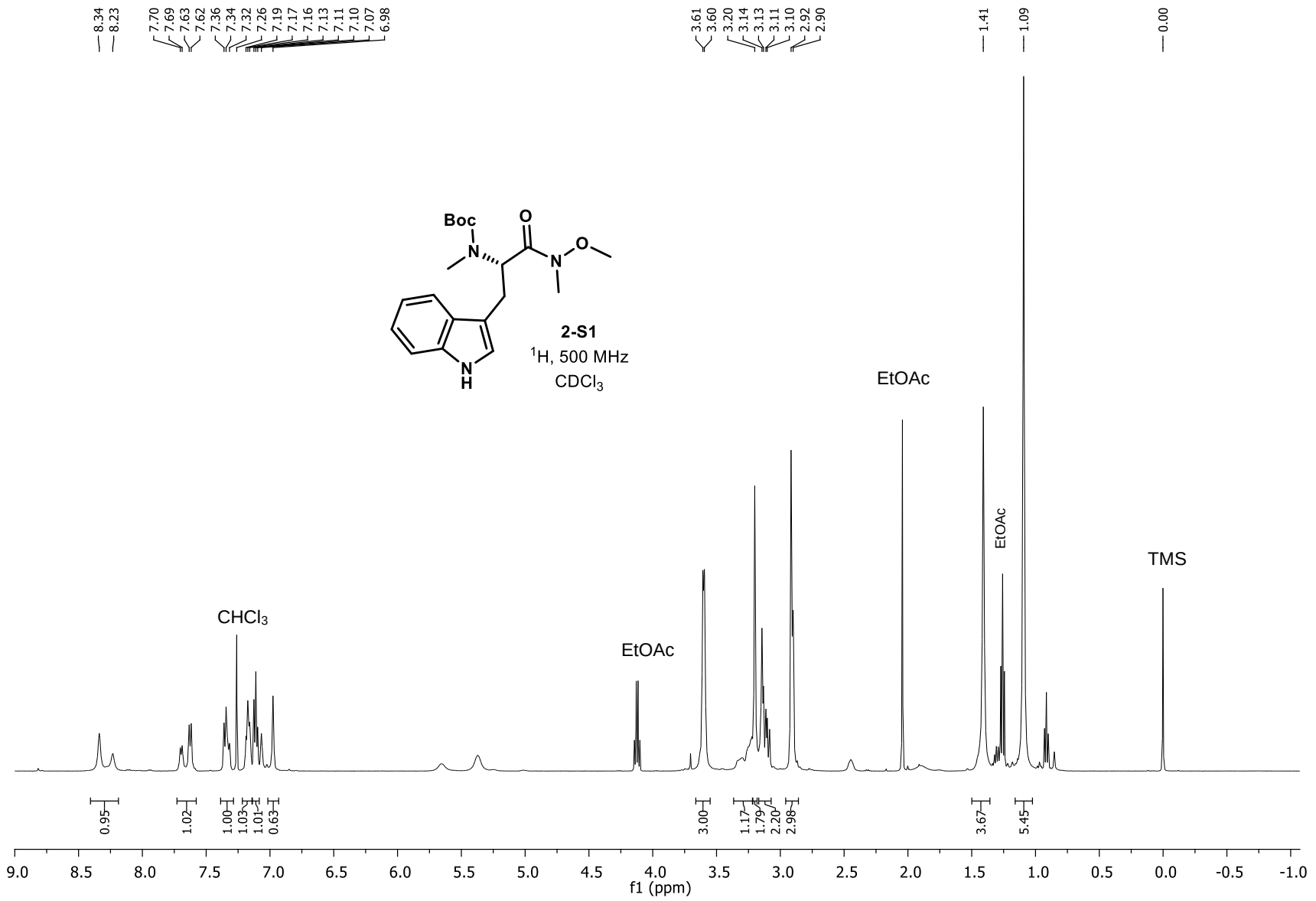
8.34
8.23
7.70
7.69
7.63
7.62
7.36
7.34
7.32
7.26
7.19
7.17
7.16
7.13
7.11
7.10
7.07
6.98
3.61
3.60
3.20
3.14
3.13
3.11
3.10
2.92
2.90
1.41
1.09
0.00
Boc
O
N
O
N
N
H
2-S1
1H, 500 MHz
CDCl3
EtOAc
EtOAc
EtOAc
TMS
CHCl3
0.95
1.02
1.00
1.03
1.01
0.63
3.00
1.17
1.79
2.20
2.98
3.67
5.45
9.0
8.5
8.0
7.5
7.0
6.5
6.0
5.5
5.0
4.5
4.0
3.5
3.0
2.5
2.0
1.5
1.0
0.5
0.0
-0.5
-1.0
f1 (ppm)

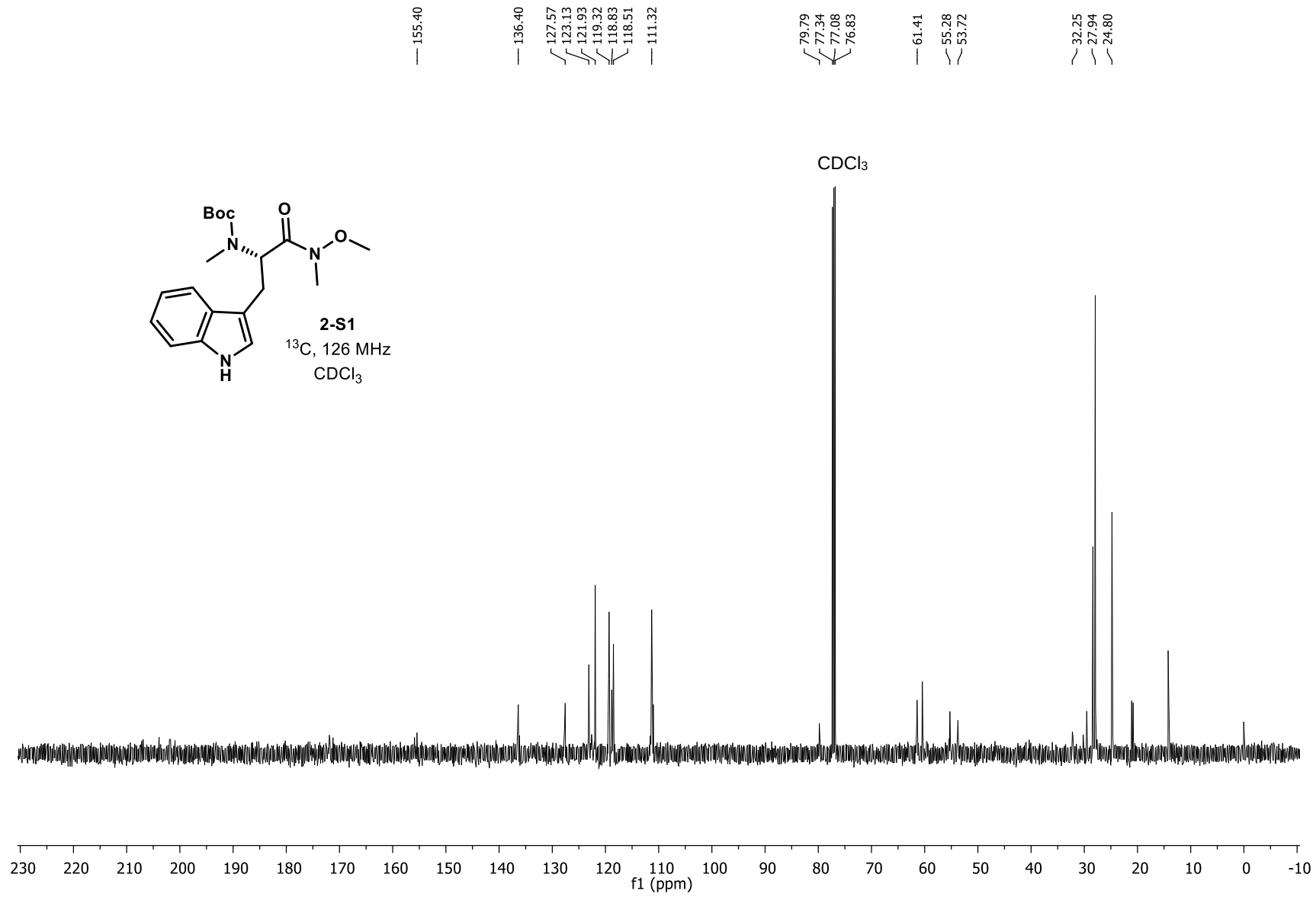
155.40
136.40
127.57
123.13
121.93
119.32
118.83
118.51
111.32
79.79
77.34
77.08
76.83
61.41
55.28
53.72
32.25
27.94
24.80
CDCl3
Boc
O
N
N
O
N
H
2-S1
13C, 126 MHz
CDCl3
230 220 210 200 190 180 170 160 150 140 130 120 110 100 90 80 70 60 50 40 30 20 10 0 -10
f1 (ppm)

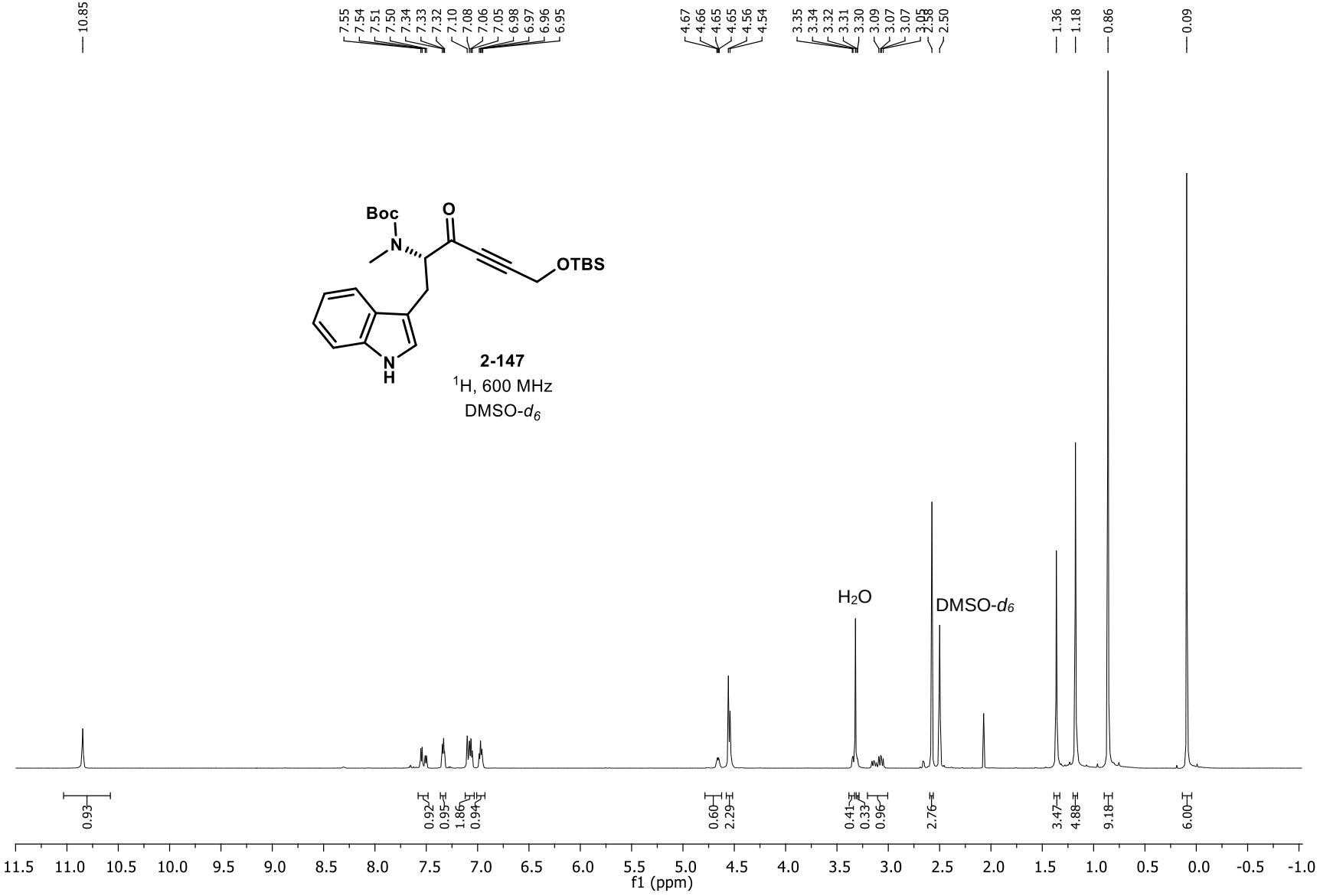
10.85
7.55
7.54
7.51
7.50
7.34
7.33
7.32
7.10
7.08
7.06
7.05
6.98
6.97
6.96
6.95
4.67
4.66
4.65
4.65
4.56
4.54
3.35
3.34
3.32
3.31
3.30
3.09
3.07
3.07
3.05
2.58
2.50
1.36
1.18
0.86
0.09
Boc
N
O
OTBS
N
H
2-147
1H, 600 MHz
DMSO-d6
H2O
DMSO-d6
0.93
0.92
0.95
1.86
0.94
0.60
2.29
0.41
0.33
0.96
2.76
3.47
4.88
9.18
6.00
11.5
11.0
10.5
10.0
9.5
9.0
8.5
8.0
7.5
7.0
6.5
6.0
5.5
5.0
4.5
4.0
3.5
3.0
2.5
2.0
1.5
1.0
0.5
0.0
-0.5
-1.0
f1 (ppm)

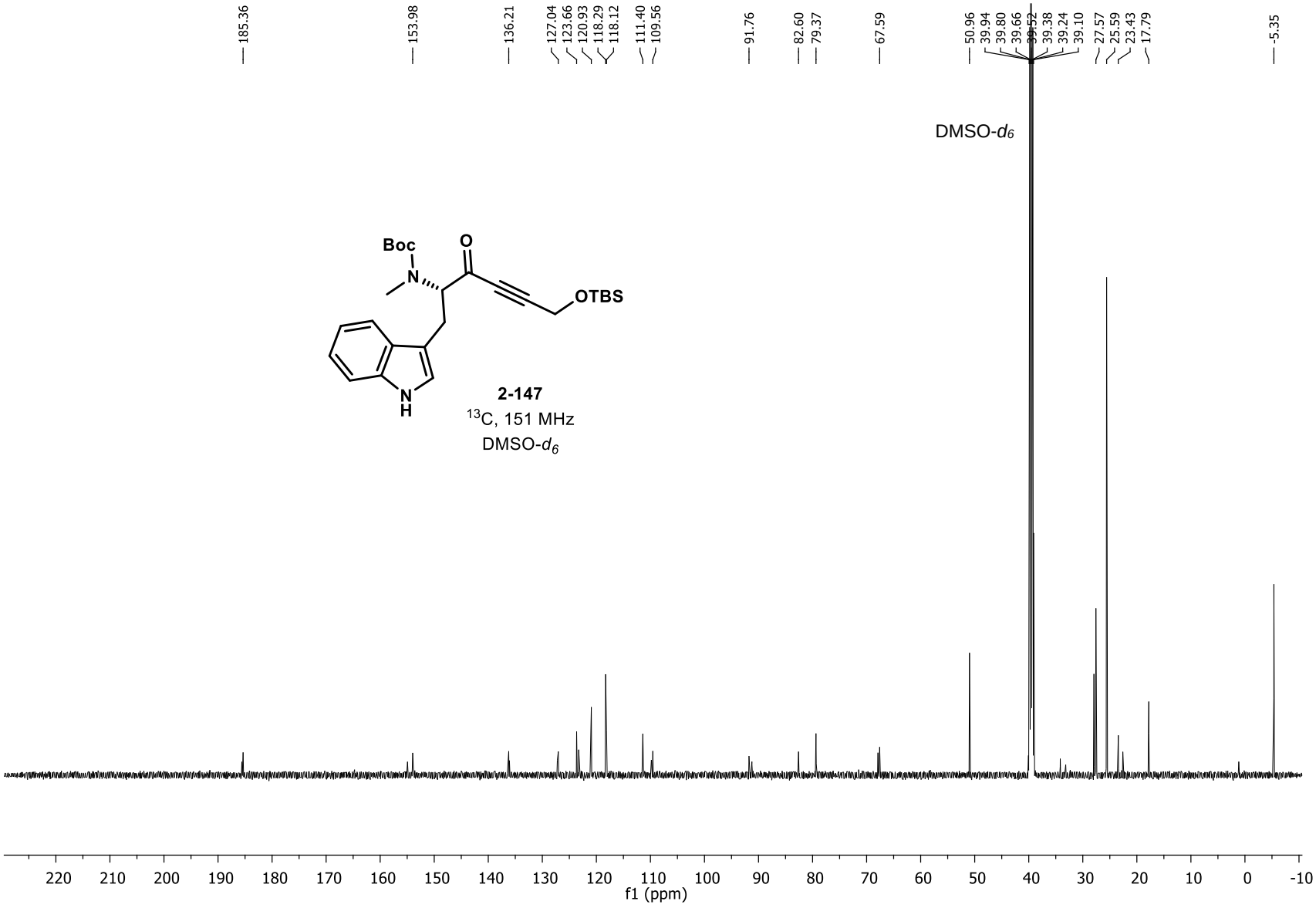
185.36
153.98
136.21
127.04
123.66
120.93
118.29
118.12
111.40
109.56
91.76
82.60
79.37
67.59
50.96
39.94
39.80
39.66
39.52
39.38
39.24
39.10
27.57
25.59
23.43
17.79
-5.35
DMSO-d6
Boc
N
O
OTBS
N
H
2-147
13C, 151 MHz
DMSO-d6
f1 (ppm)

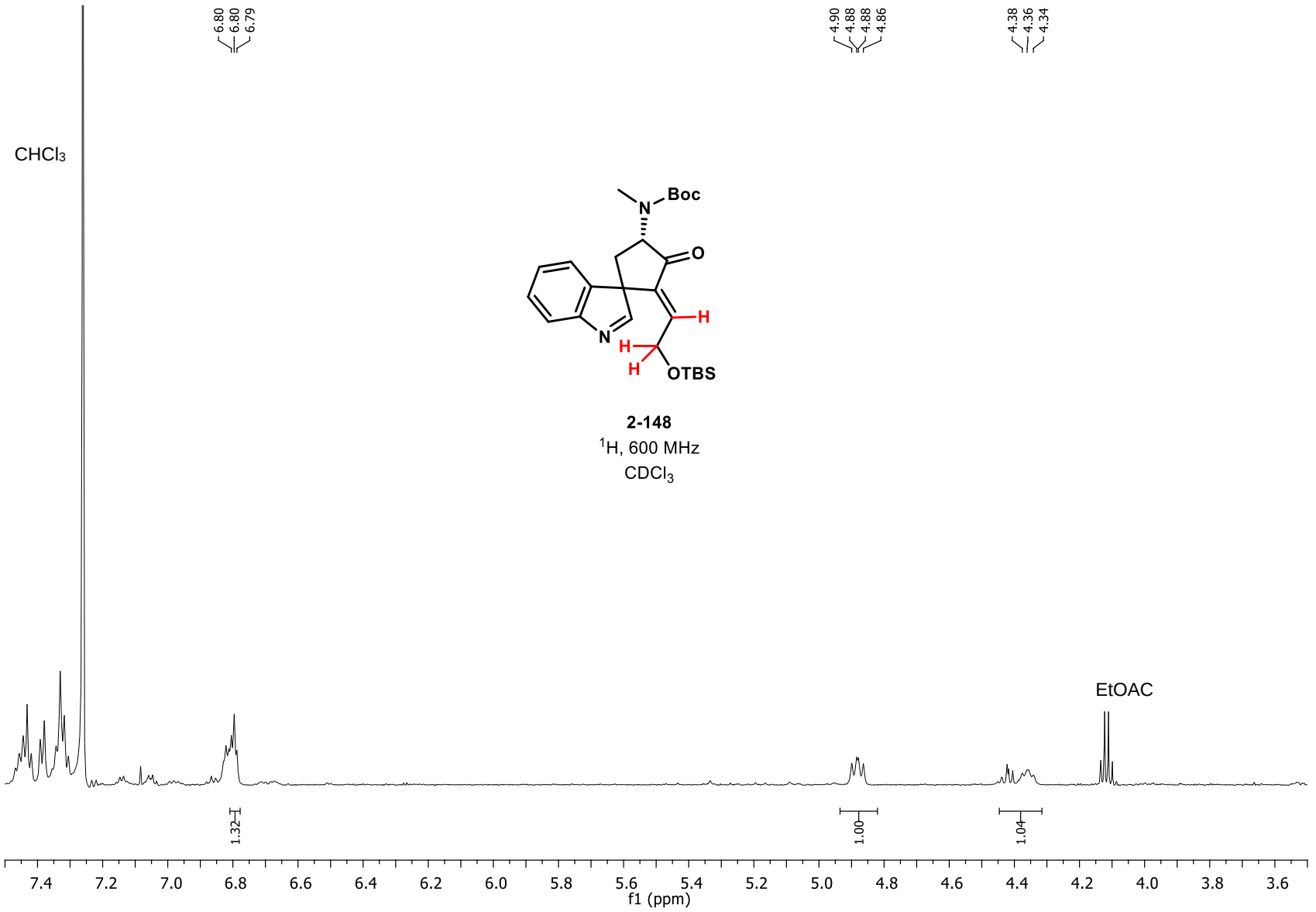

2-148

^{1}H, 600 MHz

$CDCl_3$

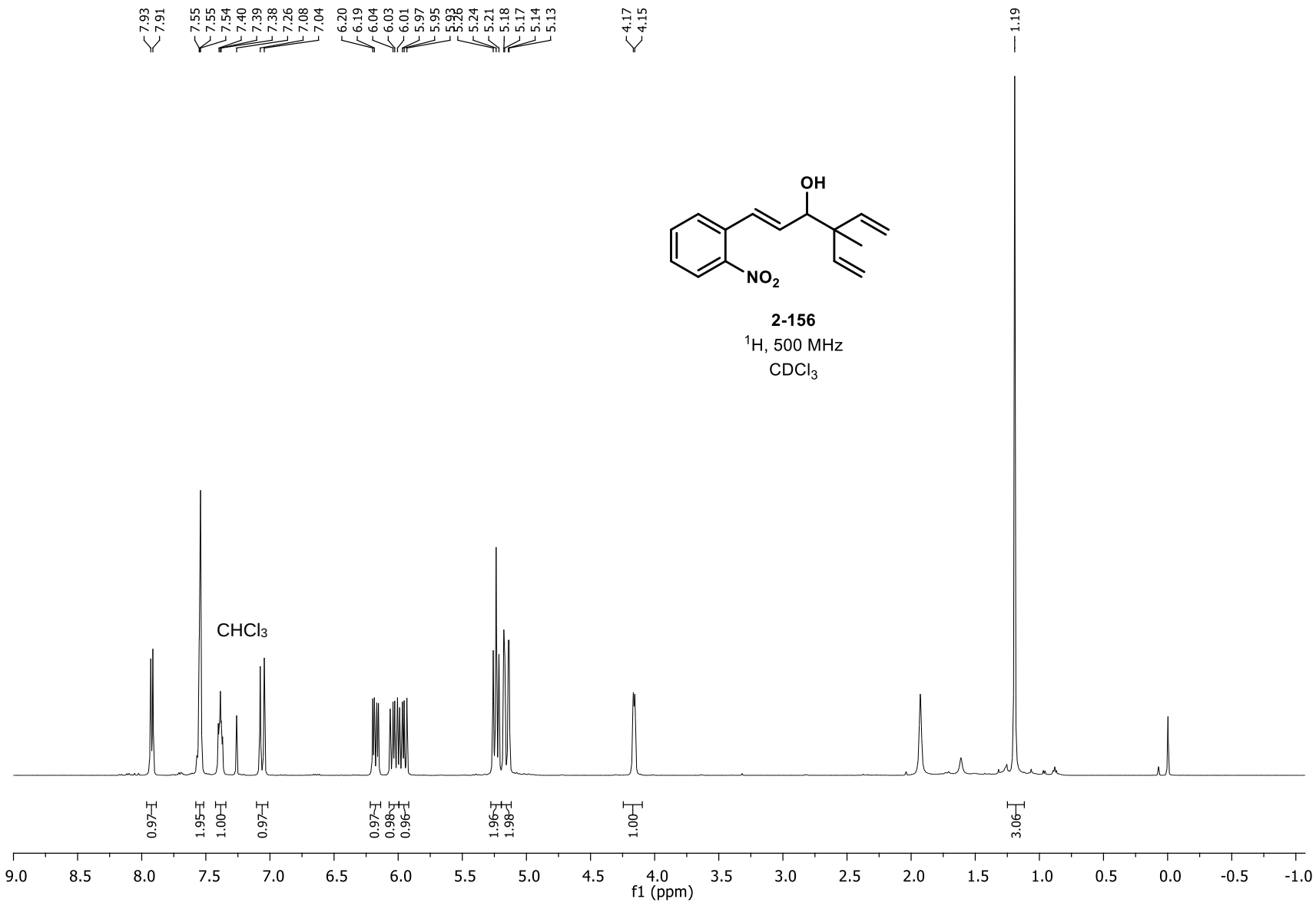
7.93
7.91
7.55
7.55
7.54
7.40
7.39
7.38
7.26
7.08
7.04
6.20
6.19
6.04
6.03
6.01
5.97
5.95
5.93
5.26
5.24
5.21
5.18
5.17
5.14
5.13
4.17
4.15
1.19
OH
NO2
2-156
1H, 500 MHz
CDCl3
CHCl3
0.97
1.95
1.00
0.97
0.97
0.98
0.96
1.96
1.98
1.00
3.06
9.0
8.5
8.0
7.5
7.0
6.5
6.0
5.5
5.0
4.5
4.0
3.5
3.0
2.5
2.0
1.5
1.0
0.5
0.0
-0.5
-1.0
f1 (ppm)

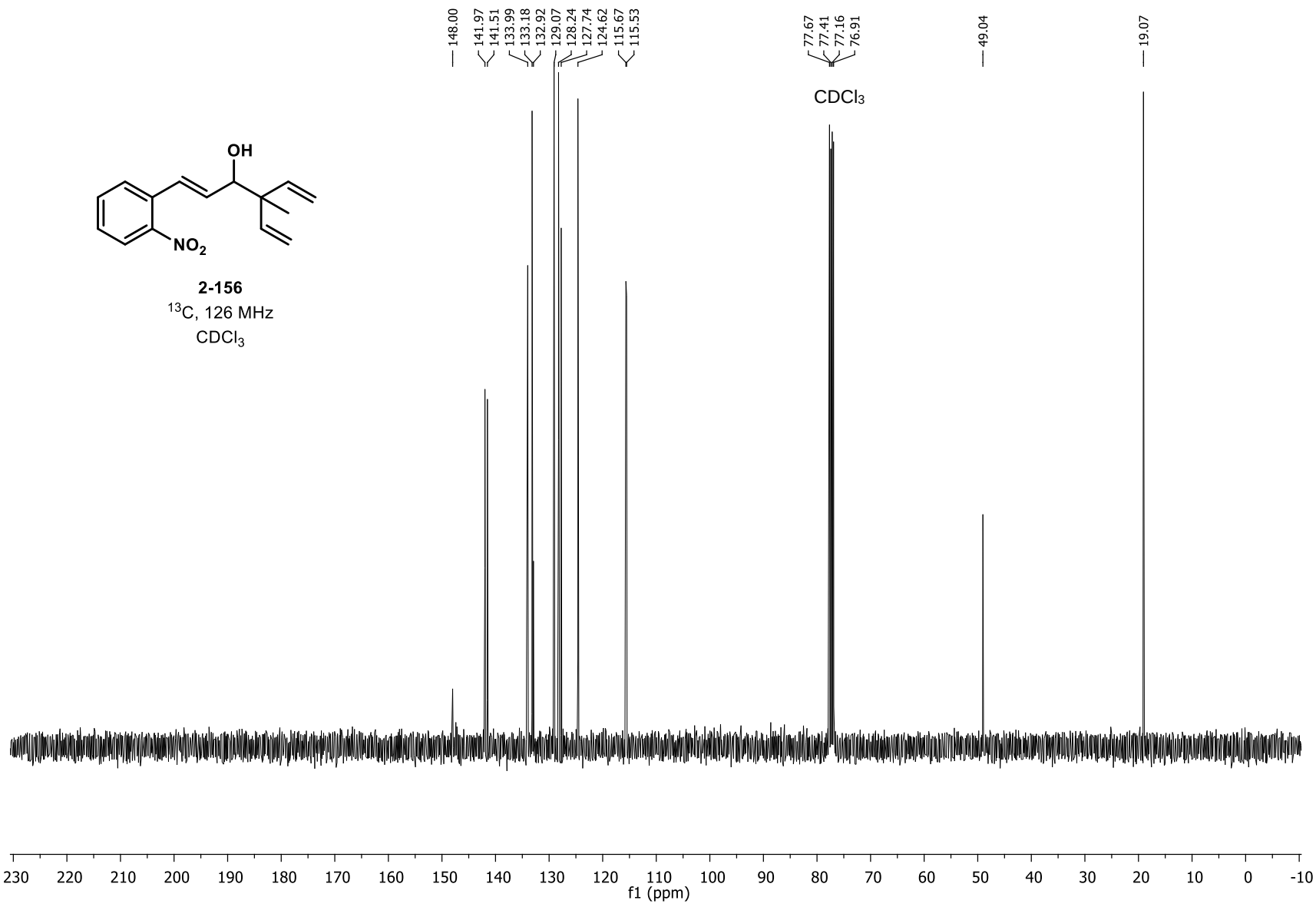
148.00
141.97
141.51
133.99
133.18
132.92
129.07
128.24
127.74
124.62
115.67
115.53
77.67
77.41
77.16
76.91
49.04
19.07
CDCl3
OH
NO2
2-156
13C, 126 MHz
CDCl3
230 220 210 200 190 180 170 160 150 140 130 120 110 100 90 80 70 60 50 40 30 20 10 0 -10
f1 (ppm)

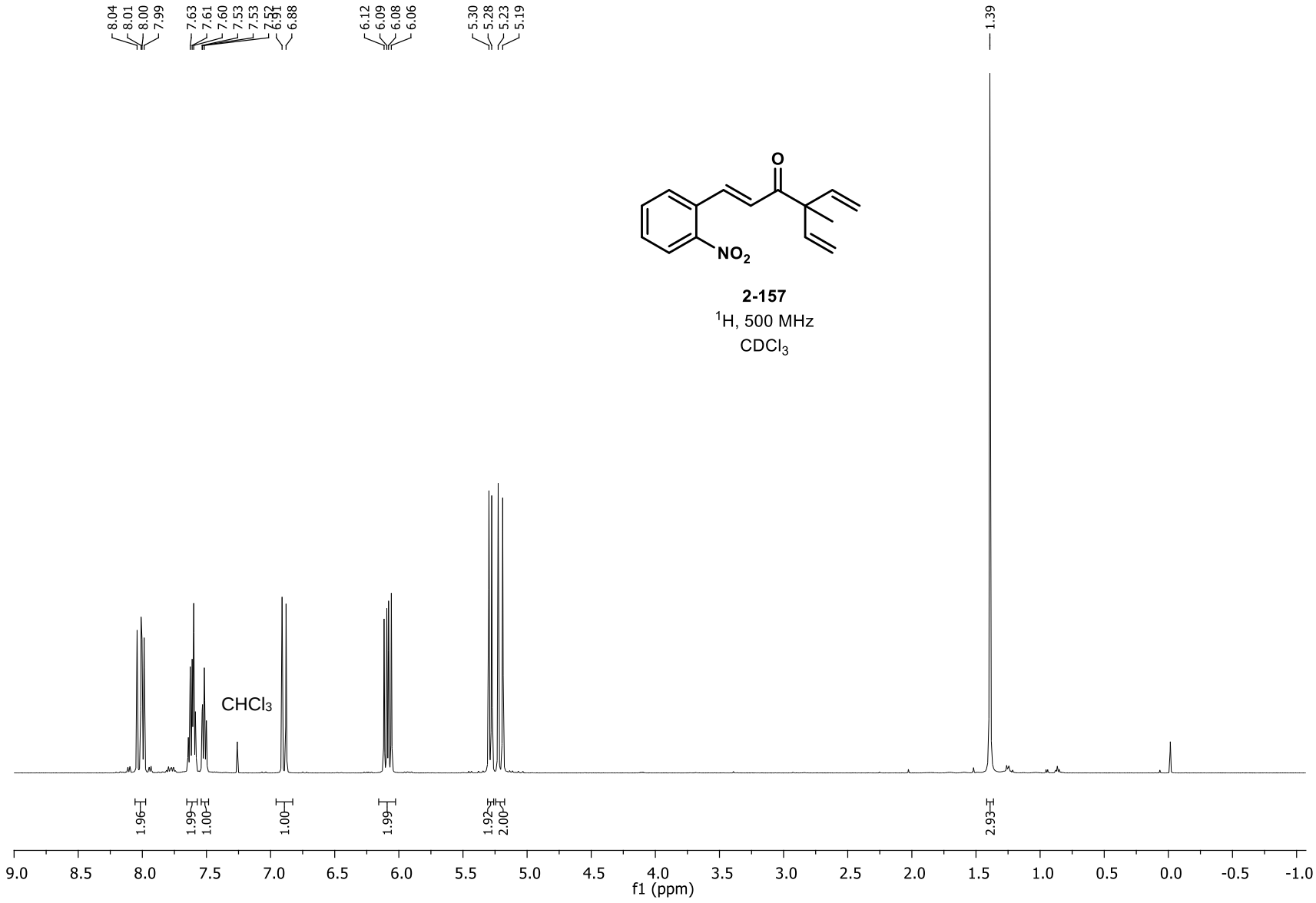
8.04
8.01
8.00
7.99
7.63
7.61
7.60
7.53
7.53
7.52
7.51
6.88
6.12
6.09
6.08
6.06
5.30
5.28
5.23
5.19
1.39
O
NO2
2-157
1H, 500 MHz
CDCl3
CHCl3
1.96
1.99
1.00
1.00
1.99
1.92
2.00
2.93
9.0
8.5
8.0
7.5
7.0
6.5
6.0
5.5
5.0
4.5
4.0
3.5
3.0
2.5
2.0
1.5
1.0
0.5
0.0
-0.5
-1.0
f1 (ppm)

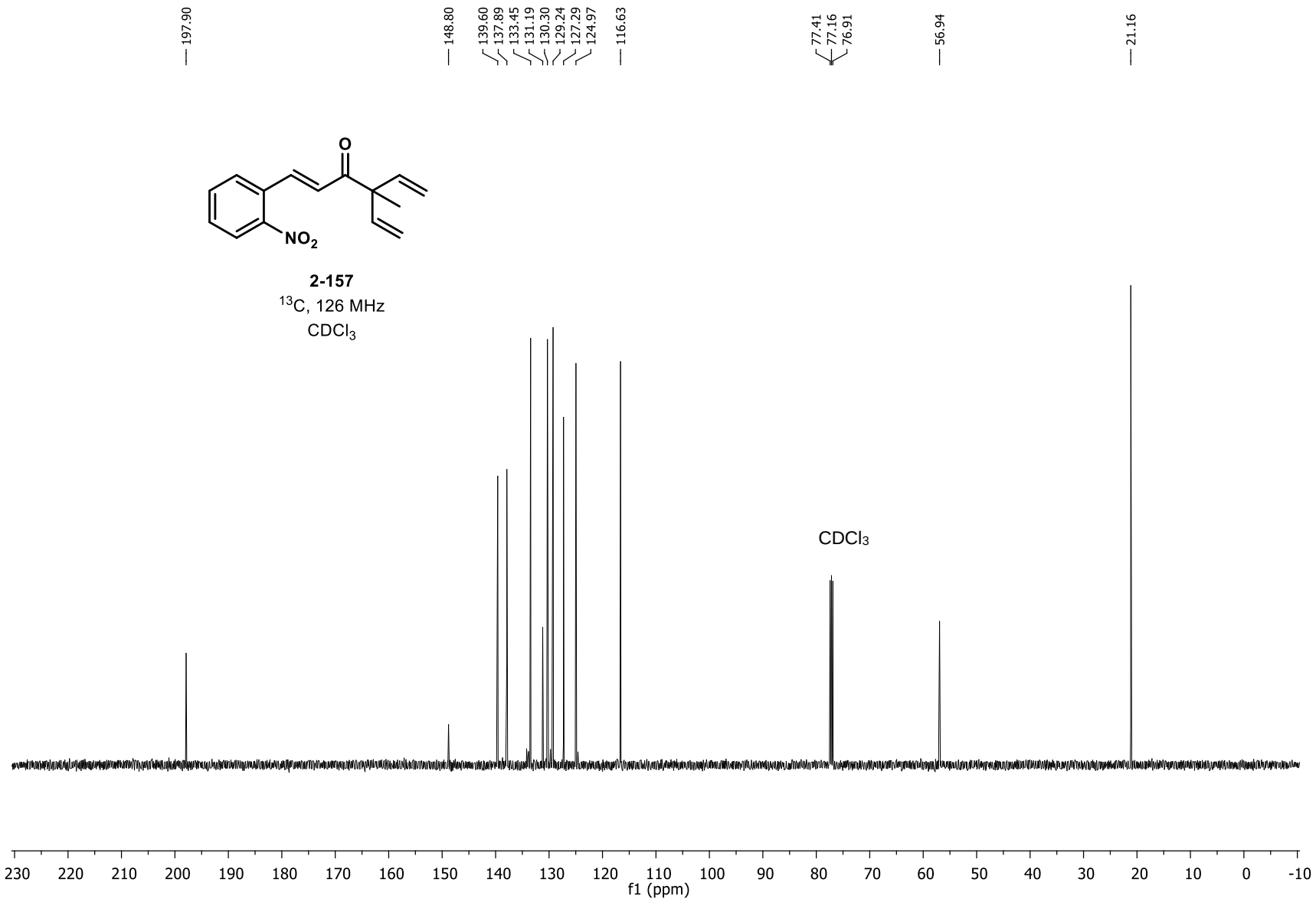
197.90
148.80
139.60
137.89
133.45
131.19
130.30
129.24
127.29
124.97
116.63
77.41
77.16
76.91
56.94
21.16
O
NO2
2-157
13C, 126 MHz
CDCl3
CDCl3
230 220 210 200 190 180 170 160 150 140 130 120 110 100 90 80 70 60 50 40 30 20 10 0 -10
f1 (ppm)

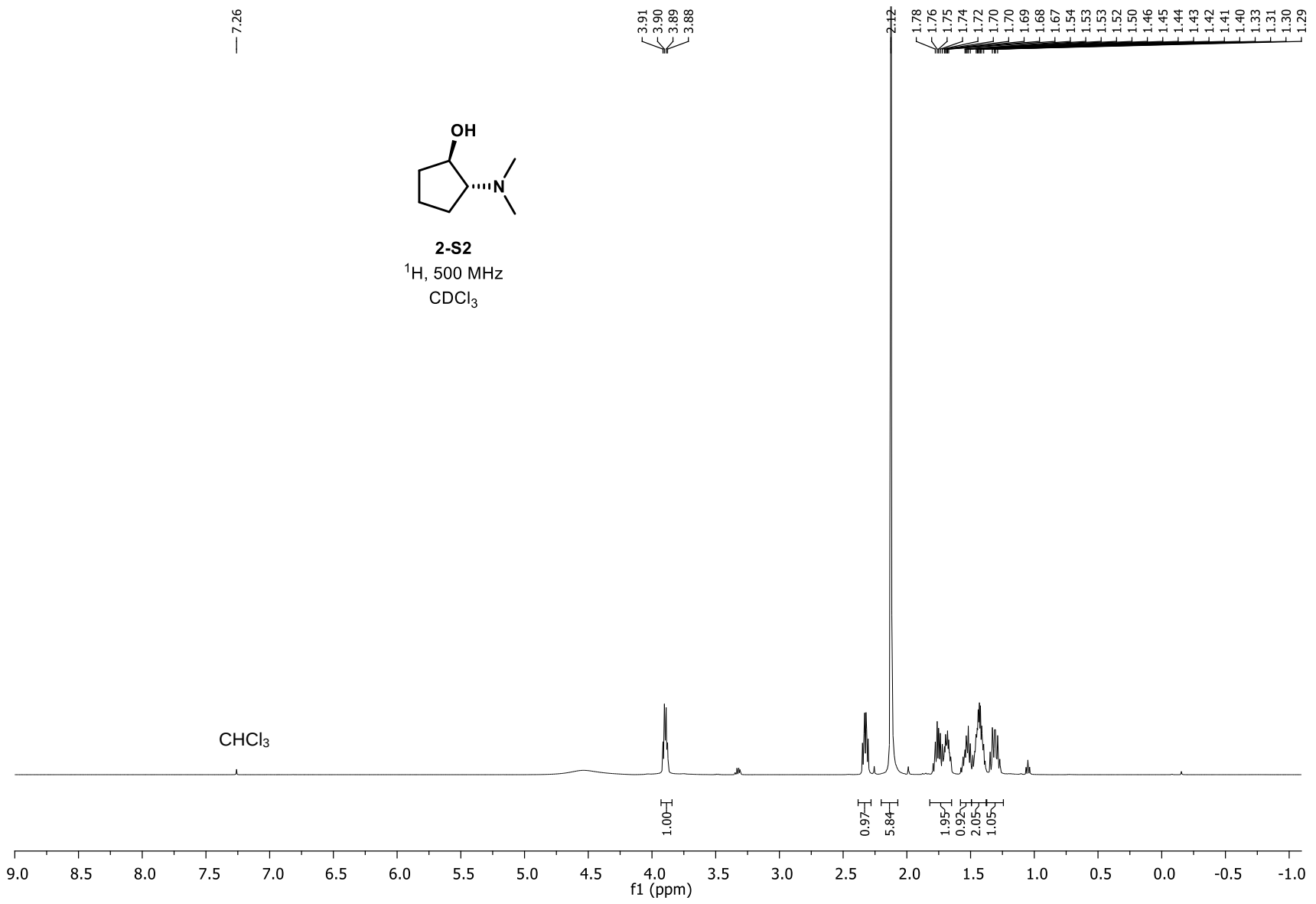
7.26
3.91
3.90
3.89
3.88
2.12
1.78
1.76
1.75
1.74
1.72
1.70
1.70
1.69
1.68
1.67
1.54
1.53
1.53
1.52
1.50
1.46
1.45
1.44
1.43
1.42
1.41
1.40
1.33
1.31
1.30
1.29
OH
N
2-S2
1H, 500 MHz
CDCl3
CHCl3
1.00
0.97
5.84
1.95
0.92
2.05
1.05
9.0
8.5
8.0
7.5
7.0
6.5
6.0
5.5
5.0
4.5
4.0
3.5
3.0
2.5
2.0
1.5
1.0
0.5
0.0
-0.5
-1.0
f1 (ppm)

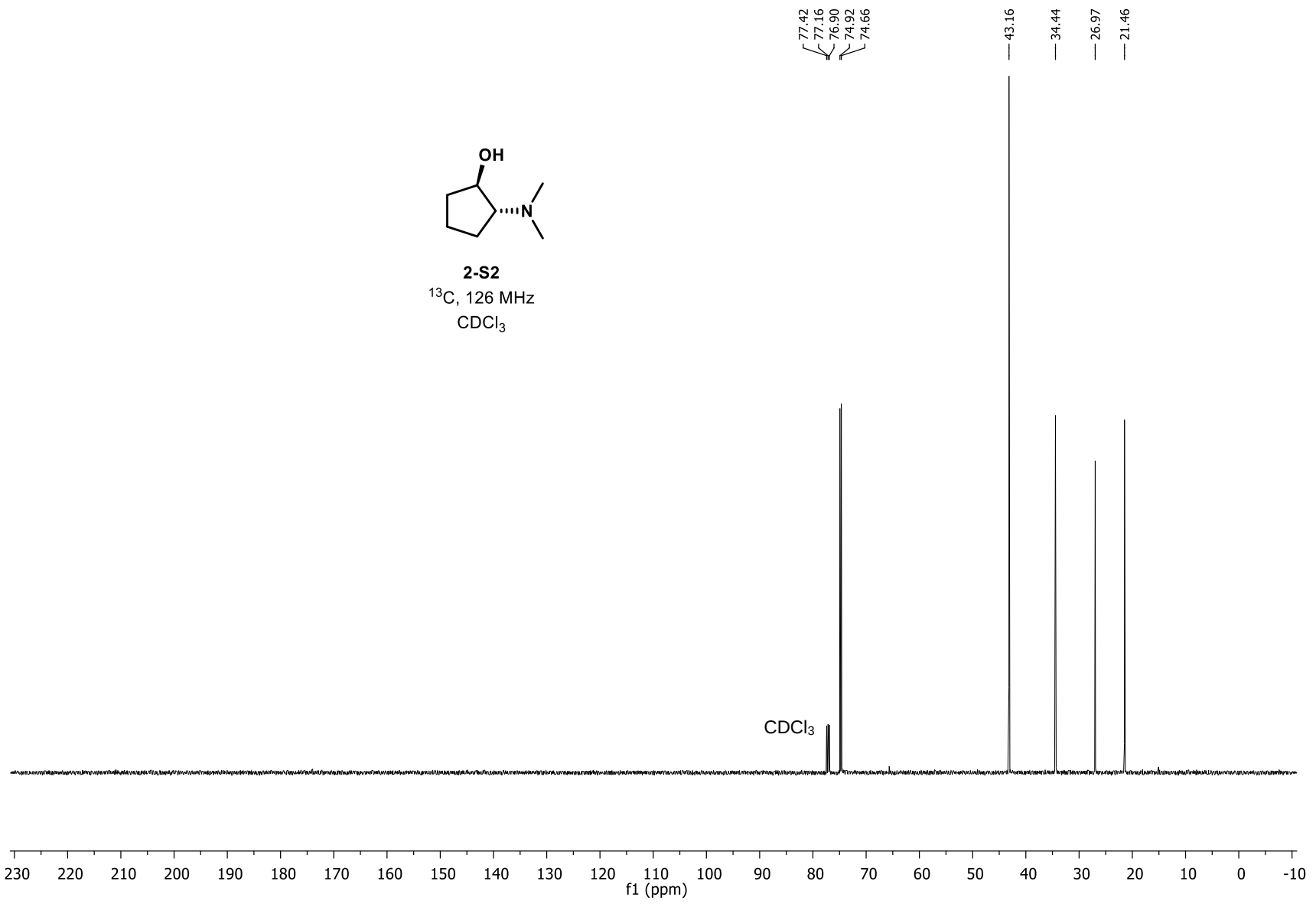
77.42
77.16
76.90
74.92
74.66
43.16
34.44
26.97
21.46
OH
N
2-S2
13C, 126 MHz
CDCl3
CDCl3
230 220 210 200 190 180 170 160 150 140 130 120 110 100 90 80 70 60 50 40 30 20 10 0 -10
f1 (ppm)

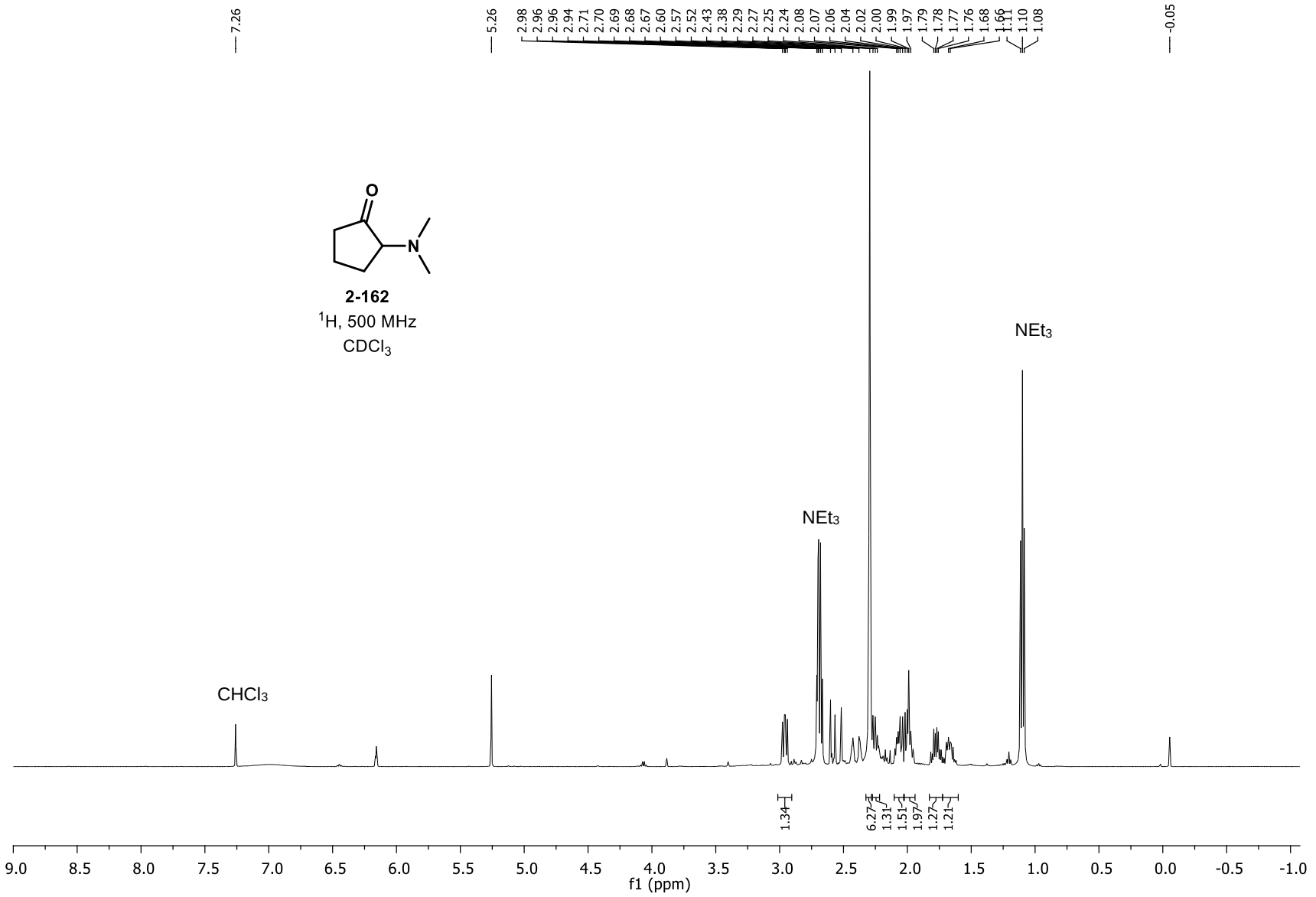
7.26
5.26
2.98
2.96
2.96
2.94
2.71
2.70
2.69
2.68
2.67
2.60
2.57
2.52
2.43
2.38
2.29
2.27
2.25
2.24
2.08
2.07
2.06
2.04
2.02
2.00
1.99
1.97
1.79
1.78
1.77
1.76
1.68
1.66
1.11
1.10
1.08
-0.05
O
N
2-162
1H, 500 MHz
CDCl3
NEt3
NEt3
CHCl3
1.34
6.27
1.31
1.51
1.97
1.27
1.21
9.0
8.5
8.0
7.5
7.0
6.5
6.0
5.5
5.0
4.5
4.0
3.5
3.0
2.5
2.0
1.5
1.0
0.5
0.0
-0.5
-1.0
f1 (ppm)

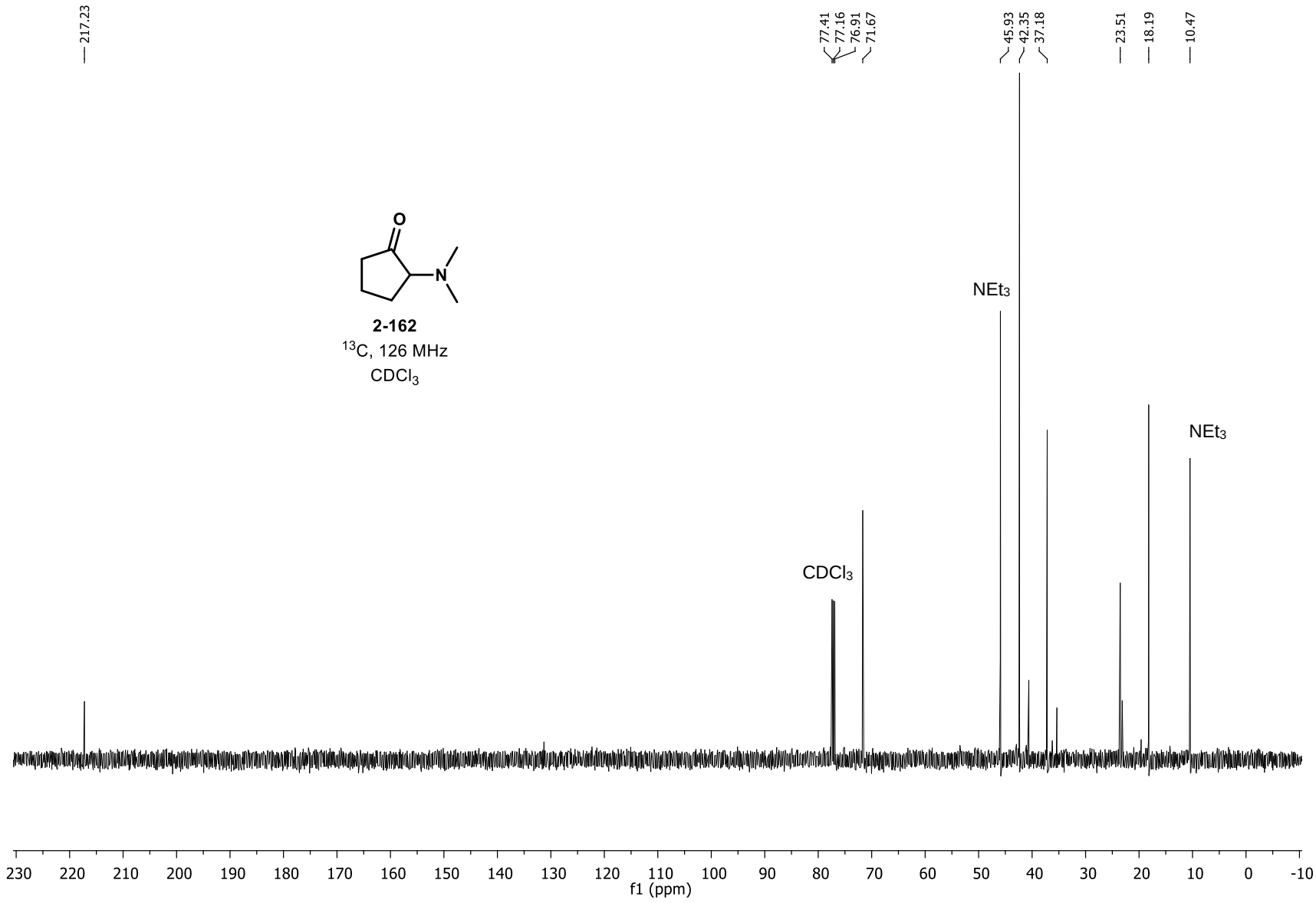
217.23
77.41
77.16
76.91
71.67
45.93
42.35
37.18
23.51
18.19
10.47
O
N
2-162
13C, 126 MHz
CDCl3
NEt3
NEt3
CDCl3
350
230 220 210 200 190 180 170 160 150 140 130 120 110 100 90 80 70 60 50 40 30 20 10 0 -10
f1 (ppm)

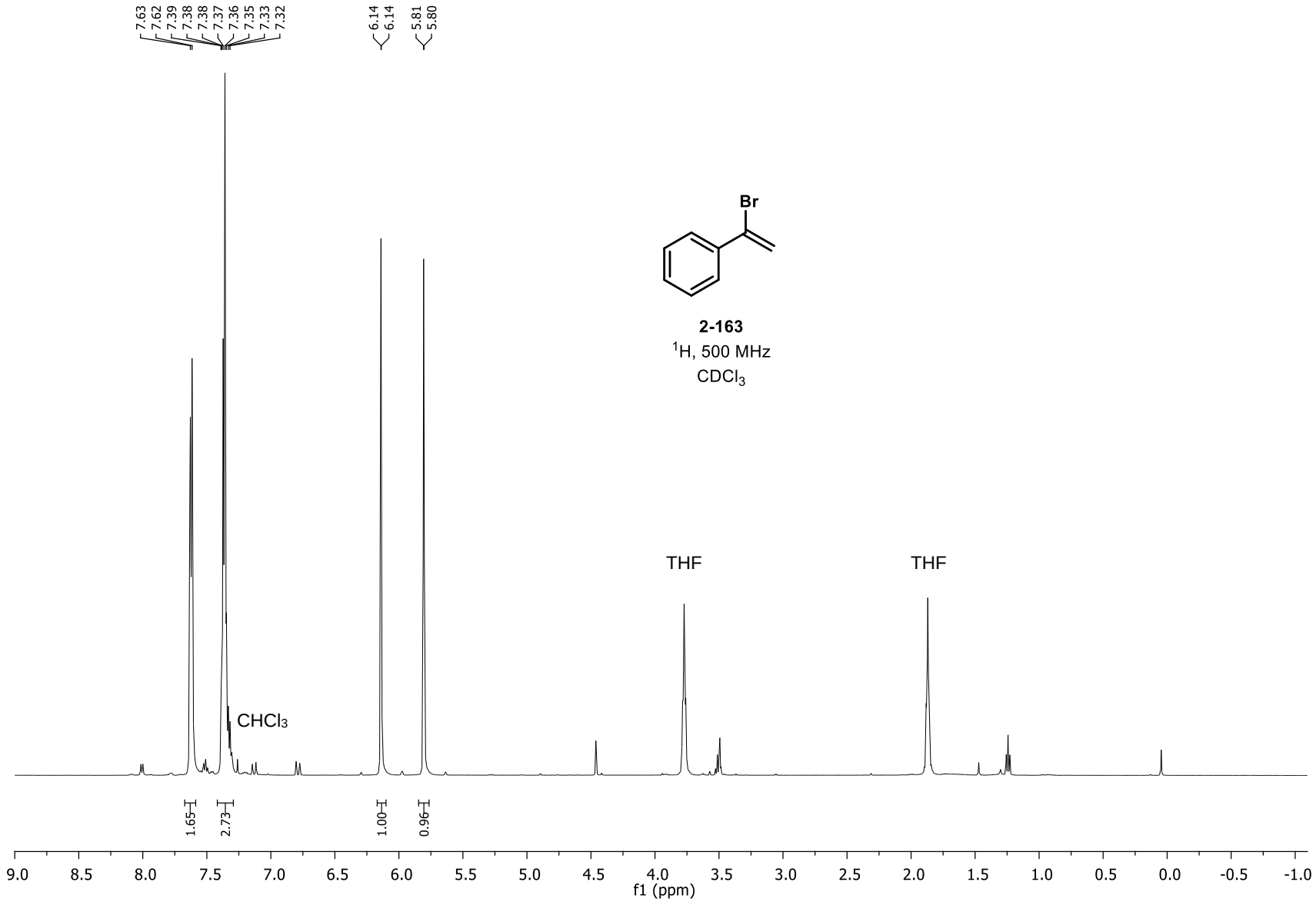
7.63
7.62
7.39
7.38
7.38
7.37
7.36
7.35
7.33
7.32
6.14
6.14
5.81
5.80
Br
2-163
1H, 500 MHz
CDCl3
THF
THF
CHCl3
1.65
2.73
1.00
0.96
9.0
8.5
8.0
7.5
7.0
6.5
6.0
5.5
5.0
4.5
4.0
3.5
3.0
2.5
2.0
1.5
1.0
0.5
0.0
-0.5
-1.0
f1 (ppm)

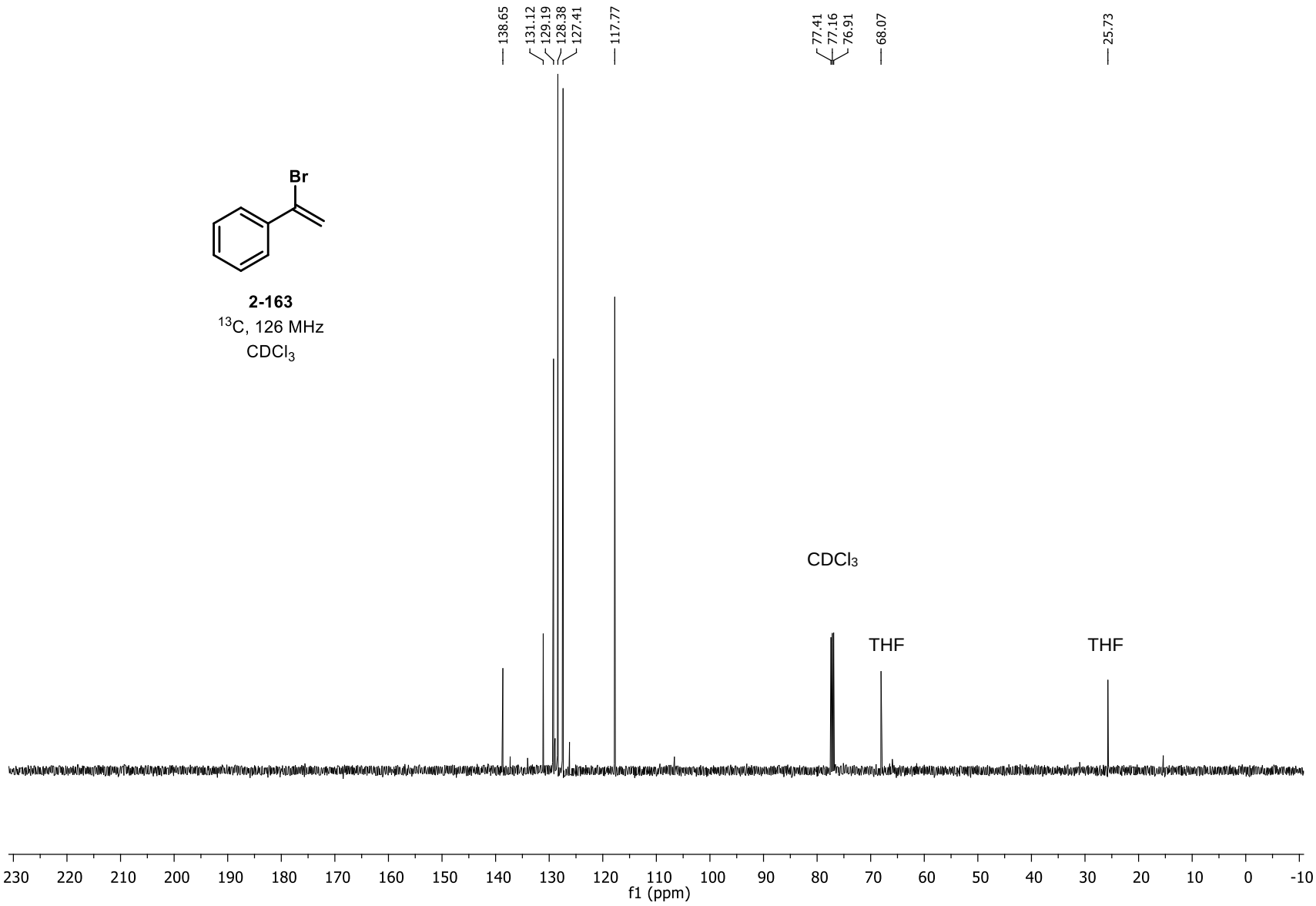
138.65
131.12
129.19
128.38
127.41
117.77
77.41
77.16
76.91
68.07
25.73
Br
2-163
13C, 126 MHz
CDCl3
CDCl3
THF
THF
230 220 210 200 190 180 170 160 150 140 130 120 110 100 90 80 70 60 50 40 30 20 10 0 -10
f1 (ppm)

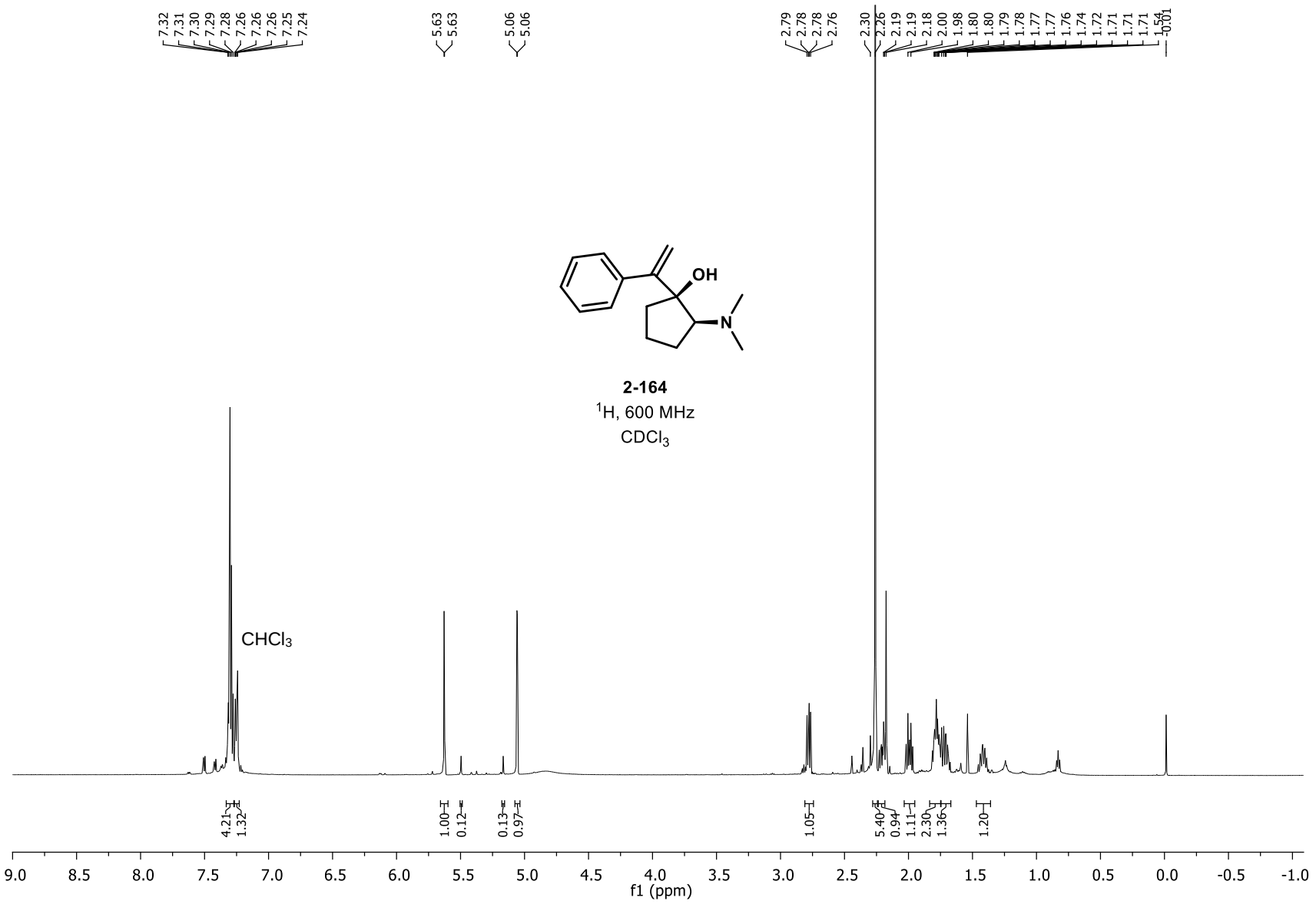
7.32
7.31
7.30
7.29
7.28
7.26
7.26
7.26
7.25
7.24
5.63
5.63
5.06
5.06
2.79
2.78
2.78
2.76
2.30
2.26
2.19
2.19
2.18
2.00
1.98
1.80
1.80
1.79
1.78
1.77
1.77
1.76
1.74
1.72
1.71
1.71
1.71
1.54
0.01
OH
N
2-164
1H, 600 MHz
CDCl3
CHCl3
4.21
1.32
1.00
0.12
0.13
0.97
1.05
5.40
0.94
1.11
2.30
1.36
1.20
9.0
8.5
8.0
7.5
7.0
6.5
6.0
5.5
5.0
4.5
4.0
3.5
3.0
2.5
2.0
1.5
1.0
0.5
0.0
-0.5
-1.0
f1 (ppm)

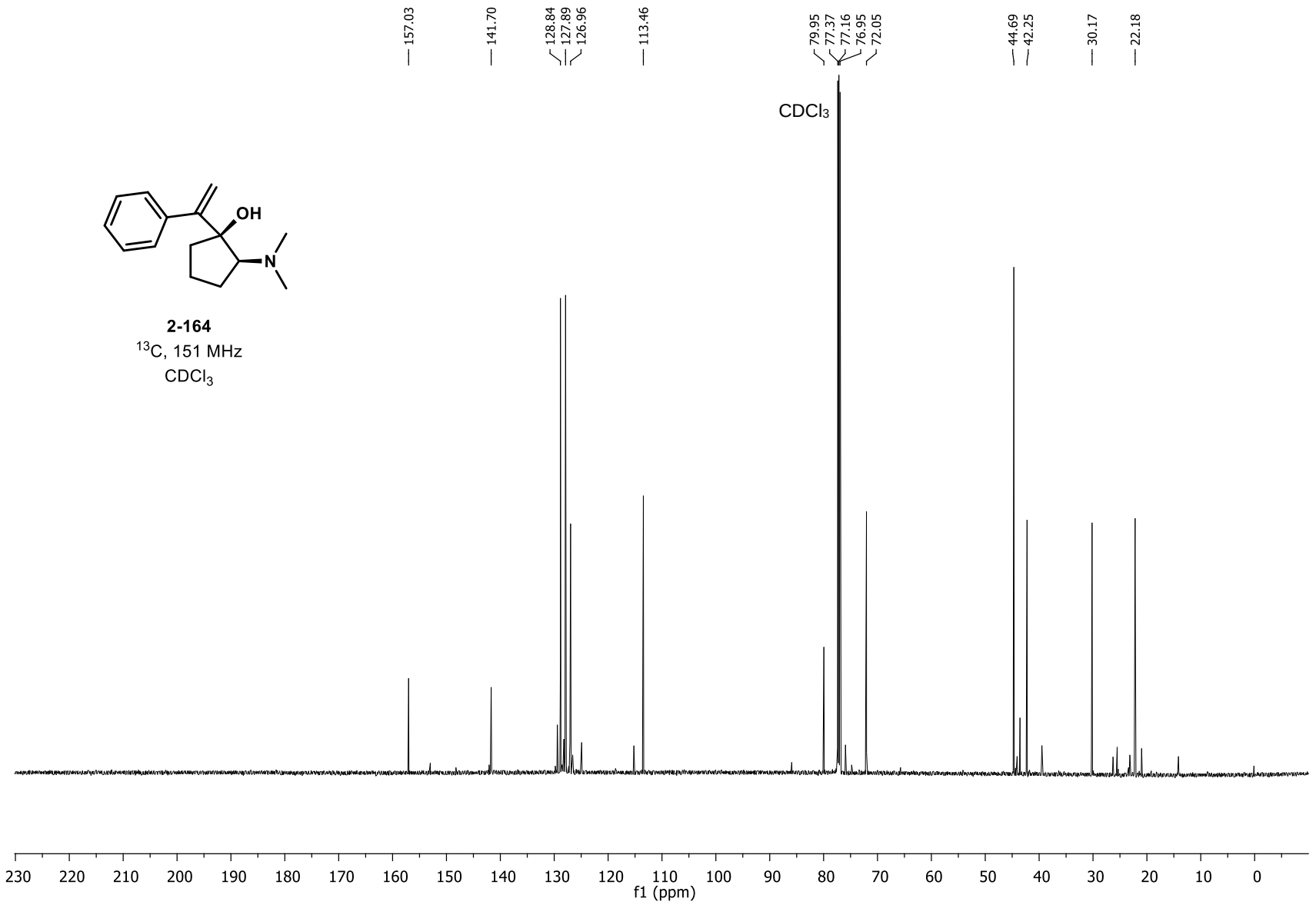
157.03
141.70
128.84
127.89
126.96
113.46
79.95
77.37
77.16
76.95
72.05
44.69
42.25
30.17
22.18
CDCl3
OH
N
2-164
13C, 151 MHz
CDCl3
230 220 210 200 190 180 170 160 150 140 130 120 110 100 90 80 70 60 50 40 30 20 10 0
f1 (ppm)

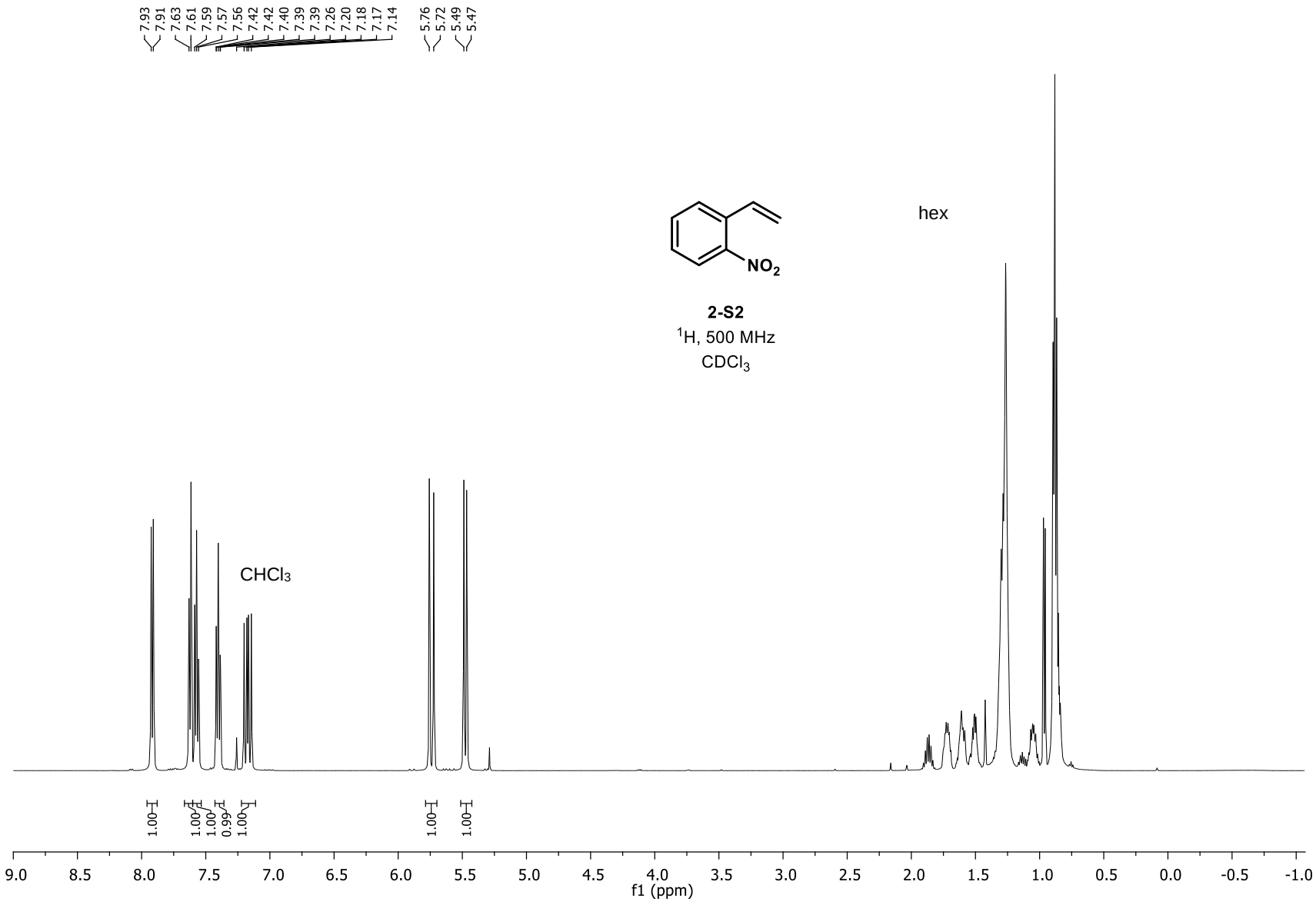
7.93
7.91
7.63
7.61
7.59
7.57
7.56
7.42
7.42
7.40
7.39
7.39
7.26
7.20
7.18
7.17
7.14
5.76
5.72
5.49
5.47
NO2
2-S2
1H, 500 MHz
CDCl3
hex
CHCl3
1.00
1.00
1.00
0.99
1.00
1.00
1.00
9.0
8.5
8.0
7.5
7.0
6.5
6.0
5.5
5.0
4.5
4.0
3.5
3.0
2.5
2.0
1.5
1.0
0.5
0.0
-0.5
-1.0
f1 (ppm)

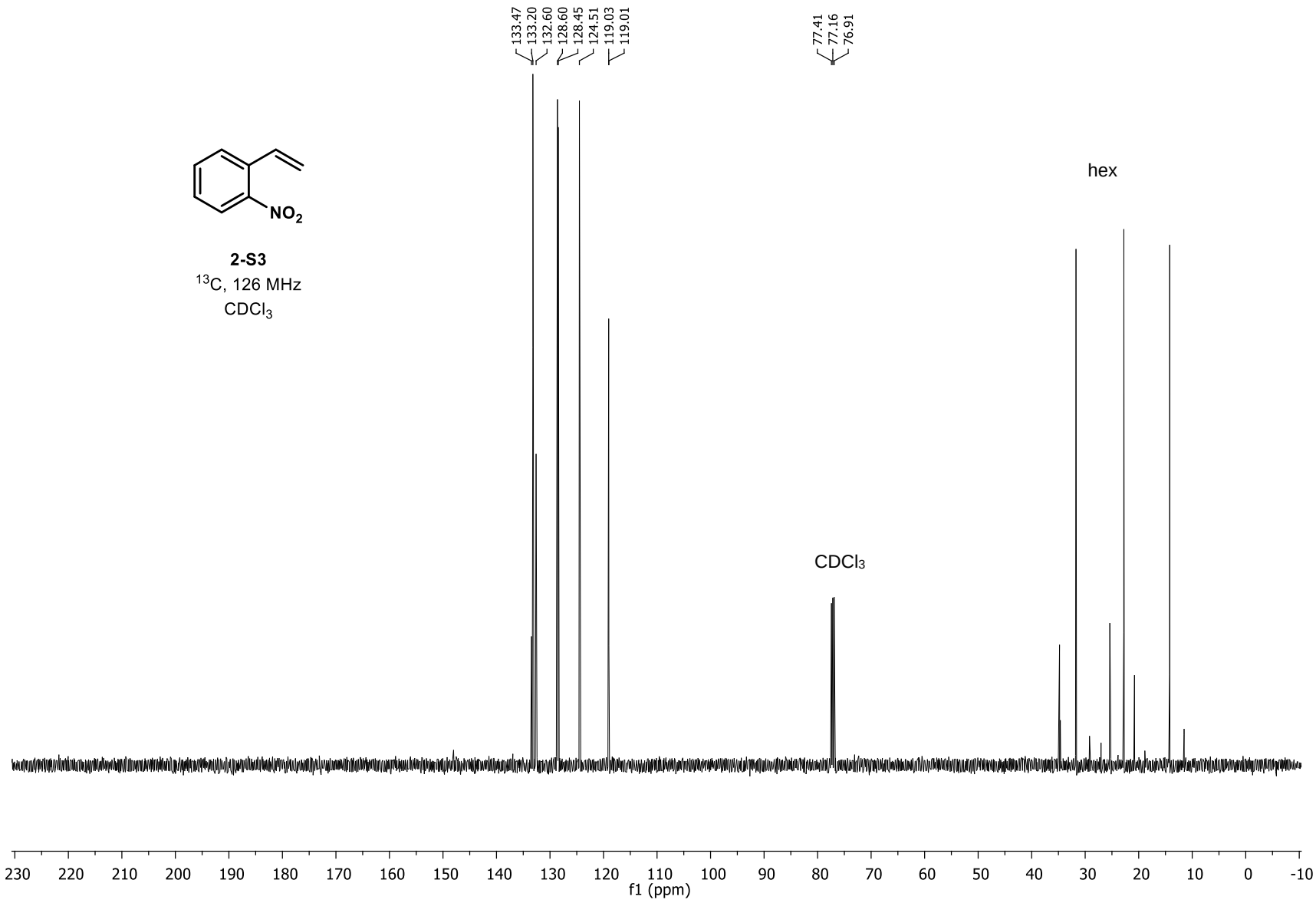
133.47
133.20
132.60
128.60
128.45
124.51
119.03
119.01
77.41
77.16
76.91
hex
CDCl3
NO2
2-S3
13C, 126 MHz
CDCl3
230 220 210 200 190 180 170 160 150 140 130 120 110 100 90 80 70 60 50 40 30 20 10 0 -10
f1 (ppm)

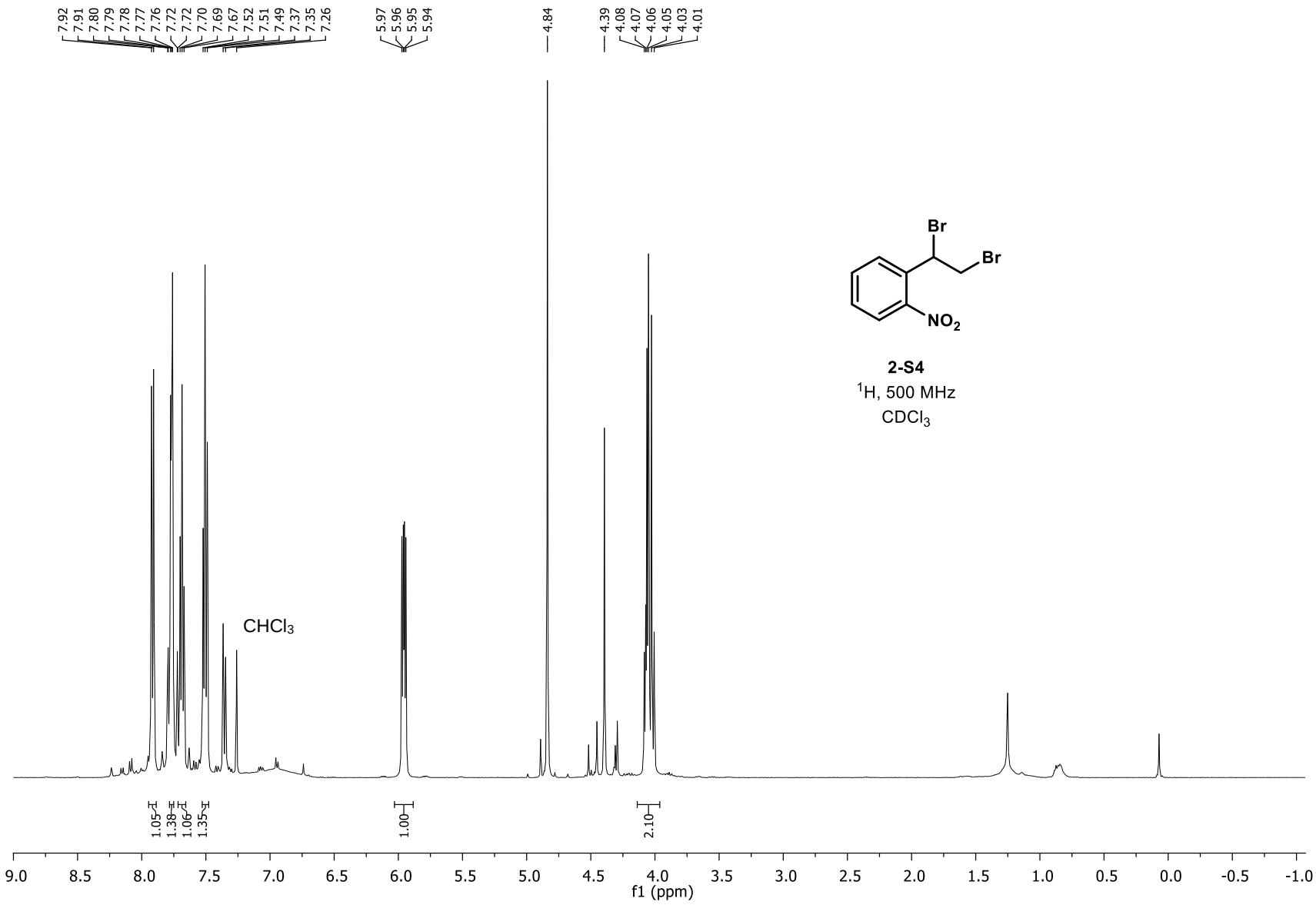
7.92
7.91
7.80
7.79
7.78
7.77
7.76
7.72
7.72
7.70
7.69
7.67
7.52
7.51
7.49
7.37
7.35
7.26
5.97
5.96
5.95
5.94
4.84
4.39
4.08
4.07
4.06
4.05
4.03
4.01
CHCl3
Br
Br
NO2
2-S4
1H, 500 MHz
CDCl3
1.05
1.38
1.06
1.35
1.00
2.10
9.0
8.5
8.0
7.5
7.0
6.5
6.0
5.5
5.0
4.5
4.0
3.5
3.0
2.5
2.0
1.5
1.0
0.5
0.0
-0.5
-1.0
f1 (ppm)

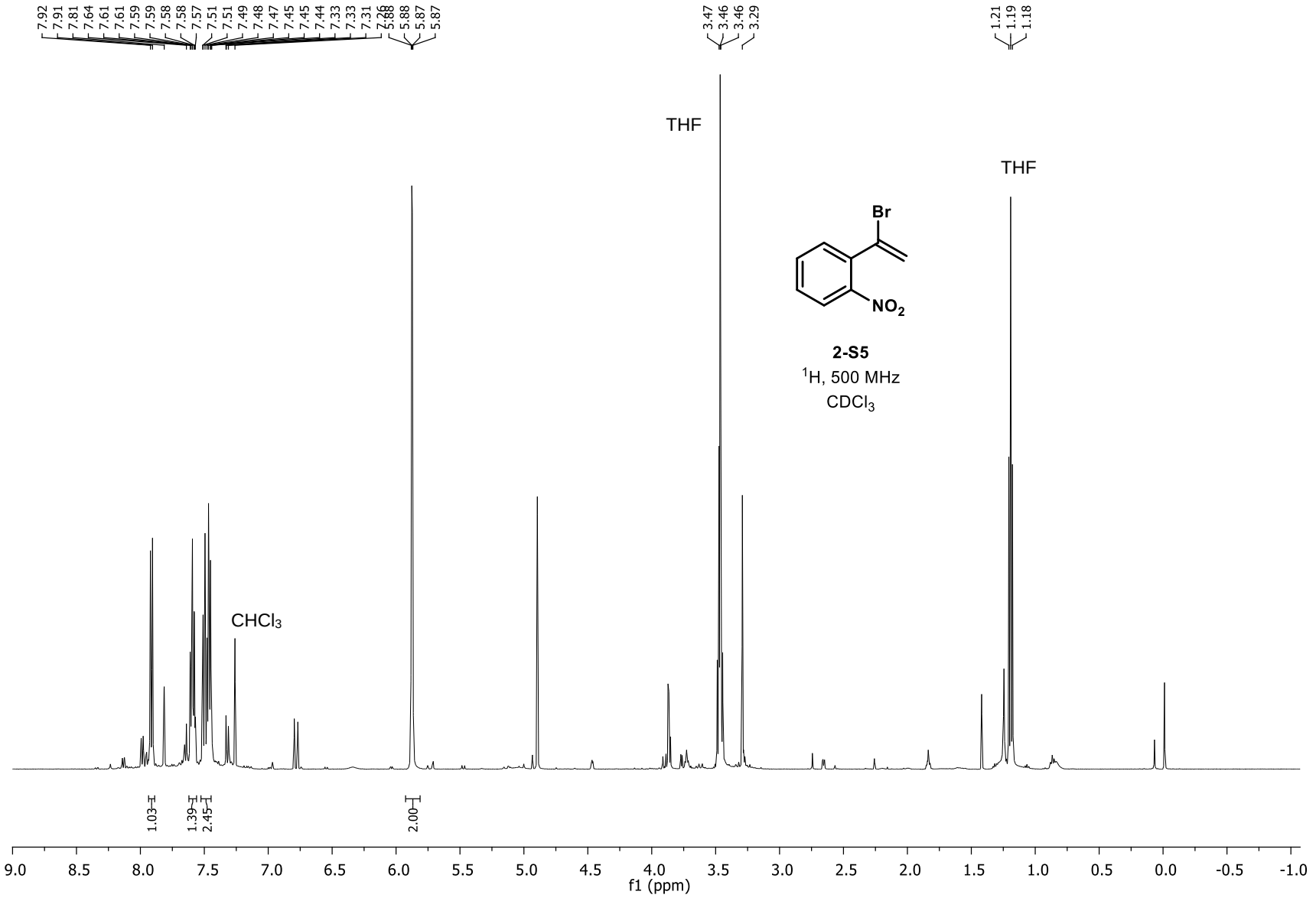
7.92
7.91
7.81
7.64
7.61
7.61
7.59
7.59
7.58
7.58
7.57
7.51
7.51
7.49
7.48
7.47
7.45
7.45
7.44
7.33
7.33
7.31
5.88
5.87
5.87
3.47
3.46
3.46
3.29
1.21
1.19
1.18
THF
THF
CHCl3
Br
NO2
2-S5
1H, 500 MHz
CDCl3
1.03
1.39
2.45
2.00
9.0
8.5
8.0
7.5
7.0
6.5
6.0
5.5
5.0
4.5
4.0
3.5
3.0
2.5
2.0
1.5
1.0
0.5
0.0
-0.5
-1.0
f1 (ppm)

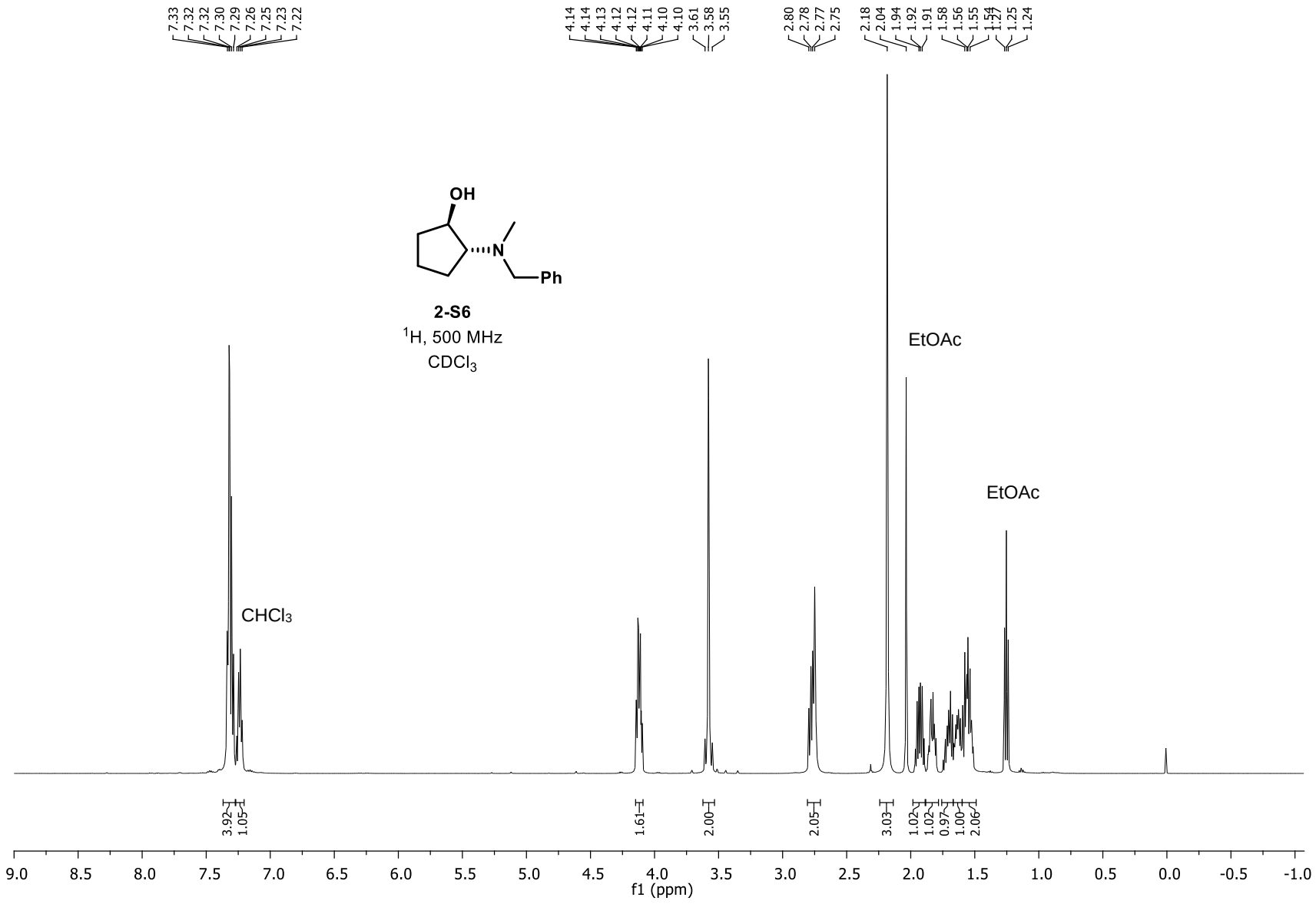
7.33
7.32
7.32
7.30
7.29
7.26
7.25
7.23
7.22
4.14
4.14
4.13
4.12
4.12
4.11
4.10
4.10
3.61
3.58
3.55
2.80
2.78
2.77
2.75
2.18
2.04
1.94
1.92
1.91
1.58
1.56
1.55
1.54
1.25
1.24
OH
N
Ph
2-S6
1H, 500 MHz
CDCl3
EtOAc
EtOAc
CHCl3
3.92
1.05
1.61
2.00
2.05
3.03
1.02
1.02
0.97
1.00
2.06
9.0
8.5
8.0
7.5
7.0
6.5
6.0
5.5
5.0
4.5
4.0
3.5
3.0
2.5
2.0
1.5
1.0
0.5
0.0
-0.5
-1.0
f1 (ppm)

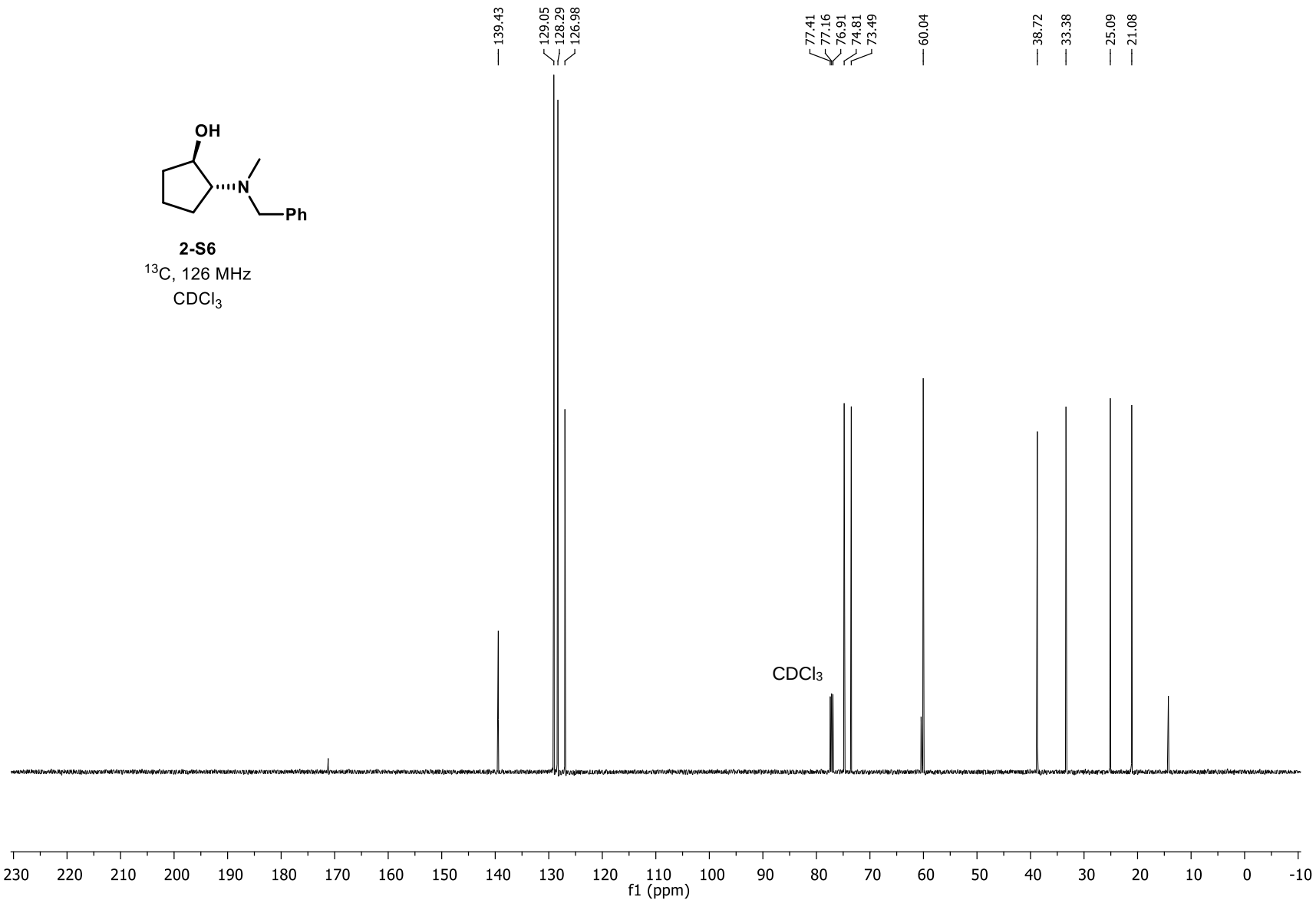
OH
N
Ph
2-S6
13C, 126 MHz
CDCl3
139.43
129.05
128.29
126.98
77.41
77.16
76.91
74.81
73.49
60.04
38.72
33.38
25.09
21.08
CDCl3
230 220 210 200 190 180 170 160 150 140 130 120 110 100 90 80 70 60 50 40 30 20 10 0 -10
f1 (ppm)

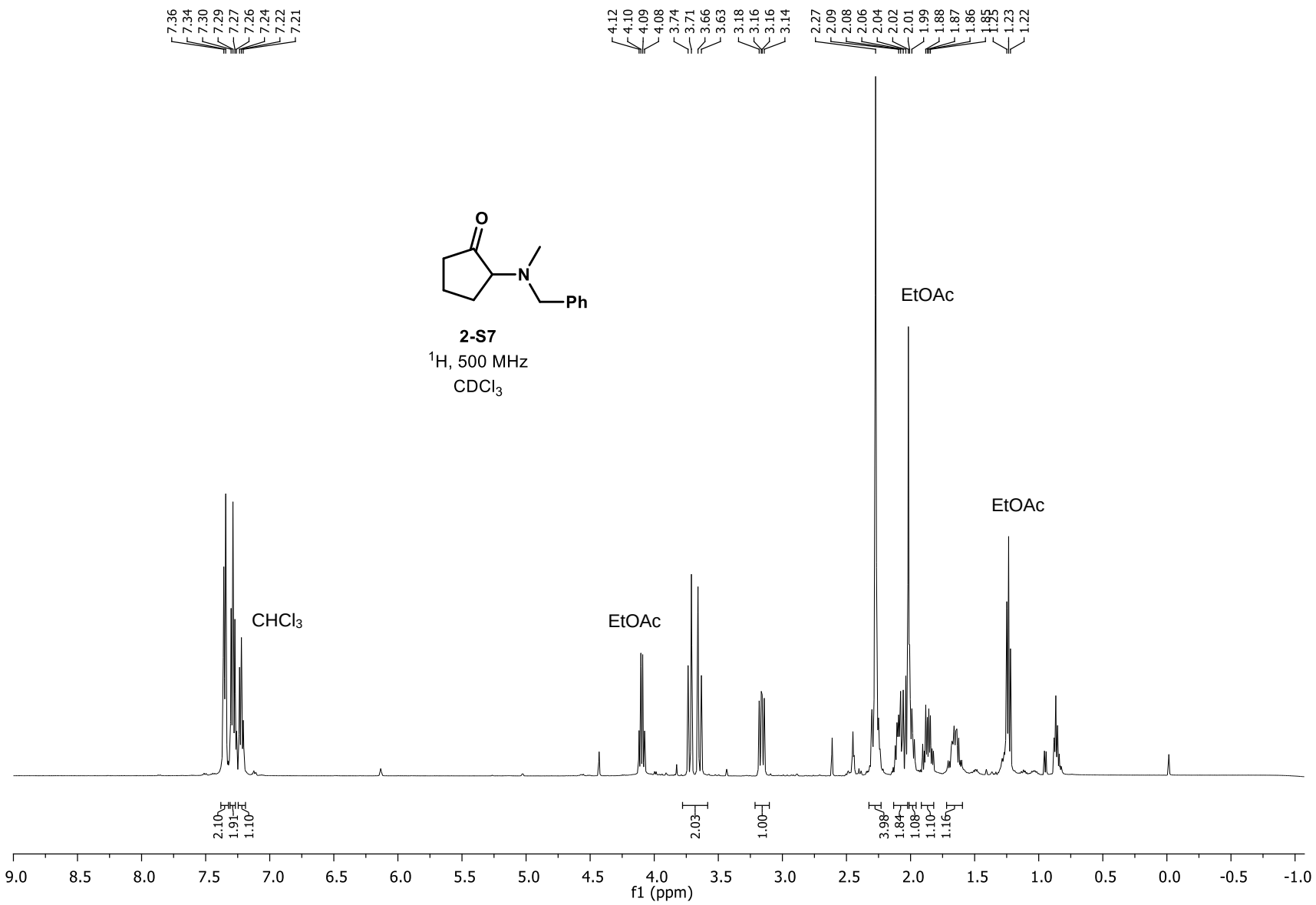
7.36
7.34
7.30
7.29
7.27
7.26
7.24
7.22
7.21
4.12
4.10
4.09
4.08
3.74
3.71
3.66
3.63
3.18
3.16
3.16
3.14
2.27
2.09
2.08
2.06
2.04
2.02
2.01
1.99
1.88
1.87
1.86
1.23
1.22
O
N
Ph
2-S7
1H, 500 MHz
CDCl3
EtOAc
EtOAc
EtOAc
CHCl3
2.10
1.91
1.10
2.03
1.00
3.98
1.84
1.08
1.10
1.16
9.0
8.5
8.0
7.5
7.0
6.5
6.0
5.5
5.0
4.5
4.0
3.5
3.0
2.5
2.0
1.5
1.0
0.5
0.0
-0.5
-1.0
f1 (ppm)

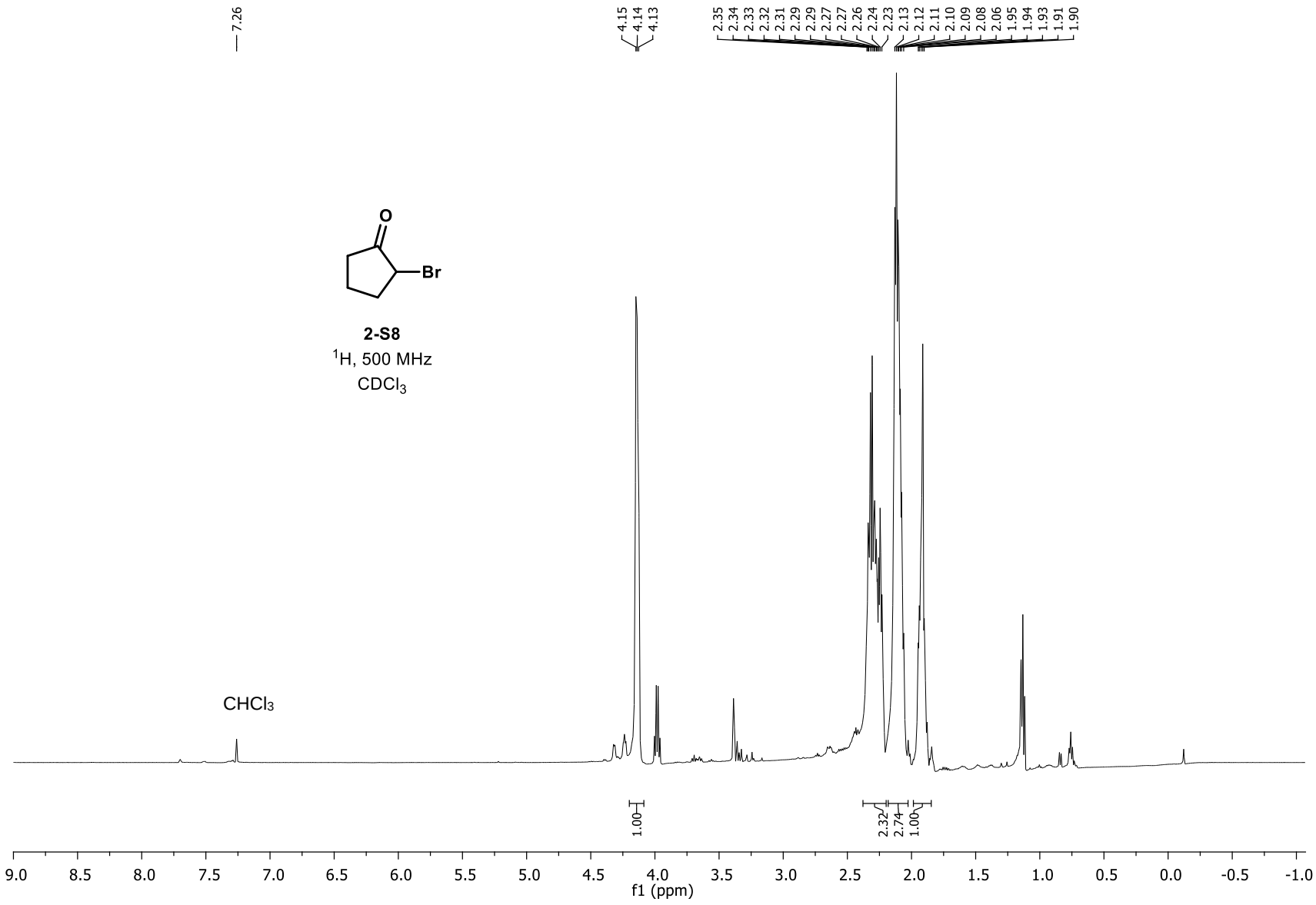
7.26
4.15
4.14
4.13
2.35
2.34
2.33
2.32
2.31
2.29
2.29
2.27
2.27
2.26
2.24
2.23
2.13
2.12
2.11
2.10
2.09
2.08
2.06
1.95
1.94
1.93
1.91
1.90
O
Br
2-S8
1H, 500 MHz
CDCl3
CHCl3
1.00
2.32
2.74
1.00
9.0
8.5
8.0
7.5
7.0
6.5
6.0
5.5
5.0
4.5
4.0
3.5
3.0
2.5
2.0
1.5
1.0
0.5
0.0
-0.5
-1.0
f1 (ppm)

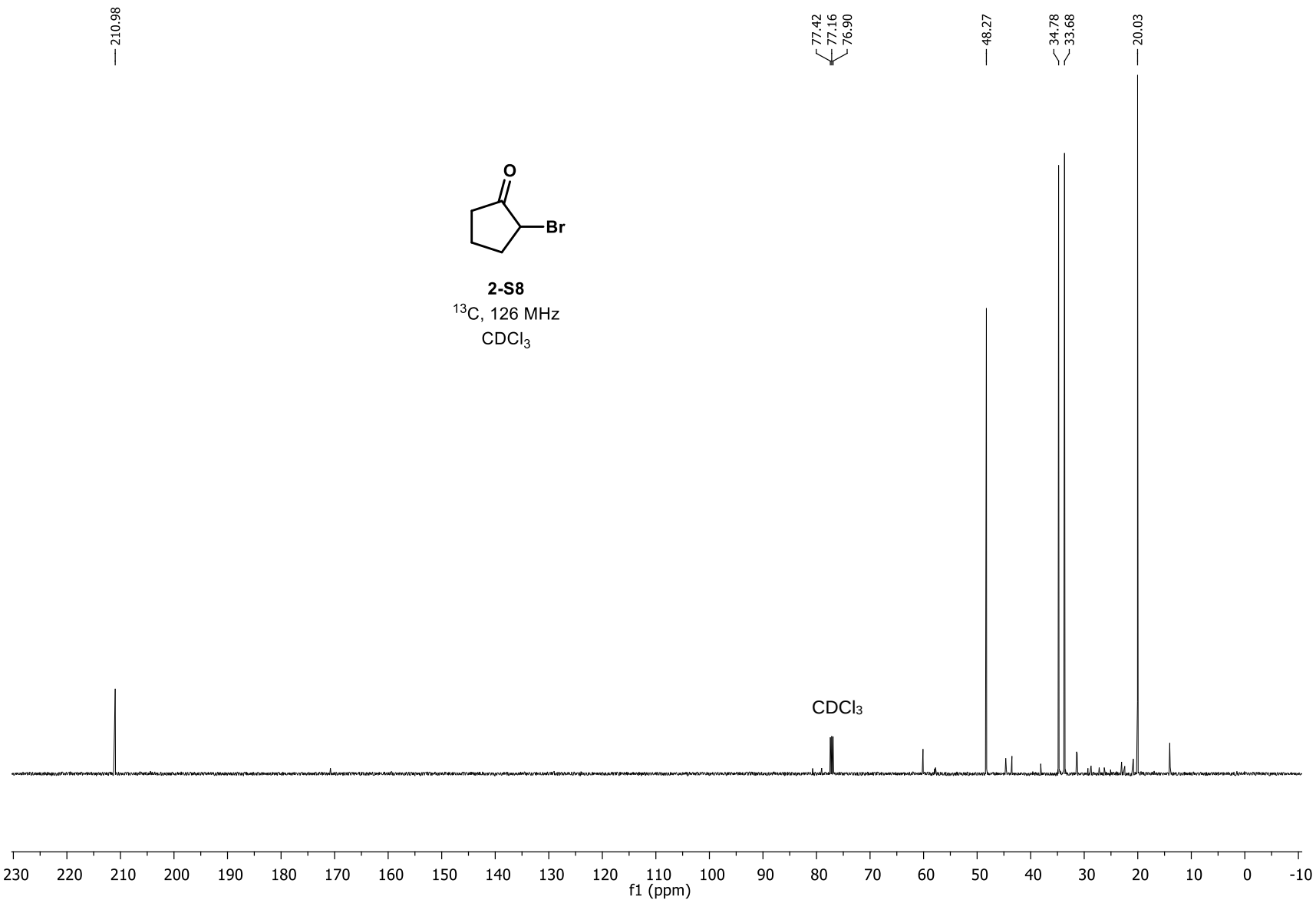
210.98
77.42
77.16
76.90
48.27
34.78
33.68
20.03
O
Br
2-S8
13C, 126 MHz
CDCl3
CDCl3
230 220 210 200 190 180 170 160 150 140 130 120 110 100 90 80 70 60 50 40 30 20 10 0 -10
f1 (ppm)

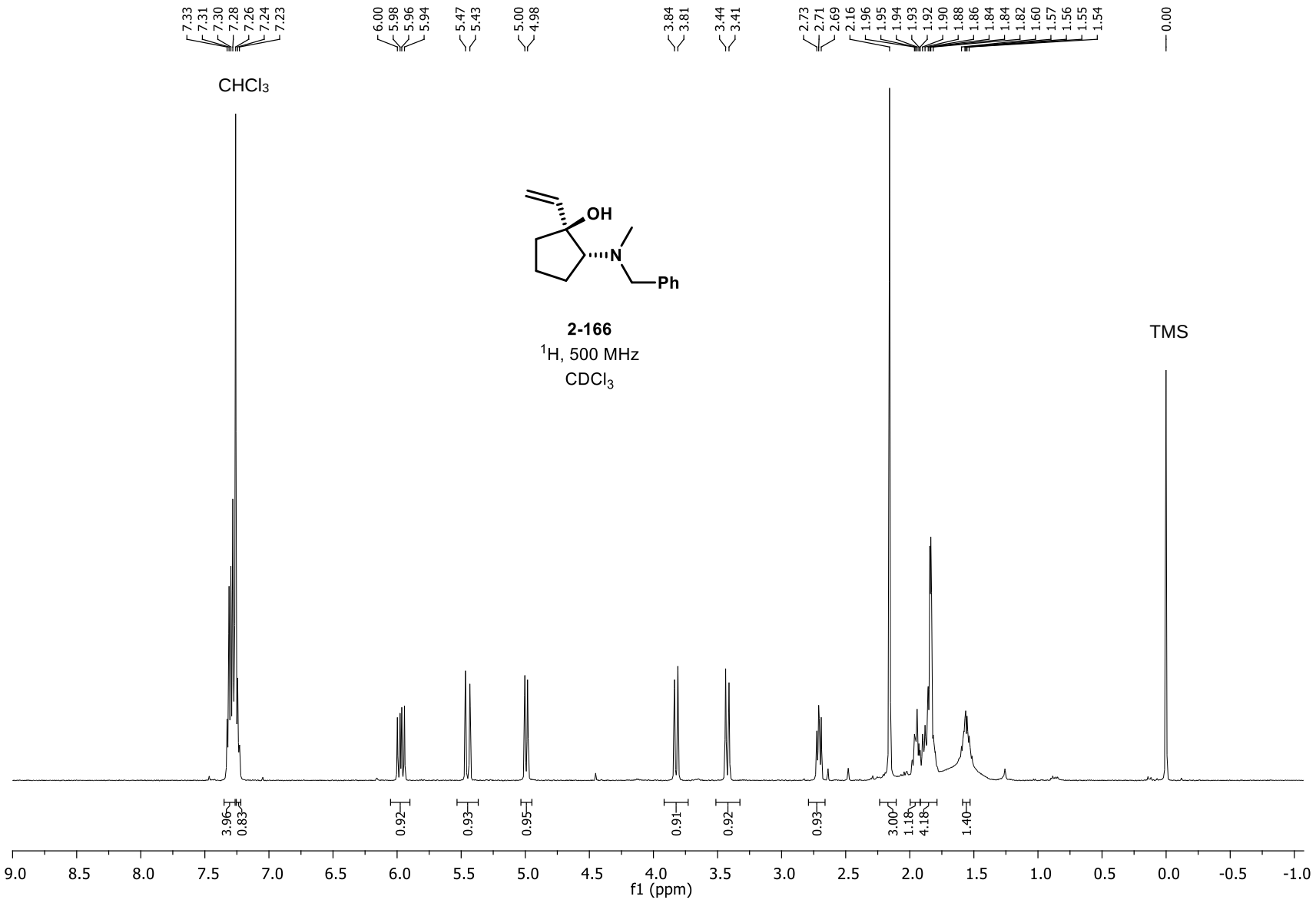
7.33
7.31
7.30
7.28
7.26
7.24
7.23
6.00
5.98
5.96
5.94
5.47
5.43
5.00
4.98
3.84
3.81
3.44
3.41
2.73
2.71
2.69
2.16
1.96
1.95
1.94
1.93
1.92
1.90
1.88
1.86
1.84
1.84
1.82
1.60
1.57
1.56
1.55
1.54
0.00
CHCl3
OH
N
Ph
2-166
1H, 500 MHz
CDCl3
TMS
3.96
0.83
0.92
0.93
0.95
0.91
0.92
0.93
3.00
1.18
4.18
1.40
9.0
8.5
8.0
7.5
7.0
6.5
6.0
5.5
5.0
4.5
4.0
3.5
3.0
2.5
2.0
1.5
1.0
0.5
0.0
-0.5
-1.0
f1 (ppm)

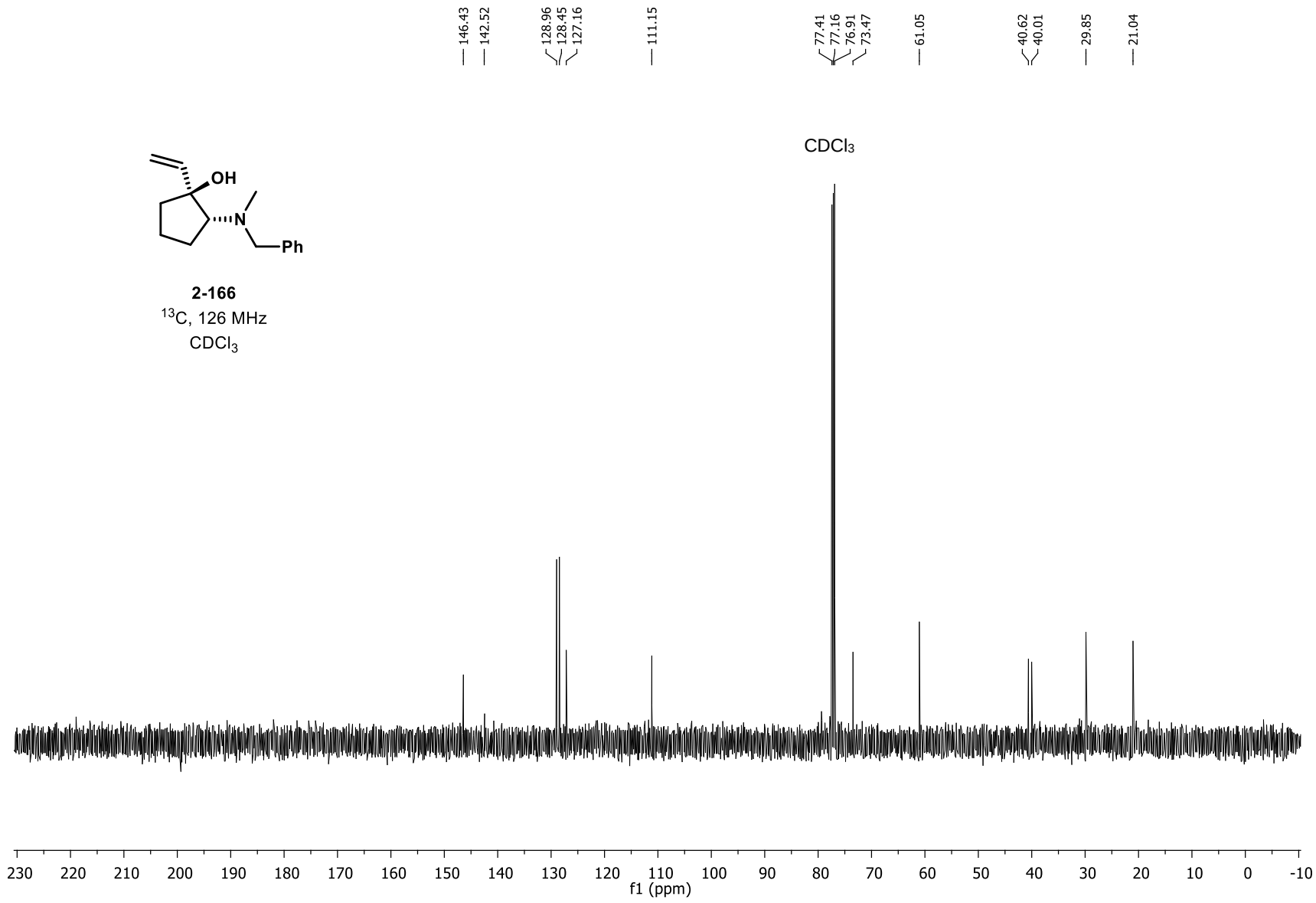
146.43
142.52
128.96
128.45
127.16
111.15
77.41
77.16
76.91
73.47
61.05
40.62
40.01
29.85
21.04
CDCl3
OH
N
Ph
2-166
13C, 126 MHz
CDCl3
230 220 210 200 190 180 170 160 150 140 130 120 110 100 90 80 70 60 50 40 30 20 10 0 -10
f1 (ppm)

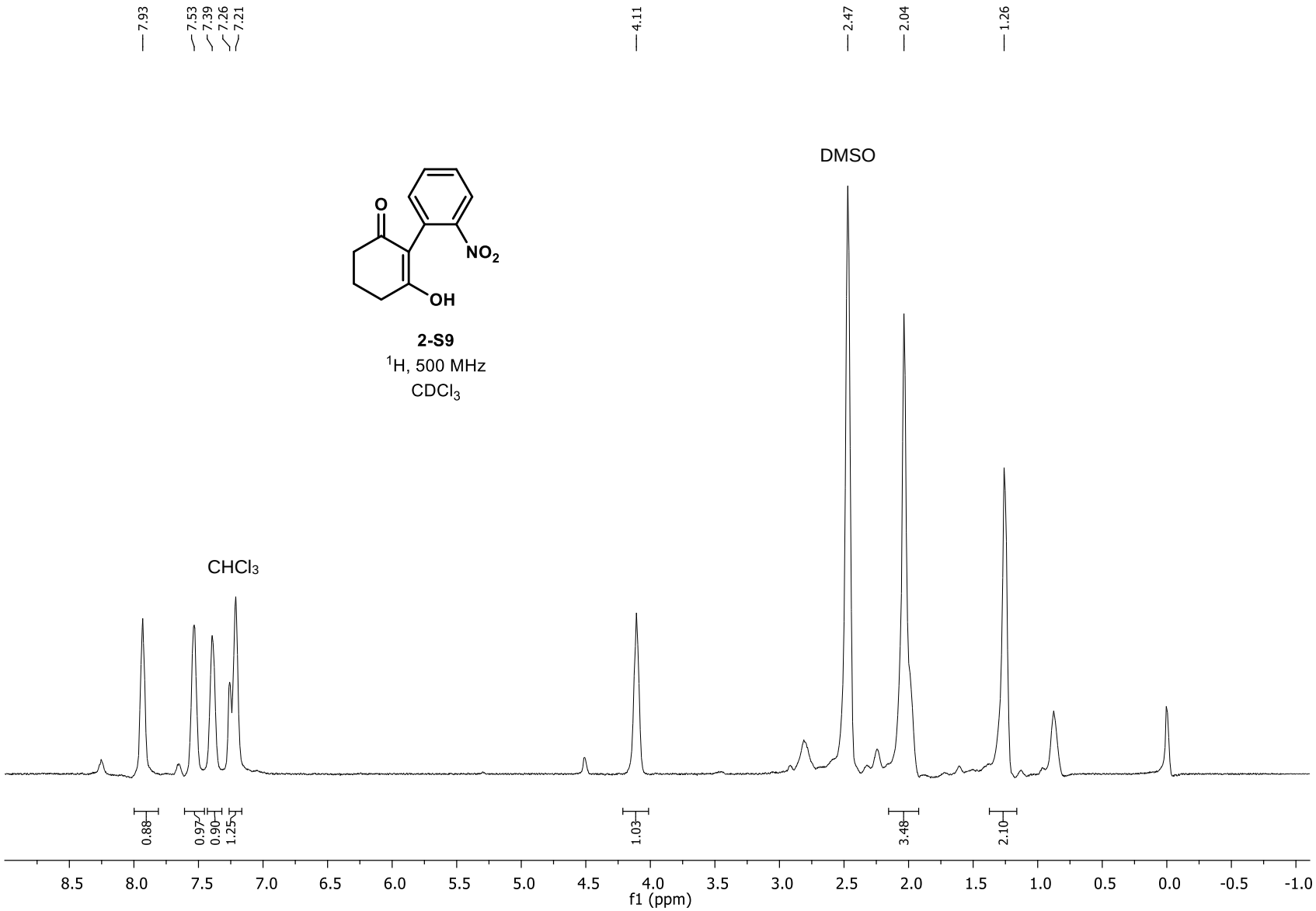
7.93
7.53
7.39
7.26
7.21
4.11
2.47
2.04
1.26
DMSO
O
NO2
OH
2-S9
1H, 500 MHz
CDCl3
CHCl3
0.88
0.97
0.90
1.25
1.03
3.48
2.10
8.5
8.0
7.5
7.0
6.5
6.0
5.5
5.0
4.5
4.0
3.5
3.0
2.5
2.0
1.5
1.0
0.5
0.0
-0.5
-1.0
f1 (ppm)

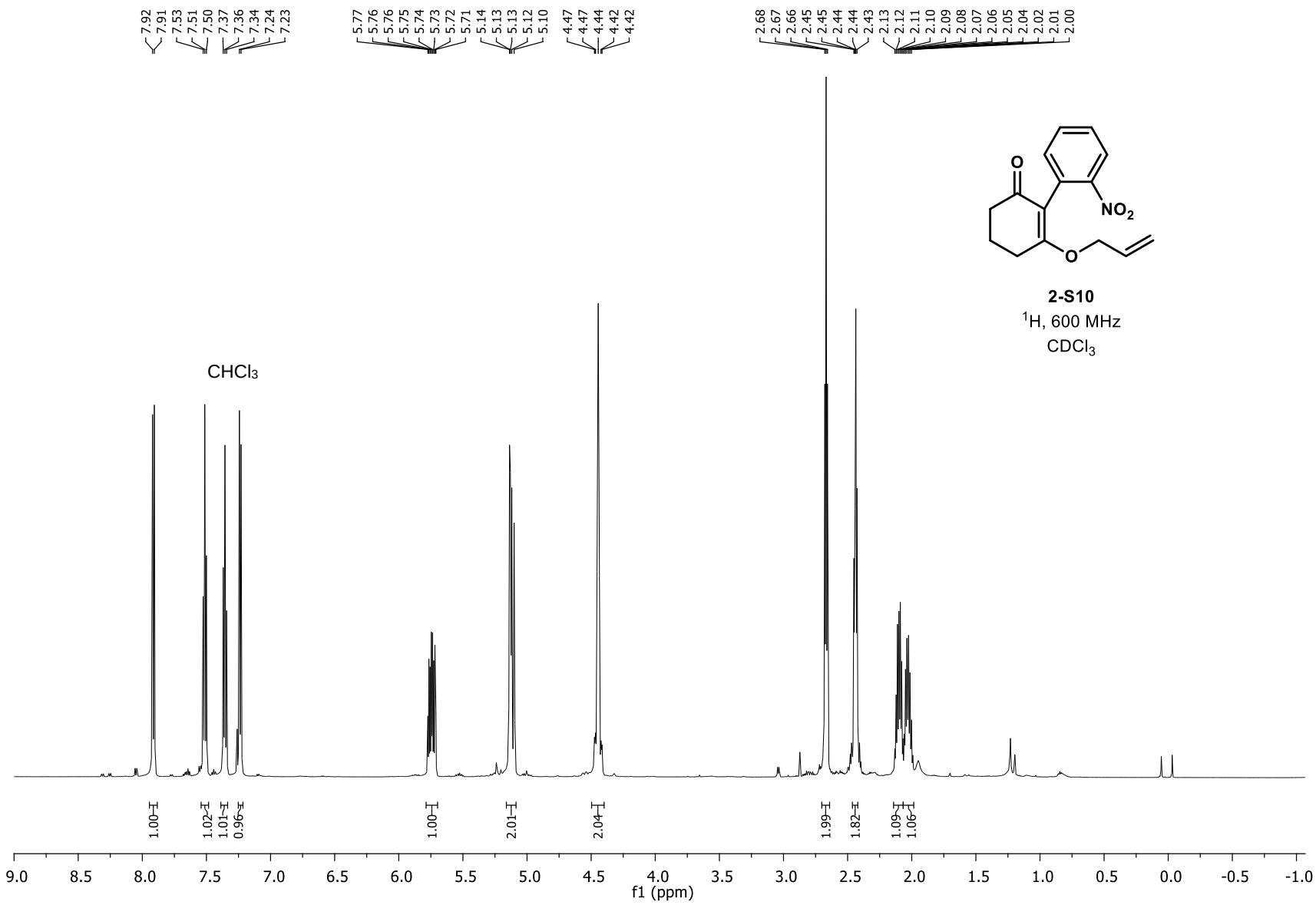
7.92
7.91
7.53
7.51
7.50
7.37
7.36
7.34
7.24
7.23
5.77
5.76
5.76
5.75
5.74
5.73
5.72
5.71
5.14
5.13
5.13
5.12
5.10
4.47
4.44
4.42
4.42
2.68
2.67
2.66
2.45
2.45
2.44
2.44
2.43
2.13
2.12
2.11
2.10
2.09
2.08
2.07
2.06
2.05
2.04
2.02
2.01
2.00
O
NO2
O
2-S10
1H, 600 MHz
CDCl3
CHCl3
1.00
1.02
1.01
0.96
1.00
2.01
2.04
1.99
1.82
1.09
1.06
9.0
8.5
8.0
7.5
7.0
6.5
6.0
5.5
5.0
4.5
4.0
3.5
3.0
2.5
2.0
1.5
1.0
0.5
0.0
-0.5
-1.0
f1 (ppm)

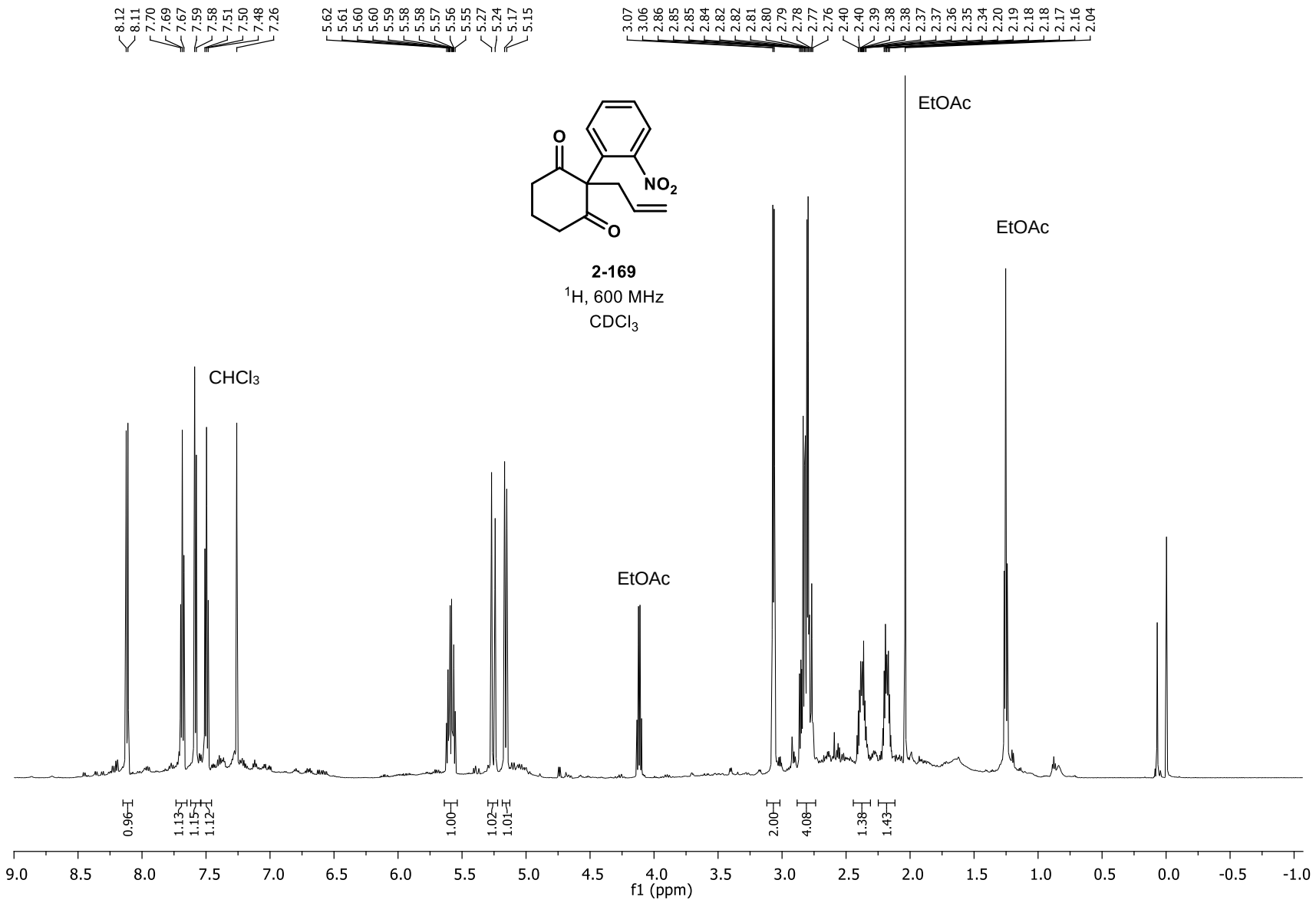
8.12
8.11
7.70
7.69
7.67
7.59
7.58
7.51
7.50
7.48
7.26
5.62
5.61
5.60
5.60
5.59
5.58
5.58
5.57
5.56
5.55
5.27
5.24
5.17
5.15
3.07
3.06
2.86
2.85
2.85
2.84
2.82
2.82
2.81
2.80
2.79
2.78
2.77
2.76
2.40
2.40
2.39
2.38
2.38
2.37
2.37
2.36
2.35
2.34
2.20
2.19
2.18
2.18
2.17
2.16
2.04
O
O
NO2
2-169
1H, 600 MHz
CDCl3
EtOAc
EtOAc
CHCl3
EtOAc
0.96
1.13
1.15
1.12
1.00
1.02
1.01
2.00
4.08
1.38
1.43
9.0
8.5
8.0
7.5
7.0
6.5
6.0
5.5
5.0
4.5
4.0
3.5
3.0
2.5
2.0
1.5
1.0
0.5
0.0
-0.5
-1.0
f1 (ppm)

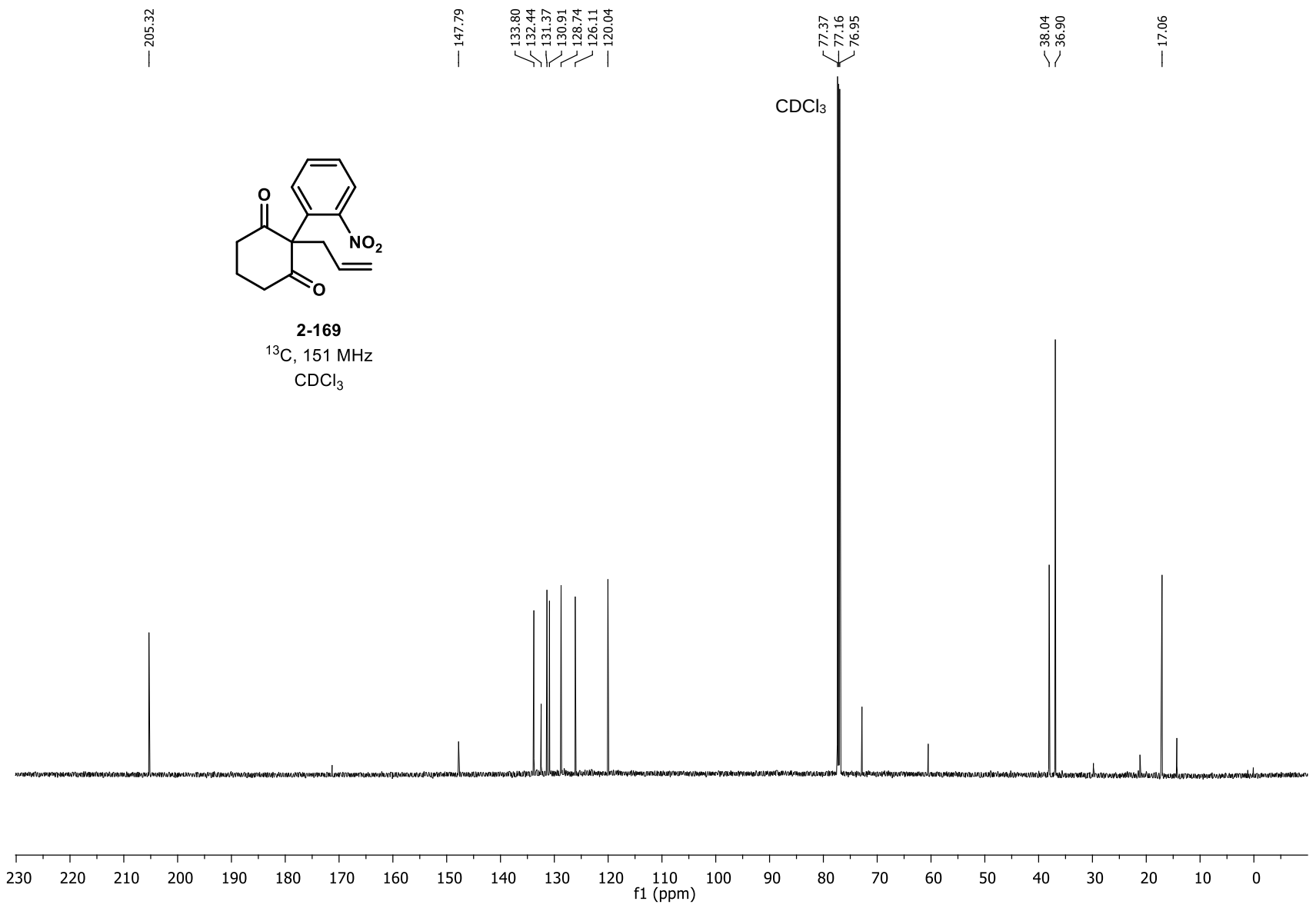
205.32
147.79
133.80
132.44
131.37
130.91
128.74
126.11
120.04
77.37
77.16
76.95
38.04
36.90
17.06
CDCl3
O
NO2
O
2-169
13C, 151 MHz
CDCl3
230
220
210
200
190
180
170
160
150
140
130
120
110
100
90
80
70
60
50
40
30
20
10
0
f1 (ppm)

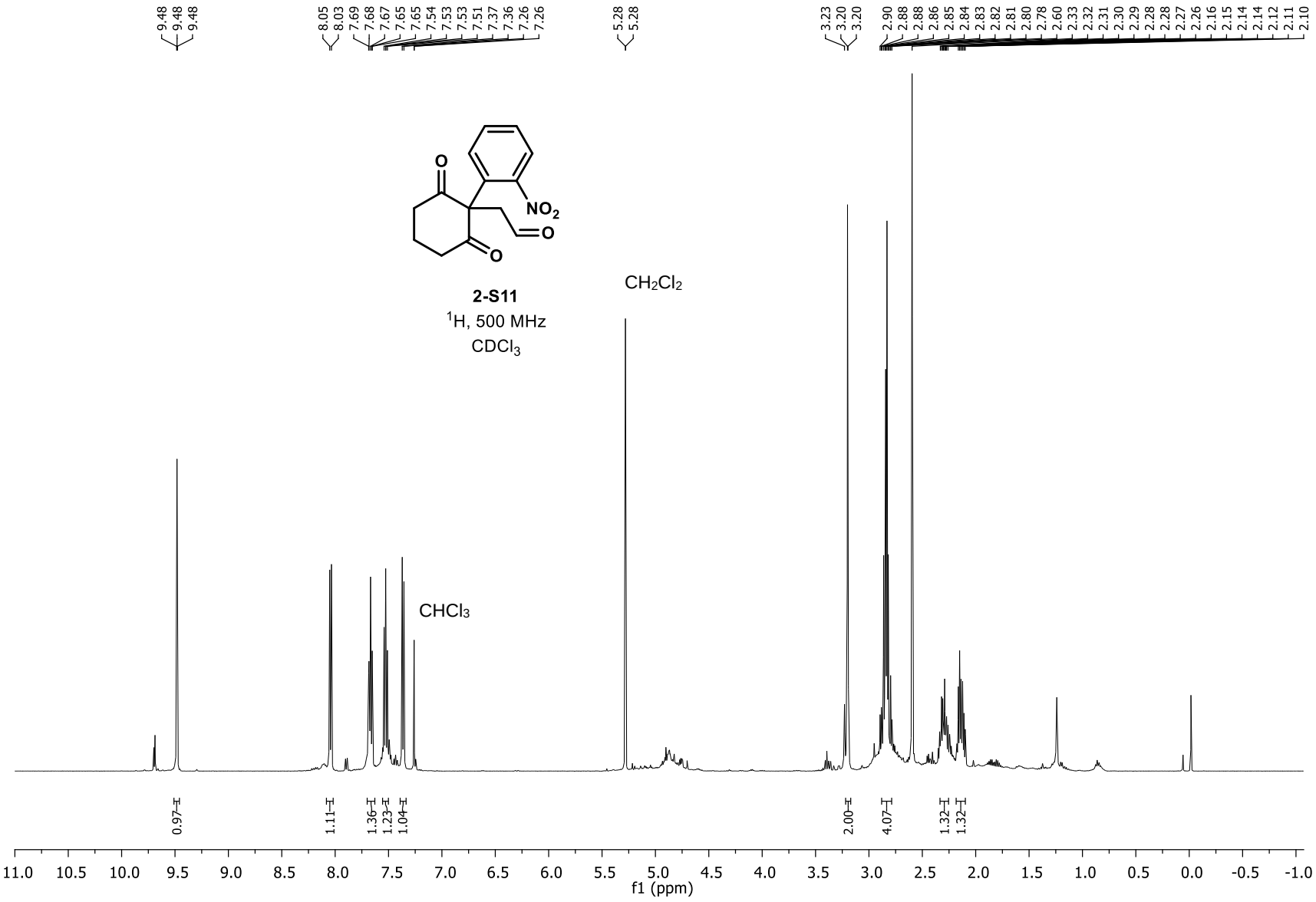
9.48
9.48
9.48
8.05
8.03
7.69
7.68
7.67
7.65
7.65
7.54
7.53
7.53
7.51
7.37
7.36
7.26
7.26
5.28
5.28
3.23
3.20
3.20
2.90
2.88
2.88
2.86
2.85
2.84
2.83
2.82
2.81
2.80
2.78
2.60
2.33
2.32
2.31
2.30
2.29
2.28
2.28
2.27
2.26
2.16
2.15
2.14
2.14
2.12
2.11
2.10
O
NO2
O
O
2-S11
1H, 500 MHz
CDCl3
CH2Cl2
CHCl3
0.97
1.11
1.36
1.23
1.04
2.00
4.07
1.32
1.32
11.0
10.5
10.0
9.5
9.0
8.5
8.0
7.5
7.0
6.5
6.0
5.5
5.0
4.5
4.0
3.5
3.0
2.5
2.0
1.5
1.0
0.5
0.0
-0.5
-1.0
f1 (ppm)

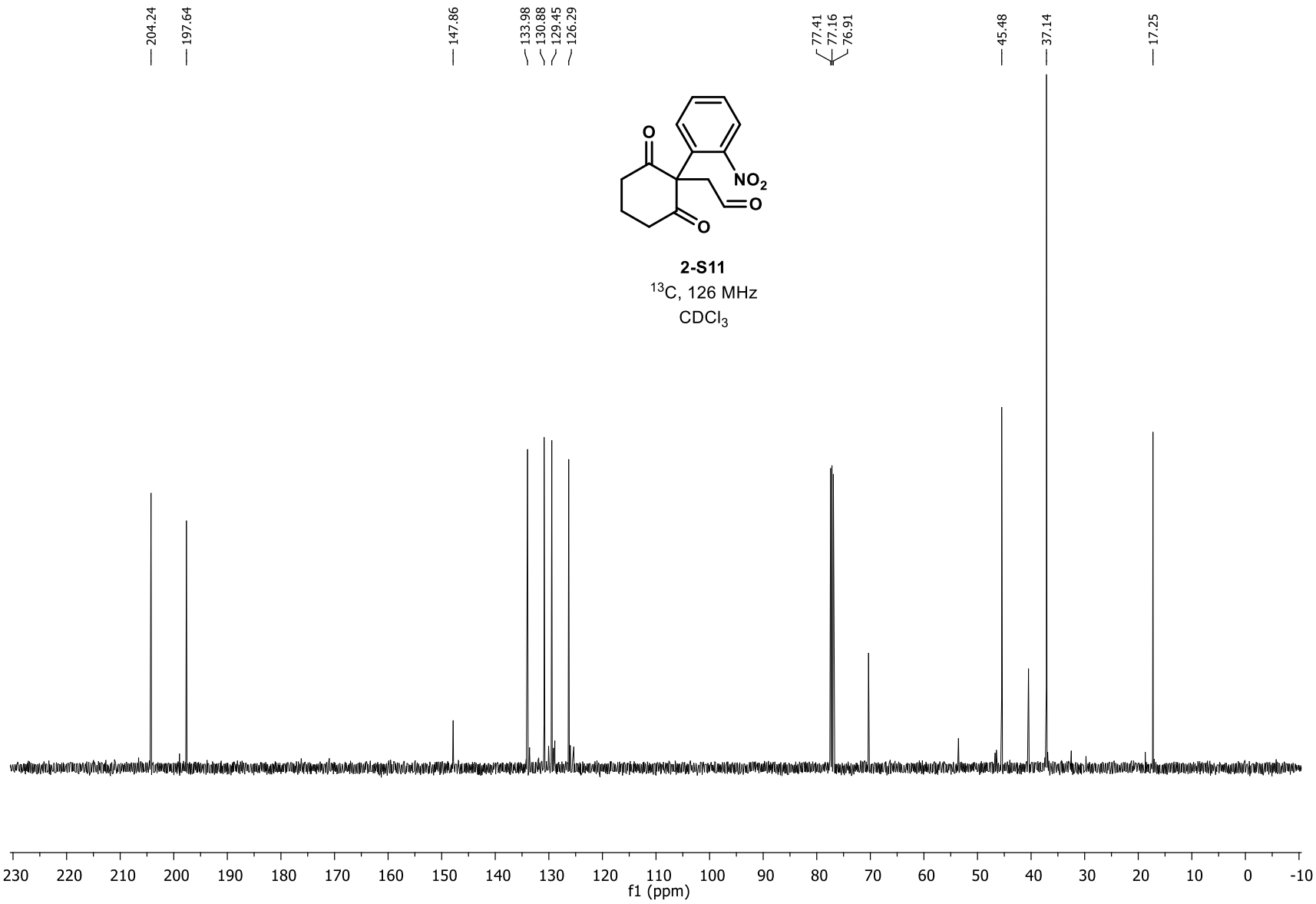
204.24
197.64
147.86
133.98
130.88
129.45
126.29
77.41
77.16
76.91
45.48
37.14
17.25
O
NO2
O
O
2-S11
13C, 126 MHz
CDCl3
230 220 210 200 190 180 170 160 150 140 130 120 110 100 90 80 70 60 50 40 30 20 10 0 -10
f1 (ppm)

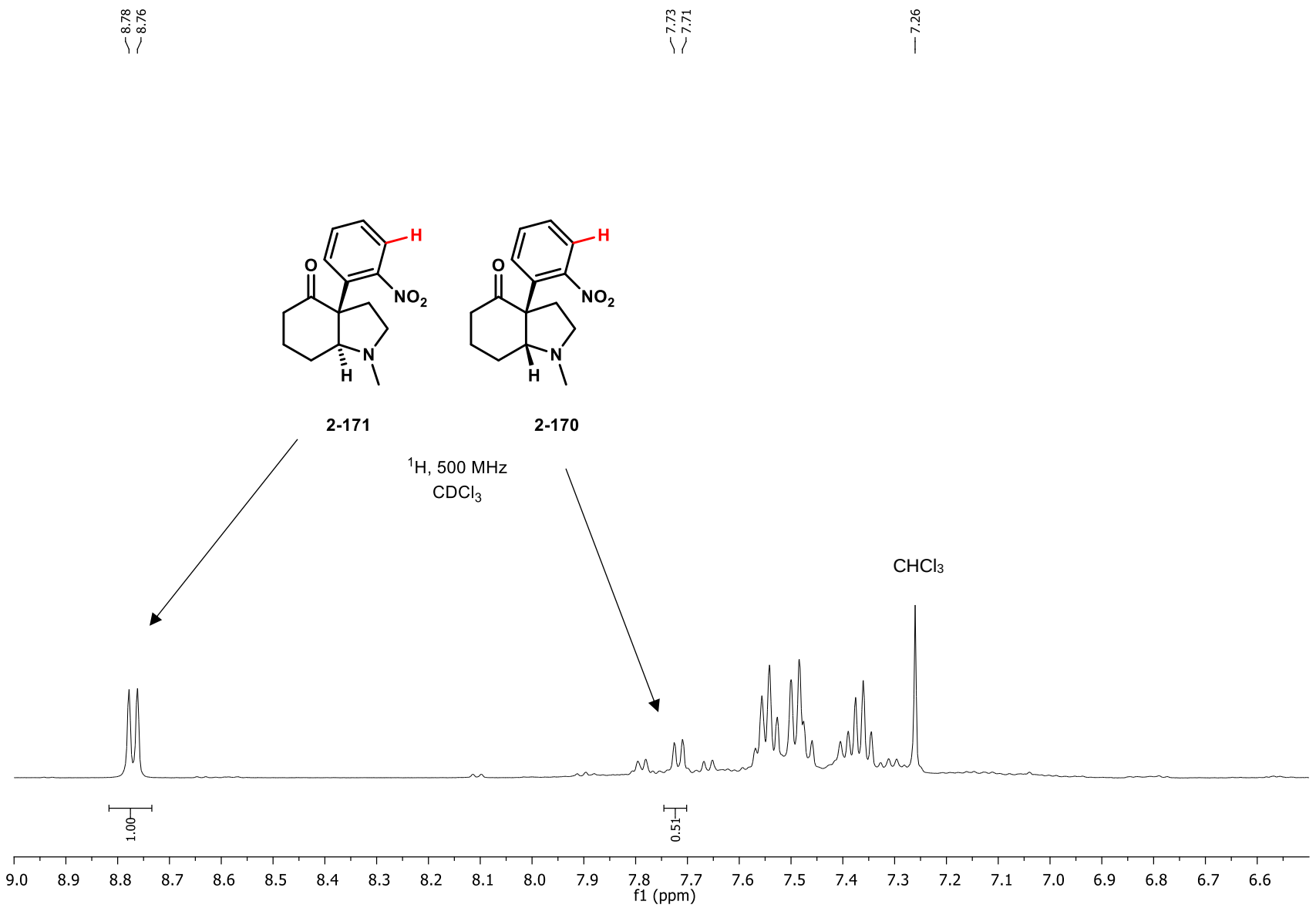
8.78
8.76
7.73
7.71
7.26
O
H
NO2
N
H
2-171
2-170
1H, 500 MHz
CDCl3
CHCl3
1.00
0.51
9.0 8.9 8.8 8.7 8.6 8.5 8.4 8.3 8.2 8.1 8.0 7.9 7.8 7.7 7.6 7.5 7.4 7.3 7.2 7.1 7.0 6.9 6.8 6.7 6.6
f1 (ppm)

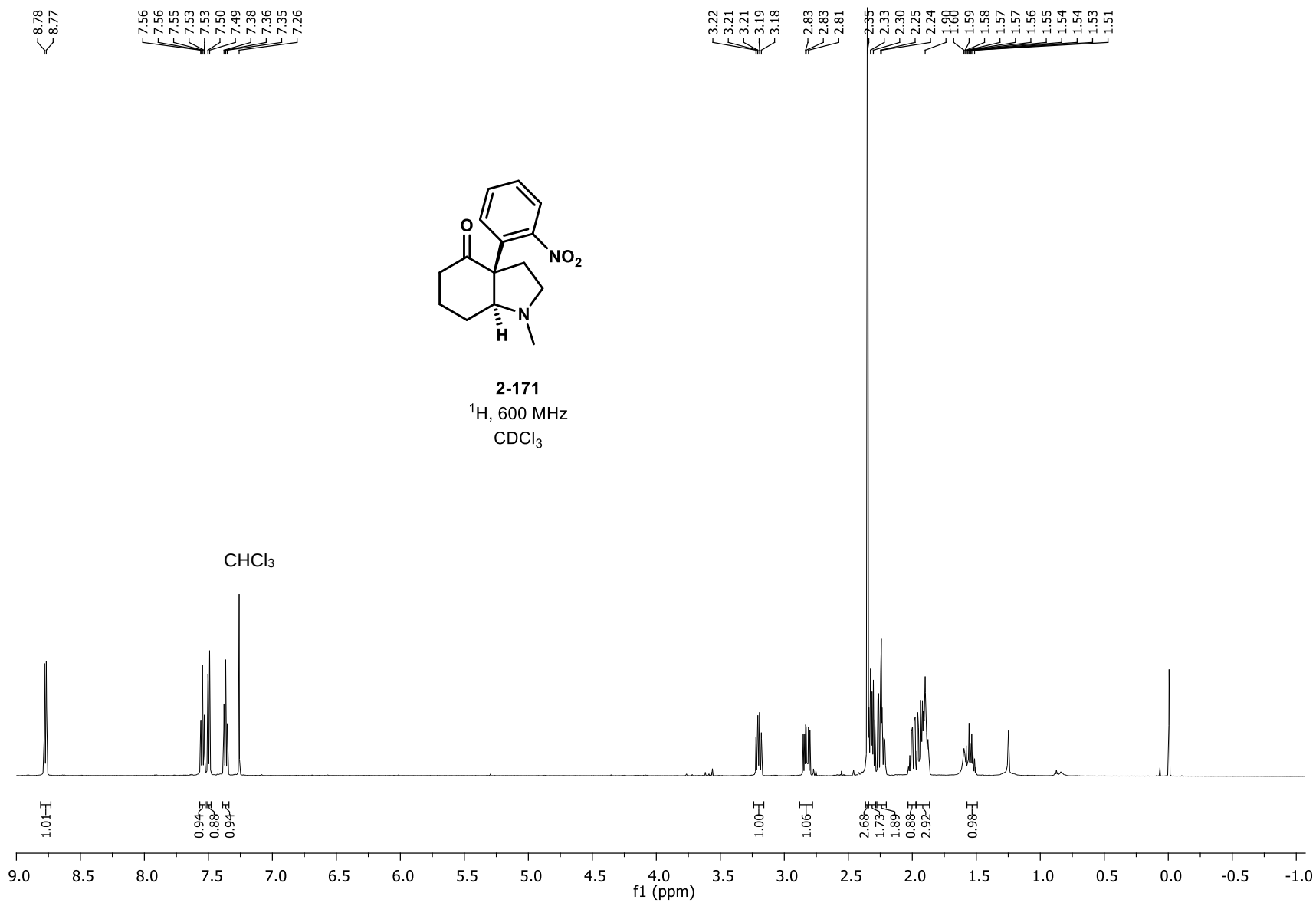
8.78
8.77
7.56
7.56
7.55
7.53
7.53
7.50
7.49
7.38
7.36
7.35
7.26
3.22
3.21
3.21
3.19
3.18
2.83
2.83
2.81
2.35
2.33
2.30
2.25
2.24
1.90
1.60
1.59
1.58
1.57
1.57
1.56
1.55
1.54
1.54
1.53
1.51
O
NO2
N
H
2-171
1H, 600 MHz
CDCl3
CHCl3
1.01
0.94
0.88
0.94
1.00
1.06
2.68
1.73
1.89
0.88
2.92
0.98
9.0
8.5
8.0
7.5
7.0
6.5
6.0
5.5
5.0
4.5
4.0
3.5
3.0
2.5
2.0
1.5
1.0
0.5
0.0
-0.5
-1.0
f1 (ppm)

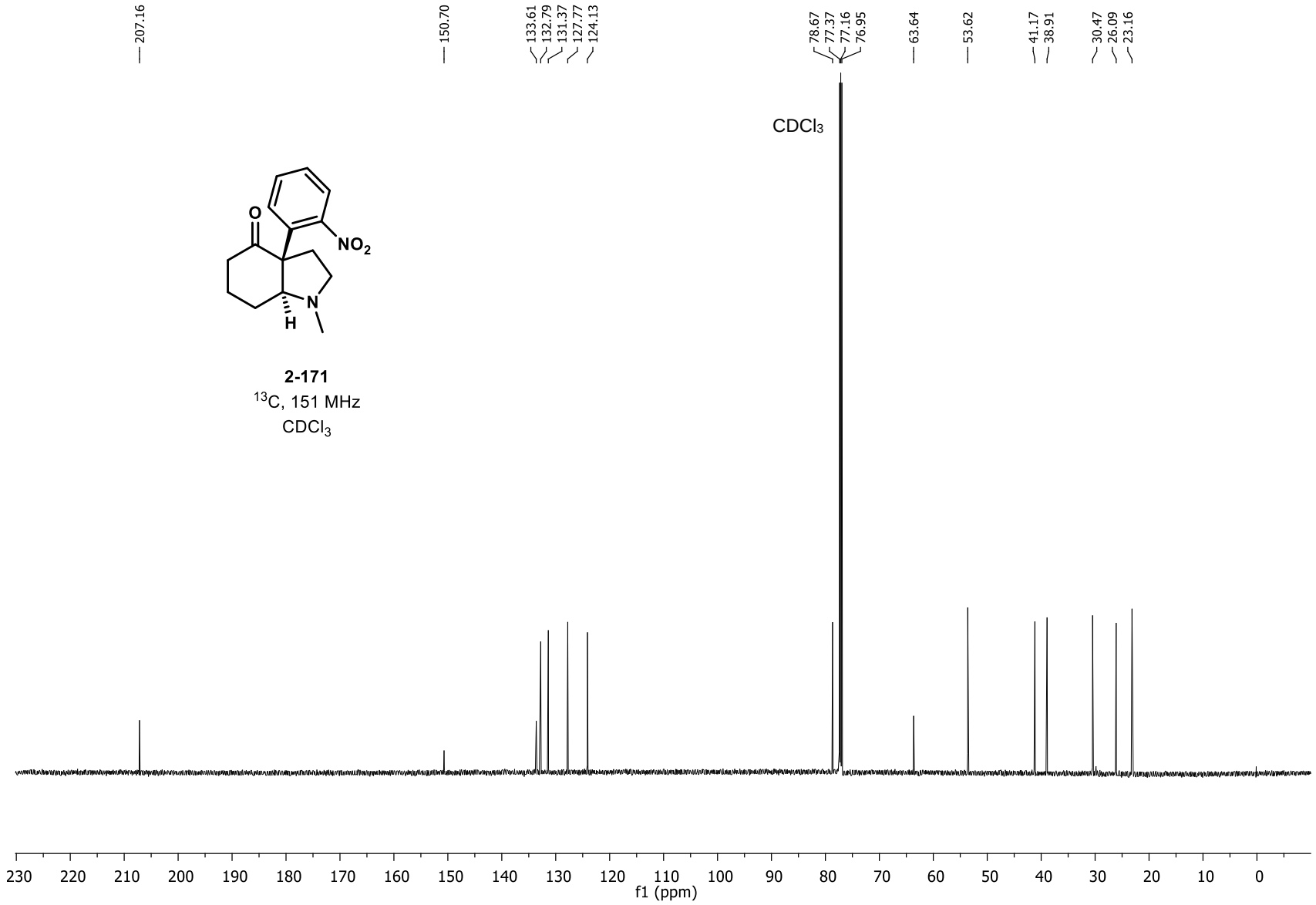
207.16
150.70
133.61
132.79
131.37
127.77
124.13
78.67
77.37
77.16
76.95
63.64
53.62
41.17
38.91
30.47
26.09
23.16
CDCl3
O
NO2
N
H
2-171
13C, 151 MHz
CDCl3
230 220 210 200 190 180 170 160 150 140 130 120 110 100 90 80 70 60 50 40 30 20 10 0
f1 (ppm)

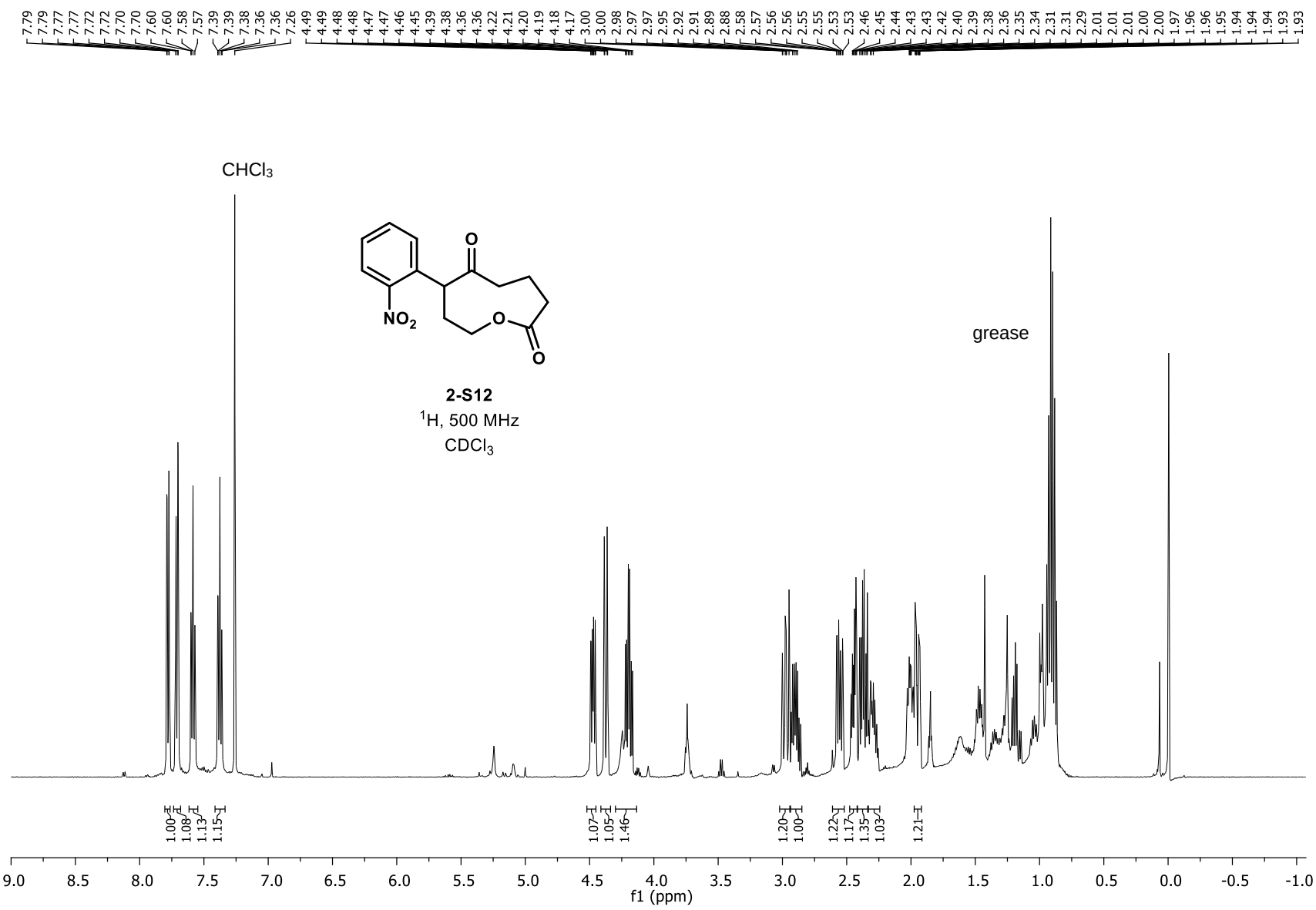
CHCl3
grease
2-S12
1H, 500 MHz
CDCl3
f1 (ppm)

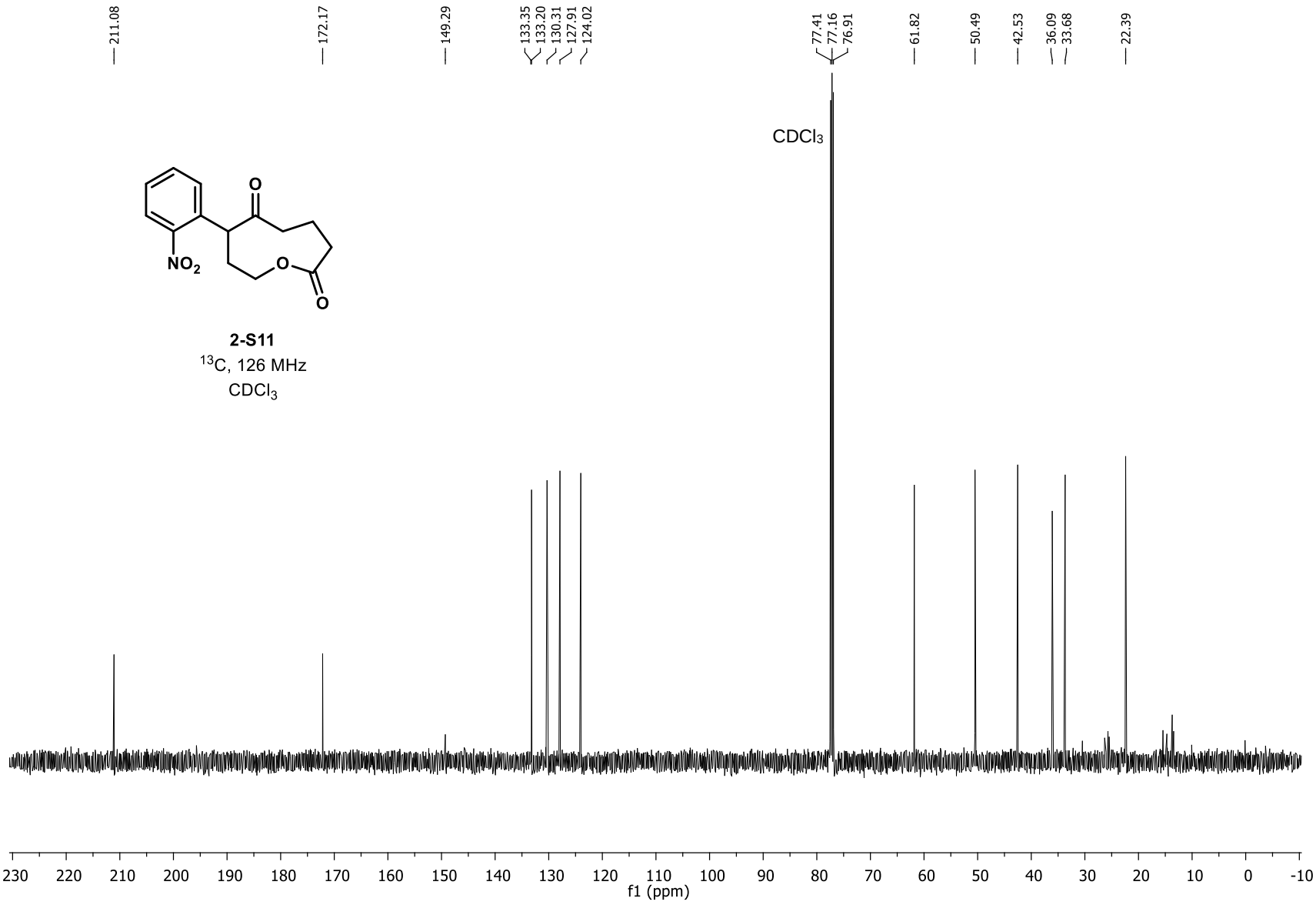
211.08
172.17
149.29
133.35
133.20
130.31
127.91
124.02
77.41
77.16
76.91
61.82
50.49
42.53
36.09
33.68
22.39
CDCl3
NO2
O
O
O
2-S11
13C, 126 MHz
CDCl3
230 220 210 200 190 180 170 160 150 140 130 120 110 100 90 80 70 60 50 40 30 20 10 0 -10
f1 (ppm)

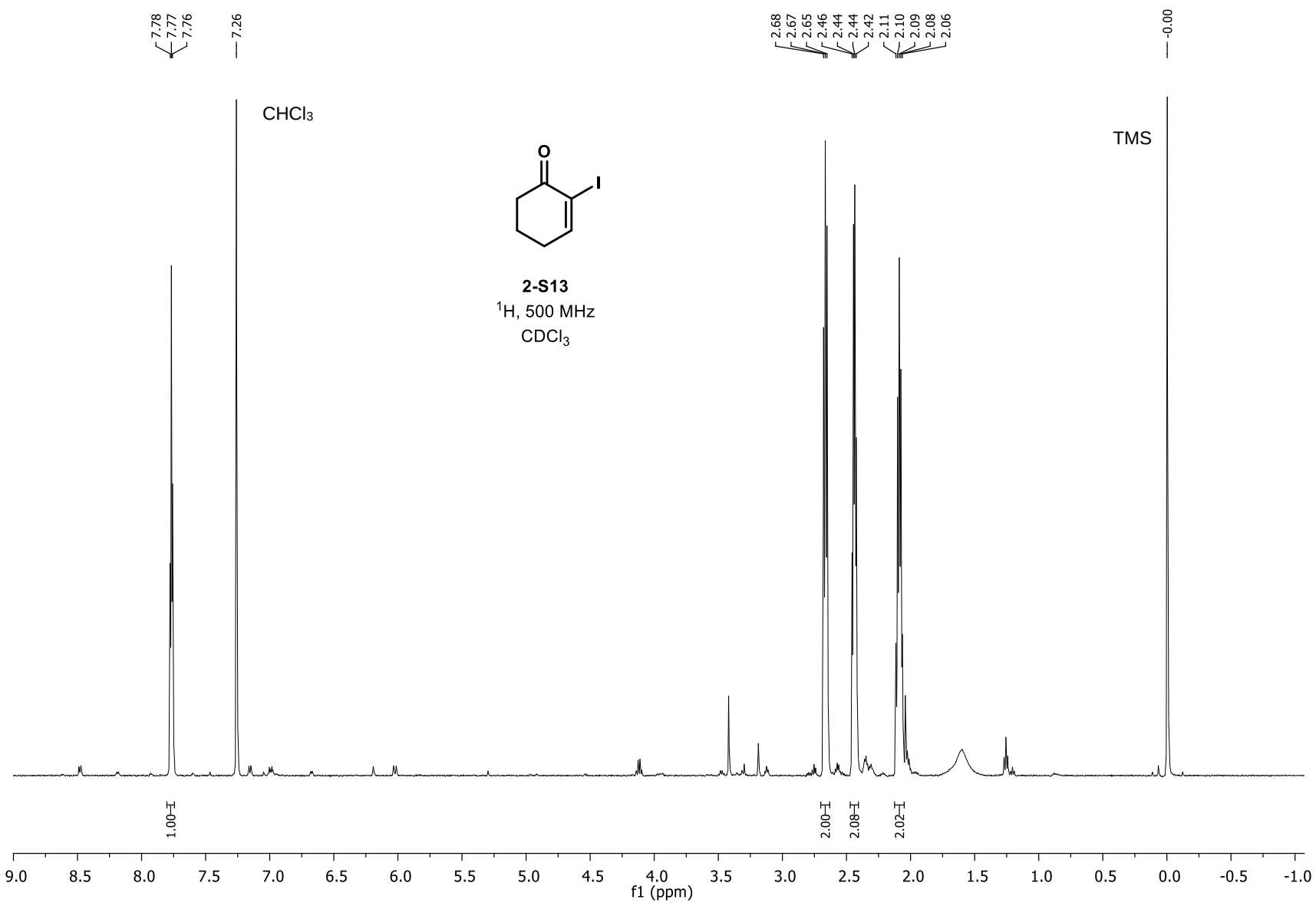
7.78
7.77
7.76
7.26
2.68
2.67
2.65
2.46
2.44
2.44
2.42
2.11
2.10
2.09
2.08
2.06
-0.00
CHCl3
TMS
O
I
2-S13
1H, 500 MHz
CDCl3
1.00
2.00
2.08
2.02
9.0
8.5
8.0
7.5
7.0
6.5
6.0
5.5
5.0
4.5
4.0
3.5
3.0
2.5
2.0
1.5
1.0
0.5
0.0
-0.5
-1.0
f1 (ppm)

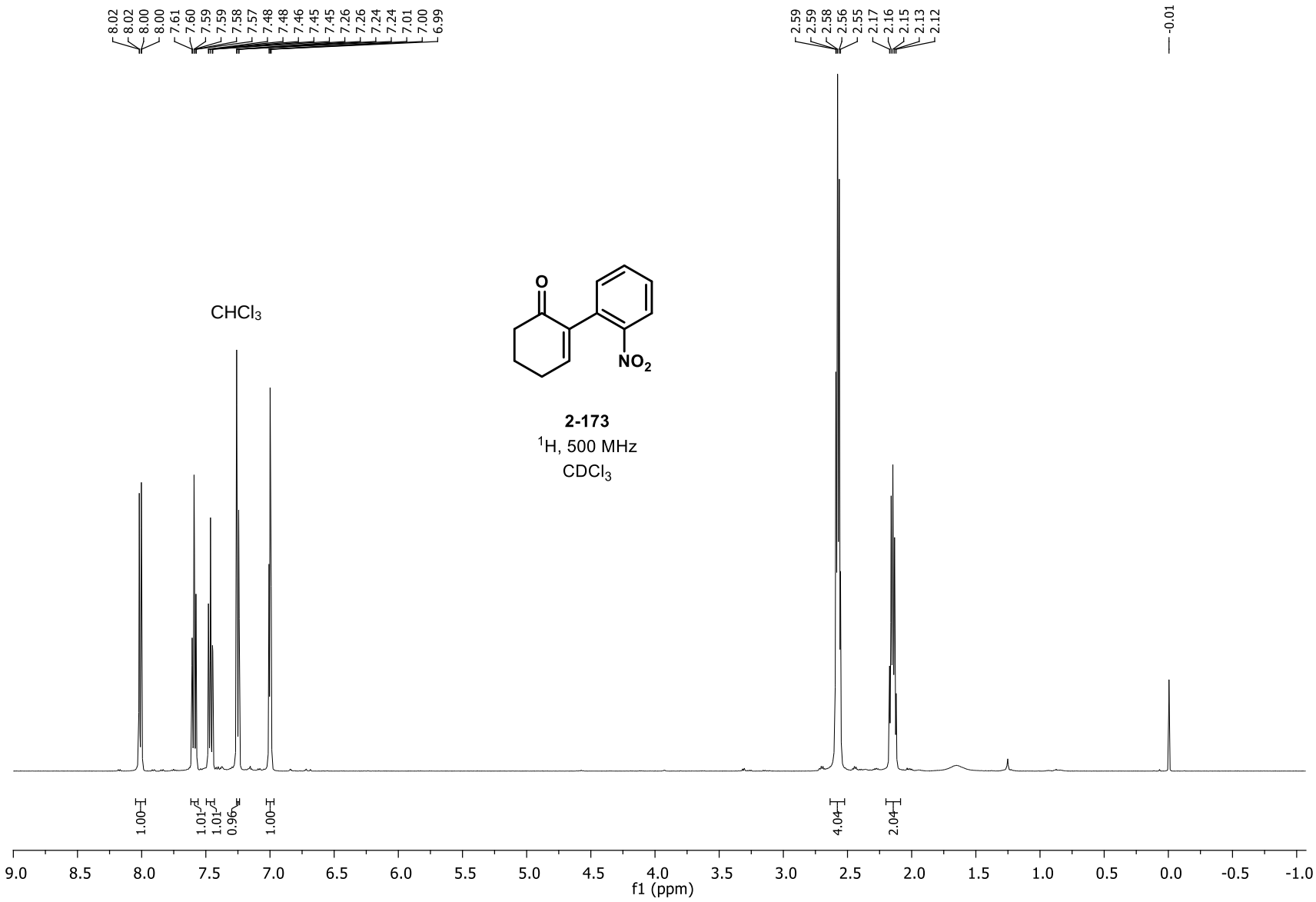
8.02
8.02
8.00
8.00
7.61
7.60
7.59
7.59
7.58
7.57
7.48
7.48
7.46
7.45
7.45
7.26
7.26
7.24
7.24
7.01
7.00
6.99
2.59
2.59
2.58
2.56
2.55
2.17
2.16
2.15
2.13
2.12
-0.01
CHCl3
O
NO2
2-173
1H, 500 MHz
CDCl3
1.00
1.01
1.01
0.96
1.00
4.04
2.04
9.0
8.5
8.0
7.5
7.0
6.5
6.0
5.5
5.0
4.5
4.0
3.5
3.0
2.5
2.0
1.5
1.0
0.5
0.0
-0.5
-1.0
f1 (ppm)

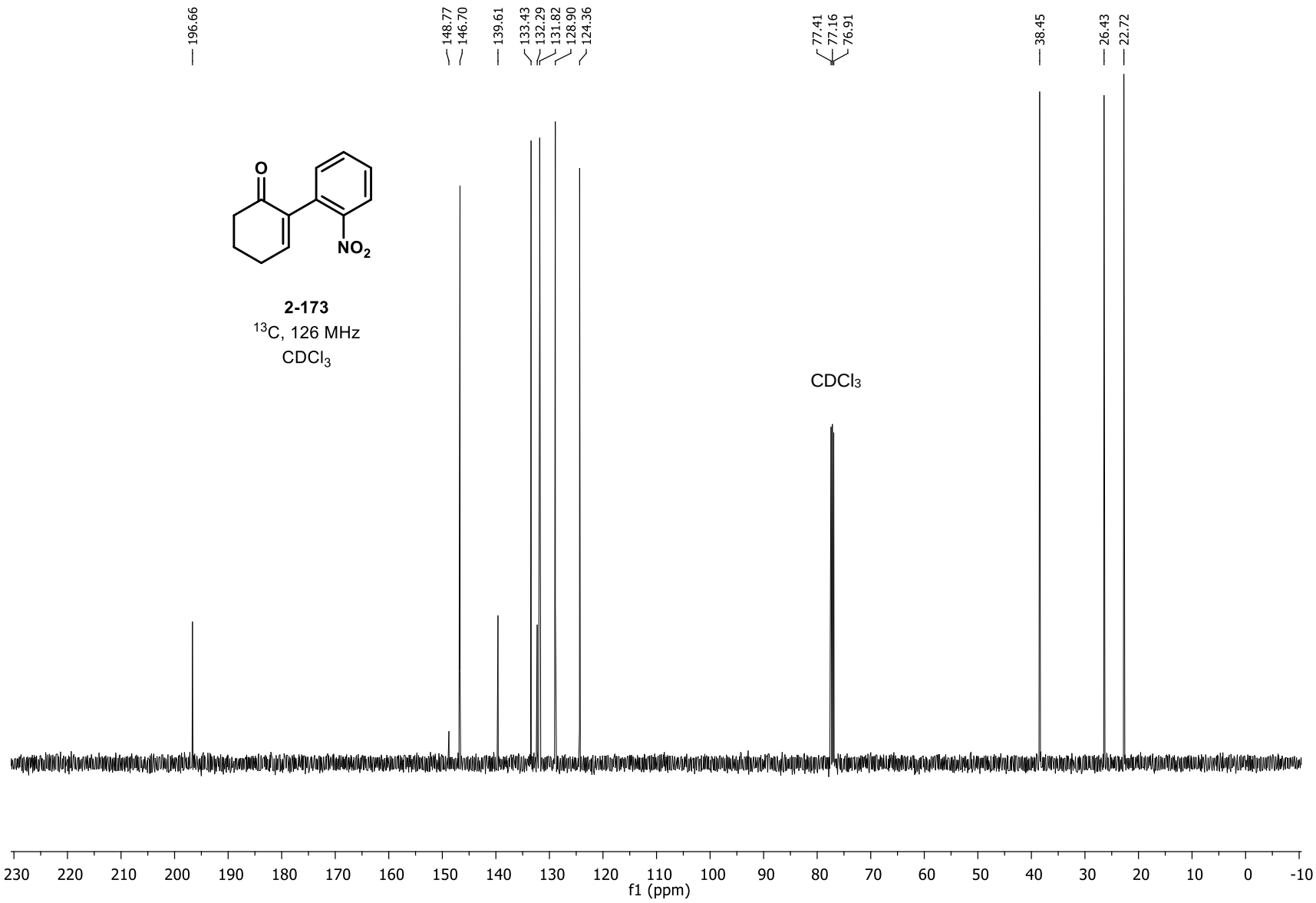
196.66
148.77
146.70
139.61
133.43
132.29
131.82
128.90
124.36
77.41
77.16
76.91
38.45
26.43
22.72
O
NO2
2-173
13C, 126 MHz
CDCl3
CDCl3
230 220 210 200 190 180 170 160 150 140 130 120 110 100 90 80 70 60 50 40 30 20 10 0 -10
f1 (ppm)

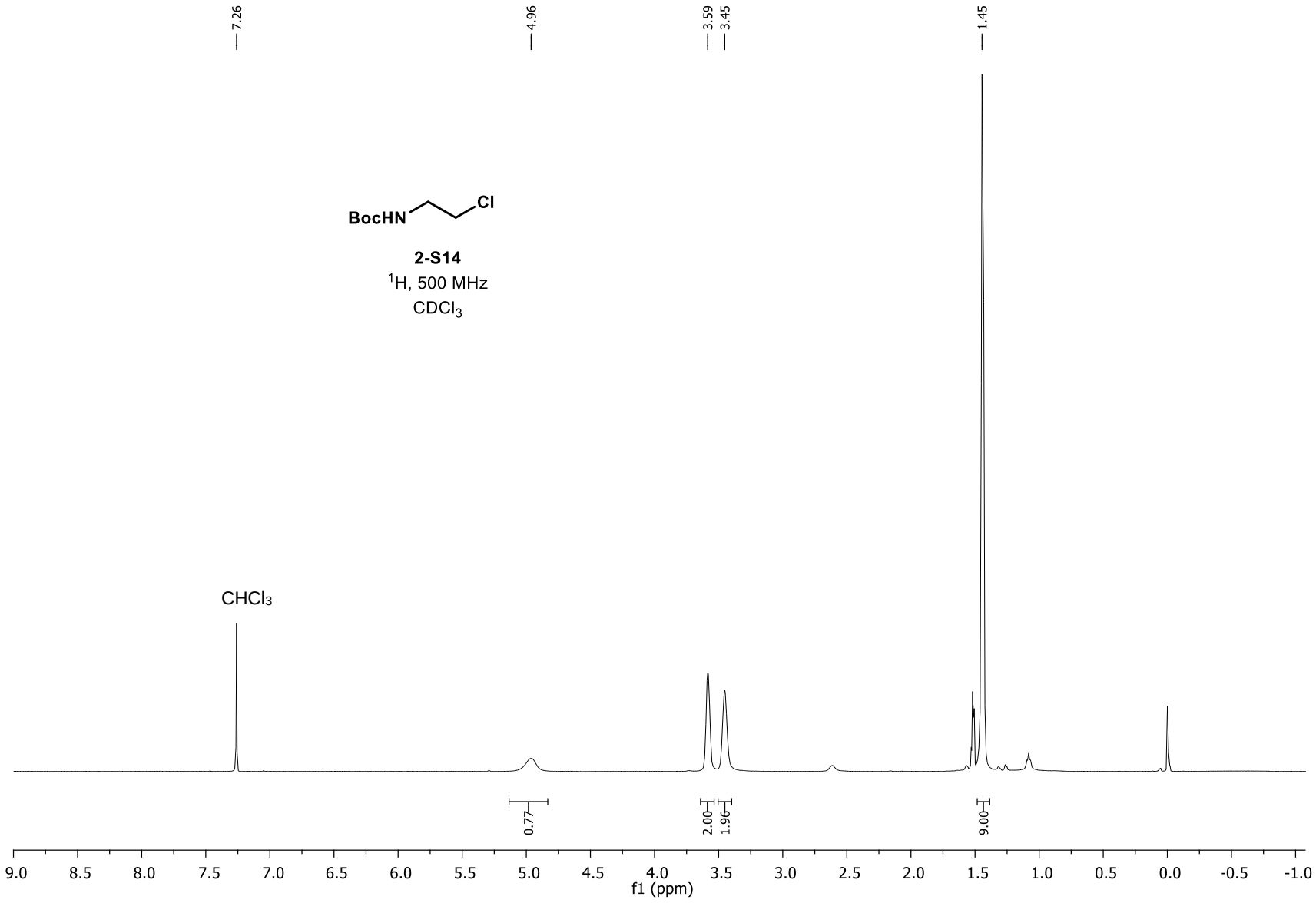
7.26
4.96
3.59
3.45
1.45
BocHN
Cl
2-S14
1H, 500 MHz
CDCl3
CHCl3
0.77
2.00
1.96
9.00
9.0
8.5
8.0
7.5
7.0
6.5
6.0
5.5
5.0
4.5
4.0
3.5
3.0
2.5
2.0
1.5
1.0
0.5
0.0
-0.5
-1.0
f1 (ppm)

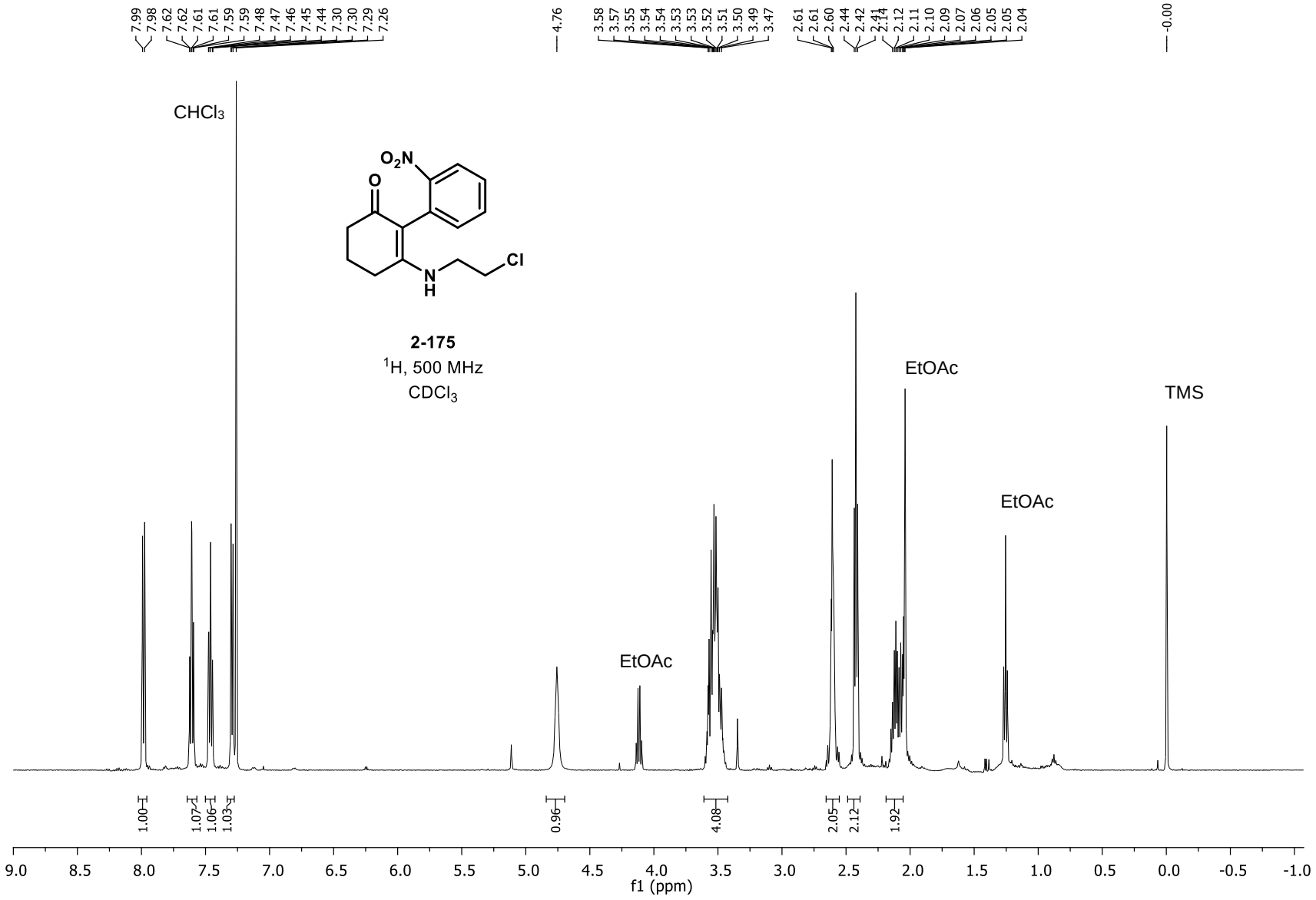
7.99
7.98
7.62
7.62
7.61
7.61
7.59
7.59
7.48
7.47
7.46
7.45
7.44
7.30
7.30
7.29
7.26
4.76
3.58
3.57
3.55
3.54
3.54
3.53
3.53
3.52
3.51
3.50
3.49
3.47
2.61
2.61
2.60
2.44
2.42
2.12
2.11
2.10
2.09
2.07
2.06
2.05
2.05
2.04
-0.00
CHCl3
O2N
O
N
H
Cl
2-175
1H, 500 MHz
CDCl3
EtOAc
EtOAc
EtOAc
TMS
1.00
1.07
1.06
1.03
0.96
4.08
2.05
2.12
1.92
9.0
8.5
8.0
7.5
7.0
6.5
6.0
5.5
5.0
4.5
4.0
3.5
3.0
2.5
2.0
1.5
1.0
0.5
0.0
-0.5
-1.0
f1 (ppm)

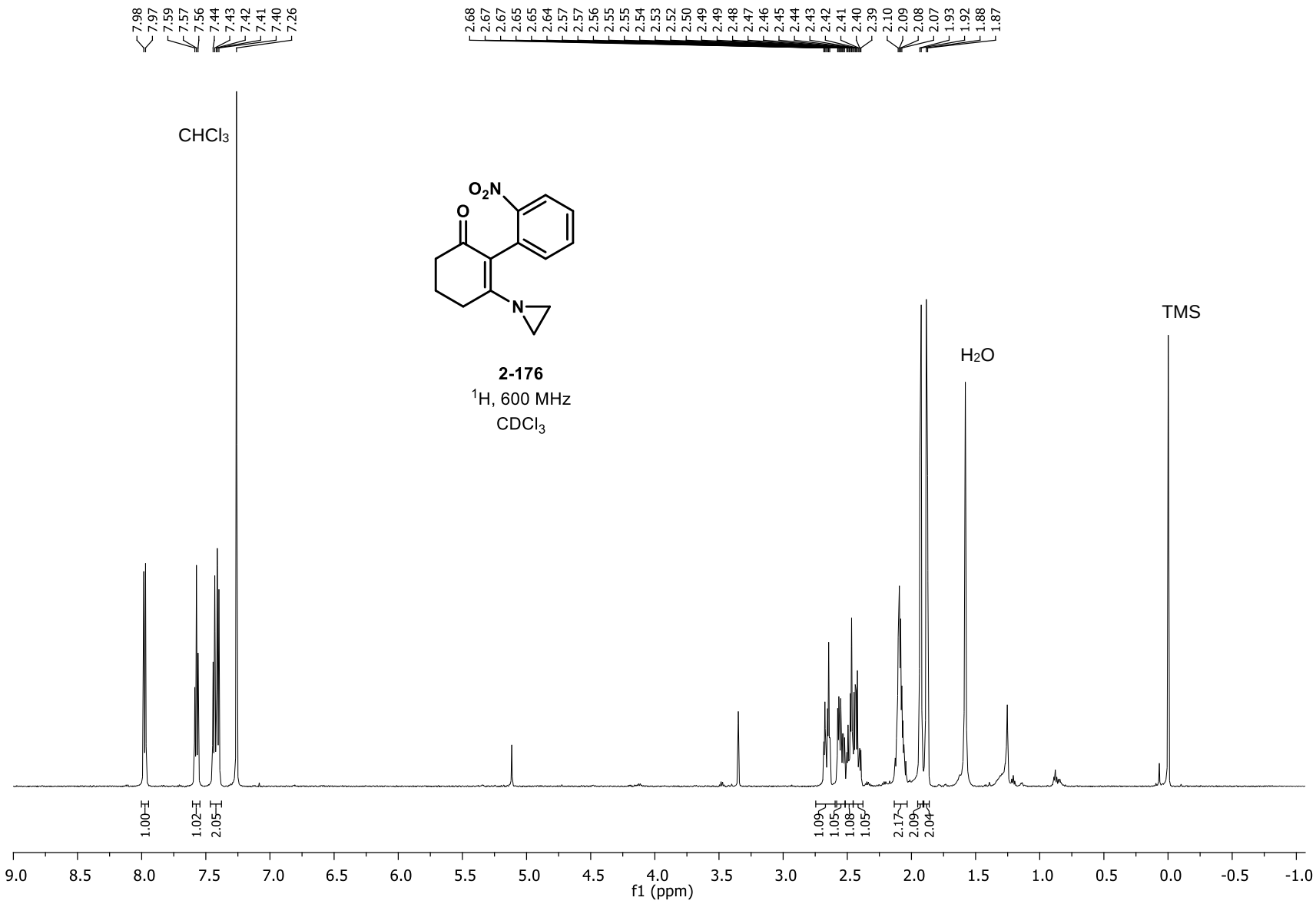
7.98
7.97
7.59
7.57
7.56
7.44
7.43
7.42
7.41
7.40
7.26
2.68
2.67
2.67
2.65
2.65
2.64
2.57
2.57
2.56
2.55
2.55
2.54
2.53
2.52
2.50
2.49
2.49
2.48
2.47
2.46
2.45
2.44
2.43
2.42
2.41
2.40
2.39
2.10
2.09
2.08
2.07
1.93
1.92
1.88
1.87
CHCl3
O2N
O
N
2-176
1H, 600 MHz
CDCl3
H2O
TMS
1.00
1.02
2.05
1.09
1.05
1.08
1.05
2.17
2.09
2.04
9.0
8.5
8.0
7.5
7.0
6.5
6.0
5.5
5.0
4.5
4.0
3.5
3.0
2.5
2.0
1.5
1.0
0.5
0.0
-0.5
-1.0
f1 (ppm)

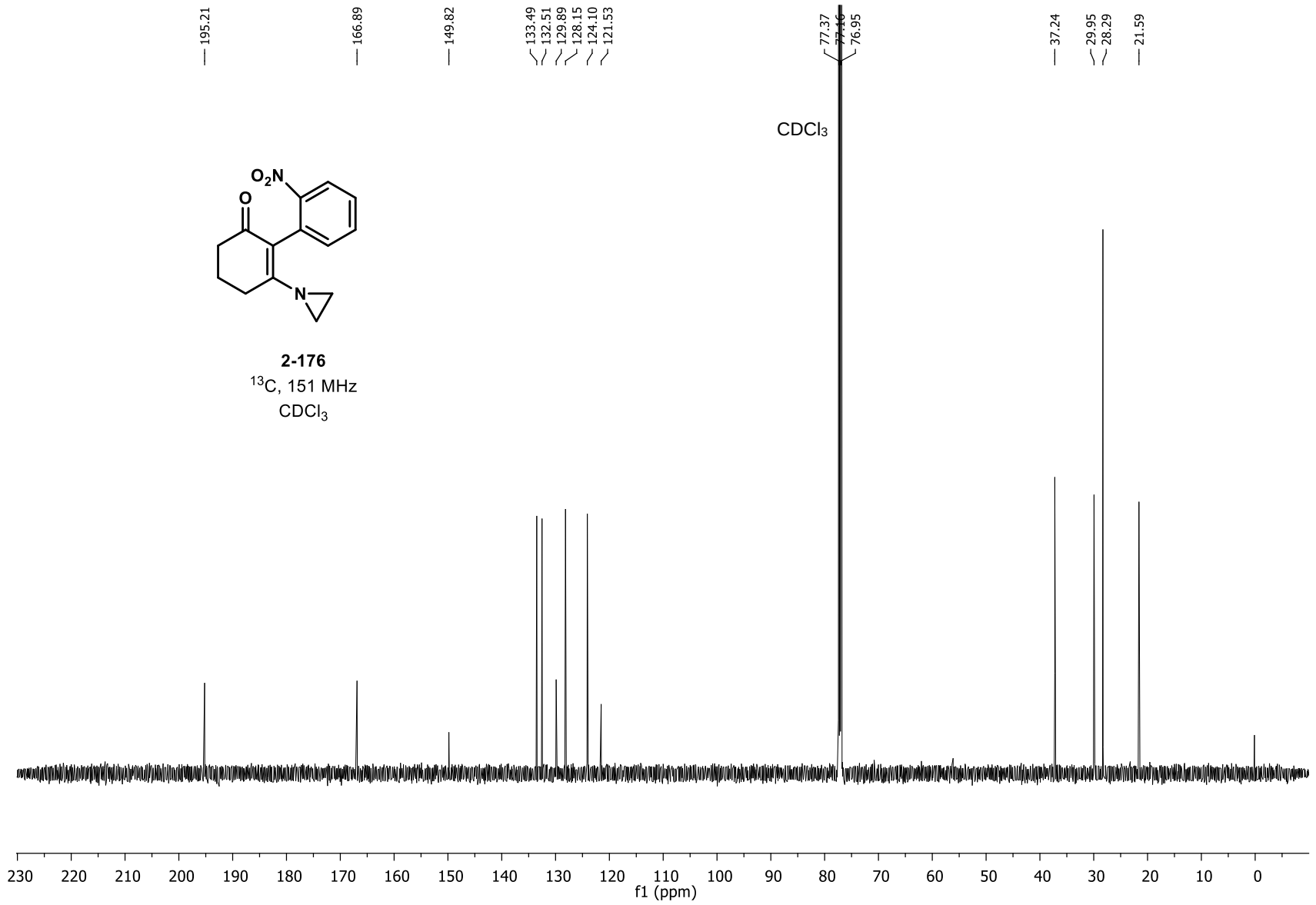
195.21
166.89
149.82
133.49
132.51
129.89
128.15
124.10
121.53
77.37
77.16
76.95
37.24
29.95
28.29
21.59
CDCl3
O2N
O
N
2-176
13C, 151 MHz
CDCl3
230 220 210 200 190 180 170 160 150 140 130 120 110 100 90 80 70 60 50 40 30 20 10 0
f1 (ppm)

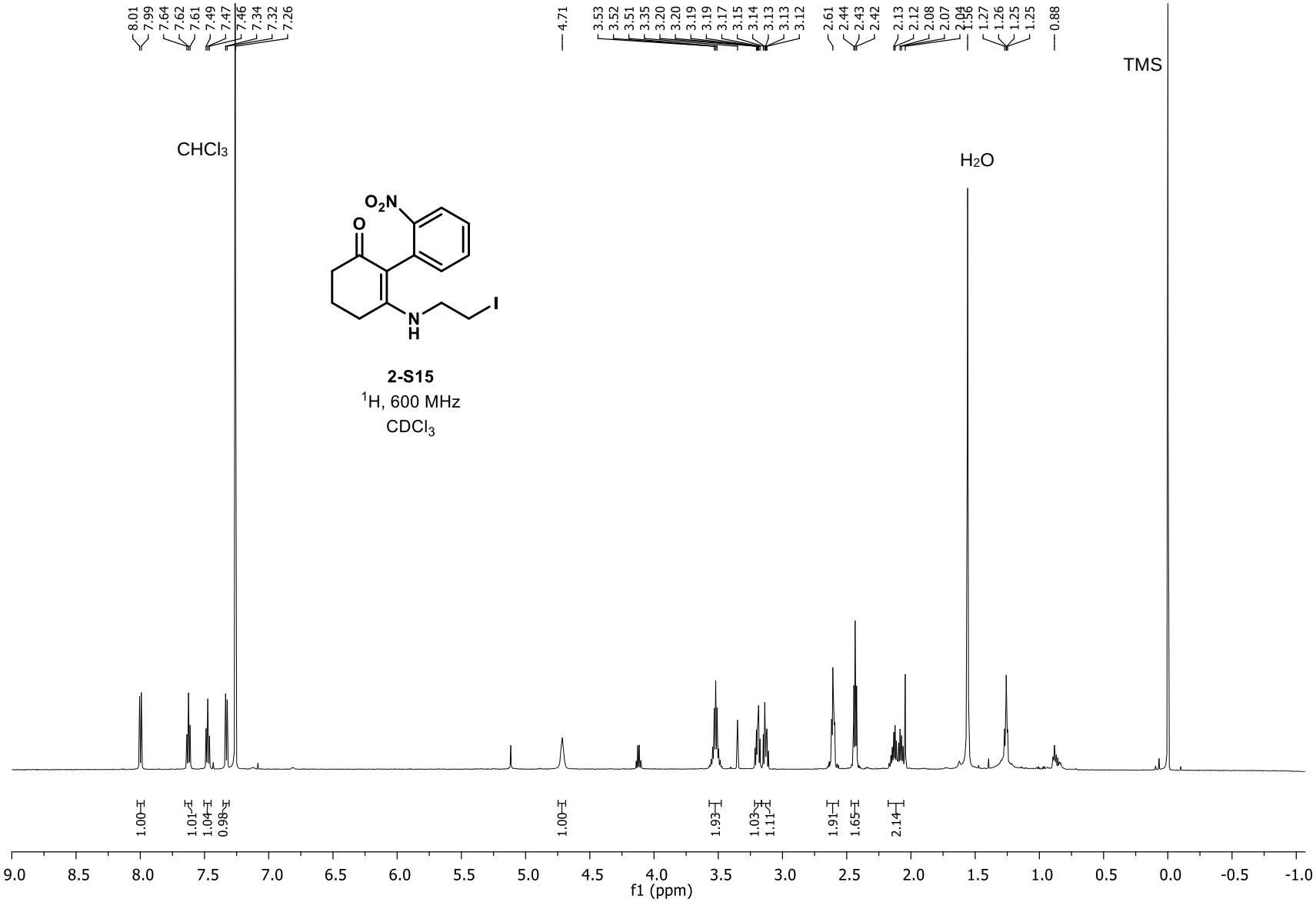
8.01
7.99
7.64
7.62
7.61
7.49
7.47
7.46
7.34
7.32
7.26
4.71
3.53
3.52
3.51
3.35
3.20
3.20
3.19
3.19
3.17
3.15
3.14
3.13
3.13
3.12
2.61
2.44
2.43
2.42
2.13
2.12
2.08
2.07
1.27
1.26
1.25
1.25
0.88
TMS
CHCl3
H2O
O2N
O
N
H
I
2-S15
1H, 600 MHz
CDCl3
1.00
1.01
1.04
0.98
1.00
1.93
1.03
1.11
1.91
1.65
2.14
9.0
8.5
8.0
7.5
7.0
6.5
6.0
5.5
5.0
4.5
4.0
3.5
3.0
2.5
2.0
1.5
1.0
0.5
0.0
-0.5
-1.0
f1 (ppm)

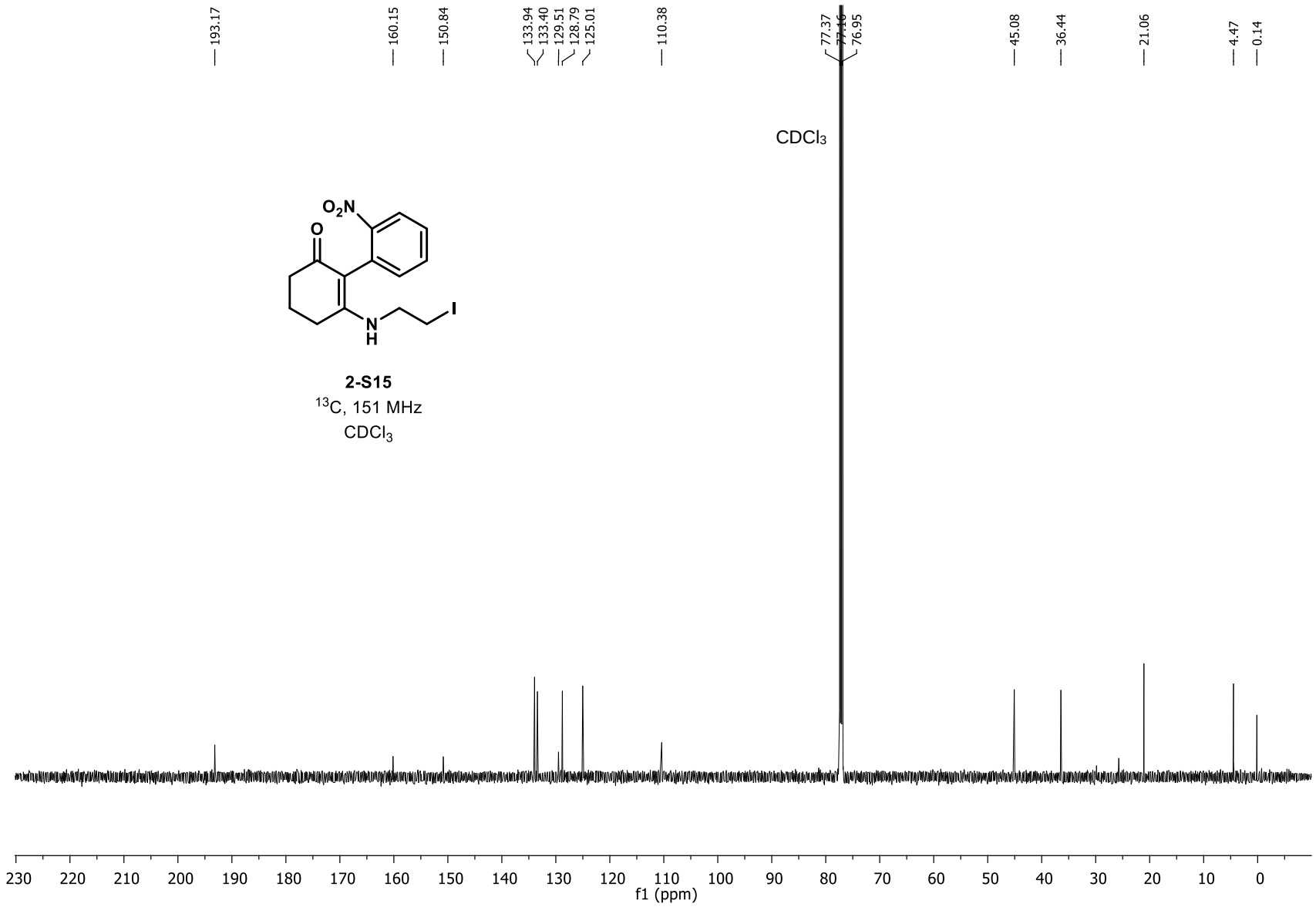
193.17
160.15
150.84
133.94
133.40
129.51
128.79
125.01
110.38
77.37
77.16
76.95
45.08
36.44
21.06
4.47
0.14
CDCl3
O2N
O
N
H
I
2-S15
13C, 151 MHz
CDCl3
230 220 210 200 190 180 170 160 150 140 130 120 110 100 90 80 70 60 50 40 30 20 10 0
f1 (ppm)

Appendix C: NMR Spectra for Chapter 3

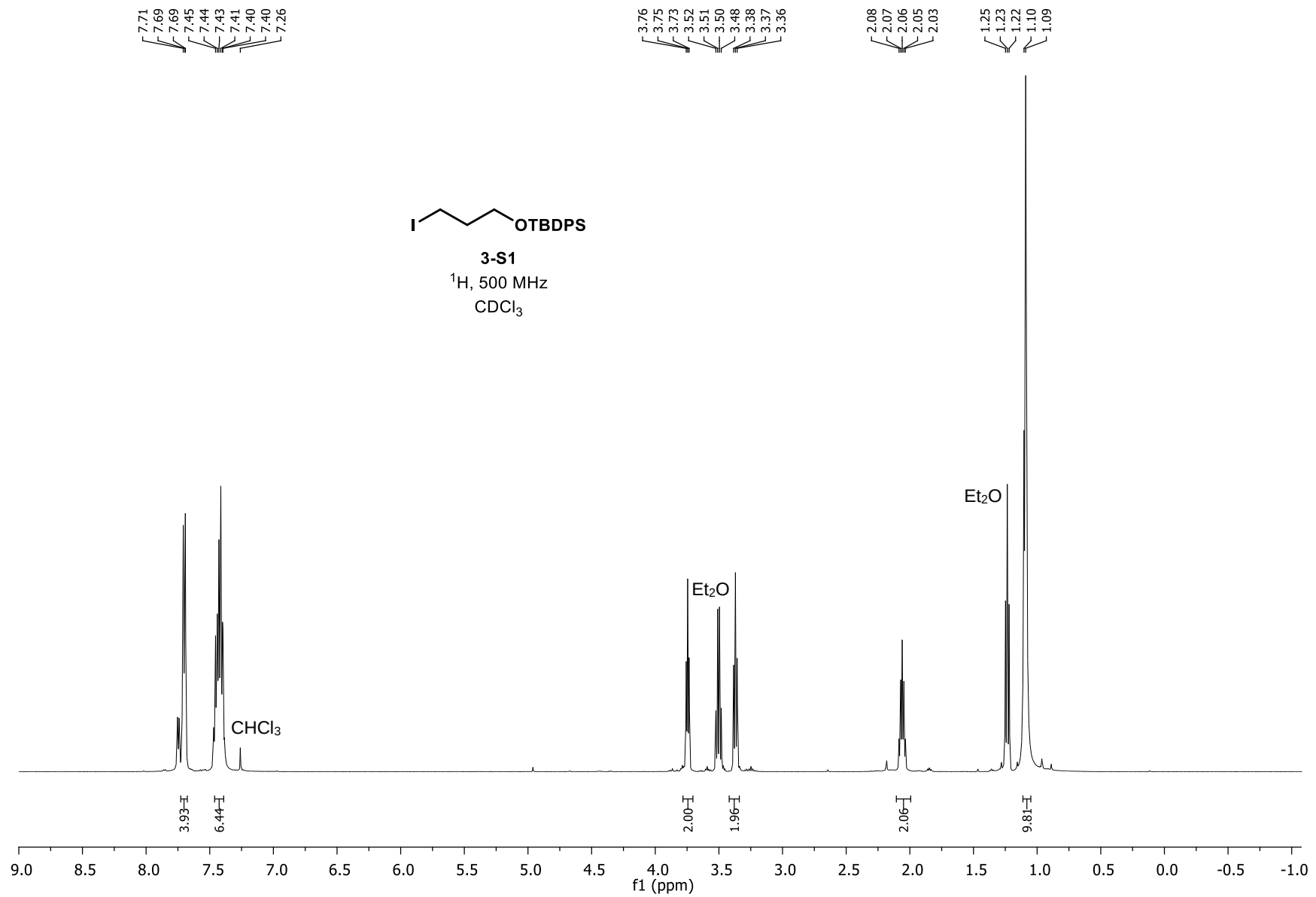
7.71
7.69
7.69
7.45
7.44
7.43
7.41
7.40
7.40
7.26
3.76
3.75
3.73
3.52
3.51
3.50
3.48
3.38
3.37
3.36
2.08
2.07
2.06
2.05
2.03
1.25
1.23
1.22
1.10
1.09
I
OTBDPS
3-S1
1H, 500 MHz
CDCl3
Et2O
Et2O
CHCl3
3.93
6.44
2.00
1.96
2.06
9.81
9.0
8.5
8.0
7.5
7.0
6.5
6.0
5.5
5.0
4.5
4.0
3.5
3.0
2.5
2.0
1.5
1.0
0.5
0.0
-0.5
-1.0
f1 (ppm)

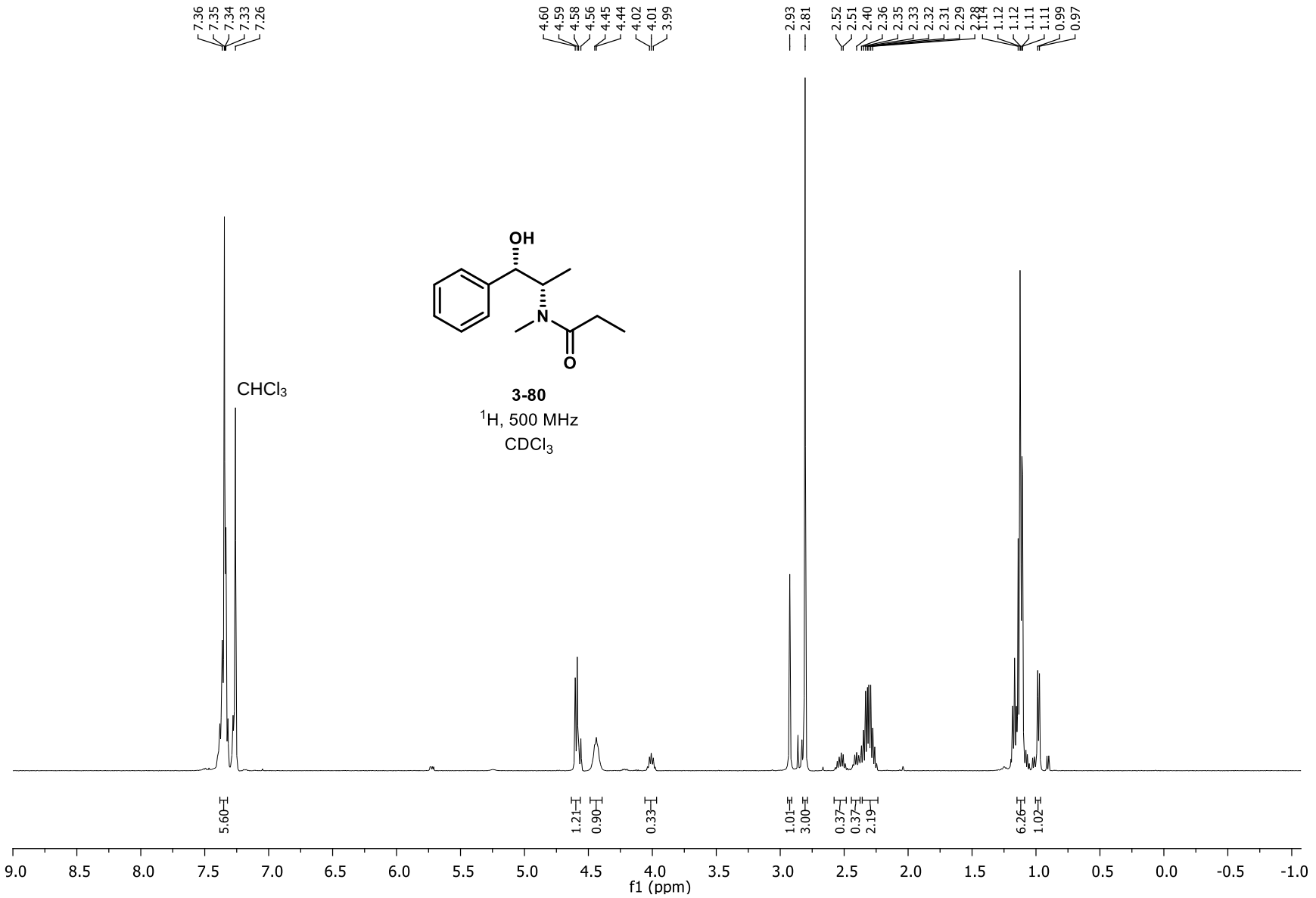
7.36
7.35
7.34
7.33
7.26
4.60
4.59
4.58
4.56
4.45
4.44
4.02
4.01
3.99
2.93
2.81
2.52
2.51
2.40
2.36
2.35
2.33
2.32
2.31
2.29
1.12
1.12
1.11
1.11
0.99
0.97
OH
N
O
CHCl3
3-80
1H, 500 MHz
CDCl3
5.60
1.21
0.90
0.33
1.01
3.00
0.37
0.37
2.19
6.26
1.02
9.0
8.5
8.0
7.5
7.0
6.5
6.0
5.5
5.0
4.5
4.0
3.5
3.0
2.5
2.0
1.5
1.0
0.5
0.0
-0.5
-1.0
f1 (ppm)

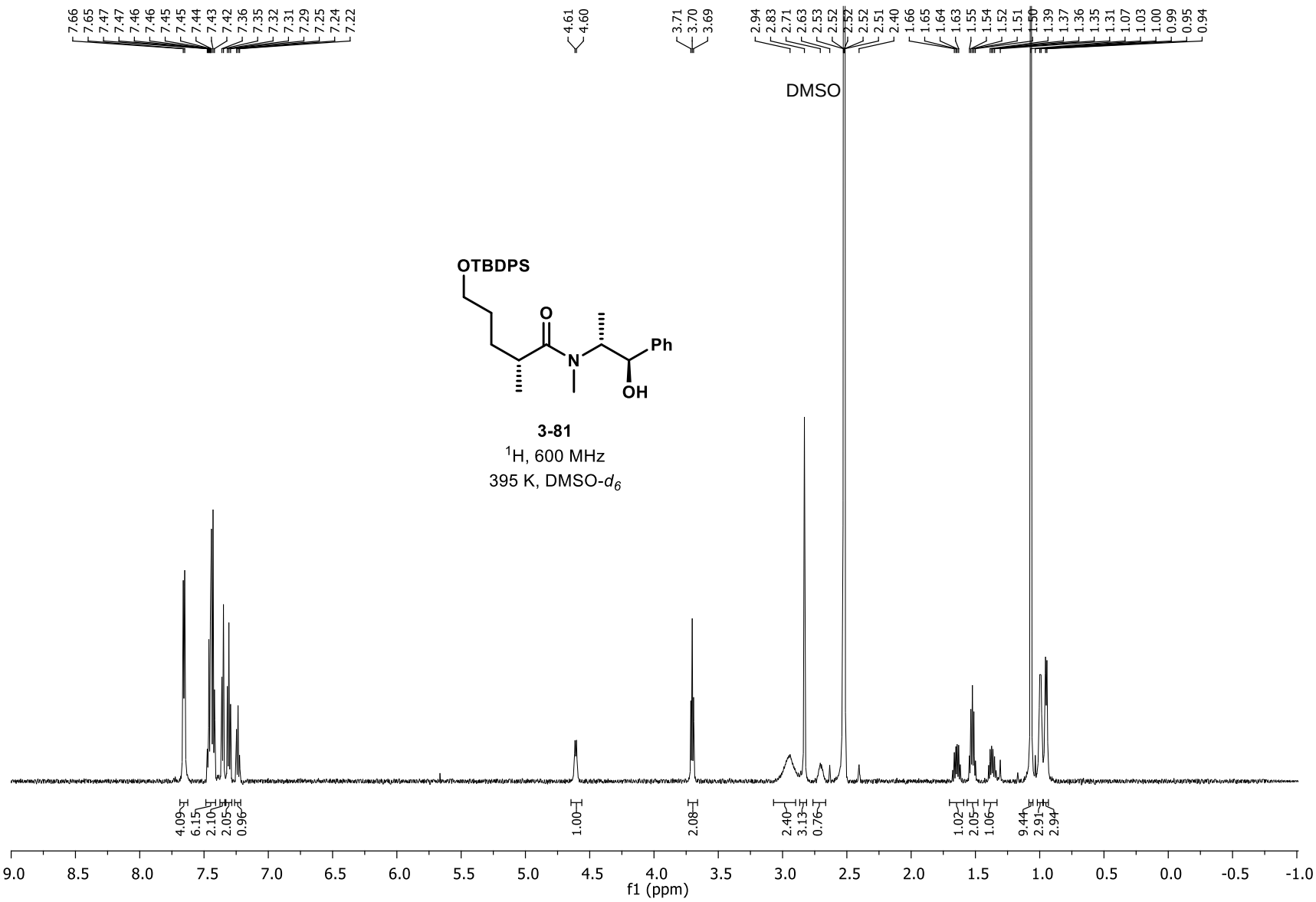
7.66
7.65
7.47
7.47
7.46
7.46
7.45
7.45
7.44
7.43
7.42
7.36
7.35
7.32
7.31
7.29
7.25
7.24
7.22
4.61
4.60
3.71
3.70
3.69
2.94
2.83
2.71
2.63
2.53
2.52
2.52
2.52
2.51
2.40
1.66
1.65
1.64
1.63
1.55
1.54
1.52
1.51
1.50
1.39
1.37
1.36
1.35
1.31
1.07
1.03
1.00
0.99
0.95
0.94
DMSO
OTBDPS
O
N
Ph
OH
3-81
1H, 600 MHz
395 K, DMSO-d6
4.09
6.15
2.10
2.05
0.96
1.00
2.08
2.40
3.13
0.76
1.02
2.05
1.06
9.44
2.91
2.94
9.0
8.5
8.0
7.5
7.0
6.5
6.0
5.5
5.0
4.5
4.0
3.5
3.0
2.5
2.0
1.5
1.0
0.5
0.0
-0.5
-1.0
f1 (ppm)

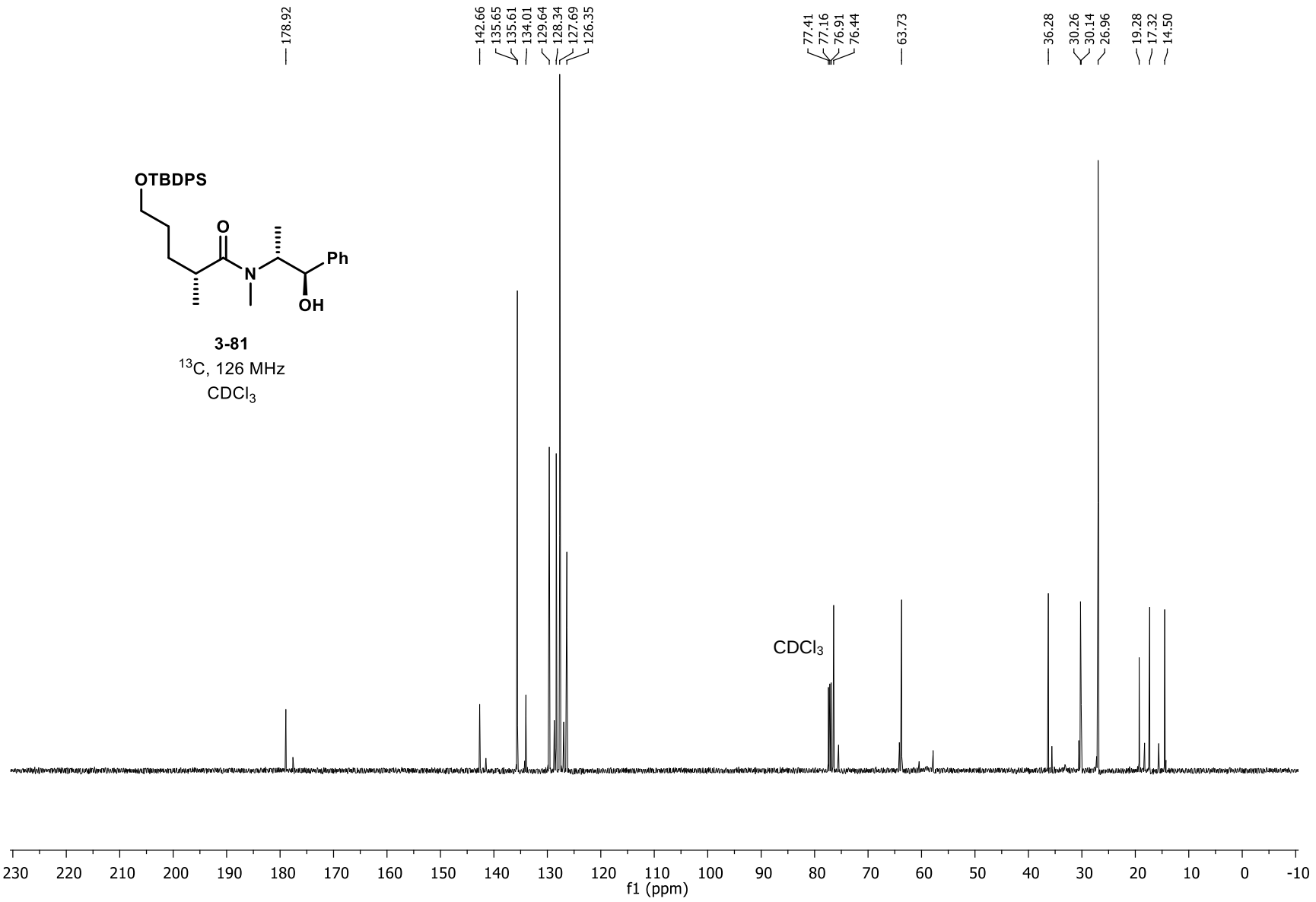
178.92
142.66
135.65
135.61
134.01
129.64
128.34
127.69
126.35
77.41
77.16
76.91
76.44
63.73
36.28
30.26
30.14
26.96
19.28
17.32
14.50
OTBDPS
O
N
Ph
OH
3-81
13C, 126 MHz
CDCl3
CDCl3
230 220 210 200 190 180 170 160 150 140 130 120 110 100 90 80 70 60 50 40 30 20 10 0 -10
f1 (ppm)

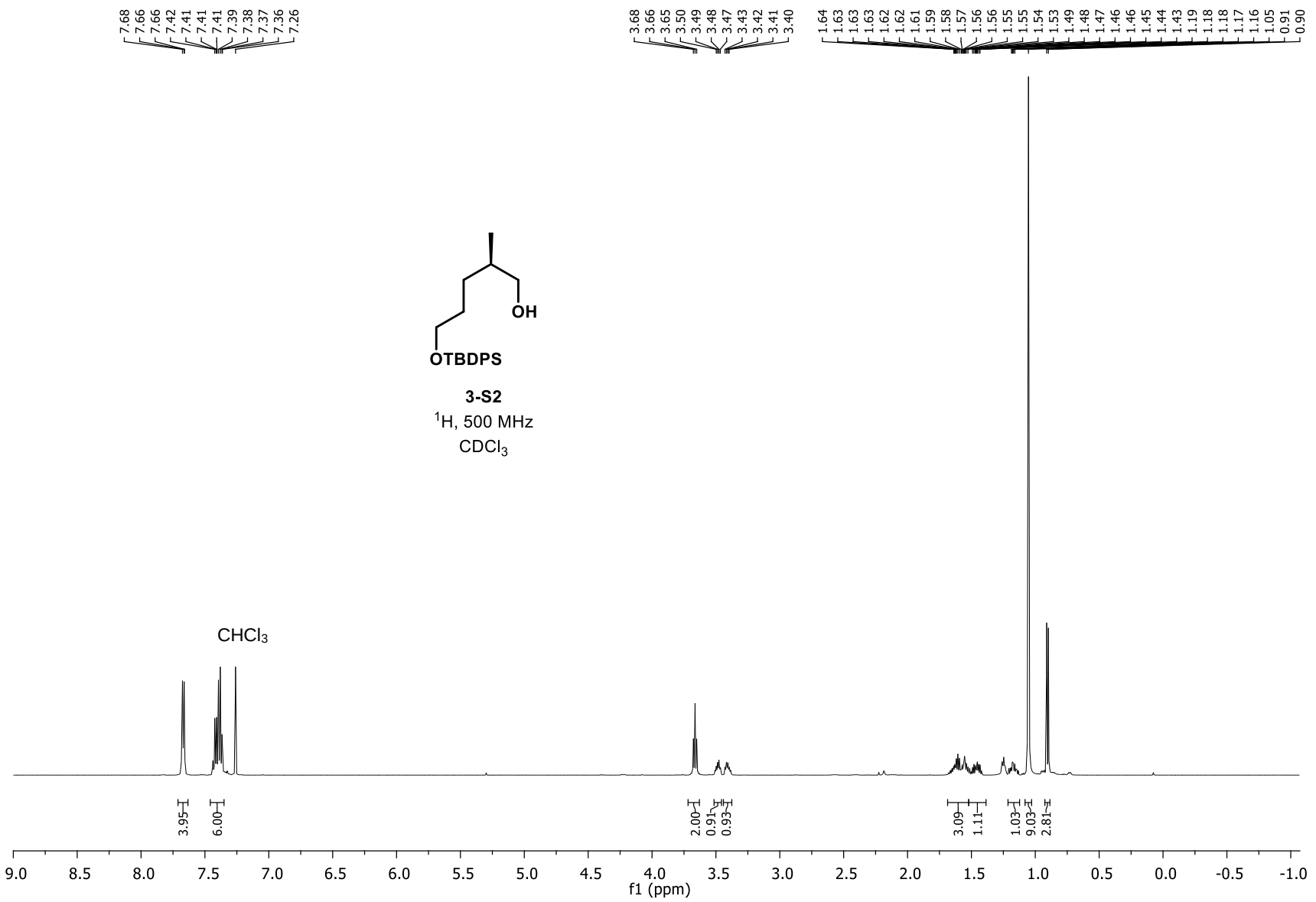
7.68
7.66
7.66
7.42
7.41
7.41
7.41
7.39
7.38
7.37
7.36
7.26
3.68
3.66
3.65
3.50
3.49
3.48
3.47
3.43
3.42
3.41
3.40
1.64
1.63
1.63
1.63
1.62
1.62
1.61
1.59
1.58
1.57
1.56
1.56
1.55
1.55
1.54
1.53
1.49
1.48
1.47
1.46
1.46
1.45
1.44
1.43
1.19
1.18
1.18
1.17
1.16
1.05
0.91
0.90
OH
OTBDPS
3-S2
1H, 500 MHz
CDCl3
CHCl3
3.95
6.00
2.00
0.91
0.93
3.09
1.11
1.03
9.03
2.81
9.0
8.5
8.0
7.5
7.0
6.5
6.0
5.5
5.0
4.5
4.0
3.5
3.0
2.5
2.0
1.5
1.0
0.5
0.0
-0.5
-1.0
f1 (ppm)

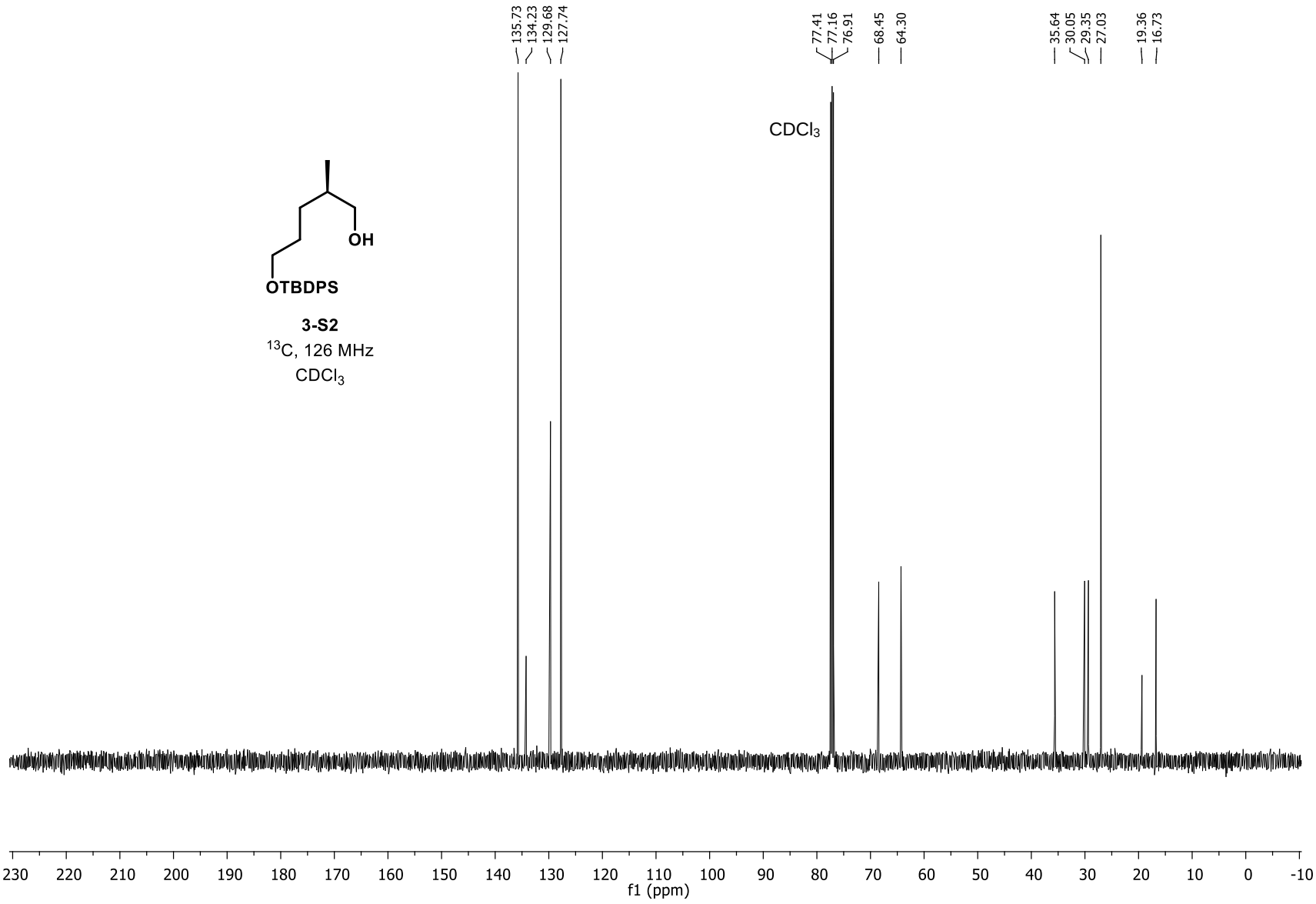
135.73
134.23
129.68
127.74
77.41
77.16
76.91
68.45
64.30
35.64
30.05
29.35
27.03
19.36
16.73
CDCl3
OH
OTBDPS
3-S2
13C, 126 MHz
CDCl3
230 220 210 200 190 180 170 160 150 140 130 120 110 100 90 80 70 60 50 40 30 20 10 0 -10
f1 (ppm)

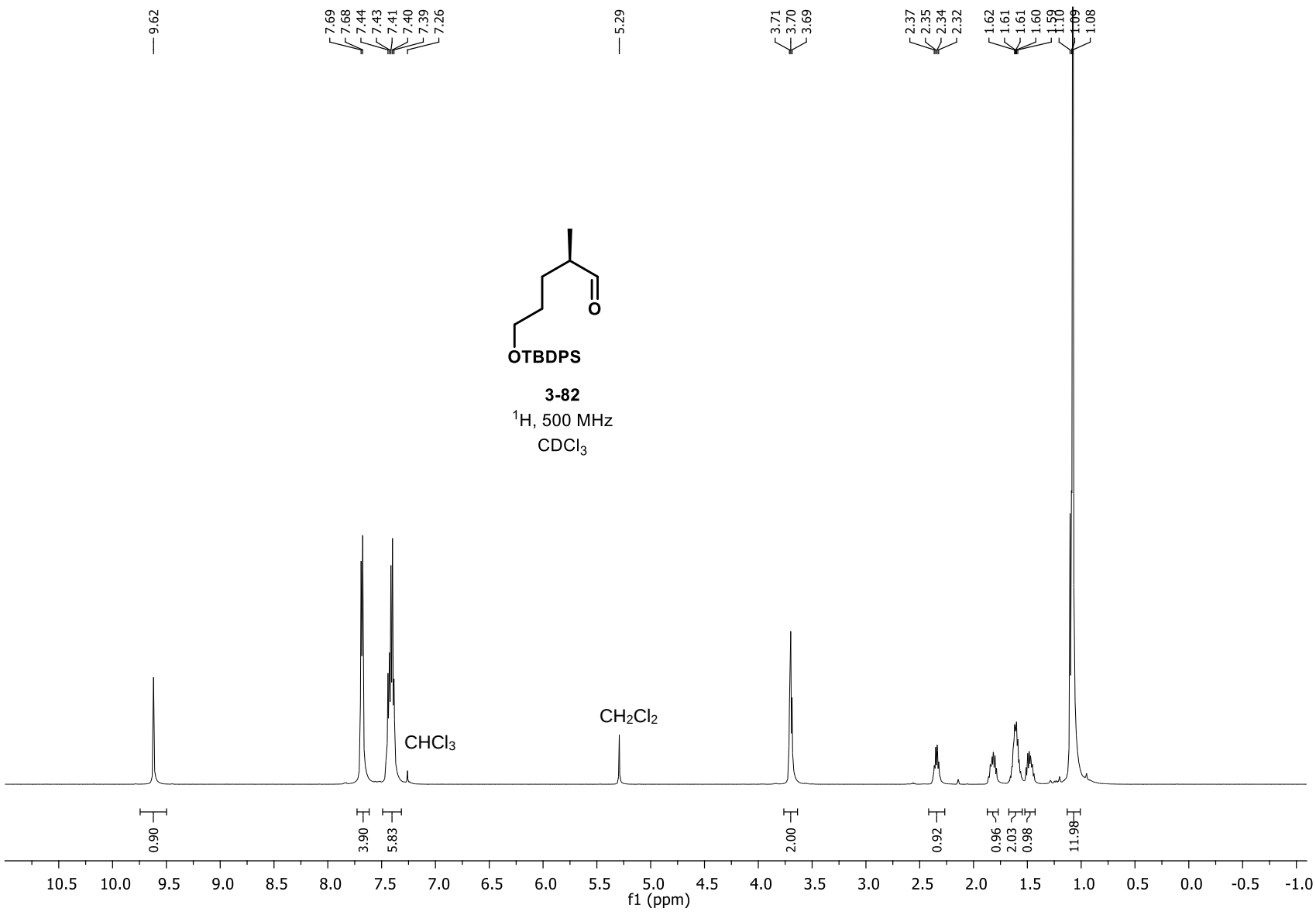
9.62
7.69
7.68
7.44
7.43
7.41
7.40
7.39
7.26
5.29
3.71
3.70
3.69
2.37
2.35
2.34
2.32
1.62
1.61
1.61
1.60
1.59
1.10
1.09
1.08
O
OTBDPS
3-82
1H, 500 MHz
CDCl3
CHCl3
CH2Cl2
0.90
3.90
5.83
2.00
0.92
0.96
2.03
0.98
11.98
10.5 10.0 9.5 9.0 8.5 8.0 7.5 7.0 6.5 6.0 5.5 5.0 4.5 4.0 3.5 3.0 2.5 2.0 1.5 1.0 0.5 0.0 -0.5 -1.0
f1 (ppm)

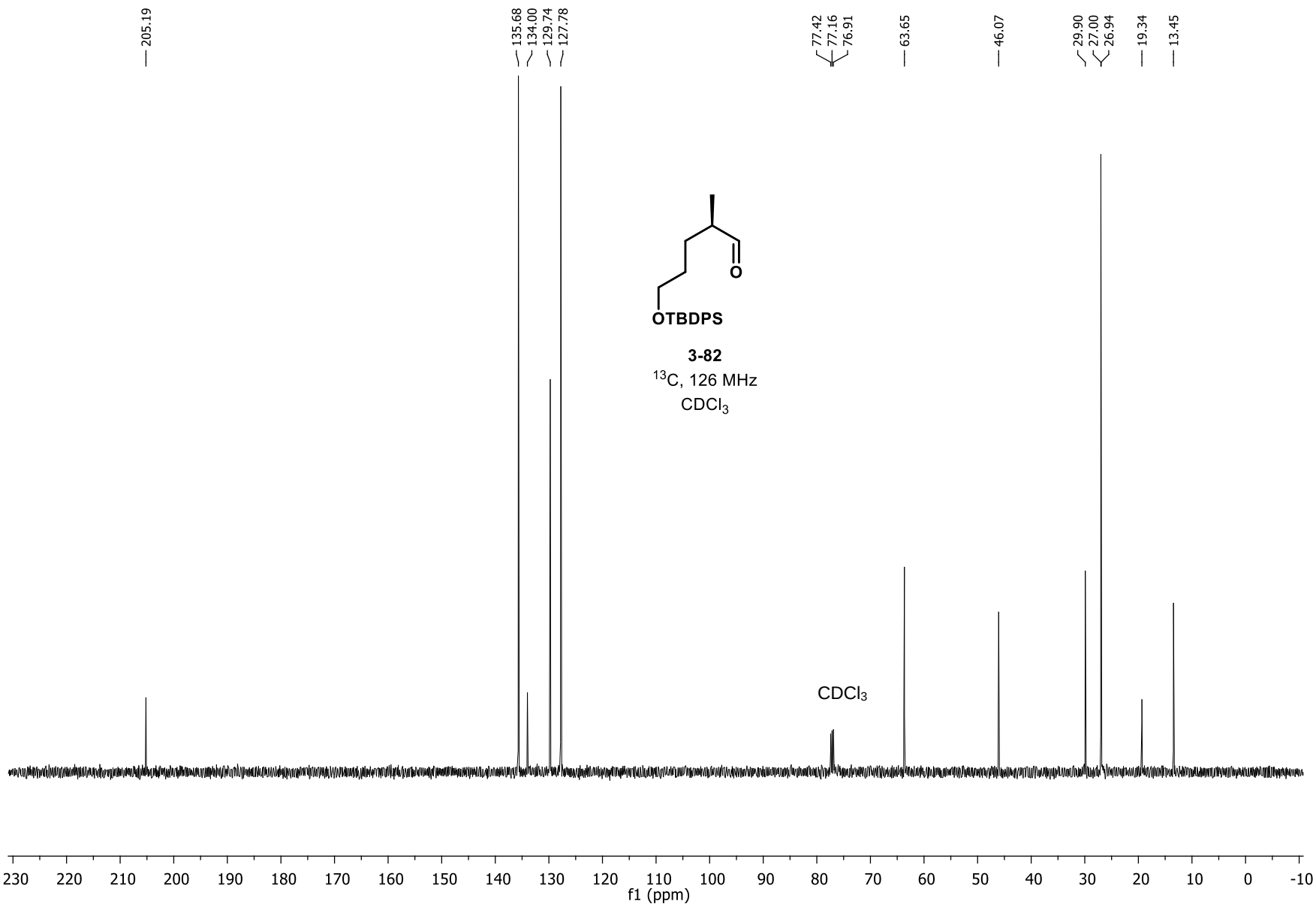
205.19
135.68
134.00
129.74
127.78
77.42
77.16
76.91
63.65
46.07
29.90
27.00
26.94
19.34
13.45
O
OTBDPS
3-82
13C, 126 MHz
CDCl3
CDCl3
230 220 210 200 190 180 170 160 150 140 130 120 110 100 90 80 70 60 50 40 30 20 10 0 -10
f1 (ppm)

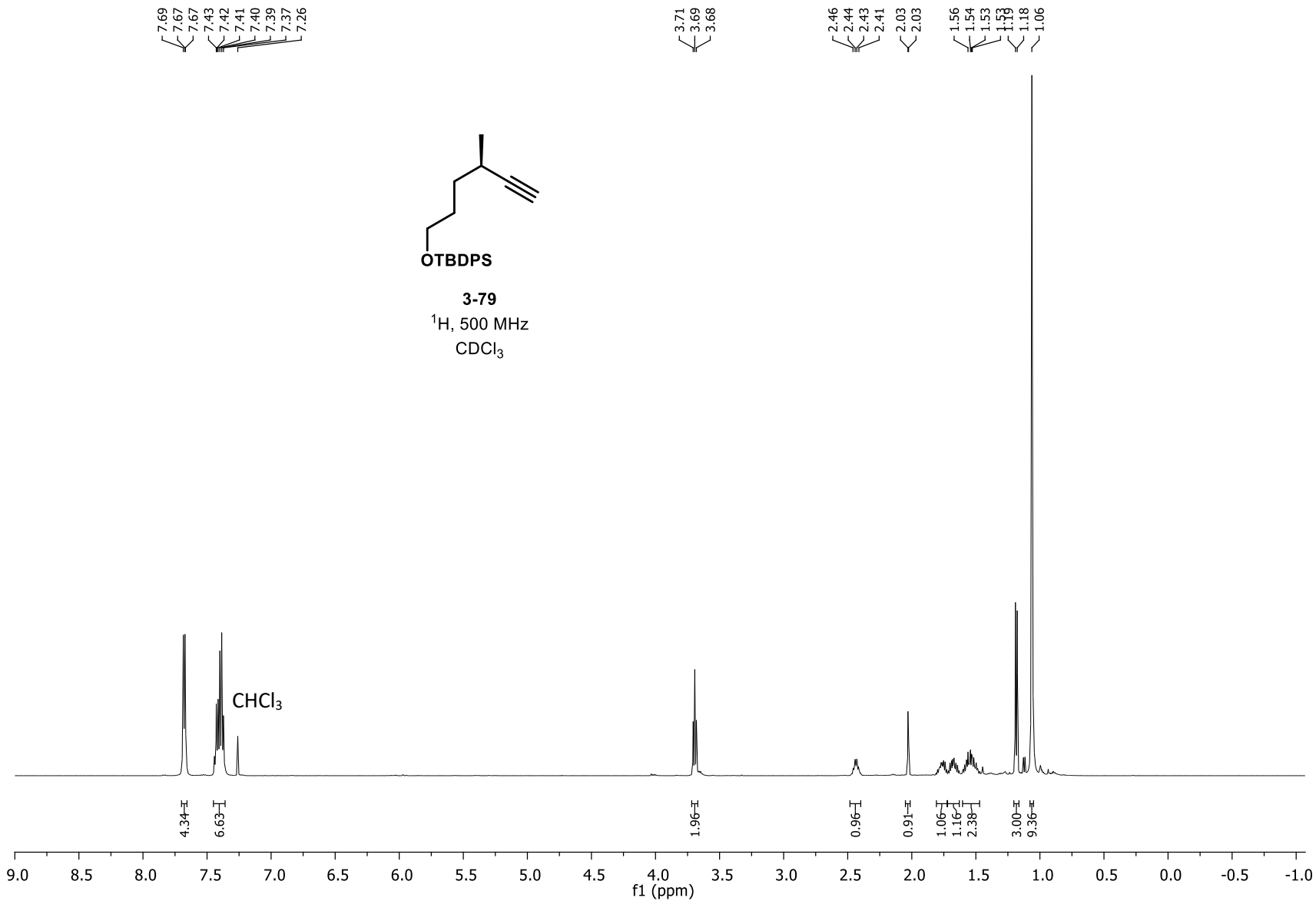
7.69
7.67
7.67
7.43
7.42
7.41
7.40
7.39
7.37
7.26
3.71
3.69
3.68
2.46
2.44
2.43
2.41
2.03
2.03
1.56
1.54
1.53
1.18
1.06
OTBDPS
3-79
1H, 500 MHz
CDCl3
CHCl3
4.34
6.63
1.96
0.96
0.91
1.06
1.16
2.38
3.00
9.36
9.0
8.5
8.0
7.5
7.0
6.5
6.0
5.5
5.0
4.5
4.0
3.5
3.0
2.5
2.0
1.5
1.0
0.5
0.0
-0.5
-1.0
f1 (ppm)

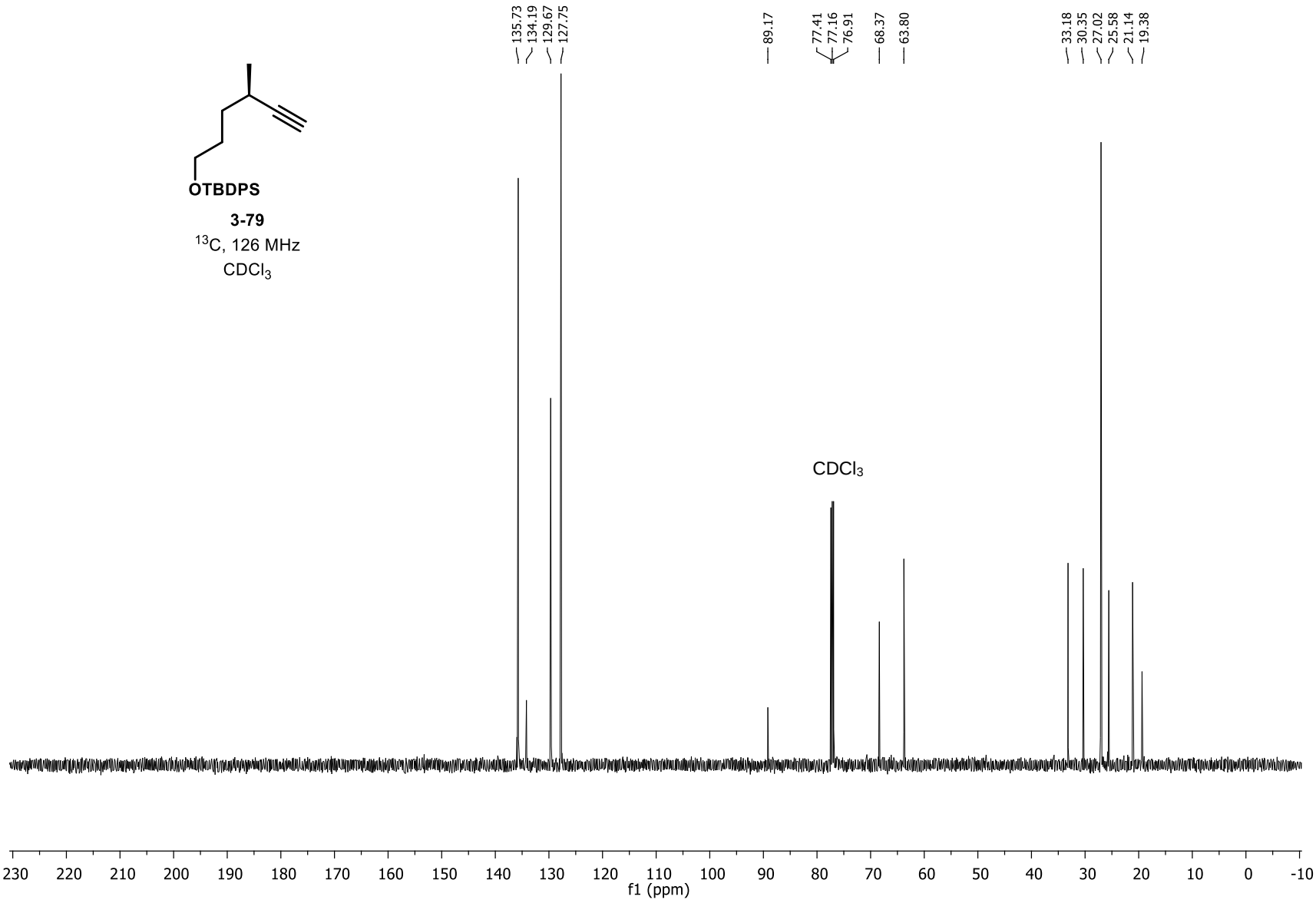
OTBDPS
3-79
^{13}C, 126 MHz
$CDCl_3$
135.73
134.19
129.67
127.75
89.17
77.41
77.16
76.91
68.37
63.80
33.18
30.35
27.02
25.58
21.14
19.38
$CDCl_3$
230 220 210 200 190 180 170 160 150 140 130 120 110 100 90 80 70 60 50 40 30 20 10 0 -10
f1 (ppm)

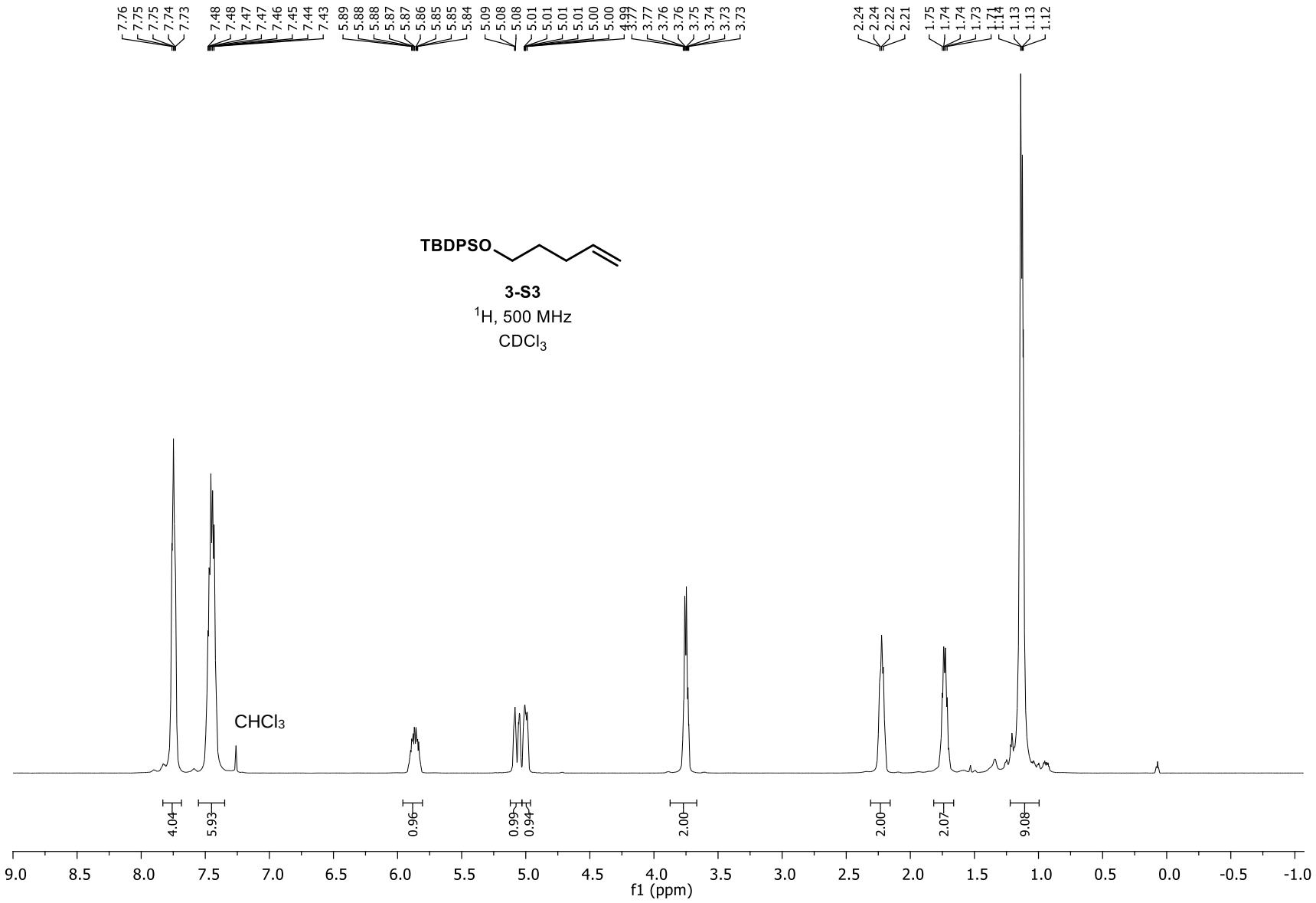
7.76
7.75
7.75
7.74
7.73
7.48
7.48
7.47
7.47
7.46
7.45
7.44
7.43
5.89
5.88
5.88
5.87
5.87
5.86
5.85
5.85
5.84
5.09
5.08
5.08
5.01
5.01
5.01
5.01
5.00
5.00
4.99
3.77
3.77
3.76
3.76
3.75
3.74
3.73
3.73
2.24
2.24
2.22
2.21
1.75
1.74
1.74
1.73
1.71
1.14
1.13
1.13
1.12
TBDPSO
3-S3
1H, 500 MHz
CDCl3
CHCl3
4.04
5.93
0.96
0.99
0.94
2.00
2.00
2.07
9.08
9.0
8.5
8.0
7.5
7.0
6.5
6.0
5.5
5.0
4.5
4.0
3.5
3.0
2.5
2.0
1.5
1.0
0.5
0.0
-0.5
-1.0
f1 (ppm)

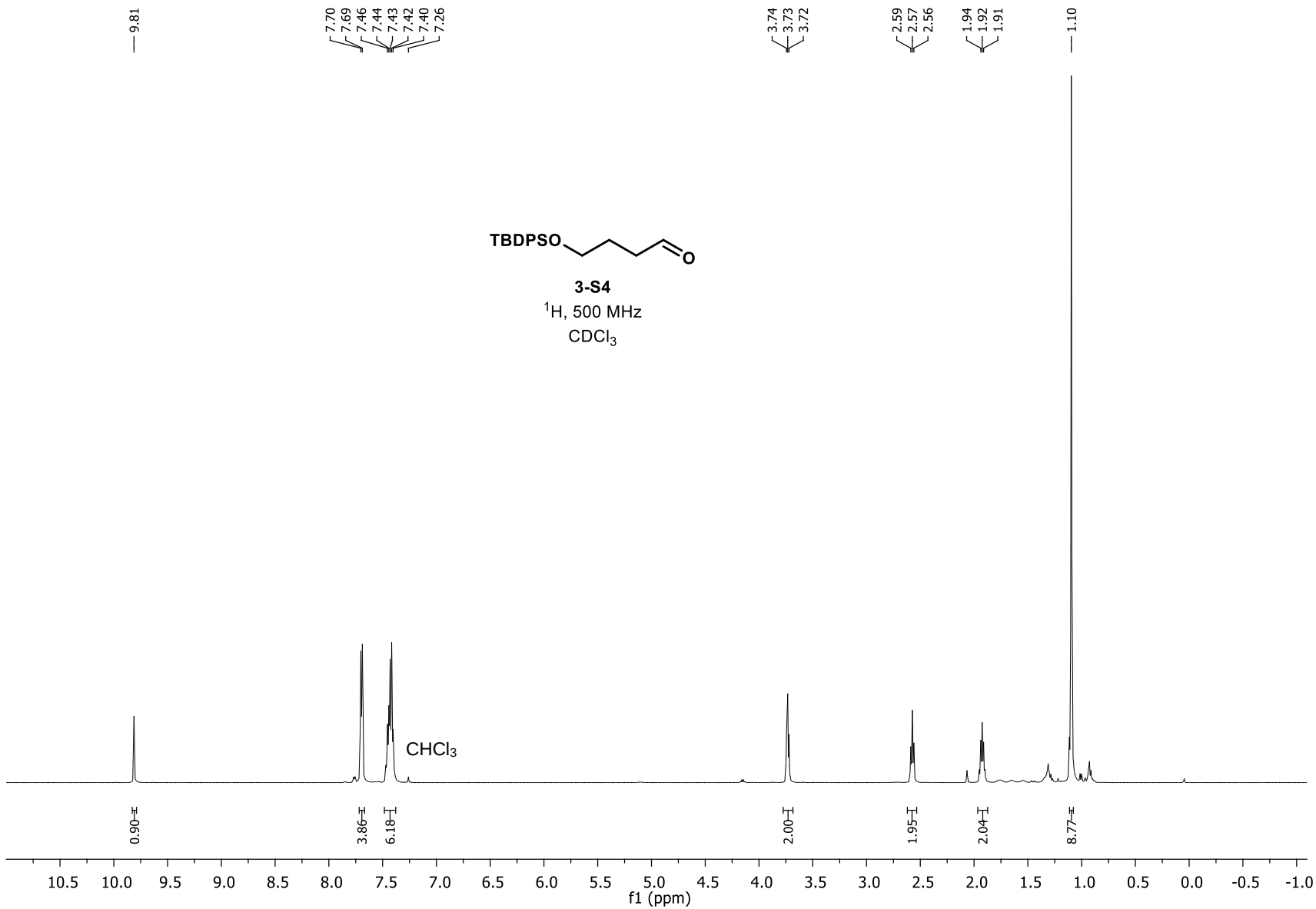
9.81
7.70
7.69
7.46
7.44
7.43
7.42
7.40
7.26
3.74
3.73
3.72
2.59
2.57
2.56
1.94
1.92
1.91
1.10
TBDPSO
O
3-S4
1H, 500 MHz
CDCl3
CHCl3
0.90
3.86
6.18
2.00
1.95
2.04
8.77
f1 (ppm)

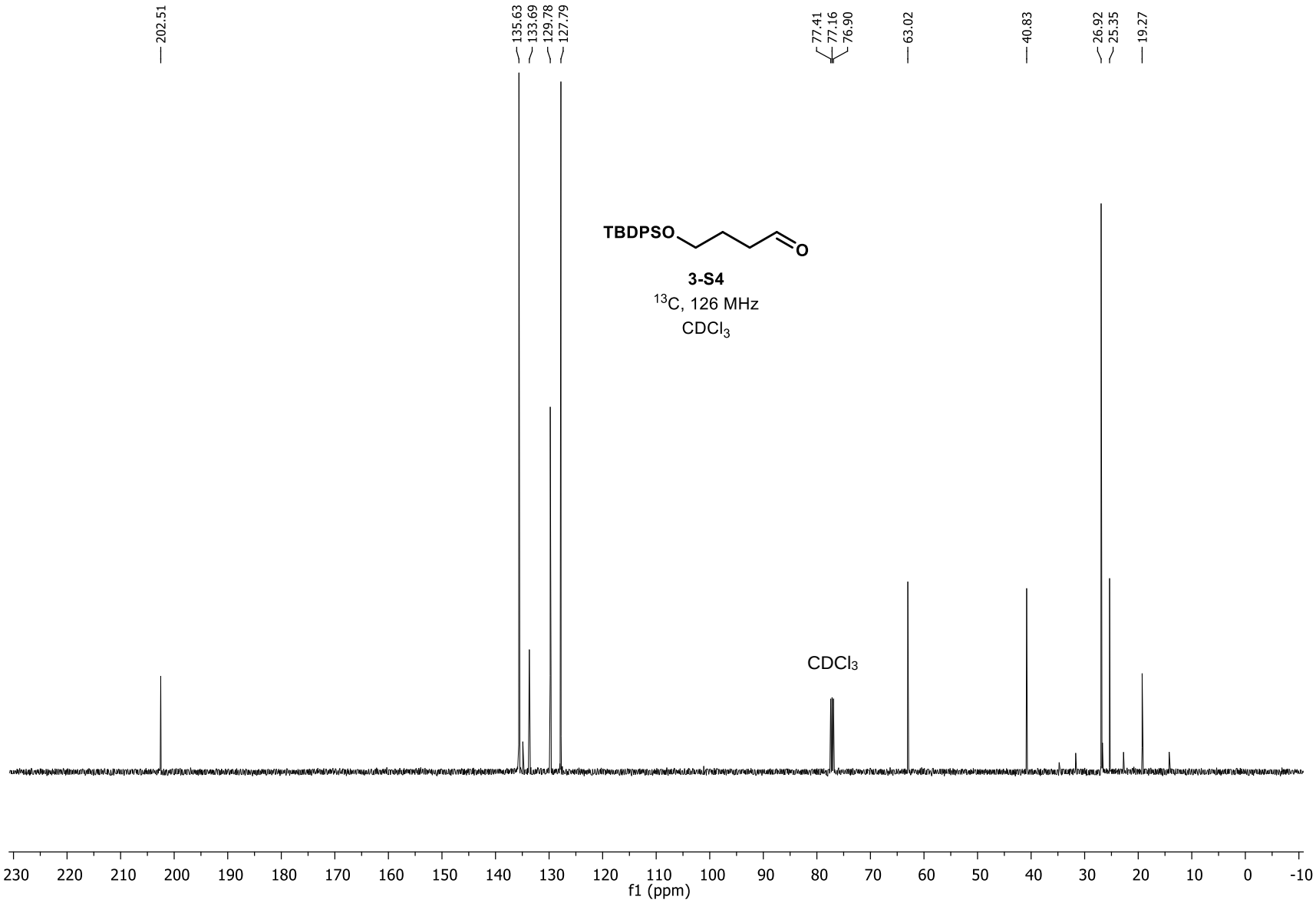
202.51
135.63
133.69
129.78
127.79
77.41
77.16
76.90
63.02
40.83
26.92
25.35
19.27
TBDPSO
O
3-S4
13C, 126 MHz
CDCl3
CDCl3
230 220 210 200 190 180 170 160 150 140 130 120 110 100 90 80 70 60 50 40 30 20 10 0 -10
f1 (ppm)

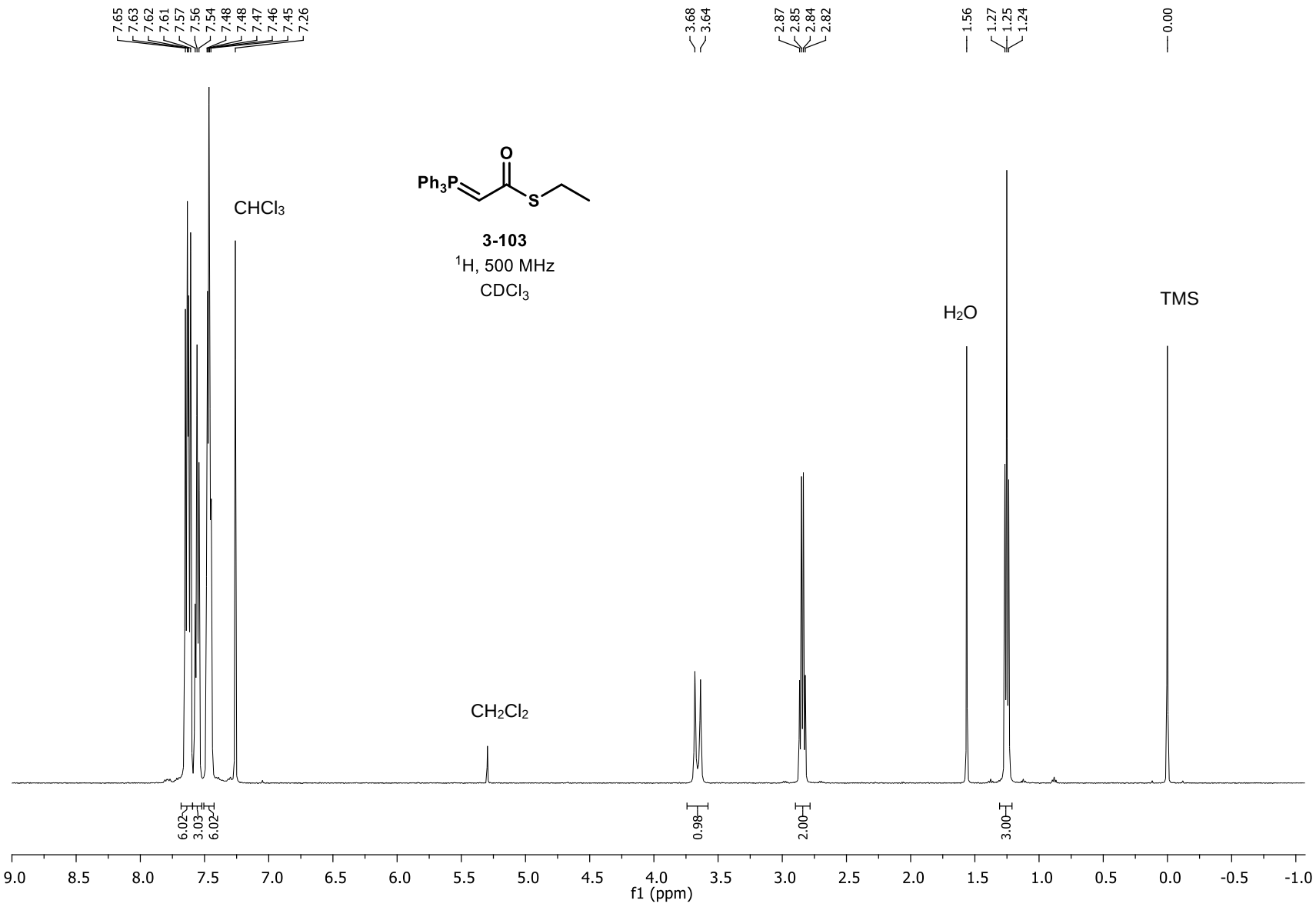
7.65
7.63
7.62
7.61
7.57
7.56
7.54
7.48
7.48
7.47
7.46
7.45
7.26
3.68
3.64
2.87
2.85
2.84
2.82
1.56
1.27
1.25
1.24
0.00
O
Ph3P
S
CHCl3
3-103
1H, 500 MHz
CDCl3
H2O
TMS
CH2Cl2
6.02
3.03
6.02
0.98
2.00
3.00
9.0
8.5
8.0
7.5
7.0
6.5
6.0
5.5
5.0
4.5
4.0
3.5
3.0
2.5
2.0
1.5
1.0
0.5
0.0
-0.5
-1.0
f1 (ppm)

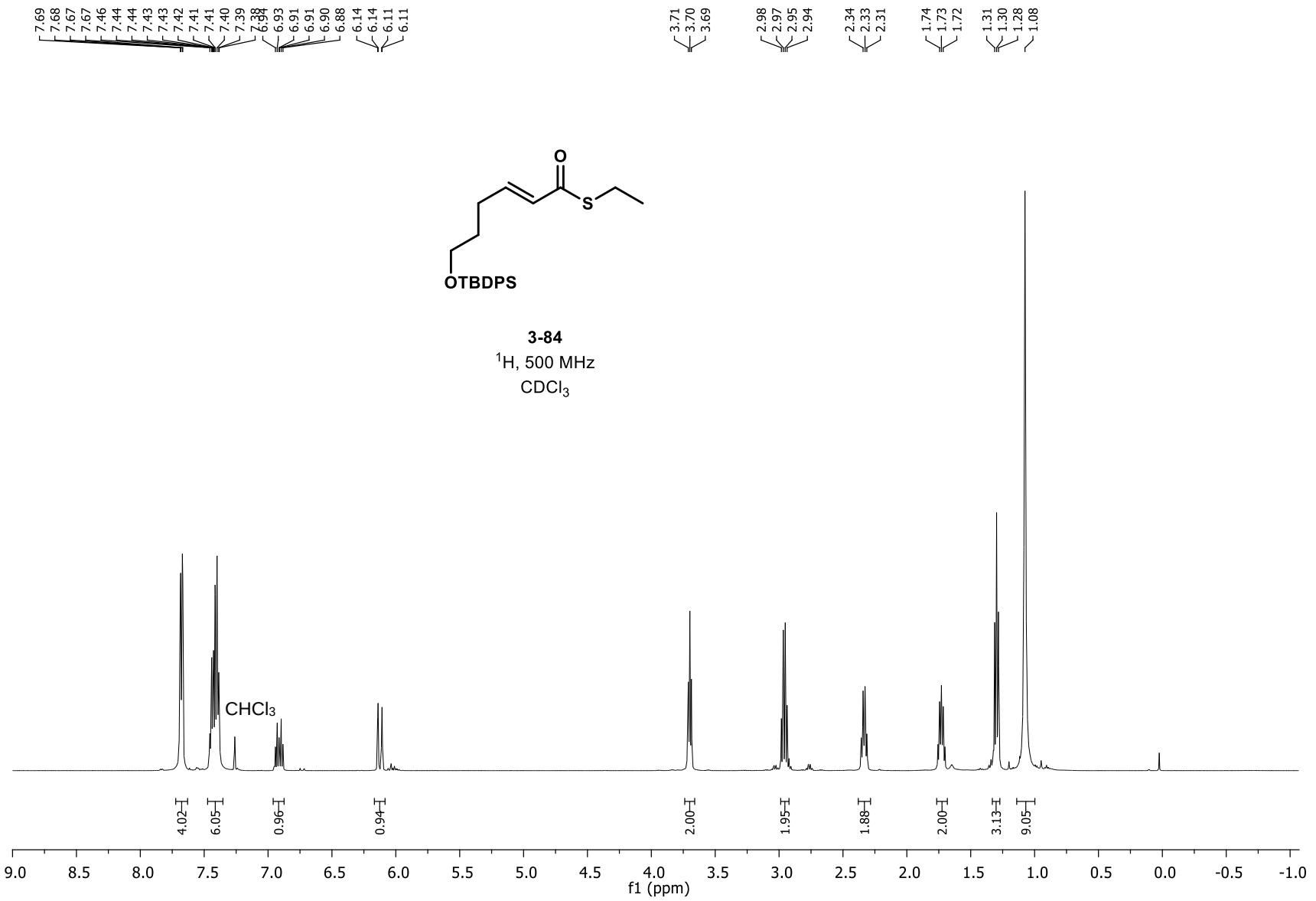
7.69
7.68
7.67
7.67
7.46
7.44
7.44
7.43
7.43
7.42
7.41
7.41
7.40
7.39
7.38
6.94
6.93
6.91
6.91
6.90
6.88
6.14
6.14
6.11
6.11
3.71
3.70
3.69
2.98
2.97
2.95
2.94
2.34
2.33
2.31
1.74
1.73
1.72
1.31
1.30
1.28
1.08
O
S
OTBDPS
3-84
1H, 500 MHz
CDCl3
CHCl3
4.02
6.05
0.96
0.94
2.00
1.95
1.88
2.00
3.13
9.05
9.0
8.5
8.0
7.5
7.0
6.5
6.0
5.5
5.0
4.5
4.0
3.5
3.0
2.5
2.0
1.5
1.0
0.5
0.0
-0.5
-1.0
f1 (ppm)

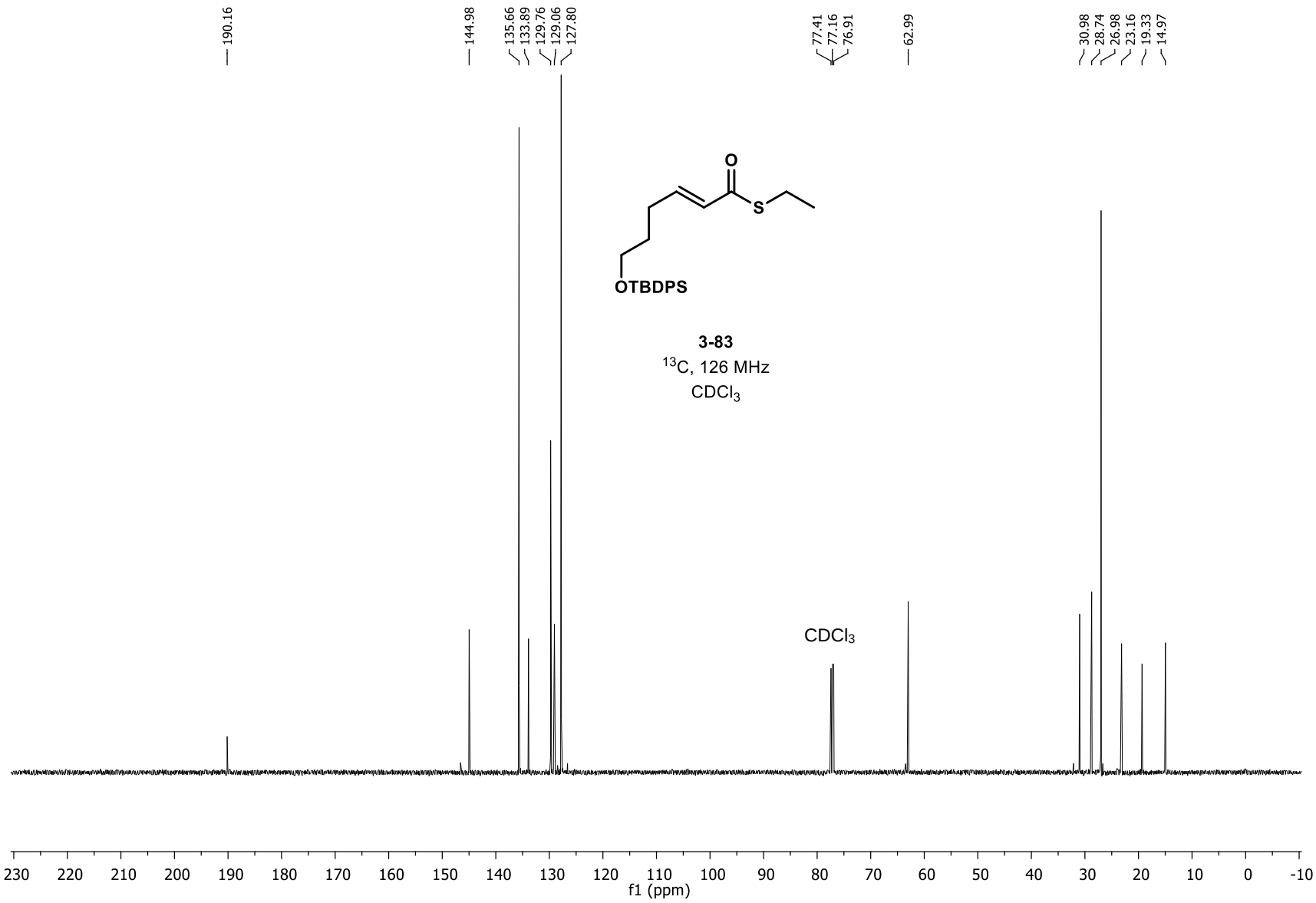
190.16
144.98
135.66
133.89
129.76
129.06
127.80
77.41
77.16
76.91
62.99
30.98
28.74
26.98
23.16
19.33
14.97
O
S
OTBDPS
3-83
13C, 126 MHz
CDCl3
CDCl3
230 220 210 200 190 180 170 160 150 140 130 120 110 100 90 80 70 60 50 40 30 20 10 0 -10
f1 (ppm)

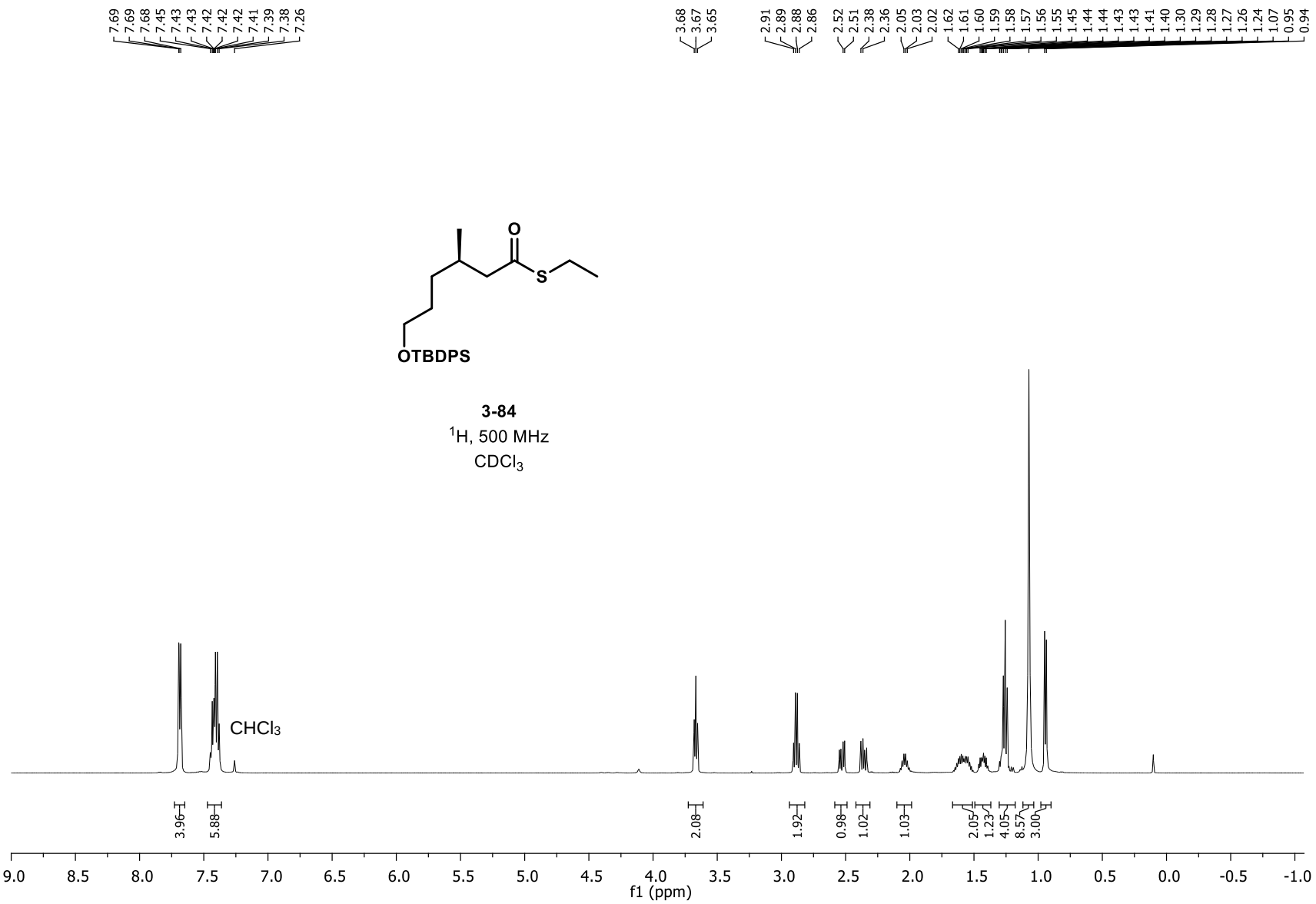
7.69
7.69
7.68
7.45
7.43
7.43
7.42
7.42
7.42
7.41
7.39
7.38
7.26
3.68
3.67
3.65
2.91
2.89
2.88
2.86
2.52
2.51
2.38
2.36
2.05
2.03
2.02
1.62
1.61
1.60
1.59
1.58
1.57
1.56
1.55
1.45
1.44
1.44
1.43
1.43
1.41
1.40
1.30
1.29
1.28
1.27
1.26
1.24
1.07
0.95
0.94
O
S
OTBDPS
3-84
1H, 500 MHz
CDCl3
CHCl3
3.96
5.88
2.08
1.92
0.98
1.02
1.03
2.05
1.23
4.05
8.57
3.00
9.0
8.5
8.0
7.5
7.0
6.5
6.0
5.5
5.0
4.5
4.0
3.5
3.0
2.5
2.0
1.5
1.0
0.5
0.0
-0.5
-1.0
f1 (ppm)

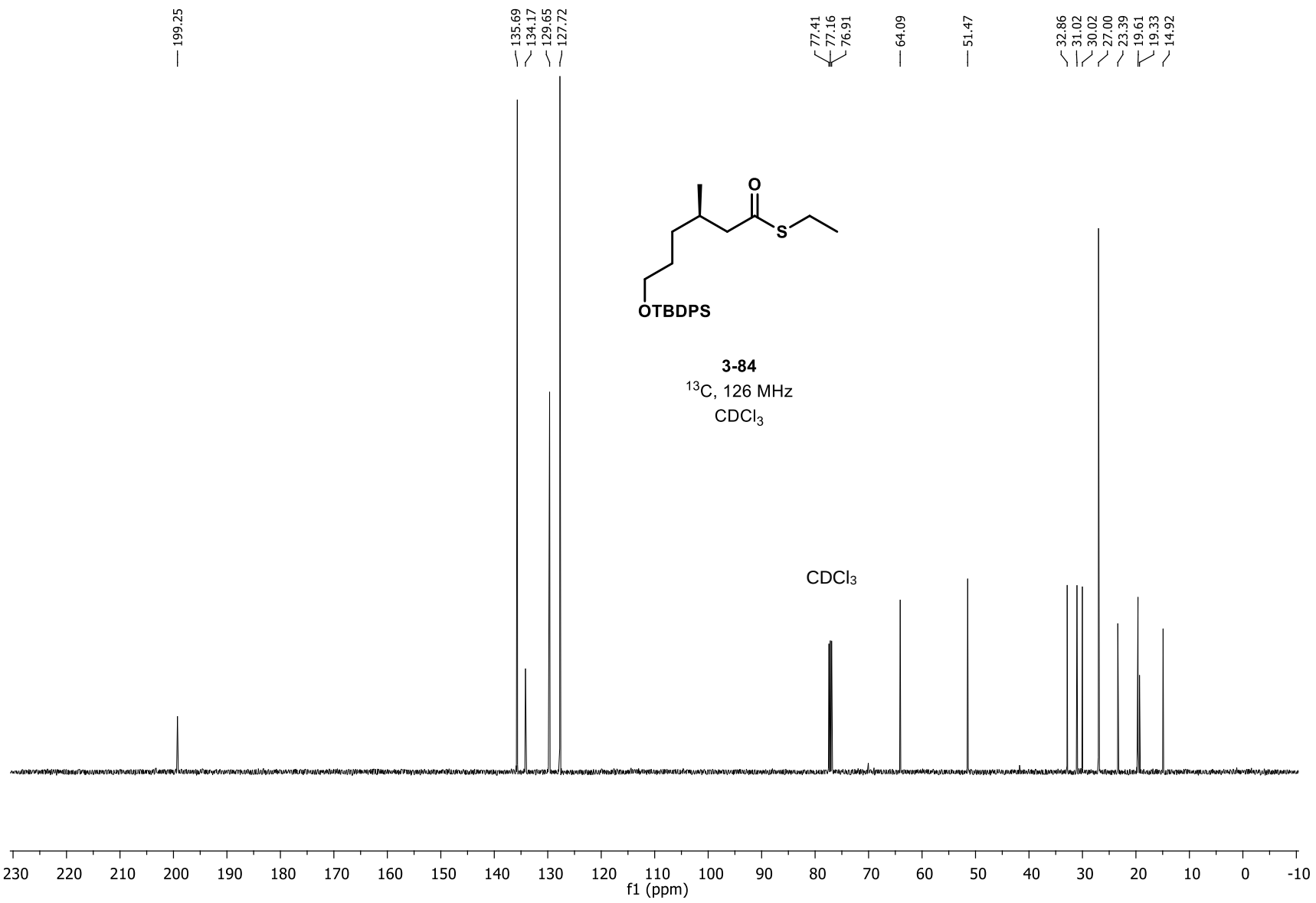
199.25
135.69
134.17
129.65
127.72
77.41
77.16
76.91
64.09
51.47
32.86
31.02
30.02
27.00
23.39
19.61
19.33
14.92
O
S
OTBDPS
3-84
13C, 126 MHz
CDCl3
CDCl3
230 220 210 200 190 180 170 160 150 140 130 120 110 100 90 80 70 60 50 40 30 20 10 0 -10
f1 (ppm)

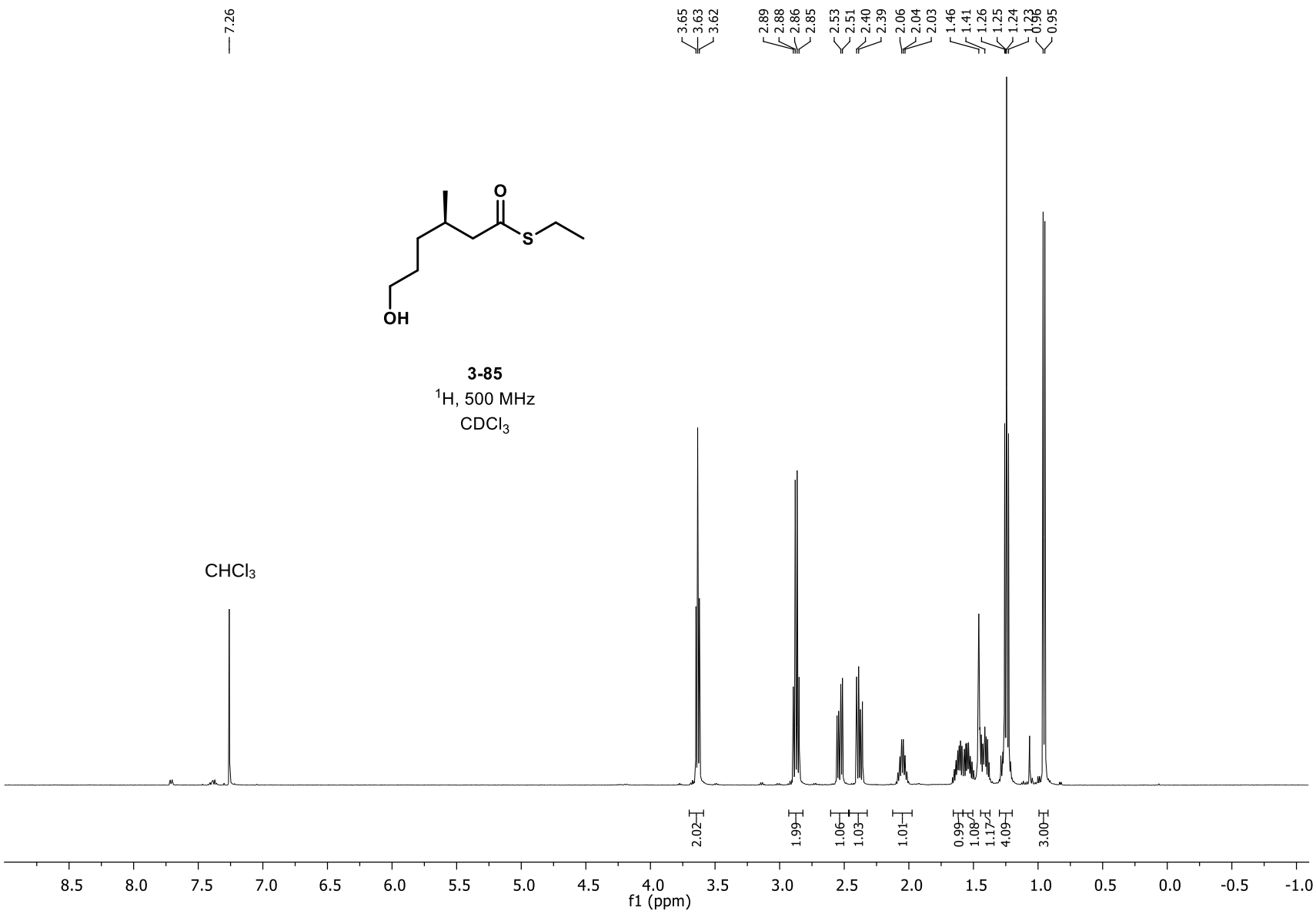
7.26
3.65
3.63
3.62
2.89
2.88
2.86
2.85
2.53
2.51
2.40
2.39
2.06
2.04
2.03
1.46
1.41
1.26
1.25
1.24
1.23
0.96
0.95
O
S
OH
3-85
1H, 500 MHz
CDCl3
CHCl3
2.02
1.99
1.06
1.03
1.01
0.99
1.08
1.17
4.09
3.00
8.5
8.0
7.5
7.0
6.5
6.0
5.5
5.0
4.5
4.0
3.5
3.0
2.5
2.0
1.5
1.0
0.5
0.0
-0.5
-1.0
f1 (ppm)

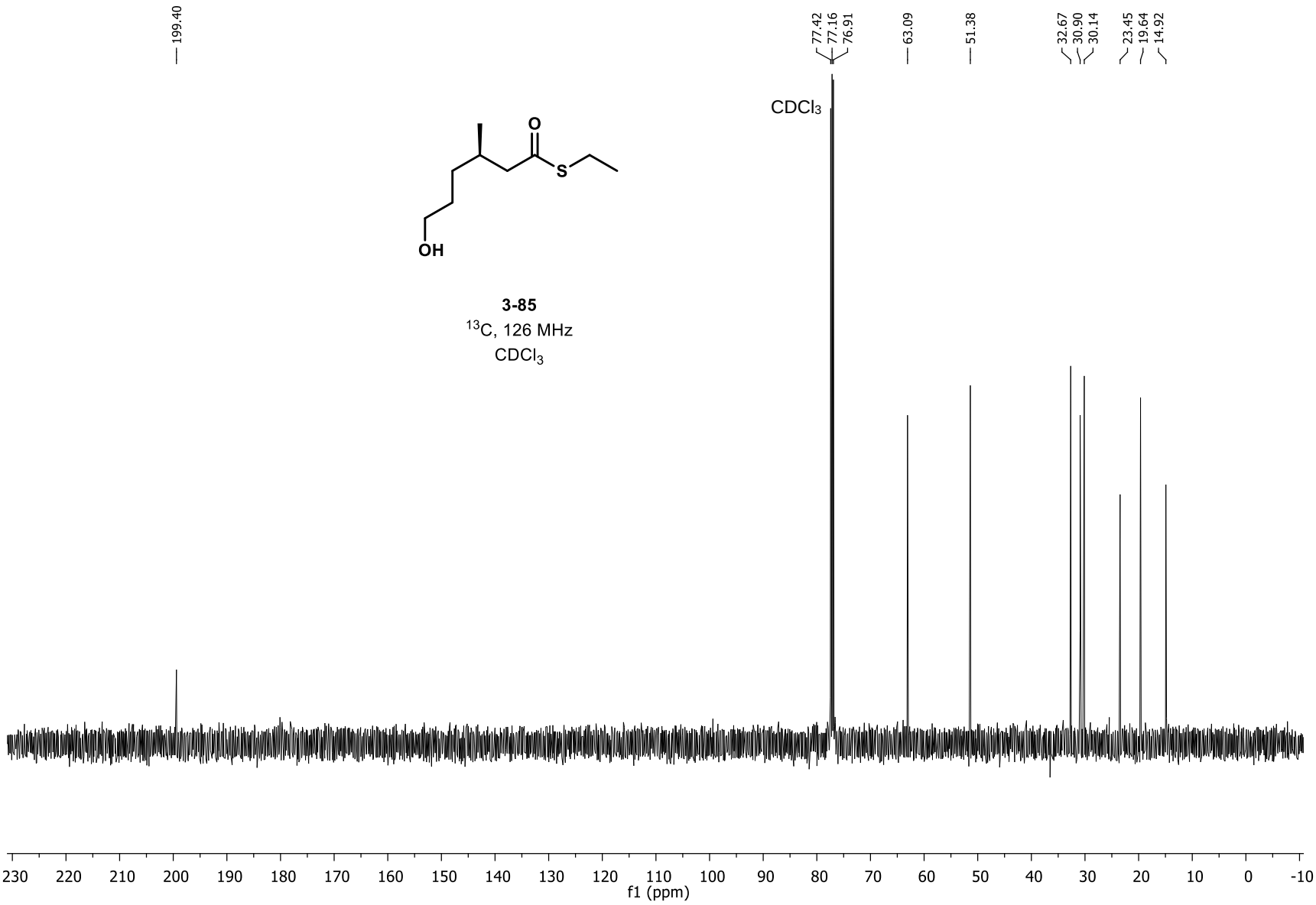
199.40
77.42
77.16
76.91
63.09
51.38
32.67
30.90
30.14
23.45
19.64
14.92
CDCl3
O
S
OH
3-85
13C, 126 MHz
CDCl3
230 220 210 200 190 180 170 160 150 140 130 120 110 100 90 80 70 60 50 40 30 20 10 0 -10
f1 (ppm)

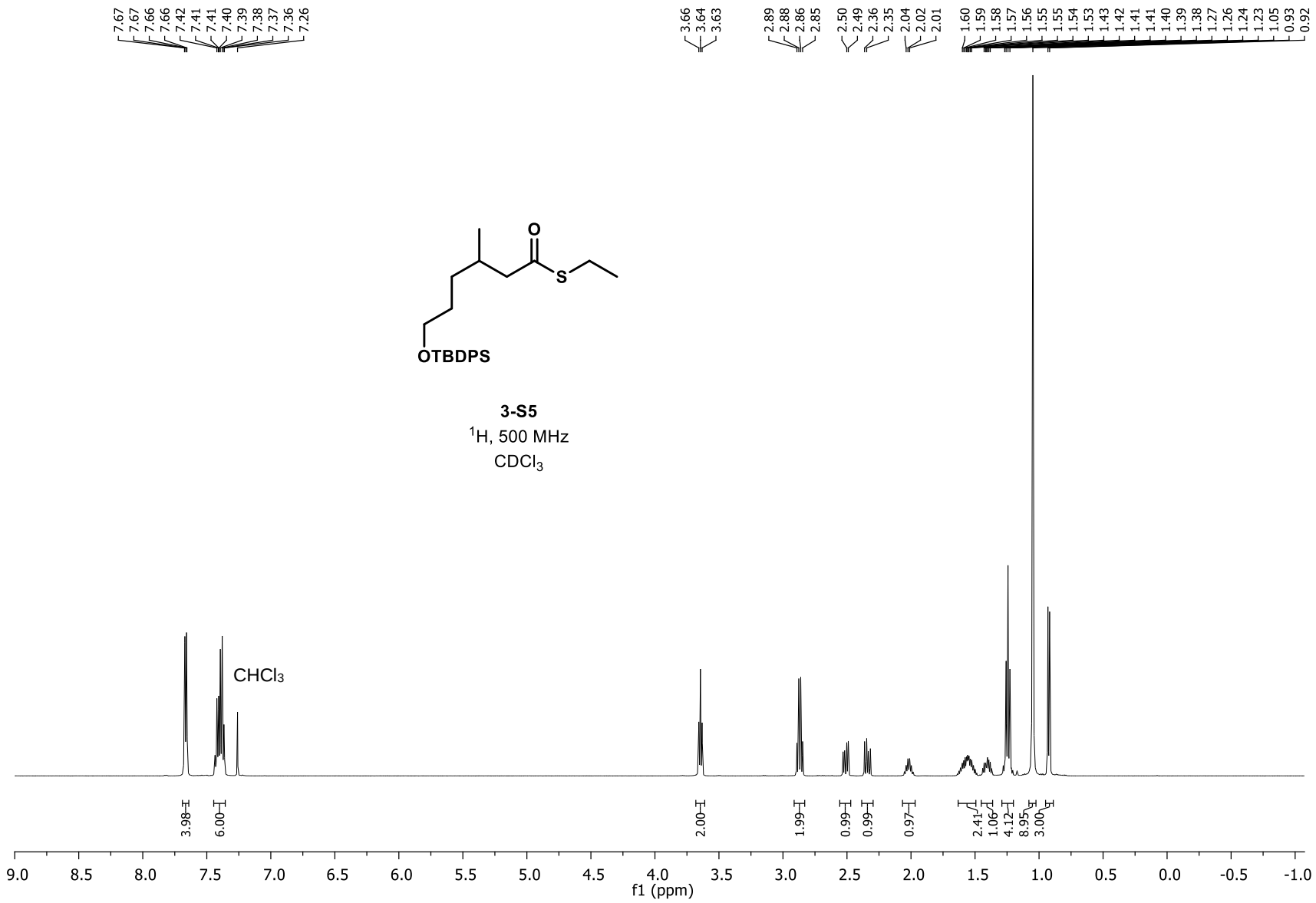
7.67
7.67
7.66
7.66
7.42
7.41
7.41
7.40
7.39
7.38
7.37
7.36
7.26
3.66
3.64
3.63
2.89
2.88
2.86
2.85
2.50
2.49
2.36
2.35
2.04
2.02
2.01
1.60
1.59
1.58
1.57
1.56
1.55
1.55
1.54
1.53
1.43
1.42
1.41
1.41
1.40
1.39
1.38
1.27
1.26
1.24
1.23
1.05
0.93
0.92
O
S
OTBDPS
3-S5
1H, 500 MHz
CDCl3
CHCl3
3.98
6.00
2.00
1.99
0.99
0.99
0.97
2.41
1.06
4.12
8.95
3.00
9.0
8.5
8.0
7.5
7.0
6.5
6.0
5.5
5.0
4.5
4.0
3.5
3.0
2.5
2.0
1.5
1.0
0.5
0.0
-0.5
-1.0
f1 (ppm)

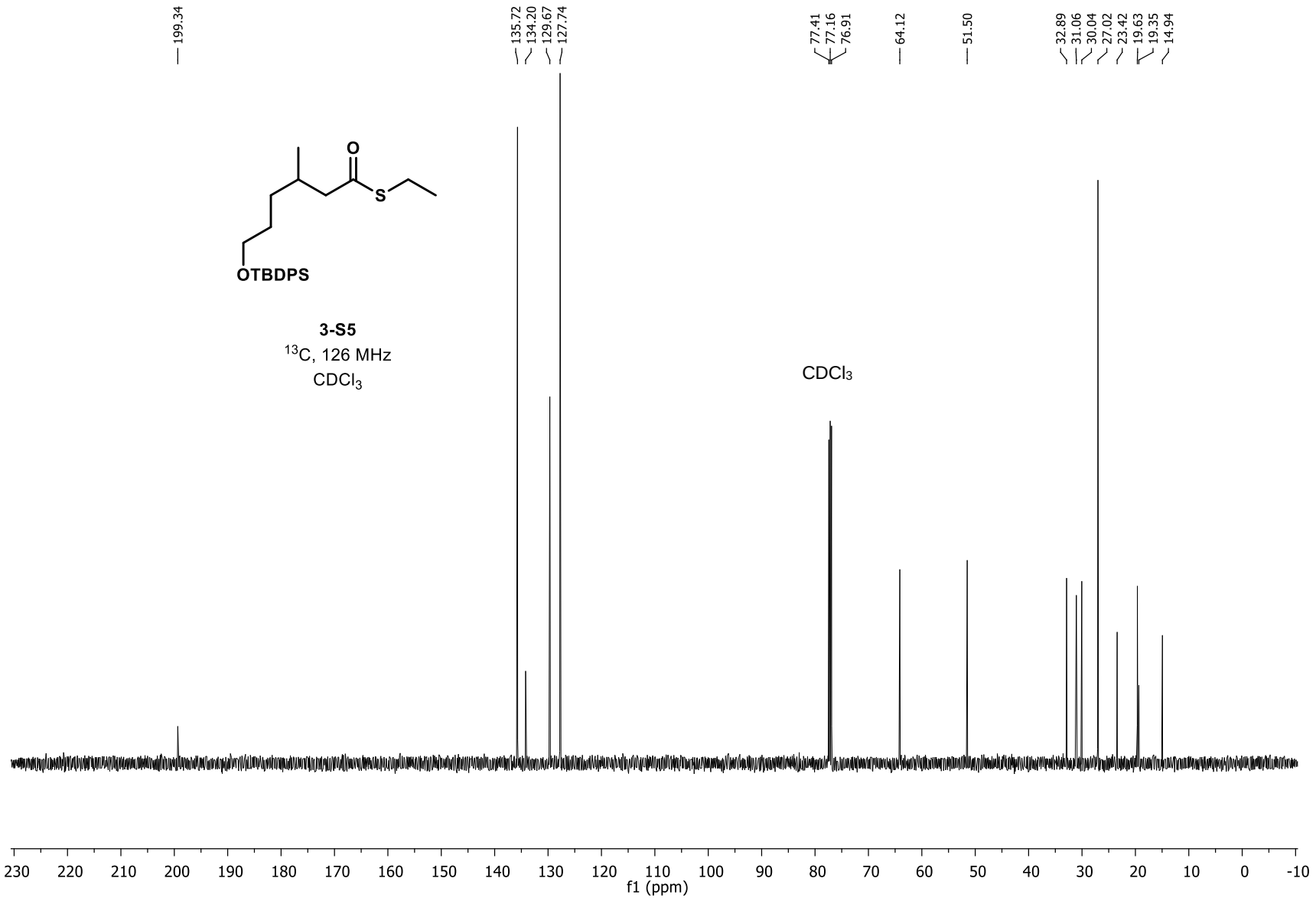
199.34
135.72
134.20
129.67
127.74
77.41
77.16
76.91
64.12
51.50
32.89
31.06
30.04
27.02
23.42
19.63
19.35
14.94
O
S
OTBDPS
3-S5
13C, 126 MHz
CDCl3
CDCl3
230 220 210 200 190 180 170 160 150 140 130 120 110 100 90 80 70 60 50 40 30 20 10 0 -10
f1 (ppm)

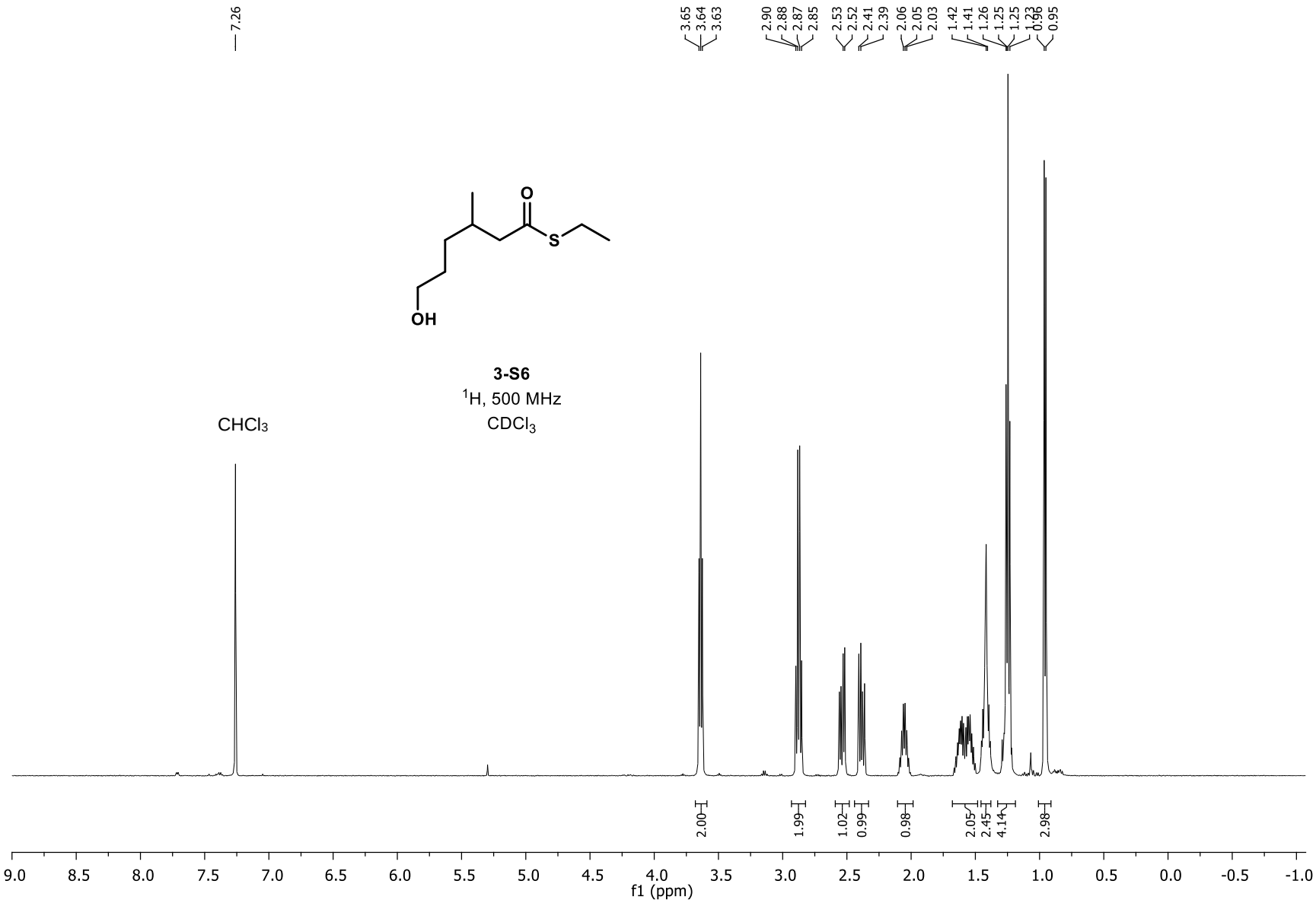
7.26
3.65
3.64
3.63
2.90
2.88
2.87
2.85
2.53
2.52
2.41
2.39
2.06
2.05
2.03
1.42
1.41
1.26
1.25
1.25
0.96
0.95
O
S
OH
3-S6
1H, 500 MHz
CDCl3
CHCl3
2.00
1.99
1.02
0.99
0.98
2.05
2.45
4.14
2.98
9.0
8.5
8.0
7.5
7.0
6.5
6.0
5.5
5.0
4.5
4.0
3.5
3.0
2.5
2.0
1.5
1.0
0.5
0.0
-0.5
-1.0
f1 (ppm)

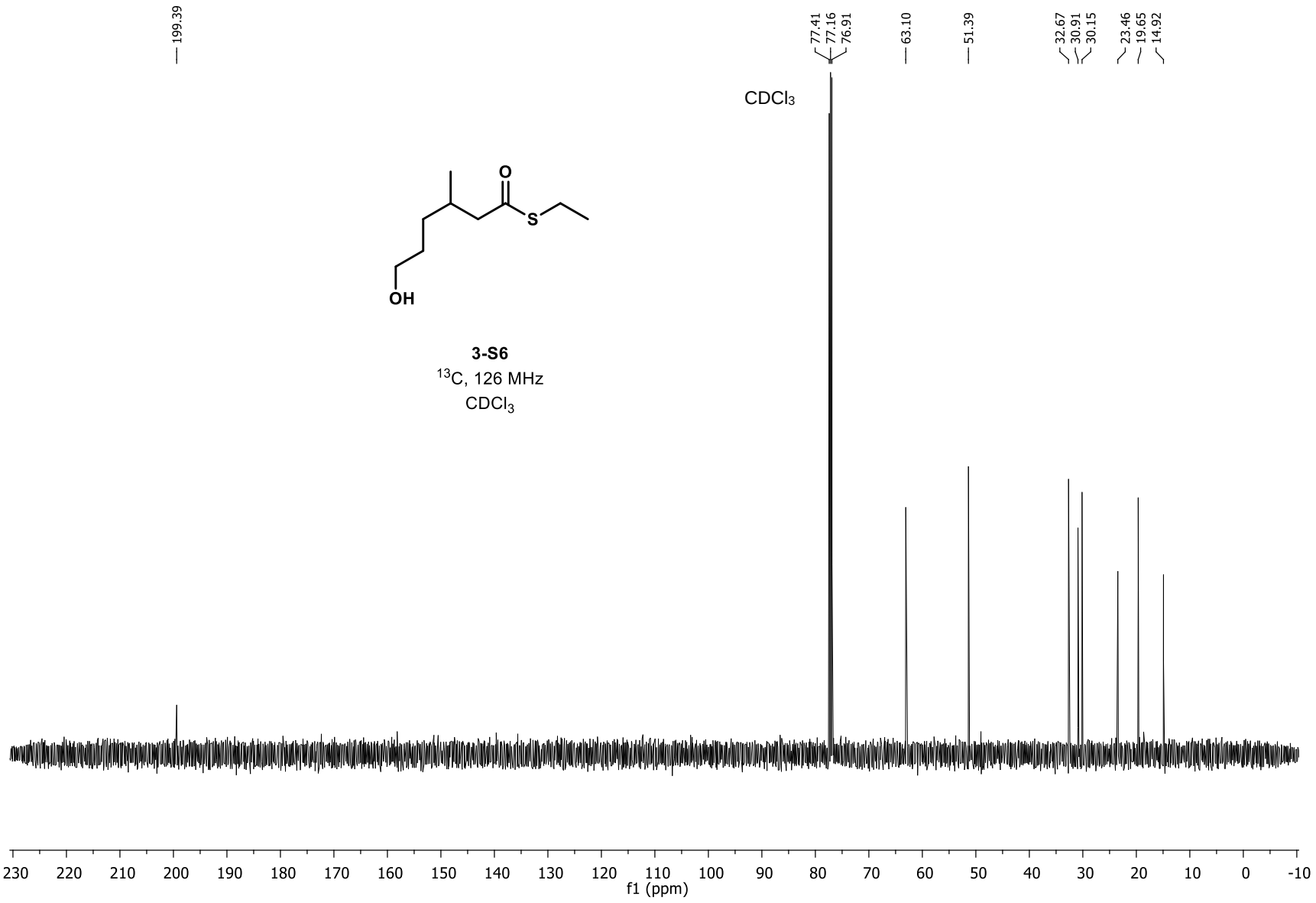
199.39
77.41
77.16
76.91
63.10
51.39
32.67
30.91
30.15
23.46
19.65
14.92
CDCl3
O
S
OH
3-S6
13C, 126 MHz
CDCl3
230 220 210 200 190 180 170 160 150 140 130 120 110 100 90 80 70 60 50 40 30 20 10 0 -10
f1 (ppm)

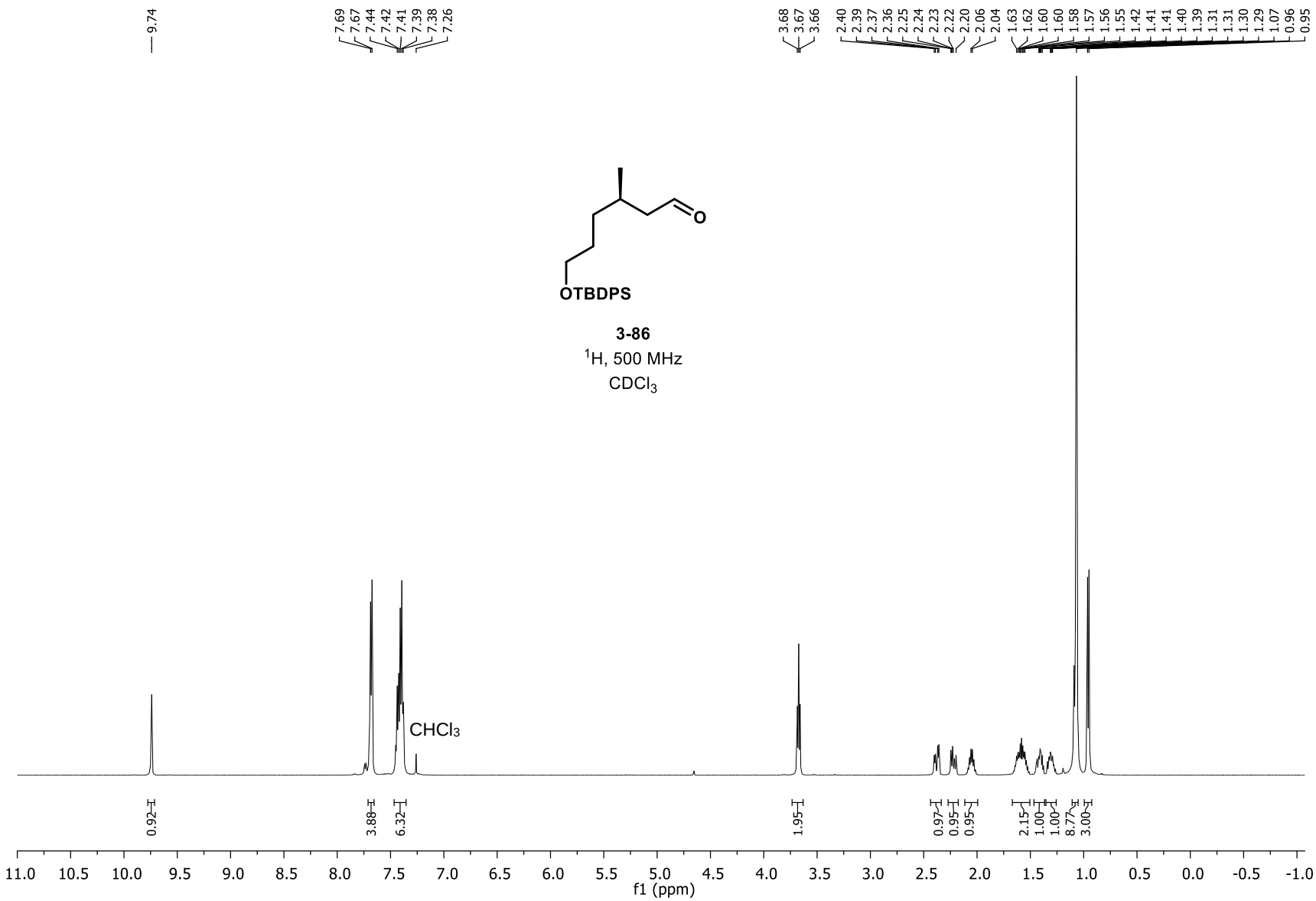
9.74
7.69
7.67
7.44
7.42
7.41
7.39
7.38
7.26
3.68
3.67
3.66
2.40
2.39
2.37
2.36
2.25
2.24
2.23
2.22
2.20
2.06
2.04
1.63
1.62
1.60
1.60
1.58
1.57
1.56
1.55
1.42
1.41
1.41
1.40
1.39
1.31
1.30
1.29
1.07
0.96
0.95
O
OTBDPS
3-86
1H, 500 MHz
CDCl3
CHCl3
0.92
3.88
6.32
1.95
0.97
0.95
0.95
2.15
1.00
1.00
8.77
3.00
11.0 10.5 10.0 9.5 9.0 8.5 8.0 7.5 7.0 6.5 6.0 5.5 5.0 4.5 4.0 3.5 3.0 2.5 2.0 1.5 1.0 0.5 0.0 -0.5 -1.0
f1 (ppm)

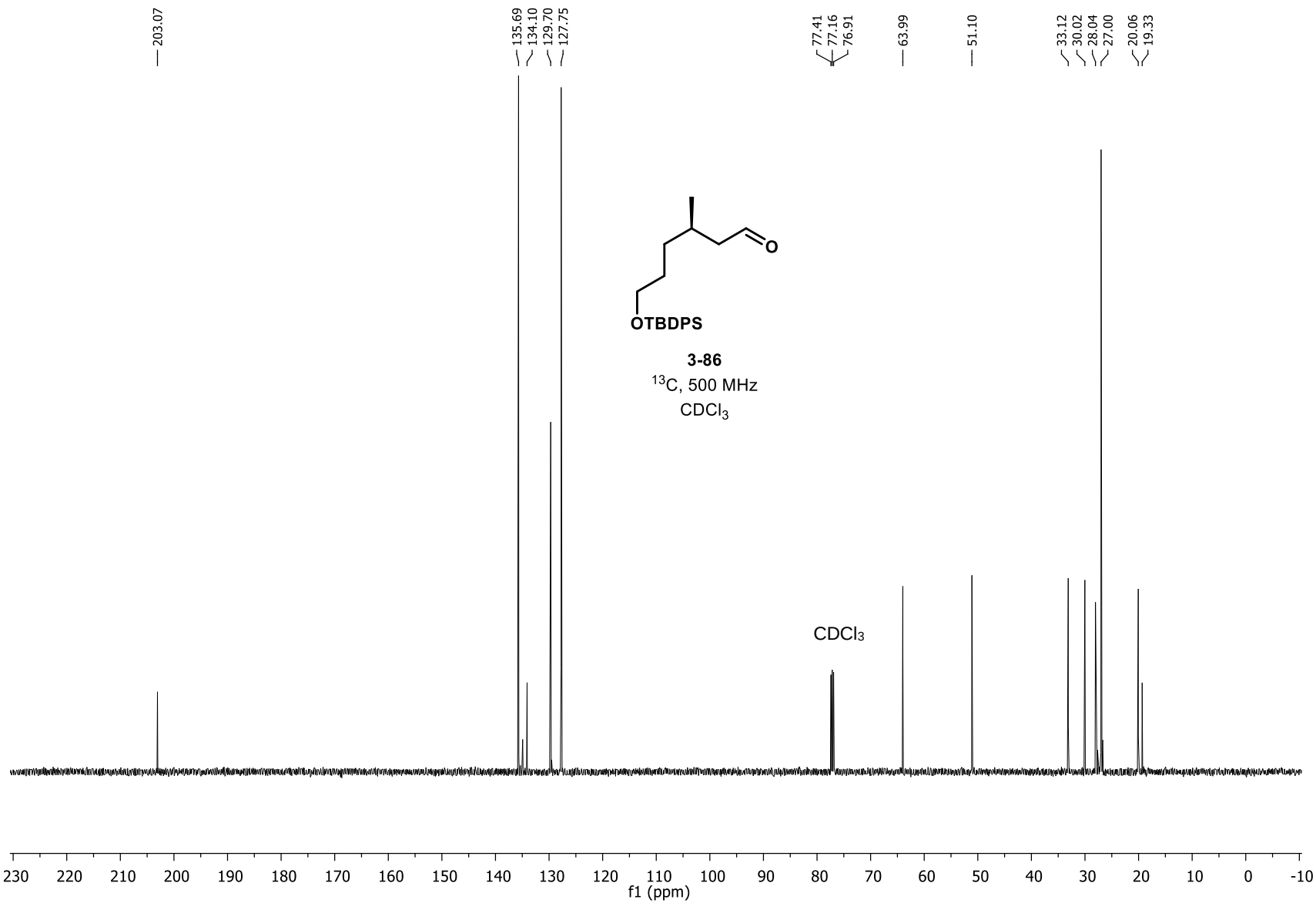
203.07
135.69
134.10
129.70
127.75
77.41
77.16
76.91
63.99
51.10
33.12
30.02
28.04
27.00
20.06
19.33
O
OTBDPS
3-86
13C, 500 MHz
CDCl3
CDCl3
230 220 210 200 190 180 170 160 150 140 130 120 110 100 90 80 70 60 50 40 30 20 10 0 -10
f1 (ppm)

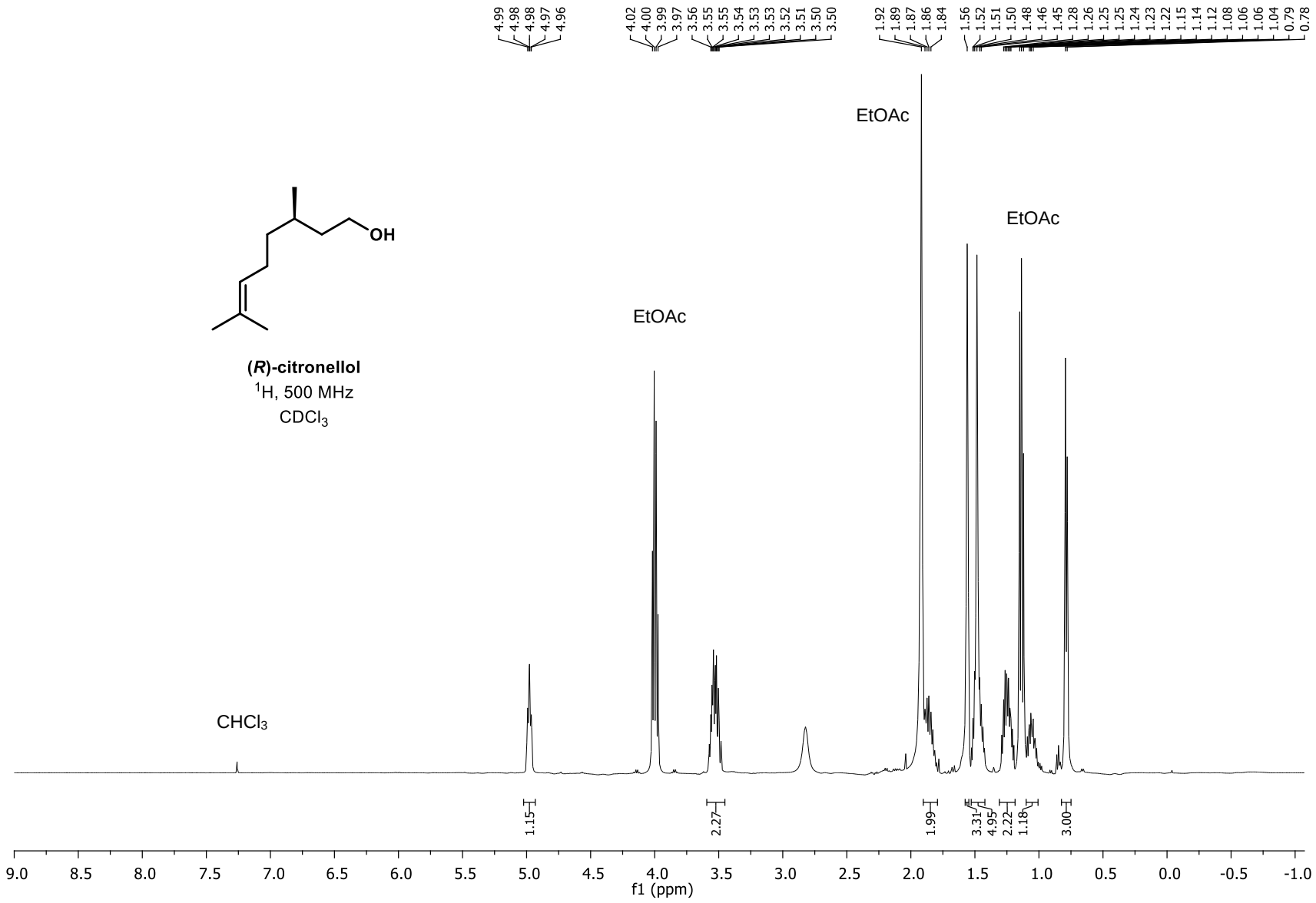
4.99
4.98
4.98
4.97
4.96
4.02
4.00
3.99
3.97
3.56
3.55
3.55
3.54
3.53
3.53
3.52
3.51
3.50
3.50
1.92
1.89
1.87
1.86
1.84
1.56
1.52
1.51
1.50
1.48
1.46
1.45
1.28
1.26
1.25
1.25
1.24
1.23
1.22
1.15
1.14
1.12
1.08
1.06
1.06
1.04
0.79
0.78
OH
(R)-citronellol
1H, 500 MHz
CDCl3
EtOAc
EtOAc
EtOAc
CHCl3
1.15
2.27
1.99
3.31
4.95
2.22
1.18
3.00
9.0
8.5
8.0
7.5
7.0
6.5
6.0
5.5
5.0
4.5
4.0
3.5
3.0
2.5
2.0
1.5
1.0
0.5
0.0
-0.5
-1.0
f1 (ppm)

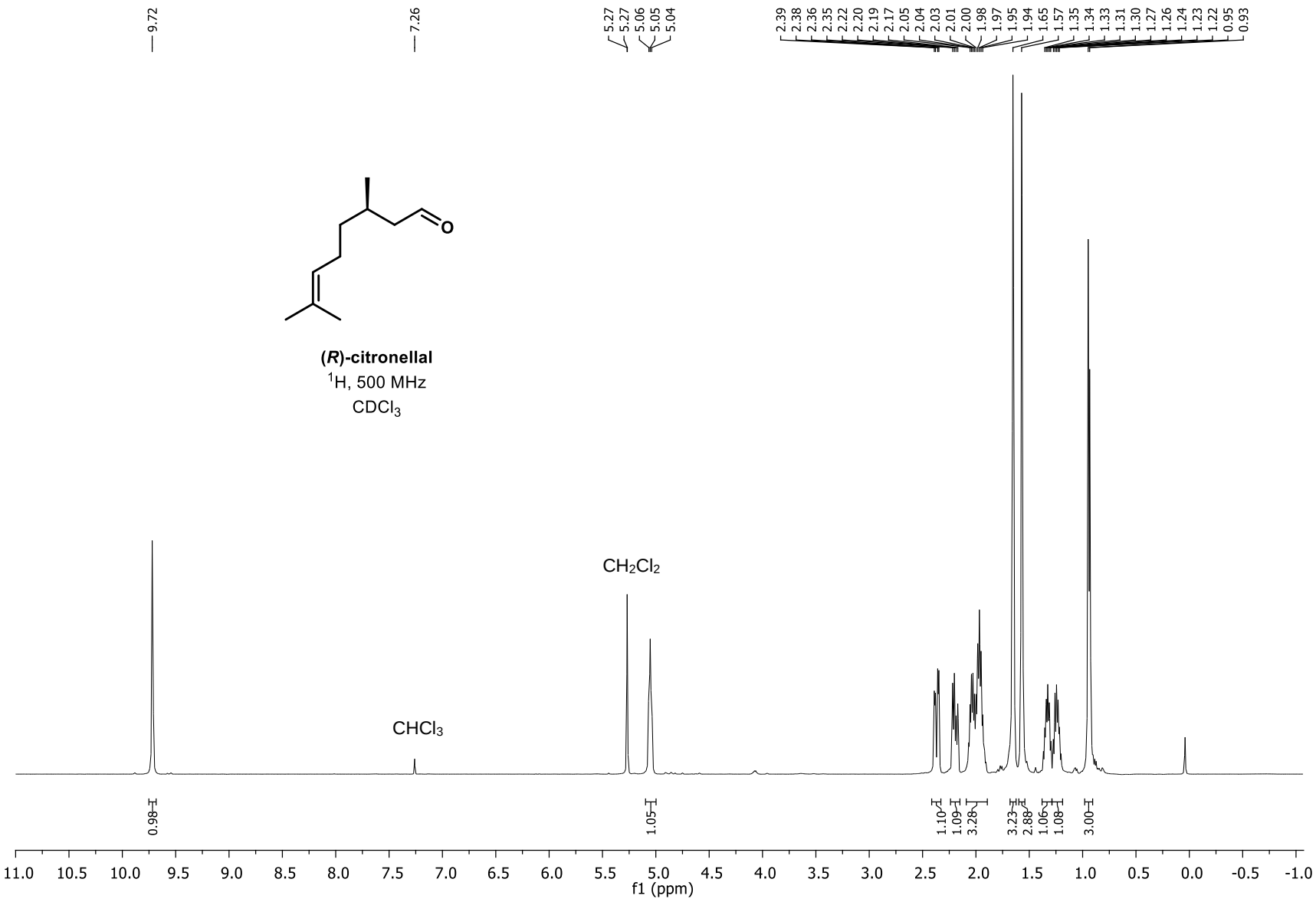
9.72
7.26
5.27
5.27
5.06
5.05
5.04
2.39
2.38
2.36
2.35
2.22
2.20
2.19
2.17
2.05
2.04
2.03
2.01
2.00
1.98
1.97
1.95
1.94
1.65
1.57
1.35
1.34
1.33
1.31
1.30
1.27
1.26
1.24
1.23
1.22
0.95
0.93
O
(R)-citronellal
1H, 500 MHz
CDCl3
CH2Cl2
CHCl3
0.98
1.05
1.10
1.09
3.28
3.23
2.88
1.06
1.08
3.00
11.0
10.5
10.0
9.5
9.0
8.5
8.0
7.5
7.0
6.5
6.0
5.5
5.0
4.5
4.0
3.5
3.0
2.5
2.0
1.5
1.0
0.5
0.0
-0.5
-1.0
f1 (ppm)

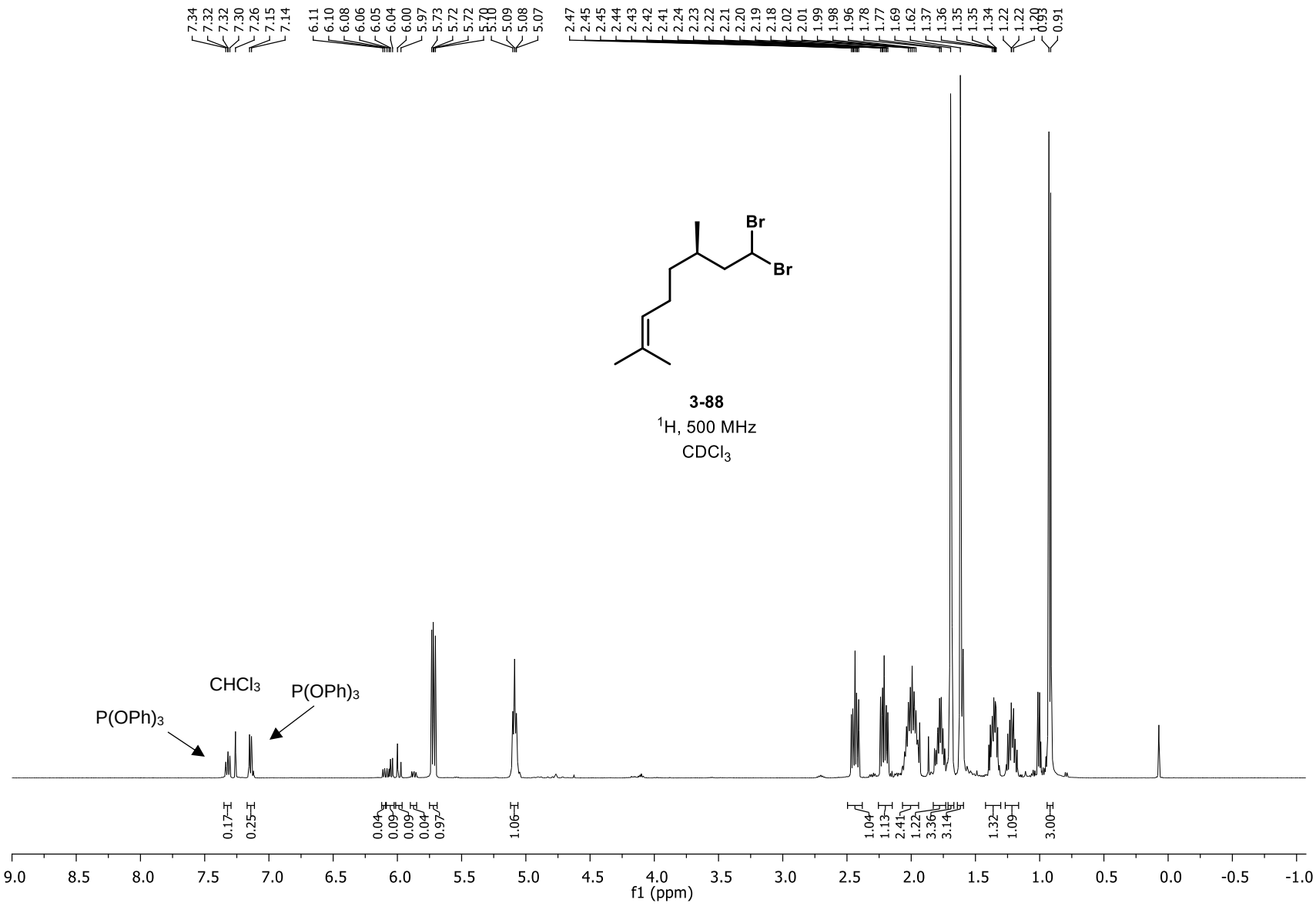
7.34
7.32
7.32
7.30
7.26
7.15
7.14
6.11
6.10
6.08
6.06
6.05
6.04
6.00
5.97
5.73
5.72
5.72
5.10
5.09
5.08
5.07
2.47
2.45
2.45
2.44
2.43
2.42
2.41
2.24
2.23
2.22
2.21
2.20
2.19
2.18
2.02
2.01
1.99
1.98
1.96
1.78
1.77
1.69
1.62
1.37
1.36
1.35
1.35
1.34
1.22
1.22
1.20
0.93
0.91
Br
Br
3-88
1H, 500 MHz
CDCl3
P(OPh)3
CHCl3
P(OPh)3
0.17
0.25
0.04
0.09
0.09
0.04
0.97
1.06
1.04
1.13
2.41
1.22
3.36
3.14
1.32
1.09
3.00
9.0
8.5
8.0
7.5
7.0
6.5
6.0
5.5
5.0
4.5
4.0
3.5
3.0
2.5
2.0
1.5
1.0
0.5
0.0
-0.5
-1.0
f1 (ppm)

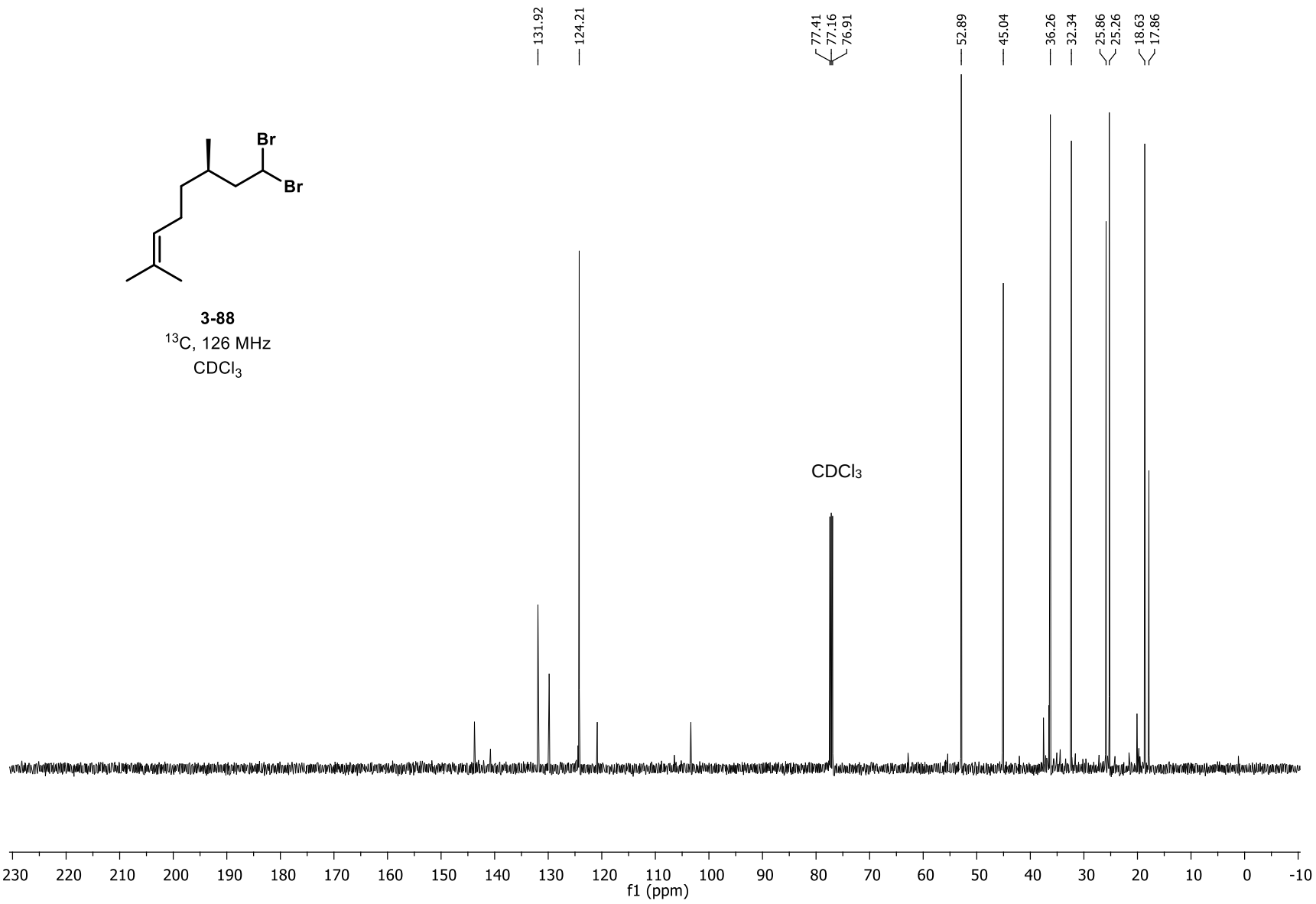
Br
Br
3-88
13C, 126 MHz
CDCl3
131.92
124.21
77.41
77.16
76.91
52.89
45.04
36.26
32.34
25.86
25.26
18.63
17.86
CDCl3
230 220 210 200 190 180 170 160 150 140 130 120 110 100 90 80 70 60 50 40 30 20 10 0 -10
f1 (ppm)

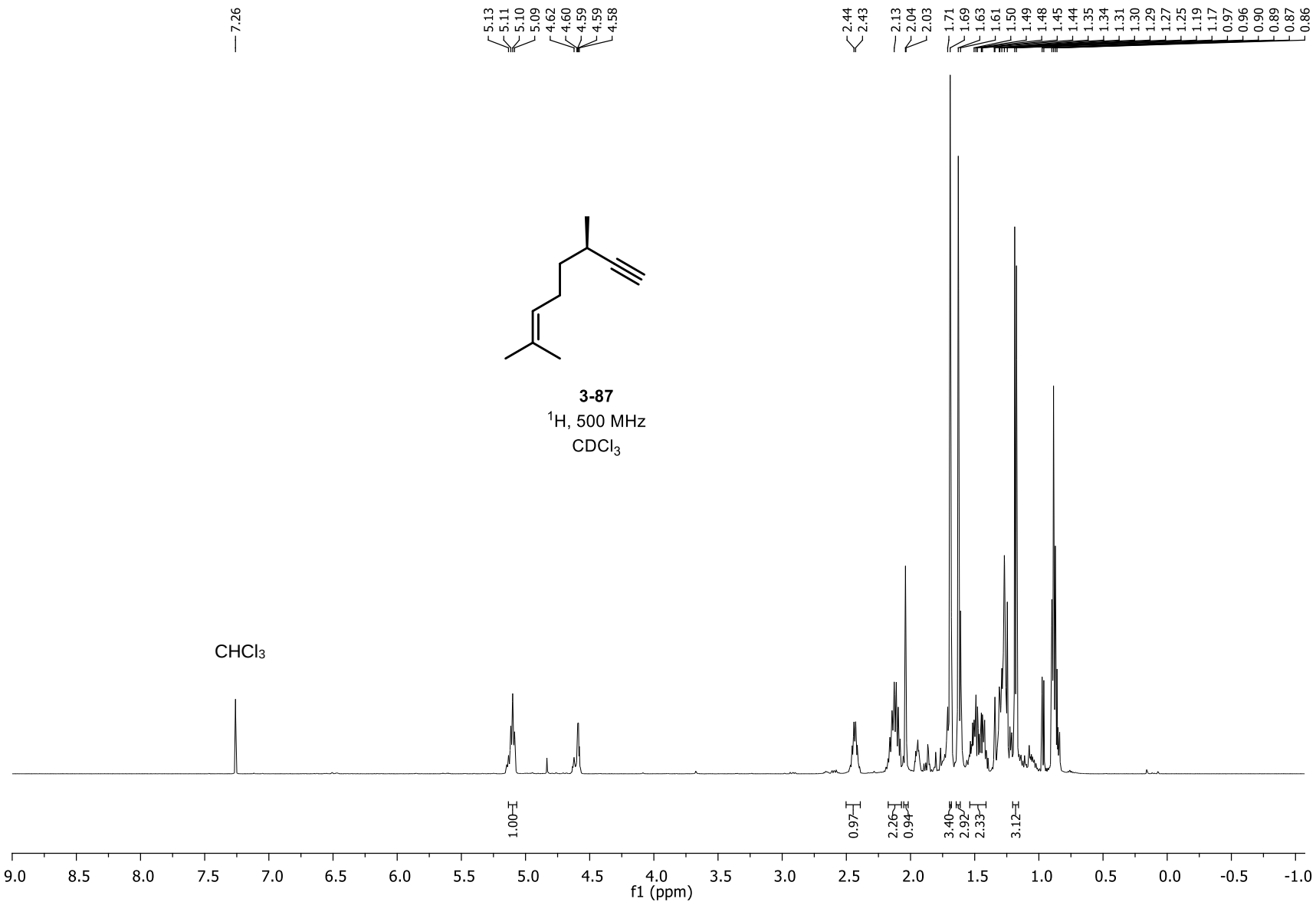
7.26
5.13
5.11
5.10
5.09
4.62
4.60
4.59
4.59
4.58
2.44
2.43
2.13
2.04
2.03
1.71
1.69
1.63
1.61
1.50
1.49
1.48
1.45
1.44
1.35
1.34
1.31
1.30
1.29
1.27
1.25
1.19
1.17
0.97
0.96
0.90
0.89
0.87
0.86
3-87
1H, 500 MHz
CDCl3
CHCl3
1.00
0.97
2.26
0.94
3.40
2.92
2.33
3.12
9.0
8.5
8.0
7.5
7.0
6.5
6.0
5.5
5.0
4.5
4.0
3.5
3.0
2.5
2.0
1.5
1.0
0.5
0.0
-0.5
-1.0
f1 (ppm)

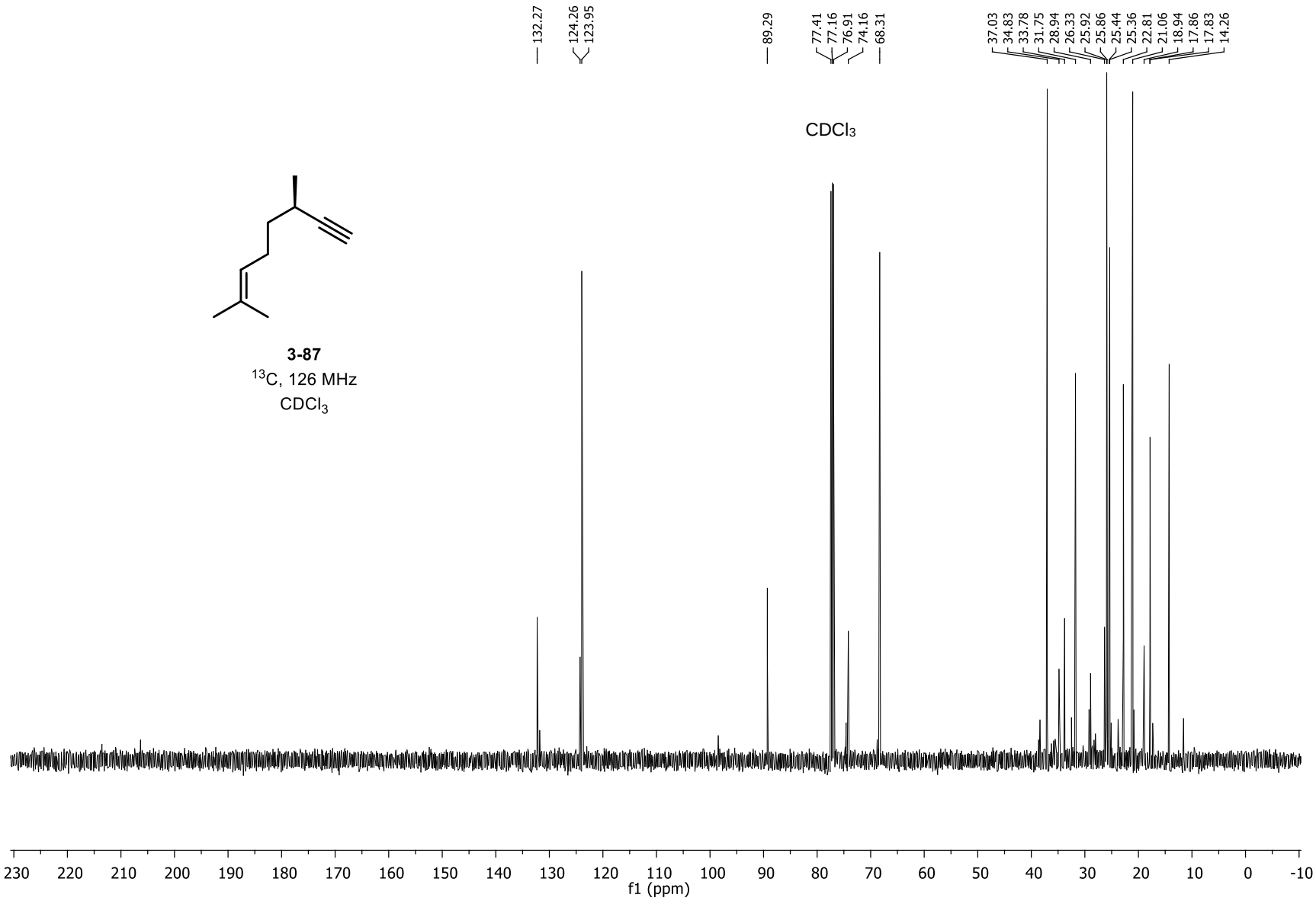
132.27
124.26
123.95
89.29
77.41
77.16
76.91
74.16
68.31
37.03
34.83
33.78
31.75
28.94
26.33
25.92
25.86
25.44
25.36
22.81
21.06
18.94
17.86
17.83
14.26
CDCl3
3-87
13C, 126 MHz
CDCl3
230 220 210 200 190 180 170 160 150 140 130 120 110 100 90 80 70 60 50 40 30 20 10 0 -10
f1 (ppm)

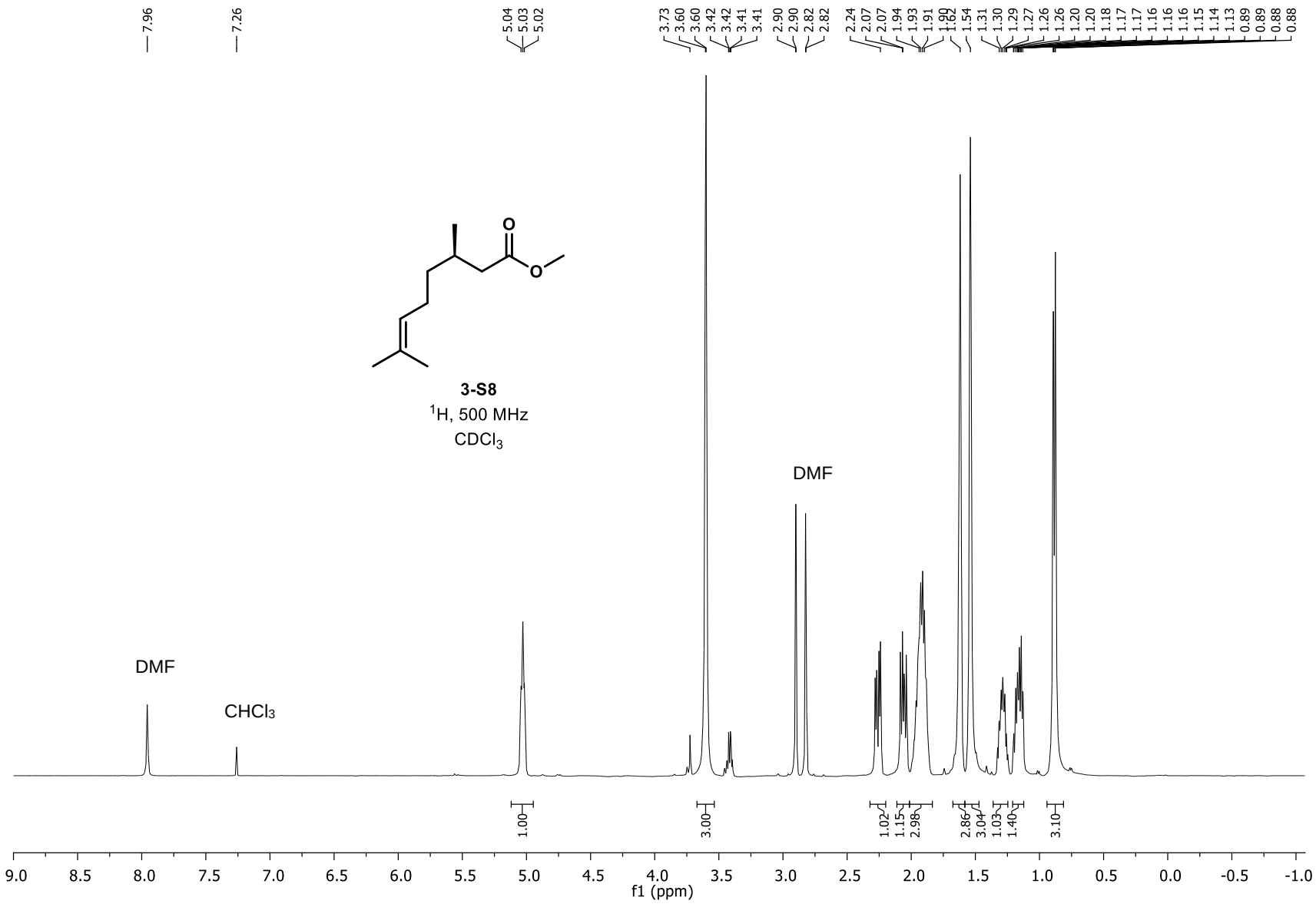
7.96
7.26
5.04
5.03
5.02
3.73
3.60
3.60
3.42
3.42
3.41
3.41
2.90
2.90
2.82
2.82
2.24
2.07
2.07
1.94
1.93
1.91
1.90
1.82
1.54
1.31
1.30
1.29
1.27
1.26
1.26
1.20
1.20
1.18
1.17
1.17
1.16
1.16
1.16
1.15
1.14
1.13
0.89
0.89
0.88
0.88
O
O
3-S8
1H, 500 MHz
CDCl3
DMF
DMF
CHCl3
1.00
3.00
1.02
1.15
2.98
2.86
3.04
1.03
1.40
3.10
9.0
8.5
8.0
7.5
7.0
6.5
6.0
5.5
5.0
4.5
4.0
3.5
3.0
2.5
2.0
1.5
1.0
0.5
0.0
-0.5
-1.0
f1 (ppm)

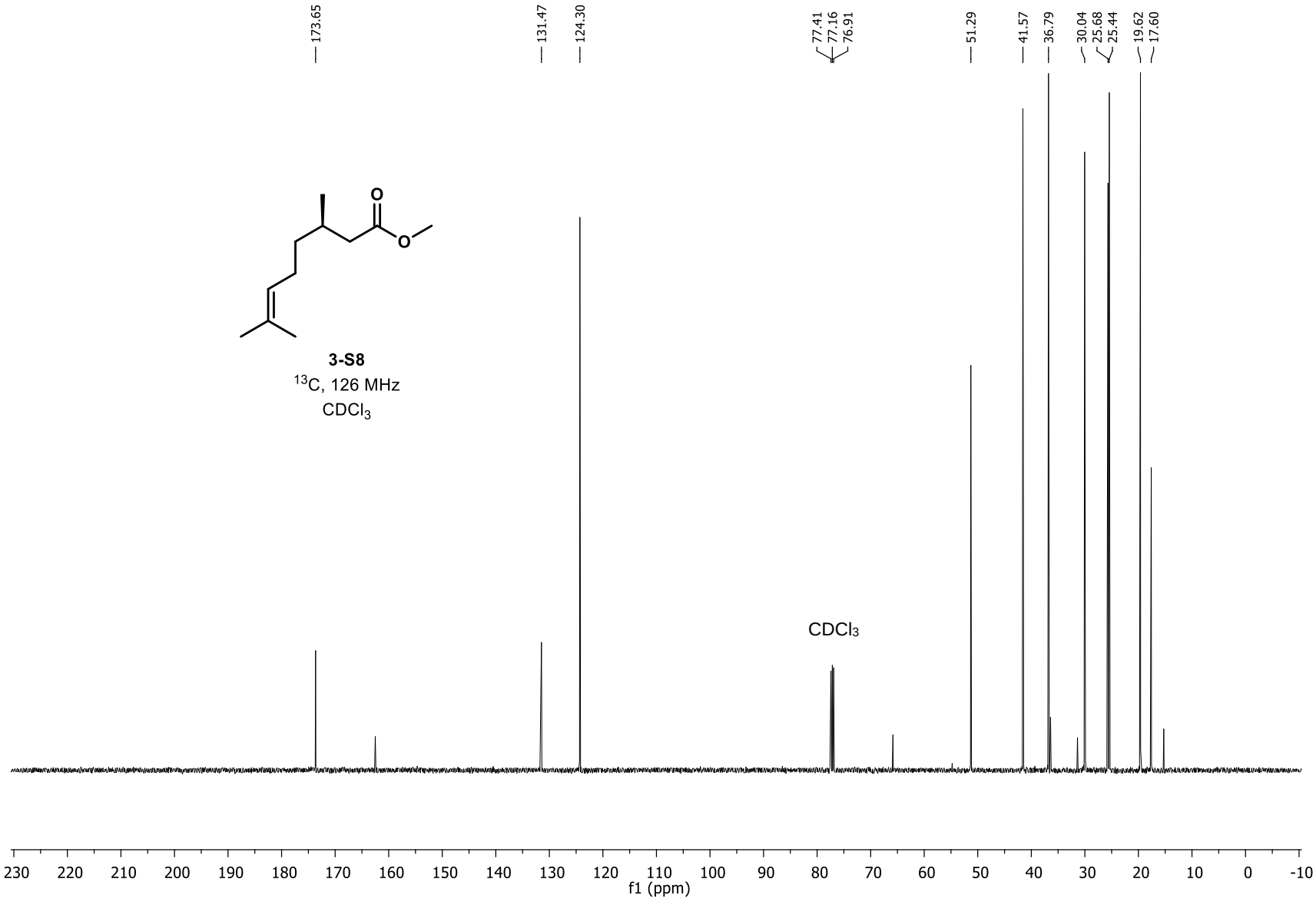
173.65
131.47
124.30
77.41
77.16
76.91
51.29
41.57
36.79
30.04
25.68
25.44
19.62
17.60
O
O
3-S8
13C, 126 MHz
CDCl3
CDCl3
230 220 210 200 190 180 170 160 150 140 130 120 110 100 90 80 70 60 50 40 30 20 10 0 -10
f1 (ppm)

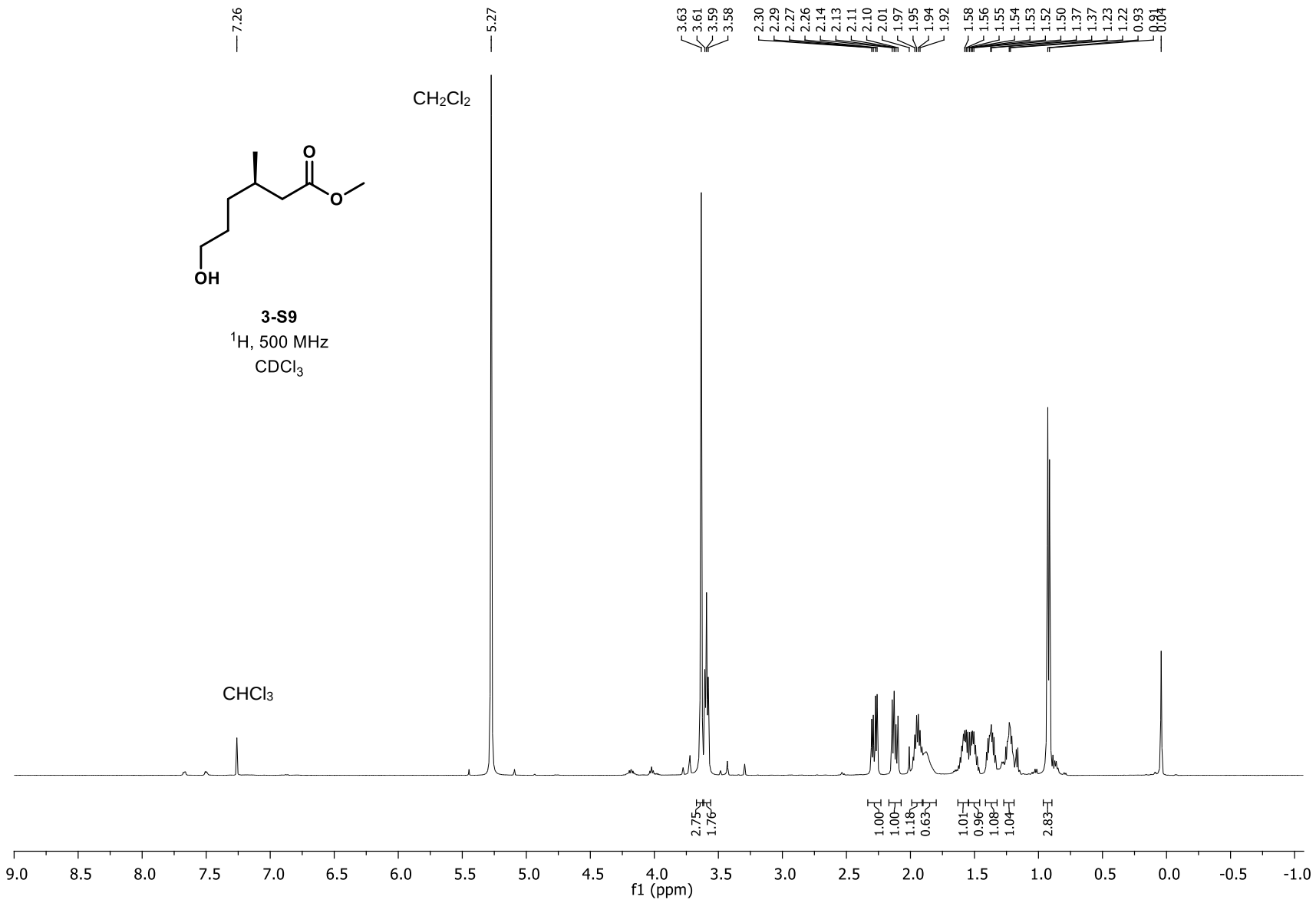
7.26
5.27
3.63
3.61
3.59
3.58
2.30
2.29
2.27
2.26
2.14
2.13
2.11
2.10
2.01
1.97
1.95
1.94
1.92
1.58
1.56
1.55
1.54
1.53
1.52
1.50
1.37
1.37
1.23
1.22
0.93
0.91
0.04
CH2Cl2
CHCl3
O
O
OH
3-S9
1H, 500 MHz
CDCl3
2.75
1.76
1.00
1.00
1.18
0.63
1.01
0.96
1.08
1.04
2.83
9.0
8.5
8.0
7.5
7.0
6.5
6.0
5.5
5.0
4.5
4.0
3.5
3.0
2.5
2.0
1.5
1.0
0.5
0.0
-0.5
-1.0
f1 (ppm)

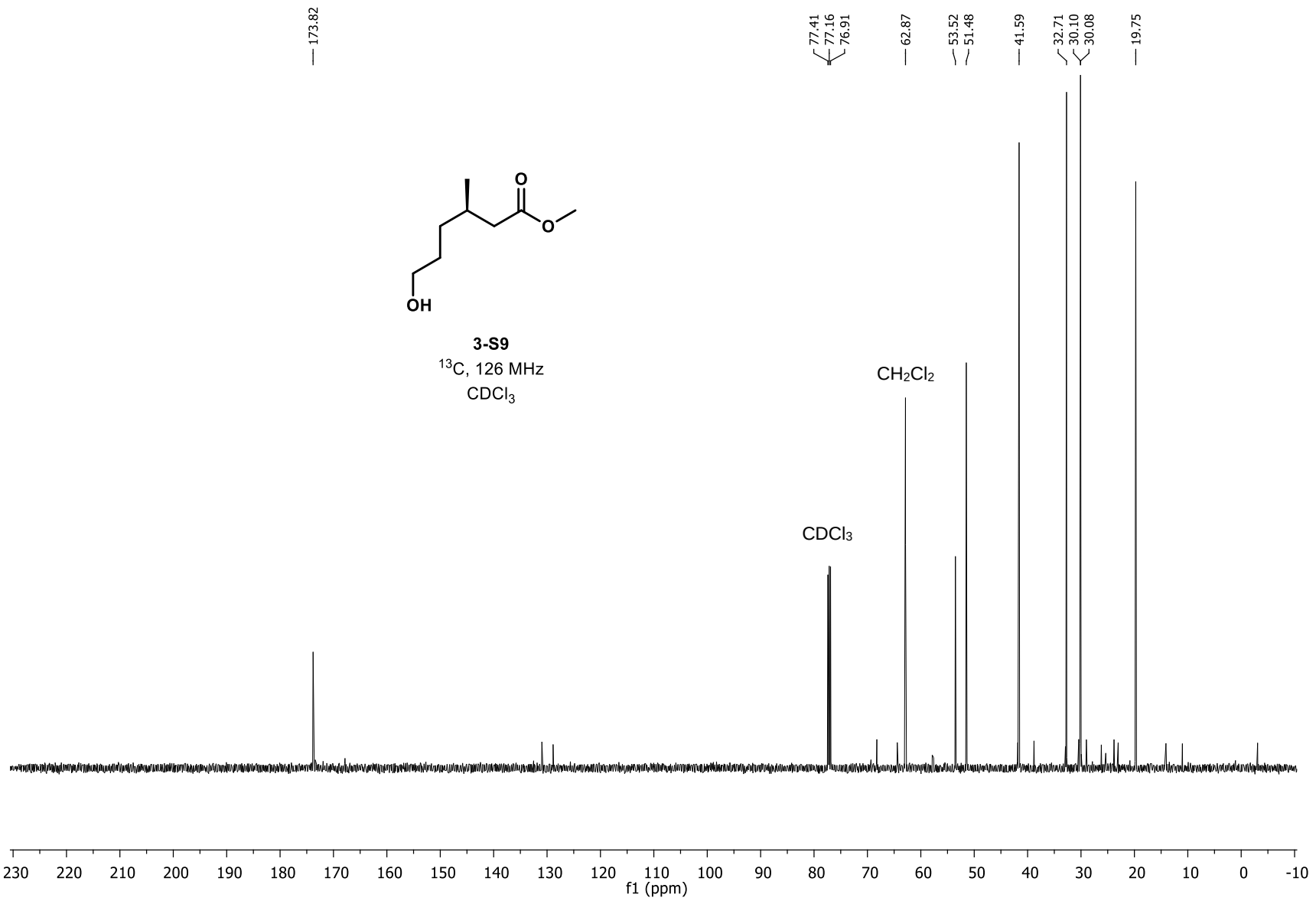
173.82
77.41
77.16
76.91
62.87
53.52
51.48
41.59
32.71
30.10
30.08
19.75
O
O
OH
3-S9
13C, 126 MHz
CDCl3
CH2Cl2
CDCl3
230 220 210 200 190 180 170 160 150 140 130 120 110 100 90 80 70 60 50 40 30 20 10 0 -10
f1 (ppm)

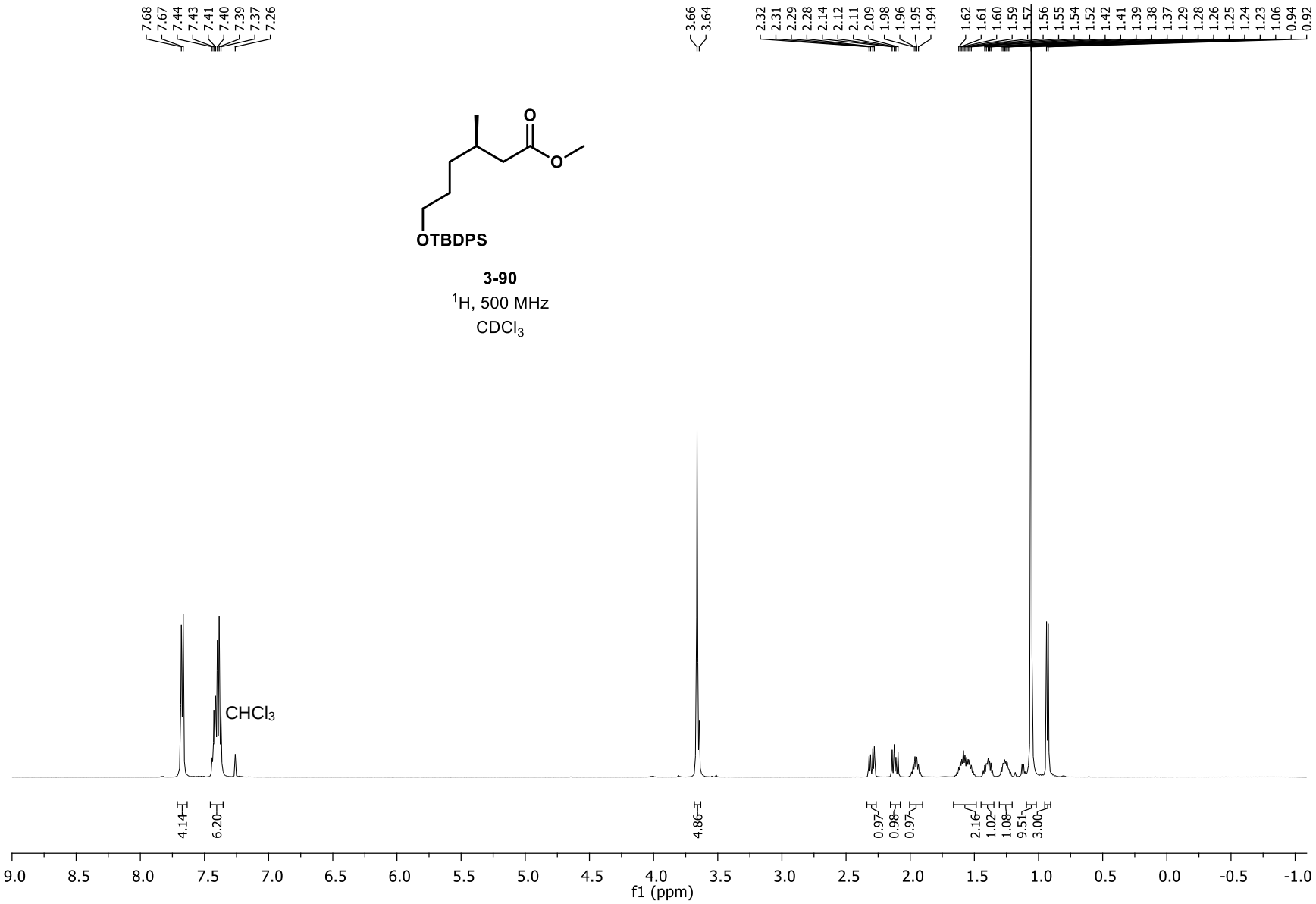
7.68
7.67
7.44
7.43
7.41
7.40
7.39
7.37
7.26
3.66
3.64
2.32
2.31
2.29
2.28
2.14
2.12
2.11
2.09
1.98
1.96
1.95
1.94
1.62
1.61
1.60
1.59
1.57
1.56
1.55
1.54
1.52
1.42
1.41
1.39
1.38
1.37
1.29
1.28
1.26
1.25
1.24
1.23
1.06
0.94
0.92
O
O
OTBDPS
3-90
1H, 500 MHz
CDCl3
CHCl3
4.14
6.20
4.86
0.97
0.98
0.97
2.16
1.02
1.08
9.51
3.00
9.0
8.5
8.0
7.5
7.0
6.5
6.0
5.5
5.0
4.5
4.0
3.5
3.0
2.5
2.0
1.5
1.0
0.5
0.0
-0.5
-1.0
f1 (ppm)

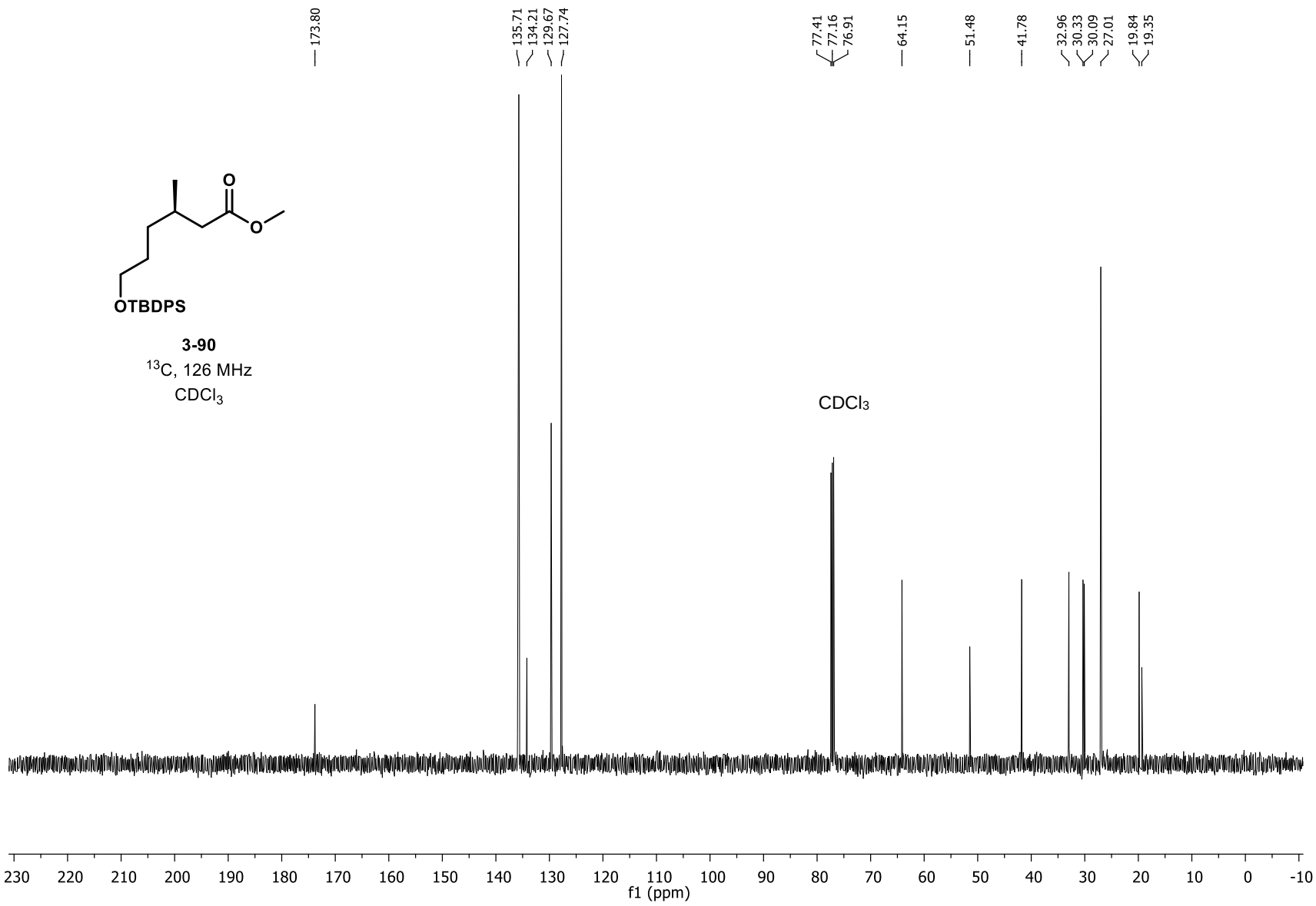
173.80
135.71
134.21
129.67
127.74
77.41
77.16
76.91
64.15
51.48
41.78
32.96
30.33
30.09
27.01
19.84
19.35
O
O
OTBDPS
3-90
13C, 126 MHz
CDCl3
CDCl3
230 220 210 200 190 180 170 160 150 140 130 120 110 100 90 80 70 60 50 40 30 20 10 0 -10
f1 (ppm)

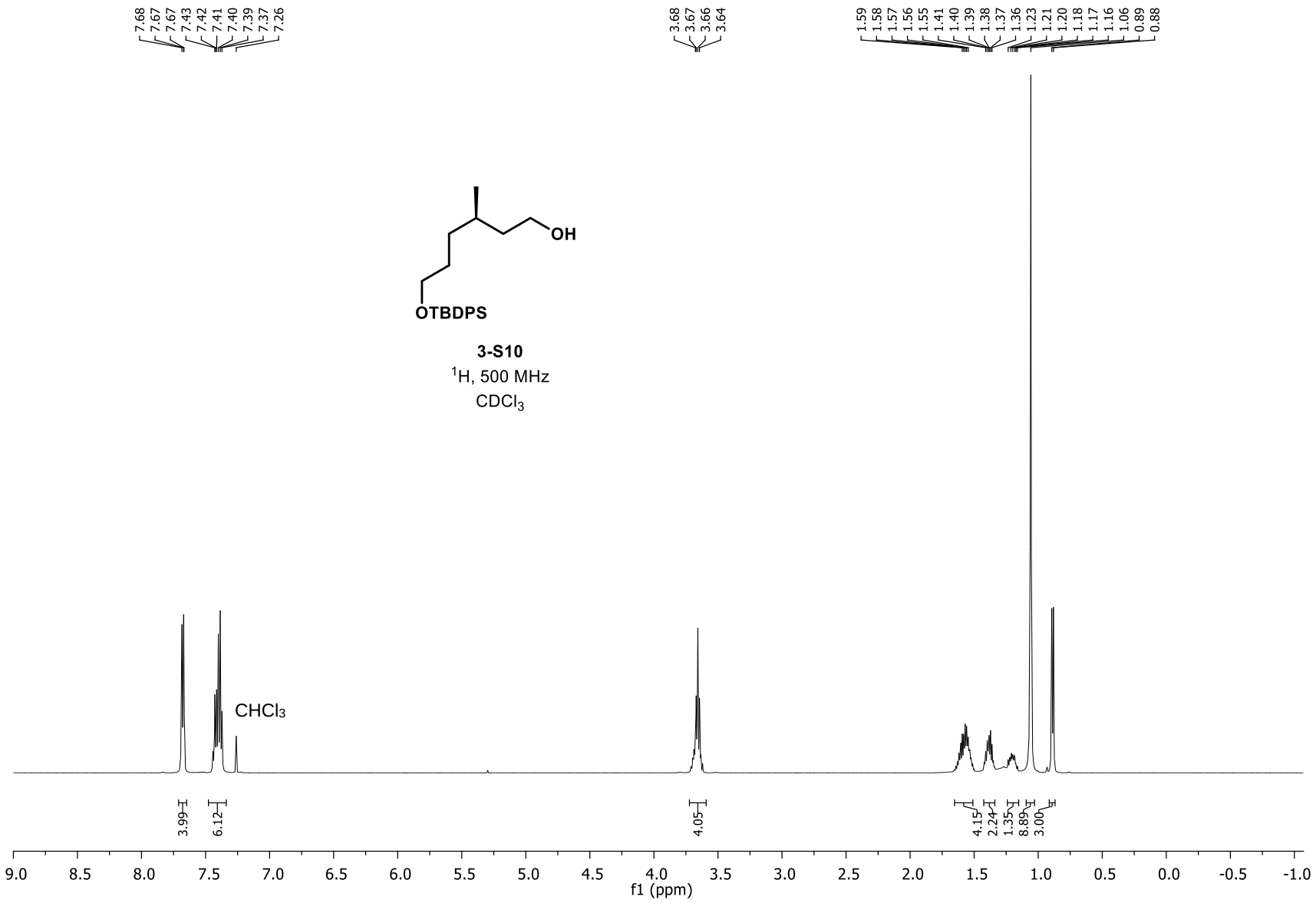
7.68
7.67
7.67
7.43
7.42
7.41
7.40
7.39
7.37
7.26
3.68
3.67
3.66
3.64
1.59
1.58
1.57
1.56
1.55
1.41
1.40
1.39
1.38
1.37
1.36
1.23
1.21
1.20
1.18
1.17
1.16
1.06
0.89
0.88
OH
OTBDPS
3-S10
1H, 500 MHz
CDCl3
CHCl3
3.99
6.12
4.05
4.15
2.24
1.35
8.89
3.00
9.0
8.5
8.0
7.5
7.0
6.5
6.0
5.5
5.0
4.5
4.0
3.5
3.0
2.5
2.0
1.5
1.0
0.5
0.0
-0.5
-1.0
f1 (ppm)

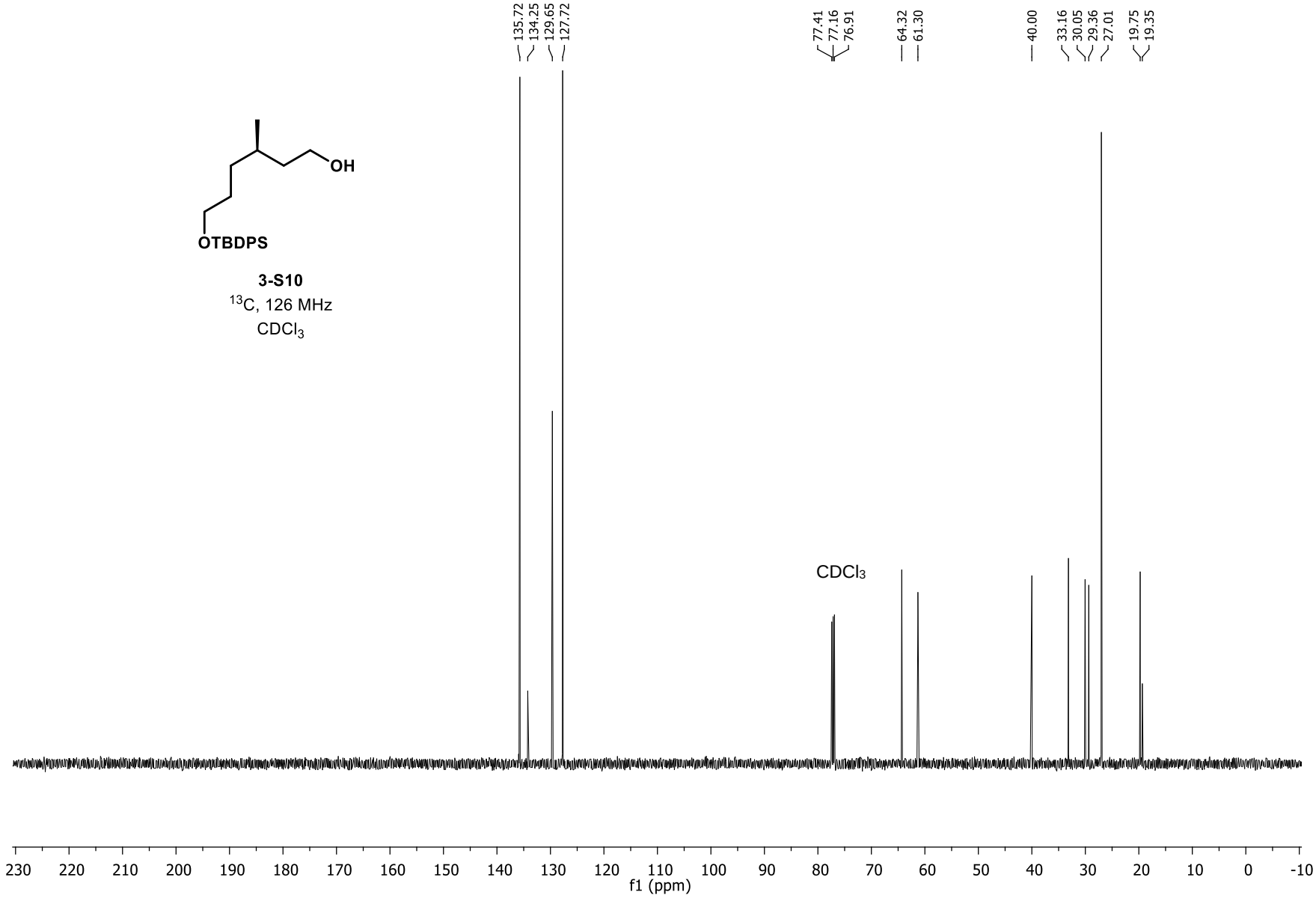
135.72
134.25
129.65
127.72
77.41
77.16
76.91
64.32
61.30
40.00
33.16
30.05
29.36
27.01
19.75
19.35
OH
OTBDPS
3-S10
13C, 126 MHz
CDCl3
CDCl3
230 220 210 200 190 180 170 160 150 140 130 120 110 100 90 80 70 60 50 40 30 20 10 0 -10
f1 (ppm)

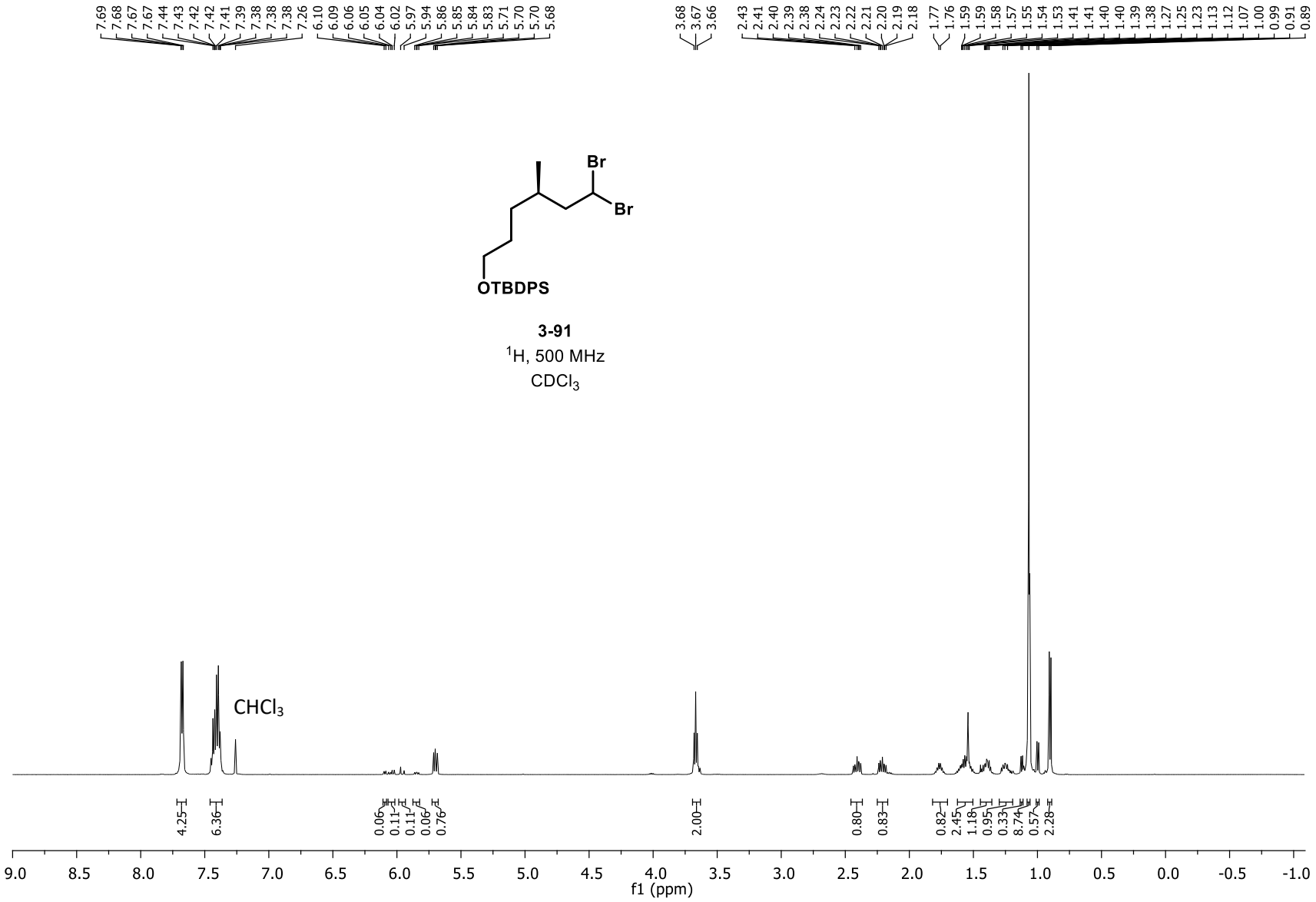
7.69 7.68 7.67 7.67 7.44 7.43 7.42 7.42 7.41 7.39 7.38 7.38 7.38 7.26
6.10 6.09 6.06 6.05 6.04 6.02 5.97 5.94 5.86 5.85 5.84 5.83 5.71 5.70 5.70 5.68
3.68 3.67 3.66
2.43 2.41 2.40 2.39 2.38 2.24 2.23 2.22 2.21 2.20 2.19 2.18
1.77 1.76 1.59 1.59 1.58 1.57 1.55 1.54 1.53 1.41 1.41 1.40 1.40 1.39 1.38 1.27 1.25 1.23 1.13 1.12 1.07 1.00 0.99 0.91 0.89
Br
Br
OTBDPS
3-91
1H, 500 MHz
CDCl3
CHCl3
4.25 6.36 0.06 0.11 0.11 0.06 0.76 2.00 0.80 0.83 0.82 2.45 1.18 0.95 0.33 8.74 0.57 2.28
9.0 8.5 8.0 7.5 7.0 6.5 6.0 5.5 5.0 4.5 4.0 3.5 3.0 2.5 2.0 1.5 1.0 0.5 0.0 -0.5 -1.0
f1 (ppm)

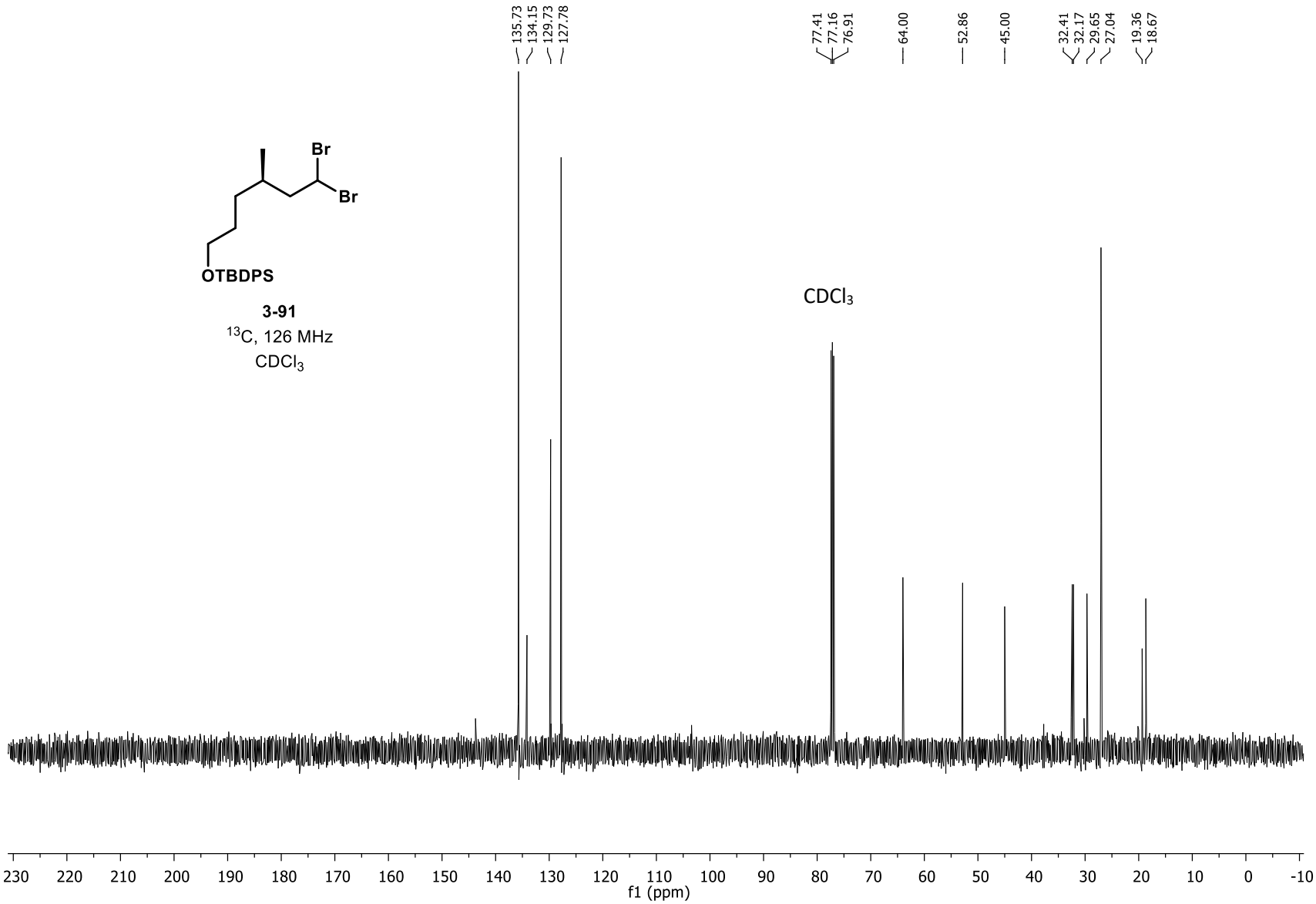
135.73
134.15
129.73
127.78
77.41
77.16
76.91
64.00
52.86
45.00
32.41
32.17
29.65
27.04
19.36
18.67
Br
Br
OTBDPS
3-91
13C, 126 MHz
CDCl3
CDCl3
230 220 210 200 190 180 170 160 150 140 130 120 110 100 90 80 70 60 50 40 30 20 10 0 -10
f1 (ppm)

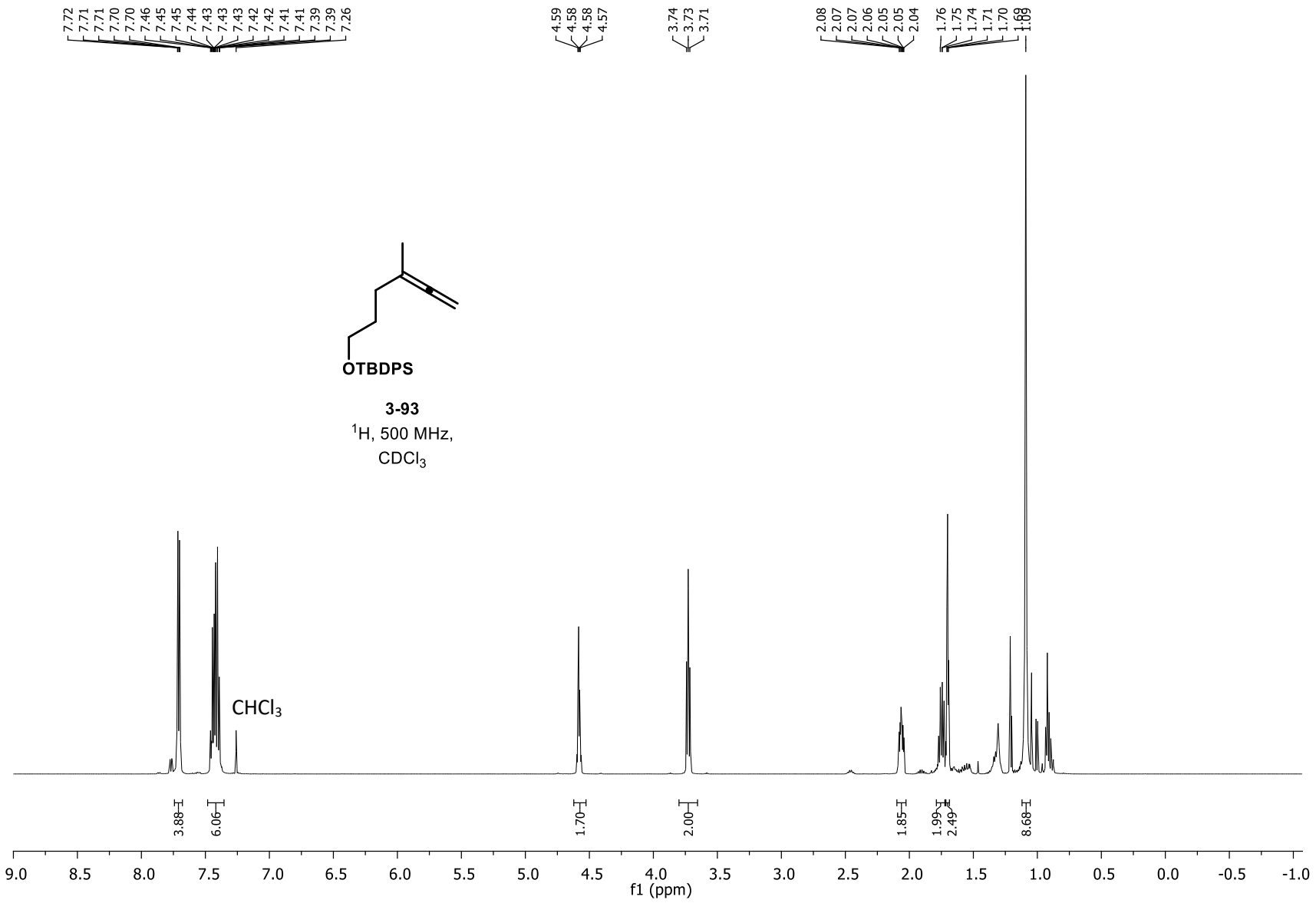
7.72
7.71
7.71
7.70
7.70
7.46
7.45
7.45
7.44
7.43
7.43
7.43
7.42
7.42
7.41
7.41
7.39
7.39
7.26
4.59
4.58
4.58
4.57
3.74
3.73
3.71
2.08
2.07
2.07
2.06
2.05
2.05
2.04
1.76
1.75
1.74
1.71
1.70
1.69
1.69
OTBDPS
3-93
1H, 500 MHz,
CDCl3
CHCl3
3.88
6.06
1.70
2.00
1.85
1.99
2.49
8.68
9.0
8.5
8.0
7.5
7.0
6.5
6.0
5.5
5.0
4.5
4.0
3.5
3.0
2.5
2.0
1.5
1.0
0.5
0.0
-0.5
-1.0
f1 (ppm)

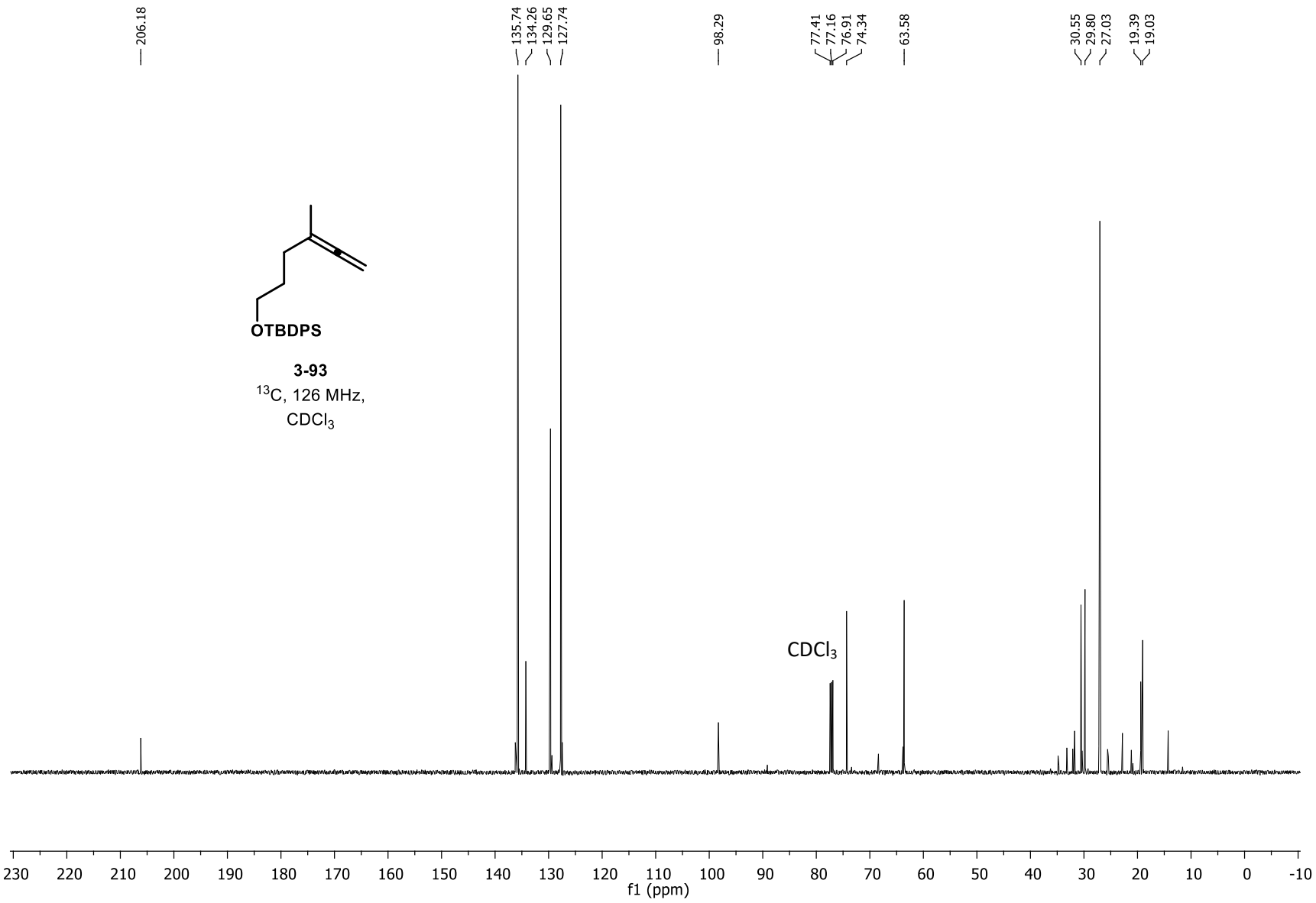
206.18
135.74
134.26
129.65
127.74
98.29
77.41
77.16
76.91
74.34
63.58
30.55
29.80
27.03
19.39
19.03
OTBDPS
3-93
13C, 126 MHz,
CDCl3
CDCl3
230 220 210 200 190 180 170 160 150 140 130 120 110 100 90 80 70 60 50 40 30 20 10 0 -10
f1 (ppm)

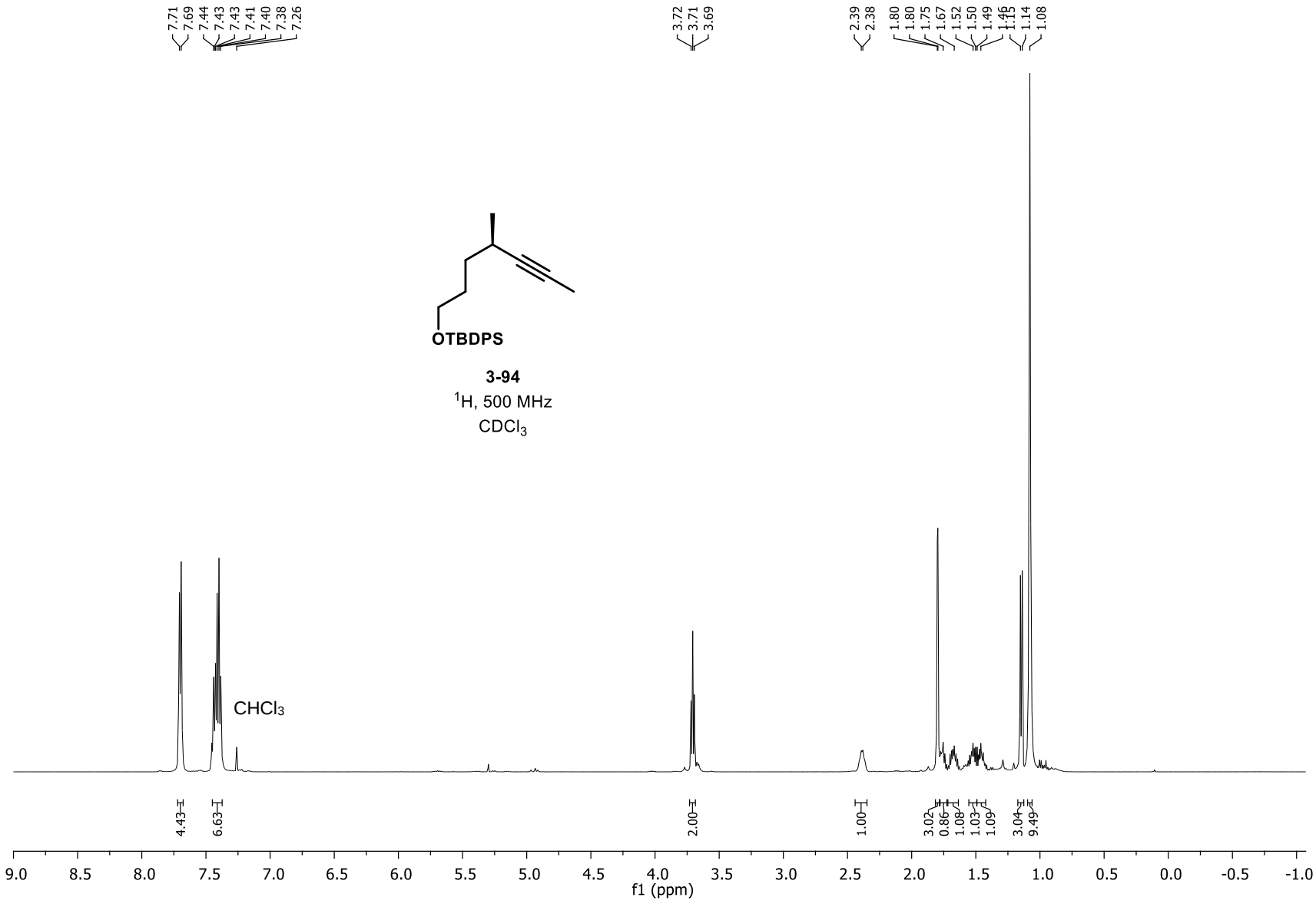
7.71
7.69
7.44
7.43
7.43
7.41
7.40
7.38
7.26
3.72
3.71
3.69
2.39
2.38
1.80
1.80
1.75
1.67
1.52
1.50
1.49
1.46
1.15
1.14
1.08
OTBDPS
3-94
1H, 500 MHz
CDCl3
CHCl3
4.43
6.63
2.00
1.00
3.02
0.86
1.08
1.03
1.09
3.04
9.49
9.0
8.5
8.0
7.5
7.0
6.5
6.0
5.5
5.0
4.5
4.0
3.5
3.0
2.5
2.0
1.5
1.0
0.5
0.0
-0.5
-1.0
f1 (ppm)

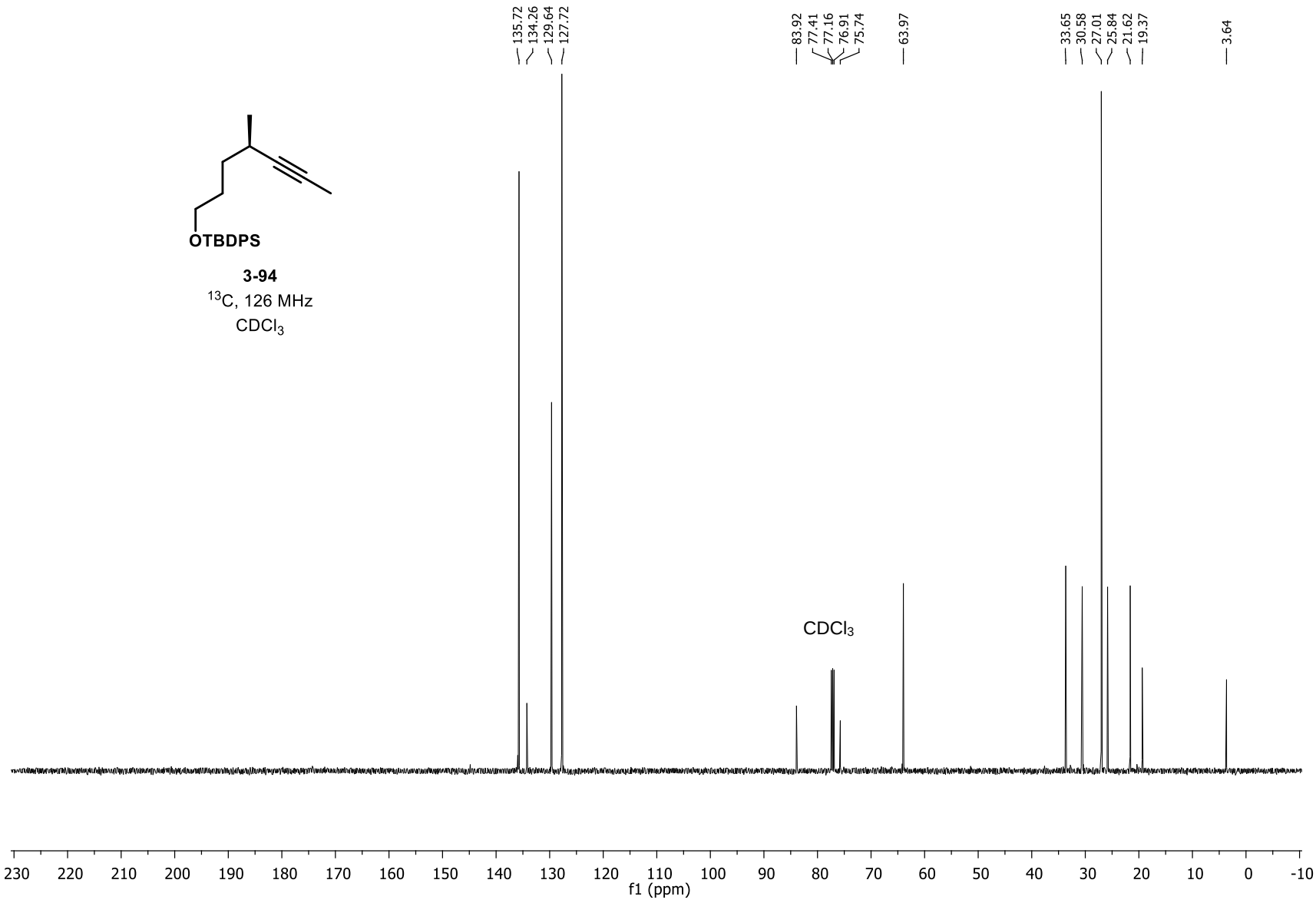
135.72
134.26
129.64
127.72
83.92
77.41
77.16
76.91
75.74
63.97
33.65
30.58
27.01
25.84
21.62
19.37
3.64
OTBDPS
3-94
13C, 126 MHz
CDCl3
CDCl3
230 220 210 200 190 180 170 160 150 140 130 120 110 100 90 80 70 60 50 40 30 20 10 0 -10
f1 (ppm)

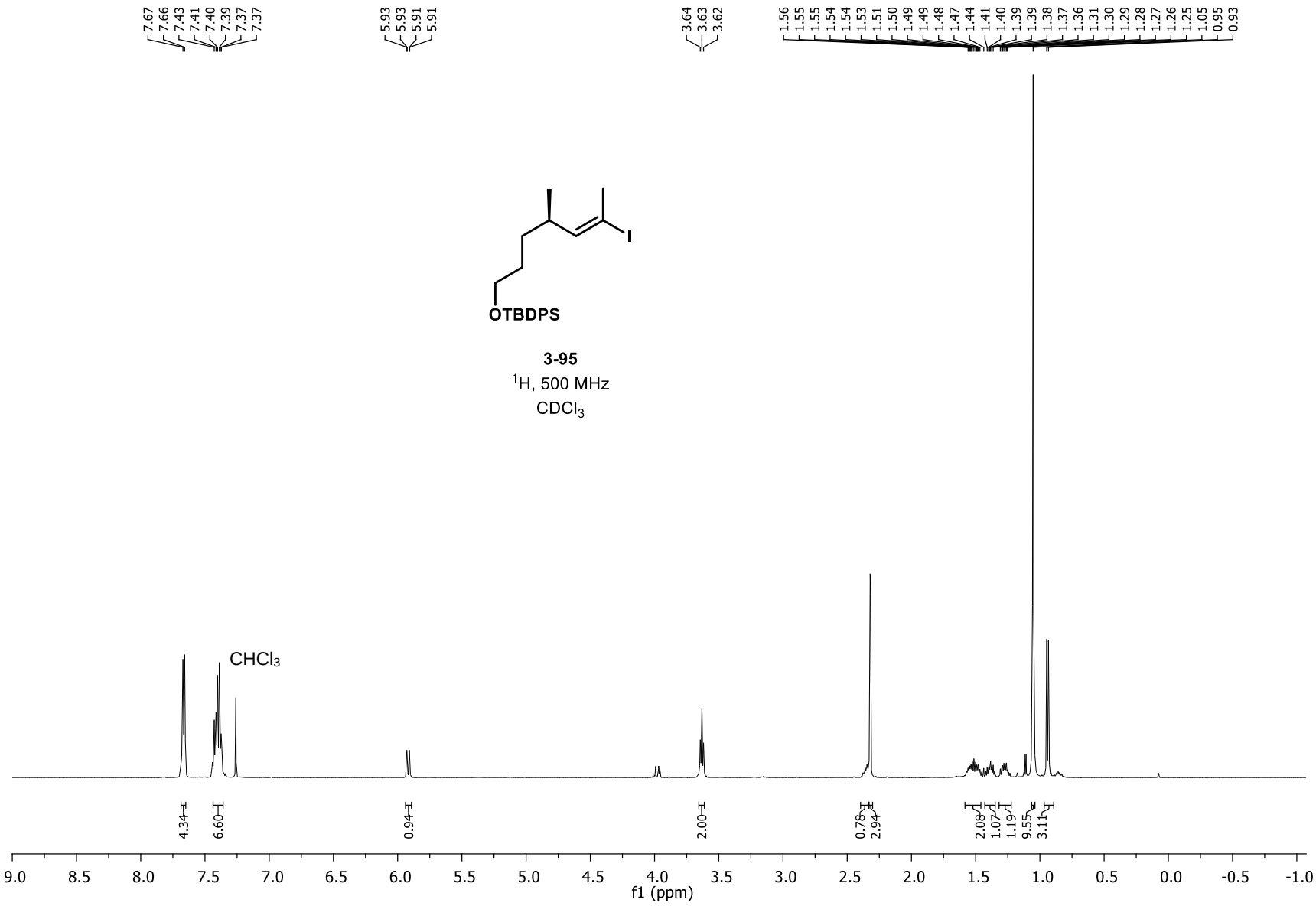
7.67
7.66
7.43
7.41
7.40
7.39
7.37
7.37
5.93
5.93
5.91
5.91
3.64
3.63
3.62
1.56
1.55
1.55
1.54
1.54
1.53
1.51
1.50
1.49
1.49
1.48
1.47
1.44
1.41
1.40
1.39
1.39
1.38
1.37
1.36
1.31
1.30
1.29
1.28
1.27
1.26
1.25
1.05
0.95
0.93
I
OTBDPS
3-95
1H, 500 MHz
CDCl3
CHCl3
4.34
6.60
0.94
2.00
0.78
2.94
2.08
1.07
1.19
9.55
3.11
9.0
8.5
8.0
7.5
7.0
6.5
6.0
5.5
5.0
4.5
4.0
3.5
3.0
2.5
2.0
1.5
1.0
0.5
0.0
-0.5
-1.0
f1 (ppm)

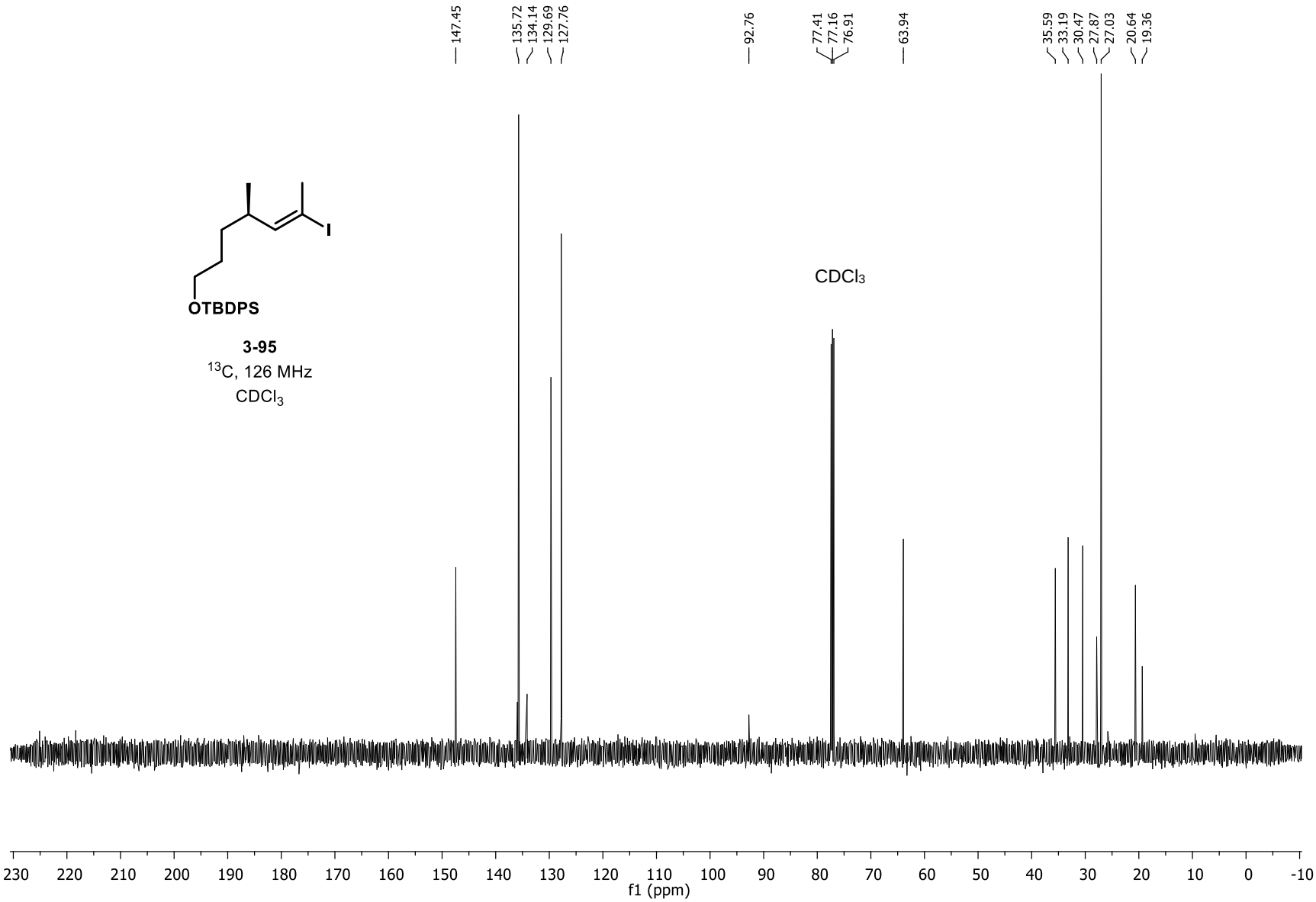
147.45
135.72
134.14
129.69
127.76
92.76
77.41
77.16
76.91
63.94
35.59
33.19
30.47
27.87
27.03
20.64
19.36
I
OTBDPS
3-95
13C, 126 MHz
CDCl3
CDCl3
230 220 210 200 190 180 170 160 150 140 130 120 110 100 90 80 70 60 50 40 30 20 10 0 -10
f1 (ppm)

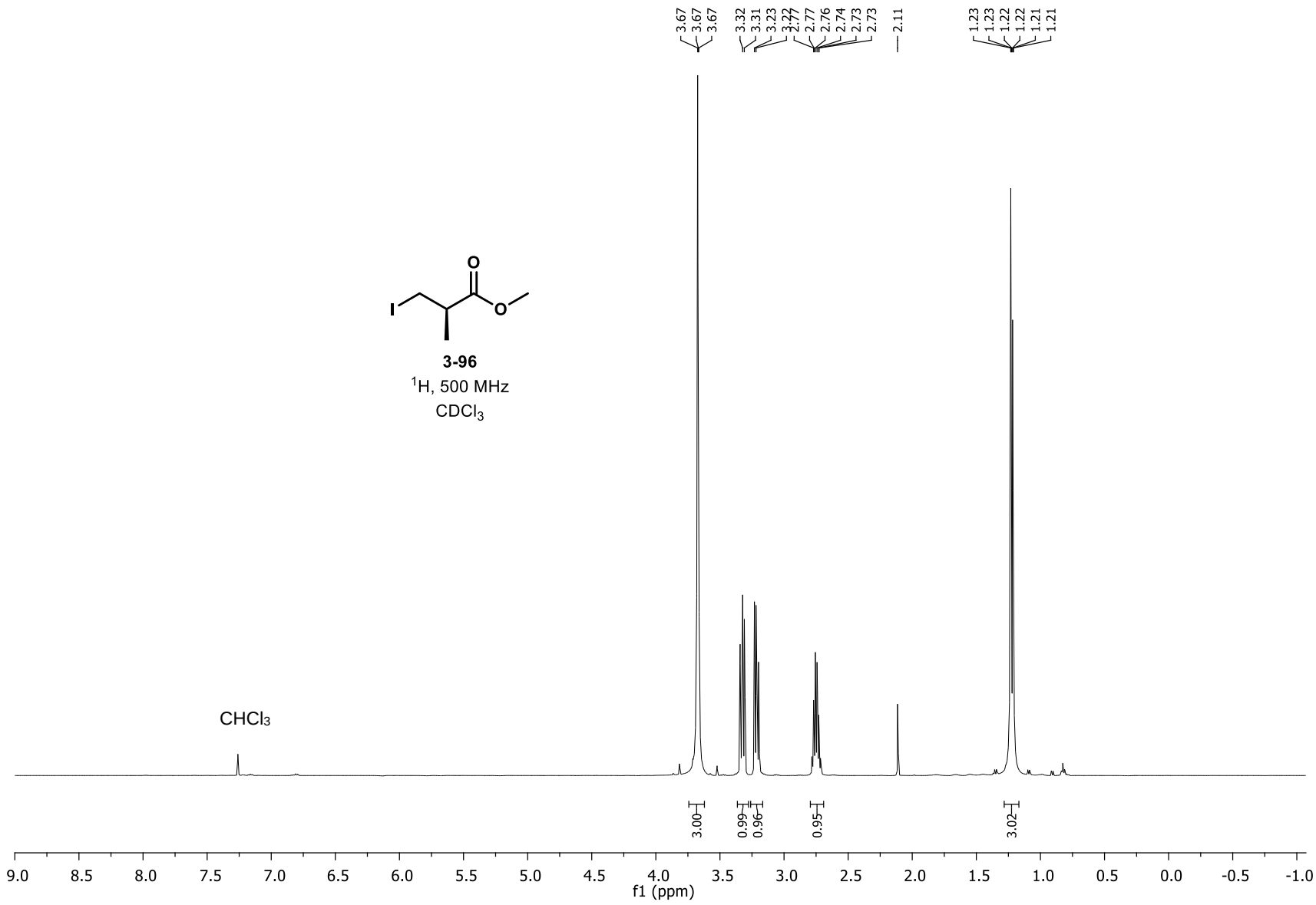
3.67
3.67
3.67
3.32
3.31
3.23
3.22
2.77
2.76
2.74
2.73
2.73
2.11
1.23
1.23
1.22
1.22
1.21
1.21
O
I
O
3-96
1H, 500 MHz
CDCl3
CHCl3
3.00
0.99
0.96
0.95
3.02
9.0
8.5
8.0
7.5
7.0
6.5
6.0
5.5
5.0
4.5
4.0
3.5
3.0
2.5
2.0
1.5
1.0
0.5
0.0
-0.5
-1.0
f1 (ppm)

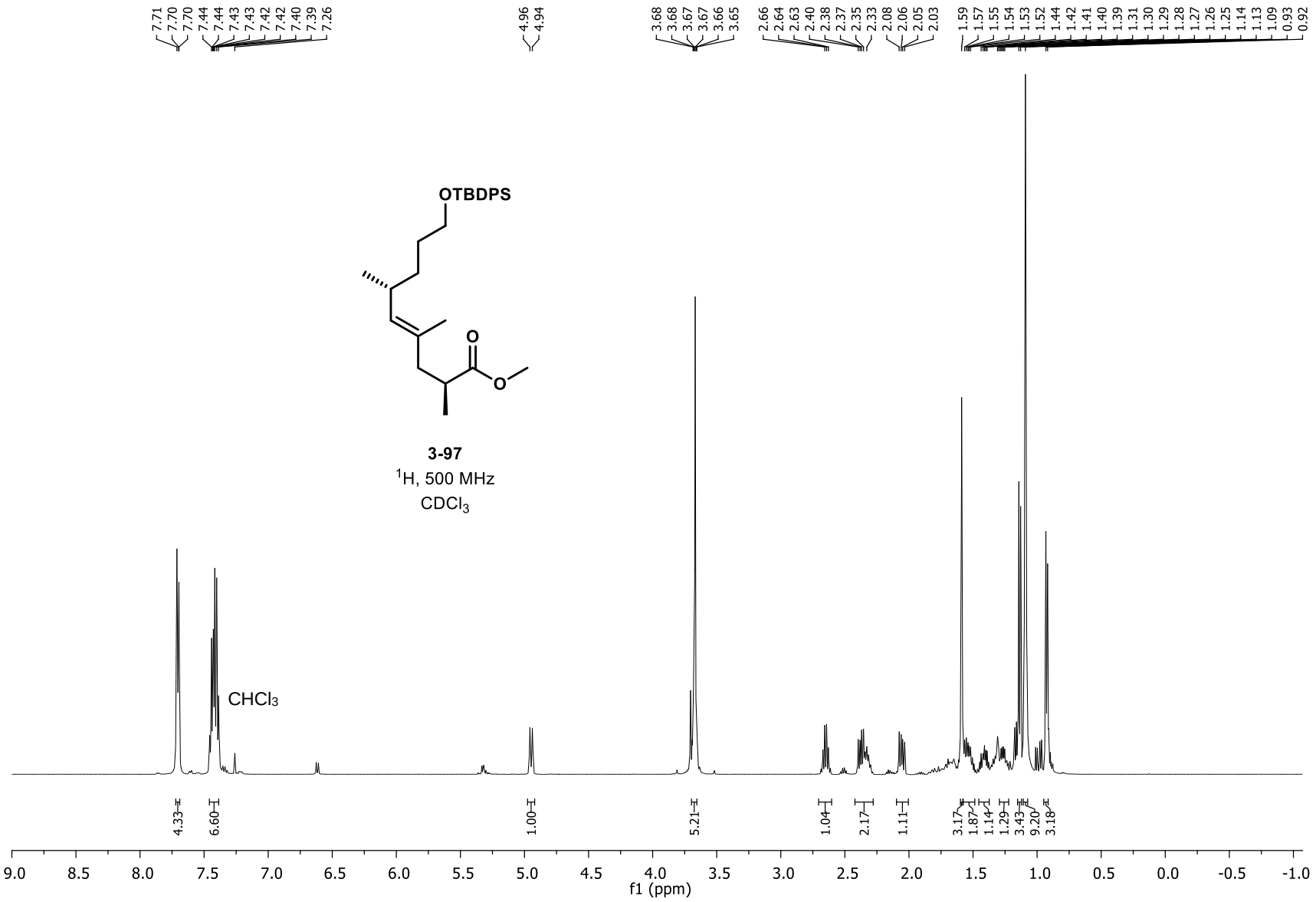
7.71
7.70
7.70
7.44
7.44
7.43
7.43
7.42
7.42
7.40
7.39
7.26
4.96
4.94
3.68
3.68
3.67
3.67
3.66
3.65
2.66
2.64
2.63
2.40
2.38
2.37
2.35
2.33
2.08
2.06
2.05
2.03
1.59
1.57
1.55
1.54
1.53
1.52
1.44
1.42
1.41
1.40
1.39
1.31
1.30
1.29
1.28
1.27
1.26
1.25
1.14
1.13
1.09
0.93
0.92
OTBDPS
O
O
3-97
1H, 500 MHz
CDCl3
CHCl3
4.33
6.60
1.00
5.21
1.04
2.17
1.11
3.17
1.87
1.14
1.29
3.43
9.20
3.18
9.0
8.5
8.0
7.5
7.0
6.5
6.0
5.5
5.0
4.5
4.0
3.5
3.0
2.5
2.0
1.5
1.0
0.5
0.0
-0.5
-1.0
f1 (ppm)

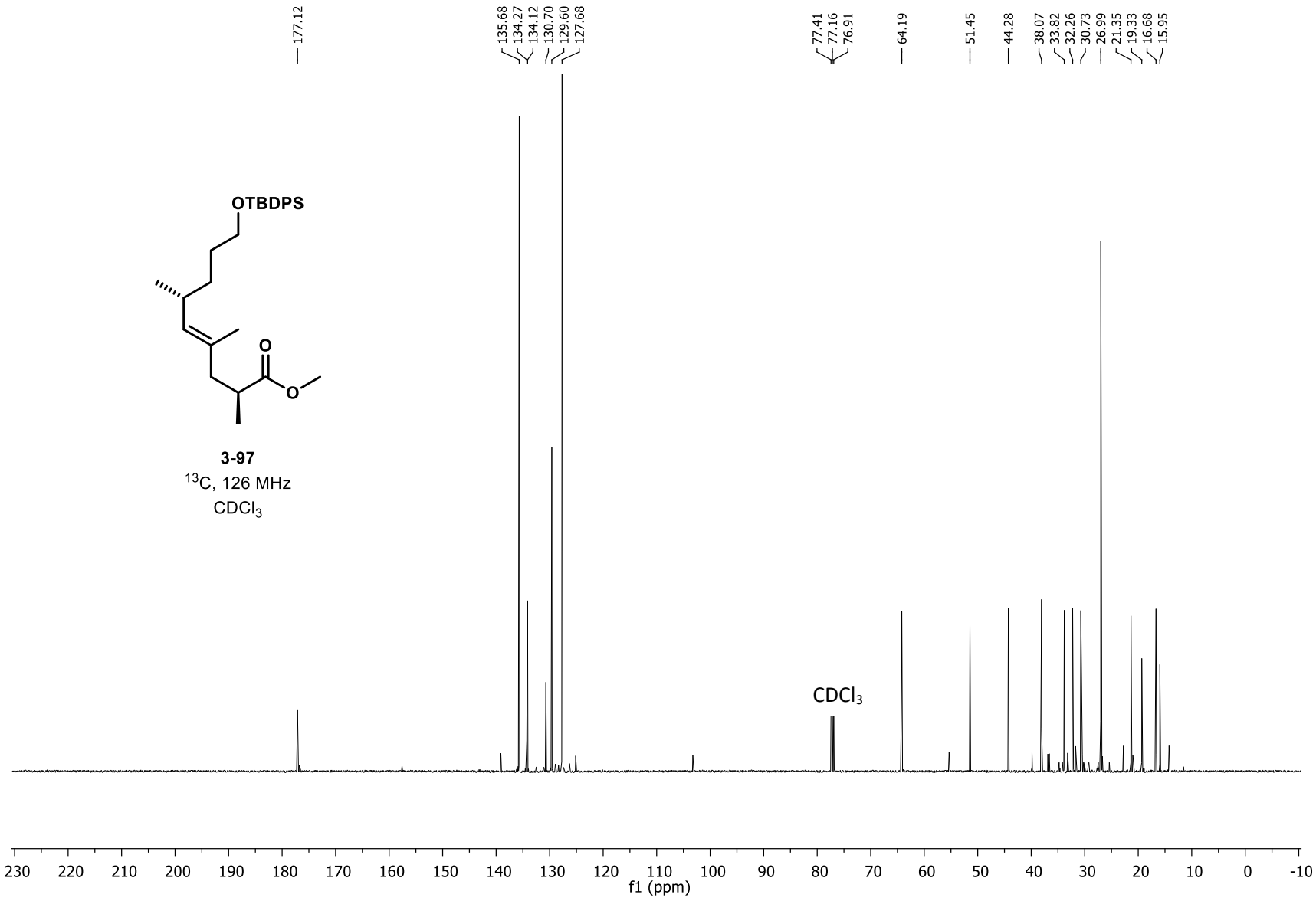
177.12
135.68
134.27
134.12
130.70
129.60
127.68
77.41
77.16
76.91
64.19
51.45
44.28
38.07
33.82
32.26
30.73
26.99
21.35
19.33
16.68
15.95
OTBDPS
O
O
3-97
13C, 126 MHz
CDCl3
CDCl3
230 220 210 200 190 180 170 160 150 140 130 120 110 100 90 80 70 60 50 40 30 20 10 0 -10
f1 (ppm)

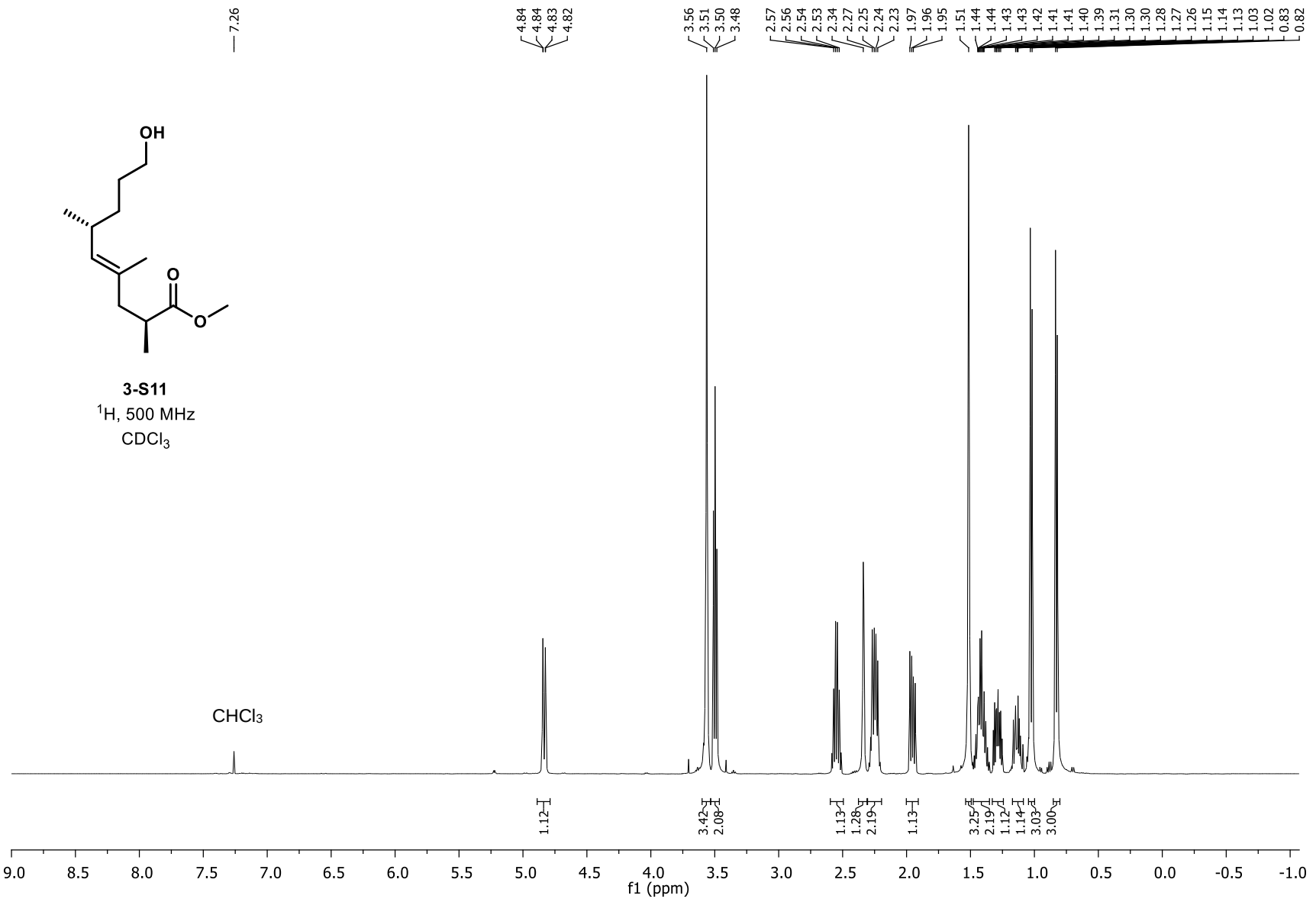
OH
O
O
3-S11
1H, 500 MHz
CDCl3
CHCl3
7.26
4.84
4.84
4.83
4.82
3.56
3.51
3.50
3.48
2.57
2.56
2.54
2.53
2.34
2.27
2.25
2.24
2.23
1.97
1.96
1.95
1.51
1.44
1.44
1.43
1.43
1.42
1.41
1.41
1.40
1.39
1.31
1.30
1.30
1.28
1.27
1.26
1.15
1.14
1.13
1.03
1.02
0.83
0.82
1.12
3.42
2.08
1.13
1.28
2.19
1.13
3.25
2.19
1.12
1.14
3.03
3.00
9.0
8.5
8.0
7.5
7.0
6.5
6.0
5.5
5.0
4.5
4.0
3.5
3.0
2.5
2.0
1.5
1.0
0.5
0.0
-0.5
-1.0
f1 (ppm)

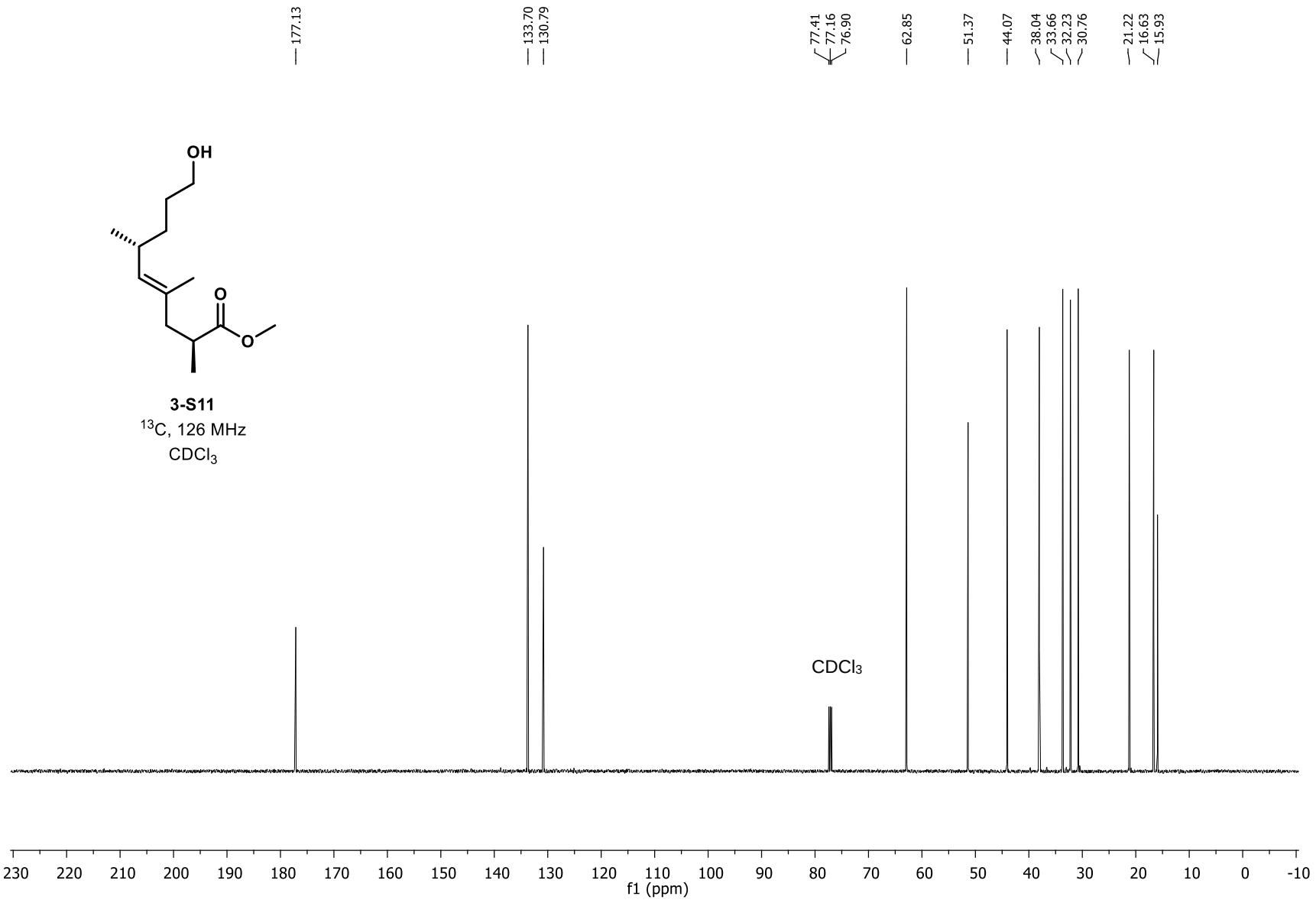
177.13
133.70
130.79
77.41
77.16
76.90
62.85
51.37
44.07
38.04
33.66
32.23
30.76
21.22
16.63
15.93
OH
O
O
3-S11
13C, 126 MHz
CDCl3
CDCl3
230 220 210 200 190 180 170 160 150 140 130 120 110 100 90 80 70 60 50 40 30 20 10 0 -10
f1 (ppm)

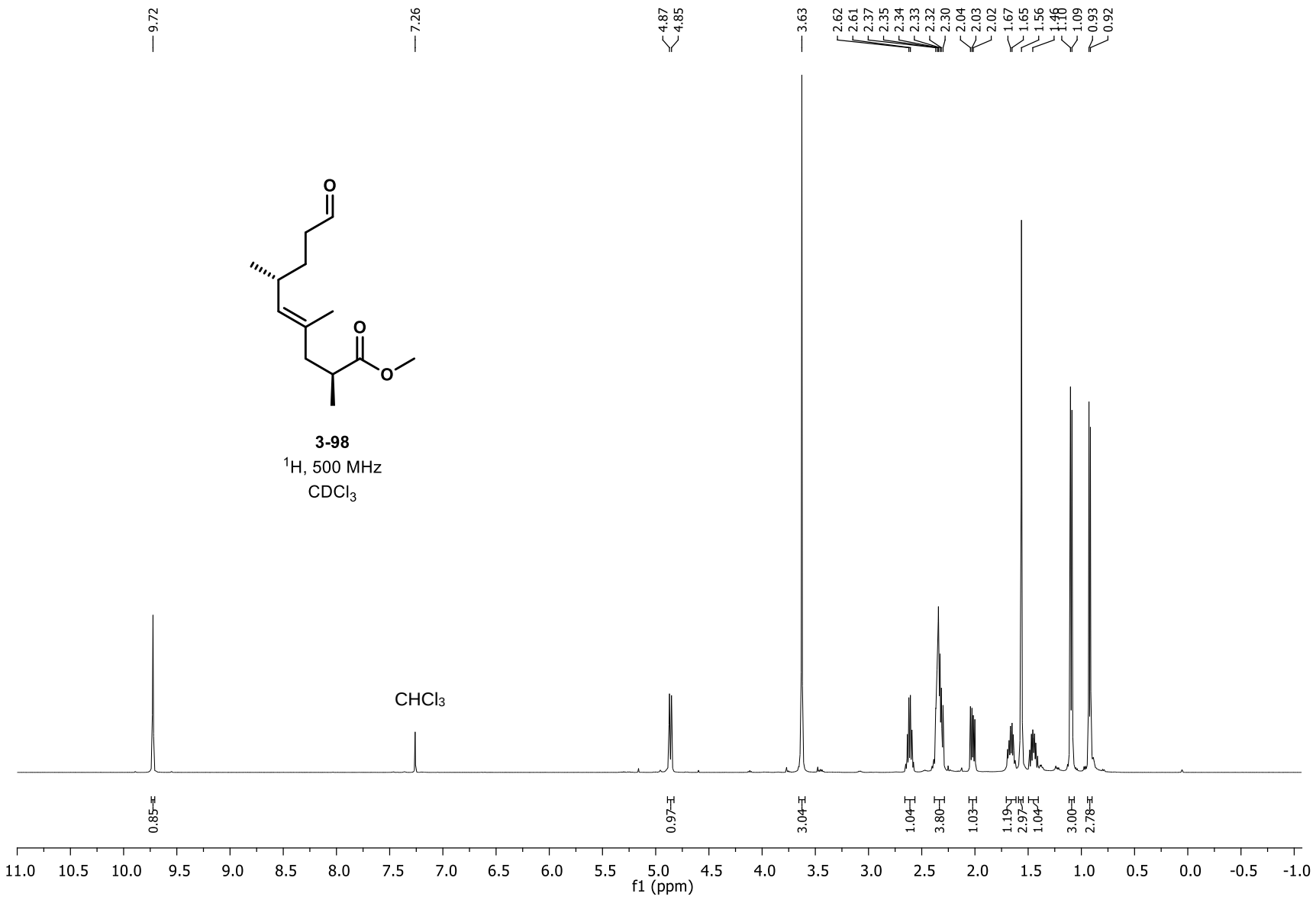
9.72
7.26
4.87
4.85
3.63
2.62
2.61
2.37
2.35
2.34
2.33
2.32
2.30
2.04
2.03
2.02
1.67
1.65
1.56
1.46
1.10
1.09
0.93
0.92
O
O
O
3-98
1H, 500 MHz
CDCl3
CHCl3
0.85
0.97
3.04
1.04
3.80
1.03
1.19
2.97
1.04
3.00
2.78
11.0 10.5 10.0 9.5 9.0 8.5 8.0 7.5 7.0 6.5 6.0 5.5 5.0 4.5 4.0 3.5 3.0 2.5 2.0 1.5 1.0 0.5 0.0 -0.5 -1.0
f1 (ppm)

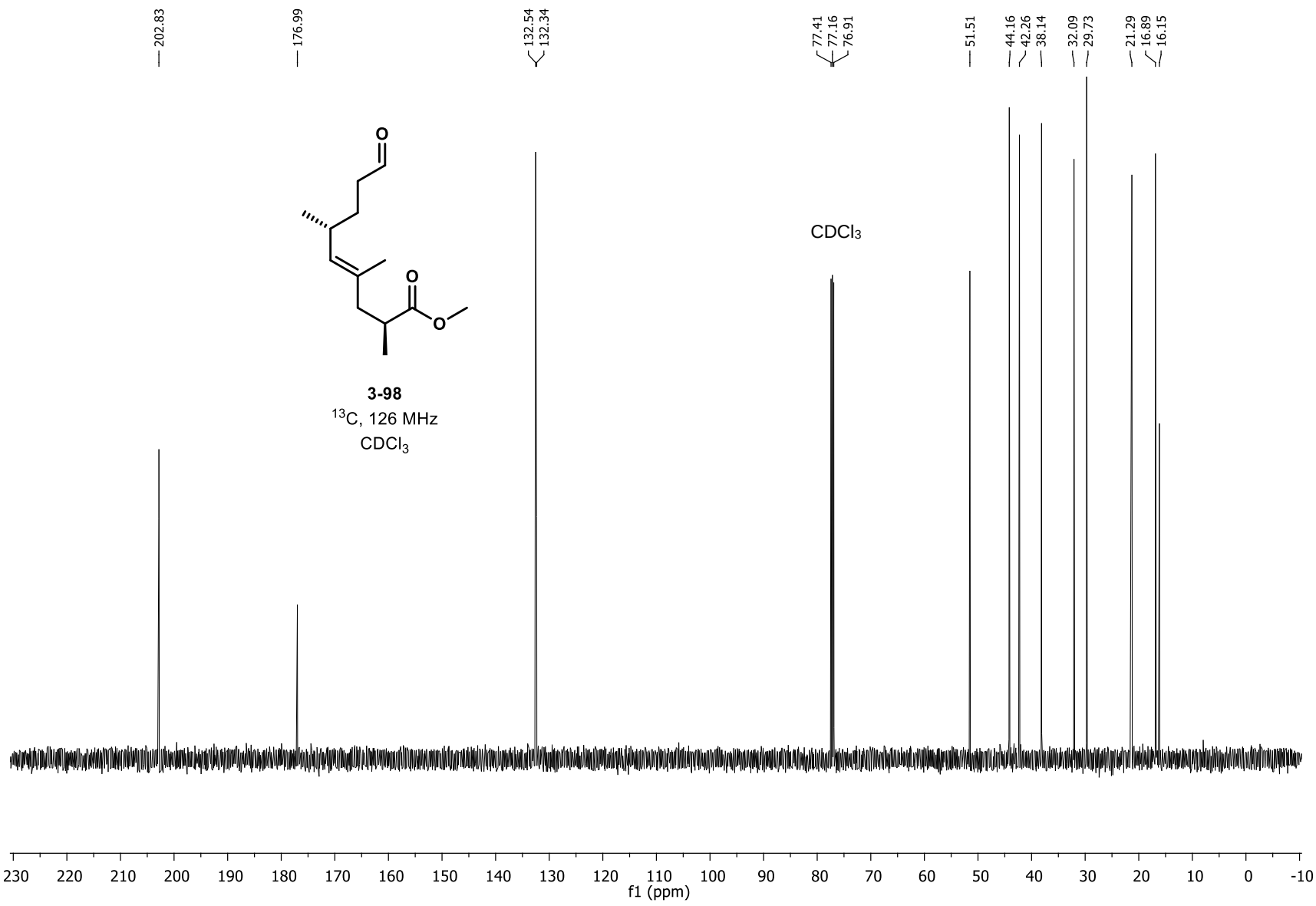
202.83
176.99
132.54
132.34
77.41
77.16
76.91
51.51
44.16
42.26
38.14
32.09
29.73
21.29
16.89
16.15
CDCl3
O
O
O
3-98
13C, 126 MHz
CDCl3
230 220 210 200 190 180 170 160 150 140 130 120 110 100 90 80 70 60 50 40 30 20 10 0 -10
f1 (ppm)

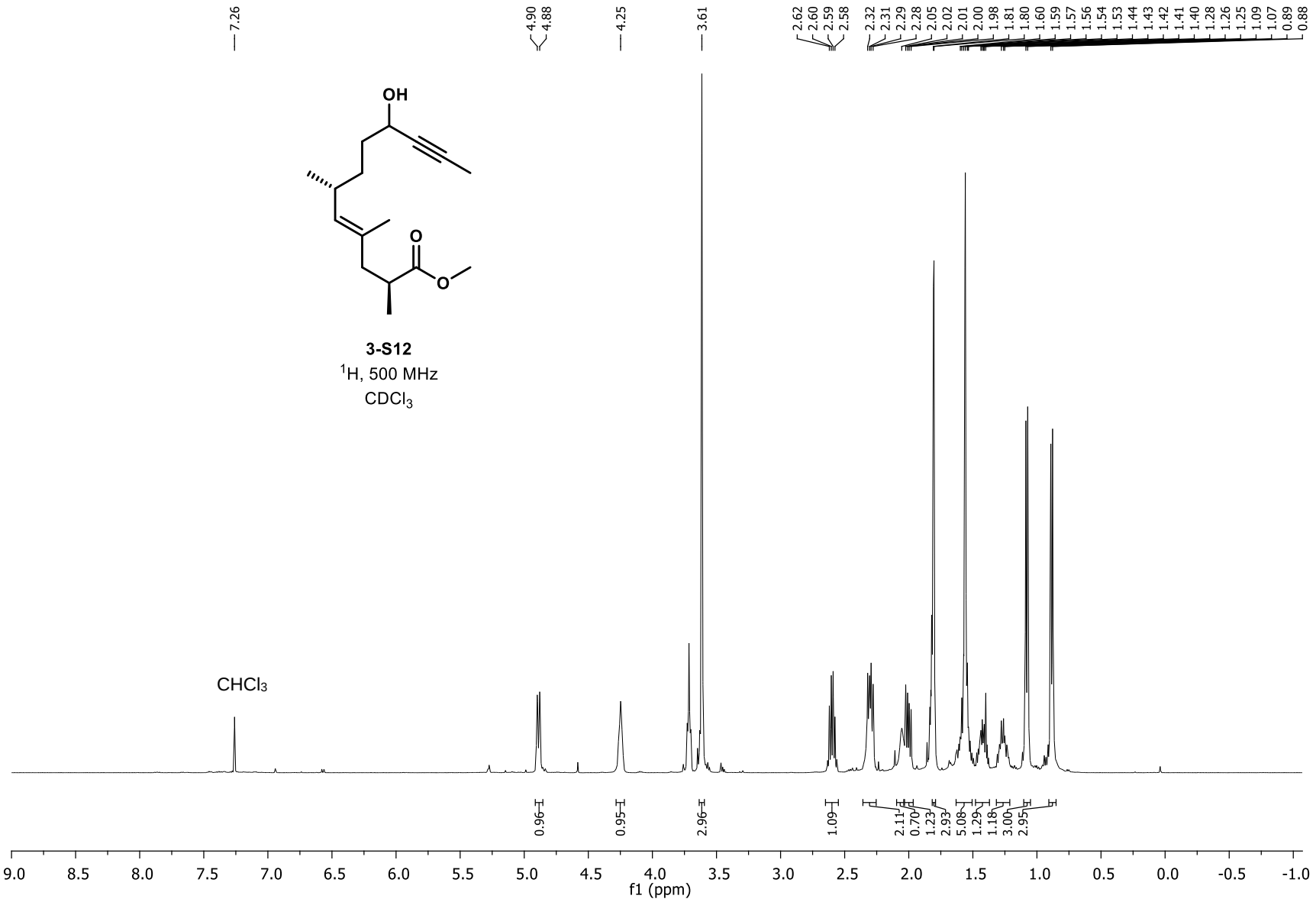
7.26
4.90
4.88
4.25
3.61
2.62
2.60
2.59
2.58
2.32
2.31
2.29
2.28
2.05
2.02
2.01
2.00
1.98
1.81
1.80
1.60
1.59
1.57
1.56
1.54
1.53
1.44
1.43
1.42
1.41
1.40
1.28
1.26
1.25
1.09
1.07
0.89
0.88
OH
O
O
3-S12
1H, 500 MHz
CDCl3
CHCl3
0.96
0.95
2.96
1.09
2.11
0.70
1.23
2.93
5.08
1.29
1.18
3.00
2.95
9.0
8.5
8.0
7.5
7.0
6.5
6.0
5.5
5.0
4.5
4.0
3.5
3.0
2.5
2.0
1.5
1.0
0.5
0.0
-0.5
-1.0
f1 (ppm)

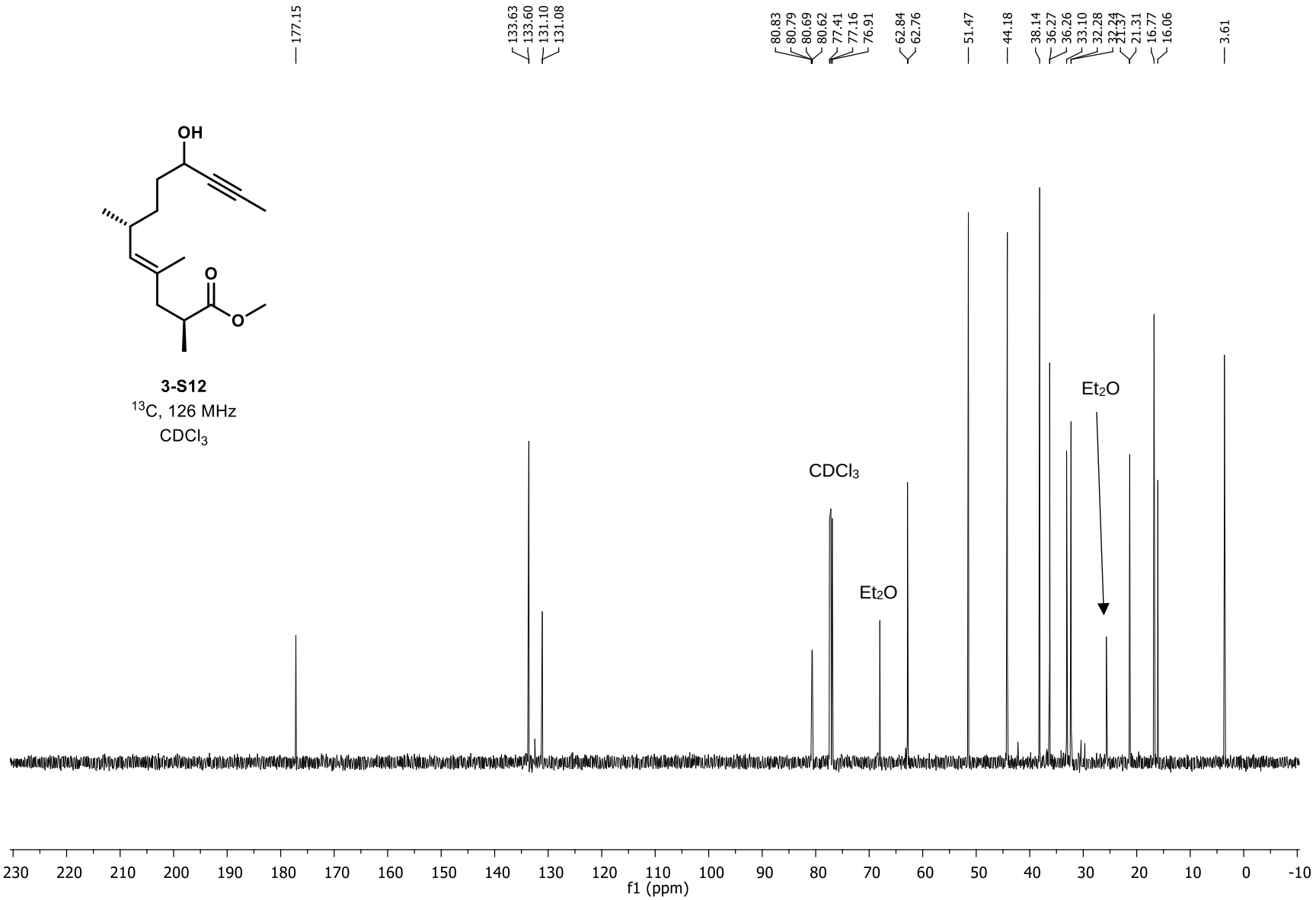
177.15
133.63
133.60
131.10
131.08
80.83
80.79
80.69
80.62
77.41
77.16
76.91
62.84
62.76
51.47
44.18
38.14
36.27
36.26
33.10
32.28
21.37
21.31
16.77
16.06
3.61
OH
O
O
3-S12
13C, 126 MHz
CDCl3
CDCl3
Et2O
Et2O
f1 (ppm)

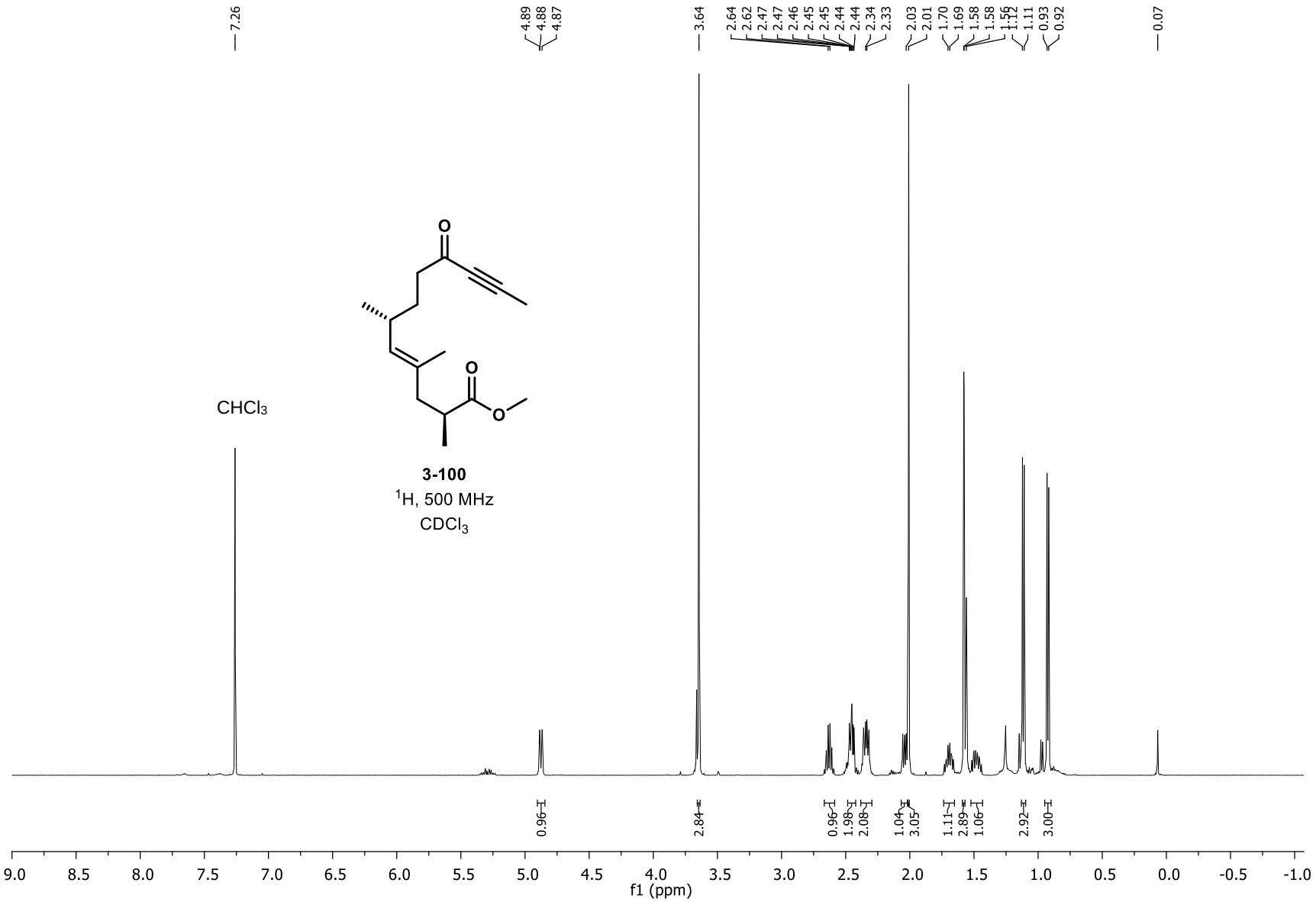
7.26
4.89
4.88
4.87
3.64
2.64
2.62
2.47
2.47
2.46
2.45
2.45
2.44
2.44
2.34
2.33
2.03
2.01
1.70
1.69
1.58
1.58
1.56
1.12
1.11
0.93
0.92
0.07
CHCl3
O
O
O
3-100
1H, 500 MHz
CDCl3
0.96
2.84
0.96
1.98
2.08
1.04
3.05
1.11
2.89
1.06
2.92
3.00
9.0
8.5
8.0
7.5
7.0
6.5
6.0
5.5
5.0
4.5
4.0
3.5
3.0
2.5
2.0
1.5
1.0
0.5
0.0
-0.5
-1.0
f1 (ppm)

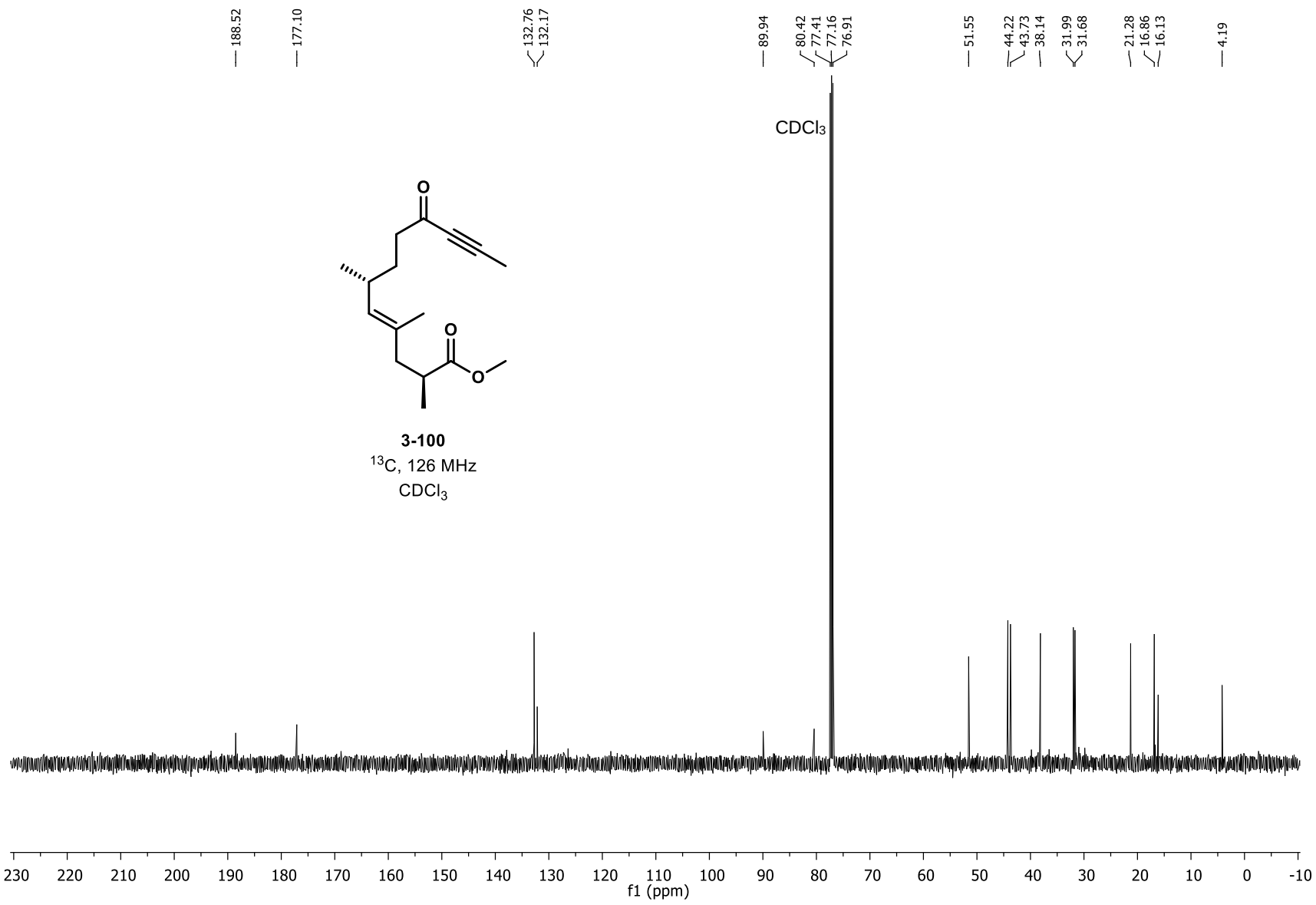
188.52
177.10
132.76
132.17
89.94
80.42
77.41
77.16
76.91
51.55
44.22
43.73
38.14
31.99
31.68
21.28
16.86
16.13
4.19
CDCl3
O
O
O
3-100
13C, 126 MHz
CDCl3
230 220 210 200 190 180 170 160 150 140 130 120 110 100 90 80 70 60 50 40 30 20 10 0 -10
f1 (ppm)

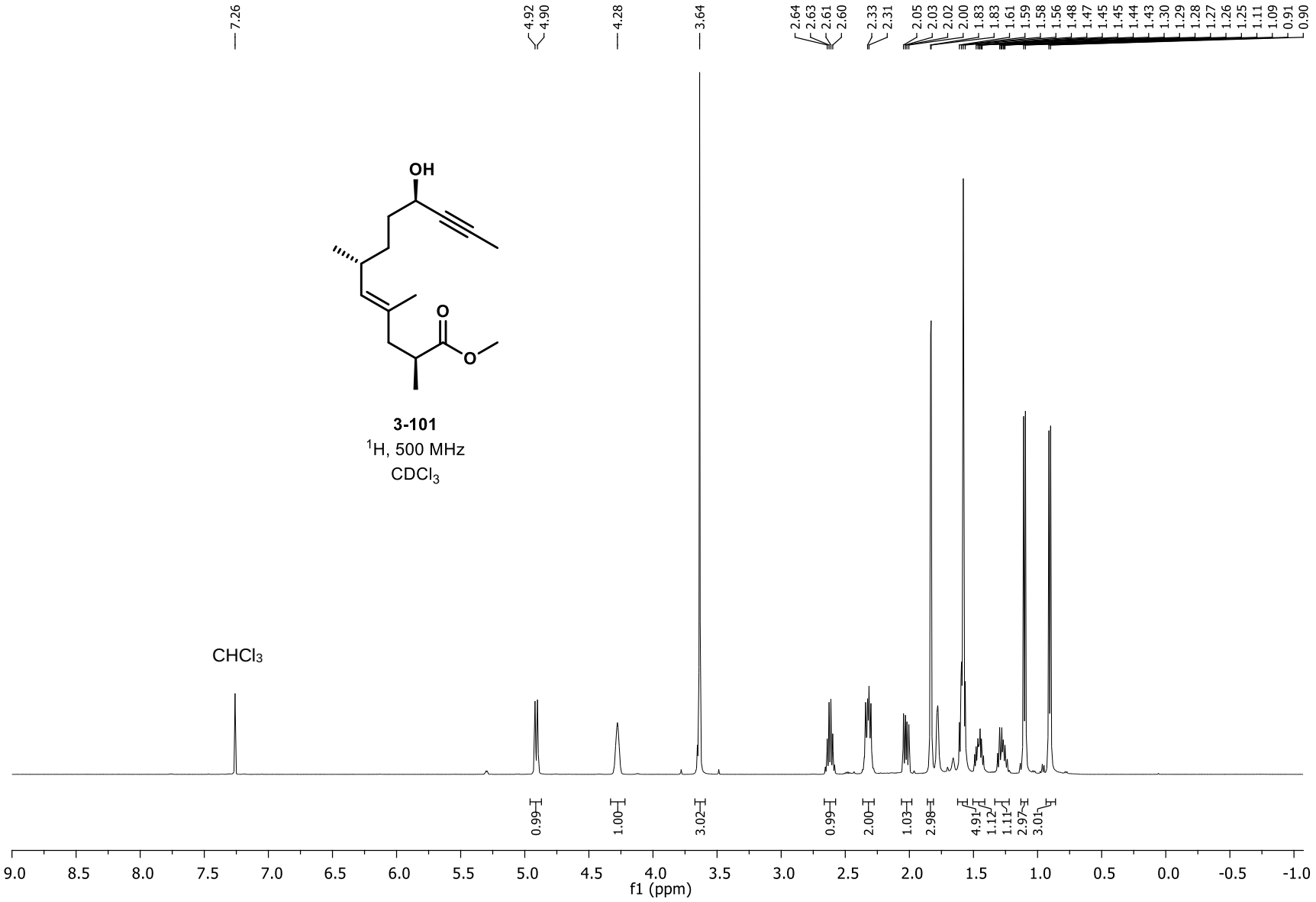
7.26
4.92
4.90
4.28
3.64
2.64
2.63
2.61
2.60
2.33
2.31
2.05
2.03
2.02
2.00
1.83
1.83
1.61
1.59
1.58
1.56
1.48
1.47
1.45
1.45
1.44
1.43
1.30
1.29
1.28
1.27
1.26
1.25
1.11
1.09
0.91
0.90
OH
O
O
3-101
1H, 500 MHz
CDCl3
CHCl3
0.99
1.00
3.02
0.99
2.00
1.03
2.98
4.91
1.12
1.11
2.97
3.01
9.0
8.5
8.0
7.5
7.0
6.5
6.0
5.5
5.0
4.5
4.0
3.5
3.0
2.5
2.0
1.5
1.0
0.5
0.0
-0.5
-1.0
f1 (ppm)

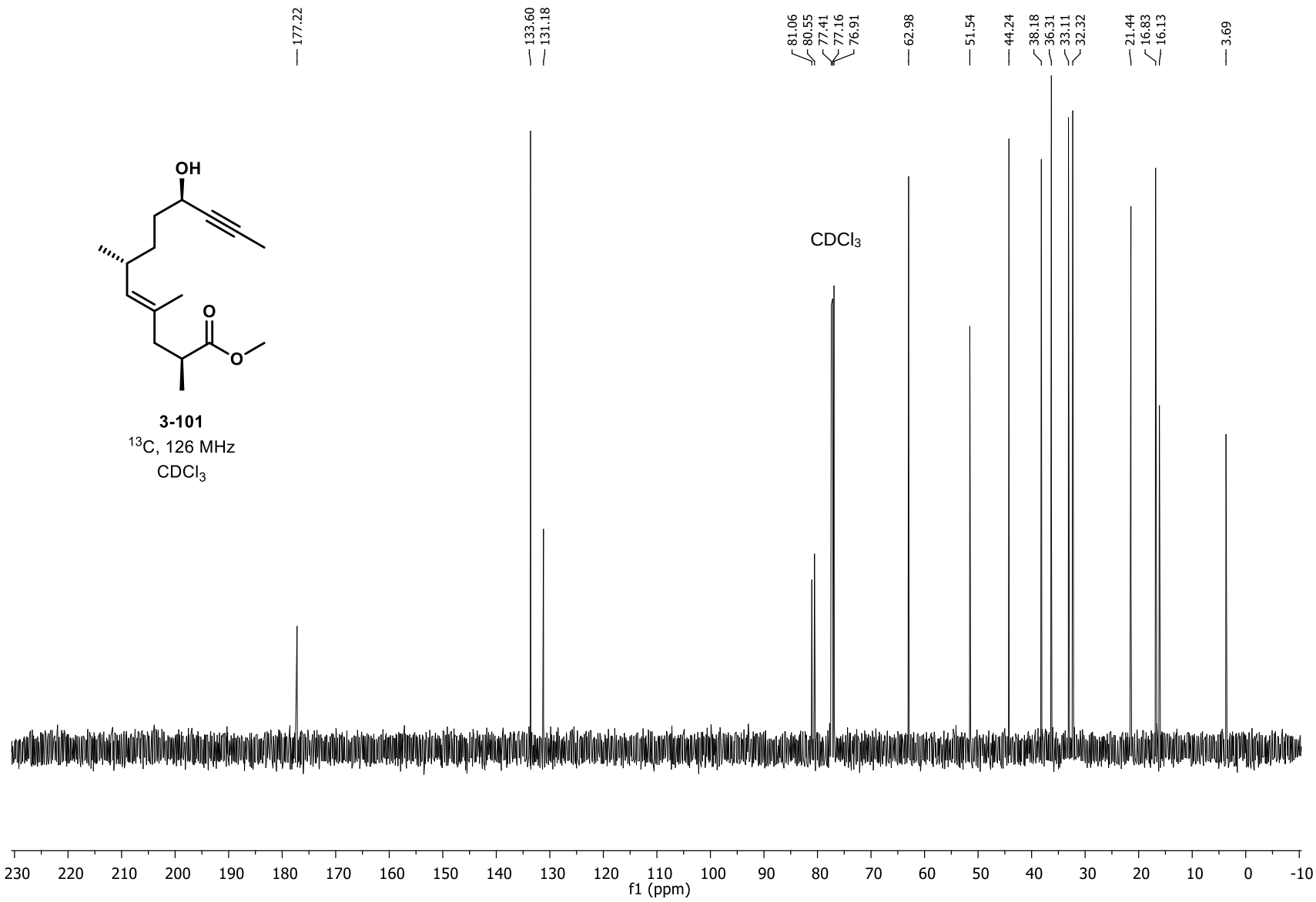
177.22
133.60
131.18
81.06
80.55
77.41
77.16
76.91
62.98
51.54
44.24
38.18
36.31
33.11
32.32
21.44
16.83
16.13
3.69
CDCl3
OH
O
O
3-101
13C, 126 MHz
CDCl3
230 220 210 200 190 180 170 160 150 140 130 120 110 100 90 80 70 60 50 40 30 20 10 0 -10
f1 (ppm)

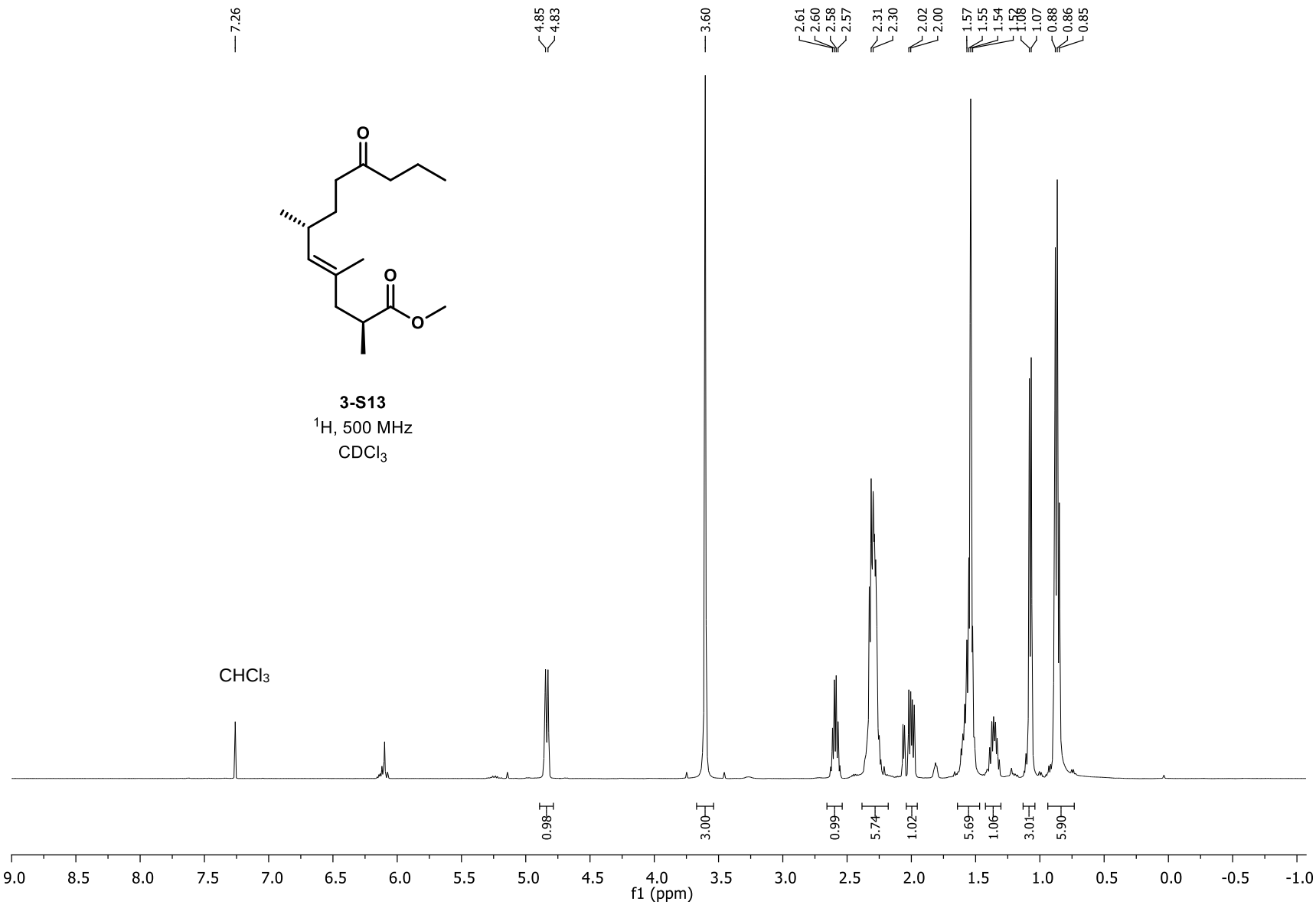
7.26
4.85
4.83
3.60
2.61
2.60
2.58
2.57
2.31
2.30
2.02
2.00
1.57
1.55
1.54
1.08
1.07
0.88
0.86
0.85
O
O
O
3-S13
1H, 500 MHz
CDCl3
CHCl3
0.98
3.00
0.99
5.74
1.02
5.69
1.06
3.01
5.90
9.0
8.5
8.0
7.5
7.0
6.5
6.0
5.5
5.0
4.5
4.0
3.5
3.0
2.5
2.0
1.5
1.0
0.5
0.0
-0.5
-1.0
f1 (ppm)

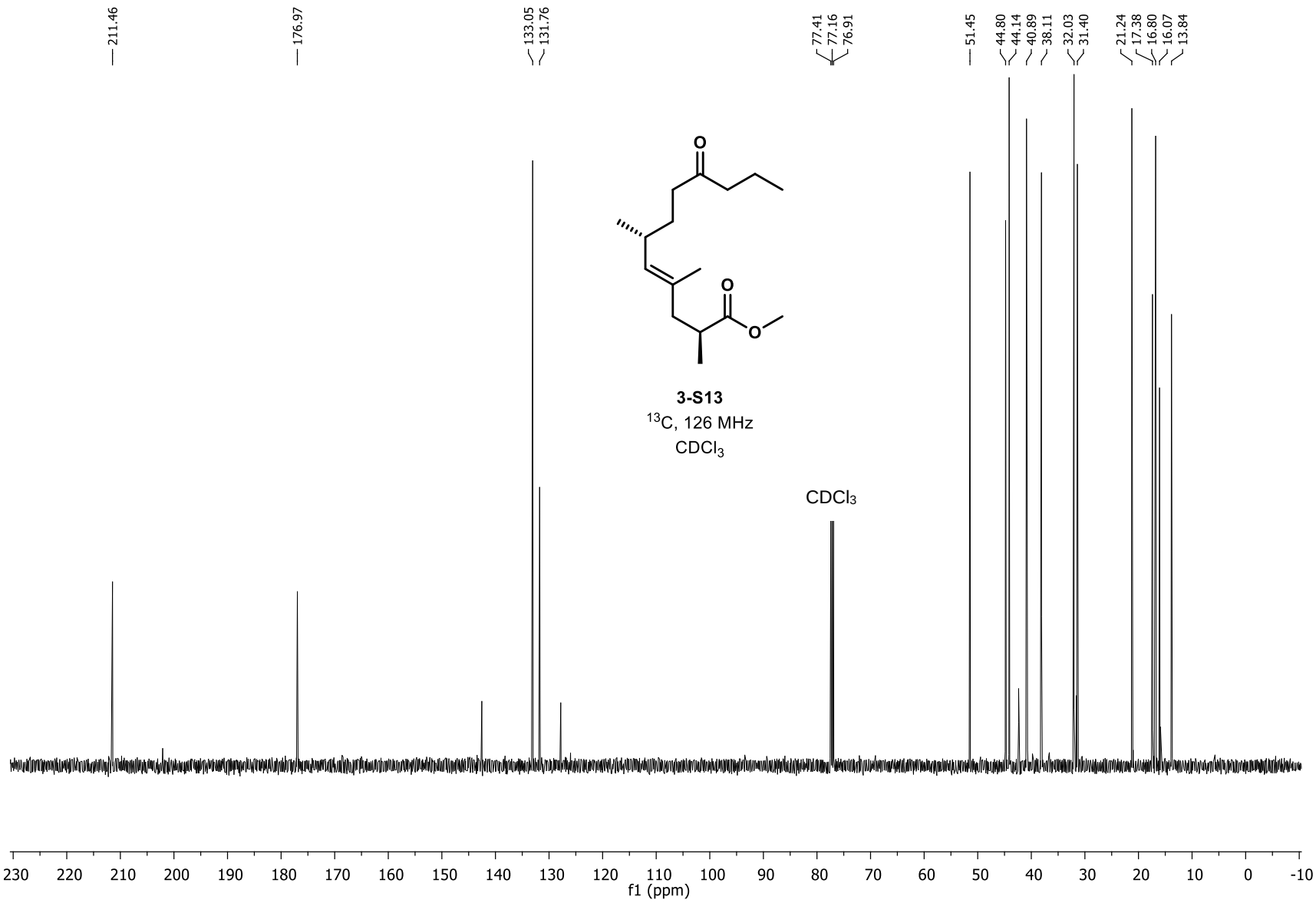
211.46
176.97
133.05
131.76
77.41
77.16
76.91
51.45
44.80
44.14
40.89
38.11
32.03
31.40
21.24
17.38
16.80
16.07
13.84
O
O
O
3-S13
13C, 126 MHz
CDCl3
CDCl3
230 220 210 200 190 180 170 160 150 140 130 120 110 100 90 80 70 60 50 40 30 20 10 0 -10
f1 (ppm)

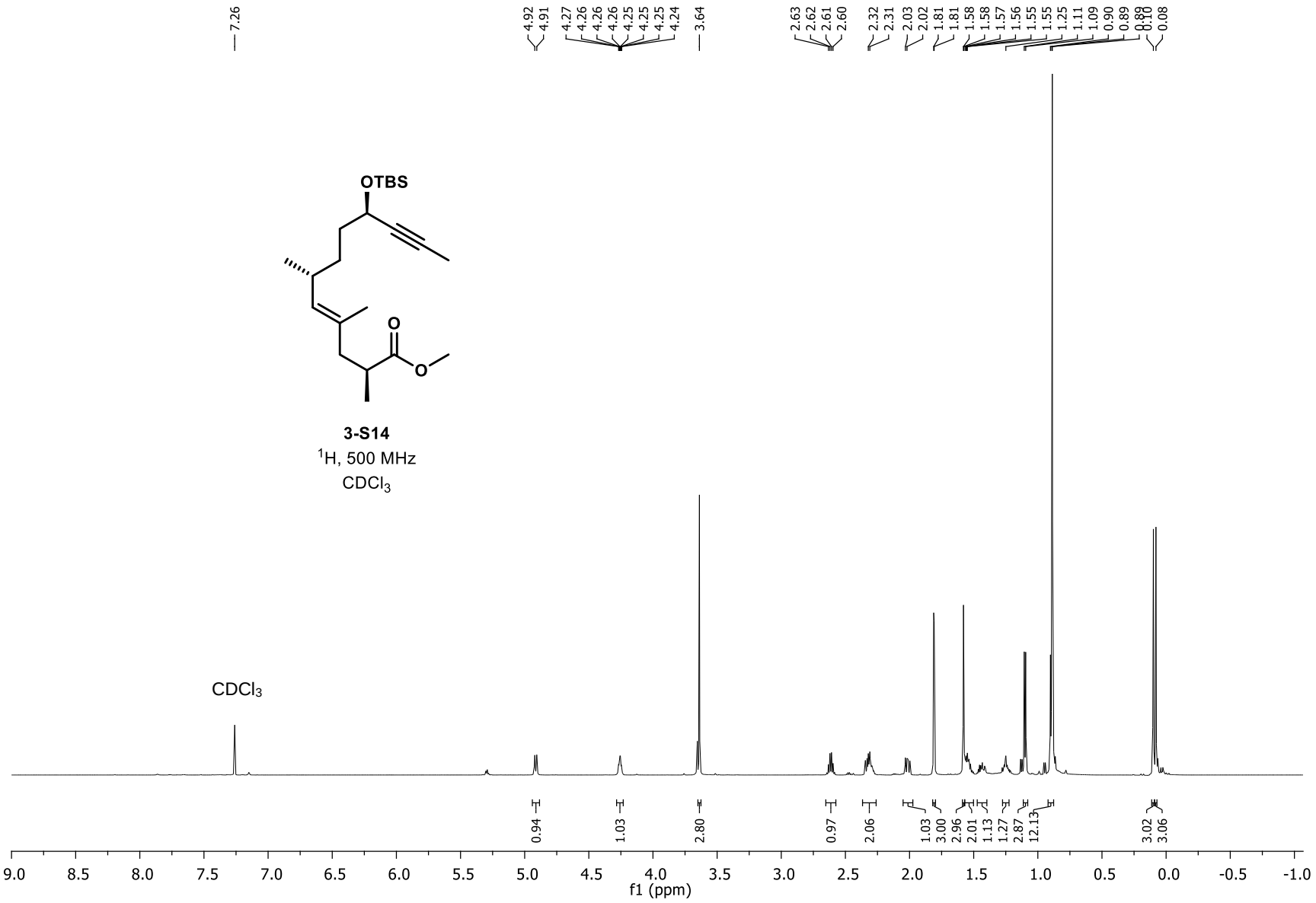
7.26
4.92
4.91
4.27
4.26
4.26
4.26
4.25
4.25
4.25
4.24
3.64
2.63
2.62
2.61
2.60
2.32
2.31
2.03
2.02
1.81
1.81
1.58
1.58
1.57
1.56
1.55
1.55
1.25
1.11
1.09
0.90
0.89
0.89
0.10
0.08
OTBS
O
O
3-S14
1H, 500 MHz
CDCl3
CDCl3
0.94
1.03
2.80
0.97
2.06
1.03
3.00
2.96
2.01
1.13
1.27
2.87
12.13
3.02
3.06
9.0
8.5
8.0
7.5
7.0
6.5
6.0
5.5
5.0
4.5
4.0
3.5
3.0
2.5
2.0
1.5
1.0
0.5
0.0
-0.5
-1.0
f1 (ppm)

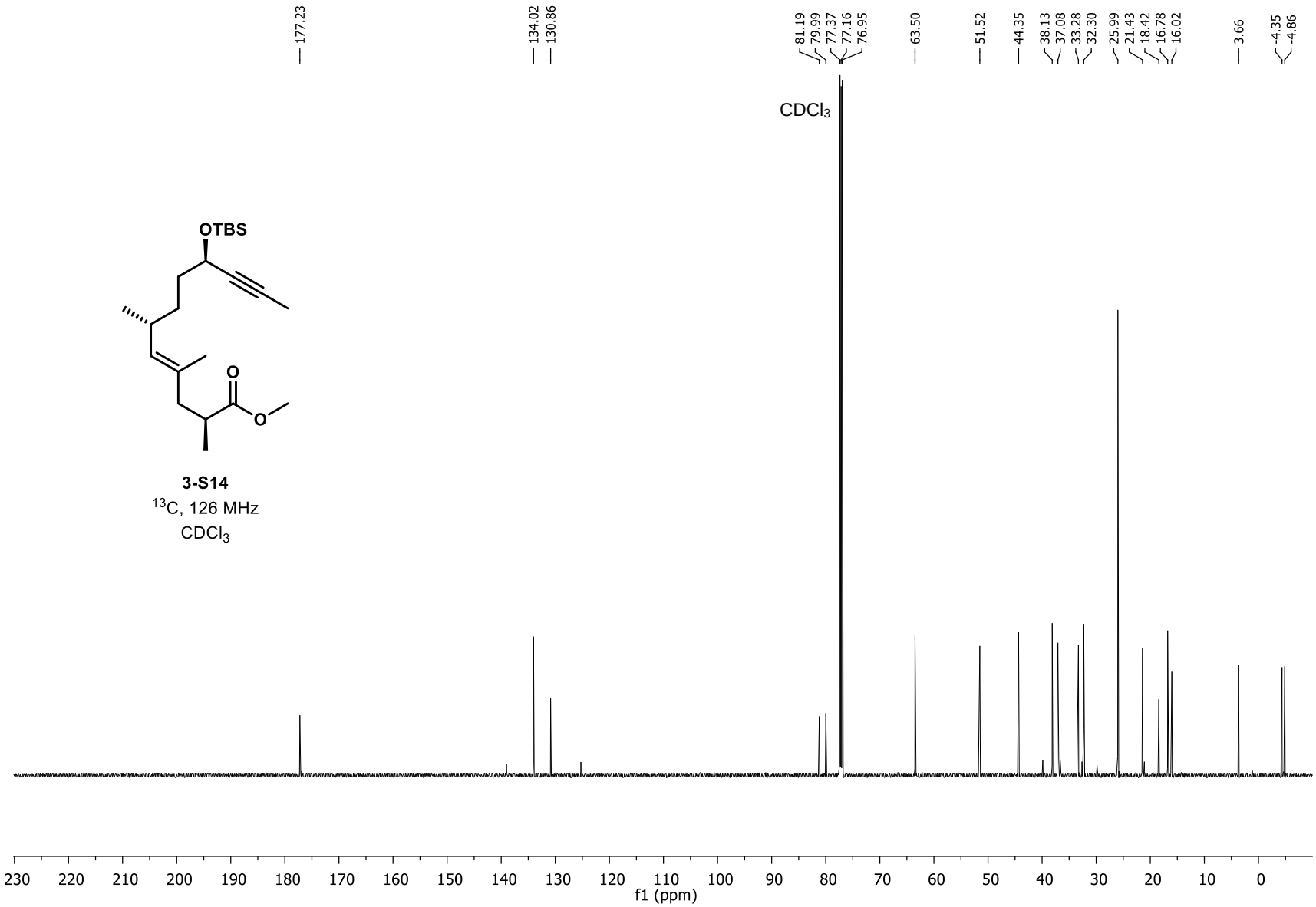
177.23
134.02
130.86
81.19
79.99
77.37
77.16
76.95
63.50
51.52
44.35
38.13
37.08
33.28
32.30
25.99
21.43
18.42
16.78
16.02
3.66
-4.35
-4.86
CDCl3
OTBS
O
O
3-S14
13C, 126 MHz
CDCl3
230 220 210 200 190 180 170 160 150 140 130 120 110 100 90 80 70 60 50 40 30 20 10 0
f1 (ppm)

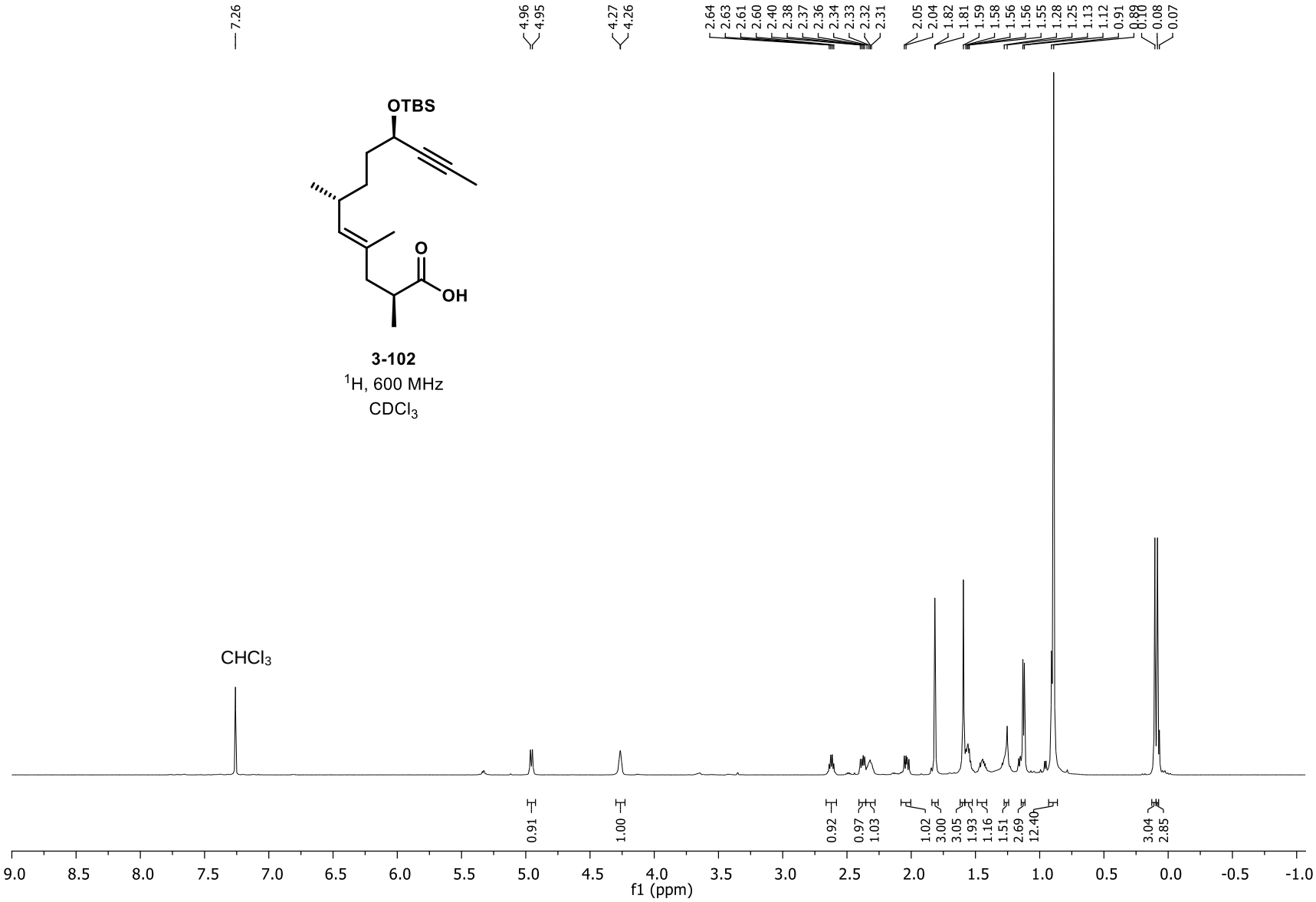
7.26
4.96
4.95
4.27
4.26
2.64
2.63
2.61
2.60
2.40
2.38
2.37
2.36
2.34
2.33
2.32
2.31
2.05
2.04
1.82
1.81
1.59
1.58
1.56
1.56
1.55
1.28
1.25
1.13
1.12
0.91
0.89
0.10
0.08
0.07
OTBS
O
OH
3-102
1H, 600 MHz
CDCl3
CHCl3
0.91
1.00
0.92
0.97
1.03
1.02
3.00
3.05
1.93
1.16
1.51
2.69
12.40
3.04
2.85
9.0
8.5
8.0
7.5
7.0
6.5
6.0
5.5
5.0
4.5
4.0
3.5
3.0
2.5
2.0
1.5
1.0
0.5
0.0
-0.5
-1.0
f1 (ppm)

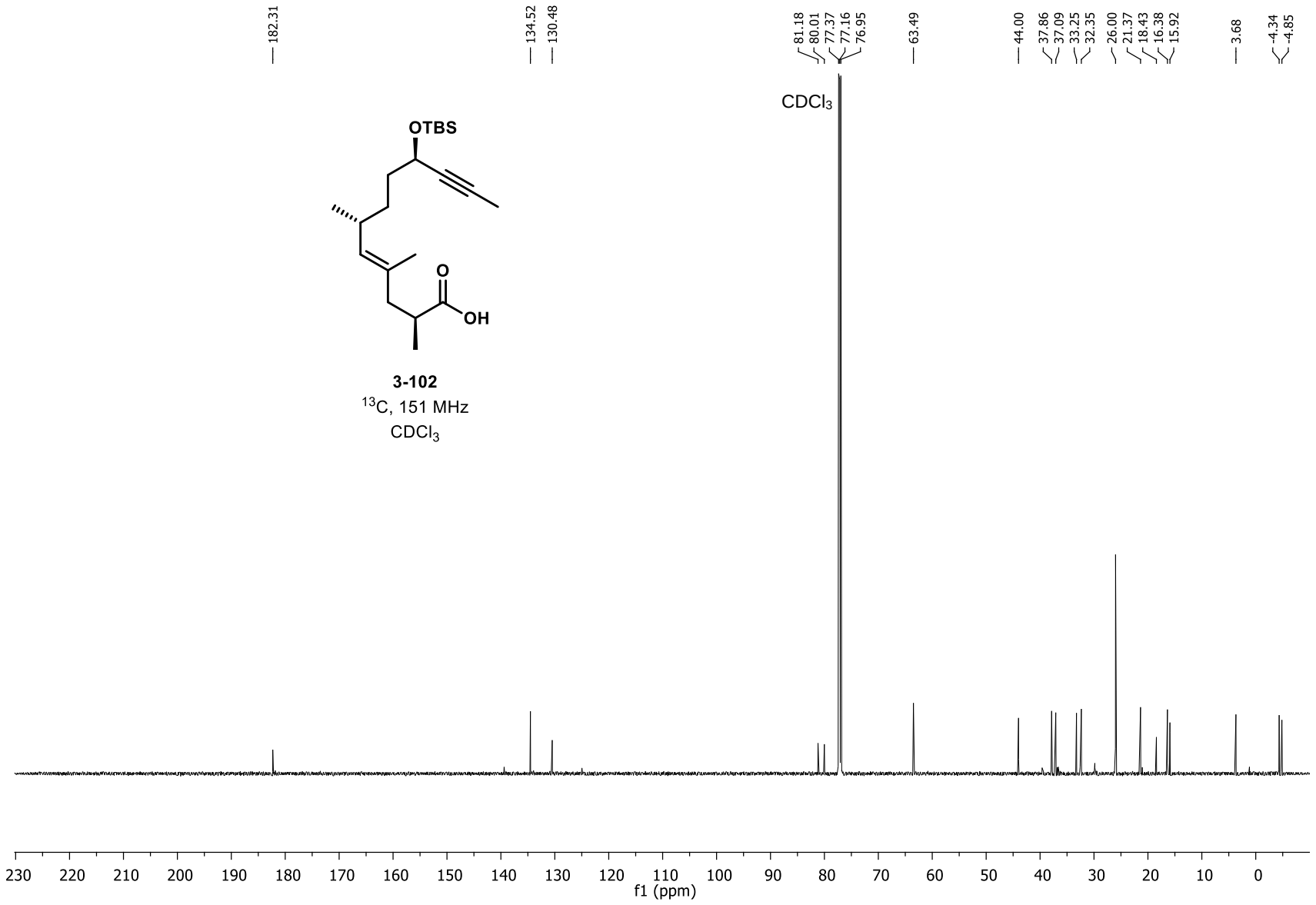
182.31
134.52
130.48
81.18
80.01
77.37
77.16
76.95
63.49
44.00
37.86
37.09
33.25
32.35
26.00
21.37
18.43
16.38
15.92
3.68
-4.34
-4.85
CDCl3
OTBS
O
OH
3-102
13C, 151 MHz
CDCl3
230 220 210 200 190 180 170 160 150 140 130 120 110 100 90 80 70 60 50 40 30 20 10 0
f1 (ppm)

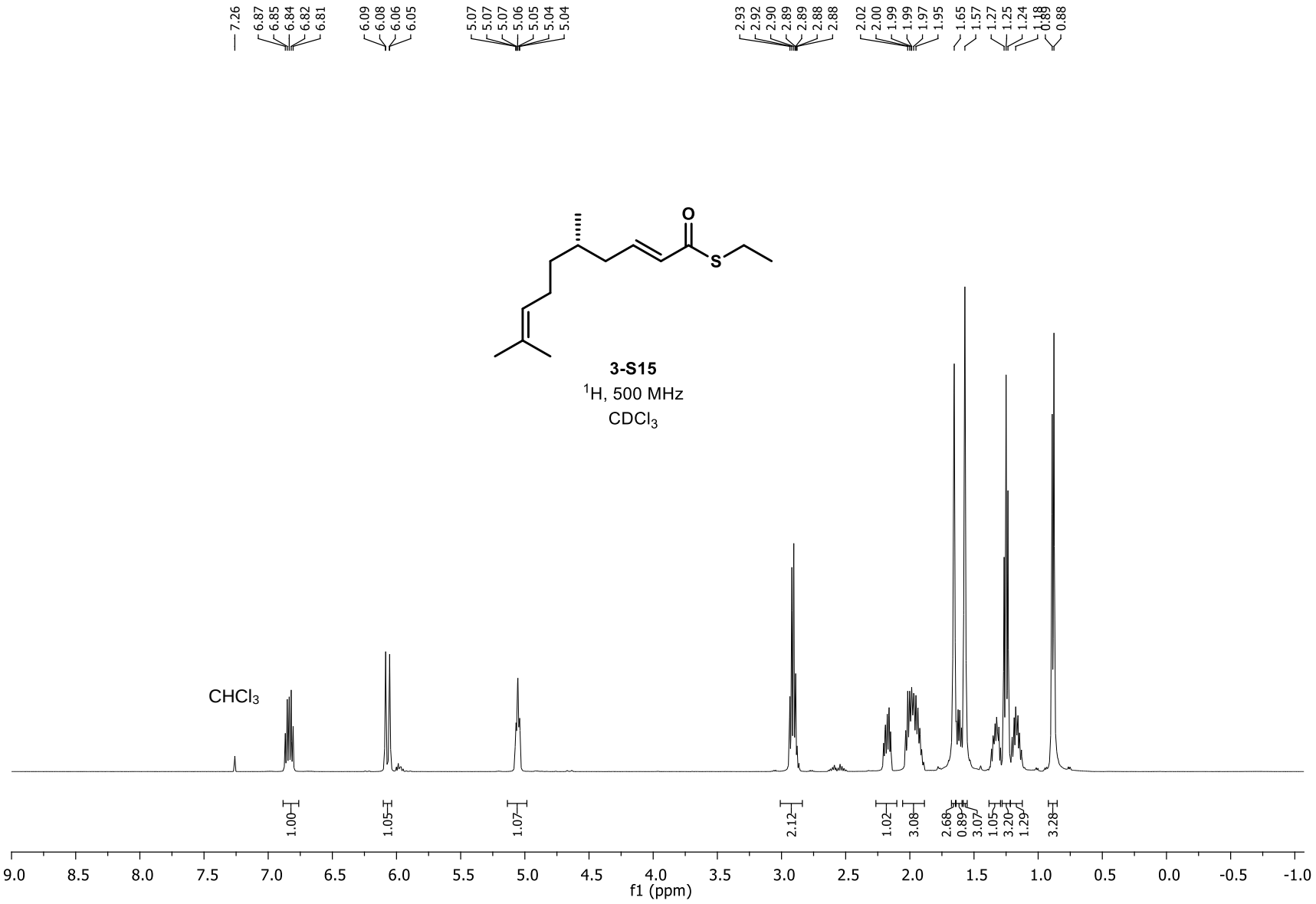
7.26
6.87
6.85
6.84
6.82
6.81
6.09
6.08
6.06
6.05
5.07
5.07
5.07
5.06
5.05
5.04
5.04
2.93
2.92
2.90
2.89
2.89
2.88
2.88
2.02
2.00
1.99
1.99
1.97
1.95
1.65
1.57
1.27
1.25
1.24
0.89
0.88
O
S
3-S15
1H, 500 MHz
CDCl3
CHCl3
1.00
1.05
1.07
2.12
1.02
3.08
2.68
0.89
3.07
1.05
3.20
1.29
3.28
9.0
8.5
8.0
7.5
7.0
6.5
6.0
5.5
5.0
4.5
4.0
3.5
3.0
2.5
2.0
1.5
1.0
0.5
0.0
-0.5
-1.0
f1 (ppm)

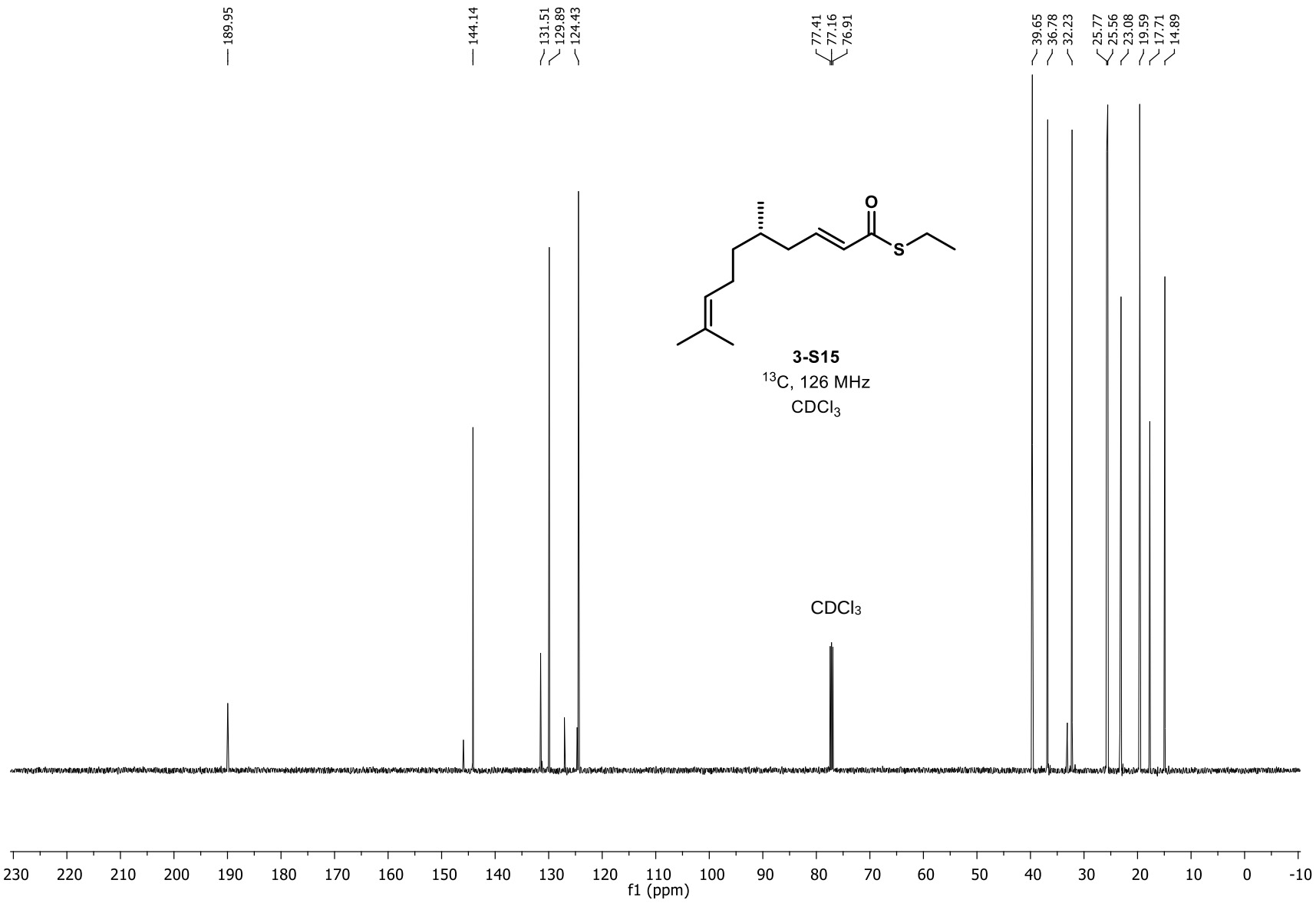
189.95
144.14
131.51
129.89
124.43
77.41
77.16
76.91
39.65
36.78
32.23
25.77
25.56
23.08
19.59
17.71
14.89
O
S
3-S15
13C, 126 MHz
CDCl3
CDCl3
230 220 210 200 190 180 170 160 150 140 130 120 110 100 90 80 70 60 50 40 30 20 10 0 -10
f1 (ppm)

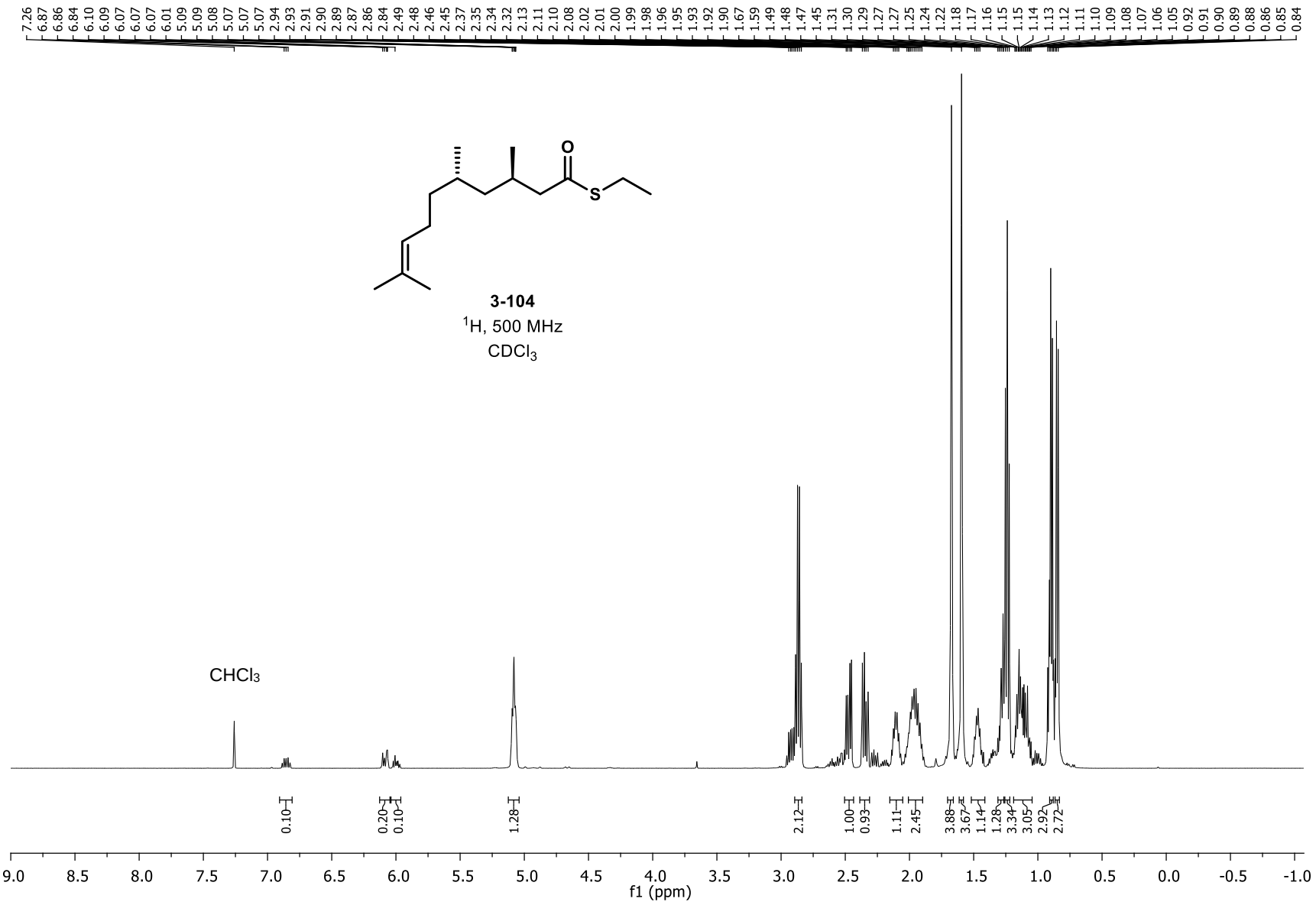
7.26 6.87 6.86 6.84 6.10 6.09 6.07 6.07 6.07 6.01 5.09 5.09 5.08 5.07 5.07 5.07 2.94 2.93 2.91 2.90 2.89 2.87 2.86 2.84 2.49 2.48 2.46 2.45 2.37 2.35 2.34 2.32 2.13 2.11 2.10 2.08 2.02 2.01 2.00 1.99 1.98 1.96 1.95 1.93 1.92 1.90 1.67 1.59 1.49 1.48 1.47 1.45 1.31 1.30 1.29 1.27 1.27 1.25 1.24 1.22 1.18 1.17 1.16 1.15 1.15 1.14 1.13 1.12 1.11 1.10 1.09 1.08 1.07 1.06 1.05 0.92 0.91 0.90 0.89 0.88 0.86 0.85 0.84
O
S
3-104
1H, 500 MHz
CDCl3
CHCl3
0.10 0.20 0.10 1.28 2.12 1.00 0.93 1.11 2.45 3.88 3.67 1.14 1.28 3.34 3.05 2.92 2.72
9.0 8.5 8.0 7.5 7.0 6.5 6.0 5.5 5.0 4.5 4.0 3.5 3.0 2.5 2.0 1.5 1.0 0.5 0.0 -0.5 -1.0
f1 (ppm)

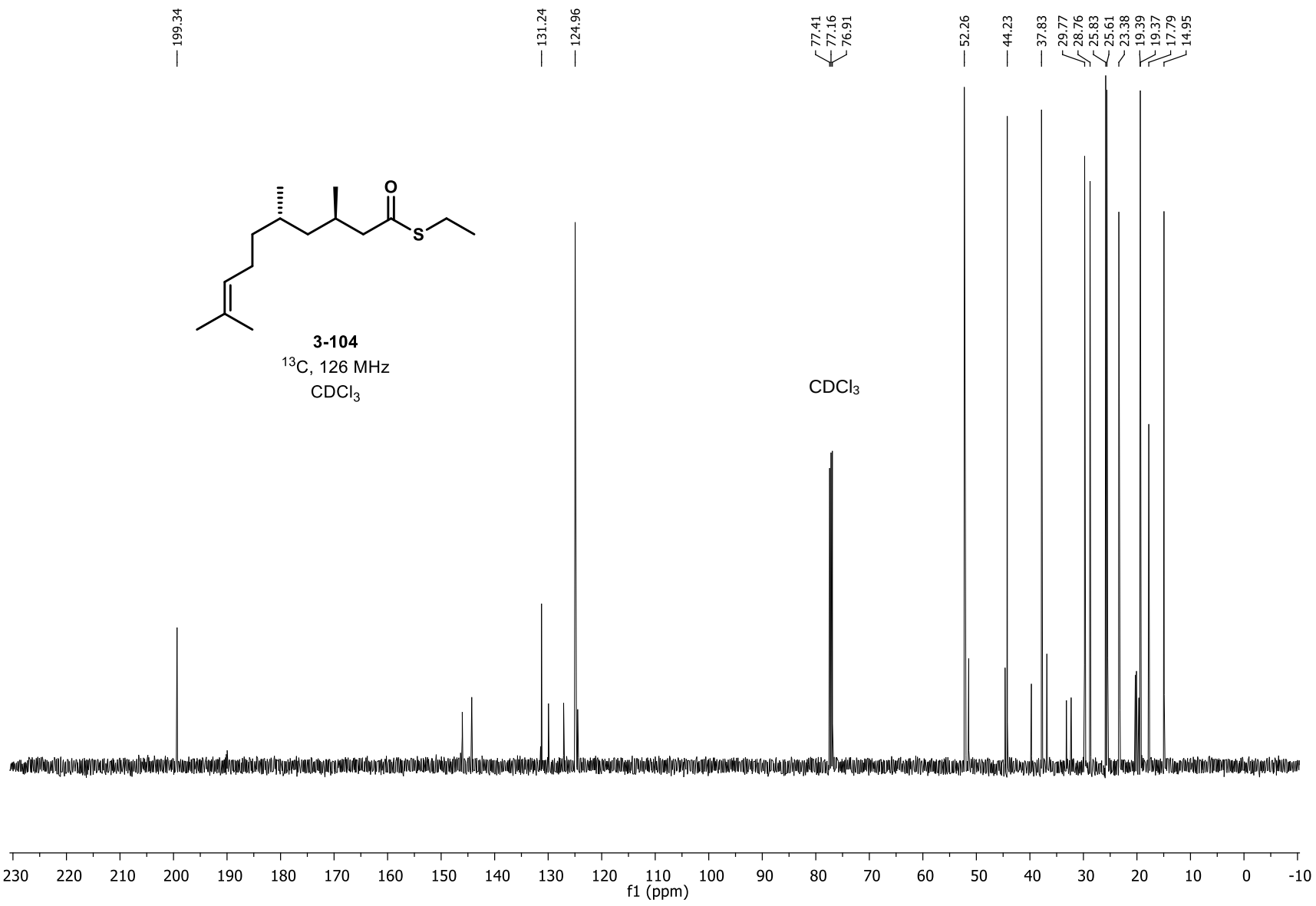
199.34
131.24
124.96
77.41
77.16
76.91
52.26
44.23
37.83
29.77
28.76
25.83
25.61
23.38
19.39
19.37
17.79
14.95
O
S
3-104
13C, 126 MHz
CDCl3
CDCl3
230 220 210 200 190 180 170 160 150 140 130 120 110 100 90 80 70 60 50 40 30 20 10 0 -10
f1 (ppm)

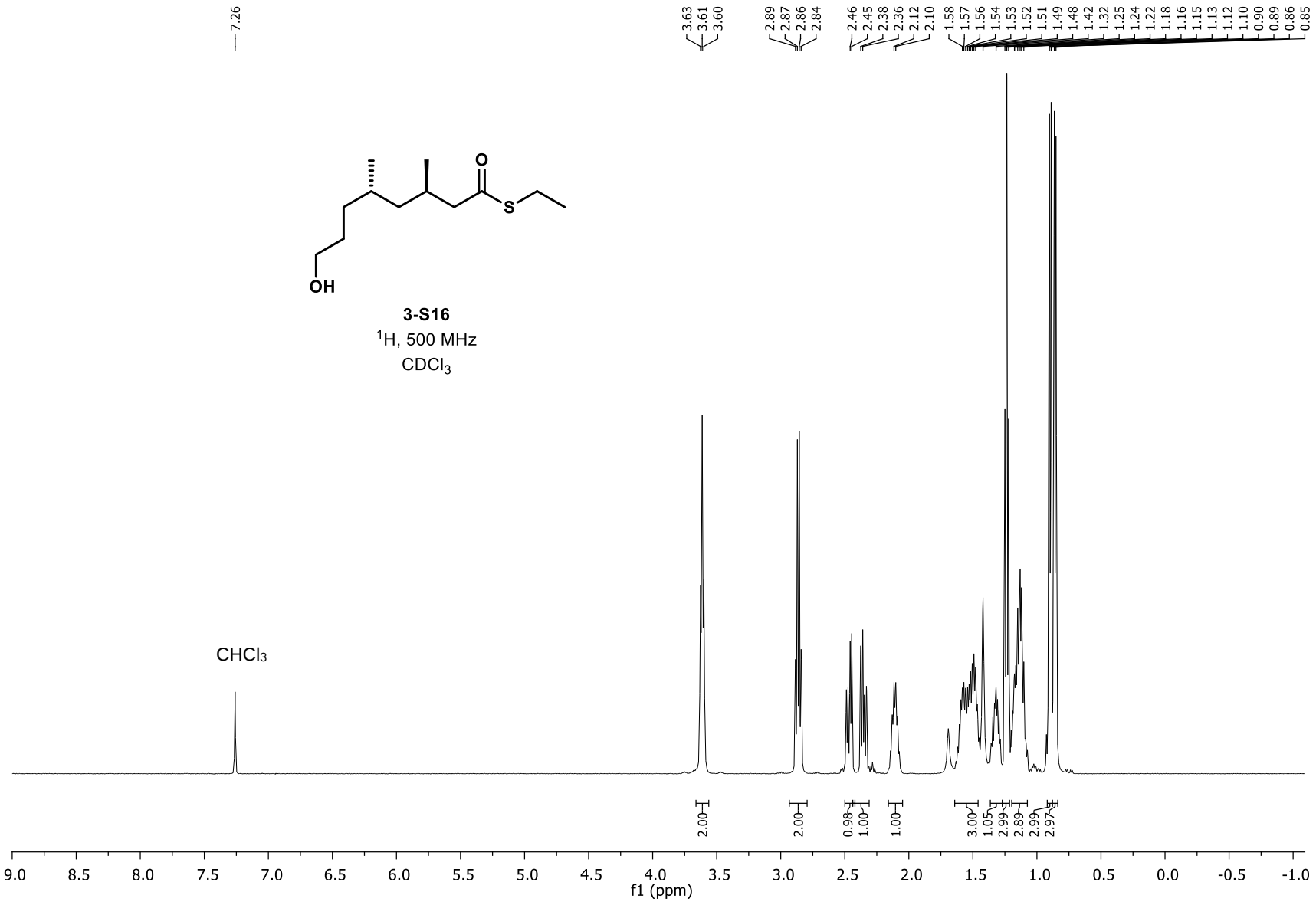
7.26
3.63
3.61
3.60
2.89
2.87
2.86
2.84
2.46
2.45
2.38
2.36
2.12
2.10
1.58
1.57
1.56
1.54
1.53
1.52
1.51
1.49
1.48
1.42
1.32
1.25
1.24
1.22
1.18
1.16
1.15
1.13
1.12
1.10
0.90
0.89
0.86
0.85
O
S
OH
3-S16
1H, 500 MHz
CDCl3
CHCl3
2.00
2.00
0.98
1.00
1.00
3.00
1.05
2.99
2.89
2.99
2.97
9.0
8.5
8.0
7.5
7.0
6.5
6.0
5.5
5.0
4.5
4.0
3.5
3.0
2.5
2.0
1.5
1.0
0.5
0.0
-0.5
-1.0
f1 (ppm)

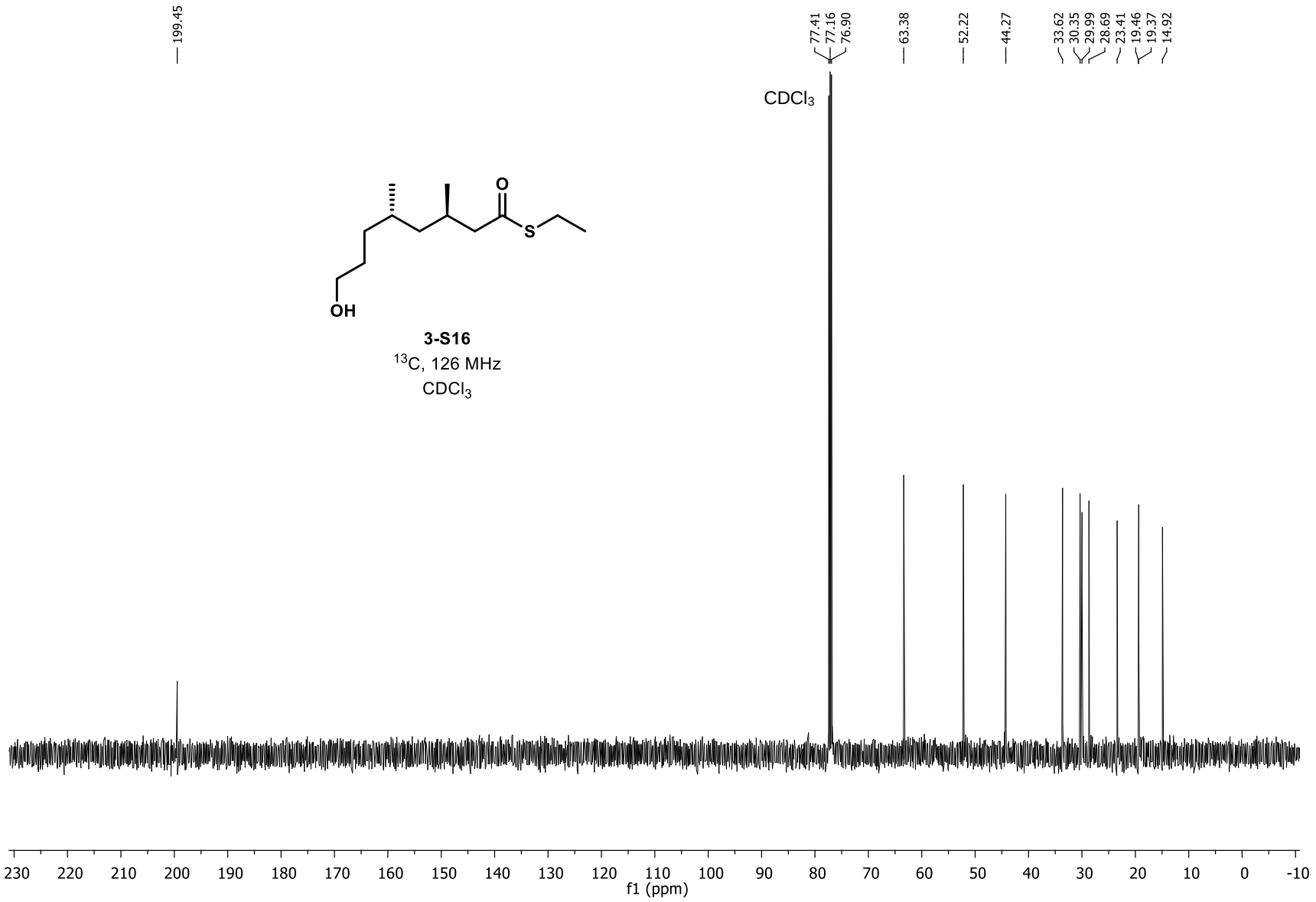
199.45
77.41
77.16
76.90
63.38
52.22
44.27
33.62
30.35
29.99
28.69
23.41
19.46
19.37
14.92
CDCl3
O
S
OH
3-S16
13C, 126 MHz
CDCl3
230 220 210 200 190 180 170 160 150 140 130 120 110 100 90 80 70 60 50 40 30 20 10 0 -10
f1 (ppm)

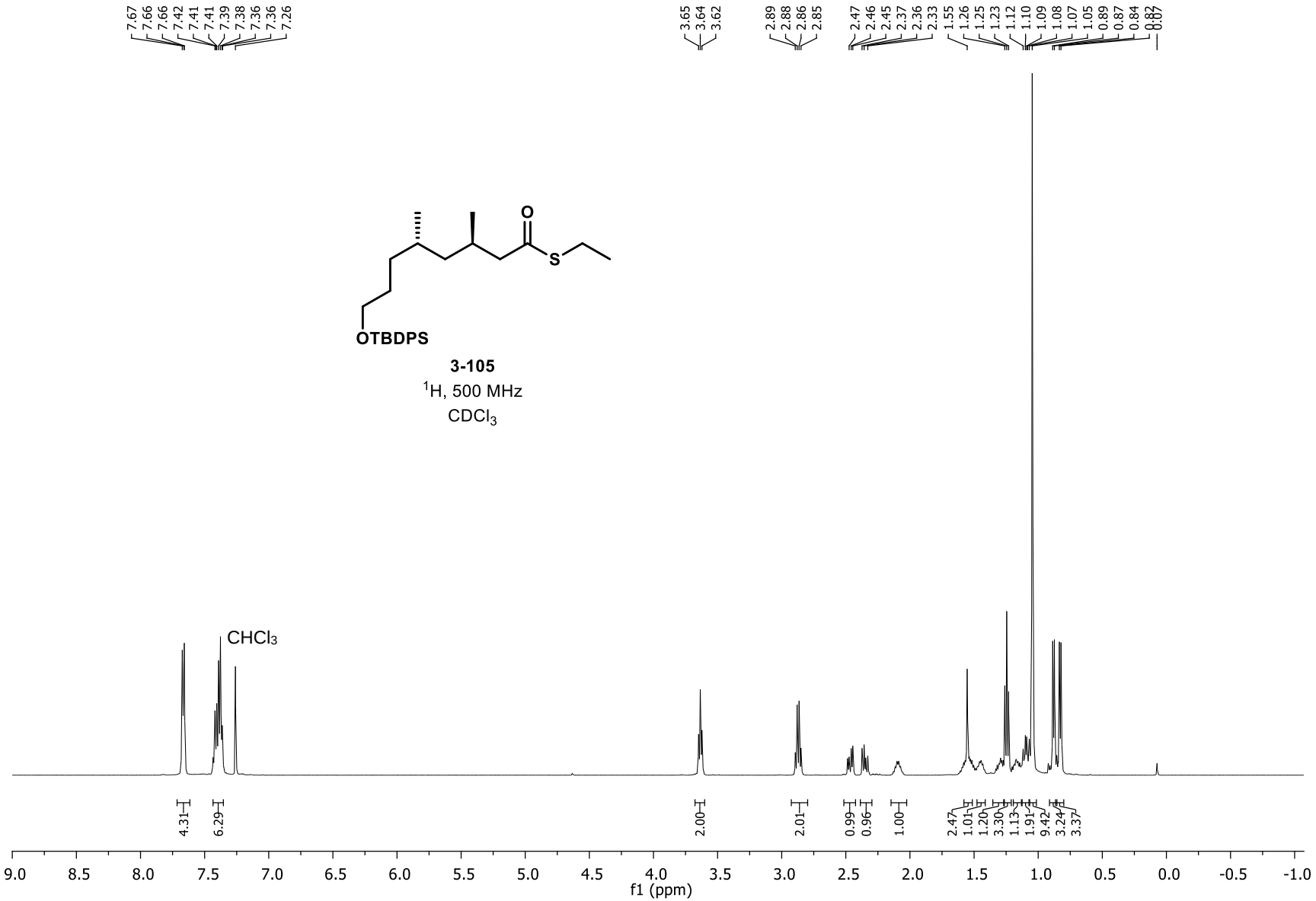
7.67
7.66
7.66
7.42
7.41
7.41
7.39
7.38
7.36
7.36
7.26
3.65
3.64
3.62
2.89
2.88
2.86
2.85
2.47
2.46
2.45
2.37
2.36
2.33
1.55
1.26
1.25
1.23
1.12
1.10
1.09
1.08
1.07
1.05
0.89
0.87
0.84
0.82
0.07
O
S
OTBDPS
3-105
1H, 500 MHz
CDCl3
CHCl3
4.31
6.29
2.00
2.01
0.99
0.96
1.00
2.47
1.01
1.20
3.30
1.13
1.91
9.42
3.24
3.37
9.0
8.5
8.0
7.5
7.0
6.5
6.0
5.5
5.0
4.5
4.0
3.5
3.0
2.5
2.0
1.5
1.0
0.5
0.0
-0.5
-1.0
f1 (ppm)

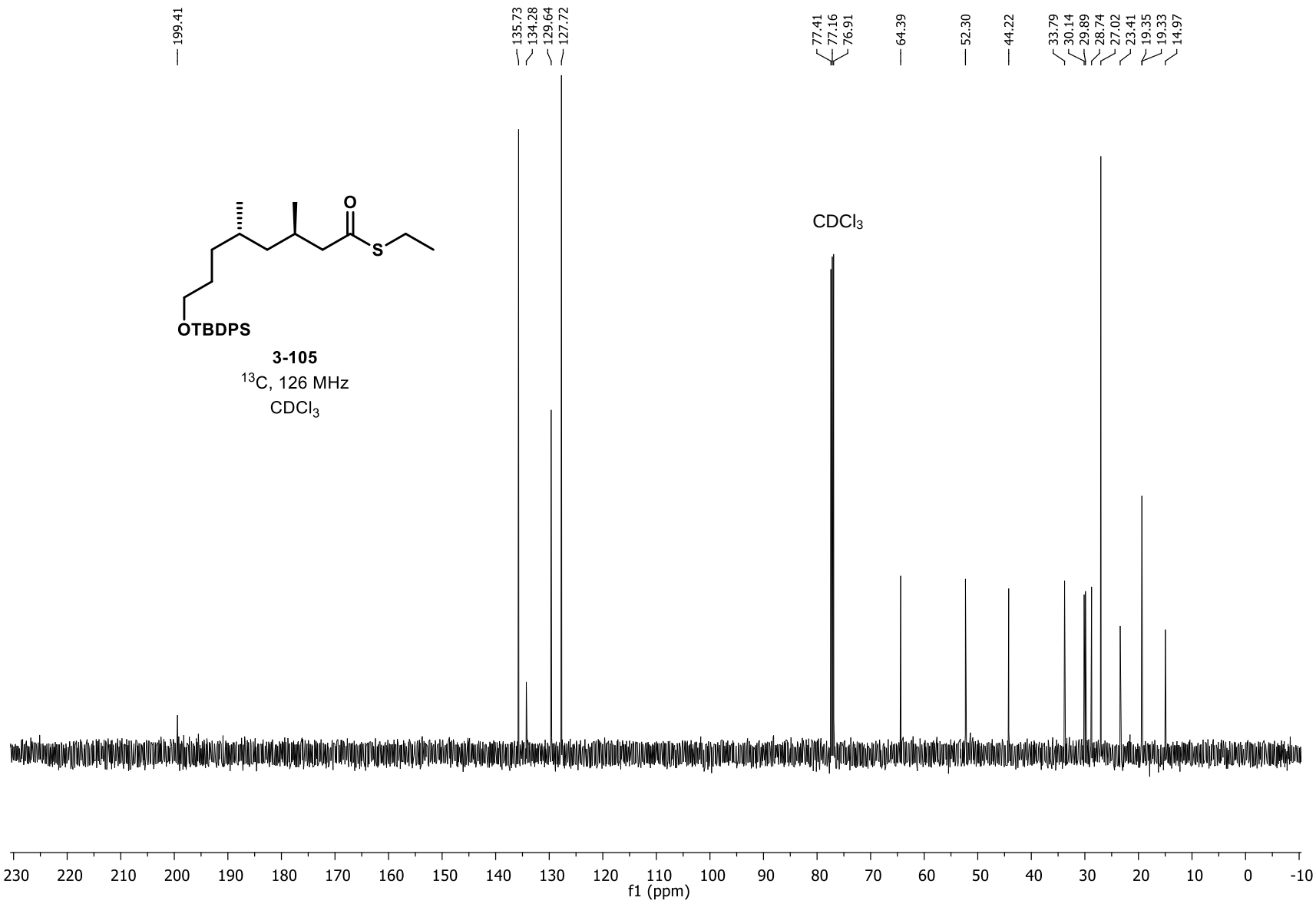
199.41
135.73
134.28
129.64
127.72
77.41
77.16
76.91
64.39
52.30
44.22
33.79
30.14
29.89
28.74
27.02
23.41
19.35
19.33
14.97
CDCl3
O
S
OTBDPS
3-105
13C, 126 MHz
CDCl3
230 220 210 200 190 180 170 160 150 140 130 120 110 100 90 80 70 60 50 40 30 20 10 0 -10
f1 (ppm)

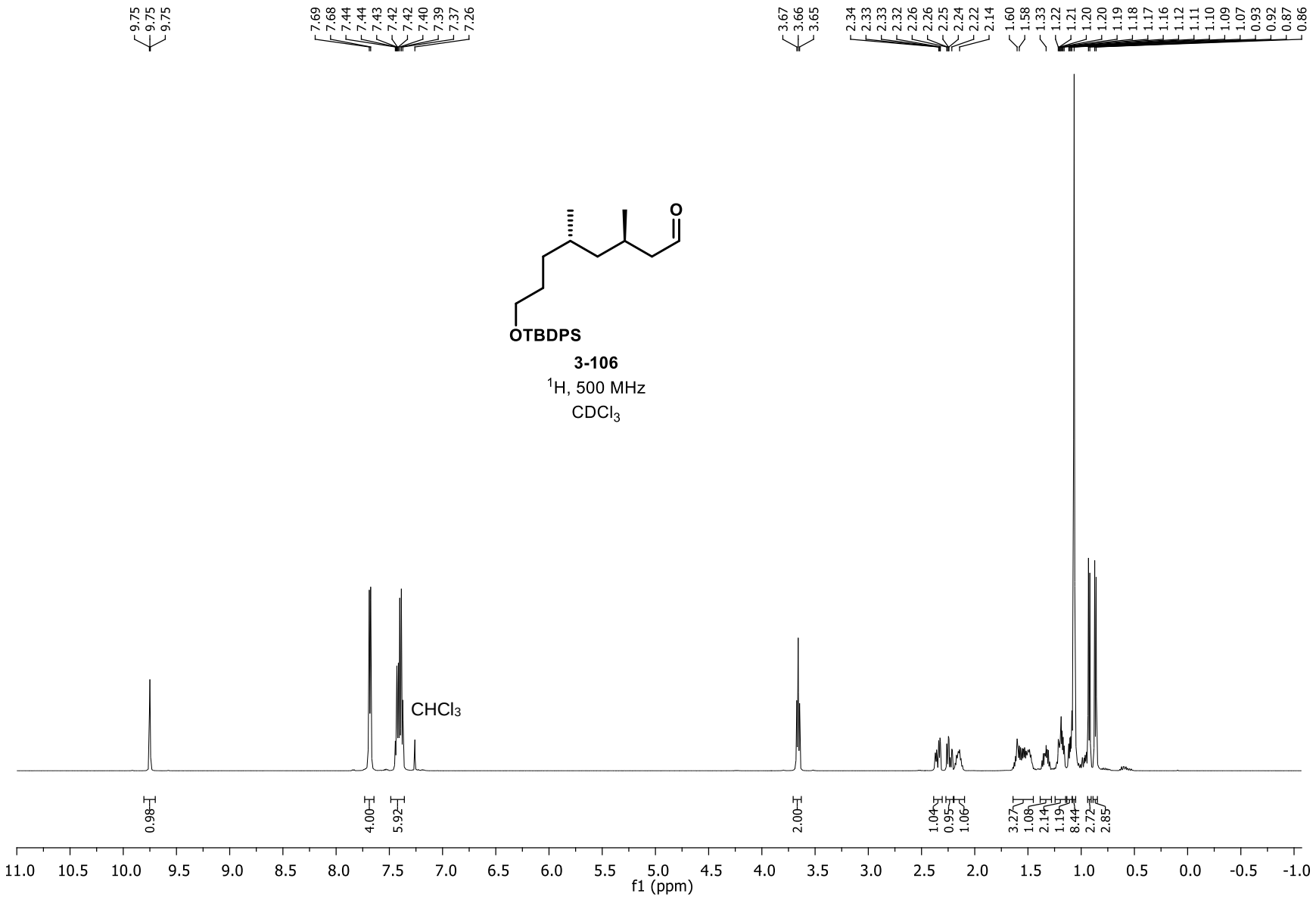
9.75
9.75
9.75
7.69
7.68
7.44
7.44
7.43
7.42
7.42
7.40
7.39
7.37
7.26
3.67
3.66
3.65
2.34
2.33
2.33
2.32
2.26
2.26
2.25
2.24
2.22
2.14
1.60
1.58
1.33
1.22
1.21
1.20
1.20
1.19
1.18
1.17
1.16
1.12
1.11
1.10
1.09
1.07
0.93
0.92
0.87
0.86
O
OTBDPS
3-106
1H, 500 MHz
CDCl3
CHCl3
0.98
4.00
5.92
2.00
1.04
0.95
1.06
3.27
1.08
2.14
1.19
8.44
2.72
2.85
11.0
10.5
10.0
9.5
9.0
8.5
8.0
7.5
7.0
6.5
6.0
5.5
5.0
4.5
4.0
3.5
3.0
2.5
2.0
1.5
1.0
0.5
0.0
-0.5
-1.0
f1 (ppm)

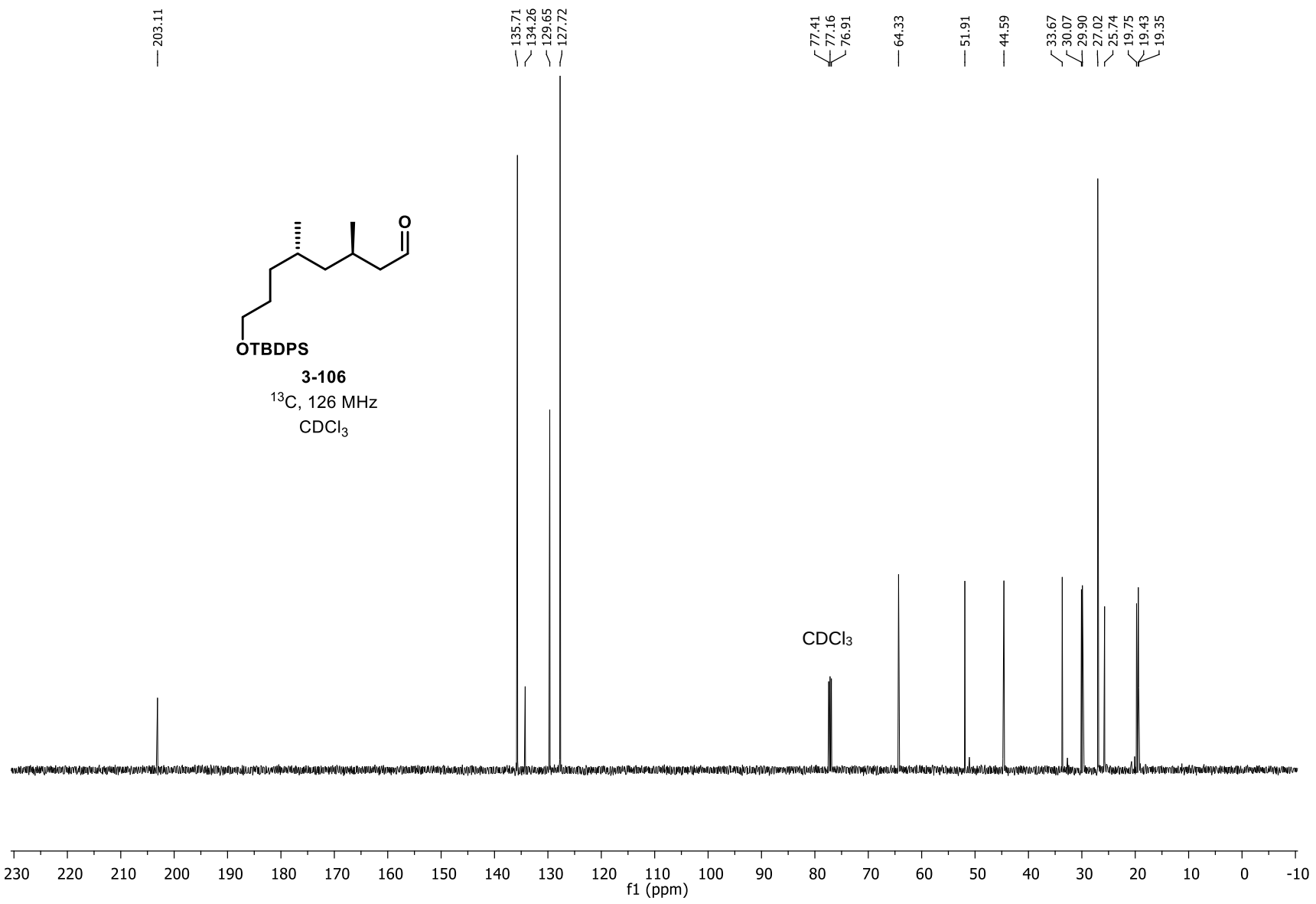
203.11
135.71
134.26
129.65
127.72
77.41
77.16
76.91
64.33
51.91
44.59
33.67
30.07
29.90
27.02
25.74
19.75
19.43
19.35
O
OTBDPS
3-106
13C, 126 MHz
CDCl3
CDCl3
230 220 210 200 190 180 170 160 150 140 130 120 110 100 90 80 70 60 50 40 30 20 10 0 -10
f1 (ppm)

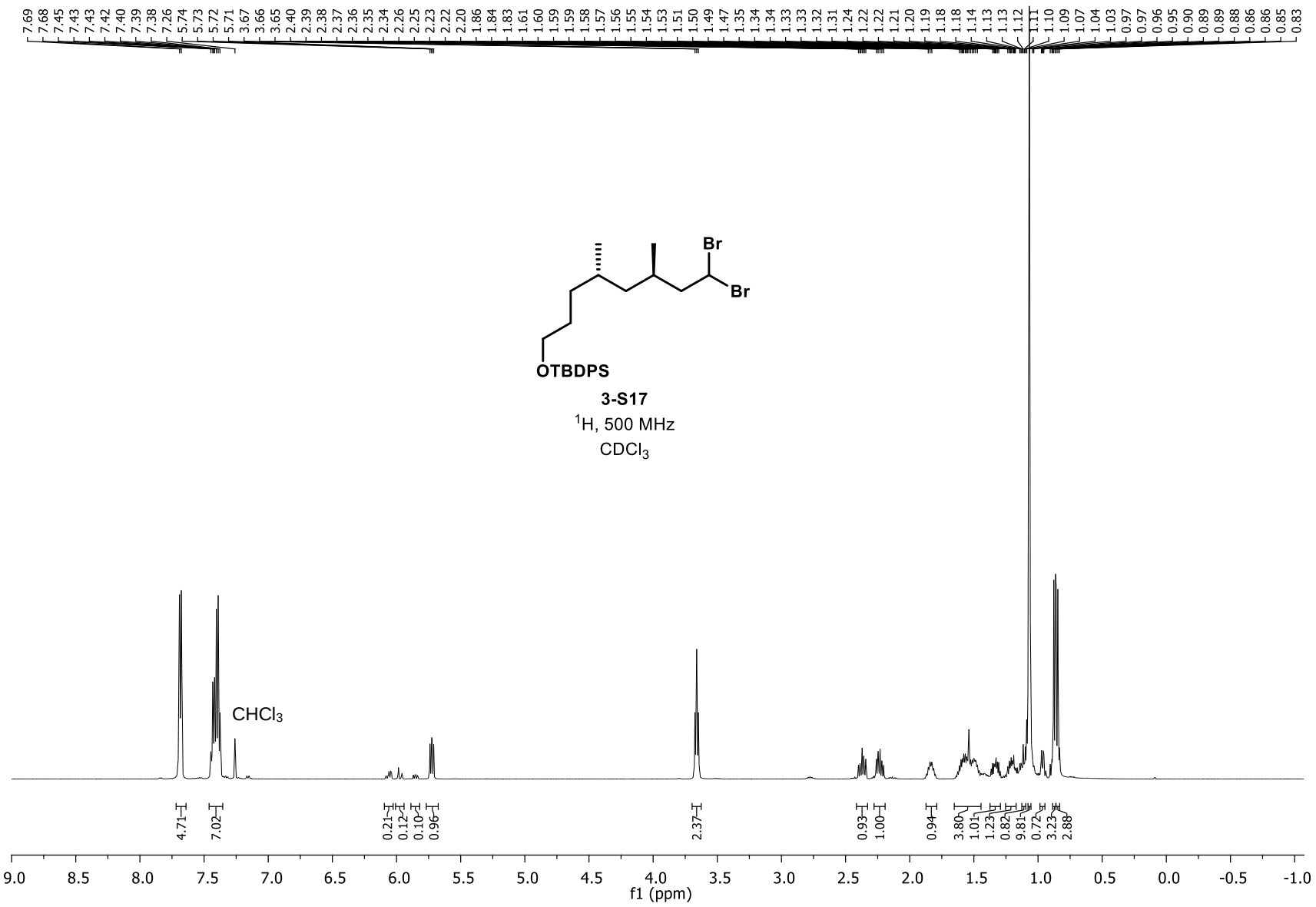
Br
Br
OTBDPS
3-S17
1H, 500 MHz
CDCl3
CHCl3
f1 (ppm)

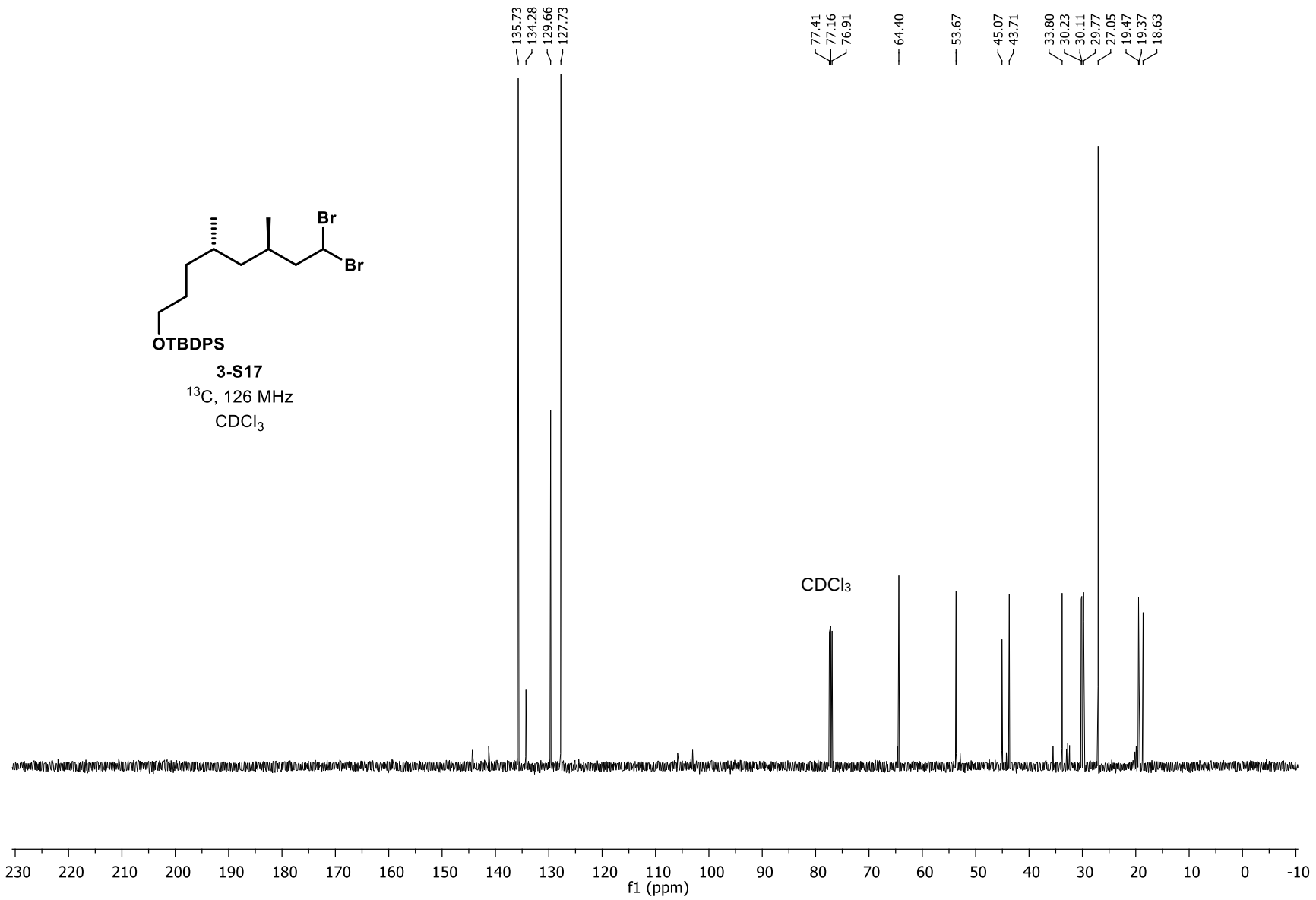
135.73
134.28
129.66
127.73
77.41
77.16
76.91
64.40
53.67
45.07
43.71
33.80
30.23
30.11
29.77
27.05
19.47
19.37
18.63
Br
Br
OTBDPS
3-S17
13C, 126 MHz
CDCl3
CDCl3
230 220 210 200 190 180 170 160 150 140 130 120 110 100 90 80 70 60 50 40 30 20 10 0 -10
f1 (ppm)

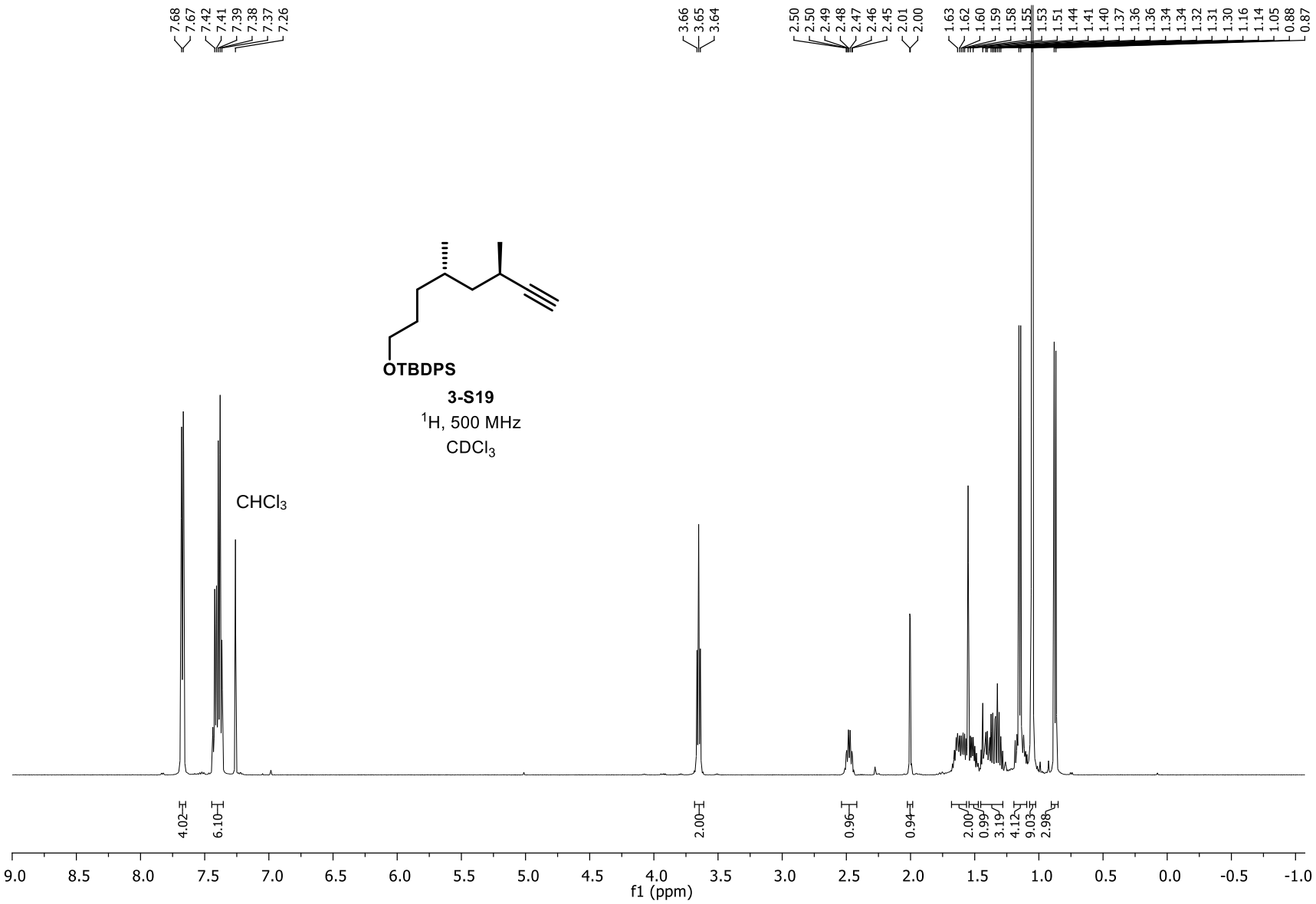
7.68
7.67
7.42
7.41
7.39
7.38
7.37
7.26
3.66
3.65
3.64
2.50
2.50
2.49
2.48
2.47
2.46
2.45
2.01
2.00
1.63
1.62
1.60
1.59
1.58
1.55
1.53
1.51
1.44
1.41
1.40
1.37
1.36
1.36
1.34
1.34
1.32
1.31
1.30
1.16
1.14
1.05
0.88
0.87
OTBDPS
3-S19
1H, 500 MHz
CDCl3
CHCl3
4.02
6.10
2.00
0.96
0.94
2.00
0.99
3.19
4.12
9.03
2.98
9.0
8.5
8.0
7.5
7.0
6.5
6.0
5.5
5.0
4.5
4.0
3.5
3.0
2.5
2.0
1.5
1.0
0.5
0.0
-0.5
-1.0
f1 (ppm)

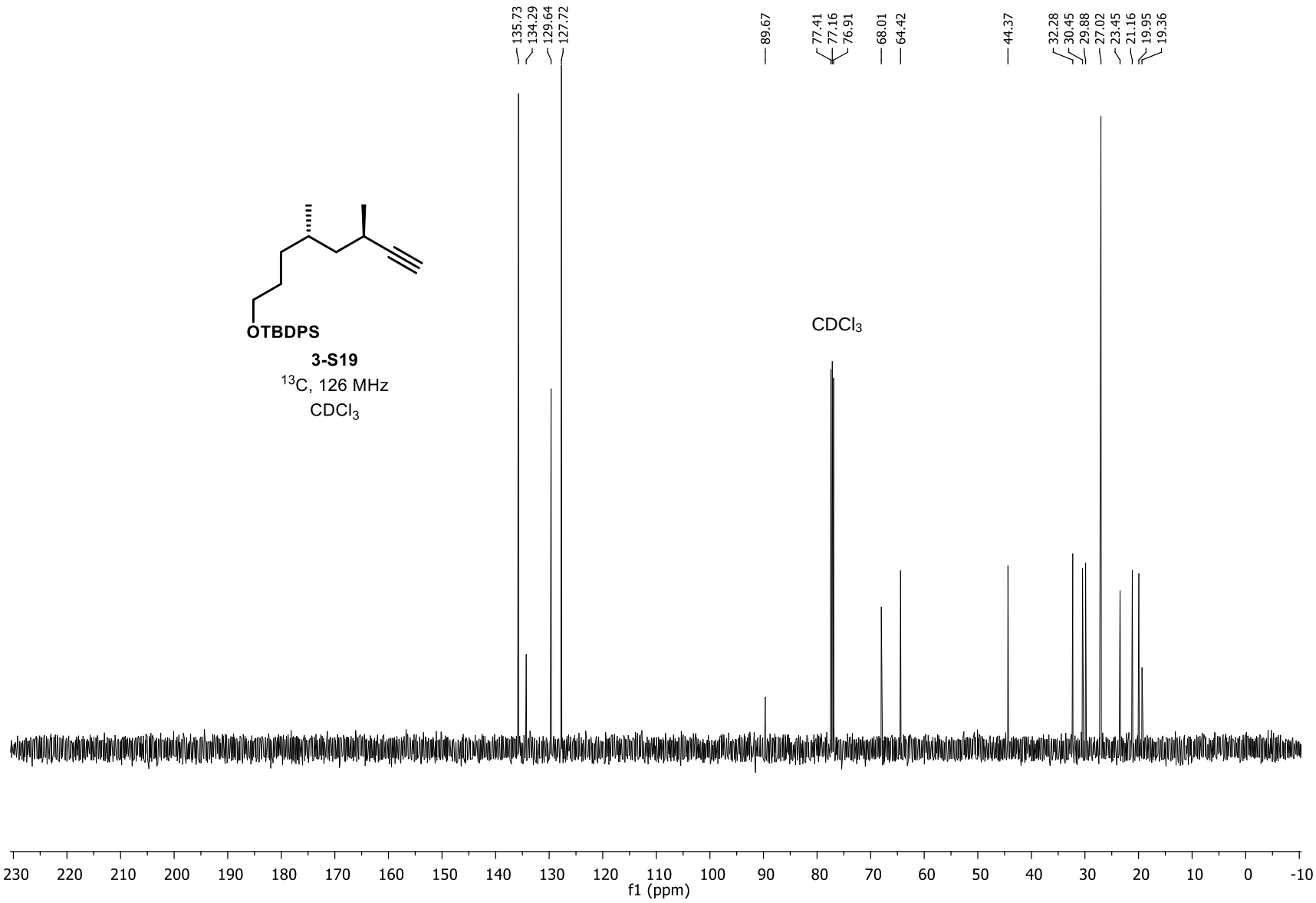
135.73
134.29
129.64
127.72
89.67
77.41
77.16
76.91
68.01
64.42
44.37
32.28
30.45
29.88
27.02
23.45
21.16
19.95
19.36
OTBDPS
3-S19
13C, 126 MHz
CDCl3
CDCl3
230 220 210 200 190 180 170 160 150 140 130 120 110 100 90 80 70 60 50 40 30 20 10 0 -10
f1 (ppm)

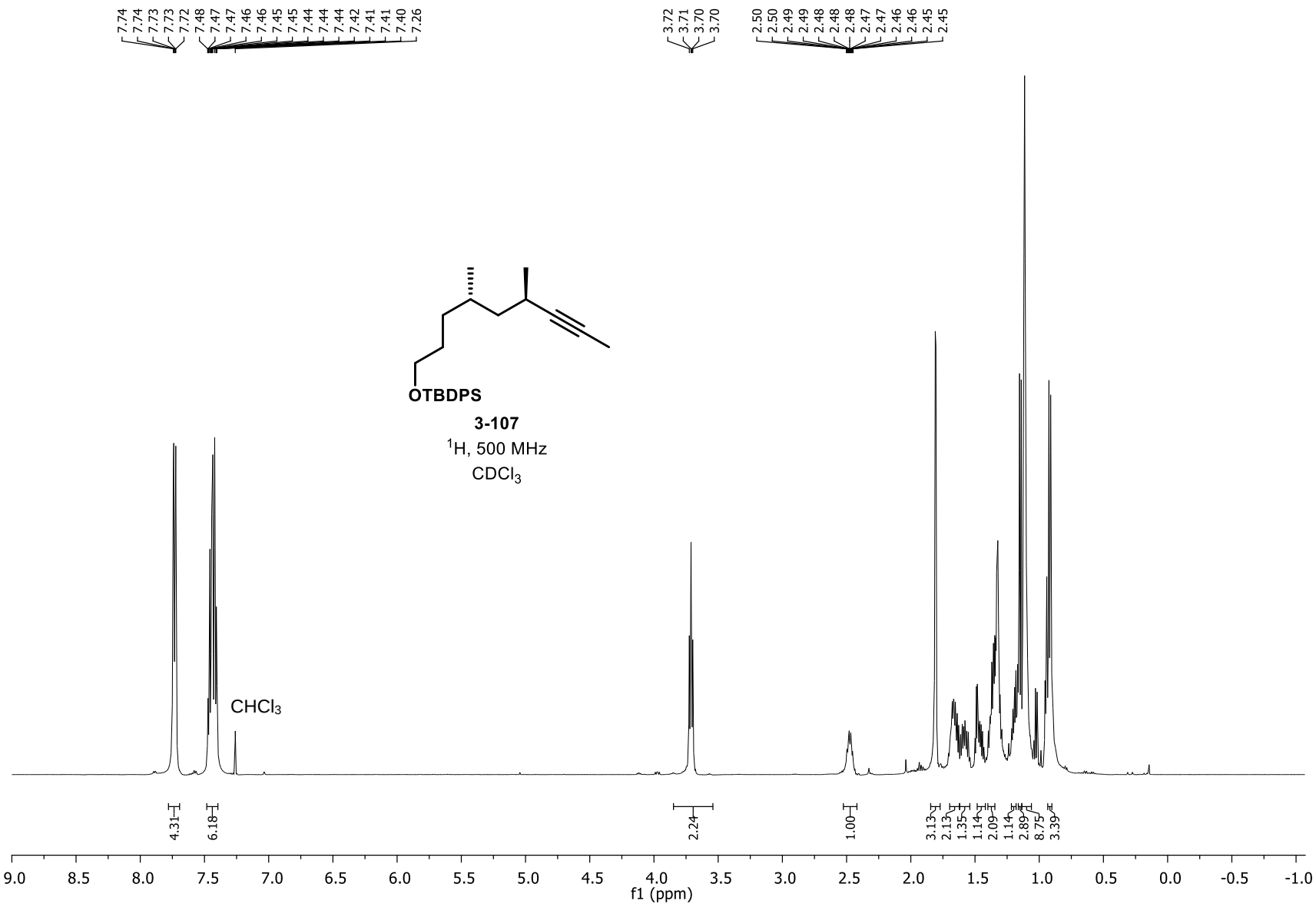
7.74
7.74
7.73
7.73
7.72
7.48
7.47
7.47
7.46
7.46
7.45
7.45
7.44
7.44
7.44
7.42
7.41
7.41
7.40
7.26
3.72
3.71
3.70
3.70
2.50
2.50
2.49
2.49
2.48
2.48
2.48
2.47
2.47
2.46
2.46
2.45
2.45
OTBDPS
3-107
1H, 500 MHz
CDCl3
CHCl3
4.31
6.18
2.24
1.00
3.13
2.13
1.35
1.14
2.09
1.14
2.89
8.75
3.39
9.0
8.5
8.0
7.5
7.0
6.5
6.0
5.5
5.0
4.5
4.0
3.5
3.0
2.5
2.0
1.5
1.0
0.5
0.0
-0.5
-1.0
f1 (ppm)

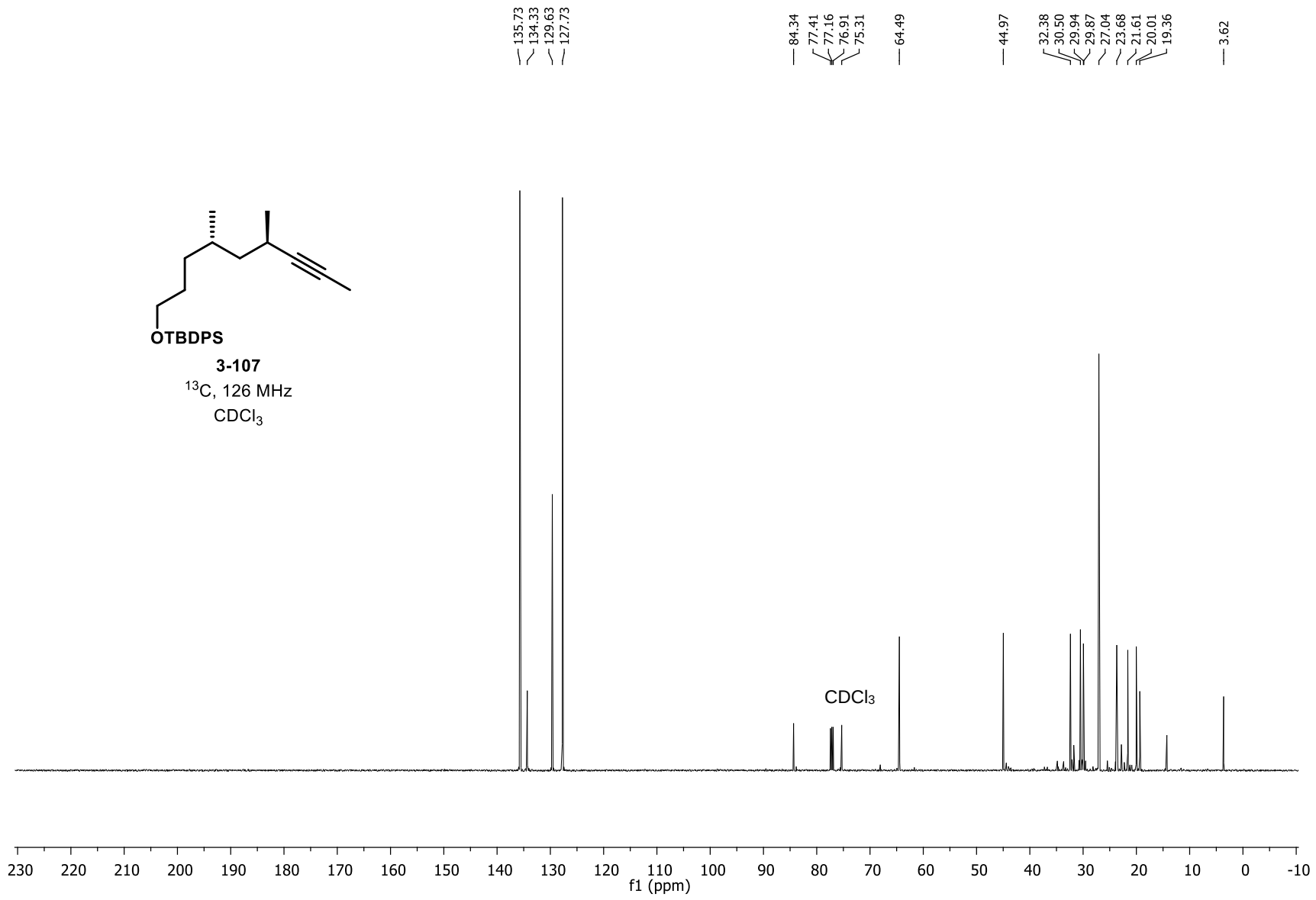
135.73
134.33
129.63
127.73
84.34
77.41
77.16
76.91
75.31
64.49
44.97
32.38
30.50
29.94
29.87
27.04
23.68
21.61
20.01
19.36
3.62
OTBDPS
3-107
13C, 126 MHz
CDCl3
CDCl3
230 220 210 200 190 180 170 160 150 140 130 120 110 100 90 80 70 60 50 40 30 20 10 0 -10
f1 (ppm)

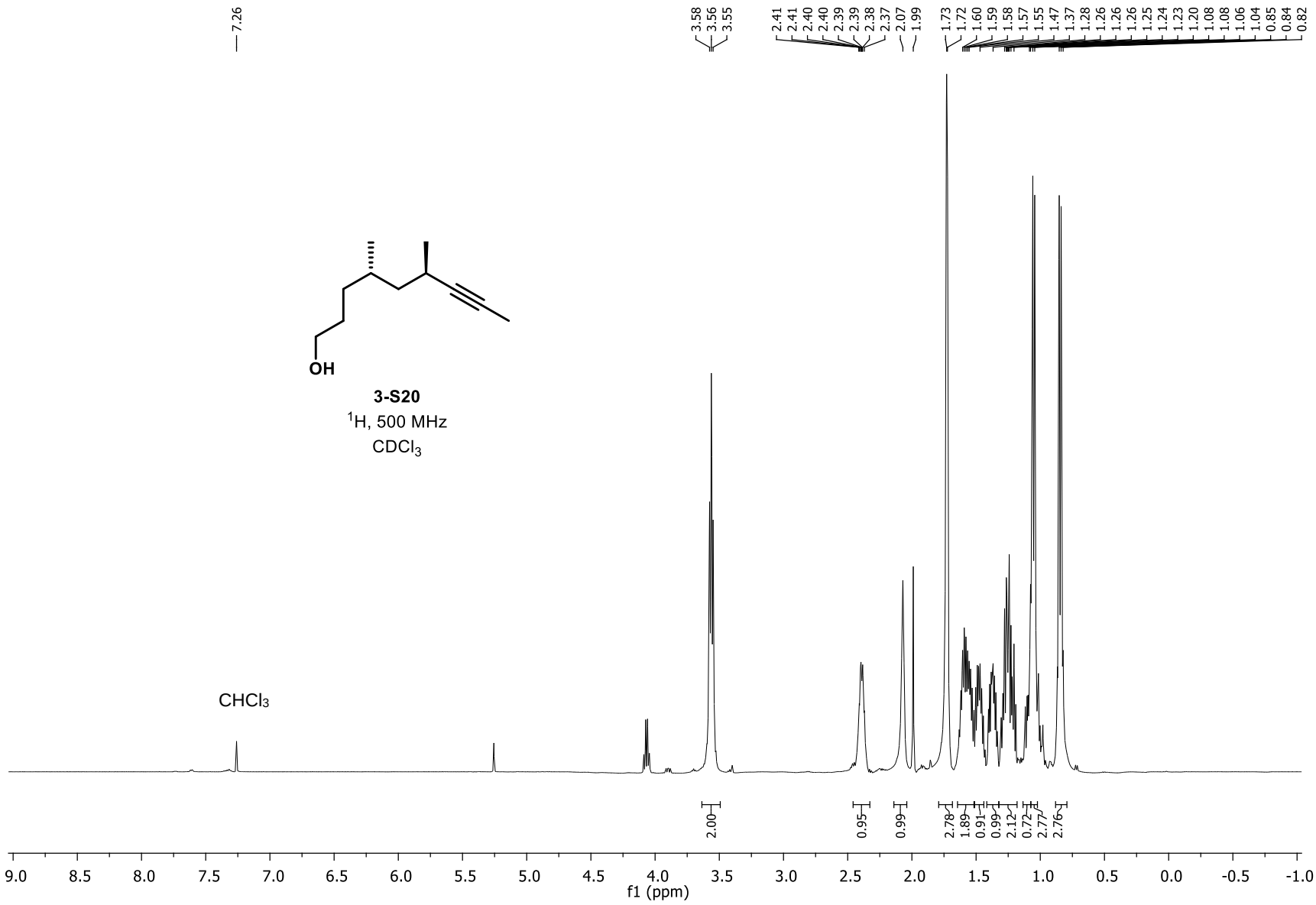
7.26
3.58
3.56
3.55
2.41
2.41
2.40
2.40
2.39
2.39
2.38
2.37
2.07
1.99
1.73
1.72
1.60
1.59
1.58
1.57
1.55
1.47
1.37
1.28
1.26
1.26
1.26
1.25
1.24
1.23
1.20
1.08
1.08
1.06
1.04
0.85
0.84
0.82
OH
3-S20
1H, 500 MHz
CDCl3
CHCl3
2.00
0.95
0.99
2.78
1.89
0.91
0.99
2.12
0.72
2.77
2.76
9.0
8.5
8.0
7.5
7.0
6.5
6.0
5.5
5.0
4.5
4.0
3.5
3.0
2.5
2.0
1.5
1.0
0.5
0.0
-0.5
-1.0
f1 (ppm)

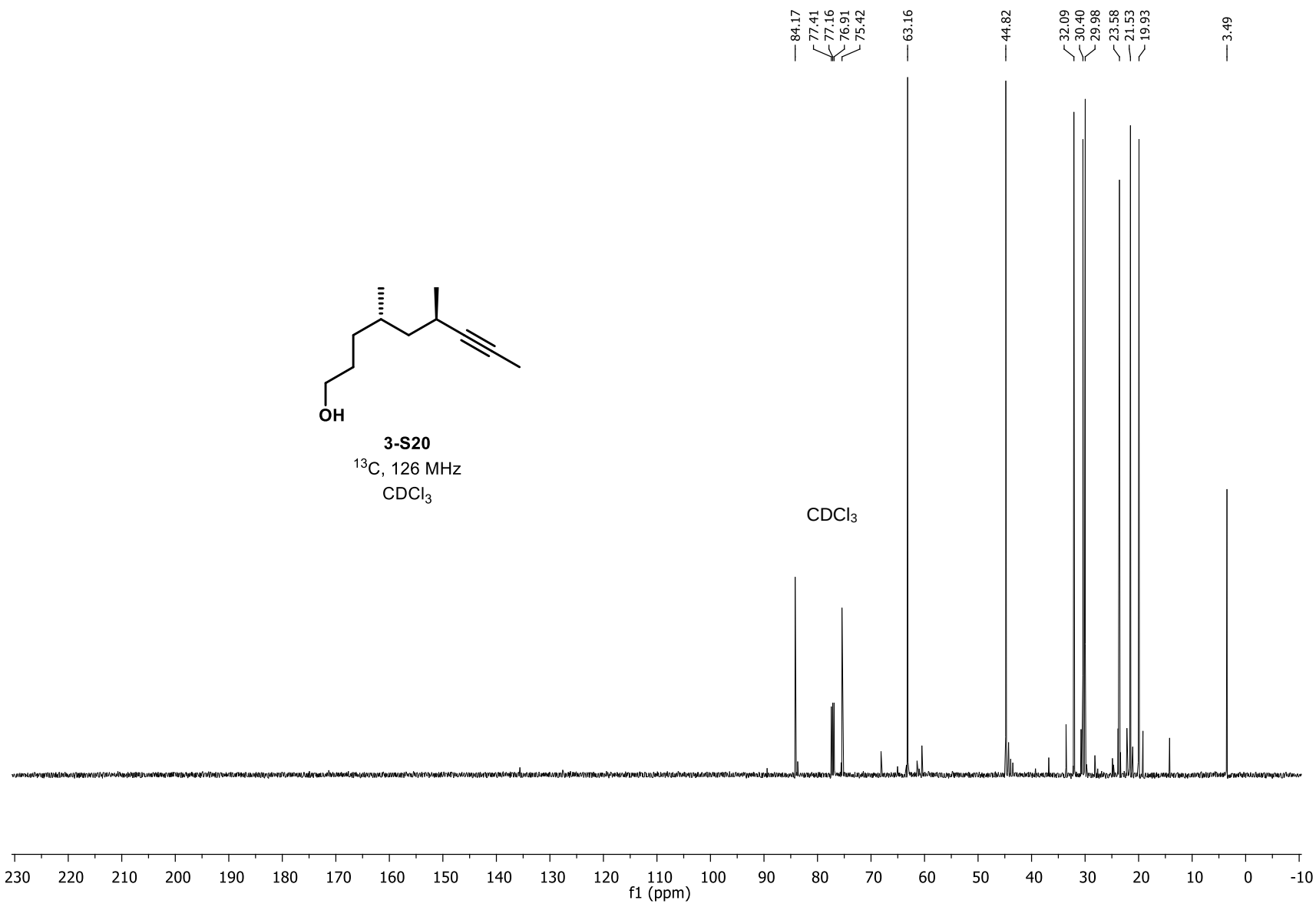
84.17
77.41
77.16
76.91
75.42
63.16
44.82
32.09
30.40
29.98
23.58
21.53
19.93
3.49
OH
3-S20
13C, 126 MHz
CDCl3
CDCl3
230 220 210 200 190 180 170 160 150 140 130 120 110 100 90 80 70 60 50 40 30 20 10 0 -10
f1 (ppm)

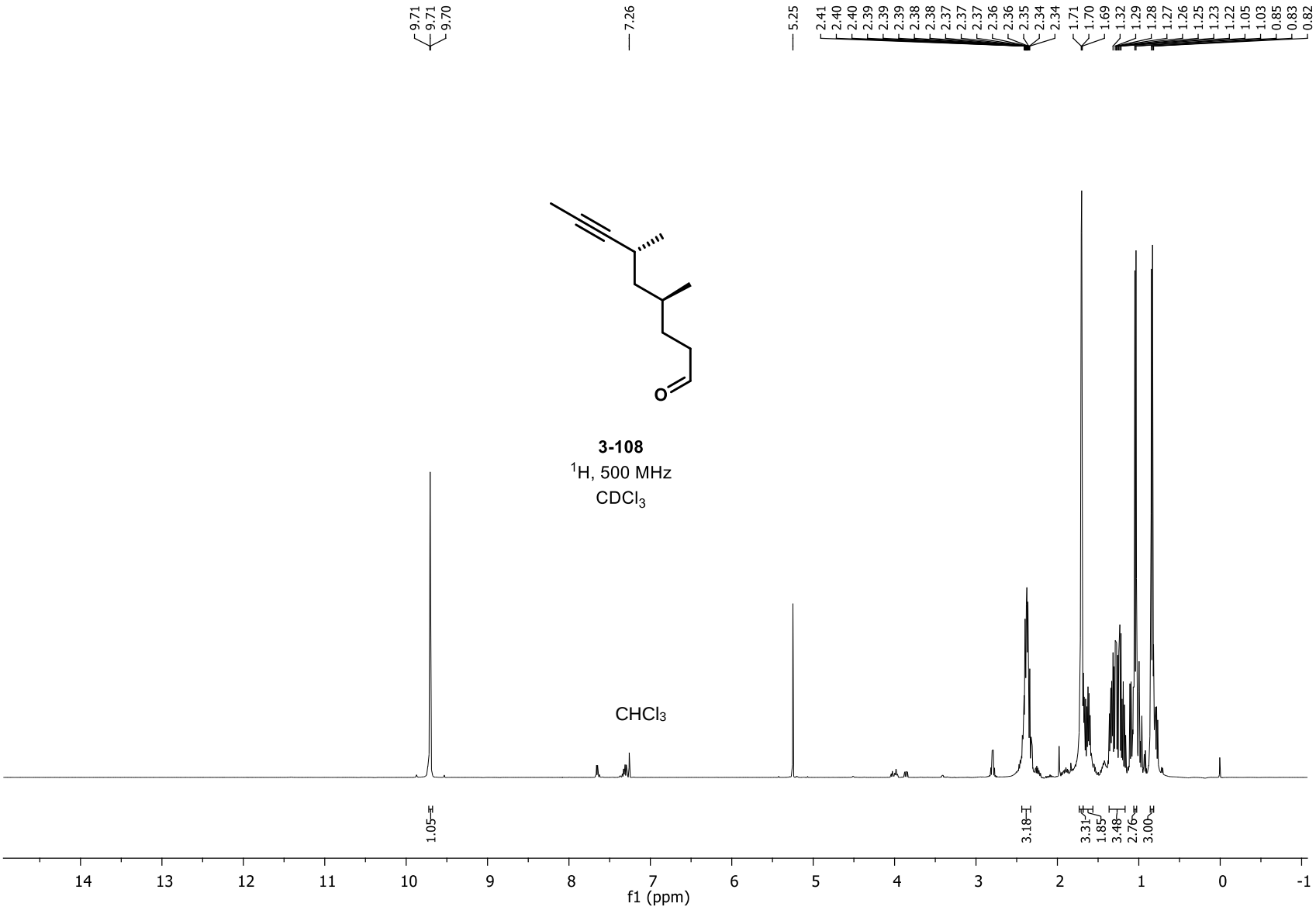
9.71
9.71
9.70
7.26
5.25
2.41
2.40
2.40
2.39
2.39
2.38
2.38
2.37
2.37
2.37
2.36
2.36
2.35
2.34
2.34
1.71
1.70
1.69
1.32
1.29
1.28
1.27
1.26
1.25
1.23
1.22
1.05
1.03
0.85
0.83
0.82
O
3-108
1H, 500 MHz
CDCl3
CHCl3
1.05
3.18
3.31
1.85
3.48
2.76
3.00
14
13
12
11
10
9
8
7
6
5
4
3
2
1
0
-1
f1 (ppm)

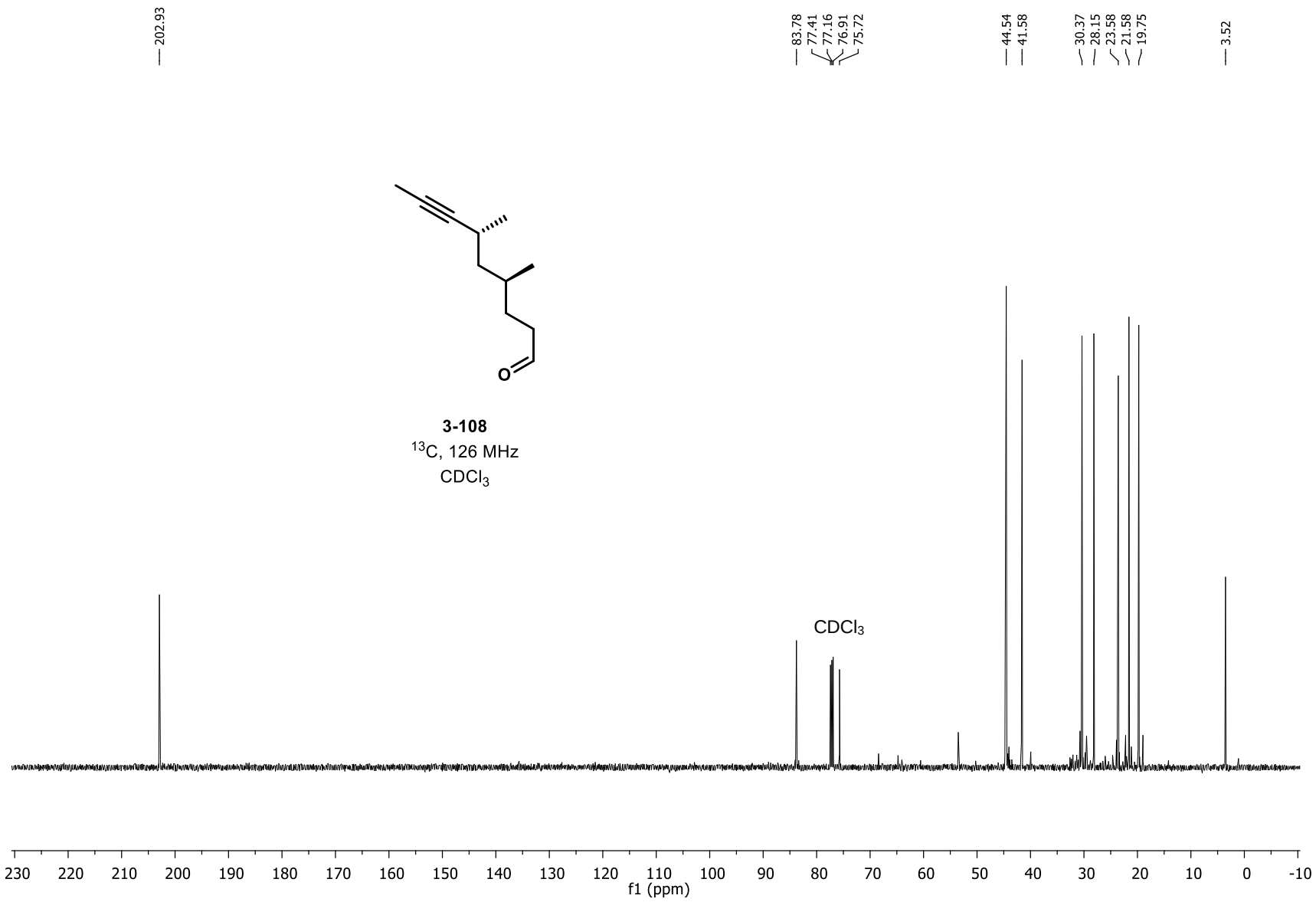
202.93
83.78
77.41
77.16
76.91
75.72
44.54
41.58
30.37
28.15
23.58
21.58
19.75
3.52
O
3-108
13C, 126 MHz
CDCl3
CDCl3
230 220 210 200 190 180 170 160 150 140 130 120 110 100 90 80 70 60 50 40 30 20 10 0 -10
f1 (ppm)

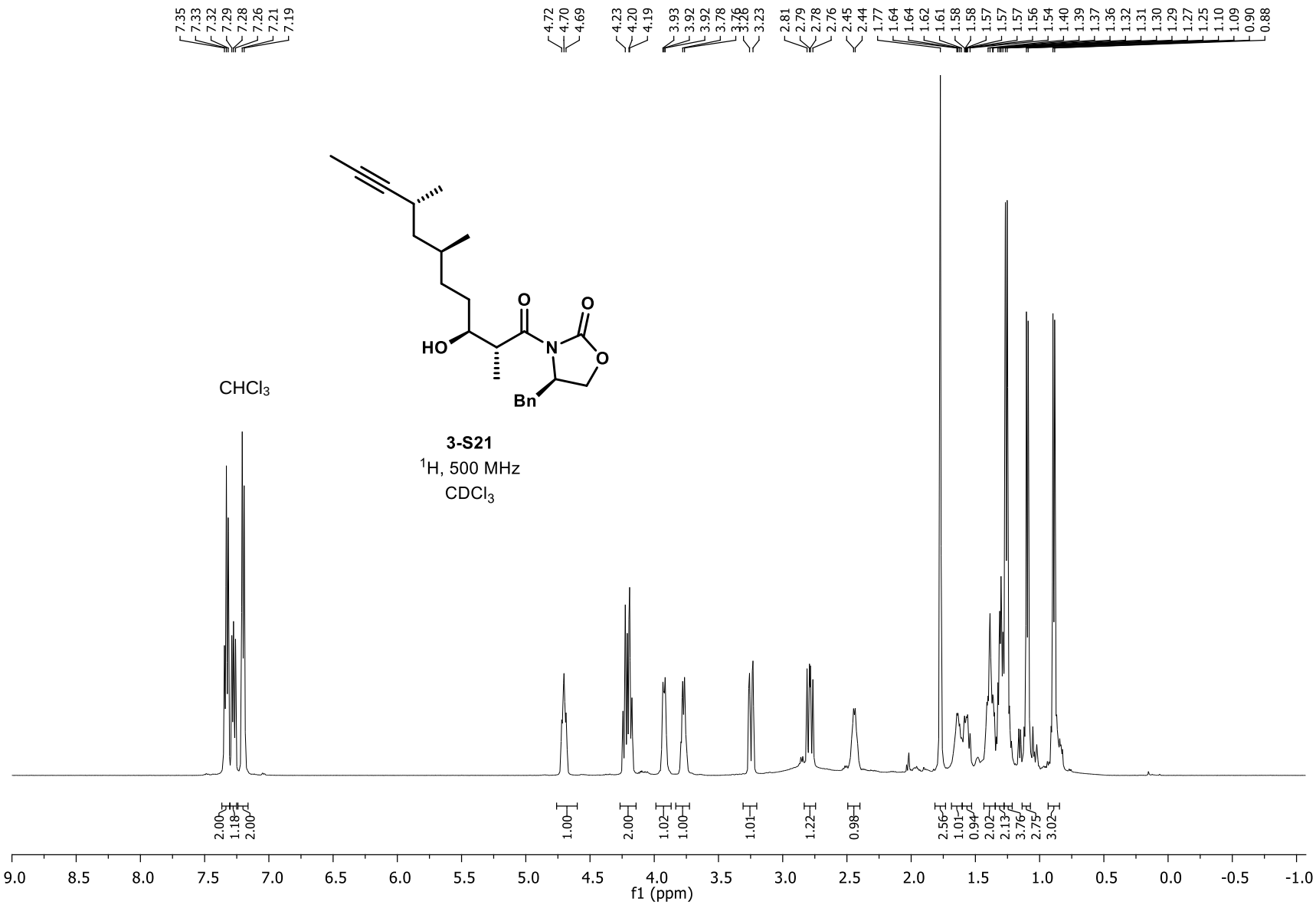
7.35
7.33
7.32
7.29
7.28
7.26
7.21
7.19
4.72
4.70
4.69
4.23
4.20
4.19
3.93
3.92
3.92
3.78
3.26
3.23
2.81
2.79
2.78
2.76
2.45
2.44
1.77
1.64
1.62
1.61
1.58
1.58
1.57
1.57
1.57
1.56
1.54
1.40
1.39
1.37
1.36
1.32
1.31
1.30
1.29
1.27
1.25
1.10
1.09
0.90
0.88
HO
O
O
N
O
Bn
CHCl3
3-S21
1H, 500 MHz
CDCl3
2.00
1.18
2.00
1.00
2.00
1.02
1.00
1.01
1.22
0.98
2.56
1.01
0.94
2.02
2.13
3.76
2.75
3.02
9.0
8.5
8.0
7.5
7.0
6.5
6.0
5.5
5.0
4.5
4.0
3.5
3.0
2.5
2.0
1.5
1.0
0.5
0.0
-0.5
-1.0
f1 (ppm)

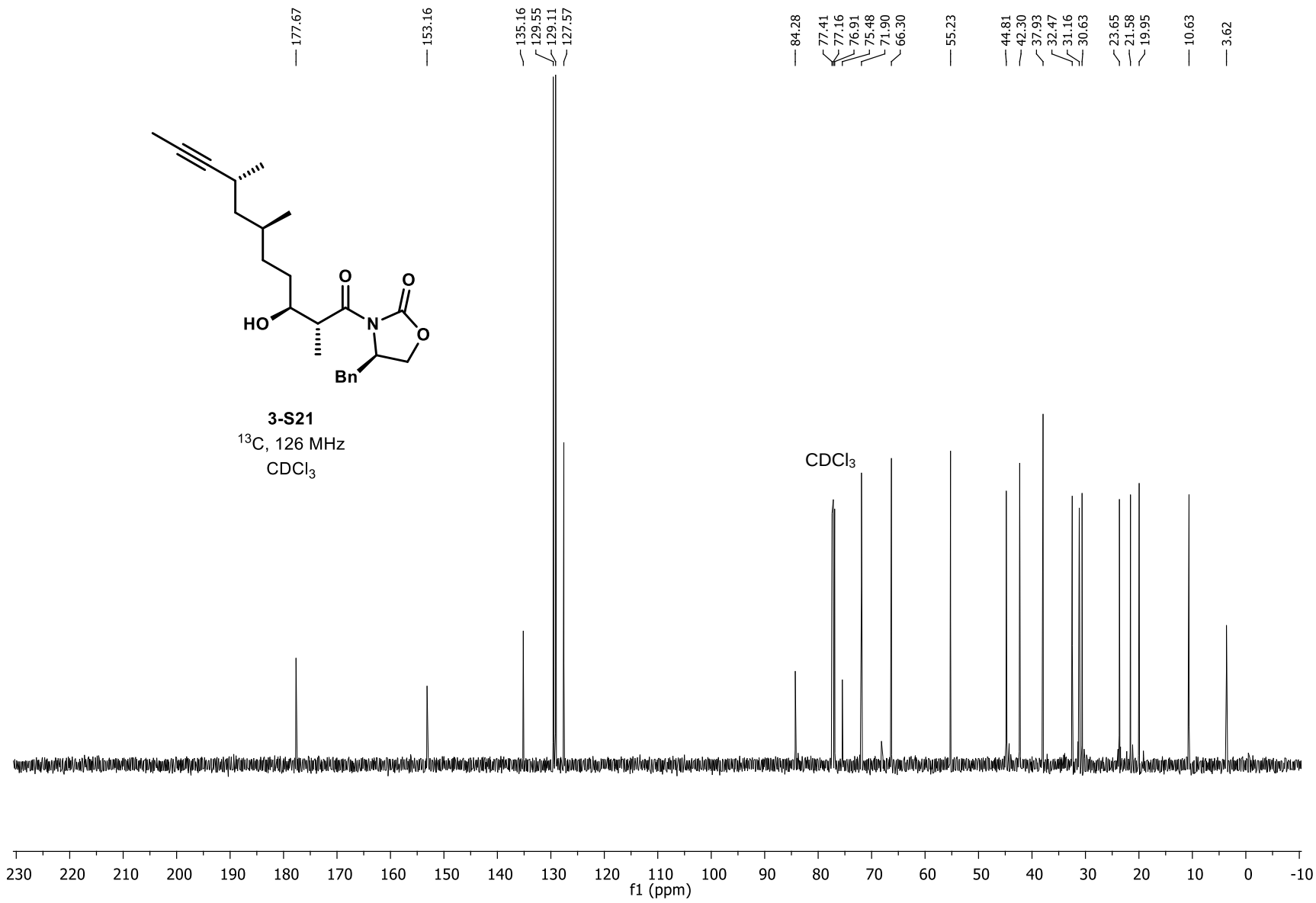
177.67
153.16
135.16
129.55
129.11
127.57
84.28
77.41
77.16
76.91
75.48
71.90
66.30
55.23
44.81
42.30
37.93
32.47
31.16
30.63
23.65
21.58
19.95
10.63
3.62
HO
O
O
N
O
Bn
3-S21
13C, 126 MHz
CDCl3
CDCl3
230 220 210 200 190 180 170 160 150 140 130 120 110 100 90 80 70 60 50 40 30 20 10 0 -10
f1 (ppm)

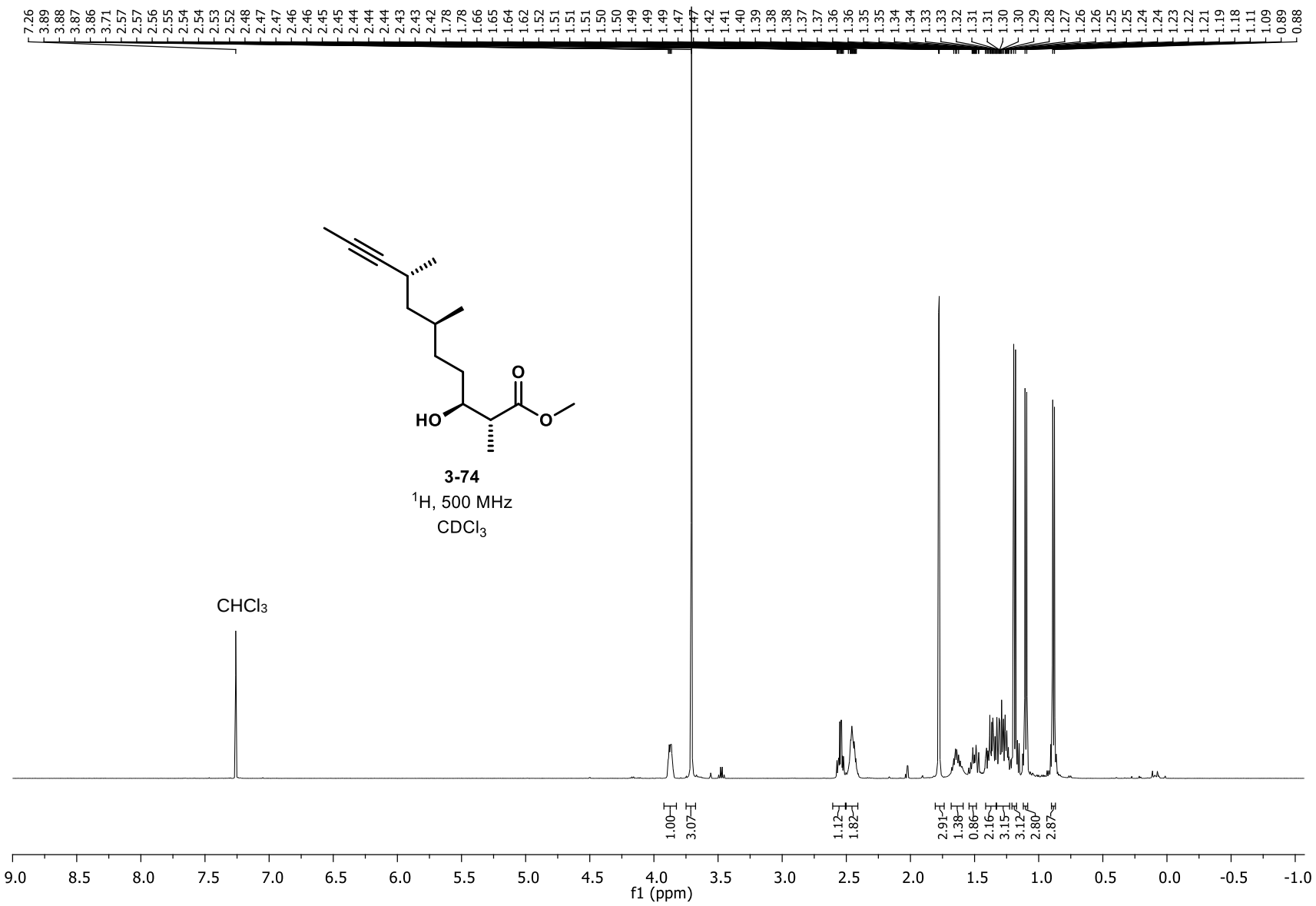
HO
O
O
3-74
1H, 500 MHz
CDCl3
CHCl3
f1 (ppm)

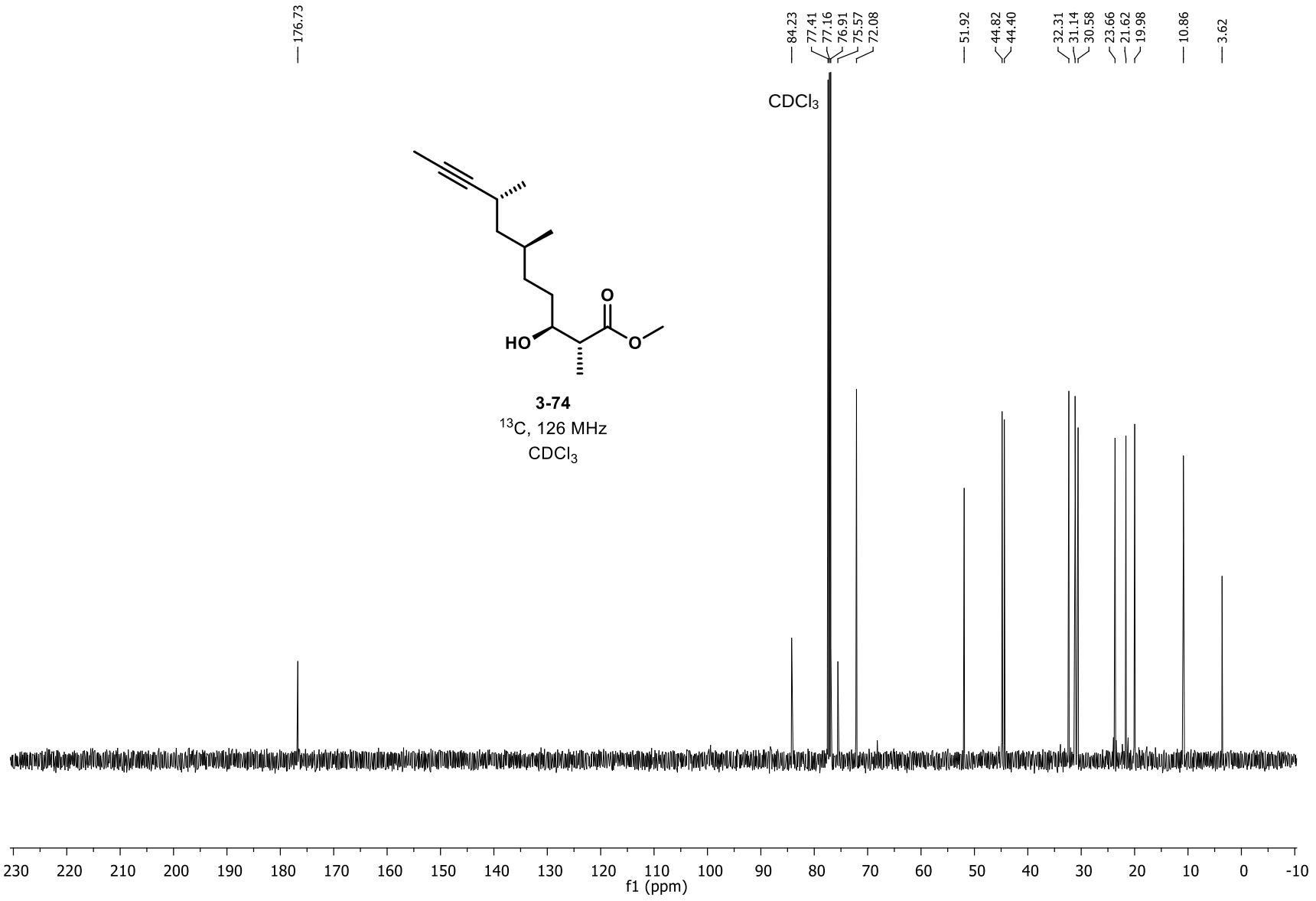
176.73
84.23
77.41
77.16
76.91
75.57
72.08
51.92
44.82
44.40
32.31
31.14
30.58
23.66
21.62
19.98
10.86
3.62
CDCl3
HO
O
O
3-74
13C, 126 MHz
CDCl3
230 220 210 200 190 180 170 160 150 140 130 120 110 100 90 80 70 60 50 40 30 20 10 0 -10
f1 (ppm)

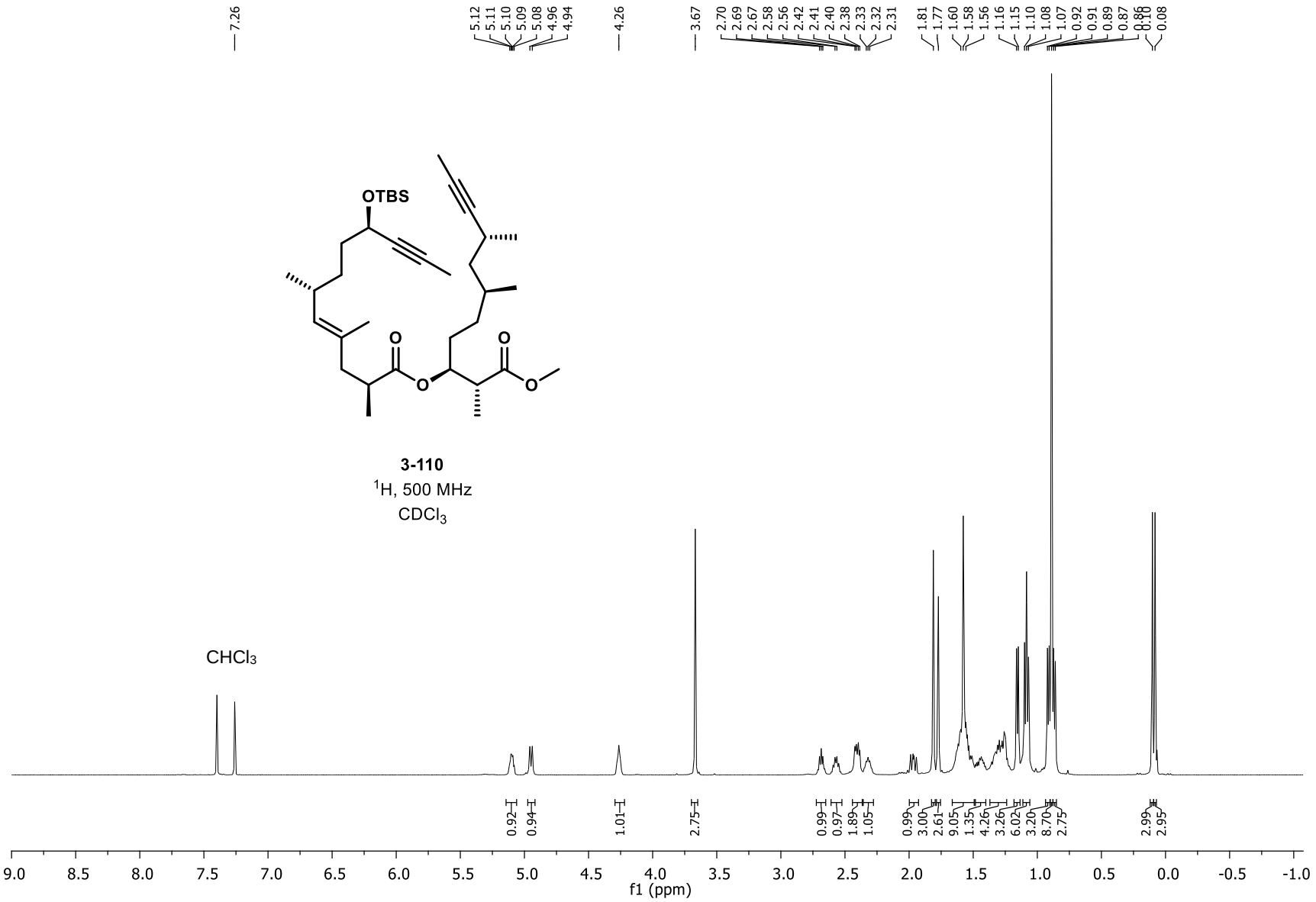
7.26
5.12
5.11
5.10
5.09
5.08
4.96
4.94
4.26
3.67
2.70
2.69
2.67
2.58
2.56
2.42
2.41
2.40
2.38
2.33
2.32
2.31
1.81
1.77
1.60
1.58
1.56
1.16
1.15
1.10
1.08
1.07
0.92
0.91
0.89
0.87
0.10
0.08
OTBS
O
O
O
O
3-110
1H, 500 MHz
CDCl3
CHCl3
0.92
0.94
1.01
2.75
0.99
0.97
1.89
1.05
0.99
3.00
2.61
9.05
1.35
4.26
3.26
6.02
3.20
8.70
2.75
2.99
2.95
9.0
8.5
8.0
7.5
7.0
6.5
6.0
5.5
5.0
4.5
4.0
3.5
3.0
2.5
2.0
1.5
1.0
0.5
0.0
-0.5
-1.0
f1 (ppm)

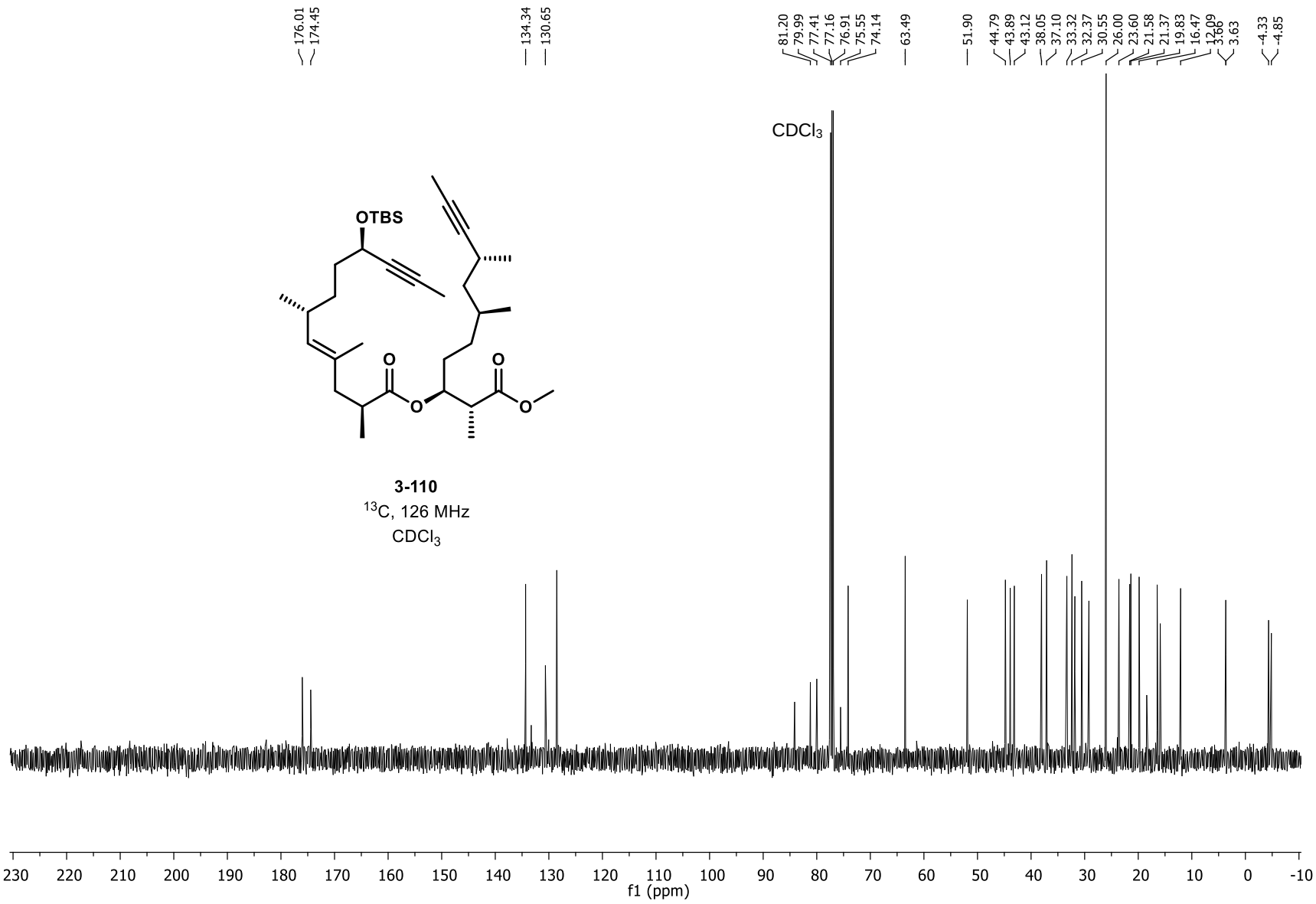
176.01
174.45
134.34
130.65
81.20
79.99
77.41
77.16
76.91
75.55
74.14
63.49
51.90
44.79
43.89
43.12
38.05
37.10
33.32
32.37
30.55
26.00
23.60
21.58
21.37
19.83
16.47
12.09
3.66
3.63
-4.33
-4.85
CDCl3
OTBS
O
O
O
O
3-110
13C, 126 MHz
CDCl3
230
220
210
200
190
180
170
160
150
140
130
120
110
100
90
80
70
60
50
40
30
20
10
0
-10
f1 (ppm)

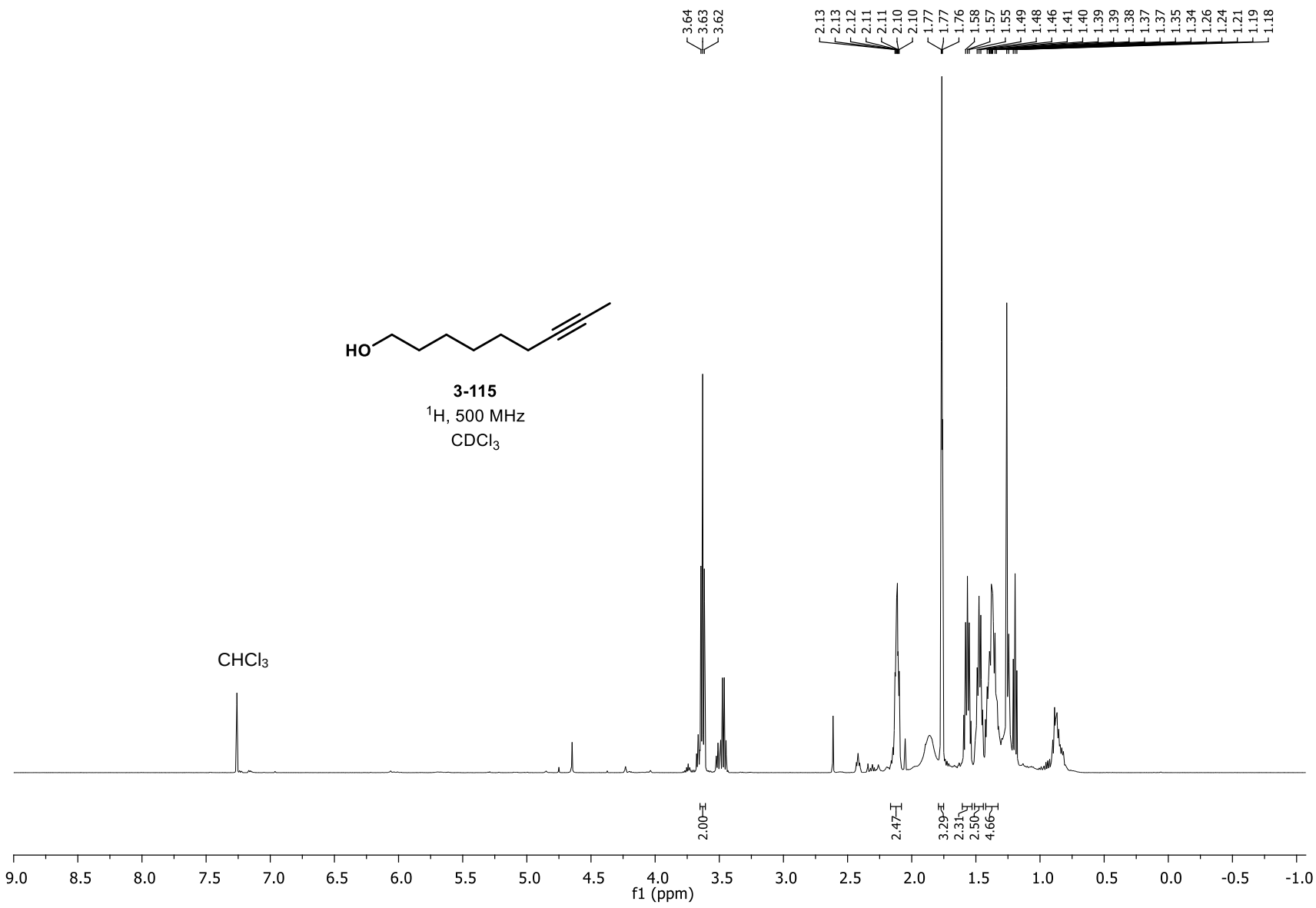
3.64
3.63
3.62
2.13
2.13
2.12
2.11
2.11
2.10
2.10
1.77
1.77
1.76
1.58
1.57
1.55
1.49
1.48
1.46
1.41
1.40
1.39
1.39
1.38
1.37
1.37
1.35
1.34
1.26
1.24
1.21
1.19
1.18
HO
3-115
1H, 500 MHz
CDCl3
CHCl3
2.00
2.47
3.29
2.31
2.50
4.66
9.0
8.5
8.0
7.5
7.0
6.5
6.0
5.5
5.0
4.5
4.0
3.5
3.0
2.5
2.0
1.5
1.0
0.5
0.0
-0.5
-1.0
f1 (ppm)

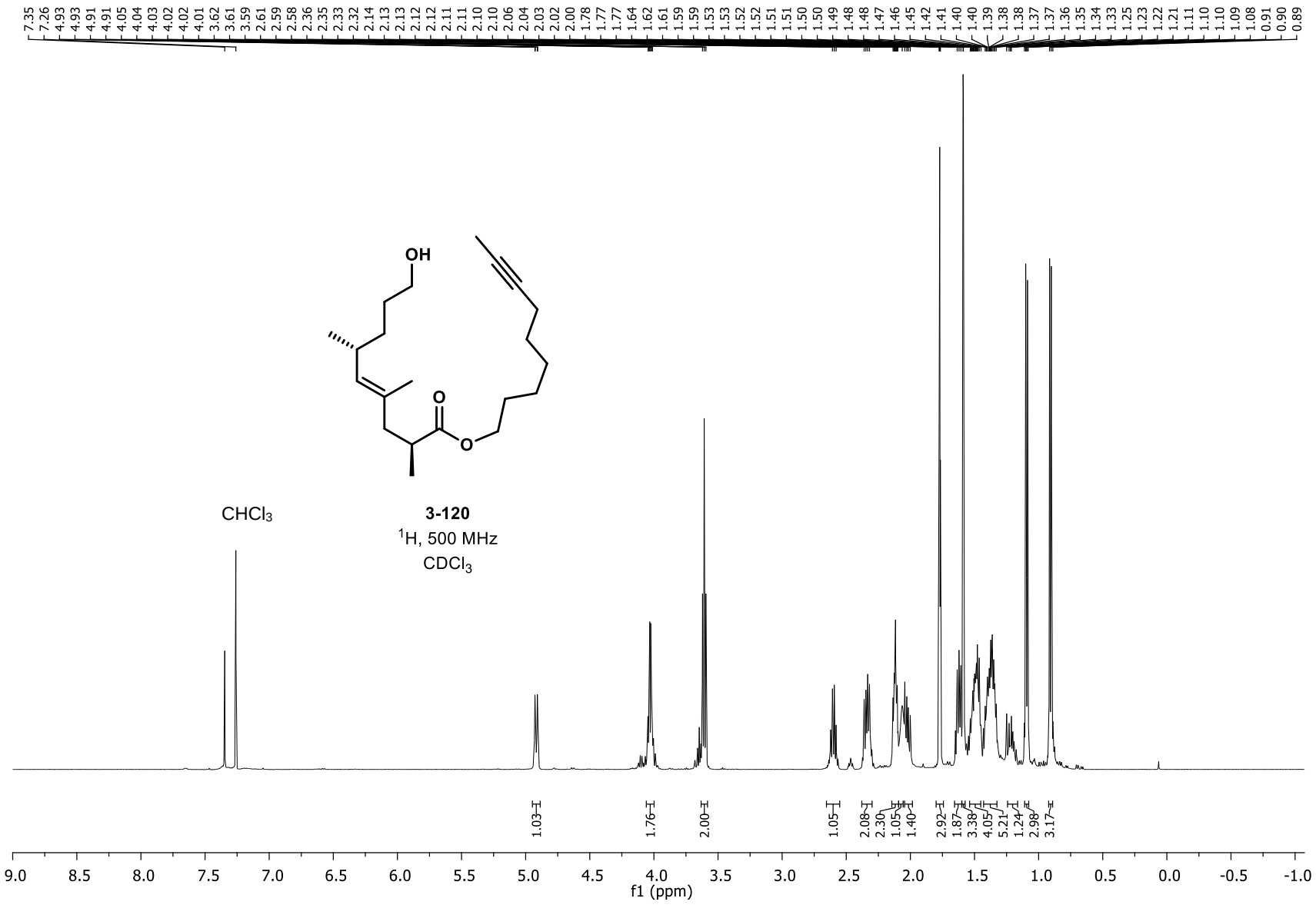
OH
O
O
CHCl3
3-120
1H, 500 MHz
CDCl3
f1 (ppm)

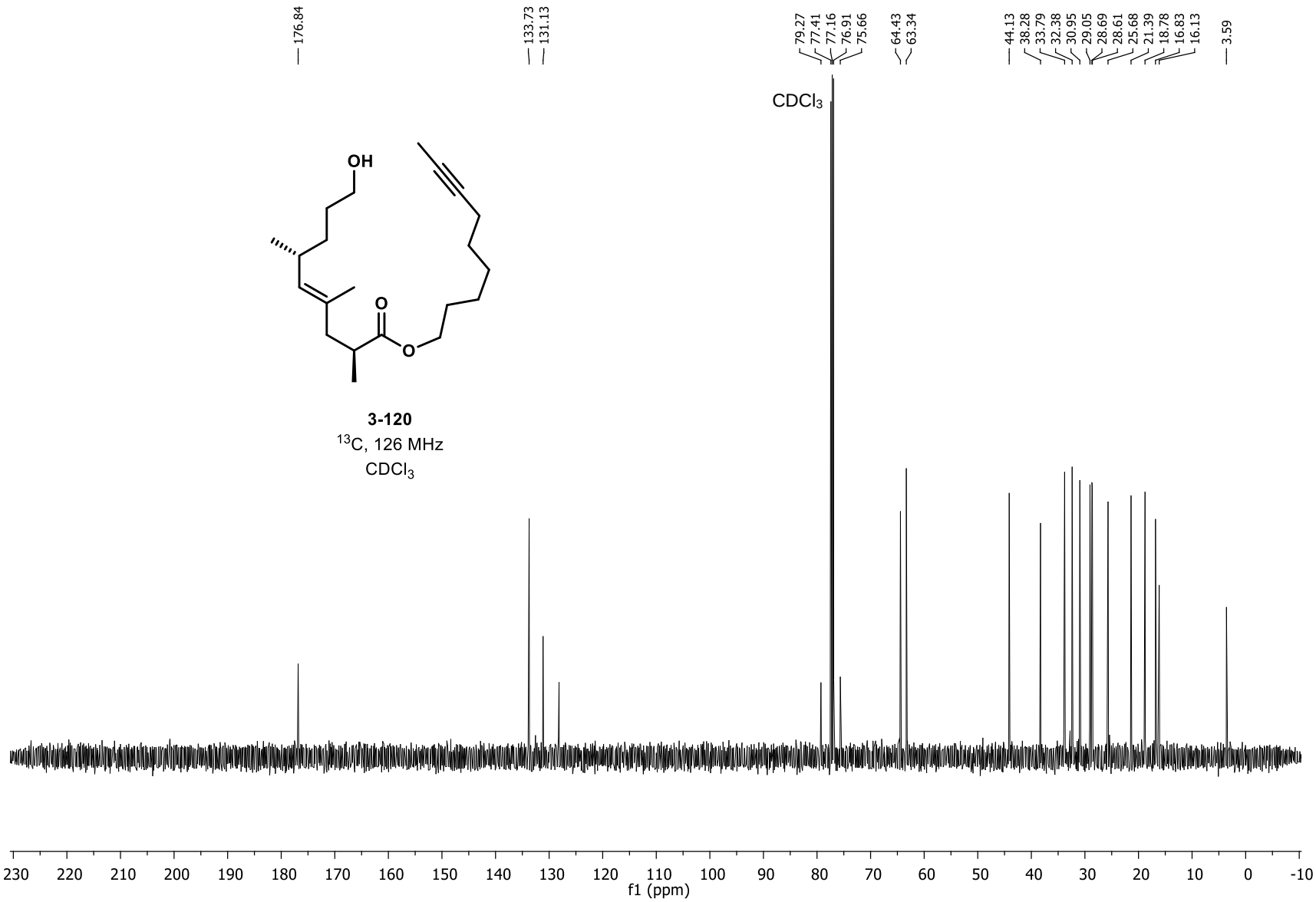
176.84
133.73
131.13
79.27
77.41
77.16
76.91
75.66
64.43
63.34
44.13
38.28
33.79
32.38
30.95
29.05
28.69
28.61
25.68
21.39
18.78
16.83
16.13
3.59
CDCl3
OH
O
O
3-120
13C, 126 MHz
CDCl3
230 220 210 200 190 180 170 160 150 140 130 120 110 100 90 80 70 60 50 40 30 20 10 0 -10
f1 (ppm)

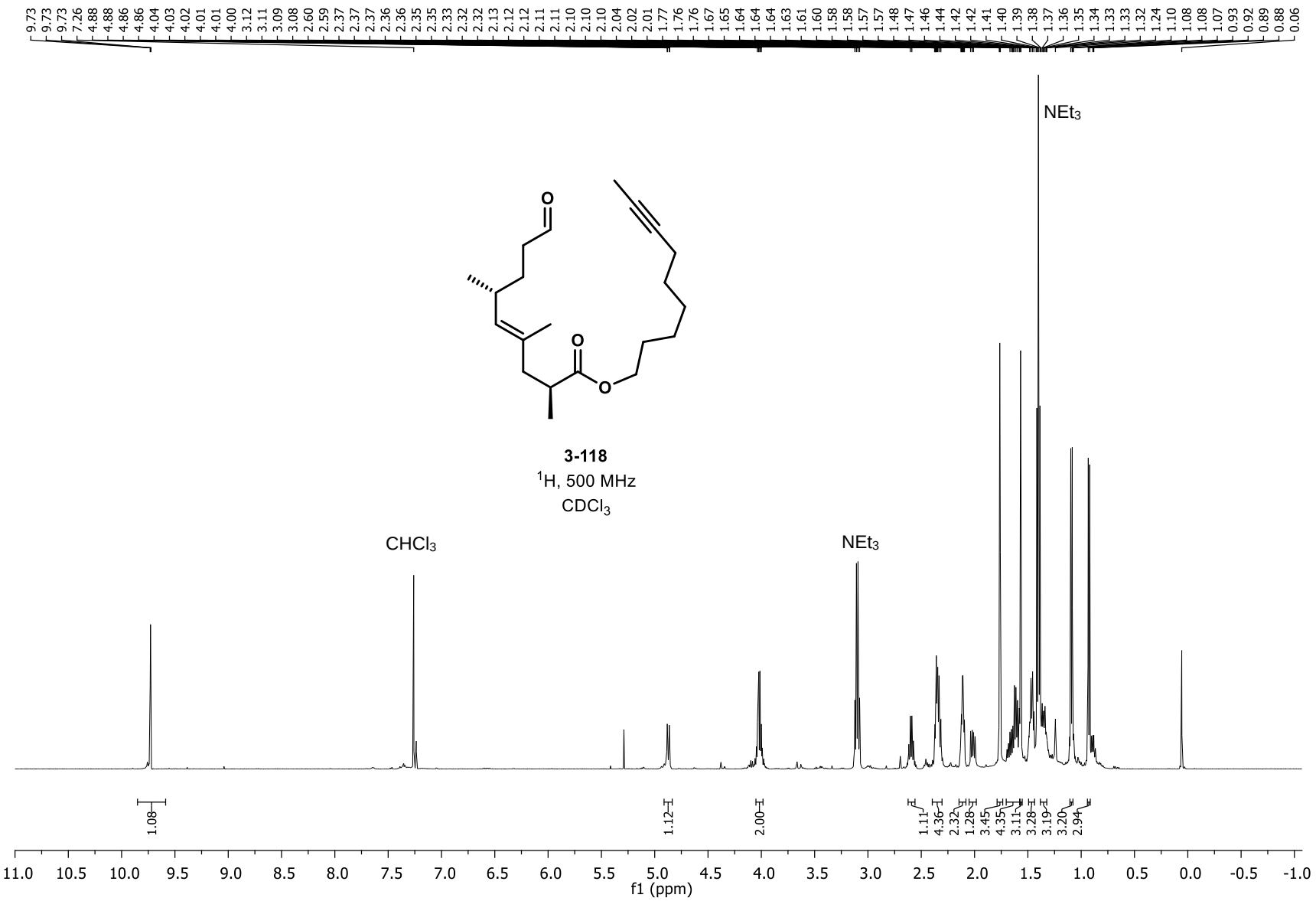
9.73 9.73 9.73 7.26 4.88 4.88 4.86 4.86 4.04 4.03 4.02 4.01 4.01 4.00 3.12 3.11 3.09 3.08 2.60 2.59 2.37 2.37 2.37 2.36 2.36 2.35 2.35 2.33 2.32 2.13 2.12 2.12 2.11 2.11 2.10 2.10 2.10 2.04 2.02 2.01 1.77 1.76 1.76 1.67 1.65 1.64 1.64 1.64 1.63 1.61 1.60 1.58 1.58 1.57 1.57 1.48 1.47 1.46 1.44 1.42 1.42 1.41 1.40 1.39 1.38 1.37 1.36 1.35 1.34 1.33 1.33 1.32 1.24 1.10 1.08 1.08 1.07 0.93 0.92 0.89 0.88 0.06
NEt3
O
O
O
3-118
1H, 500 MHz
CDCl3
CHCl3
NEt3
1.08
1.12
2.00
1.11
4.36
2.32
1.28
3.45
4.35
3.11
3.28
3.19
3.20
2.94
11.0 10.5 10.0 9.5 9.0 8.5 8.0 7.5 7.0 6.5 6.0 5.5 5.0 4.5 4.0 3.5 3.0 2.5 2.0 1.5 1.0 0.5 0.0 -0.5 -1.0
f1 (ppm)

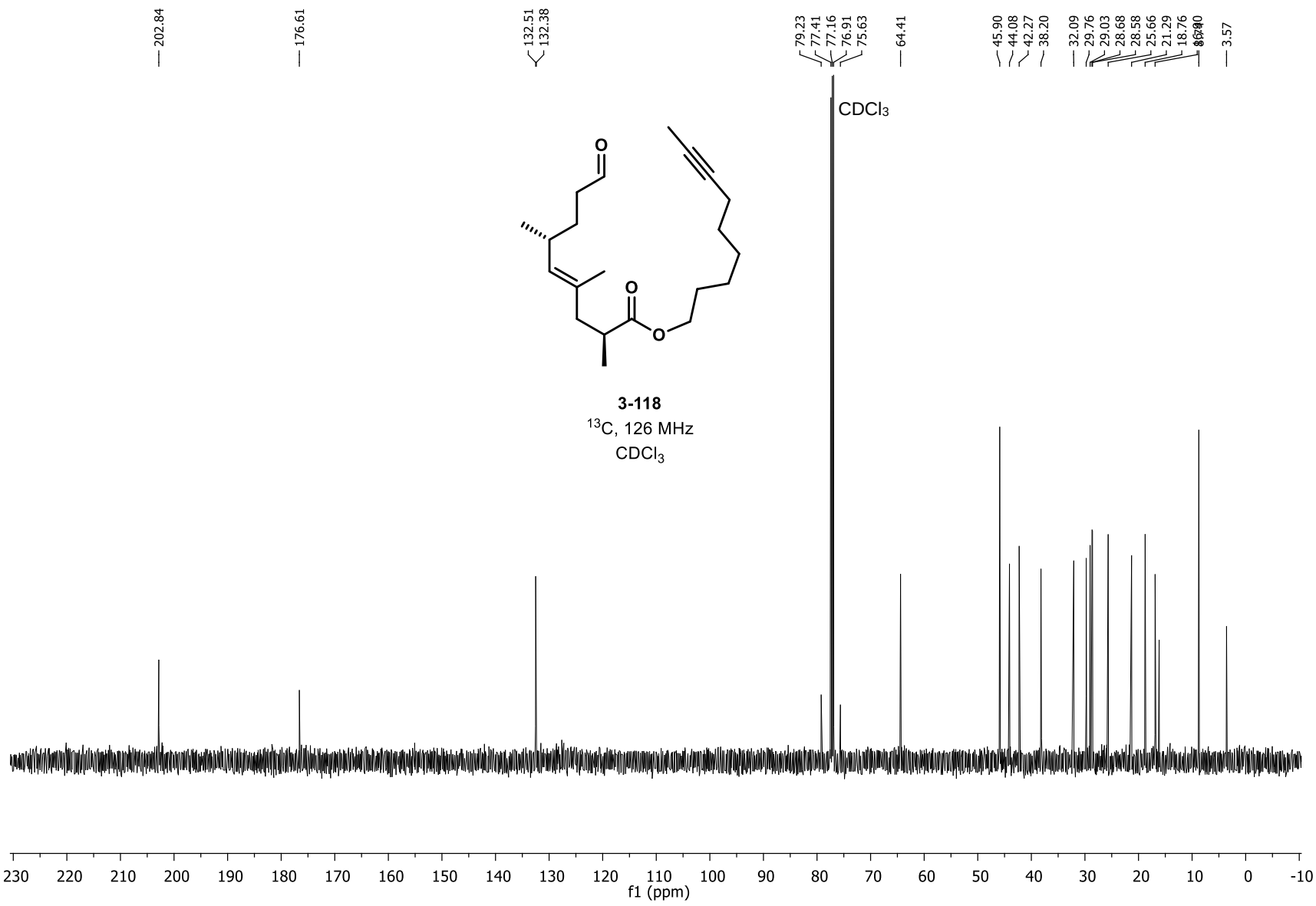
202.84
176.61
132.51
132.38
79.23
77.41
77.16
76.91
75.63
64.41
45.90
44.08
42.27
38.20
32.09
29.76
29.03
28.68
28.58
25.66
21.29
18.76
3.57
CDCl3
O
O
O
3-118
13C, 126 MHz
CDCl3
230 220 210 200 190 180 170 160 150 140 130 120 110 100 90 80 70 60 50 40 30 20 10 0 -10
f1 (ppm)

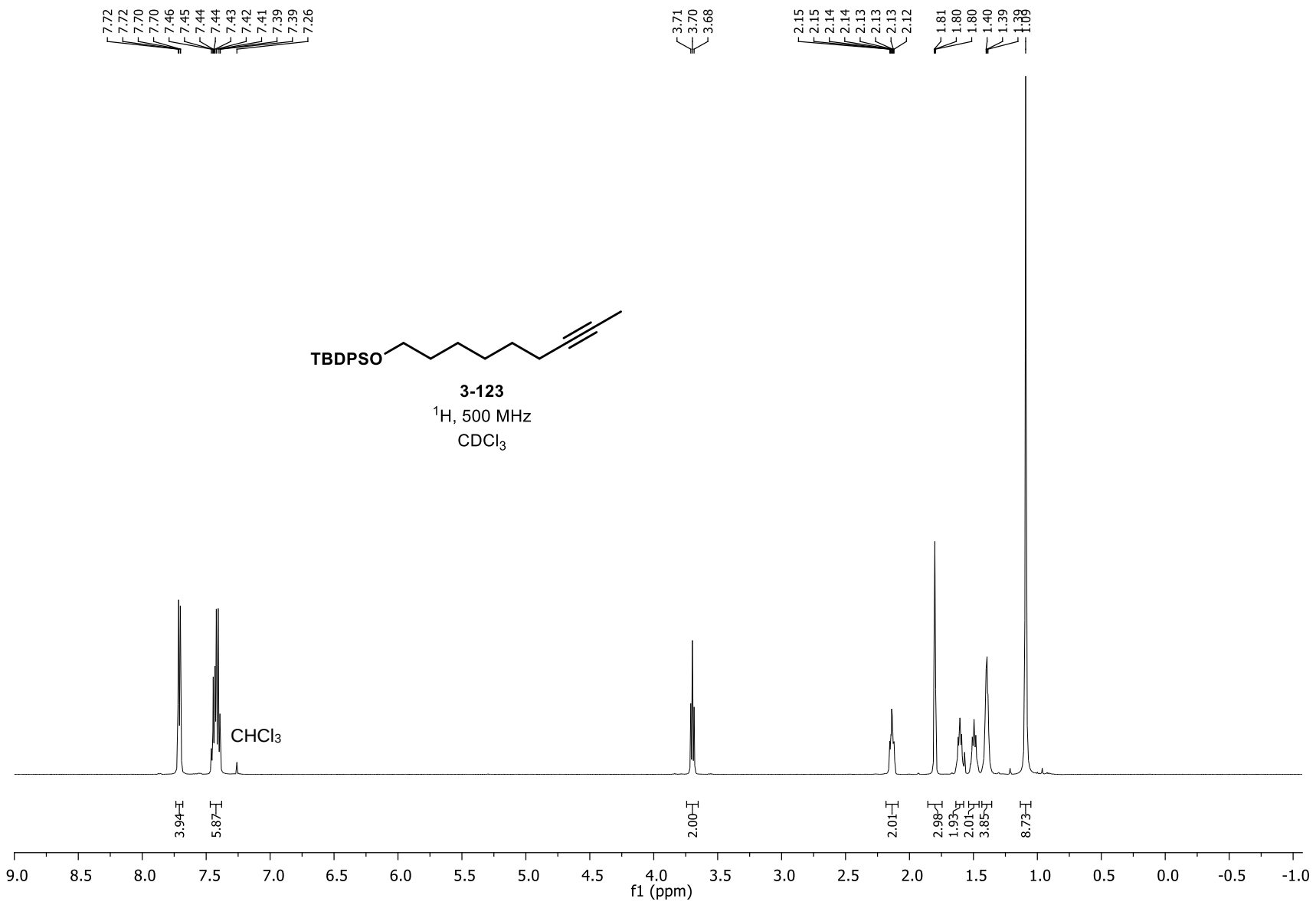
7.72
7.72
7.70
7.70
7.46
7.45
7.44
7.44
7.43
7.42
7.41
7.39
7.39
7.26
3.71
3.70
3.68
2.15
2.15
2.14
2.14
2.13
2.13
2.13
2.12
1.81
1.80
1.80
1.40
1.39
1.09
TBDPSO
3-123
1H, 500 MHz
CDCl3
CHCl3
3.94
5.87
2.00
2.01
2.98
1.93
2.01
3.85
8.73
9.0
8.5
8.0
7.5
7.0
6.5
6.0
5.5
5.0
4.5
4.0
3.5
3.0
2.5
2.0
1.5
1.0
0.5
0.0
-0.5
-1.0
f1 (ppm)

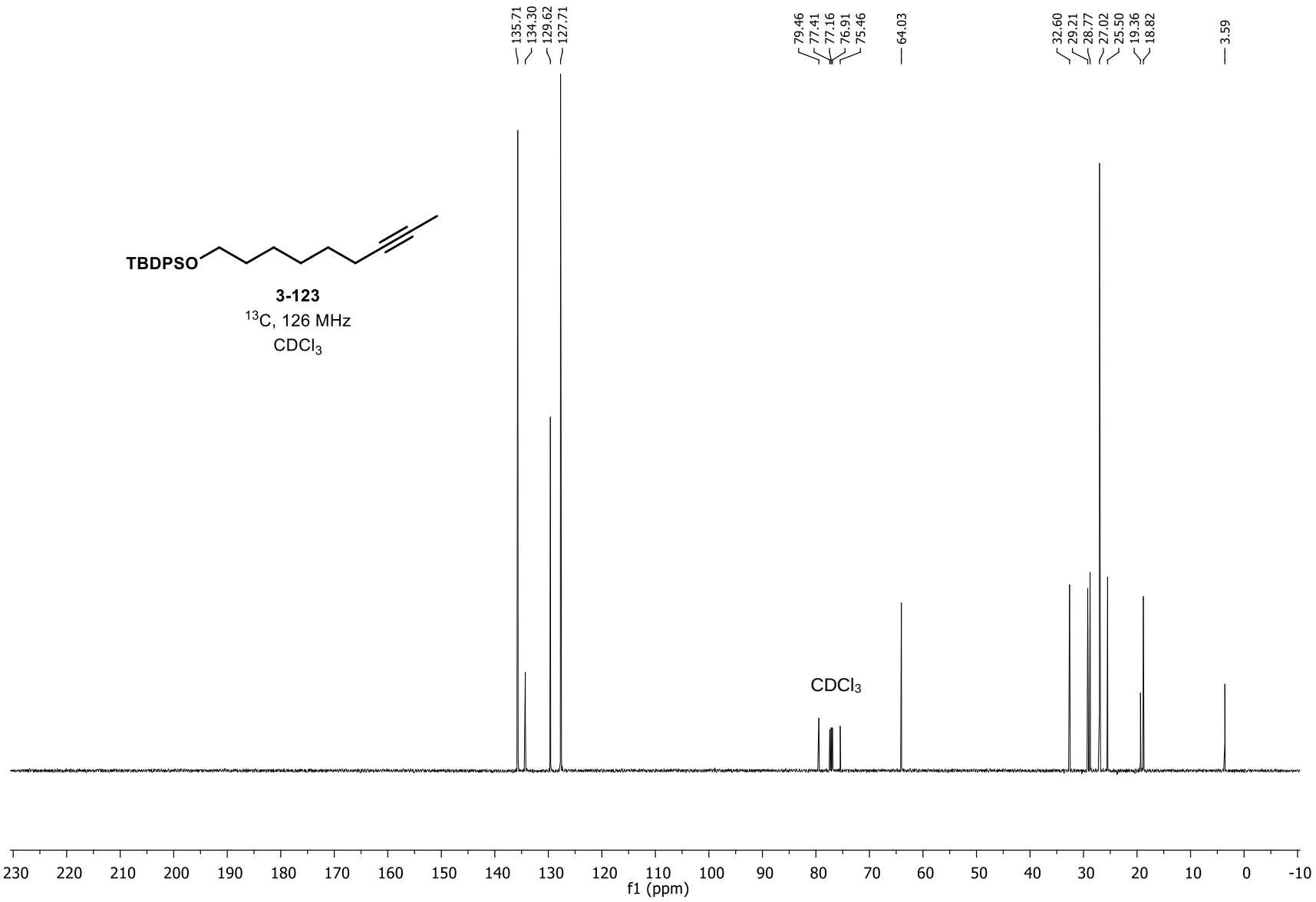
135.71
134.30
129.62
127.71
79.46
77.41
77.16
76.91
75.46
64.03
32.60
29.21
28.77
27.02
25.50
19.36
18.82
3.59
TBDPSO
3-123
13C, 126 MHz
CDCl3
CDCl3
230 220 210 200 190 180 170 160 150 140 130 120 110 100 90 80 70 60 50 40 30 20 10 0 -10
f1 (ppm)

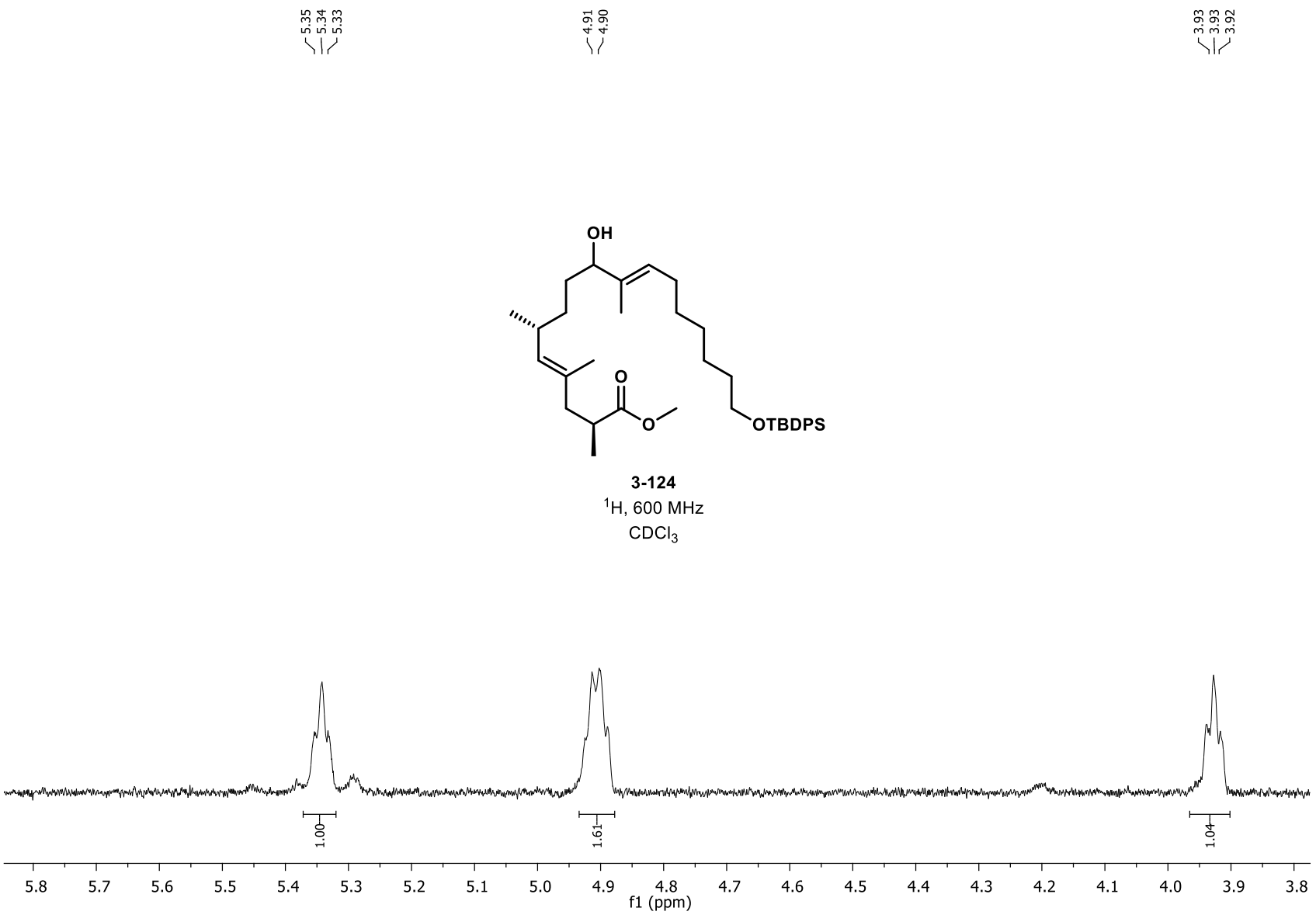

3-124

^{1}H, 600 MHz

$CDCl_3$

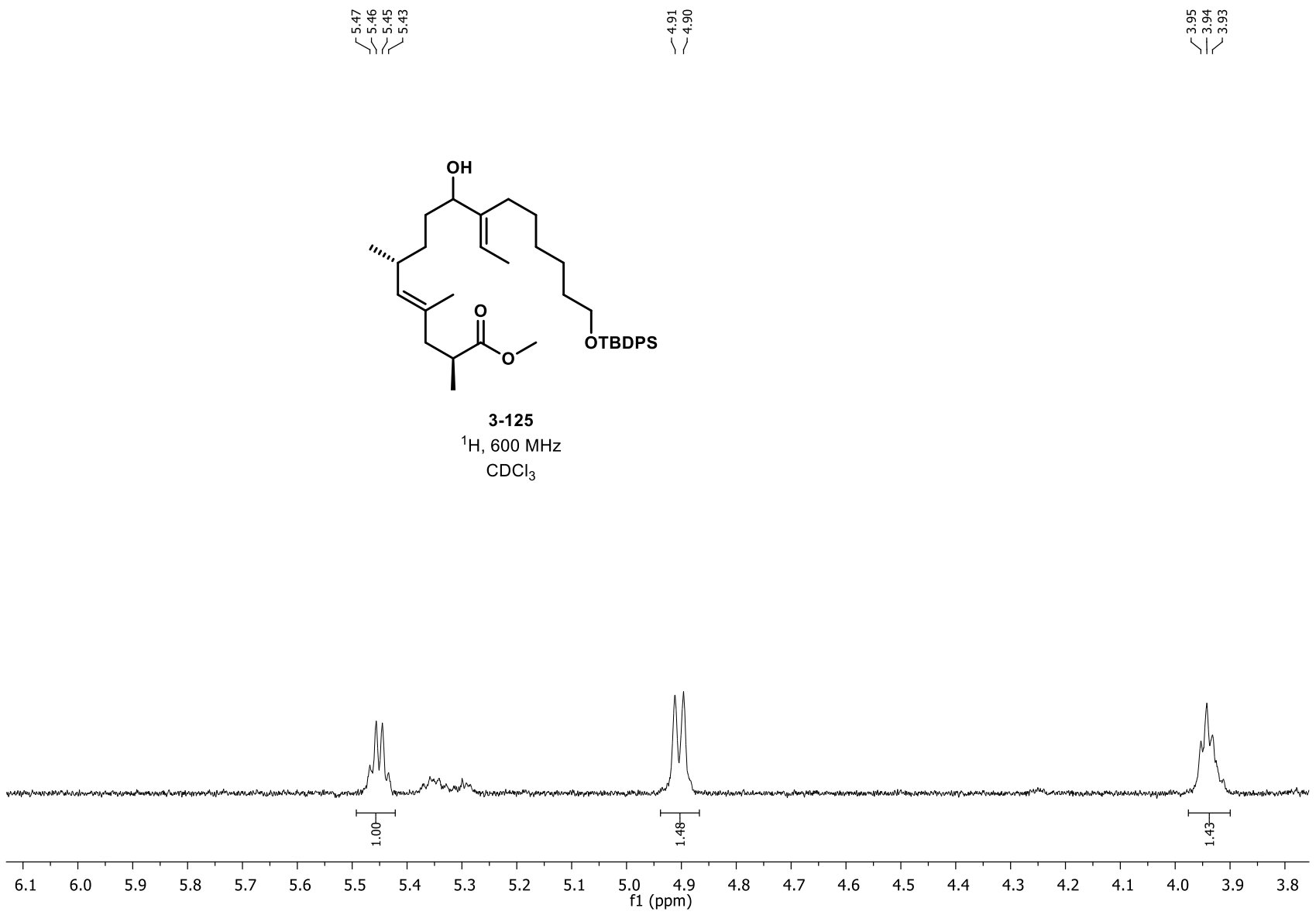

3-125

^{1}H, 600 MHz

$CDCl_3$

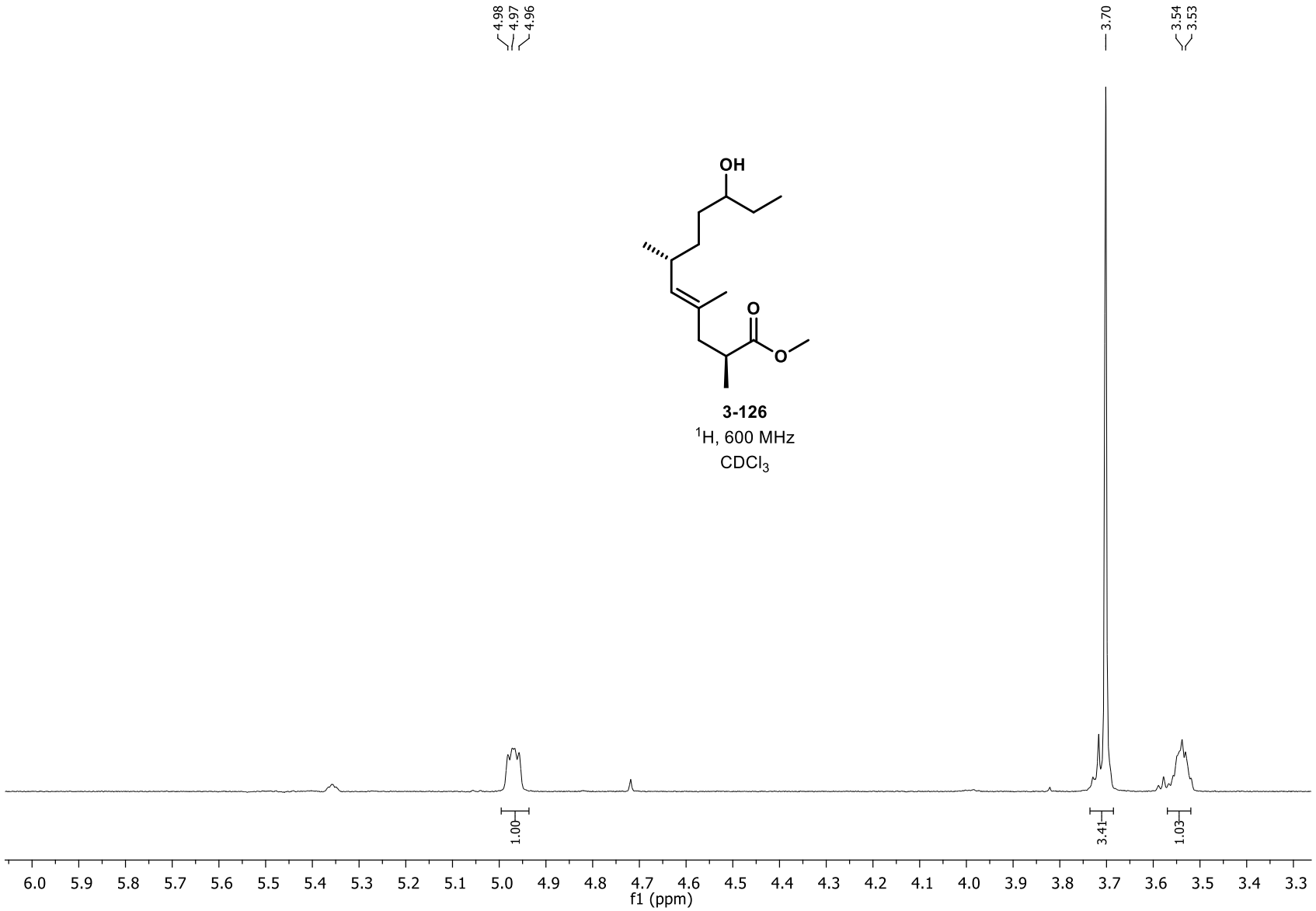
4.98
4.97
4.96
3.70
3.54
3.53
OH
O
O
3-126
1H, 600 MHz
CDCl3
1.00
3.41
1.03
6.0 5.9 5.8 5.7 5.6 5.5 5.4 5.3 5.2 5.1 5.0 4.9 4.8 4.7 4.6 4.5 4.4 4.3 4.2 4.1 4.0 3.9 3.8 3.7 3.6 3.5 3.4 3.3
f1 (ppm)

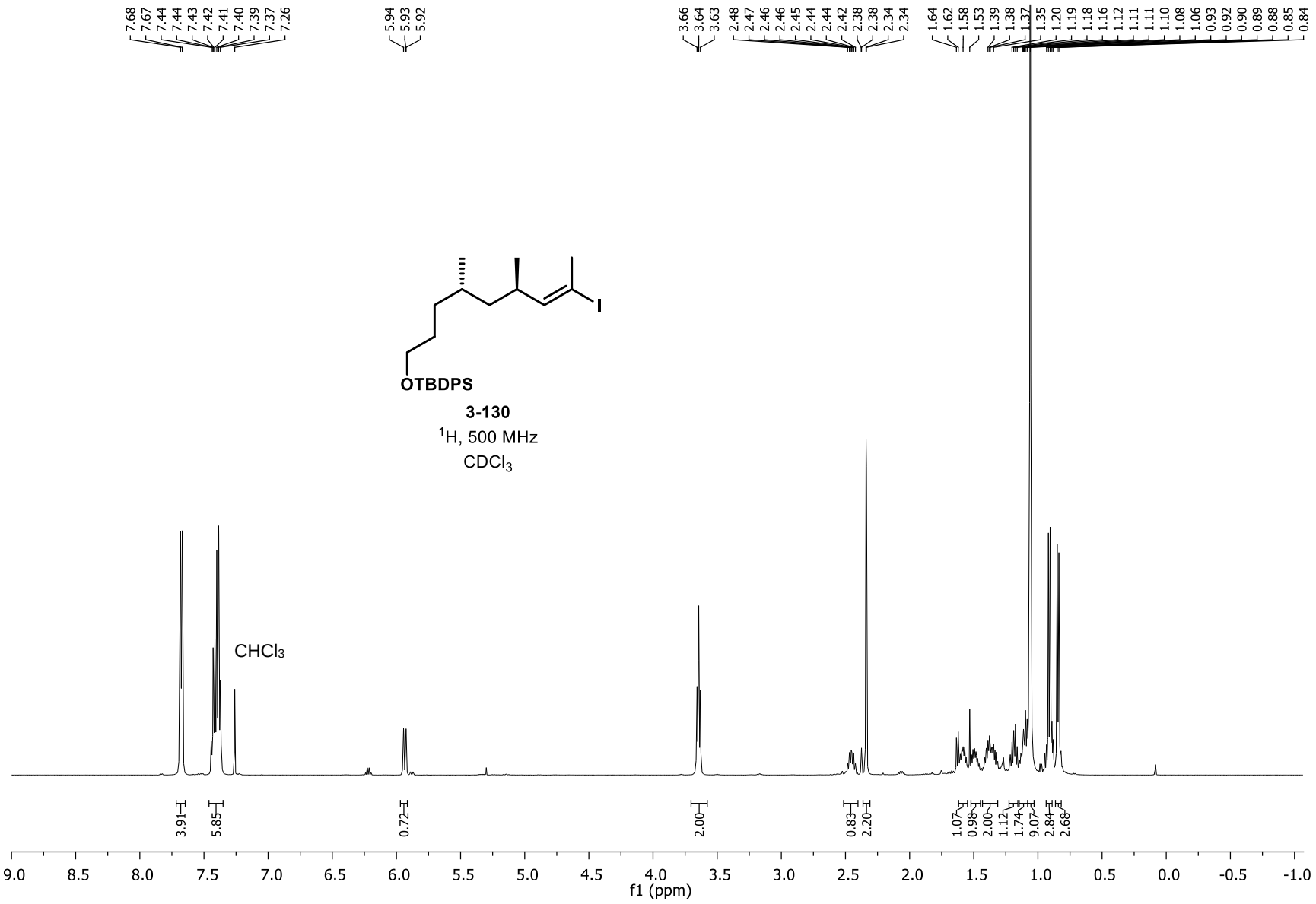
7.68
7.67
7.44
7.44
7.43
7.42
7.41
7.40
7.39
7.37
7.26
5.94
5.93
5.92
3.66
3.64
3.63
2.48
2.47
2.46
2.46
2.45
2.44
2.44
2.42
2.38
2.38
2.34
2.34
1.64
1.62
1.58
1.53
1.39
1.38
1.37
1.35
1.20
1.19
1.18
1.16
1.12
1.11
1.11
1.10
1.08
1.06
0.93
0.92
0.90
0.89
0.88
0.85
0.84
OTBDPS
3-130
1H, 500 MHz
CDCl3
CHCl3
3.91
5.85
0.72
2.00
0.83
2.20
1.07
0.98
2.00
1.12
1.74
9.07
2.84
2.68
9.0
8.5
8.0
7.5
7.0
6.5
6.0
5.5
5.0
4.5
4.0
3.5
3.0
2.5
2.0
1.5
1.0
0.5
0.0
-0.5
-1.0
f1 (ppm)

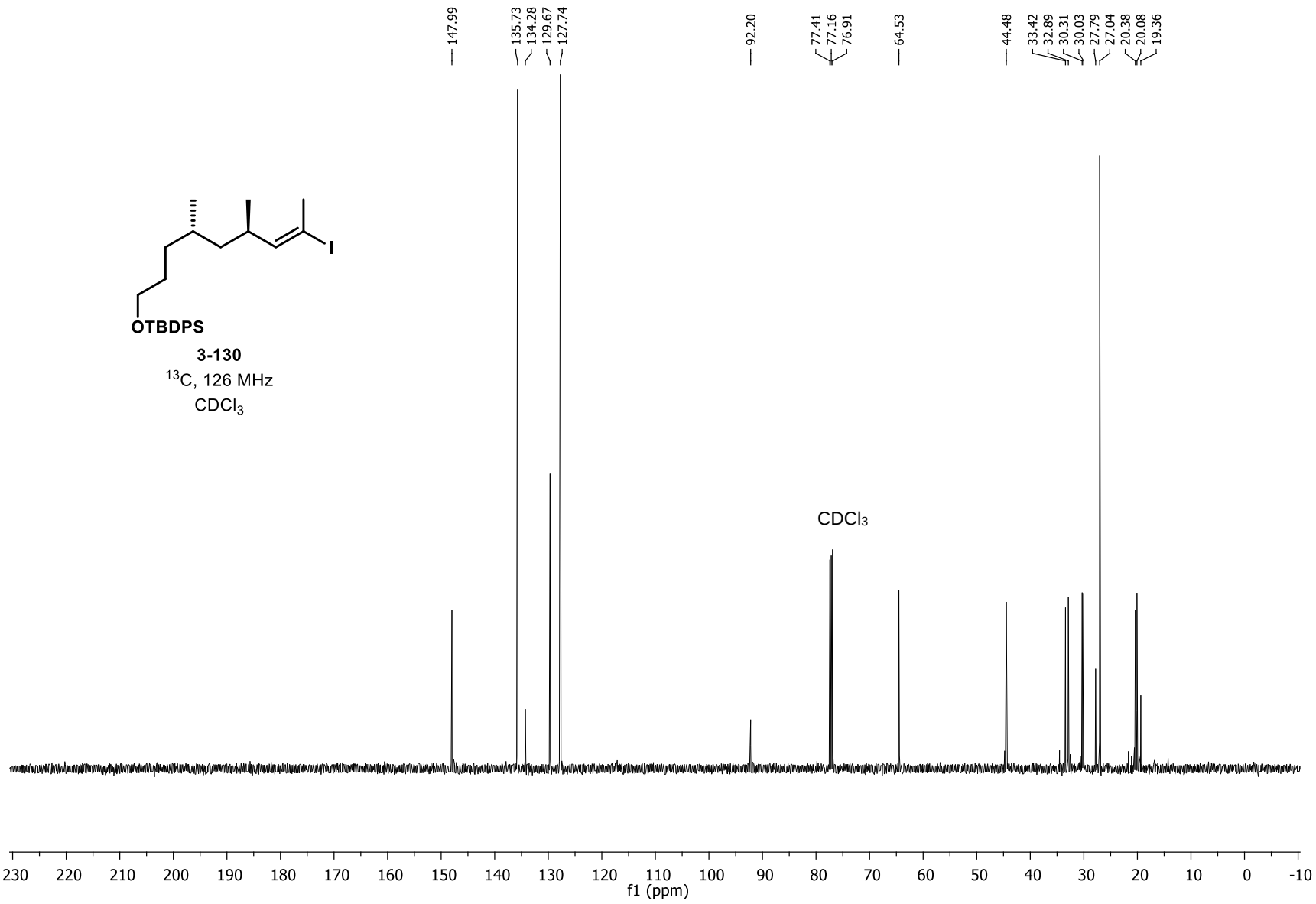
147.99
135.73
134.28
129.67
127.74
92.20
77.41
77.16
76.91
64.53
44.48
33.42
32.89
30.31
30.03
27.79
27.04
20.38
20.08
19.36
OTBDPS
3-130
13C, 126 MHz
CDCl3
CDCl3
f1 (ppm)

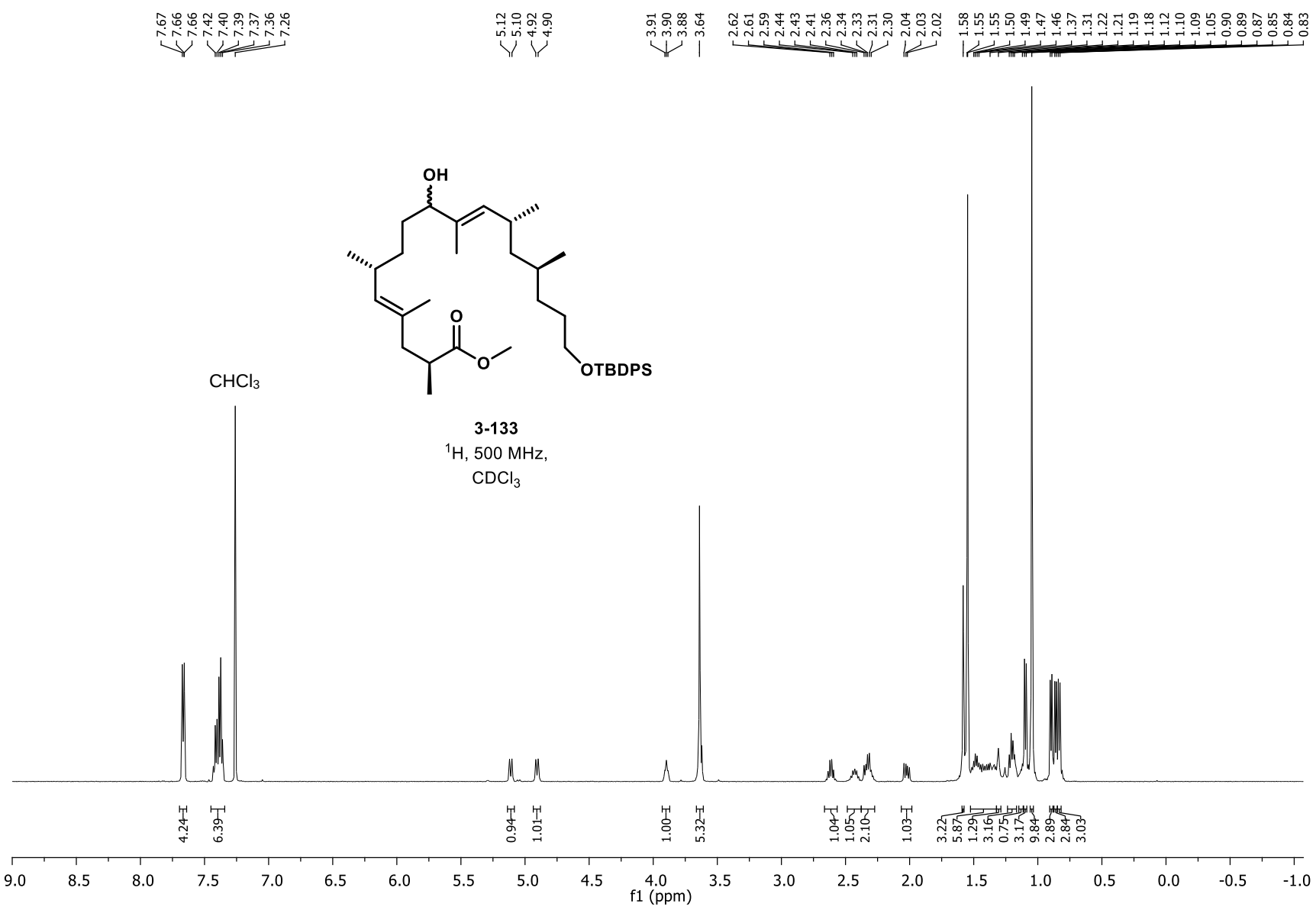
7.67
7.66
7.66
7.42
7.40
7.39
7.37
7.36
7.26
5.12
5.10
4.92
4.90
3.91
3.90
3.88
3.64
2.62
2.61
2.59
2.44
2.43
2.41
2.36
2.34
2.33
2.31
2.30
2.04
2.03
2.02
1.58
1.55
1.55
1.50
1.49
1.47
1.46
1.37
1.31
1.22
1.21
1.19
1.18
1.12
1.10
1.09
1.05
0.90
0.89
0.87
0.85
0.84
0.83
OH
O
O
OTBDPS
CHCl3
3-133
1H, 500 MHz,
CDCl3
4.24
6.39
0.94
1.01
1.00
5.32
1.04
1.05
2.10
1.03
3.22
5.87
1.29
3.16
0.75
3.17
9.84
2.89
2.84
3.03
9.0
8.5
8.0
7.5
7.0
6.5
6.0
5.5
5.0
4.5
4.0
3.5
3.0
2.5
2.0
1.5
1.0
0.5
0.0
-0.5
-1.0
f1 (ppm)

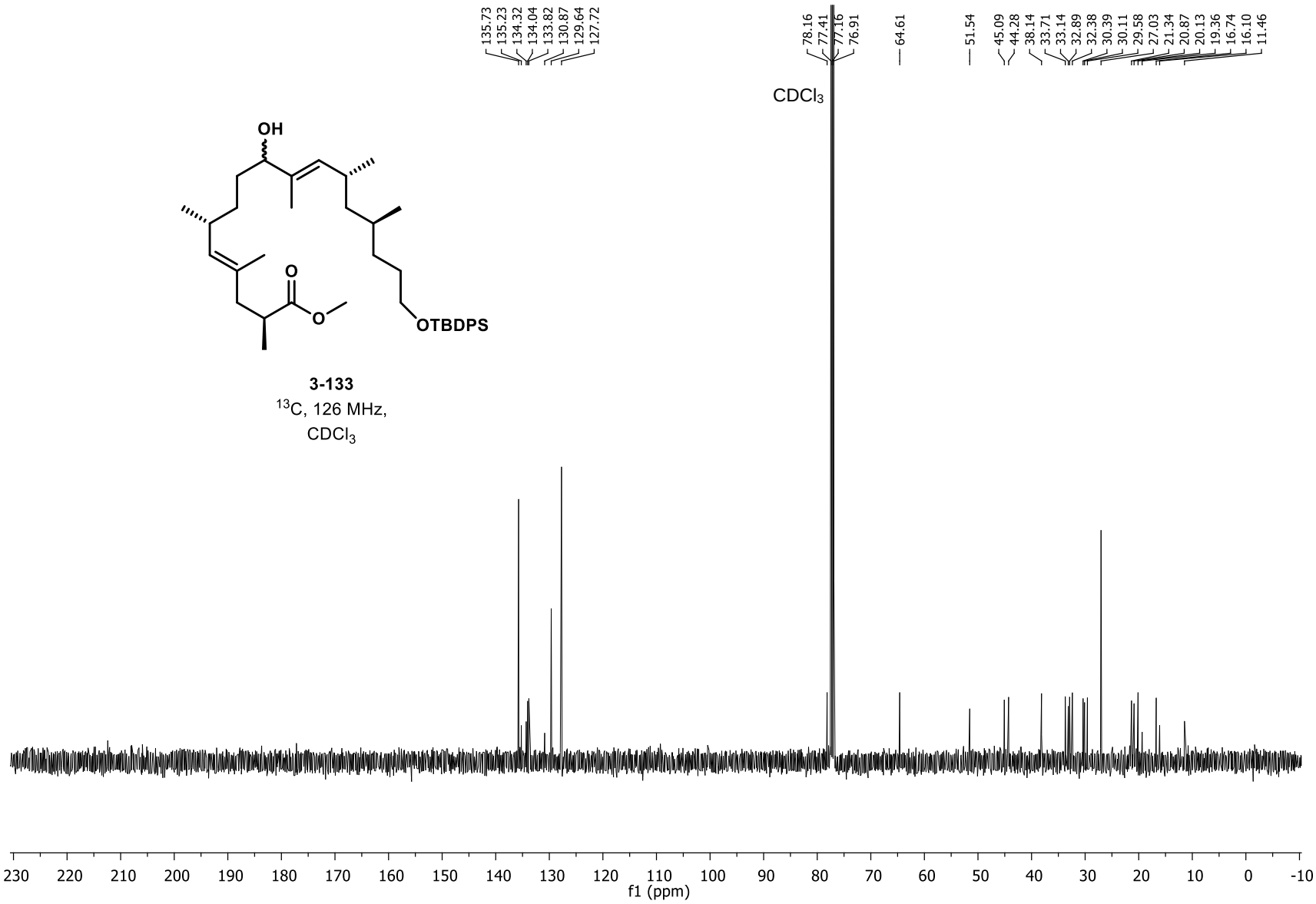
135.73
135.23
134.32
134.04
133.82
130.87
129.64
127.72
78.16
77.41
77.16
76.91
64.61
51.54
45.09
44.28
38.14
33.71
33.14
32.89
32.38
30.39
30.11
29.58
27.03
21.34
20.87
20.13
19.36
16.74
16.10
11.46
CDCl3
OH
O
O
OTBDPS
3-133
13C, 126 MHz,
CDCl3
230 220 210 200 190 180 170 160 150 140 130 120 110 100 90 80 70 60 50 40 30 20 10 0 -10
f1 (ppm)

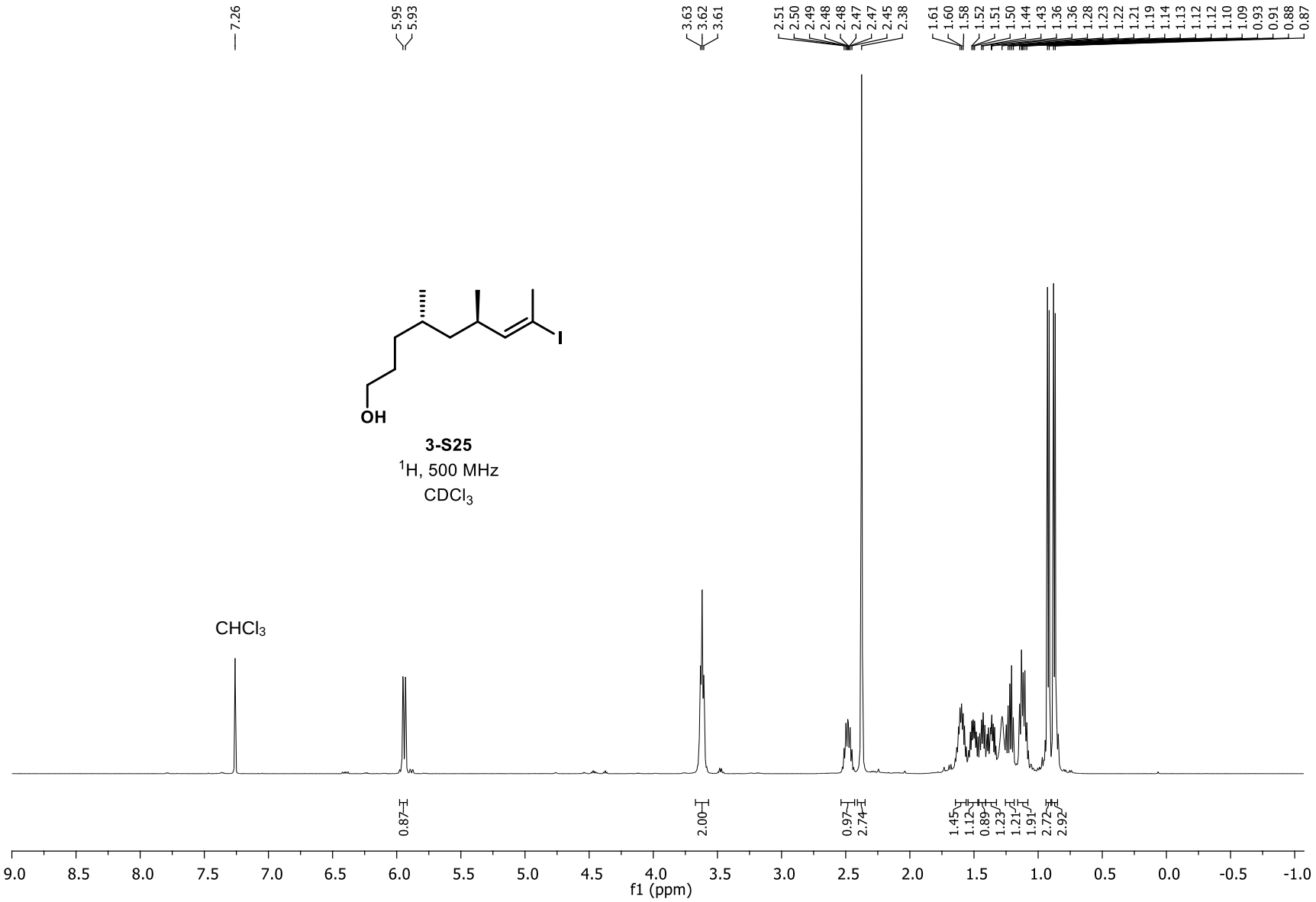
7.26
5.95
5.93
3.63
3.62
3.61
2.51
2.50
2.49
2.48
2.48
2.47
2.47
2.45
2.38
1.61
1.60
1.58
1.52
1.51
1.50
1.44
1.43
1.36
1.36
1.28
1.23
1.22
1.21
1.19
1.14
1.13
1.12
1.12
1.10
1.09
0.93
0.91
0.88
0.87
OH
3-S25
1H, 500 MHz
CDCl3
CHCl3
0.87
2.00
0.97
2.74
1.45
1.12
0.89
1.23
1.21
1.91
2.72
2.92
9.0
8.5
8.0
7.5
7.0
6.5
6.0
5.5
5.0
4.5
4.0
3.5
3.0
2.5
2.0
1.5
1.0
0.5
0.0
-0.5
-1.0
f1 (ppm)

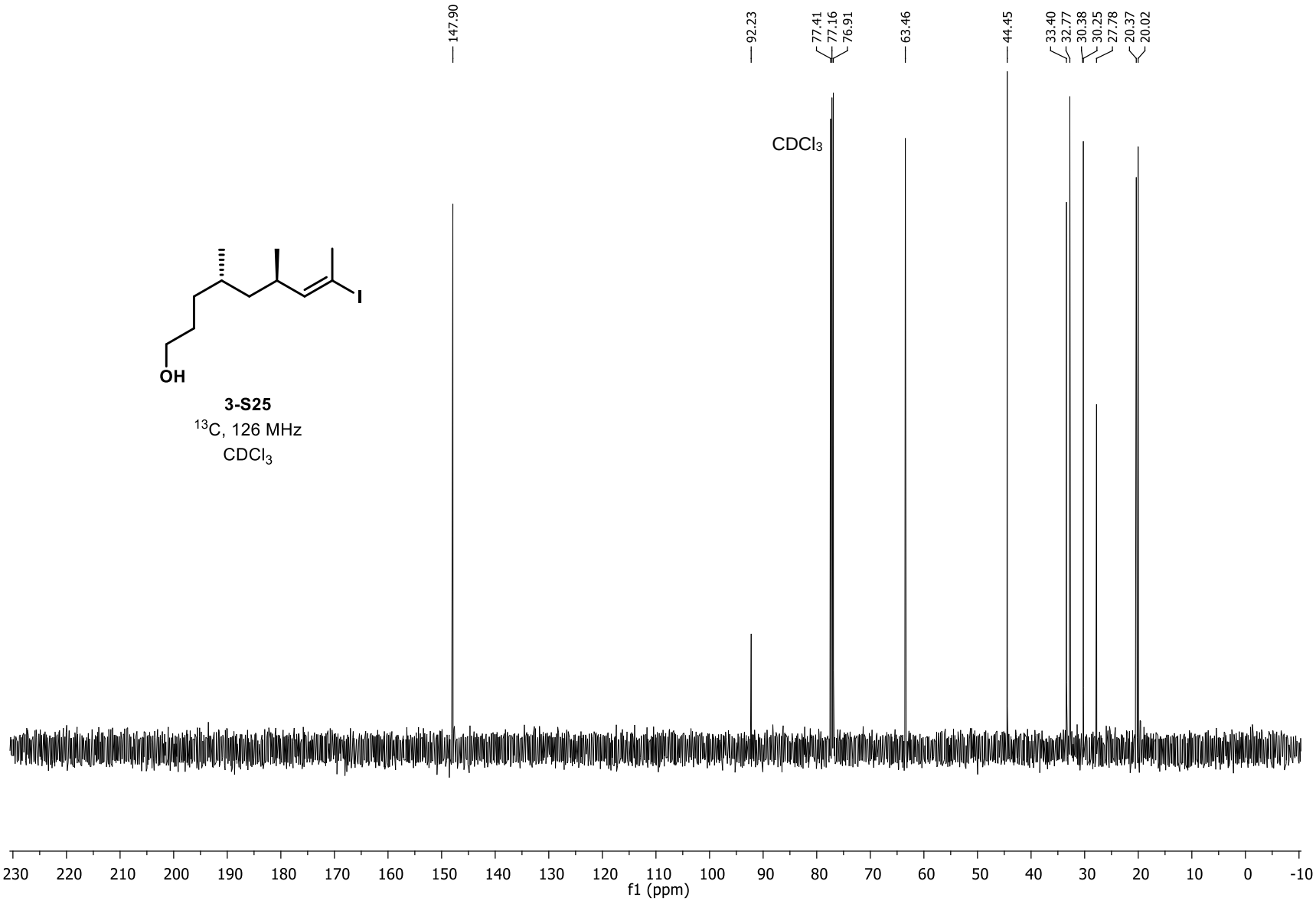
147.90
92.23
77.41
77.16
76.91
63.46
44.45
33.40
32.77
30.38
30.25
27.78
20.37
20.02
CDCl3
I
OH
3-S25
13C, 126 MHz
CDCl3
230 220 210 200 190 180 170 160 150 140 130 120 110 100 90 80 70 60 50 40 30 20 10 0 -10
f1 (ppm)

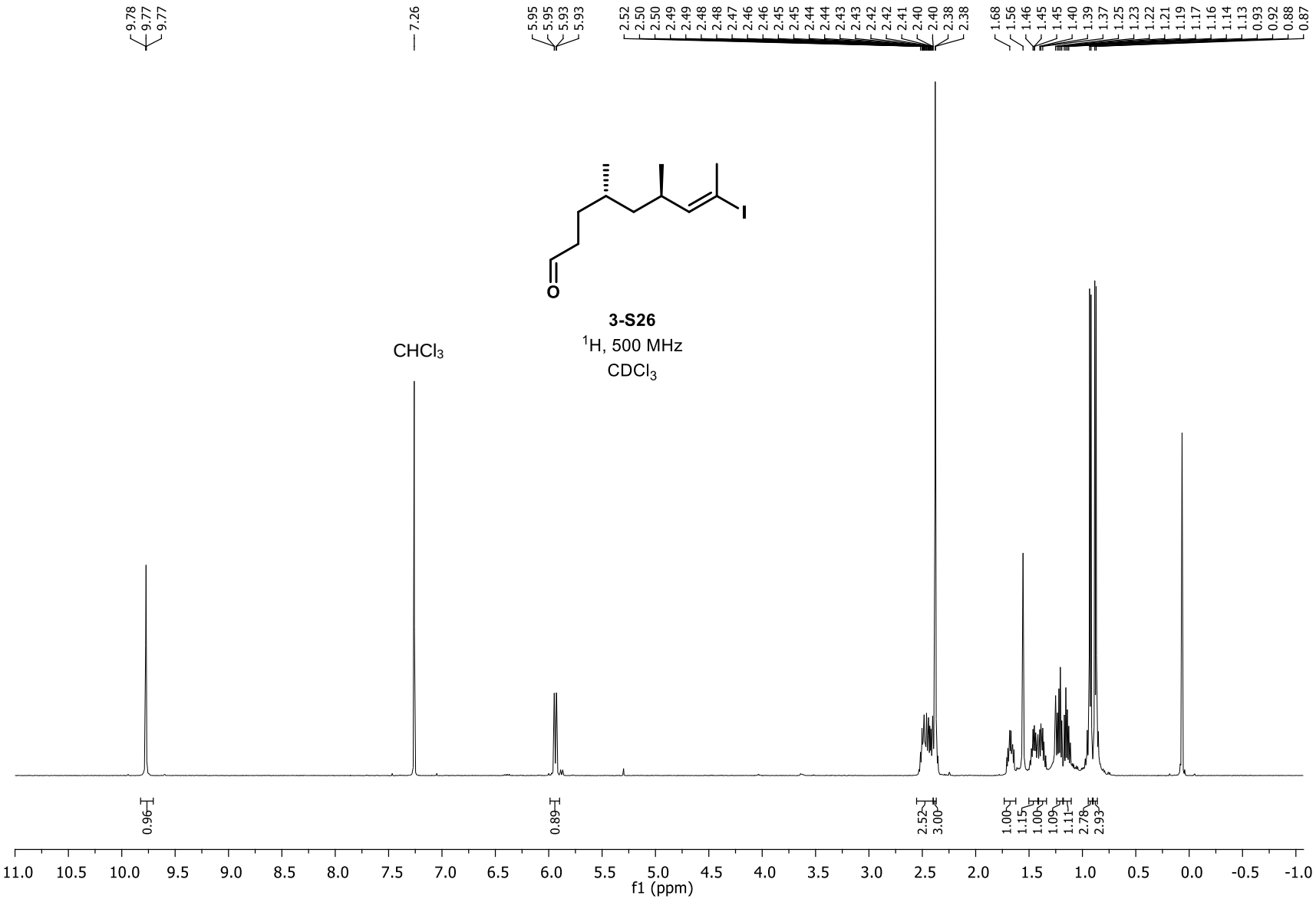
9.78
9.77
9.77
7.26
5.95
5.95
5.93
5.93
2.52
2.50
2.50
2.49
2.49
2.48
2.48
2.47
2.46
2.46
2.45
2.45
2.44
2.44
2.43
2.43
2.42
2.42
2.41
2.40
2.40
2.38
2.38
1.68
1.56
1.46
1.45
1.45
1.40
1.39
1.37
1.25
1.23
1.22
1.21
1.19
1.17
1.16
1.14
1.13
0.93
0.92
0.88
0.87
I
O
3-S26
1H, 500 MHz
CDCl3
CHCl3
0.96
0.89
2.52
3.00
1.00
1.15
1.00
1.09
1.11
2.78
2.93
11.0
10.5
10.0
9.5
9.0
8.5
8.0
7.5
7.0
6.5
6.0
5.5
5.0
4.5
4.0
3.5
3.0
2.5
2.0
1.5
1.0
0.5
0.0
-0.5
-1.0
f1 (ppm)

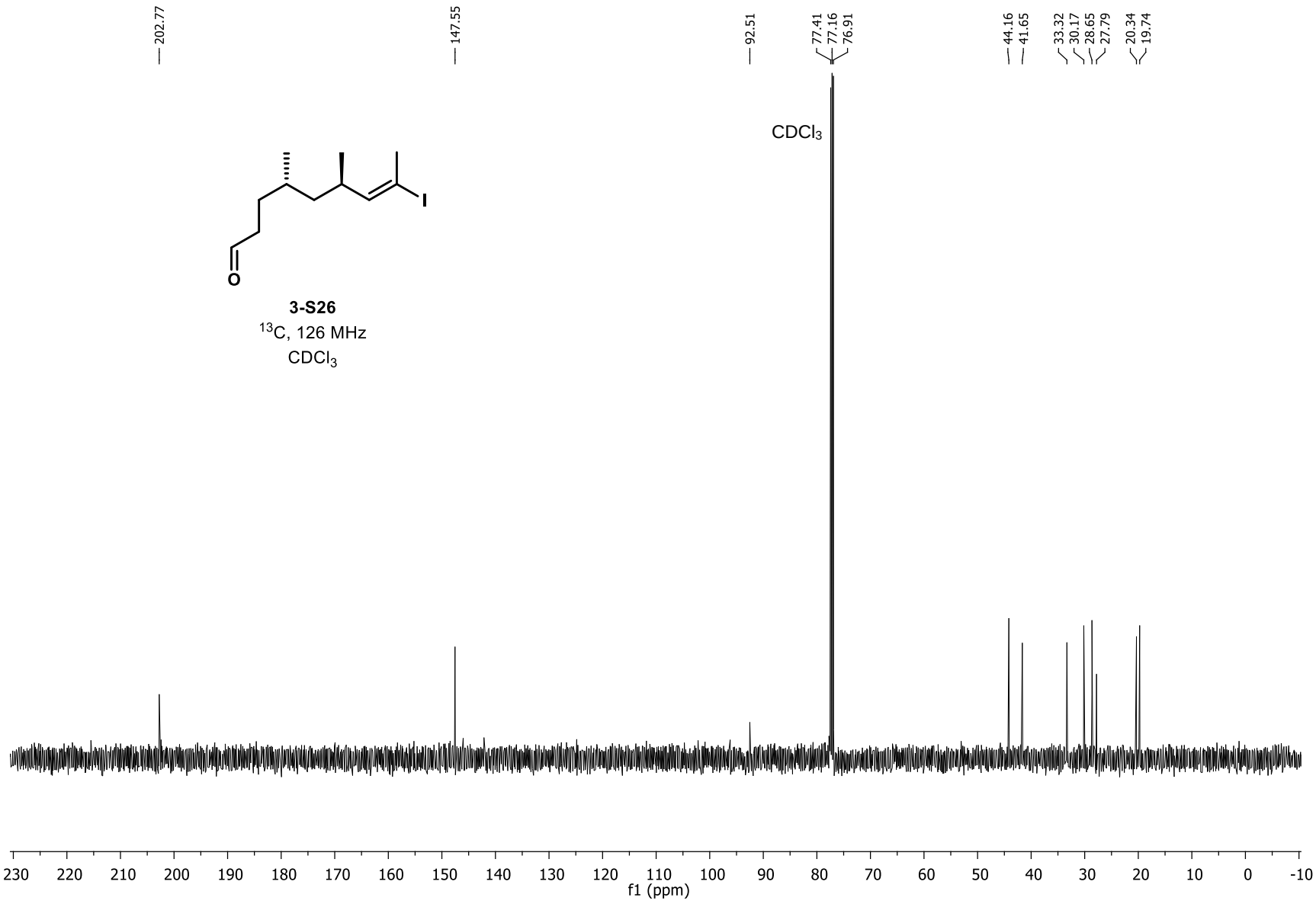
202.77
147.55
92.51
77.41
77.16
76.91
44.16
41.65
33.32
30.17
28.65
27.79
20.34
19.74
CDCl3
I
O
3-S26
13C, 126 MHz
CDCl3
230 220 210 200 190 180 170 160 150 140 130 120 110 100 90 80 70 60 50 40 30 20 10 0 -10
f1 (ppm)

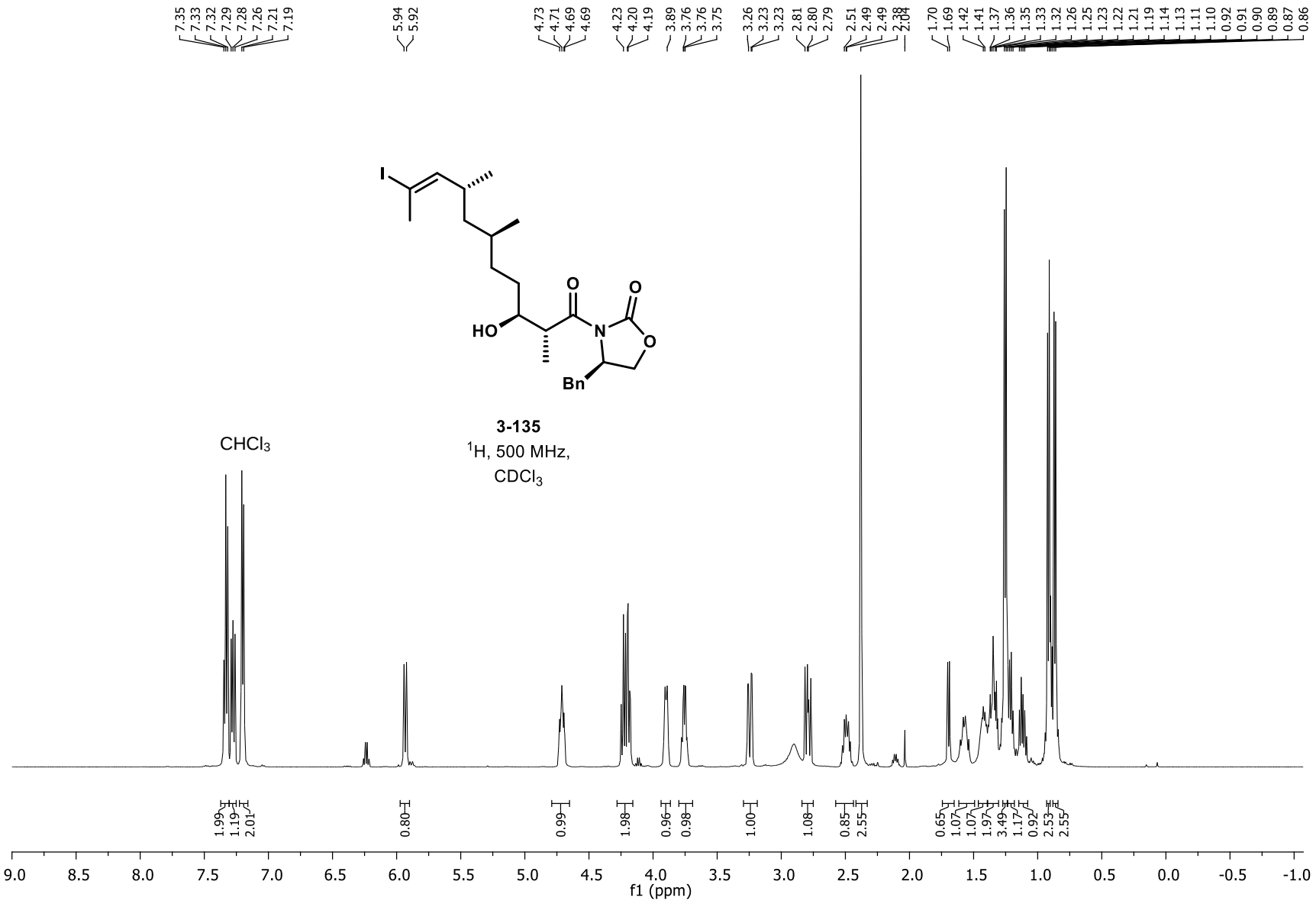
7.35
7.33
7.32
7.29
7.28
7.26
7.21
7.19
5.94
5.92
4.73
4.71
4.69
4.69
4.23
4.20
4.19
3.89
3.76
3.76
3.75
3.26
3.23
3.23
2.81
2.80
2.79
2.51
2.49
2.49
2.38
2.04
1.70
1.69
1.42
1.41
1.37
1.36
1.35
1.33
1.32
1.26
1.25
1.23
1.22
1.21
1.19
1.14
1.13
1.11
1.10
0.92
0.91
0.90
0.89
0.87
0.86
I
HO
O
O
N
O
Bn
CHCl3
3-135
1H, 500 MHz,
CDCl3
1.99
1.19
2.01
0.80
0.99
1.98
0.96
0.98
1.00
1.08
0.85
2.55
0.65
1.07
1.07
1.97
3.49
1.17
0.92
2.53
2.55
9.0
8.5
8.0
7.5
7.0
6.5
6.0
5.5
5.0
4.5
4.0
3.5
3.0
2.5
2.0
1.5
1.0
0.5
0.0
-0.5
-1.0
f1 (ppm)

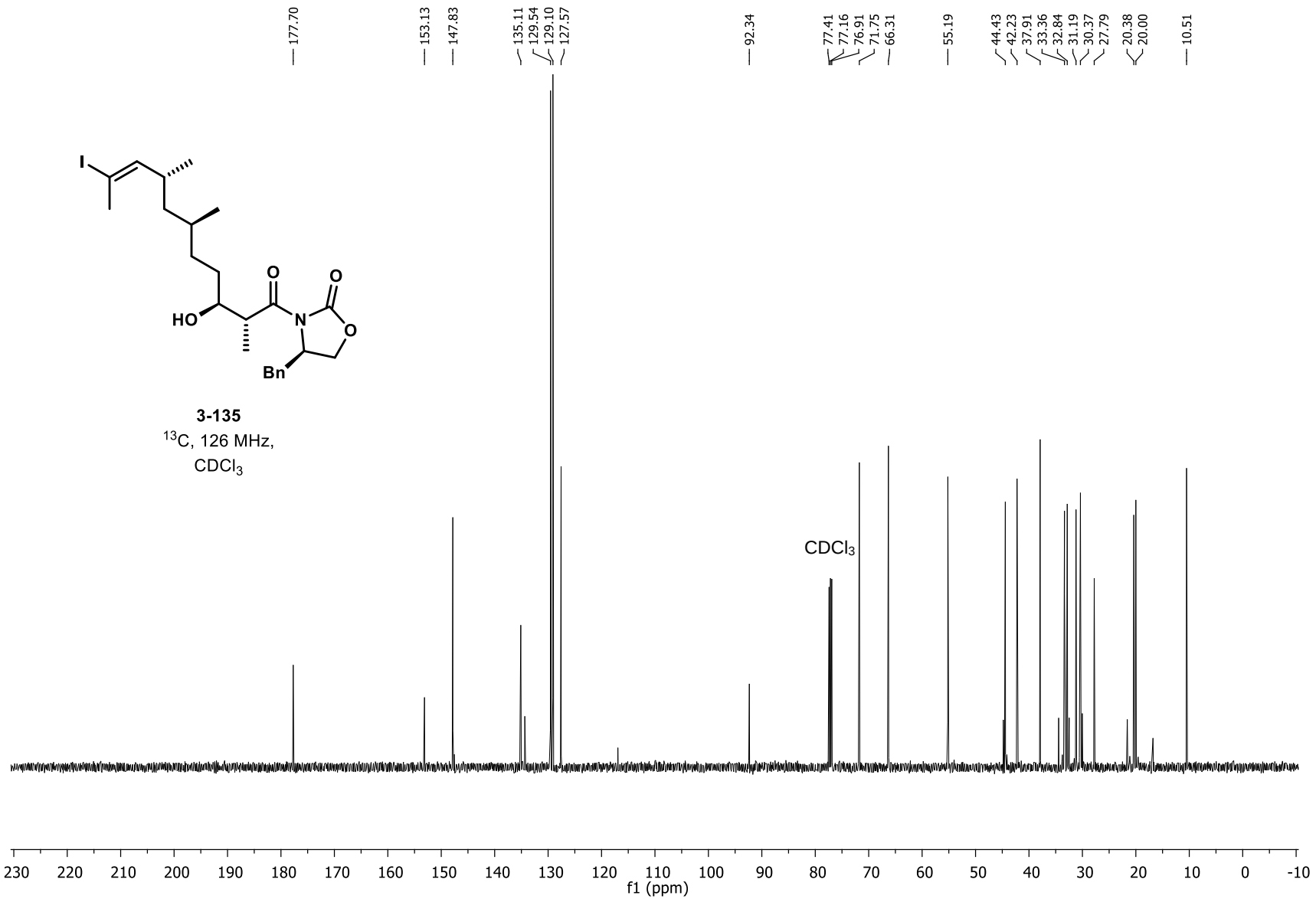
177.70
153.13
147.83
135.11
129.54
129.10
127.57
92.34
77.41
77.16
76.91
71.75
66.31
55.19
44.43
42.23
37.91
33.36
32.84
31.19
30.37
27.79
20.38
20.00
10.51
I
HO
O
O
N
O
Bn
CDCl3
3-135
13C, 126 MHz,
CDCl3
500
230 220 210 200 190 180 170 160 150 140 130 120 110 100 90 80 70 60 50 40 30 20 10 0 -10
f1 (ppm)

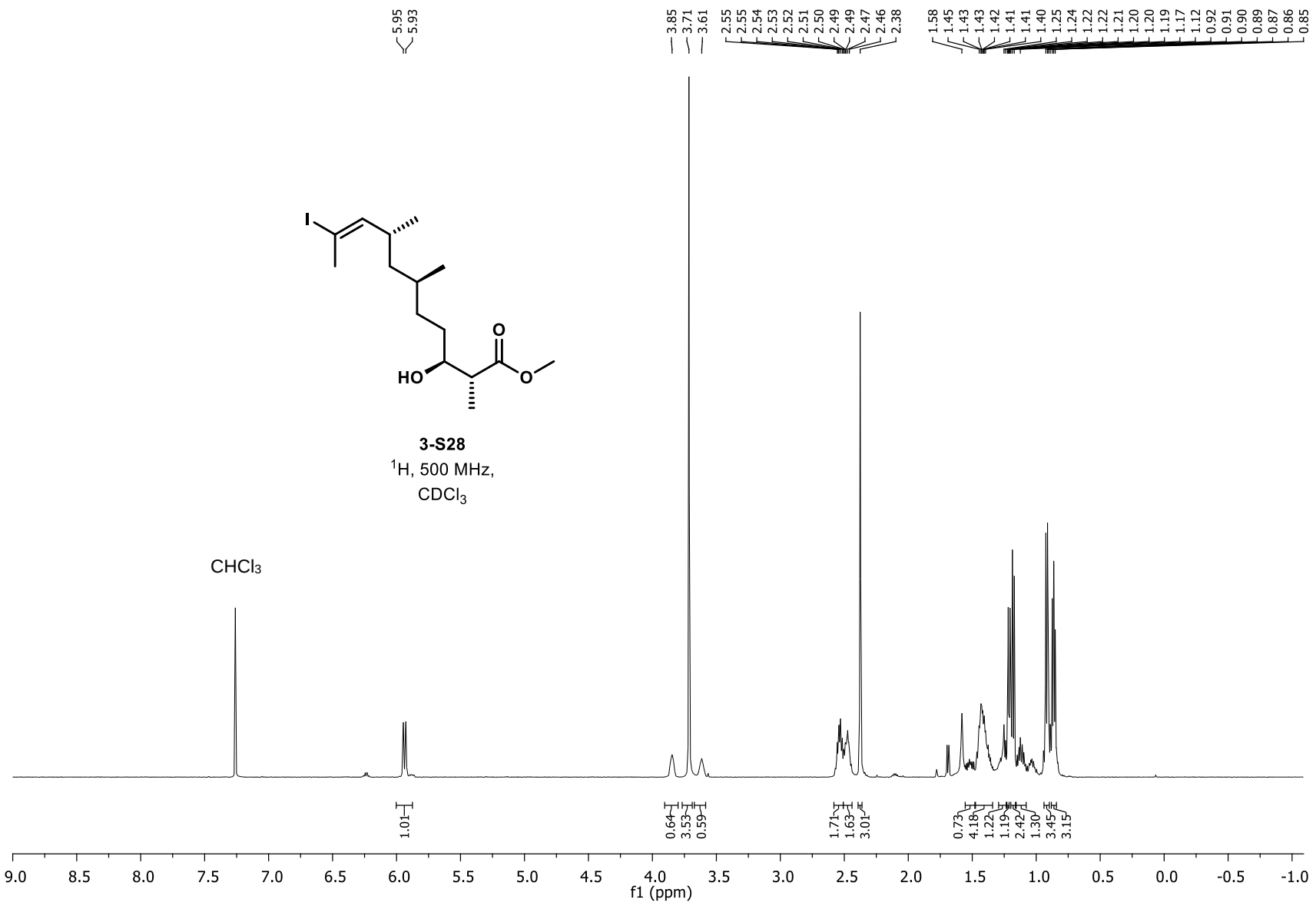

3-S28

^{1}H, 500 MHz,
$CDCl_3$

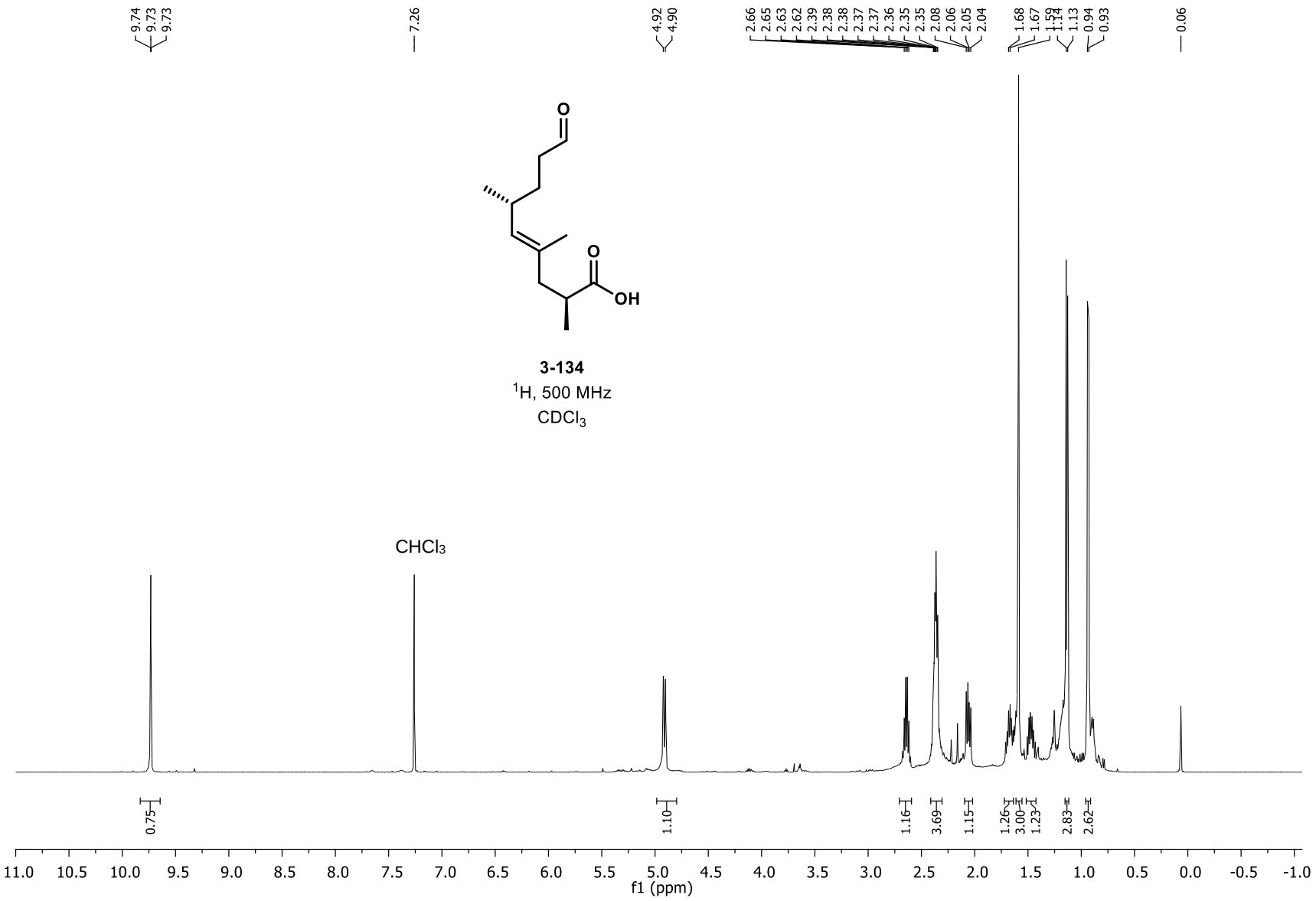
9.74
9.73
9.73
7.26
4.92
4.90
2.66
2.65
2.63
2.62
2.39
2.38
2.38
2.37
2.37
2.36
2.35
2.35
2.08
2.06
2.05
2.04
1.68
1.67
1.59
1.14
1.13
0.94
0.93
0.06
O
O
OH
3-134
1H, 500 MHz
CDCl3
CHCl3
0.75
1.10
1.16
3.69
1.15
1.26
3.00
1.23
2.83
2.62
11.0
10.5
10.0
9.5
9.0
8.5
8.0
7.5
7.0
6.5
6.0
5.5
5.0
4.5
4.0
3.5
3.0
2.5
2.0
1.5
1.0
0.5
0.0
-0.5
-1.0
f1 (ppm)

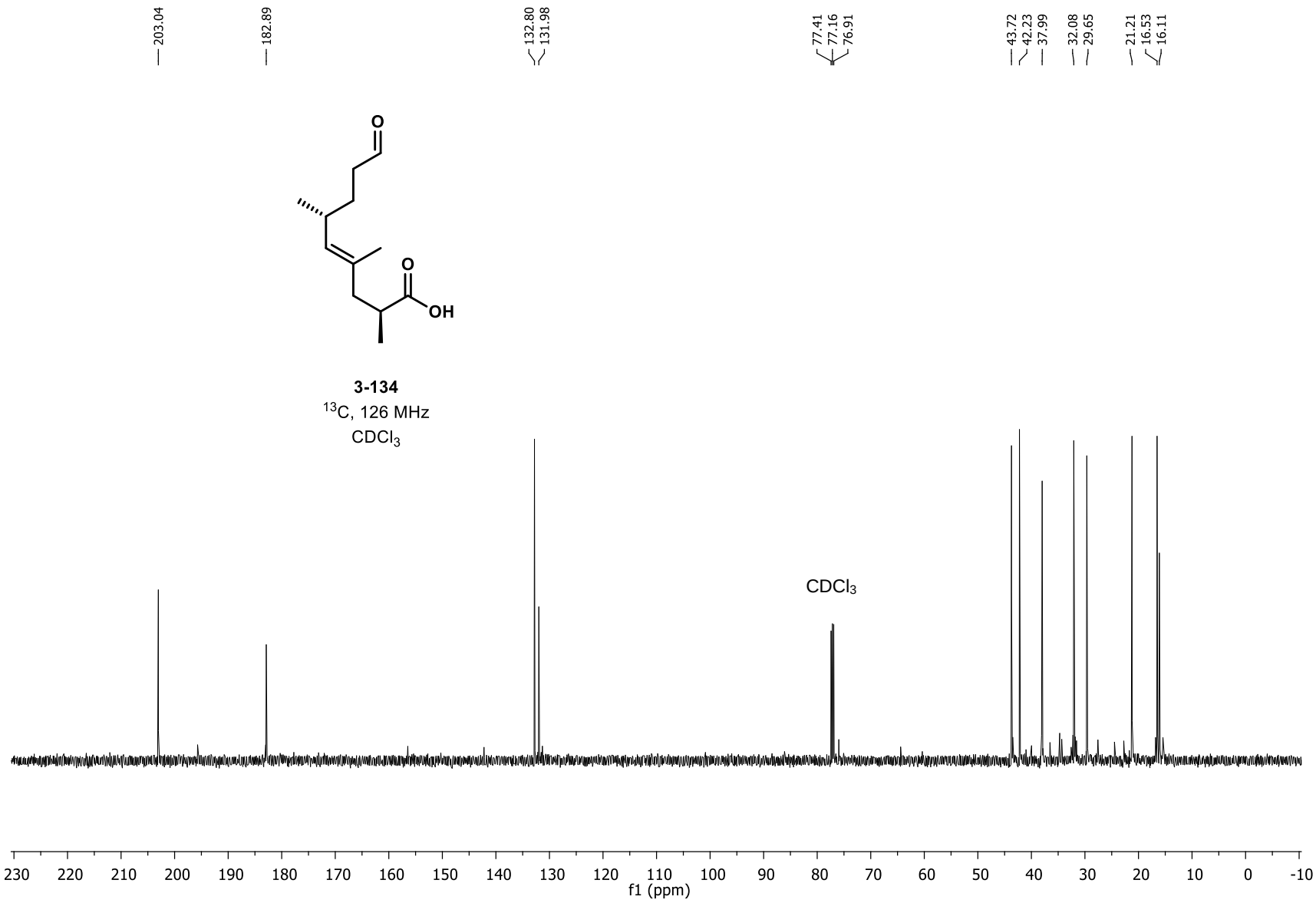
203.04
182.89
132.80
131.98
77.41
77.16
76.91
43.72
42.23
37.99
32.08
29.65
21.21
16.53
16.11
O
O
OH
3-134
13C, 126 MHz
CDCl3
CDCl3
230 220 210 200 190 180 170 160 150 140 130 120 110 100 90 80 70 60 50 40 30 20 10 0 -10
f1 (ppm)

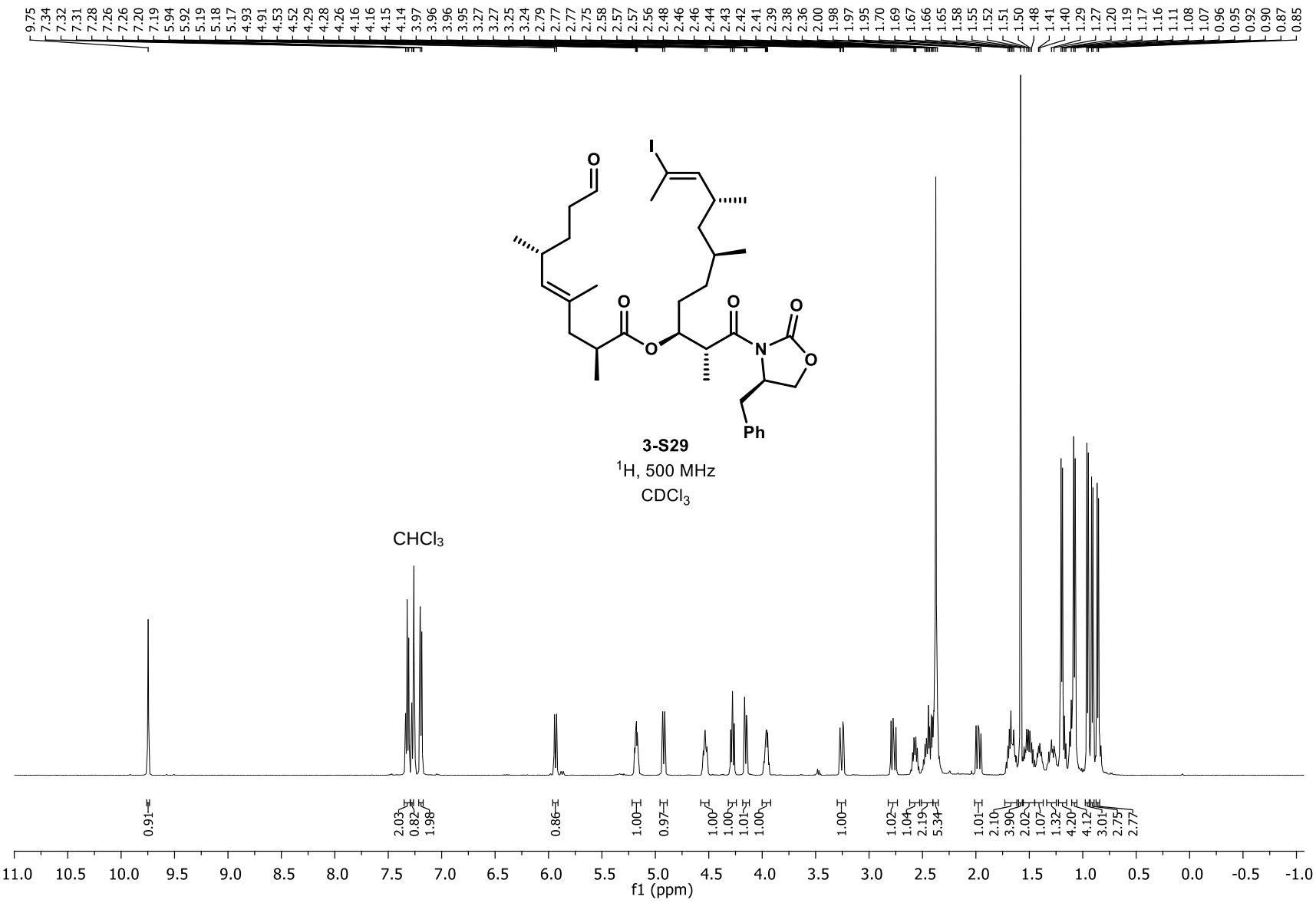
9.75 7.34 7.32 7.31 7.28 7.26 7.26 7.20 7.19 5.94 5.92 5.19 5.18 5.17 4.93 4.91 4.53 4.52 4.29 4.28 4.26 4.16 4.16 4.15 4.14 3.97 3.96 3.96 3.95 3.27 3.27 3.25 3.24 2.79 2.77 2.75 2.58 2.57 2.57 2.56 2.48 2.46 2.46 2.44 2.43 2.42 2.41 2.39 2.38 2.36 2.00 1.98 1.97 1.95 1.70 1.69 1.67 1.66 1.65 1.58 1.55 1.52 1.51 1.50 1.48 1.41 1.40 1.29 1.27 1.20 1.19 1.17 1.16 1.11 1.08 1.07 0.96 0.95 0.92 0.90 0.87 0.85
O
I
O
O
O
O
N
O
Ph
3-S29
1H, 500 MHz
CDCl3
CHCl3
0.91 2.03 0.82 1.98 0.86 1.00 0.97 1.00 1.00 1.01 1.00 1.00 1.02 1.04 2.19 5.34 1.01 2.10 3.90 2.02 1.07 1.32 4.20 4.12 3.01 2.75 2.77
11.0 10.5 10.0 9.5 9.0 8.5 8.0 7.5 7.0 6.5 6.0 5.5 5.0 4.5 4.0 3.5 3.0 2.5 2.0 1.5 1.0 0.5 0.0 -0.5 -1.0
f1 (ppm)

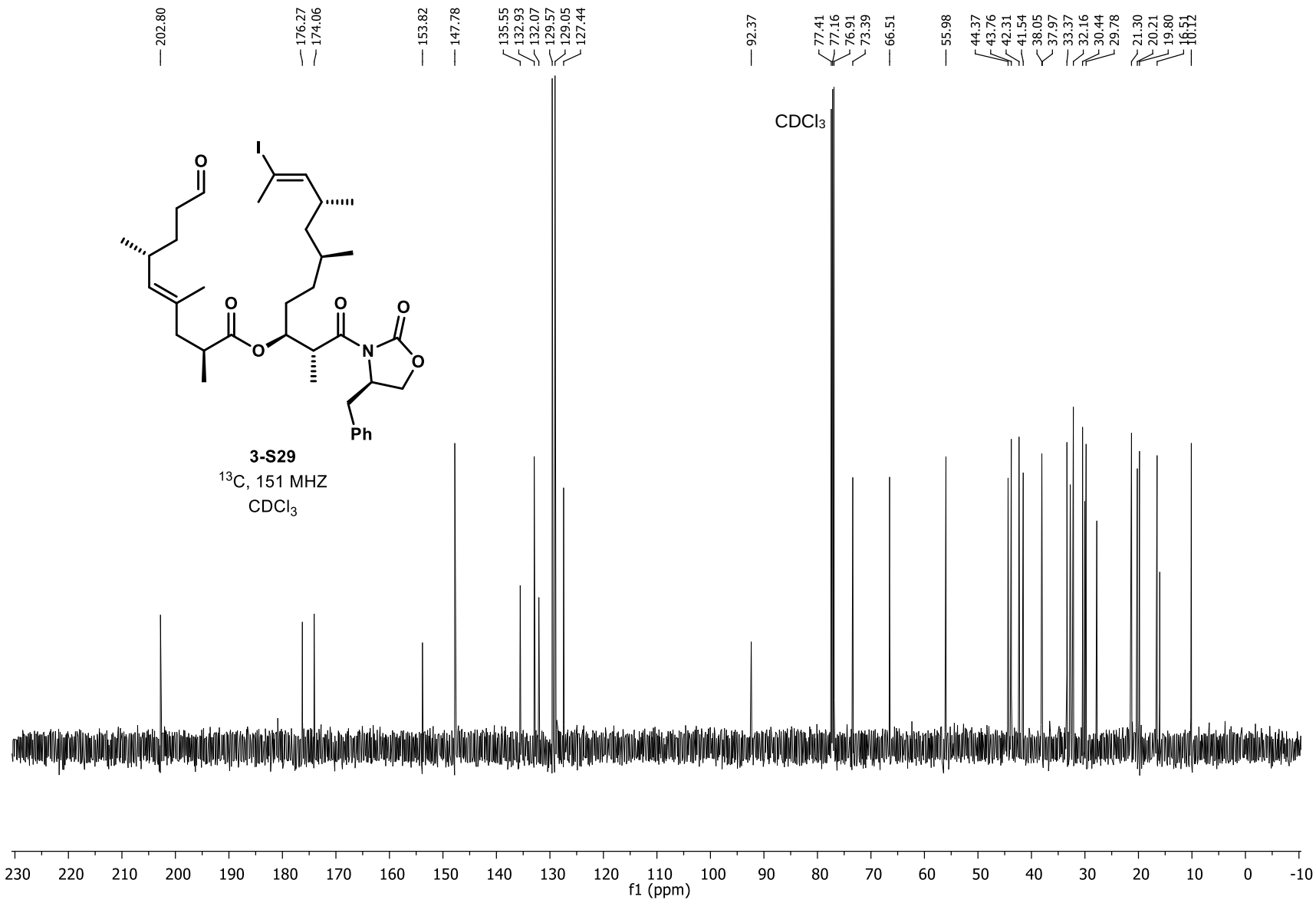
202.80
176.27
174.06
153.82
147.78
135.55
132.93
132.07
129.57
129.05
127.44
92.37
77.41
77.16
76.91
73.39
66.51
55.98
44.37
43.76
42.31
41.54
38.05
37.97
33.37
32.16
30.44
29.78
21.30
20.21
19.80
16.51
16.12
CDCl3
I
O
O
O
O
O
N
O
Ph
3-S29
13C, 151 MHZ
CDCl3
230
220
210
200
190
180
170
160
150
140
130
120
110
100
90
80
70
60
50
40
30
20
10
0
-10
f1 (ppm)

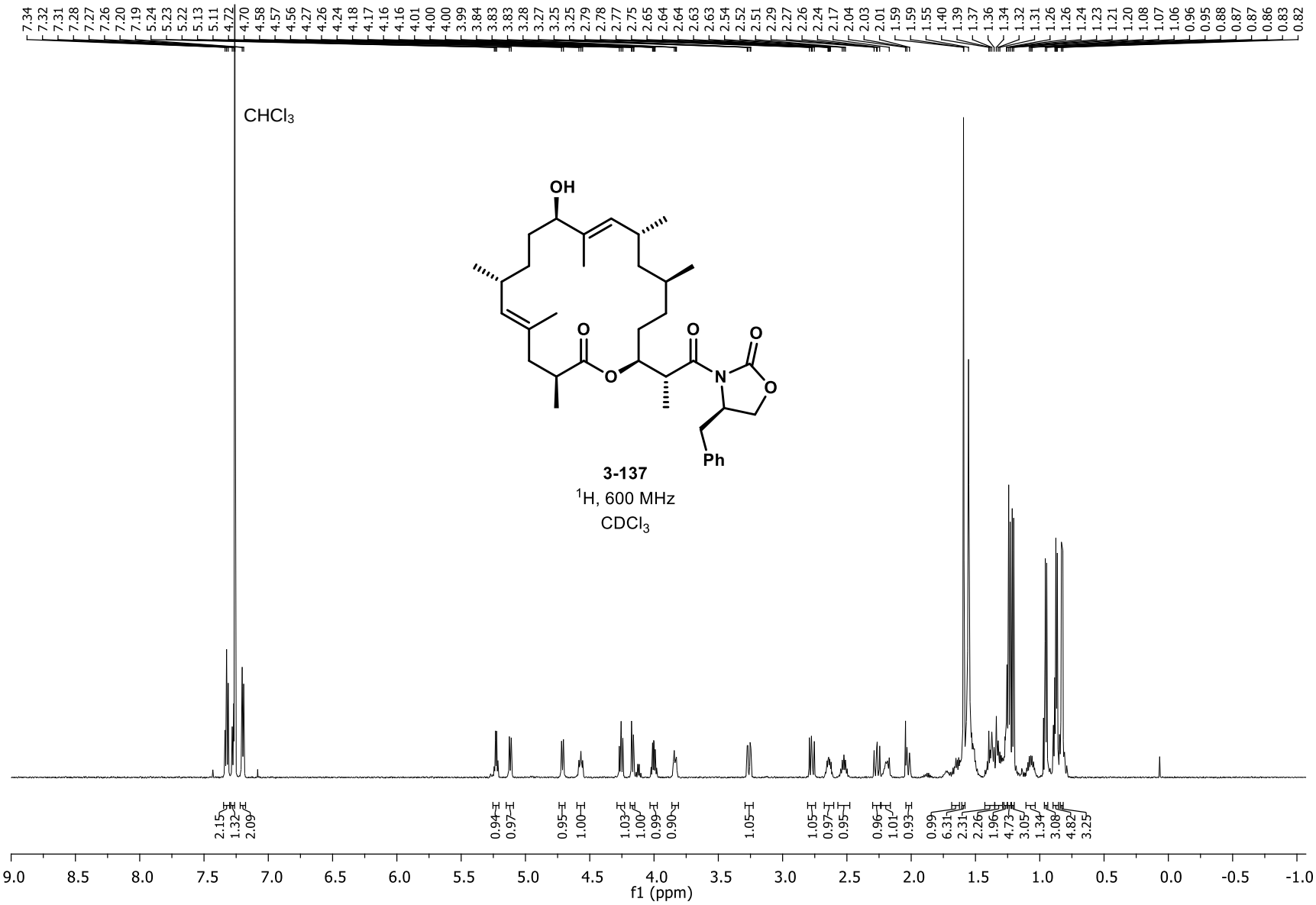
7.34 7.32 7.31 7.28 7.27 7.26 7.20 7.19 5.24 5.23 5.22 5.13 5.11 4.72 4.70 4.58 4.57 4.56 4.27 4.26 4.24 4.18 4.17 4.16 4.16 4.01 4.00 4.00 3.99 3.84 3.83 3.83 3.28 3.27 3.25 3.25 2.79 2.78 2.77 2.75 2.65 2.64 2.64 2.63 2.63 2.54 2.52 2.51 2.29 2.27 2.26 2.24 2.17 2.04 2.03 2.01 1.59 1.59 1.55 1.40 1.39 1.37 1.36 1.34 1.32 1.31 1.26 1.26 1.24 1.23 1.21 1.20 1.08 1.07 1.06 0.96 0.95 0.88 0.87 0.87 0.86 0.83 0.82
CHCl3
OH
O
O
O
O
N
O
Ph
3-137
1H, 600 MHz
CDCl3
2.15 1.32 2.09 0.94 0.97 0.95 1.00 1.03 1.00 0.99 0.90 1.05 1.05 0.97 0.95 0.96 1.01 0.93 0.99 6.31 2.31 2.26 1.96 4.73 3.05 1.34 3.08 4.82 3.25
9.0 8.5 8.0 7.5 7.0 6.5 6.0 5.5 5.0 4.5 4.0 3.5 3.0 2.5 2.0 1.5 1.0 0.5 0.0 -0.5 -1.0
f1 (ppm)

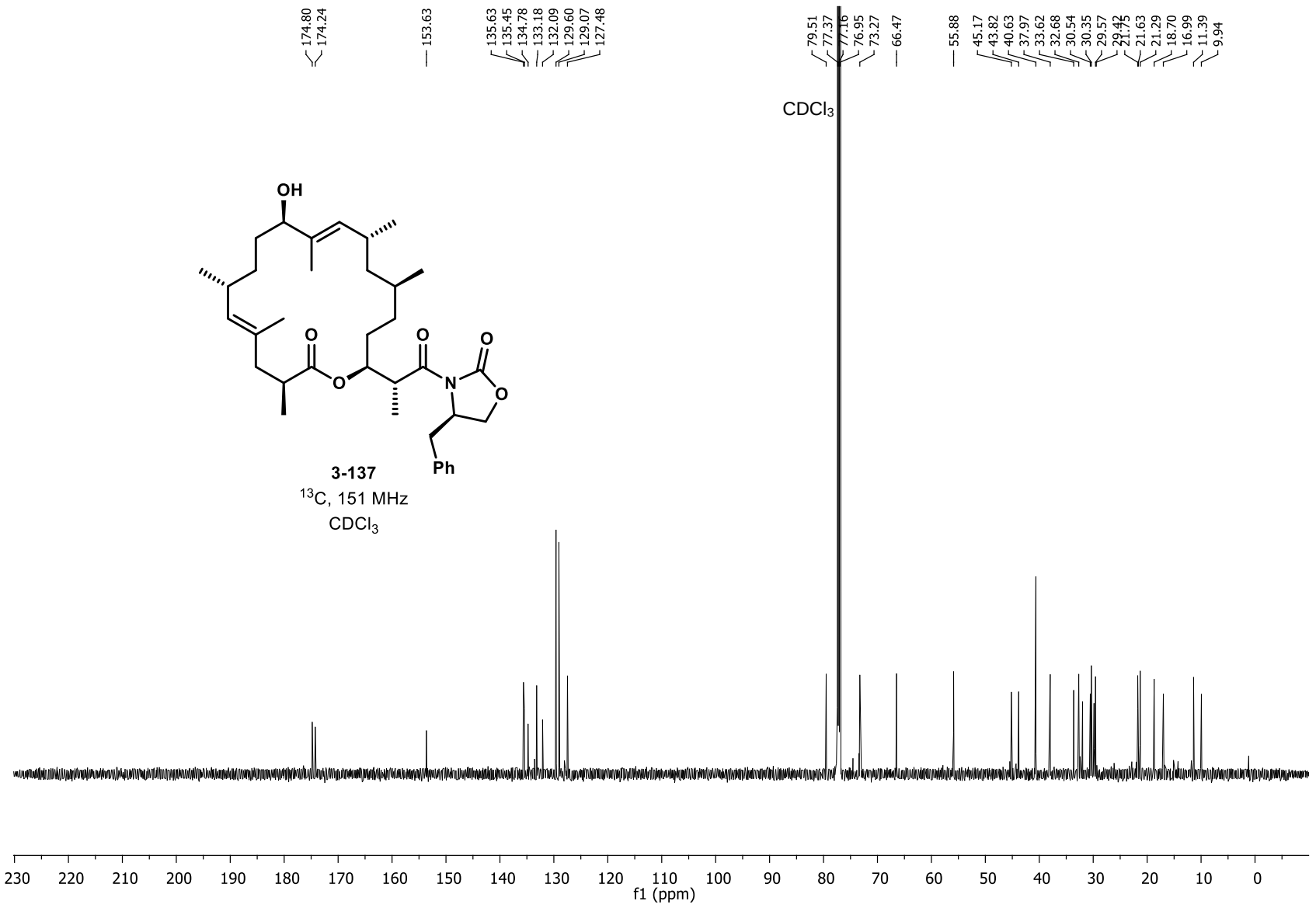
174.80
174.24
153.63
135.63
135.45
134.78
133.18
132.09
129.60
129.07
127.48
79.51
77.37
77.16
76.95
73.27
66.47
55.88
45.17
43.82
40.63
37.97
33.62
32.68
30.54
30.35
29.57
29.42
21.75
21.63
21.29
18.70
16.99
11.39
9.94
CDCl3
OH
O
O
O
O
N
O
Ph
3-137
13C, 151 MHz
CDCl3
230
220
210
200
190
180
170
160
150
140
130
120
110
100
90
80
70
60
50
40
30
20
10
0
f1 (ppm)

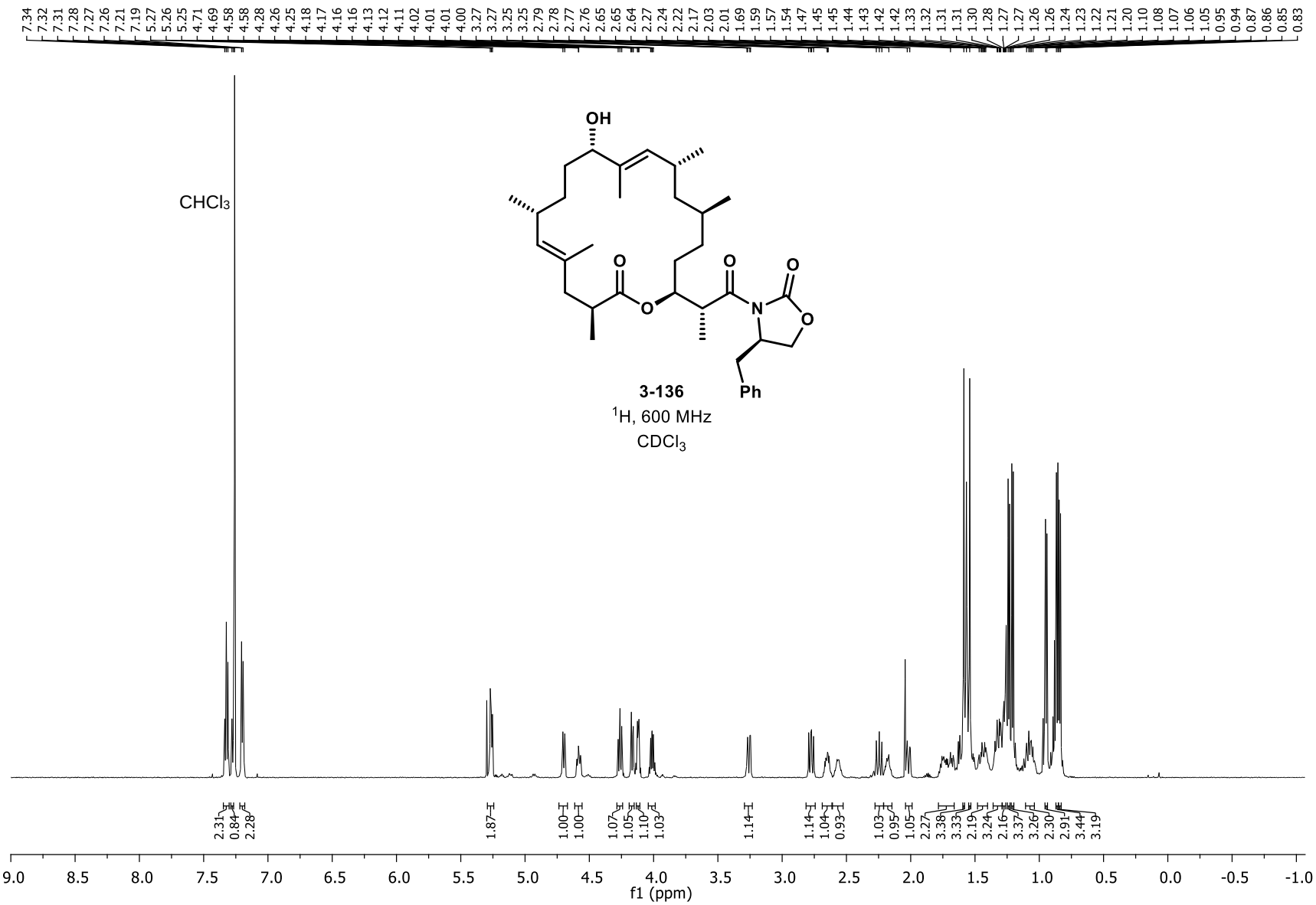
7.34 7.32 7.31 7.28 7.27 7.26 7.21 7.19 5.27 5.26 5.25 4.71 4.69 4.58 4.58 4.28 4.26 4.25 4.18 4.17 4.16 4.16 4.13 4.12 4.11 4.02 4.01 4.01 4.00 3.27 3.27 3.25 3.25 2.79 2.78 2.77 2.76 2.65 2.65 2.64 2.27 2.24 2.22 2.17 2.03 2.01 1.69 1.59 1.57 1.54 1.47 1.45 1.45 1.44 1.43 1.42 1.42 1.33 1.32 1.31 1.31 1.30 1.28 1.27 1.27 1.26 1.26 1.24 1.23 1.22 1.21 1.20 1.10 1.08 1.07 1.06 1.05 0.95 0.94 0.87 0.86 0.85 0.83
CHCl3
OH
O
O
O
O
N
O
Ph
3-136
1H, 600 MHz
CDCl3
2.31 0.84 2.28 1.87 1.00 1.00 1.07 1.05 1.10 1.03 1.14 1.14 1.04 0.93 1.03 0.95 1.05 2.27 3.38 3.33 2.19 3.24 2.16 3.37 3.26 2.30 2.91 3.44 3.19
9.0 8.5 8.0 7.5 7.0 6.5 6.0 5.5 5.0 4.5 4.0 3.5 3.0 2.5 2.0 1.5 1.0 0.5 0.0 -0.5 -1.0
f1 (ppm)

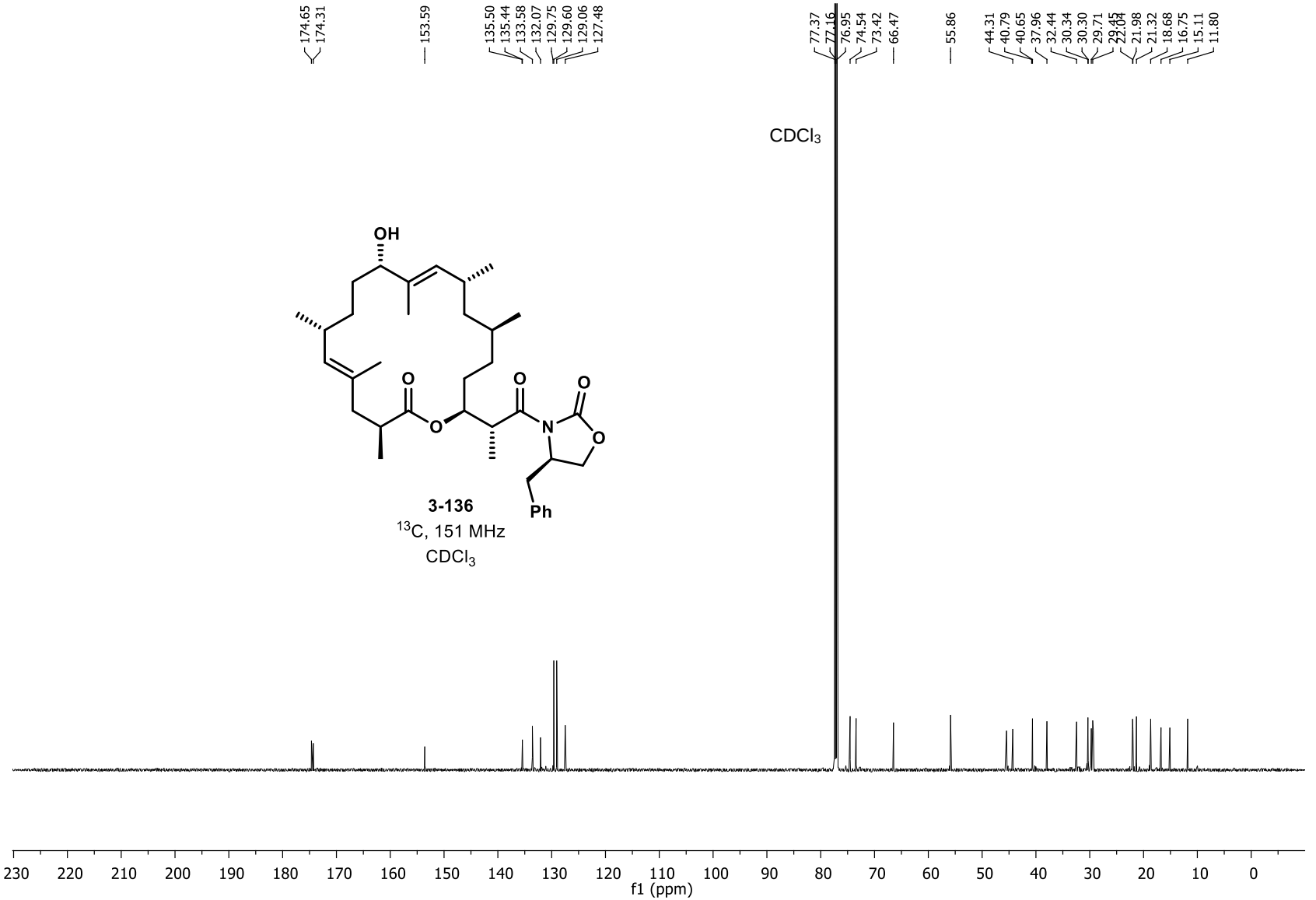
174.65
174.31
153.59
135.50
135.44
133.58
132.07
129.75
129.60
129.06
127.48
77.37
77.16
76.95
74.54
73.42
66.47
55.86
44.31
40.79
40.65
37.96
32.44
30.34
30.30
29.71
29.45
22.04
21.98
21.32
18.68
16.75
15.11
11.80
CDCl3
OH
O
O
O
O
N
O
Ph
3-136
13C, 151 MHz
CDCl3
230
220
210
200
190
180
170
160
150
140
130
120
110
100
90
80
70
60
50
40
30
20
10
0
f1 (ppm)

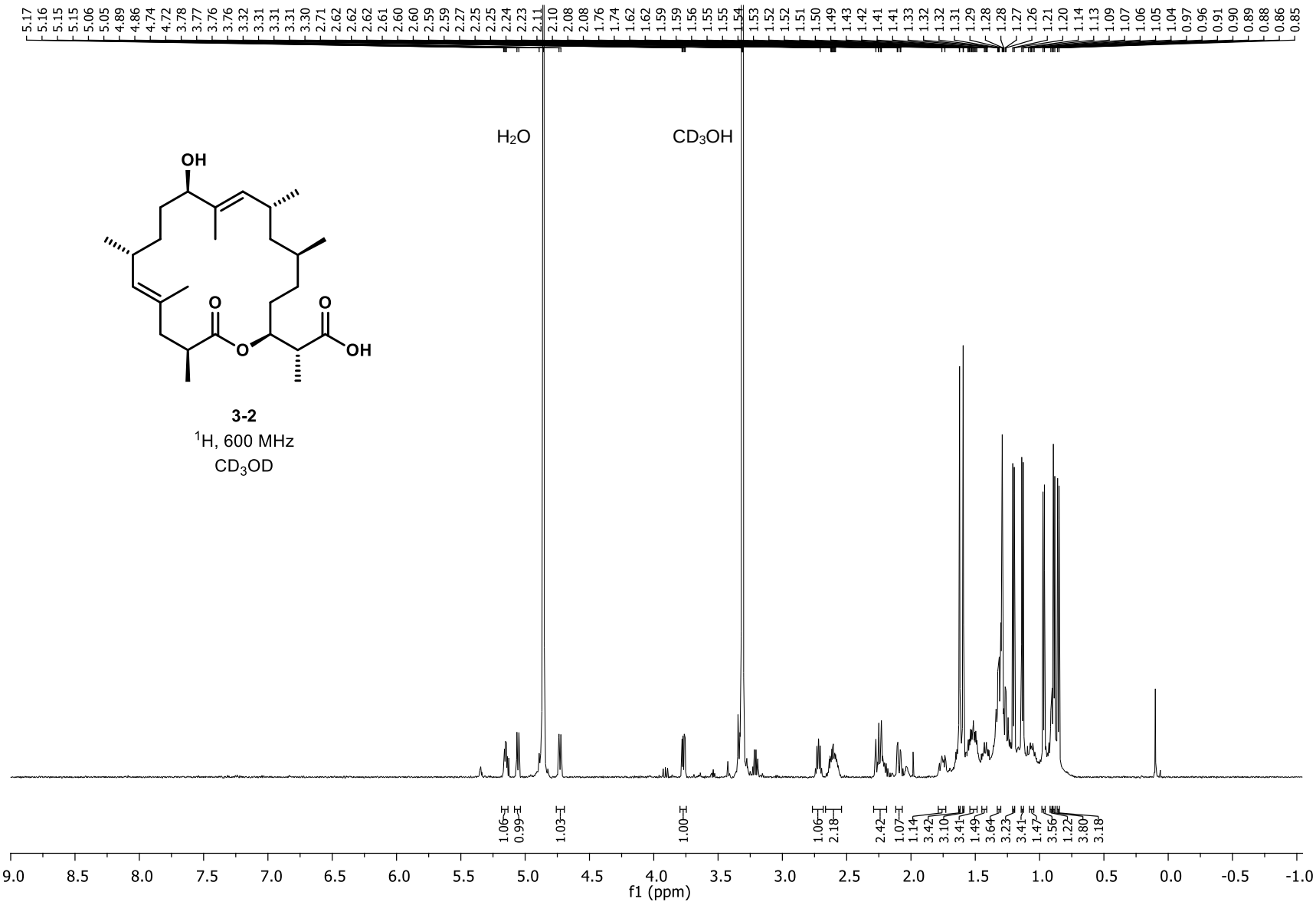
H2O
CD3OH
OH
O
O
O
OH
3-2
1H, 600 MHz
CD3OD
f1 (ppm)

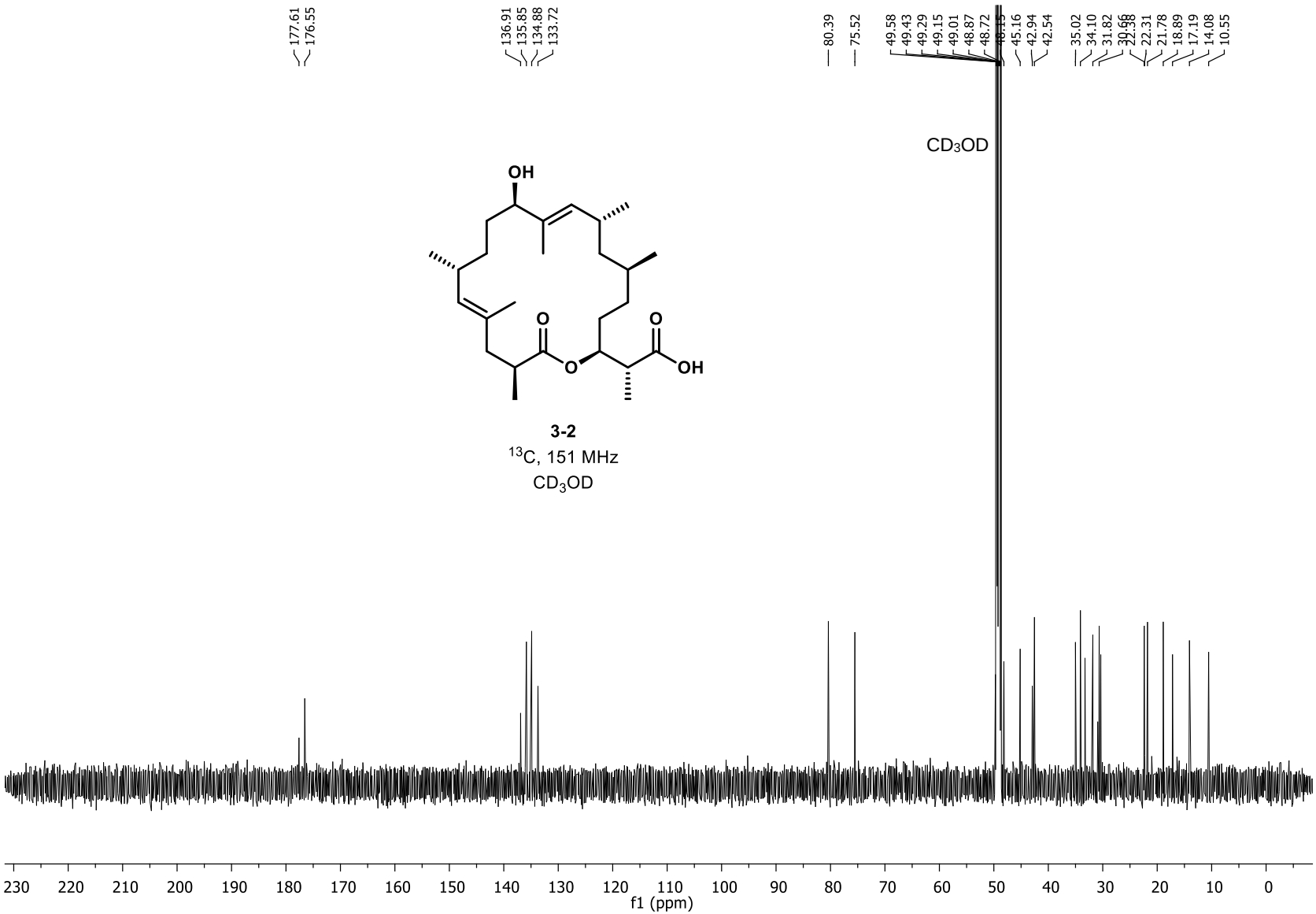
177.61
176.55
136.91
135.85
134.88
133.72
80.39
75.52
49.58
49.43
49.29
49.15
49.01
48.87
48.72
48.15
45.16
42.94
42.54
35.02
34.10
31.82
30.66
22.38
22.31
21.78
18.89
17.19
14.08
10.55
CD3OD
OH
O
O
O
OH
3-2
13C, 151 MHz
CD3OD
230 220 210 200 190 180 170 160 150 140 130 120 110 100 90 80 70 60 50 40 30 20 10 0
f1 (ppm)

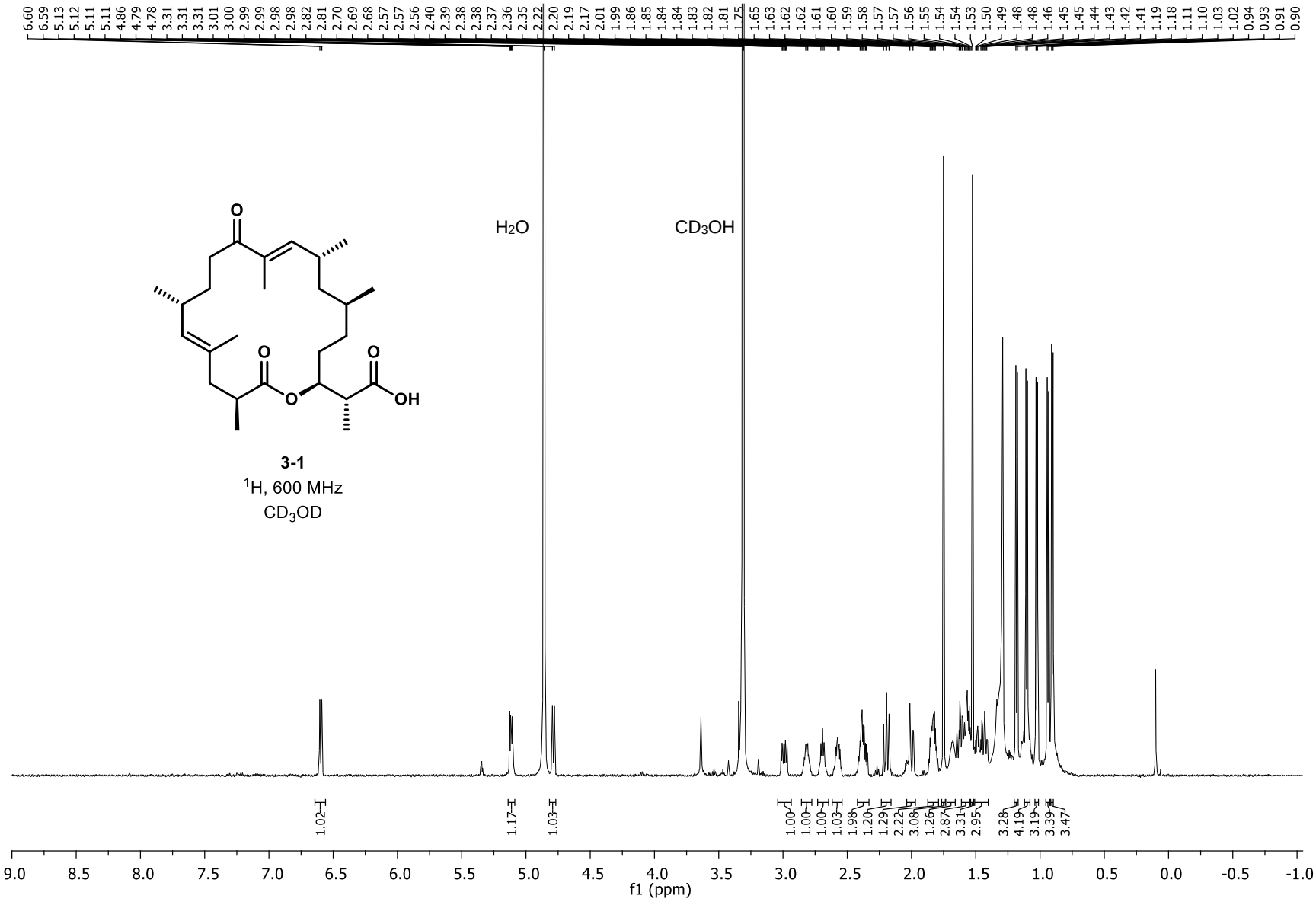
H2O
CD3OH
O
O
O
O
OH
3-1
1H, 600 MHz
CD3OD
f1 (ppm)

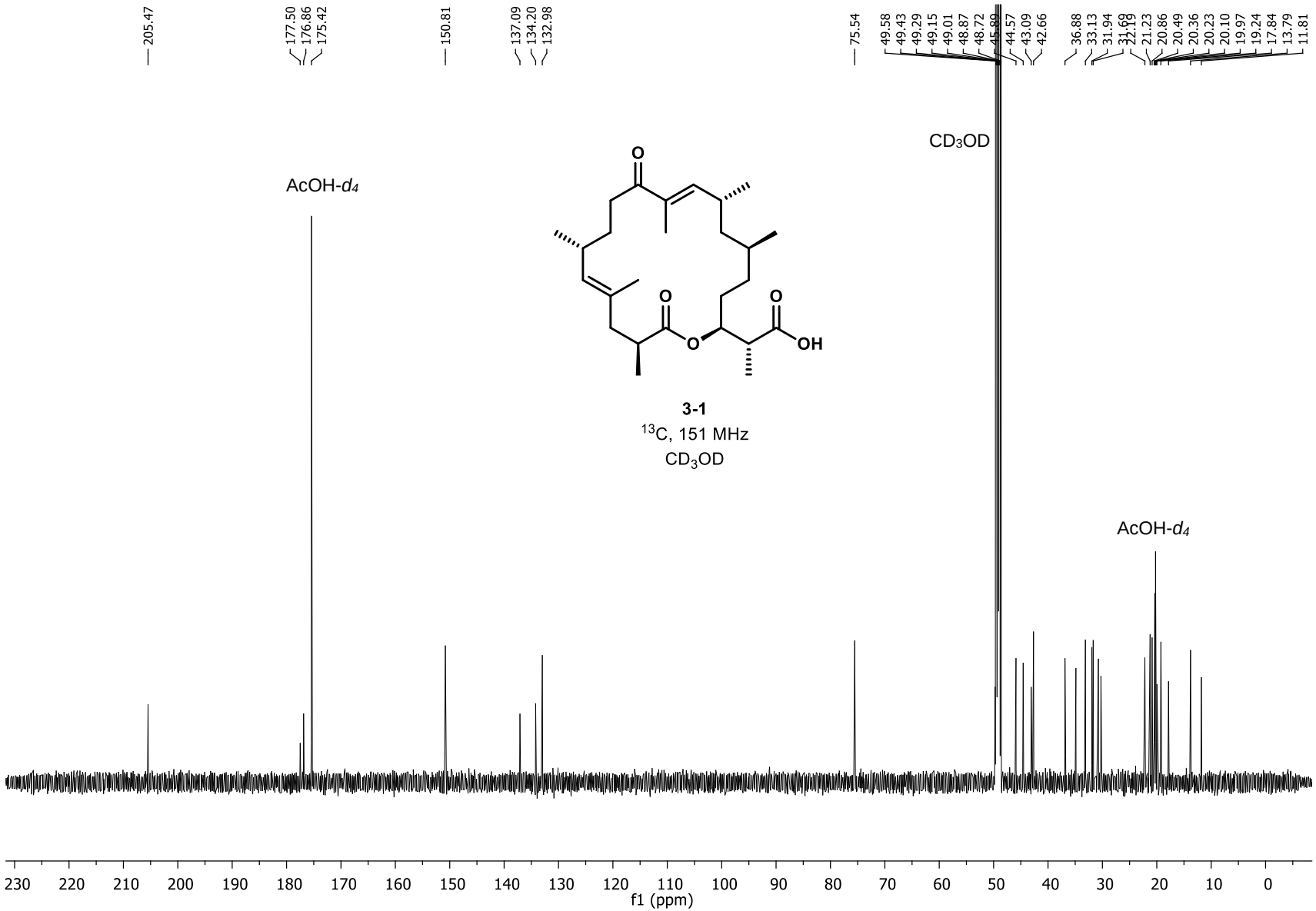
205.47
177.50
176.86
175.42
150.81
137.09
134.20
132.98
75.54
49.58
49.43
49.29
49.15
49.01
48.87
48.72
45.89
44.57
43.09
42.66
36.88
33.13
31.94
31.69
22.19
21.23
20.86
20.49
20.36
20.23
20.10
19.97
19.24
17.84
13.79
11.81
AcOH-d4
CD3OD
AcOH-d4
O
O
O
O
OH
3-1
13C, 151 MHz
CD3OD
230
220
210
200
190
180
170
160
150
140
130
120
110
100
90
80
70
60
50
40
30
20
10
0
f1 (ppm)